SD Public Utilities

Biennial Receiving Waters Monitoring and Assessment Report for the Point Loma and South Bay Ocean Outfalls

2020–2021

City of San Diego Ocean Monitoring Program
Environmental Monitoring and Technical Services Division

The City of SAN DIEGO
Public Utilities Department
Environmental Monitoring & Technical Services Division

June 30, 2022

Mr. David W. Gibson, Executive Officer
California Regional Water Quality Control Board
San Diego Region
2375 Northside Drive, Suite 100
San Diego, CA 92108

Attention: POTW Compliance Unit

Dear Mr. Gibson:

Enclosed is the 2020-2021 Biennial Receiving Waters Monitoring and Assessment Report for the Point Loma and South Bay Ocean Outfalls, as per requirements set forth in the following Orders/Permits:

(1) Order No. R9-2017-0007 for the City of San Diego's Point Loma Wastewater Treatment Plant (NPDES No. CA0107409).
(2) No. R9-2021-0011 for the City's South Bay Water Reclamation Plant (NPDES No. CA0109045).
(3) Order No. R9-2021-0001 for the United States Section of the International Boundary and Water Commission's South Bay International Wastewater Treatment Plant (NPDES No. CA0108928).

This combined report for the Point Loma and South Bay outfall regions contains data summaries, analyses, and assessments for all portions of the Ocean Monitoring Program conducted during 2020 and 2021. Additional data in support of this report will be submitted separately to either the Regional Water Quality Control Board or the California Environmental Data Exchange Network (CEDEN) in accordance with the aforementioned permits.

I certify under penalty of law that this document and all attachments were prepared under my direction or supervision in accordance with a system designed to assure that qualified personnel properly gather and evaluate the information submitted. Based on my inquiry of the person or persons who manage the system or those persons directly responsible for gathering the information, the information submitted is, to the best of my knowledge and belief, true, accurate, and complete. I am aware that there are significant penalties for submitting false information, including the possibility of fine and imprisonment for knowing violations.

If you have questions regarding this report, please call Dr. Ryan Kempster, the City's Senior Marine Biologist at (619) 758-2329.

Sincerely,

Peter S. Vroom, Ph.D.
Deputy Director, Public Utilities Department

PV/rk

cc: U.S. Environmental Protection Agency, Region 9
International Boundary and Water Commission, U.S. Section

SD Public Utilities

Biennial Receiving Waters Monitoring and Assessment Report for the Point Loma and South Bay Ocean Outfalls

2020–2021

Point Loma Wastewater Treatment Plant
(Order No. R9-2017-0007; NPDES No. CA0107409)

South Bay Water Reclamation Plant
(Order No. R9-2021-0011; NPDES No. CA0109045)

South Bay International Wastewater Treatment Plant
(Order No. R9-2021-0001; NPDES No. CA0108928)

Prepared by:
City of San Diego Ocean Monitoring Program
Environmental Monitoring & Technical Services Division, Public Utilities Department

Ryan Kempster, Managing Editor

June 2022

Table of Contents

Production Credits and Acknowledgements ..... **iii**
Table and Figure Listing ..... **iv**
Acronyms and Abbreviations ..... **xiv**

Executive Summary **1**
R. Kempster

Chapter 1. General Introduction **7**
R. Kempster

Program Requirements & Objectives 7
Background 7
Receiving Waters Monitoring 8
Special Studies & Enhanced Monitoring 10
Report Components and Organization 11
Literature Cited 11

Chapter 2. Coastal Oceanographic Conditions **15**
A. Webb, S. Jaeger, W. Enright, G. Rodriguez, C. Lantz, Z. Scott, L. Valentino

Introduction 17
Materials and Methods 16
Results and Discussion 21
Summary 35
Literature Cited 36

Chapter 3. Water Quality Compliance **47**
S. Smith, R. Kempster

Introduction 47
Materials and Methods 47
Results and Discussion 52
Summary 63
Literature Cited 67

Chapter 4. Plume Dispersion **71**
S. Jaeger, W. Enright, G. Welch, A. Webb, S. Smith, A. Feit, R. Kempster, G. Rodriguez

Introduction 71
Materials and Methods 72
Results and Discussion 78
Summary 96
Literature Cited 102

Table of Contents

Chapter 5. Sediment Quality 111
A. Latker, W. Enright

Introduction 111
Materials and Methods 112
Results 114
Discussion 131
Literature Cited 134

Chapter 6. Macrobenthic Communities 139
V. Rodriguez-Villanueva, W. Enright, R. Martinez-Lara

Introduction 139
Materials and Methods 140
Results and Discussion 141
Summary 151
Literature Cited 154

Chapter 7. San Diego Regional Benthic Conditions Assessment 159
A. Latker, W. Enright, L. Nanninga, K. Beauchamp, R. Martinez-Lara, V. Rodriguez-Villanueva

Introduction 159
Materials and Methods 161
Results 164
Discussion 181
Literature Cited 183

Chapter 8. Demersal Fishes and Megabenthic Invertebrates 189
Z. Scott, M. Lilly, M. Kasuya

Introduction 189
Materials and Methods 190
Results and Discussion 192
Summary 216
Literature Cited 218

Chapter 9. Contaminants in Marine Fishes 223
L. Valentino, A. Latker

Introduction 223
Materials and Methods 223
Results 227
Discussion 246
Literature Cited 249

Table of Contents

Appendices - Enhanced Monitoring Reports

Appendix A: Evaluation of Anthropogenic Impacts on the San Diego Coastal Kelp Forest Ecosystem (Biennial Project Report) 2020 to 2021
E. Parnell, K. Riser, B. Bulach, P.K. Dayton,
Scripps Institution of Oceanography, UC San Diego

Appendix B:Satellite & Aerial Coastal Water Quality Monitoring in the San Diego/Tijuana Region, Five Year Summary Report, 1 January 2017 - 31 December, 2021
J. Svejkovsky, M. Hess,
Ocean Imaging, Littleton, CO

Appendices - Supplemental Analyses

Appendix C: Coastal Oceanographic Conditions
Appendix D: Water Quality Compliance
Appendix E: Plume Dispersion
Appendix F: Sediment Quality
Appendix G: Macrobenthic Communities
Appendix H: San Diego Regional Benthic Conditions Assessment
Appendix I: Demersal Fishes and Megabenthic Invertebrates
Appendix J: Contaminants in Marine Fishes

Production Credits and Acknowledgements

Senior Editor: *R. Kempster*

Production Editor: *Z. Scott*

GIS Graphics: *M. Kasuya, A. Webb*

Production Team: *W. Enright, M. Lilly, L. Valentino, S. Smith, R. Kempster*

Cover Photo:
City research vessel *Oceanus* near North Coronado Island. Photo taken by Mark Phillips.

Acknowledgments:
We are grateful to the personnel of the City's Marine Biology, Marine Microbiology, and Environmental Chemistry Services Laboratories for their assistance in the collection and/or processing of all samples, and for discussions of the results. The completion of this report would not have been possible without their continued efforts and contributions. Complete staff listings for the above labs and additional details concerning relevant QA/QC activities for the receiving waters monitoring data reported herein are available upon request.

Table of Contents

How to cite this document:
City of San Diego. (2022). Biennial Receiving Waters Monitoring and Assessment Report for the Point Loma and South Bay Ocean Outfalls, 2020–2021. City of San Diego Ocean Monitoring Program, Public Utilities Department, Environmental Monitoring and Technical Services Division, San Diego, CA.

List of Tables

Chapter 1: General Introduction

1.1 NPDES permits for wastewater treatment plants run by the City of San Diego and the USIBWC 8

Chapter 2: Coastal Oceanographic Conditions

2.1 Sensor configuration and model type for RTOMS by site and depth during 2020 19
2.2 Long-term climate-related events in the Southern California Bight 40

Chapter 3: Water Quality Compliance

3.1 Depths at which seawater samples are collected for kelp and offshore stations 51
3.2 Percent compliance with STV standards during 2020 and 2021 54
3.3 Elevated bacteria densities at shore stations during 2020 and 2021 56
3.4 Elevated bacteria densities at kelp stations during 2020 and 2021 60
3.5 Elevated bacteria densities at offshore stations during 2020 and 2021 63
3.6 Percent compliance with the HF183 sampling standards 67

Chapter 4: Plume Dispersion

4.1 Summary of the numbers of reference stations, potential wastewater plume detections, and out-of-range values at offshore stations during 2020 and 2021 80
4.2 Summary of ocean conditions and observed CTD plume ranges during ScanFish surveys 97

Chapter 5: Sediment Conditions

5.1 Particle size and sediment chemistry parameters at PLOO benthic stations, 1991–2019 and 2020–2021 115
5.2 Particle size and sediment chemistry parameters at SBOO benthic stations, 1995–2019 and 2020–2021 120
5.3 Summary of sediment chemistry samples exceeding ERL and ERM thresholds, 1991–2019 and 2020–2021 124

Chapter 6: Macrobenthic Communities

6.1 Macrofaunal community parameters at PLOO benthic stations during 2020 and 2021 143
6.2 Macrofaunal community parameters at SBOO benthic stations during 2020 and 2021 144
6.3 Percent composition and abundance of major taxonomic groups during 2020 and 2021 147

Table of Contents

List of Tables (*continued*)

6.4 Ten most abundant macroinvertebrates collected at PLOO stations during 2020 and 2021 148
6.5 Ten most abundant macroinvertebrates collected at SBOO stations during 2020 and 2021 151

Chapter 7: San Diego Regional Benthic Conditions Assessment
7.1 Particle size and chemistry parameters at regional and core benthic stations during 2020 and 2021 166
7.2 Summary of particle size data for cluster groups A–H 170
7.3 Macrofaunal community parameters for regional and core stations during 2020 and 2021 175
7.4 Results for the BRI, sediment toxicity, and SQO lines of evidence for the San Diego regional and core benthic stations sampled during summer 2020 and 2021 181

Chapter 8: Demersal Fishes and Megabenthic Invertebrates
8.1 Top 15 demersal fish species collected from 18 trawls in the PLOO region during 2020 and 2021 192
8.2 Top 15 demersal fish species collected from 21 trawls in the SBOO region during 2020 and 2021 193
8.3 Demersal fish community parameters at PLOO and SBOO trawl stations during 2020 and 2021 194
8.4 Top 15 megabenthic invertebrate species collected from 18 trawls in the PLOO region during 2020 and 2021 206
8.5 Top 15 megabenthic invertebrate species collected from 21 trawls in the SBOO region during 2020 and 2021 207
8.6 Megabenthic invertebrate community parameters at PLOO and SBOO trawl stations during 2020 and 2021 208

Chapter 9: Bioaccumulation of Contaminants in Fish Tissues
9.1 Fish species collected from trawl and rig fishing zones during 2020 and 2021 226
9.2 Summary of metals in liver tissues for PLOO and SBOO trawl zones during 2020 and 2021 228
9.3 Summary of metals in liver tissues for PLOO and SBOO trawl zones, 1995–2021 230
9.4 Summary of pesticides, total PCB, total PAH, and lipids in liver tissues for PLOO and SBOO trawl zones during 2020 and 2021 234
9.5 Summary of pesticides, total PCB, total PAH, and lipids in liver tissues for PLOO and SBOO trawl zones, 1995–2021 235
9.6 Summary of metals in muscle tissues for PLOO and SBOO rig fishing zones during 2020 and 2021 239
9.7 Summary of metals in muscle tissues for PLOO and SBOO rig fishing zones, 1995–2021 241

Table of Contents

List of Tables (*continued*)

9.8 Summary of metals, pesticides, and total PCB in muscle tissues that exceeded thresholds for PLOO and SBOO rig fishing zones, 1995–2019 and during 2020 and 2021 244
9.9 Summary of pesticides, total PCB, total PAH, and lipids in muscle tissues for PLOO and SBOO rig fishing zones during 2020 and 2021 245
9.10 Summary of pesticides, total PCB, total PAH, and lipids in muscle tissues for PLOO and SBOO rig fishing zones, 1995–2021....246

List of Figures

Chapter 1: General Introduction

1.1 Receiving waters monitoring stations sampled around the PLOO and the SBOO....9

Chapter 2: Coastal Oceanographic Conditions

2.1 Location of water quality monitoring stations around the PLOO and the SBOO 17
2.2 Temperature, density, salinity, and dissolved oxygen in the PLOO region during 2020 22
2.3 Temperature, density, salinity, and dissolved oxygen in the PLOO region during 2021 23
2.4 Temperature, density, salinity, and dissolved oxygen in the SBOO region during 2020 24
2.5 Temperature, density, salinity, and dissolved oxygen in the SBOO region during 2021 25
2.6 Daily averaged temperature recorded near the PLOO by the RTOMS or thermistor array during 2020 and 2021....26
2.7 Daily averaged temperature recorded near the SBOO by the RTOMS or thermistor array during 2020 and 2021....27
2.8 Daily averaged salinity and density recorded by the PLOO RTOMS in 2020 28
2.9 Daily averaged salinity and density recorded by the SBOO RTOMS in 2020....29
2.10 Mean density for each survey conducted during 2020 and 2021 at PLOO and SBOO discharge depth stations....30
2.11 Hourly averaged DO by season at 89 m for available PLOO mooring data from 2020 to 2021....31
2.12 Hourly averaged DO by season at 26 m for available SBOO mooring data from 2020 to 2021....32
2.13 SPOT-6/7 satellite image of the San Diego region acquired April 23, 2020 depicting phtoplankton blooms....33
2.14 Temperature, DO, pH, and chlorophyll a data recorded at the SBOO RTOMS at 1 m during 2020–2021 35
2.15 Current speed and direction data, by season, from the PLOO RTOMS ADCP in 2020 36
2.16 Current speed and direction data, by season, from the SBOO RTOMS ADCP in 2020 37

Table of Contents

List of Figures (*continued*)

2.17 General current speed and direction data for select depth bins at PLOO and SBOO RTOMS locations 38
2.18 Time series of temperature, salinity, and dissolved oxygen anomalies in the PLOO and SBOO regions, 1991–2021 39

Chapter 3: Water Quality Compliance
3.1 Water quality monitoring stations sampled around the PLOO and the SBOO 49
3.2 Distribution of values at PLOO shore stations during 2020 and 2021 for running mean and median calculations, and single sample values 53
3.3 Distribution of values at SBOO shore stations during 2020 and 2021 for running mean and median calculations, and single sample values 55
3.4 Percentage of samples with elevated FIB densities in wet versus dry seasons at shore stations, 1991–2021 57
3.5 Distribution of values at PLOO kelp stations during 2020 and 2021 for running mean and median calculations, and single sample values 58
3.6 Distribution of values at SBOO kelp stations during 2020 and 2021 for running mean and median calculations, and single sample values 59
3.7 Comparison of annual rainfall to elevated FIB densities in wet versus dry seasons at kelp stations, 1991–2021 61
3.8 Landsat 8 satellite image taken on February 3, 2020 combined with bacteria levels at shore and kelp stations from February 2020 62
3.9 Distribution of values for PLOO and SBOO offshore stations during 2020 and 2021 64
3.10 Occurrence of elevated FIB at PLOO 98-m offshore stations by depth and outfall proximity, across the historical dataset 65
3.11 Occurrence of elevated FIB at SBOO 28-m offshore stations by depth and outfall proximity, across the historical dataset 66

Chapter 4: Plume Dispersion
4.1 Location of water quality monitoring stations sampled around the PLOO and the SBOO 73
4.2 ROTV tow paths for surveys conducted around the PLOO during winter 2020 and 2021 77
4.3 ROTV tow path for survey conducted around the SBOO during fall 2020, overlaid on a SPOT 6 satellite image taken on November 9, 2020 79
4.4 Distribution of stations with potential plume detections and those used as reference stations for water quality compliance calculations during 2020 and 2021 82
4.5 Depth profiles by season of the number of potential plume detections at PLOO and SBOO offshore stations during 2020 and 2021 84
4.6 Daily averaged salinity anomalies by year for each mooring sensor depth using available PLOO and SBOO RTOMS data 87
4.7 PLOO RTOMS hourly averaged ocean temperature, salinity, current speeds, chlorophyll *a*, CDOM, turbidity, and nitrate + nitrite during winter 2020 90

Table of Contents

LIST OF FIGURES (*continued*)

4.8 PLOO RTOMS hourly averaged CDOM, turbidity, nitrate + nitrite, and chlorophyll *a* shown on temperature versus salinity plots at 89 m for winter 2020....92
4.9 SBOO RTOMS hourly averaged ocean temperature, salinity, current speeds, chlorophyll *a*, CDOM, turbidity, and nitrate + nitrite during winter 2020.....93
4.10 SBOO RTOMS hourly averaged CDOM, turbidity, nitrate + nitrite, and chlorophyll *a* shown on temperature versus salinity plots at 1 m for winter 2020.....95
4.11 CDOM data from ROTV surveys of the PLOO region during winter 2020.....100
4.12 OB data from ROTV surveys of the PLOO region during winter 2020.....101
4.13 CDOM data from ROTV surveys of the PLOO region during winter 2021.....102
4.14 OB data from ROTV surveys of the PLOO region during winter 2021.....103
4.15 CDOM data from ROTV surveys of the SBOO region during winter 2020.....104
4.16 OB data from ROTV surveys of the SBOO region during winter 2020.....105

Chapter 5: Sediment Quality

5.1 Benthic stations sampled around the PLOO and SBOO.....113
5.2 Sediment composition at benthic stations during 2020 and 2021.....116
5.3 Concentrations of percent fines and various organic indicators in sediments at benthic stations, 1991–2021.....117
5.4 Distribution of select organic indicators in sediments during 2020 and 2021.....121
5.5 Distribution of select metals in sediments during 2020 and 2021.....125
5.6 Concentrations of select metals in sediments at benthic stations, 1991–2021.....128
5.7 Distribution of total DDT, total PCB and total PAH in sediments during 2020 and 2021.....130
5.8 Concentrations of DDT, total PCB, and total PAH in sediments at benthic stations, 1991–2021.....132

Chapter 6: Macrobenthic Communities

6.1 Benthic stations sampled around the PLOO and the SBOO.....141
6.2 Macrofaunal community parameters pre-discharge, post-discharge, and during 2020 and 2021.....145
6.3 Benthic Response Index, 1991–2021.....146
6.4 The five most abundant taxa at PLOO stations, 1991–2021.....149
6.5 Ecologically important indicator species collected at PLOO stations, 1991–2021...150
6.6 The five most abundant taxa at SBOO stations, 1995–2021.....151
6.7 Ecologically important indicator species collected at SBOO stations, 1995–2021...153

Chapter 7: San Diego Regional Benthic Conditions Assessment

7.1 Regional and core benthic stations sampled off San Diego and northern Baja during 2020 and 2021.....160
7.2 Scatterplot of percent fines versus depth for regional and core benthic stations during summer 2020 and 2021.....167
7.3 Ordination and cluster analysis of particle size data for regional and core benthic stations during summer 2020 and 2021.....168

Table of Contents

LIST OF FIGURES (*continued*)

7.4 Spatial distribution of particle size cluster groups A–H 169
7.5 Ordination and cluster analysis of sediment chemistry data for regional and core benthic stations during summer 2020 and 2021 172
7.6 Spatial distribution of sediment chemistry cluster groups A–F 173
7.7 Ordination and cluster analysis of macrofauna data for regional and core benthic stations during summer 2020 and 2021 176
7.8 Spatial distribution of macrofaunal cluster groups A–M.....177

Chapter 8: Demersal Fishes and Megabenthic Invertebrates
8.1 Trawl stations sampled around the PLOO and the SBOO.....190
8.2 Demersal fishes community parameters pre-discharge, post-discharge, and from 2020 and 2021 196
8.3 Ten most abundant fish species from PLOO trawl stations, 1991–2021 197
8.4 Ten most abundant fish species from SBOO trawl stations, 1995–2021.....199
8.5 Percentages of fishes collected at stations with anomalies present during 2020 and 2021 201
8.6 Results of ordination and cluster analysis of demersal fishes from PLOO trawl stations, 1991–2021 203
8.7 Results of ordination and cluster analysis of demersal fishes from SBOO trawl stations,1995–2021 204
8.8 Megabenthic invertebrates community parameters pre-discharge, post-discharge, and from 2020 and 2021 209
8.9 Ten most abundant megabenthic invertebrate species from PLOO trawl stations, 1991–2021 210
8.10 Ten most abundant megabenthic invertebrate species from SBOO trawl stations, 1995–2021 212
8.11 Results of ordination and cluster analysis of megabenthic inverterbate species from PLOO trawl stations, 1991–2021 215
8.12 Results of ordination and cluster analysis of megabenthic invertebrate species from SBOO trawl stations, 1995–2021.....217

Chapter 9: Bioaccumulation of Contaminants in Fish Tissues
9.1 Trawl and rig fishing zones sampled around the PLOO and SBOO.....224
9.2 Concentrations of metals in fish liver tissues from trawl zones, 1995–2021.....232
9.3 Concentrations of pesticides and total PCB in fish liver tissues from trawl zones, 1995–2021 236
9.4 Concentrations of metals in fish muscle tissues from rig fishing zones, 1995–2021.....242
9.5 Concentrations of pesticides and total PCB in fish muscle tissues from rig fishing zones, 1995–2021 247

Table of Contents

List of Boxes

Chapter 3: Water Quality

3.1 2019 California Ocean Plan water quality objectives for water contact areas 50
3.2 Receiving Water Baterial Compliance requirements from NPDES Permits 52

List of Appendices

Appendix C: Coastal Oceanographic Conditions

C.1 Sample dates for quarterly oceanographic surveys during 2020 and 2021 .....C1
C.2 Location, depth, and dates for each year-long deployment of the PLOO and SBOO RTOMS C2
C.3 Summary of QA/QC findings for the PLOO and SBOO RTOMS C3
C.4 Location, depth, and dates for each year-long deployment of the static moorings located at PLOO and SBOO C4
C.5 Data qualifier definitions for QC data flags.....C5
C.6 Ranges used for automated QC data flagging for each parameter for the gross range test.....C6
C.7 Annual ranges used for automated QC data flagging for each parameter, site, and depth for the climatological range test C7
C.8 Temperature near the PLOO RTOMS sensors by the thermistor array during 2020 and 2021 .....C8
C.9 Temperature near the SBOO RTOMS sensors by the thermistor array during 2020 and 2021 .....C9
C.10 Summary of temperature, salinity, DO, pH, chlorophyll a, CDOM, turbidity, nitrate + nitrite, BOD, and xCO2 at the PLOO RTOMS in fall 2021.....C10
C.11 Summary of temperature, salinity, DO, pH, chlorophyll a, CDOM, turbidity, nitrate + nitrite, BOD, and xCO2 at the SBOO RTOMS in fall 2021 .....C12
C.12 Temperature, salinity, DO, pH, chlorophyll a, CDOM, turbidity, nitrate + nitrite, BOD, and xCO2 recorded at the PLOO and SBOO RTOMS during 2020 and 2021.....C14
C.13 Seasonal buoyancy frequency in the PLOO and SBOO regions during 2020 and 2021 .....C33
C.14 pH, transmissivity, and chlorophyll *a* in the PLOO region during 2020 .....C34
C.15 pH, transmissivity, and chlorophyll *a* in the PLOO region during 2021 .....C35
C.16 pH, transmissivity, and chlorophyll *a* in the SBOO region during 2020 .....C36
C.17 pH, transmissivity, and chlorophyll *a* in the SBOO region during 2021 .....C37
C.18 Summary of current velocity magnitude and direction from the PLOO RTOMS ADCP during 2021.....C38
C.19 Summary of current velocity magnitude and direction from the SBOO RTOMS ADCP during 2021.....C41
C.20 Summary of current velocity magnitude and direction from the PLOO static ADCP during 2021.....C42
C.21 Summary of current velocity magnitude and direction from the SBOO static ADCP during 2021.....C45

Table of Contents

LIST OF APPENDICES (*continued*)

C.22 Current speed and direction data, by season, from the PLOO static ADCP in 2020 and 2021 ..... C46
C.23 Current speed and direction data, by season, from the SBOO static ADCP in 2020 and 2021 ..... C47

Appendix D: Water Quality Compliance
D.1 Water quality monitoring stations sampled around the PLOO and SBOO D3
D.2 2015 California Ocean Plan water quality objectives for water contact areas D4
D.3 Depths at which seawater samples are collected for kelp and offshore stations D5
D.4 Compliance rates for geometric mean and single sample maximum water contact standards at shore stations during 2020 and 2021 ..... D6
D.5 Elevated bacteria densities at shore stations during 2020 and 2021 ..... D7
D.6 Compliance rates for geometric mean and single sample maximum water contact standards at kelp stations during 2020 and 2021 ..... D8
D.7 Elevated bacteria densities at kelp stations during 2020 and 2021 ..... D9
D.8 Elevated bacteria densities at offshore stations during 2020 and 2021 ..... D10
D.9 Percent of samples collected from PLOO 98-m off shore stations with elevated bacteria during 2020 and 2021, compared to 1993–2019 ..... D11

Appendix E: Plume Dispersion
E.1 CDOM in the PLOO region in 2020 and 2021 ..... E1
E.2 CDOM in the SBOO region in 2020 and 2021 ..... E2
E.3 Summary of oceanographic data within potential detected plume at PLOO offshore stations during 2020 and 2021 ..... E3
E.4 CDOM and buoyancy frequency from PLOO station F30 during 2020 ..... E5
E.5 CDOM and buoyancy frequency from PLOO station F30 during 2021 ..... E6
E.6 CDOM and DO from PLOO station F30 during 2020 ..... E7
E.7 CDOM and DO from PLOO station F30 during 2021 ..... E8
E.8 CDOM and pH from PLOO station F30 during 2020 ..... E9
E.9 CDOM and pH from PLOO station F30 during 2021 ..... E10
E.10 CDOM and transmissivity from PLOO station F30 during 2020 ..... E11
E.11 CDOM and transmissivity from PLOO station F30 during 2021 ..... E12
E.12 Summary of oceanographic data within potential detected plume at SBOO offshore stations during 2020 and 2021 ..... E13
E.13 CDOM and buoyancy frequency from SBOO station I12 during 2020 ..... E15
E.14 CDOM and buoyancy frequency from SBOO station I12 during 2021 ..... E16
E.15 CDOM and DO from SBOO station I12 during 2020 ..... E17
E.16 CDOM and DO from SBOO station I12 during 2021 ..... E18
E.17 CDOM and pH from SBOO station I12 during 2020 ..... E19
E.18 CDOM and pH from SBOO station I12 during 2021 ..... E20
E.19 CDOM and transmissivity from SBOO station I12 during 2020 ..... E21
E.20 CDOM and transmissivity from SBOO station I12 during 2021 ..... E22

Table of Contents

LIST OF APPENDICES (*continued*)

E.21 Maximum daily averaged thermal gradients by depth of occurrence near PLOO and SBOO in 2020 and 2021 ..... E23
E.22 Daily averaged current speeds from the PLOO RTOMS in 2020 and static ACDP in 2021 ..... E24
E.23 Daily averaged current speeds from the SBOO RTOMS in 2020 and static ACDP in 2021 ..... E25

Appendix F: Sediment Conditions
F.1 Constituents and method detection limits for sediment samples analyzed during 2020 and 2021 ..... F1
F.2 Particle size classification of sediments during 2020 and 2021 ..... F3
F.3 Visual observations of PLOO and SBOO sediments during 2020 and 2021 ..... F4
F.4 Distribution of select metals in sediments during 2020 and 2021 ..... F6
F.5 Concentrations of select metals in sediments at benthic stations, 1991–2021 ..... F11

Appendix G: Macrobenthic Communities
G.1 Macrofaunal community parameters by grab for PLOO benthic stations sampled during 2021 ..... G1
G.2 Macrofaunal community parameters by grab for SBOO benthic stations sampled during 2021 ..... G3
G.3 Summary taxonomic listing of benthic infauna taxa identified from PLOO stations during 2021 ..... G5
G.4 Summary taxonomic listing of benthic infauna taxa identified from SBOO stations during 2021 ..... G15
G.5 Two of the five historically most abundant species recorded at PLOO stations, 1991–2021 ..... G28
G.6 Two of the five historically most abundant species recorded at SBOO stations, 1995–2021 ..... G29

Appendix H: San Diego Regional Benthic Conditions Assessment
H.1 Summary of visual observations for regional stations during 2020 and 2021 ..... H1
H.2 Summary taxonomic listing of benthic infauna taxa identified from regional stations during 2021 ..... H2
H.3 Results of spearman rank correlation of sediment parameters during summer 2020 and 2021 ..... H16
H.4 Fine particles in sediments from regional and core benthic stations during the summer 2020 and 2021 ..... H17
H.5 Distribution of select parameters in sediments from regional and core stations during summer 2020 and 2021 ..... H18
H.6 Sediment chemistry summary for sediment chemistry cluster groups A–F H29
H.7 Bioassay results for sediment toxicity testing from regional and core benthic stations during 2020 and 2021 ..... H32

Table of Contents

List of Appendices (*continued*)

H.8 Distribution of BRI values from regional and core stations summer 2020 and 2021 ..... H33
H.9 Particle size summary for each macrofauna cluster group A–M H34
H.10 Mean abundance of characteristic species found in cluster groups A–M H35

Appendix I: Demersal Fishes and Megabenthic Invertebrates

I.1 Taxonomic listing of fish species captured at PLOO trawl stations during 2020 and 2021 ..... I1
I.2 Taxonomic listing of fish species captured at SBOO trawl stations during 2020 and 2021 ..... I3
I.3 Summary of fish lengths of the four most abundant species from the PLOO region during 2020 and 2021 ..... I5
I.4 Summary of fish lengths of the four most abundant species from the SBOO region during 2020 and 2021 ..... I6
I.5 Summary of fish abnormalities and parasites at PLOO and SBOO trawl stations during 2020 and 2021 ..... I7
I.6 Description of PLOO demersal fish cluster groups A–D I8
I.7 Description of SBOO demersal fish cluster groups A–F I9
I.8 Taxonomic listing of megabenthic invertebrate species at PLOO trawl stations during 2020 and 2021 ..... I10
I.9 Taxonomic listing of megabenthic invertebrate species at SBOO trawl stations during 2020 and 2021 ..... I11
I.10 Description of PLOO megabenthic invertebrate cluster groups A–F I13
I.11 Description of SBOO megabenthic invertebrate cluster groups A–D I14

Appendix J: Contaminants in Marine Fishes

J.1 Length and weight data of fish species collected from PLOO trawl and rig fishing zones during 2020 and 2021 ..... J1
J.2 Length and weight data of fish species collected from SBOO trawl and rig fishing zones during 2020 and 2021 ..... J2
J.3 Constituents and method detection limits for liver and muscle tissue analyses from fish collected during 2020 and 2021 ..... J3
J.4 Concentrations of select metals in liver tissues of fishes collected from PLOO and SBOO trawl zones, 1995–2021 ..... J5
J.5 Concentrations of pesticides and total PAH in liver tissues of fishes collected from PLOO and SBOO trawl zones, 1995–2021 ..... J10
J.6 Concentrations of select metals in muscle tissues of fishes collected from PLOO and SBOO rig fishing zones, 1995–2021 ..... J12
J.7 Concentrations of dieldrin and total PAH in muscle tissues of fishes collected from PLOO and SBOO rig fishing zones, 1995–2021 ..... J17

Acronyms and Abbreviations

Abun	Abundance
AL	USFDA Action Limits
ADCP	Acoustic Doppler Current Profiler
ANOSIM	Analysis of Similarity
APHA	American Public Health Association
BF	Buoyancy Frequency
BM	Biomass
BOD	Biochemical Oxygen Demand
BRI	Benthic Response Index
BSQPC	B'18 Sediment Quality Planning Committee
CalCOFI	California Cooperative Fisheries Investigation
CCS	California Current System
CDIP	Coastal Data Information Program
CDOM	Colored Dissolved Organic Matter
CDPH	California Department of Public Health
CEDEN	California Environmental Data Exchange Network
CFU	Colony Forming Units
CI	Confidence Interval
CLA	City of Los Angeles
cm	centimeter
CSDTL	City of San Diego Toxicity Laboratory
CTD	Conductivity, Temperature, Depth Instrument
DDT	Dichlorodiphenyltrichloroethane
dp/dz	density gradient
DO	dissolved oxygen
Dom	Swartz dominance index
DR	Detection Rate
ELAP	Environmental Laboratory Accreditation Program
EMAP	Environmental Monitoring and Assessment Program
EMTS	Environmental Monitoring and Technical Services
ENSO	El Niño Southern Oscillation
ERL	Effects Range Low
ERM	Effects Range Median
FO	Frequency of Occurrence
F:T	Fecal to Total coliform ratio
FIB	Fecal Indicator Bacteria
FTR	Fecal to Total coliform Ratio criterion
g	gram
H'	Shannon Diversity Index
HCB	Hexachlorobenzene
HCH	Hexachlorocylclohexane
HDPE	High-density polyethylene
in	inches
IS	International Standard
J'	Pielou’s evenness index

Acronyms and Abbreviations

kg	kilogram
km	kilometer
km^2	square kilometer
L	Liter
LACSD	Los Angeles County Sanitation District
LJKF	La Jolla Kelp Forest
LOE	Line of Evidence
m	meter
MAH	Mean Abundance per Haul
MAO	Mean Abundance per Occurrence
m^2	square meter
MDL	Method Detection Limit
MEI	Multivariate ENSO Index
mg	milligram
mgd	millions of gallons per day
MIS	Median International Standard
mL	milliliter
mm	millimeter
MODIS	Moderate Resolution Imaging Spectroradiometer
MRP	Monitoring and Reporting Program
mt	metric ton
n	sample size
N	Number of observations used in a Chi-square analysis
nd	not detected
ng	nanograms
nMDS	non-metric Multidimensional Scaling
NOAA	National Oceanic and Atmospheric Administration
NPDES	National Pollutant Discharge Elimination System
NPGO	North Pacific Gyre Oscillation
ns	not sampled
NWS	National Weather Service
OB	Optical Brightener
OCSD	Orange County Sanitation District
OEHHA	California Office of Environmental Health Hazard Assessment
OI	Ocean Imaging
OMP	Ocean Monitoring Program
ONI	Oceanic Nino Index
OOR	Out-of-range
p	probability
PA	Percent Abundance
PAH	Polycyclic Aromatic Hydrocarbons
PCB	Polychlorinated Biphenyls Congeners
PDO	Pacific Decadal Oscillation
pH	Acidity/Alkalinity value
PLKF	Point Loma Kelp Forest

Acronyms and Abbreviations

PLOO	Point Loma Ocean Outfall
PLWTP	Point Loma Wastewater Treatment Plant
ppb	parts per billion
ppm	parts per million
ppt	parts per trillion
PRIMER	Plymouth Routines in Multivariate Ecological Research
psu	practical salinity units
QARTOD	Quality Assurance of Real-Time Oceanographic Data
r_s	Spearman rank correlation coefficient
RF	Rig Fishing
ROTV	Remotely Operated Towed Vehicle
RTOMS	Real-Time Oceanographic Mooring System
SABWTP	San Antonio de los Buenos Wastewater Treatment Plant
SBIWTP	South Bay International Wastewater Treament Plant
SBOO	South Bay Ocean Outfall
SBWRP	South Bay Water Reclamation Plant
SCAMIT	Southern California Association of Marine Invertebrate Taxonomists
SCB	Southern California Bight
SCBPP	Southern California Bight Pilot Project
SCCWRP	Southern California Coastal Water Research Project
SD	Standard Deviation
SDRWQCB	San Diego Regional Water Quality Control Board
SIMPER	Similarity Percentages Routine
SIMPROF	Similarity Profile Analysis
SIO	Scripps Institution of Oceanography
SL	Standard Length
sp	species (singular)
spp	species (plural)
SR	Species Richness
SSM	Single Sample Maximum
STV	Statistical Threshold Value
SWRCB	California State Water Resources Control Board
TL	Total Length
TN	Total Nitrogen
TOC	Total Organic Carbon
TSS	Total Suspended Solids
TVS	Total Volatile Solids
TZ	Trawl Zone
USEPA	United States Environmental Protection Agency
USFDA	United States Food and Drug Administration
USGS	United States Geological Survey
USIBWC	U.S. Section of the International Boundary and Water Commission
WQ	Water Quality
wt	weight
xCO2	Dissolved carbon dioxide

Acronyms and Abbreviations

XMS	Transmissivity
X2	chi sq
ZID	Zone of Initial Dilution
µg	micrograms
µm	micrometer
µM	micro-Molar
ρ	rho, test statistic for RELATE and BEST tests

This page intentionally left blank

Executive Summary

Executive Summary

The City of San Diego (City) conducts an extensive Ocean Monitoring Program to evaluate potential environmental effects associated with the discharge of treated wastewater to the Pacific Ocean via the Point Loma and South Bay Ocean Outfalls (PLOO and SBOO, respectively). Data collected are used to determine compliance with receiving water quality requirements as specified in National Pollutant Discharge Elimination System (NPDES) permits, and associated orders; these permits and orders are issued by the San Diego Regional Water Quality Control Board (SDRWQCB) and the U.S. Environmental Protection Agency (USEPA) for the City's Point Loma Wastewater Treatment Plant (PLWTP), South Bay Water Reclamation Plant (SBWRP), and the South Bay International Wastewater Treatment Plant (SBIWTP), which is operated by the U.S. Section of the International Boundary and Water Commission (USIBWC). Treated effluent from both the SBWRP and SBIWTP commingle before discharge to the ocean via the SBOO, thus a single monitoring and reporting program, approved by the SDRWQCB and USEPA, is conducted to comply with these two permits.

The principal objectives of the combined ocean monitoring efforts for both the PLOO and SBOO are to: (1) measure and document compliance with NPDES permit requirements and California Ocean Plan (Ocean Plan) water quality objectives and standards; (2) track movement and dispersion of the wastewater plumes discharged via the outfalls; (3) assess any impact of wastewater discharge on the local marine ecosystem, including effects on coastal water quality, seafloor sediments, and marine life.

Regular (core) monitoring is conducted on a weekly, quarterly, semiannual, and annual basis at a total of 142 discrete sites arranged in grids surrounding the PLOO and SBOO. The PLOO terminates at a discharge depth of around 100 m and is located approximately 7.2 km west of the PLWTP on the Point Loma peninsula. The SBOO terminates at a discharge depth of around 27 m and is located approximately 5.6 km offshore of southern San Diego, just north of the USA/Mexico border. Core monitoring in the PLOO region extends from Mission Beach southward to the tip of Point Loma along the shoreline, and from the nearshore to offshore waters from depths of around 9 to 116 m. Core monitoring of the SBOO region extends from Coronado, San Diego southward to Playa Blanca in northern Baja California, extending offshore from depths of around 9 to 55 m. In addition to monitoring at permanent core stations, an annual survey of benthic conditions (sediment quality, macrobenthic communities) is typically conducted each year at 40 randomly selected "regional" stations, which range from northern San Diego County southward to near the international border, extending offshore to depths of up to 500 m. These broader geographic surveys are useful for evaluating patterns over the entire San Diego coastal region and provide information important for distinguishing reference areas from those impacted by human activities. Additional information on background conditions for San Diego's coastal marine environment is also available from pre-discharge baseline studies conducted by the City for the PLOO region (1991–1994) and SBOO region (1995–1998).

Results of all receiving waters monitoring activities conducted for the PLOO and SBOO regions, between January 1, 2020 and December 31, 2021, are presented in this report (Chapters 2–9, Appendices A–B), and supplemental analyses are included in Appendices C–J. All raw data for the 2020-2021 sampling period have been submitted to either the SDRWQCB or the California Environmental Data Exchange Network (CEDEN) and may be accessed upon request.

Chapter 1 represents a general introduction and overview of the combined Ocean Monitoring Program for the PLOO and SBOO regions, while chapters 2–9 include results of the main monitoring

components conducted at the core and regional stations. In Chapter 2, data characterizing coastal oceanographic conditions and water mass transport for the region are evaluated. Chapter 3 presents the results of shoreline and offshore water quality compliance, including measurements of fecal indicator bacteria to assess compliance with water contact standards defined in the Ocean Plan. Chapter 4 presents the results of various plume tracking data collection efforts to assess the fate of discharged wastewater via the PLOO and SBOO. Assessments of regional benthic conditions, including benthic sediment quality (physical properties, sediment chemistry, and sediment toxicity), and the status of macrobenthic invertebrate communities are presented in Chapters 5, 6 and 7. Chapter 8 presents the results of trawling activities designed to monitor communities of bottom dwelling demersal fishes and megabenthic invertebrates. Finally, bioaccumulation assessments to measure contaminants in marine fishes are presented in Chapter 9.

In addition to the core monitoring activities described above, the City supports other projects relevant to assessing the status of receiving waters, including: (1) an ongoing long-term assessment of the health and status of San Diego's kelp forest ecosystems conducted by the Scripps Institution of Oceanography (SIO) and funded by the City (see Appendix A); (2) satellite imaging of the San Diego/Tijuana coastal region to assess wastewater plume dispersion and coastal runoff (see Appendix B).

Coastal Ocean Conditions

Oceanographic conditions, such as water temperatures, salinity, dissolved oxygen (DO) concentrations, pH, natural light levels (transmissivity or water clarity), and concentrations of chlorophyll *a* were generally within historical ranges and followed typical seasonal patterns reported for the PLOO and SBOO monitoring regions. Phytoplankton blooms, indicated by high concentrations of chlorophyll *a* (>5 µg/L), were evident at subsurface depths during spring and summer 2020 and winter through summer 2021 in the PLOO and SBOO regions. A notably large regional phytoplankton bloom in spring 2020 resulted in very high near-surface DO and pH levels, and record low observations of near-surface dissolved carbon dioxide levels. As is characteristic for these waters, conditions typically indicative of coastal upwelling were most evident during the spring, while maximum stratification or layering of the water column occurred during the spring and summer, after which the local waters became more mixed in the winter. Reductions in water clarity, or transmissivity, tended to be associated with terrestrial runoff or outflows from rivers and bays, resuspension of bottom sediments in nearshore waters due to waves or storm activity, or the presence of phytoplankton blooms. Overall, ocean conditions during the past two years were consistent with well documented patterns for southern California and northern Baja California. These findings suggest that natural factors, such as upwelling of deep ocean waters, and changes due to climatic events, such as El Niño/La Niña oscillations, continue to explain most of the temporal and spatial variability observed in the coastal waters off San Diego. As a result, proximity to either outfall is not considered a significant driver of the variations observed in oceanographic parameters discussed in Chapter 2.

Water Quality Compliance

Overall water quality compliance was typically higher in the Point Loma region than the South Bay, and higher at offshore stations compared to shore stations. Reduced compliance at shore stations, in both regions, tended to occur more frequently during the wet season. Throughout the PLOO monitoring region, overall compliance with the 2015 Ocean Plan water contact standards was over 98%, which was similar to that observed during recent years. Furthermore, compliance with the 2019 Ocean Plan water contact standards in the PLOO region was above the minimum threshold for all metrics throughout the report period. In contrast, in the SBOO region, overall compliance with the 2019 Ocean Plan water contact standards was below

the minimum threshold for all metrics except for offshore stations, which were above the minimum threshold throughout the report period. Shore stations located near the mouth of the Tijuana River and in Mexican waters near San Antonio de Los Buenos Creek have historically had higher numbers of elevated fecal indicator bacteria (FIB) samples than stations located farther to the north. It is also well established that sewage-laden discharges from the Tijuana River and San Antonio de Los Buenos Creek are likely sources of bacteria during or after storms or other periods of increased flows. The spatial and temporal distribution of elevated FIB observed during the current report period corroborate the findings of previous City reports and other studies, which suggest that the Tijuana River and other terrestrial inputs are the largest drivers of contamination in the South Bay region. To highlight the significant impact of the Tijuana River on receiving water quality, by removing the shore and kelp stations closest to the estuary mouth, the remaining stations in the SBOO region become compliant with the overall metric throughout the report period. Thus, the source of contamination in SBOO receiving waters is of known origin and likely associated with outflows from the Tijuana River and not related to wastewater discharge. Further, the general relationship between rainfall levels and elevated FIB densities in the SBOO region existed before wastewater discharge began in 1999. The low number of samples with elevated FIB near the outfall during recent years highlights the minimal impact of the wastewater discharge, which is likely a result of chlorination and the initiation of full secondary treatment that began in January 2011 at the SBWTP. As a result, we conclude that non-compliance with receiving water limitations for bacterial characteristics is primarily driven by known contaminated outflows from the Tijuana River Estuary and other non-point source runoff and not a result of wastewater discharge.

Plume Dispersion

Observations of potential plume detections from various plume tracking methods for 2020–2021 demonstrated that the PLOO effluent plume generally remained below a depth of 44 m, while the SBOO plume was generally trapped below the pycnocline during seasonal periods of water column stratification. However, unlike the PLOO plume, the SBOO plume showed potential evidence of rising to the surface when waters became more mixed and stratification broke down, typically during the winter months. Despite differences in observed plume vertical rise heights between the outfalls, both effluent plumes generally remained offshore and were transported along the coast with no evidence of nearshore movement. Although variable over space and time, the general axes of current velocities in the PLOO and SBOO regions followed a N:NW or S:SE trajectory. Thus, as effluent mixes with ambient seawater, it generally travels along the coast rather than being directed inshore toward the kelp beds, shoreline, or other recreational waters. As a result, there was no evidence that wastewater discharged to the ocean, via either the PLOO or SBOO, reached recreational waters along the shore or nearshore kelp beds. Similarly, results of water quality monitoring over the past 31 years off Point Loma, and 27 years in the South Bay, are consistent with observations from remote sensing studies (i.e., satellite imagery) over the last 20 years, which show a lack of shoreward transport of wastewater plumes from either outfall. Monitoring results are also consistent with past studies, which indicate that other sources, such as terrestrial runoff or outflows from rivers and creeks were more likely to impact coastal water quality than wastewater discharge from the outfalls, especially during and immediately after significant rain events.

Regional Benthic Conditions

Benthic habitats, and associated biological communities, found on the continental shelf and upper slope off San Diego were found to be in good condition. The results of comprehensive assessments of benthic conditions at 129 different monitoring sites, including 49 core monitoring stations (see Chapters 5 and 6) and 80 "regional" stations sampled during the

summers of 2020 and 2021 (see Chapter 7), show that the physical composition of the sediments, sediment quality, and the ecological status of the resident macrofaunal communities remain stable, with little evidence of environmental impact. Particle size composition varied throughout the region, but generally followed the typical pattern of sediments becoming finer with increasing depth.

Sediment quality was excellent throughout the entire San Diego region in summer 2020–2021. There was no evidence of degraded benthic habitats, in terms of the chemical properties of the sediments, or spatial patterns in the distribution of the different types of contaminants. Although, a number of indicators of organic loading (e.g., trace metals, pesticides, and PCBs) were detected in sediment samples throughout the San Diego region, almost all occurred at concentrations below critical thresholds, similar to that observed in previous years. Furthermore, examination of spatial patterns revealed no evidence of sediment contamination that could be attributed to local wastewater discharges via the PLOO or SBOO. This is further supported by results from sediment toxicity sampling, which revealed minimal toxicity at any of the near-ZID or regional stations tested, and these results, when integrated with benthic infauna and sediment chemistry results, demonstrated that the shelf off San Diego remains unimpacted by the PLOO or SBOO.

Benthic macrofaunal communities off San Diego also appeared to be healthy, with most assemblages appearing to be similar to those observed in the region from 1991 through 2019, and throughout southern California and northern Baja California. Although communities varied across depth and sediment gradients, there was no evidence of disturbance or significant environmental degradation that could be attributed to anthropogenic factors, such as wastewater discharge. Instead, these communities segregated by habitat characteristics, such as depth and sediment particle size, often corresponding with the "patchy" habitats reported to occur naturally in southern California's offshore coastal waters. These assemblages were typically characterized by expected abundances of pollution sensitive species (e.g., amphipods such as *Ampelisca* spp and *Rhepoxynius* spp). and pollution-tolerant species (e.g., the polychaete *Capitella teleta* and the bivalve *Solemya pervernicosa*). Other major benthic community metrics, such as species richness, macrofaunal abundance, diversity, evenness, and dominance also showed no evidence of wastewater impact or significant habitat degradation. Finally, the Benthic Response Index (BRI) further confirmed little evidence of disturbance off San Diego with 94% of all calculated BRI values being indicative of reference conditions and another 6% being characteristic of only a possible minor deviation.

Demersal Fishes and Megabenthic Invertebrates

Demersal fish and megabenthic invertebrate communities trawled off San Diego remain unaffected by wastewater discharge. Although highly variable, patterns in the abundance and distribution of individual species were similar regardless of proximity to the outfalls and were representative of similar habitats throughout the Southern California Bight (SCB). Pacific Sanddab dominated assemblages surrounding the PLOO, and Speckled Sanddab dominated assemblages surrounding the SBOO, as they have done since monitoring began in each region. Halfbanded Rockfish were also prevalent in PLOO assemblages, while California Lizardfish were also prevalent within the SBOO region during this period, as they have also done in eleven of the past thirteen years. Other commonly captured, but less abundant fishes, collected from the PLOO and SBOO regions included California Tonguefish, Dover Sole, English Sole, Longfin Sanddab, Northern Anchovy, Longspine Combfish, Shortspine Combfish, and White Croaker. Furthermore, external examinations of fish captured indicated that fish populations remained healthy off San Diego, with fewer than 0.4% of all fish having external parasites or showing any evidence of disease or other abnormalities.

Trawl-caught invertebrate assemblages were once again dominated by the pelagic red crab *Pleuroncodes planipes*, which accounted for 91% of the 166,094 megabenthic invertebrates recorded in 2020 and 2021, and was found exclusively in the PLOO region. These crabs were collected exclusively at PLOO trawl stations. In contrast to the PLOO region, no single species of invertebrate dominated SBOO trawls. Other commonly captured, but less abundant, trawl-caught invertebrates collected from the PLOO and SBOO regions included the sea urchin *Lytechinus pictus*, the shrimps *Sicyonia ingentis*, *Sicyonia penicillata*, and *Crangon nigromaculata*, the crab *Platymera gaudichaudii*, and the sea star *Astropecten californicus*. However, increasing occurrences of historically more southerly located species, such as *Octopus veligero* and *S. penicillata*, are potential indicators of large-scale climate driven effects of species distribution and occurrence, which will likely only increase in the future.

Contaminants in Marine Fishes

The accumulation of chemical contaminants in San Diego marine fishes varied across species and stations, but most values were within ranges reported previously for southern California fishes. Overall, there was no evidence of contaminant accumulation in PLOO or SBOO fishes that could be associated with wastewater discharge from either outfall, which is consistent with historical findings. Although several different trace metals, pesticides, PCB congeners, and various PAHs were detected in both liver and muscle tissues, these contaminants occurred in fishes distributed throughout both regions, with no patterns that could be attributed to wastewater discharge via the outfalls. Consequently, the occurrence of some metals and chlorinated hydrocarbons in some local fishes off San Diego is likely influenced by other factors, such as the widespread distribution of many contaminants in southern California sediments, differences in the physiology and life history traits of various species of fish, different exposure pathways, and differences in the migration pathways of various species. For example, an individual fish may be exposed to contaminants at a polluted site, but then migrate to an area that is less contaminated. This is of particular concern for fishes collected in the vicinity of the PLOO and SBOO, as there are many other nearby potential point and non-point sources of contamination.

Conclusions

The findings and conclusions for the ocean monitoring efforts conducted for the PLOO and SBOO monitoring regions, during 2020 and 2021, were consistent with previous years. There were few changes to local receiving waters, benthic sediments, or marine invertebrate and fish communities that could be attributed to wastewater discharge. Coastal water quality conditions were generally excellent throughout the region, with the exception of the South Bay shore stations, which showed the highest frequency of elevated fecal indicator bacteria. However, the spatial and temporal distribution of these observations corroborate previous findings, which suggest that the Tijuana River and other terrestrial inputs are the largest drivers of contamination in the South Bay region. Thus, there was no evidence that wastewater was a driver of nearshore contamination, and no evidence that wastewater plumes from either of the two outfalls were transported shoreward into nearshore recreational waters. There were also no clear outfall related patterns in sediment contaminant distributions or differences between invertebrate and fish assemblages at the different monitoring sites. Additionally, benthic habitats surrounding both outfalls, and throughout the entire San Diego region, remained in good overall condition, similar to reference conditions for much of the SCB. Finally, the low level of contaminant accumulation, minimal sediment toxicity, and general lack of physical anomalies or other symptoms of disease or stress in local fishes was also indicative of a healthy marine environment off San Diego.

This page intentionally left blank

Chapter 1
General Introduction

Chapter 1. General Introduction

Program Requirements & Objectives

Ocean monitoring within the Point Loma and South Bay outfall regions is conducted by the City of San Diego (City) in accordance with requirements set forth in National Pollution Discharge Elimination System (NPDES) permits and associated orders for the following: the Point Loma Wastewater Treatment Plant (PLWTP), the South Bay Water Reclamation Plant (SBWRP), and the South Bay International Wastewater Treatment Plant (SBIWTP), which is owned and operated by the U.S. Section of the International Boundary and Water Commission (USIBWC) (see Table 1.1). These documents specify the terms and conditions that allow treated effluent to be discharged to the Pacific Ocean via the Point Loma Ocean Outfall (PLOO) and South Bay Ocean Outfall (SBOO). In addition, the Monitoring and Reporting Program (MRP), included within each of these orders, defines the requirements for monitoring ocean (receiving) waters surrounding the two outfalls. These requirements include sampling design, frequency of sampling, field operations and equipment, regulatory compliance criteria, types of laboratory tests and analyses, data management and analysis, statistical methods and procedures, environmental assessment, and reporting guidelines.

The combined Ocean Monitoring Program for these regions is designed to assess the impact of wastewater discharged through the PLOO and SBOO on the coastal marine environment off San Diego. The main objectives of the program are to: (1) measure and document compliance with NPDES permit requirements and California Ocean Plan (Ocean Plan) water quality objectives and standards; (2) track movement and dispersion of the wastewater plumes discharged via the outfalls; (3) assess any impact of wastewater discharge on the local marine ecosystem, including effects on coastal water quality, seafloor sediments, and marine life.

Background

Point Loma Ocean Outfall

The City began operation of the PLWTP and original PLOO off Point Loma in 1963, at which time treated effluent was discharged approximately 3.9 km west of the Point Loma peninsula at a depth of around 60 m. The PLWTP operated as a primary treatment facility from 1963 to 1985, after which it was upgraded to advanced primary treatment between mid-1985 and July 1986. This improvement involved the addition of chemical coagulation to the treatment process, which resulted in an increase in removal of total suspended solids (TSS) to about 75%. Since then, the treatment process has continued to be improved with the addition of more sedimentation basins, expanded aerated grit removal, and refinements in chemical treatment, which together further reduced mass emissions from the plant. For example, TSS removals are now consistently greater than the 80%, as required by the NPDES permit.

The structure of the PLOO was significantly modified in the early 1990s when it was extended about 3.3 km farther offshore in order to prevent intrusion of the waste field into nearshore waters and to increase compliance with Ocean Plan standards for water-contact sports areas. Discharge from the original 60-m terminus was discontinued in November 1993 following completion of the outfall extension. Currently, the PLOO extends approximately 7.2 km west of the PLWTP to a depth of around 94 m, where the main outfall pipe splits into a Y-shaped (wye) multiport diffuser system. The two diffuser legs extend an additional 762 m to the north and south, each terminating at a depth of about 98 m. The average discharge of effluent through the PLOO in 2020-2021 was about 142 mgd (million gallons per day).

Table 1.1
NPDES permits and associated orders issued for the wastewater treatment plants run by the City of San Diego (PLWTP, SBWRP), and the USIBWC (SBIWTP).

Facility	Outfall	NPDES Permit No.	Order No.	Effective Dates
PLWTP	PLOO	CA0107409	R9-2017-0007	October 1, 2017–September 30, 2022
SBWRP	SBOO	CA0109045	R9-2021-0011[a]	July 1, 2022–June 30, 2026
SBIWTP	SBOO	CA0108928	R9-2021-0001[b]	July 1, 2022–June 30, 2026

[a] Replaced Order No. R9-2017-0023

[b] Replaced Order No. R9-2019-0012

South Bay Ocean Outfall

The SBOO is located just north of the international border between the United States and Mexico where it terminates approximately 5.6 km offshore and west of Imperial Beach at a depth of around 27 m. Unlike other southern California ocean outfalls that lie on the surface of the seafloor, the SBOO pipeline begins as a tunnel on land that extends from the SBWRP and SBIWTP facilities to the coastline, after which it continues beneath the seabed 4.3 km offshore. The outfall pipe connects to a vertical riser assembly that conveys effluent to a pipeline buried just beneath the surface of the seafloor. This subsurface pipeline then splits into a Y-shaped (wye) multiport diffuser system with the two diffuser legs each extending an additional 0.6 km to the north or south. The SBOO was originally designed to discharge wastewater through 165 diffuser ports and risers, which included one riser at the center of the wye and 82 risers spaced along each diffuser leg. Since discharge began, however, low flow rates have required closure of all ports along the northern diffuser leg and many along the southern diffuser leg in order for the outfall to operate effectively. Consequently, wastewater discharge is restricted primarily to the distal end of the southern diffuser leg and to a few intermediate points at or near the center of the wye. The average discharge of effluent through the SBOO in 2020–2021 was about 28 mgd, including about 3 mgd of secondary and tertiary treated effluent from the SBWRP, and 25 mgd of secondary treated effluent from the SBIWTP.

Receiving Waters Monitoring

The total area for the PLOO and SBOO monitoring program covers approximately 881 km^2 (~340 mi^2) of coastal marine waters from Northern San Diego County into Northern Baja California. Core monitoring for the Point Loma region is conducted at 82 stations, located from the shore to a depth of around 116 m. Core monitoring for the South Bay region is conducted at a total of 53 stations, ranging from the shore to depths of around 61 m (Figure 1.1). Each of the core monitoring stations is sampled for specific parameters as stated in their respective MRPs. A summary of the results for all quality assurance procedures performed during 2020 and 2021, in support of these requirements, can be found in City of San Diego (2021, 2022a). Data files, detailed methodologies, completed reports, and other pertinent information submitted to the San Diego Regional Water Quality Control Board (SDRWQCB), and the U.S. Environmental Protection Agency (USEPA), during these two years are available online (City of San Diego 2022b).

Prior to 1994, the City conducted an extensive ocean monitoring program off Point Loma surrounding the original 60-m discharge site. This program was subsequently expanded with the construction and operation of the deeper outfall, as discussed previously. Data from the last year of regular monitoring near the original PLOO discharge site are presented in City of San Diego (1995a), while the results of a 3-year "recovery study" are summarized in City of San Diego (1998). Additionally, a more detailed assessment of spatial and temporal patterns surrounding the original discharge site is available (Zmarzly et al. 1994). From 1991 through 1993, the City also conducted "pre-discharge" monitoring for the new PLOO discharge site in order to collect baseline data prior to wastewater discharge into these deeper waters (City of San Diego 1995a, b).

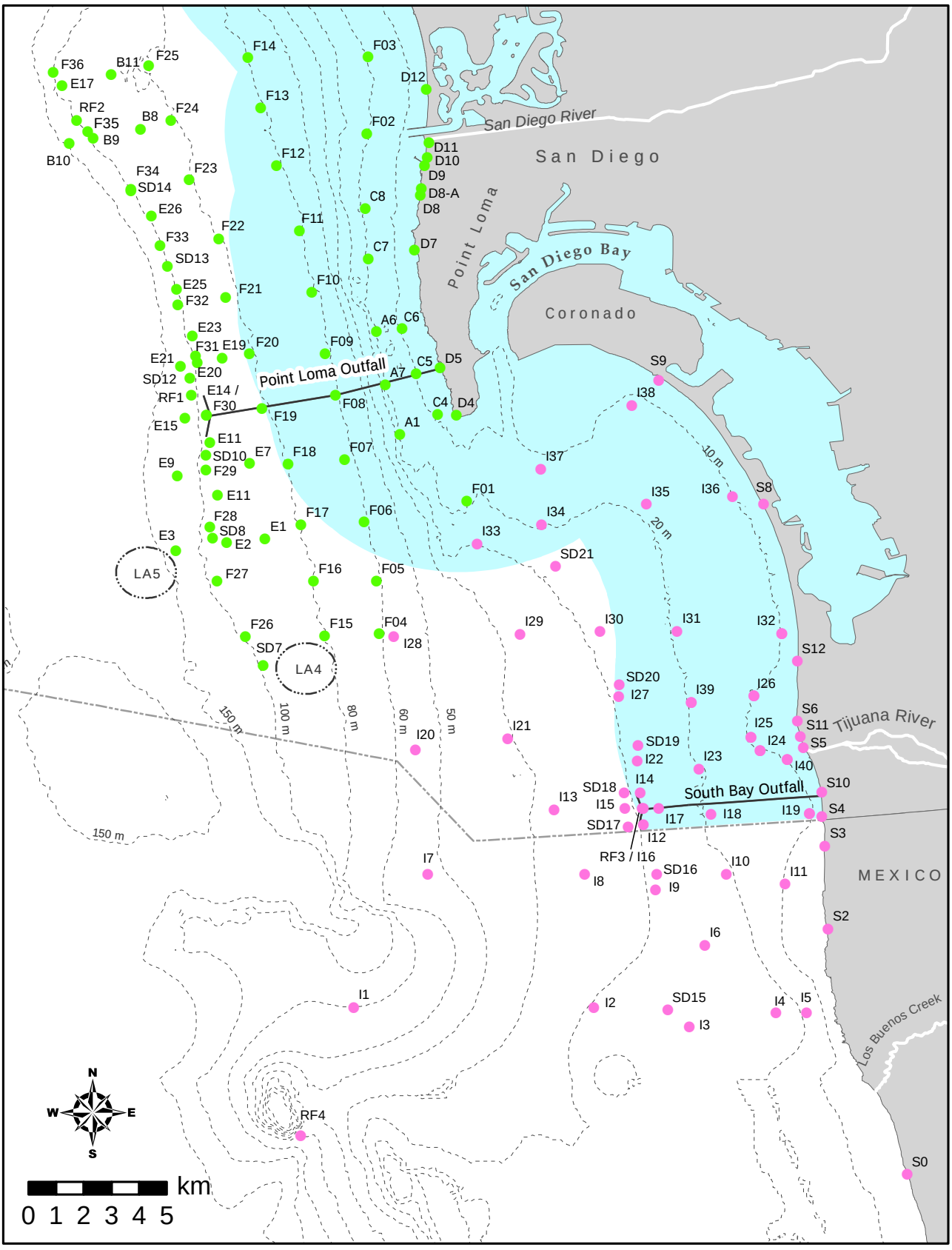

Figure 1.1
Core receiving waters monitoring stations for the PLOO (green) and SBOO (pink) as part of the City of San Diego's Ocean Monitoring Program. Light blue shading represents State jurisdictional waters.

All permit mandated ocean monitoring for the South Bay region has also been performed by the City since wastewater discharge through the SBOO began in 1999; this included pre-discharge monitoring for 3½ years (July 1995–December 1998) in order to provide background information against which post-discharge conditions could be compared (City of San Diego, 2000). Results of NPDES mandated monitoring for the extended PLOO from 1994 to 2019, and the SBOO from 1999 to 2019, are available in previous annual receiving waters monitoring reports (e.g., City of San Diego 2020). Finally, additional detailed assessments of the PLOO region have been completed as part of past modified NPDES permit renewal applications for the PLWTP submitted by the City (e.g., City of San Diego 2022c) and subsequent technical decisions issued by the USEPA (e.g., USEPA 2017).

The City has also conducted annual region-wide surveys off the coast of San Diego since 1994, either as part of regular outfall monitoring requirements (e.g., City of San Diego 1999), or as part of larger multi-agency surveys of the entire Southern California Bight (SCB) (e.g., Gillett et al. 2017). The latter include the 1994 Southern California Bight Pilot Project (SCCWRP 1998) and subsequent Bight programs from 1998 through 2018 (e.g., SCCWRP 2018). These large-scale surveys are useful for characterizing the ecological health of diverse coastal areas to distinguish reference sites from those impacted by wastewater or storm water discharges, urban runoff, or other sources of contamination. In addition to the above activities, the City participates as a member of the Region Nine Kelp Survey Consortium to fund aerial surveys of all the major kelp beds in San Diego and Orange Counties (e.g., MBC 2021).

Special Studies & Enhanced Monitoring

The City has actively participated in, or supported, numerous important special projects, or enhanced ocean monitoring studies, over the past 10 years or more. Many of these projects to date were identified as part of a scientific review of the City's Ocean Monitoring Program, conducted by the Scripps Institution of Oceanography (SIO) and other participating institutions (SIO 2004). This review evaluated the environmental monitoring needs of the region, and recommended special projects based on priorities identified. Examples of special projects currently underway, or being initiated include:

- San Diego Kelp Forest Ecosystem Monitoring Project: This project represents continuation of a long-term commitment by the City to support important research conducted on local kelp forests by SIO. This work is essential to assessing the health of San Diego's kelp forests and monitoring the effects of wastewater discharge on the local coastal ecosystem relative to other anthropogenic and natural influences (see Appendix A).

- Real-Time Oceanographic Mooring Systems (RTOMS) for the Point Loma and South Bay Ocean Outfalls: This project addresses recommendations that the City should improve monitoring of the fate and behavior of wastewater discharged to the ocean via the SBOO (Terrill et al. 2009) and PLOO (Rogowski et al. 2012a, Rogowski et al. 2012b, Rogowski et al. 2013). The project involves the deployment of RTOMS at the terminal ends of the PLOO and SBOO to provide real time data on ocean conditions. The project began in late 2015 with initial deployment of the SBOO mooring in December 2016 and the PLOO mooring in March 2018. This project is being conducted in partnership with SIO, whom presently operate a similar mooring system off Del Mar. The project is expected to significantly enhance the City's environmental monitoring capabilities in order to address current and emerging issues relevant to the health of San Diego's coastal waters, including plume dispersion, subsurface current patterns, ocean acidification, hypoxia, nutrient sources, and coastal upwelling. Additional details are available in the approved Plume Tracking Monitoring Plan for the project (City of San Diego 2018b) and Chapter 4.

- Sediment Toxicity Monitoring of the San Diego Ocean Outfall Regions: This project started with a 3-year pilot study implemented as a new joint regulatory requirement for the Point Loma and South Bay outfall regions in 2015. Findings for the 2016–2018 pilot study (City of San Diego 2015) were summarized in a final project report (City of San Diego 2019) that included recommendations for continued sampling through 2023. The findings are now being utilized as part of a Sediment Quality Triad Assessment alongside analyses of sediment chemistry and macrofaunal community data to provide a snapshot of the region's sediment quality and benthic community structure (see Chapter 7).

- Remote Sensing of the San Diego / Tijuana Coastal Region: This project represents a long-term effort, funded by the City and the USIBWC since 2002, to utilize satellite and aerial imagery to better understand regional water quality conditions off San Diego. The project is conducted by Ocean Imaging (Littleton, CO), and is focused on detecting and tracking the dispersion of wastewater plumes from local ocean outfalls and nearshore sediment plumes caused by stormwater runoff or outflows from local bays and rivers (see Appendix B).

- San Diego Regional Benthic Condition Assessment Project: This multi-phase study represents an ongoing, long-term project designed to assess the condition of continental shelf and slope habitats throughout the entire San Diego region. A preliminary summary of the deeper slope (> 200 m) results for data collected between 2003–2013 was included in Appendix C.5 of City of San Diego (2015a), while several publications covering the remainder of the project are planned for completion in late 2022.

Report Components & Organization

This report presents a comprehensive biennial assessment of the results of all receiving waters monitoring activities conducted during 2020 and 2021 for both the Point Loma and South Bay outfall regions. Included herein are results from all regular core stations that comprise the fixed-site monitoring grids surrounding the two outfalls (Figure 1.1), as well as results from the 2020-2021 summer benthic surveys of randomly selected sites that range from near the USA/Mexico border to northern San Diego County (Figure 1.2). The main components of the combined monitoring program are covered in the following sections or chapters: Executive Summary; General Introduction (Chapter 1); Coastal Oceanographic Conditions (Chapter 2); Water Quality Compliance (Chapter 3); Plume Dispersion (Chapter 4); Sediment Quality (Chapter 5); Macrobenthic Communities (Chapter 6); San Diego Regional Benthic Condition Assessment (Chapter 7); Demersal Fish and Megabenthic Invertebrate Communities (Chapter 8); Contaminants in Marine Fishes (Chapter 9). Supplemental analyses for Chapters 2–9 are included in Appendices C–J. All raw data for the 2020–2021 sampling period have been submitted to either the Regional Water Quality Control Board or the California Environmental Data Exchange Network (CEDEN) and will be provided upon request.

Literature Cited

City of San Diego. (1995a). Receiving Waters Monitoring Report for the Point Loma Ocean Outfall, 1994. City of San Diego Ocean Monitoring Program, Metropolitan Wastewater Department, Environmental Monitoring and Technical Services Division, San Diego, CA

City of San Diego. (1995b). Outfall Extension Pre-Construction Monitoring Report (July 1991–October 1992). City of San Diego Ocean Monitoring Program, Metropolitan Wastewater Department, Environmental Monitoring and Technical Services Division, San Diego, CA

City of San Diego. (1998). Recovery Stations Monitoring Report for the Original Point

Loma Ocean Outfall (1991–1996). City of San Diego Ocean Monitoring Program, Metropolitan Wastewater Department, Environmental Monitoring and Technical Services Division, San Diego, CA

City of San Diego. (1999). San Diego Regional Monitoring Report for 1994–1997. City of San Diego Ocean Monitoring Program, Metropolitan Wastewater Department, Environmental Monitoring and Technical Services Division, San Diego, CA

City of San Diego. (2000). Final Baseline Monitoring Report for the South Bay Ocean Outfall (1995–1998). City of San Diego Ocean Monitoring Program, Metropolitan Wastewater Department, Environmental Monitoring and Technical Services Division, San Diego, CA

City of San Diego. (2015). Sediment Toxicity Monitoring Plan for the South Bay Ocean Outfall and Point Loma Ocean Outfall Monitoring Regions, San Diego, California. Submitted by the City of San Diego Public Utilities Department to the San Diego Water Board and USEPA, Region IX, August 28, 2015 [approved 9/29/2015]

City of San Diego. (2018a). Biennial Receiving Waters Monitoring and Assessment Report for the Point Loma and South Bay Ocean Outfalls, 2016-2017. City of San Diego, Public Utilities Department, Environmental Monitoring and Technical Services Division, San Diego, CA.

City of San Diego. (2018b). Plume Tracking Monitoring Plan for the Point Loma and South Bay Ocean Outfall Regions, San Diego, California. Submitted by the City of San Diego Public Utilities Department to the San Diego Water Board and USEPA, Region IX, March 28, 2018 (approved 4/25/2018)

City of San Diego. (2019). Final Project Report for the Sediment Toxicity Pilot Study for the San Diego Ocean Outfall Monitoring Regions, 2016-2018. Submitted May 30, 2019 by the City of San Diego Public Utilities Department to the San Diego Regional Water Quality Control Board and U.S. Environmental Protection Agency, Region IX. 16 pp.

City of San Diego. (2020). Biennial Receiving Waters Monitoring and Assessment Report for the Point Loma and South Bay Ocean Outfalls, 2018-2019. City of San Diego, Public Utilities Department, Environmental Monitoring and Technical Services Division, San Diego, CA.

City of San Diego. (2021). Annual Receiving Waters Monitoring & Toxicity Testing Quality Assurance Report, 2020. City of San Diego Ocean Monitoring Program, Public Utilities Department, Environmental Monitoring and Technical Services Division, San Diego, CA

City of San Diego. (2022a). Annual Receiving Waters Monitoring & Toxicity Testing Quality Assurance Report, 2021. City of San Diego Ocean Monitoring Program, Public Utilities Department, Environmental Monitoring and Technical Services Division, San Diego, CA

City of San Diego. (2022b). Ocean Monitoring Reports. https://www.sandiego.gov/public-utilities/sustainability/ocean-monitoring/reports

City of San Diego. (2022c). Application for Renewal of NPDES CA0107409 and 301(h) Modified Secondary Treatment Requirements for Biochemical Oxygen Demand and Total Suspended Solids, Point Loma Ocean Outfall and Point Loma Wastewater Treatment Plant. Volumes I-X, Appendices A-U. The City of San Diego, Public Utilities Department, San Diego, CA

Gillett, D.J., L.L. Lovell, and K.C. Schiff. (2017). Southern California Bight 2013 Regional Monitoring Program: Volume VI. Benthic

Infauna. Technical Report 971. Southern California Coastal Water Research Project. Costa Mesa, CA.

[MBC] MBC Aquatic Sciences. (2021). Status of the Kelp Beds 2020, Kelp Bed Surveys: Orange, and San Diego Counties. Final Report, August 2021. MBC Aquatic Sciences, Costa Mesa CA

Rogowski, P., E. Terrill, M. Otero, L. Hazard, S.Y. Kim, P.E. Parnell, and P. Dayton. (2012a). Final Report: Point Loma Ocean Outfall Plume Behavior Study. Prepared for City of San Diego Public Utilities Department by Scripps Institution of Oceanography, University of California, San Diego, CA

Rogowski, P., E. Terrill, M. Otero, L. Hazard, and W. Middleton. (2012b). Mapping ocean outfall plumes and their mixing using Autonomous Underwater Vehicles. Journal of Geophysical Research, 117: C07016

Rogowski, P., E. Terrill, M. Otero, L. Hazard, and W. Middleton. (2013). Ocean outfall plume characterization using an Autonomous Underwater Vehicle. Water Science & Technology, 67(4): 925–933

[SCCWRP] Southern California Coastal Water Research Project. (1998). Southern California Bight 1994 Pilot Project: Volumes I-VI. Southern California Coastal Water Research Project, Westminster, CA

[SCCWRP] Southern California Coastal Water Research Project. (2018). Southern California Bight 2018 Regional Monitoring Program: Contaminant Impact Assessment Field Operations Manual. Southern California Coastal Water Research Project. Costa Mesa, CA.

[SIO] Scripps Institution of Oceanography. (2004). Point Loma Outfall Project, Final Report, September 2004. Scripps Institution of Oceanography, University of California, La Jolla, CA

Terrill, E., K. Sung Yong, L. Hazard, and M. Otero. (2009). IBWC/Surfrider – Consent Decree Final Report. Coastal Observations and Monitoring in South Bay San Diego. Scripps Institution of Oceanography, University of California, San Diego, CA.

[USEPA] United States Environmental Protection Agency. (2017). City of San Diego's Point Loma Wastewater Treatment Plant Application for a Modified NPDES Permit under Sections 301(h) and (j)(5) of the Clean Water Act. Technical Decision Document. United States Environmental Protection Agency, Region IX, San Francisco, CA

Zmarzly, D.L., T.D. Stebbins, D. Pasko, R.M. Duggan, and K.L. Barwick. (1994). Spatial patterns and temporal succession in soft-bottom macroinvertebrate assemblages surrounding an ocean outfall on the southern San Diego shelf: relation to anthropogenic and natural events. Marine Biology, 118: 293–307

This page intentionally left blank

Chapter 2
Coastal Oceanographic Conditions

Chapter 2. Coastal Oceanographic Conditions

Introduction

The City of San Diego (City) collects a comprehensive suite of oceanographic data from coastal waters surrounding the Point Loma Ocean Outfall (PLOO) and South Bay Ocean Outfall (SBOO) to characterize regional conditions and to identify possible impacts of wastewater discharge and other factors on the marine environment. These data include measurements of ocean temperature, salinity, light transmittance (transmissivity), dissolved oxygen, pH, and chlorophyll *a* throughout the water column, all of which are considered important indicators of physical and biological processes that can impact marine life (Skirrow 1975, Mann 1982, Mann and Lazier 1991). As the fate of wastewater discharged into the ocean is determined by multiple factors (e.g., outfall geometry, rate of effluent discharge, water column mixing, ocean currents, tidal flows), evaluations of physical parameters that influence the mixing potential of the water column are important components of many ocean monitoring programs (Bowden 1975, Pickard and Emery 1990).

In the nearshore coastal waters of the Southern California Bight (SCB), including the PLOO and SBOO monitoring regions, ocean conditions are influenced by multiple factors. These include: (1) large-scale climatic processes, such as El Niño Southern Oscillations (ENSO), Pacific Decadal Oscillations (PDO), and North Pacific Gyre Oscillations (NPGO), which can affect long-term trends (Peterson et al. 2006, McClatchie et al. 2008, 2009, Bjorkstedt et al. 2010, 2011, 2012, Wells et al. 2013, NOAA/NWS 2022); (2) the California Current System, coupled with local gyres that transport distinct water masses into and out of the SCB (Lynn and Simpson 1987, Leising et al. 2014); (3) seasonal changes in local weather patterns (Bowden 1975, Skirrow 1975, Pickard and Emery 1990), which are a primary driver of water column stratification typically observed off San Diego and in coastal waters throughout the rest of southern California (Terrill et al. 2009, Rogowski et al. 2012a,b, 2013). These seasonal patterns include typically warmer and more stratified waters in the dry season, from May through September, and cooler, more weakly stratified and well-mixed waters, in the wet season, from October through April (e.g., City of San Diego 2022a, Hess 2019, 2020).

Understanding changes in oceanographic conditions due to natural processes, such as the seasonal patterns described above, is of utmost importance since they will likely affect the transport and distribution of wastewater, storm water, and other nearshore plumes. In the PLOO and SBOO monitoring regions, nearshore plumes include sediment or turbidity plumes associated with outflows from local bays, major rivers, lagoons and estuaries, discharges from storm drains or other point sources, surface runoff from local watersheds, seasonal upwelling, and variable ocean currents or eddies. Outflow plumes from the San Diego River, San Diego Bay, and the Tijuana River can contribute significantly to patterns of nearshore turbidity, sediment deposition, and bacterial contamination (see Largier et al. 2004, Terrill et al. 2009, Svejkovsky 2010, 2017, Hess 2018, 2019, 2020).

In order to assess conditions on a comprehensive spatial scale, quarterly water quality surveys have historically been conducted across the two outfall regions (beginning in 1991 at PLOO and 1995 at SBOO). Subsequent studies of the fate and behavior of wastewater discharged to the ocean via the SBOO (Terrill et al. 2009) and the PLOO (Rogowski et al. 2012a,b, 2013) included recommendations to use real-time oceanographic mooring systems (RTOMS) and advanced sampling technologies to better understand nearshore coastal water quality and the impacts of local ocean currents and tidal fluxes on effluent plume dynamics. This higher temporal resolution data collection began in 2017

at SBOO and in 2018 at PLOO (City of San Diego 2018a, 2020). While quarterly surveys provide a snapshot of conditions across a large regional area, the RTOMS provide near-continuous information on how ocean conditions change over time near the two ocean outfalls. As such, some variations in ranges and seasonal comparisons between quarterly surveys and RTOMS data are expected, and differences between these sampling approaches are discussed in relevant sections.

This chapter presents analysis and interpretation of the oceanographic monitoring data collected during 2020 and 2021 for the coastal waters surrounding the PLOO and SBOO. The primary goals of this chapter are to: (1) summarize coastal oceanographic conditions in these regions to provide information on the state of local receiving waters; (2) determine if water clarity, pH or dissolved oxygen are significantly altered at any point outside of the Zone of Initial Dilution (ZID) as a result of the outfall discharge; (3) evaluate local ocean conditions off the coast of San Diego within the context of regional climatic processes. In addition, results of remote sensing observations (e.g., satellite imagery) are combined with measurements of physical oceanographic parameters to provide further insight on the horizontal transport of surface waters off San Diego. The results reported herein are also referred to in subsequent chapters to explain patterns of fecal indicator bacteria distributions and plume dispersion (see Chapters 3 and 4) as well as other changes in the local marine environment (see Chapters 5–9).

Materials and Methods

Quarterly CTD surveys

Data Collection

A total of 69 offshore water quality monitoring stations were sampled quarterly to assess coastal oceanographic conditions in the two outfall regions (Figure 2.1). These include 36 stations surrounding the PLOO and 33 stations surrounding the SBOO. The PLOO stations are designated F1–F36 and are located along or adjacent to the 18, 60, 80, and 98-m depth contours. The SBOO stations are designated I1–I18, I20–I23, I27–I31, and I33–I38, and are located along the 9, 19, 28, 38 and 55-m depth contours, respectively. All 69 stations were monitored during winter (February), spring (May), summer (August), and fall (November) in 2020 and 2021, and were sampled over a four-day period during each survey (Appendix C.1). Sampling at an additional eight kelp bed stations off Point Loma (i.e., stations A1, A6, A7, C4–C8) and seven kelp/nearshore stations in the South Bay region (i.e., stations I19, I24–I26, I32, I39, I40) was conducted four to five times per month to meet bacterial monitoring requirements (see Chapter 3). However, only data collected at these 15 kelp bed stations that occurred within one week of the quarterly offshore stations are analyzed in this chapter (see Appendix C.1).

Oceanographic data were collected using a SeaBird SBE 25 Plus conductivity, temperature, and depth instrument (CTD). The CTD was lowered through the water column at each station to collect continuous measurements of water temperature, conductivity (used to calculate salinity), pressure (used to calculate depth), dissolved oxygen (DO), pH, transmissivity (a proxy for water clarity), chlorophyll *a* fluorescence (a proxy for phytoplankton), and colored dissolved organic material (CDOM). Vertical profiles of each parameter were constructed for each station per survey by averaging the data values recorded within each 1-m depth bin. This level of data reduction ensures that physical measurements used in subsequent analyses will correspond to discrete sampling depths required for bacterial monitoring (see Chapter 3). Visual observations of weather and water conditions were recorded just prior to each CTD cast. These observations were previously reported in monthly receiving waters monitoring reports submitted to the San Diego Regional Water Quality Control Board (see City of San Diego 2020–2022a,b).

Data Analysis

Water column parameters were summarized as quarterly means pooled over all stations by the

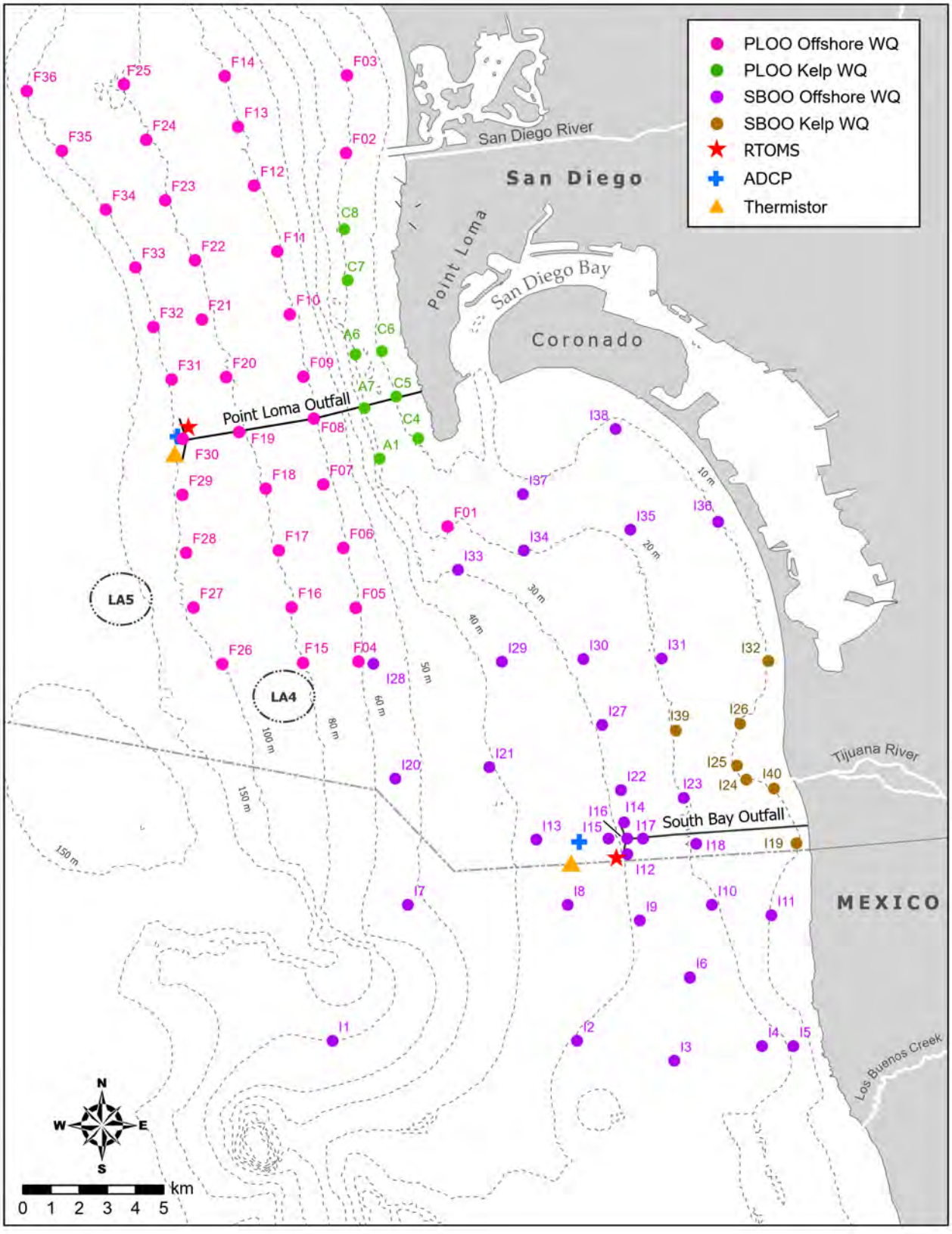

Figure 2.1
Locations of CTD water quality monitoring stations and mooring sites (RTOMS, ADCP, and thermistor arrays) sampled around the PLOO and SBOO as part of the City of San Diego's Ocean Monitoring Program.

following depth layers: 1–20 m, 21–60 m, 61–80 m, 81–98 m (PLOO), and 1–9 m, 10–19 m, 20–28 m, 29–38 m, 39–55 m (SBOO). The top layer is herein referred to as surface water, while the subsurface layers account for mid and bottom waters. Unless otherwise noted, analyses were performed using R (R Core Team, 2021) and various functions within the reshape2, Rmisc, mixOmics, tidyverse, Hmisc, RODBC, and oce packages (Wickham 2007, Hope 2013, Rohart et al. 2017, Wickham et al. 2019, Harrell 2021, Ripley and Lapsley 2021, Kelley and Richards 2022).

Vertical density profiles were constructed from CTD data to depict the pycnocline (i.e., depth layer where the density gradient was greatest) for each survey and to illustrate seasonal changes in water column stratification. Data for these density profiles were limited to stations located along the 98-m depth contour in the PLOO region (i.e., stations F26–F36) and the 28-m depth contour in the SBOO region (i.e., stations I2, I3, I6, I9, I12, I14I17, I22, I27, I30, I33) to prevent masking trends that occur when data from multiple depth contours are combined. Buoyancy frequency (BF), a measure of the static stability of the water column, was used to quantify the magnitude of stratification for each station per survey and was calculated as follows:

$$BF = \sqrt{(g/\rho * (d\rho/dz))}$$

where g is the acceleration due to gravity, ρ is the seawater density, and dρ/dz is the density gradient (Mann and Lazier 1991). The depth of maximum BF was used as a proxy for the depth at which stratification was the greatest.

Additionally, time series of anomalies for water temperature, salinity, and DO were calculated to evaluate regional oceanographic events within the context of large-scale climatic processes (i.e., ENSO events). These analyses were limited to data from the discharge depth stations for each outfall, with all water column depths combined. Anomalies were then calculated as the difference between the quarterly historical average and quarterly means for each year.

RTOMS

Data Collection

Two real-time oceanographic mooring systems were deployed at the terminal ends of the PLOO and SBOO (Figure 2.1), in partnership with Scripps Institution of Oceanography (SIO). The PLOO RTOMS was anchored at a depth of approximately 95 m, just east of the northern diffuser leg, and the SBOO RTOMS was anchored at a depth of approximately 30 m, just west of the southern diffuser leg terminus (Appendix C.2). Each mooring was deployed for a period of approximately one year. The last complete PLOO deployment occurred from October 7, 2019 to September 29, 2020, and the last SBOO deployment occurred from December 18, 2019 to December 17, 2020. The current and ongoing PLOO and SBOO deployments began on November 3, 2021. RTOMS data presented here includes only data collected in real-time from all deployments, with the exception of data downloaded after PLOO mooring recovery, which was used to backfill a two-week gap during a period of a cell modem failure (February 14 to March 3, 2020). RTOMS data are not available for much of 2021 due to supply chain disruptions and work limitations for collaborators at SIO related to the COVID-19 pandemic, in addition to catastrophic engine failure of the City's primary monitoring vessel used for deployments (City of San Diego 2022b). For a summary of data issues and instrument problems for 2021, see Appendix C.3 and for 2020, see Addendum 2-1 in City of San Diego (2021).

Each RTOMS was outfitted with a series of instruments/sensors at fixed depths (Table 2.1). Critical parameters that were measured on a real-time basis, by both systems, included temperature, conductivity (salinity), total pH, DO, dissolved carbon dioxide (xCO_2), nitrogen (nitrate + nitrite), chlorophyll *a*, CDOM, biological oxygen demand (BOD), and current direction and velocity. For 2021, in order to better target potential plumes at the PLOO, the bottom instrument package ('cage-2') and associated measurements were relocated from 89 m to 75 m depth (Table 2.1). Note that pH is reported in total scale (pH_T) from RTOMS with a more accurate calibration and measurement method

Table 2.1

Sensor configuration and model type for RTOMS by site and depth during 2020. For 2021, sensors were relocated to the following locations for PLOO: nitrate + nitrite moved to 30 m from 1 m, bottom package (cage-2) moved to 75 m from 90 m (all parameters), and temperature, conductivity, dissolved oxygen retained at 90 m.

Sensor Depth		
PLOO	**SBOO**	**Parameters Measured (Sensor Types)**
1 m (surface)	1 m (surface)	Temperature, conductivity, pH (total), DO (Sea-Bird SeapHOx)
		Ocean currents (RDI 300kHz ADCP)
		Partial pressure of carbon dioxide (Pro-Oceanus pCO_2 System)
		Chlorophyll *a*, CDOM, turbidity (Sea-Bird ECO triplet)
		Nitrate + nitrite (Sea-Bird SUNA V2)
10 m	10 m	Temperature, conductivity (Sea-Bird MicroCAT)
	18 m	Temperature, conductivity, DO (Sea-Bird MicroCAT ODO)
		Chlorophyll *a*, CDOM, turbidity (Sea-Bird ECO triplet)
20 m		Temperature, conductivity (Sea-Bird MicroCAT)
	26 m (cage)	Temperature, conductivity, pH, DO (Sea-Bird SeapHOx)
		Chlorophyll *a*, CDOM, turbidity (Sea-Bird ECO triplet)
		Nitrate + nitrite (Sea-Bird SUNA V2)
		BOD (Chelsea UviLux)
30 m (cage-1)		Temperature, conductivity, pH, DO (Sea-Bird SeapHOx)
		Chlorophyll *a*, CDOM, turbidity (Sea-Bird ECO triplet)
		BOD (Chelsea UviLux)
45 m		Temperature, conductivity (Sea-Bird MicroCAT)
60 m		Temperature, conductivity (Sea-Bird MicroCAT)
75 m		Temperature, conductivity (Sea-Bird MicroCAT)
89 m (cage-2)		Temperature, conductivity, pH, DO (Sea-Bird Deep SeapHOx)
		Chlorophyll *a*, CDOM, turbidity (Sea-Bird ECO triplet)
		Nitrate + nitrite (Sea-Bird SUNA V2)
		BOD (Chelsea UviLux)

for seawater, while pH has been reported in National Bureau of Standards (NBS) scale from CTD casts; it is not recommended to convert between these scales (Marion et al. 2011). In general, pH_T ranges reported by RTOMS may be lower than those recorded by the CTD, and any pH comparisons should be interpreted with caution due to method differences. All parameters were recorded at 10-minute intervals, with the exception of nitrate + nitrite, which was recorded at 1-hour intervals, and xCO_2, which was recorded at 10-hour intervals. Beginning in November 2021, xCO_2 sampling increased to 1-hour intervals, due to additional power available from a solar panel upgrade at both moorings.

Temperature and ocean current data from static moorings were used to supplement data gaps between RTOMS deployments. These non-telemetered (static) upward-facing bottom-mounted acoustic doppler current profilers (ADCPs) (Teledyne RD Instruments 300 KHz Workhorse Monitor) and thermistor (Onset Tidbit temperature loggers) string arrays were moored near the RTOMS at the terminal end of the PLOO and SBOO (Figure 2.1, Appendix C.4), as part of the original Moored Observation System Pilot Study (Storms et al. 2006). Data from completed static mooring deployments are available throughout much of 2020 and 2021.

These instrument packages are much smaller and less logistically challenging to retrieve and deploy compared to RTOMS. Data from ADCPs were collected every five minutes in 4-m depth bins, ranging from 9 to 93 m at the PLOO and from 6 to 30 m at the SBOO. Temperature data were collected from vertical series of thermistors every 10 minutes from duplicate arrays at the PLOO (100 m) and a single array at the SBOO (36 m). The thermistors were deployed on mooring lines at each site starting at 2 m above the seafloor and extending through the water column every 4 m to within 6 m of the surface.

Data Processing and Analysis

Prior to conducting analyses, RTOMS data were subject to a comprehensive suite of quality assurance/ quality control (QA/QC) procedures following Quality Assurance of Real-Time Oceanographic Data (QARTOD) methodologies (US IOOS 2017, 2020). This collaborative effort was developed to address data quality issues of the U.S. Integrated Ocean Observing System (US IOOS) community and provides recommendations for applying automated data qualifier flags specific to each parameter Methodology for ADCP data differed slightly and is described separately. For all other RTOMS data, QARTOD tests were applied to all data prior to analysis (Appendices C.5–C.7, City of San Diego 2020, 2021). In addition to these automated tests, all data were reviewed manually and flagged to identify questionable data, which may result from biofouling, interference from bubbles, sensor drift, or other malfunctions. Major data and sensor problems are highlighted by parameter and location (Appendix C.3, City of San Diego 2021), and a detailed log of data flagged manually by parameter, site, depth, and date range is available upon request. When possible, additional QA/QC procedures analyzing quarterly CTD casts to validate data from RTOMS sensors, and seawater samples to validate nitrate + nitrate results were conducted. After review, all data that were flagged as suspect or bad were excluded from further analyses and are not presented in this report.

Analyses were performed in R (R Core Team 2021) using functions within various packages (i.e., zoo, reshape2, Rmisc, mixOmics, tidyverse, scales, pracma, data.table, gtools) (Zeileis and Grothendieck 2005, Wickham 2007, Hope 2013, Rohart et al. 2017, Wickham et al. 2019, Wickham and Seidel 2020, Borchers 2021, Dowle and Srinivasan 2021, Warnes et al. 2021). Annual time series of raw and daily-averaged data were plotted at each depth and site for all parameters, with the exception of ADCP data (described subsequently). Contour plots were generated in MATLAB (2016) using default settings, which display fixed isolines, and fill areas between isolines with constant colors. Density calculations and temperature-salinity plots were created using the SEAWATER toolbox library for MATLAB, version 3.3.1 (Morgan and Pender 2014). Vertical profiles were constructed for daily-averages of temperature, salinity, and density, as these parameters had the most coverage through the water column. Density and thermal gradients were calculated by differences in daily-averaged values between sensors and dividing by the depth. In addition, summary statistics were completed at each depth and site with the following seasonal periods that align with quarterly water quality sampling: winter (January–March); spring (April–June); summer (July–September); fall (October–December). Large data gaps were identified as seasons with < 40% data recovery, based on expected number of samples for sensor-specific sampling intervals, and were excluded from summary analyses.

Ocean current data collected by ADCP were checked for quality by eliminating those measurements that did not meet echo intensity criteria (i.e., minimum correlation among the four beams of > 75%). Following this initial screening, tidal frequency data were removed using the PL33 filter (Alessi et al. 1984), compass direction was corrected to true north (+12.8 degrees), and data were hourly averaged. For all RTOMS and ADCP deployments in 2020, and all static ADCP deployments in 2020 and 2021, data were summarized as counts of observed velocities by season and select depth bins. The deployment of the RTOMS-based ADCP instrumentation in 2021 was not of sufficient duration to be summarized in this manner. The generalized axes of current

direction and magnitude were determined by linear regression of 2020 RTOMS-based ADCP northern versus eastern velocities for select depth bins. Data not reported previously were summarized by season and depth bin.

Data collected during 2020 were reported previously (City of San Diego 2021), and applicable all raw data for the 2020–2021 sampling period have been submitted to either the Regional Water Quality Control Board or the California Environmental Data Exchange Network (CEDEN) and may be accessed upon request.

Results and Discussion

Oceanographic Conditions in 2020–2021

Water Temperature

Ocean temperatures recorded during the 2020–2021 quarterly CTD surveys followed expected seasonal patterns throughout the PLOO and SBOO regions, ranging from a minimum of 9.7 to a maximum of 15.9°C in winter, 9.7 to 20.1°C in spring, 10.5 to 23.9°C in summer, and 10.8 to 19.2°C in fall (Figures 2.2–2.5, City of San Diego 2021). Regardless of the year or season, water temperature decreased throughout the water column with increasing depth. Surface waters during the summer were typically the warmest, and deeper waters during the spring were the coldest. Over the past two years, maximum water temperatures were recorded in surface waters of both regions during summer 2020 (PLOO: 23.9°C; SBOO: 23.8°C). Conversely, the coldest water temperatures were recorded in the deepest waters of both regions (PLOO: 81–98 m stations; SBOO: 39–55 m stations) during spring 2020 and winter 2021 in the PLOO region (9.7°C), and spring 2021 in the SBOO region (10.4°C).

Ocean temperatures observed by RTOMS and thermistor arrays showed similar seasonal patterns and comparable ranges to quarterly CTD surveys. Temperatures recorded during 2020–2021 from moorings near the PLOO and SBOO ranged from a minimum of 9.6 to a maximum of 17.9°C in winter, 9.3 to 22.5°C in spring, 9.8 to 25.5°C in summer, and 10.4 to 21.8°C in fall (Figures 2.6–2.7, Appendices C.8–C.12, City of San Diego 2021). The warmest seasonal mean water temperatures were recorded at the surface in both regions during summer 2020 (PLOO: 21.2°C; SBOO: 19.8°C), with maximums occurring in late August (PLOO: 25.5°C; SBOO: 24.4°C) (City of San Diego 2021). Conversely, the coldest seasonal mean water temperatures were recorded in the deepest locations for both RTOMS (PLOO: 89 m; SBOO: 26 m) during spring 2020 (PLOO: 10.1°C; SBOO: 11.7°C), with minimums occurring in late April (PLOO: 9.3°C; SBOO: 10.6°C). Overall, cooler temperatures (< 9.8°C) occurred during the winter and spring of both years at deep depths (>60 m), and warmer temperatures (>22°C) occurred near the surface in the summer of both years and in spring 2020. As a result of higher frequency sampling, maximum surface summer temperatures from moorings were up to 1.6°C higher than observations from any sites during quarterly surveys.

Salinity

Salinities recorded during the 2020–2021 quarterly surveys also followed expected seasonal patterns throughout the PLOO and SBOO regions, ranging from a minimum of 32.18 to a maximum of 34.12 ppt in winter, 33.44 to 34.28 ppt in spring, 33.27 to 33.95 ppt in summer, and 33.27 to 33.89 ppt in fall (Figures 2.2–2.5, City of San Diego 2021). Within the PLOO region, the highest salinity values (>34.0 ppt) were typically recorded at bottom depths (80 and 98-m stations) during spring 2020 and winter 2021. Similarly, high salinities in the SBOO region (>33.8 ppt) were recorded at bottom depths (55-m stations) during spring 2020, and winter and spring 2021. High salinity values, associated with deep waters during the spring in both the PLOO and SBOO regions, corresponded with the coldest temperatures, as described previously. Taken together, these results support the observation that local coastal upwelling appears to be strongest during the spring months (Jackson 1986). Unusual, elevated salinity appeared at near surface depths at some stations during spring 2020 (Figures 2.2, 2.4), likely influenced by excess organic matter from very high phytoplankton concentrations

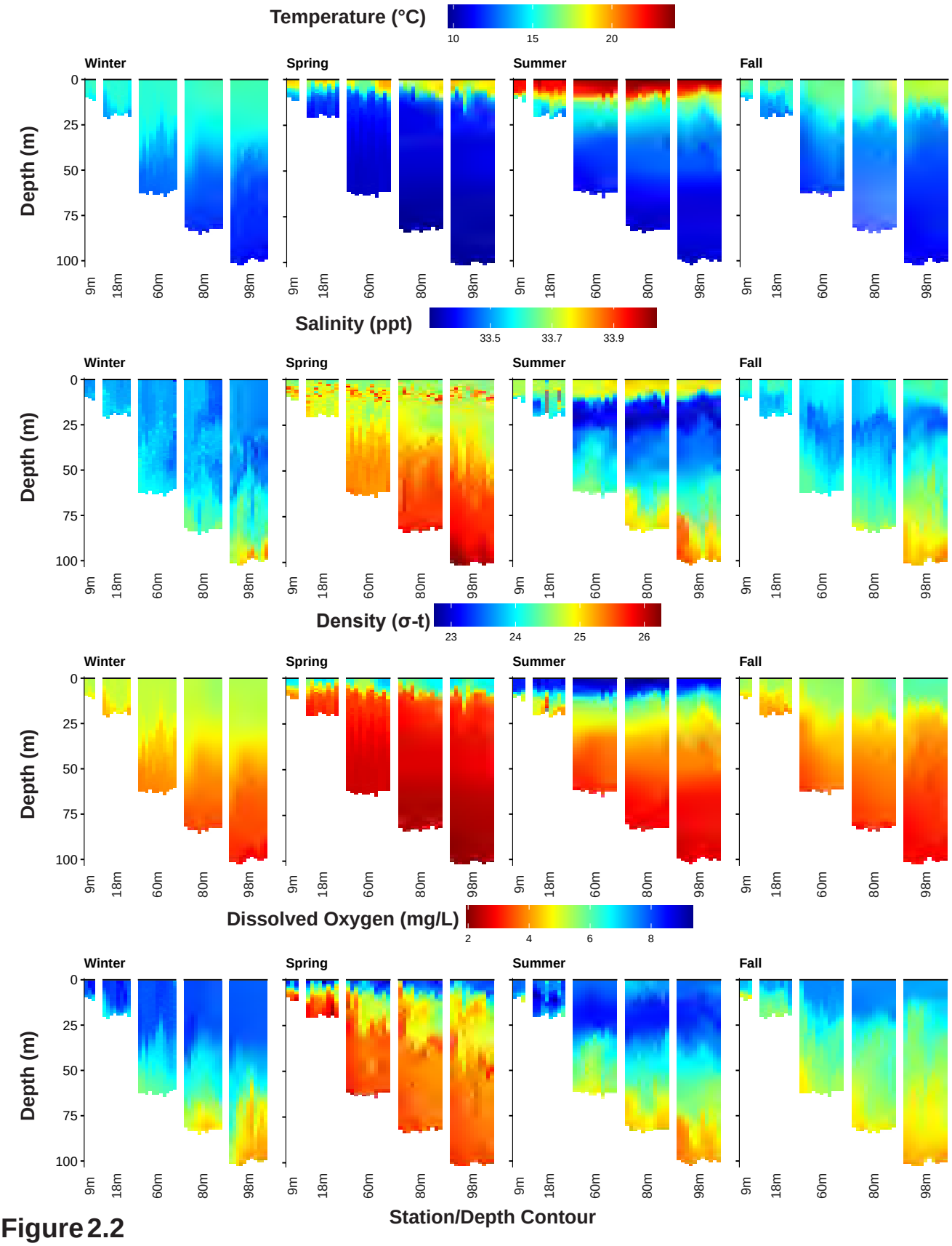

Figure 2.2

Temperature, density, salinity, and dissolved oxygen recorded in the PLOO region during 2020. Data are 1-m binned values per depth for each station and were collected over 4–5 days during each quarterly survey. Stations are depicted from north to south along each depth contour.

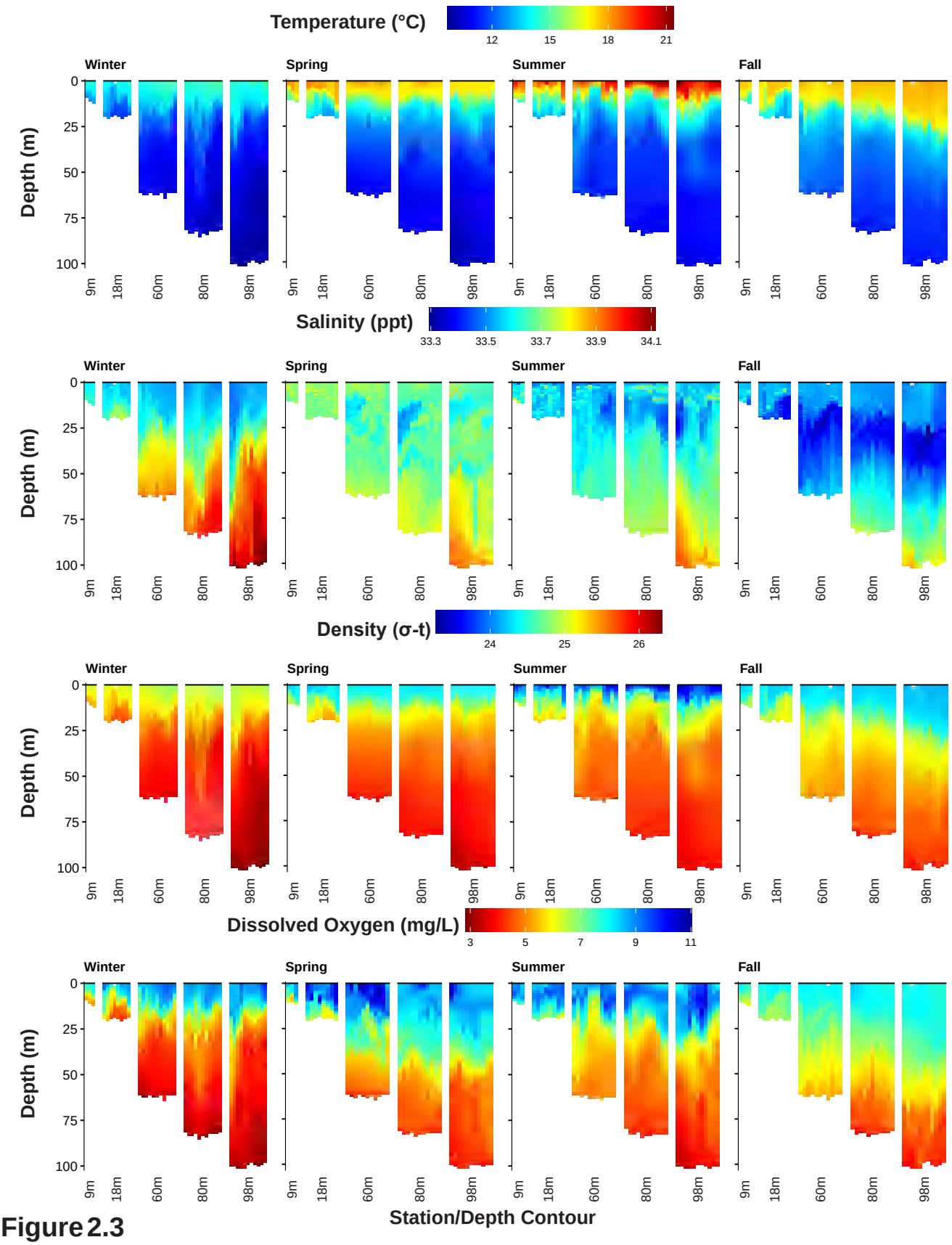

Figure 2.3

Temperature, density, salinity, and dissolved oxygen recorded in the PLOO region during 2021. Data are 1-m binned values per depth for each station and were collected over 4–5 days during each quarterly survey. Stations are depicted from north to south along each depth contour.

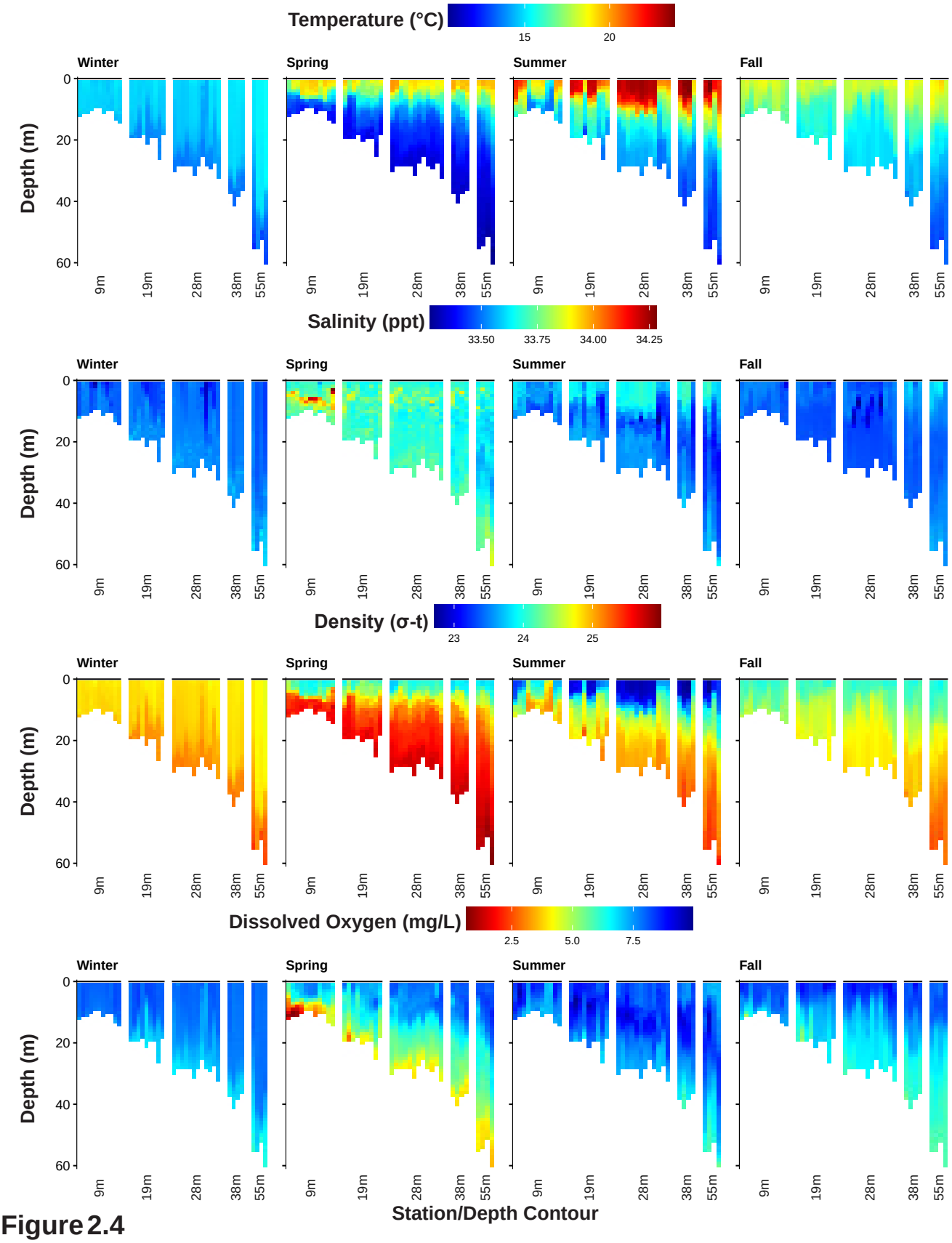

Figure 2.4

Temperature, density, salinity, and dissolved oxygen recorded in the SBOO region during 2020. Data are 1-m binned values per depth for each station and were collected over 4–5 days during each quarterly survey. Stations are depicted from north to south along each depth contour.

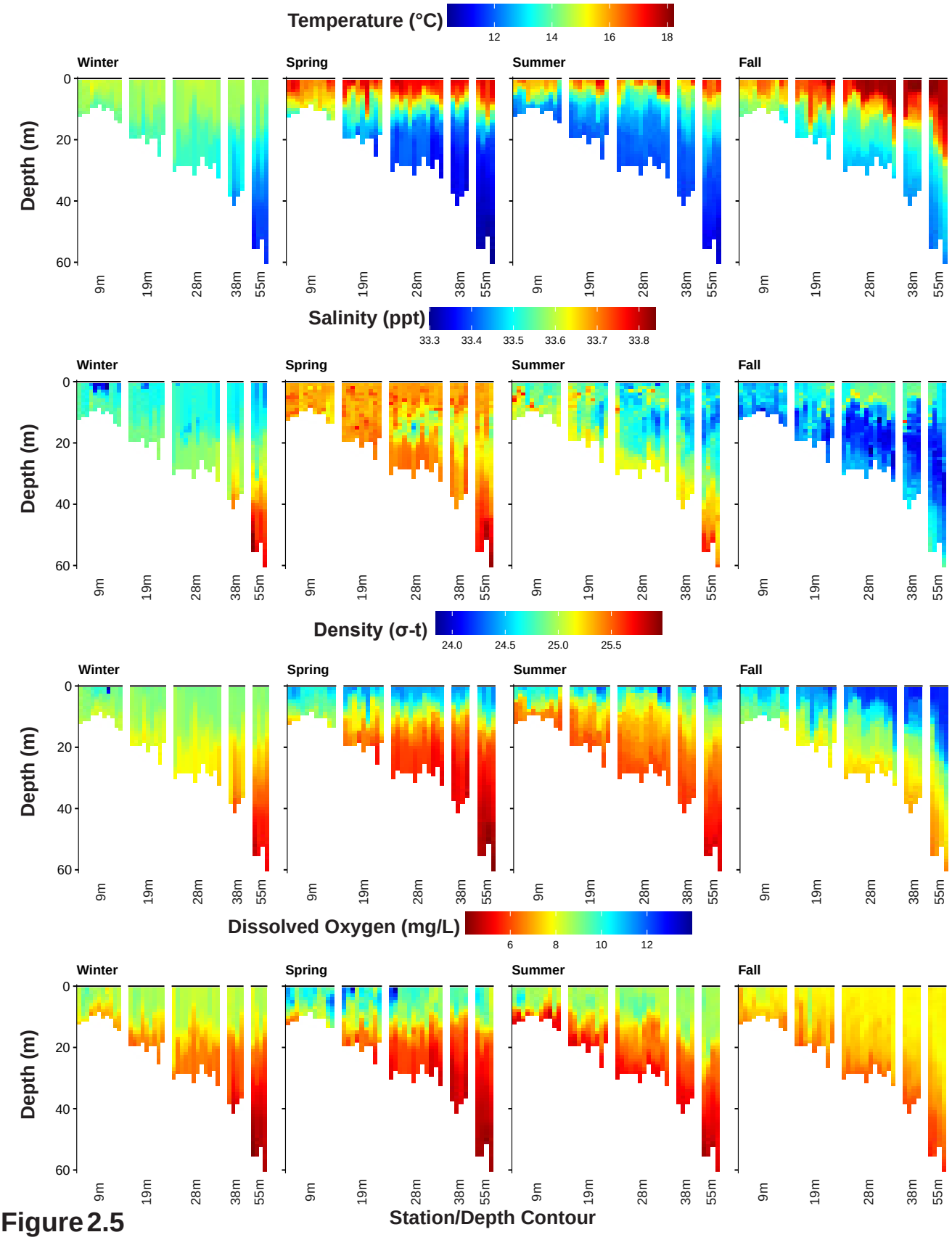

Figure 2.5

Temperature, density, salinity, and dissolved oxygen recorded in the SBOO region during 2021. Data are 1-m binned values per depth for each station and were collected over 4–5 days during each quarterly survey. Stations are depicted from north to south along each depth contour.

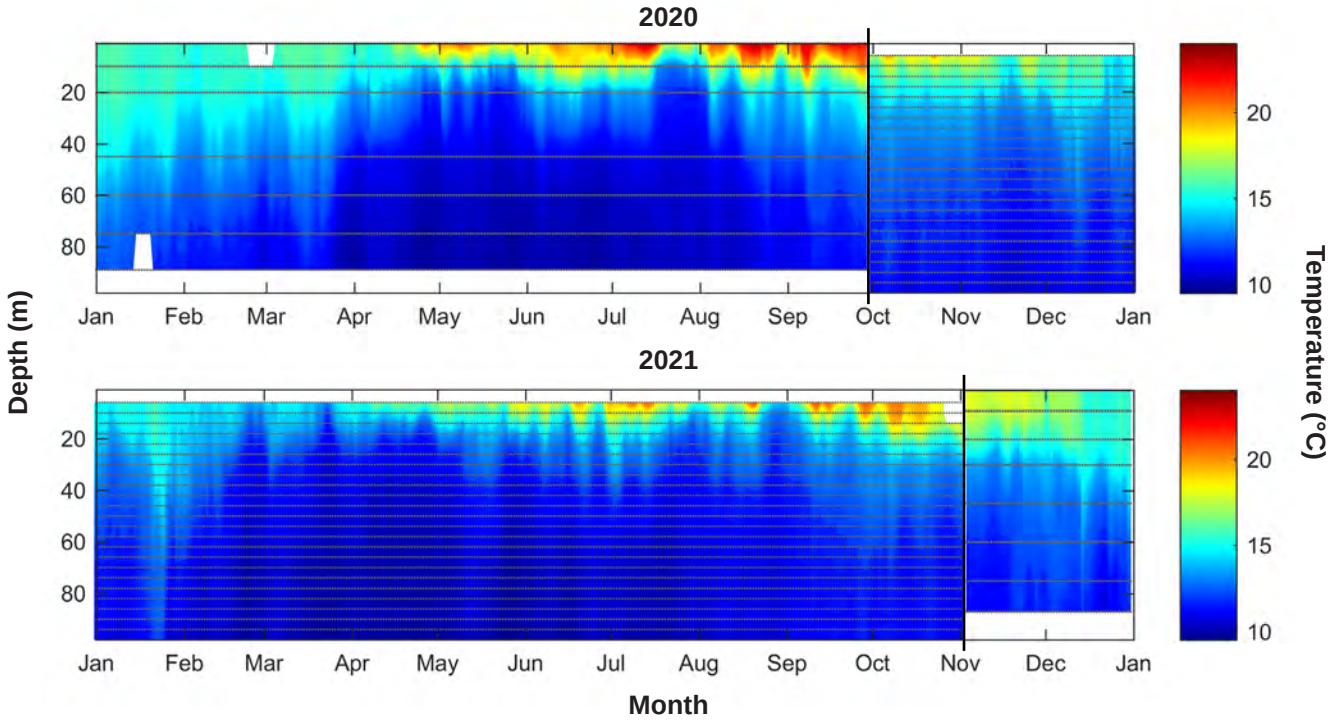

Figure 2.6

Daily averaged temperature recorded near the PLOO by the RTOMS or thermistor array during 2020 and 2021. Horizontal gray lines indicate depths at which sensors were located. Vertical black lines indicate time periods when thermistor array data were used to replace RTOMS data missing due to instrument failure or gap between deployments (i.e., 9/30/20–11/2/21). Additional missing data shown as white spaces.

fouling the conductivity cell, and is unlikely a true measure of elevated salinity.

Low salinity values in the PLOO (< 33.5 ppt) and SBOO (< 33.3 ppt) regions were limited to mostly surface waters in winter and fall in the PLOO region, with some occurrences in summer 2021 in both regions (Figures 2.2–2.5). Similarly, during winter and spring in the SBOO region, low salinities were also recorded at some surface depths (9 and 18-m stations), but less uniformly than what was observed in the PLOO region. Given the proximity of these SBOO locations to the mouth of the Tijuana River, and the infrequency of the low salinity events, they may be correlated with winter rain events and the resultant influx of fresh water input into local receiving waters (Hess 2019, NOAA/NWS 2022).

Salinities observed from moorings near the PLOO and SBOO ranged from a minimum of 32.89 to a maximum of 33.84 PSU (Practical Salinity Unit) in winter, 32.12 to 33.94 PSU in spring, 32.97 to 33.87 PSU in summer during 2020, and 33.04 to 33.87 PSU during fall 2021 (Figures 2.8–2.9, Appendices C.10–C.12, City of San Diego 2021). As described in Materials and Methods, salinity data from moorings is not available from fall 2020 through summer 2021. The highest seasonal mean salinity (PLOO: 33.66 PSU) was recorded near the surface during summer 2020 (City of San Diego 2021), likely due to evaporation caused by atmospheric warming (Jones et. al 2002) and corresponded to high mean summer temperatures. High seasonal mean salinities (>33.6 PSU) also occurred at depth at both sites during spring 2020 (PLOO: 75–89 m; SBOO: 26 m), with maximums occurring in late April (PLOO: 33.94 PSU; SBOO: 33.84 PSU). This time period overlaps with the coldest temperatures, and supports the same indication of spring upwelling as observed by quarterly surveys. The lowest seasonal mean salinity (PLOO: 33.3 PSU) was recorded near bottom depths (89 m) during winter 2020, likely influenced by the PLOO effluent plume due to the proximity of the mooring to the outfall discharge (see Chapter 4). Minimum salinity values were recorded in spring

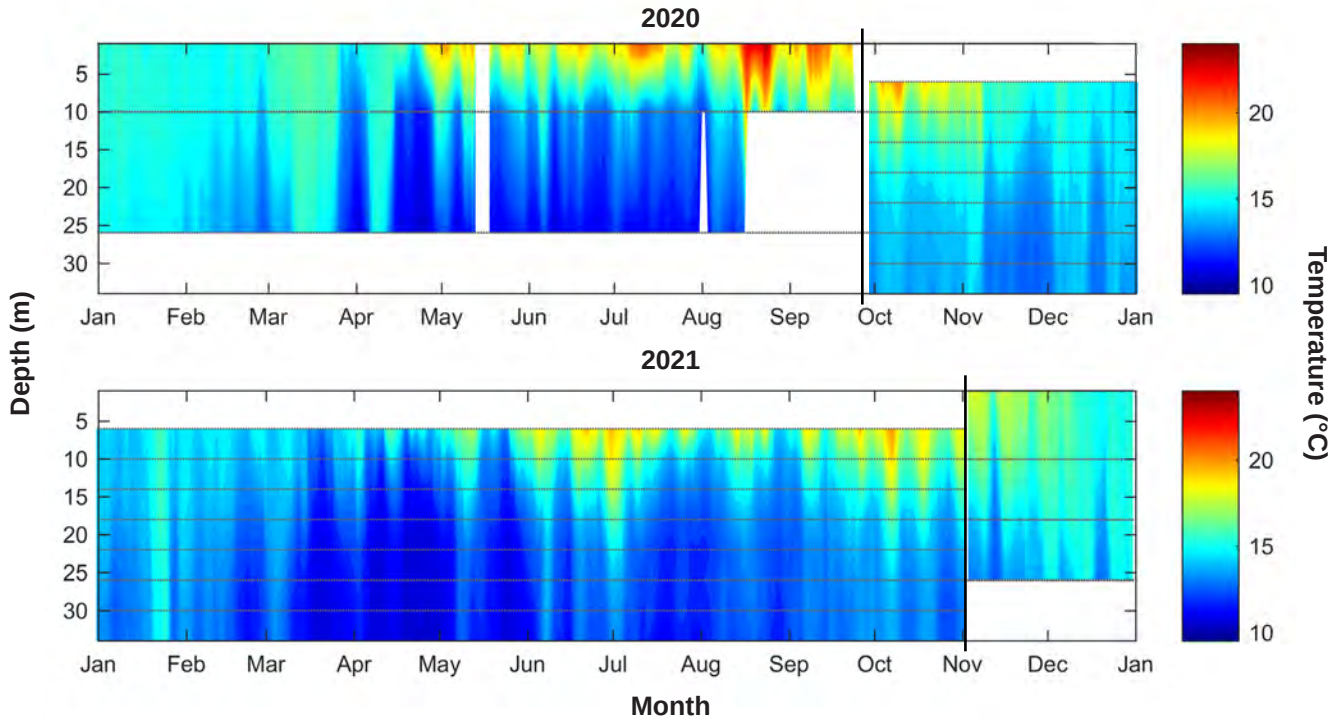

Figure 2.7

Daily averaged temperature recorded near the SBOO by the RTOMS or thermistor array during 2020 and 2021. Horizontal gray lines indicate depths at which sensors were located. Vertical black lines indicate time periods when thermistor array data were used to replace RTOMS data missing due to instrument failure or gap between deployments (i.e., 9/24/20–11/2/21). Additional missing data shown as white spaces.

2020 at both sites at the surface (PLOO: 32.12 PSU; SBOO: 32.90 PSU) and may be influenced by rain events as described previously.

Density and Ocean Stratification

Seasonal changes in thermal stratification over the past two years were mirrored by density stratification of the water column during each survey (Figures 2.2–2.5). These results align with regional studies showing that density in shallow coastal waters of southern California, and elsewhere, is primarily influenced by temperature differences, since salinity is relatively uniform (Bowden 1975, Jackson 1986, Pickard and Emery 1990). Additionally, maximum buoyancy frequency for both regions ranged from a minimum of 4.92 to a maximum of 6.68 cycles/min during the winter, 9.39 to 15.74 cycles/min during the spring, 11.42 to 14.60 cycles/min during the summer, and 8.56 to 9.38 cycles/min during the fall (Figure 2.10, Appendix C.13). As expected, the depth of the pycnocline also varied by season. Shallower pycnocline depths (≤ 11 m) occurred in spring and summer, which typically corresponded to greater stratification, although moderate stratification was observed during fall in the SBOO region in both 2020 and 2021.

Observations from the RTOMS provided an extensive temporal record of stratification changes near the ocean outfalls due to density differences when RTOMS data were available. Densities at the PLOO RTOMS were lowest (< 23.3 kg/m^3) near the surface from July through September in 2020, and highest (> 26 kg/m^3) from late March through early July 2020 in deeper waters (≥ 60 m) (Figure 2.8, City of San Diego 2021). Similarly, the lowest densities (< 23.3 kg/m^3) at the SBOO RTOMS were recorded near the surface from August through September in 2020, and highest densities (> 25.7 kg/m^3) from early April through July 2020 at the bottom depth (26 m) (Figure 2.9, City of San Diego 2021). Density gradients were dominated by changes in temperature as discussed above, which had greater data coverage due to thermistor array deployments (Figures 2.6–2.7). At PLOO and SBOO over the past two years, moderate thermal stratification

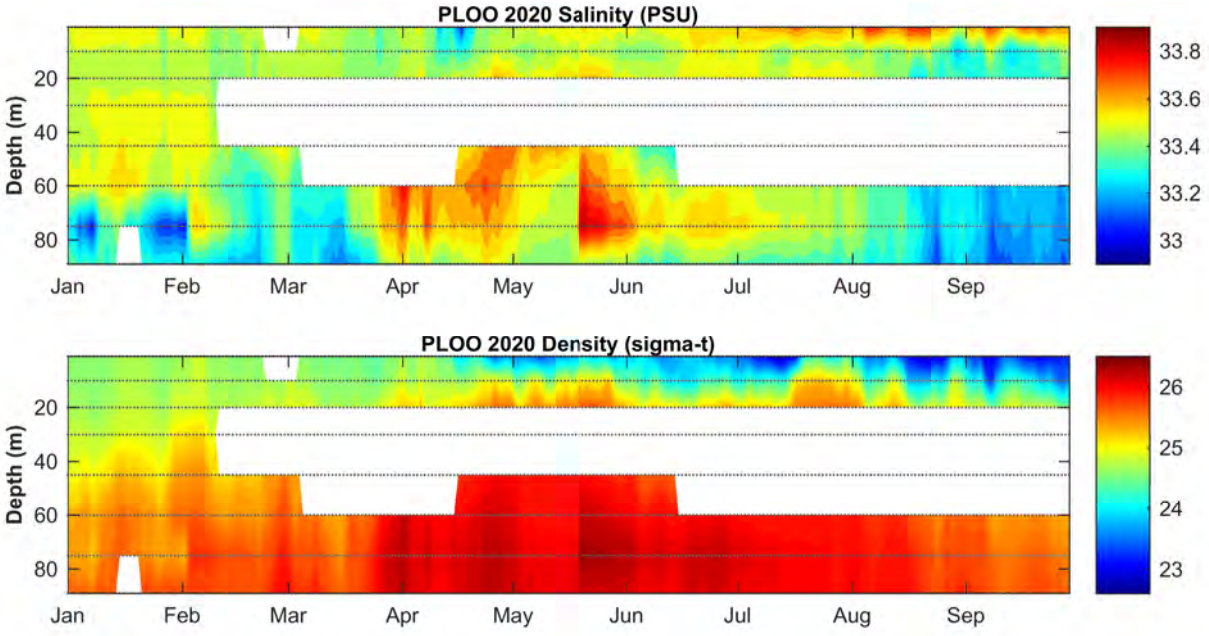

Figure 2.8
Daily averaged salinity and density recorded by the PLOO RTOMS from January through September 2020. Horizontal gray lines indicate depths at which sensors were located. Missing data due to instrument failure or loss shown as white spaces.

(gradients >0.2°C/m) persisted for much of April through November in the upper water column (PLOO: < 30 m; SBOO: < 22 m), with the strongest stratification (gradients >0.5°C/m) occurring intermittently in spring and summer months (see Chapter 4, Appendix E.21).

Dissolved Oxygen and pH

Levels of DO and pH in the coastal waters off San Diego generally followed expected patterns in 2020 and 2021 that corresponded to seasonal fluctuations in water mass inputs. Additionally, changes in DO and pH tended to be closely linked, since both parameters reflect fluctuations in dissolved carbon dioxide, an indicator of biological activity in coastal waters (Skirrow 1975). Concentrations of DO across the PLOO and SBOO regions ranged from a minimum of 2.8 to a maximum of 10.0 mg/L in winter, 0.6 to 13.9 mg/L in spring, 3.3 to 10.6 mg/L in summer, and 3.7 to 9.3 mg/L in fall. The recorded pH ranged from a minimum of 7.7 to a maximum of 8.3 in winter, 7.5 to 8.5 in spring, 7.7 to 8.3 in summer, and 7.6 to 8.3 in fall (Figures 2.2–2.5, Appendices C.14–C.17, City of San Diego 2021). Maximum DO and pH were recorded in surface waters of both regions during spring 2021 (PLOO: 11 mg/L and 8.4; SBOO: 14 mg/L and 8.5) (Figures 2.2–2.5, Appendices C.14–C.17, City of San Diego 2021). Conversely, minimum DO and pH were recorded in the bottom depths of nearshore stations (9 and 18-m stations) of both regions during spring 2020 (PLOO: 1.9 mg/L and 7.6; SBOO: 0.6 mg/L and 7.6), likely due to the upwelling of cold, saline, oxygen-poor water moving inshore similar to the pattern described previously for temperature and salinity.

Changes in DO and pH at the PLOO and SBOO RTOMS were also generally aligned and showed similar seasonal patterns to quarterly CTD surveys. Concentrations of DO observed during 2020 ranged from a minimum of 2.2 to a maximum of 9.8 mg/L in winter, 2.1 to 22.5 mg/L in spring, 3 to 11 mg/L in summer, and during fall 2021 from 3.1 to 10.1 mg/L (Appendices C.10–C.12, City of San Diego 2021). Similarly, pH_T (total scale) recorded during 2020 ranged from a minimum of 7.6 to a maximum of 8.2 in winter, 7.4 to 8.9 in spring, 7.6 to 8.2 in summer, and during fall 2021 from 7.8 to 8.2 pH units (Appendices C.10–C.12, City of San Diego 2021).

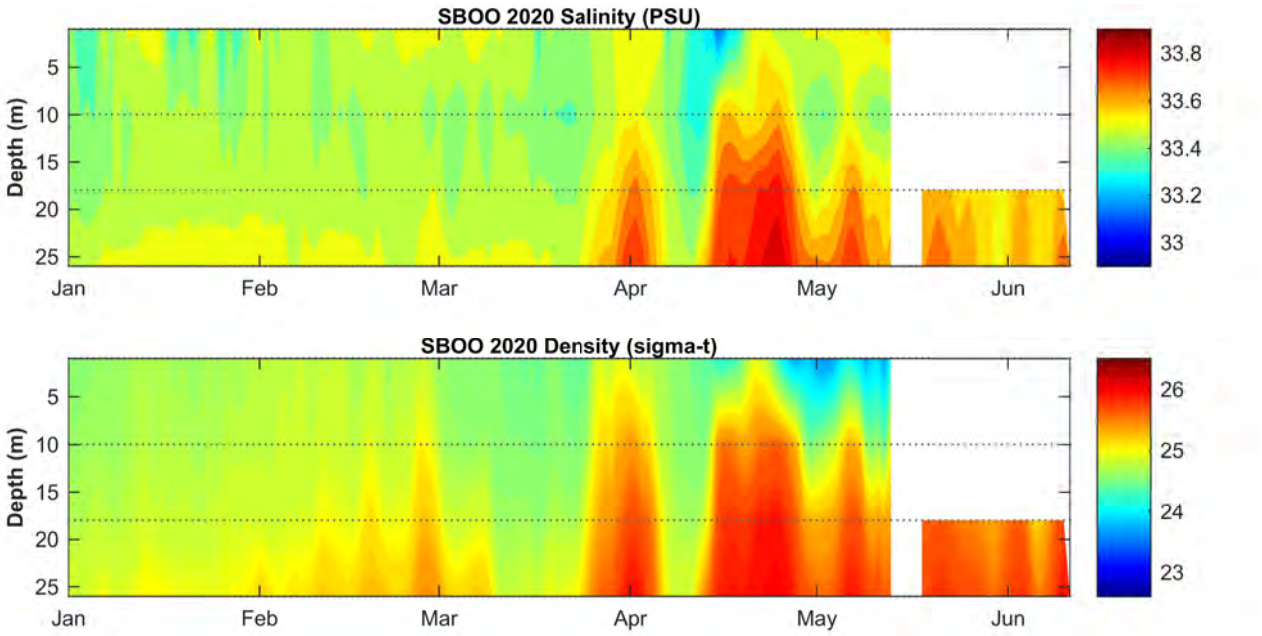

Figure 2.9
Daily averaged salinity and density recorded by the SBOO RTOMS from January through June 2020. Horizontal gray lines indicate depths at which sensors were located. Missing data due to instrument failure or loss shown as white spaces.

As described in Materials and Methods, DO and pH_T data from moorings are not available from fall 2020 through summer 2021, and generally RTOMS sensors report slightly lower pH values compared to quarterly CTD surveys due to difference in pH units (total scale and NBS units, respectively).

The highest DO and pH_T levels were observed from both RTOMS at the surface in early May 2020 (PLOO: 22.5 mg/L and 8.9; SBOO: 23.3 mg/L and 8.6) (Appendix C.12, City of San Diego 2021). Quarterly CTD sampling occurred in late May in 2020 (Appendix C.1), which did not overlap during the peak periods in DO and pH_T levels observed by the RTOMS. These maximum values exceeded all previously reported RTOMS data (City of San Diego 2020) and corresponded to an unprecedented, large regional spring phytoplankton bloom in April/May 2020 (Anderson and Hepner-Medina 2020). Conversely, the lowest DO and pH_T levels were observed at deep depths in early April 2020 (PLOO: 2.1 mg/L and 7.6; SBOO: 3.4 mg/L and 7.4). At the PLOO, the lowest DO values (< 3 mg/L) at deep depths were closely associated with the coldest and highest salinity water masses (Figure 2.11). Similarly, low DO values at the bottom depth at the SBOO were generally recorded in coldest, saline waters, although some low DO values were also observed at moderate salinities and cool temperatures (Figure 2.12). These observations further support the role of upwelling in the spring as a significant driver of local conditions.

Dissolved CO_2

Surface seawater carbon dioxide levels (xCO_2) recorded from the RTOMS generally aligned with surface DO and pH_T levels. Concentrations of xCO_2 ranged from a minimum of 59 to a maximum of 477 ppm, as observed at the PLOO from winter through summer 2020, and from 61 to 565 ppm at the SBOO in all 2020 and fall 2021 (Appendices C.10–C.12, City of San Diego 2021). As described in Materials and Methods, data are not available from fall 2020 through summer 2021. The lowest seasonal mean levels were observed during spring 2020 at both RTOMS PLOO: 272 ppm; SBOO: 297 ppm) (City of San Diego 2021). Minimum values occurred in early May 2020 that were lower than all previously reported mooring data (City of San Diego 2020)

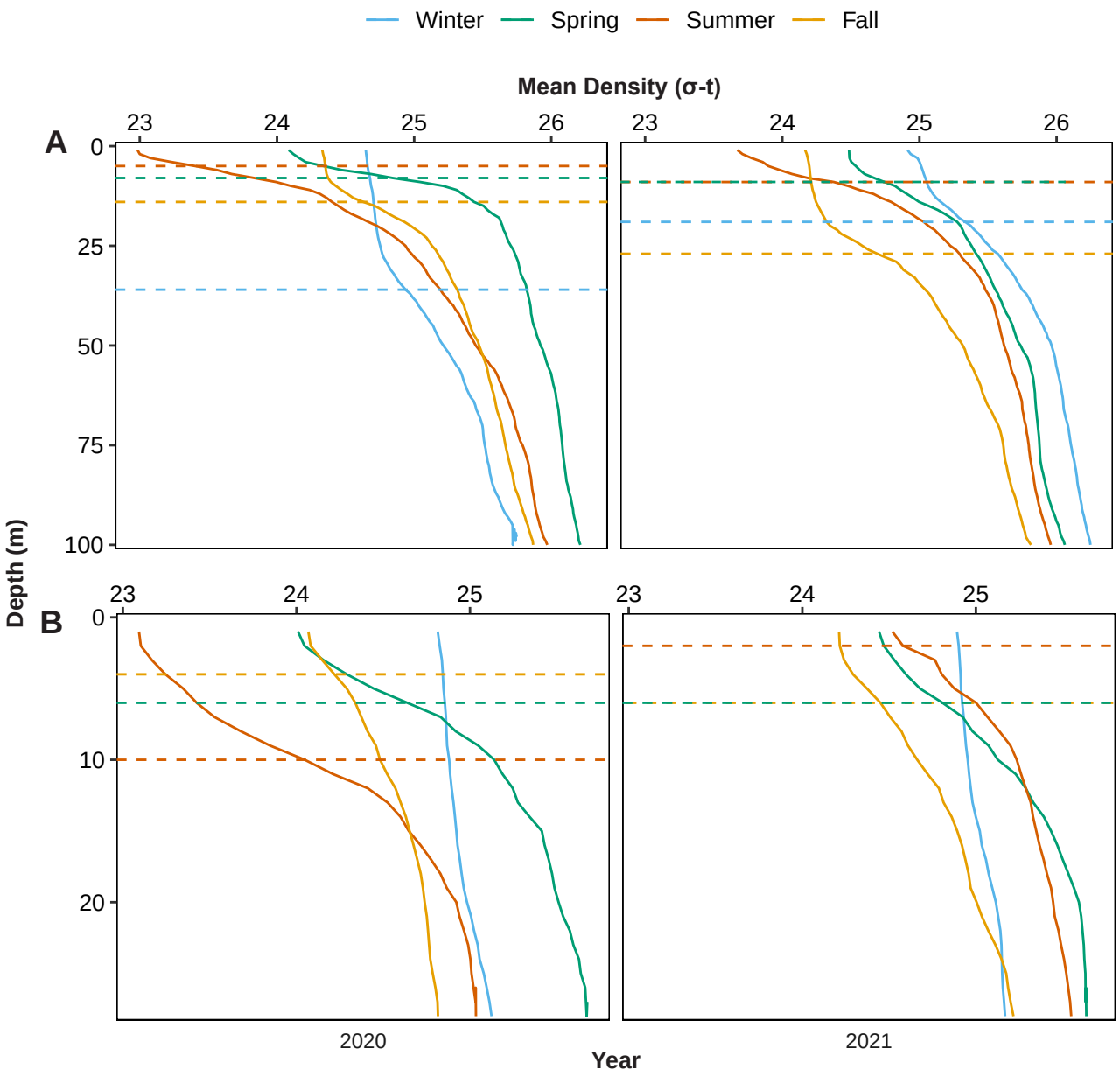

Figure 2.10

Mean density for each survey conducted during 2020 and 2021 at (A) PLOO discharge depth stations (n = 11) and (B) SBOO discharge depth stations (n = 13). Horizontal dashed lines indicate depth of maximum buoyancy frequency. Dashed line not shown for buoyancy frequencies less than 5.5 cycles/minute indicating a well mixed water column.

due to the large regional phytoplankton bloom as described above for DO and pH_T levels. The highest seasonal mean (398 ppm) was observed in fall 2020 at the SBOO mooring. Generally, the largest short-term variability (> 100 ppm change between days) was observed during the spring and summer at both moorings, while winter generally shows more stable daily values (Appendix C.12). These observations show similar seasonal variability and ranges to the closest near-coastal SIO carbon mooring (California Current Ecosystem mooring 2, NOAA/PMEL 2022), with the exception of April/May 2020 where observations at PLOO and SBOO decreased below 200 ppm during the near coastal regional bloom. Generally, biological productivity and surface water temperatures drive large seasonal amplitudes in pCO_2 (Sutton et al. 2019).

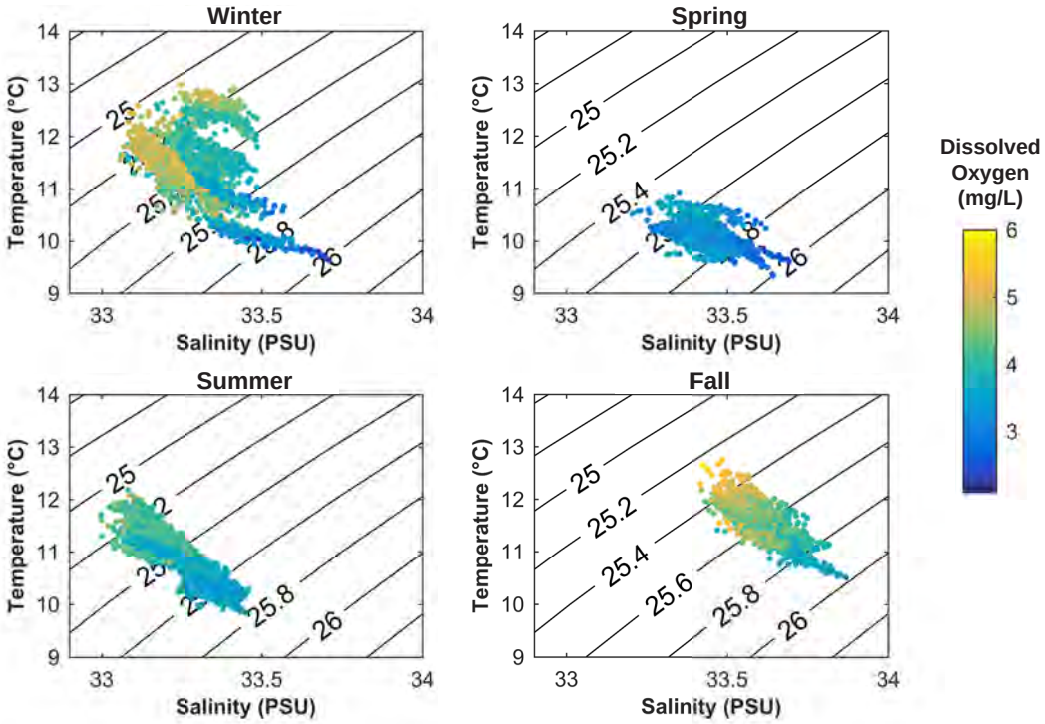

Figure 2.11

Hourly averaged DO by season shown on temperature versus salinity plots at 89 m for all available PLOO mooring data from 2020 to 2021. Isopycnals and corresponding σ-t values shown by black lines.

Transmissivity

Although water clarity (transmissivity) ranged widely, from a minimum of 22 to a maximum of 94% throughout the PLOO and SBOO regions, values were generally quite high, exceeding 84% during most of 2020 and 2021 (Appendices C.14–C.17). During winter and fall, low transmissivity (< 75%) was most often observed at shallow monitoring stations, located close to shore, where the influence of waves, currents, and land-based turbidity plumes was most acute. For example, reduced water clarity in winter 2020 at the 9-m SBOO stations coincided with increased turbidity along the coast that was likely due to concurrent rain activity and large waves (CDIP 2022). Other concentrations of low transmissivity during spring/summer surveys in both regions appeared to be associated with high concentrations of chlorophyll *a*, possibly indicative of dense accumulations of phytoplankton cells (see next section), most obvious during spring 2020. Finally, low transmissivity values were also occasionally observed in bottom waters at stations located along all depth contours indicating a possible resuspension of soft sediments caused by the CTD approaching or hitting the seafloor.

***Chlorophyll* a**

Concentrations of chlorophyll *a* ranged from a minimum of < 0.1 to a maximum of 31.8 µg/L across the PLOO and SBOO regions in 2020 and 2021 (Appendices C.14–C.17). Elevated chlorophyll *a* levels (> 5 µg/L) were recorded at depths from the surface to 25 m along all depth contours in the PLOO region during spring 2020, and to depths associated with (or just below) the mixed layer. These elevated values were associated with a large and prolonged phytoplankton red tide bloom located in the SCB and northern Baja California (Figure 2.13; Ocean Imaging 2021, Weber et al. 2021, Anderson and Hepner-Medina 2020). Elevated levels were also recorded at depths from ~5 to 25 m along all depth contours in the PLOO region during winter, spring, and summer 2021, as well as from ~5 to 25 m along all depth contours in the SBOO region during spring and summer 2021. Elevated chlorophyll *a* levels at these depths reflect the tendency for phytoplankton to accumulate along natural barriers

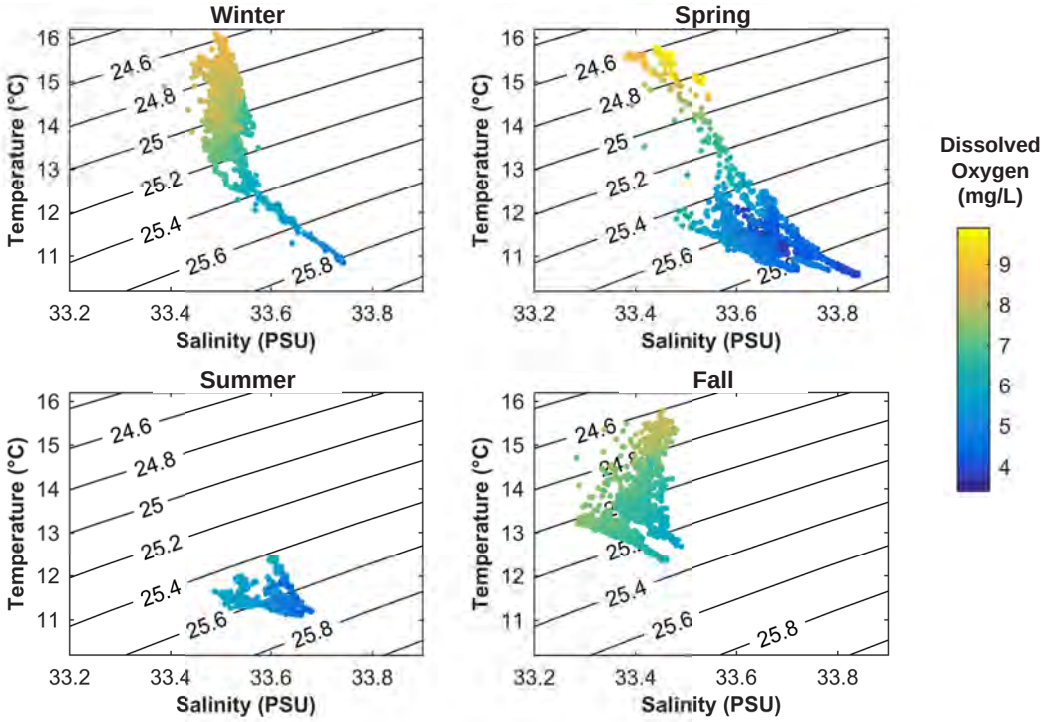

Figure 2.12
Hourly averaged DO by season shown on temperature versus salinity plots at 26 m for all available SBOO mooring data from 2020 to 2021. Isopycnals and corresponding σ-t values shown by black lines.

such as isopycnals near the thermocline, where deeper water nutrients are available and light is not yet limiting (Lalli and Parsons 1993).

Chlorophyll *a* observed at the PLOO and SBOO moorings ranged from a minimum of < 0.1 to a maximum of > 29.4 µg/L through winter and spring 2020 and fall 2021 (Appendices C.10–C.12, City of San Diego 2021). Data are not available from fall 2020 through summer 2021 while RTOMS were not deployed, and multiple sensor failures occurred in the summer of 2020 (City of San Diego 2021). Generally, the highest chlorophyll *a* values occurred near the surface during spring 2020 at PLOO and SBOO (>29.4 µg/L), with elevated levels occurring at mid depths during the same time period (PLOO: up to 14.7 µg/L at 30 m; SBOO: up to 12.6 µg/L at 18 and 26 m). As described for the quarterly surveys, these elevated levels were due to a large regional red tide bloom during April and May 2020, with associated higher than normal DO and pH_T levels and record low xCO_2 concentrations reported from the moorings near the surface (Figure 2.14). During RTOMS deployments in 2020 and earlier, chlorophyll sensors were configured with a maximum threshold of 30 µg/L, so higher values were not captured as described by quarterly surveys. This sensor issue was corrected for RTOMS deployments in 2021 (Appendix C.116). In addition, accumulation of phytoplankton tends to be patchy both horizontally and vertically in the water column, so maximum chlorophyll concentrations may have occurred at depths or locations where no mooring sensors were present.

Nitrate (plus Nitrite)

Nitrate + nitrate concentrations observed at the RTOMS from winter through summer 2020 and fall 2021 at the PLOO ranged from < 2.0 to 39.2 µM, and from < 2.0 to 25.4 µM at the SBOO (Appendices C.10–C.12, City of San Diego 2021). Data are not available from fall 2020 through summer 2021 while RTOMS were not deployed, and other data gaps occurred due to sensor failures (City of San Diego 2021). The lowest seasonal mean levels were observed during the spring and summer of 2020 near the surface

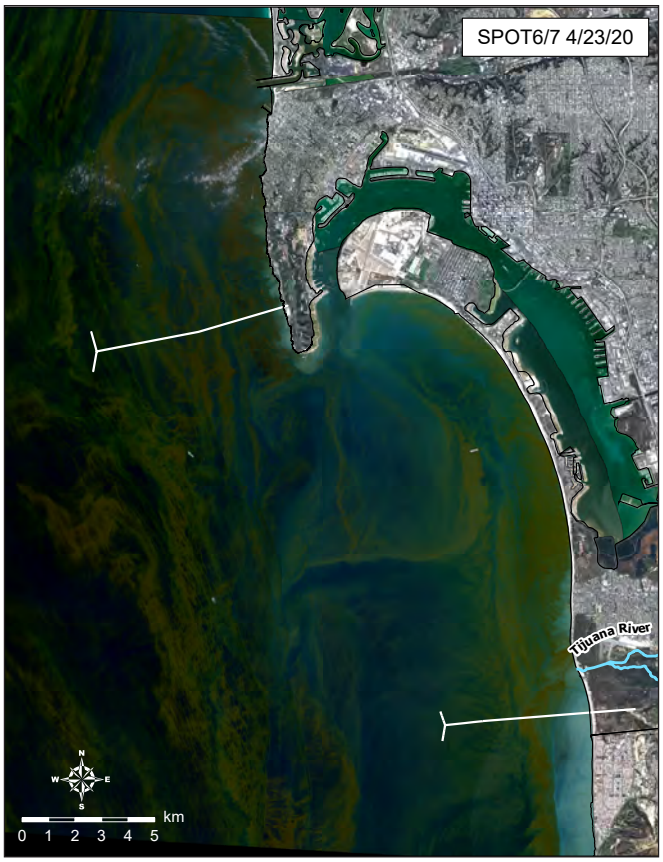

Figure 2.13
SPOT-6/7 satellite image of the San Diego region acquired April 23, 2020 (Ocean Imaging 2021) depicting phtoplankton blooms.

at both moorings (< 2 µM), likely due to uptake from phytoplankton. Generally, nitrate + nitrite concentrations increased with increasing depth and higher salinities, with the highest seasonal mean occurring in the fall of 2021 at PLOO (21.3 µM at 75 m) (Appendix C.10). These observations generally showed similar ranges to that of historical data (1969–2020) from nearby regional stations reported by the California Cooperative Oceanic Fisheries Investigations (CalCOFI) surveys, where the lowest nitrate levels occurred near the surface (<10 m: <0.1–11.2 µM) and higher levels occurred at depth, associated with higher salinities (70–130 m: <0.1–33.4 µM) (CalCOFI 2022, Weber et. al 2021

Summary of Ocean Currents in 2020–2021

Direction and Velocity of Subsurface Currents

Ocean currents surrounding the PLOO and SBOO varied by depth and season during the 2020–2021 reporting period. Seasonal mean current velocities (by 2-m depth bin in 2020 and 1-m depth bin in 2021) at the PLOO, from January through September 2020, ranged from a minimum of 53 to a maximum of 159 mm/s during winter, 72 to 270 mm/s during spring, and 73 to 173 mm/s during summer (City of San Diego 2021) while in fall of 2021, mean velocities (by 1-m depth bin) ranged from 17 to 117 mm/s (Appendix C.18). Seasonal mean current velocities (by 1-m depth bin) at the SBOO during 2020 ranged from a minimum of 42 to a maximum of 117 mm/s during winter, 48 to 147 mm/s during spring, 41 to 109 mm/s during summer, and 33 to 68 mm/s in the fall (City of San Diego 2021) while mean currents ranged from 58 to 164 in fall of 2021 (Appendix C.19). The highest seasonal mean current velocities typically occurred in near-surface waters during the spring at both the PLOO, and SBOO. Generally, for all seasons, the highest mean current velocities occurred in the upper 20 m at the PLOO and the upper 10 m at the SBOO. Below these thresholds, velocities decreased with depth around both outfalls, with the lowest mean velocities roughly 15 m from the bottom at the PLOO and 5 m from the bottom at the SBOO. Currents predominantly flowed along a north-northwest/south-southeast axis of variation, regardless of season or outfall location (Figures 2.15, 2.16). Additionally, linear regression of all current direction observations for select depth bins show that along-coast currents tend to dominate (Figure 2.17). These results are consistent with observations from the nearby bottom-mounted static ADCPs at both locations (Appendices C.20–C.23), and previous studies conducted in the region (Winant and Bratkovich 1981, Rogowski et al. 2012a).

Historical Assessment of Oceanographic Conditions

A review of temperature, salinity, and DO anomalies from all discharge depth stations sampled from 1991 through 2021 demonstrates how the PLOO and SBOO regions have responded to long-term climate-related changes in the SCB (Figure 2.18). Overall, these results are consistent with largescale temporal patterns in the California Current System (CCS)

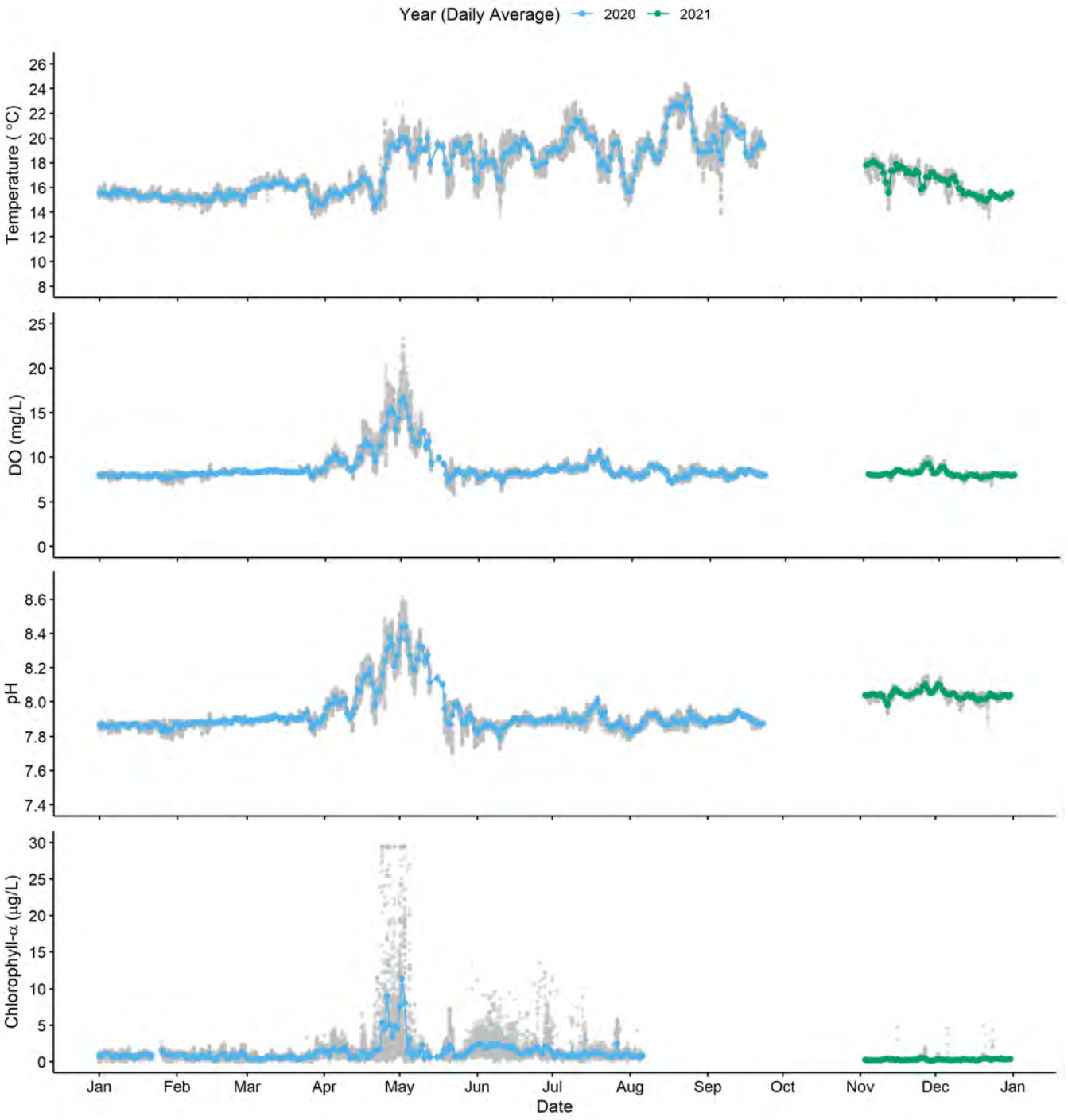

Figure 2.14

Temperature, DO, pH, and chlorophyll a data recorded at the SBOO RTOMS at 1 m during 2020–2021. Data presented as daily averages shown in color and raw values shown in gray.

associated with ENSO, PDO and NPGO events (Peterson et al. 2006, McClatchie et al. 2008, 2009, Bjorkstedt et al. 2010, 2011, 2012, Wells et al. 2013, Leising et al. 2014, 2015, Thompson et al. 2018, 2019, Harvey et al. 2021, Weber et al. 2021, NOAA/NWS 2022). Several major events in the CCS have affected SCB coastal waters since 1997 (Table 2.2). Temperature and salinity data for the entire San Diego region were overall consistent with the CCS events in Table 2.2, but there have been some notable deviations from these trends. For example, while the CCS was experiencing a warming trend through

2006, the PLOO region experienced cooler than normal conditions during much of 2005 and 2006. Conditions in San Diego waters during 2005–2006 were more consistent with observations from northern Baja California where water temperatures were well below the decadal mean (Peterson et al. 2006). Ocean temperatures were also warmer than the long-term average during winter through summer 2016. These results corresponded to El Niño conditions that lasted until spring 2016 before switching to being relatively cool in November 2016, a pattern that corresponded well with a La Niña that lasted from late 2016 through winter 2017. Deviations from the long-term average were minor, reflecting the ENSO neutral conditions that endured for most of 2017 (NOAA/NWS 2022). Ocean temperatures observed throughout the water column were warmer than the historical average during most of 2018, as confirmed by both CTD surveys and RTOMS (City of San Diego 2020), and closer to average conditions during 2019 for the PLOO region in particular.

In contrast, the CCS north of Monterey Bay showed surface water temperatures far above average in summer and fall 2019, consistent with a regionwide marine heat wave, as well as positive PDO and negative NPGO phases. With the switch to negative PDO and MEI phases in 2020, overall ocean temperatures were roughly average, with surface temperatures above average in 2020. Despite the negative PDO and MEI phases, the 2020 heatwave affected the Southern California Bight region similarly to 2014, with surface temperatures above average in 2020 (Weber et al. 2021). Surface temperatures were 0.5 to 3.0°C above normal in 2020, with the exception of fall in the PLOO region, while 2021 was more typical, with the exception of a cooler than normal summer in the SBOO region. Above average salinity observed during 2018 through 2021 was consistent with conditions all along the west coast, shifting from lower than normal salinities during the warm period of 2014–2016. These anomalous conditions were remotely observed moving towards the SCB prior to 2018, suggesting a shifting balance of water mass source waters being responsible for these temperature and salinity anomalies, which have remained through 2021 (Thompson et al. 2018, 2019, Harvey et al. 2021, Weber et al. 2021).

Historical trends in local DO concentrations reflect several periods during which lower than normal DO has corresponded with low water temperatures and high salinity (Figure 2.18). The alignment of these anomalies is generally consistent with cold, saline, less oxygenated ocean waters, which coincided with higher than normal salinities (e.g., 2002, 2005–2012, 2019–2021). The overall decrease observed in DO in the PLOO and SBOO regions through 2012 was also observed throughout the entire CCS and deep North Pacific and was thought to be linked to changing ocean climate (Bjorkstedt et al. 2012). However, no significant long-term trend has been shown over the last 70 years in the North Pacific shelf depths (Schmidtko et al. 2017). These large negative anomalies have been absent since mid-2013 in the PLOO and SBOO regions, but were present for some of 2020 and 2021 in the PLOO region.

Summary

Oceanographic conditions in the PLOO and SBOO regions, during 2020 and 2021, in general followed typical seasonal patterns for the coastal waters off San Diego, with a notable large regional phytoplankton bloom in spring 2020 that resulted in very high near-surface DO and pH levels and record low near-surface xCO_2 levels observed by the RTOMS. Maximum water column stratification occurred during spring and summer months, whereas waters were well mixed or weakly stratified in the winter. Ocean conditions indicative of local coastal upwelling, such as relatively cold, dense waters with low DO and pH at subsurface depths, were most evident during the spring months of both years and winter months of 2021. Phytoplankton blooms, indicated by high concentrations of chlorophyll *a* (> 5 µg/L), were evident at subsurface depths during spring and summer 2020 and winter through summer 2021 in the PLOO and SBOO regions, including the notably large bloom in spring 2020. Ocean currents varied seasonally and generally trended

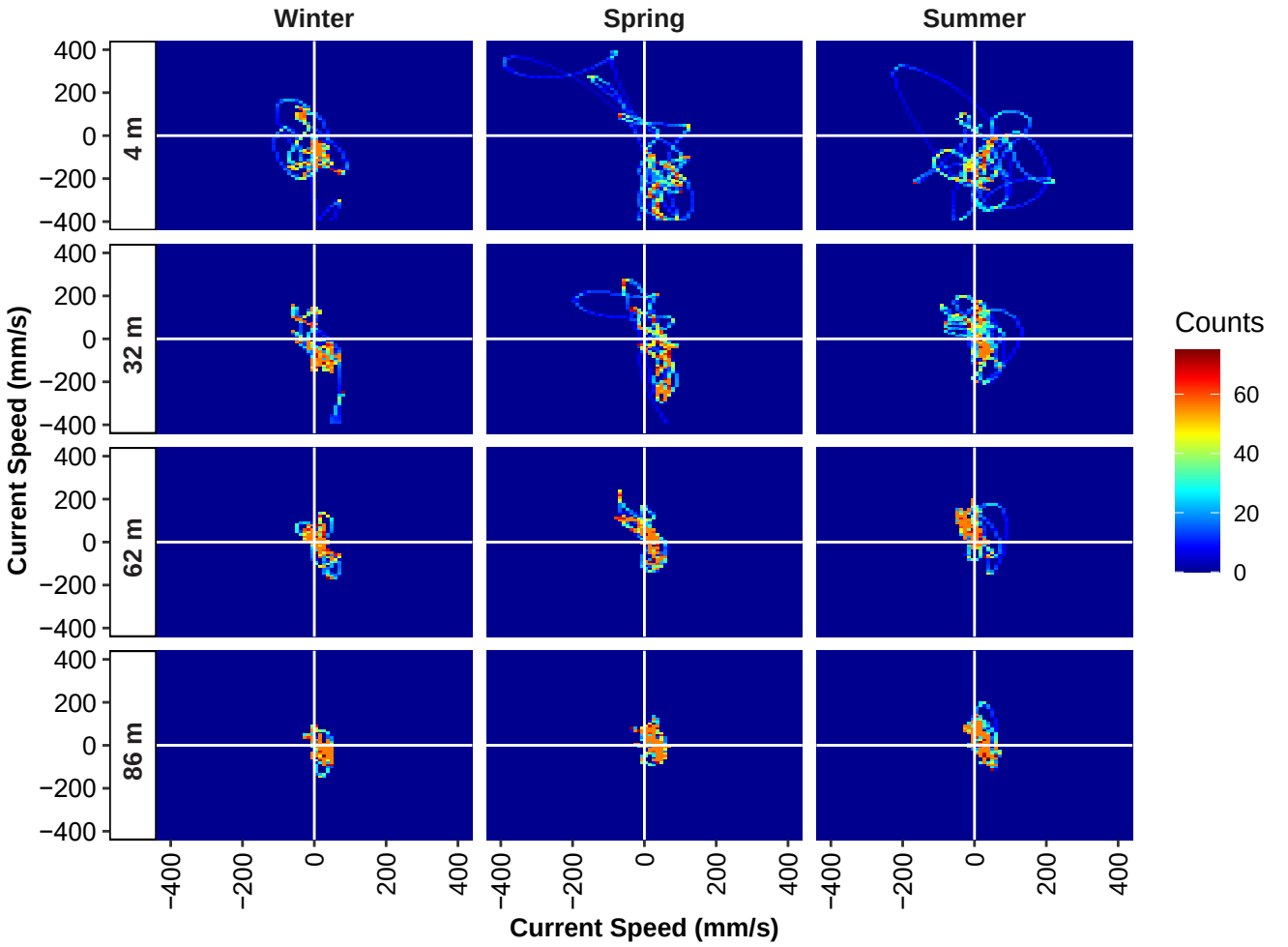

Figure 2.15

Frequency distribution (counts) by season of current speed (mm/s) and direction from 2020 at the PLOO RTOMS ADCP location at representative depth bins. The deployment ended prior to the fall season. On the x-axis, positive values indicate an eastward direction while negative values indicate a westward direction. On the y-axis, positive values indicate a northward direction while negative values indicate a southward direction.

similar to findings reported previously for the San Diego region (City of San Diego 2015a,b, 2016a,b, 2018b, 2020, 2022a,b) and are generally consistent with conditions and long-term trends in the SCB (Peterson et al. 2006, McClatchie et al. 2008, 2009, Bjorkstedt et al. 2010, 2011, 2012, Wells et al. 2013, Leising et al. 2014, 2015, NOAA/NWS 2022), and northern Baja California waters (Peterson et al. 2006). These observations suggest that overall, the temporal and spatial variability observed in oceanographic conditions for coastal San Diego is explained by a combination of local (e.g., coastal upwelling, rain-related runoff) and large-scale oceanographic-climatic processes (e.g., ENSO, PDO, NPGO). As a result, proximity to either outfall is not considered a significant driver of the variations observed in oceanographic parameters discussed in this chapter.

Literature Cited

Alessi, C.A., R. Beardsley, R. Limeburner, and L.K. Rosenfeld. (1984). CODE-2: Moored Array and Large-Scale Data Report. Woods Hole Oceanographic Institution Technical Report. 85–35: 21.

Anderson, C. and M. Hepner-Medina. (2020). SCCOOS Red Tide Bulletin: Spring 2020. Newsletter, published May 8th 2020. https://sccoos.org/california-hab-bulletin/red-tide/.

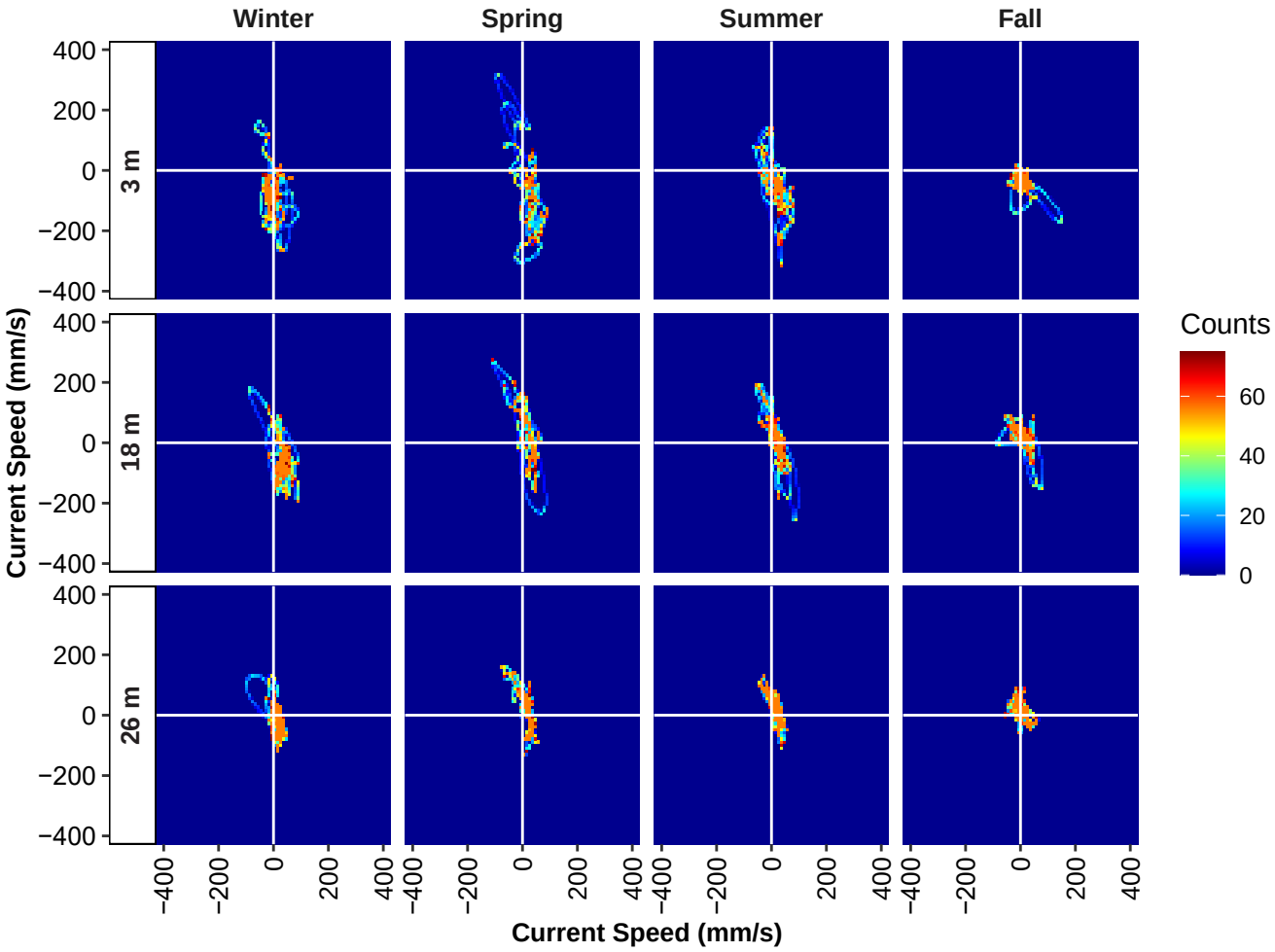

Figure 2.16
Frequency distribution (counts) by season of current speed (mm/s) and direction from 2020 at the SBOO RTOMS ADCP location at representative depth bins. On the x-axis, positive values indicate an eastward direction while negative values indicate a westward direction. On the y-axis, positive values indicate a northward direction while negative values indicate a southward direction.

Bjorkstedt, E.P., R. Goericke, S. McClatchie, E. Weber, W. Watson, N. Lo, B. Peterson, B. Emmett, J. Peterson, R. Durazo, G. Gaxiola-Castro, F. Chavez, J.T. Pennington, C.A. Collins, J. Field, S. Ralston, K. Sakuma, S.J. Bograd, F.B. Schwing, Y. Xue, W.J. Sydeman, S.A. Thompson, J.A. Santora, J. Largier, C. Halle, S. Morgan, S.Y. Kim, K.B.P. Merkins, J.A. Hildebrand, and L.M. Munger. (2010). State of the California Current 2009–2010: Regional variation persists through transition from La Niña to El Niño (and back?). California Cooperative Oceanic Fisheries Investigations (CalCOFI) Reports, 51: 39–69.

Bjorkstedt, E.P., R. Goericke, S. McClatchie, E. Weber, W. Watson, N. Lo, B. Peterson, B. Emmett, R. Brodeur, J. Peterson, M. Litz, J. Gómez-Valdés, G. Gaxiola-Castro, B. Lavaniegos, F. Chavez, C.A. Collins, J. Field, K. Sakuma, S.J. Bograd, F.B. Schwing, P. Warzybok, R. Bradley, J. Jahncke, G.S. Campbell, J.A. Hildebrand, W.J. Sydeman, S.A. Thompson, J.L. Largier, C. Halle, S.Y. Kim, and J. Abell. (2011). State of the California Current 2010–2011: Regionally variable responses to a strong (but fleeting?) La Niña. California Cooperative Oceanic Fisheries Investigations (CalCOFI) Reports, 52: 36–68.

Bjorkstedt, E.P., R. Goericke, S. McClatchie, E. Weber, W. Watson, N. Lo, W.T. Peterson, R.D. Brodeur, T. Auth, J. Fisher, C. Morgan, J. Peterson, J. Largier, S.J. Bograd, R. Durazo, G. Gaxiola-

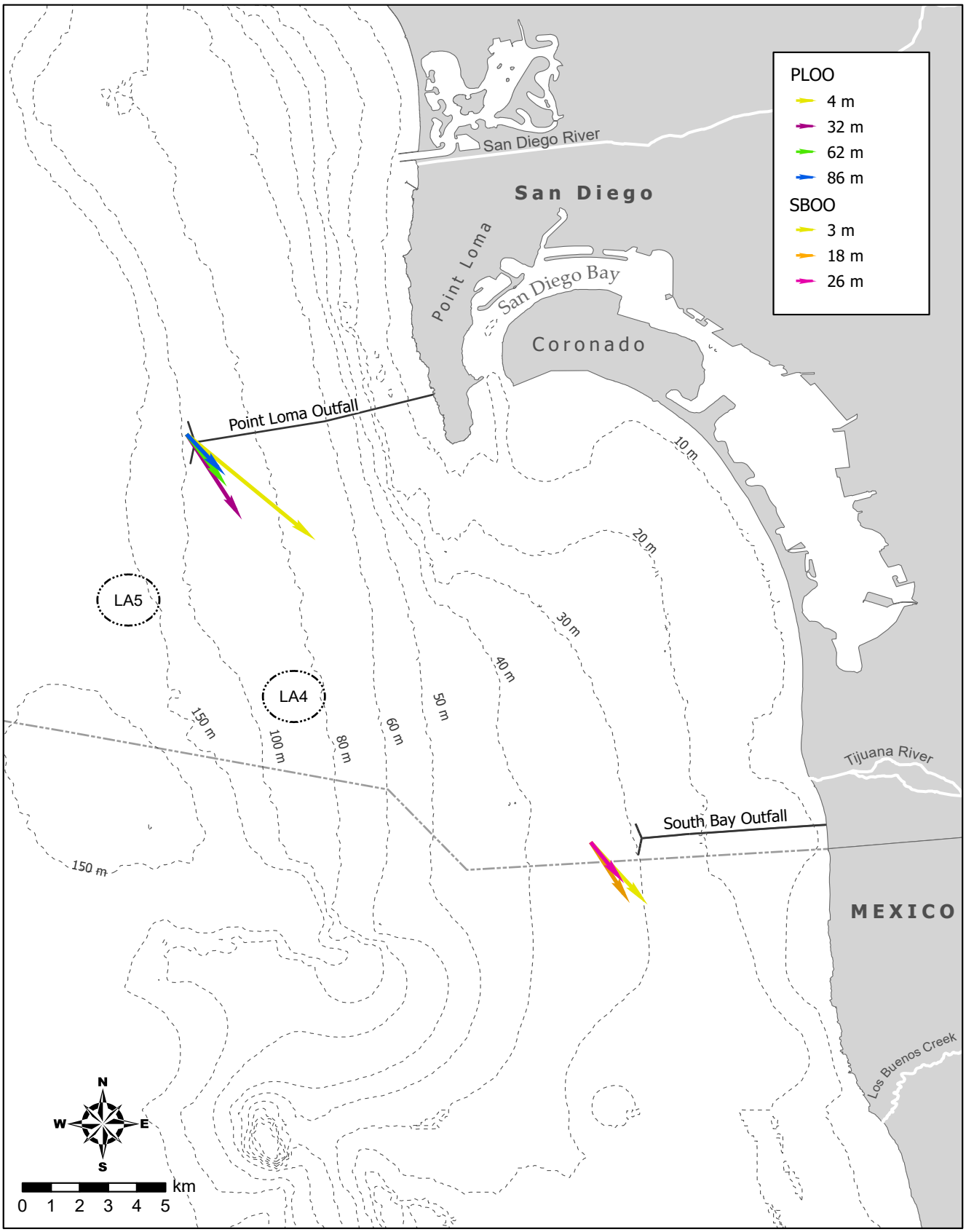

Figure 2.17
Generalized current speed and direction as determined by linear regression of all velocities for select depth bins at PLOO and SBOO RTOMS locations during the 2020 deployment. Length of arrow reflects relative current speed.

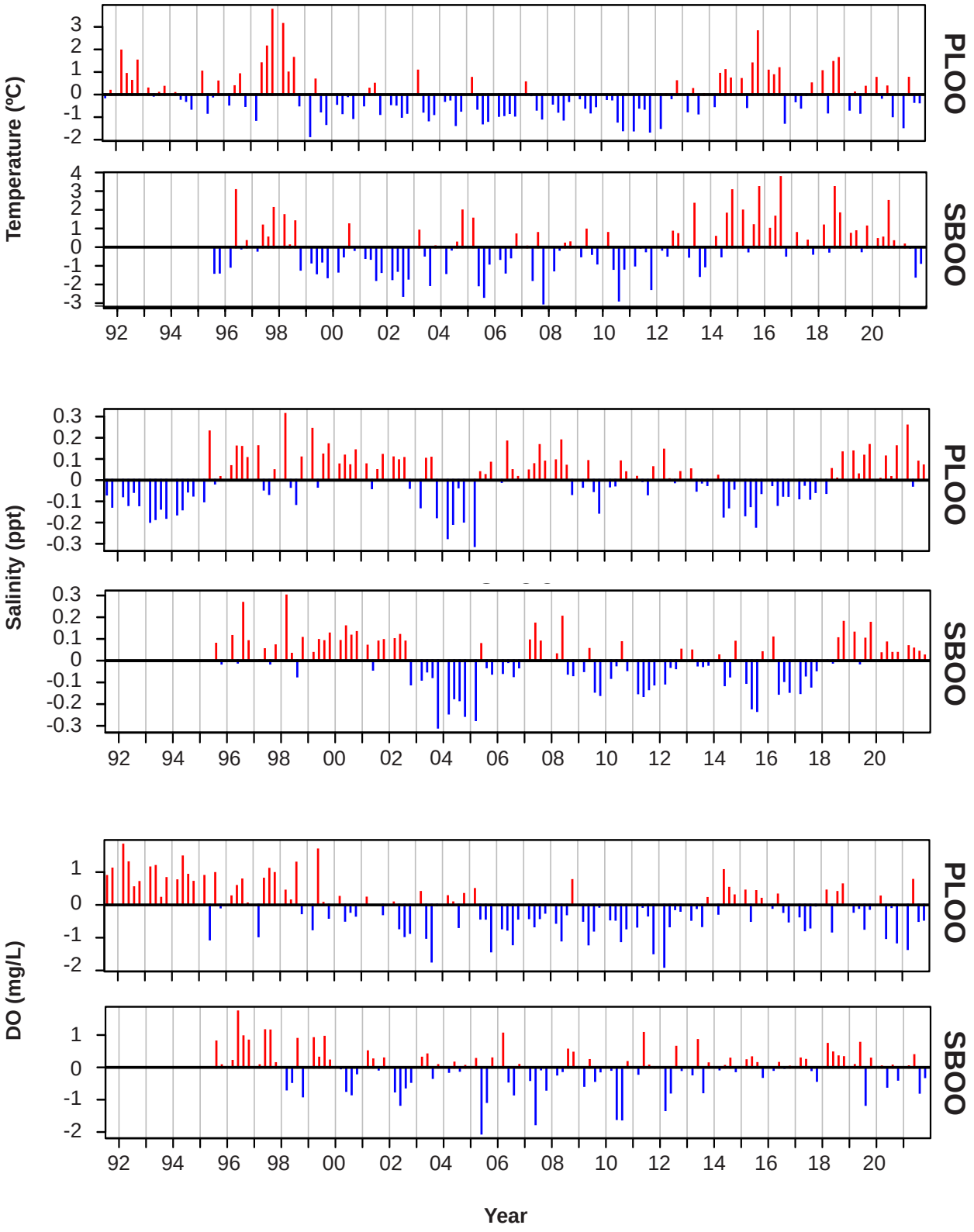

Figure 2.18

Time series of temperature, salinity, and dissolved oxygen (DO) anomalies from 1991 through 2021 at PLOO discharge depth stations (n = 11) and SBOO discharge depth stations (n = 13), all depths combined. Monitoring at the SBOO stations began in 1995.

Table 2.2

Long-term climate-related events in the Southern California Bight. El Niño Southern Oscillation (ENSO); Pacific Decadal Oscillation (PDO); California Current System (CCS); North Pacific Gyre Oscillation (NPGO); Multivariate ENSO Index (MEI)

Approximate Timespan	Large-Scale Climatic Event
1997-1998	Colossal El Niño
1998-2002	Phase change to (-) ENSO and (-) PDO indices to cold conditions
2002-2006	Return to warm ocean conditions in CCS
2002-2004	Intrusion of subarctic waters into CSS with lower than normal salinities
2007	Moderate to strong La Niña, negative PDO cooling event, positive NPGO indicating increased flow of cold, nutrient-rich water from the north
2010	Moderate to strong La Niña
2013-2014	Phase change to (+) PDO , (-) NPGO, and (+) MEI, resulting in region-wide warming
2014-2015	Largest marine heatwave (Blob) in NE Pacific
2015	Colossal El Niño
2016-2018	Weak La Niña to neutral ENSO conditions
2018-2019	Weak El Niño
2019	Marine heatwave in the CCS
2020	Marine heatwave offshore in the CCS (second largest to Blob)
2021	Marine heatwave mostly offshore in the CCS
2020-2021	Phase change to (-) PDO and (-) MEI, with weak La Niña

Castro, B. Lavaniegos, F.P. Chavez, C.A. Collins, B. Hannah, J. Field, K. Sakuma, W. Satterthwaite, M. O'Farrell, S. Hayes, J. Harding, W.J. Sydeman, S.A. Thompson, P. Warzybok, R. Bradley, J. Jahncke, R.T. Golightly, S.R. Schneider, R.M. Suryan, A.J. Gladics, C.A. Horton, S.Y. Kim, S.R. Melin, R.L. DeLong, and J. Abell. (2012). State of the California Current 2011–2012: Ecosystems respond to local forcing as La Niña wavers and wanes. California Cooperative Oceanic Fisheries Investigations (CalCOFI) Reports, 53: 41–76.

Borchers, H.W. (2021). pracma: Practical Numerical Math Functions. R package version 2.3.6. https://CRAN.R-project.org/package=pracma

Bowden, K.F. (1975). Oceanic and Estuarine Mixing Processes. In: J.P. Riley and G. Skirrow (eds.). Chemical Oceanography, 2nd Ed., Vol.1. Academic Press, San Francisco, CA. p 1–41.

[CalCOFI] California Cooperative Oceanic Fisheries Investigations (2022). Archive of nutrient bottle data, January 1969–January 2020. https://calcofi.org/data/oceanographic-data/bottle-database/.

[CDIP] Coastal Data Information Program (2022). Archive of offshore wave buoy data. http://cdip.ucsd.edu.

City of San Diego. (2015a). Point Loma Ocean Outfall Annual Receiving Waters Monitoring and Assessment Report, 2014. City of San Diego Ocean Monitoring Program, Public Utilities Department, Environmental Monitoring and Technical Services Division, San Diego, CA.

City of San Diego. (2015b). South Bay Ocean Outfall Annual Receiving Waters Monitoring and Assessment Report, 2014. City of San Diego Ocean Monitoring Program, Public Utilities Department, Environmental Monitoring and Technical Services Division, San Diego, CA.

City of San Diego. (2016a). Point Loma Ocean Outfall Annual Receiving Waters Monitoring

and Assessment Report, 2015. City of San Diego Ocean Monitoring Program, Public Utilities Department, Environmental Monitoring and Technical Services Division, San Diego, CA.

City of San Diego. (2016b). South Bay Ocean Outfall Annual Receiving Waters Monitoring and Assessment Report, 2015. City of San Diego Ocean Monitoring Program, Public Utilities Department, Environmental Monitoring and Technical Services Division, San Diego, CA.

City of San Diego. (2018a). Plume Tracking Monitoring Plan for the Point Loma and South Bay Ocean Outfall Regions, San Diego, California. Submitted by the City of San Diego Public Utilities Department to the San Diego Water Board and USEPA, Region IX, March 28, 2018 (approved 4/25/2018).

City of San Diego. (2018b). Biennial Receiving Waters Monitoring and Assessment Report for the Point Loma and South Bay Ocean Outfalls, 2016–2017. City of San Diego Ocean Monitoring Program, Public Utilities Department, Environmental Monitoring and Technical Services Division, San Diego, CA.

City of San Diego. (2020–2022a). Monthly Receiving Waters Monitoring Reports for the Point Loma Ocean Outfall (Point Loma Wastewater Treatment Plant), January 2020–December 2021. City of San Diego Ocean Monitoring Program, Public Utilities Department, Environmental Monitoring and Technical Services Division, San Diego, CA.

City of San Diego. (2020–2022b). Monthly Receiving Waters Monitoring Reports for the South Bay Ocean Outfall (South Bay Water Reclamation Plant), January 2020–December 2021. City of San Diego Ocean Monitoring Program, Public Utilities Department, Environmental Monitoring and Technical Services Division, San Diego, CA.

City of San Diego. (2020). Biennial Receiving Waters Monitoring and Assessment Report for the Point Loma and South Bay Ocean Outfalls, 2018–2019. City of San Diego Ocean Monitoring Program, Public Utilities Department, Environmental Monitoring and Technical Services Division, San Diego, CA.

City of San Diego. (2021). Interim Receiving Waters Monitoring Report for the Point Loma and South Bay Ocean Outfalls, 2020. City of San Diego Ocean Monitoring Program, Public Utilities Department, Environmental Monitoring and Technical Services Division, San Diego, CA.

City of San Diego. (2022a). Appendix P. Oceanography. In: Application for Renewal of NPDES CA0107409 and 301(h) Modified Secondary Treatment Requirements, Point Loma Ocean Outfall. Volume X, Appendices O thru U. Public Utilities Department, Environmental Monitoring and Technical Services Division, San Diego, CA.

City of San Diego. (2022b). Plume Tracking Monitoring Plan Progress Report for the Point Loma and South Bay Ocean Outfall Regions, San Diego, California; Report Period: January–December 2021. Submitted by the City of San Diego Public Utilities Department to the San Diego Water Board and USEPA, Region IX, March 3, 2020.

Dowle, M. and A. Srinivasan. (2021). data.table: Extension of `data.frame`. R package version 1.14.2. https://CRAN.R-project.org/package=data.table

Harrell, F.E., Jr. (2021). Hmisc: Harrell Miscellaneous. R package version 4.6-0. http://CRAN.R-project.org/package=Hmisc.

Harvey, C.J., N. Garfield, G.D. Williams, and N. Tolimieri, editors. (2021). Ecosystem Status Report of the California Current for 2020–21: A Summary of Ecosystem Indicators

Compiled by the California Current Integrated Ecosystem Assessment Team (CCIEA). U.S. Department of Commerce, NOAA Technical Memorandum NMFS-NWFSC-170.

Hess, M. (2018). Satellite & Aerial Coastal Water Quality Monitoring in the San Diego/Tijuana Region: Annual Summary Report 1 January 2017–31 December 2018. Littleton, CO.

Hess, M. (2019). Satellite & Aerial Coastal Water Quality Monitoring in the San Diego/Tijuana Region: Annual Summary Report 1 January 2018–31 December 2019. Littleton, CO.

Hess, M. (2020). Satellite & Aerial Coastal Water Quality Monitoring in the San Diego/Tijuana Region: Annual Summary Report 1 January 2019–31 June 2019. Littleton, CO.

Hope, R.M. (2013). Rmisc: Ryan Miscellaneous. R package version 1.5. http://CRAN.R-project.org/package=Rmisc.

Jackson, G.A. (1986). Physical Oceanography of the Southern California Bight. In: R. Eppley (ed.). Plankton Dynamics of the Southern California Bight. Springer Verlag, New York. p 13–52.

Jones, B., M.A. Noble, and T.D. Dickey. (2002). Hydrographic and particle distributions over the Palos Verdes continental shelf: Spatial, seasonal and daily variability. Continental Shelf Research. 22: 945–965.

Kelley, D. and C. Richards. (2022). oce: Analysis of Oceanographic Data. R package version 1.5.0. http://CRAN.R-project.org/package=oce.

Lalli, C.M. and T.R. Parsons. (1993). Biological Oceanography: an introduction. Pergamon, New York.

Largier, J., L. Rasmussen, M. Carter, and C. Scearce. (2004). Consent Decree–Phase One Study Final Report. Evaluation of the South Bay International Wastewater Treatment Plant Receiving Water Quality Monitoring Program to Determine Its Ability to Identify Source(s) of Recorded Bacterial Exceedances. Scripps Institution of Oceanography, University of California, San Diego, CA.

Leising, A.W., I.D. Schroeder, S.J. Bograd, E.P. Bjorkstedt, J. Field, K. Sakuma, J. Abell, R.R. Robertson, J. Tyburczy, W.T. Peterson, R. Brodeur, C. Barcelo, T.D. Auth, E.A. Daly, G.S. Campbell, J.A. Hildebrand, R.M. Suryan, A.J. Gladics, C.A. Horton, M. Kahru, M. Manzano-Sarabia, S. McClatchie, E.D. Weber, W. Watson, J.A. Santora, W.J. Sydeman, S.R. Melin, R.L. DeLong, J. Largier, S.Y. Kim, F.P. Chavez, R.T. Golightly, S.R. Schneider, P. Warzybok, R. Bradley, J. Jahncke, J. Fisher, and J. Peterson. (2014). State of the California Current 2013-2014: El Niño Looming. California Cooperative Oceanic Fisheries Investigations (CalCOFI) Reports, 55: 51–87.

Leising, A.W., I.D. Schroeder, S.J. Bograd, J. Abell, R. Durazo, G. Gaxiola-Castro, E.P. Bjorkstedt, J. Field, K. Sakuma, R.R. Robertson, R. Goericke, W.T. Peterson, R.D. Brodeur, C. Barceló, T.D. Auth, E.A. Daly, R.M. Suryan, A.J. Gladics, J.M. Porquez, S. McClatchie, E.D. Weber, W. Watson, J.A. Santora, W.J. Sydeman, S.R. Melin, F.P. Chavez, R.T. Golightly, S.R. Schneider, J. Fisher, C. Morgan, R. Bradley, and P. Warybok. (2015). State of the California Current 2014-2015: Impacts of the Warm-Water "Blob". California Cooperative Oceanic Fisheries Investigations (CalCOFI) Reports, 56: 31–69.

Lynn, R.J. and J.J. Simpson. (1987). The California Current System: The Seasonal Variability of its Physical Characteristics. Journal of Geophysical Research, 92(C12): 12947–12966.

Mann, K.H. (1982). Ecology of Coastal Waters, A Systems Approach. University of California Press, Berkeley.

Mann. K.H. and J.R.N. Lazier. (1991). Dynamics of Marine Ecosystems, Biological–Physical Interactions in the Oceans. Blackwell Scientific Publications, Boston.

Marion, G.M, F.J. Millero, M.F. Camões, P. Spitzer, R. Feistel, and C.-T.A. Chen. (2011). pH of seawater. Marine Chemistry. 126: 89–96.

MATLAB. (2016). Version R2016a. The MathWorks Inc., Natick, Massachusetts. URL https://www.mathworks.com/products/matlab.html.

McClatchie, S., R. Goericke, J.A. Koslow, F.B. Schwing, S.J. Bograd, R. Charter, W. Watson, N. Lo, K. Hill, J. Gottschalck, M. l'Heureux, Y. Xue, W.T. Peterson, R. Emmett, C. Collins, G. Gaxiola-Castro, R. Durazo, M. Kahru, B.G. Mitchell, K.D. Hyrenbach, W.J. Sydeman, R.W. Bradley, P. Warzybok, and E. Bjorkstedt. (2008). The state of the California Current, 2007–2008: La Niña conditions and their effects on the ecosystem. California Cooperative Oceanic Fisheries Investigations (CalCOFI) Reports, 49: 39–76.

McClatchie, S., R. Goericke, J.A. Koslow, F.B. Schwing, S.J. Bograd, R. Charter, W. Watson, N. Lo, K. Hill, J. Gottschalck, M. l'Heureux, Y. Xue, W.T. Peterson, R. Emmett, C. Collins, J. Gomez-Valdes, B.E. Lavaniegos, G. Gaxiola-Castro, B.G. Mitchell, M. Manzano-Sarabia, E. Bjorkstedt. S. Ralston, J. Field, L. Rogers-Bennet, L. Munger, G. Campbell, K. Merkens, D. Camacho, A. Havron, A. Douglas, and J. Hildebrand. (2009). The state of the California Current, Spring 2008–2009: Cold conditions drive regional differences in coastal production. California Cooperative Oceanic Fisheries Investigations (CalCOFI) Reports, 50: 43–68.

Morgan, P. and L. Pender. (2014). SEAWATER library for calculating EOS-80 properties of seawater in MATLAB. CSIRO Marine Research, version 3.3.1. http://www.cmar.csiro.au/datacentre/ext_docs/seawater.htm.

[NOAA/NWS] National Oceanic and Atmospheric Administration/National Weather Service. (2022). Climate Weather Linkage Website. http://www.cpc.ncep.noaa.gov/products/precip/CWlink/MJO/enso.shtml.

[NOAA/PMEL] National Oceanic and Atmospheric Administration/Pacific Marine Environmental Laboratory (2022). Carbon group data from California Current Ecosystem Mooring 2 (CCE2). https://www.ncei.noaa.gov/access/ocean-carbon-acidification-data-system/oceans/Moorings/CCE2.html

Ocean Imaging. (2021). Ocean Imaging Corporation archive of aerial and satellite-derived images. http://www.oceani.com/SanDiegoWater/index.html.

Peterson, B., R. Emmett, R. Goericke, E. Venrick, A. Mantyla, S.J. Bograd, F.B. Schwing, R. Hewitt, N. Lo, W. Watson, J. Barlow, M. Lowry, S. Ralston, K.A. Forney, B.E. Lavaniegos, W.J. Sydeman, D. Hyrenbach, R.W. Bradley, P. Warzybok, F. Chavez, K. Hunter, S. Benson, M. Weise, J. Harvey, G. Gaxiola-Castro, and R. Durazo. (2006). The state of the California Current, 2005–2006: Warm in the north, cool in the south. California Cooperative Oceanic Fisheries Investigations (CalCOFI) Reports, 47: 30–74.

Pickard, D.L. and W.J. Emery. (1990). Descriptive Physical Oceanography. 5th Ed. Pergamon Press, Oxford.

R Core Team. (2021). R: A language and environment for statistical computing. R Foundation for Statistical Computing, Vienna, Austria. URL https://www.R-project.org/.

Ripley, B. and M. Lapsley. (2021). RODBC: ODBC Database Access. R package version 1.3-19. http://CRAN.R-project.org/package=RODBC.

Rogowski, P., E. Terrill, M. Otero, L. Hazard, S.Y. Kim, P.E. Parnell, and P. Dayton. (2012a). Final Report: Point Loma Ocean Outfall Plume Behavior Study. Prepared for City of San Diego Public Utilities Department by Scripps Institution of Oceanography, University of California, San Diego, CA.

Rogowski, P., E. Terrill, M. Otero, L. Hazard, and W. Middleton. (2012b). Mapping ocean outfall plumes and their mixing using Autonomous Underwater Vehicles. Journal of Geophysical Research, 117: C07016.

Rogowski, P., E. Terrill, M. Otero, L. Hazard, and W. Middleton. (2013). Ocean outfall plume characterization using an Autonomous Underwater Vehicle. Water Science & Technology, 67(4): 925–933.

Rohart F., B. Gautier, A. Singh, and K-A Le Cao. (2017) mixOmics: An R package for 'omics feature selection and multiple data integration. PLoS computational biology, 13(11):e1005752.

Schmidtko, S., L. Stramma, M. Visbeck. (2017). Decline in global oceanic oxygen content during the past five decades. Nature, 542(7641): 335-339.

Skirrow, G. (1975). Chapter 9. The Dissolved Gases–Carbon Dioxide. In: Chemical Oceanography. J.P. Riley and G. Skirrow, eds. Academic Press, London. Vol. 2. p 1–181.

Storms, W.E., T.D Stebbins, and P.E. Parnell. (2006). San Diego Moored Observation System Pilot Study Workplan for Pilot Study of Thermocline and Current Structure off Point Loma, San Diego, California. City of San Diego, Metropolitan Wastewater Department, Environmental Monitoring and Technical Services Division, and Scripps Institution of Oceanography, La Jolla, CA.

Sutton, A. J., R. A. Feely, S. Maenner-Jones, S. Musielwicz, J. Osborne, C. Dietrich, N. Monacci, J. Cross, R. Bott, A. Kozyr, A. J. Andersson, N. R. Bates, W. Cai, M. F. Cronin, E. H. De Carlo, B. Hales, S. D. Howden, C. M. Lee, D. P. Manzello, M. J. McPhaden, M. Meléndez, J. B. Mickett, J. A. Newton, S. E. Noakes, J. H. Noh, S. R. Olafsdottir, J. E. Salisbury, U. Send, T. W. Trull, D. C. Vandemark, R. A. Weller. (2019). Autonomous seawater pCO2 and pH time series from 40 surface buoys and the emergence of anthropogenic trends. Earth System Science Data, 11(1): 421–439.

Svejkovsky, J. (2010). Satellite and Aerial Coastal Water Quality Monitoring in the San Diego/Tijuana Region: Annual Summary Report for: 1 January 2009–31 December 2009. Solana Beach, CA.

Svejkovsky J. (2017). Satellite and Aerial Coastal Water Quality Monitoring in the San Diego/Tijuana Region: Annual Summary Report for: 1 January 2016–31 December 2016. Solana Beach, CA.

Terrill, E., K. Sung Yong, L. Hazard, and M. Otero. (2009). IBWC/Surfrider–Consent Decree Final Report. Coastal Observations and Monitoring in South Bay San Diego. Scripps Institution of Oceanography, University of California, San Diego, CA.

Thompson, A.R., I.D. Schroeder, S.J. Bograd, E.L. Hazen, M.G. Jacox, A. Leising, B.K. Wells, J. Largier, J. Fisher, E. Bjorkstedt, R.R. Robertson, F.P. Chavez, M. Kahru, R. Goericke, S. McClatchie, C.E. Peabody, T. Baumgartner, B.E. Lavaniegos, J. Gomez-Valdes, R.D. Brodeur, E.A. Daly, C.A. Morgan, T.D. Auth, B.J. Burke, J. Field, K. Sakuma, E.D. Weber, W. Watson, J. Coates,

R. Schoenbaum, L. Rogers-Bennett, R.M. Suryan, J. Dolliver, S. Loredo, J. Zamon, S.R. Schneider, R.T. Golightly, P. Warzybok, J. Jahncke, J.A. Santora, S. A. Thompson, W. Sydeman, and S.R. Melin. (2018). State of the California Current 2017-2018: Still Not Quite Normal in the North and Getting Interesting in the South. California Cooperative Oceanic Fisheries Investigations (CalCOFI) Reports, 59: 1-66.

Thompson, A.R., I.D. Schroeder, S.J. Bograd, E.L. Hazen, M.G. Jacox, A. Leising, B.K. Wells, J. Fisher, K. Jacobson, S. Zemen, E. Bjorkstedt, R.R. Robertson, M. Kahru, R. Goericke, C.E. Peabody, T. Baumgartner, B.E. Lavaniegos, L.E. Miranda, E. Gomez-Ocampo, J. Gomez-Valdez, T. Auth, E.A. Daly, C.A. Morgan, B.J. Burke, J.C. Field, K.M. Sakuma, E.D. Weber, W. Watson, J.M. Porquez, J. Dolliver, D. Lyons, R.A. Orben, J. Zamon, P. Warzybok, J. Jahncke, J.A. Santora, S. A. Thompson, B. Hoover, W. Sydeman, and S.R. Melin. (2019). State of the California Current 2018-2019: a Novel Anchovy Regime and a New Marine Heat Wave? California Cooperative Oceanic Fisheries Investigations (CalCOFI) Reports, 60: 1-65.

[US IOOS] U.S. Integrated Ocean Observing System. (2017). Manual for the Use of Real-Time Oceanographic Data Quality Control Flags, Version 1.1. Silver Spring, MD, U.S. Department of Commerce, National Oceanic and Atmospheric Administration, National Ocean Service, Integrated Ocean Observing System, 43 pp.

[US IOOS] U.S. Integrated Ocean Observing System (2020). Quality Assurance/Quality Control of Real Time Oceanographic Data. https://ioos.noaa.gov/project/qartod/.

Warnes, G.R., B. Bolker, T. Lumley. (2021). gtools: Various R Programming Tools. R package version 3.9.2. https://CRAN.R-project.org/package=gtools

Weber, E.D., T.D. Auth, S. Baumann-Pickering, T.R. Baumgartner, E.P. Bjorkstedt, S.J. Bograd, B.J. Burke, J.L. Cadena-Ramirez, E.A. Daly, M. de la Cruz, H. Dewar, J.C. Field, J.L. Fisher, A. Giddings, R. Goericke, E. Gomez-Ocampo, J. Gomez-Valdes, E.L. Hazen, J. Hildebrand, C.A. Horton, K.C. Jacobson, M.G. Jacox, J. Jahncke, M. Kahru, R.M. Kudela, B.E. Lavaniegos, A. Leising, S.R. Melin, L.E. Miranda-Bojorquez, C.A. Morgan, C.F. Nickels, R.A. Orben, J.M. Porquez, E.J. Portner, R.R. Robertson, D.L. Rudnick, K.M. Sakuma, J.A. Santora, I.D. Schroeder, O.E. Snodgrass, W.J. Sydeman, A.R. Thompson, S.A. Thompson, J.S. Trickey, J. Villegas-Mendoza, P. Warzybok, W. Watson, and S.M. Zeman. (2021). State of the California Current 2019-2020: Back to the Future with Marine Heatwaves? Frontiers in Marine Science, 8: 1-23.

Wells, B.K., I.D. Schroeder, J.A. Santora, E.L. Hazen, S.J. Bograd, E.P. Bjorkstedt, V.J. Loeb, S. McClatchie, E.D. Weber, W. Watson, A.R. Thompson, W.T. Peterson, R.D. Brodeur, J. Harding, J. Field, K. Sakuma, S. Hayes, N. Mantua, W.J. Sydeman, M. Losekoot, S.A. Thompson, J. Largier, S.Y. Kim, F.P. Chavez, C. Barcelo, P. Warzybok, R. Bradley, J. Jahncke, R. Goericke, G.S. Campbell, J.A. Hildebrand, S.R. Melin, R.L. DeLong, J. Gomez-Valdes, B. Lavaniegos, G. Gaxiola-Castro, R.T. Golightly, S.R. Schneider, N. Lo, R.M. Suryan, A.J. Gladics, C.A. Horton, J. Fisher, C. Morgan, J. Peterson, E.A. Daly, T.D. Auth, and J. Abell. (2013). State of the California Current 2012-2013: no such thing as an “average” year. California Cooperative Oceanic Fisheries Investigations (CalCOFI) Reports, 54: 37–71.

Wickham, H. (2007). Reshaping Data with the reshape Package. Journal of Statistical Software, 21(12): 1–20. URL http://www.jstatsoft.org/v21/i12/.

Wickham, H., M. Averick, J. Bryan, W. Chang, L. D'Agostino McGowan, R. François, G.Grolemund, A. Hayes, L. Henry, J. Hester, M. Kuhn, T. Lin Pedersen, E. Miller, S. Milton Bache, K. Müller, J. Ooms, D. Robinson, D. P. Seidel, V. Spinu, K. Takahashi, D. Vaughan, C. Wilke, K. Woo, H. Yutani. (2019). Welcome to the tidyverse. Journal of Open Source Software, 4(43), 1686, https://doi.org/10.21105/joss.01686.

Wickham, H. and D. Seidel. (2020). scales: Scale Functions for Visualization. R package version 1.1.1. https://CRAN.R-project.org/package=scales

Winant, C. and A. Bratkovich. (1981). Temperature and currents on the southern California shelf: A description of the variability. Journal of Physical Oceanography, 11: 71–86.

Zeileis, A. and G Grothendieck. (2005). zoo: S3 Infrastructure for Regular and Irregular Time Series. Journal of Statistical Software,14(6), 1-27. https://doi.org/10.18637/jss.v014.i06

Chapter 3
Water Quality Compliance

Chapter 3. Water Quality Compliance

Introduction

The City of San Diego (City) conducts extensive monitoring along the shoreline (beaches), nearshore (e.g., kelp forests), and other offshore coastal waters surrounding the Point Loma and South Bay Ocean Outfalls (PLOO and SBOO, respectively) to characterize regional water quality conditions and to identify possible impacts of wastewater discharge, or other contaminant sources, on the marine environment. Densities of fecal indicator bacteria (FIB), including total coliforms, fecal coliforms, and *Enterococcus*, are measured and evaluated to provide information about the dispersion of potentially contaminated water throughout the regions surrounding the two outfalls. Evaluation of these data may also help to identify the source of bacterial contamination throughout the region. In addition, the City's water quality monitoring efforts are designed to assess compliance with the bacterial water contact standards and other physical and chemical water quality objectives specified in the California Ocean Plan (Ocean Plan) that are intended to help protect the beneficial uses of State ocean waters (SWRCB, 2019).

Multiple sources of bacterial contamination exist in the Point Loma and South Bay monitoring regions and being able to separate any impact that may be associated with wastewater discharge from other point, or non-point, sources of contamination is often challenging. Examples include outflows from the San Diego River, San Diego Bay, the Tijuana River, and the San Antonio de Los Buenos Creek in northern Baja California (Largier et al., 2004, Nezlin et al., 2007, Gersberg et al., 2008, Terrill et al., 2009). Likewise, storm water discharges and terrestrial runoff from local watersheds during storms, or other wet weather events, can also flush sediments and contaminants into nearshore coastal waters (Noble et al., 2003, Reeves et al., 2004, Sercu et al., 2009, Griffith et al., 2010). Moreover, decaying kelp and seagrass (beach wrack), sediments and sludge accumulating in storm drains, and sandy beach sediments themselves can serve as reservoirs for bacteria until release into coastal waters by returning tides, rain events, or other disturbances (Gruber et al., 2005, Martin and Gruber, 2005, Noble et al., 2006, Yamahara et al. 2007, Phillips et al. 2011). Further, the presence of shore birds and their droppings has been associated with high bacterial counts that may impact nearshore water quality (Grant et al. 2001, Griffith et al. 2010).

This chapter presents an analysis and assessment of bacterial distribution patterns collected during 2020 and 2021, at more than 100 permanent water quality monitoring stations surrounding the PLOO and SBOO. The primary goals are to: (1) document bacteriological conditions off San Diego; (2) distinguish elevated bacteriological signals that may result from the PLOO and SBOO wastewater plumes versus other possible sources of contamination; (3) assess compliance with Ocean Plan water contact standards; (4) dentify any unknown sources of fecal bacteria contamination and determine if human fecal waste is the cause. Results of remote sensing observations (i.e., satellite imagery) for the San Diego and Tijuana regions are also evaluated to provide insight into the transport and dispersal of wastewater and other types of surface water plumes during the study period. To better understand potential impacts of a wastewater plume on ocean conditions, Chapter 4 discusses natural chemical tracers that can be leveraged to detect and distinguish an outfall's effluent signal from other non-point sources.

Materials and Methods

Field Sampling

Shore stations

Seawater samples were collected weekly at 19 shoreline stations to monitor concentrations of FIB in waters adjacent to public beaches

(Figure 3.1). Sixteen of these stations are in California State waters and are therefore subject to Ocean Plan water contact standards (SWRCB 2019) (Box 3.1). Eight PLOO stations (D4, D5, D7, D8-A/D8-B, D9, D10, D11, D12) are located from Mission Beach southward to the tip of Point Loma. Due to access issues, station D8-A replaced D8 in July 2016 and station D8-B replaced D8-A in March 2018. Sampling at station D8-A resumed in December 2020. Due to recent access issues at D8-A, sampling resumed at D8-B during February 2021. Eight SBOO stations (S4, S5, S6, S8, S9, S10, S11, S12) are located between the USA/Mexico border and Coronado, while the other three SBOO shoreline stations (S0, S2, S3) are located south of the border and are not subject to Ocean Plan standards. Following an internal investigation of suspicious data, conducted by the City, a report was provided to the San Diego Regional Water Quality Control Board (SDRWQCB) on October 22, 2020, which detailed the removal of suspicious data collected between 2019 and 2020. As a result, a total of 35 samples[1] (including resamples) from 2020 were removed from further analysis and, thus, not included in this report.

Seawater samples were collected from the surf zone at each of the above stations in sterile 250 mL bottles, after which they were transported on blue ice to the City's Marine Microbiology Laboratory and analyzed to determine concentrations of three types of FIB (i.e., total coliform, fecal coliform, *Enterococcus* bacteria). In addition, weather conditions and visual observations of water color and clarity, surf height, and human or animal activity were recorded at the time of sample collection. Wind speed and direction were measured using a hand-held anemometer with a compass. These observations were previously reported in monthly receiving waters monitoring reports submitted to the SDRWQCB (see City of San Diego 2020–2022). These reports are available online (City of San Diego 2022a).

1 The Oct 22, 2020 report to SDRWQCB detailed the removal of 27 samples. Upon further investigation, 8 additional samples were removed.

Kelp and offshore stations

Fifteen stations located in relatively shallow waters within or near the Point Loma or Imperial Beach kelp beds (i.e., referred to as "kelp" stations herein) were monitored weekly to assess water quality conditions and Ocean Plan compliance in nearshore areas used for recreational activities such as SCUBA diving, surfing, fishing, and kayaking (Figure 3.1). These included PLOO stations C4, C5 and C6 located along the 9-m depth contour near the inner edge of the Point Loma kelp forest, PLOO stations A1, A6, A7, C7, and C8 located along the 18-m depth contour near the outer edge of the Point Loma kelp forest, SBOO stations I25, I26, and I39 located at depths of 9–18 m contiguous to the Imperial Beach kelp bed, and SBOO stations I19, I24, I32, and I40 located in other nearshore waters along the 9-m depth contour.

An additional 69 offshore stations were sampled quarterly over consecutive days in winter (February or March), spring (May), summer (August), and fall (November) to monitor water quality conditions and to estimate dispersion of the PLOO and SBOO wastewater plumes (Figure 3.1). These included 36 stations surrounding the PLOO, and 33 stations surrounding the SBOO. The PLOO stations are designated F1–F36 and are located along or adjacent to the 18, 60, 80, and 98-m depth contours. Seawater samples for FIB were collected at all of these stations. The SBOO stations are designated I1–I18, I20–I23, I27–I31, and I33–I38 and are located along the 9, 19, 28, 38 and 55-m depth contours, respectively. Only a subset of SBOO sites (n = 21; I3, I5, I7, I8, I9, I10–I14, I16, I18, I20–I23, I30, I33, I36–I38), are sampled for FIB. Additionally, 15 of the PLOO stations (F01–F03, F06–F14, F18–F20) and 15 of the SBOO stations (I12, I14, I16–I18, I22–I23, I27, I31, I33–I38) are located within State jurisdictional waters (i.e., within 3 nautical miles of shore) and therefore subject to the Ocean Plan compliance standards.

Seawater samples for FIB analyses were collected from three to five discrete depths at the kelp and offshore stations as indicated in Table 3.1. These samples were typically collected using a rosette sampler fitted with Niskin bottles surrounding a

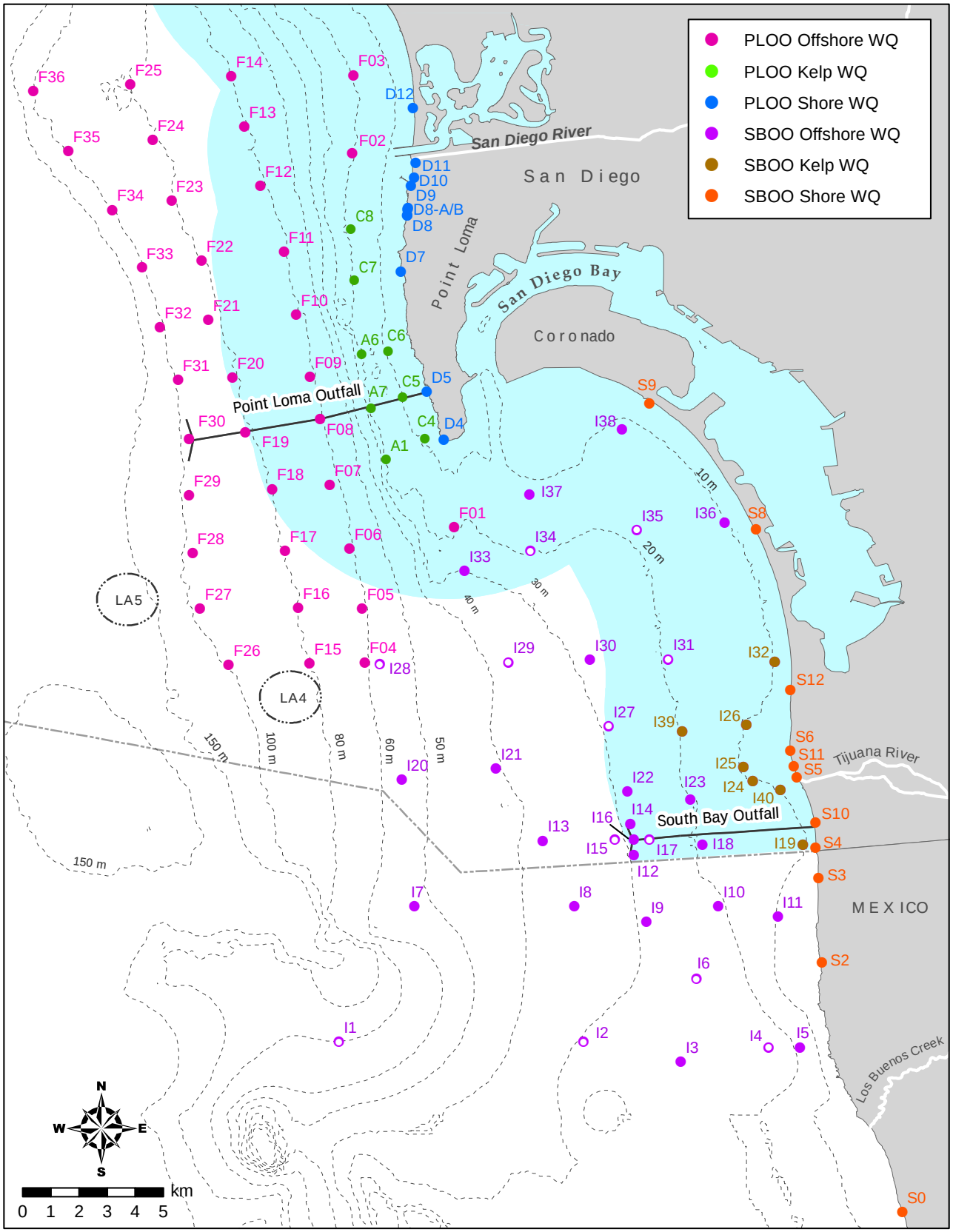

Figure 3.1
Water quality (WQ) monitoring station locations sampled around the PLOO and SBOO as part of the City of San Diego's Ocean Monitoring Program. Open circles are sampled by CTD only. Light blue shading represents State jurisdictional waters.

Box 3.1

Water quality objectives for water contact areas, California Ocean Plan (SWRCB 2019).

A. Bacterial Characteristics – Water Contact Standards; CFU = colony forming units.

(a) *Fecal Coliforms:*
   1) A 30-day geometric mean of fecal coliform density shall not exceed 200 CFU/100 mL, calculated based on the five most recent samples from each site
   2) A single sample maximum of fecal coliform density shall not exceed 400 CFU/100 mL.

(b) *Enterococcus*:
   1) A 42-day geometric mean of *Enterococcus* density shall not exceed 30 CFU/100 mL, calculated weekly
   2) A statistical threshold value of *Enterococcus* density shall not exceed 110 CFU/100 mL in more than 10% of samples per calendar month.

(c) *Total Coliforms:*
   1) The median of total coliform density shall not exceed 70 CFU/100 mL*.
   2) A statistical threshold value of total coliform density shall not exceed 230 CFU/100 mL in more than 10% of samples.

B. Physical Characteristics

(a) Floating particulates and oil and grease shall not be visible.
(b) The discharge of waste shall not cause aesthetically undesirable discoloration of the ocean surface.
(c) Natural light shall not be significantly reduced at any point outside of the initial dilution zone as the result of the discharge of waste.

C. Chemical Characteristics

(a) The dissolved oxygen concentration shall not at any time be depressed more than 10% from what occurs naturally, as a result of the discharge of oxygen demanding waste materials.
(b) The pH shall not be changed at any time more than 0.2 units from that which occurs naturally.

D. A time period is not specified for the total coliforms running median calculation. For the purposes of this report, the median was calculated over a 30-day running window,

central Conductivity, Temperature, and Depth (CTD) instrument, although replacement samples due to misfires or other causes may have been collected from a separate follow-up cast using stand-alone Van Dorn bottles if necessary. All weekly kelp/nearshore samples and quarterly offshore SBOO samples were analyzed for all three types of FIB, while the quarterly offshore PLOO samples were only analyzed for *Enterococcus* per permit requirements. All samples were refrigerated at sea and then transported on blue ice to the City's Marine Microbiology Laboratory for processing and analysis. Oceanographic data were collected simultaneously with the water samples at each station (see Chapter 2). Visual observations of weather, sea conditions, and human or animal activity were also recorded at the time of sampling. These latter observations were reported previously in monthly receiving waters monitoring reports submitted to the SDRWQCB (see City of San Diego 2020–2022).

Laboratory Analyses

The City Marine Microbiology Laboratory follows guidelines issued by the U.S. Environmental Protection Agency (USEPA) Water Quality Office, State Water Resources Control Board (SWRCB) including the 2019 Ocean Plan and Environmental Laboratory Accreditation Program (ELAP) with respect to sampling and analytical procedures (Bordner et al. 1978, APHA 2012, USEPA 2014). All bacterial analyses were initiated within eight hours of sample collection and conformed to standard membrane filtration techniques, for which the laboratory is certified (ELAP Field of Testing 126).

Table 3.1

Depths from which seawater samples are collected for bacteriological analysis from kelp and offshore stations.

Station Contour	PLOO Sample Depth (m)								
	1	3	9	12	18	25	60	80	98
Kelp Bed									
9-m	x	x	x						
18-m	x			x	x				
Offshore									
18-m	x			x	x				
60-m	x					x	x		
80-m	x					x	x	x	
98-m	x					x	x	x	x

Station Contour	SBOO Sample Depth (m)							
	2	6	9/11	12	18	27	37	55
Kelp Bed								
9-m	x	x	x[a]					
18-m	x			x	x			
Offshore								
9-m	x	x	x[a]					
18-m	x			x	x			
28-m	x				x	x		
38-m	x				x		x	
55-m	x				x			x

[a] Stations I25, I26, I32, and I40 sampled at 9 m; stations I11, I19, I24, I36, I37, and I38 sampled at 11 m

FIB densities were determined and validated in accordance with USEPA and APHA guidelines (Bordner et al. 1978, APHA 2012, USEPA 2014). Plates with FIB densities above or below the ideal counting range were given greater than (>), greater than or equal to (≥), less than (<), or estimated (e) qualifiers. However, all qualifiers were dropped, and densities were treated as discrete values, when determining compliance with Ocean Plan standards.

Quality assurance tests were performed routinely on bacterial samples to ensure that analyses and sampling variability did not exceed acceptable limits. Laboratory and field duplicate bacteriological samples were processed according to method requirements to measure analyst precision and variability between samples, respectively. Results of these procedures were reported under separate cover (City of San Diego 2021a, 2022b).

Data Analyses

Bacteriology

Compliance with the running geometric mean standards for fecal coliforms and *Enterococcus* was assessed using running 30-day and 42-day windows, respectively. Compliance with the median standard for total coliforms was assessed over a running 30-day window[2]. Compliance with the statistical threshold value (STV) metric for total coliforms and *Enterococcus* was calculated at monthly intervals. Compliance calculations were limited to shore, kelp and offshore stations located within State waters, excluding resamples. In all instances, compliance was rounded to the nearest whole number (e.g., 99.5% equates to 100%). For the purpose of visualization, to assess temporal and spatial trends, and to assess compliance with the HF183 sampling standards (Box 3.2), elevated FIB was determined by the number of analyses in which FIB concentrations exceeded the threshold established by the 2019 Ocean Plan's water quality bacterial objectives for single sample maximum (SSM) or STV benchmark levels (SWRCB 2019)[3] (Box 3.1). Due to the nature of the STV metric, elevated FIB does not necessarily indicate out-of-compliance for individual analyses of *Enterococcus* and total

2 The 2019 Ocean Plan does not specify a time frame for the analysis of the total coliform median calculation. For the purpose of the analyses discussed herein, a 30-day running median was calculated.

3 In previous years, analyses were conducted per sample, but due to changes in the Ocean Plan water quality standards this was no longer deemed appropriate.

Box 3.2

Receiving Water Bacterial Compliance (NPDES Permit No. CA0109045, Order No. R9-2021-0011; NPDES Permit No. CA0108928, Order No. R9-2021-0001).

Receiving water monitoring for human marker HF183 and effluent monitoring for fecal indicator bacteria may be required if any of the following conditions are true, and if the source of contamination is unknown.

A. The overall compliance rate with the receiving water limitations for bacterial characteristics is below 90% within a rolling one-year period.
B. A single monitoring location exceeds the bacteria receiving water limitations more than 50% of the time within a rolling one-year period for offshore monitoring locations.
C. A single monitoring location exceeds the bacteria receiving water limitations more than 50% of the time within a rolling quarterly period for kelp/nearshore monitoring locations.

coliform densities. Compliance with the HF183 sampling metrics was calculated as the proportion of analyses showing elevated FIB within the rolling window specified in Box 3.2, assessed daily over the report period. To also comply with the 2015 Ocean Plan water quality bacterial objectives required by the National Pollutant Discharge Elimination System (NPDES) permit for the Point Loma Wastewater Treatment Plant (NPDES No. CA0107409; Order No. R9-2017-0007), additional analyses, and their associated methods, are presented in Appendix D.

Bacterial densities were compared to rainfall data from Lindbergh Field, San Diego, CA (NOAA 2022). Satellite images of the San Diego coastal region were provided by Ocean Imaging of Solana Beach, California and were used to aid in the analysis and interpretation of water quality data (see Appendix C). All analyses were performed using R (R Core Team 2019) and various functions within the gtools, Hmisc, psych, reshape2, RODBC, tidyverse, ggpubr, quantreg, and openxlsx packages (Wickham 2007, 2017, Harrell et al. 2015, Warnes et al. 2015, Revelle 2015, Ripley and Lapsley 2017, Kassambara 2019, Koenker 2019, Schauberger and Walker 2019). Data collected during 2020 were reported previously (City of San Diego 2021b), and all raw data for the 2020–2021 sampling period have been submitted to either the Regional Water Quality Control Board or the California Environmental Data Exchange Network (CEDEN), and may be accessed upon request.

Results and Discussion

Bacteriological Compliance and Distribution

Shore stations

Seawater samples collected from the eight PLOO shore stations were 100% compliant with the 42-day *Enterococcus* geometric mean standard and the 30-day fecal coliform geometric mean standard, while the total coliform median standard was in compliance 90% of the time over the report period (Figure 3.2A). Compliance with the fecal coliform SSM standard at these sites was 100% (Figure 3.2B). The STV for *Enterococcus* was in compliance in 62–100% of stations each month, while the STV for total coliforms compliance rate was 50–100% (Figure 3.2B, Table 3.2). In contrast, compliance rates were more variable during these two years at the eight SBOO shore stations located in State waters. For example, compliance with the total coliform median standard was 49%, compliance for the 30-day geometric mean of fecal coliforms was 78%, and compliance for the six-week geometric mean standard for *Enterococcus* was 63% (Figure 3.3A). Furthermore, compliance with the SSM for fecal coliforms was 67% (Figure 3.3B), and STV compliance for both total coliforms and *Enterococcus* ranged from 0–100% of stations in compliance each month (Figure 3.3B, Table 3.2). However, it is important to note that six of these eight stations (S4, S5, S6, S10, S11, S12) are located near or within areas listed as 'impaired waters', and are not expected to comply with State water contact standards (State of California 2010).

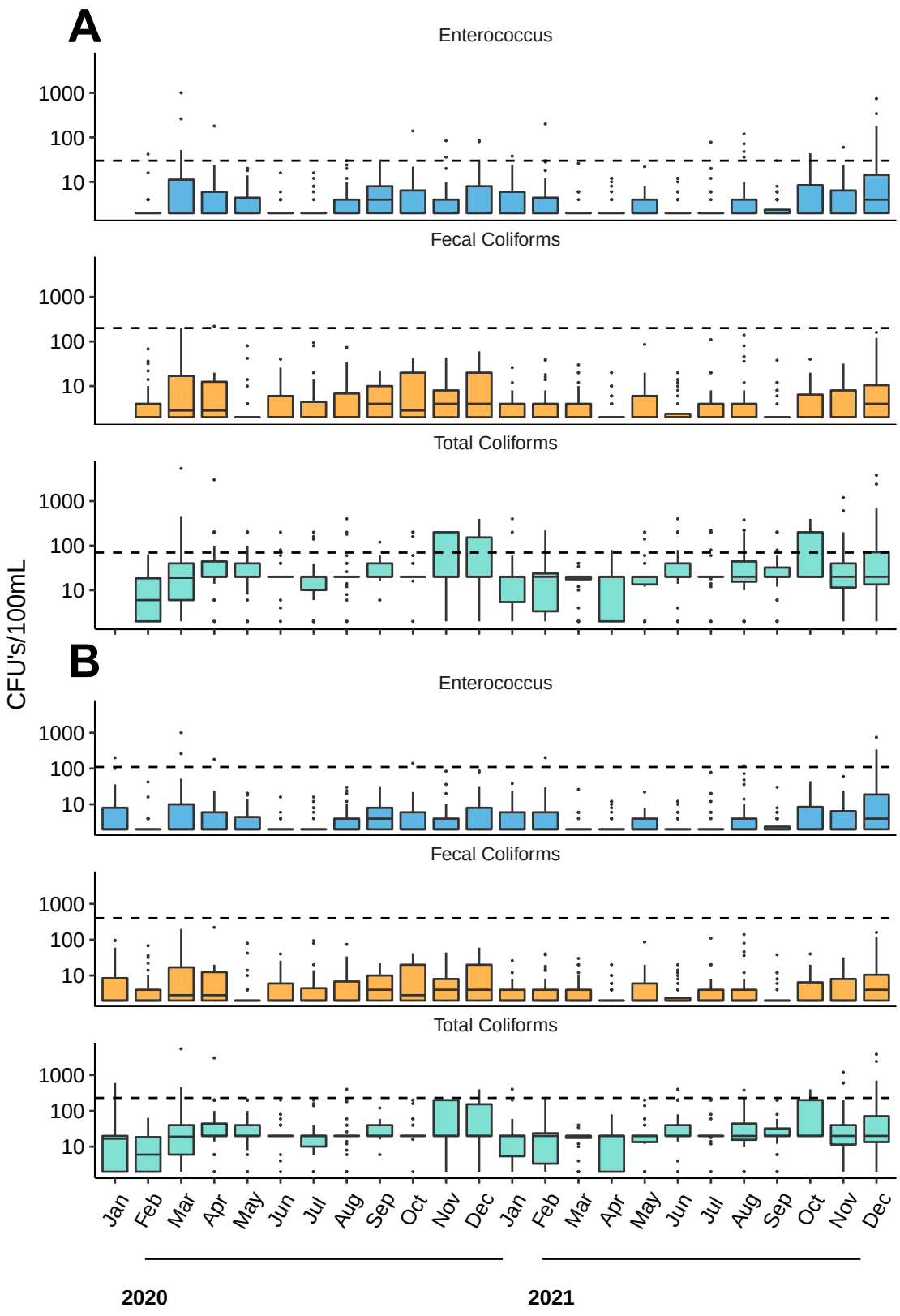

Figure 3.2

Distribution of values at PLOO shore stations during 2020 and 2021, binned monthly, for (A) running mean and median calculations and (B) single sample values. Dashed line represents the water contact standard compliance threshold*. Boxes = median, upper and lower quantiles; whiskers = 1.5x interquartile range, dots = outliers. *STV compliance is calculated separately and shown in Table 3.2.

Table 3.2

Percent compliance with STV standards across all months in the reporting period, binned by year and region.

Enterococcus

Year	Project		Jan	Feb	Mar	Apr	May	Jun	Jul	Aug	Sep	Oct	Nov	Dec
2020	**PLOO**	*Shore*	88	100	73	88	100	100	100	100	100	88	100	100
		Kelp	100	100	100	100	100	100	100	100	100	100	100	100
		Offshore	—	100	—	—	94	—	—	100	—	—	83	—
	SBOO	*Shore*	72	38	0	0	12	50	50	38	25	100	75	100
		Kelp	14	43	71	14	86	100	86	43	29	100	100	100
		Offshore	—	100	—	—	100	—	—	100	—	—	100	—
2021	**PLOO**	*Shore*	100	94	100	100	100	100	100	88	100	100	100	62
		Kelp	100	100	100	100	100	100	100	100	100	100	100	100
		Offshore	—	100	—	—	83	—	—	83	—	—	75	—
	SBOO	*Shore*	62	25	25	38	100	100	88	100	38	62	88	25
		Kelp	57	43	100	86	86	100	100	100	57	100	100	57
		Offshore	—	90	—	—	100	—	—	100	—	—	100	—

Total Coliforms

Year	Project		Jan	Feb	Mar	Apr	May	Jun	Jul	Aug	Sep	Oct	Nov	Dec
2020	**PLOO**	*Shore*	75	100	87	88	100	100	100	88	100	100	100	75
		Kelp	88	100	100	100	100	100	100	100	100	100	100	100
	SBOO	*Shore*	72	38	0	0	12	38	38	25	25	75	50	75
		Kelp	14	29	0	14	71	86	57	29	29	100	57	100
		Offshore	—	90	—	—	100	—	—	100	—	—	100	—
2021	**PLOO**	*Shore*	88	100	100	100	100	88	100	88	100	88	88	50
		Kelp	100	100	88	100	100	100	100	100	100	100	100	100
	SBOO	*Shore*	62	12	25	50	100	38	62	100	25	62	100	12
		Kelp	43	14	43	43	14	71	100	86	29	86	100	14
		Offshore	—	90	—	—	100	—	—	100	—	—	100	—

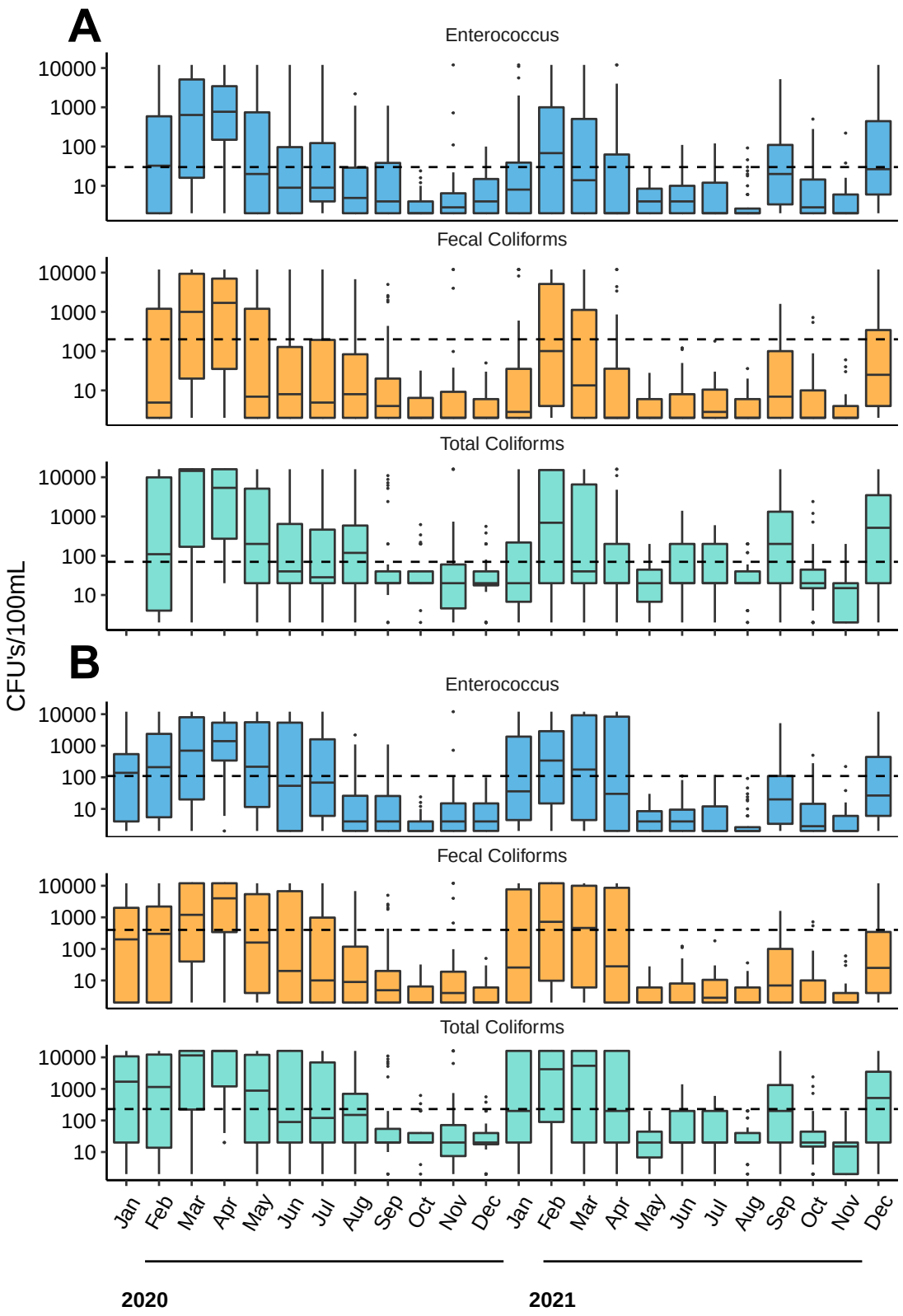

Figure 3.3

Distribution of values at SBOO shore stations during 2020 and 2021, binned monthly, for (A) running mean and median calculations and (B) single sample values. Dashed line represents the water contact standard compliance threshold*. Boxes = median, upper and lower quantiles; whiskers = 1.5x interquartile range, dots = outliers. *STV compliance is calculated separately and shown in Table 3.2.

Table 3.3

Number of analyses showing elevated FIB (eFIB) collected from shore stations during wet and dry seasons, and percent occuring in the wet season (% wet) during 2020 and 2021. Rain data are from Lindbergh Field, San Diego, CA. Stations are listed north to south from top to bottom. Stations not listed had no analyses showing elevated FIB during the report period.

	Seasons		
Station	**Wet**	**Dry**	**% Wet**
PLOO			
D12	1	0	100
D11	9	2	82
D10	3	2	60
D9	4	0	100
D8-B	8	0	100
SBOO			
S9	13	1	93
S8	17	3	85
S12	20	16	56
S6	36	25	59
S11	38	32	54
S5	85	45	65
S10	90	20	82
S4	86	18	83
S3	85	16	84
S2	72	19	79
S0	145	86	63
Rain (inches)	10.96	4.72	70
Total eFIB	712	285	71
Total Analyses	3378	2508	57

Of the 5886 analyses run on seawater samples collected at the PLOO and SBOO shore stations in 2020–2021 (not including resamples), about 17% (n=997) had elevated FIB (Table 3.3). A large majority (71%) of the shore samples with elevated FIB were collected during the wet seasons when rainfall totaled 10.96 inches over both years. This general relationship between rainfall and elevated bacterial levels at shore stations has been evident since water quality monitoring began in both regions (Figure 3.4). Further analyses of data from PLOO and SBOO shore stations indicate that the occurrence of a sample with elevated FIB was significantly more likely during the wet season than during the dry season (15% versus 5%, respectively; n=80,871, $\chi 2 = 4721.8$, $p < 0.0001$).

Regionally, elevated FIB densities occurred most often at SBOO shore stations S4, S5, S10, and S11 located near the mouth of the Tijuana River, as well as in northern Baja California waters at stations S0, S2, and S3 over the past two years (Table 3.3). Results from historical analyses also indicated that elevated FIB occurred more frequently at stations near the Tijuana River and south of the border near San Antonio de Los Buenos Creek, than at other PLOO or SBOO shore stations, especially during the wet seasons (Figure 3.4). Over the past several years, high FIB densities at these stations have consistently corresponded to outflows from the Tijuana River and San Antonio de Los Buenos Creek, typically following rain events (City of San Diego 2020). In addition, several sanitary sewer overflow events impacted the Tijuana River Valley during 2020 and 2021 (USIBWC 2020–2021). Each overflow event lasted from one to 50 days, with an average length of two days, and an average overflow of 86.3 million gallons impacting the main channel of the Tijuana River.

Kelp bed stations

Seawater samples from the PLOO kelp stations were 100% compliant with the median standard for total coliforms, the 30-day geometric mean standard for fecal coliforms, the six-week standard for *Enterococcus* (Figure 3.5A), and the SSM for fecal coliforms (Figure 3.5B). Compliance with the STV metric for total coliforms ranged from 88–100% of stations in compliance each month while compliance with the *Enterococcus* STV standard was 100% (Table 3.2). In the SBOO region, as was noted above for the shore stations, compliance rates were variable at the seven kelp bed, or nearshore, stations. For example, compliance in the SBOO kelp stations with the median standard for total coliforms was 79% over the report period, while compliance with the 30-day geometric mean for fecal coliforms was 96% and 89% for the six-week geometric mean

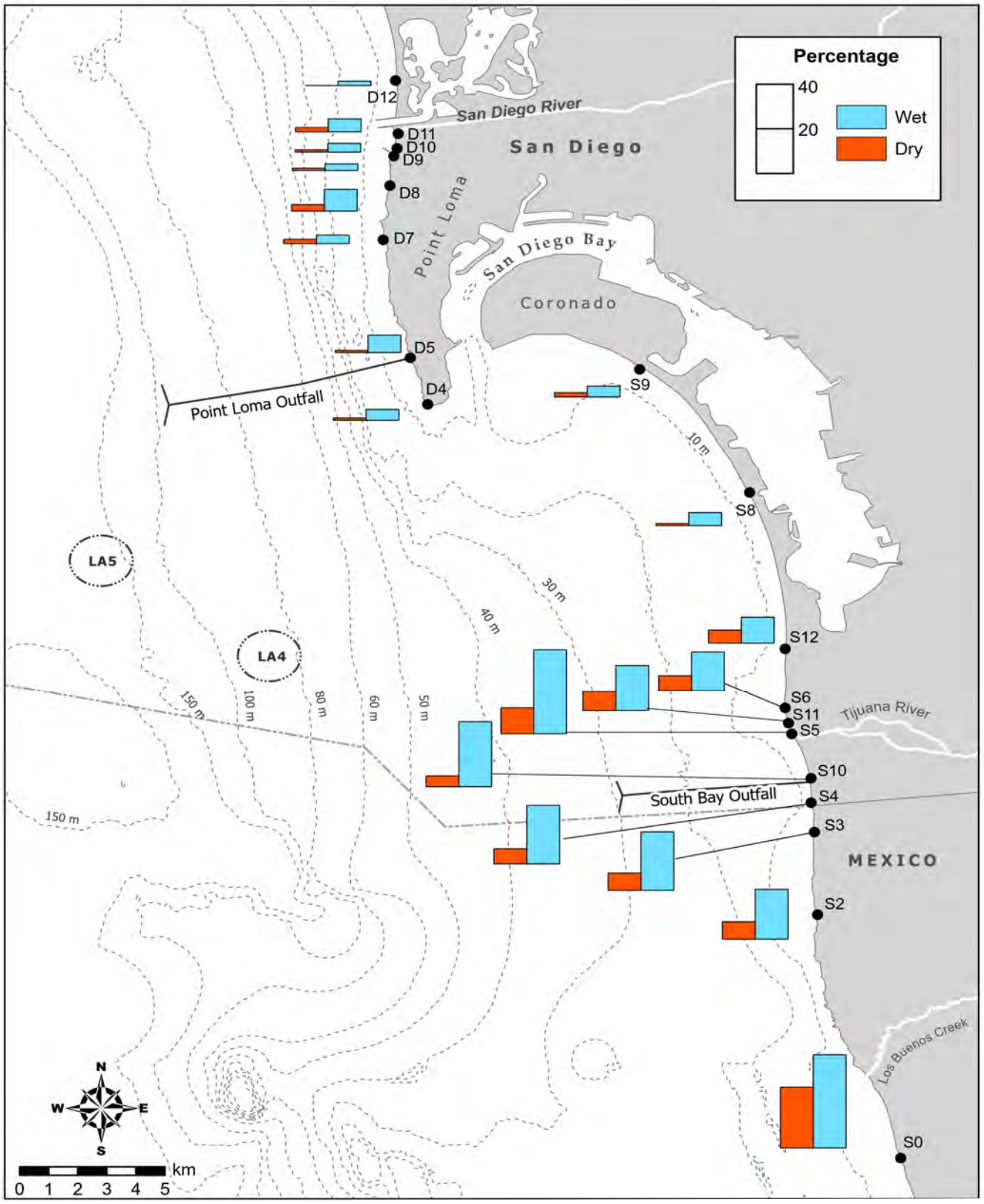

Figure 3.4
Percentage of samples with elevated FIB densities in wet versus dry seasons at shore stations from 1991 through 2021. Shore sampling in the SBOO region began in 1995.

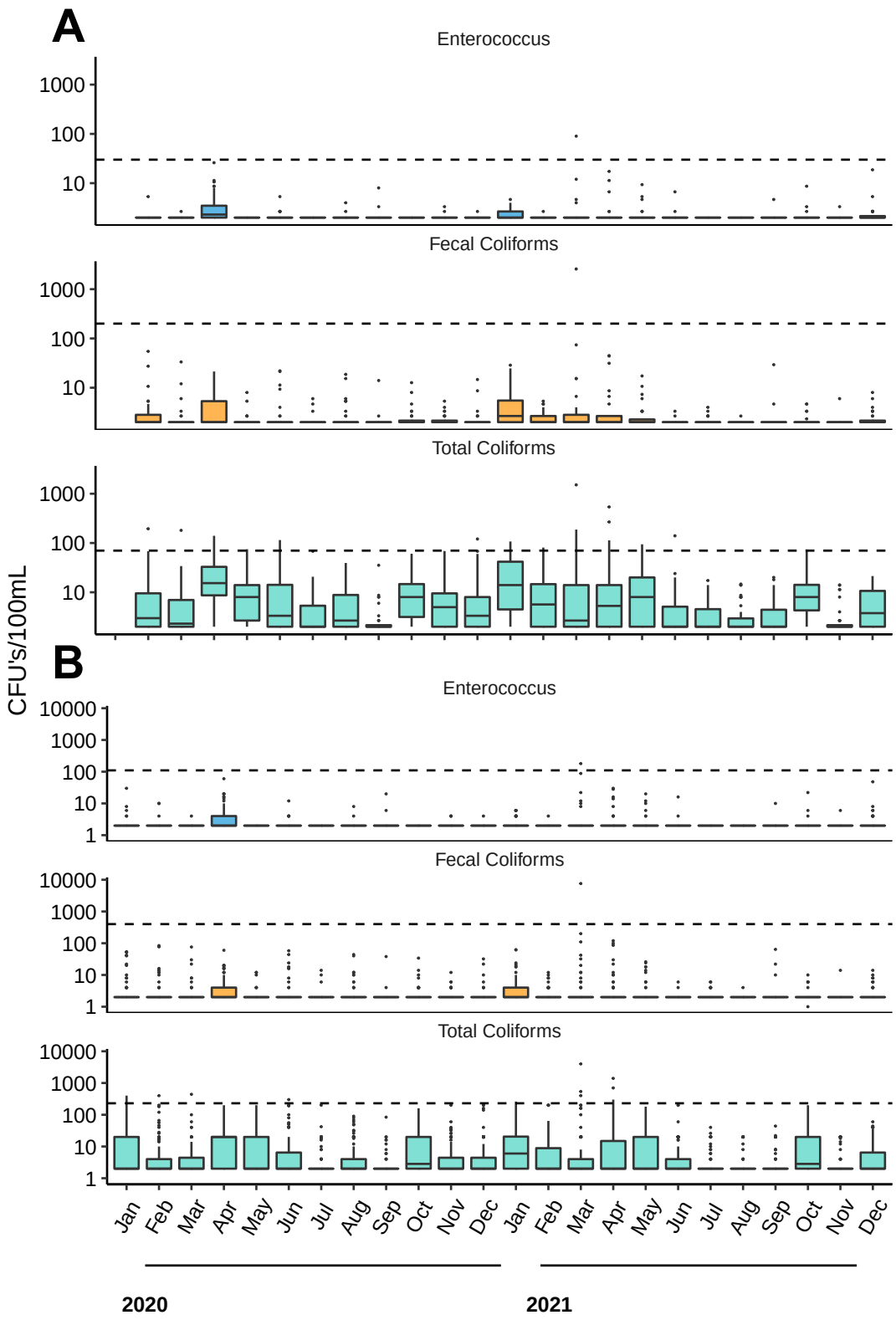

Figure 3.5

Distribution of values at PLOO kelp stations during 2020 and 2021, binned monthly, for (A) running mean and median calculations and (B) single sample values. Dashed line represents the water contact standard compliance threshold*. Boxes = median, upper and lower quantiles; whiskers = 1.5x interquartile range, dots = outliers. *STV compliance is calculated separately and shown in Table 3.2.

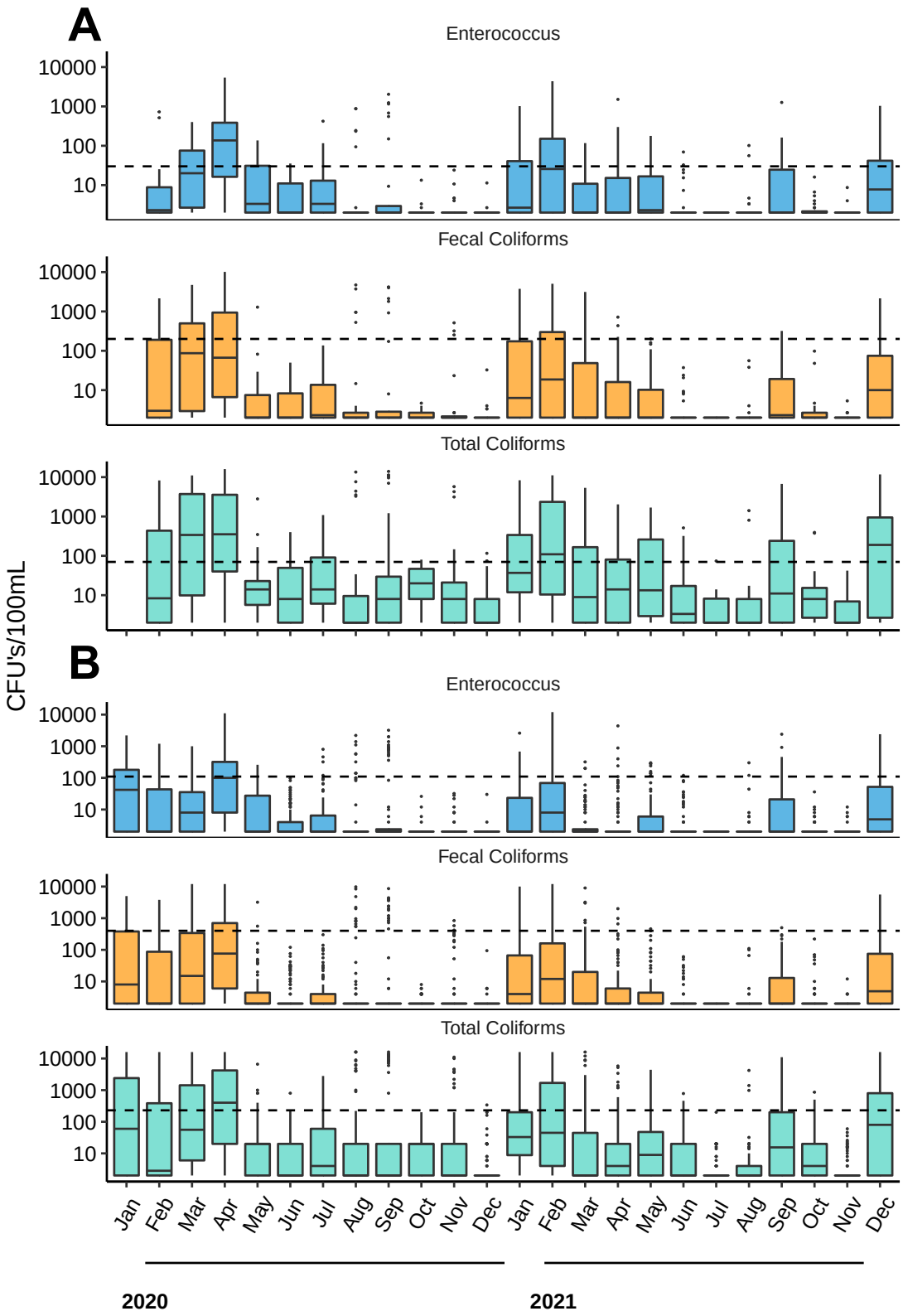

Figure 3.6

Distribution of values at SBOO kelp stations during 2020 and 2021, binned monthly, for (A) running mean and median calculations and (B) single sample values. Dashed line represents the water contact standard compliance threshold*. Boxes = median, upper and lower quantiles; whiskers = 1.5x interquartile range, dots = outliers. *STV compliance is calculated separately and shown in Table 3.2.

Table 3.4

Number of analyses showing elevated FIB (eFIB) collected from kelp stations during wet and dry seasons, and percent occuring in the wet season (% wet) during 2020 and 2021. See Table 3.3 for rain data. Within each contour stations are listed from north to south. Stations not listed had no analyses showing elevated FIB during the report period.

	Seasons		
	Wet	Dry	% Wet
PLOO			
18-m Depth Contour			
C7	4	0	100
A6	3	1	75
A7	3	0	100
A1	4	0	100
SBOO			
9-m Depth Contour			
I32	49	7	88
I26	51	21	71
I25	58	26	69
I24	94	35	73
I40	142	37	79
I19	177	44	80
18-m Depth Contour			
I39	12	8	60
Total eFIB	361	127	74
Total Analyses	8235	5940	58

standard for *Enterococcus* (Figure 3.6A). The SSM standard for fecal coliforms was met in 92% of samples (Figure 3.6B), and the STV standard for total coliforms ranged from 0–100%, while the STV for *Enterococcus* ranged from 14–100% (Table 3.2).

Of the 14,175 analyses run on samples collected at the PLOO and SBOO kelp stations in 2020–2021, approximately 3% (n=488) had elevated FIB, of which 74% occurred during the wet season (Table 3.4). However, analysis of water quality monitoring data collected at PLOO kelp stations over the course of the monitoring program (since 1991) shows that the difference in the occurrence of elevated FIB between wet and dry seasons is, though statistically significant, small in magnitude, indicating that rainfall has little impact on water quality in the PLOO region (2.9% in the dry season versus 3.7% in the wet season; n=164,508, $\chi 2=1296.7$, $p<0.0001$). Instead, the likelihood of encountering elevated FIB at these stations was significantly higher before the PLOO was extended to its present discharge site in late 1993 (13% versus <1%; n=164,508, $\chi 2=521.78$, $p<0.0001$) (see Figure 3.7). The influence of rainfall on FIB has been much more pronounced in the SBOO region over the past 25 years (Figure 3.7), with elevated FIB significantly more likely to occur at these stations during the wet season than during the dry season (10% versus <2%, respectively; n=59,180, $\chi 2=3153.3$, $p<0.0001$). As at the shore stations, high FIB densities at the SBOO kelp stations have historically corresponded to outflows from the Tijuana River and San Antonio de Los Buenos Creek following rain events in the area (City of San Diego 2009–2016b, 2018). Such rain-driven turbidity plumes have often been observed in satellite images of the region overlapping SBOO kelp stations with elevated FIB counts (e.g., Figure 3.8). The higher incidence of elevated FIB at the SBOO kelp bed stations during the wet season of 2020 and 2021 was also likely related to a series of large sewage spills that originated in Tijuana before spreading through the Tijuana River Valley and eventually reaching ocean waters and moving offshore (see USIBWC 2020–2021).

Offshore stations

Of the 2640 analyses run on samples collected at these stations in the PLOO and SBOO over the past two years, only about 4% (n=103) had elevated FIB, 58% of which occurred during the wet season (Table 3.5). The STV standard for *Enterococcus* at the 15 PLOO offshore stations located within State of California jurisdictional waters where Ocean Plan water contact standards apply ranged from 75–100% over the report period (Figure 3.9A, Table 3.2). Additionally, the 10 SBOO stations located within State of California jurisdictional waters were 98% compliant with the SSM standard for fecal coliforms (Figure 3.9B), and were 90–100% in compliance with the STV standard for both the total coliforms and *Enterococcus* (Table 3.2).

Most of the offshore analyses showing elevated FIB (n=103) in 2020–2021 occurred in the PLOO region

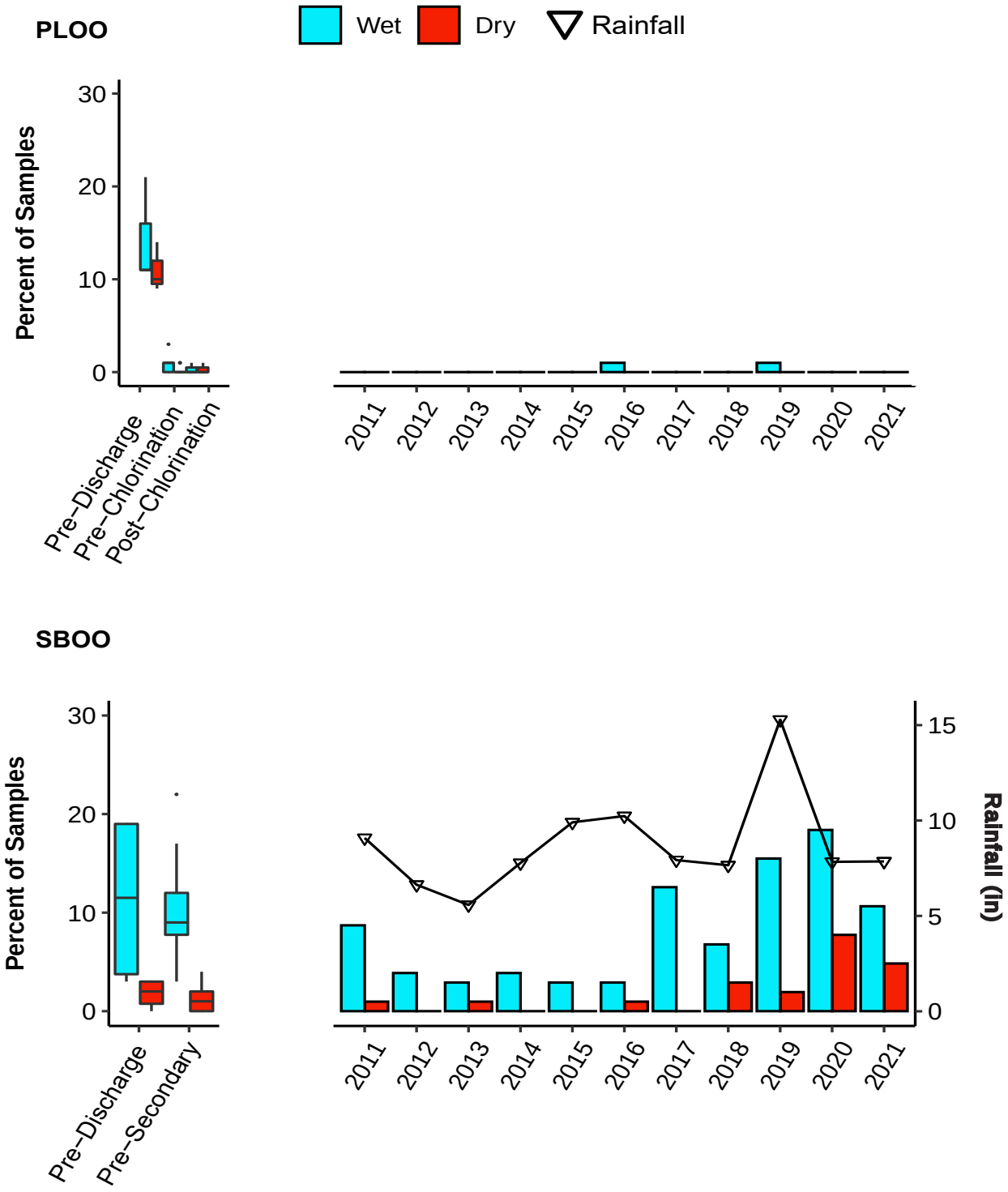

Figure 3.7

Comparison of annual rainfall with occurance of elevated FIB densities in wet (blue bars) versus dry (red bars) seasons at PLOO and SBOO kelp stations over the last decade. Boxed data show the distriution of % exceedances for each season over monitoring periods pre-dating the last decade. For PLOO, the Pre-Discharge period spanned from 1991 until the extension of the outfall to its current location in 1993. Chlorination of PLOO effluent began in 2008. For SBOO, Pre-Discharge data were collected in 1999, and secondary treatment began in 2011. Rain data are from Lindberg Field, San Diego, CA.

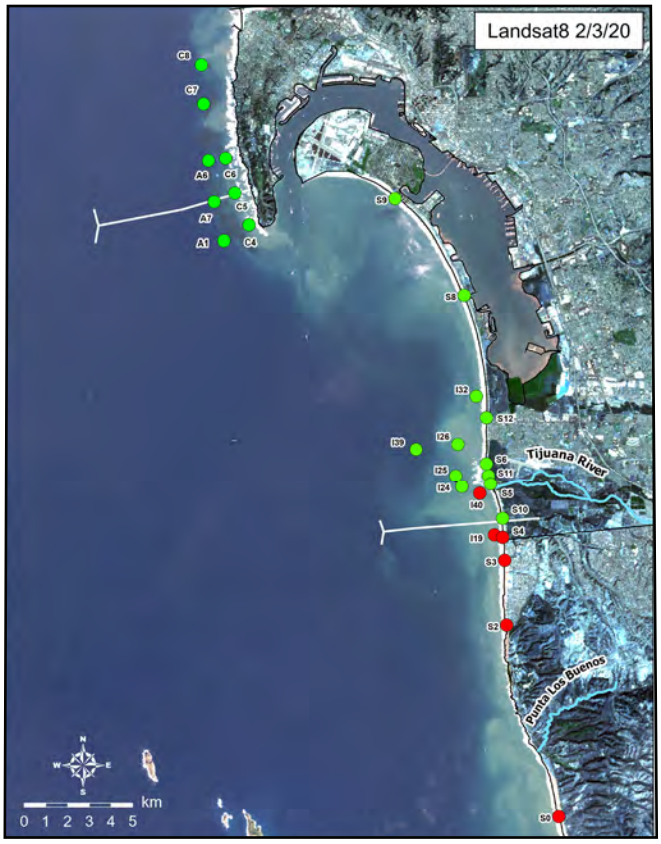

Figure 3.8
Landsat 8 satellite image showing the PLOO and SBOO regions on February 3rd, 2020 (Ocean Imaging 2020) combined with bacteria levels sampled at shore and kelp stations sampled on February 4th and 5th, respectively. Green circles indicate FIB met and red circles indicate at least one analysis with FIB exceeding water contact standards. Turbid waters correspond to an 826 million gallon sewage spill that started on January 24th and lasted until February 9th (IBWC 2021). Offshore stations sampled later in February had no exeedances.

(n=65) (Table 3.5). These high counts were from depths of 60 m or deeper, with 97% from stations located along the 80 or 98-m depth contours, and 27% from stations F29, F30, and F31 located within 1000 m of the PLOO discharge site (i.e., nearfield stations). These results suggest that the PLOO wastewater plume continues to be restricted to relatively deep, offshore waters throughout the year. Additionally, there were no signs of wastewater at any of the 36 offshore PLOO stations based on visual observations of the surface. This conclusion is consistent with historical remote sensing observations that have provided no indication of the PLOO plume reaching surface waters (see Appendix B: Svejkovsky and Hess 2022).

The above findings are also consistent with historical ocean monitoring results, which revealed that <4% of samples collected at depths of ≤25 m from the PLOO 98-m (i.e., discharge depth) stations had elevated levels of *Enterococcus* during the pre-chlorination years (1993–2008) (Figure 3.10). This percentage dropped to <1% at these depths following the initiation of partial chlorination at the Point Loma Wastewater Treatment Plant (PLWTP) in 2008 (City of San Diego 2009) and was zero during the current reporting period. Overall, detection of elevated *Enterococcus* has been significantly more likely at the three nearfield stations (F29, F30, F31) than at any other 98-m site (11% versus 6%, respectively; n=6905, $\chi 2=1030.8$, $p<0.0001$). The addition of chlorination significantly decreased the number of samples with elevated *Enterococcus* at these three stations (i.e., 17% before versus 9% after, n=1095, $\chi 2=46.31$, $p<0.0001$), and the other 98-m stations (9% before versus 3% after; n=5810, $\chi 2=348.38$, $p<0.0001$).

In the SBOO region, 38 analyses of offshore samples had elevated FIB during the two-year reporting period (Table 3.5). Historically, elevated bacterial levels were more likely at the three nearfield stations (i.e., I12, I14, I16) when compared to other SBOO 28-m (i.e., discharge depth) stations (10% versus 3%; n=18,351, $\chi 2=22.24$, $p<0.0001$) (Figure 3.11). These samples were predominately collected at a depth of 18 m. With the exception of 2017, the number of samples with elevated FIB collected from nearfield stations has decreased to ≤2 samples per year since secondary treatment was initiated at the South Bay Wastewater Treatment Plant in January 2011. These results demonstrate improved water quality near the outfall compared to previous years.

Receiving Water Bacterial Compliance

Compliance with receiving water limitations for bacterial characteristics (Box 3.2) in the PLOO region were above the minimum threshold for all metrics (for each parameter) throughout the report period (Table 3.6). In contrast, in the SBOO region, overall compliance was below the minimum threshold (i.e., 90%) for fecal coliforms on 378 of the 731 days (52% days out of compliance) in the report period, 460 days (63%) for *Enterococcus*, and

Table 3.5

Number of analyses showing elevated FIB (eFIB) collected from offshore stations during wet and dry seasons, and percent occuring in the wet season (% wet) during 2020 and 2021. See Table 3.3 for rain data. Within each contour stations are listed from north to south. Stations not listed had no analyses showing elevated FIB during the report period.

	Seasons		
	Wet	**Dry**	**% Wet**
PLOO			
60-m Depth Contour			
F15	1	0	100
F11	0	1	0
80-m Depth Contour			
F25	2	1	67
F24	1	2	33
F23	0	1	0
F22	1	2	33
F21	2	2	50
F20	3	3	50
F19	2	3	40
F18	1	0	100
F17	1	1	50
100-m Depth Contour			
F36	1	0	100
F34	1	0	100
F33	4	2	67
F32	2	3	40
F31*	2	3	40
F30*	3	6	33
F29*	1	2	33
F28	1	1	50
F27	2	0	100
F26	1	0	100
SBOO			
9-m Depth Contour			
I11	8	4	67
I5	16	5	76
18-m Depth Contour			
I23	4	0	100
I10	0	1	0
Total eFIB	60	43	58
Total Analyses	1320	1320	50

* Nearfield station

on all of the 731 days (100%) in the report period for total coliforms (Table 3.6). Stations with the highest occurrence of elevated FIB were shore and nearshore stations located close to the mouth of the Tijuana River Estuary. Furthermore, compliance with the kelp station metric was below the minimum threshold for fecal coliforms at station I19 on one or more days in the report period, stations I19 and I40 for enterococcus, and at I19, I24, and I40 for total coliforms. However, compliance with the offshore station metric in the SBOO region was above the minimum threshold for each parameter, throughout the report period (Table 3.6). To highlight the significant impact of the Tijuana River on receiving water quality, by removing the ten stations with the highest FIB counts, which also happen to be ten of the 11 closest shore and kelp stations to the estuary mouth (S4, S5, S6, S10, S11, S12, I19, I40, I24, I25), the remaining stations in the SBOO region become compliant with the overall metric (for each parameter) throughout the report period. Thus, the source of contamination in SBOO receiving waters is of known origin and likely associated with outflows from the Tijuana River and not related to wastewater discharge.

Summary

Compliance with all standards for FIB was typically higher at the PLOO and SBOO kelp beds, and other offshore stations, compared to the shore stations, and tended to be higher at PLOO stations than at the SBOO stations. Reduced compliance at shore stations, in both regions, tended to occur during the wet season. Historically, elevated FIB along the shore, or at the kelp bed stations, have typically been associated with storm activity (rain), heavy recreational use, the presence of seabirds, and decaying kelp or surfgrass (e.g., City of San Diego 2009–2022). Exceptions to the above patterns have occurred over the years due to specific events. For example, elevated bacteria observed at the PLOO shore and kelp stations in 1992 followed a catastrophic rupture of the outfall that occurred within the Point Loma kelp forest (Tegner et al. 1995). A more frequent source of known contamination in the SBOO region has been cross-border transportation of sewage

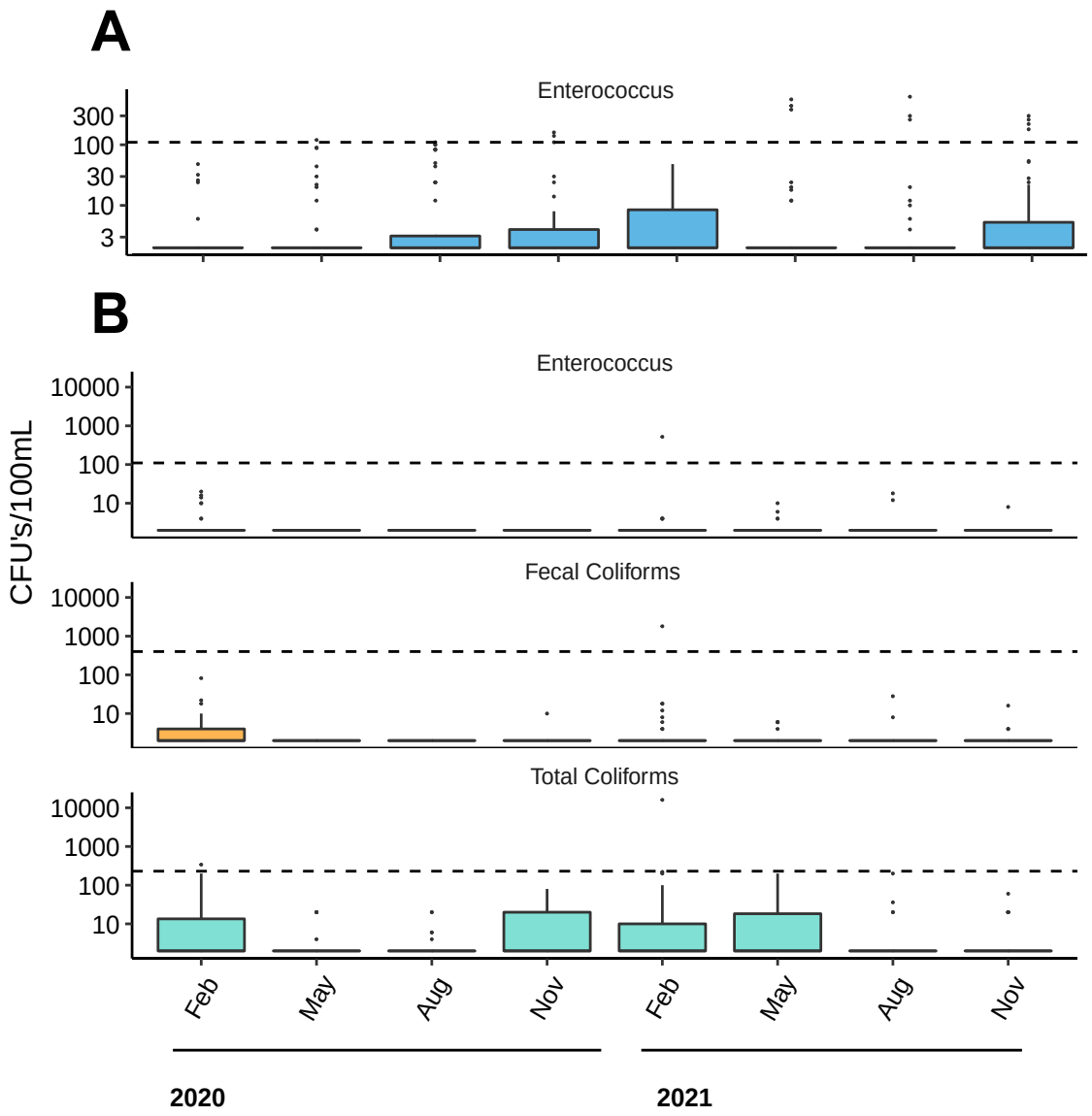

Figure 3.9

Distribution of values for PLOO (A) and SBOO (B) offshore stations during 2020 and 2021, binned monthly. Dashed line represents the water contact standard compliance threshold*. Boxes = median, upper and lower quantiles; whiskers = 1.5x interquartile range, dots = outliers. *STV compliance is calculated separately and shown in Table 3.2. Only Enterococcus is measured at PLOO offshore stations.

that originate from spills in Tijuana, Mexico such as the 7.6 billion gallon spill that occurred in April 2020 (USIBWC 2020–2021).

The spatial and temporal distribution of elevated FIB observed during the current report period corroborate the findings of previous City reports and other studies, which suggest that the Tijuana River and other terrestrial inputs are the largest drivers of contamination in the South Bay region (Svejkovsky and Jones 2001, Noble et al. 2003, Gersberg et al. 2004, 2006, 2008, Largier et al. 2004, Terrill et al. 2009, Svejkovsky and Hess 2022). For example, coastal runoff from rivers and creeks were more likely to impact coastal water quality than wastewater discharge from the outfall, especially during and immediately after significant rain events (Svejkovsky and Jones 2001, Terrill et al. 2009). Shore stations located near the mouths of the Tijuana River and in Mexican waters near San Antonio de Los Buenos Creek have historically had higher numbers of elevated FIB samples than

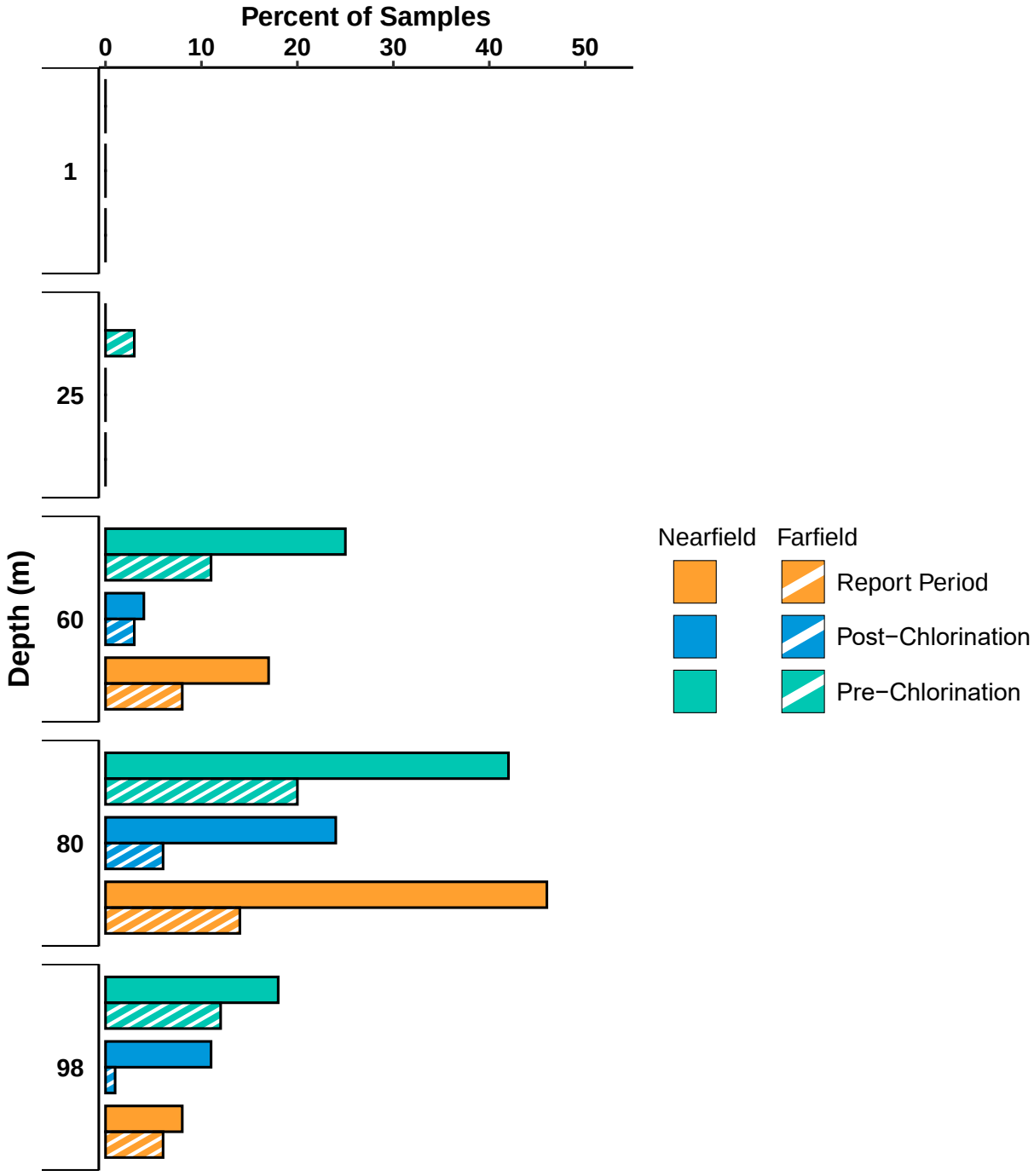

Figure 3.10
Percent of analyses of samples collected from PLOO 98-m offshore stations with elevated FIB. Samples from 2020 and 2021 are compared to those collected since the onset of discharge in 1993. Data for offshore stations in the PLOO region were only collected for seven months prior to discharge from the present location with no exceedances. Therefore, the Pre-Discharge group has been omitted.

stations located farther to the north. It is also well established that sewage-laden discharges from the Tijuana River and San Antonio de Los Buenos Creek are likely sources of bacteria during or after storms or other periods of increased flows (Svejkovsky and Jones 2001, Noble et al. 2003, Gersberg et al. 2004, 2006, 2008, Largier et al. 2004, Terrill et al. 2009, Svejkovsky and Hess 2022). Further, the general relationship between rainfall levels and elevated FIB densities in the SBOO

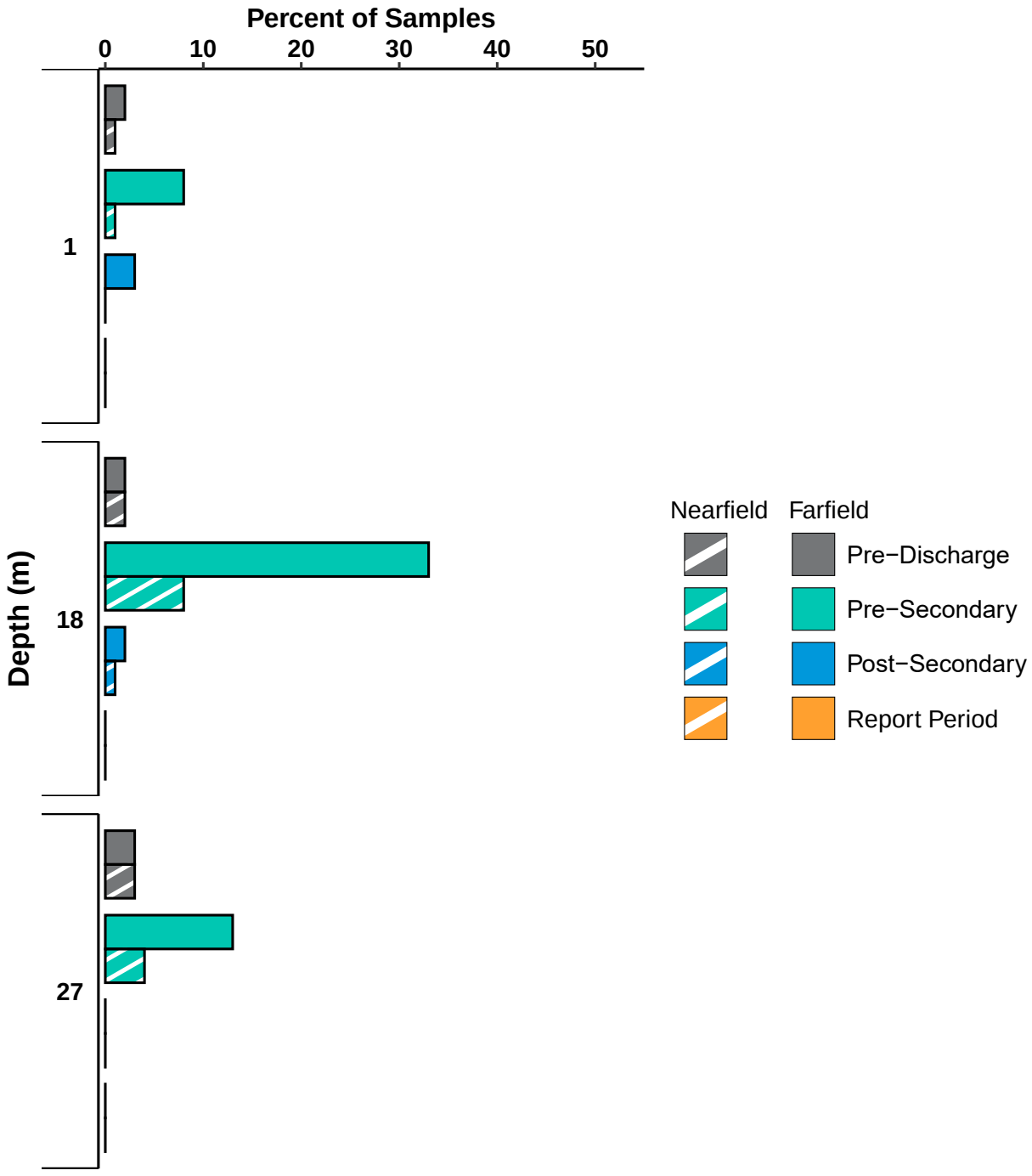

Figure 3.11
Percent of analyses of samples collected from SBOO 28-m offshore stations with elevated FIB. Samples from 2020 and 2021 are compared to those collected since the onset of monitoring in the South Bay in 1995.

region existed before wastewater discharge began in 1999 (City of San Diego 2000). The low number of samples with elevated FIB near the outfall during recent years is likely a result of chlorination and the initiation of full secondary treatment that began in January 2011 at the South Bay International Treatment Plant. As a result, we conclude that non-compliance with receiving water limitations for bacterial characteristics is primarily driven by known contaminated outflows from the Tijuana River Estuary and other non-point source runoff and not a result of wastewater discharge.

Table 3.6

Percent compliance with the HF183 sampling standards, calculated as the proportion of rolling window calcualtions, taken daily over the report period, showing compliance rates above the threshold established for each metric (90% overall, 50% kelp, 50% offshore). In the case of kelp and offshore compliance metrics, any stations with compliance <100% are listed individually.

PLOO

	Fecal Coliforms	Total Coliforms	*Enterococcus*
Overall	100	100	100
Kelp	100	100	100
Offshore	100	100	100

SBOO

	Fecal Coliforms	Total Coliforms	*Enterococcus*
Overall	48	0	37
Kelp			
9-m contour stations			
I19	99	76	90
I24	100	92	100
I40	100	79	93
Offshore	100	100	100

Literature Cited

[APHA] American Public Health Association. (2012). Standard Methods for the Examination of Water and Wastewater, 22ndt edition. E.W. Rice, R. Baird, A. Eaton and L. Clesceri (eds.). American Public Health Association, American Water Works Association, and Water Pollution Control Federation.

Bordner, R., J. Winter, and P. Scarpino, eds. (1978). Microbiological Methods for Monitoring the Environment: Water and Wastes, EPA Research and Development, EPA-600/8-78-017.

City of San Diego. (2000). International Wastewater Treatment Plant Final Baseline Ocean Monitoring Report for the South Bay Ocean Outfall (1995–1998). City of San Diego Ocean Monitoring Program, Metropolitan Wastewater Department, Environmental Monitoring and Technical Services Division, San Diego, CA.

City of San Diego. (2009). Annual Receiving Waters Monitoring Report for the Point Loma Ocean Outfall, 2008. City of San Diego Ocean Monitoring Program, Metropolitan Wastewater Department, Environmental Monitoring and Technical Services Division, San Diego, CA.

City of San Diego. (2020). Biennial Receiving Waters Monitoring and Assessment Report for the Point Loma and South Bay Ocean Outfalls, 2018-2019. City of San Diego Ocean Monitoring Program, Public Utilities Department, Environmental Monitoring and Technical Services Division, San Diego, CA.

City of San Diego. (2020–2022). Monthly Receiving Waters Monitoring Reports for the South Bay Ocean Outfall (South Bay Water Reclamation Plant), January 2020–December 2021. City of San Diego Ocean Monitoring Program, Public Utilities Department, Environmental Monitoring and Technical Services Division, San Diego, CA.

City of San Diego. (2021a). Annual Receiving Waters Monitoring and Toxicity Testing Quality Assurance Report, 2020. City of San Diego Ocean Monitoring Program, Public Utilities Department, Environmental Monitoring and Technical Services Division, San Diego, CA.

City of San Diego. (2021b). Interim Receiving Waters Monitoring Report for the Point Loma Ocean Outfall and South Bay Ocean Outfalls, 2020. City of San Diego Ocean Monitoring Program, Public Utilities Department, Environmental Monitoring and Technical Services Division, San Diego, CA.

City of San Diego. (2022a). Ocean Monitoring Reports. https://www.sandiego.gov/public-utilities/sustainability/ocean-monitoring/reports

City of San Diego. (2022b). Annual Receiving Waters Monitoring and Toxicity Testing Quality Assurance Report, 2021. City of San Diego Ocean Monitoring Program, Public Utilities Department, Environmental Monitoring and Technical Services Division, San Diego, CA.

Gersberg, R.M., D. Daft, and D. Yorkey. (2004). Temporal pattern of toxicity in runoff from the Tijuana River Watershed. Water Research, 38: 559–568.

Gersberg, R.M., M.A. Rose, R. Robles-Sikisaka, and A.K. Dhar. (2006). Quantitative detection of hepatitis a virus and enteroviruses near the United States-Mexico Border and correlation with levels of fecal indicator bacteria. Applied and Environmental Microbiology, 72: 7438–7444.

Gersberg, R., J. Tiedge, D. Gottstein, S. Altmann, K. Watanabe, and V. Luderitz. (2008). Effects of the South Bay Ocean Outfall (SBOO) on beach water quality near the USA-Mexico border. International Journal of Environmental Health Research, 18: 149–158.

Grant, S.B., B.F. Sanders, A. Boehm, J. Redman, R. Kim, A. Chu, M. Gouldin, C. McGee, N. Gardiner, B. Jones, J. Svejkovsky, and G. Leipzig. (2001). Generation of enterococci bacteria in a coastal saltwater marsh and its impact on surf zone water quality. Environmental Science Technology, 35: 2407–2416.

Griffith, J., K.C. Schiff, G. Lyon, and J. Fuhrman. (2010). Microbiological water quality at non-human influenced reference beaches in southern California during wet weather. Marine Pollution Bulletin, 60: 500–508.

Gruber, S., L. Aumand, and A. Martin. (2005). Sediments as a reservoir of indicator bacteria in a coastal embayment: Mission Bay, California, Technical paper 0506. Weston Solutions, Inc. Presented at StormCon 2005. Orlando, FL, USA. July 2005.

Harrell, F.E. Jr, C. Dupont et al. (2015). Hmisc: Harrell Miscellaneous. R package version 3.17-0. http://CRAN.R-project.org/package=Hmisc.

Kassambara, A. (2019). ggpubr: 'ggplot2' Based Publication Ready Plots. R package version 0.2.4. https://CRAN.R-project.org/package=ggpubr.

Koenker, R. (2019). quantreg: Quantile Regression. R package version 5.52. https://CRAN.R-project.org/package=quantreg.

Largier, J., L. Rasmussen, M. Carter, and C. Scearce. (2004). Consent Decree – Phase One Study Final Report. Evaluation of the South Bay International Wastewater Treatment Plant Receiving Water Quality Monitoring Program to Determine Its Ability to Identify Source(s) of Recorded Bacterial Exceedances. Scripps Institution of Oceanography, University of California, San Diego, CA.

Martin, A., and S. Gruber. (2005). Amplification of indicator bacteria in organic debris on southern California beaches. Technical Paper 0507.

Weston Solutions, Inc. Presented at StormCon 2005. Orlando, FL, USA. July 2005.

Nezlin, N.P., P.M. DiGiacomo, S.B. Weisberg, D.W. Diehl, J.A. Warrick, M.J. Mengel, B.H. Jones, K.M. Reifel, S.C. Johnson, J.C. Ohlmann, L. Washburn, and E.J. Terrill. (2007). Southern California Bight 2003 Regional Monitoring Program: V. Water Quality. Southern California Coastal Water Research Project. Costa Mesa, CA.

[NOAA] National Oceanic and Atmospheric Administration. (2022). National Climatic Data Center. https://www.ncdc.noaa.gov/cdo-web/search

Noble, R.T., D.F. Moore, M.K. Leecaster, C.D. McGee, and S.B. Weisberg. (2003). Comparison of total coliform, fecal coliform, and Enterococcus bacterial indicator response for ocean recreational water quality testing. Water Research, 37: 1637–1643.

Noble, M.A., J.P. Xu, G.L. Robertson, and K.L. Rosenfeld. (2006). Distribution and sources of surfzone bacteria at Huntington Beach before and after disinfection of an ocean outfall–A frequency-domain analysis. Marine Environmental Research, 61: 494–510.

Phillips, C.P., H.M. Solo-Gabriele, A.J. Reneiers, J.D. Wang, R.T. Kiger, and N. Abdel-Mottaleb. (2011). Pore water transport of enterococci out of beach sediments. Marine Pollution Bulletin, 62: 2293–2298.

R Core Team. (2019). R: A language and environment for statistical computing. R Foundation for Statistical Computing, Vienna, Austria. URL https://www.R-project.org/.

Reeves, R.L., S.B. Grant, R.D. Mrse, C.M. Copil Oancea, B.F. Sanders, and A.B. Boehm. (2004). Scaling and management of fecal indicator bacteria in runoff from a coastal urban watershed in southern California. Environmental Science and Technology, 38: 2637–2648.

Revelle, W. (2015). psych: Procedures for Personality and Psychological Research, Northwestern University, Evanston, Illinois, USA, http://CRAN.R-project.org/package=psych version 1.5.8.

Ripley, B. and M. Lapsley. (2017). RODBC: ODBC Database Access. R package version 1.3-12. http://CRAN.R-project.org/package=RODBC.

Schauberger, P and A. Walker (2019). openxlsx: Read, Write and Edit xlsx Files. R package version 4.1.4. https://CRAN.R-project.org/package=openxlsx.

Sercu, B., L.C. Van de Werfhorst, J. Murray, and P.A. Holden. (2009). Storm drains are sources of human fecal pollution during dry weather in three urban southern California watersheds. Environmental Science and Technology, 43: 293–298.

State of California. (2010). Integrated Report (Clean Water Act Section 303(d) List/305(b) Report). http://www.waterboards.ca.gov/water_issues/programs/tmdl/integrated2010.shtml.

Svejkovsky, J. and B. Jones. (2001). Detection of coastal urban storm water and sewage runoff with synthetic aperture radar satellite imagery. Eos, Transactions, American Geophysical Union, 82, 621–630.

Svejkovsky, J. and Hess, M. (2022). Satellite & Aerial Coastal Water Quality Monitoring in the San Diego/Tijuana Region: Five Year Summary Report: 1 January 2017 – 31 December 2021. Littleton, CO.

[SWRCB] California State Water Resources Control Board. (2019). California Ocean Plan, Water Quality Control Plan, Ocean Waters of California. California Environmental Protection Agency, Sacramento, CA.

Tegner, M.J., P.K. Dayton, P.B. Edwards, K.L. Riser, D.B. Chadwick, T.A. Dean, and L. Deysher. (1995). Effects of a large sewage spill on a kelp

forest community: Catastrophe or disturbance? Marine Environmental Research, 40: 181–224.

Terrill, E., K. Sung Yong, L. Hazard, and M. Otero. (2009). IBWC/Surfrider – Consent Decree Final Report. Coastal Observations and Monitoring in South Bay San Diego. Scripps Institution of Oceanography, University of California, San Diego, CA.

[USEPA] United States Environmental Protection Agency. (2014). Method 1600: Enterococci in Water by Membrane Filtration Using membrane-Enterococcus Indoxyl-β-D-Glucoside Agar (mEI). EPA Document EPA-821-R-14-011. Office of Water (4303T), Washington, DC.

[USIBWC] Unites States International Boundary Water Commission (2020-2021). Transboundary Flow Reports. https://www.waterboards.ca.gov/sandiego/water_issues/programs/tijuana_river_valley_strategy/spill_report.html

Warnes, G., B. Bolker, and T. Lumley. (2015). gtools: Various R Programming Tools. R package version 3.5.0. http://CRAN.R-project.org/package=gtools.

Wickham, H. (2007). Reshaping Data with the reshape Package. Journal of Statistical Software, 21(12), 1-20. URL http://www.jstatsoft.org/v21/i12/.

Wickham, H. (2017). tidyverse: Easily Install and Load the 'Tidyverse'. R package version 1.2.1. https://CRAN.R-project.org/package=tidyverse.

Yamahara, K.M., B.A. Layton, A.E. Santoro, and A.B. Boehm. (2007). Beach sands along the California coast are diffuse sources of fecal bacteria to coastal waters. Environmental Science and Technology, 41: 4515–4521.

Chapter 4
Plume Dispersion

Chapter 4. Plume Dispersion

Introduction

The City of San Diego (City) collects a comprehensive suite of oceanographic data in nearshore (e.g., kelp forests) and offshore coastal waters surrounding the Point Loma and South Bay Ocean Outfalls (PLOO and SBOO, respectively) to identify the presence of discharged treated wastewater effluent ('plume') and characterize regional water quality conditions. A range of specialized equipment are used to facilitate this data collection both temporally and spatially, including a conductivity, temperature, and depth (CTD) instrument package deployed weekly at nearshore stations, and quarterly at offshore stations; two real-time oceanographic mooring systems (RTOMS) anchored near the terminal ends of the PLOO and SBOO; and a remotely operated towed vehicle (ROTV) deployed quarterly in the PLOO and SBOO regions. The ability to monitor over a large spatial scale using a CTD and continuously in real-time using RTOMS, and to track potential wastewater discharge directly using an ROTV, ensures that the City has the most comprehensive suite of tools available to both assess plume dispersion and predict potential shoreward movement of wastewater plumes.

The specialized equipment utilized for plume tracking come equipped with auxiliary instruments that help to distinguish an outfall's effluent signal from ambient ocean water. For example, colored dissolved organic material (CDOM) has proven useful in identifying wastewater plumes from the PLOO and SBOO in the San Diego region (Terrill et al. 2009, Rogowski et al. 2012a,b, 2013). The reliability of plume detection can be further improved by combining measurements of CDOM with additional parameters (e.g., low chlorophyll *a* concentrations), thus facilitating evaluation of possible wastewater impacts on coastal waters.

Historically, the City has assessed the presence of effluent plumes via quarterly CTD surveys alone, which provide discrete measurements over a large spatial scale, but lack the temporal and spatial resolution that may be necessary to fully assess plume behavior and the ocean conditions that impact plume dispersion. Following an independent review of the City's Ocean Monitoring Program (SIO 2004), the Scripps Institution of Oceanography (SIO) was contracted to develop and conduct enhanced monitoring intended to provide an improved understanding of physical circulation and current movement patterns in local coastal waters surrounding the PLOO. Initially, non-telemetered moored temperature loggers (thermistor arrays) and acoustic doppler current profilers (ADCPs) were utilized to characterize the thermocline structure and current regime in the area surrounding the PLOO (Storms et al. 2006). The use of these "static" moorings was later expanded to include both the PLOO and SBOO regions where the resultant data have been a valuable part of the City's annual receiving waters reports (e.g., City of San Diego 2020a, 2021).

Subsequent studies of the fate and behavior of wastewater discharged to the ocean via the SBOO (Terrill et al. 2009) and the PLOO (Rogowski et al. 2012a,b, 2013) included recommendations to use RTOMS and advanced mobile sampling technologies (i.e., ROTVs or autonomous underwater vehicles) to better understand nearshore coastal water quality and the impacts of local ocean currents and tidal fluxes on effluent plume dynamics. The ability to monitor in near real-time is an essential component of wastewater plume tracking, as it provides the City with the opportunity to predict potential shoreward movement of wastewater plumes, which may otherwise present a hazard to people utilizing recreational waters along the shoreline. Furthermore, real-time monitoring allows the City to quickly identify issues with mooring

equipment to facilitate long-term maintenance. Used in conjunction with the RTOMS, optimized and adaptive sampling using ROTV surveys can improve evaluation of plume dispersion from outfalls. Based on these recommendations, the City, U.S. Section of the International Boundary and Water Commission (USIBWC), San Diego Regional Water Quality Control Board (SDRWQCB) and U.S. Environmental Protection Agency (USEPA) reached an agreement that real-time monitoring should be developed for the PLOO and SBOO regions. Therefore, between 2017 and 2021, the City developed and carried out the Plume Tracking Monitoring Plan (PTMP) for the Point Loma and South Bay Ocean Outfall Regions (City of San Diego 2018a, 2020b, 2022a). As of July 1, 2021, the PTMP was included as a requirement in the National Pollutant Discharge Elimination System (NPDES) permit for the South Bay International Wastewater Treatment Plant (SBIWTP) and the South Bay Water Reclamation Plant (SBWRP).

This chapter presents the initial analysis and interpretation of plume tracking data collected by CTD, RTOMS, and ROTV in 2020 and 2021 in the PLOO and SBOO regions. The primary goals of this chapter are to: (1) provide in-depth evaluations, interpretations, discussions, and conclusions concerning wastewater plume behavior in receiving waters; (2) determine if the wastewater plume is encroaching upon receiving water areas used for swimming, surfing, diving, and shellfish harvesting; (3) assess the fate of the discharged wastewater plume.

Materials and Methods

CTD

Deployment and Configuration

Oceanographic data were collected using a Sea-Bird SBE 25 Plus CTD. The CTD was lowered through the water column at each station to collect continuous measurements of water temperature, conductivity (used to calculate salinity), pressure (used to calculate depth), dissolved oxygen (DO), pH, transmissivity (a proxy for water clarity), chlorophyll *a* fluorescence (a proxy for phytoplankton), and colored dissolved organic material (CDOM). Vertical profiles of each parameter were constructed for each station, per survey, by averaging the data values recorded within each 1-m depth bin (see Chapter 2).

Data Collection

Fifteen stations located in relatively shallow waters within or near the Point Loma or Imperial Beach kelp beds (i.e., referred to as "kelp" stations herein) were monitored weekly to assess water quality conditions and California Ocean Plan (Ocean Plan) (SWRCB 2019) compliance in nearshore areas used for recreational activities such as SCUBA diving, surfing, fishing, and kayaking (Figure 4.1). These included PLOO stations C4, C5, and C6, located along the 9-m depth contour near the inner edge of the Point Loma kelp forest, PLOO stations A1, A6, A7, C7, and C8, located along the 18-m depth contour near the outer edge of the Point Loma kelp forest, SBOO stations I25, I26, and I39, located at depths of 9–18 m contiguous to the Imperial Beach kelp bed, and SBOO stations I19, I24, I32, and I40 located in other nearshore waters along the 9-m depth contour.

An additional 69 offshore stations were sampled quarterly over consecutive days in winter (February), spring (May), summer (August), and fall (November) to monitor water quality conditions and to estimate dispersion of the PLOO and SBOO wastewater plumes (Figure 4.1). These included 36 stations surrounding the PLOO, and 33 stations surrounding the SBOO. The PLOO stations are designated F1–F36 and are located along or adjacent to the 18, 60, 80, and 98-m depth contours. The SBOO stations are designated I1–I18, I20–I23, I27–I31, and I33–I38, and are located along the 9, 19, 28, 38 and 55-m depth contours, respectively. Fifteen of the PLOO stations (F01–F03, F06–F14, F18–F20) and 15 of the SBOO stations (I12, I14, I16–I18, I22–I23, I27, I31, I33–I38) are located within State jurisdictional waters (i.e., within 3 nautical miles of shore) and therefore subject to Ocean Plan compliance standards (see Chapter 3 for further details).

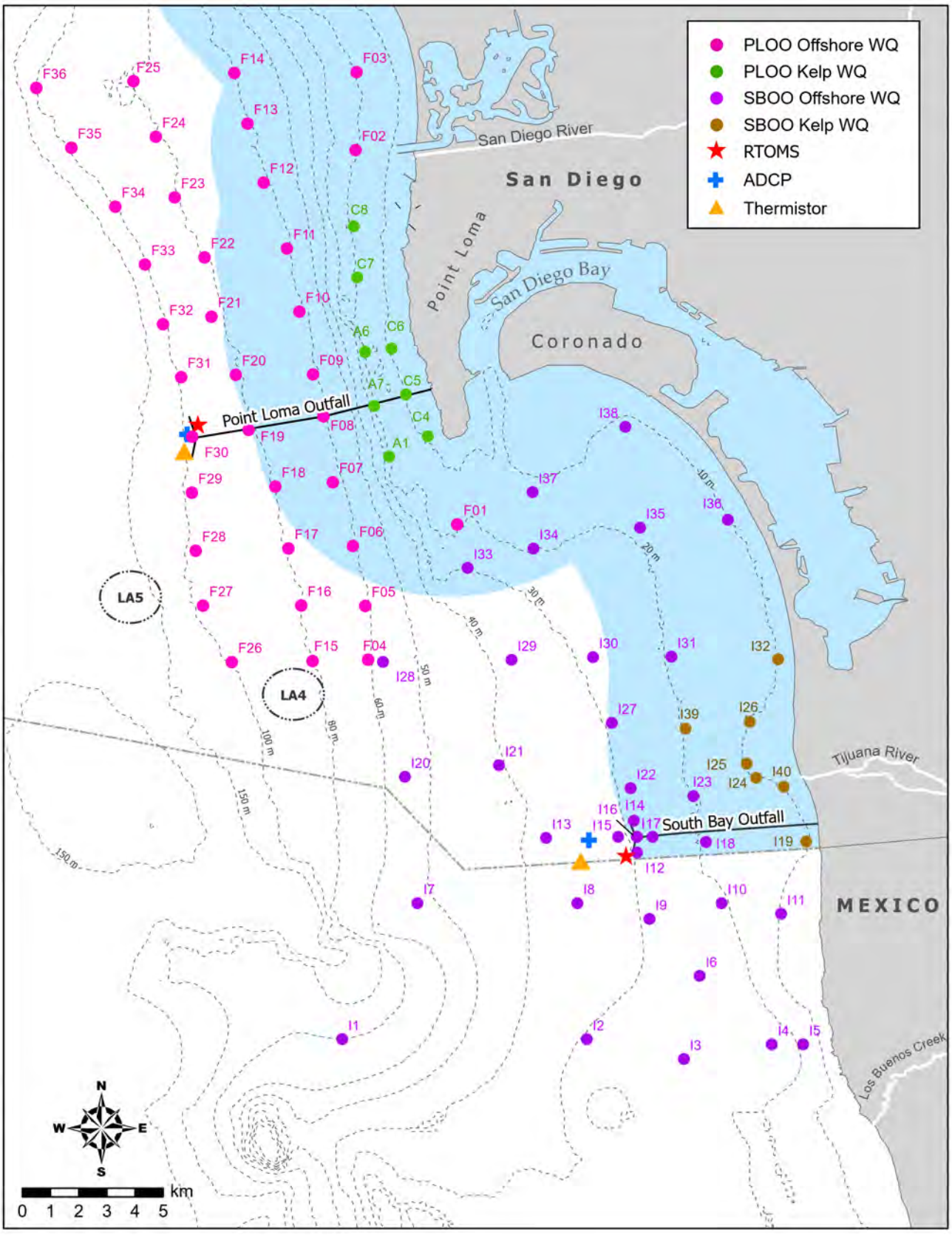

Figure 4.1
Oceanographic mooring and monitoring station locations around the PLOO and SBOO sampled as part of the City of San Diego's Ocean Monitoring Program. Light blue shading represents State jurisdictional waters.

Data Analyses

Presence or absence of the wastewater plume at the PLOO and SBOO offshore stations was estimated by evaluating a combination of oceanographic parameters (i.e., detection criteria). All stations along the 9-m depth contour were excluded from these analyses, due to the potential for coastal runoff or sediment resuspension in shallow nearshore waters to confound any CDOM signal that could be associated with plume dispersion from the outfalls (Appendices E.1, E.2). Previous monitoring results have consistently shown that the PLOO plume remains trapped below the pycnocline with no evidence of surfacing throughout the year (City of San Diego 2020a, Rogowski et al. 2012a, b, 2013, Hess 2019, 2020, 2021). In contrast, the SBOO plume stays trapped below the pycnocline during seasonal periods of water column stratification but may rise to the surface when waters become more mixed and stratification breaks down. Water column stratification and pycnocline depth were quantified using buoyancy frequency (BF, cycles/min) calculations for each quarterly survey. This measure of the water column's static stability was used to quantify the magnitude of stratification for each survey and was calculated as follows:

$$BF = \sqrt{g/\rho} * (d\rho/dz)$$

where g is the acceleration due to gravity, ρ is the seawater density, and dρ/dz is the density gradient (Mann and Lazier 1991). The depth of maximum BF was used as a proxy for the depth at which stratification was the greatest. If the water column was determined to be stratified (i.e., maximum BF > 5.5 cycles/min), subsequent analyses were limited to depths below the pycnocline.

Identification of potential plume signal was determined for each quarterly survey at each monitoring station based on a combination of CDOM, chlorophyll *a*, and salinity levels, as well as a visual review of the overall water column profile. Detection thresholds for the PLOO and SBOO stations were set adaptively for each quarter according to the criteria described in City of San Diego (2016a,b). It should be noted that these thresholds are based on observations of ocean properties specific to the distinct PLOO and SBOO monitoring regions, and thus constrained to only those regions. Finally, water column profiles were visually interpreted to remove stations with spurious signals (e.g., CDOM signals near the seafloor that were likely caused by sediment resuspension). All analyses were performed using R (R Core Team 2021) and various functions within the reshape2, Rmisc, RODBC, oce, and tidyverse packages (Wickham 2007, Hope 2013, Ripley and Lapsley 2017, Kelley and Richards 2019, Wickham et al. 2019). Further confirmation of these CTD-based parameters as being indicative of the effluent plume was determined by comparison of potential plume detections with fecal indicator bacteria (FIB) data at the same stations and similar depths (see Chapter 3).

The effect of any potential "plume detection" on local water quality, during each quarterly survey, was evaluated by comparing mean values of DO, pH, and transmissivity within the possible plume boundaries to thresholds calculated for the same depths from reference stations. For each quarter, stations with all CDOM values below the 85th percentile of that region's values were considered "reference". Individual non-reference stations were then determined to be out-of-range (OOR) compared to the reference stations if values exceeded narrative water quality standards defined in the Ocean Plan (see Box 3.1, Chapter 3). For example, the Ocean Plan defines OOR thresholds for DO as a 10% reduction from naturally-occurring concentrations, for pH as a 0.2 pH unit change, and for transmissivity as below the lower 95% confidence interval from the mean. For purposes of this report, "naturally" is defined for DO as the mean concentration minus one standard deviation (see Nezlin et al. 2016).

RTOMS

Deployment and Configuration

The RTOMS are anchored buoys suspended in the water column configured with a range of instruments, collecting near continuous oceanographic data and providing near real-time information of changing

conditions. The RTOMS are outfitted with a series of instruments at various depths throughout the water column (see Chapter 2, Table 2.1). Critical parameters that were measured on a real-time basis included temperature, conductivity (salinity), total pH, DO, dissolved carbon dioxide (xCO_2), nitrate (nitrate + nitrite), chlorophyll *a*, CDOM, backscatter (turbidity), biological oxygen demand (BOD), and current direction and velocity. Parameters were recorded at 10-minute intervals, with the exception of nitrate + nitrite, which was recorded at 1-hour intervals, and xCO_2, which was recorded at 10-hour intervals. Beginning in November 2021, xCO_2 sampling increased to 1-hour intervals, due to additional power available from a solar panel upgrade at both moorings.

Data Collection

Two RTOMS were anchored near the terminal ends of the PLOO and SBOO (nearfield), at a distance far enough from the diffuser ports to be outside the area of active plume rise. The PLOO RTOMS was anchored at a depth of approximately 95 m, just east of the northern diffuser leg, and the SBOO RTOMS was anchored at a depth of approximately 30 m, just west of the southern diffuser leg terminus (Figure 4.1). Each mooring was deployed for a period of approximately one year, with a gap in deployments for much of 2021 (see Chapter 2).

In addition, temperature and ocean current data from static moorings were used to supplement data gaps between RTOMS deployments (from September 30, 2020 to November 2, 2021 at the PLOO; from December 17, 2020 to November 2, 2021 at the SBOO). These non-telemetered (static) upward-facing bottom-mounted ADCPs (Teledyne RD Instruments 300 KHz Workhorse Monitor) and thermistor (Onset Tidbit temperature loggers) string arrays were moored near the RTOMS at the terminal ends of the PLOO and SBOO (Figure 4.1; see Chapter 2 for details).

Data Processing and Analysis

Prior to conducting analyses, RTOMS data were subject to a comprehensive suite of quality assurance/ quality control (QA/QC) procedures following Quality Assurance of Real-Time Oceanographic Data (QARTOD) methodologies (see Chapter 2). After review, all data that were flagged as suspect or bad were excluded from further analyses and are not presented in this report.

Ocean current data analyses were performed in R (R Core Team 2021) using functions within various packages (i.e., reshape2, Rmisc, mixOmics, tidyverse, scales, pracma, and gtools) (Wickham 2007, Hope 2013, Le Cao et al. 2017, Wickham et al. 2019, Wickham and Seidel 2020, Borchers 2021, Warnes et al. 2021). Specifically, after data QA/QC, tidal frequency data were removed using the PL33 filter (Alessi et al. 1984) and then hourly averaged. Plots and analyses for all other RTOMS data were completed in MATLAB (2016). Contour plots were generated for parameters with sufficient vertical coverage in the water column using default settings, which display fixed isolines and fill areas between isolines with constant colors. Density calculations and temperature-salinity plots were created using the SEAWATER toolbox library for MATLAB, version 3.3.1 (Morgan and Pender 2014).

Temperature gradients were evaluated from RTOMS and thermistor data to illustrate daily and seasonal changes in thermal stratification. Vertical gradients were calculated by the daily average temperature difference between adjacent sensors in the water column (e.g., from 6 to 10 m at thermistor arrays) and then dividing by the depth between sensors. Depths of the maximum daily temperature gradients were used to evaluate stratification, with moderate stratification defined as greater than 0.2°C/m gradients.

During time periods when the wastewater effluent plumes overlap with the fixed locations of the RTOMS, observations may be assessed for potential plume detections. In order to compare potential freshwater signals from effluent plumes to background ocean salinity levels, time series anomalies of RTOMS salinity were calculated and compared to historical salinity data from CTD surveys. Since there were no equivalent moorings deployed in similar ocean water masses to use as a

farfield reference site on the same time scale, this approach provided a baseline comparison to typical salinity ranges by region and depth. The historical CTD salinity data included data from the last two decades (2001–2021) and excluded data from nearfield stations (F29, F30, F31 for PLOO; I12, I14, I15, I16 for SBOO). Historical CTD data averages and percentiles were calculated within a similar depth range for each mooring sensor (1–3 m for the surface bin for both RTOMS; other target depths spanned ±3 m for PLOO and ±1 m for SBOO). Salinity anomalies from RTOMS data were then calculated as the difference between the historical CTD average for each depth range and the daily means for each RTOMS sensor depth. Relatively low subsurface salinities (33.2–33.5 Practical Salinity Unit [PSU]) are frequently observed in the San Diego region (City of San Diego 2020a), likely influenced by seasonal evaporation at the surface and the incursion of the low salinity and low temperature Pacific Subarctic water mass within the California Current System (Lynn and Simpson 1987, Jones et al. 2002). Therefore, RTOMS salinity anomalies were compared to minimum CTD salinity observations at each depth range using the 99th percentile, in order to assess for high likelihood of potential influence from freshwater effluent plumes.

While previous studies in the region used salinity signatures to estimate effluent dilution near outfalls (e.g., Washburn et al. 1992), more recent work has improved upon the impracticality of discerning effluent plumes using salinity signatures alone by examining additional identifying characteristics such as elevated CDOM (Rogowski et al. 2012a,b, 2013, City of San Diego 2016a). Initial analyses of other parameters (i.e., CDOM, turbidity, nitrate + nitrite, BOD) that may aid in potential plume detections by the PLOO and SBOO RTOMS are presented, where an example is highlighted for each site along with challenges in deciphering plume signals. Further work will be completed to evaluate potential wastewater plume detections by RTOMS throughout the year in future reports.

ROTV

Deployment and Configuration

The ScanFish III is a wing-shaped ROTV that is towed behind the sampling vessel using a "live-wire" tow cable with ethernet communication capabilities to surface computing platforms aboard the sampling vessel. The surface computing platforms control the ROTV and process, display, and record data as the data are collected. Using surface communication, the ROTV can be programmed to sample a variable depth range in the water column, moving in an undulating pattern from ocean surface to seabed, or moving in a fixed depth or terrain-following mode. Its large payload enables a variety of modular sensors to be outfitted to the vehicle frame. The City's current package includes a Sea-Bird SBE 25 Plus CTD with a Sea-Bird pump, temperature, conductivity, DO, and CDOM sensors, and three Turner Designs Cyclops-7F fluorometers tuned for CDOM, Tryptophan and Optical Brightener (OB) measurements, and a Chelsea BOD sensor.

During all surveys, vessel speed while towing the ROTV was kept below 11 knots. The tow cable payout varied from 200 to 600 m depending on the depth of the transect and vessel speed. Data from the ROTV were continuously monitored in real-time to ensure instrument function. Fathometer readings from both the ROTV and the shipboard instruments were also closely monitored to ensure capture of the largest possible portion of the water column without damage to the ROTV. To prevent altimeter errors, the ROTV was typically flown no less than 10–15 m below the surface, especially after May 2020, when shallow depths were determined to be a cause of altimeter failure. To prevent collision with the seafloor, the ROTV was kept 5–15 m from the bottom.

Data Collection

City staff have been evaluating the use of the ROTV for plume tracking as part of an ongoing project (City of San Diego 2020b, 2022a,b). The initial goal of the project was to compare towed

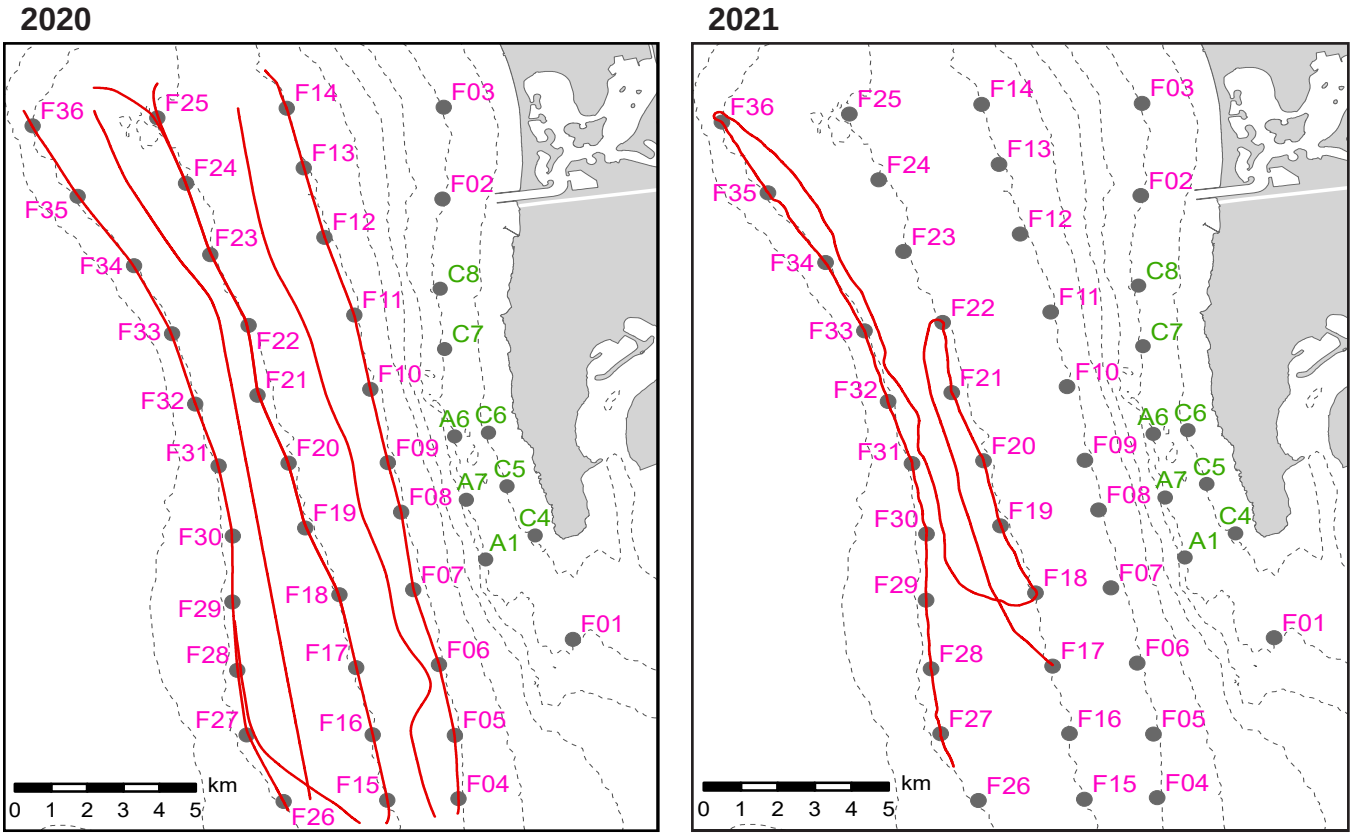

Figure 4.2

The ROTV tow path for surveys conducted in the PLOO region during the winter of 2020 and 2021. In 2020, sampling was conducted parallel to the regular offshore water quality stations. In 2021, the sampling path was altered to concentrate sampling in the area where the plume was observed in the data by observers on the vessel in real-time.

CTD measurements from the ROTV to traditional fixed grid vertical-profile CTD measurements during each quarterly water quality sampling period in 2020 and 2021. Surveys were initially conducted solely in the PLOO region to help develop ROTV survey methods. The PLOO region was surveyed during winter (February 18–19, 2020 and February 23, 2021), spring (May 19–21, 2020, May 19, 2021, and June 3, 2021), summer (August 18–20, 2020), and fall (November 10–13, 2020). ROTV efforts in the first three quarters of 2020 were focused on cross-validation of ROTV data against CTD data collected during quarterly offshore surveys. As such, the ROTV tows were conducted in parallel with regular quarterly water quality sampling. The ROTV was towed through water quality stations along the 98, 80, and 60-m transects each quarter over three consecutive days, except for the month of May 2020, during which the 60-m transect and portions of the 80-m transect were not captured due to instrument failure after the first day of sampling. Beginning in November 2020, ROTV surveys were conducted adaptively, so survey efforts were focused on areas and depths where there was evidence of the potential PLOO plume (typically where elevated CDOM and/or OB values were observed in real-time). ROTV surveys did not, therefore, follow the same spatial pattern as surveys conducted in other quarters. For example, the winter 2020 (February) PLOO ROTV survey track followed the fixed grid station isobaths, while the winter 2021 survey track was adjusted in real-time in order to maximize observations of potential plume signals (Figure 4.2). The City has a single vessel, the M/V *Oceanus,* equipped with a conducting winch capable of ROTV towing. In July

2021, the *Oceanus* suffered catastrophic engine failure resulting in being out of service until May 2022. Due to the loss of this sampling capability, ROTV surveys were not completed during summer and fall 2021.

The ROTV surveys in the SBOO region have proven to be significantly more problematic than the PLOO surveys due to the complicated hydrography, proximity of multiple sources of organic material (i.e., Tijuana River, San Diego Bay), shallower depths in comparison to the PLOO region survey area, and a high abundance of fishing gear and abandoned equipment in the area during all times of the year. During the SBOO fall survey in 2020, the ROTV became entangled in fishing gear, resulting in contact with the seafloor and significant damage to the ROTV structure. Because of these issues, results from ROTV surveys were limited to summer (August 8) and fall (November 3–4) of 2020. To help distinguish potential wastewater plume signals from other freshwater plumes, some surveys were compared with satellite imagery taken from a similar timeframe (Figure 4.3) (Ocean Imaging 2020).

Data Processing and Analysis

Data from the ROTV were processed and displayed in real-time via onboard computers, and were checked for anomalous sensor readings that may have indicated either possible plume detection or equipment malfunction during data collection. For analyses presented herein, data outside of climatological ranges established for RTOMS QA/QC were flagged as suspect and removed from analysis, as were data that appeared suspect upon initial manual review. Further QA/QC protocols for ROTV data are in development.

Data from the ROTV surveys were analyzed using the R programming language (R Core Team 2021), employing functions within various packages (i.e., tidyverse, marelac, fields) (Wickham et al. 2019, Soetaert et al. 2020, Nychka et al. 2021). In order to visualize the spatial extent of potential plume signals from data collected during ROTV surveys, heat maps of the data from single transects (isobaths) were created by interpolating data between points using a locally estimated scatterplot smoothing (LOESS) regression using the R package "stats" (R Core Team 2021) and were overlaid with the ROTV track showing the actual location of the ROTV measurements in the water column.

Within the array of data collected during the ROTV surveys, CDOM and OB were found to have the strongest correlation to potential plume signatures (Cao et al. 2009, Terrill et al. 2009, Rogowski et al. 2012a,b, 2013). OB fluorescence has similar confounding issues as CDOM which limit its interpretation of these data in the absence of chlorophyll *a* fluorescence measurements (Cao et al. 2009, Hagedorn and Weisberg 2009). However, ongoing refinement of ROTV sensor technology integration and data analysis methodologies may lead to increasingly reliable plume detection. For the purposes of this initial analysis, only CDOM and OB values were plotted along select depth contours for both the PLOO and SBOO regions.

Results and Discussion

Potential Plume Signals Determined via CTD

PLOO Region

The dispersion of the treated wastewater plume from the PLOO and its effects on natural light (% transmissivity), DO, and pH levels were assessed by evaluating the results of 328 CTD profile casts performed in 2020 and 2021. Based on the criteria described previously (City of San Diego 2016a,b), potential evidence of a plume signal was detected 42 times during the year from 17 different stations, while up to 21 stations were identified as reference sites during each quarterly survey (Table 4.1, Figure 4.4, Appendix E.3). No stations were identified as reference sites during May 2020 in the PLOO region due to an exceptional regionwide phytoplankton bloom (see Chapter 2). Decaying phytoplankton are a significant source of CDOM (e.g., Rochelle-Newall and Fisher 2002, Romera-Castillo et al. 2010) and their prevalence created conditions where CDOM values from all

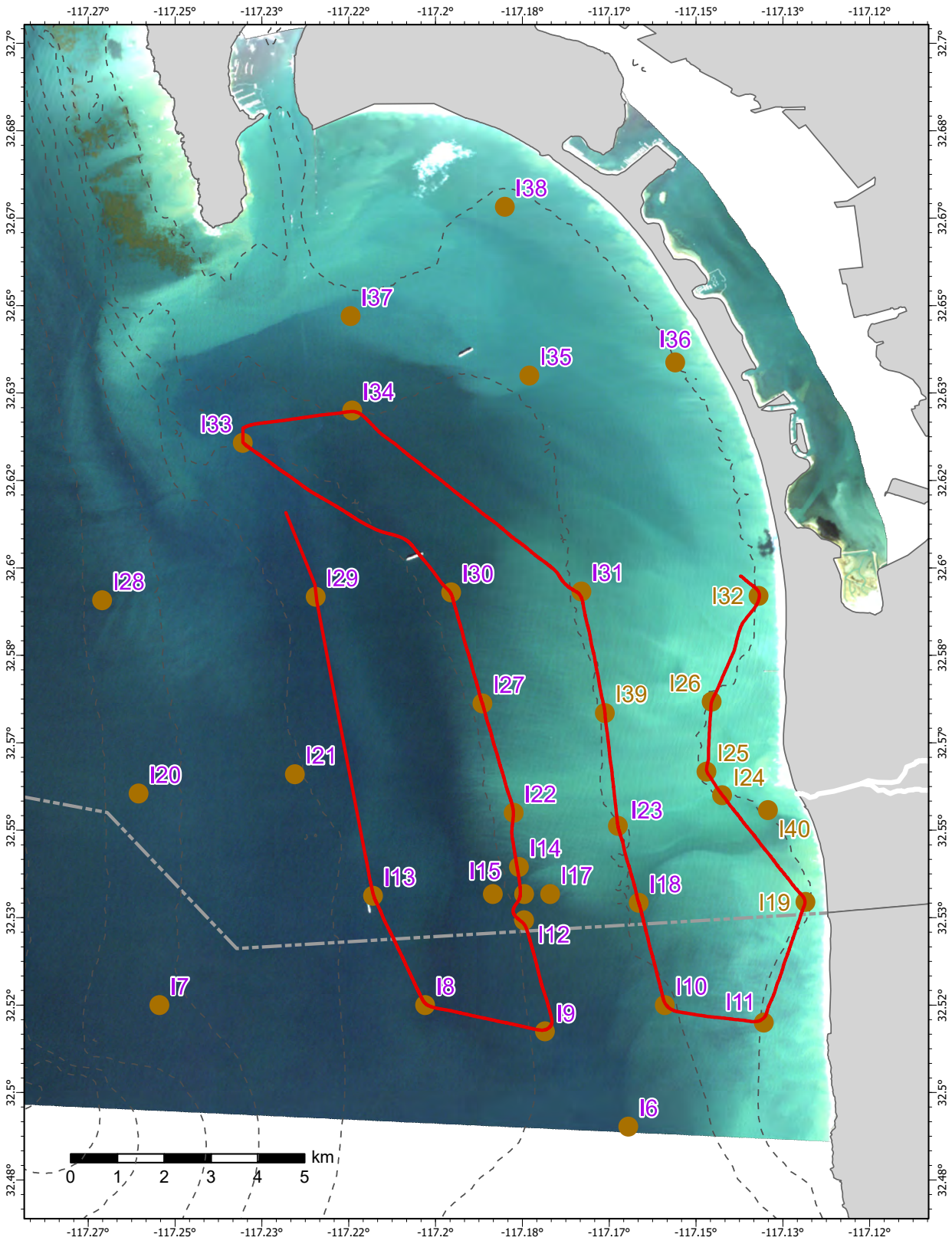

Figure 4.3

The ROTV tow path for the fall 2020 survey in the SBOO region. Sampling was conducted parallel to the regular offshore water quality stations.The tow path is overlaid on an image taken by the Spot 6 satellite on November 9th, 2020 (Ocean Imaging 2020). Turbid water is seen extending from the shoreline out across the tow path.

Table 4.1

Summary of the numbers of reference stations, potential wastewater plume detections, and out-of-range values at offshore stations during 2020 and 2021. DO = dissolved oxygen; XMS = transmissivity.

PLOO

	Reference Stations	Potential Plume Detections	Out of Range		
			DO	pH	XMS
2020					
Feb	21	8	8	0	2
May	0[a]	2	0	0	0
Aug	16	5	0	0	0
Nov	19	6	1	0	1
2021					
Feb	17	5	0	0	1
May	12	4	0	0	4
Aug	17	4	0	0	3
Nov	20	8	0	0	0
Detection Rate (%)		13	3	0	3
Total Count		42	9	0	11
Total Samples		328	328	328	328

SBOO

	Reference Stations	Potential Plume Detections	Out of Range		
			DO	pH	XMS
2020					
Feb	20	2	0	0	1
May	11	4	1	0	4
Aug	10	4	0	0	2
Nov	14	6	2	0	0
2021					
Feb	13	4	0	0	0
May	15	3	0	0	0
Aug	18	5	0	0	0
Nov	11	3	0	0	2
Detection Rate (%)		13	1	0	4
Total Count		31	3	0	9
Total Samples		232	232	232	232

[a] Due to the exceptional algal bloom in May 2020, no sites in the PLOO region were appropriate as reference stations

stations exceeded the 85th percentile at some point in their water column profile. In August 2020, all reference stations were shallower than potential plume detection depths, preventing comparisons of reference values for compliance evaluation. About 40% of casts showing possible plume detections (n = 17) occurred at the three stations located closest to the outfall (F29, F30, F31), equating to a detection rate of 71% at these nearfield sites over the past two years. All other possible detections occurred at stations along the 80 or 98-m depth contours, located between 13 km to the north and 8 km to the south of the outfall. Overall, the variation in plume dispersion observed near Point Loma in 2020 and 2021 appeared similar to flow-mediated dispersal patterns reported previously for the region (Rogowski et al. 2012a,b, 2013).

The width and rise height of potential PLOO plume detections varied between stations throughout the year (Figure 4.5, Appendix E.3). Despite fluctuations in depth of the pycnocline, plume detections remained below 44 m even during periods of weak water column stratification. Additionally, detection depths were similar between nearfield and farfield stations. This finding aligns with historical satellite imagery observations that have not shown visual evidence of the plume surfacing (e.g., Svejkovsky 2010, Hess 2019, 2020, 2021). About 62% (n = 26) of the potential plume detections corresponded with elevated *Enterococcus* densities, all of which were collected at depths at or below 60 m (City of San Diego 2020–2022a).

Of the 42 potential plume signals that occurred during the reporting period, a total of 20 out-of-range (OOR) events were identified at various stations throughout the year, which consisted of 11 OOR events for natural light and 9 OOR events for DO (Table 4.1, Appendix E.3). Representative quarterly profiles from station F30 are shown in Appendices E.4–E.11. There were no OOR events for pH. Only two of the natural light OOR events and one of the OOR events for DO occurred at stations located within State jurisdictional waters where Ocean Plan compliance standards apply (i.e., stations F18–F20).

SBOO Region

The dispersion of the SBOO plume and its effects on natural light, DO and pH levels were assessed by evaluating the results of 232 CTD profile casts performed in 2020 and 2021. Potential evidence of a plume signal was detected 31 times during the reporting period from 17 different stations, while 10–20 stations were identified as reference sites during each quarterly survey (Table 4.1, Figure 4.4, Appendix E.12). About 45% of the possible detections (n = 14) occurred at nearfield stations (i.e., I12, I14, I15, I16). None of these plume detections were associated with elevated FIB (City of San Diego 2020–2022b). Other potential plume signals at farfield stations may be associated with their proximity to known sources of organic matter. For example, station I34 is located within the influence of San Diego Bay tidal pumping, while stations I23 and I27 are located within the possible influence of Tijuana River outflows.

The width and rise height of potential SBOO plume detections varied between stations throughout the reporting period (Figure 4.5, Appendix E.12). Unlike the observations at the PLOO, potential SBOO plume signals were detected throughout the water column, ranging from 2 to 29 m with a median depth of 13 m. However, as with the PLOO, potential plume detection depths in the SBOO region were similar between nearfield and farfield stations.

The effects of the SBOO wastewater plume on the three physical water quality indicators described above were calculated for each station and depth where a possible plume signal was detected (Table 4.1, Appendix E.12). Representative profiles from station I12 are shown in Appendices E.13–E.20. Of the 31 potential plume signals that occurred during the reporting period, a total of 9 OOR events were identified for transmissivity, while three OOR events occurred for DO. There were no OOR events for pH. Ten of the 12 OOR events occurred at stations within State jurisdictional waters where Ocean Plan compliance

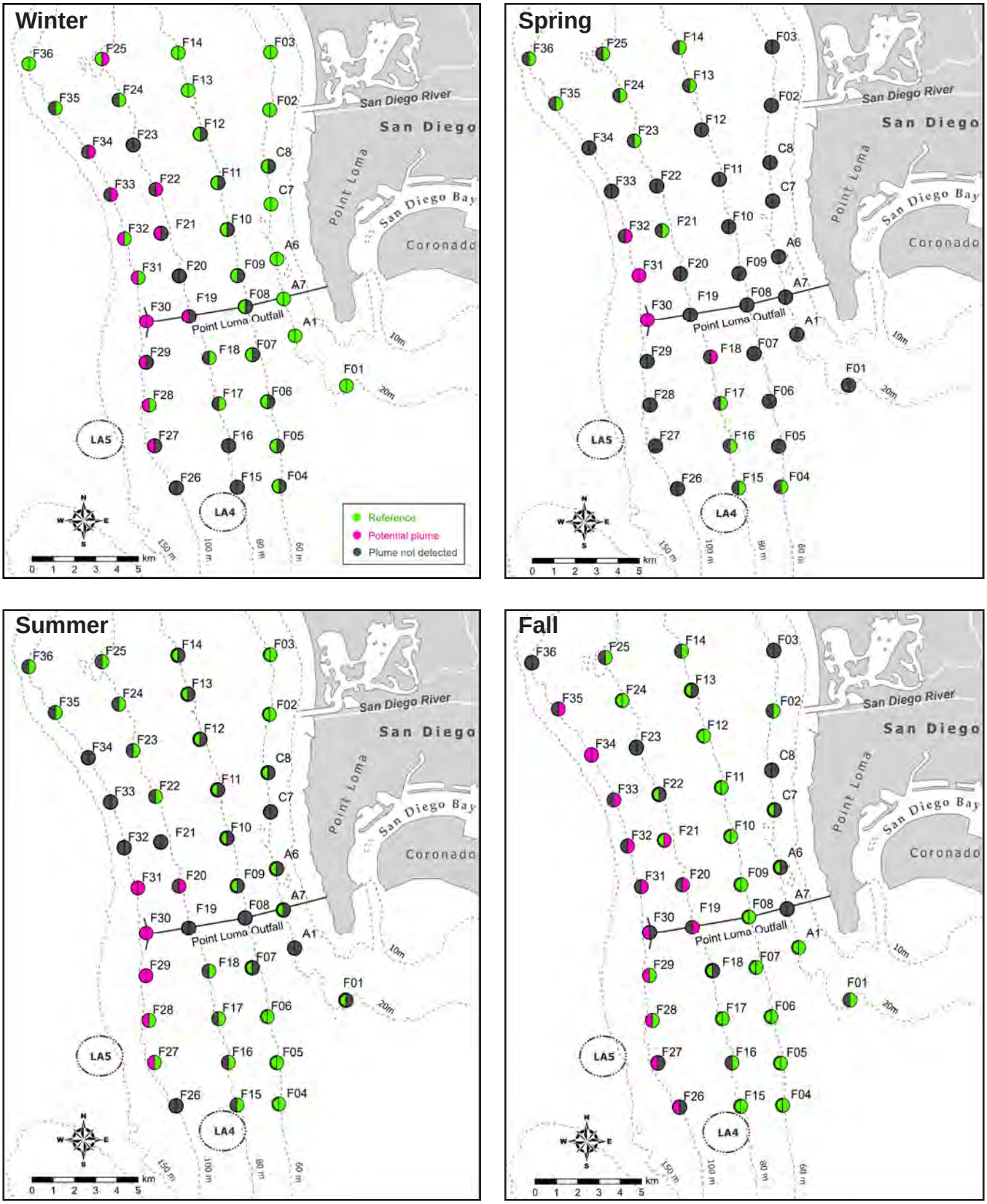

Figure 4.4

Distribution of stations meeting potential plume criteria (pink) and those used as reference stations (green) near the PLOO (this page) and SBOO (facing page) during quarterly surveys in 2020 (left half of pie) and 2021 (right half).

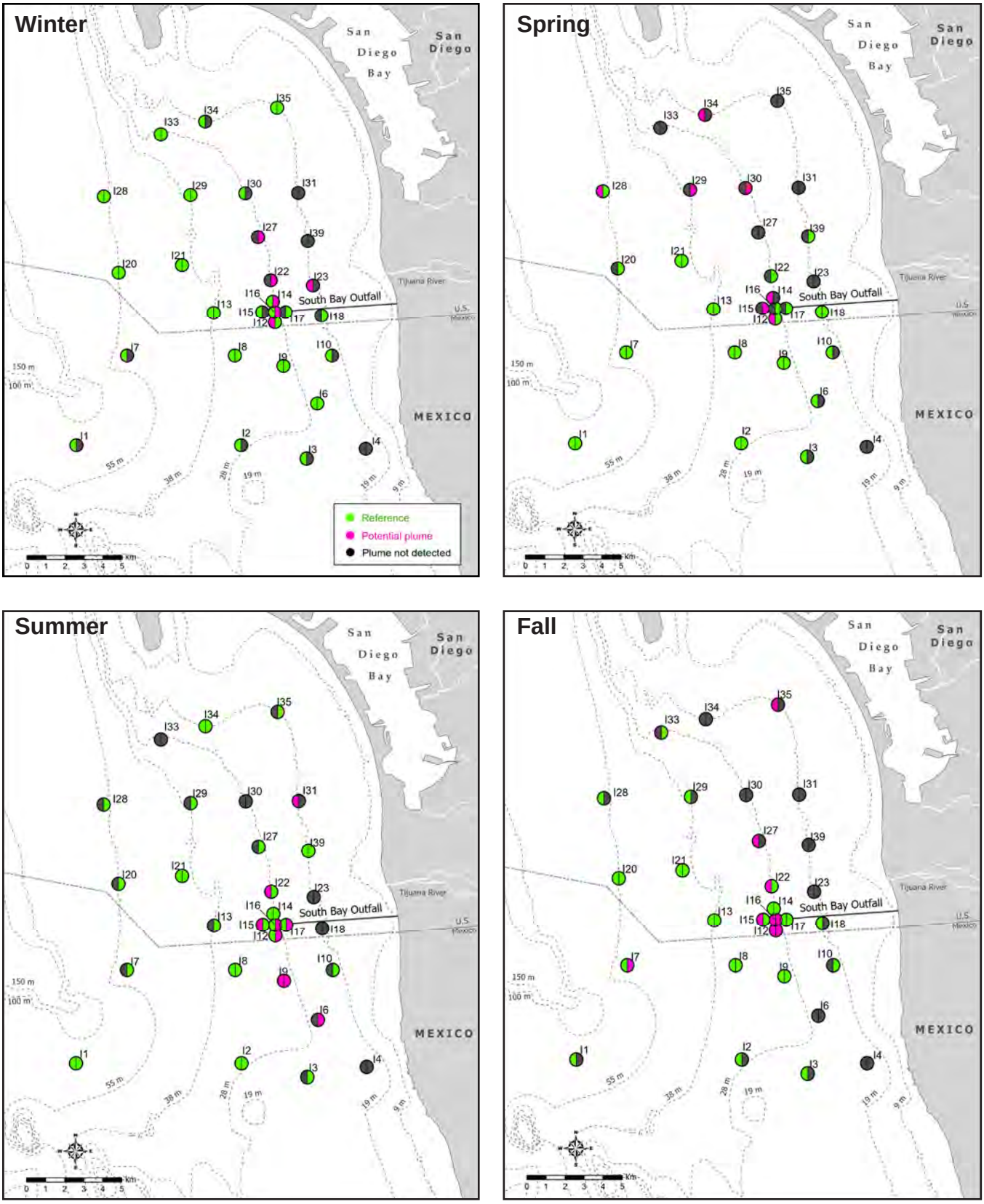

Figure 4.4 *continued*

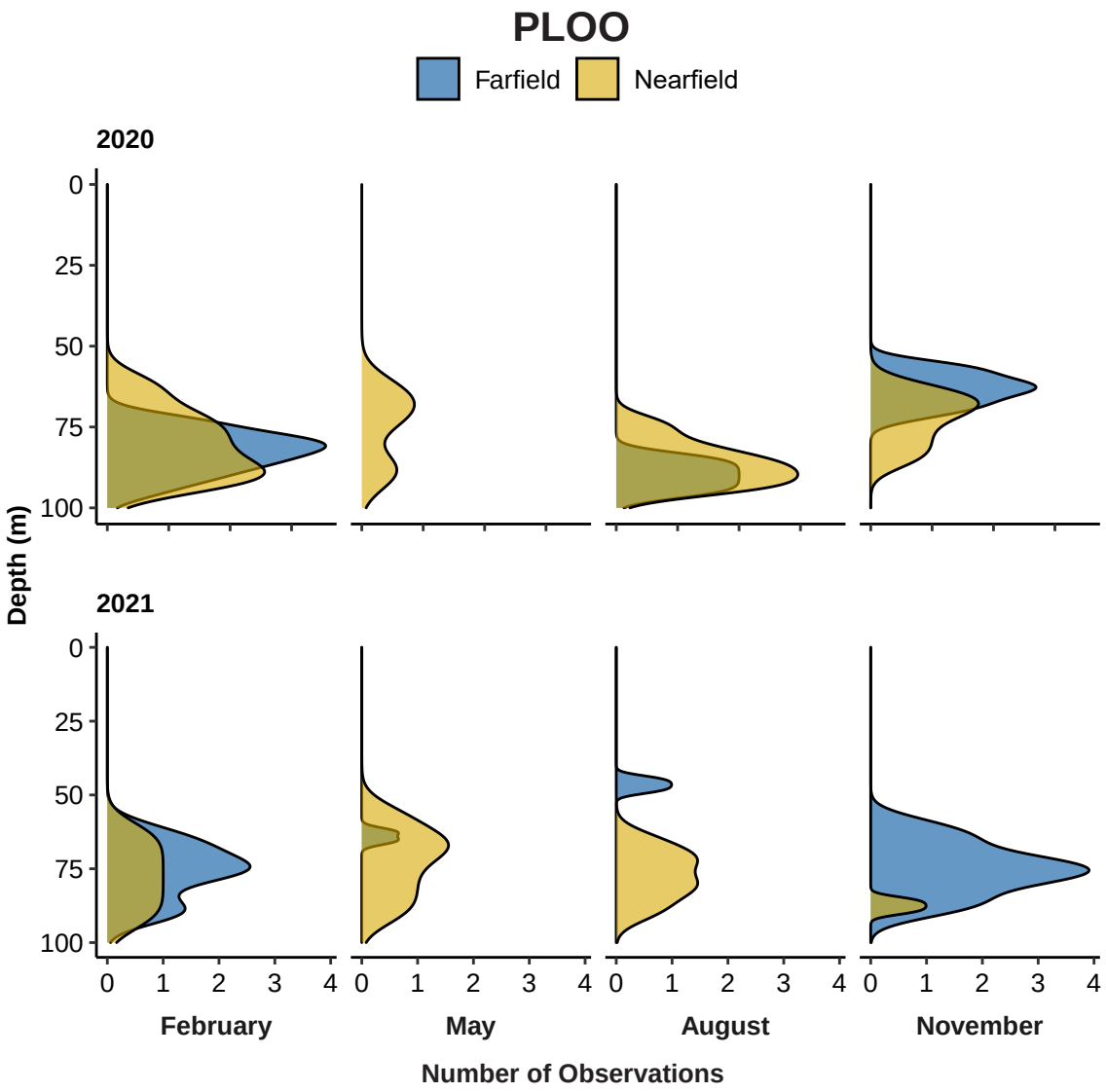

Figure 4.5
Depth profiles by season of the number of potential plume detections at PLOO and SBOO offshore stations during 2020 and 2021. Nearfield stations for PLOO are F29, F30, F31; nearfield stations for SBOO are I12, I14, I15, I16. Histograms smoothed using a kernel density estimate.

standards apply, with four of these events occurring at nearfield stations I12, I14, I15, or I16.

Receiving Waters Conditions and Potential Plume Signals Determined via RTOMS

Receiving Waters Conditions

Ocean conditions surrounding the PLOO and SBOO RTOMS that could potentially affect the dispersion of wastewater plumes, such as ocean currents and density structure of the water column, were generally within historical ranges and align with expected seasonality patterns for the region (see Chapter 2; Terrill et al. 2009, Rogowski et al. 2012a, City of San Diego 2022c).

Changes in ocean stratification are primarily influenced by water column temperature structure in the region, where larger differences in temperature between depths (thermal gradients) result in stronger stratification (see Chapter 2; Bowden 1975, Jackson 1986, Pickard and Emery 1990). The weakest thermal stratification (<0.2°C/m) was observed during late fall and winter months (December through February) in 2020 and 2021, with daily maximum thermal gradients occurring more frequently at mid

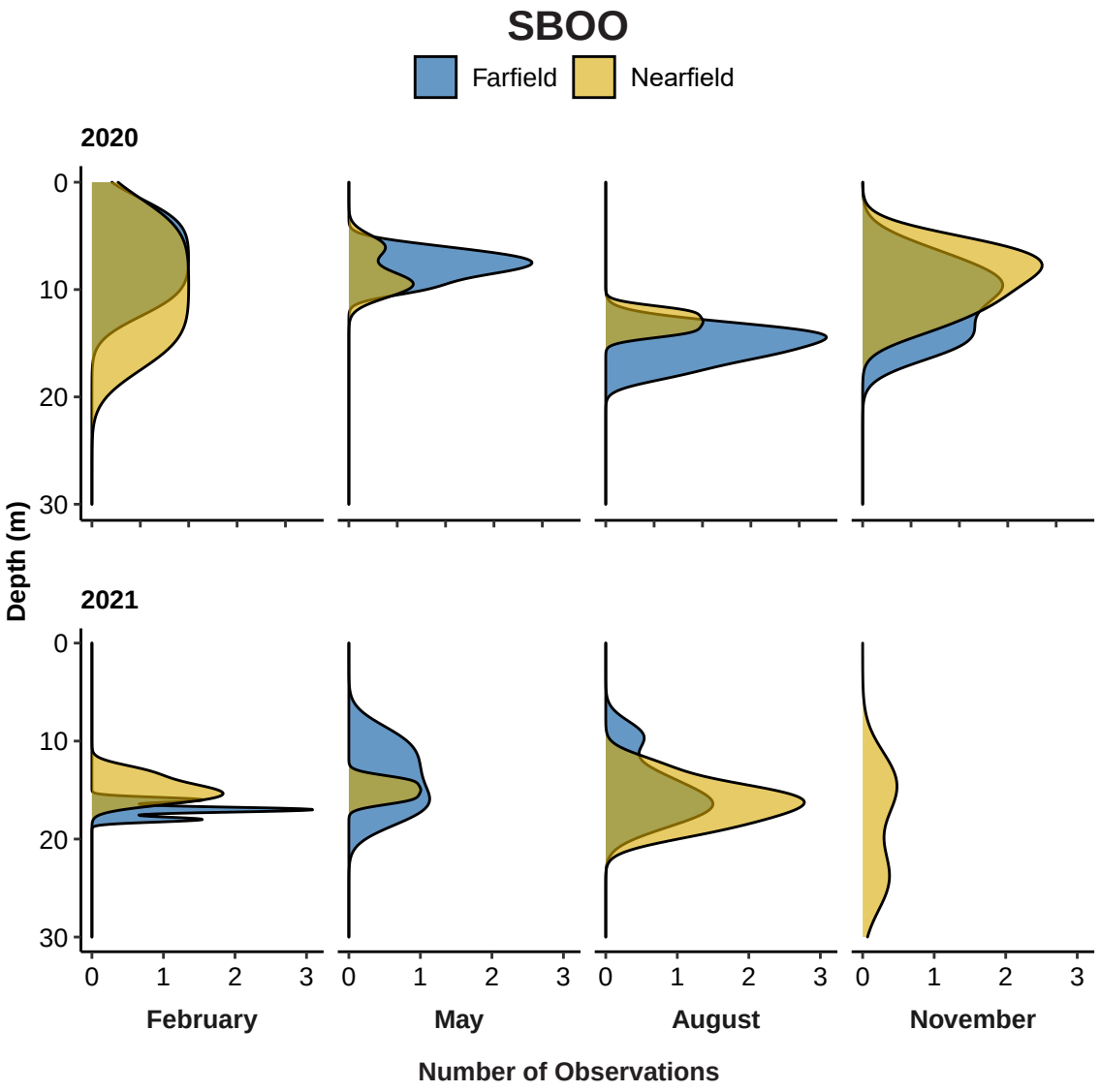

Figure 4.5 *continued*

to deep depths (PLOO: 26–70m; SBOO: 22–34m) (Appendix E.21). Conversely, moderate (>0.2°C/m) to strong (>0.5°C/m) daily thermal stratification persisted from spring to fall (April through October) in 2020 and 2021 at shallower depths (PLOO and SBOO: <10 to 18m), with more variability in stratification occurring during transition months in the spring and fall (March and November) of both years. As described in the CTD results in this chapter, previous monitoring results have consistently shown that the PLOO plume remains at depth even during periods of weak stratification, while the SBOO plume may have a greater likelihood of reaching the surface during these periods when the water column is more mixed (Figure 4.5).

Ocean currents predominantly flowed along a north-northwest/south-southeast axis of variation near the PLOO and SBOO (Appendices E.22, E.23). Generally, along-coast currents tended to dominate, regardless of season (see Chapter 2). Variability in currents occurred throughout 2020 to 2021, with distinct periods of predominantly N:NW and S:SE directed currents throughout the water column from days to weeks at a time (Appendices E.22, E.23). Transitions in current direction and speed often indicate a shift in local conditions that may also result in further mixing of the water column, especially when there is increased vertical shear (i.e., one section of the water column moving in a different direction than the other part of the water column)

(see Pickard and Emery 1990). Additionally, ocean currents in the vicinity of the outfalls can influence the initial rise height and horizontal dispersion of the wastewater effluent plumes, as well as the rate of transport of effluent out of the discharge area on longer time scales (days to weeks) (City of San Diego 2022c).

PLOO Region

At the PLOO RTOMS, the lowest salinity values (daily average values <33.2 PSU) were observed from 60 to 89 m in the winter and late summer of 2020 (Figure 2.8, Chapter 2). Anomalously low salinity measurements from the PLOO RTOMS have occurred at these deep depths throughout prior deployments regardless of season and are lower than what has historically been reported from CTD data or the more recent ROTV surveys (Figure 4.6). In addition, these depths of lowest salinities overlaped with other observations of potential PLOO plume rise heights (Figure 4.5; Rogowski et al. 2012a). Given the proximity of the mooring to the PLOO, these low salinity values at deep depths (>45 m) may likely be attributable to the effluent plume. Additionally, the observations by the RTOMS of record-low salinities in deep waters near the PLOO were likely due to the increased frequency of sampling that captured a larger range of variability, as well as a potential reduction in mixing between the freshwater effluent plume and ocean water masses by the equipment itself. For example, the mooring instruments are suspended passively in the water column at a fixed location, while large towed or profiling packages such as the ROTV or CTD rosette may result in turbulence and additional mixing as moved through the water (e.g., Paver et al. 2020). Given these factors, it is expected that the potential presence of the plume may be better discerned using salinity at the RTOMS as a supplement to other methods.

Auxiliary measurements from RTOMS, such as CDOM, were also assessed to assist with possible plume detection. Time periods with a strong potential for plume detection (e.g., low salinities at typical plume depths) and fewer confounding factors (such as during dry periods or low phytoplankton concentrations) may be targeted initially to identify other possible plume characteristics. As one example, near the PLOO in late January to early February 2020, possible plume detections were evident from low salinity values at depths from 60 to 89 m (Figure 4.7). Beginning February 3, the plume appeared to be advected away from the sensors by a shift in currents to a more south-easterly direction. During the same period, drops in salinity at 89 m coincided with slightly elevated CDOM and turbidity levels that were not observed at mid-depth (30 m) (Figure 4.7). Nitrate + nitrite measurements were relatively low for this time period compared to other periods (Appendix C.12, City of San Diego 2021), which align with the typical PLOO effluent's relatively low nitrate proportion of nitrogen (see City of San Diego 2020–2022c, CSWRCB 2022). This range falls within a similar range of ambient ocean nitrate levels (see Weber et al. 2021). Generally, higher nitrate levels were observed in cold, high salinity water masses during winter 2020, while slightly elevated CDOM levels tended to occur at warmer temperatures and lower salinities (Figure 4.8). This supports the role of upwelling in bringing cold, saline, nutrient-rich, oxygen-poor water masses into the region (see Chapter 2, Weber et al. 2021). During the PLOO RTOMS deployments in 2020–2021, BOD levels were not found to be a useful indicator of possible plume presence (see Appendix C.12). Overall, salinity observations, used in conjunction with CDOM, turbidity, and chlorophyll *a* levels, provide potential evidence of effluent plume signals at the PLOO RTOMS and further work will be completed to better evaluate these detections throughout the year.

SBOO Region

At the SBOO RTOMS, the detection of potential SBOO plume signals was often not discernable solely by examining salinity values. The lowest salinity anomalies, where daily average values were significantly less than 33.1 PSU, occurred in the first SBOO RTOMS deployment from 10 to 18 m in the summer and early fall of 2017, and were not observed in subsequent years (Figure 4.6). Auxiliary mooring measurements that could aid in plume detection, such as CDOM, were not available

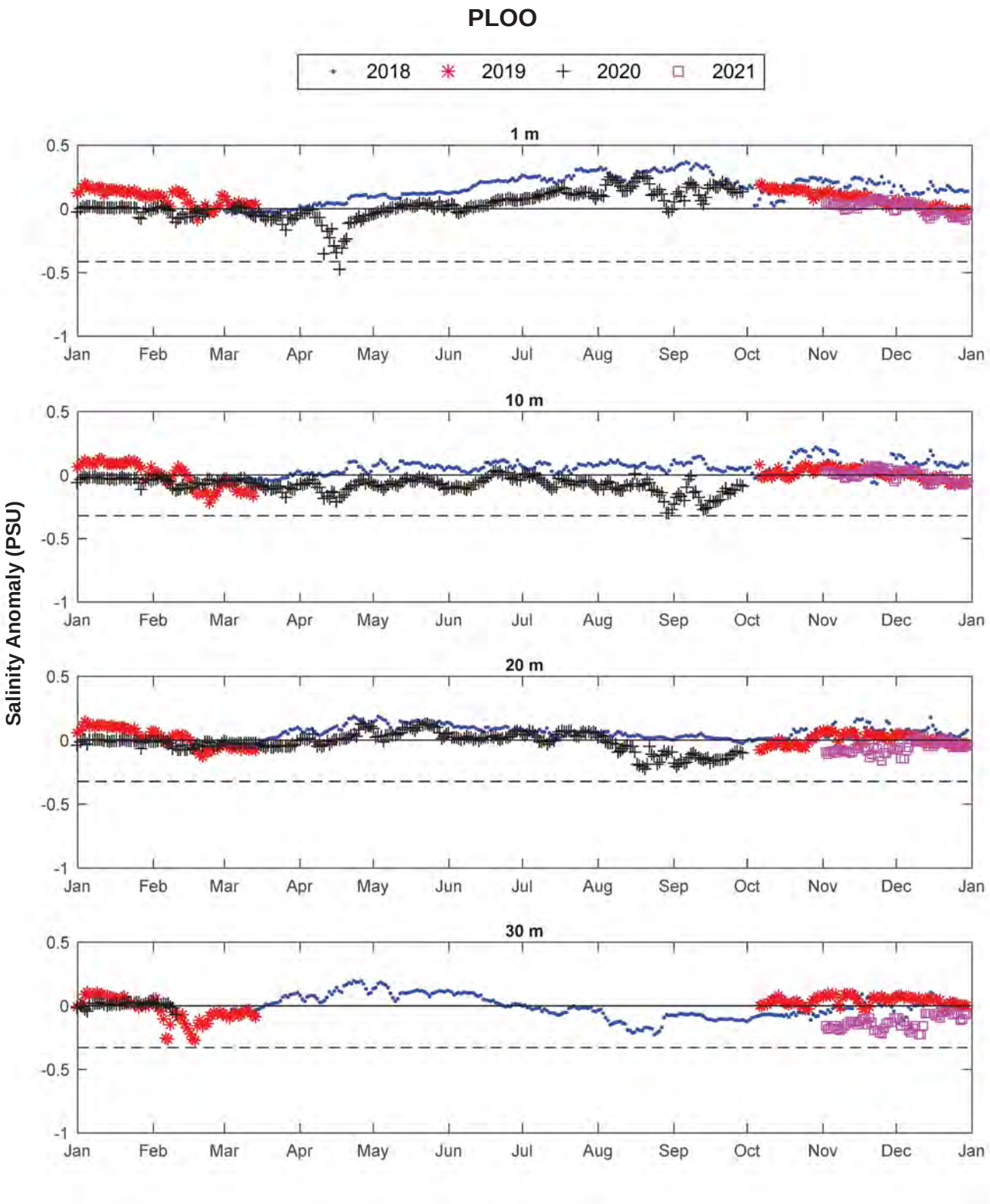

Figure 4.6

Daily averaged salinity anomalies by year for each mooring sensor depth using available RTOMS data (2018–2021 for PLOO and 2017–2021 for SBOO). Anomalies calculated from historical CTD survey data from 2001–2021 for each monitoring region and depth range, excluding nearfield stations (see text). Dashed line indicates 99th percentile minimum from CTD survey data.

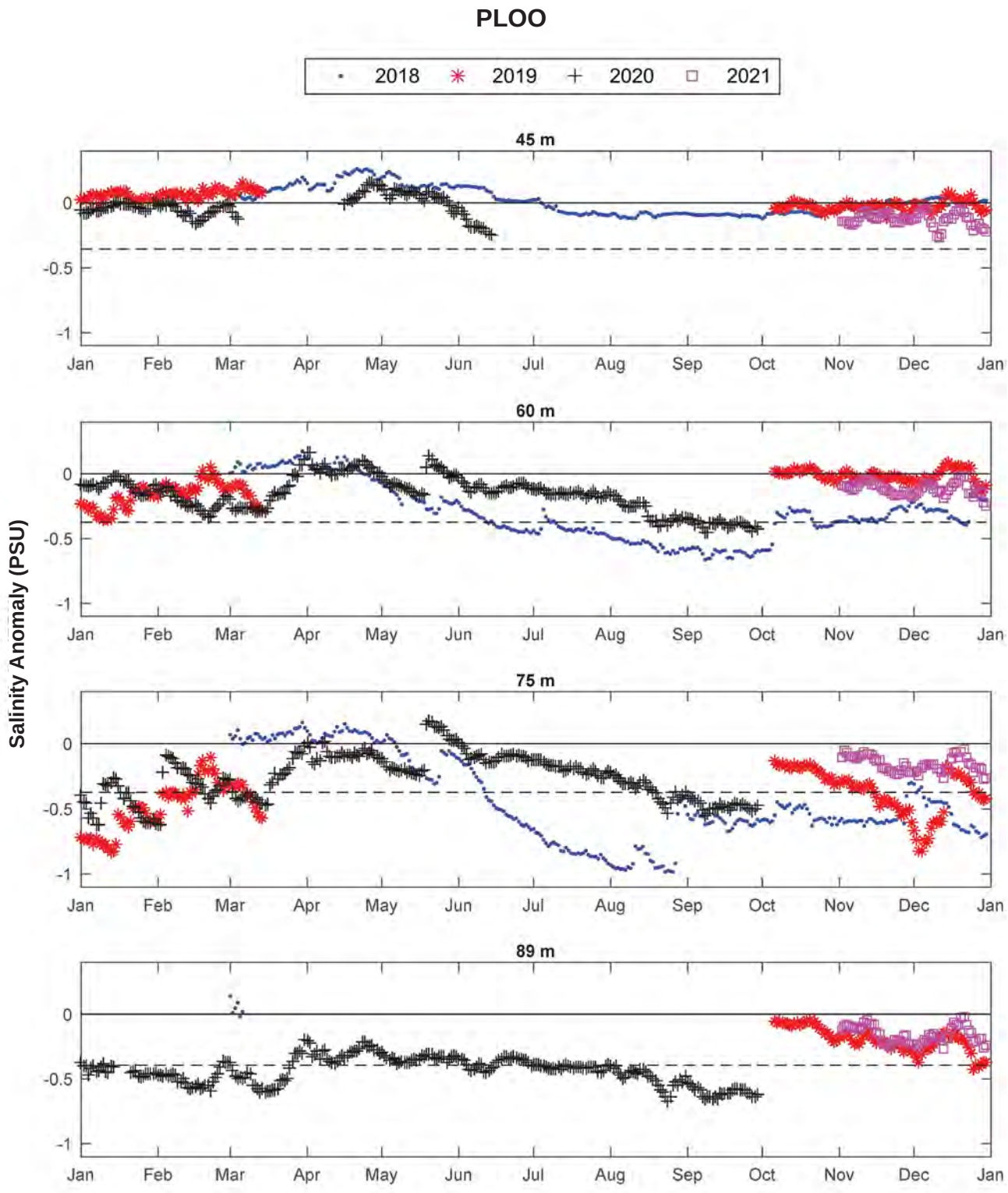

Figure 4.6 *continued*

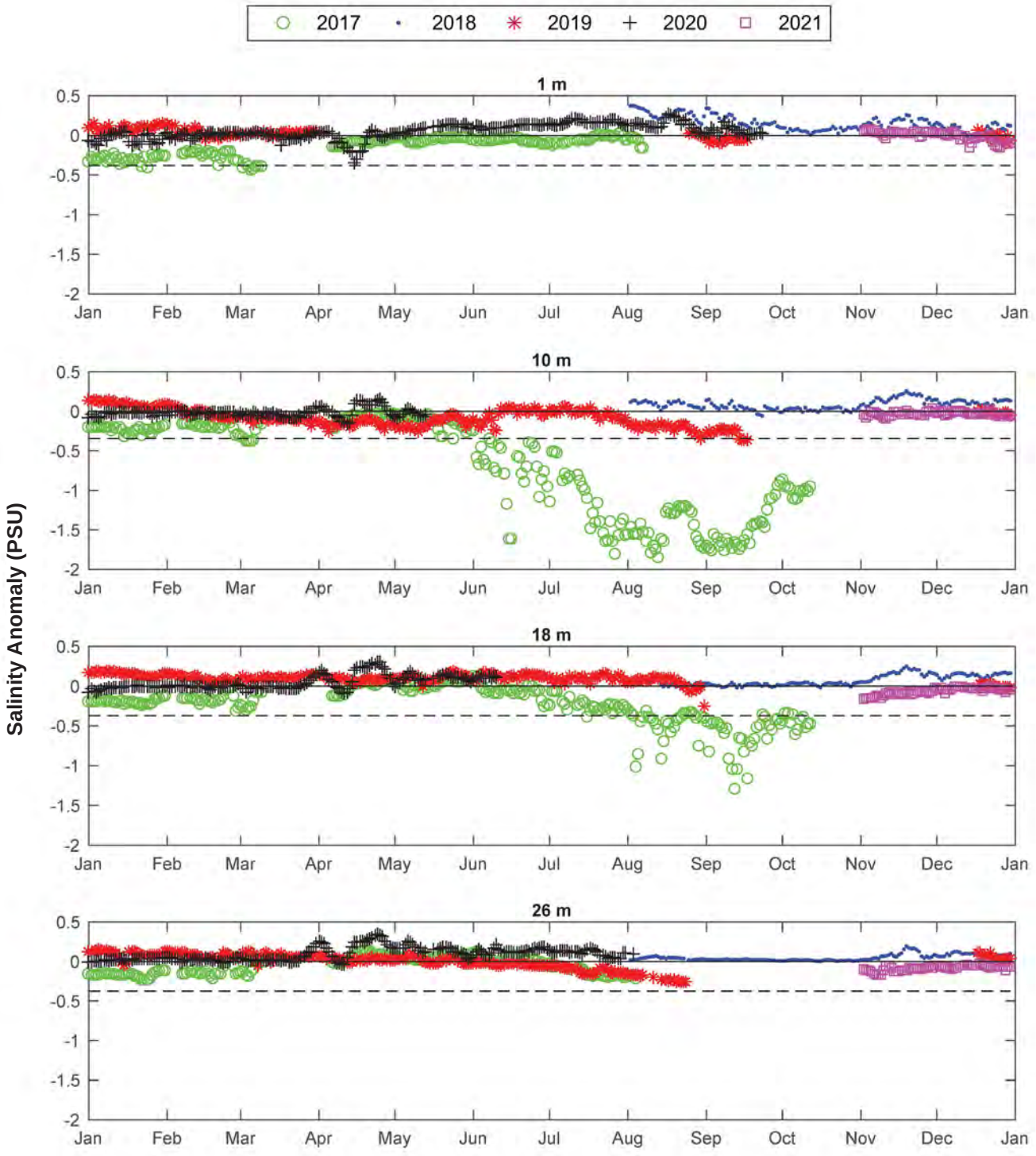

Figure 4.6 *continued*

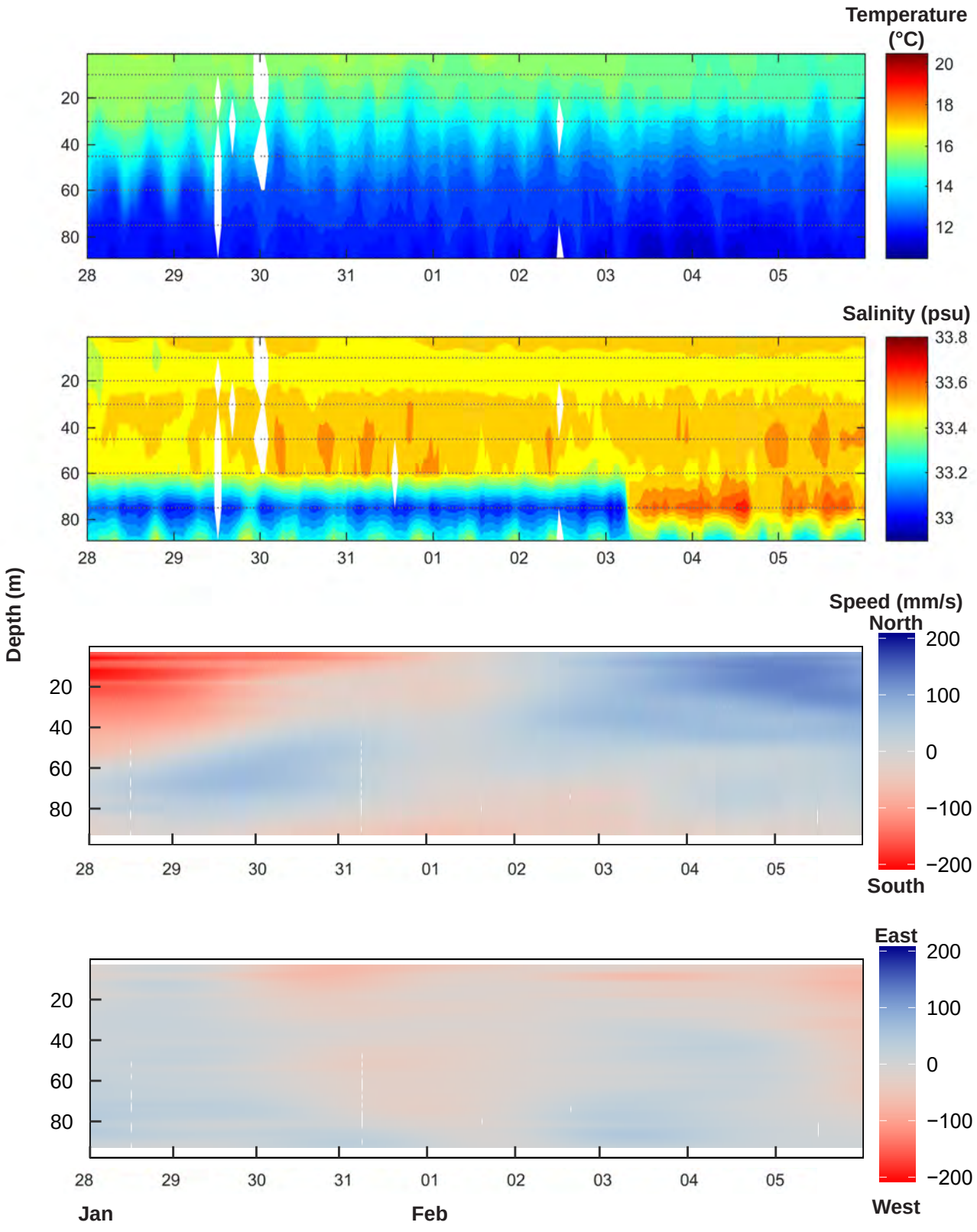

Figure 4.7

PLOO RTOMS hourly averaged ocean temperature, salinity, and current speeds (tides removed) interpolated for entire water column plus chlorophyll *a* (chl), CDOM, turbidity, and nitrate + nitrite for select depths during the week of January 28–February 5, 2020. Gaps and white areas indicate loss of data due to instrumentation issues or failure to meet data quality criteria (see text).

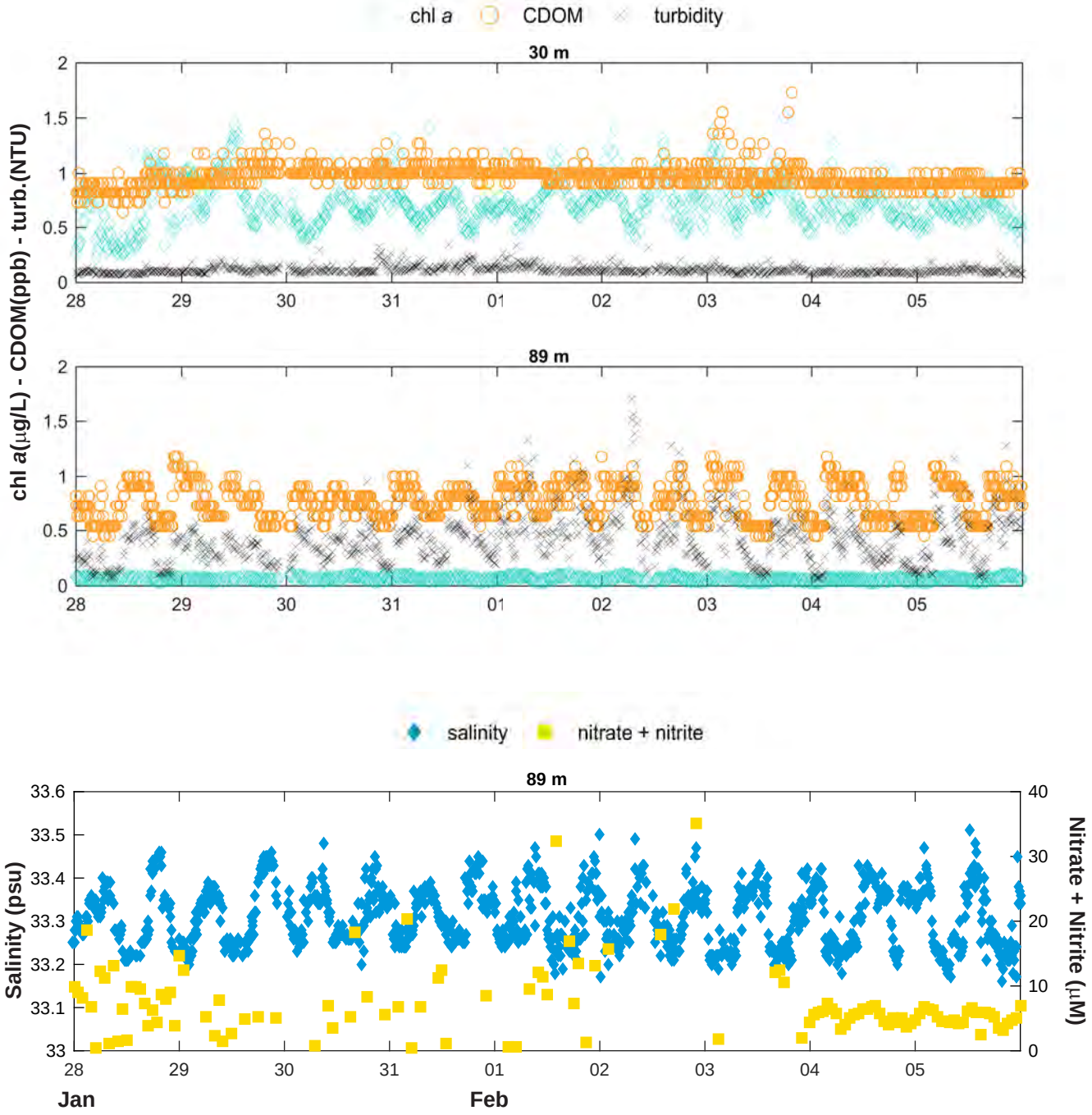

Figure 4.7 *continued*

at these depths during the same time period. In order to target possible plume characteristics, time periods were examined in the same manner as the PLOO RTOMS data (e.g., during dry periods and low phytoplankton concentrations) where other parameters, in addition to salinity, were available. As one example, during late January to early February 2020 near the SBOO, weak stratification and currents alternating between southeasterly and northwesterly occurred on the same days as observations of slightly reduced salinity near the surface and mid depths (1–10 m) (Figure 4.9). Additionally, these lower salinity periods coincided with slightly elevated CDOM, turbidity, and nitrate + nitrite levels at the surface, while these characteristics were not observed at the deepest sensor depth (26 m) of the mooring (Figure 4.9). Taken together, these near surface signals may

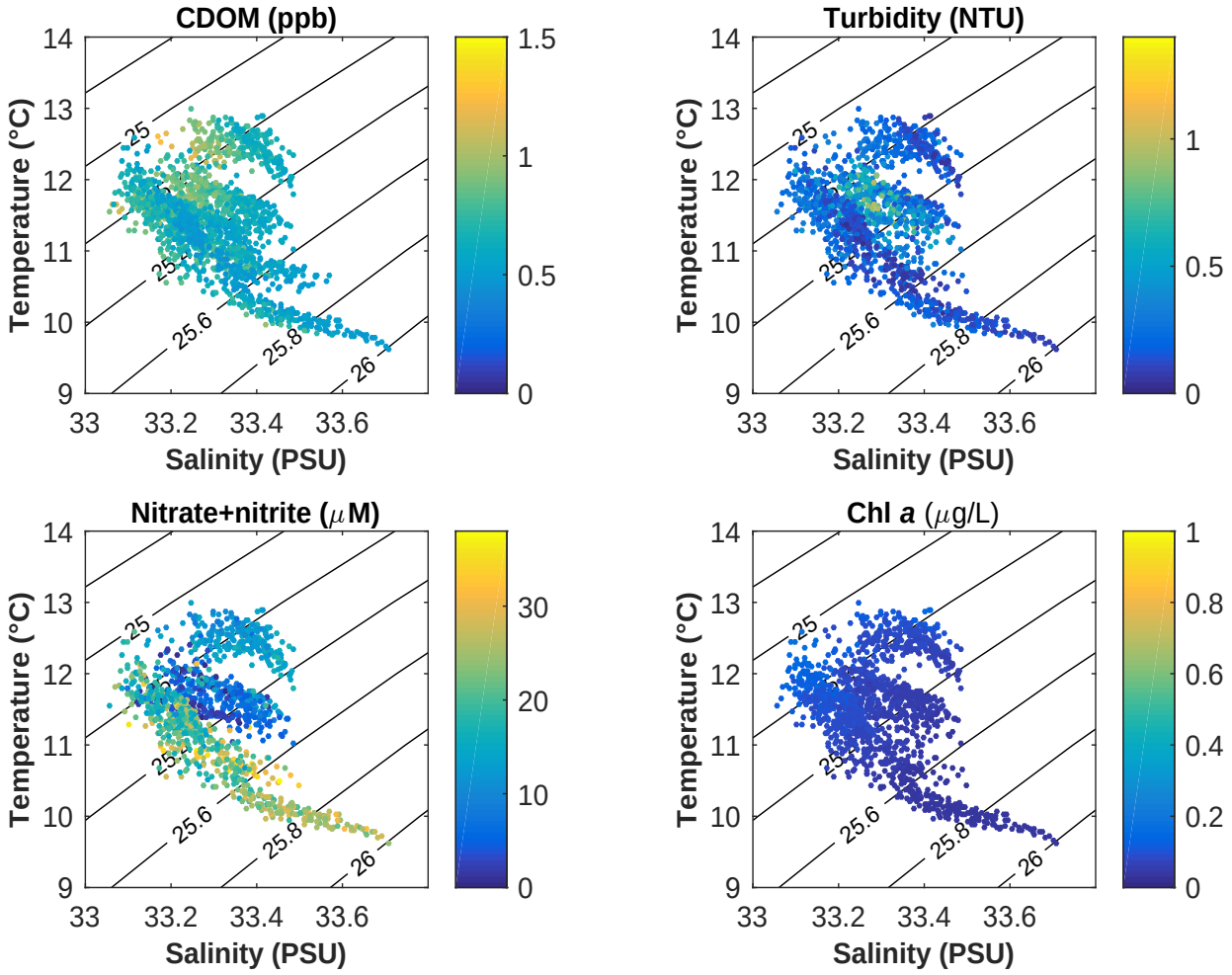

Figure 4.8

PLOO RTOMS hourly averaged CDOM, turbidity, nitrate + nitrite, and chlorophyll *a* shown on temperature versus salinity plots at 89 m for winter 2020 (January–March). Isopycnals and corresponding σ-t values shown by black lines.

possibly be attributed to effluent plume influence. Overall, higher nitrate and CDOM levels were observed with slightly lower salinities at the surface during winter 2020 (Figure 4.10). In contrast to the PLOO, treated effluent from the SBWRP and SBIWTP discharged through the SBOO generally contained concentrations of nitrate higher than ambient ocean nitrate levels (for effluent levels, see City of San Diego 2020–2022d, CSWRCB 2022; for ocean levels, see Weber et al. 2021). Depending on the conditions and mixing regime, nitrate may be another potential indicator of SBOO plume presence. However, other confounding factors such as coastal runoff and influence from the Tijuana River estuary may also bring water masses into the region that are less saline, CDOM, and nutrient-rich, resulting in a complex environment in the SBOO region (e.g., Figure 4.3; Hess 2019, 2020, 2021). During the SBOO RTOMS deployments in 2020–2021, BOD levels were relatively stable over time and did not appear to show possible plume influence (Appendix C.12). Further analyses with additional RTOMS data and other available data will be completed in the future to address these challenges with determining potential SBOO plume signals.

Potential Plume Signals Determined via ROTV

PLOO Region

Within the PLOO region, CDOM and OB values offered viable visual signals of potential plume

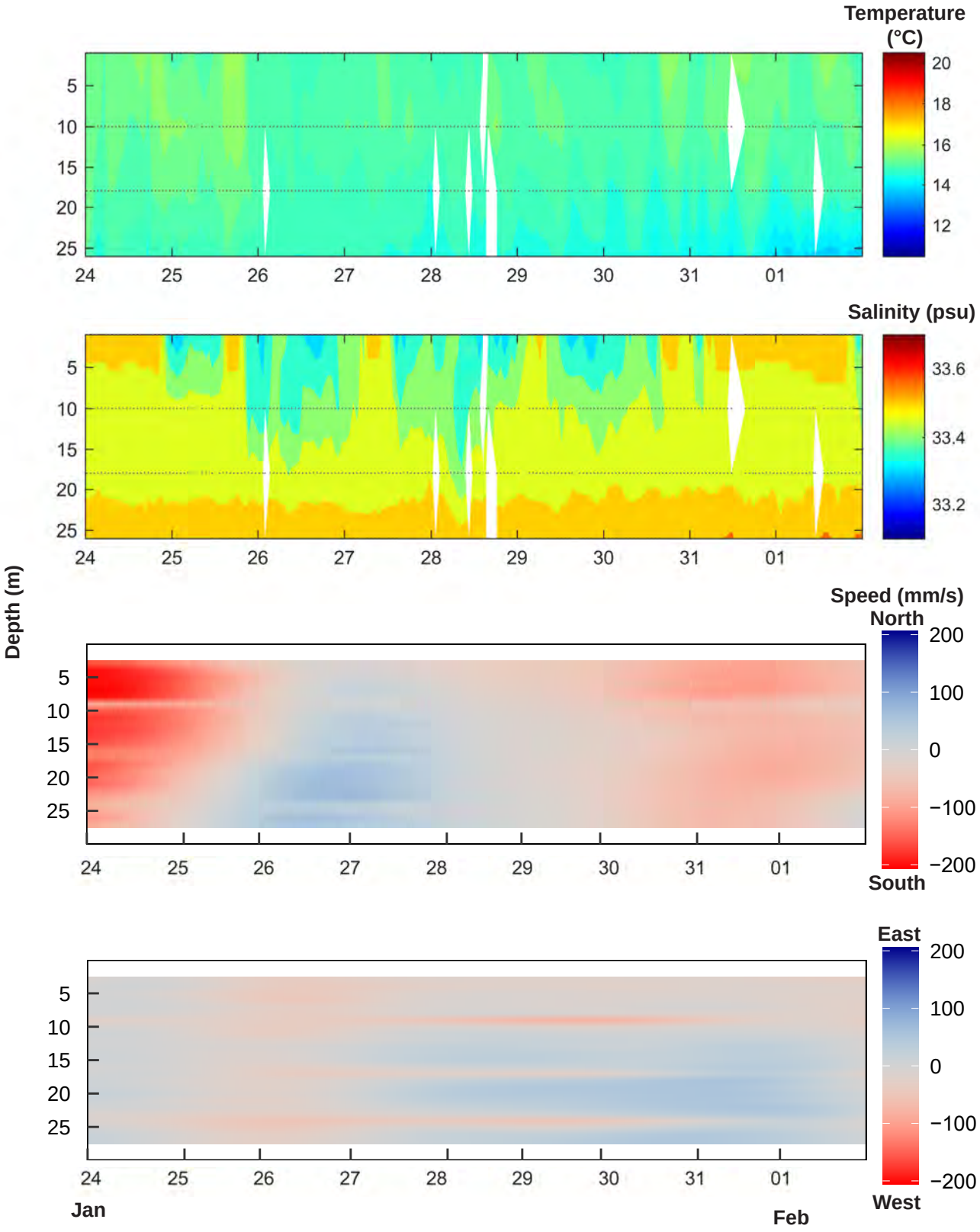

Figure 4.9

SBOO RTOMS hourly averaged ocean temperature, salinity, and current speeds (tides removed) interpolated for entire water column plus chlorophyll *a* (chl), CDOM, turbidity, and nitrate + nitrite for select depths during the week of January 24–February 1, 2020. Gaps and white areas indicate loss of data due to instrumentation issues or failure to meet data quality criteria (see text).

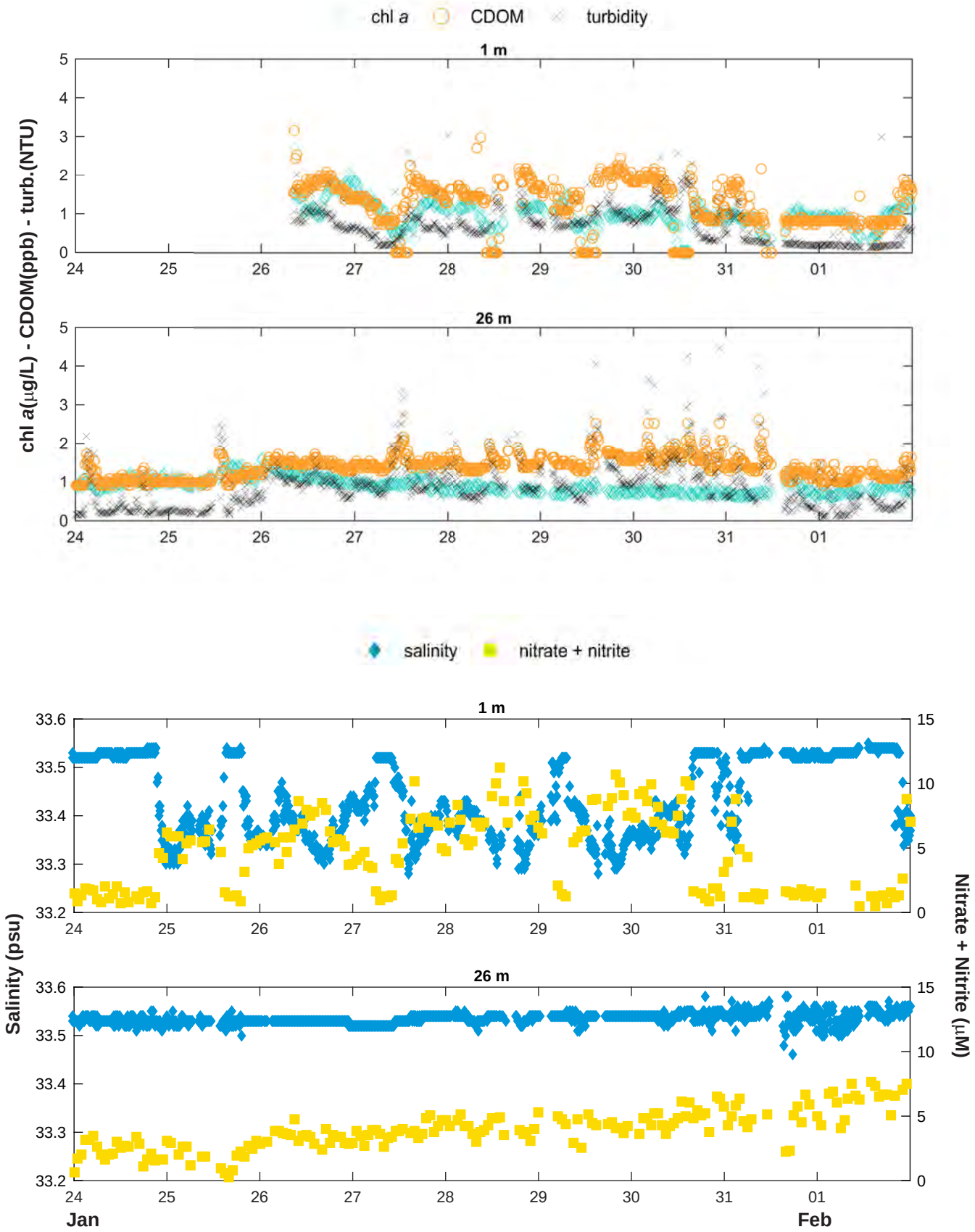

Figure 4.9 *continued*

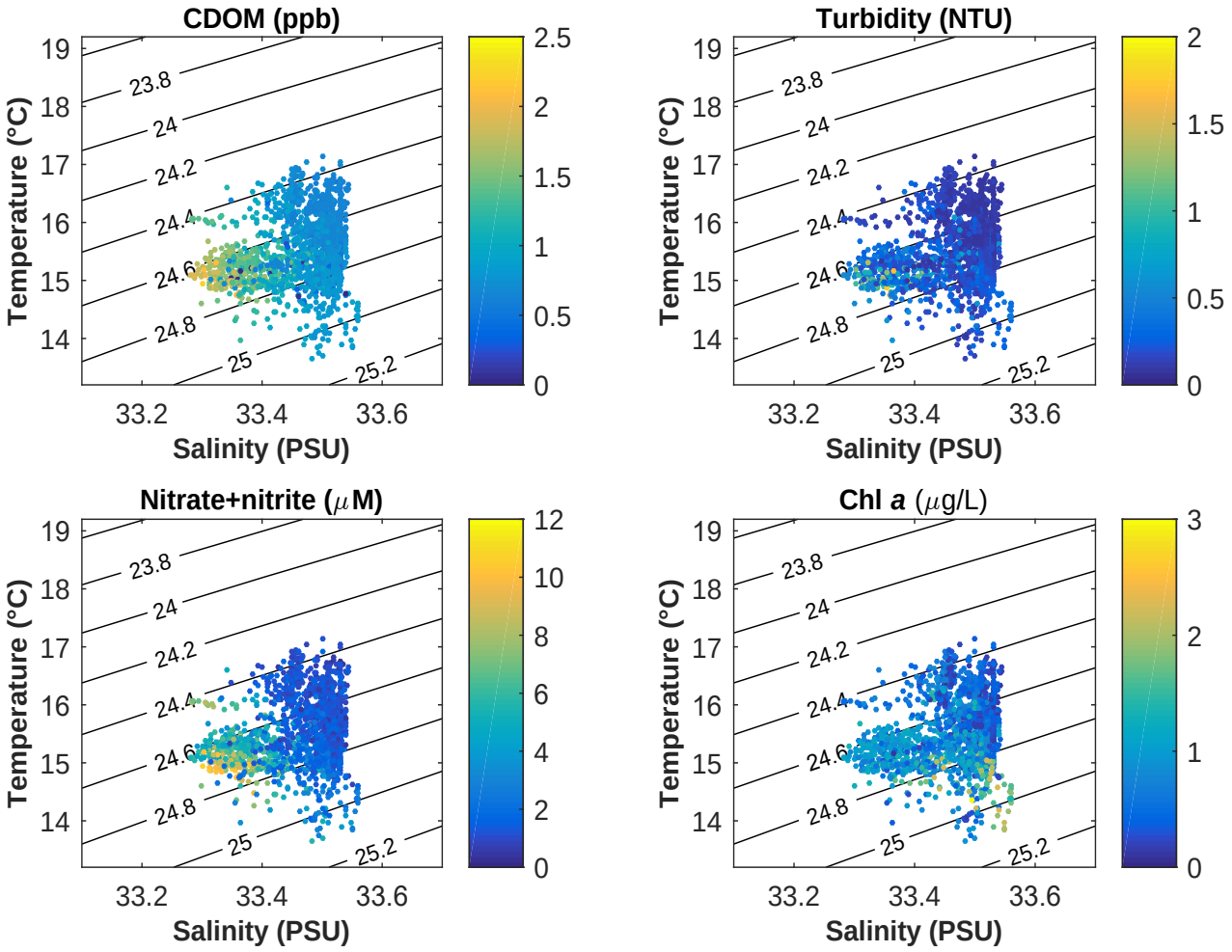

Figure 4.10

SBOO RTOMS hourly averaged CDOM, turbidity, nitrate + nitrite, and chlorophyll *a* shown on temperature versus salinity plots at 1 m for winter 2020 (January–March). Isopycnals and corresponding σ-t values shown by black lines.

signatures. During sampling in 2020–2021, ROTV surveys captured a large range of ocean conditions (Table 4.2). As an example of the capability of the ROTV for plume mapping, survey tracks were analyzed from winter 2020 and winter 2021 (Figure 4.2). Results from these surveys demonstrated the most distinct possible plume signatures (CDOM >1.0 parts per billion [ppb]), where CDOM and OB measurements aligned with each other and offered possible validation of potential plume signatures (Figures 4.11–4.14). As with RTOMS results described in the previous section, BOD and tryptophan levels measured during 2020 and 2021 ROTV surveys were not found to be reliable indicators of plume presence.

During winter 2020, the potential plume signal along the 100-m transect rose slightly in the water column to approximately 55 m as it moved sightly northward from the outfall (Figures 4.11, 4.12). There also appeared to be some potential plume signal south of the outfall and close to the seafloor. Along the 80-m transect, the potential plume signature was much weaker and remained close to the seafloor. A plume signature was not observed along the 60-m transect. During winter 2021, the potential plume signature along the 100-m transect again rose slightly in the water column and dispersed in a more northerly direction from the outfall (Figures 4.13, 4.14). Similar to 2020, the potential plume signature was much weaker

inshore along the 80-m transect; however, during this ROTV survey, it rose to approximately 45 m in the water column.

These examples of distinct potential plume signatures occurred during the winter months when other confounding environmental factors were not present (i.e., phytoplankton blooms, water column stratification). During the winters of 2020 and 2021, ocean conditions were weakly stratified (Table 4.2), so stratification likely played a minimal role in plume dispersion patterns described above. However, as described in the RTOMS section, ocean currents likely influenced plume dispersion patterns, both on short time scales in the immediate vicinity of discharge as well as on the rate of transport of effluent out of the discharge area on longer time scales (days to weeks). In the weeks preceding the winter 2020 ROTV survey, ocean currents were southeast and then remained in a consistent weak north-northwest direction during the sampling week (Table 4.2, Appendix E.22), which corresponds to potential plume signature patterns (Figures 4.11, 4.12). Prior to the winter 2021 ROTV survey, ocean currents alternated from south-southeast to north-northwest and then transitioned to a more northerly direction during the sampling week (Table 4.2, Appendix E.22); however, potential plume signatures were concentrated north of the outfall only during the ROTV survey (Figures 4.13, 4.14). With the presence of additional environmental factors during ROTV surveys conducted in other times of the year, such as phytoplankton blooms and strong stratification, interpreting potential PLOO plume signatures was more problematic.

SBOO Region

Within the SBOO region, CDOM and OB values measured with the ROTV may offer viable signals of potential SBOO plume presence; however, from ROTV surveys collected to date, distinct SBOO plume signatures were not identified. The SBOO ROTV surveys were limited in number due to complications resulting from a more compressed sampling depth range, the presence of commercial fishing equipment, and ROTV equipment failure. Additionally, SBOO ROTV surveys completed thus far occurred during a limited range of ocean conditions (Table 4.2). Further, there are many factors present in the SBOO region that can adversely affect locating potential SBOO plume signatures, such as nearshore currents, a relatively shallow outfall depth (28 m), shore-based sources of CDOM and OB (i.e., the Tijuana River outflow, San Diego Bay, other non-point source runoff), nearshore turbidity, and phytoplankton blooms. When the entire water column is weakly stratified and well mixed, as is often the case in the SBOO region from late fall to early spring (see Chapter 2), tracking the transport of water sources is further complicated due to mixing of surface and deep waters. As an example of the difficulties in determining potential SBOO plume signatures, during the fall 2020 SBOO ROTV survey, high concentrations of CDOM and OB were observed throughout the survey area at various depths (Figures 4.15, 4.16). This was also reflected in satellite imagery taken around the same time (November 2020) highlighting multiple sediment turbidity plumes throughout the region (Figure 4.3). However, none of these observations could be strongly linked to a potential SBOO plume signature.

Summary

Historically, the City has evaluated the fate and dispersal of treated wastewater effluent plumes through quarterly and weekly monitoring of a fixed grid of stations utilizing CTD instrumentation and bacteriological evidence (e.g., City of San Diego 2020a). Although this technique covers a large spatial area, the infrequent temporal sampling rate limits observations to just a few "snapshots" in time. This limited timeframe may not capture sporadic events, such as storm-driven transport or other oceanographic phenomena. To address this issue, the City installed non-telemetered ADCP and thermistor instrumentation to document hydrographic conditions in the immediate vicinity of the outfalls over much finer timescales (Storms et al. 2006). Although variable over space and time, the general axes of current velocities were consistently observed to follow N:NW or S:SE

Table 4.2

Summary of ocean conditions from RTOMS and static instrumentation as well as observed plume ranges from quarterly CTD surveys during days that ScanFish surveys were completed. Deep currents are defined as measurements from > 60 m depth for PLOO and from > 19 m depth for SBOO. nd = not detected.

		Stratification [a]			Currents [b]			Plume Detections	
Region	Quarter	Qualitative	Max ΔT (°C) (surface-bottom)	Max thermocline depth (m)	Dominant alongshore current	Dominant cross-shore current	Mean deep current speed (mm/s)	Max observed plume width (m)	Min observed plume depth (m)
PLOO									
	2020								
	Winter	Weak	4.4	nd	Very Weak North	Very Weak Variable	6	36	59
	Spring	Strong	8.7	<10	Weak South	Weak East	19	15	61
	Summer	Strong	12.8	<20	Transition: Moderate North to Weak South	Transition: Very Weak West to Very Weak East	40	24	72
	Fall	Moderate	6.3	<22	Moderate South	Weak East	68	27	55
	2021								
	Winter	Weak	4.1	nd	Transition: Moderate South to Weak North	Transition: Weak East to Weak West	43	36	59
	Spring	Moderate to Strong	7.4	<10	Generally South (some very weak North mid-column)	Very Weak East	21	40	54
	Summer	Strong	7.9	<14	Transition: Moderate North to Moderate South	Transition: Weak West to Very Weak East	43	—	—

[a] PLOO RTOMS data not available in November 2020 or all of 2021. Thermocline calculated from static thermistor data (from 4 to 98 m depth, spaced 4 m apart). See description in Chapter 2.

[b] RTOMS data not available in February or November. Current measurements from static ADCP (4 m bins, upward facing). See description in Chapter 2.

Table 4.2 *continued*

Region	Quarter	Stratification [a]			Currents [b]			Plume Detections	
		Qualitative	Max ΔT (°C) (surface-bottom)	Max thermocline depth (m)	Dominant alongshore current	Dominant cross-shore current	Mean deep current speed (mm/s)	Max observed plume width (m)	Min observed plume depth (m)
SBOO									
	2020								
	Summer	Strong	8.2	<10	Transition: Strong North to Strong South	Transition: Very Weak West to Weak East	20	5	12
	Fall	Moderate	3.7	<14	Transition: Weak North to Strong South back to Weak surface South and Weak bottom North	Transition: Very Weak West to East (Moderate surface)	23	7	5

[a] PLOO RTOMS data not available in November 2020 or all of 2021. Thermocline calculated from static thermistor data (from 4 to 98 m depth, spaced 4 m apart). See description in Chapter 2.

[b] RTOMS data not available in February or November. Current measurements from static ADCP (4 m bins, upward facing). See description in Chapter 2.

trajectories. This has indicated that as effluent mixes with ambient seawater, it generally travels along the coast rather than being directed inshore toward the shoreline, kelp beds, or other recreational waters. The ADCP data have improved temporal coverage of conditions in the area; however, the 4-month recovery cycle for the data has rendered it useful only to understand events in retrospect and has not included auxiliary measurements for potential plume characterization.

More recently, real-time data have become available via the City's RTOMS, which include a variety of instrumentation at multiple depths providing near-continuous information from a single platform. These observations have enhanced the assessment of environmental conditions and the potential impacts of oceanographic and anthropogenic events in coastal waters. While not possible to understand the dispersion and spatial extent of plumes using RTOMS alone, these near-continuous data may show potential vertical spread of plumes as well as events that would otherwise be missed by fixed grid surveys. For example, they provided the ability to capture greater variability and extreme events, such as the intense regional harmful algal bloom in spring 2020 (see Chapter 2; Anderson and Hepner-Medina 2020). In addition, these high frequency data at a single, fixed location provide context on the state and variability of the receiving waters into which the PLOO and SBOO discharge. For example, the rise height of the effluent plume is highly dependent on density structure and stratification of the water column, as well as ambient currents (Rogowski et al. 2012a,b, 2013, City of San Diego 2022b,c). Stronger currents may result in greater initial mixing while weaker currents may result in shallower rise heights depending on stratification. Other local ocean dynamics, such as internal waves, can result in further mixing and impact observed plume rise heights (Rogowski et al. 2012a). These data can be further used to validate predictive models that seek to characterize changes, which may cause environmental degradation. While initial RTOMS results presented show examples of potential indicators of effluent plume signals, one challenge remains: there is no equivalent farfield reference mooring station in similar water masses to use for comparison at the same time scales. Thus, it is difficult to confirm plume presence as well as any possible plume effects on DO, pH, or natural light water quality indicators (also note that moorings are located outside State jurisdictional waters where Ocean Plan compliance standards do not apply). To strengthen the ability to discern plume signals, additional data collection over multiple depths and further analyses are planned.

To complement the operations of the RTOMS, the ROTV may allow the City to develop a truly adaptive and dynamic sampling program that will be able to appropriately evaluate the extent of plume dispersion. Using real-time information on ocean stratification, currents, and potential plume detections from the RTOMS, targeted ROTV surveys may be completed for adaptive sampling and mapping of the plumes as needed. Furthermore, as ROTV data appeared to generally agree qualitatively with CTD data (City of San Diego 2022b), this potentially presents a more focused and higher resolution method for tracking plumes over a large spatial scale. While initial results from ROTV surveys in the PLOO region showed strong potential for distinguishing PLOO plume signals, a similar evaluation of SBOO plume detections remains problematic. ROTV sampling has been more challenging in the SBOO region due to technical issues, logistical challenges, and environmental factors, which may hinder the usefulness of this technique for SBOO plume tracking purposes. Specifically, the frequent occurrence of obstacles and abandoned fishing gear caused significant damage to the ROTV and technical challenges such as altimeter issues in the shallower depths resulted in fewer successful surveys in the SBOO region. An assessment of the effectiveness of the ROTV is currently ongoing and due for completion in mid-2022. Future work is planned to improve potential plume detections, including refinement of ROTV sensor technology integration and additional data analysis methodologies.

Despite the different spatial and temporal coverages of the CTD, RTOMS, and ROTV instrument

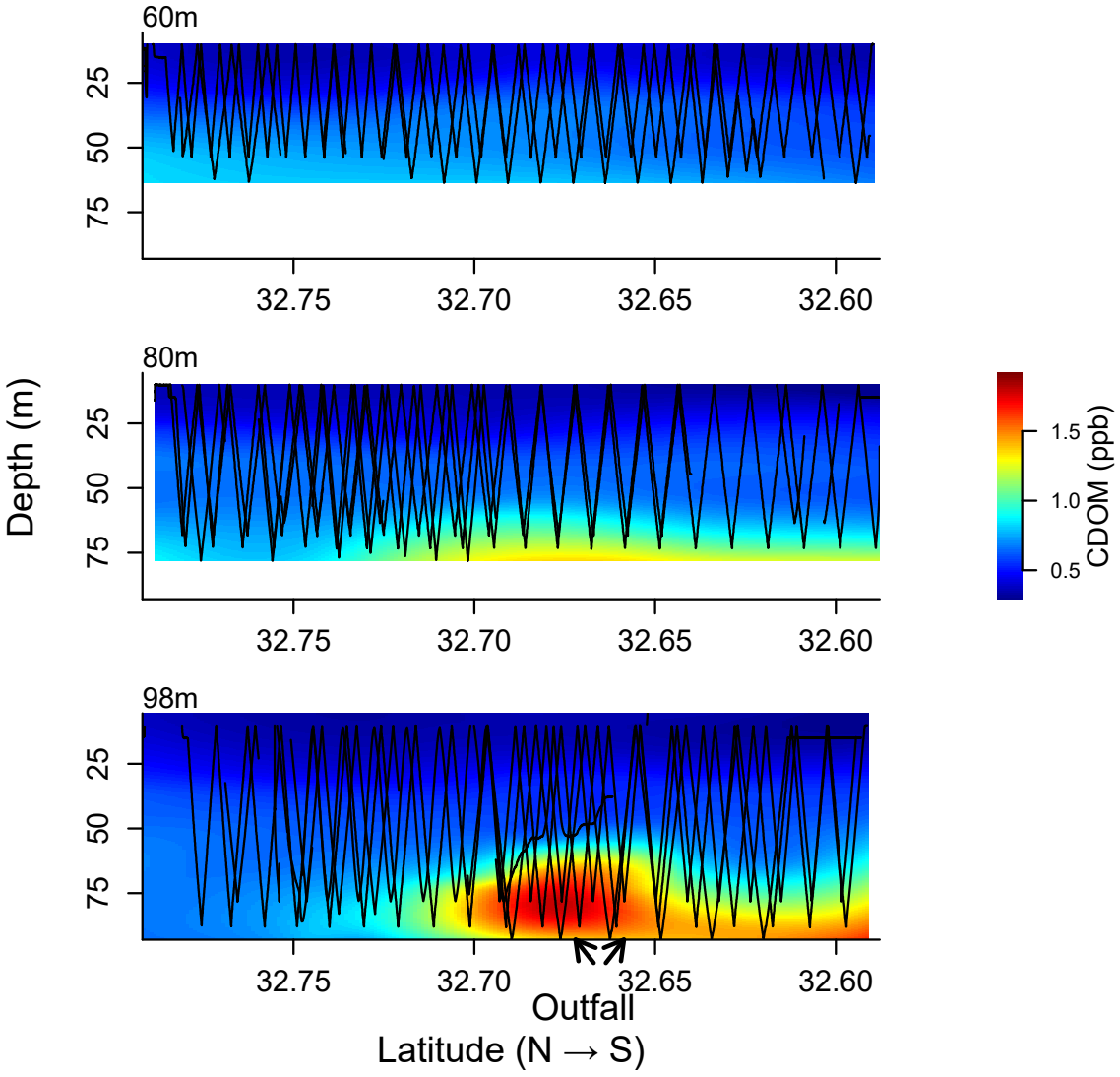

Figure 4.11
CDOM data from ROTV surveys of the PLOO region conducted during the winter 2020. Data are interpolated over the water column using a LOESS regression. Black lines indicate the position of the ROTV in the water column. The two active ends of the outfall's wye are indicated by arrows along the 98-m isobath.

packages utilized by the City, all observations from 2020–2021 demonstrated that the Point Loma effluent plume generally remained offshore below a depth of 44 m, and was transported along the coast. This finding concurs with prior plume tracking studies (Rogowski et al. 2012a,b, 2013), as well as historical satellite imagery observations that have not shown visual evidence of the plume surfacing (e.g., Svejkovsky 2010, Hess 2019, 2020, 2021). These observations support previous studies showing that there is no evidence that wastewater discharged to the ocean via the current configuration of the PLOO has ever reached the shoreline or had any significant impact on recreational waters (City of San Diego 2022b,c).

Within the shallower SBOO region, past studies have shown that other sources, such as coastal runoff

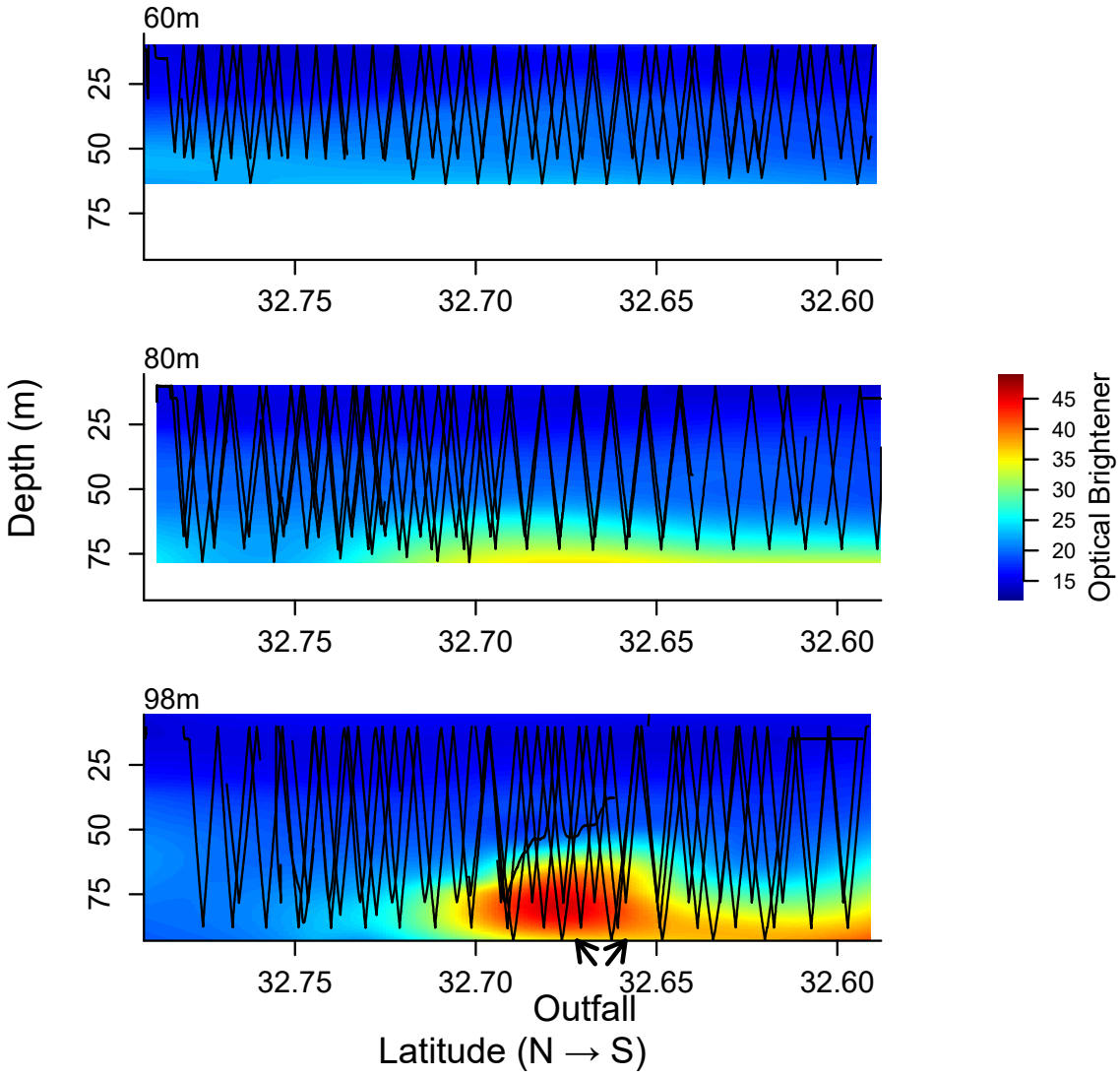

Figure 4.12
Optical Brightener data from ROTV surveys of the PLOO region conducted during the winter 2020. Data are interpolated over the water column using a LOESS regression. Black lines indicate the position of the ROTV in the water column. The two active ends of the outfall's wye are indicated by arrows along the 98-m isobath.

from rivers and creeks, were more likely to impact coastal water quality than wastewater discharge from the outfall, especially during and immediately after significant rain events (see Chapter 3; Svejkovsky and Jones 2001, Terrill et al. 2009). The San Diego Bay and the Tijuana River estuary often deliver less saline, CDOM- and nutrient-rich water masses, resulting in a complex environment in the SBOO region. It is also well established that sewage-laden discharges from the Tijuana River and Los Buenos Creek are likely sources of contaminated water during or after storms or other periods of increased flows (see Chapter 3). These factors confound efforts to decipher SBOO effluent plume signals from other coastal influences. While the SBOO plume generally stays trapped below the pycnocline during seasonal periods of water column stratification, it may rise to the surface

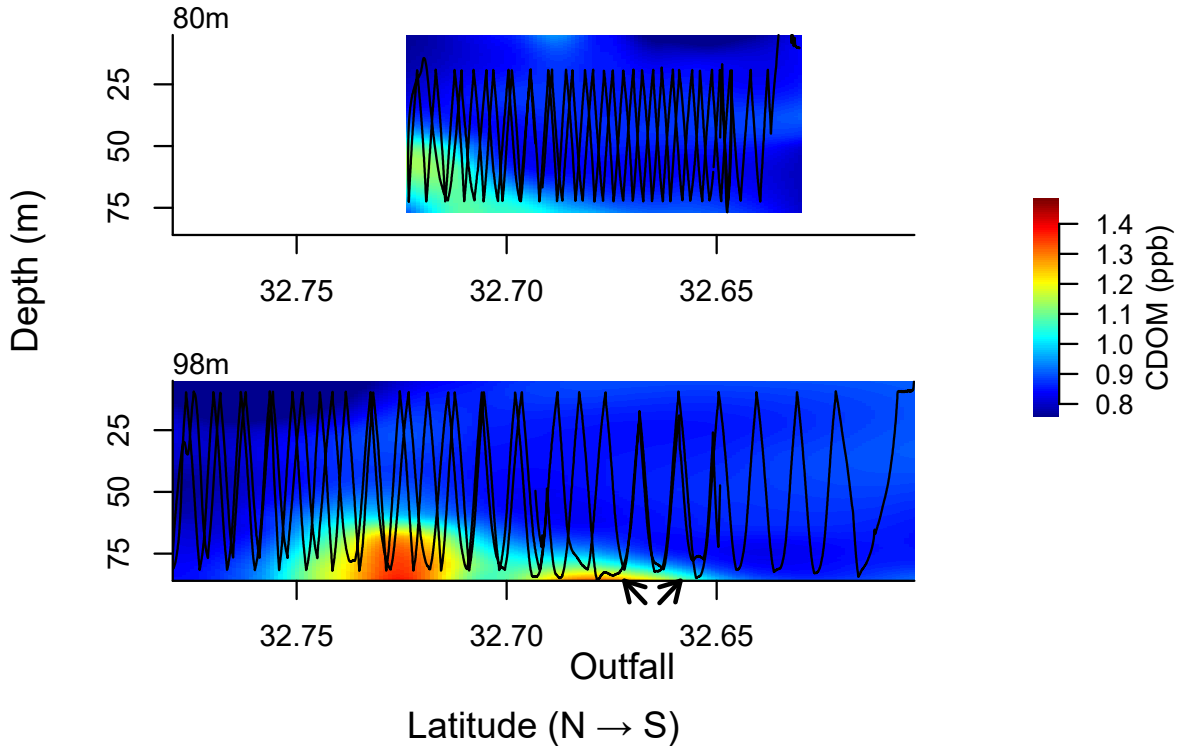

Figure 4.13
CDOM data from ROTV surveys of the PLOO region conducted during the winter of 2021. Data are interpolated over the water column using a LOESS regression. Black lines indicate the position of the ROTV in the water column. The two active ends of the outfall's wye are indicated by arrows along the 98-m isobath.

when waters become more mixed and stratification breaks down (Terrill et al. 2009, Hess 2019, 2020, 2021, City of San Diego 2020a). However, given predominant along-shore currents, it does not appear that wastewater discharged via the SBOO reaches the shoreline or impacts recreational waters, particularly compared to other coastal inputs (Largier et al. 2004, Terrill et al. 2009).

Literature Cited

Alessi, C.A., R. Beardsley, R. Limeburner, and L.K. Rosenfeld. (1984). CODE-2: Moored Array and Large-Scale Data Report. Woods Hole Oceanographic Institution Technical Report. 85–35: 21.

Anderson, C. and M. Hepner-Medina. (2020). SCCOOS Red Tide Bulletin: Spring 2020. Newsletter, published May 8th 2020. https://sccoos.org/california-hab-bulletin/red-tide/.

Borchers, H.W. (2021). pracma: Practical Numerical Math Functions. R package version 2.3.3. https://CRAN.R-project.org/package=pracma.

Bowden, K.F. (1975). Oceanic and Estuarine Mixing Processes. In: J.P. Riley and G. Skirrow (eds.). Chemical Oceanography, 2nd Ed., Vol.1. Academic Press, San Francisco, CA. p 1–41.

Cao, Y., J.F. Griffith, and S.B. Weisberg. . (2009). Evaluation of optical brightener photodecay

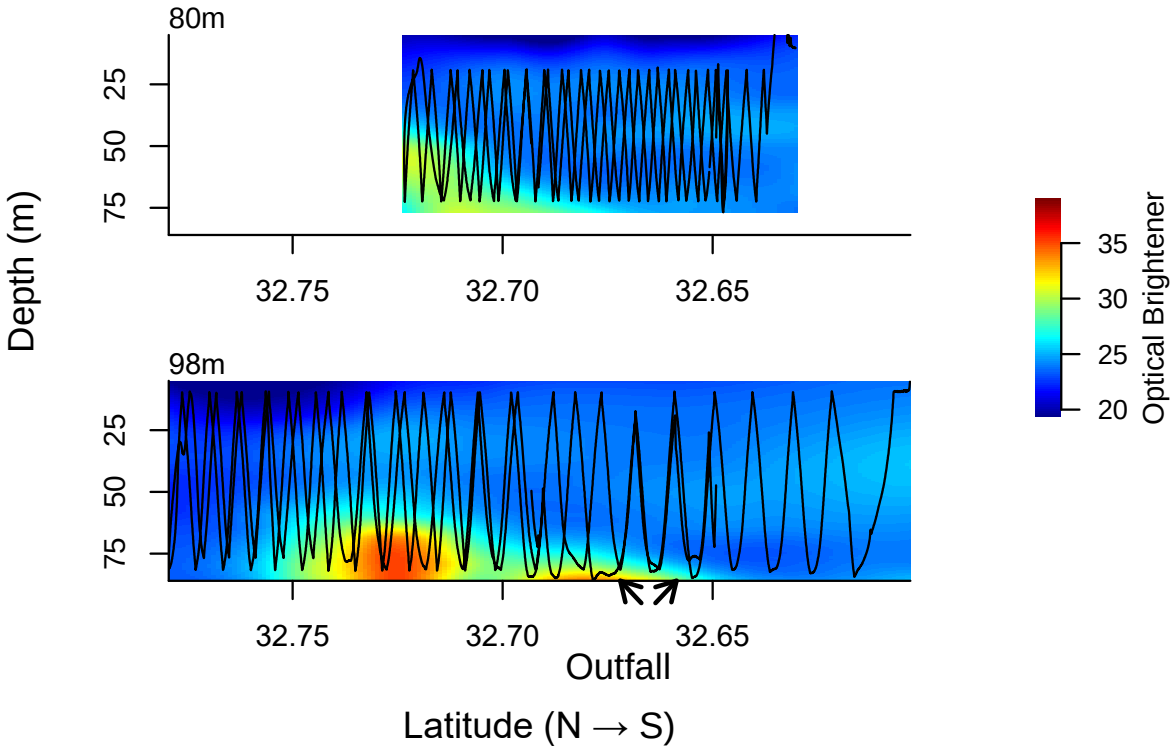

Figure 4.14
Optical Brightener data from ROTV surveys of the PLOO region conducted during the winter of 2021. Data are interpolated over the water column using a LOESS regression. Black lines indicate the position of the ROTV in the water column. The two active ends of the outfall's wye are indicated by arrows along the 98-m isobath.

characteristics for detection of human fecal contamination. Water Research, 43(8), 2273–2279.

City of San Diego. (2016a). Point Loma Ocean Outfall Annual Receiving Waters Monitoring and Assessment Report, 2015. City of San Diego Ocean Monitoring Program, Public Utilities Department, Environmental Monitoring and Technical Services Division, San Diego, CA.

City of San Diego. (2016b). South Bay Ocean Outfall Annual Receiving Waters Monitoring and Assessment Report, 2015. City of San Diego Ocean Monitoring Program, Public Utilities Department, Environmental Monitoring and Technical Services Division, San Diego, CA.

City of San Diego. (2018a). Plume Tracking Monitoring Plan for the Point Loma and South Bay Ocean Outfall Regions, San Diego, California. Submitted by the City of San Diego Public Utilities Department to the San Diego Water Board and USEPA, Region IX, March 28, 2018 (approved 4/25/2018).

City of San Diego. (2018b). Biennial Receiving Waters Monitoring and Assessment Report for the Point Loma and South Bay Ocean Outfalls, 2016–2017. City of San Diego Ocean Monitoring Program, Public Utilities

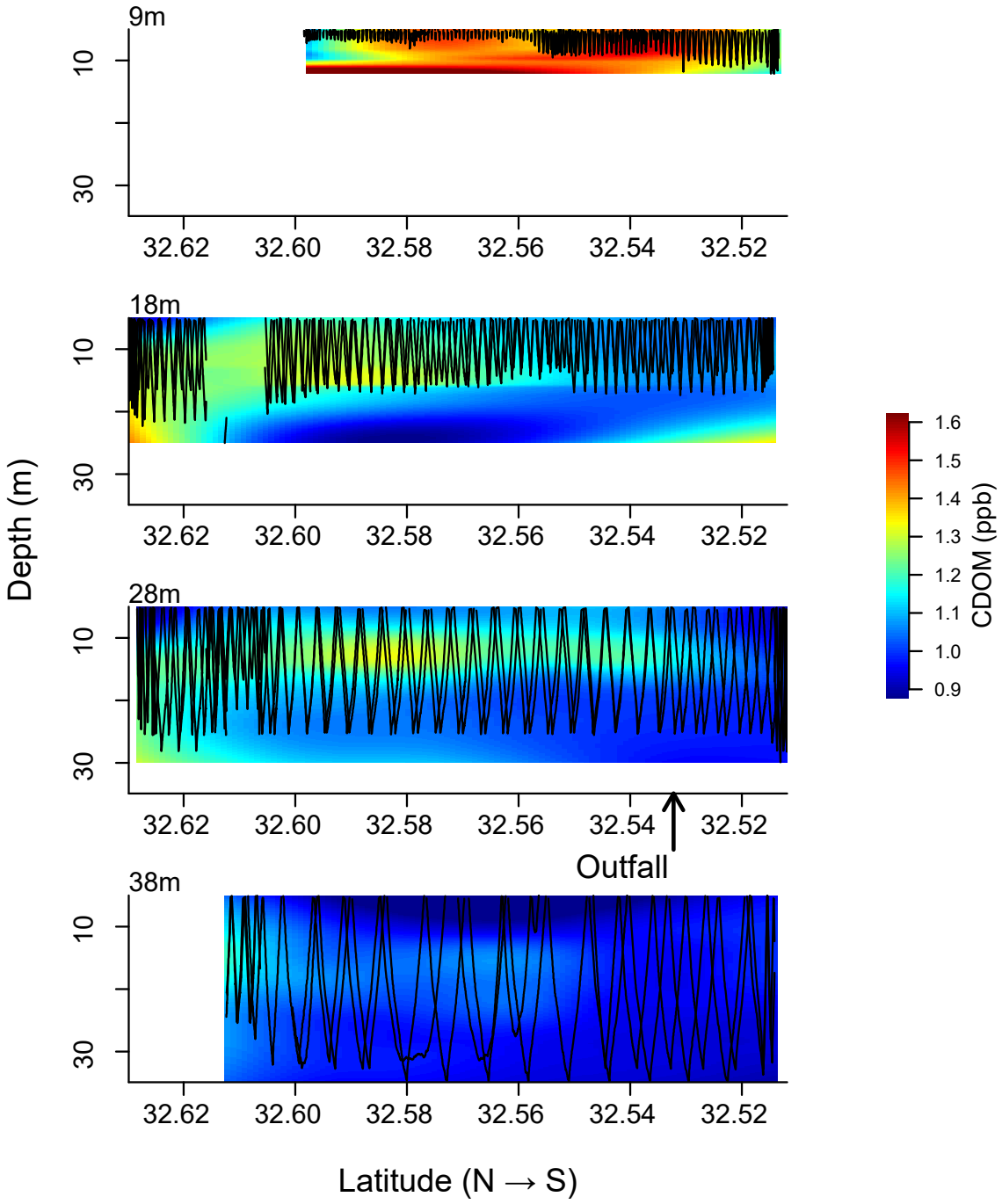

Figure 4.15
CDOM data from ROTV surveys of the SBOO region conducted during the fall of 2020. Data are interpolated over the water column using a LOESS regression. Black lines indicate the position of the ROTV in the water column. The active end of the outfall's wye is indicated by the arrow along the 28-m isobath.

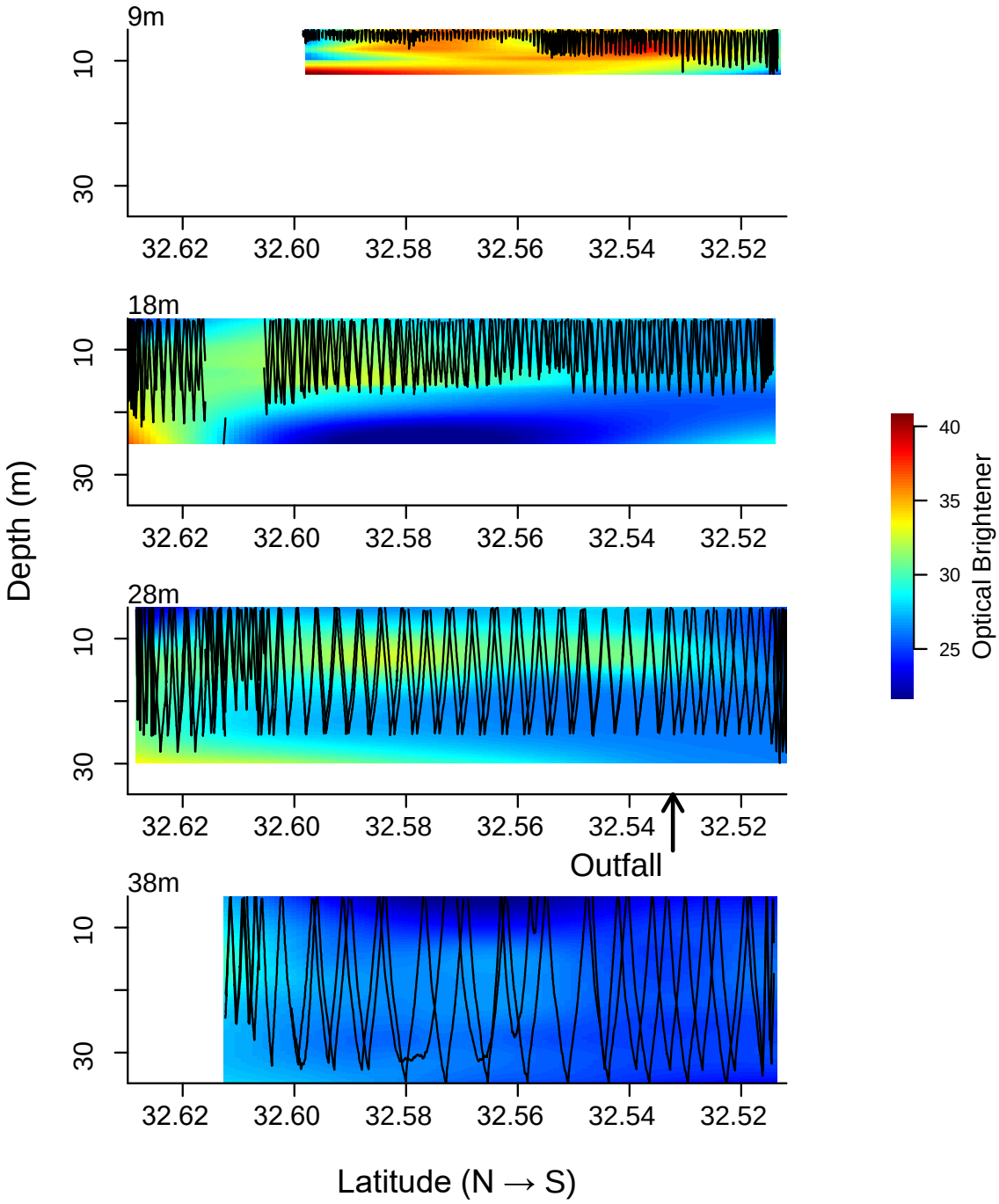

Figure 4.16
Oprtical Brightener data from ROTV surveys of the SBOO region conducted during the fall of 2020. Data are interpolated over the water column using a LOESS regression. Black lines indicate the position of the ROTV in the water column. The active end of the outfall's wye is indicated by the arrow along the 28-m isobath.

Department, Environmental Monitoring and Technical Services Division, San Diego, CA.

City of San Diego. (2020a). Biennial Receiving Waters Monitoring and Assessment Report for the Point Loma Ocean Outfall and South Bay Ocean Outfall, 2018-2019. City of San Diego Ocean Monitoring Program, Public Utilities Department, Environmental Monitoring and Technical Services Division, San Diego, CA.

City of San Diego. (2020b). Plume Tracking Monitoring Plan Progress Report for the Point Loma and South Bay Ocean Outfall Regions, San Diego, California; Report Period: January–December 2019. Submitted by the City of San Diego Public Utilities Department to the San Diego Water Board and USEPA, Region IX, March 3, 2020.

City of San Diego. (2020–2022a). Monthly Receiving Waters Monitoring Reports for the Point Loma Ocean Outfall (Point Loma Wastewater Treatment Plant), January 2020–December 2021. City of San Diego Ocean Monitoring Program, Public Utilities Department, Environmental Monitoring and Technical Services Division, San Diego, CA.

City of San Diego. (2020–2022b). Monthly Receiving Waters Monitoring Reports for the South Bay Ocean Outfall (South Bay Water Reclamation Plant), January 2020–December 2021. City of San Diego Ocean Monitoring Program, Public Utilities Department, Environmental Monitoring and Technical Services Division, San Diego, CA.

City of San Diego. (2020–2022c). Monthly Monitoring Reports for the Point Loma Wastewater Treatment Plant and Ocean Outfall, January 2020–December 2021. City of San Diego, Public Utilities Department, Environmental Monitoring and Technical Services Division, San Diego, CA.

City of San Diego. (2020–2022d). Monthly Monitoring Reports for the South Bay Water Reclamation Plant and Ocean Outfall, January 2020–December 2021. City of San Diego, Public Utilities Department, Environmental Monitoring and Technical Services Division, San Diego, CA.

City of San Diego. (2021). Interim Receiving Waters Monitoring Report for the Point Loma and South Bay Ocean Outfalls, 2020. City of San Diego Ocean Monitoring Program, Public Utilities Department, Environmental Monitoring and Technical Services Division, San Diego, CA.

City of San Diego. (2022a). Plume Tracking Monitoring Plan Progress Report for the Point Loma and South Bay Ocean Outfall Regions, San Diego, California; Report Period: January – December 2021. Submitted by the City of San Diego Public Utilities Department to the San Diego Water Board and USEPA, Region IX, March 3, 2020.

City of San Diego. (2022b). Appendix D. Plume Behavior and Tracking Summary. In: Report of Waste Discharge and Application for Renewal of NPDES CA 0107409 and 301(h) Modified Secondary Treatment Requirements. Volume VI, Appendices D–G. Public Utilities Department, San Diego, CA.

City of San Diego. (2022c). Appendix P. Oceanography. Appendix Q. Initial Dilution Simulation Models. In: Report of Waste Discharge and Application for Renewal of NPDES CA 0107409 and 301(h) Modified Secondary Treatment Requirements. Volume X, Appendices O–U. Public Utilities Department, San Diego, CA.

[CSWRCB] California State Water Resources Control Board, Office of Information Management and Analysis (2022). California Integrated Water Quality System Project, Water Quality Effluent Electronic Self-Monitoring Report (eSMR) Data. https://data.ca.gov/dataset/water-quality-effluent-electronic-self-monitoring-report-esmr-data.

Hagedorn, C. and S.B. Weisberg. (2009). Chemical-based fecal source tracking methods: Current status and guidelines for evaluation. Reviews in Environmental Science and Bio/Technology 8(3):275-287.

Hess, M. (2019). Satellite & Aerial Coastal Water Quality Monitoring in the San Diego/Tijuana Region: Annual Summary Report 1 January 2018 – 31 December 2018. Littleton, CO.

Hess, M. (2020). Satellite & Aerial Coastal Water Quality Monitoring in the San Diego/Tijuana Region: Annual Summary Report 1 January 2019 – 31 December 2019. Littleton, CO.

Hess, M. (2021). Satellite & Aerial Coastal Water Quality Monitoring in the San Diego/Tijuana Region: Annual Summary Report 1 January 2020 – 31 December 2020. Littleton, CO.

Hope, R.M. (2013). Rmisc: Ryan Miscellaneous. R package version 1.5. http://CRAN.R-project.org/package=Rmisc.

Jackson, G.A. (1986). Physical Oceanography of the Southern California Bight. In: R. Eppley (ed.). Plankton Dynamics of the Southern California Bight. Springer Verlag, New York. p 13–52.

Jones, B., M.A. Noble, and T.D. Dickey. (2002). Hydrographic and particle distributions over the Palos Verdes continental shelf: Spatial, seasonal and daily variability. Continental Shelf Research. 22: 945–965.

Kelley, D. and C. Richards. (2019). oce: Analysis of Oceanographic Data. R package version 1.1-1. http://CRAN.R-project.org/package=oce.

Largier, J., L. Rasmussen, M. Carter, and C. Scearce. (2004). Consent Decree – Phase One Study Final Report. Evaluation of the South Bay International Wastewater Treatment Plant Receiving Water Quality Monitoring Program to Determine Its Ability to Identify Source(s) of Recorded Bacterial Exceedances. Scripps Institution of Oceanography, University of California, San Diego, CA.

Le Cao, K-A., F. Rohart, I. Gonzalez, S. Dejean, B. Gautier, F. Bartolo, P. Monget, J. Coquery, F. Yao, and B. Liquet. (2017). mixOmics: Omics. R package version 6.8.0. https://CRAN.R-project.org/package=mixOmics.

Lynn, R.J. and J.J. Simpson. (1987). The California Current System: The Seasonal Variability of its Physical Characteristics. Journal of Geophysical Research. 92(C12): 12947–12966.

Mann. K.H. and J.R.N. Lazier. (1991). Dynamics of Marine Ecosystems, Biological–Physical Interactions in the Oceans. Blackwell Scientific Publications, Boston.

MATLAB. (2016). Version R2016a. The MathWorks Inc., Natick, Massachusetts. URL https://www.mathworks.com/products/matlab.html.

Morgan, P., and L. Pender. (2014). SEAWATER library for calculating EOS-80 properties of seawater in MATLAB. CSIRO Marine Research, version 3.3.1. http://www.cmar.csiro.au/datacentre/ext_docs/seawater.htm.

Nezlin, N.P, J.A.T. Booth, C. Beegan, C.L. Cash, J.R. Gully, A. Latker, M.J. Mengel, G.L. Robertson, A. Steele, and S.B. Weisberg. (2016). Assessment of wastewater impact on dissolved oxygen around southern California's submerged ocean outfalls. Regional Studies in Marine Science. In Press.

Nychka, D., R. Furrer, J. Paige, S. Sain. (2021). "fields: Tools for spatial data." R package version 13.3, https://github.com/dnychka/fieldsRPackage.

Ocean Imaging. (2020). Ocean Imaging Corporation archive of aerial and satellite-derive images. http://www.oceani.com/SanDiegoWater/index.html.

Paver, C.R., L.A. Codispoti, V.J. Coles, and L.W. Cooper. (2020). Sampling errors arising from carousel entrainment and insufficient flushing of oceanographic samples bottles. Limnology & Oceanography: Methods, 18: 311–326.

Pickard, D.L. and W.J. Emery. (1990). Descriptive Physical Oceanography. 5th Ed. Pergamon Press, Oxford.

R Core Team. (2021). R: A language and environment for statistical computing. R Foundation for Statistical Computing, Vienna, Austria. URL https://www.R-project.org/.

Ripley, B. and M. Lapsley. (2017). RODBC: ODBC Database Access. R package version 1.3-12. http://CRAN.R-project.org/package=RODBC.

Rochelle-Newall, E.W. and T.R. Fisher. (2002). Production of chromophoric dissolved organic matter fluorescence in marine and estuarine environments: an investigation into the role of phytoplankton. Marine Chemistry, 77: 7–21.

Rogowski, P., E. Terrill, M. Otero, L. Hazard, S.Y. Kim, P.E. Parnell, and P. Dayton. (2012a). Final Report: Point Loma Ocean Outfall Plume Behavior Study. Prepared for City of San Diego Public Utilities Department by Scripps Institution of Oceanography, University of California, San Diego, CA.

Rogowski, P., E. Terrill, M. Otero, L. Hazard, and W. Middleton. (2012b). Mapping ocean outfall plumes and their mixing using Autonomous Underwater Vehicles. Journal of Geophysical Research, 117: C07016.

Rogowski, P., E. Terrill, M. Otero, L. Hazard, and W. Middleton. (2013). Ocean outfall plume characterization using an Autonomous Underwater Vehicle. Water Science & Technology, 67(4): 925–933.

Romera-Castillo, C., H. Sarmento, X.A. Álvarez-Salgado, J.M. Gasol, and C. Marrasé. (2010). Production of chromophoric dissolved organic matter by marine phytoplankton. Limnology and Oceanography, 55: 446–454.

[SIO] Scripps Institution of Oceanography. (2004). Point Loma Outfall Project, Final Report, September 2004. Scripps Institution of Oceanography, University of California, La Jolla, CA.

Soetaert, K., T. Petzoldt, F. Meysman, and L. Meire. (2020). "marelac: tools for aquatic sciences" R package version 2.1.10. https://CRAN.R-project.org/package=marelac.

Storms, W.E., T.D Stebbins, and P.E. Parnell. (2006). San Diego Moored Observation System Pilot Study Workplan for Pilot Study of Thermocline and Current Structure off Point Loma, San Diego, California. City of San Diego, Metropolitan Wastewater Department, Environmental Monitoring and Technical Services Division, and Scripps Institution of Oceanography, La Jolla, CA.

Svejkovsky, J. (2010). Satellite and Aerial Coastal Water Quality Monitoring in the San Diego/Tijuana Region: Annual Summary Report, 1 January 2009–31 December 2009. Ocean Imaging, Solana Beach, CA.

Svejkovsky, J. and B. Jones. (2001). Detection of coastal urban storm water and sewage runoff with synthetic aperture radar satellite imagery. Eos, Transactions, American Geophysical Union, 82, 621–630.

[SWRCB] California State Water Resources Control Board. (2019). California Ocean Plan, Water Quality Control Plan, Ocean Waters of California. California Environmental Protection Agency, Sacramento, CA.

Terrill, E., K. Sung Yong, L. Hazard, and M. Otero. (2009). IBWC/Surfrider – Consent Decree Final Report. Coastal Observations and Monitoring in South Bay San Diego. Scripps

Institution of Oceanography, University of California, San Diego, CA.

Warnes, G., B. Bolker, and T. Lumley. (2021). gtools: Various R Programming Tools. R package version 3.5.0. http://CRAN.R-project.org/package=gtools.

Washburn, L., B.H. Jones, A. Bratkovich, T.D. Dickey, and M.S. Chen. (1992). Mixing, dispersion, and resuspension in vicinity of ocean wastewater plume. Journal of Hydraulic Engineering, 118: 38–58.

Weber, E.D., T.D. Auth, S. Baumann-Pickering, T.R. Baumgartner, E.P. Bjorkstedt, S.J. Bograd, B.J. Burke, J.L. Cadena-Ramirez, E.A. Daly, M. de la Cruz, H. Dewar, J.C. Field, J.L. Fisher, A. Giddings, R. Goericke, E. Gomez-Ocampo, J. Gomez-Valdes, E.L. Hazen, J. Hildebrand, C.A. Horton, K.C. Jacobson, M.G. Jacox, J. Jahncke, M. Kahru, R.M. Kudela, B.E. Lavaniegos, A. Leising, S.R. Melin, L.E. Miranda-Bojorquez, C.A. Morgan, C.F. Nickels, R.A. Orben, J.M. Porquez, E.J. Portner, R.R. Robertson, D.L. Rudnick, K.M. Sakuma, J.A. Santora, I.D. Schroeder, O.E. Snodgrass, W.J. Sydeman, A.R. Thompson, S.A. Thompson, J.S. Trickey, J. Villegas-Mendoza, P. Warzybok, W. Watson, and S.M. Zeman. (2021). State of the California Current 2019-2020: Back to the Future with Marine Heatwaves? Frontiers in Marine Science, 8: 1-23.

Wickham, H. (2007). Reshaping Data with the reshape Package. Journal of Statistical Software, 21(12), 1-20, http://www.jstatsoft.org/v21/i12/.

Wickham, H., M. Averick, J. Bryan, W. Chang, L. D'Agostino McGowan, R. François, G. Grolemund, A. Hayes, L. Henry, J. Hester, M. Kuhn, T. Lin Pedersen, E. Miller, S. Milton Bache, K. Müller, J. Ooms, D. Robinson, D. P. Seidel, V. Spinu, K. Takahashi, D. Vaughan, C. Wilke, K. Woo, H. Yutani. (2019). Welcome to the tidyverse. Journal of Open Source Software, 4(43), 1686, https://doi.org/10.21105/joss.01686.

Wickham, H. and D. Seidel. (2020). scales: Scale Functions for Visualization. R package version 1.1.1. https://CRAN.R-project.org/package=scales.

This page intentionally left blank

Chapter 5
Sediment Quality

Chapter 5. Sediment Quality

Introduction

Ocean sediment samples are analyzed by the City of San Diego (City) as part of the Ocean Monitoring Program to examine the effects of wastewater discharge from the Point Loma Ocean Outfall (PLOO) and South Bay Ocean Outfall (SBOO), and other anthropogenic inputs, on the marine benthic environment. Analyses of various sediment contaminants are conducted as anthropogenic inputs to the marine ecosystem, including municipal wastewater, can lead to increased concentrations of pollutants within the local environment. The relative proportions of sand, silt, clay, and other particle size parameters are also examined as concentrations of some compounds are known to be directly linked to sediment composition (Emery 1960, Eganhouse and Venkatesan 1993). Physical and chemical sediment characteristics are also analyzed as they define the primary microhabitats for benthic macroinvertebrates (macrofauna) that live within or on the seafloor, and therefore influence the distribution and presence of various species. For example, differences in sediment composition and organic loading impact the burrowing, tube building, and feeding abilities of infaunal invertebrates, thus affecting benthic community structure (Gray 1981, Snelgrove and Butman 1994). Many demersal fish species are also associated with specific sediment types that reflect the habitats of their preferred invertebrate prey (Cross and Allen 1993). Thus, understanding changes in sediment condition and quality over time and space is crucial to assessing corresponding changes in benthic invertebrate and demersal fish populations (see Chapters 6 and 8, respectively).

Both natural and anthropogenic factors affect the composition, distribution, and stability of seafloor sediments on the continental shelf. Natural factors that affect sediment conditions include geologic history, strength and direction of bottom currents, exposure to wave action, seafloor topography, inputs from rivers and bays, beach erosion, runoff, bioturbation by fish and benthic invertebrates, and decomposition of calcareous organisms (Emery 1960). These processes affect the size and distribution of sediment particles, as well as the chemical composition of sediments. For example, erosion from coastal cliffs and shores, and flushing of terrestrial sediment and debris from bays, rivers, and streams strongly influence the overall organic content and particle size of coastal sediments (Emery 1960). These inputs can also contribute to the deposition and accumulation of trace metals, or other contaminants, on the sea floor. In addition, primary productivity by phytoplankton, and decomposition of marine and terrestrial organisms, are major sources of organic loading in coastal shelf sediments (Mann 1982, Parsons et al. 1990).

Municipal wastewater outfalls, such as the PLOO and SBOO off San Diego, are one of many anthropogenic sources, which may influence sediment characteristics through the discharge of treated effluent, and the subsequent deposition of a wide variety of organic and inorganic compounds. Some of the most commonly detected contaminants discharged via ocean outfalls are trace metals, pesticides, and various indicators of organic loading such as organic carbon, nitrogen, and sulfides (Anderson et al. 1993). In particular, organic enrichment, due to wastewater discharge, is of concern as it may impair habitat quality for resident marine organisms and, thus, disrupt ecological processes (Gray 1981). Lastly, the physical presence of a large outfall, and associated ballast materials (e.g., rock, sand) on the seafloor, may alter the hydrodynamic regime in surrounding areas, thus affecting sediment movement and transport, as well as the structure of local fish and invertebrate communities.

This chapter presents analysis and interpretation of sediment particle size, and chemistry data, collected, during 2020 and 2021, from core benthic monitoring stations throughout the PLOO and SBOO regions. The three primary goals of this chapter are to: (1) document sediment conditions at core monitoring

stations; (2) identify if concentrations of pollutants in marine sediments are at levels that would degrade the benthic communities; (3) identify possible effects of wastewater discharge on sediment quality; (4) identify other potential natural or anthropogenic sources of sediment contamination. For additional information, a broader regional assessment of benthic conditions throughout the entire San Diego region is presented in Chapter 7.

Materials and Methods

Field Sampling

Benthic samples analyzed in this chapter were collected at a total of 49 core monitoring stations, located at inner shelf (≤ 30 m) to middle shelf (> 30 –120 m) depths, surrounding the PLOO and SBOO, during winter (January) and summer (July) of 2020 and 2021 (Figure 5.1). The PLOO sites include 12 primary core stations located along the 98-m discharge depth contour, and 10 secondary core stations located along or adjacent to the 88-m or 116-m depth contours. The SBOO sites include 12 primary core stations located along the 28-m discharge depth contour, and 15 secondary core stations located along or adjacent to the 19, 38, or 55-m depth contours. Stations located within 1000 m of the boundary of the zone of initial dilution (ZID), for either outfall, are considered to represent near-ZID conditions. These include PLOO stations E11, E14, E15 and E17, and SBOO stations I12, I14, I15 and I16.

Samples for benthic analyses were collected using a double 0.1-m^2 Van Veen grab, with one grab per cast used for sediment quality analyses, and one grab per cast used for benthic community analysis (see Chapters 6 and 7). Visual observations of weather, sea conditions, and human/animal activity were also recorded at the time of sampling. Criteria established by the U.S. Environmental Protection Agency (USEPA) to ensure consistency of these types of samples were followed with regard to sample disturbance and depth of penetration (USEPA 1987). Sub-samples for particle size and sediment chemistry analyses were taken from the top 2 cm of the sediment surface and handled according to standard guidelines (USEPA 1987, SCCWRP 2018).

Laboratory Analyses

All sediment chemistry and particle size analyses were performed at the City's Environmental Chemistry Services Laboratory. Detailed analytical protocols are available upon request. Briefly, sediment sub-samples were analyzed on a dry weight basis to determine concentrations of various indictors of organic loading (biochemical oxygen demand, total organic carbon, total nitrogen, total sulfides, total volatile solids), 18 trace metals, nine chlorinated pesticides, 42 polychlorinated biphenyl compound congeners (PCBs), and 24 polycyclic aromatic hydrocarbons (PAHs). Data were limited to values above the method detection limit (MDL) for each parameter (Appendix F.1).

Particle size analysis was performed using either a Horiba LA-950V2 laser scattering particle analyzer or a set of nested sieves. The Horiba measures particles ranging in size from 0.5 to 2000 µm. Coarser sediments were removed and quantified prior to laser analysis by screening samples through a 2000 µm mesh sieve. These data were later combined with the Horiba results to obtain a complete distribution of particle sizes totaling 100%, and then classified into 11 sub-fractions and four main size fractions based on the Wentworth scale (Folk 1980) (see Appendix F.2). When a sample contained substantial amounts of coarse sand, gravel, shell hash or other large materials that could damage the Horiba analyzer, or where the general distribution of sediments would be poorly represented by laser analysis, a set of nested sieves was used with mesh sizes of 2000 µm, 1000 µm, 500 µm, 250 µm, 125 µm, 75 µm, and 63 µm to divide the samples into seven sub-fractions.

Data Analyses

Data for each parameter analyzed during 2020 were reported previously (City of San Diego

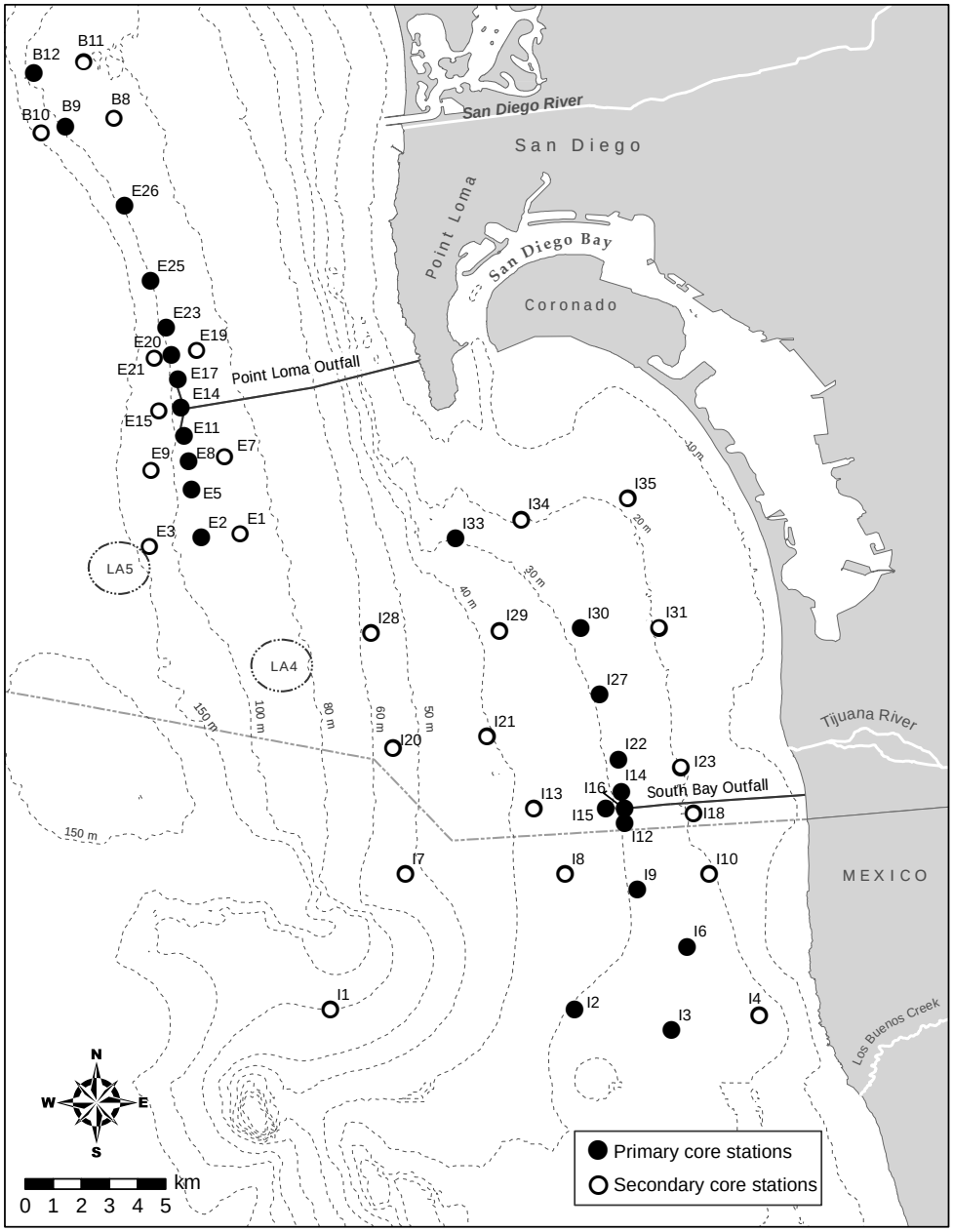

Figure 5.1
Benthic station locations sampled around the PLOO and SBOO as part of the City of San Diego's Ocean Monitoring Program.

2021), and all raw data for the 2020–2021 sampling period have been submitted to either the Regional Water Quality Control Board or the California Environmental Data Exchange Network (CEDEN) and will be provided upon request.

Data summaries for the various sediment parameters included detection rate, minimum, maximum, and mean values for all samples combined by outfall region (i.e., PLOO, SBOO). Historical summaries were generated using data from current primary and secondary core stations but limited to samples collected during winter and summer surveys. This represents a change from previous reports where historical summaries were limited to primary core stations. For chemistry parameters, all means were calculated using detected values only, with no substitutions made for non-detects in the data (i.e., analyte concentrations < MDL). Limiting analyses to detected values (i.e., excluding non-

detects) is considered a conservative way of handling contaminant concentrations as it creates a strong upward bias in the data and respective summary statistics, and therefore may represent a worst-case scenario (e.g., see Helsel 2005a, b, 2006 for discussions of non-detect data). In contrast to previous reports (e.g., City of San Diego 2020), estimated values that fell below method detection limits but were confirmed by mass-spectrometry were excluded from all data (1991–2021). Instead, estimated values were treated as non-detects for this report. Total chlordane, total DDT (tDDT), total hexachlorocyclohexane (tHCH), total PCB (tPCB), and total PAH (tPAH) were calculated for each sample as the sum of all individual constituents with reported values. When applicable, contaminant concentrations were compared to the Effects Range Low (ERL) and Effects Range Median (ERM) sediment quality guidelines of Long et al. (1995). The ERLs represent chemical concentrations below which adverse biological effects are rarely observed, while values above ERLs, but below ERMs, represent levels at which effects occasionally occur. Concentrations above the ERM indicate likely biological effects, although these may not always be validated by toxicity testing results (Schiff and Gossett 1998). Analyses were performed using R (R Core Team 2021) and various functions within the zoo, reshape2, plyr, stringr, Rmisc, ROBDC, tidyr, ggpubr, vegan, psych, tidyverse, ggplot2, and dplyr (Zeileis and Grothendieck 2005, Wickham 2007, 2011, 2019, Hope 2013, Ripley and Lapsley 2017, Wickham and Henry 2018, Kassambara 2019, Oksanen et al. 2019, Revelle 2019, Wickham et al. 2019a,b, 2020).

Results

Particle Size Distribution

Ocean sediments sampled at the core PLOO stations during 2020 and 2021 were composed primarily of fine silts and clays (fine particles, or percent fines), plus fine sands. Percent fines ranged from 17.3 to 73.1% per sample, while fine sands ranged from 17.9 to 63.1%, medium-coarse sands ranged from < 1 to 28.3%, and coarse particles ranged from 0 to 38.6% (Table 5.1). Coarser particles often included shell hash, black sand, and/or gravel (Appendix F.3). Overall, there were no spatial patterns in sediment composition relative to proximity to the PLOO discharge site over the past two years (Figure 5.2). For example, most samples from the near-ZID stations (E11, E14, E15, and E17) had proportions of fine particles that fell within the range of the farfield stations (35.7–61.9% versus 37.6–73.1% per sample, respectively). Two samples from station E14 and one sample from station E11 had comparatively coarse sediments. Sediments at station E14 in winter 2020 had just 17.3% fines, with 34.2% fine sands, 10.0% medium-coarse sand, and 38.6% coarse particles, while sediments in winter 2021 had 53.8% fine particles, 35.4% fine sands, 7.7% medium-coarse sands, and 3.2% coarse particles. Sediments at station E11 in summer 2020 had 39.6% fine particles, 45.9% fine sands, 5.2% medium-coarse sands, and 9.3% coarse particles. Sediments from farfield stations that also had larger proportions of medium-coarse sands ($\geq$11.0% per sample) and/or coarse particles ($\geq$ 3.2% per sample) included one sample from station E1, two samples from station E2, three samples from station E3, one sample from station E5, three samples from station E9, and three samples from station B12.

There was no evidence that fine sediments have been accumulating over time at any of the nearfield or farfield primary core PLOO stations since wastewater discharge began at the current discharge site in late 1993 (Figure 5.3). Instead, temporal variability of sediment composition at these sites has been primarily in the sand and coarse fractions (see City of San Diego 2014a, 2022a). This variability has corresponded to occasional patches of coarse sands (e.g., black sand) or larger particles (e.g., gravel, shell hash). For example, black sands have been observed at stations E9, E15, and E14 over the years (e.g., City of San Diego 2020) possibly due in part to the presence of ballast or bedding material near the outfall (City of San Diego 2022a). In addition to the sporadic occurrence of coarser sediments at a few stations, a sudden, region-wide increase in fine particles was observed starting in winter 2019. This abrupt change remains unexplained.

Table 5.1

Summary of particle sizes and chemistry concentrations in sediments from PLOO benthic stations sampled historically (1991–2019) and during the current reporting period (2020–2021). Data include the total number of samples analyzed (n), detection rate (DR, %), minimum, maximum, and mean values for the entire survey area during each time period. For chemistry parameters, minimum and maximum values were calculated based on all samples, whereas means were calculated on detected values only; nd = not detected.

	Historical (1991–2019)					Current (2020–2021)				
Parameter	**n**	**DR**	**Min**	**Max**	**Mean**	**n**	**DR**	**Min**	**Max**	**Mean**
Particle Size (%)										
Coarse Particles	1153	28	0	64.2	1.4	88	17	0.0	38.6	1.5
Med-Coarse Sands	1153	95	0	66.5	3.7	88	100	0.1	28.3	3.4
Fine Sands	1153	100	0	85.6	53.1	88	100	17.9	63.1	39.0
Fine Particles	1153	100	0	80.9	41.7	88	100	17.3	73.1	56.1
Organic Indicators										
BOD (ppm)	1014	99.9	nd	980	304	48	100	148	546	270
Sulfides (ppm)	1173	96	nd	108.0	5.0	87	72	nd	30.8	6.0
TN (% weight)	1107	99	nd	0.192	0.052	88	100	0.032	0.113	0.052
TOC (% weight)	1108	100	0.13	4.85	0.68	88	100	0.28	3.49	0.77
TVS (% weight)	1172	100	0.2	5.4	2.4	76	100	1.2	4.5	2.2
Metals (ppm)										
Aluminum	1065	100	3130	31,800	9527	88	100	3910	11,000	6546
Antimony	1157	47	nd	13.90	1.81	88	100	0.29	2.85	0.93
Arsenic	1175	100	0.75	8.82	3.04	88	100	1.77	8.25	2.85
Barium	669	100	10.3	155.0	37.3	88	100	11.2	54.1	27.1
Beryllium	1175	45	nd	6.760	0.458	88	74	nd	0.370	0.176
Cadmium	1175	47	nd	6.270	0.624	88	50	nd	0.114	0.061
Chromium	1175	99.9	nd	40.6	17.4	88	100	9.9	26.8	15.1
Copper	1175	99.9	nd	82.4	8.2	88	100	3.4	17.0	6.1
Iron	1109	100	4840	31,900	13,072	88	100	6300	24,300	10,484
Lead	1175	66	nd	326.0	6.0	88	100	1.9	7.5	3.3
Manganese	976	100	32	319	102	88	100	45	139	78
Mercury	1158	66	nd	0.142	0.031	88	100	0.008	0.057	0.025
Nickel	1175	96	nd	29.0	7.3	88	100	2.5	10.0	5.3
Selenium	1175	50	nd	0.90	0.28	88	10	nd	0.54	0.32
Silver	1175	13	nd	67.4	1.7	88	1	nd	0.072	0.072
Thallium	1175	9	nd	113.0	11.1	88	0	—	—	—
Tin	976	65	nd	42.00	1.38	88	89	nd	1.46	0.76
Zinc	1175	99.9	nd	176.0	30.3	88	100	16.5	52.5	25.4
Pesticides (ppt)										
Total DDT	1150	50	nd	63,580	1354	88	100	93	2216	469
Total Chlordane	1150	1	nd	2000	383	88	6	nd	223	122
Total HCH	1150	1	nd	980	231	88	0	—	—	—
HCB	957	5	nd	3300	773	74	9	nd	490	238
Endrin aldehyde	1150	0	nd	970	970	88	0	—	—	—
Mirex	1150	0	nd	66	66	88	0	—	—	—
Total PCB (ppt)	841	19	nd	60,730	2392	87	57	nd	59,355	2161
Total PAH (ppb)	1155	22	nd	9751.3	129.9	88	48	nd	239.5	56.9

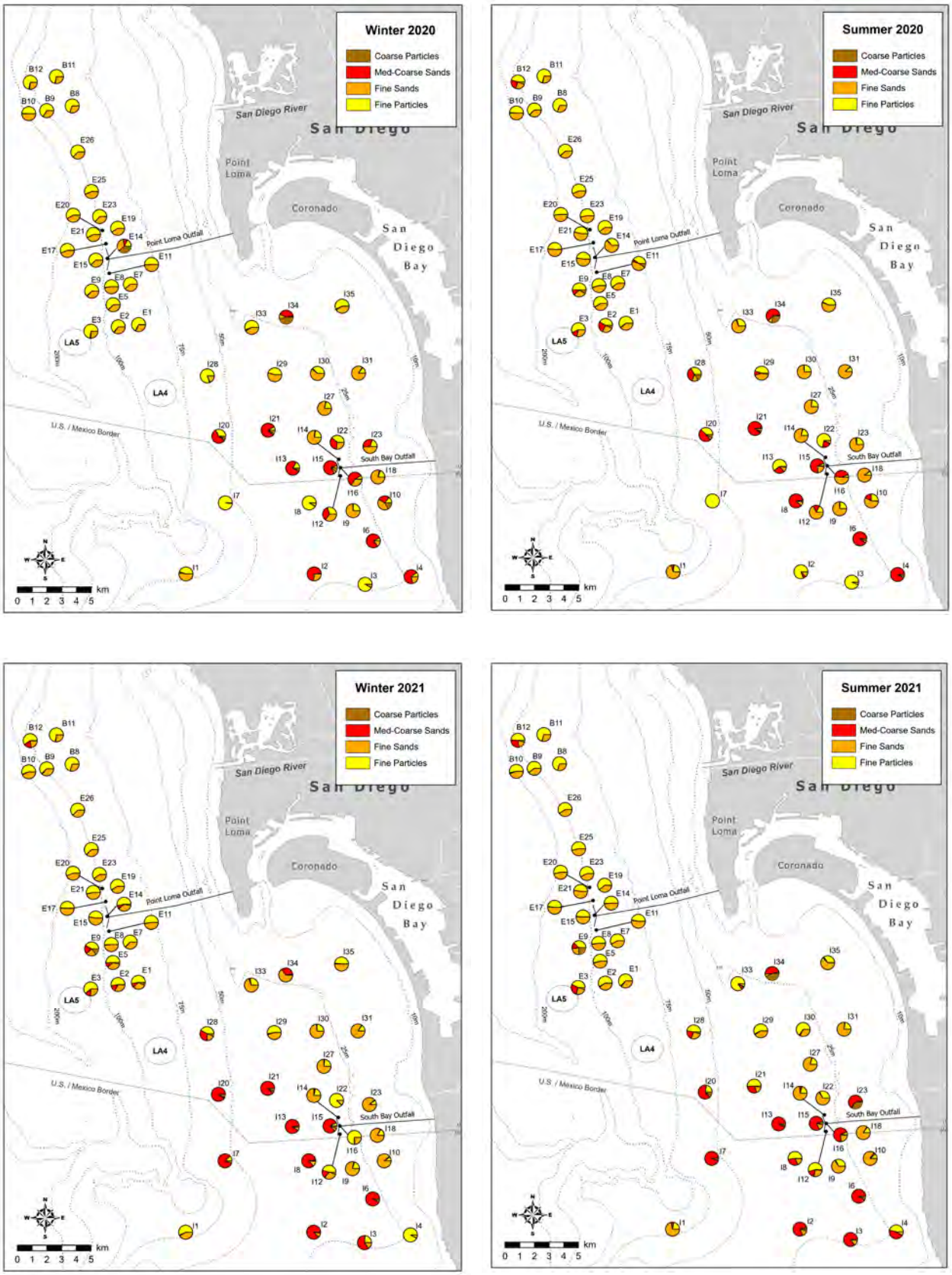

Figure 5.2
Sediment composition at PLOO and SBOO benthic stations during winter and summer surveys of 2020 and 2021.

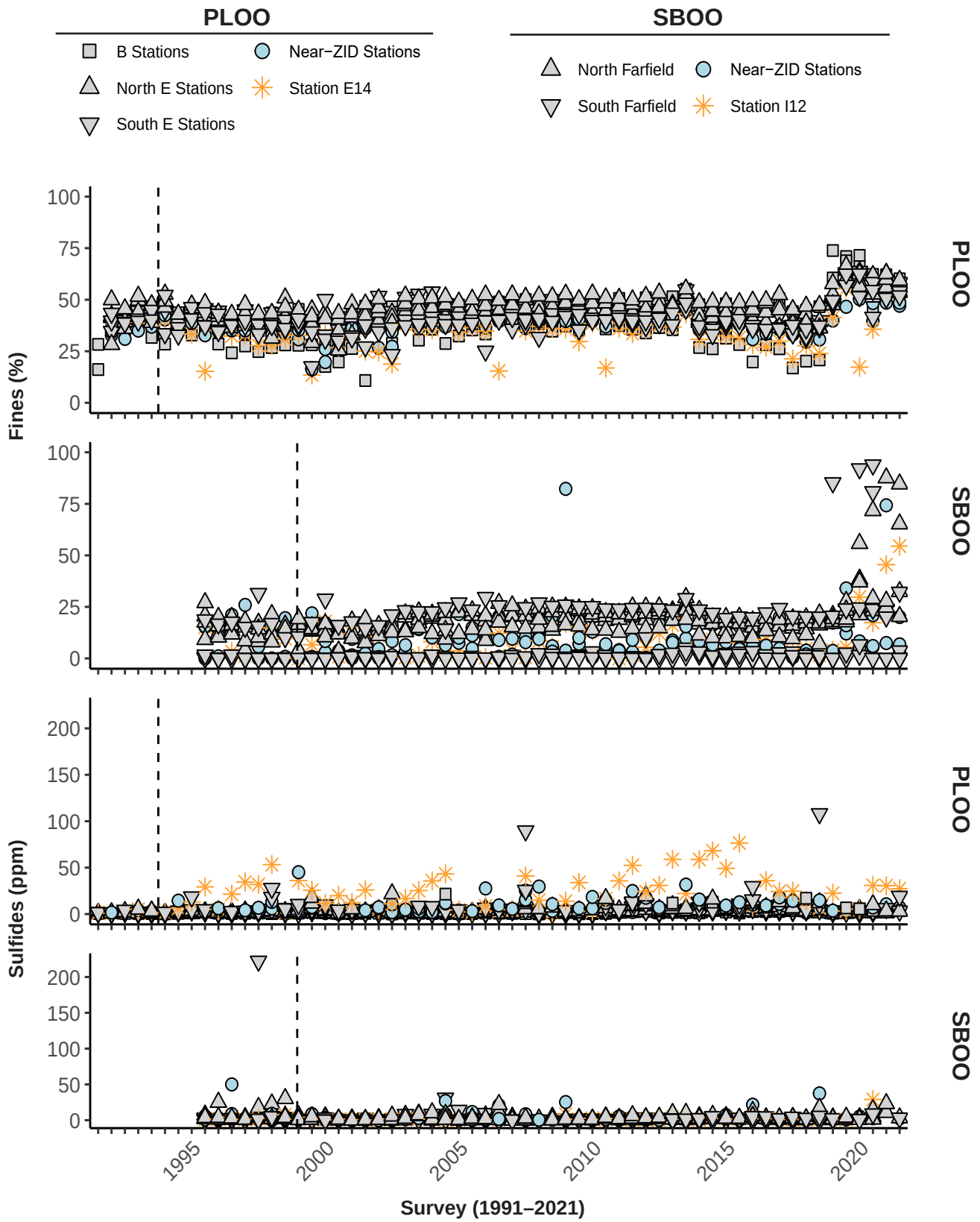

Figure 5.3

Percent fines and concentrations of organic indicators in sediments sampled during winter and summer surveys at PLOO primary core stations from 1991 through 2021 and at SBOO primary core stations from 1995 through 2021. Data represent detected values from each station, n ≤ 12 samples per survey. Dashed lines indicate onset of discharge from the PLOO or SBOO. Biochemical Oxygen Demand (BOD) only measured at PLOO stations.

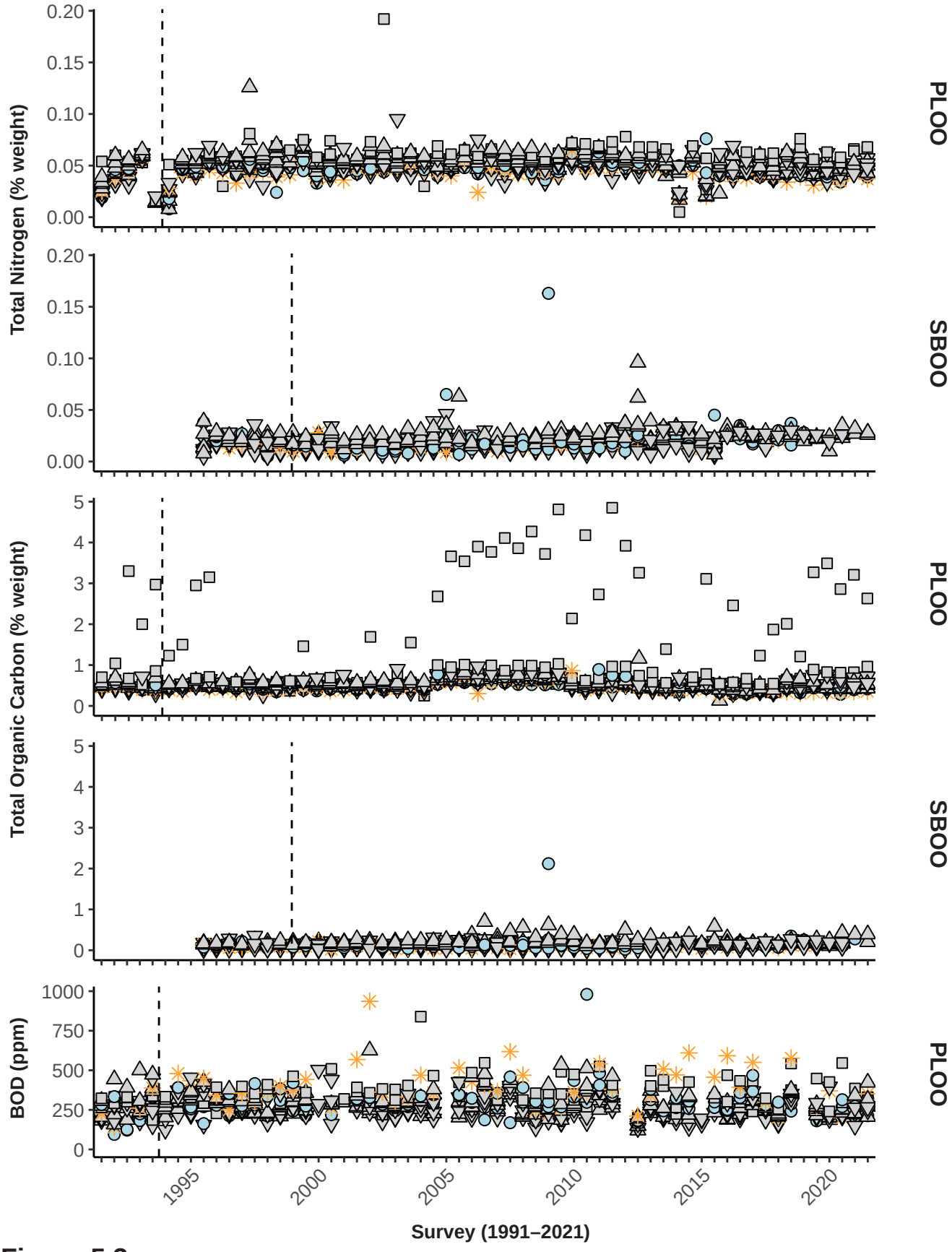

Figure 5.3 *continued*

In contrast to the PLOO region, seafloor sediments were much more diverse at the SBOO monitoring sites during 2020 and 2021. Percent fines ranged from 0 to 100% per sample at these stations, while fine sands ranged from 0 to 89.2%, medium-coarse sands ranged from 0 to 94.5%, and coarse particles ranged from 0 to 46.1% (Table 5.2). Coarser particles at the SBOO stations often comprised shell hash, red relict sands, black sand, gravel or cobble (Appendix F.3). There were no spatial patterns in sediment composition relative to proximity to the SBOO discharge site over the past two years (Figure 5.2). Similar to the rest of the SBOO region, sediments from near-ZID stations (I12, I14, I15, and I16) were highly variable, with proportions of fine particles ranging from 4.0–74.3%, fine sands ranging from 5.9–78.1%, medium-coarse sands ranging from 1.0–79.8%, and coarse particles ranging from 0–10.0%. Stations I15 and I16 tended to have larger proportions of medium-coarse sands than stations I12 and I14 (mean = 60.1% versus 12.4%, respectively). It is interesting to note that fine particles also appeared to increase starting in winter 2019 at some SBOO primary core stations. Previous analysis of particle size data revealed considerable temporal variability at some sites within the SBOO region and relative stability at others, with no clear patterns evident relative to depth, proximity to the outfall, or other sources of nearshore sediment plumes, such as San Diego Bay and the Tijuana River (City of San Diego 2014b).

Indicators of Organic Loading

Detection rates and concentrations of the various indicators of organic loading in benthic sediments, surrounding the PLOO and SBOO, varied both within and between regions during 2020 and 2021 (Tables 5.1, 5.2). Only the parameter total volatile solids (TVS) was detected in all sediment samples from both regions. In contrast, total nitrogen (TN) and total organic carbon (TOC) were detected in 100% of the PLOO sediment samples, but only in 31% and 55% of the SBOO samples, respectively. Detection rates for sulfides were 72% in the PLOO region and 33% in the SBOO region. Although not a required parameter for any of the PLOO or SBOO permits, biochemical oxygen demand (BOD) has long been measured by the City at PLOO benthic stations; this parameter was detected in all PLOO primary core station sediments sampled during 2020 and 2021. Detection rates for these parameters were similar to, or lower than, those recorded historically since monitoring began. Lower detection rates likely reflect changes in MDLs; for example, the MDL for sulfides went from 0.14 ppm in summer 2017 to 2.2 ppm in summer 2021.

Sediments off Point Loma, in 2020 and 2021, had BOD concentrations $\leq$ 546 ppm per sample, while sulfides were $\leq$ 30.8 ppm, TN was $\leq$ 0.113% weight, TOC was $\leq$ 3.49% weight, and TVS was $\leq$ 4.5% weight per sample (Table 5.1). The highest concentrations of TN, TOC, and TVS were consistently detected in sediments from the northern 'B' stations located at least 10 km north of the PLOO (Figure 5.4). In contrast, BOD and sulfide distributions were more variable over this period. The highest concentrations of BOD occurred in two samples from northern station B12, and one sample from northern station E20. The highest concentrations of sulfides occurred in three samples from station E14. In general, only sulfide and BOD have shown any changes in concentrations near the PLOO that appear consistent with possible organic enrichment (Figure 5.3) (see also City of San Diego 2022a,b).

Sediments surrounding the SBOO, in 2020 and 2021, had sulfide concentrations $\leq$ 28.9 ppm per sample, while TN concentrations were $\leq$ 0.076% weight, TOC concentrations were $\leq$ 4.37% weight, and TVS concentrations were $\leq$ 2.0% weight per sample (Table 5.2). There was little evidence of any significant organic enrichment near the SBOO discharge site during these two years; the highest concentrations of the various organic loading indicators were widely distributed throughout the region (Figure 5.4). For TOC, TN and TVS, variable concentrations may be linked to regional differences in sediment particle composition since these parameters can co-vary with the amount of percent fines (see City of San Diego 2014b and Chapter 7). In contrast to the overall survey area,

Table 5.2

Summary of particle sizes and chemistry concentrations in sediments from SBOO benthic stations sampled historically (1995–2019) and during the current reporting period (2020–2021). Data include the total number of samples analyzed (n), detection rate (DR, %), minimum, maximum, and mean values for the entire survey area during each time period. For chemistry parameters, minimum and maxium values were calculated based on all samples, whereas means were calculated on detected values only; nd = not detected.

	Historical (1995–2019)					Current (2020–2021)				
Parameter	**n**	**DR**	**Min**	**Max**	**Mean**	**n**	**DR**	**Min**	**Max**	**Mean**
Particle Size (%)										
Coarse Particles	1302	44	0	56.8	2.8	108	44	0	46.1	3.1
Med-Coarse Sands	1302	99	0	99.8	35.1	108	97	0	94.5	30.6
Fine Sands	1302	100	0	97.4	50.6	108	99	0	89.2	37.2
Fine Particles	1302	88	0	95.3	11.5	108	91	0	100	29.0
Organic Indicators										
Sulfides (ppm)	1306	82	nd	222.0	2.9	108	33	nd	28.9	6.6
TN (% weight)	1307	88	nd	0.200	0.000	108	31	nd	0.076	0.031
TOC (% weight)	1307	97	nd	6.90	0.20	108	55	nd	4.37	0.36
TVS (% weight)	1274	100	0.2	39.8	0.9	81	100	0.2	2.0	0.9
Metals (ppm)										
Aluminum	1307	100	495	30,100	4650	108	100	575	7220	3082
Antimony	1307	33	nd	6.40	0.71	108	74	0.00	1.31	0.58
Arsenic	1307	99	nd	11.90	2.43	108	100	0.58	10.50	2.48
Barium	903	100	0.9	177.0	20.0	108	99	nd	38.9	14.5
Beryllium	1307	38	nd	3.09	0.21	108	58	nd	0.134	0.070
Cadmium	1307	29	nd	2.00	0.14	108	12	nd	0.073	0.044
Chromium	1307	99.9	nd	39.0	9.8	108	100	2.3	13.4	8.3
Copper	1307	76	nd	99.2	3.5	108	49	nd	5.1	2.6
Iron	1307	100	559	29,300	6279	108	100	998	8820	4871
Lead	1307	65	nd	20.0	2.3	108	100	0.7	3.2	1.6
Manganese	1280	100	5.2	621	65	108	100	5	101	41
Mercury	1278	28	nd	0.135	0.011	108	44	nd	0.020	0.008
Nickel	1307	76	nd	22.8	3.0	108	97	nd	5.0	1.7
Selenium	1307	15	nd	0.62	0.22	108	0	—	—	—
Silver	1307	13	nd	11.20	0.98	108	0	—	—	—
Thallium	1307	7	nd	18.0	2.5	108	0	—	—	—
Tin	1280	49	nd	4.50	0.87	108	96	nd	1.89	0.33
Zinc	1307	95	nd	136.0	13.7	108	100	1.6	41.3	10.1
Pesticides (ppt)										
Total DDT	1264	15	nd	23,380	1062	108	40	nd	3493	378
Total Chlordane	1264	0.2	nd	600	331	108	2	nd	174	111
Total HCH	1264	1	nd	3550	695	108	3	nd	218	87
HCB	916	7	nd	6200	727	88	5	nd	412	276
Dieldrin	1264	0.1	nd	60	60	108	0	—	—	—
Endrin	1264	0.1	nd	133	133	108	0	—	—	—
Beta-Endosulfan	1264	0.1	nd	820	820	108	0	—	—	—
Total PCB (ppt)	1109	3.2	nd	106,390	3901	108	12	nd	1173	471
Total PAH (ppb)	1283	12.1	nd	1819.5	90.3	108	19	nd	37	15

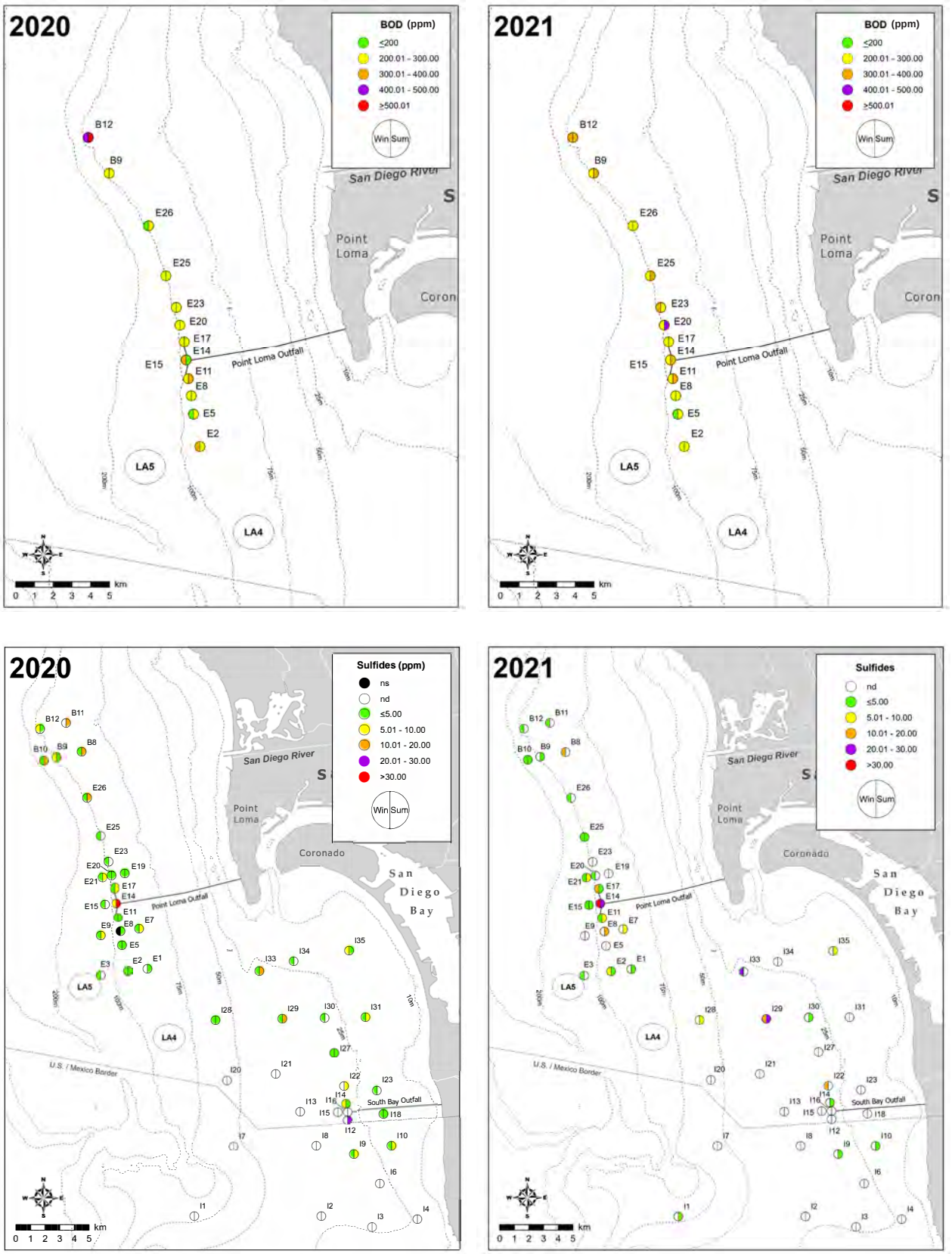

Figure 5.4
Distribution of select organic loading indicators in sediments from the PLOO and SBOO regions during winter and summer surveys of 2020 and 2021. BOD is only measured at PLOO primary core stations during summer surveys; nd = not detected; ns = not sampled.

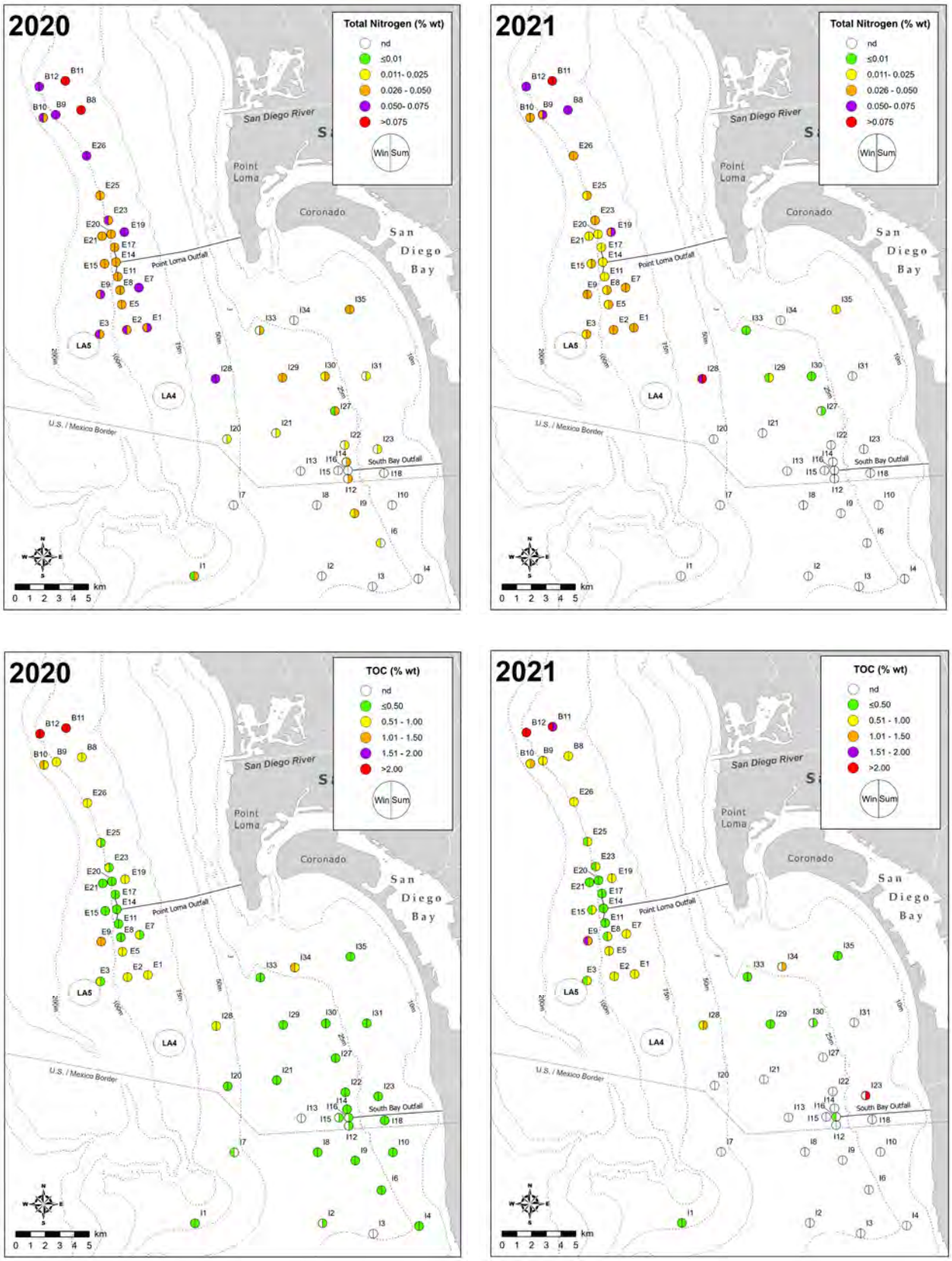

Figure 5.4 *continued*

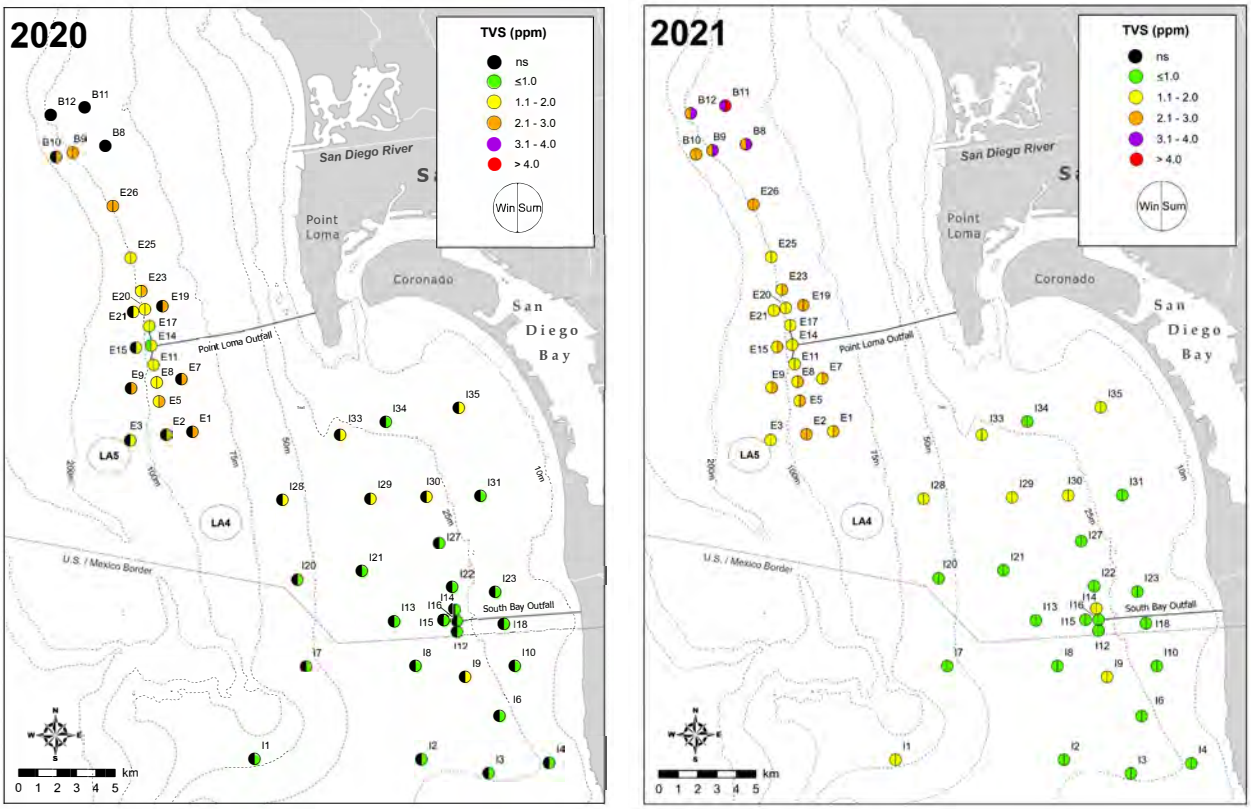

Figure 5.4 *continued*

concentrations of these organic indicators have been less variable at the SBOO primary core stations, with no patterns indicative of organic enrichment being evident since wastewater discharge began in early 1999 (Figure 5.3). For both regions, all reported concentrations of TN and TOC over the past 25–29 years generally fell within ranges reported regionally off San Diego (e.g., Chapter 7; see also City of San Diego 2022b), and elsewhere in the Southern California Bight (SCB) (e.g., Dodder et al. 2016, Du et al. 2020).

Trace Metals

Seven of the 18 trace metals analyzed were detected in all sediment samples collected at the PLOO and SBOO core benthic stations, in 2020 and 2021, including: aluminum, arsenic, chromium, iron, lead, manganese, and zinc (Tables 5.1, 5.2). Antimony, barium, nickel, and tin also had high detection rates in both regions (≥ 74%).

Beryllium, cadmium, copper, and mercury were found more often in the PLOO region (DR = 50–100%) than in the SBOO region (DR = 12–58%). Detection rates for selenium also varied considerably between regions, ranging from 10% at the PLOO stations to only 5% at the SBOO stations. Selenium and silver were detected in 10% and 1% of PLOO samples, respectively, and none of the SBOO samples. Thallium was not detected in any samples collected during the 2-year reporting period.

Of the nine metals with published ERLs and ERMs (Long et al. 1995), only arsenic was reported at levels above its threshold during 2020 or 2021 (Table 5.3). Arsenic exceeded its ERL in a sediment sample collected from PLOO farfield station B11 in summer 2021, and in three samples from SBOO farfield station I21 collected from summer 2020 through summer 2021. None of these exceeded the ERM for arsenic. In addition to low overall values, metal concentrations varied in sediments throughout the two regions, with no discernible patterns relative to proximity to either outfall. For example, several of the highest concentrations of aluminum, antimony, arsenic, barium, beryllium,

Table 5.3

Summary of samples with chemistry concentrations that exceeded Effects Range Low (ERL) and Effects Range Median (ERM) thresholds (see Long et al 1995) in sediments from PLOO and SBOO benthic stations sampled historically (1991–2019) and during the current reporting period (2020–2021). Data include the percent of samples that exceeded the ERL (%ERL) and ERM (%ERM) threholds during each time period. See Tables 5.1 and 5.2 for total number of samples analyzed.

			PLOO				SBOO			
	Thresholds		1991–2019		2020–2021		1995–2019		2020–2021	
Parameter	ERL	ERM	%ERL	%ERM	%ERL	%ERM	%ERL	%ERM	%ERL	%ERM
Metals (ppm)										
Arsenic	8.2	70.0	0.1	0	1.1	0	2.6	0	2.8	0
Cadmium	1.2	9.6	7.7	0	0	0	0.2	0	0	0
Chromium	81	370	0	0	0	0	0	0	0	0
Copper	34	270	0.3	0	0	0	0.2	0	0	0
Lead	46.7	218.0	0.2	0.1	0	0	0	0	0	0
Mercury	0.15	0.71	0	0	0	0	0	0	0	0
Nickel	20.9	51.6	0.1	0	0	0	0.1	0	0	0
Silver	1.0	3.7	5.9	0.6	0	0	3.8	1.1	0	0
Zinc	150	410	0.1	0	0	0	0	0	0	0
Pesticides (ppt)										
tDDT	1580	461,000	9.3	0.1	1.1	0	2.1	0	2.8	0
tPAH	4022	44,792	0.1	0	0	0	0	0	0	0

chromium, copper, iron, lead, manganese, mercury, nickel, tin and zinc were found in sediments from one or more of the northern 'B' stations or southern 'E' stations within the PLOO region (e.g., Figure 5.5, see also Appendix F.4). As with TOC, TN and TVS, this pattern may be linked to regional differences in sediment particle composition since several of these metals can co-vary with the amount of percent fines (see City of San Diego 2014b and Chapter 7). Only cadmium tended to be highest near the PLOO, with the three highest values ($\geq$0.083) recorded in sediments from near-ZID station E14. Note, though, that the maximum value recorded at these sites (0.114 ppm) was well below the ERL of 1.2 ppm. Within the SBOO region, farfield station I35 had relatively high values of antimony, barium, manganese, and tin, while farfield station I29 had high values of barium and tin, farfield stations I6, I7, I13, and I21 had high values of arsenic, farfield station I9 had high values of barium, and station I33 had high values of tin in one or more samples over the past two years.

Historically, detection rates have been relatively high for several different metals at PLOO and SBOO stations. For example, aluminum, arsenic, barium, chromium, copper, iron, manganese, nickel, and zinc have been detected in $\geq$ 76% of the sediment samples collected in these areas since monitoring began (Tables 5.1, 5.2). Concentrations of chromium and mercury have remained below their ERLs, while exceedances for arsenic, cadmium, copper, lead, nickel, silver, and zinc have also been rare (historical rates $\leq$ 5.9% within each region; Table 5.3). Concentrations of the remaining metals have been extremely variable with most being detected within ranges reported regionally off San Diego (e.g., Chapter 7; see also City of San Diego 2022b), and elsewhere in the Southern California Bight (SCB) (e.g., Dodder et al. 2016, Du et al. 2020). While high metal concentrations have been occasionally recorded in sediments collected from both PLOO and SBOO near-ZID stations, no discernible long-term patterns have been identified that could be associated with proximity to either outfall or to the onset of wastewater discharge (Figure 5.6, Appendix F.5).

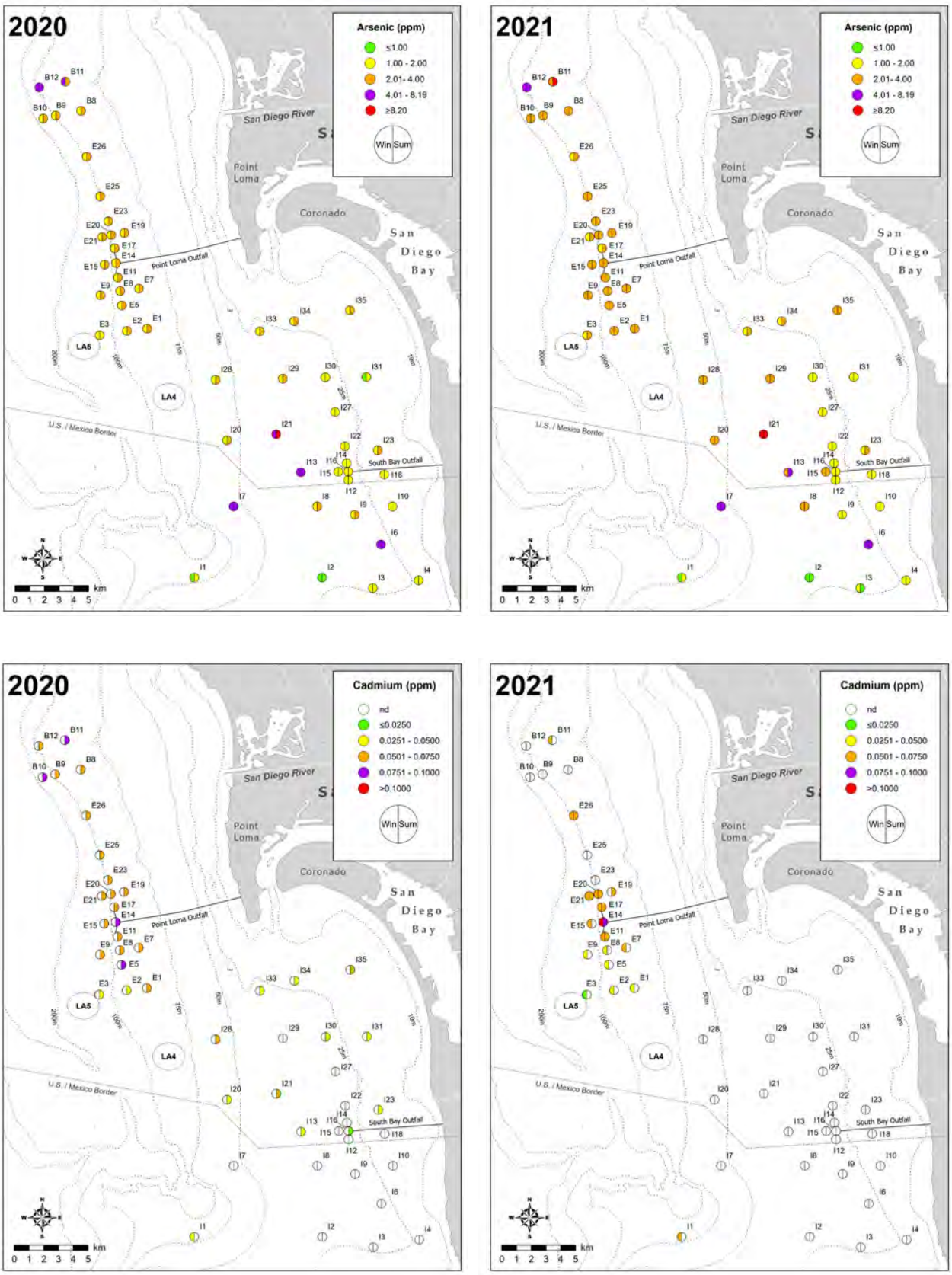

Figure 5.5
Distribution of select metals (ppm) in sediments from the PLOO and SBOO regions during winter and summer surveys of 2020 and 2021.

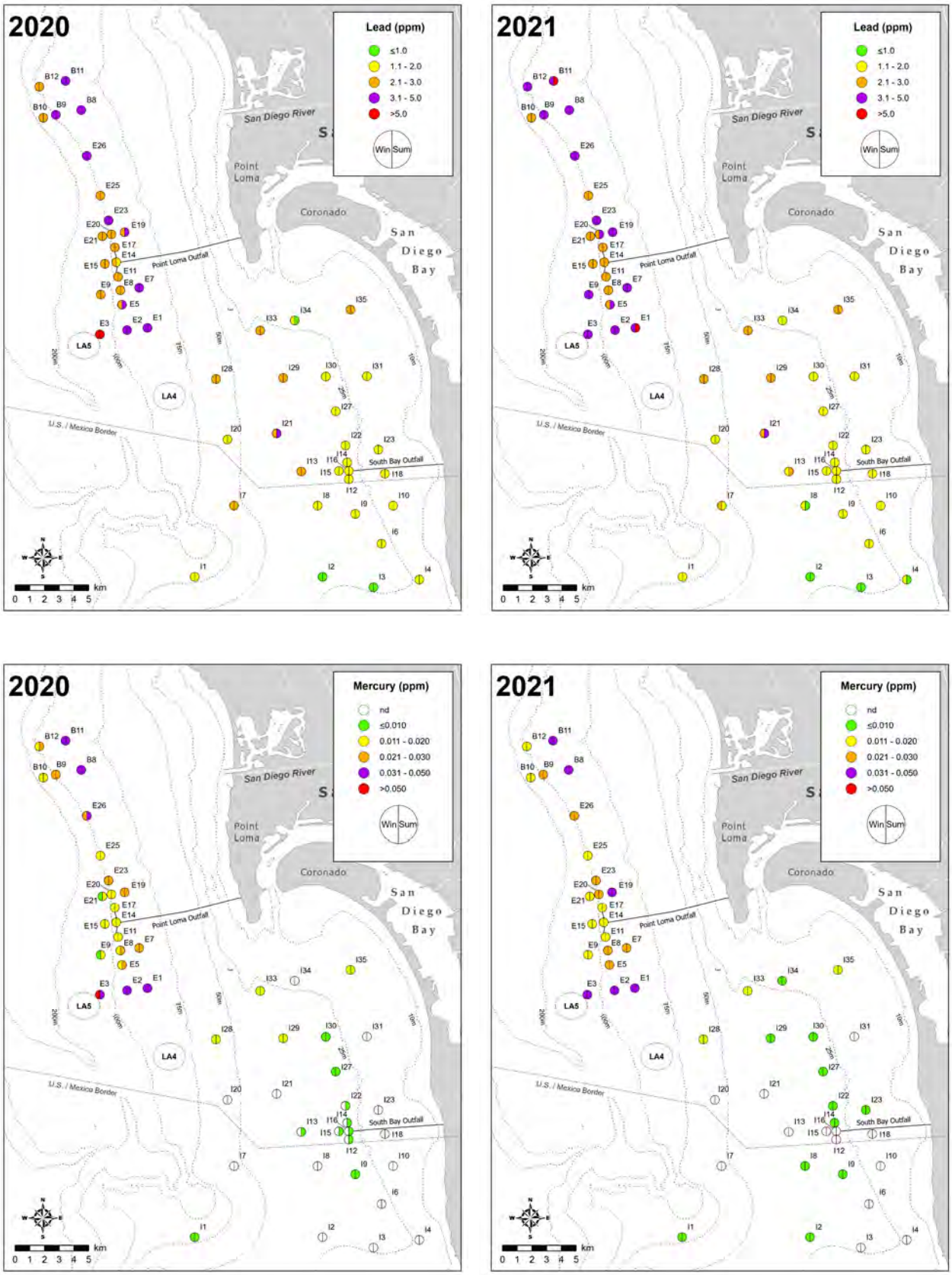

Figure 5.5 *continued*

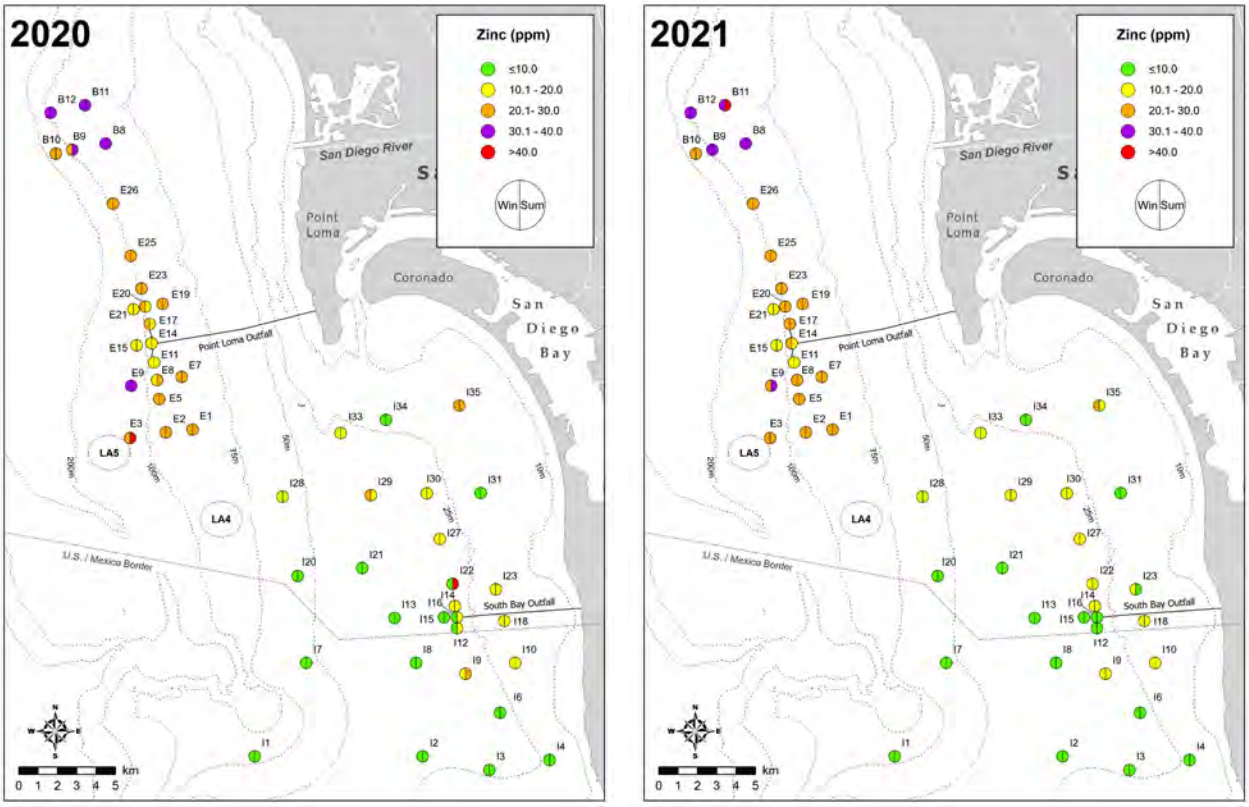

Figure 5.5 *continued*

Pesticides, PCBs, PAHs

A total of four chlorinated pesticides were detected in benthic sediments off San Diego during 2020 and 2021, including chlordanes, DDT, hexachlorobenzene (HCB), and HCH (Tables 5.1, 5.2). The most common of these pesticides, DDT, was detected in 100% of the PLOO samples and 40% of the SBOO samples, with total DDT concentrations $\leq$ 2216 ppt and $\leq$ 3493 ppt per region, respectively. The second most common pesticide, HCB, was detected in 9% of PLOO and 5% SBOO samples, with concentrations $\leq$ 490 ppt and $\leq$ 412 ppt per region, respectively. Chlordanes had a detection rate of 6% for PLOO samples but was found in only 2% of the SBOO samples, with a maximum concentration of 223 ppt for both regions. HCH was detected in 3% of SBOO samples, with concentrations $\leq$ 218 ppt; this pesticide was not detected in sediments from the PLOO region. Aldrin, dieldrin, endosulfan (*alpha*, *beta*, endosulfan sulfate), endrin and endrin aldehyde, and mirex were not detected in any PLOO or SBOO sediment samples during this reporting period.

The spatial distribution of these pesticides varied in sediments from throughout the two regions over the past two years, with no discernible patterns relative to either outfall (e.g., Figure 5.7). For example, similar to many of the metals, the many of highest DDT values were found in sediments from the northern 'B' or southern 'E' PLOO stations. Four samples had DDT values that exceeded the ERL threshold of 1580 ppt. These exceedances occurred at PLOO farfield station E7 in summer 2021, SBOO farfield station I28 in winter 2020, and SBOO farfield station I29 in winter and summer 2020.

During the 2020–2021 reporting period, PCBs were detected in 57% of sediment samples from the PLOO region at concentrations up to 59,355 ppt, and in 12% of samples from the SBOO region, at concentrations up to 1173 ppt (Tables 5.1, 5.2). See Chapter 7 for further assessment of the high total PCB values recorded during this period.

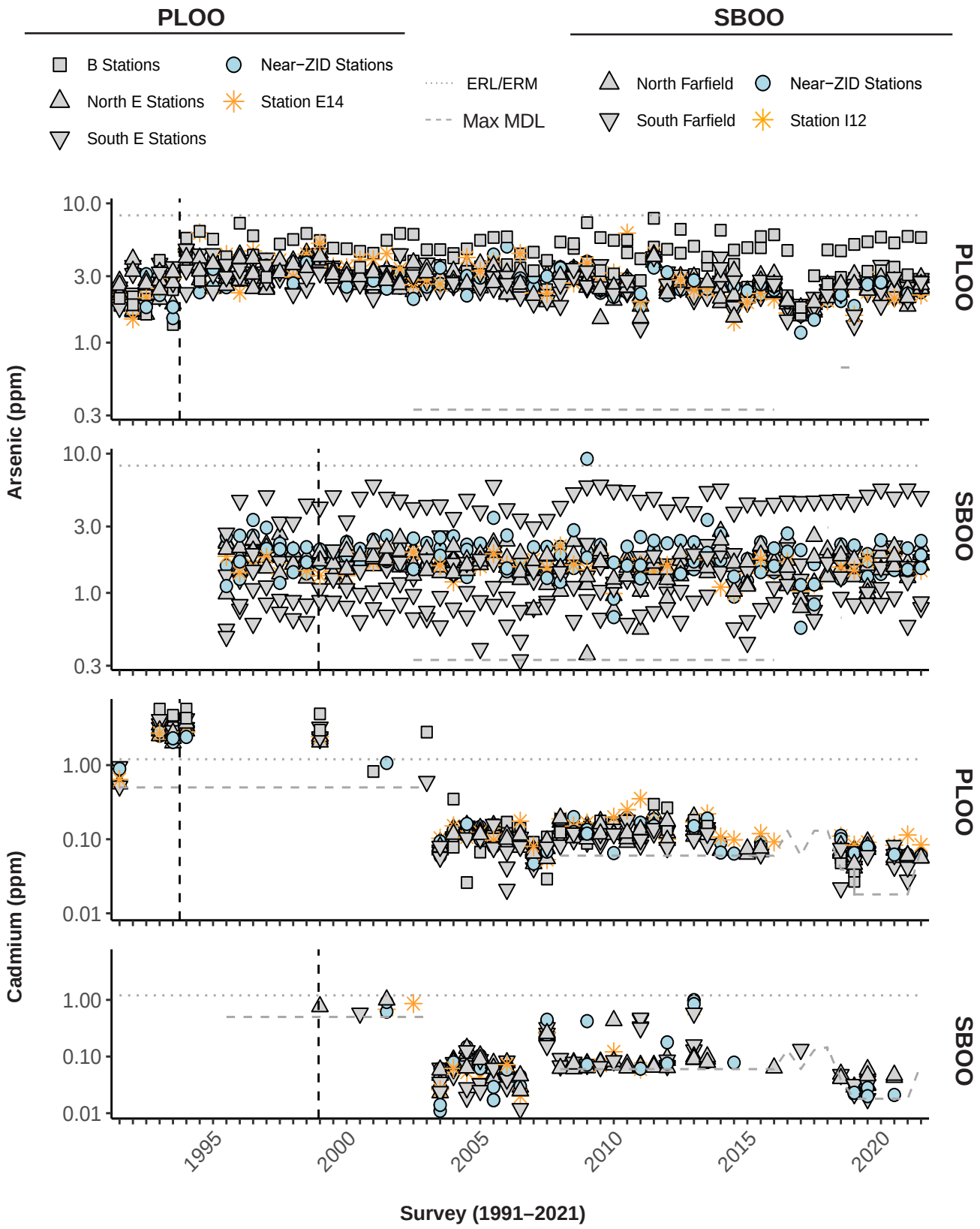

Figure 5.6

Concentrations of select metals in sediments sampled during winter and summer surveys at PLOO primary core stations from 1991 through 2021 and at SBOO primary core stations from 1995 through 2021. Data represent detected values from each station, n≤12 samples per survey. Dashed lines indicate onset of discharge from the PLOO or SBOO. Thresholds included (ERLs, ERMs) when relevant (see Table 5.3), along with the maximum MDL per survey.

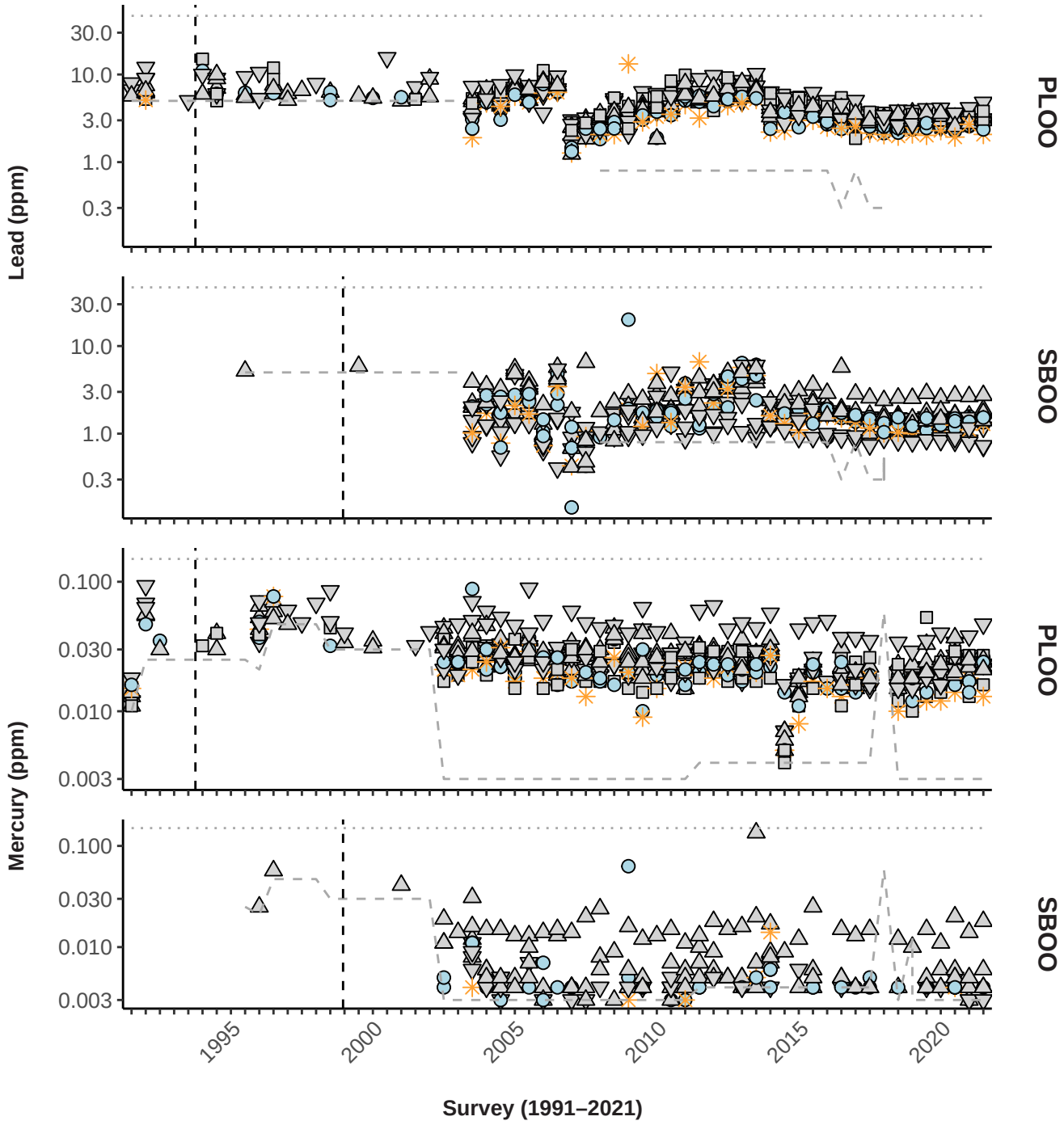

Figure 5.6 *continued*

Total PAH was also detected more frequently in the PLOO region (48%) versus the SBOO region (19%), at concentrations ≤ 239.5 ppb at all stations, well below the ERL threshold of 4022 ppb. Concentrations of total PCB and total PAH varied in sediments from throughout the two regions over the past two years, with no discernible patterns relative to either outfall. Instead, both contaminant types tended to be highest at the southern 'E' PLOO stations (Figure 5.7).

Although historical comparisons of pesticide, PCB and PAH results indicate higher detection rates in 2020–2021 versus previous years (Tables 5.1, 5.2), these apparent recent increases should be viewed with caution, since they

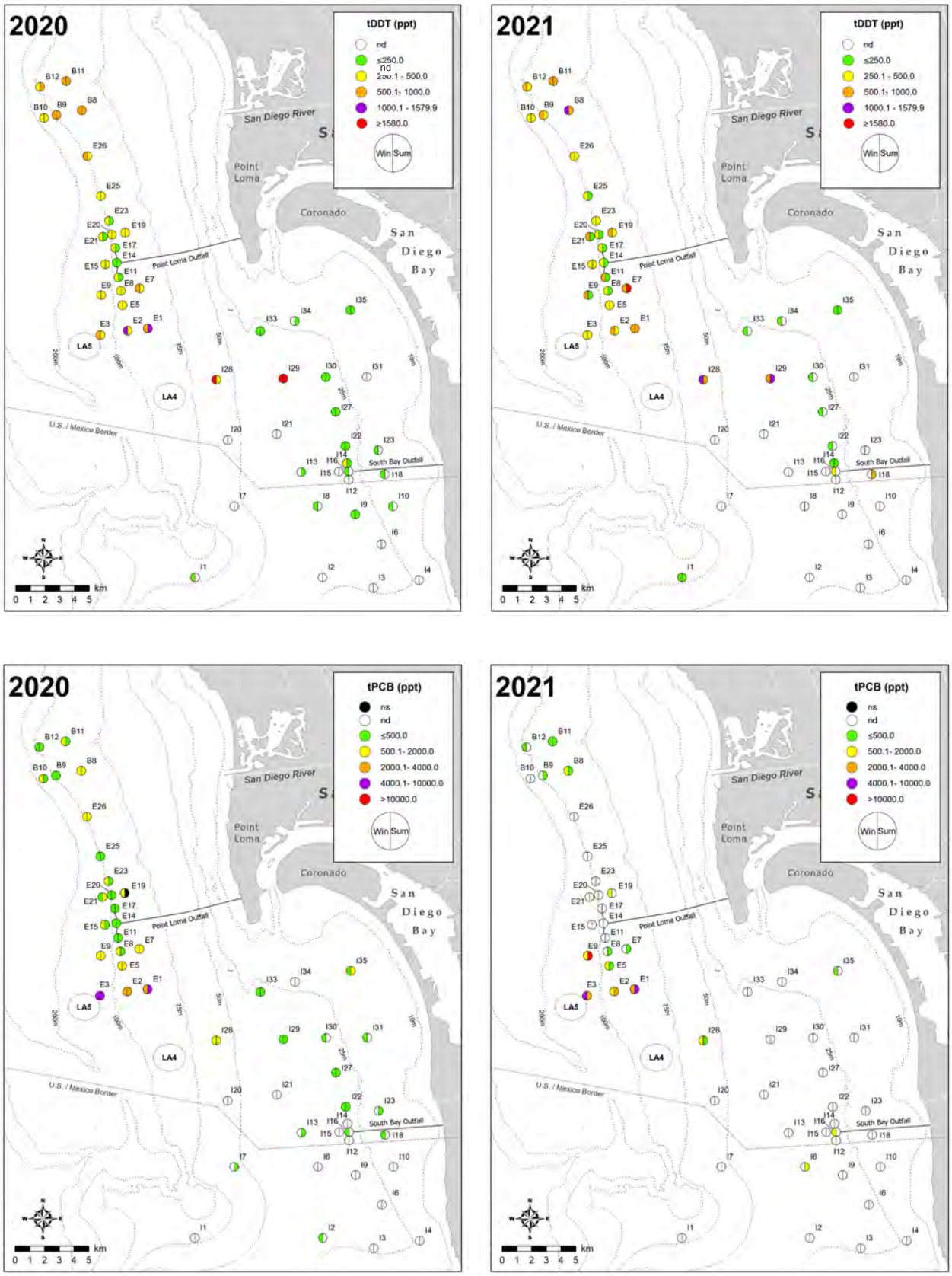

Figure 5.7
Distribution of total DDT, total PCB and total PAH in sediments from the PLOO and SBOO regions during winter and summer surveys of 2020 and 2021; nd = not detected; na = not analyzed.

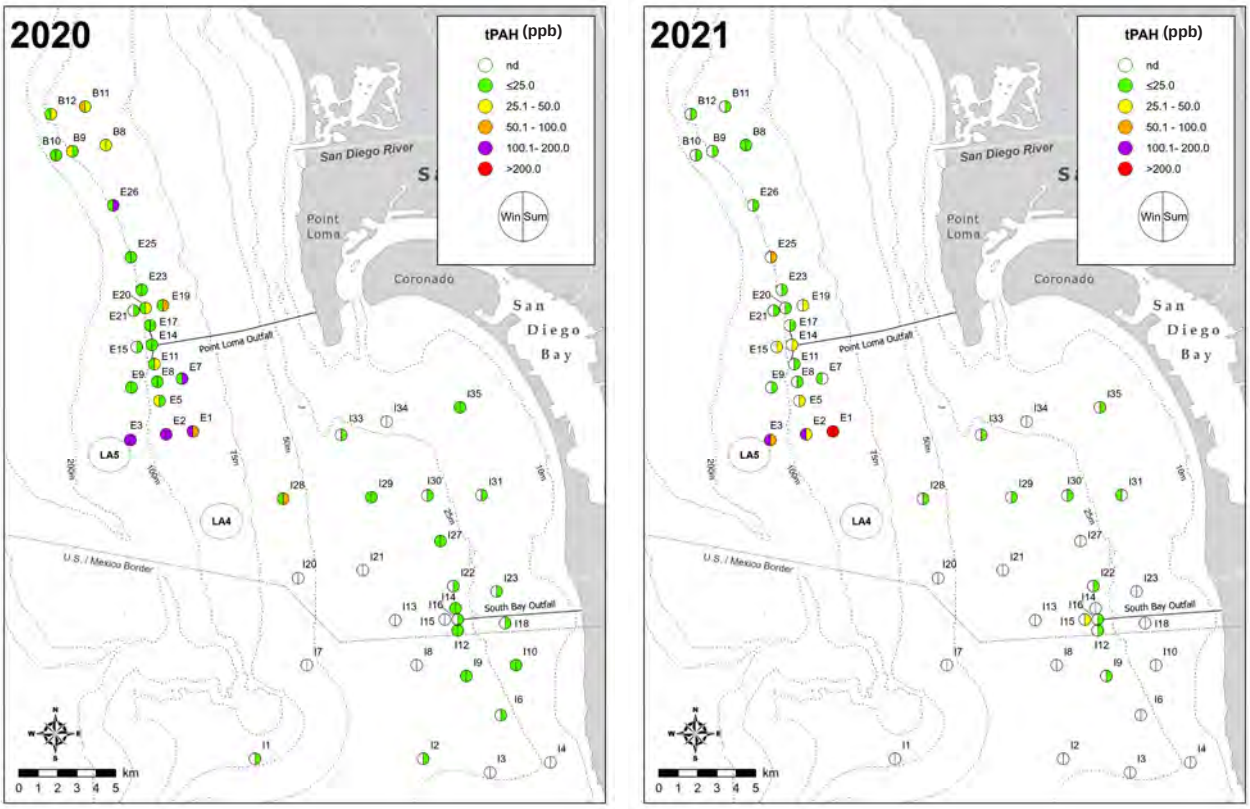

Figure 5.7 *continued*

are most likely due to improved methods that increase the likelihood of detecting these parameters (Dodder et al. 2016). In addition, pesticide, PCB and PAH concentrations have been consistently low, with total DDT exceeding its ERL in just 9.3% of the samples collected in the PLOO region, and 2.1% of the samples in the SBOO region between 1991 or 1995 – 2019 (Table 5.3). Total PAH exceeded its ERL in 0.1% of the samples from PLOO stations, and neither DDT or PAH have ever exceeded their ERMs. These thresholds do not exist for PCBs measured as congeners. For both regions, all reported concentrations of total DDT, chlordanes, total PCB, and total PAHs were generally within values reported regionally off San Diego (e.g., Chapter 7; see also City of San Diego 2022b), and well below maximum values reported elsewhere in the SCB (e.g., Dodder et al. 2016, Du et al. 2020). Finally, changes in DDT, PCB and PAH demonstrated no discernible long-term patterns that can be associated with wastewater discharge via either outfall (Figure 5.8).

Discussion

Particle size composition during the current reporting period (2020–2021) at PLOO and SBOO stations varied as expected by outfall region and depth stratum (e.g., Emery 1960, MBCES 1988), and was generally consistent with results of previous surveys off San Diego (e.g., City of San Diego 2020, 2022a,b). Within the PLOO region, percent fines (silt and clay) and fine sands continued to comprise the largest proportion of sediments. Within the SBOO region, sands continued to comprise the largest proportion of sediments, with the relative amounts of coarser and finer particles varying among sites. No spatial relationship was evident between sediment particle size composition and proximity to the SBOO discharge site, while only minor deviations were found near the PLOO. Further, there has not been any substantial accumulation of fine particles at any of the near-ZID stations or elsewhere since wastewater discharge began at the current PLOO discharge site in late 1993 or the SBOO discharge site in early 1999. Instead, a sudden increase

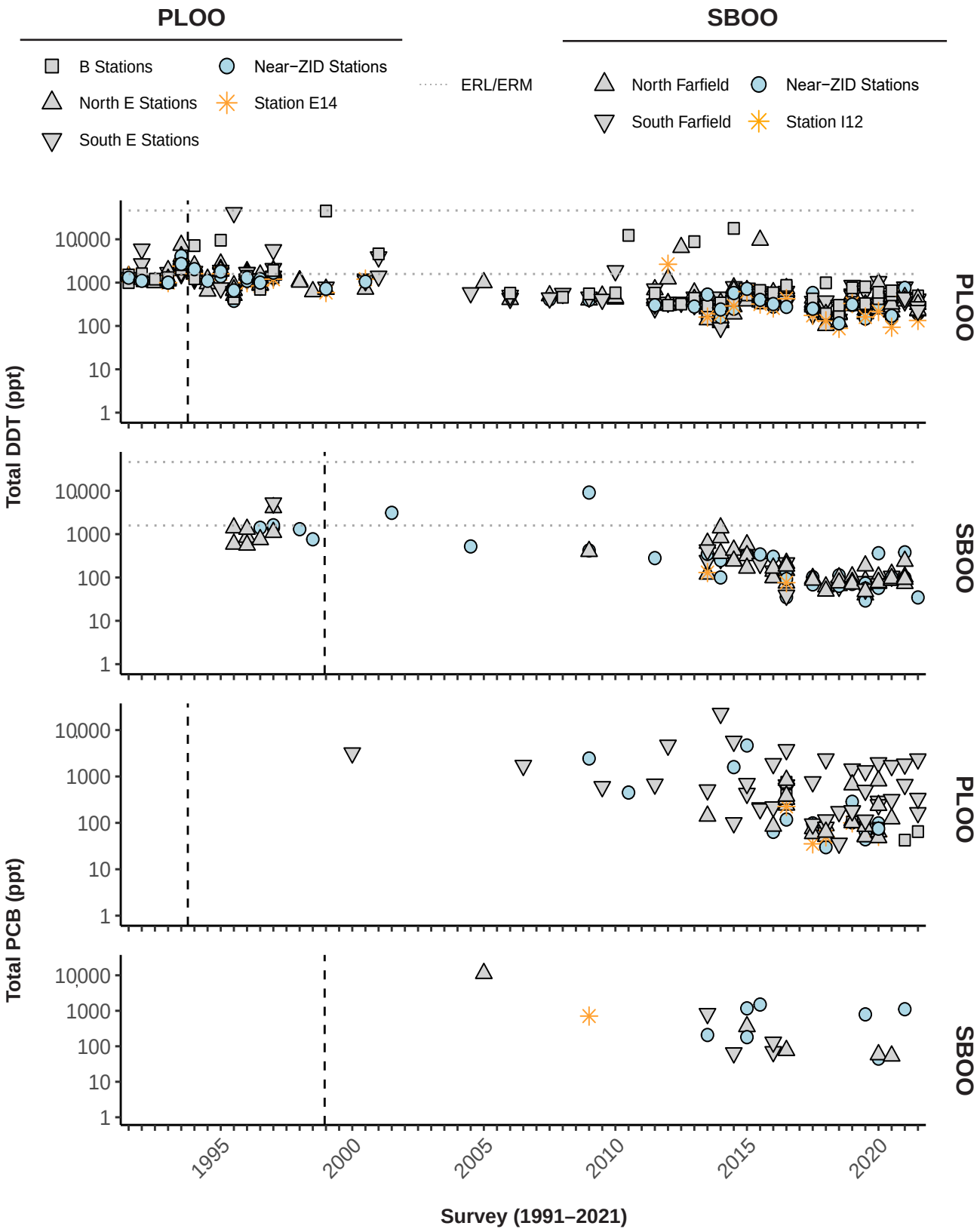

Figure 5.8

Concentrations of total DDT, total PCB, and total PAH in sediments sampled during winter and summer surveys at PLOO primary core stations from 1991 through 2021 and at SBOO primary core stations from 1995 through 2021. Data represent detected values from each station, n≤12 samples per survey. Dashed lines indicate onset of discharge from the PLOO or SBOO. Thresholds included (ERLs, ERMs) when relevant (see Table 5.3).

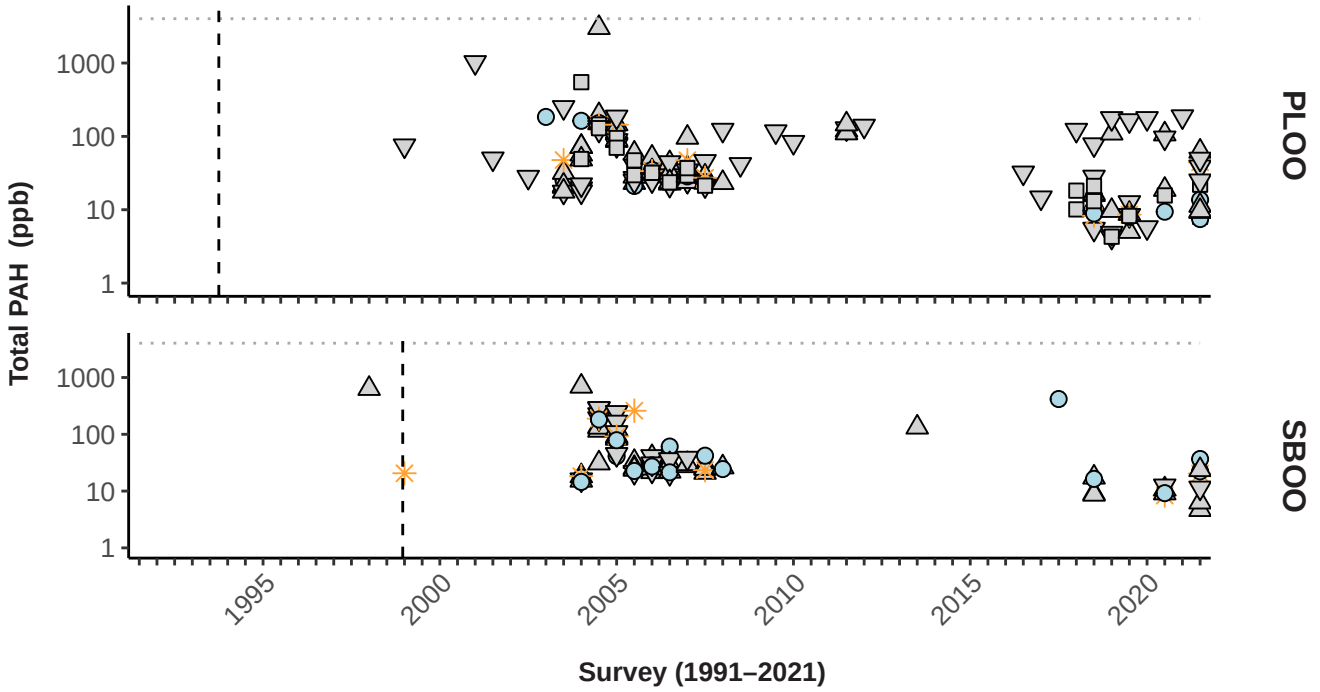

Figure 5.8 *Continued*

in fine particles was observed across the entire PLOO region and part of the SBOO region starting in winter 2019 that has persisted through summer 2021. Further investigation is required to determine the origins of this dramatic change.

The diversity of sediment types in these areas reflect multiple geologic origins and complex patterns of transport and deposition. Variability in the composition of Point Loma sediments is likely affected by both anthropogenic and natural influences, including outfall construction or ballast materials, offshore disposal of dredged materials, and recent deposition of sediment and detrital materials (Emery 1960, Parnell et al. 2008, City of San Diego 2022a). For example, the PLOO lies within the Mission Bay littoral cell (Patsch and Griggs 2007), which has natural sources of sediments, such as outflows from Mission Bay, the San Diego River, and San Diego Bay. However, fine particles may also travel in suspension across littoral cell borders up and down the coast (e.g., Farnsworth and Warrick 2007, Svejkovsky 2013), thus widening the range of potential sediment sources to the region. Additionally, the presence of relict red sands at some stations in the SBOO region is indicative of minimal sediment deposition in recent years (Emery 1960). Several SBOO stations are also located within or near an accretion zone for sediments moving within the Silver Strand littoral cell (MBC-ES 1988, Patsch and Griggs 2007). Therefore, higher proportions of fine sands, silts, and clays at these sites are also likely associated with the transport of fine materials originating from the Tijuana River, the Silver Strand beach, and to a lesser extent from San Diego Bay (MBC-ES 1988).

Various organic loading indicators, trace metals, pesticides, PCBs, and PAHs were detected in sediment samples collected throughout the PLOO and SBOO regions in 2020 and 2021. However, concentrations of these parameters were below ERM thresholds, mostly below ERL thresholds, and typically within historical ranges at regional sites (e.g., City of San Diego 2020, 2022b). Additionally, values for most sediment parameters remained within ranges typical for other areas of the southern California continental shelf (see Schiff and Gossett 1998, City of San Diego 2000, 2022b, Noblet et al. 2002, Schiff et al. 2006, 2011, Maruya and Schiff 2009, Dodder et al. 2016, Du et al. 2020).

There have been few, if any, clear spatial patterns consistent with outfall discharge effects on sediment

chemistry values over the past several years, with concentrations of most contaminants at near-ZID sites falling within the range of values observed at farfield stations. The only exceptions off San Diego have been slightly higher sulfide and BOD levels measured in sediments near the PLOO discharge site (see also City of San Diego 2022a). Instead, the highest concentrations of several organic indicators, trace metals, pesticides, PCBs, and PAHs have historically occurred in sediments from southern and/or northern farfield stations. The driver of elevated contaminants at the northern PLOO stations is unknown, while sediments from the southern PLOO stations are known to be impacted by the dumping of dredged materials destined originally for the LA-5 dredged disposal dumpsite (Anderson et al. 1993, Steinberger et al. 2003, Parnell et al. 2008). In the SBOO region, relatively high values of most parameters could be found distributed throughout the region, and several organic indicators and metals co-occurred in samples characterized by finer sediments. This association is expected due to the known correlation between particle size and concentrations of these chemical parameters (Eganhouse and Venkatesan 1993).

The broad distribution of various contaminants in sediments throughout the PLOO and SBOO regions is likely derived from several sources. Mearns et al. (1991) described the distribution of contaminants, such as arsenic, mercury, DDT, and PCBs as being ubiquitous in the SCB. Additionally, Brown et al. (1986) concluded that there may be no coastal areas in southern California that are sufficiently free of chemical contaminants to be considered reference sites. This has been supported by more recent surveys of SCB continental shelf habitats (Schiff and Gossett 1998, Noblet et al. 2002, Schiff et al. 2006, 2011, Dodder et al. 2016, Du et al. 2020). The lack of contaminant-free reference areas clearly pertains to the PLOO and SBOO regions as demonstrated by the presence of many contaminants in sediments prior to wastewater discharge (see City of San Diego 2000, 2022a). In addition, historical assessments of benthic sediments off the coast of Los Angeles have shown that as wastewater treatment improved, sediment conditions were more likely affected by other factors (Stein and Cadien 2009). Such factors may include bioturbative re-exposure of buried legacy sediments (Niedoroda et al. 1996, Stull et al. 1996), large storms that assist redistribution of legacy contaminants (Sherwood et al. 2002), and stormwater discharges (Schiff et al. 2006, Nezlin et al. 2007). Possible non-outfall sources and pathways of contaminant dispersal off San Diego include transport of contaminated sediments from San Diego Bay via tidal exchange, offshore disposal of dredged sediments, nearshore turbidity plumes emanating from the Tijuana River, and surface runoff from local watersheds (Parnell et al. 2008).

In conclusion, there was no evidence of fine particle loading related to wastewater discharge via the PLOO or SBOO, during the current reporting period, or since the discharge originally began through either outfall in the 1990s. Likewise, contaminant concentrations at near-ZID stations were generally within the range of variability observed throughout both outfall regions and do not appear to be reflect any significant organic enrichment. The only sustained effects have been restricted to a few sites located within 200 m of the PLOO (near-ZID stations E11, E14 and E17). These minor effects include small increases in sulfide and BOD concentrations (City of San Diego 2022). Finally, the quality of PLOO and SBOO sediments in 2020 and 2021 was similar to previous years with overall contaminant concentrations remaining relatively low compared to available thresholds, or values found in other southern California coastal areas (Schiff and Gossett 1998, Noblet et al. 2002, Schiff et al. 2006, 2011, Maruya and Schiff 2009, Dodder et al. 2016, Du et al. 2020). Consequently, there is presently no evidence to suggest that wastewater discharge via the PLOO or SBOO is affecting the quality of benthic sediments off San Diego to the point that it may degrade resident marine biological communities (i.e., Chapters 6–8).

Literature Cited

Anderson, J.W., D.J. Reish, R.B. Spies, M.E. Brady, and E.W. Segelhorst. (1993). Human

Impacts. In: M.D. Dailey, D.J. Reish, and J.W. Anderson (eds.). Ecology of the Southern California Bight: A Synthesis and Interpretation. University of California Press, Berkeley, CA. p 682–766.

Brown, D.A., R.W. Gossett, G.P. Hershelman, C.G. Word, A.M. Westcott, and J.N. Cross. (1986). Municipal wastewater contamination in the Southern California Bight: Part I–metal and organic contaminants in sediments and organisms. Marine Environmental Research, 18: 291–310.

City of San Diego. (2000). International Wastewater Treatment Plant Final Baseline Ocean Monitoring Report for the South Bay Ocean Outfall (1995–1998). City of San Diego Ocean Monitoring Program, Metropolitan Wastewater Department, Environmental Monitoring and Technical Services Division, San Diego, CA.

City of San Diego. (2014a). Point Loma Ocean Outfall Annual Receiving Waters Monitoring and Assessment Report, 2013. City of San Diego Ocean Monitoring Program, Public Utilities Department, Environmental Monitoring and Technical Services Division, San Diego, CA.

City of San Diego. (2014b). South Bay Ocean Outfall Annual Receiving Waters Monitoring and Assessment Report, 2013. City of San Diego Ocean Monitoring Program, Public Utilities Department, Environmental Monitoring and Technical Services Division, San Diego, CA.

City of San Diego. (2020). Biennial Receiving Waters Monitoring and Assessment Report for the Point Loma and South Bay Ocean Outfalls, 2018–2019. City of San Diego, Public Utilities Department, Environmental Monitoring and Technical Services Division, San Diego, CA.

City of San Diego. (2021). Interim Receiving Waters Monitoring Report for the Point Loma and South Bay Ocean Outfalls, 2020. City of San Diego, Public Utilities Department, Environmental Monitoring and Technical Services Division, San Diego, CA.

City of San Diego. (2022a). Appendix C.1 Benthic Sediments, Invertebrates and Fishes. In: Application for Renewal of NPDES CA0107409 and 301(h) Modified Secondary Treatment Requirements Point Loma Ocean Outfall. Volume V, Appendices C thru D. Public Utilities Department, Environmental Monitoring and Technical Services Division, San Diego, CA.

City of San Diego. (2022b). Appendix C.2 San Diego Benthic Tolerance Intervals; 24-Year San Diego Regional Benthic Assessment and Reference Tolerance Intervals. In: Application for Renewal of NPDES CA0107409 and 301(h) Modified Secondary Treatment Requirements Point Loma Ocean Outfall. Volume V, Appendices C thru D. Public Utilities Department, Environmental Monitoring and Technical Services Division, San Diego, CA.

Cross, J.N. and L.G. Allen. (1993). Fishes. In: M.D. Dailey, D.J. Reish, and J.W. Anderson (eds.). Ecology of the Southern California Bight: A Synthesis and Interpretation. University of California Press, Berkeley, CA. p 459–540.

Dodder, N., K. Schiff, A. Latker, C-L Tang. (2016). Southern California Bight 2013 Regional Monitoring Program: IV. Sediment Chemistry. Southern California Coastal Water Research Project, Westminster, CA.

Du, B., C.S. Wong, K. Mclaughlin, and K. Schiff. (2020). Southern California Bight 2018 Regional Monitoring Program: II. Sediment Chemistry. Southern California Coastal Water Research Project, Westminster, CA.

Eganhouse, R.P. and M.I. Venkatesan. (1993). Chemical Oceanography and Geochemistry.

In: M.D. Dailey, D.J. Reish, and J.W. Anderson (eds.). Ecology of the Southern California Bight: A Synthesis and Interpretation. University of California Press, Berkeley, CA. p 71–189.

Emery, K.O. (1960). The Sea off Southern California. John Wiley, New York, NY.

Farnsworth, K.L. and J.A. Warrick. (2007). Sources, dispersal, and fate of fine sediment supplied to coastal California. U.S. Geological Survey Scientific Investigations Report 2007–5254. Reston, VA.

Folk, R.L. (1980). Petrology of Sedimentary Rocks. Hemphill, Austin, TX.

Gray, J.S. (1981). The Ecology of Marine Sediments: An Introduction to the Structure and Function of Benthic Communities. Cambridge University Press, Cambridge, England.

Helsel, D.R. (2005a). More than obvious: better methods for interpreting nondetect data. Environmental Science & Technology (October 15, 2005), 419A–423A.

Helsel, D.R. (2005b). Nondetects and Data Analysis: Statistics for Censored Environmental Data. John Wiley, New York.

Helsel, D.R. (2006). Fabrication data: how substituting values for nondetects can ruin results, and what can be done about it. Chemosphere 65: 2434–2439.

Hope, R.M. (2013). Rmisc: Ryan Miscellaneous. R package version 1.5. http://CRAN.R-project.org/package=Rmisc.

Kassambara, A. (2019). ggpubr: 'ggplot2' Based Publication Ready Plots. R package version 0.2.5. https://CRAN.R-project.org/package=ggpubr.

Long, E.R., D.L. MacDonald, S.L. Smith, and F.D. Calder. (1995). Incidence of adverse biological effects within ranges of chemical concentration in marine and estuarine sediments. Environmental Management, 19: 81–97.

[MBC-ES] MBC Applied Environmental Sciences and Engineering-Science. (1988). Part F: Biological studies. In: Tijuana Oceanographic Engineering Study, Volume 1. Ocean Measurement Program. Prepared for the City of San Diego, CA.

Mann, K.H. (1982). The Ecology of Coastal Marine Waters: A Systems Approach. University of California Press, Berkeley, CA.

Maruya, K.A. and K. Schiff. (2009). The extent and magnitude of sediment contamination in the Southern California Bight. Geological Society of America Special Paper, 454: 399–412.

Mearns, A.J., M. Matta, G. Shigenaka, D. MacDonald, M. Buchman, H. Harris, J. olas, and G. Lauenstein. (1991). Contaminant Trends in the Southern California Bight: Inventory and Assessment. NOAA Technical Memorandum NOS ORCA 62. Seattle, WA.

Nezlin, N.P., P.M. DiGiacomo, S.B. Weisberg, D.W. Diehl, J.A. Warrick, M.J. Mengel, B.H. Jones, K.M. Reifel, S.C. Johnson, J.C. Ohlmann, L. Washburn, and E.J. Terrill. (2007). Southern California Bight 2003 Regional Monitoring Program: V. Water Quality. Southern California Coastal Water Research Project. Costa Mesa, CA.

Niedoroda, A.W., D.J.P. Swift, C.W. Reed, and J.K. Stull. (1996). Contaminant dispersal on the Palos Verdes continental margin. Science of the Total Environment, 179: 109–133.

Noblet, J.A., E.Y. Zeng, R. Baird, R.W. Gossett, R.J. Ozretich, and C.R. Phillips. (2002). Southern California Bight 1998 Regional Monitoring Program: VI. Sediment Chemistry. Southern California Coastal Water Research Project, Westminster, CA.

Oksanen, J., F.G. Blanchet, R. Kindt, P. Legendre, P.R. Minchin, R.B. O'Hara, G.L. Simpson, P. Solymos, M.H.H. Stevens, and H. Wagner. (2019). vegan: Community Ecology Package. R package version 2.5-6. http://CRAN.R-project.org/package=vegan.

Parnell, P.E., A.K. Groce, T.D. Stebbins, and P.K. Dayton. (2008). Discriminating sources of PCB contamination in fish on the coastal shelf off San Diego, California (USA). Marine Pollution Bulletin, 56: 1992–2002.

Parsons, T.R., M. Takahashi, and B. Hargrave. (1990). Biological Oceanographic Processes 3rd Edition. Pergamon Press, Oxford.

Patsch, K. and G. Griggs. (2007). Development of Sand Budgets for California's Major Littoral Cells. Institute of Marine Sciences, University of California, Santa Cruz, CA.

R Core Team. (2021). R: A language and environment for statistical computing. R Foundation for Statistical Computing, Vienna, Austria. URL https://www.R-project.org/.

Revelle, W. (2019) psych: Procedures for Personality and Psychological Research, Northwestern University, Evanston, Illinois, USA, https://CRAN.R-project.org/package=psych Version = 1.9.12.31.

Ripley, B. and M. Lapsley. (2017). RODBC: ODBC Database Access. R package version 1.3-12. http://CRAN.R-project.org/package=RODBC.

[SCCWRP] Southern California Coastal Water Research Project. (2018). Southern California Bight 2018 Regional Monitoring Program: Contaminant Impact Assessment Field Operations Manual. Southern California Coastal Water Research Project. Costa Mesa, CA.

Schiff, K.C. and R.W. Gossett. (1998). Southern California Bight 1994 Pilot Project: III. Sediment Chemistry. Southern California Coastal Water Research Project. Westminster, CA.

Schiff, K., R. Gossett, K. Ritter, L. Tiefenthaler, N. Dodder, W. Lao, and K. Maruya. (2011). Southern California Bight 2008 Regional Monitoring Program: III. Sediment Chemistry. Southern California Coastal Water Research Project, Costa Mesa, CA.

Schiff, K., K. Maruya, and K. Christenson. (2006). Southern California Bight 2003 Regional Monitoring Program: II. Sediment Chemistry. Southern California Coastal Water Research Project, Westminster, CA.

Sherwood, C.R., D.E. Drake, P.L. Wiberg, and R.A. Wheatcroft. (2002). Prediction of the fate of p,p-DDE in sediment on the Palos Verdes shelf, California, USA. Continental Shelf Research, 32: 1025–1058.

Snelgrove, P.V.R. and C.A. Butman. (1994). Animal-sediment relationships revisited: cause versus effect. Oceanography and Marine Biology Annual Review, 32: 111–177.

Stein, E.D. and D.B. Cadien. (2009). Ecosystem response to regulatory and management actions: The Southern California experience in long-term monitoring. In: K. Schiff (ed.). Southern California Coastal Water Research Project Annual Report 2009. Southern California Coastal Water Research Project, Costa Mesa, CA.

Steinberger, A., E. Stein, and K. Schiff. (2003). Characteristics of dredged material disposal to the Southern California Bight between 1991 and 1997. In: Southern California Coastal Water Research Project Biennial Report 2001–2002. Long Beach, CA. p 50–60.

Stull, J.K., D.J.P. Swift, and A.W. Niedoroda. (1996). Contaminant dispersal on the Palos Verdes Continental margin. Science of the Total Environment, 179: 73–90.

Svejkovsky, J. (2013). Satellite and Aerial Coastal Water Quality Monitoring in the San Diego/ Tijuana Region: Annual Summary Report, 1 January, 2012–31 December, 2012. Ocean Imaging, Solana Beach, CA.

[USEPA] United States Environmental Protection Agency. (1987). Quality Assurance and Quality Control for 301(h) Monitoring Programs: Guidance on Field and Laboratory Methods. EPA Document 430/9-86-004. Office of Marine and Estuary Protection, Washington, DC.

Wickham, H. (2007). Reshaping Data with the reshape Package. Journal of Statistical Software, 21(12), 1–20. URL http://www.jstatsoft.org/v21/i12/.

Wickham, H. (2011). The Split-Apply-Combine Strategy for Data Analysis. Journal of Statistical Software, 40(1), 1–29. URL http://www.jstatsoft.org/v40/i01/.

Wickham, H. (2019). stringr: Simple, Consistent Wrappers for Common String Operations. R package version 1.4.0. https://CRAN.R-project.org/package=stringr.

Wickham, H., R. Francois, L. Henry and K. Müller. (2020). dplyr: A Grammar of Data Manipulation. R package version 1.2.0. https://CRAN.R-project.org/package=dplyr.

Wickham, H., M. Averick, J. Bryan, W. Chang, L. D'Agostino McGowan, R. François, G.Grolemund, A. Hayes, L. Henry, J. Hester, M. Kuhn, T. Lin Pedersen, E. Miller, S. Milton Bache, K. Müller, J. Ooms, D. Robinson, D. P. Seidel, V. Spinu, K. Takahashi, D. Vaughan, C. Wilke, K. Woo, H. Yutani. (2019a). Welcome to the tidyverse. Journal of Open Source Software, 4(43), 1686, https://doi.org/10.21105/joss.01686.

Wickham, H., W. Chang, L. Henry, T.L. Pedersen, K. Takahashi, C. Wilke, K. Woo, (2019b). Ggplot2: Create Elegant Data Visualizations Using the Grammar of Graphics. Version 3.2.0. Rstudio. URL https://ggplot2.tidyverse.org/.

Wickham H. and L. Henry. (2018). tidyr: Easily Tidy Data with 'spread()' and 'gather()' Functions. R package version 0.7.2. https://CRAN.R-project.org/package=tidyr.

Wickham, H., Francois, L. Henry and K. Müller (2020). dplyr: A Grammar of Data Manipulation. R package version 0.8.5. https://CRAN.R-project.org/package=dplyr.

Zeileis, A and G. Grothendieck. (2005). zoo: S3 Infrastructure for Regular and Irregular Time Series. Journal of Statistical Software, 14(6), 1–27. URL http://www.jstatsoft.org/v14/i06/

Chapter 6
Macrobenthic Communities

Chapter 6. Macrobenthic Communities

Introduction

The City of San Diego (City) conducts extensive monitoring of soft-bottom marine macrobenthic communities at permanent (core) monitoring sites surrounding the Point Loma Ocean Outfall (PLOO) and South Bay Ocean Outfall (SBOO). Additionally, a number of randomly selected (regional) stations, distributed throughout the broader San Diego coastal region are sampled in order to characterize the status of the local marine ecosystem and to identify any possible effects of wastewater discharge or other anthropogenic or natural influences. Benthic macrofauna (e.g., worms, crabs, clams, brittle stars, other small invertebrates) are targeted when monitoring seafloor habitats, because such organisms play important ecological roles in coastal marine ecosystems off southern California, and throughout the world (e.g., Fauchald and Jones 1979, Thompson et al. 1993a, Snelgrove et al. 1997). As many macrobenthic species live relatively long and stationary lives, their populations may exhibit the effects of pollution, or other disturbances over time (Hartley 1982, Bilyard 1987). The response of many of these species to environmental stressors is also well documented, and thus monitoring changes in discrete populations, or more complex communities, can help identify areas impacted by anthropogenic inputs (Pearson and Rosenberg 1978, Bilyard 1987, Warwick 1993, Smith et al. 2001). For example, pollution-tolerant species are often opportunistic, successfully colonizing impacted areas, and can therefore displace more sensitive species. In contrast, populations of pollution-sensitive species will typically decrease in response to contamination, oxygen depletion, nutrient loading, or other forms of environmental degradation (Gray 1979). For these reasons, the assessment of benthic community structure has become a major component of many ocean monitoring programs (e.g., Gillett et al. 2017).

The City relies on a suite of ecological indices to evaluate potential changes in local marine macrobenthic communities. Biological indices, such as the Benthic Response Index (BRI), Shannon Diversity Index (H'), and Swartz Dominance Index (Dom) are used as important metrics of community structure (e.g., Smith et al. 2001). The use of multiple measures of community health also provides better resolution than the evaluation of single parameters, some of which include established benchmarks for determining environmental impacts caused by anthropogenic influences. Collectively, these data are used to evaluate whether macrobenthic assemblages from habitats with comparable depth and sediment particle size are similar, or whether impacts from local ocean outfalls, or other sources, may be occurring. For example, minor organic enrichment due to wastewater discharge should be evident through increases in species richness and abundance in macrofaunal assemblages. Additionally, more severe impacts should result in decreases in the overall number of species, coupled with increases in dominance by a few pollution-tolerant species (Pearson and Rosenberg 1978).

This chapter presents analysis and interpretation of macrofaunal data collected at core benthic monitoring stations throughout the PLOO and SBOO regions, during 2020 and 2021. Included are descriptions of the different macrobenthic communities present in these two regions, along with comparisons of spatial patterns and long-term changes over time. The three primary goals of the chapter are to: (1) characterize and document the benthic assemblages present during the reporting period; (2) assess whether benthic communities are degraded as a result of wastewater discharge; (3) identify other potential natural or anthropogenic sources of variability in the San Diego coastal marine ecosystem. A broader regional assessment of benthic conditions throughout the entire San Diego region, based on a subset of data reported in this chapter

combined with a suite of randomly selected stations sampled during the summers of 2020 and 2021 is presented in Chapter 7.

Materials and Methods

Field Sampling

Benthic samples analyzed in this chapter were collected at a total of 49 core monitoring stations located at inner shelf (≤ 30 m) to middle shelf (> 30–120 m) depths, surrounding the PLOO and SBOO, during winter (January) and summer (July) of 2020 and 2021 (Figure 6.1). The PLOO sites include 12 primary core stations located along the 98-m discharge depth contour, and 10 secondary core stations located along or adjacent to the 88-m or 116-m depth contours. The SBOO sites include 12 primary core stations located along the 28-m discharge depth contour, and 15 secondary core stations located along or adjacent to the 19, 38, or 55-m depth contours. Stations located within 1000 m of the boundary of the Zone of Initial Dilution (ZID) for either outfall are considered to represent near-ZID conditions. These include PLOO stations E11, E14, E15, and E17, and SBOO stations I12, I14, I15, and I16. All other stations are considered farfield.

Samples for benthic analyses were collected using a double 0.1 m^2 Van Veen grab, with one grab per cast used for sediment quality analysis (see Chapters 5 and 7) and one grab per cast used for benthic community analysis. Criteria established by the U.S. Environmental Protection Agency (USEPA) to ensure consistency of these types of samples were followed with regard to sample disturbance and depth of penetration (USEPA 1987). Samples for infauna analysis were transferred to a wash table aboard ship, rinsed with seawater, and then sieved through a 1.0-mm mesh screen in order to remove as much sediment as possible. The macroinvertebrates (macrofauna or infauna) retained on the screen were transferred to sample jars, relaxed for 30 minutes in a magnesium sulfate solution, and then fixed with buffered formalin. The preserved samples were then transferred back to the City's Marine Biology Laboratory. After a minimum of 72 hours, but no more than 10 days in formalin, each sample was thoroughly rinsed with fresh water and transferred to 70% ethanol for final preservation. All organisms were separated from the raw material (e.g., sediment grunge, shell hash, debris) and sorted into the following six taxonomic groups by an external contract lab: Annelids (e.g., polychaete and oligochaete worms), Arthropods (e.g., crustaceans, pycnogonids), Molluscs (e.g., bivalves, gastropods, scaphopods), non-ophiuroid Echinoderms (e.g., sea urchins, sea stars, sea cucumbers), ophiuroids (i.e., brittle stars), and other phyla (e.g., Platyhelminthes, Nemertea, Cnidaria). The sorted macrofaunal samples were then returned to the City's Marine Biology Laboratory where all animals were identified to species or to the lowest taxon possible by staff marine biologists. All identifications followed nomenclatural standards established by the Southern California Association of Marine Invertebrate Taxonomists (SCAMIT 2018).

Data Analyses

Macrofaunal community parameter data for each PLOO and SBOO core station sampled in 2021 are listed in Appendices G.1 and G.2 while taxonomic listings of all specimens identified are listed in Appendices G.3 and G.4. The following community metrics were determined for each station and expressed per 0.1-m^2 grab: species richness (number of species or distinct taxa), abundance (number of individuals), Shannon Diversity Index (H'), Pielou's Evenness Index (J'), Swartz Dominance Index (Dom) (see Swartz et al. 1986, Ferraro et al. 1994), and Benthic Response Index (BRI) (see Smith et al. 2001). Unless otherwise noted, the above analyses were performed using the computational software package R (R Core Team 2021) and various functions within the ggpubr, reshape2, Rmisc, RODBC, scales, tidyverse, and vegan packages (Kassambara 2019, Wickham 2007, 2017, 2018, Hope 2013, Oksanen et al. 2017, Ripley and Lapsley 2017). Data collected during 2020 were reported previously (City of San Diego 2021), and all raw data for the 2020–2021 sampling period have been submitted to either the Regional Water Quality

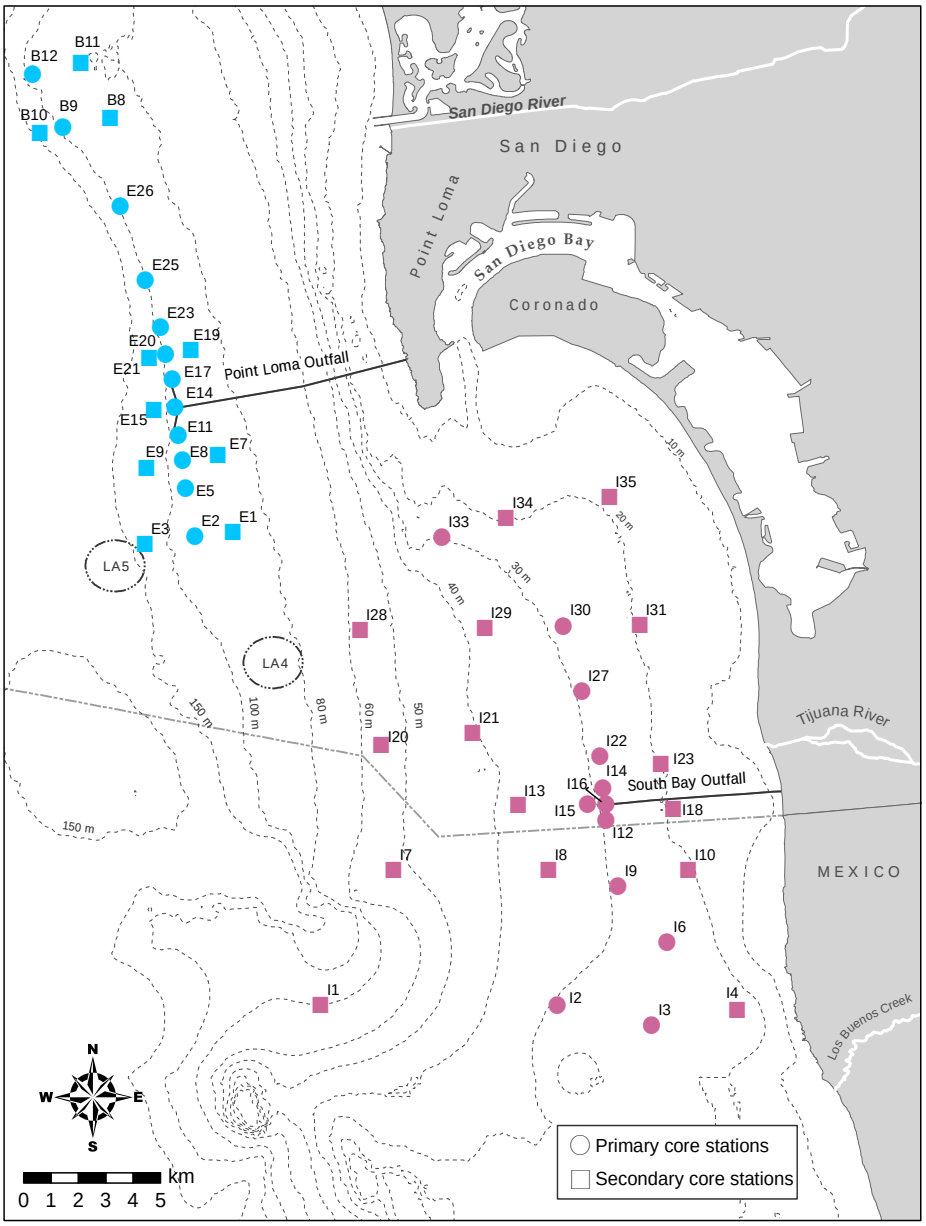

Figure 6.1
Benthic station locations sampled around the PLOO (blue) and SBOO (magenta) as part of the City of San Diego's Ocean Monitoring Program.

Control Board or the California Environmental Data Exchange Network (CEDEN) and may be accessed upon request.

Results and Discussion

Community Parameters

Species richness

A total of 915 different taxa were identified from 196 grabs collected at 22 core PLOO stations and 27 core SBOO stations during 2020 and 2021 (Appendices G.1, G.2, City of San Diego 2021). Approximately 78% (n = 716) of these taxa were fully identified to species, while the remainder could only be identified to genus or higher taxonomic levels. From the relatively deeper (88–116 m) mid-shelf waters off Point Loma, 583 taxa were identified during this period, of which at least 454 (78%) were distinct species. In contrast, 755 taxa were identified from the shallower (19–55 m) inner to mid-shelf stations in the SBOO region. Of these, 594 (78%) were distinct species. Most taxa occurred at multiple stations, although 18% (n = 165) of the PLOO taxa and 22% (n = 202) of the SBOO taxa were recorded

only once. Eleven new taxa were reported that had not previously been recorded by the City's Ocean Monitoring Program, including nine polychaetes, one ascidian and one nemertean.

During 2020 and 2021, species richness ranged from a mean of 64 to 109 taxa per grab at the PLOO stations, and 27 to 144 taxa per grab at the SBOO stations (Tables 6.1 and 6.2, respectively). The greatest number of taxa (n = 122), collected from a single grab, in the PLOO region was identified at northern farfield station B11 during summer of 2021, while the fewest taxa (n = 54) were identified during winter of 2020 at near-ZID station E11 (see Appendix B.21 in City of San Diego 2021). In the SBOO region, the winter sample from 2021 at northern station I28 had the greatest number of taxa (n = 163), while near-ZID station I15 from winter of 2020 had the fewest taxa identified (n = 17) (see Appendix B.22 in City of San Diego 2021). These values were similar to the historical range of 19–198 taxa per grab for mid-shelf stations reported from 1994 through 2020 at regional stations (City of San Diego 2022). Comparisons of these parameters among near-ZID stations, versus northern and southern farfield stations, sampled during pre-discharge, historical post-discharge, and current discharge periods did not reveal any clear spatial patterns that could be attributed to wastewater discharge (Figure 6.2).

Macrofaunal abundance

A total of 59,255 macrofaunal animals were recorded for all core PLOO and SBOO stations sampled during 2020 and 2021. Mean abundance ranged from 282 to 508 animals in the PLOO region and from 56 to 667 animals in the SBOO region (Tables 6.1, 6.2, respectively). As shown for species richness, there were no clear patterns in abundance relative to their proximity to either outfall (see Figure 6.2). The highest abundance, per grab, in the PLOO region occurred during winter of 2021 at near-ZID stations E11 and E17 (n = 645), while the lowest abundance occurred at northern station E21 in summer of 2021 (n = 215) (Appendix G.1). In the SBOO region, the highest abundance occurred in the summer 2021 at northern inshore station I34 (n = 913), while the lowest abundance was observed at near-ZID station I15 (n = 30) in winter of 2020 (see Appendix G.2 in City of San Diego 2021). These values were similar to the range of 47 to 1467 organisms per grab reported at mid-shelf stations from 1994 to 2020 (City of San Diego 2022).

Species diversity, evenness, and dominance

Shannon Diversity Index (H') values ranged from a mean of 3.2 to 4.2 at the PLOO stations, and 2.8 to 4.3 at the SBOO stations, during 2020 and 2021 (Tables 6.1, 6.2, respectively). In the PLOO region, the highest diversity per grab sample occurred at northern farfield stations B11 and B12 in summer 2021 and southern farfield station E3 in winter and summer 2021 (H' = 4.3) (Appendix G.1), and the lowest diversity was observed at northern station E21 in the summer of 2020 (H' = 2.9) (see Appendix B.21 in City of San Diego 2021). In the SBOO region, the highest diversity per grab sample occurred at northern farfield station I28 in winter 2021 (H' = 4.5) (Appendix G.2), and the lowest diversity was observed at near-ZID stations I12 and I16 in winter of 2020 (H' = 2.3) (see Appendix B.22 in City of San Diego 2021).

Pielou's Evenness Index (J') values ranged from a mean of 0.77 to 0.90 in the PLOO region, and 0.72 to 0.90 in the SBOO region (Tables 6.1, 6.2, respectively). In the PLOO region, the highest evenness values per grab sample occurred at northern farfield stations B12 and B9 in winter and summer 2021 respectively, as well as southern farfield station E3 in winter and summer 2021 (J' = 0.91) (Appendix G.1), and the lowest evenness values occurred at northern station E21 in summer of 2020 (J' = 0.70) (see Appendix B.21 in City of San Diego 2021). In the SBOO region, the highest evenness occurred at near ZID station I15 in winter of 2021 (J' = 0.95), and the lowest value occurred at northern station I20 in summer of 2021 (J' = 0.63) (Appendix G.2).

Swartz Dominance Index values ranged from a mean of 16 to 43 taxa at PLOO stations, and 9 to 49 taxa at SBOO stations (Table 6.1, 6.2, respectively). In the PLOO region, the highest dominance (i.e., lowest index value) per grab sample occurred at northern station E21 in summer 2020 (11) (see Appendix

Table 6.1

Summary of macrofaunal community parameters for PLOO benthic stations sampled during 2020 and 2021. Data for each station are expressed as biennial means (n = 4). SR = species richness; Abun = abundance; H' = Shannon diversity index; J' = Pielou's evenness; Dom = Swartz dominance; BRI = Benthic Response Index; CI = confidence interval. Stations are listed north to south from top to bottom for each depth contour.

	Station	SR	Abun	H'	J'	Dom	BRI
88-m Depth Contour	B11	102	314	4.1	0.89	39	12
	B8	78	332	3.6	0.83	23	8
	E19	80	499	3.4	0.78	17	12
	E7	85	425	3.8	0.84	26	12
	E1	96	450	3.8	0.83	26	9
98-m Depth Contour	B12	106	360	4.2	0.89	40	10
	B9	90	321	3.9	0.88	32	12
	E26	89	406	3.7	0.83	26	12
	E25	78	508	3.4	0.78	18	10
	E23	84	500	3.6	0.80	21	12
	E20	76	436	3.4	0.79	18	13
	E17[a]	86	504	3.5	0.78	20	16
	E14[a]	74	474	3.4	0.80	18	30
	E11[a]	73	450	3.5	0.80	20	16
	E8	86	404	3.8	0.86	28	10
	E5	89	396	3.8	0.84	26	10
	E2	104	441	3.9	0.84	32	12
116-m Depth Contour	B10	84	282	3.9	0.88	31	14
	E21	64	356	3.2	0.77	16	14
	E15[a]	74	441	3.4	0.79	17	15
	E9	105	392	4.0	0.86	37	12
	E3	109	325	4.2	0.90	43	12
All Grabs	Mean	87	410	3.7	0.83	26	13
	95% CI	3	21	0.1	0.01	2	1
	Minimum	54	215	2.9	0.70	11	4
	Maximum	122	645	4.3	0.91	49	33

[a] Near-ZID station

B.21 in City of San Diego 2021), and the lowest dominance (i.e., highest index value) occurred at northern farfield station B11 in summer of 2021 (49) (Appendix G.1). In the SBOO region, the highest dominance occurred at southern farfield station I3 and northern farfield station I34 in winter of 2020 (6) (see Appendix B.22 in City of San Diego 2021), and the lowest dominance occurred at northern station I28 in summer of 2021 (55) (Appendix G.2).

Overall, these results indicate that the PLOO and SBOO benthic communities remain characterized by relatively diverse assemblages of evenly distributed species. Values for all three of the above parameters in 2020 and 2021 (Appendices G.1, G.2, City of San Diego 2021), were within historical ranges (see City of San Diego 2022), and there remain no patterns that appear related to wastewater discharge in either region (see Figure 6.2).

Table 6.2

Summary of macrofaunal community parameters for SBOO benthic stations sampled during 2020 and 2021. Data for each station are expressed as biennial means (n=4 grabs). SR=species richness; Abun=abundance; H'=Shannon diversity index; J'=Pielou's evenness; Dom=Swartz dominance; BRI=Benthic Response Index; CI=confidence interval. Stations are listed north to south from top to bottom for each depth contour.

	Station	SR	Abun	H'	J'	Dom	BRI
19-m Depth Contour	I35	73	242	3.8	0.88	27	27
	I34	53	667	2.8	0.72	9	17
	I31	48	152	3.2	0.84	17	17
	I23	68	290	3.4	0.82	21	20
	I18	50	168	3.4	0.87	21	15
	I10	52	128	3.5	0.89	22	18
	I4	27	56	3.0	0.90	14	8
28-m Depth Contour	I33	88	221	4.0	0.90	36	24
	I30	62	174	3.7	0.88	26	24
	I27	57	176	3.4	0.86	21	21
	I22	55	140	3.4	0.87	24	22
	I14[a]	78	212	3.9	0.89	32	22
	I16[a]	51	190	3.1	0.79	17	15
	I15[a]	40	126	2.9	0.82	16	15
	I12[a]	52	157	3.1	0.80	19	12
	I9	62	162	3.7	0.89	26	24
	I6	34	142	2.8	0.79	11	9
	I2	37	142	2.8	0.78	11	18
	I3	38	151	2.8	0.77	10	10
38-m Depth Contour	I29	120	408	4.2	0.87	42	15
	I21	48	148	3.3	0.87	19	6
	I13	44	144	3.3	0.86	17	8
	I8	40	112	3.1	0.85	16	16
55-m Depth Contour	I28	144	494	4.3	0.88	49	15
	I20	70	419	3.1	0.75	17	8
	I7	49	144	3.3	0.85	20	5
	I1	74	235	3.7	0.86	28	15
All Grabs	Mean	60	215	3.4	0.84	22	16
	95% CI	5	32	0.1	0.01	2	1
	Minimum	17	30	2.3	0.63	6	-6
	Maximum	163	913	4.5	0.95	55	29

[a] Near-ZID station

Benthic Response Index

The BRI is an important tool for evaluating anthropogenic impacts on coastal seafloor habitats off southern California: BRI values less than 25 are considered indicative of reference conditions (i.e., not impacted by natural and/or anthropogenic disturbance), values between 25 and 34 represent possible minor deviation from reference conditions, and values greater than 34 represent increasing levels of degradation (Smith et al. 2001). Overall, 94% (n = 184) of all individual benthic samples collected in the combined PLOO and SBOO regions during 2020 and 2021 were characteristic of reference conditions (Appendices G.1, G.2, City of San Diego 2021). No stations had BRI values considered indicative of degradation (i.e., all stations had a BRI $\leq$ 34).

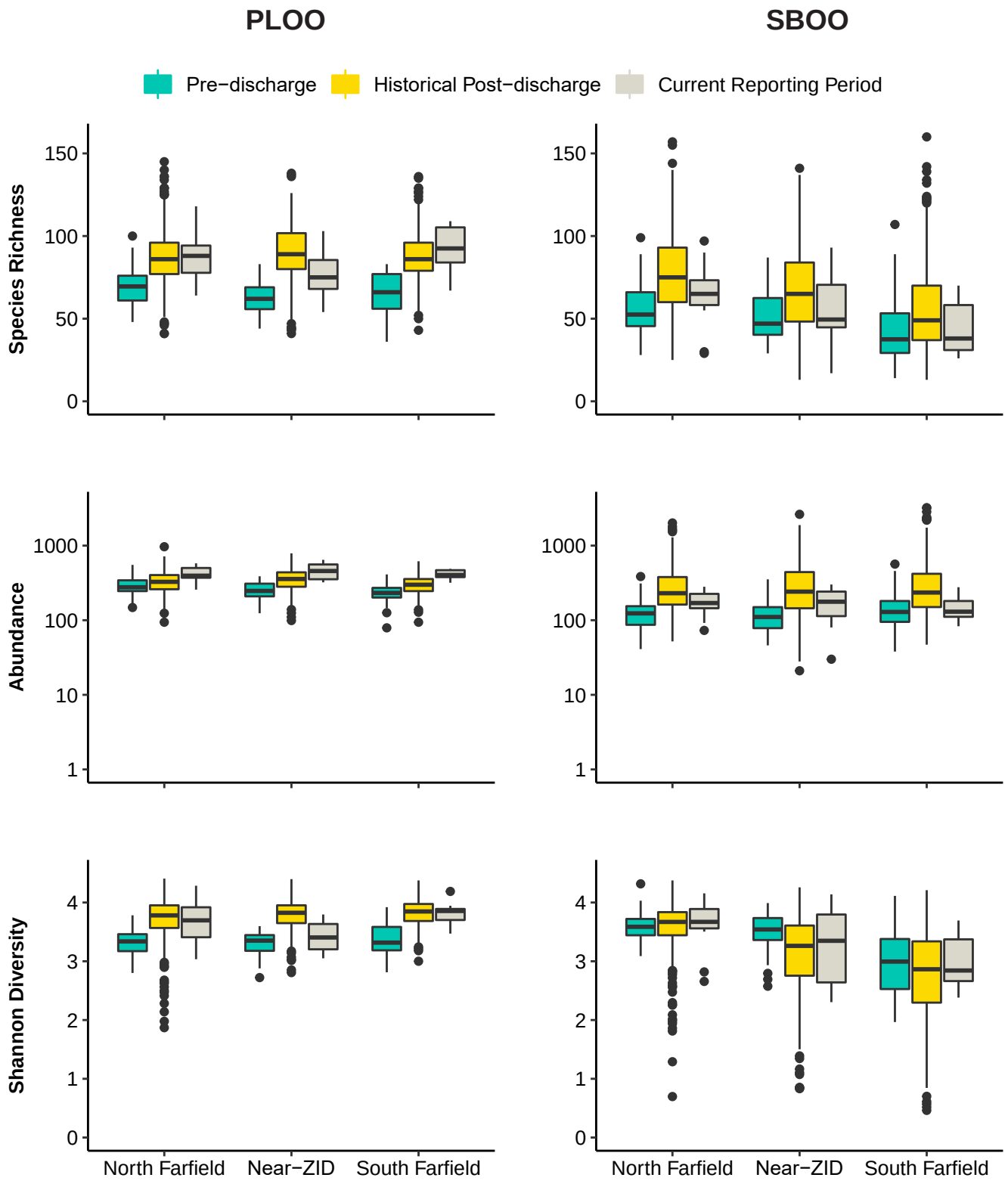

Figure 6.2

Species richness, abundance, and diversity (H') of benthic infauna collected from PLOO and SBOO north farfield, near-ZID, and south farfield primary core stations during pre-discharge, historical post-discharge, and current reporting period; Boxes = median, upper, and lower quantiles; whiskers = 1.5x interquantile range; circles = outliers; see Chapter 1 for description of pre- versus post-discharge time periods for the two outfalls.

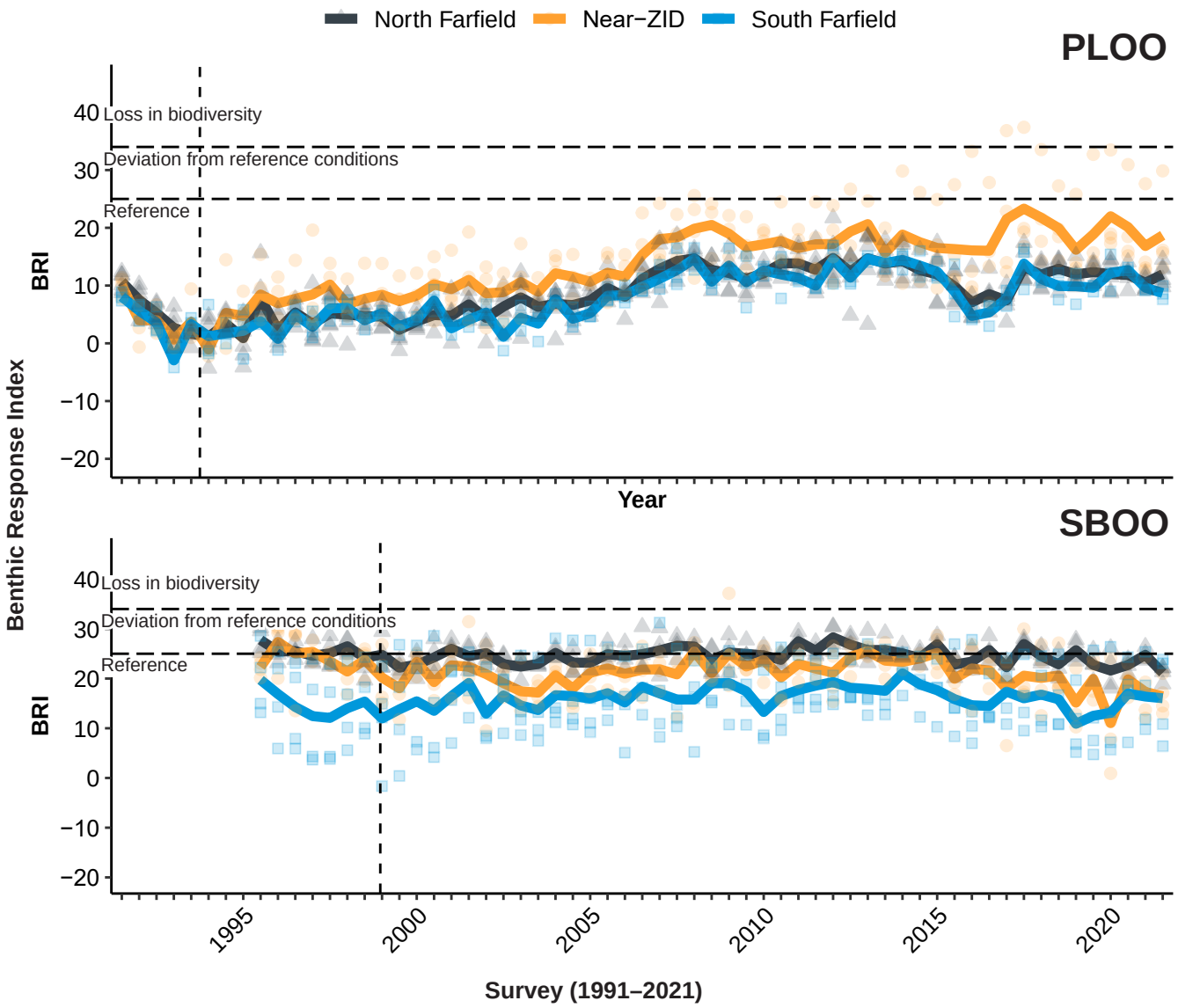

Figure 6.3

Benthic Response Index at PLOO and SBOO north farfield, near-ZID, and south farfield primary core stations sampled from 1991 through 2021. For each station group, mean BRI per survey is shown by the solid line ($n \leq 8$) while BRI per station is shown by the symbols. Vertical dashed lines indicate onset of wastewater discharge at each outfall.

Almost all of the individual samples (95%) in the PLOO region had BRI values indicative of reference conditions. Only near-ZID station E14, with individual BRI scores ranging from 28 to 33, appeared to show evidence of slight deviation from reference conditions (Appendix G.1, City of San Diego 2021). The other three PLOO near-ZID stations (E11, E15, E17) all had BRI values only slightly higher than sites located farther from the outfall (an average of 16 versus 11, respectively). Station E14 was distinguished from the other primary core "E" stations, located along the 98-m PLOO discharge depth contour, as it had a higher proportion of coarse sediment particles and lower proportion of very fine particles (see Chapter 5). This difference in habitat may contribute to the slightly elevated BRI scores at station E14, as it may decrease the presence of certain pollution-sensitive species (e.g., the brittle star *Amphiodia urtica*) that are known to prefer finer sediments (Bergen 1995). No other spatial patterns relative to depth or sediments were observed (see Figures 5.2, 6.3, Tables 6.1, 6.2).

Table 6.3

Percent composition and abundance of major taxonomic groups in PLOO and SBOO benthic grabs sampled during 2020 and 2021. Percentages may not add up to 100 due to rounding artifacts.

	PLOO		SBOO	
Phyla	**Species (%)**	**Abundance (%)**	**Species (%)**	**Abundance (%)**
Annelida (Polychaeta)	53	64	50	64
Arthropoda (Crustacea)	18	8	20	17
Echinodermata	4	10	4	3
Mollusca	14	14	15	7
Other Phyla	10	3	12	9

In the SBOO region, BRI values ranged from -6 at northern station I21 to 29 at northern station I35 during 2021, with about 93% of these being indicative of reference conditions (Appendix G.2, City of San Diego 2021). No SBOO samples had BRI values > 34 that would indicate environmental degradation. Individual sample BRI values corresponding to possible minor deviation from reference conditions (≥ 25) occurred at five stations (I9, I22, I30, I33, I35) (Appendix G.2, City of San Diego 2021). The slightly higher BRI values at these stations are not unexpected, due to naturally higher levels of organic matter that may occur at depths < 30 m (Smith et al. 2001). Historically, BRI values at the near-ZID SBOO stations have been similar to values observed for northern farfield SBOO stations, while BRI has been consistently lower at the southern farfield SBOO stations (Figure 6.3). Although these southern stations are also located along the 28-m depth contour, their sediments favor the presence of aggregations of the sand dollar, *Dendraster terminalis*, a pollution sensitive species that yields low BRI values.

Species of Interest

Dominant taxa

Annelid polychaete worms were the dominant taxonomic group found in both the PLOO and SBOO regions during 2020–2021, accounting for 53% and 50% of all taxa collected, respectively (Table 6.3). Crustaceans accounted for 18 to 20% of the taxa per region, molluscs for 14 to 15%, echinoderms 4% in both regions, and all other taxa combined equated to 10 to 12%. Polychaetes were also the most abundant organisms encountered, accounting for 64% of all macrofauna in both the PLOO and SBOO regions. Crustaceans, molluscs, echinoderms, and "other phyla" each contributed to ≤ 17% of the total abundance in each region. Overall, the percentage of taxa that occurred within each of the above major taxa groups, and their relative abundances, have shown little change since monitoring began (City of San Diego 2022) and are similar to the rest of the Southern California Bight (SCB) (see Ranasinghe et al. 2012, Gillett et al. 2017).

The 10 most abundant taxa in the PLOO region during 2020–2021 included seven species of polychaetes, one species of bivalve, and two ophiuroids (Table 6.4). Together, these species accounted for about 43% of all invertebrates identified during this period. The numerically dominant polychaetes included the spionids *Spiophanes duplex, Spiophanes kimballi* and *Prionospio jubata,* capitellids in the genus *Mediomastus*, and the maldanids *Praxillella pacifica* and Euclymeninae sp A. The dominant bivalve was *Axinopsida serricata,* while the brittle star *Amphiodia urtica* was the dominant ophiuroid. *Amphiodia urtica* populations have been declining across the region since monitoring at the current stations began in 1991, and especially since the warm water period of 2015–2017 (see Chapter 2, Figure 2.18). However, they are still a dominant taxon, accounting for approximately 5% of all invertebrates collected in the region and occurring in 91% of grabs with a mean abundance of approximately 19 individuals per grab. Historically, *Amphiodia urtica* and *Spiophanes duplex* (Figure 6.4), as well as *Proclea* sp A (Figure 6.5) have also been numerically dominant.

Table 6.4

The 10 most abundant macroinvertebrate taxa collected from PLOO benthic stations during 2020 and 2021. Data are expressed as percent abundance (number of individuals per species/total abundance of all species), frequency of occurrence (percentage of grabs in which a species occurred), and abundance per grab (mean number of individuals per grab, n = 88).

Species	Taxonomic Classification	Percent Abundance	Frequency of Occurrence	Abundance per Grab
Spiophanes duplex	Polychaeta: Spionidae	10	99	42
Axinopsida serricata	Mollusca: Bivalvia	8	89	35
Mediomastus sp	Polychaeta: Capitellidae	5	100	22
Amphiodia urtica	Echinodermata: Ophiuroidea	5	91	19
Paradiopatra parva	Polychaeta: Onuphidae	3	99	14
Spiophanes kimballi	Polychaeta: Spionidae	3	90	11
Prionospio jubata	Polychaeta: Spionidae	3	100	11
Amphiuridae	Echinodermata: Ophiuroidea	2	92	10
Praxillella pacifica	Polychaeta: Maldanidae	2	93	9
Euclymeninae sp A	Polychaeta: Maldanidae	2	93	9

However, other historically dominant species, the oweniid *Myriochele striolata* and the terebellid, *Phisidia sanctaemariae,* were not as abundant during the most recent reporting period (Appendix G.5). *Proclea* sp A and *M. striolata* have not been abundant in the region since 2005, while *P. sanctaemariae* has been largely absent since 2000.

The 10 most abundant taxa in the SBOO region during 2020–2021, included eight polychaetes, one tanaid, and members of the phylum Nematoda (Table 6.5). The dominant polychaetes included the spionids *Spiophanes norrisi* and *S. duplex*, the capitellid *Mediomastus* sp, the sabellid *Jasmineira* sp B, the dorvilleid *Protodorvillea gracilis*, the phyllodocid *Hesionura coineaui difficilis*, the amphinomid *Paramphinome* sp, and the sigalionid *Sigalion spinosus*. The dominant tanaid was represented by the species complex *Chondrochelia dubia,* while the other most abundant group was Nematoda. The polychaete worm *Spiophanes norrisi* was the most abundant of all these species during the past two years, accounting for 7% of invertebrates collected in the SBOO area and occurring in 94% of all grabs. Although not as numerous as in previous surveys, *S. norrisi* has remained the most abundant species recorded in the SBOO region since 2007 (Figure 6.6), with up to 3009 individuals found in a single grab from station I6 during the summer of 2010 (City of San Diego 2011). Aside from *S. duplex*, all other taxa collected during the current reporting period averaged six individuals or fewer per grab (Table 6.5). Three other numerically dominant species occurred in ≥ 72% of the samples, including *Spiophanes duplex, Chondrochelia dubia* Cmplx, and *Sigalion spinosus* (Table 6.5). The remaining six of the top 10 taxa occurred in 3–61% of the samples with average abundances per grab of 3–6 animals. Historically, the polychaetes *S. norrisi*, *S. duplex*, and *Mediomastus* sp (Figure 6.6), along with the cirratulid *Kirkegaardia siblina* and the maldanid species Euclymeninae sp A were the most numerically dominant taxa (Appendix G.6).

Indicator species

Several species known to be useful indicators of environmental change that occur in the PLOO and SBOO regions include the capitellid polychaete *Capitella teleta*, amphipods in the genera *Ampelisca* and *Rhepoxynius*, the bivalve *Solemya pervernicosa*, the terebellid polychaete *Proclea* sp A, and the brittle star *Amphiodia urtica*. For example, increased abundances of pollution-tolerant species such as *C. teleta* and *S. pervernicosa* and decreased

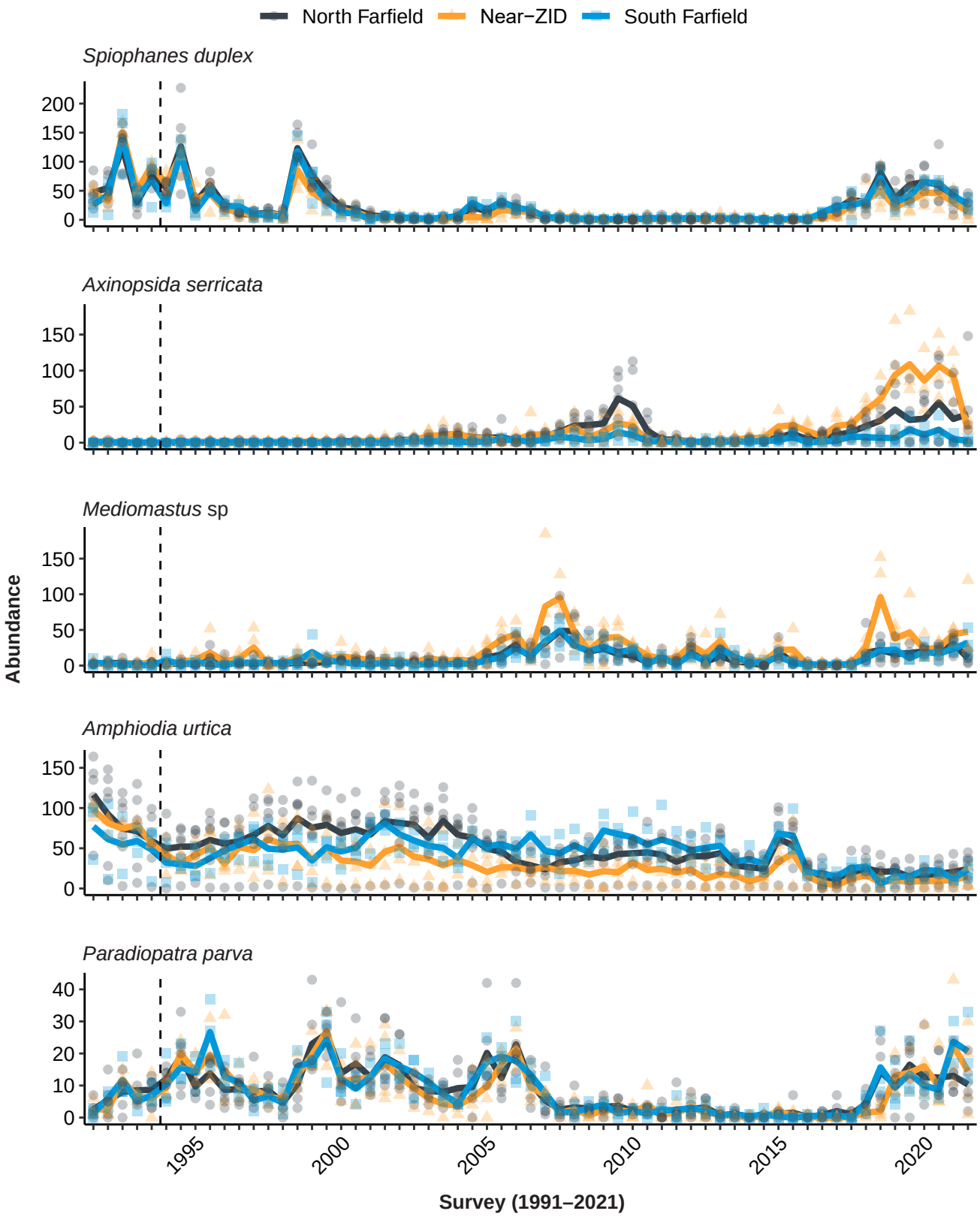

Figure 6.4

Abundances of the five most numerically dominant species recorded during 2020 and 2021 (presented in order) at PLOO north farfield, near-ZID, and south farfield primary core stations from 1991 through 2021. For each station group, mean abundance per survey is shown by the solid line ($n \leq 8$) while abundance per station is shown by the symbols. Dashed lines indicate onset of wastewater discharge.

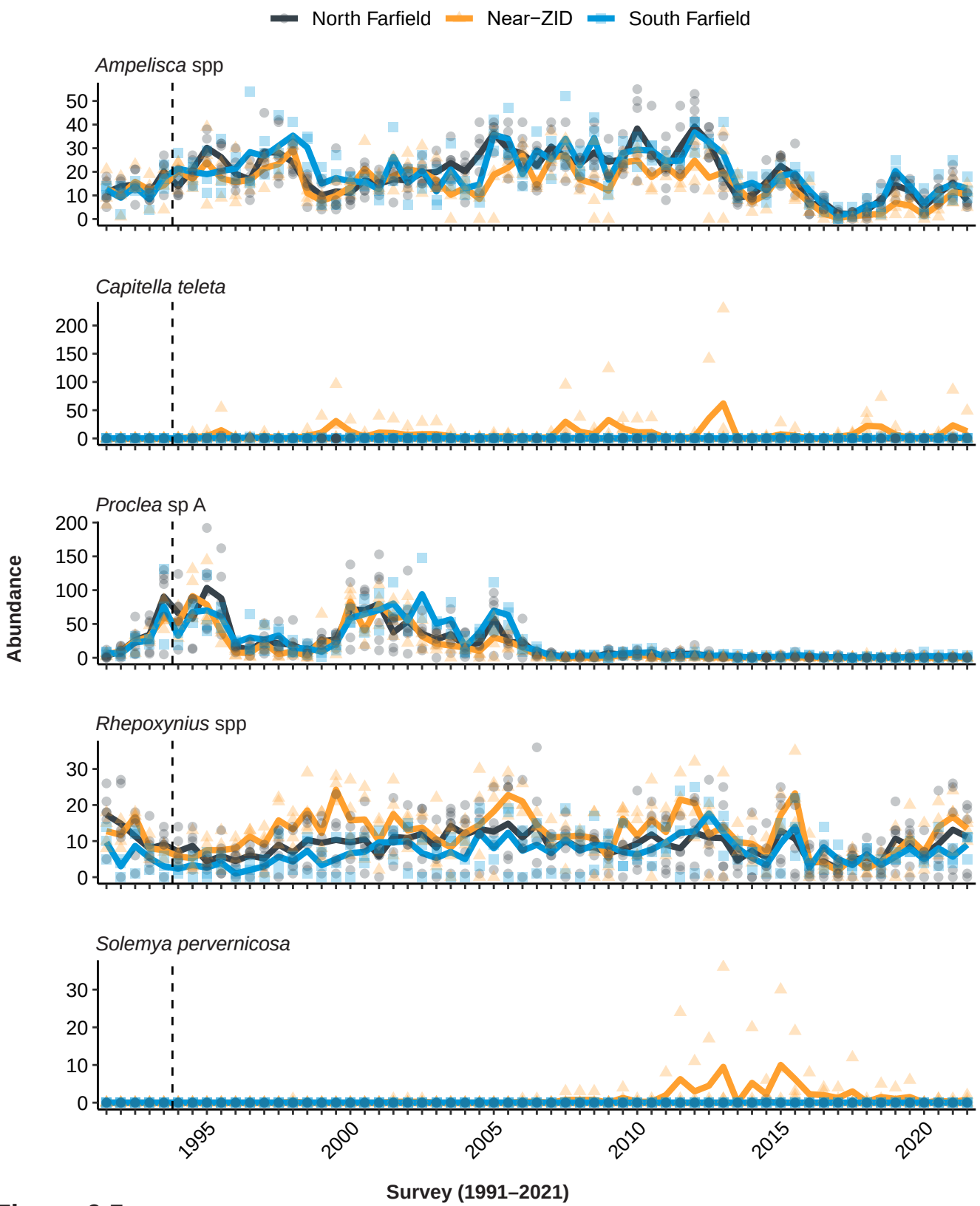

Figure 6.5

Abundances of representative ecologically important indicator taxa collected at PLOO north farfield, near-ZID, and south farfield primary core stations from 1991 through 2021. For each station group, mean abundance per survey is shown by the solid line ($n \leq 8$) while abundance per station is shown by the symbols. Dashed lines indicate onset of wastewater discharge.

Table 6.5

The 10 most abundant macroinvertebrate taxa collected from SBOO benthic stations during 2020 and 2021. Data are expressed as percent abundance (number of individuals per species/total abundance of all species), frequency of occurrence (percentage of grabs in which a species occurred), and abundance per grab (mean number of individuals per grab, n = 108).

Species	Taxonomic Classification	Percent Abundance	Frequency of Occurrence	Abundance per Grab
Spiophanes norrisi	Polychaeta: Spionidae	7	94	14
Spiophanes duplex	Polychaeta: Spionidae	6	78	14
Mediomastus sp	Polychaeta: Capitellidae	3	58	6
Jasmineira sp B	Polychaeta: Sabellidae	3	16	6
Protodorvillea gracilis	Polychaeta: Dorvilleidae	2	35	5
Chondrochelia dubia Cmplx	Arthropoda: Tanaidacea	2	72	5
Nematoda		2	61	4
Hesionura coineaui difficilis	Polychaeta: Phyllodocidae	2	6	3
Paramphinome sp	Polychaeta: Amphinomidae	1	3	3
Sigalion spinosus	Polychaeta: Sigalionidae	1	74	3

abundances of pollution-sensitive taxa such as *A. urtica*, *Proclea* sp A, *Ampelisca* spp, and *Rhepoxynius* spp are often indicative of organic enrichment and may indicate habitats impacted by human activity (Barnard and Ziesenhenne 1961, Anderson et al. 1998, Linton and Taghon 2000, Smith et al. 2001, Kennedy et al. 2009, McLeod and Wing 2009). During 2020 and 2021, a total of 217 individuals of *C. teleta* were found in samples collected across the entire region distributed among 26 different sites (stations B11, B12, E2, E5, E7, E8, E9, E11, E14, E15, E17, E20, E21, E25, E26, I2, I3, I9, I14, I20, I28, I29, I33, I34, I35), while a total of 14 individuals of *S. pervernicosa* were identified in samples from eight different sites (stations E1, E11, E14, E17, I14, I22, I28, I29). Despite occasionally exceeding regional tolerance intervals of 0 to 1 animal per grab (see City of San Diego 2022), abundances of *C. teleta* and *S. pervernicosa* remained characteristic of relatively undisturbed habitats (Figures 6.5, 6.7). For example, *C. teleta* commonly reaches densities as high as 600 individuals per 0.1m^2 grab in polluted sediments (Reish 1957, Swartz et al. 1986). Changes in abundances of *Ampelisca* and *Rhepoxynius* amphipod species varied at all PLOO primary core stations regardless of proximity to the outfall, and may have been influenced by the presence of large populations of pelagic red crabs from 2016 to 2019 (Figure 6.5, see Chapter 8).

Summary

Analyses of macrofaunal data for the 2020–2021 reporting period demonstrate that wastewater discharged through the Point Loma and South Bay outfalls has not negatively impacted macrobenthic communities in the coastal waters off San Diego. Values for most community parameters are similar at stations located both near to and far from the discharge areas. Major community metrics, such as species richness, abundance, diversity, evenness, and dominance were within historical ranges reported for the San Diego region (City of San Diego 2022), and were representative of those characteristic of similar SCB benthic habitats (Barnard and Ziesenhenne 1961, Jones 1969, Fauchald and Jones 1979, Thompson et al. 1987, 1993b, Zmarzly et al. 1994, Diener and Fuller 1995, Bergen et al. 1998, 2000, 2001, Ranasinghe et al. 2003, 2007, 2010, 2012, Mikel et al. 2007, Gillett et al. 2017). BRI values

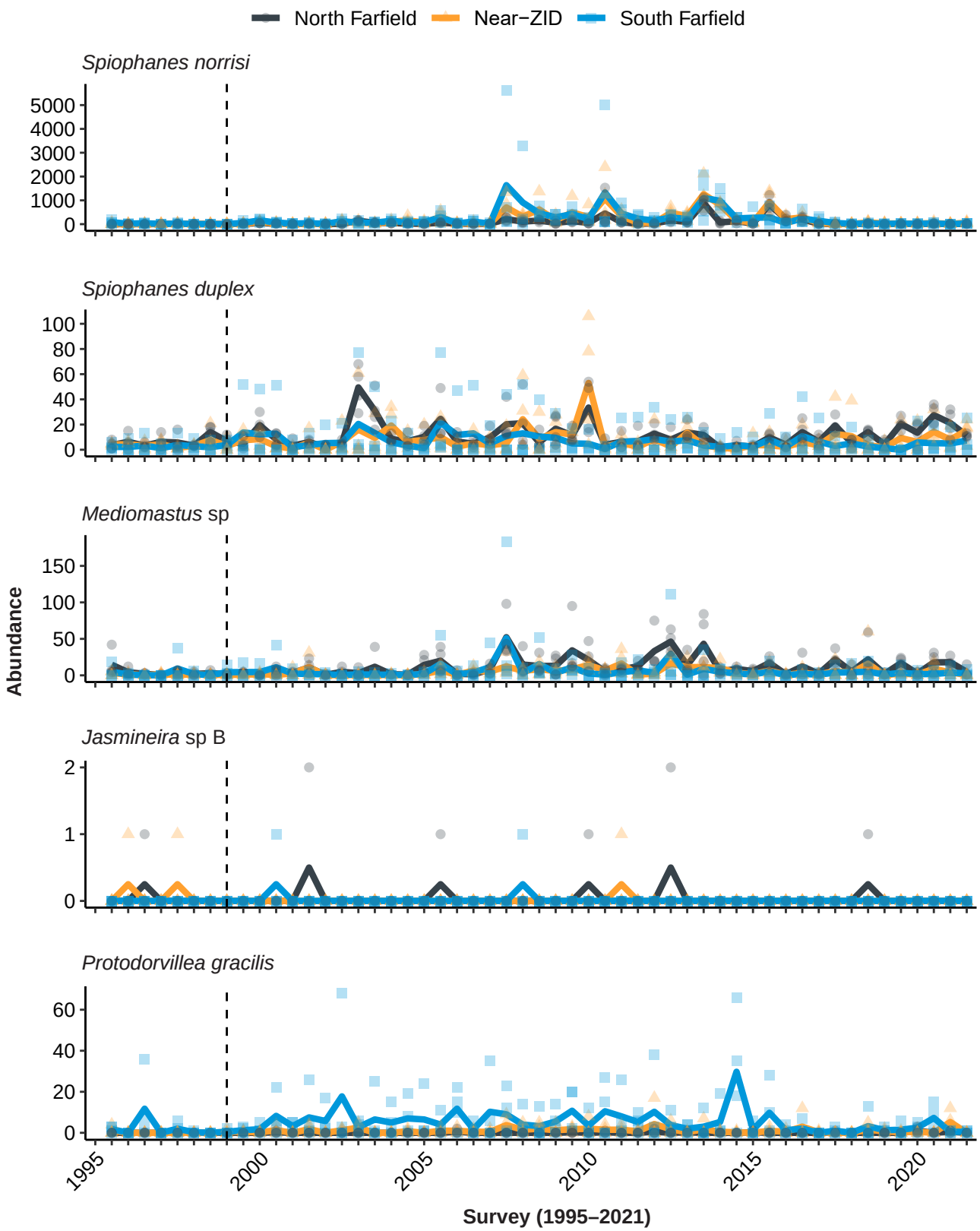

Figure 6.6

Abundances of the five most numerically dominant species (presented in order) recorded during 2020 and 2021 at SBOO north farfield, near-ZID, and south farfield primary core stations from 1995 through 2021. For each station group, mean abundance per survey is shown by the solid line ($n \leq 8$) while abundance per station is shown by the symbols. Dashed lines indicate onset of wastewater discharge.

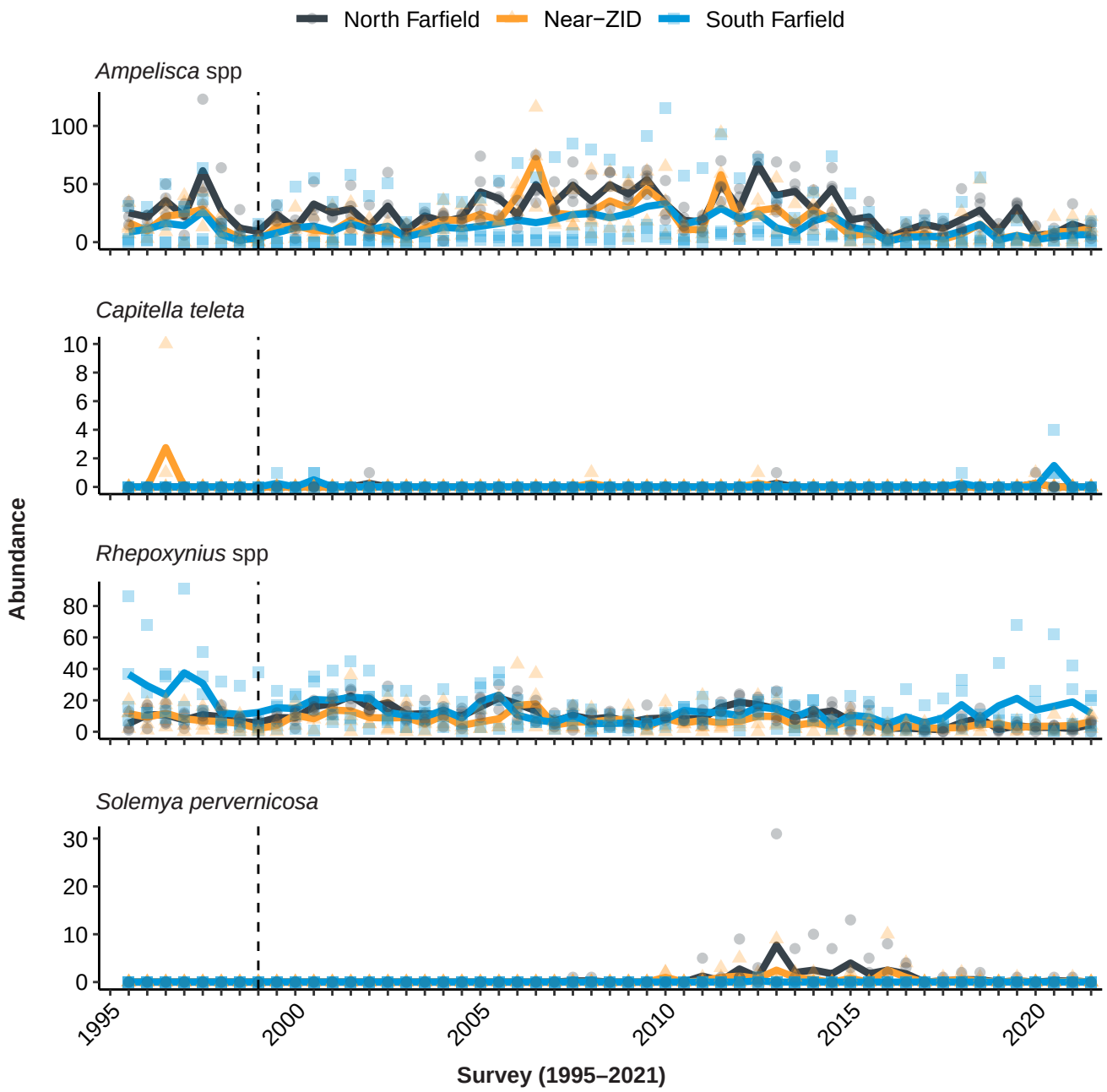

Figure 6.7

Abundances of representative ecologically important indicator taxa collected at SBOO north farfield, near-ZID, and south farfield primary core stations from 1995 through 2021. For each station group, mean abundance per survey is shown by the solid line (n ≤ 8) while abundance per station is shown by the symbols. Dashed lines indicate onset of wastewater discharge.

for 94% of the PLOO sites and 93% of the SBOO sites were considered characteristic of undisturbed habitats, while the remaining stations had values suggesting only a possible minor deviation from reference conditions. Additionally, BRI values at the shallower stations less than 28 m in the SBOO region have typically been higher than BRI values for deeper water stations since monitoring began. However, this pattern is not unexpected, since naturally higher levels of organic matter often occur closer to shore and particle sizes tend to be coarser (see Chapter 5). A similar phenomenon has been reported across the SCB where Smith et al. (2001) found a pattern of lower BRI values at

mid-depth stations (25–130 m) versus shallower (10–35 m) or deeper (110–324 m) sites.

Changes in populations of pollution-sensitive and pollution-tolerant species, or other indicators of benthic condition, provide little or no evidence of habitat degradation in either outfall region. For example, the brittle star *Amphiodia urtica* is a well-known dominant species of the mid-shelf in fine sediment habitats in the SCB, which is known to be sensitive to environmental changes near wastewater outfalls (Swartz et al. 1986). However, abundances of *A. urtica* off Point Loma remained within the range of natural variation in SCB populations (Gillett et al. 2017). Additionally, populations of opportunistic species, such as the polychaete *Capitella teleta* and the bivalve *Solemya pervernicosa,* remained low during 2020 and 2021, while populations of pollution-sensitive amphipods in the genera *Ampelisca* and *Rhepoxynius* have generally varied similarly between near-ZID and farfield stations. Furthermore, although spionid polychaetes are often abundant in other coastal areas of the world that possess high levels of organic matter (Díaz-Jaramillo et al. 2008), in the SCB these worms are known to be a stable, dominant component of many healthy environments with normal levels of organic inputs (Rodríguez-Villanueva et al. 2003). Thus, the presence of large populations of *Spiophanes norrisi* observed at many SBOO stations since 2007 is not considered to be indicative of habitat degradation related to wastewater discharge. Instead, population fluctuations of this spionid, in recent years, may correspond to natural changes in large-scale oceanographic conditions. Further support for this hypothesis is shown by the continued relatively low abundances of *S. norrisi* at all station groups during 2020 and 2021, compared to what would be expected at negatively impacted areas.

In conclusion, benthic macrofaunal communities appear to be in good condition overall throughout the PLOO and SBOO regions. Communities remain largely similar to those observed prior to outfall operations and are representative of natural communities from similar habitats on the southern California continental shelf. Overall, 94% of all benthic sites surveyed for the combined region, in 2020 and 2021, were classified as being in reference condition, based on assessments using the BRI. The few, slightly elevated, BRI values found at near-ZID stations, or along and shallower than the outfall discharge depth contour, generally fit historical patterns that have existed since before operation of either outfall began. More moderate indicators of increasing disturbance at PLOO near-ZID station E14 remain highly localized and below the threshold of community degradation. Thus, no significant effects of wastewater discharge on the local macrobenthic communities off San Diego could be identified during this past 2-year reporting period.

Literature Cited

Anderson, B.S., J.W. Hunt, B.M. Philips, S. Tudor, R. Fairey, J. Newman, H.M. Puckett, M. Stephenson, E.R. Long, and R.S. Tjeerdema. (1998). Comparison of marine sediment toxicity test protocols for the amphipod *Rhepoxynius abronius* and the polychaete worm *Nereis* (*Neanthes*) *arenaceodentata*. Environmental Toxicology and Chemistry. 17(5): 859–866.

Barnard, J.L. and F.C. Ziesenhenne. (1961). Ophiuroidea communities of southern Californian coastal bottoms. Pacific Naturalist, 2: 131–152.

Bergen, M. (1995). Distribution of Brittlestar Amphiodia (Amphispina) spp. in the Southern California Bight in 1956 to 1959. Bulletin of the Southern California Academy of Sciences. 94(3): 190–203.

Bergen, M., S.B. Weisberg, D. Cadien, A. Dalkey, D. Montagne, R.W. Smith, J.K. Stull, and R.G. Velarde. (1998). Southern California Bight 1994 Pilot Project: IV. Benthic Infauna. Southern California Coastal Water Research Project, Westminster, CA.

Bergen, M., D.B. Cadien, A. Dalkey, D.E. Montagne, R.W. Smith, J.K. Stull, R.G. Velarde, and S.B. Weisberg. (2000). Assessment of benthic

infaunal condition on the mainland shelf of southern California. Environmental Monitoring Assessment, 64: 421–434.

Bergen, M., S.B. Weisberg, R.W. Smith, D.B. Cadien, A. Dalkey, D.E. Montagne, J.K. Stull, R.G. Velarde, and J.A. Ranasinghe. (2001). Relationship between depth, sediment, latitude, and the structure of benthic infaunal assemblages on the mainland shelf of southern California. Marine Biology, 138: 637–647.

Bilyard, G.R. (1987). The value of benthic infauna in marine pollution monitoring studies. Marine Pollution Bulletin, 18(11): 581–585.

City of San Diego. (2011). Annual Receiving Waters Monitoring Report for the South Bay Ocean Outfall (South Bay Water Reclamation Plant), 2010. City of San Diego Ocean Monitoring Program, Public Utilities Department, Environmental Monitoring and Technical Services Division, San Diego, CA.

City of San Diego. (2021). Interim Receiving Waters Monitoring Report for the Point Loma and South Bay Ocean Outfalls, 2020. City of San Diego Ocean Monitoring Program, Public Utilities Department, Environmental Monitoring and Technical Services Division, San Diego, CA.

City of San Diego. (2022). Appendix C2: San Diego Benthic Tolerance Intervals. In: Report of Waste Discharge and Application for Renewal of NPDES CA 0107409 and 301(h) Modified Secondary Treatment Requirements. Volume V: Appendix C. City of San Diego Public Utilities Department, San Diego, CA.

Díaz-Jaramillo, M., P. Muñoz, V. Delgado-Blas, and C. Bertrán. (2008). Spatio-temporal distribution of spionids (Polychaeta-Spionidae) in an estuarine system in south-central Chile. Revista Chilena de Historia Natural, 81: 501–514.

Diener, D.R. and S.C. Fuller. (1995). Infaunal patterns in the vicinity of a small coastal wastewater outfall and the lack of infaunal community response to secondary treatment. Bulletin of the Southern California Academy of Science, 94: 5–20.

Fauchald, K. and G.F. Jones. (1979). Variation in community structures on shelf, slope, and basin macrofaunal communities of the Southern California Bight. Report 19, Series 2. In: Southern California Outer Continental Shelf Environmental Baseline Study, 1976/1977 (Second Year) Benthic Program. Principal Investigators Reports, Vol. II. Science Applications, Inc. La Jolla, CA.

Ferraro, S.P., R.C. Swartz, F.A. Cole, and W.A. Deben. (1994). Optimum macrobenthic sampling protocol for detecting pollution impacts in the Southern California Bight. Environmental Monitoring and Assessment, 29: 127–153.

Gillett, D.J., L.L. Lovell and K.C. Schiff. (2017). Southern California Bight 2013 Regional Monitoring Program: Volume VI. Benthic Infauna. Technical Report 971. Southern California Coastal Water Research Project. Costa Mesa, CA.

Gray, J.S. (1979). Pollution-induced changes in populations. Philosophical Transactions of the Royal Society of London (Series B), 286: 545–561.

Hartley, J.P. (1982). Methods for monitoring offshore macrobenthos. Marine Pollution Bulletin, 12: 150–154.

Hope, R.M. (2013). Rmisc: Ryan Miscellaneous. R package version 1.5. http://CRAN.R-project.org/package=Rmisc.

Jones, G.F. (1969). The benthic macrofauna of the mainland shelf of southern California. Allan Hancock Monographs of Marine Biology, 4: 1–219.

Kassambara, A. (2019). ggpubr: 'ggplot2' Based Publication Ready Plots. R package version 0.2.2. https://CRAN.R-project.org/package=ggpubr.

Kennedy, A.J., J.A. Stevens, G.R. Lotufo, J.D. Farrar, M.R. Reiss, R.K. Kropp, J. Doi, and T.S. Bridges. (2009). A comparison of acute and chronic toxicity methods for marine sediments. Marine Environmental Research, 68: 118–127.

Linton, D.L. and G.L. Taghon. (2000). Feeding, growth, and fecundity of *Capitella* sp. I in relation to sediment organic concentration. Marine Ecology Progress Series, 205: 229–240.

McLeod, R.J. and S.R. Wing. (2009). Strong pathways for incorporation of terrestrially derived organic matter into benthic communities. Estuarine, Coastal and Shelf Science, 82: 645–653.

Mikel T.K., J.A Ranasinghe, and D.E. Montagne. (2007). Characteristics of benthic macrofauna of the Southern California Bight. Appendix F. Southern California Bight 2003 Regional Monitoring Program, SCCWRP, Costa Mesa, CA.

Oksanen, J., F. G. Blanchet, R. Kindt, P. Legendre, P. R. Minchin, R. B. O'Hara, G. L. Simpson, P. Solymos, M. H. H. Stevens and H. Wagner (2017). vegan: Community Ecology Package. R package version 2.3-1. http://CRAN.R-project.org/package=vegan.

Pearson, T.H. and R. Rosenberg. (1978). Macrobenthic succession in relation to organic enrichment and pollution of the marine environment. Oceanography and Marine Biology Annual Review, 16: 229–311.

R Core Team (2021). R: A language and environment for statistical computing. R Foundation for Statistical Computing, Vienna, Austria. URL https://www.R-project.org/.

Ranasinghe, J.A., D.E. Montagne, R.W. Smith, T.K. Mikel, S.B. Weisberg, D. Cadien, R. Velarde, and A. Dalkey. (2003). Southern California Bight 1998 Regional Monitoring Program: VII. Benthic Macrofauna. Southern California Coastal Water Research Project, Westminster, CA.

Ranasinghe, J.A., A.M. Barnett, K. Schiff, D.E. Montagne, C. Brantley, C. Beegan, D.B. Cadien, C. Cash, G.B. Deets, D.R. Diener, T.K. Mikel, R.W. Smith, R.G. Velarde, S.D. Watts, and S.B. Weisberg. (2007). Southern California Bight 2003 Regional Monitoring Program: III. Benthic Macrofauna. Southern California Coastal Water Research Project, Costa Mesa, CA.

Ranasinghe, J.A., K.C. Schiff, D.E. Montagne, T.K. Mikel, D.B. Cadien, R.G. Velarde, and C.A. Brantley. (2010). Benthic macrofaunal community condition in the Southern California Bight, 1994–2003. Marine Pollution Bulletin, 60: 827–833.

Ranasinghe, J.A., K.C. Schiff, C.A. Brantley, L.L. Lovell, D.B. Cadien, T.K. Mikel, R.G. Velarde, S. Holt, and S.C. Johnson. (2012). Southern California Bight 2008 Regional Monitoring Program: VI. Benthic Macrofauna. Technical Report No. 665, Southern California Coastal Water Research Project, Costa Mesa, CA.

Reish, D. J. (1957). The relationship of the polychaetous annelid *Capitella capitata* (Fabricius) to waste discharges of biological origin. In: C.M. Tarzwell (ed.). Biological Problems in Water Pollution. U.S. Public Health Service, Washington, DC. p 195–200.

Ripley, B. and M. Lapsley. (2017). RODBC: ODBC Database Access. R package version 1.3-15. http://CRAN.R-project.org/package=RODBC.

Rodríguez-Villanueva, V., R. Martínez-Lara, and V. Macías Zamora. (2003). Polychaete community structure of the northwestern coast of Mexico: patterns of abundance and distribution. Hydrobiologia, 496: 385–399.

[SCAMIT] Southern California Association of Marine Invertebrate Taxonomists. (2018). A taxonomic listing of benthic macro- and megainvertebrates from infaunal and epibenthic monitoring programs in the Southern California Bight,

edition 12. Southern California Association of Marine Invertebrate Taxonomists, Natural History Museum of Los Angeles County Research and Collections, Los Angeles, CA.

Smith, R.W., M. Bergen, S.B. Weisberg, D. Cadien, A. Dalkey, D. Montagne, J.K. Stull, and R.G. Velarde. (2001). Benthic response index for assessing infaunal communities on the southern California mainland shelf. Ecological Applications, 11(4): 1073–1087.

Snelgrove, P.V.R., T.H. Blackburn, P.A. Hutchings, D.M. Alongi, J.F. Grassle, H. Hummel, G. King, I. Koike, P.J.D. Lambshead, N.B. Ramsing, and V. Solis-Weiss. (1997). The importance of marine sediment biodiversity in ecosystem processes. Ambio, 26: 578–583.

Swartz, R.C., F.A. Cole, and W.A. Deben. (1986). Ecological changes in the Southern California Bight near a large sewage outfall: benthic conditions in 1980 and 1983. Marine Ecology Progress Series, 31: 1–13.

Thompson, B.E., J.D. Laughlin, and D.T. Tsukada. (1987). 1985 reference site survey. Technical Report No. 221, Southern California Coastal Water Research Project, Long Beach, CA.

Thompson, B., J. Dixon, S. Schroeter, and D.J. Reish. (1993a). Chapter 8. Benthic invertebrates. In: M.D. Dailey, D.J. Reish, and J.W. Anderson (eds.). Ecology of the Southern California Bight: A Synthesis and Interpretation. University of California Press, Berkeley, CA.

Thompson, B.E., D. Tsukada, and D. O'Donohue. (1993b). 1990 reference site survey. Technical Report No. 269, Southern California Coastal Water Research Project, Long Beach, CA.

[USEPA] United States Environmental Protection Agency. (1987). Quality Assurance and Quality Control (QA/QC) for 301(h) Monitoring Programs: Guidance on Field and Laboratory Methods. EPA Document 430/9-86-004. Office of Marine and Estuarine Protection.

Warwick, R.M. (1993). Environmental impact studies on marine communities: pragmatical considerations. Australian Journal of Ecology, 18: 63–80.

Wickham, H. (2007). Reshaping Data with the reshape Package. Journal of Statistical Software, 21(12), 1-20. URL http://www.jstatsoft.org/v21/i12/.

Wickham, H. (2017). tidyverse: Easily Install and Load the 'Tidyverse'. R package version 1.2.1. https://CRAN.R-project.org/package=tidyverse.

Wickham, H. (2018). scales: Scale Functions for Visualization. R package version 1.0.0. https://CRAN.R-project.org/package=scales

Zmarzly, D.L., T.D. Stebbins, D. Pasko, R.M. Duggan, and K.L. Barwick. (1994). Spatial patterns and temporal succession in soft-bottom macroinvertebrate assemblages surrounding an ocean outfall on the southern San Diego shelf: Relation to anthropogenic and natural events. Marine Biology, 118: 293–307.

This page intentionally left blank

Chapter 7
San Diego Regional
Benthic Condition Assesssment

Chapter 7. San Diego Regional Benthic Condition Assessment

Introduction

The City of San Diego (City) has conducted annual surveys of randomly selected (regional) benthic stations off the coast of San Diego since 1994 (see Chapter 1). The location of these regional surveys typically range from offshore of Del Mar in northern San Diego County southward to the USA/Mexico border. An array of 40 stations are selected each year using a probability-based, random stratified sampling design as described in Bergen (1996), Stevens (1997), and Stevens and Olsen (2004). During 1995–1997, 1999–2002, and 2005–2007, the surveys off San Diego were restricted to continental shelf depths < 200 m. However, beginning in 2009, the survey area was expanded to include deeper habitats along the upper continental slope (200–500 m). No separate San Diego regional survey was conducted in 2004 due to sampling for a special sediment mapping project (Stebbins et al. 2004), while the 1994, 1998, 2003, 2008, 2013, and 2018 regional surveys were conducted as part of the larger Southern California Bight (SCB) Regional Monitoring Program (Bergen et al. 1998, 2001, Schiff and Gossett 1998, Noblet et al. 2002, Schiff et al. 2006, 2011, Maruya and Schiff 2009, Ranasinghe et al. 2003, 2007, 2010, 2012, Dodder et al. 2016, Gillett et al. 2017, SCCWRP 2018, Du et al. 2020). In total more than 960 samples from 911 different regional stations have been sampled off San Diego over the past 28 years (1994–2021).

This chapter presents an overall assessment of regional benthic conditions on the continental shelf and upper slope off San Diego during 2020–2021. Included are analyses of sediment particle size, sediment chemistry, sediment toxicity, and macrofaunal community data collected from a total of 80 regional and 49 core benthic stations sampled during summer 2020 and 2021. These data provide a snapshot of the region's sediment quality and benthic community structure across the major depth strata defined by the SCB regional monitoring programs (e.g., SCCWRP 2018). Additional analysis of spatial patterns, winter vs. summer differences, and long-term changes over time at the core Point Loma Ocean Outfall (PLOO) and South Bay Ocean Outfall (SBOO) stations are presented in Chapters 5 and 6.

In an effort to provide a more comprehensive assessment of sediment quality in this region, sediment toxicity results have been integrated with other lines of evidence (LOEs), including sediment chemistry and benthic community structure. These LOEs were integrated using a framework adopted by the State of California to assess sediment quality within enclosed bays and estuaries (SWRCB 2009; Bay et al. 2013), but with the same modifications used for the coastal shelf as part of Southern California Bight (SCB) Regional Monitoring Program surveys (i.e., Bight regional surveys; see B13CIA 2017). These modifications included applying the results from the 10-day amphipod sediment toxicity test prescribed by the Sediment Toxicity Monitoring Plan (versus the two sediment toxicity tests available for embayments) (City of San Diego 2015a) and the benthic response index (BRI) that was developed specifically for evaluation of benthic macrofaunal (e.g., worms, crabs, clams, brittle stars, other small invertebrates) communities in offshore waters (Bergen et al. 2000, Smith et al. 2001). The same two sediment chemistry assessment indices developed for embayments were used, even though these indices have not been calibrated or validated for continental shelf sediments, as these are the best tools currently available (B13CIA 2017). The integration of each line of evidence using the State of California's sediment quality assessment framework resulted in the classification of each site into one of five potential categories: (1) unimpacted; (2) likely unimpacted; (3) possibly impacted; (4) likely impacted; (5) clearly impacted. The State Water Board considers the first two categories as healthy, or representative of conditions undisturbed by pollutants in sediment (SWRCB 2009, B13CIA 2017).

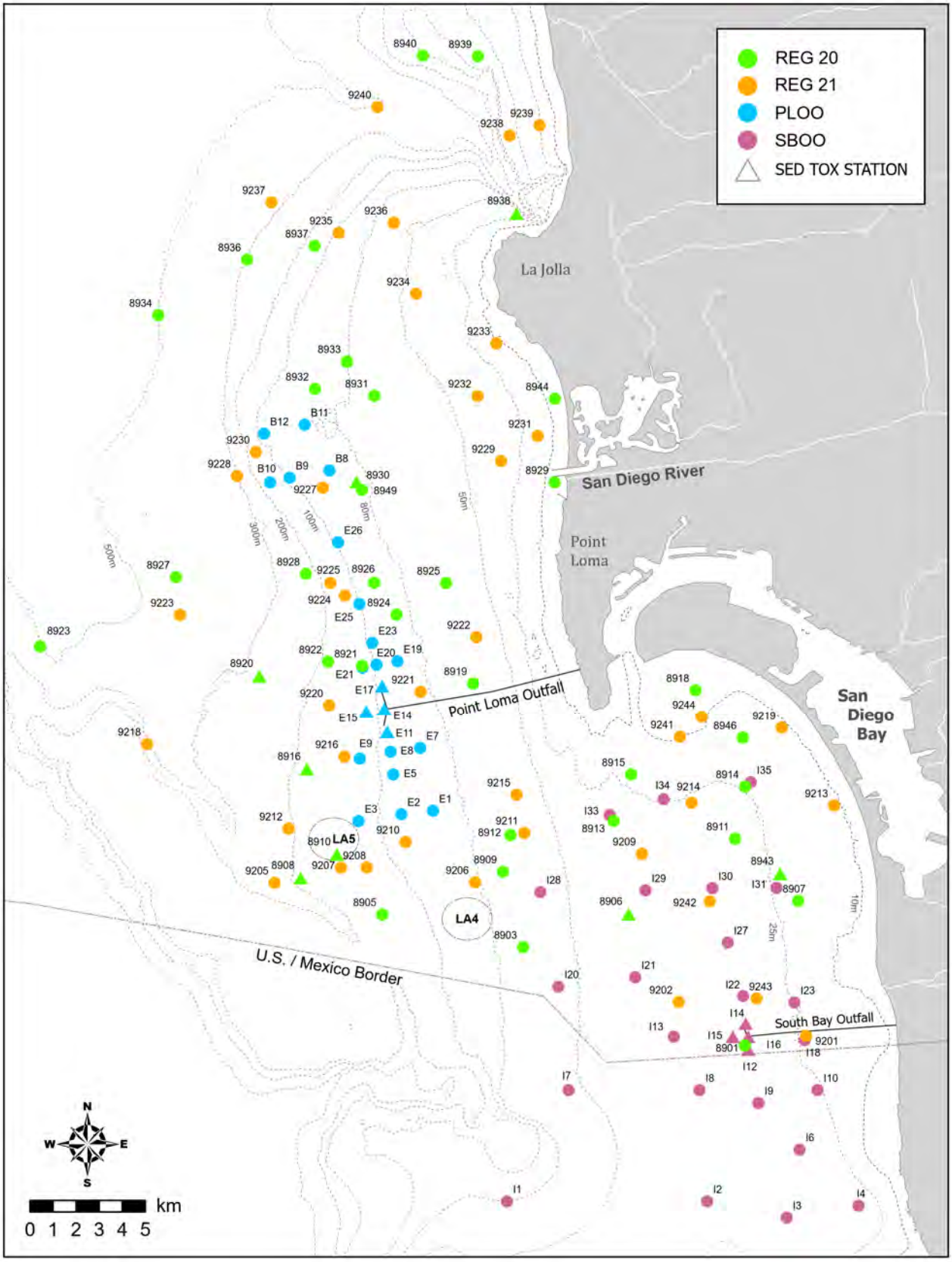

Figure 7.1
Distribution of 80 regional and 49 core (PLOO/SBOO) benthic stations sampled off San Diego and northern Baja California during summer 2020 and 2021.

The primary objectives of this chapter are to: (1) describe the overall condition and quality of the diverse benthic habitats that occur in the offshore coastal waters off San Diego; (2) characterize sediment quality, sediment toxicity, and the health of the soft-bottom marine benthos in the region; (3) gain a better understanding of regional variation in order to distinguish between the effects of anthropogenic and natural factors; (4) put into context the results of more frequent sampling at permanent (core) monitoring sites surrounding the PLOO and SBOO.

Materials and Methods

Collection and Processing of Samples

Benthic samples analyzed in this chapter were collected during the summer of 2020 and 2021 at 129 stations that ranged from Del Mar southward to below the USA/Mexico border (Figure 7.1). A total of 80 of these stations were selected using a probability-based random stratified sampling design as described in Bergen (1996), Stevens (1997), and Stevens and Olsen (2004). These "regional" stations were sampled at depths ranging from 7 to 523 m spanning four distinct depth strata off southern California. These included 23 regional stations along the inner shelf (7–30 m), 33 regional stations along the mid-shelf (30–120 m), 11 regional stations along the outer shelf (120–200 m), and 13 regional stations on the upper slope (200–523 m). In addition to the above, the results of summer sampling at the 49 core PLOO and SBOO monitoring stations located at inner to mid-shelf depths as described in Chapters 5 and 6 are also analyzed in this chapter. Stations located within 1000 m of the boundary of the zone of initial dilution (ZID) for either outfall are considered to represent near-ZID conditions. These include PLOO stations E11, E14, E15, E17, SBOO stations I12, I14, I15, I16, and regional station 8822 near the PLOO.

Samples for benthic analyses were collected using a double 0.1-m^2 Van Veen grab, with one grab per cast used for sediment quality analysis (see Chapter 5), one grab per cast used for benthic community analysis (see Chapter 6), and subsequent grabs used for sediment toxicity testing where required. Visual observations of weather, sea conditions, and human/animal activity were also recorded at the time of sampling. Criteria established by the U.S. Environmental Protection Agency (USEPA) to ensure consistency of these types of samples were followed with regard to sample disturbance and depth of penetration (USEPA 1987).

Sub-samples for particle size and sediment chemistry analyses were taken from the top 2 cm of the sediment surface and handled according to standard guidelines (USEPA 1987, SCCWRP 2018). For infauna analysis, sediment from an entire grab was transferred to a wash table aboard ship, rinsed with seawater, and then sieved through a 1.0-mm mesh screen in order to remove as much sediment as possible. The macroinvertebrates retained on the screen were transferred to sample jars, relaxed for 30 minutes in a magnesium sulfate solution, and then fixed with buffered formalin. The preserved samples were then transferred back to the City's Marine Biology Laboratory. After a minimum of 72 hours, but no more than 10 days, in formalin, each sample was thoroughly rinsed with fresh water and transferred to 70% ethanol for final preservation.

For sediment toxicity samples, a plastic (high-density polyethylene [HDPE], polycarbonate, or Teflon) or stainless-steel scoop was used to collect sediment from the top 2 cm of the undisturbed surface material in the grab. Contact with sediment within 1 cm of the sides of the grab was avoided in order to minimize cross-contamination. In most cases, multiple grabs were required to obtain enough sediment for toxicity testing (i.e., up to 6 L of sediment). If more than one grab was required, sediment from each grab was added to a Teflon bag and homogenized thoroughly using either a clean Teflon or plastic spoon, or by kneading the sample within the bag. Once collected, the toxicity samples were stored in the dark at 4°C in the laboratory for no longer than four weeks prior to testing.

Laboratory Analyses

Sediment Particle Size

All sediment chemistry and particle size analyses were performed at the City's Environmental

Chemistry Services Laboratory. Particle size analysis was performed using either a Horiba LA-950V2 laser scattering particle analyzer or a set of nested sieves. The Horiba measures particles ranging in size from 0.5 to 2000 µm. Coarser sediments were removed and quantified prior to laser analysis by screening samples through a 2000 µm mesh sieve. These data were later combined with the Horiba results to obtain a complete distribution of particle sizes totaling 100%, and then classified into 11 sub-fractions and four main size fractions based on the Wentworth scale (Folk 1980) (see Appendix F.2). When a sample contained substantial amounts of coarse sand, gravel, shell hash or other large materials that could damage the Horiba analyzer or where the general distribution of sediments would be poorly represented by laser analysis, a set of nested sieves with mesh sizes of 2000 µm, 1000 µm, 500 µm, 250 µm, 125 µm, 75 µm and 63 µm was used to divide the samples into seven sub-fractions. See Appendix H.1 for visual observations for each regional station; see Appendix F.3 for visual observations for each PLOO and SBOO core station.

Sediment Chemistry

A detailed description of the analytical protocols is available upon request. Briefly, sediment sub-samples were analyzed on a dry weight basis to determine concentrations of various indictors of organic loading (i.e., biochemical oxygen demand, total organic carbon, total nitrogen, total sulfides, total volatile solids), 18 trace metals, 9 chlorinated pesticides, 42 polychlorinated biphenyl compound congeners (PCBs), and 24 polycyclic aromatic hydrocarbons (PAHs) (see Appendix F.2).

Sediment Toxicity Testing

A detailed description of the sediment toxicity testing protocols can be found in City of San Diego (2022b). Briefly, all sediment toxicity testing was conducted by the City of San Diego Toxicology Laboratory (CSDTL) using the marine amphipod *Eohaustorius estuarius*. The 10-day amphipod tests were conducted in accordance with EPA 600/R-94/0925 (USEPA 1994) and the procedures approved for Southern California Bight 2018 Regional Monitoring Program (Bight'18 Toxicology Committee 2018). Juvenile *E. estuarius* were exposed for 10 days to both test and control sediments. Response criteria included amphipod mortality, emergence from sediment during exposure, and, if considered a measurement of interest, the ability of amphipods to rebury in clean sediment at the end of the bioassay. In addition, a reference toxicant test (using seawater only) was conducted concurrently and under identical environmental conditions as the sediment toxicity tests to determine test organism sensitivity.

Macrobenthic Assemblages

All organisms were separated from the raw material (e.g., sediment grunge, shell hash, debris) and sorted into the following six taxonomic groups by an external contract lab: Annelids (e.g., polychaete and oligochaete worms), Arthropods (e.g., crustaceans and pycnogonids), Molluscs (e.g., clams, snails, and scaphopods), non-ophiuroid Echinoderms (e.g., sea urchins, sea stars, and sea cucumbers), Ophiuroids (i.e., brittle stars), and other phyla (e.g., flatworms, nemerteans, and cnidarians). The sorted macrofaunal samples were then returned to the City's Marine Biology Laboratory where all animals were identified to species, or to the lowest taxon possible, by City Marine Biologists. All identifications followed nomenclatural standards established by the Southern California Association of Marine Invertebrate Taxonomists (SCAMIT 2018; see Appendix H.2.

Data Analyses

Data for each parameter analyzed during 2020 were reported previously (City of San Diego 2021), and all raw data for the 2020–2021 sampling period have been submitted to either the Regional Water Quality Control Board or the California Environmental Data Exchange Network (CEDEN) and will be provided upon request.

Sediment Chemistry

Data summaries for the various sediment parameters included detection rate, minimum, maximum, and mean values. For chemistry parameters, all means were calculated using detected values only, with no substitutions made for non-detects in the data (analyte concentrations < method detection limit [MDL]). Limiting analyses to detected values (i.e., excluding non-detects) is considered a conservative way of handling contaminant concentrations as it creates

a strong upward bias in the data and respective summary statistics, and therefore may represent a worst-case scenario (e.g., see Helsel 2005a, b, 2006 for discussions of non-detect data). For continuity, and in contrast to previous reports (e.g., City of San Diego 2020), estimated values that fell below method detection limits but were confirmed by mass-spectrometry were excluded from all data (1991–2021). Estimated values were treated as non-detects for this report. Total chlordane, total DDT (tDDT), total hexachlorocyclohexane (tHCH), total PCB (tPCB), and total PAH (tPAH) were calculated for each sample as the sum of all individual constituents with reported values. When applicable, contaminant concentrations were compared to the Effects Range Low (ERL) and Effects Range Median (ERM) sediment quality guidelines (Long et al. 1995). The ERLs represent chemical concentrations below which adverse biological effects are rarely observed, while values above the ERL but below the ERM represent levels at which effects occasionally occur. Concentrations above the ERM indicate likely biological effects, although these are not always validated by toxicity testing (Schiff and Gossett 1998). Unless stated otherwise, analyses were performed using R (R Core Team 2021) and various functions within the zoo, reshape2, plyr, stringr, Rmisc, ROBDC, tidyr, ggpubr, vegan, psych, tidyverse, ggplot2, and dplyr (Zeileis and Grothendieck 2005, Wickham 2007, 2011, 2019b, Hope 2013, Ripley and Lapsley 2017, Wickham and Henry 2018, Kassambara 2019, Oksanen et al. 2019, Revelle 2019, Wickham et al. 2019a,b, 2020).

Spearman rank correlations were calculated to assess if values for the various parameters co-varied in the sediments. This non-parametric analysis accounts for non-detects in the data without the use of value substitutions (Helsel 2005b). However, depending on the data distribution, the instability in rank-based analyses may intensify with increased censoring (Conover 1980). Therefore, a criterion of $<50\%$ non-detects was used to screen eligible constituents for this analysis.

Sediment Toxicity Testing

All data were analyzed in accordance with procedures outlined in Sections 12 and 13 of EPA 600/R-94/0925 using the acceptability criterion of $\geq 90\%$ mean control survival at test termination. Additional information and the standard operation procedures for sediment toxicity testing are provided in Appendix B of the CSDTL's Quality Assurance Manual (City of San Diego 2022b).

Macrobenthic Assemblages

The following community metrics were determined for each station and expressed per 0.1-m^2 grab: species richness (number of species or distinct taxa), abundance (number of individuals), Shannon Diversity Index (H'), Pielou's Evenness Index (J'), Swartz dominance index (see Swartz et al. 1986, Ferraro et al. 1994), and BRI (see Smith et al. 2001). Due to limitations in the validation dataset, BRI values were not calculated for samples collected at depths <10 m or >200 m (Smith et al. 2001). Unless otherwise noted, analyses were performed using the computational software package R (R Core Team 2021) and various functions within the reshape2, Rmisc, RODBC, tidyr, ggpubr, vegan, scales, tidyverse (Wickham 2007, Hope 2013, Ripley and Lapsley 2017, Wickham and Henry 2018, Kassambara 2019, Oksanen et al. 2019, Wickham 2019a, Wickham et al. 2019a).

Sediment Quality Triad Assessment

Following instructions provided in Bay et al. (2013), benthic macrofauna and sediment chemistry results were combined with sediment toxicity results from the 16 stations where sediment toxicity was conducted to determine relevant condition categories. The benthic community LOE was determined by assigning condition categories to each sample collected at acceptable depths as follows: BRI values <25 = reference conditions, 25–33 = minor deviation from reference conditions, 34–43 = moderate disturbance, 44–71 = high disturbance (defined as loss in community function in Smith et al. 2001), and >72 = defaunation. The sediment toxicity LOE was determined by assigning scores to samples using the following thresholds: percent control $\geq 90\%$ = nontoxic, $\geq 82\%$ = low toxicity, and $\geq 59\%$ = moderate toxicity, $<59\%$ = high toxicity. The sediment chemistry LOE was determined by using the California Logistic Regression Model Index (LRM) and the Chemical Score Index (CSI) to calculate scores for each sample with sufficient parameters analyzed (i.e., all but

PCB 8 and PCB 195), calculating the mean score as (LRM + CSI)/2, and assigning the overall integrated chemistry category LOE as follows: mean score ≤1.0=minimal exposure, 1.1–2.0=low exposure, 2.1–3.0=moderate exposure, and 3.1–4.0=high exposure.

After the scores were converted to LOE categories, they were combined using the integration framework defined in Bay et al (2013). This framework is based on a conceptual approach that addresses two key elements: (1) is there biological degradation at the site, and (2) is chemical exposure at the site high enough to potentially result in a biological response? (see SWRCB 2009, Bay and Weisberg 2012). Station assessment (site condition) categories were assigned using benthic community condition as determined by the BRI (reference, or low, moderate, high disturbance), sediment toxicity (non-toxic, or low, moderate, high toxicity), and sediment chemistry exposure (minimal, low, moderate, high) according to Table 6.1 in Bay et al (2013). For example, if a sample had a benthic community in reference condition, the sediments were found to be nontoxic, and the sediment chemistry exposure was minimal, then the station assessment (site condition) was deemed unimpacted. There is a total of 64 combinations resulting in the five categories: (1) unimpacted; (2) likely unimpacted; (3) possibly impacted; (4) likely impacted; (5) clearly impacted. The station assessment could also be inconclusive (e.g., reference benthic conditions plus moderate sediment toxicity exposure plus high sediment chemistry exposure).

Multivariate Analyses

Multivariate analyses were performed using PRIMER v7 software to examine spatial and temporal patterns in particle size, sediment chemistry, and macrofaunal data collected at the 129 regional and core stations sampled during summer 2020 and 2021 (Clarke et al. 2008, Clarke et al. 2014). These included ordination and hierarchical agglomerative clustering (cluster analysis) with group-average linking and similarity profile analysis (SIMPROF) to confirm the non-random structure of the resultant cluster dendrograms. Prior to these analyses, proportions of silt and clay sub-fractions were combined as percent fines to accommodate sieved samples, while sediment chemistry data were normalized after non-detects (see above) were converted to "0" and macrofaunal abundance data were square-root transformed to lessen the influence of overly abundant species and increase the importance (or presence) of rare species. Measures of similarity used as the basis for clustering included Euclidean distance for particle size and sediment chemistry data, and the Bray-Curtis measure of similarity for macrofaunal data. Major ecologically-relevant clusters receiving SIMPROF support were retained, and similarity percentages analysis (SIMPER) was used to determine which sub-fractions, chemical parameter, or species were responsible for the greatest contributions to within-group similarity (characteristic species) and between-group dissimilarity for retained clusters.

BEST tests, using the BVSTEP procedure, were conducted to determine which subset of sediment sub-fractions, chemical parameters, or species best described patterns within the dendrograms resulting from each of the above cluster analyses. Additional BEST tests, using the BIO-ENV procedure, were conducted to: (1) determine which subsets of sediment sub-fractions were the best explanatory variables for the similarity between the particle size and sediment chemistry resemblance matrices; (2) determine which subsets of sediment sub-fractions were the best explanatory variables for similarity between the particle size and macrofaunal resemblance matrices. To determine whether sediment chemistry concentrations or macrofaunal communities varied by sediment particle size sub-fractions, a RELATE test was used to compare patterns in the matrices with patterns in the particle size Euclidean distance matrix.

RESULTS

Regional Sediment Quality

Particle Size Composition

Ocean sediments were diverse at the 129 benthic stations sampled during the 2020 and 2021 summer surveys. The proportion of fine silt and clay particles (combined as 'fine particles' or 'percent fines') ranged from a minimum of 0 to a maximum of 100% per sample, while fine sands ranged from 0 to 89.2%,

medium-coarse sands ranged from 0 to 94.5%, and coarse particles ranged from 0 to 49.9% (Table 7.1). Overall, and as expected, sediment composition varied by depth and region (e.g., City of San Diego 2020). For example, the amount of percent fines at regional stations increased with depth, with a mean of 20.9% per sample along the inner shelf, 53.5% along the mid-shelf, 61.1% along the outer shelf, and 73.8% along the upper slope. Furthermore, correlation analysis confirmed that percent fines tended to increase with depth throughout the San Diego area (Figure 7.2, Appendix H.3), but not as strongly as previously reported (e.g., $r_s = 0.64$ for samples collected in summer 2020 and 2021, versus $r_s = 0.76$ for samples collected in summer 2016 and 2017; see City of San Diego 2018). These results are due to several exceptions to this overall pattern during the current reporting period, where percent fines were higher or lower than expected by depth. Exceptions were found at several inner and mid-shelf SBOO stations (i.e., stations I2, I3, I4, I6, I7, I13, I22, I33), regional station 8918 located southeast of the entrance to San Diego Bay at a depth of 8 m, regional station 9233 located off north Pacific Beach at a depth of 14 m, and regional station 9218 located on the eastern edge of the Coronado Bank at a depth of 292 m (Appendix H.4).

Cluster and ordination analyses of the sediment particle size data, described above, resulted in eight ecologically-relevant SIMPROF-supported clusters (groups A–H) (Figures 7.3, 7.4, Table 7.2). According to BEST/BVSTEP results ($\rho = 0.983$, $p = 0.001$, number of permutations = 999), these eight clusters were primarily distinguished by differing proportions of coarse sand (e.g., particle size groups A, B, C, D vs groups E, F, G, H), very fine sand (e.g., particle size groups B and D), and fine particles (e.g., particle size groups A and B). Additionally, these groups were distributed to some degree by depth strata, but more so by monitoring region. For example, cluster groups C, D, F, G and H primarily occurred at inner- and mid-shelf depths within the SBOO monitoring region. Cluster group B, however, primarily occurred at mid-shelf, outer shelf, and upper slope depths within the PLOO monitoring region. Sediments collected from station E14 in summer 2020, one of eight samples collected from PLOO near-ZID stations, had smaller proportions of fine particles than other surrounding mid-shelf stations (group D versus group B), while the eight samples collected from SBOO near-ZID stations I12, I14, I15, and I16 fell into four different clusters (groups B, C, D, H) that were characterized by varying proportions of fine particles and sand. The main characteristics and distribution of each of the eight particle size cluster groups are described below.

Particle size cluster group A comprised seven sediment samples that were collected at depths ranging from 27 to 491 m (Figures 7.3, 7.4). Four of these samples were from stations I2, I3, I7 and I33 located on the inner and mid-shelf within the SBOO region, while three samples were from regional stations 8927, 8934, 9223 located on the upper slope offshore of La Jolla and Point Loma at depths from 437 to 491 m. Sediments represented by this cluster group were distinguished from all others by having the largest proportion of fine particles (mean = 87.5% per sample), the second lowest proportion of fine sand (mean = 2.8% per sample), and the lowest proportion of medium sand (mean = 1.6% per sample and coarse sand (mean = 0.5% per sample), with no very coarse sand or granules present (Table 7.2).

Particle size cluster group B was the largest group, comprising 102 sediment samples from 81 stations widely distributed throughout the entire survey area at depths ranging from 8 to 523 m (Figures 7.3, 7.4). This group encompassed 77% (n = 75) of samples collected along the mid-shelf, including 95% (n = 42) of samples from PLOO near-ZID and farfield stations. Group B also encompassed 91% (n = 10) of samples collected along the outer shelf, 77% (n = 10) of samples collected on the upper slope, but just 12% (n = 7) of samples collected on the inner shelf. These sediments had the second largest proportion of fine particles (mean = 58.5% per sample) and very fine sand (mean = 26.5% per sample), and the second smallest proportion of medium sand (mean = 2.5% per sample) (Table 7.2). It also averaged 9.4% fine sand, 2.3% coarse sand, 0.7% very coarse sand, with no granules present.

Particle size cluster group C comprised four sediment samples that were collected at inner shelf depths ranging from 10 to 28 m (Figures 7.3, 7.4). Three of

Table 7.1

Summary of particle sizes and chemistry concentrations in sediments from San Diego regional (Reg) and core benthic stations sampled during summer 2020 and 2021. Data include detection rate (DR; %), minimum, maximum, and mean values for the entire survey area, as well as mean value by depth stratum. For chemistry parameters, minimum and maximum values were calculated using all samples, whereas means were calculated with detected values only; n = number of samples; nd = not detected.

					Depth Strata						
					Inner Shelf		Mid-Shelf			Outer Shelf	Upper Slope
	2020–2021 Survey Area				SBOO	Reg	PLOO	SBOO	Reg	Reg	Reg
Parameter	**DR**	**Min**	**Max**	**Mean**	**n=17**	**n=23**	**n=22**	**n=10**	**n=33**	**n=11**	**n=13**
Particle Size (%)											
Coarse particles	28	0	49.9	2.4	3	4.5	1.5	3.6	1.4	1	0.3
Med-coarse sands	99	0	94.5	14.5	25.9	17.8	3.4	41.7	7.4	3.9	2.5
Fine sands	99	0	89.2	39.4	44.8	56.8	39	19.2	37.8	34	23.4
Fine particles	97	0	100	43.7	26.3	20.9	56.1	35.5	53.5	61.1	73.8
Organic Indicators											
Sulfides (ppm)	66	nd	87.6	12.5	5.9	13	6	9	14.9	11.8	25.5
TN (% weight)	75	nd	0.27	0.062	0.026	0.03	0.052	0.039	0.056	0.077	0.171
TOC (% weight)	83	nd	4.37	0.83	0.37	0.53	0.77	0.33	0.69	1.13	2.52
TVS (% weight)	100	0.4	9.5	2.1	0.9	0.9	2.2	0.8	2.3	3.4	6.6
Trace Metals (ppm)											
Aluminum	100	597	15,700	5766	3655	3356	6546	2108	7001	9003	11,864
Antimony	89	nd	2.38	0.81	0.62	0.43	0.93	0.52	0.77	0.87	1.25
Arsenic	100	0.8	9.31	2.58	1.9	1.9	2.85	3.47	2.5	2.35	2.94
Barium	100	0.3	120	27.7	18.5	19.4	27.1	7.5	33.6	43.8	69.3
Beryllium	62	nd	0.426	0.136	0.076	0.053	0.176	0.06	0.15	0.186	0.347
Cadmium	38	nd	0.467	0.087	0.042	0.056	0.061	0.046	0.09	0.121	0.237
Chromium	100	2.3	41.9	13.6	8.3	7.6	15.1	8.3	15.5	19.7	30.6
Copper	85	nd	34.5	6.7	2.5	2.5	6.1	3.5	6.7	14.6	16.6
Iron	100	1030	24,300	8845	4829	4958	10,484	4942	10,695	13,678	17,377
Lead	100	0.7	72.7	3.3	1.5	1.5	3.3	1.9	3.8	11.2	5.3
Manganese	100	5	191	71	50	57	78	26	87	102	125
Mercury	78	nd	0.134	0.029	0.007	0.008	0.025	0.01	0.034	0.058	0.06
Nickel	99	nd	21.7	4.6	1.9	1.7	5.3	1.5	5.5	8.1	13.9
Selenium	7	nd	1.07	0.62	—	—	0.32	—	0.29	0.44	0.7
Silver	1	nd	0.102	0.087	—	—	0.072	—	—	—	0.102
Thallium	4	nd	0.223	0.177	—	0.153	—	—	0.199	0.211	0.173
Tin	87	nd	3.08	0.64	0.35	0.3	0.76	0.29	0.81	1.18	1.25
Zinc	100	1.6	79.2	21.8	11.5	12	25.4	7.7	26.1	39	47.9
Pesticides (ppt)											
Total DDT	67	nd	4072	690	129	106	469	952	685	897	2169
Total HCH	1	nd	61	61	87	—	—	—	61	—	—
Total Chlordane	4	nd	1058	325	48	49	122	174	94	544	1058
Hexachlorobenzene	3	nd	1940	585	276	182	238	—	—	1940	—
Total PCB (ppt)	37	nd	167,680	6165	260	3946	2161	718	1917	9447	14,686
Total PAH (ppb)	60	nd	736.9	61.9	12.9	19.6	56.9	18.3	63	152.6	122.5

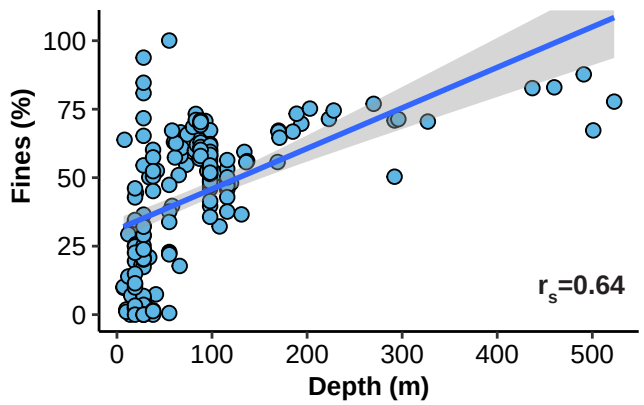

Figure 7.2
Scatterplot of concentrations of fine particles (Fines) versus depth for sediments collected from San Diego regional and core benthic stations during summer 2020 and 2021. Shaded area indicates 95% confidence interval.

these samples were collected from regional stations 8915, 9219, and 9244 located south of the entrance to San Diego Bay and offshore of Coronado Beach, while one sample was collected at SBOO near-ZID station I16 in 2020. Sediments represented by this cluster group had the largest proportion of fine sand (mean = 39.9% per sample) and the second largest proportion of medium sand (mean = 24.9% per sample) (Table 7.2). It also averaged 8.3% fine particles, 12.5% very fine sand, 10.6% coarse sand, 3.5% very coarse sand, and 0.4% granules.

Particle size cluster group D was the second largest group, comprising 39 sediment samples from 32 stations, also widely distributed off San Diego at depths from 7 to 98 m (Figures 7.3, 7.4). This group encompassed 58% (n = 33) of samples collected along the inner shelf and 37% (n = 20) of samples collected from SBOO stations. Group D sediments had the largest proportion of very fine sand (mean = 47.0% per sample) and the second highest proportion of fine sand (mean = 25.1%) (Table 7.2). They also averaged 23.1% fine particles, 4.1% medium sand, 0.7% coarse sand, 0.1% very coarse sand, with no granules present.

Particle size cluster group E comprised two sediment samples, one collected at regional station 9233 located on the inner shelf off north Pacific Beach at 14 m depth, and one collected at SBOO station I17 at 52 m depth (Figures 7.3, 7.4). Sediments represented by this cluster group had the largest proportion of coarse sand (mean = 83.3% per sample), the third largest proportion of very coarse sand (mean = 5.0% per sample), and the smallest proportions of fine particles (mean = 0.3% per sample), very fine sand (mean = 0% per sample) and fine sand (mean = 0.4% per sample) (Table 7.2). These sediments also averaged 11.0% medium sand, with no granules present.

Particle size cluster group F comprised seven sediment samples collected at depths ranging from 55 to 131 m (Figures 7.3, 7.4). Three of these samples were collected from SBOO stations I20 and I28 at a depth of 55 m, one sample was collected at regional station 8903 located southeast of the LA4 dumpsite at a depth of 66 m, one sample was collected from regional station 8940 located off Del Mar at a depth of 108 m, one sample was collected from PLOO station E9, and one sample was collected from regional station 9208 located southeast of the LA-5 dredge materials disposal site at a depth of 131 m. Group F sediments had the second largest proportion of very coarse sand (mean = 13.0% per sample) and granules (mean = 0.7% per sample), the third largest proportion of fine particles (mean = 31.1% per sample) and coarse sand (mean = 34.7% per sample), and the third smallest proportion of fine sand (mean = 4.6% per sample) (Table 7.2).

Particle size cluster group G comprised five sediment samples collected at inner shelf depths ranging from 10 to 29 m (Figures 7.3, 7.4). Two samples were collected from SBOO station I34, one sample from SBOO station I23 in summer 2021, one sample from regional station 9241 located south of the entrance to San Diego Bay, and one sample from regional station 9229 located off Mission Beach. Sediments represented by group G were distinguished from all other groups by having the largest proportion of very coarse sand (mean = 20.6% per sample) and granules (mean = 16.1% per sample), the third largest proportion of medium sand (mean = 22.0% per sample), and the third smallest proportion of fine particles (mean = 2.8% per sample) and very fine sand (mean = 2.1% per sample) (Table 7.2).

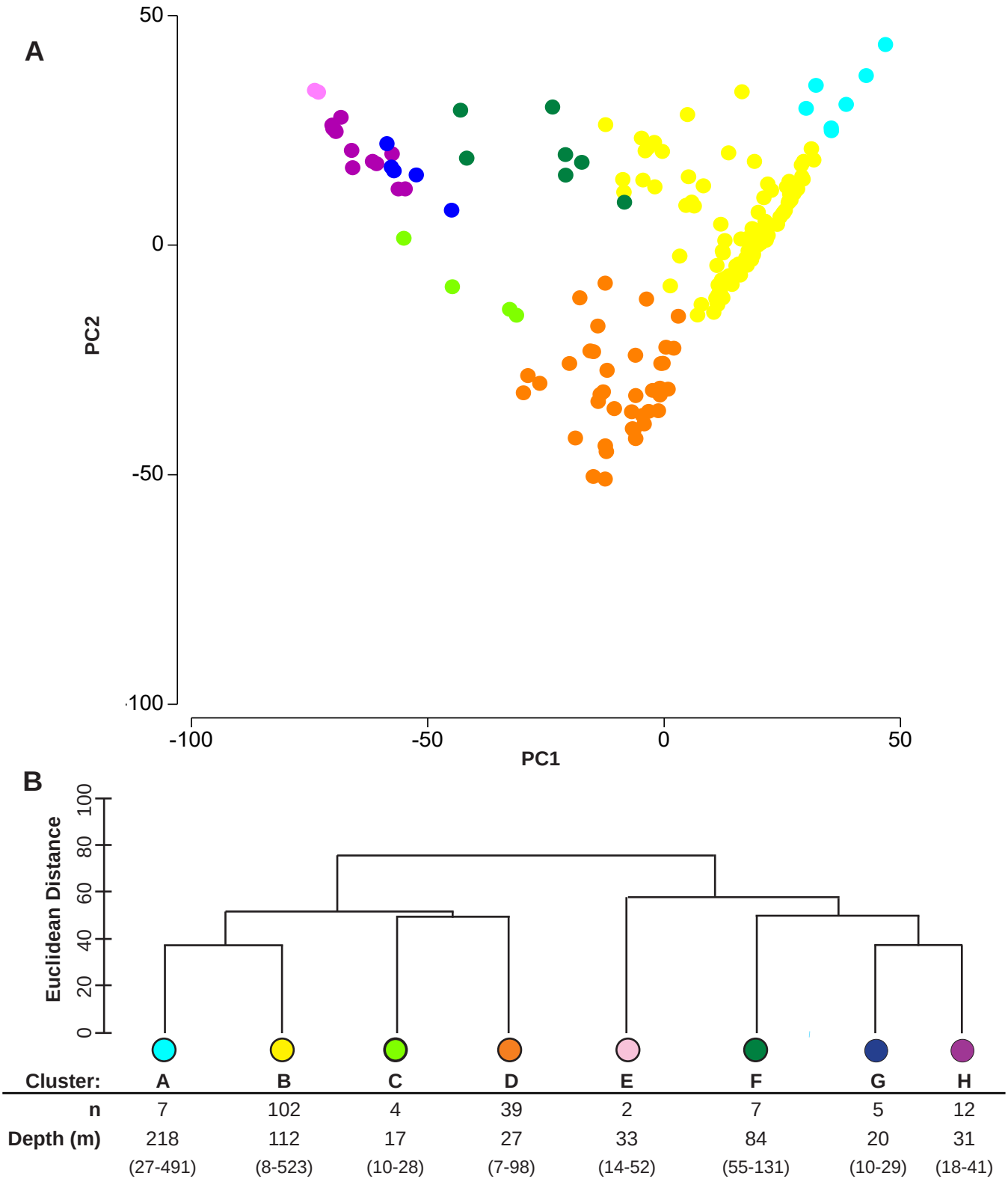

Figure 7.3

Results of ordination and cluster analysis of particle size sub-fraction data from San Diego regional and core benthic stations sampled during summer 2020 and 2021. Results are presented as (A) two-dimensional Principal Components (PC) Analysis ordination and (B) a dendrogram of main cluster groups. Depth presented as means (ranges) calculated over all stations within a cluster group (n).

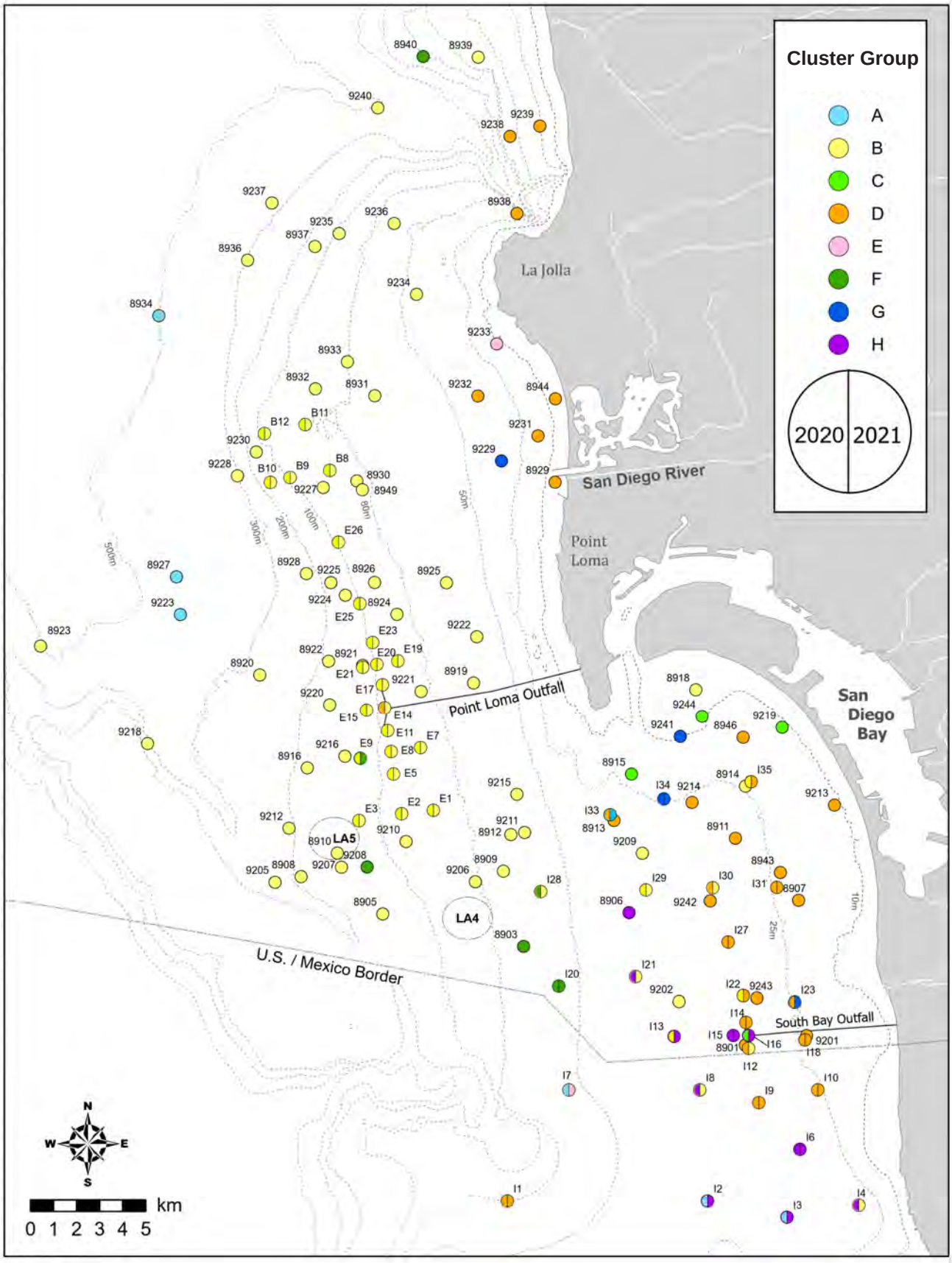

Figure 7.4
Spatial distribution of particle size cluster groups A–H defined in Figure 7.3.

Table 7.2

Particle size (%) summary for each particle size cluster group A–H (defined in Figure 7.3). Data are presented as means (ranges) calculated over all samples within a cluster group (n). VF = very fine; F = fine; M = medium; C = coarse; VC = very coarse.

	Particle Size Cluster Group							
	A	**B**	**C**	**D**	**E**	**F**	**G**	**H**
n	7	102	4	39	2	7	5	12
Depth (m)	218 (27-491)	112 (8-523)	17 (10-28)	27 (7-98)	33 (14-52)	84 (55-131)	20 (10-29)	31 (18-41)
Fines	87.5 (80.9-100.1)	58.5 (39.6-77.8)	8.3 (1.0-13.9)	23.1 (6.9-39.7)	0.3 (0-0.6)	31.1 (17.8-37.6)	2.8 (1.9-4.3)	2.5 (0-7.4)
VFSand	7.6 (0-14.1)	26.5 (3.7-42.5)	12.5 (4.7-17.9)	47 (16.9-68.8)	0 —	9.8 (2.6-18.3)	2.1 (0.3-7.0)	1.4 (0.2-4.3)
FSand	2.8 (0-6.1)	9.4 (3.3-17.5)	39.9 (32.6-46.0)	25.1 (12.8-44.8)	0.4 (0.3-0.4)	4.6 (2.4-8.0)	5.4 (0.6-9.0)	8.9 (2.6-17.7)
MSand	1.6 (0-6.2)	2.5 (0.1-32.2)	24.9 (15.0-33.7)	4.1 (0-16.3)	11.0 (9.0-13.1)	6.1 (0.3-12.1)	22.0 (13.2-31.1)	44.1 (28.2-57.2)
CSand	0.5 (0-3.2)	2.3 (0-20.0)	10.6 (2.8-22.7)	0.7 (0-8.9)	83.3 (81.4-85.2)	34.7 (14.4-52.6)	30.9 (20.4-43.9)	39.3 (21.1-59.4)
VCSand	0 —	0.7 (0-8.9)	3.5 (0-9.1)	0.1 (0-2.7)	5 (4.6-5.4)	13 (7.8-25.5)	20.6 (15.4-25.8)	3.8 (2.1-8.1)
Granules	0 —	0 (0-0.4)	0.4 (0-1.5)	0 —	0 —	0.7 (0-2.9)	16.1 (11.7-27.0)	0 —

Particle size cluster group H was the third largest group, comprising 12 sediment samples from 10 stations, all of which were located within the SBOO monitoring region at depths from 18 to 41 m (Figures 7.3, 7.4). This group included sediments from SBOO stations I2, I3, I4, I6, I8, I13, I15, I16, and I21, and regional station 8906 located to the north of station I21. These sediments had the largest proportion of medium sand (mean = 44.1% per sample), the second largest proportion of coarse sand (mean = 39.3% per sample), and the second smallest proportion of fine particles (mean = 2.5% per sample) and very fine sand (mean = 1.4% per sample) (Table 7.2). They also averaged 8.9% fine sand, 3.8% very coarse sand, with no granules present.

Sediment Chemistry

As with sediment particle size composition, regional patterns of sediment contamination during summer 2020 and 2021 were similar to patterns seen in previous years (e.g., City of San Diego 2018, 2020). There was no evidence of degraded sediment quality in the general San Diego region. While various indictors of organic loading, trace metals, chlorinated pesticides, PCBs, and PAHs were detected at variable concentrations in sediment samples collected throughout the region, almost all contaminants occurred at levels below both ERL and ERM thresholds, within tolerance intervals calculated for the PLOO region, and within historical ranges (Table 7.1; see also Chapter 5 and City of San Diego 2022a). Of the 178 samples collected during these surveys, only 12% (n = 22) had elevated concentrations of a parameter with available thresholds. Arsenic exceeded its ERL in a total of three samples, including two samples collected from SBOO farfield station I21 in summer 2020 and 2021, and one sample collected from PLOO farfield station B11 in summer 2021 (Appendix H.5). Copper exceeded its ERL in a single sediment sample collected from regional station 8910 located within the LA-5 dredge materials disposal site at a depth of 169 m. Lead exceeded its ERL in a single sample collected from regional station 8905 located south of the LA-5 disposal site at a depth of 134 m. Nickel exceeded its ERL in a single sample collected from regional station 8934 located on the upper slope

off Point La Jolla at a depth of 491 m. Total DDT exceeded its ERL in a total of 14 sediment samples, including one sample from PLOO farfield station E7 in summer 2021, one sample from SBOO farfield station I29 in summer 2020, two samples from regional stations located along the mid-shelf (stations 9202, 9206), one regional station located along the outer shelf (stations 8910) and nine samples from regional stations located along the upper slope (stations 8920, 8923, 8927, 8934, 8936, 9212, 9223, 9237).

As in previous surveys (e.g., City of San Diego 2018, 2020), several parameters had increasing concentrations across depth strata, mimicking the pattern described above for percent fines (Table 7.1). For example, total nitrogen at regional stations averaged 0.030% wt per sample along the inner shelf, 0.056% wt along the mid-shelf, 0.077% wt along the outer shelf, and 0.171% wt along the upper slope. Additionally, total volatile solids, aluminum, beryllium, chromium, copper, iron, lead, nickel, and zinc had a significant, positive correlation ($r^s > 0.70$) with depth (Appendix H.3, select examples Appendix H.5).

Cluster and ordination analyses of the sediment chemistry data, described above, resulted in six ecologically-relevant SIMPROF-supported clusters (groups A–F) (Figures 7.5, 7.6). According to BEST/BVSTEP results 0.953, $p = 0.001$, number of permutations = 999), these six cluster groups were primarily distinguished by 13 specific indicators: arsenic, barium, beryllium, chromium, copper, lead, nickel, silver, thallium, total organic carbon, total volatile solids, and total PAH (Appendix H.6). According to RELATE results ($\rho = 0.166$, $p = 0.001$, number of permutations = 999), overall patterns in combined sediment chemistry concentrations were only very weakly linked to sediment particle size composition. Fine particles were most highly correlated to the distribution of sediment chemistry parameters (BEST/BIOENV, $\rho = 0.289$, $p = 0.001$, number of permutations = 999). This weak association is due to the combination of parameters that tend to co-vary with percent fines (e.g., total nitrogen, aluminum, mercury, nickel), and those that do not, such as sulfides, total organic carbon, arsenic, and total PCB (Appendices H.2, H.3, H.4). The distribution and main characteristics of each cluster group are described below.

Sediment chemistry group E included 90% (n = 161) of the samples analyzed during summer 2020 and 2021 (Figures 7.5, 7.6). These samples were collected from a wide range of inner to upper slope stations that spanned the entire San Diego region at depths ranging from 7 to 327 m. Included in this group were all 16 samples collected from the near-ZID PLOO and SBOO sites, as well as one other near-ZID regional station. Sediments represented by this group averaged just 40.8% fine particles, and characteristic parameters tended to be found in lower concentrations relative to the other sediment cluster groups (Appendix H.6). According to SIMPER results, 19 analytes accounted for 53% of the within-group similarity for group E, including (in order of increasing contribution): total HCH (not detected), selenium (mean = 0.29 ppm), total chlordane (mean = 111 ppt), lead (mean = 2.64 ppm), total PCB (mean = 4158 ppt), TVS (mean = 1.7% wt), TN (mean = 0.05% wt), silver (mean = 0.070 ppm), cadmium (mean = 0.070 ppm), nickel(mean = 3.7 ppm), total DDT (mean = 489 ppt), copper (mean = 5.3 ppm), chromium (mean = 12.0 ppm), barium (mean = 23.9 ppm), mercury (mean = 0.020 ppm), TOC (mean = 0.65% wt), zinc (mean = 19.0 ppm), total PAH (mean = 48.1 ppb), and tin (mean = 0.57 ppm). It is likely that this cluster group represents background conditions for continental shelf habitats in the San Diego region.

Sediment chemistry group F comprised 13 sediment samples collected at outer shelf and upper slope depths ranging from 189 to 523 m (Figures 7.5, 7.6). This group of stations had the second largest proportion of percent fines (mean = 73.6% per sample) (Appendix H.6). According to SIMPER, sediments represented by group F were distinguished from group E by higher concentrations of selenium (mean = 0.66 ppm), TVS (mean = 6.6% wt), TN (mean = 0.170% wt), nickel (mean = 14.1 ppm), cadmium (mean = 0.240 ppm), total DDT (mean = 2021 ppt), chromium (mean = 30.2 ppm), barium (mean = 68.3 ppm), TOC (mean = 2.55% wt), zinc (mean = 49.5 ppm), copper (mean = 16.0 ppm), and sulfides (mean = 23.0 ppm). Several of these parameters had a significant, positive correlation ($r^s > 0.70$) with percent fines and/or depth (Appendix H.3)

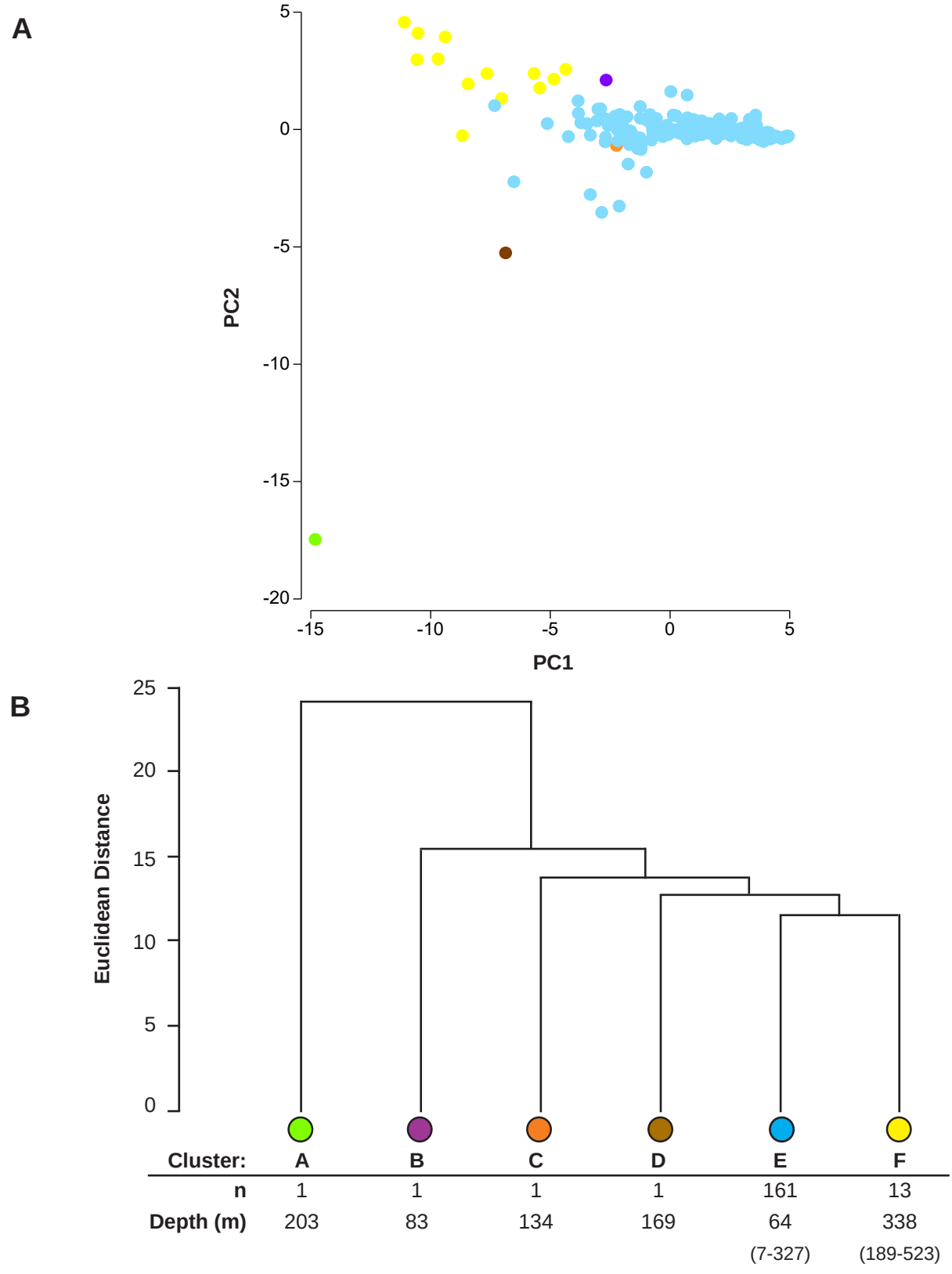

Figure 7.5

Results of ordination and cluster analysis of sediment chemistry data from San Diego regional and core benthic stations sampled during summer 2020 and 2021. Results are presented as (A) two-dimensional Principal Components Analysis ordination and (B) a dendrogram of main cluster groups. Depth presented as means (ranges) calculated over all stations within a cluster group (n).

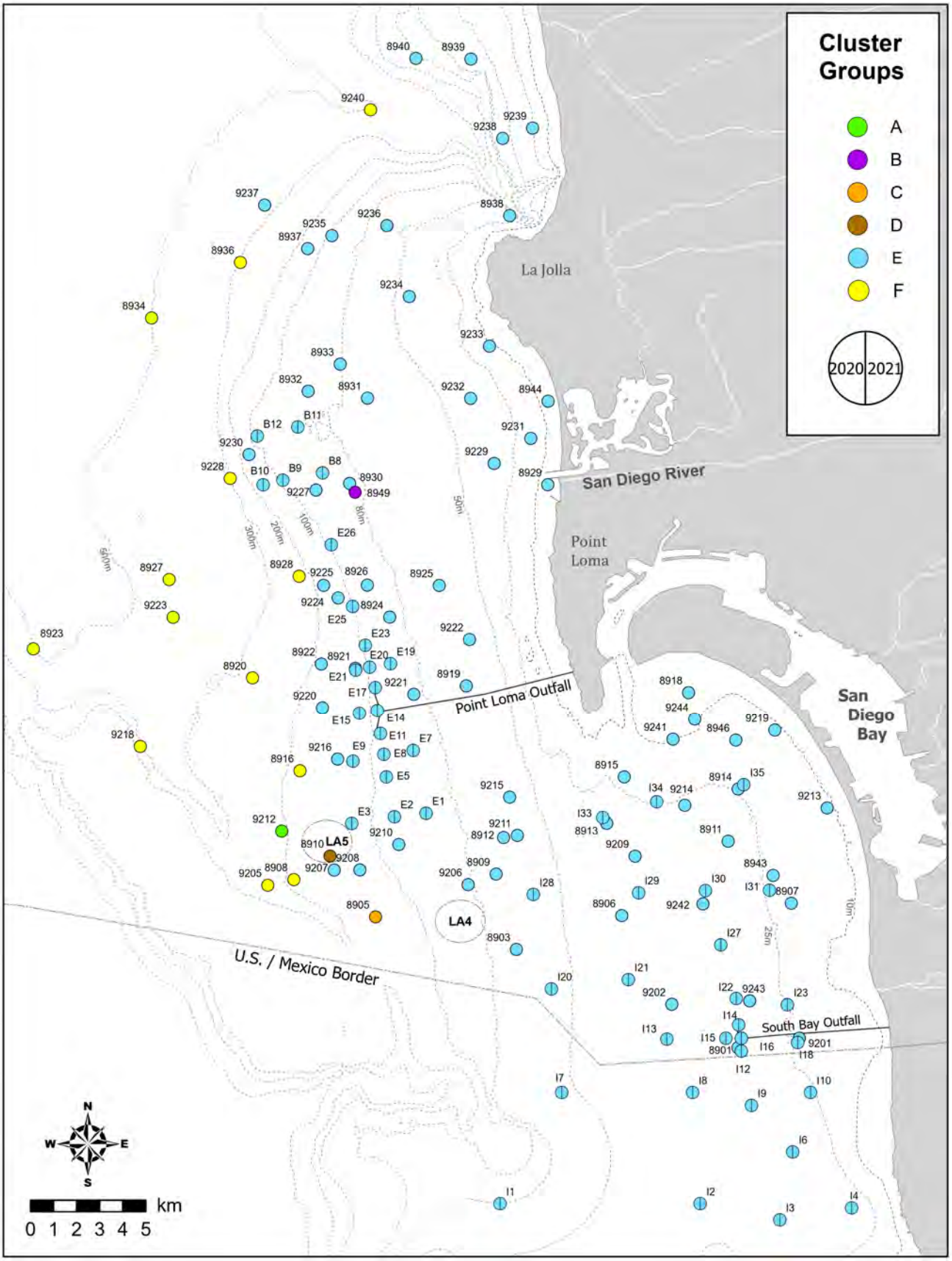

Figure 7.6
Spatial distribution of sediment chemistry cluster groups A–F defined in Figure 7.5.

Sediment chemistry cluster groups A–D represented unique "outlier" groups with one sample each that differed from group E, primarily due to very high values of just a few select contaminants (Figures 7.5, 7.6, Appendix H.6). For example, sediments from regional station 9212 (sediment chemistry group A), located on the west side of the LA-5 dredge materials disposal site at 203 m depth on the upper slope, were distinguished by the highest concentrations of total PCB (167,680 ppt), silver (0.102 ppm), total PAH (736.9 ppb), and tin (3.08 ppm). In contrast, sediments from regional station 8949 (sediment chemistry group B), located directly offshore of the mouth of the San Diego River at a depth of 83 m, were distinguished by the highest (only detected) concentration of total HCH (61 ppt). Sediments from regional station 8905 (sediment chemistry group C), located southeast of the LA-5 disposal site at 134 m depth, was distinguished by the highest concentration of lead (72.7 ppm). Sediments from regional station 8910 (sediment chemistry group D), located at 169 m on the outer shelf within the LA-5 disposal site, were distinguished by the highest concentrations of copper (34.5 ppm) and mercury (0.081 ppm), and the second highest concentration of total chlordane (918 ppt) and total PAH (290.0 ppb).

Sediment Toxicity

During summer 2020, sediments were collected and tested for toxicity at eight regional stations that ranged in depth from 19 to 270 m (Figure 7.1). During summer 2021, sediments were collected for toxicity testing from the four near-ZID PLOO stations (depth = 98 m) and the four near-ZID SBOO stations (depth = 28 m). Mean survival rates for the regional stations ranged from 92 to 99%, while mean survival rates for PLOO near-ZID stations ranged from 89 to 98%, and mean survival rates for SBOO near-ZID stations ranged from 97 to 99% (Appendix H.7). The lowest mean survival rates (≤95%) occurred on the outer shelf at regional stations 8910 and 8908, and at PLOO near-ZID stations E14 and E17. Station 8910 corresponded to sediment chemistry cluster group D, while the remaining sites landed in the cluster group indicative of background conditions (group E; see previous section).

Regional Macrobenthic Communities

A total of 51,869 macrobenthic invertebrates were identified from the 178 grabs collected during summer 2020 and 2021 surveys at depths ranging from 7 to 523 m off San Diego. Of the 955 taxa recorded, 80% (n = 762) were identified to the level of species, while the rest could only be identified to higher taxonomic levels. Macrofaunal community structure varied across both the continental shelf and slope: with species richness ranging from 16 to 188 taxa per grab; macrofaunal abundance ranging from 25 to 1180 individuals per grab; Shannon Diversity Index (H') ranging from 0.3 to 4.4 per grab; Pielou's Evenness Index (J') ranging from 0.12 to 0.96 per grab; and Swartz Dominance Index ranging from 1 to 55 per grab (Table 7.3). Reported values for each parameter, and the variation observed between strata, generally correspond to findings reported previously for the San Diego region (e.g., City of San Diego 2018, 2020). For example, species richness and abundance values were lowest at upper slope stations. As has also been reported previously, BRI values off San Diego have generally been indicative of reference, or non-impacted, conditions (BRI < 25) (Smith et al. 2001). This remained true for the 2020 and 2021 summer surveys with 94% of samples (n = 153), collected from BRI-validated depths, having BRI values indicative of reference condition (Appendix H.8). A total of nine samples (~6%) had slightly elevated BRI values between 25–34, which may indicate a minor deviation from reference condition; these samples were collected at near-ZID PLOO station E14, SBOO farfield stations I35, and regional stations 8914, 8938, 8946, 9219, 9220, and 9225. None of the stations sampled in summer 2020 and 2021 had BRI values >34, which would indicate increasing levels of disturbance or environmental degradation.

Cluster and ordination analyses of the macrofaunal data, described above, resulted in 13 ecologically-relevant SIMPROF-supported cluster groups (groups A–M) (Figures 7.7, 7.8). These macrofauna cluster groups included from 1 to 84 grabs. The composition of each cluster group varied in terms of the specific taxa present and their relative abundance,

Table 7.3

Macrofaunal community summary statistics calculated for San Diego regional and core benthic stations sampled during summer 2020 and 2021. Data are presented as means (ranges) by stratum; n = number of grabs; SR = species richness; Abun = abundance; H' = Shannon diversity index; J' = Pielou's evenness; Dom = Swartz dominance; BRI = benthic response index.

Stratum		n	SR	Abun	H'	J'	Dom	BRI[a]
Inner Shelf								
	SBOO	34	62 (29-99)	249 (63-913)	3.4 (2.6-4.2)	0.84 (0.67-0.93)	22 (8-41)	18 (5-27)
	Regional	23	46 (16-113)	196 (25-645)	3.0 (0.3-4.0)	0.79 (0.12-0.96)	17 (1-37)	19 (2-31)
	All Inner Shelf	57	56 (16-113)	227 (25-913)	3.2 (0.3-4.2)	0.82 (0.12-0.96)	20 (1-41)	18 (2-31)
Middle Shelf								
	PLOO	44	89 (60-122)	398 (215-636)	3.7 (2.9-4.3)	0.83 (0.70-0.91)	28 (11-49)	13 (7-31)
	SBOO	20	70 (39-135)	241 (120-434)	3.4 (2.6-4.4)	0.81 (0.63-0.92)	24 (8-55)	13 (4-24)
	Regional	33	89 (53-188)	375 (122-1180)	3.7 (2.8-4.3)	0.82 (0.68-0.92)	27 (10-46)	14 (8-25)
	All Middle Shelf	97	85 (39-188)	358 (120-1180)	3.6 (2.6-4.4)	0.83 (0.63-0.92)	27 (8-55)	13 (4-31)
Outer Shelf								
	Regional	11	56 (33-84)	256 (172-348)	3.1 (2.3-3.8)	0.77 (0.65-0.86)	15 (5-28)	19 (11-27)
Upper Slope								
	Regional	13	34 (17-53)	108 (39-304)	2.8 (2.0-3.3)	0.81 (0.52-0.94)	12 (5-22)	—
	All Stations	178	70 (16-188)	291 (25-1180)	3.4 (0.3-4.4)	0.82 (0.12-0.96)	23 (1-55)	15 (2-31)

[a]BRI statistic not calculated for stations located at depths < 10 m or > 200 m

as well as depth and sediment composition. For example, the macrofaunal assemblages represented by cluster groups B, C, D, E, G, H, and I occurred along the inner and mid-shelf at depths of 8–55 m, with all but six samples located within the SBOO monitoring region. Macrofaunal assemblages associated with cluster group K, the largest group (n = 84), spanned a significant portion of the middle and outer shelf off San Diego. Assemblages associated with cluster groups A, J, L, and M represented a total of 20 samples that occurred along the outer shelf and upper slope at depths of 169–523 m.

Similar patterns of variation occurred in the macrofaunal and sediment similarity/dissimilarity matrices used to generate cluster dendrograms (RELATE $\rho = 0.593$, $p = 0.001$, number of permutations = 999). The sediment sub-fractions that were most highly correlated with the macrofaunal communities included coarse sand, granules, medium sand, and fine particles (BEST/BIOENV $\rho = 0.596$, $p = 0.001$, number of permutations = 999). Of these sub-fractions, fine particles accounted for most of the variation (corr. = 0.521). According to BEST/BVSTEP ($\rho = 0.95$, $p = 0.001$, number of permutations = 999), a total of 29 species best described the overall pattern (gradient) of the cluster dendrogram, including the polychaetes *Praxillella pacifica,* Euclymeninae sp A, *Spiophanes duplex, Spiophanes kimballi, Spiophanes norrisi, Phyllodoce hartmanae, Prionospio jubata, Prionospio dubia, Prionospio pygmaeus, Pectinaria californiensis, Paradiopatra parva, Mediomastus* sp*, Goniada maculata, Kirkegaardia siblina, Phyllochaetopterus*

A

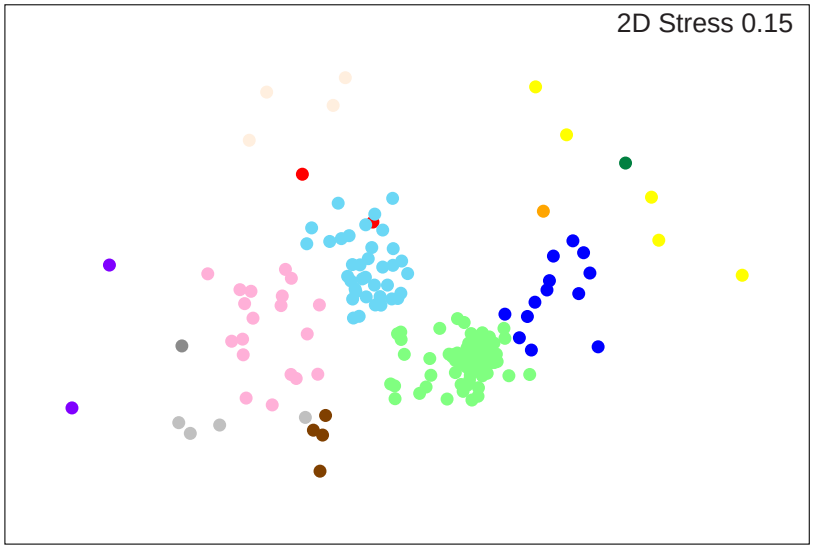

B

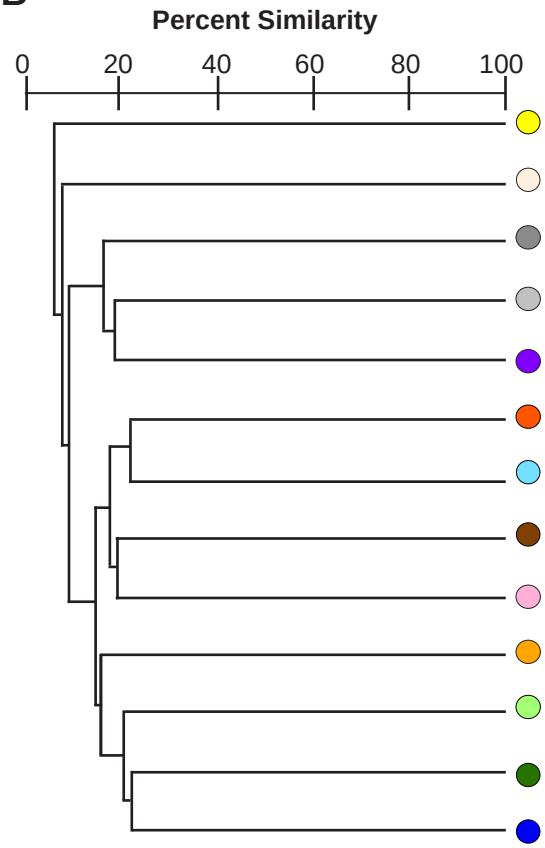

Cluster Group	n	Depth Range (m)	Community Metric	
			SR	Abun
A	5	437-523	28	71
B	4	8-12	18	185
C	1	18	32	63
D	4	19-29	70	684
E	2	10-14	25	238
F	2	7-7	36	178
G	38	15-34	66	200
H	4	52-55	64	242
I	19	18-41	47	178
J	1	292	42	84
K	84	34-137	90	385
L	1	270	20	69
M	13	169-327	45	206

Figure 7.7

Results of ordination and cluster analysis of macrofauna data from San Diego regional and core benthic stations sampled during summer 2020 and 2021. Results are presented as (A) nMDS ordination and (B) a dendrogram of main cluster groups. Data are mean values over all stations in each group (n); SR = species richness; Abun = abundance. Cluster groups are named in order of increasing depth.

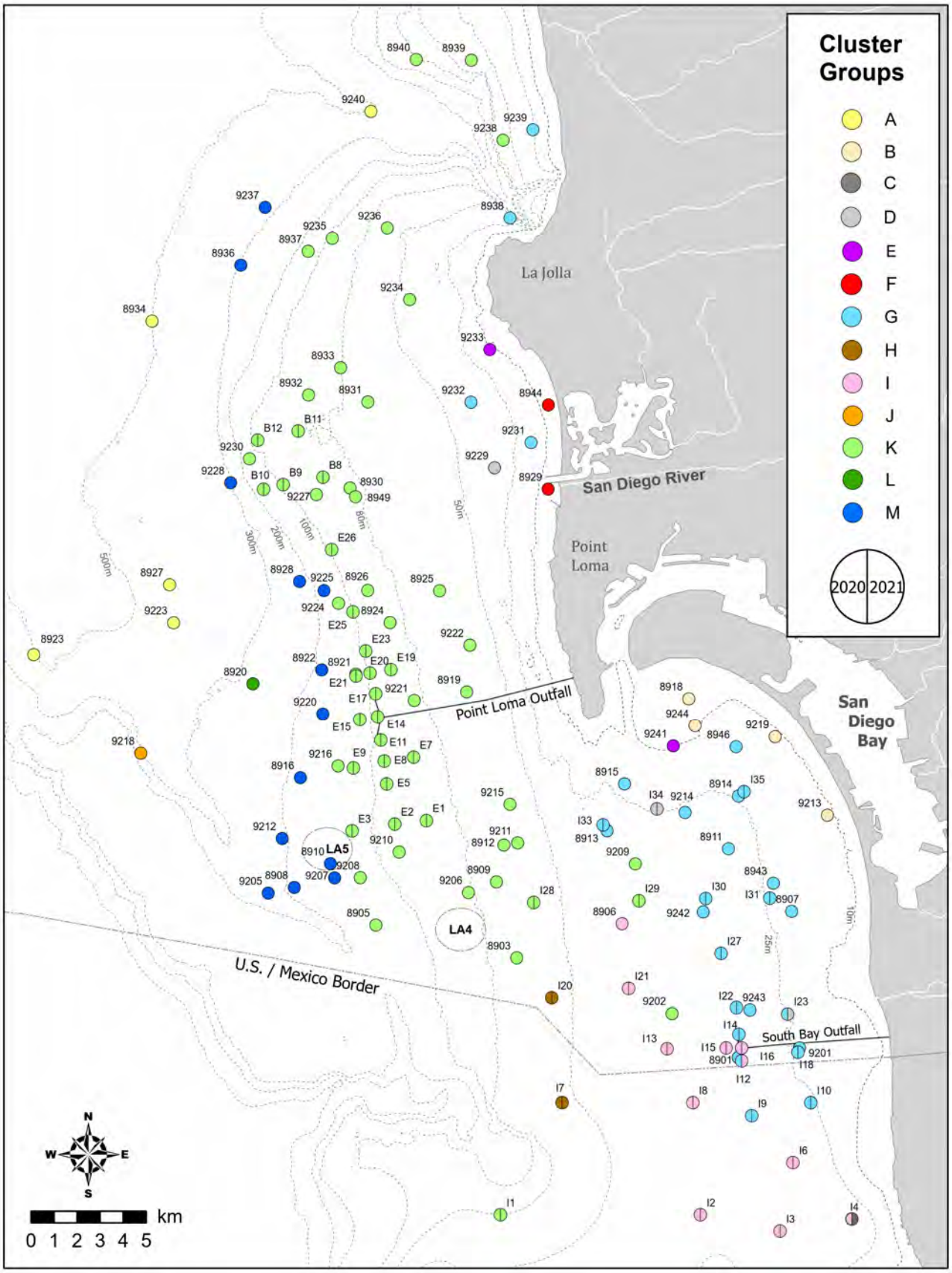

Figure 7.8
Spatial distribution of macrofaunal cluster groups A–M defined in Figure 7.7.

limicolus, Petaloclymene pacifica, and *Hesionura coineaui difficilis,* the amphipods *Ampelisca brevisimulata, Ampelisca careyi, Ampelisca cristata cristata, Ampelisca pugetica,* and *Rhepoxynius menziesi,* the tanaid *Chondrochelia dubia* Cmplx, ophiuroids in the family Amphiuridae, the sand dollar *Dendraster terminalis,* the bivalves *Nuculana* sp A and *Tellina* sp B, the scaphapod *Gadila aberrans,* and the nemertean *Tubulanus polymorphus*. The main characteristics and distribution of each cluster group are described below.

Macrofauna cluster groups B–F represented small groups (1–4 grabs per cluster) of assemblages found on the inner shelf during summer 2020 and 2021, each associated with varying sediment composition (Figures 7.7, 7.8). For example, Group D comprised four grabs collected at depths from 19 to 29 m from SBOO farfield stations I23 (summer 2021) and I34 (summer 2020 and 2021), and from regional station 9229 located offshore of Mission Beach. Compared to all other cluster groups, sediments from group D sites had the largest proportions of very coarse sand (mean = 21.9% per grab) and granules (mean = 16.7% per grab), relatively large proportions of medium sand (mean = 20.7% per grab) and coarse sand (mean = 30.2% per grab), along with very small proportions of fine particles (mean = 3.1% per grab) (Appendix H.9). According to SIMPER, group D assemblages were characterized by relatively high numbers of Nematoda (mean = 54 per grab), and the polychaetes *Protodovillea gracilis* (mean = 76 per grab), *Pisione* sp (mean = 54 per grab), and *Lumbrineris latrelli* (mean = 28 per grab) (Appendix H.10). The polychaete *Hesionura coineaui difficilis* was also characteristic of this group (mean = 57 per grab). Group E comprised two regional sites (9233, 9241) that also had sediments with very small amounts of fine particles (mean = 1% per grab), but had the largest proportion of coarse sand (mean = 59.5% per grab), with slightly less medium sand (mean = 18.2% per grab), very coarse sand (mean = 10.4% per grab), and granules (mean = 16.7% per grab). Group E assemblages were characterized by the second highest numbers of Nematoda (mean = 20 per grab) and the polychaete *Pisione* sp (mean = 14 per grab), along with the highest number of the nemertean *Cephalothrix* sp (mean = 5 per grab). Regional station 9233 was located just south of Point La Jolla at a depth of 14 m, while regional station 9241 was located south of the entrance to San Diego Bay at a depth of 10 m. Group F comprised two regional stations, each located at a depth of 7 m; station 8929 was located just south of the entrance to San Diego River and station 8944 was located off north Pacific Beach. Sediments from these sites were primarily sand (mean = 34.1% very fine sand, 39.2% fine sand, 11.7% medium sand per grab), with slightly more fine particles (mean = 10% per grab) and much less coarse sand (mean = 3.6% per grab) and very coarse sand (mean = 1.3% per grab) than groups D and E, with no granules present. Assemblages represented by group F were characterized by the highest numbers of the nemertean *Carinoma mutabilis* (mean = 8 per grab) and the snail *Callianax baetica* (mean = 16 per grab), and the second highest number of the polychaete *Spiophanes duplex* (mean = 26 grab). Group B included a total of four grabs collected from regional stations 8918, 9213, 9219, and 9244 located along the Coronado "Silver Strand" beach at depths ranging from 8 to 12 m. Sediments from these four sites were similar to those associated with group F, but with more fine particles (mean = 27.0% per grab), slightly more medium sand (mean = 15.9% per grab), and less very fine sand (mean = 21.1% per grab) and fine sand (mean = 26.5%). Group B assemblages were characterized by the highest numbers of the polychaetes *Prionospio pygmaeus* (mean = 154 per grab) and *Goniada littorea* (mean = 3 grab). Finally, group C represented a unique assemblage present at SBOO farfield station I4 sampled in summer 2021 that had sediments with a mix of fine particles (46%) and medium sand (32.2%), and the highest numbers of the sand dollar *Dendraster terminalis* (n = 9), the ascidian *Cnemidocarpa rhisopus* (n = 6), the polychaetes *Scoloplos acemeceps* (n = 4) and *Ophelia pulchella* (n = 2), the amphipod *Rhepoxynius lucubrans* (n = 3), the cumacean *Mesolamprops bispinosus* (n = 2), Oligochaeta (n = 2), and the bivalve *Simomactra falcata* (n = 2) relative to all other clusters.

Macrofauna cluster groups G (n=38) and I (n=19) were the second and third largest groups, together accounting for 77% of all grabs collected on the inner shelf during summer 2020 and 2021, and for 74% (n=40) of the grabs collected from SBOO stations during these two surveys (Figures 7.7, 7.8). Group G comprised grabs from SBOO near-ZID stations I12 and I14, SBOO farfield stations I9, I10, I18, I22, I23, I27, I30, I31, I33, and I35, and 16 regional stations primarily interspersed within the SBOO region at depths from 15 to 34 m. Sediments from these grabs had the largest proportions of very fine sand (mean=44.6% per grab), relatively small proportions of fine particles (mean=27.7% per grab), fine sand (mean=22.3% per grab), medium sand (mean=4.1% per grab), coarse sand (mean=1.1% per grab), and only trace amounts (<1% per grab) of very coarse sand and granules (Appendix H.9). Assemblages represented by group G were characterized by the highest numbers of the polychaete *Sigalion spinosus* (mean=6 per grab) and the scaphopod *Gadila aberrans* (mean=6 per grab), along with relatively high numbers of the polychaetes *Spiophanes duplex* (mean=18 per grab), *S. norrisi* (mean=11 per grab), and *Mediomastus* sp (mean=13 per grab) (Appendix H.10). Group I comprised grabs from SBOO near-ZID stations I12, I16, I15, SBOO farfield stations I2, I3, I4, I6, I8, I13, and I21, and regional station 8906. Whereas group G stations were located surrounding, to the north, and inshore of the terminus of the SBOO, group I stations were located surrounding, to the south, and offshore of the terminus of the SBOO. Additionally, and in contrast to group G, sediments from these sites had relatively small proportions of very fine sand (mean=3.8% per grab) and large amounts of medium sand (mean=32.6% per grab), coarse sand (mean=28.1% per grab) and very coarse sand (mean=2.8% per grab). Assemblages represented by group I were characterized by the highest numbers of *Spiophanes norrisi* (mean=38 per grab), the amphipods *Rhepoxynius heterocuspidatus* (mean=8 per grab) and *Ampelisca cristata cristata* (mean=4 per grab), the second highest number of *Dendraster terminalis* (mean=7 per grab), and relatively high numbers of the polychaete *Spiochaetopterus costarum* Cmplx (mean=4 per grab).

Macrofauna cluster group H represented assemblages from four grabs collected from two SBOO farfield stations (stations I7, I20) located on the mid-shelf at depths of 52 and 55 m (Figures 7.7, 7.8). Sediments from these four grabs varied in terms of particle size, with proportions of fine particles ranging from <1 to 100% (Appendix H.9). According to SIMPER, Group H assemblages were characterized by the highest numbers of the polychaetes *Jasmineira* sp B (mean=72 per grab), and *Mooreonuphis* sp SD1 (mean=15 per grab), and the amphipod *Byblis millsi* (mean=4 per grab) (Appendix H.10). *Spiophanes norrisi* (mean=3 per grab) and *Polycirrus* sp A (mean =3 per grab) were also characteristic of this group.

Macrofauna cluster group K was the largest group (n = 84), representing assemblages from 82% of all grabs collected on the mid-shelf during summer 2020 and 2021, including 100% of grabs from PLOO near-ZID and farfield stations (Figures 7.7, 7.8). Overall, depths of group K sites ranged from 34 to 137 m. Sediments associated with this cluster group were largely a mix of fine particles (mean=53.9% per grab), very fine sand (mean=28.5% per grab) and fine sand (mean=10.5% per grab), with relatively small amounts of medium sand (mean=1.9% per grab), coarse sand (mean=3.5% per grab), very coarse sand (mean=1.6% per grab), with trace amounts (<1% per grab) granules (Appendix H.9). Group K averaged 90 taxa and 385 individuals per grab. The five most characteristic taxa for cluster group K were *Spiophanes duplex* (mean=39 per grab), *Mediomastus* sp (mean=16 per grab), *Amphiodia urtica* (mean=20 per grab), *Paradiopatra parva* (mean=13 per grab), and *Prionospio jubata* (mean=8 per grab) (Appendix H.10). These were the highest numbers of these species found across all cluster groups.

Macrofauna cluster group M represented deep water assemblages sampled from 13 sites located on the outer shelf and upper slope at depths between 169 and 327 m west of Point La Jolla (regional stations 8936, 9237), the San Diego River (regional station 9228), and Point Loma (regional stations 8916, 8922, 8928, 9220, 9225), and within or west of the boundaries of the LA-5 dredge

materials disposal site (8910, 8908, 9205, 9207, 9212) (Figures 7.7, 7.8). As with group K, group M sediments were also largely a mix of fine particles and fine sand, but with slightly more fine particles (mean = 69.1% per grab), slightly less very fine sand (mean = 23.1% per grab) and fine sand (mean = 7.0% per grab), only trace (<1% per grab) amounts of medium sand, and no coarse sand, very coarse sand, or granules present (Appendix H.9). Assemblages associated with this group averaged 45 taxa and 206 individuals per grab, and were characterized by the polychaetes *Phyllochaetopterus limicolus* (mean = 39 per grab), *Mediomastus* sp (mean = 14 per grab), *Paraprionospio alata* (mean = 11 per grab), *Spiophanes kimballi* (mean = 12 per grab), and the bivalve *Axinopsida serricata* (mean = 22 per grab) (Appendix H.10). These were the highest numbers of *P. limicolus* and *A. serricata* found across all cluster groups.

Macrofauna cluster groups A, J and L represented small groups (1–5 grabs per cluster) of assemblages found on the upper slope during summer 2020 and 2021 (Figures 7.7, 7.8). Group L represented a unique assemblage present at regional station 8920 located northwest of the PLOO at a depth of 270 m. Sediments from this site also had high proportions of fine particles (n = 77%) (Appendix H.9), but characteristic (abundant) species included fewer *Prionnospio ehlersi* (n = 3) than group A assemblages, along with the highest numbers of the polychaetes *Paraprionospio alata* (n = 33) and *Cossura* sp A (n = 2) and the scaphopod *Compressidens stearnsii* (n = 2), compared to all other groups (Appendix H.10). Group J represented a unique assemblage present at regional station 9218 located on the inner edge of the Coronado Bank at a depth of 292 m. In contrast to groups A and L, sediments from this site had moderate amounts of fine particles (50%), and abundant species included the polychaetes *Phyllochaetopterus limicolus* (n = 13) and *Mediomastus* sp (n = 10). This assemblage also had the highest numbers of the polychaetes *Fauveliopsis* sp SD1 (n = 8), *Ampharete acutifrons* (n = 5), *Aricidea (Aricidea) wassi* (n = 2), *Drilonereis falcata* (n = 2), and *Decamastus gracilis* (n = 2), the solitary bryozoan *Ascorhiza occidentalis* (n = 2), as well as the ohiuroid *Amphiodia digitata* (n = 5). Group A represented the deepest assemblages sampled during summer 2020 and 2021. This group included a total of five grabs collected from regional stations 8923, 8927, 8934, 9223, and 9240 at depths ranging from 437 to 523 m. Sediments from these sites had the largest proportion of fine particles (mean = 79.7% per grab) compared to all other groups. According to SIMPER, the five most characteristic species for cluster group A were the polychaetes *Prionospio ehlersi* (mean = 7 per grab), *Bipalponephtys cornuta* (mean = 4 per grab), and *Eclysppe trilobata* (mean = 3 per grab), the bivalve *Yoldiella nana* (mean = 5 per grab), and the scaphopod *Rhabdus rectius* (mean = 1 per grab) (Appendix H.10). Relative to other groups, these were the highest numbers of *P. ehlersi*, *Y. nana*, and *B. cornuta.*

Integrated Benthic Conditions Assessment

Overall, benthic community conditions were excellent off San Diego during summer 2020 and 2021. Sediment toxicity was absent (percent control = 90-100%, condition ≥90% = non-toxic) at each of the 16 samples tested (Table 7.4). Fifteen of these samples (94%) had combined sediment chemistry concentrations indicative of minimal exposure. The only exception occurred at station 8916, which had concentrations indicative of low exposure. This station was located offshore of the PLOO and north of the LA-5 disposal site at a depth of 189 m. Of the limited parameters included in the SQO calculations, sediments from station 8916 had the fifth highest concentration of copper (19.6 ppm), the fourth highest concentration of lead (7.56 ppm), second highest concentration of mercury (0.107 ppm), the highest concentration of zinc (79.2 ppm), the fifth highest concentration of total PAH (251.6 ppb), and the seventh highest concentration of total PCB (5777 ppt), of all sediments sampled during summer 2020 and 2021. However, none of the available ERLs were exceeded at this site.

BRI scores were available for 15 of the 16 sediment toxicity stations, with values ranging from 8.71 to 29.86 (Table 7.4). Thirteen stations had scores indicative of reference stations (i.e., < 25). The two stations with scores indicating possible minor

Table 7.4

Results for the benthic response index (BRI), sediment toxicity, and sediment quality objective (SQO) lines of evidence for San Diego regional and core benthic stations sampled during summer 2020 and 2021 at which sediment toxicity testing was conducted. Cond = condition; TR = test result; TC = test control; %C = percent control; LRM = logistic regression model; CSI = chemical score index; Ref = reference; MD = minor deviation from reference conditions; NT = non-toxic; ME = minimal exposure; LE = low exposure; NA = not available (see text).

		Depth	Fines	BRI		Sediment Toxicity				SQOs			Site
Survey	Station	(m)	(%)	Value	Cond	TR	TC	%C	Cond	LRM	CSI	Cond	Condition
2020	8906	41	13.6	16.26	Ref	96	95	101	NT	0.05	1.00	ME	Unimpacted
	8908	194	51.1	16.67	Ref	92	95	97	NT	0.23	1.06	ME	Unimpacted
	8910	169	51.7	22.31	Ref	93	95	98	NT	0.29	1.03	ME	Unimpacted
	8916	189	53.3	24.71	Ref	96	95	101	NT	0.37	1.11	LE	Unimpacted
	8920	270	55.9	NA	NA	97	95	102	NT	0.26	1.06	ME	(Incomplete)
	8930	83	55.1	8.71	Ref	98	95	103	NT	0.21	1.06	ME	Unimpacted
	8938	28	54.2	26.90	MD	99	95	104	NT	0.06	1.00	ME	Unimpacted
	8943	19	37.0	20.28	Ref	98	95	103	NT	0.05	1.00	ME	Unimpacted
2021	E11	98	47.1	16.12	Ref	98	99	99	NT	0.11	1.00	ME	Unimpacted
	E14	98	51.1	29.86	MD	95	99	96	NT	0.10	1.00	ME	Unimpacted
	E15	98	48.7	15.66	Ref	98	99	99	NT	0.12	1.00	ME	Unimpacted
	E17	98	48.5	13.13	Ref	89	99	90	NT	0.12	1.00	ME	Unimpacted
	I12	28	54.5	17.12	Ref	98	99	99	NT	0.06	1.00	ME	Unimpacted
	I14	28	20.1	21.05	Ref	97	99	98	NT	0.10	1.00	ME	Unimpacted
	I15	28	4.0	14.51	Ref	99	99	100	NT	0.04	1.00	ME	Unimpacted
	I16	28	6.8	13.02	Ref	98	99	99	NT	0.04	1.00	ME	Unimpacted

deviation from reference conditions were PLOO near-ZID station E14 in summer 2021 and regional station 8938, located adjacent to the La Jolla Canyon at a depth of 28 m. There was no indication of sediment contamination at station 8938, as no ERLs were exceeded at this station, combined SQO scores were indicative of minimal exposure, and station 8938 did not fall out as an outlier in the sediment chemistry or macrofaunal cluster analyses. In contrast, sediments from station E14 have been known to have relatively high sulfides and biochemical oxygen demand (BOD) values periodically over the years. For example, station E14 had the third highest BOD concentration during the summer of 2021. However, as with station 8938, no ERLs were exceeded at this station, combined SQO scores were indicative of minimal exposure, and station E14 did not fall out as an outlier in the sediment chemistry or macrofaunal cluster analyses. Thus, all BRI scores, when integrated with SQOs and sediment toxicity scores, resulted in 100% of the stations assessed in summer 2020 and 2021 deemed as unimpacted.

Discussion

Benthic habitats and associated macrofaunal communities found on the continental shelf and upper slope off San Diego remained in good condition during the 2020–2021 reporting period. Overall, this regional assessment is consistent with the findings from the more extensive sampling of the core PLOO and SBOO stations reported in Chapter 5 for sediment quality and Chapter 6 for macrofaunal communities.

The physical composition of the sediments at the regional and core benthic stations, sampled during the summer 2020 and 2021, was typical for this portion of the southern California coast (Emery 1960), and is consistent with results of previous surveys off San Diego (e.g., City of San Diego 2018, 2020, 2022a). Overall, particle size composition varied as expected by outfall region and depth stratum. For example, stations sampled along the inner and mid-shelf within

the SBOO monitoring area tended to be composed of medium and coarse sands, whereas stations sampled along the middle and outer shelf within the PLOO region were typically characterized by much finer sediments (see also Chapter 5). Much of the variability in particle size distributions off San Diego is likely related to the complexities of local seafloor geology, topography, and current patterns all of which can significantly affect sediment transport and deposition (Emery 1960, Patsch and Griggs 2007).

Sediment quality was excellent throughout the entire San Diego region in summer 2020–2021. There was no evidence of degraded benthic habitats, in terms of the chemical properties of the sediments, or spatial patterns in the distribution of the different types of contaminants, which may accumulate over time (e.g., organic indicators, trace metals). In addition, results of sediment toxicity testing in offshore San Diego waters revealed minimal toxicity at any of the near-ZID or regional stations tested, and these results, when integrated with benthic infauna and sediment chemistry results, demonstrated that the shelf off San Diego remains unimpacted by the PLOO or SBOO.

Sediment contamination patterns during the current reporting period were also similar to those seen in previous years. Although, a number of indicators of organic loading (e.g., trace metals, pesticides, and PCBs) were detected in sediment samples throughout the San Diego region, almost all occurred at concentrations below critical ERL and ERM thresholds, similar to that observed in previous years (e.g., City of San Diego 2018, 2020, 2022a). Furthermore, examination of spatial patterns revealed no evidence of sediment contamination that could be attributed to local wastewater discharges via the PLOO or SBOO. Instead, concentrations of total nitrogen and several trace metals were found to increase with increasing depth and, to a lesser degree, with increased percent fines. However, this association is expected, due to the known correlation between sediment size and concentrations of organics and trace metals (Eganhouse and Venkatesan 1993). Finally, concentrations of these contaminants in San Diego waters remained relatively low compared to other coastal areas located off southern California (Schiff and Gossett 1998, Noblet et al. 2002, Schiff et al. 2006, 2011, Maruya and Schiff 2009, Dodder et al. 2016, Du et al 2020).

Macrofaunal communities in the San Diego region also appeared healthy in summer 2020–2021, with assemblages consistent with those observed during previous regional surveys conducted from 1994 to 2019 (City of San Diego 2010–2013, 2015b, 2016, 2018, 2020, 2022a). BRI results revealed little evidence of disturbance off San Diego, with 94% of all calculated BRI values being indicative of reference condition and another 6% being characteristic of only a possible minor deviation. These results reflect assemblages characterized by expected abundances of pollution sensitive species, such as the amphipods *Ampelisca* spp and *Rhepoxynius* spp., expected abundances of pollution tolerant species, such as the polychaete *Capitella teleta* and the bivalve *Solemya pervernicosa* (see also Chapter 6). Comparison of the results for other major benthic community metrics (e.g. species richness, macrofaunal abundance, diversity, evenness, and dominance) also showed no evidence of wastewater impact or significant habitat degradation during the 2020 and 2021 surveys. Furthermore, values for each of these community structure metrics remain within, or near, the range of tolerance intervals calculated for their specific habitats (see City of San Diego 2022a).

Most of the macrofaunal assemblages identified in summer 2020–2021 segregated by habitat characteristics such as depth and sediment particle size, often corresponding with the "patchy" habitats reported to occur naturally across the SCB (Fauchald and Jones 1979, Jones 1969, Bergen et al. 2000, Mikel et al. 2007). Several of the inner to mid-shelf assemblages described in this chapter were similar to those previously described in other shallow habitats across southern California (Barnard 1963, Jones 1969, Thompson et al. 1987, 1993a,b, MBC 1988, Mikel et al. 2007). These assemblages occurred in sandy sediments and were characterized by several species of polychaetes, including the spionids *Spiophanes norrisi* and *Spiophanes duplex*, and the capitellid *Mediomastus* sp. However, differences between these groups were probably driven by minor variations in sediment type (e.g., shell hash, relict red sand) or depth that differentially

affected populations of the resident species. The middle to outer shelf strata off San Diego were dominated by macrofauna cluster group K, which represented assemblages from 78% of the samples analyzed at these depths during the current reporting period. These assemblages occurred in sediments with close to 40% fines and larger proportions of very fine and fine sand. Benthic communities dominated by polychaete worms such as *S. duplex* have long been common off Point Loma, and in similar seafloor habitats in other areas of southern California (Jones 1969, Fauchald and Jones 1979, Thompson et al. 1987, 1993a,b, Zmarzly et al. 1994, Diener and Fuller 1995, Bergen et al. 1998, 2000, 2001, Mikel et al. 2007, City of San Diego 2022a). The even finer sediments of upper slope stations sampled off San Diego in summer 2020–2021 were characterized by macrofaunal assemblages with much lower total abundances and fewer species than at most shelf stations. This pattern is similar to results reported previously for the region since regular monitoring of these deeper slope habitats began (e.g., City of San Diego 2010–2013, 2015b, 2016, 2018, 2020, 2022a).

Although benthic habitats and their associated macrofaunal communities continue to vary across depth and sediment gradients throughout the San Diego region, there was no evidence of disturbance or environmental degradation in 2020–2021, which may be attributed to anthropogenic factors, such as wastewater discharge via the PLOO or SBOO, or other point sources. Macrobenthic communities appeared to be in good condition overall, with none of the sites surveyed showing evidence consistent with environmental disturbance. This result is similar to findings in Gillett et al.(2017) who reported that at least 98% of the entire SCB mainland shelf is in good condition, based on BRI data from bight-wide regional monitoring program.

Literature Cited

Barnard, J.L. (1963). Relationship of benthic Amphipoda to invertebrate communities of inshore sublittoral sands of southern California. Pacific Naturalist, 3: 439–467.

Bay, S.M., D.J. Greenstein, J.A. Ranasinghe, D.W. Diehl, and A.E. Fetscher. (2013). Sediment Quality Assessment Technical Support Manual. Technical Report 777. Southern California Coastal Water Research Project. Costa Mesa, CA.

Bay S.M. and S.B. Weisberg. (2012). Framework for interpreting sediment quality triad data. Integrated Environ Assess Manag 8:589-596.

Bergen, M. (1996). The Southern California Bight Pilot Project: Sampling Design. In: M.J. Allen, C. Francisco, D. Hallock (Eds.). Southern California Coastal Water Research Project: Annual Report 1994–1995. Southern California Coastal Water Research Project, Westminster, CA.

Bergen, M., D.B. Cadien, A. Dalkey, D.E. Montagne, R.W. Smith, J.K. Stull, R.G. Velarde, and S.B. Weisberg. (2000). Assessment of benthic infaunal condition on the mainland shelf of southern California. Environmental Monitoring Assessment, 64: 421–434.

Bergen, M., S.B. Weisberg, D. Cadien, A. Dalkey, D. Montagne, R.W. Smith, J.K. Stull, and R.G. Velarde. (1998). Southern California Bight 1994 Pilot Project: IV. Benthic Infauna. Southern California Coastal Water Research Project, Westminster, CA.

Bergen, M., S.B. Weisberg, R.W. Smith, D.B. Cadien, A. Dalkey, D.E. Montagne, J.K. Stull, R.G. Velarde, and J.A. Ranasinghe. (2001). Relationship between depth, sediment, latitude, and the structure of benthic infaunal assemblages on the mainland shelf of southern California. Marine Biology, 138: 637–647.

[B13CIA] Bight '13 Contaminant Impact Assessment Planning Committee. (2017). Southern California Bight 2013 Regional Monitoring Program: Volume VIII. Contaminant Impact Assessment Synthesis Report. Technical Report 973. Southern California Coastal Water Research Project. Costa Mesa, CA.

Bight'18 Toxicology Committee. (2018). Bight'18 Toxicology Laboratory Manual. Southern California Bight 2018 Regional Monitoring Program. Southern California Coastal Water Research Project. Costa Mesa, CA.

City of San Diego. (2010). Annual Receiving Waters Monitoring Report for the South Bay Ocean Outfall (South Bay Water Reclamation Plant), 2009. City of San Diego Ocean Monitoring Program, Public Utilities Department, Environmental Monitoring and Technical Services Division, San Diego, CA.

City of San Diego. (2011). Annual Receiving Waters Monitoring Report for the South Bay Ocean Outfall (South Bay Water Reclamation Plant), 2010. City of San Diego Ocean Monitoring Program, Public Utilities Department, Environmental Monitoring and Technical Services Division, San Diego, CA.

City of San Diego. (2012). Annual Receiving Waters Monitoring Report for the South Bay Ocean Outfall (South Bay Water Reclamation Plant), 2011. City of San Diego Ocean Monitoring Program, Public Utilities Department, Environmental Monitoring and Technical Services Division, San Diego, CA.

City of San Diego. (2013). Annual Receiving Waters Monitoring Report for the South Bay Ocean Outfall (South Bay Water Reclamation Plant), 2012. City of San Diego Ocean Monitoring Program, Public Utilities Department, Environmental Monitoring and Technical Services Division, San Diego, CA.

City of San Diego. (2015a). Sediment Toxicity Monitoring Plan for the South Bay Ocean Outfall and Point Loma Ocean Outfall Monitoring Regions, San Diego, California. Submitted by the City of San Diego Public Utilities Department to the San Diego Water Board and USEPA, Region IX, August 28, 2015 [approved 9/29/2015].

City of San Diego. (2015b). South Bay Ocean Outfall Annual Receiving Waters Monitoring and Assessment Report, 2014. City of San Diego Ocean Monitoring Program, Public Utilities Department, Environmental Monitoring and Technical Services Division, San Diego, CA.

City of San Diego. (2016). South Bay Ocean Outfall Annual Receiving Waters Monitoring and Assessment Report, 2015. City of San Diego Ocean Monitoring Program, Public Utilities Department, Environmental Monitoring and Technical Services Division, San Diego, CA.

City of San Diego. (2018). Biennial Receiving Waters Monitoring and Assessment Report for the Point Loma and South Bay Ocean Outfalls, 2016–2017. City of San Diego, Public Utilities Department, Environmental Monitoring and Technical Services Division, San Diego, CA.

City of San Diego. (2020). Biennial Receiving Waters Monitoring and Assessment Report for the Point Loma and South Bay Ocean Outfalls, 2018–2019. City of San Diego, Public Utilities Department, Environmental Monitoring and Technical Services Division, San Diego, CA.

City of San Diego. (2021). Interim Receiving Waters Monitoring Report for the Point Loma and South Bay Ocean Outfalls, 2020. City of San Diego, Public Utilities Department, Environmental Monitoring and Technical Services Division, San Diego, CA.

City of San Diego. (2022a). Appendix C. Ocean Benthic Conditions. In: Application for Renewal of NPDES CA0107409 and 301(h) Modified Secondary Treatment Requirements, Point Loma Ocean Outfall. Volume V, Appendix C. Public Utilities Department, Environmental Monitoring and Technical Services Division, San Diego, CA.

City of San Diego. (2022b). Quality Assurance Manual for Toxicity Testing. City of San Diego Toxicology Laboratory, Environmental

Monitoring and Technical Services Division, Public Utilities Department, San Diego, CA.

Clarke, K.R., R.N. Gorley, P.J. Somerfield, and R.M. Warwick. (2014). Change in marine communities: an approach to statistical analysis and interpretation, 3rd edition. PRIMER-E, Plymouth, England.

Clarke, K.R., P.J. Somerfield, and R.N. Gorley. (2008). Testing of null hypotheses in exploratory community analyses: similarity profiles and biota-environment linkage. Journal of Experimental Marine Biology and Ecology, 366: 56–69.

Conover, W.J. (1980). Practical Nonparametric Statistics, 2nd ed. John Wiley & Sons, Inc., New York, NY.

Diener, D.R. and S.C. Fuller. (1995). Infaunal patterns in the vicinity of a small coastal wastewater outfall and the lack of infaunal community response to secondary treatment. Bulletin of the Southern California Academy of Science, 94: 5–20.

Dodder, N., K. Schiff, A. Latker, and C-L Tang. (2016). Southern California Bight 2013 Regional Monitoring Program: IV. Sediment Chemistry. Southern California Coastal Water Research Project, Westminster, CA.

Du, B., C.S. Wong, K. Mclaughlin, and K. Schiff. (2020). Southern California Bight 2018 Regional Monitoring Program: II. Sediment Chemistry. Southern California Coastal Water Research Project, Westminster, CA.

Eganhouse, R.P. and M.I. Venkatesan. (1993). Chemical Oceanography and Geochemistry. In: M.D. Dailey, D.J. Reish, and J.W. Anderson (eds.). Ecology of the Southern California Bight: A Synthesis and Interpretation. University of California Press, Berkeley, CA. p 71–189.

Emery, K. O. (1960). The Sea Off Southern California. John Wiley, New York, NY.

Fauchald, K. and G.F. Jones. (1979). Variation in community structures on shelf, slope, and basin macrofaunal communities of the Southern California Bight. Report 19, Series 2. In: Southern California Outer Continental Shelf Environmental Baseline Study, 1976/1977 (Second Year) Benthic Program. Principal Investigators Reports, Vol. II. Science Applications, Inc. La Jolla, CA.

Ferraro, S.P., R.C. Swartz, F.A. Cole, and W.A. Deben. (1994). Optimum macrobenthic sampling protocol for detecting pollution impacts in the Southern California Bight. Environmental Monitoring and Assessment, 29: 127–153.

Folk, R.L. (1980). Petrology of Sedimentary Rocks. Hemphill, Austin, TX.

Gillett, D.J., L.L. Lovell, and K.C. Schiff. (2017). Southern California Bight 2013 Regional Monitoring Program: Volume VI. Benthic Infauna. Technical Report 971. Southern California Coastal Water Research Project. Costa Mesa, CA.

Helsel, D.R. (2005a). More than obvious: better methods for interpreting nondetect data. Environmental Science & Technology (October 15, 2005), 419A-423A.

Helsel, D.R. (2005b). Nondetects and Data Analysis: Statistics for Censored Environmental Data. John Wiley, New York.

Helsel, D.R. (2006). Fabrication data: how substituting values for nondetects can ruin results, and what can be done about it. Chemosphere 65: 2434-2439.

Hope, R.M. (2013). Rmisc: Ryan Miscellaneous. R package version 1.5. http://CRAN.R-project.org/package=Rmisc.

Jones, G.F. (1969). The benthic macrofauna of the mainland shelf of southern California. Allan Hancock Monographs of Marine Biology, 4: 1–219.

Kassambara, A. (2019). ggpubr: Based Publication Ready Plots R package version 0.2.1 http://www.sthda.com/english/rpkgs/ggpubr.

Long, E.R., D.L. MacDonald, S.L. Smith, and F.D. Calder. (1995). Incidence of adverse biological effects within ranges of chemical concentration in marine and estuarine sediments. Environmental Management, 19(1): 81–97.

Maruya, K.A. and K. Schiff. (2009). The extent and magnitude of sediment contamination in the Southern California Bight. Geological Society of America Special Paper, 454: 399–412.

[MBC] MBC Applied Environmental Sciences and Engineering-Science. (1988). Part F: Biological studies. In: Tijuana Oceanographic Engineering Study, Volume 1. Ocean Measurement Program. Prepared for the City of San Diego, CA.

Mikel T.K., J.A Ranasinghe, and D.E. Montagne. (2007). Characteristics of benthic macrofauna of the Southern California Bight. Appendix F. Southern California Bight 2003 Regional Monitoring Program, SCCWRP, Costa Mesa, CA.

Noblet, J.A., E.Y. Zeng, R. Baird, R.W. Gossett, R.J. Ozretich, and C.R. Phillips. (2002). Southern California Bight 1998 Regional Monitoring Program: VI. Sediment Chemistry. Southern California Coastal Water Research Project, Westminster, CA.

Oksanen, J., F.G. Blanchet, R. Kindt, P. Legendre, P.R. Minchin, R.B. O'Hara, G.L. Simpson, P. Solymos, M.H.H. Stevens, and H. Wagner. (2019). vegan: Community Ecology Package. R package version 2.5-6. http://CRAN.R-project.org/package=vegan.

Patsch, K. and G. Griggs. (2007). Development of Sand Budgets for California's Major Littoral Cells. Institute of Marine Sciences, University of California, Santa Cruz, CA.

R Core Team. (2021). R: A language and environment for statistical computing. R Foundation for Statistical Computing, Vienna, Austria. URL https://www.R-project.org/.

Ranasinghe, J.A., A.M. Barnett, K. Schiff, D.E. Montagne, C. Brantley, C. Beegan, D.B. Cadien, C. Cash, G.B. Deets, D.R. Diener, T.K. Mikel, R.W. Smith, R.G. Velarde, S.D. Watts, and S.B. Weisberg. (2007). Southern California Bight 2003 Regional Monitoring Program: III. Benthic Macrofauna. Southern California Coastal Water Research Project. Costa Mesa, CA.

Ranasinghe, J.A., D. Montagne, R.W. Smith, T.K. Mikel, S.B. Weisberg, D. Cadien, R. Velarde, and A. Dalkey. (2003). Southern California Bight 1998 Regional Monitoring Program: VII. Benthic Macrofauna. Southern California Coastal Water Research Project. Westminster, CA.

Ranasinghe, J.A., K.C. Schiff, C.A. Brantley, L.L. Lovell, D.B. Cadien, T.K. Mikel, R.G. Velarde, S. Holt, and S.C. Johnson. (2012). Southern California Bight 2008 Regional Monitoring Program: VI. Benthic Macrofauna. Technical Report No. 665, Southern California Coastal Water Research Project, Costa Mesa, CA.

Ranasinghe, J.A., K.C. Schiff, D.E. Montagne, T.K. Mikel, D.B. Cadien, R.G. Velarde, and C.A. Brantley. (2010). Benthic macrofaunal community condition in the Southern California Bight, 1994–2003. Marine Pollution Bulletin, 60: 827–833.

Revelle, W. (2019) psych: Procedures for Personality and Psychological Research, Northwestern University, Evanston, Illinois, USA, https://CRAN.R-project.org/package=psych Version = 1.9.12.31.

Ripley, B. and M. Lapsley. (2017). RODBC: ODBC Database Access. R package version 1.3-12. http://CRAN.R-project.org/package=RODBC.

[SCAMIT] Southern California Association of Marine Invertebrate Taxonomists. (2018). A taxonomic listing of benthic macro- and megainvertebrates from infaunal and epibenthic monitoring programs in the Southern California Bight, edition 12. Southern California Association of Marine Invertebrate Taxonomists, Natural History Museum of Los Angeles County Research and Collections, Los Angeles, CA.

[SCCWRP] Southern California Coastal Water Research Project. (2018). Southern California Bight 2018 Regional Monitoring Program: Contaminant Impact Assessment Field Operations Manual. Southern California Coastal Water Research Project. Costa Mesa, CA.

Schiff, K.C. and R.W. Gossett. (1998). Southern California Bight 1994 Pilot Project: III. Sediment Chemistry. Southern California Coastal Water Research Project. Westminster, CA.

Schiff, K., R. Gossett, K. Ritter, L. Tiefenthaler, N. Dodder, W. Lao, and K. Maruya. (2011). Southern California Bight 2008 Regional Monitoring Program: III. Sediment Chemistry. Southern California Coastal Water Research Project, Costa Mesa, CA.

Schiff, K., K. Maruya, and K. Christenson. (2006). Southern California Bight 2003 Regional Monitoring Program: II. Sediment Chemistry. Southern California Coastal Water Research Project, Westminster, CA.

Smith, R.W., M. Bergen, S.B. Weisberg, D. Cadien, A. Dalkey, D. Montagne, J.K. Stull, and R.G. Velarde. (2001). Benthic response index for assessing infaunal communities on the southern California mainland shelf. Ecological Applications, 11(4): 1073–1087.

[SWRCB] State Water Resource Control Board. (2009). Water Quality Control Plan for Enclosed Bays and Estuaries – Part 1 Sediment Quality. Resolution Number 2008-0070, State Water Resources Control Board, Sacramento, CA.

Stebbins, T.D., K.C. Schiff, and K. Ritter. (2004). San Diego Sediment Mapping Study: Workplan for Generating Scientifically Defensible Maps of Sediment Conditions in the San Diego Region. City of San Diego, Metropolitan Wastewater Department, Environmental Monitoring and Technical Services Division, and Southern California Coastal Water Research Project, Westminster, CA.

Stevens Jr., D.L. (1997). Variable density grid-based sampling designs for continuous spatial populations. Environmetrics, 8: 167–195.

Stevens Jr., D.L. and A.R. Olsen. (2004). Spatially-balanced sampling of natural resources in the presence of frame imperfections. Journal of the American Statistical Association, 99: 262–278.

Swartz, R.C., F.A. Cole, and W.A. Deben. (1986). Ecological changes in the Southern California Bight near a large sewage outfall: benthic conditions in 1980 and 1983. Marine Ecology Progress Series, 31: 1–13.

Thompson, B.E., J.D. Laughlin, and D.T. Tsukada. (1987). 1985 reference site survey. Technical Report No. 221, Southern California Coastal Water Research Project, Long Beach, CA.

Thompson, B., J. Dixon, S. Schroeter, and D.J. Reish. (1993a). Chapter 8. Benthic invertebrates. In: M.D. Dailey, D.J. Reish, and J.W. Anderson (eds.). Ecology of the Southern California Bight: A Synthesis and Interpretation. University of California Press, Berkeley, CA.

Thompson, B.E., D. Tsukada, and D. O'Donohue. (1993b). 1990 reference site survey. Technical Report No. 269, Southern California Coastal Water Research Project, Long Beach, CA.

[USEPA] United States Environmental Protection Agency. (1987). Quality Assurance and Quality Control (QA/QC) for 301(h) Monitoring Programs: Guidance on Field and Laboratory Methods. EPA Document 430/9-86-004. Office of Marine and Estuarine Protection.

[USEPA] United States Environmental Protection Agency. (1994). Methods for assessing the toxicity of sediment-associated contaminants with estuarine and marine amphipods. EPA/600/R-94/025. Office of Research and Development, UEPA. Narragansett, RI.

Wickham, H. (2007). Reshaping Data with the reshape Package. Journal of Statistical Software, 21(12), 1-20. URL http://www.jstatsoft.org/v21/i12/.

Wickham, H. (2011). The Split-Apply-Combine Strategy for Data Analysis. Journal of Statistical Software, 40(1), 1-29. URL http://www.jstatsoft.org/v40/i01/.

Wickham, H. (2019a). Scales: Scale Functions for Visualization Rstudio. R package version 1.1.0. https://scales.r-lib.org/.

Wickham, H. (2019b). stringr: Simple, Consistent Wrappers for Common String Operations. R package version 1.4.0. https://CRAN.R-project.org/package=stringr.

Wickham, H., M. Averick, J. Bryan, W. Chang, L. D'Agostino McGowan, R. François, G.Grolemund, A. Hayes, L. Henry, J. Hester, M. Kuhn, T. Lin Pedersen, E. Miller, S. Milton Bache, K. Müller, J. Ooms, D. Robinson, D. P. Seidel, V. Spinu, K. Takahashi, D. Vaughan, C. Wilke, K. Woo, H. Yutani. (2019a). Welcome to the tidyverse. Journal of Open Source Software, 4(43), 1686, https://doi.org/10.21105/joss.01686.

Wickham, H., W. Chang, L. Henry, T.L. Pedersen, K. Takahashi, C. Wilke, K. Woo, (2019b). Ggplot2: Create Elegant Data Visualizations Using the Grammar of Graphics. Version 3.2.0. Rstudio. URL https://ggplot2.tidyverse.org/.

Wickham, H. and L. Henry (2018). tidyr: Easily Tidy Data with 'spread()' and 'gather()' Functions. R package version 0.7.0. https://CRAN.R-project.org/package=tidyr.

Wickham, H., R. Francois, L. Henry and K. Müller (2020). dplyr: A Grammar of Data Manipulation. R package version 0.7.2. https://CRAN.R-project.org/package=dplyr.

Zeileis, A and G. Grothendieck. (2005). zoo: S3 Infrastructure for Regular and Irregular Time Series. Journal of Statistical Software, 14(6), 1-27. URL http://www.jstatsoft.org/v14/i06/.

Zmarzly, D.L., T.D. Stebbins, D. Pasko, R.M. Duggan, and K.L. Barwick. (1994). Spatial patterns and temporal succession in soft-bottom macroinvertebrate assemblages surrounding an ocean outfall on the southern San Diego shelf: Relation to anthropogenic and natural events. Marine Biology, 118: 293–307.

Chapter 8
Demersal Fishes and Megabenthic Invertebrates

Chapter 8. Demersal Fishes and Megabenthic Invertebrates

Introduction

The City of San Diego (City) collects bottom dwelling (demersal) fishes, and relatively large (megabenthic) surface dwelling invertebrates, by otter trawl to examine the potential effects of wastewater discharge, or other natural and/or anthropogenic disturbances, on the marine environment around the Point Loma and South Bay Ocean Outfalls (PLOO and SBOO, respectively). These fish and invertebrate communities are targeted for monitoring as they are known to play critical ecological roles on the southern California coastal shelf (e.g., Allen et al. 2006, Thompson et al. 1993a,b). Trawled species typically live on or near the seafloor, and are therefore exposed to sediment conditions, which may be affected by both point and non-point sources such as discharges from ocean outfalls, runoff from watersheds, outflows from rivers and bays, or the disposal of dredged sediments (see Chapter 5: Sediment Quality). For these reasons, assessment of bottom dwelling fish and invertebrate communities has become an important focus of ocean monitoring programs throughout the world, but especially in the Southern California Bight (SCB) where they have been sampled extensively on the mainland shelf for the past four decades (e.g., Stein and Cadien 2009).

In healthy coastal marine ecosystems, demersal fish and megabenthic invertebrate communities vary widely and are influenced by many natural factors. For example, prey availability, seafloor topography, sediment composition, and changes in water temperatures associated with large scale oceanographic events, such as El Niño, may affect migration patterns or the recruitment of certain fish species (Cross et al. 1985, Helvey and Smith 1985, Karinen et al. 1985, Murawski 1993, Stein and Cadien 2009). Population fluctuations may also be due to the mobile nature of many species (e.g., fish schools, urchin aggregations). Therefore, an understanding of natural background conditions is essential to determine whether observed differences, or changes in community structure, may be related to anthropogenic activity. Pre-discharge and regional monitoring efforts by the City and others since 1991 provide baseline information on the variability of demersal fish and megabenthic invertebrate communities in the San Diego region critical for such comparative analyses (e.g., Allen et al. 1998, 2002, 2007, 2011, City of San Diego 1995, 1998, 2000, Walther et al. 2017).

The City relies on a suite of scientifically-accepted indices and statistical analyses to evaluate changes in local fish and invertebrate communities. These include univariate measures of community structure, such as species richness, abundance, and diversity while multivariate analyses are used to detect spatiotemporal differences among communities (e.g., Warwick 1993). The use of multiple types of analyses allows for more robust inference than relying on single parameters for determining anthropogenic environmental impacts. In addition, the examination of trawl-caught fishes for evidence of physical abnormalities or diseases is informative as they can be indicators of degraded habitats (e.g., Cross and Allen 1993, Stein and Cadien 2009). Collectively, these data are used to determine whether demersal fish and megabenthic invertebrate assemblages from habitats with comparable depth and sediment characteristics are similar, or if observable impacts from wastewater discharge or other sources have occurred.

This chapter presents analysis and interpretation of demersal fish and megabenthic invertebrate data collected at designated monitoring stations throughout the PLOO and SBOO regions, during 2020 and 2021. Included are descriptions of the different fish and invertebrate communities present in these two regions during the reporting period, along with comparisons of spatial patterns and long-term changes over time. The four primary

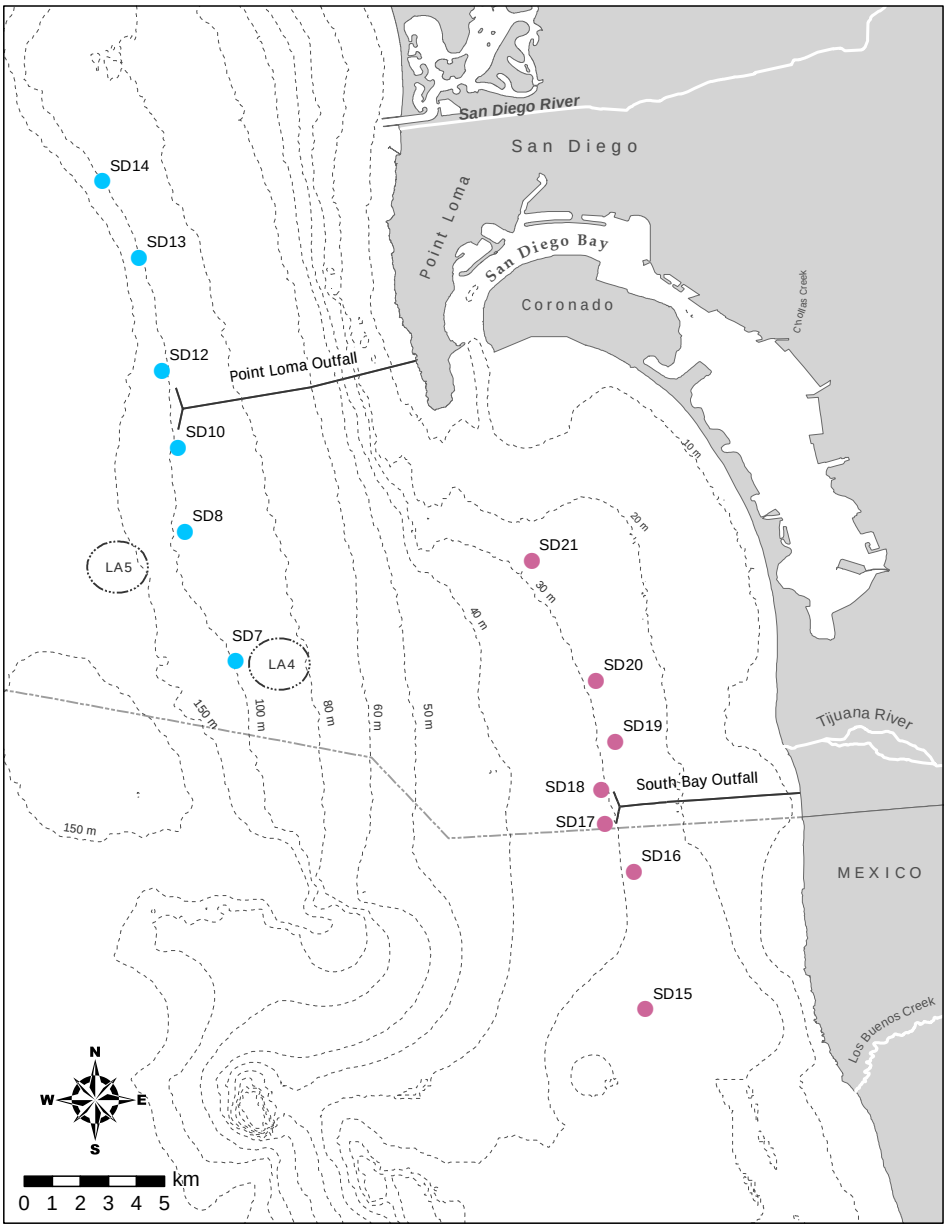

Figure 8.1
Trawl station locations sampled around the Point Loma and South Bay Ocean Outfalls as part of the City of San Diego's Ocean Monitoring Program.

goals of this chapter are to: (1) characterize and document the demersal fish and megabenthic invertebrate assemblages present during the current reporting period; (2) determine the presence or absence of impacts on these assemblages that may be associated with wastewater discharge from the PLOO and SBOO; (3) identify other potential natural or anthropogenic sources of variability in the San Diego coastal marine ecosystem; (4) determine if the populations of selected species of fish and invertebrates are changing over time.

Materials and Methods

Field Sampling

Trawls were conducted at 13 stations, throughout the PLOO and SBOO regions, to monitor demersal fishes and megabenthic invertebrates during winters and summers of 2020 and 2021 (Figure 8.1). These included six PLOO stations located along the

100-m depth contour (discharge depth), ranging from 9 km south to 8 km north of the outfall, and seven SBOO stations located along the 28-m depth contour (discharge depth), ranging from 7 km south to 8.5 km north of the outfall. The two PLOO stations (SD10, SD12) and two SBOO stations (SD17, SD18) located within 1 km of the outfall structures are considered to represent nearfield conditions.

A single trawl was performed at each station, during each survey, using a 7.6-m Marinovich otter trawl fitted with a 1.3-cm cod-end mesh net. Standard sampling procedures required towing the net for a total of at least 10 minutes bottom time per trawl, at a speed of around 2 knots, along a predetermined heading that follows the isobath at each station. A pressure-temperature sensor was attached to one of the trawl doors to measure water temperature, depth, and time of the individual trawls; these data were used to confirm acceptability of the trawl. The catch from each successful trawl was sorted, recorded, and immediately returned to the water to minimize mortality whenever possible. All individual fish and invertebrates captured were identified to species, or to the lowest taxon possible, based on accepted taxonomic protocols for the region (Eschmeyer and Herald 1998, Page et al. 2013, SCAMIT 2018). If an animal could not be accurately identified to species in the field, it was returned to the laboratory for further identification where possible. The total number of individuals and total biomass (kg, wet weight) were recorded for each species of fish. Additionally, each fish was inspected for the presence of physical abnormalities (e.g., tumors, lesions, fin erosion, discoloration) or external parasites (e.g., copepods, cymothoid isopods, leeches). The length of each individual fish was measured to the nearest centimeter to determine size class; total length (TL) was measured for cartilaginous fishes while standard length (SL) was measured for bony fishes (SCCWRP 2018). For invertebrates, the total number of individuals was recorded for each species. In contrast to previous years, parasitic invertebrates no longer attached to their hosts, including the cymothoid isopod *Elthusa vulgaris* and leeches in the subclass Hirudinea, were recorded as present/absent rather than being counted individually, and are, therefore, no longer included in the analyses presented herein. This change aligns with Bight methods (SCCWRP 2018). Visual observations of weather, sea conditions, and human and animal activity were also recorded at the time of sampling.

Data Analyses

Population characteristics of fish and invertebrate species between regions were summarized as percent abundance (PA; number of individuals per species/total abundance of all species), frequency of occurrence (FO; percentage of stations at which a species was collected), mean abundance per haul (MAH; number of individuals per species/total number of sites sampled), and mean abundance per occurrence (MAO; number of individuals per species/number of sites at which the species was collected). Additionally, the following community structure parameters were calculated per station for fishes and invertebrates separately: species richness (number of species), total abundance (number of individuals per species), and the Shannon Diversity Index (H'). For fishes, total biomass was also calculated per station. These analyses were performed using R (R Core Team 2019) and various functions within the dplyr, ggalt, ggplot2, ggpubr, gtools, plyr, psych, reshape2, Rmisc, RODBC, R.utils, stats, stringr, sqldf, and vegan packages (Bengtsson 2003, Wickham 2007, 2011, 2016, Hope 2013, Grothendieck 2014, Oksanen et al. 2015, Ripley and Lapsley 2015, Warnes et al. 2015, Revelle 2017, Kassambara 2018, 2019, Wickham and Francois 2016, Wickham et al. 2018).

To determine if the populations of fish and invertebrates are changing over time, multivariate analyses were performed in PRIMER v7 software using fish and invertebrate abundance data collected from 10-minute trawls conducted in the PLOO and SBOO regions from 1991 through 2021 (see Clarke 1993, Warwick 1993, Clarke et al. 2014). Prior to these analyses, all data were limited to summer surveys to reduce variability from natural seasonal variations.

Additionally, data were square-root transformed to characterize the natural variability in species abundance more accurately. Additional multivariate analyses included Bray-Curtis measure of dissimilarity to serve as the basis for ordination (non-metric multidimensional scaling; nMDS) and hierarchical agglomerative clustering (cluster analysis) with group-average linking. Similarity profile analysis (SIMPROF) was used to confirm the non-random structure of the resultant cluster dendrogram (Clarke et al. 2008), with major ecologically-relevant clusters receiving SIMPROF support retained as cluster groups. A BEST test using the BVSTEP procedure was conducted to determine which subset of species best described patterns within the resulting cluster dendrograms. Similarity percentages analysis (SIMPER) was used to determine which species were responsible for > 70% of the contributions to within-group similarity (characteristic species) by cluster group to support cluster group selection.

Data collected during 2020 were reported previously (City of San Diego 2021), and all raw data for the 2020–2021 sampling period have been submitted to either the Regional Water Quality Control Board or the California Environmental Data Exchange Network (CEDEN) and may be accessed upon request.

Results and Discussion

Demersal Fish Populations in 2020–2021

A total of 11,839 fishes were captured from the 52 trawls conducted within the PLOO and SBOO monitoring regions during 2020 and 2021, representing at least 44 different species from 20 families in the PLOO, and 34 species from 21 families in SBOO (Appendices I.1, I.2). Pacific Sanddabs continued to dominate PLOO demersal fish assemblages over the past two years, occurring in every haul and accounting for 47% of the fishes collected across trawls in that region (Table 8.1). Halfbanded Rockfish were also numerically dominant in PLOO assemblages during this period, occurring in 83% of the trawls and accounting for 12% of the fishes collected. Though Dover Sole and Shortspine Combfish were present in 100% of trawls, they only accounted for 10% and 3% of fishes collected, respectively. Other species of fish that were collected in at least 85% of the trawls, but in relatively low mean abundance (≤ 15/haul), included Longfin Sanddab, English Sole, Longspine Combfish, and Hornyhead Turbot. Fish assemblages in the SBOO region were dominated by Speckled Sanddabs, which occurred in all trawls and accounted for 45% of the fishes collected, and by California Lizardfish, which occurred in 79% of the hauls and accounted for 15% of the fishes collected (Table 8.2). Though California Tonguefish occurred in 75% of trawls, it only accounted for 3% of the fishes collected. Other species that were collected in at least 50% of the trawls, but in relatively low numbers (≤ 22/haul), included Longfin Sanddab and Hornyhead Turbot. Rare species in both regions that are not included in Tables 8.1 and 8.2 can be found in Appendices I.1 and I.2.

Table 8.1
Top 15 most abundant demersal fish species collected from 18 trawls conducted in the PLOO region during 2020 and 2021. PA = percent abundance; FO = frequency of occurrence; MAH = mean abundance per haul; MAO = mean abundance per occurrence.

Species	PA	FO	MAH	MAO
Pacific Sanddab	47	100	142	142
Halfbanded Rockfish	12	83	37	45
Dover Sole	10	100	29	29
Longfin Sanddab	5	92	15	16
English Sole	4	92	13	14
Longspine Combfish	4	88	12	14
Yellowchin Sculpin	4	38	11	29
Shortspine Combfish	3	100	10	10
Stripetail Rockfish	2	71	7	10
Plainfin Midshipman	1	71	4	6
Hornyhead Turbot	1	88	3	4
Bigmouth Sole	1	83	3	4
California Tonguefish	1	67	3	4
Pink Seaperch	1	71	2	3
Slender Sole	1	29	2	7

More than 99% of the fishes collected in the PLOO and SBOO monitoring regions were < 30 cm in length. The only species collected from PLOO stations with individuals measuring ≥ 30 cm were California Skate, California Lizardfish, Fantail Sole, Wolf-eel, and California Halibut (Appendix I.1). Within the SBOO region, species with individuals measuring ≥ 30 cm included Shovelnose Guitarfish, Thornback, Round Stingray, and California Halibut (Appendix I.2).

The four most abundant fishes in the PLOO region showed spatiotemporal variation in lengths (Appendix I.3). Pacific Sanddab, which are the most dominant species in PLOO, showed the greatest variation in lengths, ranging from 3–26 cm in length across the 3404 individuals collected (Appendix I.1). Longfin Sanddab also showed considerable variation in lengths, ranging from 4–24 cm in length across the 355 individuals collected. On the contrary, Halfbanded Rockfish showed little variation in length across surveys, apart from at station SD13 in summer 2020 where individuals ranged from 5–18 cm in length. Like Pacific Sanddab, Dover Sole showed moderate variation in length across surveys, with larger individuals generally being collected during summer surveys. Overall, fish lengths varied across species and stations, with no notable patterns in relation to proximity to the PLOO discharge site.

Similarly, the four most abundant fishes in the SBOO region also exhibited spatiotemporal variation in lengths, though not to the same degree as in the PLOO region (Appendix I.4). Speckled Sanddab showed little variation in length, ranging from 4–12 cm across the 2051 individuals collected (Appendix I.2). California Lizardfish, however, showed substantial variation in length, with the majority of the largest individuals (21–27 cm) being collected in summer of 2020. Though Northern Anchovy were only collected in winter of 2021, 613 individuals were collected at sizes ranging from 6–12 cm, with no apparent pattern across stations. Longfin Sanddab, most of which were collected during summer surveys, showed moderate variation in lengths, with most individuals measuring between 9–13 cm. As in the PLOO region, overall, there were no notable patterns in lengths of fishes observed relative to their proximity to the SBOO discharge site.

Table 8.2

Top 15 most abundant demersal fish species collected from 21 trawls conducted in the SBOO region during 2020 and 2021. PA = percent abundance; FO = frequency of occurrence; MAH = mean abundance per haul; MAO = mean abundance per occurrence.

Species	PA	FO	MAH	MAO
Speckled Sanddab	45	100	73	73
California Lizardfish	15	79	25	32
Northern Anchovy	13	18	22	123
Longfin Sanddab	13	68	22	32
California Tonguefish	3	75	5	6
White Croaker	2	21	3	12
Pacific Sardine	1	4	2	62
Yellowchin Sculpin	1	29	2	7
Hornyhead Turbot	1	57	2	3
English Sole	1	36	1	4
Pacific Sanddab	1	25	1	5
California Halibut	1	46	1	2
Plainfin Midshipman	1	36	1	2
Pipefish Unidentified	<1	21	1	3
Specklefin Midshipman	<1	32	1	2

Demersal Fish Community Structure Parameters

No notable spatial patterns in demersal fishes community parameters were observed relative to the proximity of the PLOO or SBOO discharge sites during 2020–2021 (Table 8.3). Results were generally consistent with previous findings for the two regions, and elsewhere in the SCB (e.g., Allen et al. 1998, 2002, 2007, 2011, City of San Diego 1995, 1998, Walther et al. 2017, Wisenbaker et al. 2021); mean species richness and diversity were consistently low (SR ≤ 16 species; H' ≤ 1.6, respectively); and fish abundance and biomass remained variable among both nearfield and farfield stations and between surveys over the past two years, with values ranging from 19–929 fishes/haul and 0.5–29.1 kg/haul, respectively.

Table 8.3

Summary of demersal fish community parameters for PLOO and SBOO trawl stations sampled during 2020 and 2021. Data are included for species richness, abundance, diversity (H'), and biomass (kg, wet weight).

	Station	2020		2021		2020		2021	
		Winter	Summer	Winter	Summer	Winter	Summer	Winter	Summer
		Species Richness				*Abundance*			
PLOO	SD7	17	14	15	17	221	126	353	288
PLOO	SD8	22	13	18	11	453	229	202	152
PLOO	SD10	14	19	17	20	184	327	310	275
PLOO	SD12	6	17	17	22	51	174	272	708
PLOO	SD13	12	21	13	13	151	929	370	446
PLOO	SD14	12	16	18	13	119	274	285	356
SBOO	SD15	5	5	10	3	48	38	219	51
SBOO	SD16	7	9	14	5	68	183	605	255
SBOO	SD17	7	5	8	5	100	19	82	241
SBOO	SD18	9	8	7	9	66	80	110	288
SBOO	SD19	9	12	6	10	153	194	57	235
SBOO	SD20	8	11	6	11	162	299	62	285
SBOO	SD21	15	10	11	11	144	178	71	291
		Diversity				*Biomass*			
PLOO	SD7	2.0	1.6	1.4	1.7	3.4	2.9	4.6	6.9
PLOO	SD8	1.7	1.3	2.2	1.8	7.2	3.6	5.9	2.2
PLOO	SD10	1.5	2.0	1.9	1.6	9.2	8.0	6.5	4.6
PLOO	SD12	1.1	1.8	2.0	1.4	0.6	8.5	8.5	22.5
PLOO	SD13	1.5	1.5	1.7	1.4	5.3	29.1	10.1	14.1
PLOO	SD14	1.7	1.4	2.0	1.2	5.9	7.7	14.1	7.4
SBOO	SD15	0.5	0.6	0.6	0.7	1.2	0.5	4.4	0.5
SBOO	SD16	0.9	1.2	0.6	1.1	1.0	3.9	5.6	3.0
SBOO	SD17	1.2	1.4	1.3	0.9	1.2	0.5	2.2	1.5
SBOO	SD18	1.5	0.9	1.2	1.1	6.3	0.8	4.3	3.2
SBOO	SD19	1.5	1.2	0.6	1.3	2.2	3.6	0.6	11.2
SBOO	SD20	1.4	1.3	0.6	1.4	3.1	6.1	1.1	5.9
SBOO	SD21	1.9	1.6	1.5	1.3	7.2	4.9	2.7	5.3

Within the PLOO region, the largest 10% of hauls occurred at station SD13 in summer 2020 and station SD12 in summer 2021 (Table 8.3). These two hauls included substantial numbers of Pacific Sanddab (153–469/haul) and Dover Sole (41–57/haul) (City of San Diego 2021). The heaviest 10% of hauls occurred during summer 2020 at station SD13 (29.1 kg) largely due to the collection of 13.7 kg of Halfbanded Rockfish, and summer 2021 at station SD12 (22.5 kg) largely due to 16.9 kg of Pacific Sanddab (Table 8.3; City of San Diego 2021). The smallest 10% of hauls occurred in the winter 2020 at stations SD12 and SD14 (Table 8.3). These hauls included relatively few Pacific Sanddabs (33–64/haul), Halfbanded Rockfish (0–5/haul), and low numbers of all other species (≤ 15 individuals per species). The lightest 10% of trawls were collected from station SD12 in winter 2020 and station SD8 in summer 2021 (City of San Diego 2021). Though the light haul during winter 2020 did correspond to high numbers of the red crab *Pleuroncodes planipes* (45,712 individuals), there were no *P. planipes* in the light haul in summer 2021.

Within the SBOO region, the largest hauls occurred during summer 2020 at station SD20 and winter 2021 at station SD16 (Table 8.3). Hauls during these trawls comprised 159 and 40 Speckled Sanddab, respectively, while the haul at SD16 was dominated by Northern Anchovy (524 individuals). The smallest hauls occurred at stations SD15 and SD17 during summer 2020, co-occurring with some of the lowest species richness and biomass values recorded over the past two years (City of San Diego 2021). Biomass at SBOO trawl stations ranged from 0.5–11.2 kg and tended to reflect the total number of individuals collected (Table 8.3), with one exception; the trawl from station SD19 during summer 2021 weighed 11.2 kg and included 5.8 kg of large California Halibut (4 individuals).

Historical comparisons indicate no noteworthy spatial patterns in demersal fishes community parameters relative to their proximity to the nearfield sites, nor to the onset of wastewater discharge that began in in the PLOO and SBOO regions in 1994 and 1999, respectively (Figure 8.2). Since the initiation of discharge, mean species richness and diversity values for demersal fishes collected from PLOO and SBOO stations have remained low (SR $\leq$ 15 species; H' $\leq$ 1.6, respectively). However, there has been considerably greater variability in abundance, with post-discharge hauls generally having a greater abundances of fishes. The latter was largely due to population fluctuations of a few numerically dominant species in each region (Figures 8.3, 8.4). For example, differences in overall trawl catch abundances tend to track changes in Pacific Sanddab populations at the PLOO stations, and Speckled Sanddab populations at the SBOO stations, since these two species have been numerically dominant in these regions since monitoring began. In addition, occasional spikes in abundances within the PLOO region have been due to population fluctuations of other common species, such as Halfbanded Rockfish, Yellowchin Sculpin, Longspine Combfish, Dover Sole, California Lizardfish, Stripetail Rockfish, Plainfin Midshipman, Longfin Sanddab, and Shortspine Combfish (Figure 8.3). In contrast, periodic spikes within the SBOO region have been due to population dynamics of California Lizardfish, Longfin Sanddab, White Croaker, Yellowchin Sculpin, California Tonguefish, Hornyhead Turbot, Roughback Sculpin, Northern Anchovy, and Longspine Combfish (Figure 8.4). Population dynamics of these species and communities over time do not appear to be associated with wastewater discharge from either outfall.

Physical Abnormalities and Parasitism in Demersal Fishes

Demersal fishes populations appeared healthy in the PLOO and SBOO regions in 2020–2021, with abnormalities reported for just 0.04% of fishes collected. Generally, eye parasites appear to occur more frequently in the PLOO region, whereas abnormalities (e.g., deformation, tumor, lesion), and gill and external parasites appear to occur more frequently in the SBOO region (Figure 8.5). As abnormalities or parasites were present across nearly all sites, there does not appear to be a relationship between these anomalies and proximity to either outfall. There were no incidences of fin rot on any fishes sampled during the last two years, while other recorded abnormalities were limited to: (1) three instances of tumors: two found in winter 2021 on individuals of Dover Sole collected from stations SD8 and SD10, and one found in summer 2020 on a Speckled Sanddab collected from station SD20; (2) a skeletal deformity, found in winter 2020 at station SD21 on a Speckled Sanddab; (3) one leech, found in winter 2021 at station SD20 on a Thornback (Appendix I.5).

Evidence of parasitism was also very low (0.4%) for trawl-caught fishes from both outfall regions over the past two years (Appendix I.5). Incidences included: (1) the copepod eye parasite *Phrixocephalus cincinnatus*, which was present on 33 PLOO fishes including Pacific Sanddab, Fantail Sole, Dover Sole, and Hornyhead Turbot; (2) the cymothoid isopod *Elthusa vulgaris* (a gill parasite of fishes), which was present either externally or in the gills of 10 fishes including Pacific Sanddab, California Scorpionfish, and Speckled Sanddab collected in both regions (Appendix I.5). Several

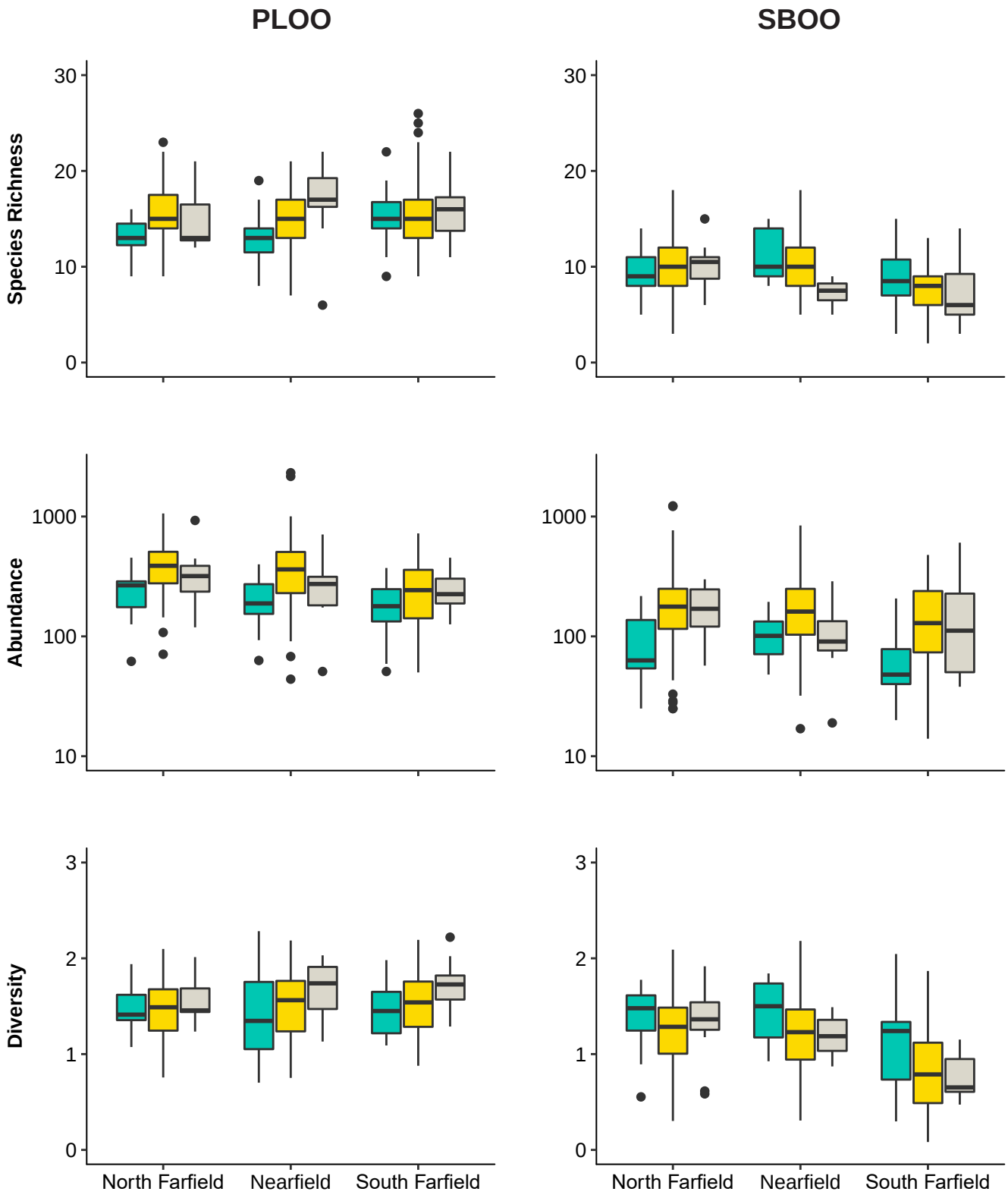

Figure 8.2

Species richness, abundance, and diversity (H') of demersal fishes collected from PLOO and SBOO north farfield, nearfield, and south farfield during pre-discharge (green), historical post-discharge (yellow), and current post-discharge (grey) periods. Data limited to 10-minute trawls. Boxes = median, upper, and lower quantiles; whiskers = 1.5x interquantile range; circles = outliers; see text for description of pre- versus post-discharge periods for the two outfalls.

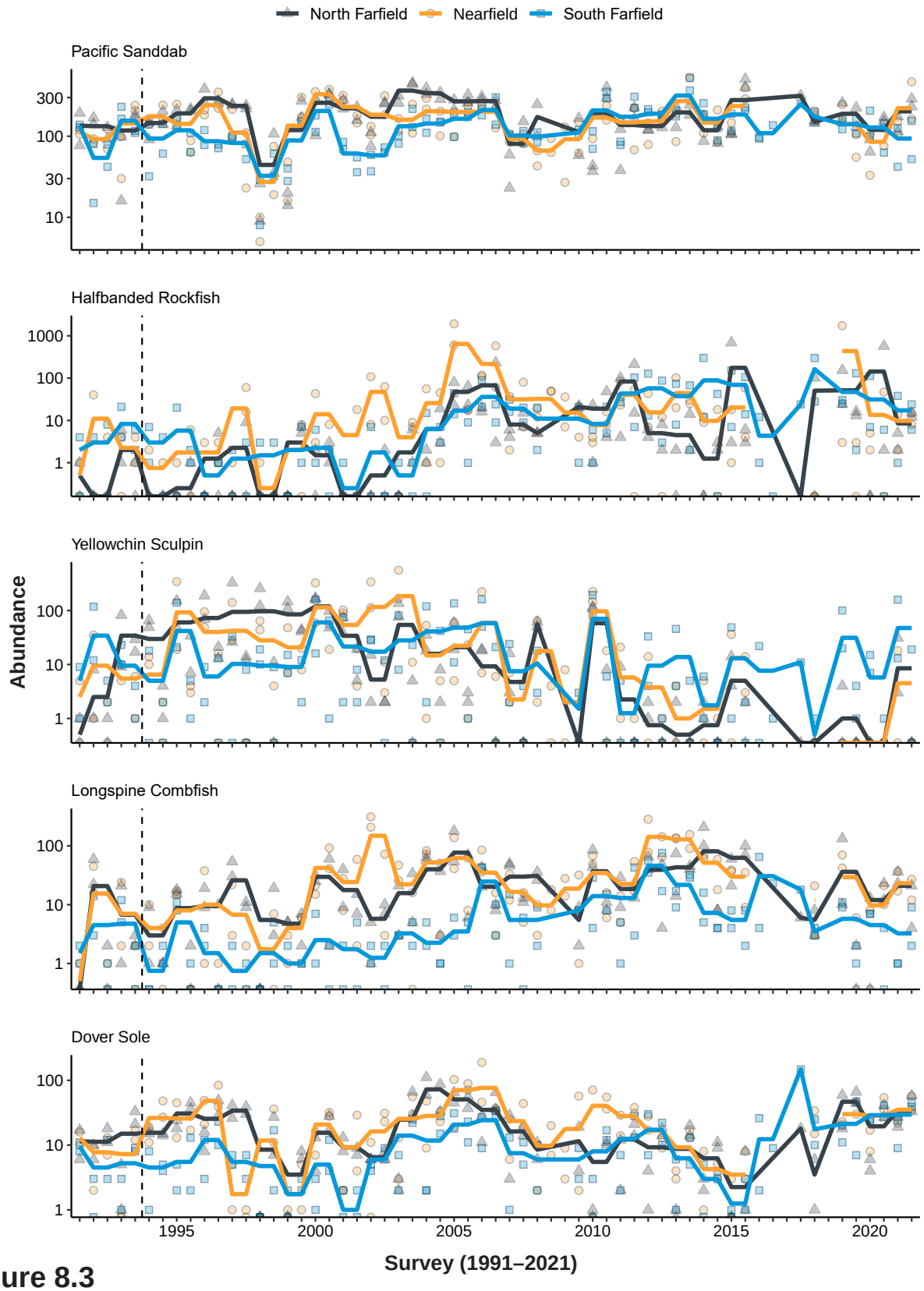

Figure 8.3

The ten most abundant demersal fish species (presented in order) collected from PLOO trawl stations sampled from 1991 through 2021. Data are limited to 10-minute trawls and are presented as quarterly means (lines) and total values per haul for north farfield (triangles), nearfield (circles), and south farfield (squares) stations. Dashed lines indicate onset of wastewater discharge.

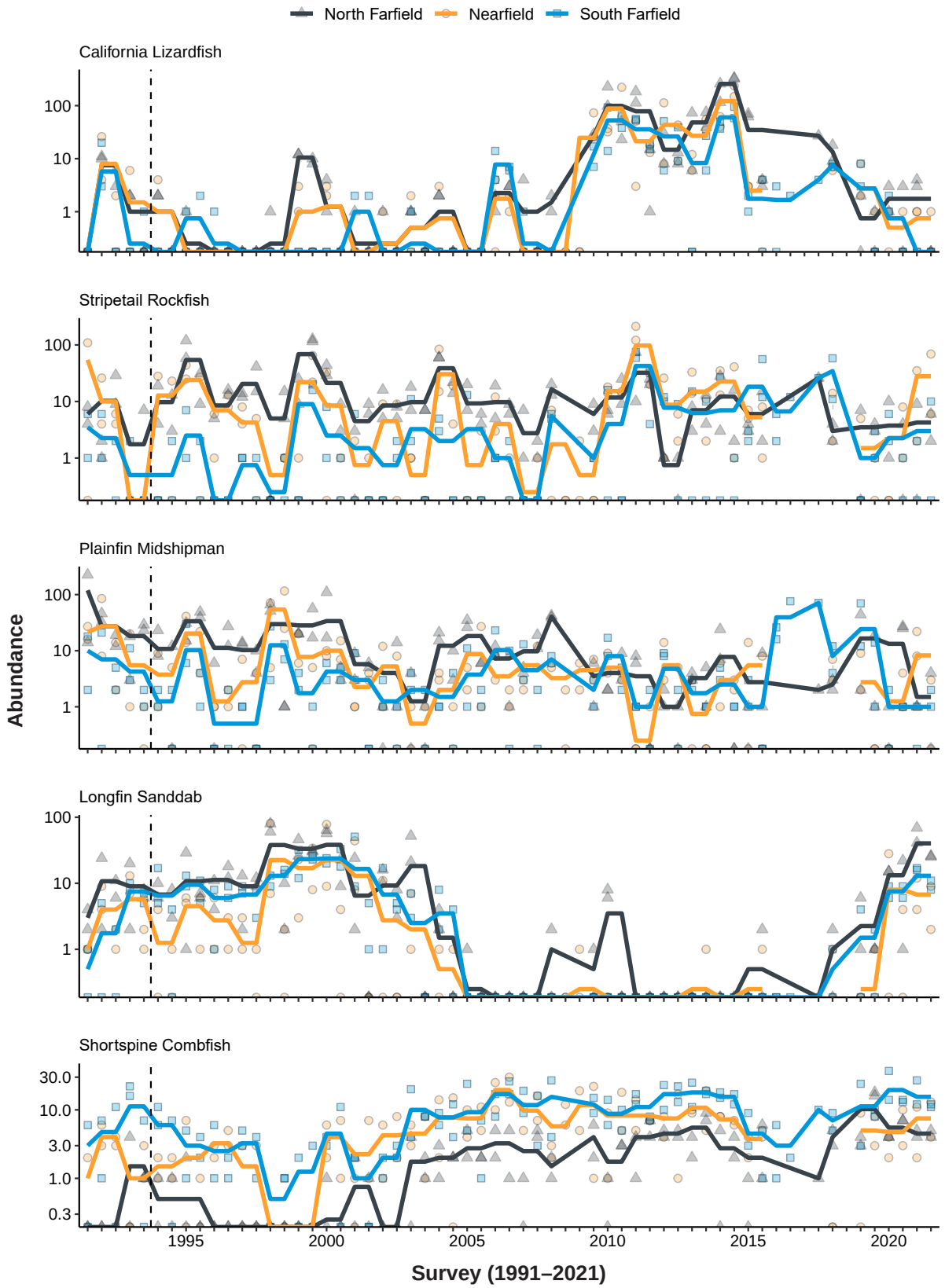

Figure 8.3 *continued*

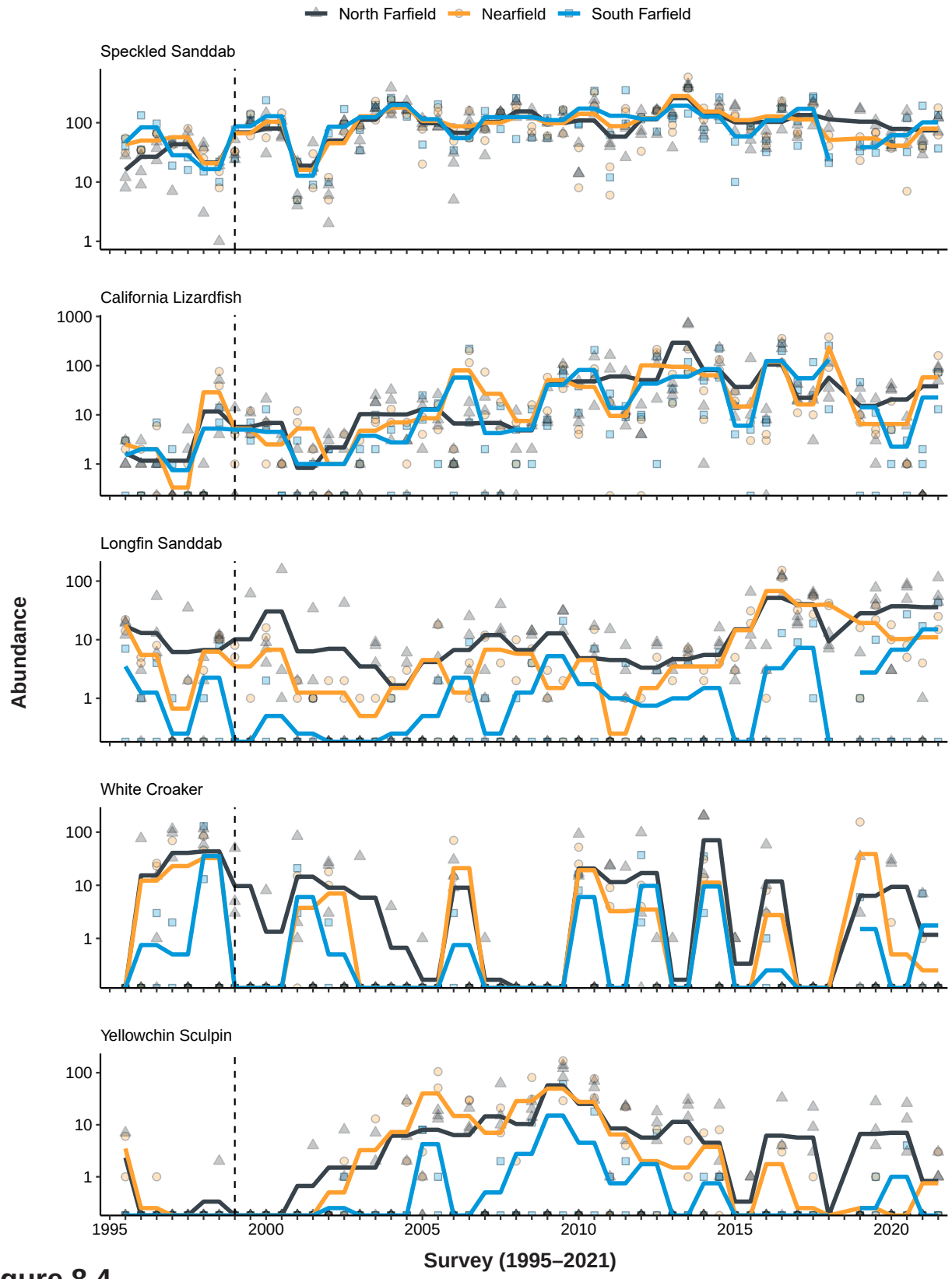

Figure 8.4

The ten most abundant demersal fish species (presented in order) collected from SBOO trawl stations sampled from 1995 through 2021. Data are limited to 10-minute trawls and are presented as quarterly means (lines) and total values per haul for north farfield (triangles), nearfield (circles), and south farfield (squares) stations. Dashed lines indicate onset of wastewater discharge.

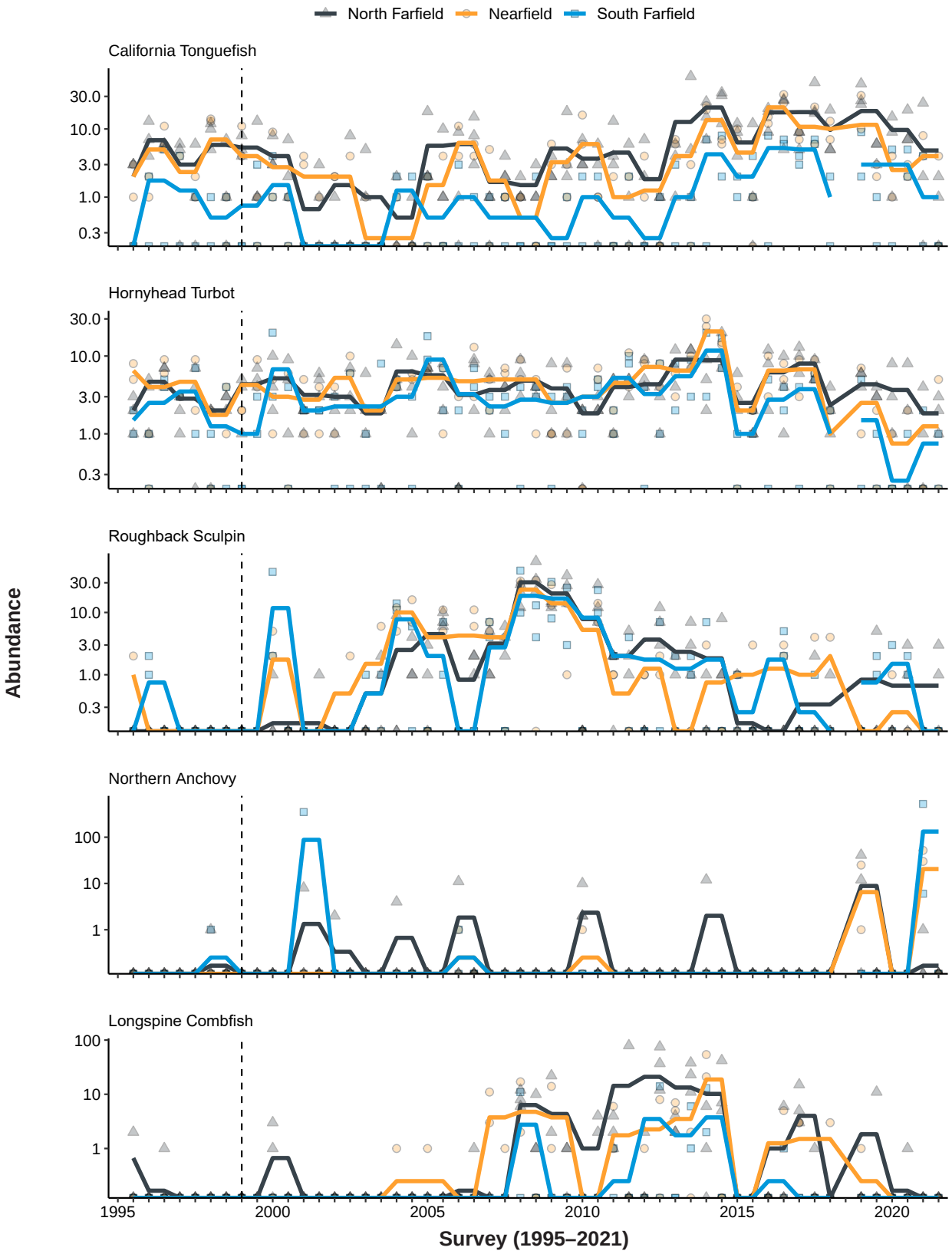

Figure 8.4 *continued*

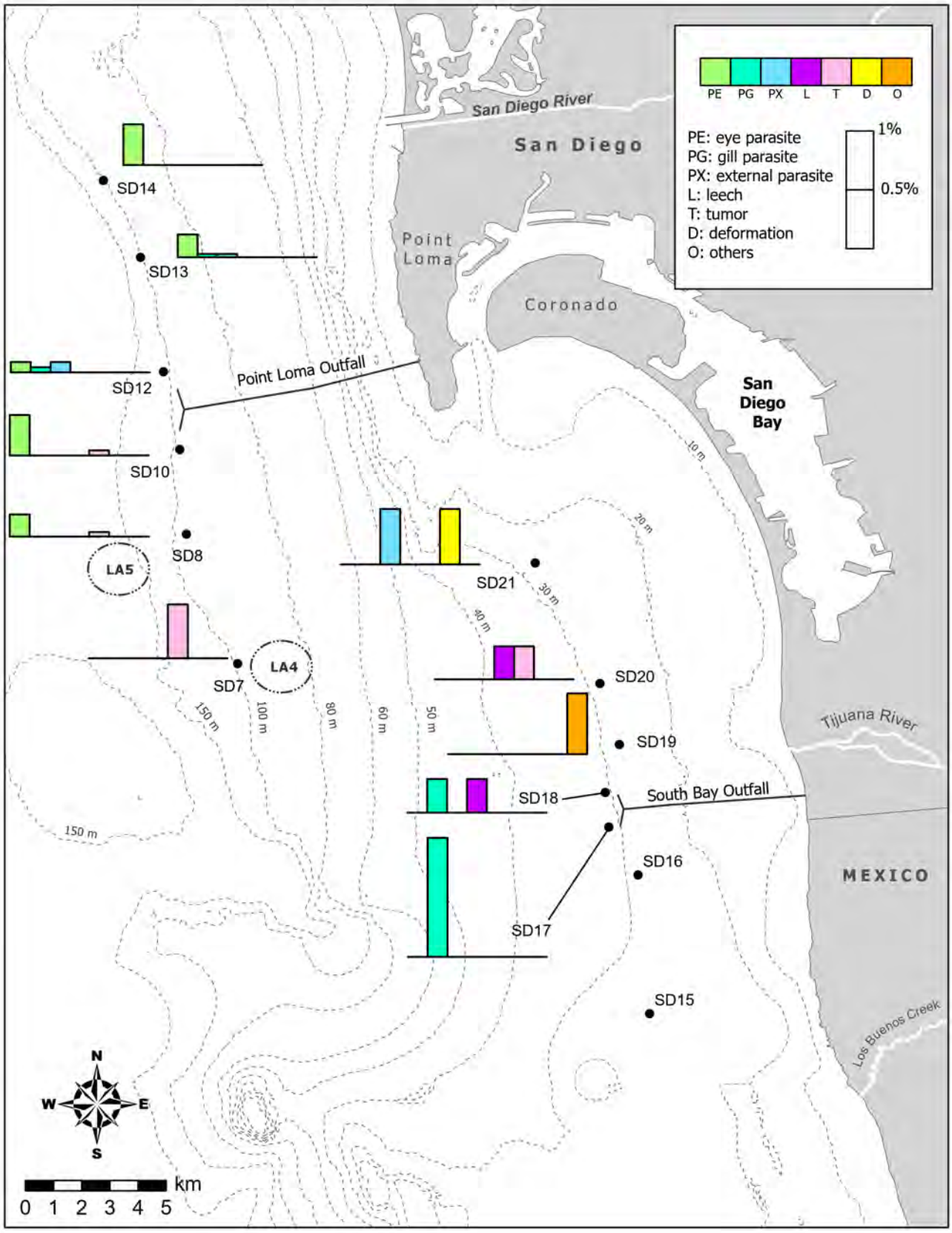

Figure 8.5
Percentages of fishes collected at stations with anomalies present during 2020 and 2021. PE = eye parasite; PG = gill parasite; PX = external parasite; L = leech; T = tumor; D = deformation; O = others.

additional *E. vulgaris* specimens were noted as being present during each survey. Since *E. vulgaris* often become detached from their hosts during retrieval and sorting of the trawl catch, it is unknown which fishes were parasitized by these isopods. However, *E. vulgaris* is known to be especially common on Pacific and Speckled Sanddab, and California Lizardfish in southern California waters where it may reach infestation rates of 3% and 80%, respectively (see Brusca 1978, 1981).

Classification of Demersal Fishes Assemblages

PLOO Region

Cluster and ordination analyses of a total of 167 trawls resulted in four ecologically-relevant SIMPROF-supported groups, or types of assemblages, in the PLOO region over the past 31 years (cluster groups A–D; Figure 8.6, Appendix I.6). These assemblages represented from 1 to 132 hauls each and varied in both species richness and abundance per haul. A BEST/BVSTEP ($\rho = 0.952$, $p \leq 0.001$, number of permutations = 999) test implicated Bay Goby, California Lizardfish, Dover Sole, English Sole, Halfbanded Rockfish, Longfin Sanddab, Longspine Combfish, Pacific Sanddab, Pink Seaperch, Plainfin Midshipman, Shortspine Combfish, Slender Sole, Spotfin Sculpin, Stripetail Rockfish, and Yellowchin Sculpin as being influential to the overall pattern (gradient) of the cluster dendrogram. Overall, the data show that when sites are compared over time, the outfall sites are not different from the farfield sites (Figure 8.6). Instead, assemblages appeared to be influenced by the distribution of the more abundant species or unique characteristics of specific station locations (e.g., habitat differences). For example, assemblages from stations SD7 and SD8 located south of the outfall often grouped apart from the remaining stations between 1993 and 2002, and station SD7 remained unique in 2007, 2016, and 2020 (see group C). The species composition and main descriptive characteristics of each of the four cluster groups are included below.

Cluster group A represented a unique assemblage sampled at nearfield trawl station SD12 in 1998 (Figure 8.6, Appendix I.6). The assemblage represented by cluster group A was characterized by the highest species richness (16 species/haul), second highest total abundance (261/haul), and third highest mean abundance of Pacific Sanddabs of any cluster group (75/haul). Plainfin Midshipman ($\bar{x}$ = 116/haul) and Gulf Sanddab ($\bar{x}$ = 5/haul) also contributed to the dissimilarity between this and other cluster groups.

Cluster group B was the largest group, representing assemblages from a total of 132 hauls that were conducted across the entire monitoring period (Figure 8.6). Approximately 41% (n = 20) of the trawls conducted from 1991 through 1998 were in this cluster group, including mostly nearfield and north farfield station assemblages. After 1998, this was the dominant cluster group across all stations, apart from three assemblages in cluster group C at station SD7 in 2007, 2016, and 2020. Assemblages in cluster group B averaged 15 species of fish, 361 individuals, and 212 Pacific Sanddab per haul (Figure 8.6, Appendix I.6). Along with Pacific Sanddabs, Dover Sole ($\bar{x}$ = 26/haul), Halfbanded Rockfish ($\bar{x}$ = 27/haul), Longspine Combfish ($\bar{x}$ = 18/haul), and Shortspine Combfish ($\bar{x}$ = 6/haul) were the other four most characteristic species of these assemblages.

Cluster group C was the second largest cluster group, representing assemblages from a total of 32 hauls that included 54% (n = 48) of the trawls conducted from 1991 through 1998 (Figure 8.6). Trawls at station SD7 in 2001, 2002, 2007, 2016, and 2020 were also included in this cluster group. These assemblages averaged 13 species and 148 individuals per haul. The most characteristic species of cluster group C were Pacific Sanddab ($\bar{x}$ = 86/haul), Plainfin Midshipman ($\bar{x}$ = 16/haul), Dover Sole ($\bar{x}$ = 10/haul), and Longfin Sanddab ($\bar{x}$ = 5/haul) (Appendix I.6).

Cluster group D represented two unique assemblages sampled at nearfield station SD10 in 1997 and south farfield station SD8 in 2001(Figure 8.6). These assemblages included the smallest hauls, averaging just 10 species and 47 individuals per haul, and had

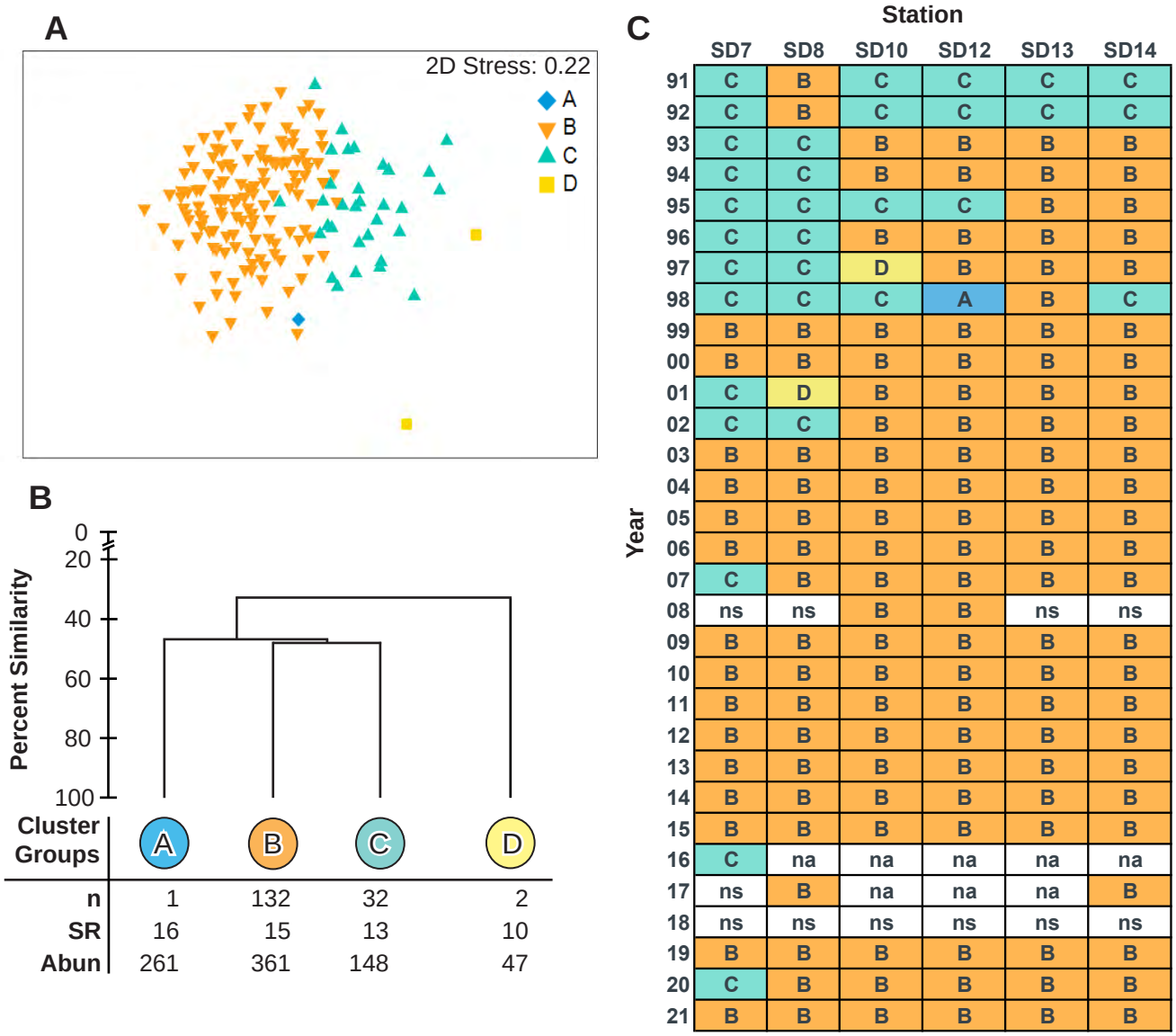

Figure 8.6

Results of ordination and cluster analysis of demersal fish assemblages from PLOO trawl stations sampled from 1991 through 2021. Data are limited to 10-minute trawls from summer surveys and presented as (A) nMDS ordination; (B) a dendrogram of main cluster groups; (C) a matrix showing distribution of cluster groups over time; n = number of hauls; SR = mean species richness; Abun = mean abundance; na = not analyzed; ns = not sampled.

the lowest average Pacific Sanddab abundance (30/haul). (Appendix I.6).

SBOO Region

Cluster and ordination analyses of a total of 182 trawls resulted in six ecologically-relevant SIMPROF-supported groups, or types of assemblages in the South Bay outfall region over the past 27 years (cluster groups A–F; Figure 8.7, Appendix I.7). These assemblages represented from 1 to 103 hauls each and represented a wide range of mean species richness (6–15 species/haul) and mean abundances (49–315/haul). A BEST/BVSTEP test ($\rho = 0.957$, $p \leq 0.001$, number of permutations = 999) implicated California Lizardfish, California Tonguefish, English Sole, Hornyhead Turbot, Longfin Sanddab, Roughback Sculpin, Speckled Sanddab, Spotted Turbot, and Yellowchin Sculpin as being influential to the overall pattern (gradient) of the cluster dendrogram. Overall, there were no discernable patterns associated with proximity to the SBOO

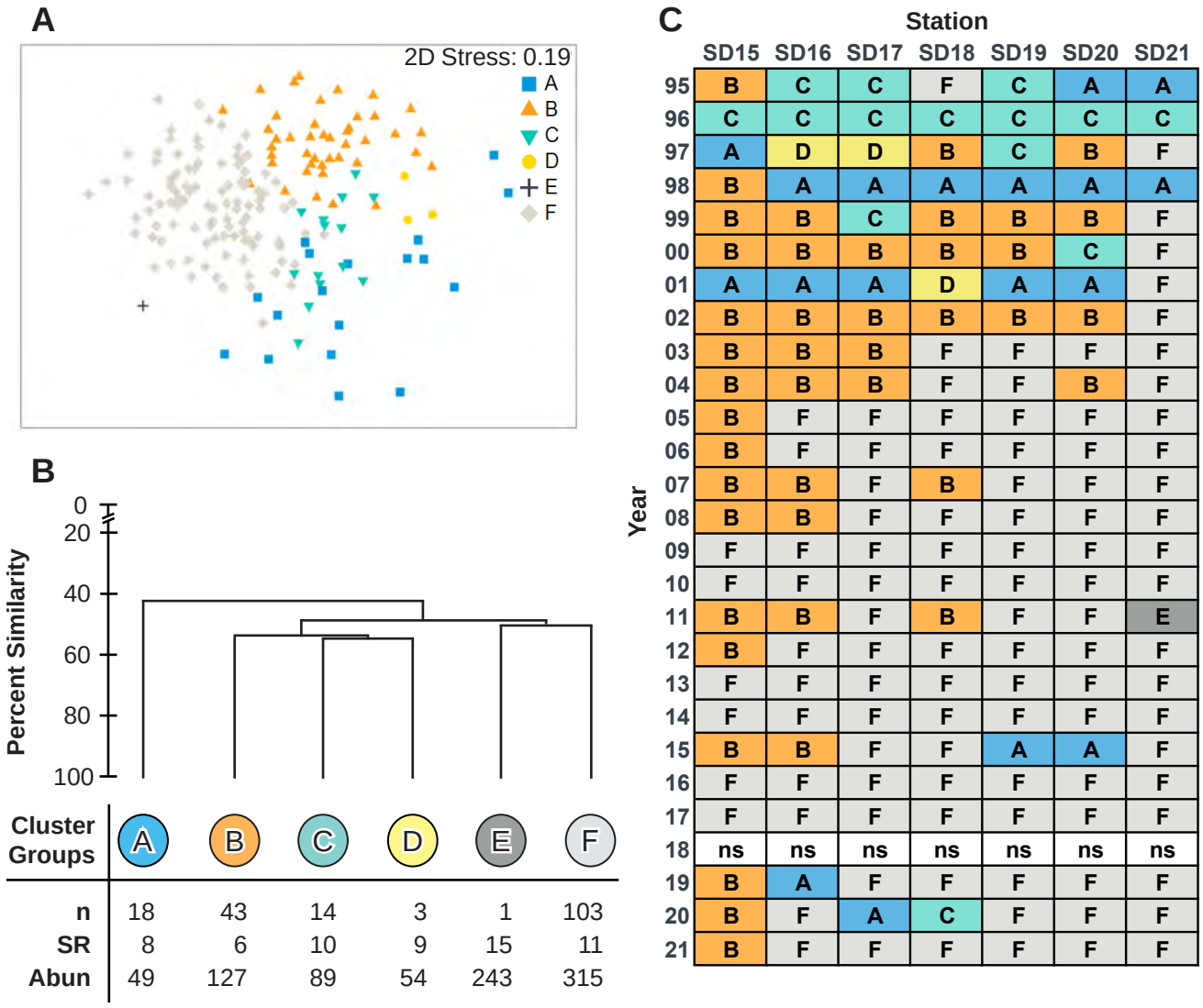

Figure 8.7

Results of ordination and cluster analysis of demersal fish assemblages from SBOO trawl stations sampled from 1995 through 2021. Data are limited to 10-minute trawls from summer surveys and presented as (A) nMDS ordination; (B) a dendrogram of main cluster groups; (C) a matrix showing distribution of cluster groups over time; n = number of hauls; SR = mean species richness; Abun = mean abundance; ns = not sampled.

discharge site. Instead, as observed in the PLOO region, SBOO fishes assemblages appear to be influenced by the distribution of the more abundant species or the unique characteristics of a specific station location. For example, cluster group A was distinguished by comparatively low abundances of Speckled Sanddab that generally coincided with or followed warm water El Niño events in 1994–1995, 1997–1998 and 2014–2016 (NOAA/NWS 2022). Furthermore, more hauls appear to group into cluster F over time, suggesting historical El Niño events and more recent above-average temperatures may be causing shifts in the region's communities (see Chapter 2: Ocean Conditions). Additionally, station SD15, located farthest south of the SBOO in northern Baja California waters, often grouped apart from the remaining stations (see cluster group B), possibly due to habitat differences such as sandier sediments (see Chapter 5: Sediment Quality). The species composition and main descriptive characteristics of each of the six cluster groups are included below.

Cluster group A comprised 18 hauls, including 28% (n = 14) of trawls between 1995 through 2001, and assemblages at north farfield stations SD19

and SD20 in 2015, south farfield station SD16 in 2019, and nearfield station SD17 in 2020 (Figure 8.7). Assemblages in this cluster group averaged 8 species and 49 individuals per haul and had the fewest number of Speckled Sanddab ($\bar{x}$ = 17/haul). Low numbers of California Lizardfish ($\bar{x}$ = 13/haul), Longfin Sanddab ($\bar{x}$ = 7/haul), and Hornyhead Turbot ($\bar{x}$ = 2/haul) were also characteristic of these trawls (Appendix I.7).

Cluster group B comprised 43 hauls, including 63% (n = 17) of the trawls from station SD15 and 33% (n = 9) of the trawls from station SD16 over the past 27 years (Figure 8.7). This cluster group also included 38% (n = 15) of the trawls conducted at stations SD17–SD20 from 1997 through 2004. The remaining two hauls from group B occurred at nearfield station SD18 in 2007 and 2011. This type of assemblage never occurred at station SD21. The assemblages represented by cluster group B averaged 6 species and 127 fishes per haul. These assemblages had the highest average numbers of Speckled Sanddab ($\bar{x}$ = 111/haul) (Appendix I.7).
Cluster group C represented assemblages from 14 trawls that included 30% (n = 13) of the trawls conducted across stations from 1995 through 2000, and one trawl conducted at nearfield station SD18 in 2020 (Figure 8.7). During summer 1996, all stations belonged to this cluster group, and their similar community compositions may be related to the warm water El Niño events in 1994–1995 (NOAA/NWS 2018). This cluster group averaged 10 species and 89 fishes per haul. The most characteristic species for this group were Speckled Sanddab ($\bar{x}$ = 53/haul), Longfin Sanddab ($\bar{x}$ = 10/haul), and Hornyhead Turbot ($\bar{x}$ = 5/haul) (Appendix I.7).

Cluster group D comprised 3 trawls, including south farfield station SD16 and SD17 conducted in 1997, and nearfield station SD18 conducted in 2001 (Figure 8.7). Assemblages represented by cluster group D averaged 9 species, 54 individuals, and 35 Speckled Sanddab per haul (Figure 8.7, Appendix I.7). In addition to Speckled Sanddab, the most characteristic species for this group were Hornyhead Turbot ($\bar{x}$ = 7/haul) and Spotted Turbot ($\bar{x}$ = 3/haul).

Cluster group E represented a unique assemblage at north farfield station SD21 conducted in 2011 (Figure 8.7). This assemblage had the highest species richness (15 species/haul) and abundance (243/haul), and the highest mean abundances of Longspine Combfish ($\bar{x}$ = 79/haul) and White Croaker ($\bar{x}$ = 22/haul) (Appendix I.7). These two species contributed to at least 18% and 9% of the dissimilarity to other cluster groups, respectively. Other species found in high abundances include Specked Sanddab ($\bar{x}$ = 26/haul), California Lizardfish ($\bar{x}$ = 75/haul), and Longfin Sanddab ($\bar{x}$ = 8/haul). California Lizardfish contributed to at least 11% of the dissimilarity to other cluster groups.

Cluster group F was the largest cluster group comprising 103 hauls spanning the entire monitoring period. This cluster group represented 11% (n = 6) of the hauls at nearfield and north farfield stations from 1995 through 2002, and 86% (n = 97) of all hauls conducted from 2003 through 2020 (Figure 8.7). Assemblages represented by cluster group F averaged 11 species and 315 individuals per haul, the highest average total abundance of all cluster groups. As the largest cluster group, these assemblages represented great variation in species richness (5–15 species/haul) and total abundance (96–1229/haul), as well as the highest average abundance (157/haul) and highest abundances (up to 587/haul) of Speckled Sanddab (Appendix I.7). This group was also characterized by the highest average abundances of California Lizardfish ($\bar{x}$ = 81/haul, up to a max of 726/haul) and Longfin Sanddab ($\bar{x}$ = 25/haul). Though not a characteristic species of cluster group F, Yellowchin Sculpin were collected in greatest abundances from hauls in this cluster group, which contributed to 5% of the dissimilarity to other cluster groups.

Of trawls conducted in the summers of 2020 and 2021, about 71% belonged to cluster group F and were characterized by moderate abundances (43–178/haul) of Speckled Sanddab. Likewise, the spike in California Lizardfish in 2021 across all stations except SD15 resulted in these hauls clustering alongside those from 2006 on, when as many as

726 California Lizardfish were collected in a haul. Hauls from summer 2020 at farfield stations SD16 and SD19–SD21 also belonged to this cluster group and were characterized by moderate abundances of Speckled Sanddab and Longfin Sanddab.

Megabenthic Invertebrate Populations in 2020–2021

A total of 166,094 invertebrates were captured from the 52 trawls conducted within the PLOO and SBOO monitoring regions in 2020–2021, representing 78 taxa from seven phyla (Annelida, Arthropoda, Brachiopoda, Echinodermata, Mollusca, Cnidaria, Silicea) (Appendices I.8, I.9). The pelagic red crab *Pleuroncodes planipes* continued to dominate PLOO trawl-caught invertebrates during the current reporting period, occurring in 33% of the hauls and accounting for 92% of the invertebrates collected (Table 8.4). In contrast, the sea urchin *Lytechinus pictus* occurred in 92% of the PLOO trawls, but only accounted for 6% of the total catch. Other species that were collected in at least 50% of the trawls, but in low numbers (≤ 56/haul), included the shrimp *Sicyonia ingentis*, the crab *Platymera gaudichaudii*, and the sea star *Astropecten californicus*. The mass migration of *P. planipes* in to the PLOO region, which peaked between 2016 and 2020 at stations SD12 and SD13, was thought to be associated with localized ecological changes as during this time, the presence of historically influential species decreased as did species richness and diversity (City of San Diego 2018, 2020). In 2014 and 2015, stations SD12 and SD13 were primarily dominated by the sea urchins *L. pictus* and *Strongylocentrotus fragilis* along with the sea pen *Acanthoptilum* sp, the brittle star *Ophiura luetkenii*, and the shrimp *Sicyonia ingentis*. Species richness at these stations ranged from 8 to 13 species per haul and diversity ranged from 0.2 to 1.5 (City of San Diego 2015, 2016). Following the sharp increase in abundance of *P. planipes*, species richness and diversity at SD12 and SD13 decreased to a range of 4 to 7 species per haul and 0.03 to 0.8, respectively during 2018 to 2020 (City of San Diego 2019, 2020, 2021). As of 2021, *P. planipes* have reduced in number and a gradual return to background conditions appears evident, although species richness is still relatively low. Diversity has improved and now ranges from 0.1 to 1.5 at SD12 and SD13 (Table 8.6).

Table 8.4
Top 15 most abundant megabenthic invertebrate species collected from 18 trawls conducted in the PLOO region during 2020 and 2021. PA = percent abundance; FO = frequency of occurrence; MAH = mean abundance per haul; MAO = mean abundance per occurrence.

Species	PA	FO	MAH	MAO
Pleuroncodes planipes	92	33	6317	18,952
Lytechinus pictus	6	92	431	470
Sicyonia ingentis	1	75	56	75
Platymera gaudichaudii	<1	58	19	33
Astropecten californicus	<1	62	2	3
Luidia foliolata	<1	42	1	4
Paguroidea	<1	4	1	32
Luidia asthenosoma	<1	25	1	5
Ophiothrix spiculata	<1	12	1	9
Apostichopus californicus	<1	46	1	1
Paguristes bakeri	<1	12	1	5
Ophiura luetkenii	<1	25	1	2
Luidia armata	<1	25	1	2
Neocrangon zacae	<1	17	1	3
Ophiopholis bakeri	<1	12	<1	3

In contrast to the PLOO region, no single species dominated SBOO trawls over the past two years. Rather, four species occurred in more than 50% of the hauls and accounted for 4% to 36% of the total catch, including the shrimps *Crangon nigromaculata* and *Sicyonia penicillata,* the sea star *A. californicus,* and the sea urchin *L. pictus* (Table 8.5). Rare species in both regions that are not included in Tables 8.4 and 8.5 can be found in Appendices I.8 and I.9.

Megabenthic Invertebrate Community Structure Parameters

No notable spatial patterns in megabenthic invertebrate community parameters were observed relative to the proximity of the PLOO or SBOO discharge sites during 2020–2021. Results were generally consistent with previous findings for the two regions and elsewhere in the SCB (e.g., Allen et al. 1998, 2002, 2007, 2011, City of

San Diego 1995, 1998, Walther et al. 2017, Wisenbaker et al. 2021). For example, species richness and diversity were consistently low (SR ≤ 15; H' ≤ 2.2), whereas abundance remained highly variable among both nearfield and farfield stations and between surveys over the past two years, with values ranging from 7 to 46,255 individuals/haul (Table 8.6).

Within the PLOO region, species richness and diversity varied both over time and across stations, both nearfield and farfield. Much of this variation may be correlated with the population dynamics of *Pleuroncodes planipes* and *Lytechinus pictus*, which collectively accounted for 98% of the invertebrates collected during 2020 and 2021 (Table 8.4). For instance, some of the lowest diversity values in the region (H' ≤ 0.03–0.1), were seen during winter 2020, when *P. planipes* was collected in excessive abundances (≥ 23,890/haul) for four of the six stations. However, during 2021, *P. planipes* was not seen in any PLOO hauls, but *L. pictus* abundances rose to 4272 individuals sampled in the winter and 2551 individuals sampled in the summer, effectively replacing *P. planipes* as the dominant species.

Within the SBOO region, overall species richness and diversity were higher than seen in the PLOO region, due to a lack of one or two species dominating the area. For instance, the three most abundant species in the SBOO region, the shrimp *Crangon nigromaculata*, the sea star *Astropecten californicus*, and the brittle star *Ophiothrix spiculata*, only accounted for 63% of the total abundance (Table 8.5). The highest diversity (H' = 2.2) and third highest species richness (13 species/haul) were seen at SD17 in the winter of 2020. This was accounted for by the fact that 13 species were present and no one species had an abundance greater than 8 individuals. Conversely, the lowest species richness (3 species/haul) and diversity (H' = 0.2) were seen at stations SD19 and SD20 in the summer of 2021. This is explained by the presence of relatively high abundances of the sea star *A. californicus* at these stations (83/haul and 51/haul respectively) (Table 8.6).

Table 8.5
Top 15 most abundant megabenthic invertebrate species collected from 21 trawls conducted in the SBOO region during 2020 and 2021. PA = percent abundance; FO = frequency of occurrence; MAH = mean abundance per haul; MAO = mean abundance per occurrence.

Species	PA	FO	MAH	MAO
Crangon nigromaculata	36	68	26	39
Astropecten californicus	18	86	13	15
Ophiothrix spiculata	9	32	7	20
Philine auriformis	7	46	5	11
Lytechinus pictus	5	57	4	7
Sicyonia penicillata	4	54	3	5
Crangon alba	3	18	2	14
Lovenia cordiformis	3	29	2	8
Portunus xantusii	2	50	2	3
Dendraster terminalis	2	21	1	6
Heptacarpus stimpsoni	2	11	1	11
Luidia armata	1	46	1	2
Pyromaia tuberculata	1	39	1	2
Pagurus spilocarpus	1	25	<1	2
Suberites sp	<1	29	<1	1

Historical comparisons indicate no notable spatial patterns in megabenthic invertebrate community parameters relative to the proximity of the PLOO or SBOO discharge sites, or to the onset of wastewater discharge that began in 1994 or 1999, respectively (Figure 8.8). Over the past 27–31 years (the length of time current data sets have been collected for the SBOO and PLOO region, respectively), mean species richness has remained below 24 per haul and mean diversity has remained below 2.3 per haul collectively for both regions. However, there has been considerably greater variability in mean abundance (10−5613 individuals/haul). The latter was largely due to population fluctuations of a few numerically dominant species in each region (Figures 8.9, 8.10). For example, differences in overall megabenthic invertebrate abundances at the PLOO stations tended to track population changes of the pelagic red crab *P. planipes*, the sea urchins *L. pictus* and *Strongylocentrotus fragilis*, the brittle star *Ophiura luetkenii*, the sea stars *Luidia foliolata* and *A. californicus*, the sea pen *Acanthoptilum* sp, the sea cucumber *Apostichopus californicus*, the shrimp *Sicyonia ingentis* and the crab *Platymera*

Table 8.6

Summary of megabenthic invertebrate community parameters for PLOO and SBOO trawl stations sampled during 2020 and 2021. Data are included for species richness, abundance, diversity (H').

	Station	2020 Winter	2020 Summer	2021 Winter	2021 Summer	2020 Winter	2020 Summer	2021 Winter	2021 Summer
		Species Richness				***Abundance***			
PLOO	SD7	7	9	8	9	24	28	85	76
PLOO	SD8	13	9	13	9	1092	1010	3917	1494
PLOO	SD10	9	6	10	7	24,242	839	50	1048
PLOO	SD12	5	4	5	4	46,255	11,558	15	178
PLOO	SD13	7	6	4	2	34,371	137	7	14
PLOO	SD14	7	5	8	3	36,118	1164	345	9
SBOO	SD15	10	9	15	8	45	46	116	60
SBOO	SD16	7	9	14	12	33	49	141	34
SBOO	SD17	13	10	11	12	34	75	141	39
SBOO	SD18	7	9	15	11	23	47	79	42
SBOO	SD19	7	2	15	3	64	48	277	87
SBOO	SD20	5	6	9	3	33	41	79	54
SBOO	SD21	6	5	11	6	46	32	222	31
		Diversity							
PLOO	SD7	1.8	1.7	1.3	1.6				
PLOO	SD8	0.3	0.1	0.1	0.1				
PLOO	SD10	0.1	0.1	1.8	0.1				
PLOO	SD12	0.1	0.3	1.5	0.1				
PLOO	SD13	0.03	0.4	1.3	0.4				
PLOO	SD14	0.1	0.3	0.3	1.0				
SBOO	SD15	1.6	1.6	1.7	1.6				
SBOO	SD16	1.4	1.3	0.9	2.0				
SBOO	SD17	2.2	0.8	0.5	2.0				
SBOO	SD18	1.5	1.4	1.7	1.5				
SBOO	SD19	1.3	0.4	1.3	0.2				
SBOO	SD20	1.2	0.6	0.9	0.2				
SBOO	SD21	1.0	0.6	0.6	1.1				

gaudichaudii (Figure 8.9). Differences in overall abundances at SBOO stations also tended to track population changes of *P. planipes* and *L. pictus* but these two species were not as dominant as in the PLOO region. Other species with strong influence in the SBOO region were the sea star *A. californicus*, the shrimps *Crangon nigromaculata* and *Sicyonia penicillata*, the snail *Philine auriformis*, the sand dollar *Dendraster terminalis*, the brittle star *O. spiculata*, the swimming crab *Portunus xantusii*, and the elbow crab *Latulambrus occidentalis.* An ecologically interesting note is the recently consistent presence of *S. penicillata* in the SBOO region. *S. penicillata* has a documented range of Puntarenas, Costa Rica in the south to Punta Canoas, Mexico in the north, with noted incursions in to the SCB only during El Niño events (Jensen 2014). However, since the 2014–2016 El Niño, *S. pencillata* appears to have established a resident population and has been seen with increased frequency and abundance in SBOO trawls (Figure 8.10). None of the observed changes appear to be associated with wastewater discharge from either outfall.

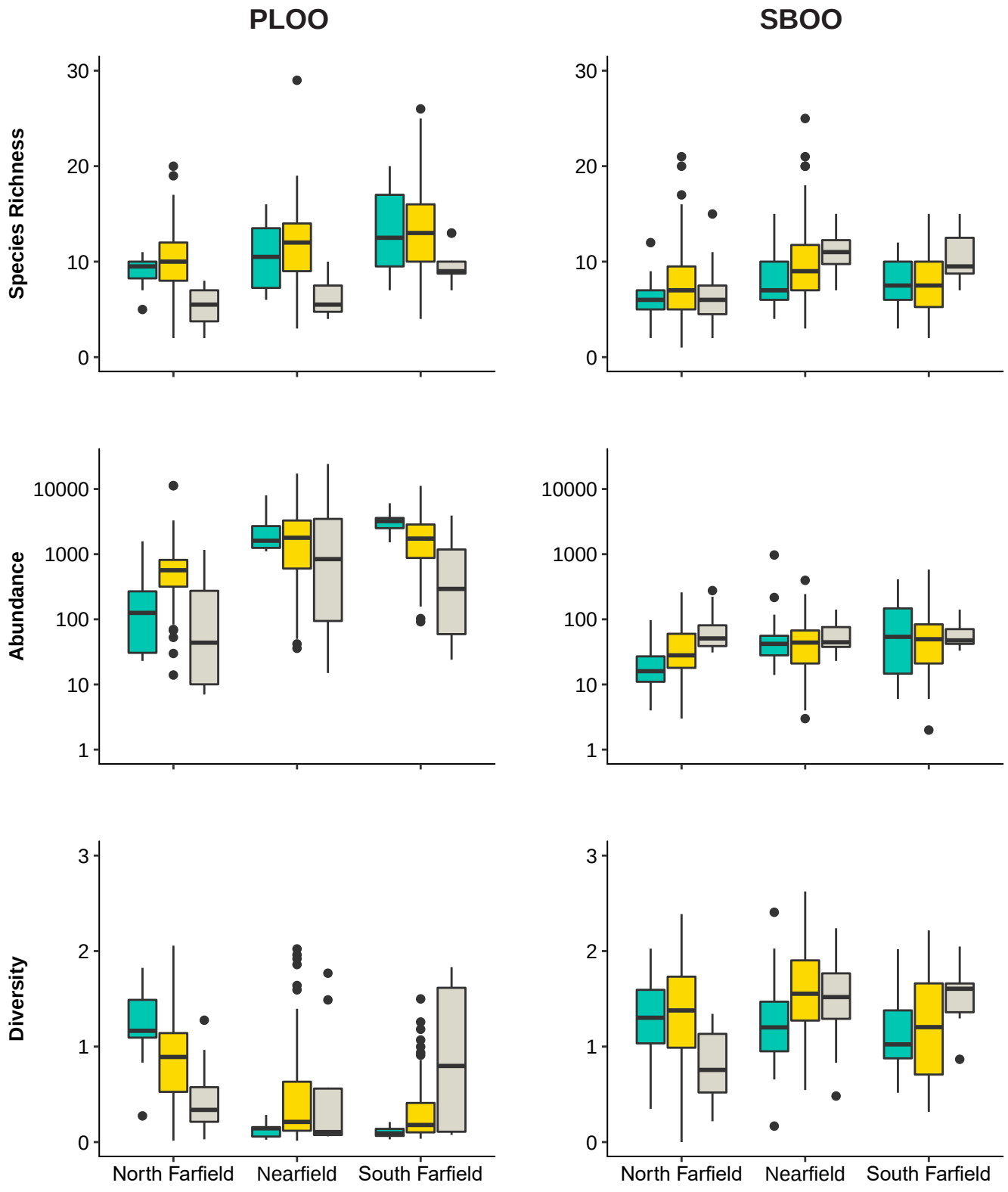

Figure 8.8

Species richness, abundance, and diversity (H') of megabenthic invertebrates collected from PLOO and SBOO north farfield, nearfield, and south farfield trawl stations during pre-discharge (green), historical post-discharge (yellow), and current post-discharge (grey) periods. Data are limited to 10-minute trawls. Boxes = median, upper, and lower quantiles; whiskers = 1.5x interquantile range; circles = outliers; see text for description of pre- versus post-discharge periods for the two outfalls.

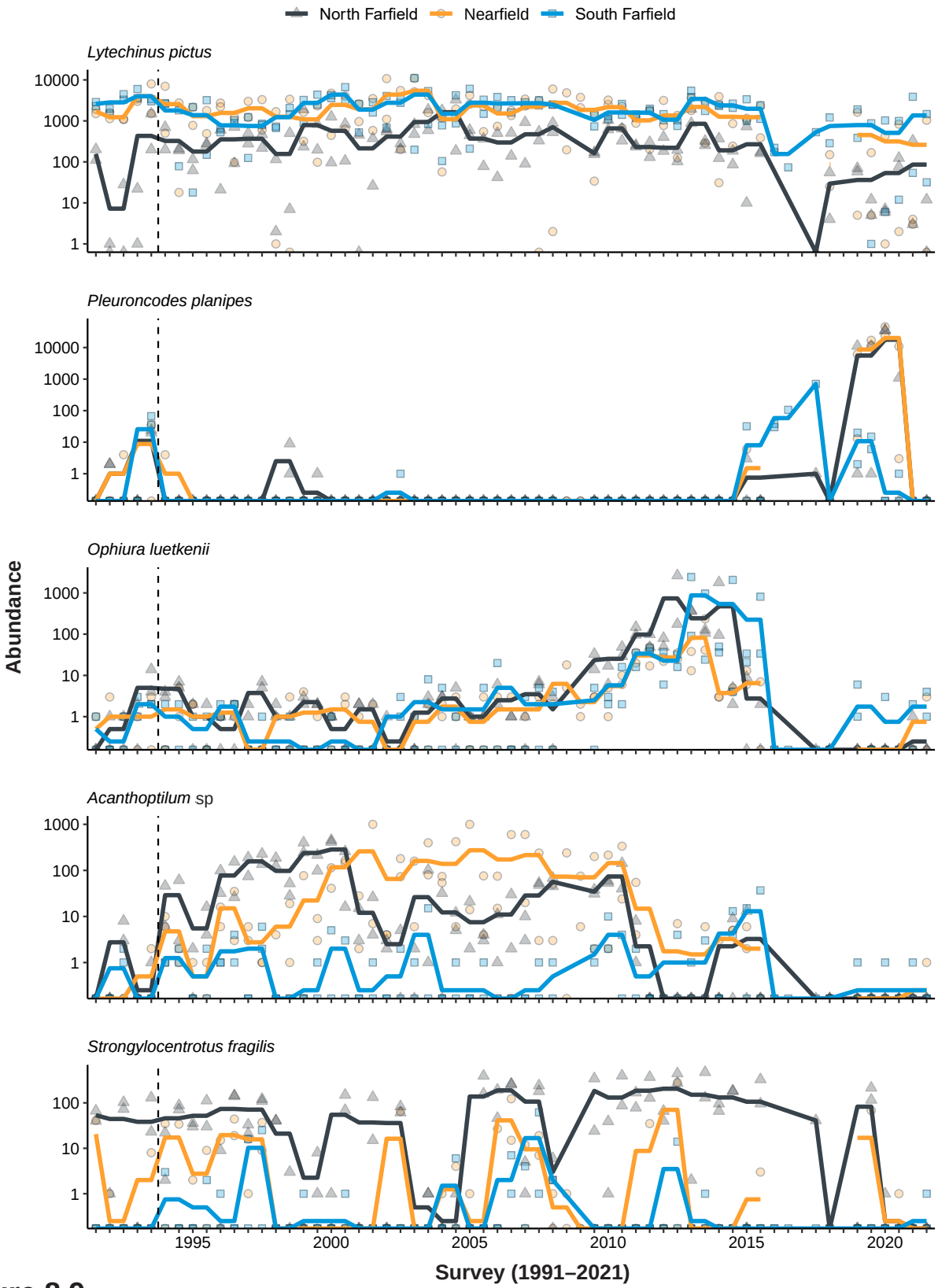

Figure 8.9

The ten most abundant megabenthic invertebrate species (presented in order) collected from PLOO trawl stations sampled from 1991 through 2021. Data are limited to 10-minute trawls and are presented as quarterly means (lines) and total values per haul for north farfield (triangles), nearfield (circles), and south farfield (squares) stations. Dashed lines indicate onset of wastewater discharge.

Figure 8.9 *continued*

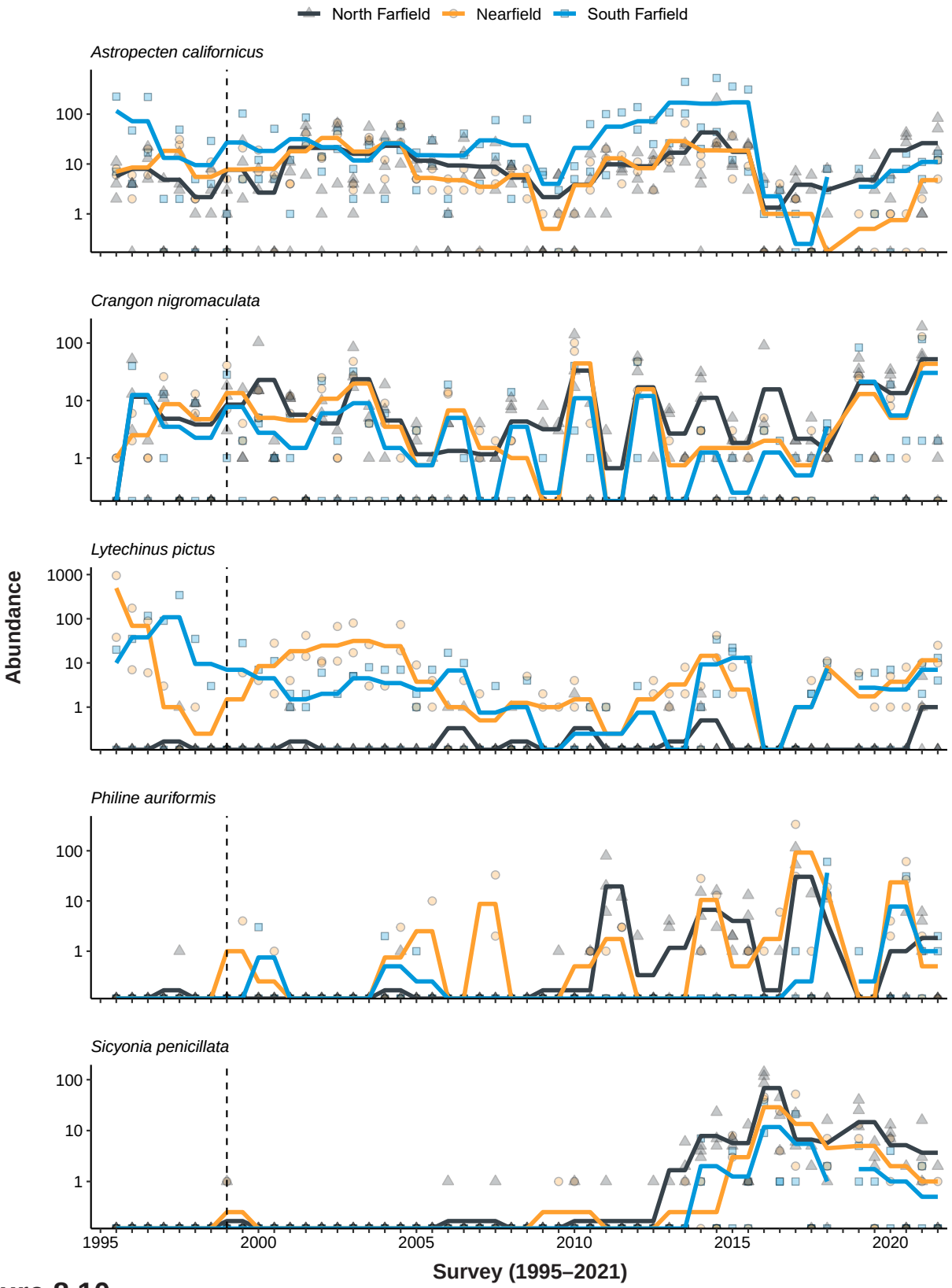

Figure 8.10

The ten most abundant megabenthic invertebrate species (presented in order) collected from SBOO trawl stations sampled from 1995 through 2021. Data are limited to 10-minute trawls and are presented as quarterly means (lines) and total values per haul for north farfield (triangles), nearfield (circles), and south farfield (squares) stations. Dashed lines indicate onset of wastewater discharge.

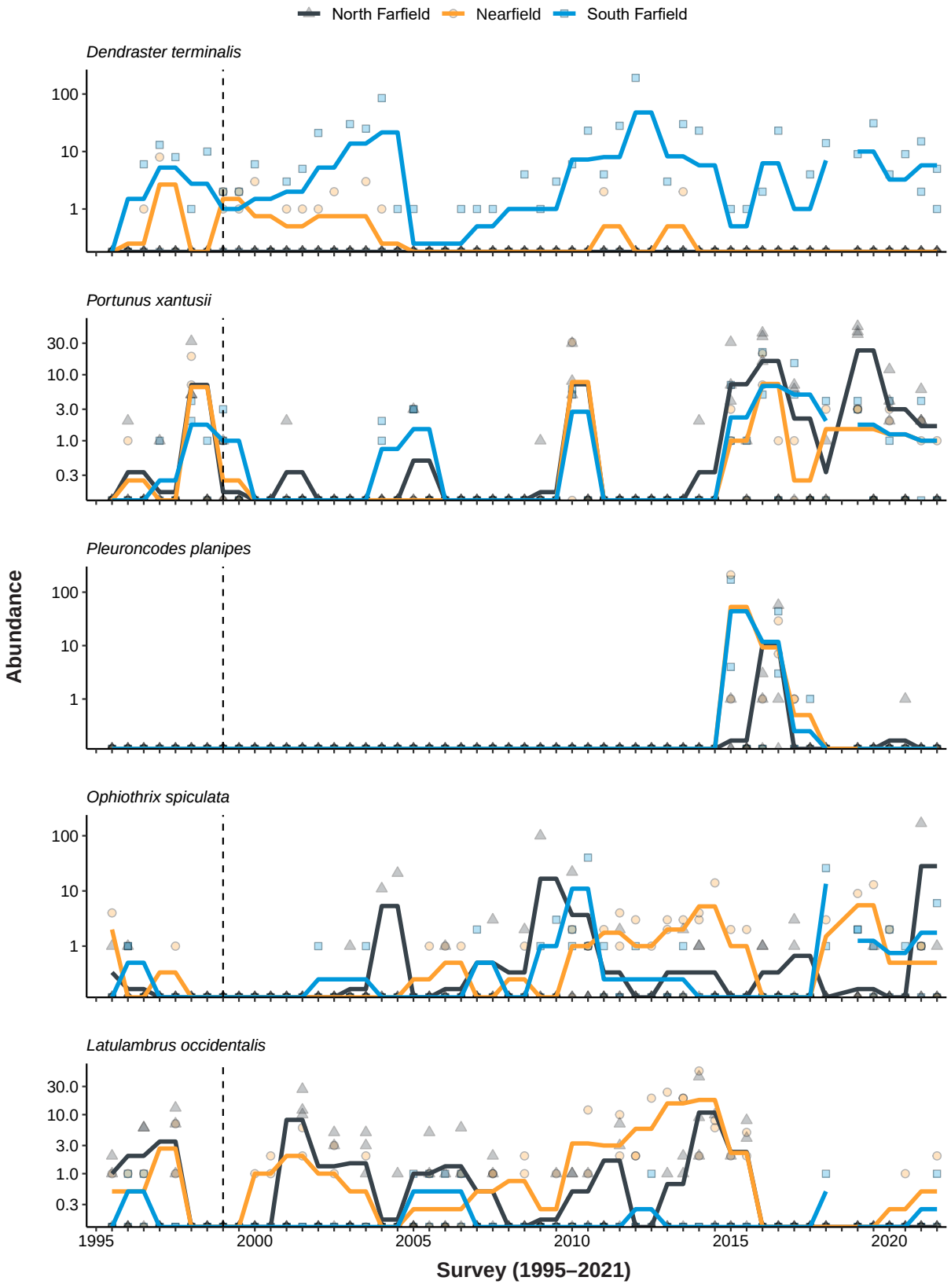

Figure 8.10 *continued*

Classification Analysis of Invertebrate Assemblages

PLOO Region

Cluster and ordination analyses of a total of 167 trawls resulted in six ecologically-relevant SIMPROF-supported groups or types of megabenthic invertebrate assemblages in the PLOO region over the past 31 years (cluster groups A–F). These assemblages represented from 1 to 97 hauls each, and varied in terms of species present, as well as the relative abundances per haul. A BEST/BVSTEP test ($\rho = 0.967$, $p \leq 0.001$, number of permutations = 999) implicated the sea pen *Acanthoptilum* sp, the sea urchins *Lytechinus pictus* and *Strongylocentrotus fragilis*, and the pelagic red crab *Pleuroncodes planipes*, as being influential to the overall pattern (gradient) of the cluster dendrogram. Overall, there were no discernible patterns associated with proximity to the PLOO discharge site. Instead, assemblages appear influenced by the distribution of the more abundant species or the unique characteristics of specific station locations. For example, stations SD13 and SD14 located north of the PLOO often grouped apart from the remaining stations (cluster group E) (Figure 8.11). The species composition and main descriptive characteristics of each of the six cluster groups are included below.

Cluster groups A and B were small "outlier" clusters that only occurred in the last 3–5 years; cluster group A occurred from 2019–2021 and cluster group B occurred from 2016–2020 (Figure 8.11). Cluster group A consisted of assemblages from 5 hauls and was tied for the lowest species richness (5 species/haul). It was primarily characterized by the shrimp *Sicyonia ingentis (*$\bar{x}$ = 49/haul), as well as *L. pictus (*$\bar{x}$ = 5/haul), the sea star *Luidia foliolata (*$\bar{x}$ = 2/haul) and the octopus *Octopus veligero (*$\bar{x}$ = 1/haul) (Appendix I.10). One of the more interesting characteristic species of cluster group A was *Octopus veligero*. While only 8 individuals were sampled in July 2021, its presence was distinctive. This species is historically rare in the SCB and is currently considered a transient. It was previously assumed that its presence in the region was linked to El Niño events, but further analysis did not support this association (Lilly, 2004). The last time it was seen in the San Diego region was in 2013 (n = 1). In 2021 it was sampled at nearfield stations SD10 (n = 1) and SD12 (n = 1), and north farfield stations SD13 (n = 2) and SD14 (n = 4). Cluster group B consisted of assemblages from 7 hauls and tied for the lowest mean species richness (5 species/haul). It was primarily dominated by *P. planipes (*$\bar{x}$ = 7514/haul) (Figure 8.11, Appendix I.10).

Cluster group C was comprised of one trawl at north farfield station SD14 in 2012. It had the second highest average abundance (3204/haul) and was heavily influenced by a large haul of the brittle star *Ophiura luetkenii* (2640 individuals). Other characteristic species included *L. pictus* (102 individuals), *S. fragilis* (442 individuals), *L. foliolata* (11 individuals), and *Astropecten californicus* (1 individual) (Figure 8.11, Appendix I.10).

Cluster group D was the largest group, representing assemblages from a total of 97 hauls. The majority of these hauls occurred at south farfield stations SD7 and SD8, and nearfield station SD10 (Figure 8.11). These assemblages had the highest average species richness (13 species/haul), but over time species richness was highly variable, ranging from 6-29 species per haul. Abundance also varied greatly over the years from 399–8026 individuals per haul with the mean abundance being 2260 individuals per haul. This group was characterized by the highest average number of *L. pictus* (2126/haul) (Appendix I.10).

Cluster group E was the second largest group, representing assemblages from a total of 50 hauls. The majority of these hauls occurred at the north farfield stations SD13 and SD14. These group E assemblages averaged 11 species per haul and 443 individuals per haul (Figure 8.11). The two most characteristic species of group E were *L. pictus* ($\bar{x}$ = 230/haul) and *S. fragilis* ($\bar{x}$ = 134/haul) (Appendix I.10).

Cluster group F comprised 7 hauls and had the second lowest average abundance ($\bar{x}$ = 150/haul).

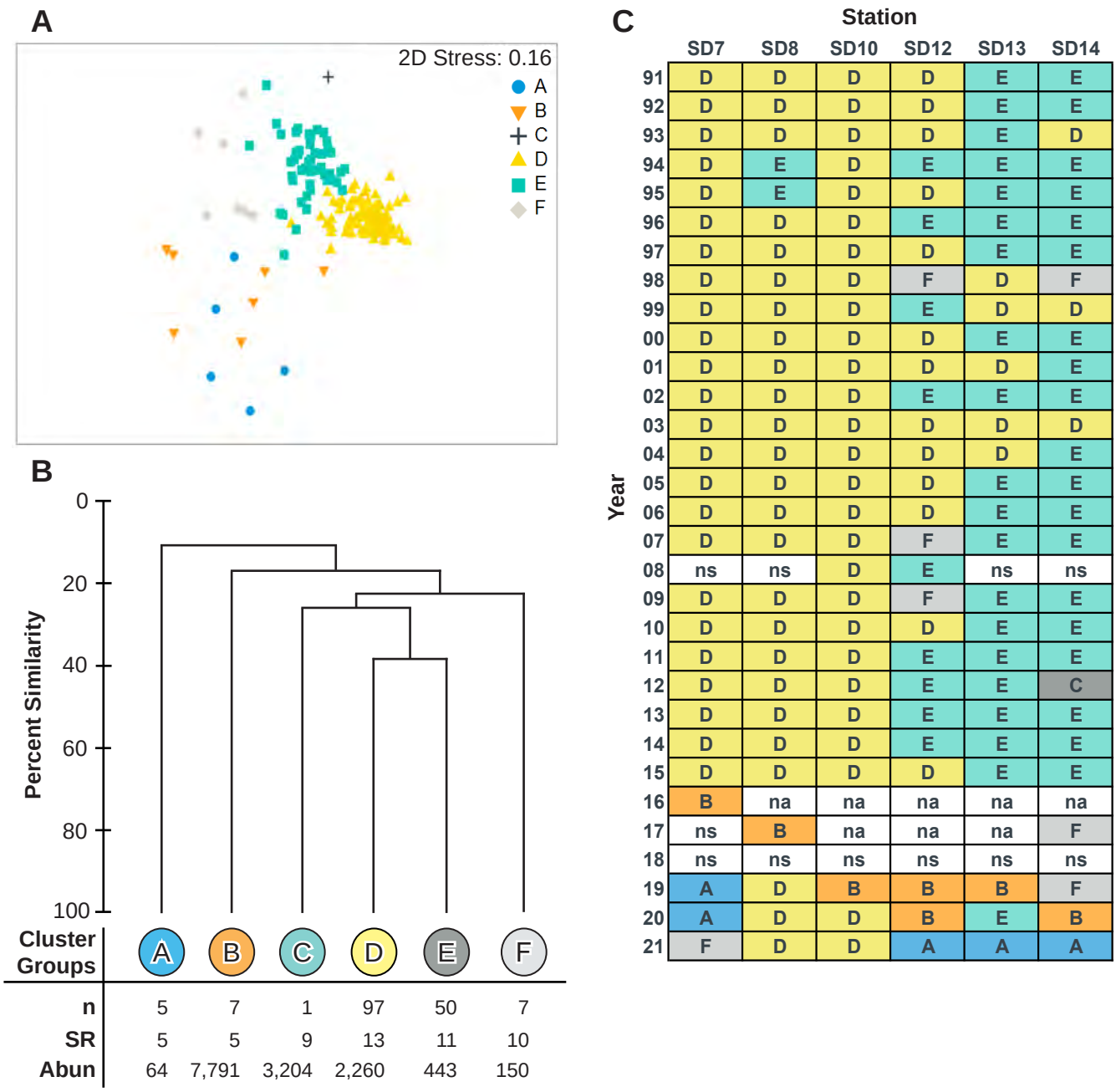

Figure 8.11

Results of ordination and cluster analysis of megabenthic invertebrate assemblages from PLOO trawl stations sampled from 1991 through 2021. Data are limited to 10-minute trawls from summer surveys and presented as (A) nMDS ordination; (B) a dendrogram of main cluster groups; (C) a matrix showing distribution of cluster groups over time; n = number of hauls; SR = mean species richness; Abun = mean abundance; na = not analyzed; ns=not sampled.

It was primarily influenced by the relatively high abundance of the sea pen *Acanthoptilum sp* ($\bar{x}$ = 69/haul) but other characteristic species of this cluster group included, *L. pictus* ($\bar{x}$ = 11/haul), *S. fragilis* ($\bar{x}$ = 40/haul), *S. ingentis* ($\bar{x}$ = 11/haul), and *A. californicus* ($\bar{x}$ = 5/haul). (Figure 8.11, Appendix I.10).

SBOO Region

Cluster and ordination analyses of a total of 182 trawls resulted in four ecologically-relevant SIMPROF-supported groups or types of megabenthic invertebrate assemblages in the SBOO region over the past 27 years (cluster groups A–D; Figure 8.12, Appendix I.11). These

assemblages represented from 1 to 159 hauls each, and varied in terms of species present, as well as the relative abundances of individual species. A BEST/BVSTEP test ($\rho = 0.95$, $p \leq 0.001$, number of permutations = 999) implicated the sea stars *Astropecten californicus*, *Pisaster brevispinus,* and *Luidia armata,* the shrimps *Crangon nigromaculata* and *Sicyonia penicillata,* the sand dollar *Dendraster terminalis,* the snails *Kelletia kelletii* and *Philine auriformis,* the dorid *Acanthodoris brunnea,* the cephalopod *Octopus rubescens,* the crabs *Latulambrus occidentalis*, *Metacarcinus gracilis, Pyromaia tuberculata*, and *Platymera gaudichaudii,* the urchin *Lytechinus pictus,* and the brittle star *Ophiothrix spiculata,* as being influential to the overall pattern (gradient) of the cluster dendrogram.

Overall, there were no discernible patterns associated with proximity to the SBOO discharge site (Figure 8.12). Instead, assemblages appear influenced by the distribution of the more abundant species during specific time periods (groups A and D) versus background conditions (group C). The species composition and main descriptive characteristics of each of the four cluster groups are included below.

SBOO invertebrate cluster groups A and B represented small "outlier" clusters that included one or two hauls. Cluster group A comprised 2 hauls from north farfield stations SD20 and SD21 in 2000, which averaged 4 species and 7 individuals per haul, respectively (Figure 8.12). These assemblages were primarily characterized by *C. nigromaculata* ($\bar{x}$ = 2/haul). Cluster group B represented a unique assemblage that occurred at south farfield station SD15 in 2009. This assemblage had 8 species and 84 individuals, of which 72 were specimens of the brittle star *Ophiura luetkenii*. Other characteristic species included *O. spiculata* (3/haul), *D. terminalis* (3/haul), the shrimp *Crangon alba* (2/haul), and the snail *Megastraea turbanica* (1/haul). (Appendix I.11).

SBOO invertebrate cluster group C comprised 159 hauls and was found at all stations a majority of the time between 1995 and 2021, likely reflecting background conditions within the region (Figure 8.12). Assemblages represented by cluster group C averaged 8 species per haul and 63 individuals per haul, but over time there was variability in both parameters with species richness ranging from 1–25 species per haul and abundance ranging from 2–975 individuals per haul. This cluster group was primarily characterized by *A. californicus* ($\bar{x}$ = 30/haul) and *P. brevispinus* ($\bar{x}$ = 1/haul) (Appendix I.11).

SBOO invertebrate cluster group D represented assemblages from a total of 6 hauls sampled in 2000, 2017, and 2019 (Figure 8.12). It occurred at south farfield (SD15 and SD16) and nearfield (SD17 and SD18) stations. Average species richness of hauls in this cluster was 8 species per haul and average abundance was 14 individuals per haul. The most characteristic species for cluster group D assemblages were *L. pictus* ($\bar{x}$ = 2/haul), *Crossata ventricosa* ($\bar{x}$ = 1/haul), *P. gaudichaudii* ($\bar{x}$ = <1/haul), and *K. kelletii* ($\bar{x}$ = <1/haul) (Appendix I.11).

Summary

Demersal fishes and megabenthic invertebrate populations monitored in 2020 and 2021 do not show evidence of negative impacts associated with proximity to wastewater discharge from the PLOO and SBOO. Community parameters are similar at stations located both near and far from the outfall discharge sites in both regions. Major community metrics, such as species richness, abundance, and diversity were generally within historical ranges reported for the San Diego region (City of San Diego 1995, 1998, 2000, 2022), and were representative of those characteristic of similar habitats throughout the SCB (e.g., Allen et al. 1998, 2002, 2007, 2011, Walther et al. 2017).

Over the past two years, Pacific Sanddab dominated assemblages surrounding the PLOO, and Speckled Sanddab dominated assemblages surrounding the SBOO, as they have done so since monitoring began in each region. Halfbanded Rockfish were also

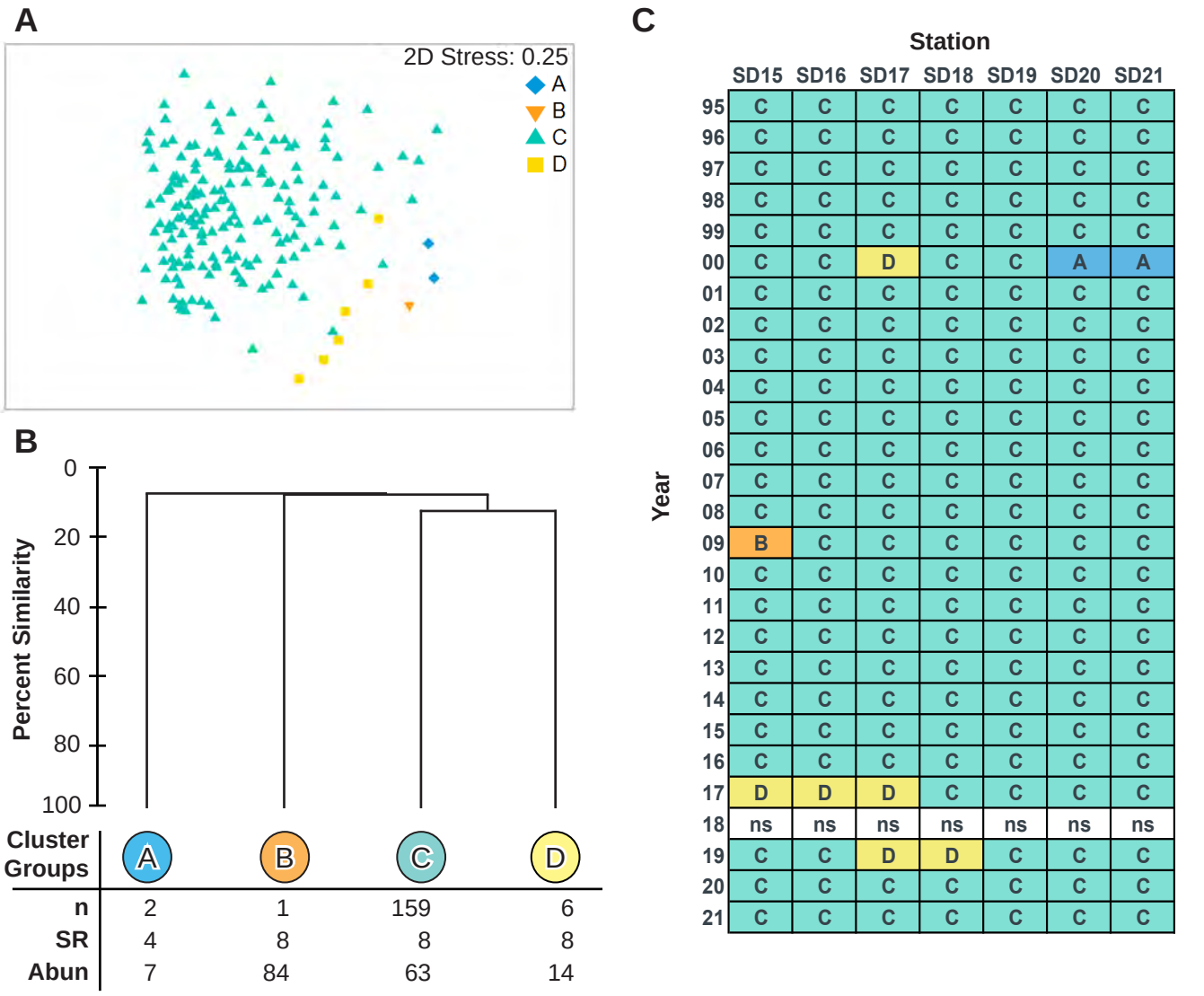

Figure 8.12

Results of ordination and cluster analysis of megabenthic invertebrate assemblages from SBOO trawl stations sampled from 1995 through 2021. Data are limited to 10-minute trawls from summer surveys and presented as (A) non-metric multi-dimensional scaling ordination; (B) a dendrogram of main cluster groups; (C) a matrix showing distribution of cluster groups over time; n = number of hauls; SR = mean species richness; Abun = mean abundance; ns = not sampled.

prevalent in PLOO assemblages during 2020–2021, while California Lizardfish were also prevalent within the SBOO region during this period, as they have also done so in eleven of the past thirteen years. Other commonly captured, but less abundant fishes, collected from the PLOO and SBOO regions included California Tonguefish, Dover Sole, English Sole, Longfin Sanddab, Northern Anchovy, Longspine Combfish, Shortspine Combfish, and White Croaker.

Of the 166,094 megabenthic invertebrates encountered during 2020 and 2021, 91% were the pelagic red crab *Pleuroncodes planipes,* collected exclusively at PLOO trawl stations. The arrival of large populations of *P. planipes* in the SCB is thought to be associated with El Niño events (Gordon 2015, Samenow 2015, Gartman et. al. 2016) with populations only remaining in the region for 1 to 2-year periods. However, this latest incursion of *P. planipes* remained in the San Diego region for five years (2015–2020) and may be indicative of a large scale climate-driven

effect on invertebrate population dynamics in the SCB. In contrast to the PLOO region, no single species of invertebrate dominated SBOO trawls over the past two years. Other commonly captured, but less abundant, trawl-caught invertebrates collected from the PLOO and SBOO regions included the sea urchin *Lytechinus pictus,* the shrimps *Sicyonia ingentis, S. penicillata,* and *Crangon nigromaculata,* the crab *Platymera gaudichaudii,* and the sea star *Astropecten californicus.* However, increasing occurrences of historically more southerly located species, such as *Octopus veligero* and *S. penicillata*, are potential indicators of large-scale climate driven effects of species distribution and occurrence, which will likely only increase in the future.

The abundance and distribution of species varied similarly at stations located near and far from the outfalls in both regions. The high degree of variability in these assemblages during this reporting period was similar to that observed in previous years, including before wastewater discharge began through either outfall (City of San Diego 1995, 1998, 2000, 2022). Furthermore, this sort of variability has been observed in similar habitats elsewhere off the coast of southern California (Allen et al. 1998, 2002, 2007, 2011, Walther et al. 2017). Consequently, changes in local community structure of these fishes and invertebrates are more likely due to natural factors, such as changes in ocean temperatures associated with El Niño or other large-scale oceanographic events. Finally, the rarity of disease indicators, or other physical abnormalities, in local fishes suggests that populations in the Point Loma and South Bay outfall regions continue to be unimpacted by wastewater discharge.

Literature Cited

Allen, L.G., D.J. Pondella II, and M.H. Horn. (2006). The Ecology of Marine Fishes: California and Adjacent Waters. University of California Press, Berkeley, CA.

Allen, M.J., S.L. Moore, K.C. Schiff, D. Diener, S.B. Weisburg, J.K. Stull, A. Groce, E. Zeng, J. Mubarak, C.L. Tang, R. Gartman, and C.I. Haydock. (1998). Assessment of demersal fish and megabenthic invertebrate assemblages on the mainland shelf of Southern California in 1994. Southern California Coastal Water Research Project, Westminster, CA.

Allen, M.J., A.K. Groce, D. Diener, J. Brown, S.A. Steinert, G. Deets, J.A. Noblet, S.L. Moore, D. Diehl, E.T. Jarvis, V. Raco-Rands, C. Thomas, Y. Ralph, R. Gartman, D. Cadien, S.B. Weisberg, and T. Mikel. (2002). Southern California Bight 1998 Regional Monitoring Program: V. Demersal Fishes and Megabenthic Invertebrates. Southern California Coastal Water Research Project, Westminster, CA.

Allen, M.J., T. Mikel, D.B. Cadien, J.E. Kalman, E.T. Jarvis, K.C. Schiff, D.W. Diehl, S.L. Moore, S. Walther, G. Deets, C. Cash, S. Watts, D.J. Pondella II, V. Raco-Rands, C. Thomas, R. Gartman, L. Sabin, W. Power, A.K. Groce, and J.L. Armstrong. (2007). Southern California Bight 2003 Regional Monitoring Program: IV. Demersal Fishes and Megabenthic Invertebrates. Southern California Coastal Water Research Project. Costa Mesa, CA.

Allen, M.J., D.B. Cadien, E. Miller, D.W. Diehl, K. Ritter, S.L. Moore, C. Cash, D.J. Pondella, V. Raco-Rands, C. Thomas, R. Gartman, W. Power, A.K. Latker, J. Williams, J.L. Armstrong, and K. Schiff. (2011). Southern California Bight 2008 Regional Monitoring Program: Volume IV. Demersal Fishes and Megabenthic Invertebrates. Southern California Coastal Water Research Project, Costa Mesa, CA.

Bengtsson, H. (2003). R.utils: The R.oo package - Object-Oriented Programming with References Using Standard R Code, Proceedings of the 3rd International Workshop on Distributed Statistical Computing (DSC 2003), ISSN 1609-395X, Hornik, K.; Leisch, F. & Zeileis, A.

Brusca, R.C. (1978). Studies on the cymothoid fish symbionts of the eastern Pacific (Crustacea: Cymothoidae). II. Systematics and biology of Livoneca vulgaris Stimpson 1857. Occasional Papers of the Allan Hancock Foundation. (New Series), 2: 1–19.

Brusca, R.C. (1981). A monograph on the Isopoda Cymothoidae (Crustacea) of the eastern Pacific. Zoological Journal of the Linnean Society, 73: 117–199.

City of San Diego. (1995). Outfall Extension Pre-Construction Monitoring Report (July 1991–October 1992). City of San Diego Ocean Monitoring Progra, Metropolitan Wastewater Department, Environmental Monitoring and Technical Services Division, San Diego, CA.

City of San Diego. (1998). San Diego Regional Monitoring Report for 1994–1997. City of San Diego Ocean Monitoring Program, Metropolitan Wastewater Department, Environmental Monitoring and Technical Services Division, San Diego, CA.

City of San Diego. (2000). International Wastewater Treatment Plant Final Baseline Ocean Monitoring Report for the South Bay Ocean Outfall (1995–1998). City of San Diego Ocean Monitoring Program, Metropolitan Wastewater Department, Environmental Monitoring and Technical Services Division, San Diego, CA.

City of San Diego. (2015). Point Loma Ocean Outfall Annual Receiving Waters Monitoring and Assessment Report, 2014. City of San Diego Ocean Monitoring Program, Public Utilities Department, Environmental Monitoring and Technical Services Division, San Diego, CA.

City of San Diego. (2016). Point Loma Ocean Outfall Annual Receiving Waters Monitoring and Assessment Report, 2015. City of San Diego Ocean Monitoring Program, Public Utilities Department, Environmental Monitoring and Technical Services Division, San Diego, CA.

City of San Diego. (2018). Biennial Receiving Waters Monitoring and Assessment Report for the Point Loma and South Bay Ocean Outfalls, 2016–2017. City of San Diego Ocean Monitoring Program, Public Utilities Department, Environmental Monitoring and Technical Services Division, San Diego, CA.

City of San Diego. (2019). Interim Receiving Waters Monitoring Report for the Point Loma Ocean Outfall and South Bay Ocean Outfalls, 2018. City of San Diego Ocean Monitoring Program, Public Utilities Department, Environmental Monitoring and Technical Services Division, San Diego, CA.

City of San Diego. (2020). Biennial Receiving Waters Monitoring and Assessment Report for the Point Loma and South Bay Ocean Outfalls, 2018–2019. City of San Diego Ocean Monitoring Program, Public Utilities Department, Environmental Monitoring and Technical Services Division, San Diego, CA.

City of San Diego. (2021). Interim Receiving Waters Monitoring Report for the Point Loma Ocean Outfall and South Bay Ocean Outfalls, 2020. City of San Diego Ocean Monitoring Program, Public Utilities Department, Environmental Monitoring and Technical Services Division, San Diego, CA.

City of San Diego. (2022). Appendix C.1 Benthic Sediments, Invertebrates, and Fishes. In: Application for Renewal of NPDES CA0107409 and 301(h) Modified Secondary Treatment Requirements Point Loma Ocean Outfall. Volume V, Appendix C. Public Utilities Department, Environmental Monitoring and Technical Services Division, San Diego, CA.

Clarke, K.R. (1993). Non-parametric multivariate analyses of changes in community structure. Australian Journal of Ecology, 18: 117–143.

Clarke, K.R., R.N. Gorley, P.J. Somerfield, and R.M. Warwick. (2014). Change in marine

communities: an approach to statistical analysis and interpretation, 3rd edition. PRIMER-E, Plymouth, England.

Clarke, K.R., P.J. Somerfield, and R.N. Gorley. (2008). Testing of null hypotheses in exploratory community analyses: similarity profiles and biota-environment linkage. Journal of Experimental Marine Biology and Ecology, 366: 56–69.

Cross, J.N. and L.G. Allen. (1993). Chapter 9. Fishes. In: M.D. Dailey, D.J. Reish, and J.W. Anderson (eds.). Ecology of the Southern California Bight: A Synthesis and Interpretation. University of California Press, Berkeley, CA. 459–540.

Cross, J.N., J.N. Roney, and G.S. Kleppel. (1985). Fish food habits along a pollution gradient. California Fish and Game, 71: 28–39.

Eschmeyer, W.N. and E.S. Herald. (1998). A Field Guide to Pacific Coast Fishes of North America. Houghton and Mifflin Company, New York.

Gartman, R., A.K. Latker, A. Brownlee, W. Enright, T. Stebbins. (2016). INVASION – the pelagic red crab, Pleuroncodes planipes, takes over the continental shelf off San Diego, California! 2016 Annual CalCOFI meeting. Dec 5-7. San Diego, CA. (Poster).

Gordon, J. (2015). Thousands of tuna crabs invade San Diego's beaches and it's thought that El Nino is to Blame. http://www.dailymail.co.uk/news/article-3122203/Thousands-tuna-crabs-invade-San-Diego-s-beaches-s-thought-El-Ni-o-blame.html

Grothendieck, G. (2014). sqldf: Perform SQL Selects on R Data Frames. R package version 0.4-10. http://CRAN.R-project.org/package=sqldf.

Helvey, M. and R.W. Smith. (1985). Influence of habitat structure on the fish assemblages associated with two cooling-water intake structures in southern California. Bulletin of Marine Science, 37: 189–199.

Hope, R.M. (2013). Rmisc: Ryan Miscellaneous. R package version 1.5. http://CRAN.R-project.org/package=Rmisc.

Jensen, G.C. (2014). Crabs and Shrimps of the Pacific Coast. A Guide to Shallow Water Decapods from Southeastern Alaska to the Mexican Border. MolaMarine Publication. WA. 240 pp.

Karinen, J.B., B.L. Wing, and R.R. Straty. (1985). Records and sightings of fish and invertebrates in the eastern Gulf of Alaska and oceanic phenomena related to the 1983 El Niño event. In: W.S. Wooster and D.L. Fluharty (eds.). El Niño North: El Niño Effects in the Eastern Subarctic Pacific Ocean. Washington Sea Grant Program, Seattle, WA. 253–267.

Kassambara, A. (2018). ggpubr: Based Publication Ready Plots R package version 0.2. http://www.sthda.com/english/rpkgs/ggpubr.

Kassambara, A. (2019). ggalt: 'ggplot2' Based Publication Ready Plots. alboukadel.kassambara@gmail.com.

Lilly, M. (2004). Octopus veligero: Permanent Resident or Fair-Weather Friend? The Festivus. Vol XXXVI(1): pp 3-8.

Murawski, S.A. (1993). Climate change and marine fish distribution: forecasting from historical analogy. Transactions of the American Fisheries Society, 122: 647–658.

[NOAA/NWS] National Oceanic and Atmospheric Administration/National Weather Service. (2022). Climate Prediction Center Website. https://origin.cpc.ncep.noaa.gov/products/analysis_monitoring/ensostuff/ONI_v5.php

Oksanen, J., F.G. Blanchet, R. Kindt, P. Legendre, P.R. Minchin, R.B. O'Hara, G.L. Simpson, P. Solymos, M. Henry, H. Stevens and H. Wagner. (2015). vegan: Community Ecology Package. R package version 2.3-0. http://CRAN.R-project.org/package=vegan.

Page, L., M., H. Espinosa-Pérez, L. T. Findley, C. R. Gilbert, R. N. Lea, N. E. Mandrak, R. L. Mayden, and J. S. Nelson. (2013). Common and Scientific names of fishes from the United States, Canada and Mexico. Special Publication 34. The American Fisheries Society, Bethesda, Maryland.

R Core Team. (2019). R: A language and environment for statistical computing. R Foundation for Statistical Computing, Vienna, Austria. URL https://www.R-project.org/.

Revelle, W. (2017) psych: Procedures for Personality and Psychological Research, Northwestern University, Evanston, Illinois, USA, https://CRAN.R-project.org/package=psych Version = 1.7.5.

Ripley, B. and M. Lapsley. (2015). RODBC: ODBC Database Access. R package version 1.3-12. http://CRAN.R-project.org/package=RODBC.

Samenow, J. (2015). Washington Post. https://www.washingtonpost.com/news/capital-weather-gang/wp/2015/06/17/red-crabs-swarm-southern-california-linked-to-warm-blob-in-pacific/?utm_term=.0632ac357d58

[SCAMIT] Southern California Association of Marine Invertebrate Taxonomists. (2018). A taxonomic listing of benthic macro- and megainvertebrates from infaunal and epibenthic monitoring programs in the Southern California Bight, edition 12. Southern California Associations of Marine Invertebrate Taxonomists, Natural History Museum of Los Angeles County, Research and Collections, Los Angeles, CA.

[SCCWRP] Southern California Coastal Water Research Project. (2018). Southern California Bight 2018 Regional Monitoring Program: Contaminant Impact Assessment Field Operations Manual. Southern California Coastal Water Research Project. Costa Mesa, CA.

Stein, E.D. and D.B. Cadien. (2009). Ecosystem response to regulatory and management actions: The southern California experience in long-term monitoring. Marine Pollution Bulletin, 59: 91–100.

Thompson, B., J. Dixon, S. Schroeter, and D.J. Reish. (1993a). Chapter 8. Benthic invertebrates. In: M.D. Dailey, D.J. Reish, and J.W. Anderson (eds.). Ecology of the Southern California Bight: A Synthesis and Interpretation. University of California Press, Berkeley, CA. 369–458.

Thompson, B., D. Tsukada, and J. Laughlin. (1993b). Megabenthic assemblages of coastal shelves, slopes, and basins off Southern California. Bulletin of the Southern California Academy of Sciences, 92: 25–42.

Walther, S.M., J.P. Williams, A. Latker, D.B. Cadien, D.W. Diehl, K. Wisenbaker, E. Miller, R. Gartman, C. Stransky and K. Schiff. (2017). Southern California Bight 2013 Regional Monitoring Program: Volume VII. Demersal Fishes and Megabenthic Invertebrates. Southern California Coastal Water Research Project. Costa Mesa, CA.

Warnes, G.R., B. Bolker, and T. Lumley. (2015). gtools: Various R Programming Tools. R package version 3.4.2. http://CRAN.R-project.org/package=gtools.

Warwick, R.M. (1993). Environmental impact studies on marine communities: pragmatical considerations. Australian Journal of Ecology, 18: 63–80.

Wickham, H. (2007). Reshaping Data with the reshape Package. Journal of Statistical

Software, 21(12), 1-20. URL http://www.jstatsoft.org/v21/i12/.

Wickham, H. (2011). The Split-Apply-Combine Strategy for Data Analysis. Journal of Statistical Software, 40(1), 1-29. URL http://www.jstatsoft.org/v40/i01/.

Wickham, H. (2016). stringr: Simple, Consistent Wrappers for Common String Operations. R package version 1.1.0. https://CRAN.R-project.org/package=stringr.

Wickham, H. and R. Francois. (2016). dplyr: A Grammar of Data Manipulation. R package version 0.5.0. https://CRAN.R-project.org/package=dplyr.

Wickham, H., W. Chang, L. Henry, T. L. Pedersen, K. Takahashi, C. Wilke, K. Woo, (2018). Ggplot2: Create Elegant Data Visualisations Using the Grammar of Graphics. Version 3.1.0. Rstudio. URL https://ggplot2.tidyverse.org/.

Wisenbaker, K., K. McLaughlin, D. Diehl, A. Latker, K. Stolzenbach, R. Gartman, K. Schiff. (2021). Southern California Bight 2018 Regional Monitoring Program: Volume IV. Demersal Fishes and Megabenthic Invertebrates. Technical Report #1183. Southern California Coastal Water Research Project. Costa Mesa, CA.

Chapter 9
Contaminants in Marine Fishes

Chapter 9. Contaminants in Marine Fishes

Introduction

Bottom dwelling (demersal) fishes are collected by the City of San Diego (City) as part of the Ocean Monitoring Program to evaluate the presence of contaminants in their tissues, which may result from the discharge of wastewater through the Point Loma Ocean Outfall (PLOO) and South Bay Ocean Outfall (SBOO). Anthropogenic inputs to coastal waters can result in increased concentrations of pollutants within the local marine environment, which may subsequently accumulate in the tissues of fishes and their prey. Such accumulation occurs through the biological uptake and retention of chemicals derived via various exposure pathways, including the absorption of dissolved chemicals directly from seawater, and the ingestion/ assimilation of pollutants contained in different food sources (Connell 1988, Cardwell 1991, Rand 1995, USEPA 2000). In addition, demersal fishes may accumulate contaminants through the ingestion of suspended particulates or sediments because of their proximity to the seafloor. For this reason, contaminant levels in the tissues of these bottom dwelling fishes throughout the Southern California Bight (SCB) are often linked to those found in the surrounding environment (Schiff and Allen 1997), thus making these types of assessments useful in biomonitoring programs.

This portion of the City's Ocean Monitoring Program consists of two components: (1) analyzing liver tissues from mostly trawl-caught fishes; (2) analyzing muscle tissues from fishes collected by hook and line (rig fishing). Species targeted by trawling activities (see Chapter 8) are considered representative of the general demersal fish community off San Diego. The chemical analysis of liver tissues in target species of these fishes is important for assessing population effects because this is the organ where contaminants typically bioaccumulate. In contrast, species targeted for capture by rig fishing represent fish that are more characteristic of a typical sport fisher's catch and are therefore considered to be of recreational and commercial importance, and thus directly relevant to human health concerns. Consequently, muscle samples are analyzed from these fishes as this is the tissue most often consumed by humans. All liver and muscle tissue samples collected were analyzed for contaminants specified in the National Pollutant Discharge Elimination System (NPDES) discharge permits that govern monitoring requirements for the PLOO and SBOO regions (see Chapter 1).

This chapter presents analysis and interpretation of all chemical analyses performed on the tissues of fishes collected in the PLOO and SBOO regions during 2020 and 2021. The primary goals of this chapter are to: (1) document levels of contaminant loading in local demersal fishes to establish if concentrations accumulate to levels that may degrade marine communities and/or be harmful to human health; (2) identify whether any contaminant bioaccumulation detected in local fishes is changing over time and if the health of fish is changing as a result; (3) identify potential natural and anthropogenic sources of pollutants to the San Diego coastal marine environment that may play a role in contaminant bioaccumulation.

Materials and Methods

Fishes were collected in fall (October) 2020 and 2021 from a total of nine trawl zones (TZ1–TZ9) and four rig fishing zones (RF1–RF4) that span the PLOO and SBOO monitoring regions (Figure 9.1). Each trawl zone represents an area centered on (within a 1-km radius of) one or two trawl stations as specified in Chapter 8. Trawl Zone 1 includes the "nearfield" area of PLOO stations SD10 and SD12, which are located just south and north of the outfall discharge site, respectively. Trawl Zone 2 includes the area surrounding northern "farfield" PLOO stations SD13 and SD14. Trawl Zone 3

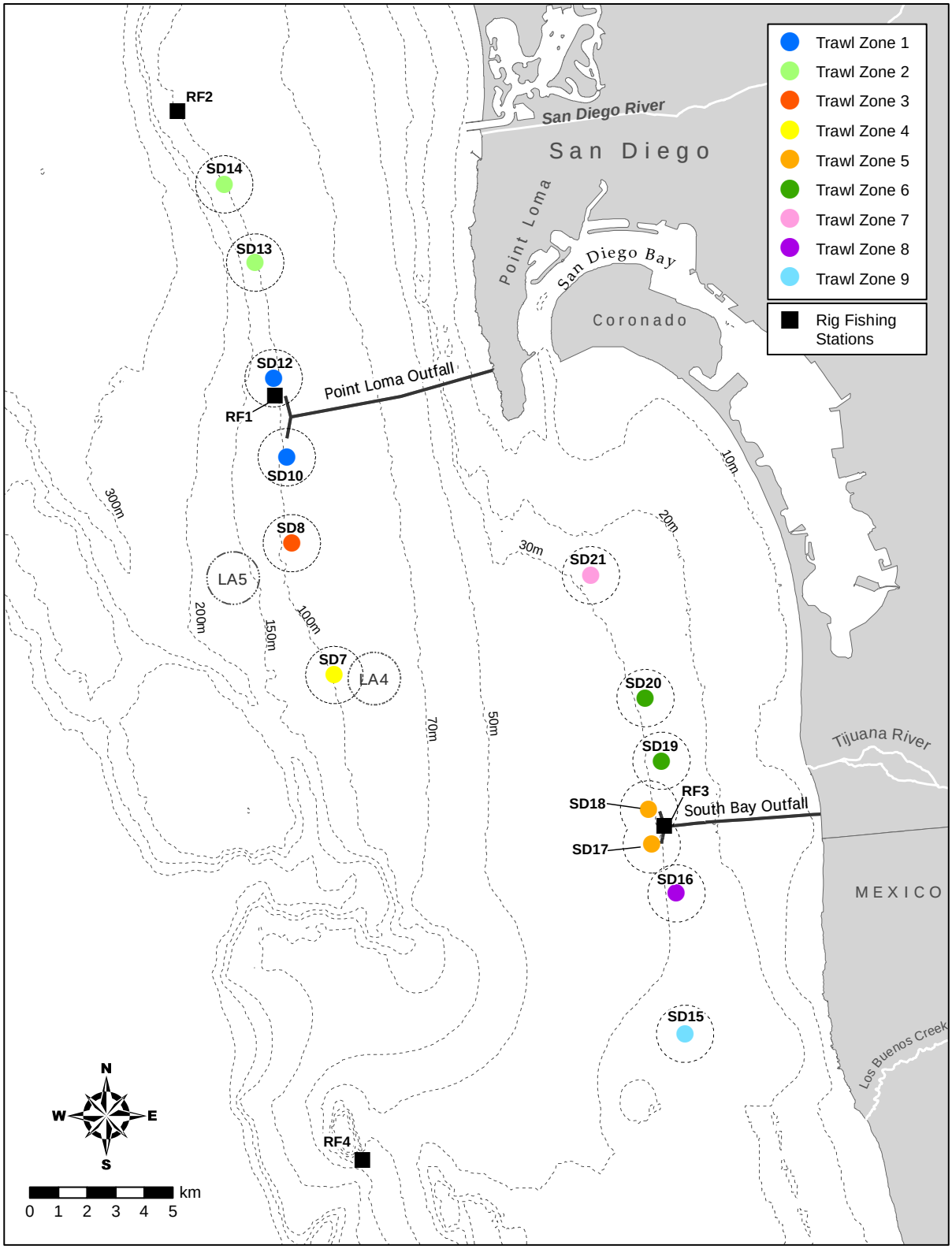

Figure 9.1
Trawl and rig fishing zone locations sampled around the PLOO and SBOO as part of the City of San Diego's Ocean Monitoring Program.

represents the area surrounding "farfield" PLOO station SD8, which is located south of the outfall near the LA-5 dredged material disposal site. Trawl Zone 4 is the area surrounding "farfield" PLOO station SD7 located several kilometers south of the outfall. Trawl Zone 5 includes the area surrounding SBOO stations SD17 and SD18, which are located just south and north of the outfall discharge site, respectively. Trawl Zone 6 includes the area surrounding northern SBOO stations SD19 and SD20, while Trawl Zone 7 includes the area surrounding northern SBOO station SD21. Trawl Zone 8 represents the area surrounding southern SBOO station SD16, while Trawl Zone 9 represents the area surrounding southern SBOO station SD15. Rig Fishing Zones 1–4 represent the areas within a 1-km radius of the nominal coordinates for stations RF1, RF2, RF3, and RF4. Stations RF1 and RF3 are located within 1 km of the PLOO and SBOO discharge sites, respectively, and are considered the "nearfield" rig fishing sites. In contrast, station RF2 is located about 11 km northwest of the PLOO, while station RF4 is located about 13.2 km southeast of the SBOO. These two sites are considered "farfield" or reference stations for the analyses herein. Efforts to collect target species by trawl were limited to five 10-minute (bottom time) trawls per site, while rig fishing effort was limited to 5 hours at each station. Occasionally, insufficient numbers of target species are obtained despite this effort; during 2020, this resulted in inadequate amounts of tissue at Trawl Zone 9 to complete three full composite samples.

A total of 14 species of fish were collected for analysis of liver and muscle tissues during the 2020 and 2021 surveys (Table 9.1). Five different species of flatfish were collected from the nine trawl zones for analysis of liver tissues, including Pacific Sanddab (*Citharichthys sordidus*), Longfin Sanddab (*Citharichthys xanthostigma*), English Sole (*Parophrys vetulus*), Hornyhead Turbot (*Pleuronichthys verticalis*), and Spotted Turbot (*Pleuronichthys ritteri*). These flatfish were collected from regular trawls at the SBOO stations, and by alternative hook and line methods at the PLOO stations. An additional nine species of fish were collected for analysis of muscle tissues at the rig fishing stations using standard hook and line fishing techniques. These species included California Scorpionfish (*Scorpaena guttata*), Brown Rockfish (*Sebastes auriculatus*), Flag Rockfish (*Sebastes rubrivinctus*), Gopher Rockfish (*Sebastes carnatus*), Speckled Rockfish (*Sebastes ovalis*), Starry Rockfish (*Sebastes constellatus*), Treefish (*Sebastes serriceps*), Olive Rockfish (*Sebastes serranoides*), and Vermilion Rockfish (*Sebastes miniatus*).

Only fishes with standard lengths ≥11cm were retained to ensure the collection of sufficient tissue for analysis while minimizing total catch necessary. These fishes were sorted into three composite samples per station, with a minimum of three individuals in each composite. All fishes were wrapped in aluminum foil, labeled, sealed in re-sealable plastic bags, placed on dry ice, and then transported to the City's Marine Biology Laboratory where they were stored at -20°C prior to dissection and tissue processing.

Tissue Processing and Chemical Analyses

All dissections were performed according to standard techniques for tissue analysis. A brief summary follows, but detailed methods are available in City of San Diego (2020b). Prior to dissection, each fish was partially defrosted, cleaned with a paper towel to remove loose scales and excess mucus, and the standard length (cm) and weight (g) were recorded (Appendices J.1, J.2). Dissections were carried out on Teflon® pads that were cleaned between samples. The liver or muscle tissues from each fish were removed and placed in separate glass jars for each composite sample, sealed, labeled, and stored in a freezer at -20°C prior to chemical analyses.

All tissue analyses were performed at the City's Environmental Chemistry Laboratory. Detailed analytical protocols are available upon request. Briefly, all fish tissue samples were analyzed on a wet weight basis to determine the concentrations of 18 different trace metals, nine

Table 9.1
Species of fish collected from each PLOO and SBOO trawl and rig fishing zone during 2020–2021.

	Zone	Composite 1	Composite 2	Composite 3
PLOO				
2020	Rig Fishing Zone 1 (RF1)	Vermilion Rockfish	Vermilion Rockfish	Vermilion Rockfish
	Rig Fishing Zone 2 (RF2)	Starry Rockfish	Starry Rockfish	Mixed Rockfish [a]
	Trawl Zone 1 (TZ1)	Pacific Sanddab	Pacific Sanddab	Pacific Sanddab
	Trawl Zone 2 (TZ2)	Pacific Sanddab	Pacific Sanddab	Pacific Sanddab
	Trawl Zone 3 (TZ3)	Pacific Sanddab	Pacific Sanddab	Pacific Sanddab
	Trawl Zone 4 (TZ4)	Pacific Sanddab	Pacific Sanddab	Longfin Sanddab
2021	Rig Fishing Zone 1 (RF1)	Vermilion Rockfish	Vermilion Rockfish	Vermilion Rockfish
	Rig Fishing Zone 2 (RF2)	Starry Rockfish	Starry Rockfish	Mixed Rockfish [b]
	Trawl Zone 1 (TZ1)	Pacific Sanddab	Pacific Sanddab	Pacific Sanddab
	Trawl Zone 2 (TZ2)	Pacific Sanddab	Pacific Sanddab	Pacific Sanddab
	Trawl Zone 3 (TZ3)	Pacific Sanddab	Pacific Sanddab	Pacific Sanddab
	Trawl Zone 4 (TZ4)	Pacific Sanddab	Pacific Sanddab	Pacific Sanddab
SBOO				
2020	Rig Fishing Zone 3 (RF3)	California Scorpionfish	Mixed Rockfish [c]	Mixed Rockfish [d]
	Rig Fishing Zone 4 (RF4)	Mixed Rockfish [e]	California Scorpionfish	California Scorpionfish
	Trawl Zone 5 (TZ5)	Longfin Sanddab	Hornyhead Turbot	Spotted Turbot
	Trawl Zone 6 (TZ6)	Longfin Sanddab	Longfin Sanddab	Longfin Sanddab
	Trawl Zone 7 (TZ7)	Longfin Sanddab	Longfin Sanddab	Longfin Sanddab
	Trawl Zone 8 (TZ8)	Hornyhead Turbot	Longfin Sanddab	California Scorpionfish
	Trawl Zone 9 (TZ9)	Spotted Turbot	No sample	No sample
2021	Rig Fishing Zone 3 (RF3)	California Scorpionfish	California Scorpionfish	Mixed Rockfish [f]
	Rig Fishing Zone 4 (RF4)	Gopher Rockfish	Gopher Rockfish	California Scorpionfish
	Trawl Zone 5 (TZ5)	Longfin Sanddab	Longfin Sanddab	Hornyhead Turbot
	Trawl Zone 6 (TZ6)	Longfin Sanddab	Longfin Sanddab	Hornyhead Turbot
	Trawl Zone 7 (TZ7)	Longfin Sanddab	Longfin Sanddab	Hornyhead Turbot
	Trawl Zone 8 (TZ8)	Longfin Sanddab	Longfin Sanddab	Longfin Sanddab
	Trawl Zone 9 (TZ9)	Hornyhead Turbot	English Sole	Spotted Turbot [g]

[a] Includes Flag, Speckled, and Starry Rockfish; [b] includes Vermilion and Flag Rockfish; [c] includes Treefish and Gopher Rockfish; [d] includes Brown and Olive Rockfish; [e] includes Treefish and Gopher Rockfish; [f] includes Brown and Vermilion Rockfish; [g] missing all metals, except mercury, due to insufficient sample volume

chlorinated pesticides and their constituents, 42 polychlorinated biphenyl compound congeners (PCBs), and 24 polycyclic aromatic hydrocarbons (PAHs). Data were limited to values above the method detection limit (MDL) for each parameter (Appendix J.3).

Data Analyses

Data for each chemical parameter analyzed in PLOO and SBOO fish tissues sampled during 2020 were reported previously (City of San Diego 2021), and all raw data for the 2020–2021 sampling

period have been submitted to either the Regional Water Quality Control Board or the California Environmental Data Exchange Network (CEDEN) and will be provided upon request.

Data summaries for each parameter include detection rate, minimum, maximum, and mean values for all samples combined by species for each outfall region. All means were calculated using detected values only, with no substitutions made for non-detects (analyte concentrations <MDL). Limiting analyses to detected values (i.e., excluding non-detects) is considered a conservative way of handling contaminant concentrations as it creates a strong upward bias in the data and respective summary statistics, and therefore may represent a worst-case scenario (e.g., see Helsel 2005a, b, 2006 for discussions of non-detect data). For continuity, and in contrast to previous reports (e.g., City of San Diego 2020a), estimated values that fell below method detection limits, but were confirmed by mass-spectrometry, were excluded from all data (1995–2021). Estimated values were treated as non-detects for this report. No fish tissue samples were collected during 2018 due to a resource exchange granted by the San Diego Regional Water Quality Control Board for participation in the region-wide Bight'18 sampling project. Total chlordane, total DDT (tDDT), total hexachlorocyclohexane (tHCH), total PCB (tPCB), and total PAH (tPAH) were calculated for each sample as the sum of all constituents with reported values for individual constituents. For comparative historical analyses, data were limited as follows: (1) fall (October) surveys only; (2) data collected after 1994; (3) specific species feeding guilds (e.g., mixed sanddabs, mixed rockfish) (see Allen et al. 2002) or the most frequently collected species (City of San Diego 2020a). Data collected from the PLOO region prior to 1995 were excluded due to incompatible methods used by the external contract lab at the time (see City of San Diego 2015). Barred Sand Bass were also included in the historical analyses because it was the only species collected at SBOO station RF3 in 1995. Previously, a variety of laboratory technical issues resulted in a significant amount of non-reportable fish tissue chemistry data (City of San Diego 2020a) and historical comparisons involving these parameters should therefore be interpreted with caution. Data analyses were performed using R (R Core Team 2021) using various functions within the zoo, reshape2, plyr, scales, tidyverse, vegan, psych, and ggpubr packages (Zeileis and Grothendieck 2005, Wickham 2007, 2011, 2019, Oksanen et al. 2019, Revelle 2019, Wickham et al. 2019, Kassambara 2020).

Contaminant levels in muscle tissue samples were compared to state, national, and international limits and standards to address seafood safety and public health issues. These included: (1) fish contaminant goals for chlordane, DDT, methylmercury, selenium, and PCBs developed by the California Office of Environmental Health Hazard Assessment (OEHHA) (Klasing and Brodberg 2008); (2) action limits on the amount of mercury, DDT, and chlordane in seafood that can be sold for human consumption, which are set by the U.S. Food and Drug Administration (USFDA) (Mearns et al. 1991); (3) international standards for acceptable concentrations of various metals and DDT (Mearns et al. 1991).

Results

Contaminants in Fish Liver Tissues

Trace Metals

Thirteen of the 18 trace metals analyzed were detected in fish liver tissue samples from PLOO and SBOO trawl zones in 2020–2021, including: arsenic, beryllium, cadmium, chromium, copper, iron, lead, manganese, mercury, nickel, selenium, tin, and zinc (Table 9.2). Arsenic, cadmium, copper, iron, mercury, and zinc were detected in all fish liver samples at concentrations ≤154 ppm. Detection rates for manganese and selenium were slightly less at 52– 96% per region at concentrations ≤2.35 ppm, while lead, nickel, beryllium, and chromium were detected at rates ≤17% per region at concentrations ≤0.36 ppm. Tin was detected in 42% of liver samples from the PLOO region at concentrations ≤7.96 ppm but was not detected in samples from the SBOO region. Aluminum, antimony, barium, silver, and thallium were not detected in any fish liver tissue samples from either region during 2020–2021.

Table 9.2

Summary of metals (ppm) in liver tissues of fishes collected from PLOO and SBOO trawl zones during 2020–2021. Data include the number of detected values (n), minimum, maximum, and mean[a] detected concentrations for each species, and the total number of samples, detection rate (DR%), and maximum value for all species within each region; nd = not detected.

		Al	Sb	As	Ba	Be	Cd	Cr	Cu	Fe
PLOO	Longfin Sanddab									
	n	0	0	1	0	0	1	0	1	1
	Min	—	—	11.1	—	—	3.36	—	7.82	135
	Max	—	—	11.1	—	—	3.36	—	7.82	135
	Mean	—	—	11.1	—	—	3.36	—	7.82	135
	Pacific Sanddab									
	n	0	0	23	0	1	23	1	23	23
	Min	—	—	2.3	—	nd	2.11	nd	1.57	62
	Max	—	—	10.8	—	0.019	4.60	0.20	8.19	136
	Mean	—	—	5.2	—	0.019	2.83	0.20	4.58	94
	Total Samples	24	24	24	12	24	24	24	24	24
	DR%	0	0	100	0	4	100	4	100	100
	Max	—	—	11.1	0	0.019	4.6	0.20	8.19	136
SBOO	California Scorpionfish									
	n	0	0	1	0	0	1	0	1	1
	Min	—	—	1.8	—	—	4.30	—	30.10	154
	Max	—	—	1.8	—	—	4.30	—	30.10	154
	Mean	—	—	1.8	—	—	4.30	—	30.10	154
	English Sole									
	n	0	0	1	0	0	1	0	1	1
	Min	—	—	4.6	—	—	0.54	—	5.36	119
	Max	—	—	4.6	—	—	0.54	—	5.36	119
	Mean	—	—	4.6	—	—	0.54	—	5.36	119
	Hornyhead Turbot									
	n	0	0	6	0	0	6	0	6	6
	Min	—	—	3.4	—	—	3.77	—	6.21	48
	Max	—	—	6.5	—	—	6.61	—	14.20	85
	Mean	—	—	4.8	—	—	5.23	—	8.47	70
	Longfin Sanddab									
	n	0	0	17	1	4	17	2	17	17
	Min	—	—	3.4	0	nd	0.45	nd	3.12	44
	Max	—	—	12.1	0.603	0.022	2.97	0.22	9.14	117
	Mean	—	—	5.8	0.603	0.020	1.21	0.21	6.42	84
	Spotted Turbot									
	n	0	0	2	0	0	2	0	2	2
	Min	—	—	11.4	—	—	2.00	—	12.50	133
	Max	—	—	21.2	—	—	4.20	—	19.50	149
	Mean	—	—	16.3	—	—	3.10	—	16.00	141
	Total Samples	27	27	27	27	27	27	27	27	27
	DR%	0	0	100	4	15	100	7	100	100
	Max	—	—	21.2	0.603	0.022	6.61	0.22	30.10	154

[a] Minimum and maximum values were based on all samples, whereas means were calculated from detected values only

Table 9.2 *continued*

		Pb	Mn	Hg	Ni	Se	Ag	Tl	Sn	Zn
PLOO	Longfin Sanddab									
	n	0	1	1	0	0	0	0	0	1
	Min	—	0.61	0.175	—	—	—	—	—	34.6
	Max	—	0.61	0.175	—	—	—	—	—	34.6
	Mean	—	0.61	0.175	—	—	—	—	—	34.6
	Pacific Sanddab									
	n	4	22	23	2	18	0	0	10	23
	Min	nd	nd	0.097	nd	nd	—	—	nd	18.6
	Max	0.36	1.24	0.202	0.121	2.35	—	—	7.96	35.1
	Mean	0.30	0.89	0.140	0.089	1.84	—	—	7.96	26.5
	Total Samples	24	24	24	24	24	24	12	24	24
	DR%	17	96	100	8	75	0	0	42	100
	Max	0.36	1.24	0.202	0.121	2.35	—	—	7.96	35.1
SBOO	California Scorpionfish									
	n	0	1	1	0	0	0	0	0	1
	Min	—	0.67	0.174	—	—	—	—	—	141.0
	Max	—	0.67	0.174	—	—	—	—	—	141.0
	Mean	—	0.67	0.174	—	—	—	—	—	141.0
	English Sole									
	n	0	1	1	0	1	0	0	0	1
	Min	—	0.99	0.021	—	2.26	—	—	—	26.8
	Max	—	0.99	0.021	—	2.26	—	—	—	26.8
	Mean	—	0.99	0.021	—	2.26	—	—	—	26.8
	Hornyhead Turbot									
	n	0	6	6	1	4	0	0	0	6
	Min	—	0.77	0.075	nd	nd	—	—	—	49.3
	Max	—	1.49	0.117	0.147	1.86	—	—	—	75.5
	Mean	—	1.01	0.101	0.147	1.42	—	—	—	60.8
	Longfin Sanddab									
	n	0	16	17	0	9	0	0	0	17
	Min	—	nd	0.028	—	nd	—	—	—	13.5
	Max	—	1.19	0.092	—	2.30	—	—	—	27.0
	Mean	—	0.81	0.048	—	1.67	—	—	—	21.0
	Spotted Turbot									
	n	1	2	3	0	0	0	0	0	2
	Min	nd	1.49	0.076	—	—	—	—	—	57.4
	Max	0.29	1.58	0.102	—	—	—	—	—	73.6
	Mean	0.29	1.54	0.090	—	—	—	—	—	65.5
	Total Samples	27	27	28	27	27	27	13	27	27
	DR%	4	96	100	4	52	0	0	0	100
	Max	0.29	1.58	0.174	0.147	2.30	—	—	—	141.0

Detection rates have been relatively high for several different metals in liver tissues of fishes collected at trawl zones since 1995 (Table 9.3). Cadmium, copper, iron, manganese, mercury, selenium, and zinc were detected in ≥88% of all Sanddab, Scorpionfish, and Hornyhead Turbot liver samples analyzed from the PLOO and SBOO trawl zones over the past 27 years. Detection rates for other metals varied by species. For example, arsenic was detected in ≥86% of all Sanddab and

Table 9.3

Summary of metals (ppm) in liver tissues of fishes collected from PLOO and SBOO trawl zones from 1995 through 2021. Data include the total number of samples (n), detection rate (DR%), minimum, maximum, and mean[a] detected concentrations for each guild or species; nd = not detected.

		Al	Sb	As	Ba	Be	Cd	Cr	Cu	Fe	Pb	Mn	Hg	Ni	Se	Ag	Tl	Sn	Zn
PLOO	Mixed Sanddabs																		
	n	331	331	331	210	331	331	331	323	331	331	331	333	331	332	331	307	331	331
	DR%	59	15	91	59	12	94	59	100	100	17	98	90	17	98	24	25	52	100
	min	nd	nd	nd	nd	nd	nd	nd	0.9	27.0	nd	nd	nd	nd	nd	nd	nd	nd	8.6
	max	44.6	9.7	123.0	15.2	0.18	19.20	22.80	28.7	233.0	8.8	5.5	0.579	18.90	4.37	2.2	6.4	277.0	74.2
	mean	12.0	1.4	5.2	0.3	0.02	4.13	0.64	5.3	97.1	0.9	0.8	0.099	0.68	1.17	0.2	1.6	4.0	24.2
	California Scorpionfish																		
	n	104	104	104	42	104	104	104	104	104	104	104	106	104	106	104	104	104	104
	DR%	88	12	44	95	10	94	55	100	100	14	88	94	25	99	41	14	26	100
	min	nd	nd	nd	nd	nd	nd	nd	4.1	29.6	nd	nd	nd	nd	nd	nd	nd	nd	20.5
	max	59.8	1.7	8.1	0.6	0.06	6.92	5.34	81.1	481.0	8.1	2.5	0.695	2.67	2.82	1.2	5.3	3.4	207.0
	mean	13.6	0.9	2.3	0.1	0.01	2.64	0.92	22.9	178.9	1.4	0.6	0.175	0.42	0.88	0.3	4.2	1.3	97.4
SBOO	Hornyhead Turbot																		
	n	137	137	137	117	137	137	137	137	137	137	137	137	137	138	137	129	137	137
	DR%	62	8	91	53	4	99	76	100	100	15	99	98	16	98	75	19	58	100
	min	nd	nd	nd	0	nd	nd	nd	2.3	19.4	nd	nd	nd	nd	nd	nd	nd	nd	23.0
	max	27.8	1.8	25.0	0.3	0.02	12.00	7.67	41.7	263.0	3.3	3.2	0.407	4.61	3.38	1.3	3.8	88.2	233.0
	mean	7.0	1.1	4.3	0.1	0.01	3.95	0.40	7.9	56.2	0.6	1.1	0.108	0.50	0.86	0.2	1.7	2.1	62.1
	Longfin Sanddab																		
	n	174	174	174	127	174	174	174	174	174	174	174	174	174	175	174	157	174	174
	DR%	57	15	86	45	6	92	60	100	100	12	97	88	19	95	40	29	56	100
	min	nd	nd	nd	0	nd	nd	nd	1.4	33.0	nd	nd	nd	nd	nd	nd	nd	nd	10.3
	max	49.0	2.4	12.1	0.6	0.04	9.31	3.56	23.2	449.0	14.3	2.0	0.438	1.59	2.30	1.6	2.7	4.6	109.0
	mean	12.6	0.9	5.5	0.2	0.02	1.86	0.43	6.2	76.9	1.1	1.0	0.083	0.44	0.92	0.2	0.9	1.5	23.4

[a] Minimum and maximum values were calculated based on all samples, whereas means were calculated from detected values only

Hornyhead Turbot liver samples, but only 44% of Scorpionfish samples. Aluminum and barium were detected in 88% and 95% of all California Scorpionfish, respectively, and 47–62% of Sanddab and Hornyhead Turbot samples. Chromium, silver, and tin were detected in 76%, 75%, and 58% of Hornyhead Turbot samples, respectively, and 24–60% of California Scorpionfish and Sanddab samples. Antimony, beryllium, lead, nickel, and thallium were detected in ≤29% of all samples from both regions.

Metal concentrations have also been highly variable over these past 27 years, with most being detected within ranges reported elsewhere in the SCB (e.g., Mearns et al. 1991, CLA 2015, OCSD 2018, McLaughlin et al 2020). While relatively high values of various metals have been occasionally recorded in liver tissues from fishes collected from nearfield zones, when compared to farfield zones, there were no discernable intra-species patterns that could be associated with proximity to either outfall (Figure 9.2, Appendix J.4).

Pesticides

Two chlorinated pesticides were detected in fish liver tissue samples from PLOO and SBOO trawl zones in 2020–2021 (Table 9.4). Total DDT was detected in all samples from PLOO and 96% in the SBOO region, at concentrations ≤751.3 ppb. Total chlordane was detected in 75% of the PLOO samples and 21% of the SBOO samples, at concentrations ≤13.3 ppb. The pesticides (or pesticide constituents) tHCH, hexachlorobenzene, mirex, dieldrin, aldrin, alpha-endosulfan, beta-endosulfan, endosulfan sulfate, endrin, and endrin aldehyde were analyzed but not detected in any liver samples from fishes collected from either region.

DDT was the most frequently detected pesticide in liver tissues from trawl-zone fishes since 1995 with rates between 98–99% per species (or species group) (Table 9.5). In contrast, long-term detection rates were 5–36% for HCB, 1–31% for total chlordane, 0–6% for total HCH, ≤1% for mirex and ≤2% for aldrin, dieldrin, and endrin. In contrast, endrin aldehyde, alpha endosulfan, beta-endosulfan, and endosulfan sulfate, have been analyzed but never detected in any liver tissue samples from PLOO or SBOO trawl zones. As with metals, pesticide concentrations have been highly variable over time, with most being detected at levels within ranges reported elsewhere in the SCB (e.g., Allen et al. 1998, 2002, Mearns et al. 1991, LACSD 2016, McLaughlin et al 2020). While relatively high values of various pesticides have been occasionally recorded in liver tissues from nearfield zones, when compared to farfield zones, there were no discernable intra-species patterns that could be associated with proximity to either outfall (Figure 9.3, Appendix J.5).

PCBs

PCBs were detected in all fish liver tissue samples from PLOO and 71% in SBOO trawl zones in 2020–2021, at concentrations ≤868.3 ppb (Table 9.4). Since 1995, PCBs have been detected in 93–99% of the liver samples from Sanddabs and Scorpionfish, and in 46% of the liver samples from Hornyhead Turbot (Table 9.5), with total PCB concentrations generally within ranges reported elsewhere in the Southern California Bight (e.g., Allen et al. 1998, Mearns et al. 1991, LACSD 2016, McLaughlin et al 2020). There were no discernable intra-species patterns that could be associated with proximity to either outfall over the past 27 years (Figure 9.3).

PAHs

PAHs were not detected in any liver tissue samples from PLOO or SBOO trawl zones in 2020–2021 (Table 9.4). Historically, PAHs have been detected in ≤13% of the liver tissue samples from Sanddabs, Scorpionfish, and Hornyhead Turbot analyzed since 1995 (Table 9.5), with total PAH concentrations generally within ranges reported elsewhere in the Southern California Bight (e.g., Allen et al. 1998, Mearns et al. 1991, LACSD 2016). There were no discernable intra-species patterns that could be associated with proximity to either outfall during the years that PAH was analyzed (Appendix J.5).

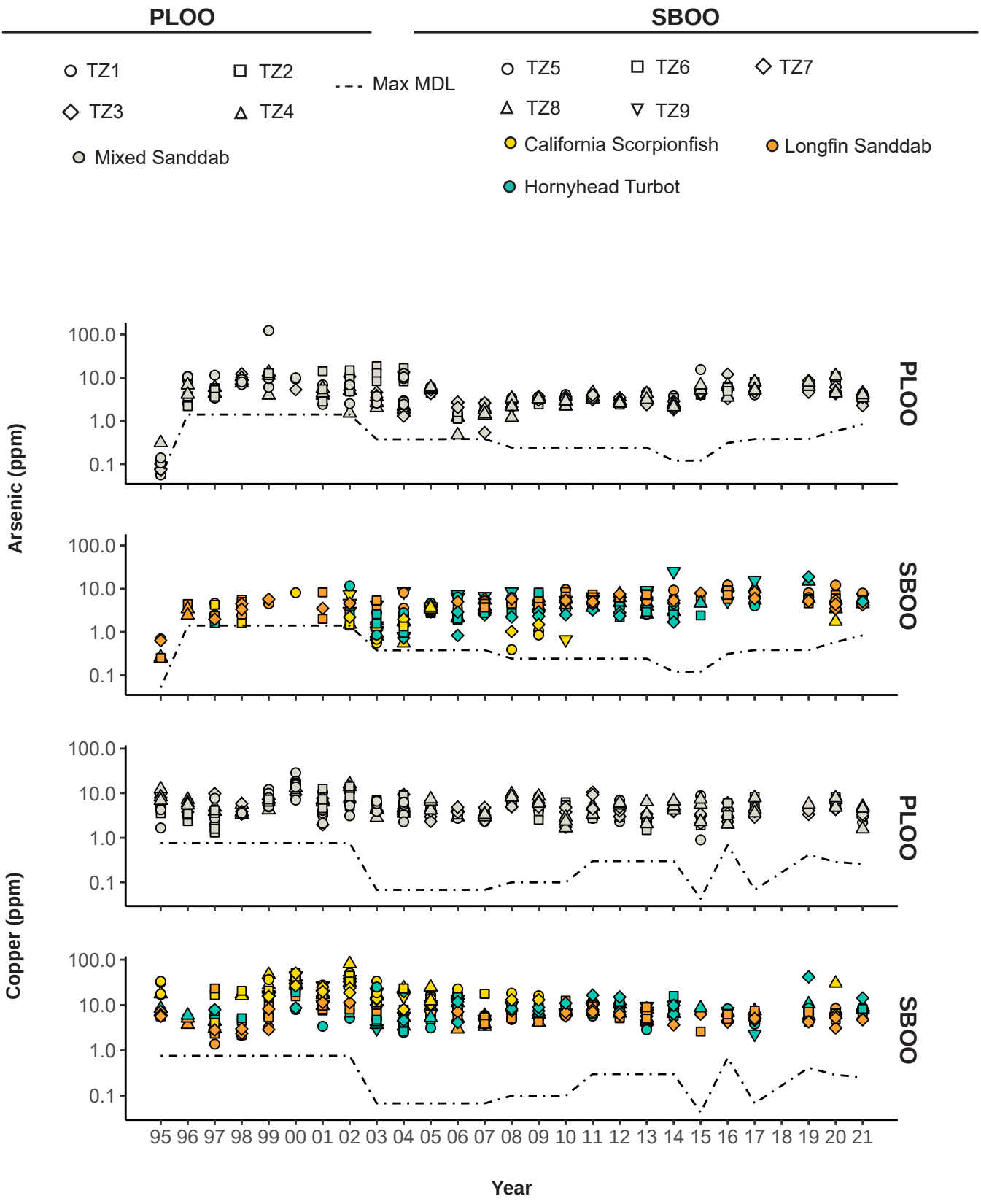

Figure 9.2

Concentrations of select metals in liver tissues of fishes collected from PLOO and SBOO trawl zones from 1995 through 2021. Zones TZ1 and TZ5 are considered nearfield. No samples were collected in 2018 as described in text.

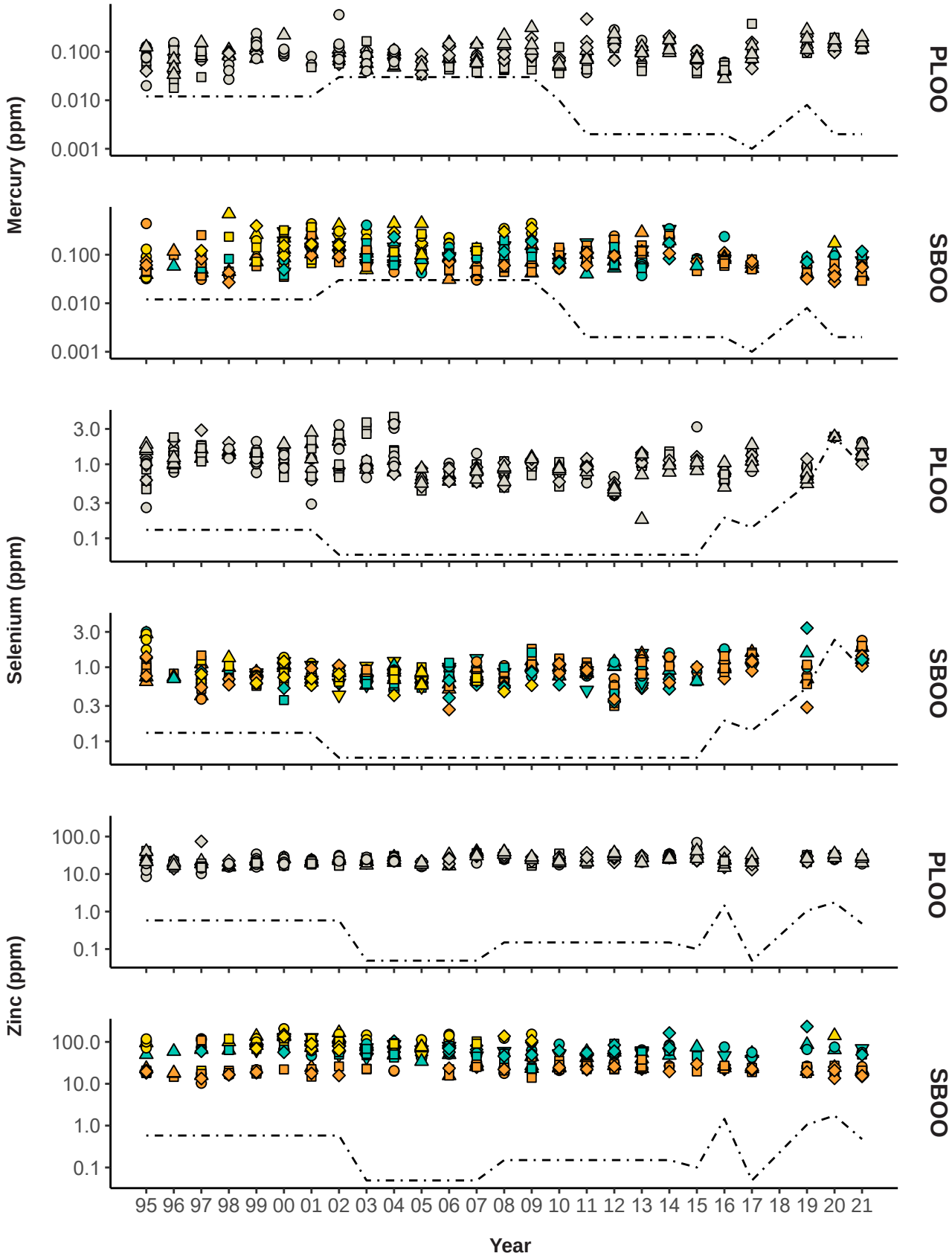

Figure 9.2 *continued*

Table 9.4

Summary of pesticides (ppb), total PCB (ppb), total PAH (ppb), and lipids (% weight) in liver tissues of fishes collected from PLOO and SBOO trawl zones during 2020–2021. Data include the number of detected values (n), minimum, maximum, and mean [a] detected concentrations for each species, and the total number of samples, detection rate (DR%), and maximum value for all species; nd = not detected

		Pesticides				
		tChlordane	tDDT	tPCB	tPAH	Lipids
PLOO	Longfin Sanddab					
	n	1	1	1	0	1
	Min	4.3	358.4	580.9	—	35.2
	Max	4.3	358.4	580.9	—	35.2
	Mean	4.3	358.4	580.9	—	35.2
	Pacific Sanddab					
	n	17	23	23	0	23
	Min	nd	133.6	93.3	—	17.7
	Max	13.3	751.3	868.3	—	40.9
	Mean	6.9	324.4	431.8	—	29.3
	Total Samples	24	24	24	18	24
	DR%	75	100	100	0	100
	Max	13.3	751.3	868.3	0	40.9
SBOO	California Scorpionfish					
	n	1	1	1	0	1
	Min	3.1	151.1	62.9	—	9.0
	Max	3.1	151.1	62.9	—	9.0
	Mean	3.1	151.1	62.9	—	9.0
	English Sole					
	n	0	1	0	0	1
	Min	—	14.6	—	—	10.9
	Max	—	14.6	—	—	10.9
	Mean	—	14.6	—	—	10.9
	Hornyhead Turbot					
	n	0	6	1	0	6
	Min	—	24.2	nd	—	3.6
	Max	—	53.9	4.2	—	30.4
	Mean	—	31.6	4.2	—	14.2
	Longfin Sanddab					
	n	5	17	17	0	17
	Min	nd	115.1	37.8	—	15.3
	Max	4.1	246.9	234.5	—	40.4
	Mean	2.8	171.1	109.9	—	31.4
	Spotted Turbot					
	n	0	2	1	0	3
	Min	—	nd	nd	—	2.4
	Max	—	17.4	7.6	—	4.7
	Mean	—	12.1	7.6	—	3.2
	Total Samples	28	28	28	15	28
	DR%	21	96	71	0	100
	Max	4.1	246.9	234.5	0	40.4

[a] Minimum and maximum values were based on all samples, whereas means were calculated from detected values only

Table 9.5

Summary of pesticides (ppb), total PCB (ppb), total PAH (ppb), and lipids (% weight) in liver tissues of fishes collected from PLOO and SBOO trawl zones from 1995 through 2021. Data include total number of samples (n), detection rate (DR%), minimum, maximum, and mean[a] detected concentrations per guild or species; nd = not detected; tChlor = total chlordane.

		Pesticides										
		Aldrin	tChlor	tDDT	Dieldrin	Endrin	HCB	tHCH	Mirex	tPCB	tPAH	Lipids
PLOO	Mixed Sanddab											
	n	329	340	340	317	317	320	340	340	341	160	337
	DR%	0	31	98	2	0	26	6	0	99	13	100
	min	—	nd	nd	nd	—	nd	nd	nd	nd	nd	6.9
	max	—	94.0	3800.0	15.8	—	120.0	22.0	48.0	3179.5	1353.0	69.6
	mean	—	16.6	696.4	6.2	—	7.8	4.7	48.0	431.3	212.2	37.5
	California Scorpionfish											
	n	94	94	94	94	94	93	94	94	108	72	106
	DR%	2	13	98	2	2	5	3	0	93	0	100
	min	nd	nd	nd	nd	nd	nd	nd	—	nd	—	6.4
	max	19.0	122.0	15,503.0	63.0	66.0	37.3	278.0	—	2187.9	—	45.4
	mean	12.1	35.0	1243.0	38.5	55.0	12.2	137.0	—	298.3	—	19.6
SBOO	Hornyhead Turbot											
	n	140	143	143	138	138	137	143	143	145	126	142
	DR%	0	1	99	0	0	10	0	0	46	5	100
	min	—	nd	nd	—	—	nd	—	—	nd	nd	0.1
	max	—	32.0	2802.0	—	—	41.0	—	—	828.4	330.5	32.2
	mean	—	26.2	125.5	—	—	9.7	—	—	50.7	133.7	9.8
	Longfin Sanddab											
	n	168	171	171	159	159	152	171	171	175	139	174
	DR%	0	20	99	0	0	36	2	1	99	4	100
	min	—	nd	nd	—	—	nd	nd	nd	nd	nd	6.2
	max	—	120.0	3600.0	—	—	51.3	3.2	2.0	6781.9	43,167	62.4
	mean	—	10.5	619.0	—	—	4.4	2.5	1.8	526.3	8678.3	35.5

[a] Minimum and maximum values were based on all samples, whereas means were calculated from detected values only

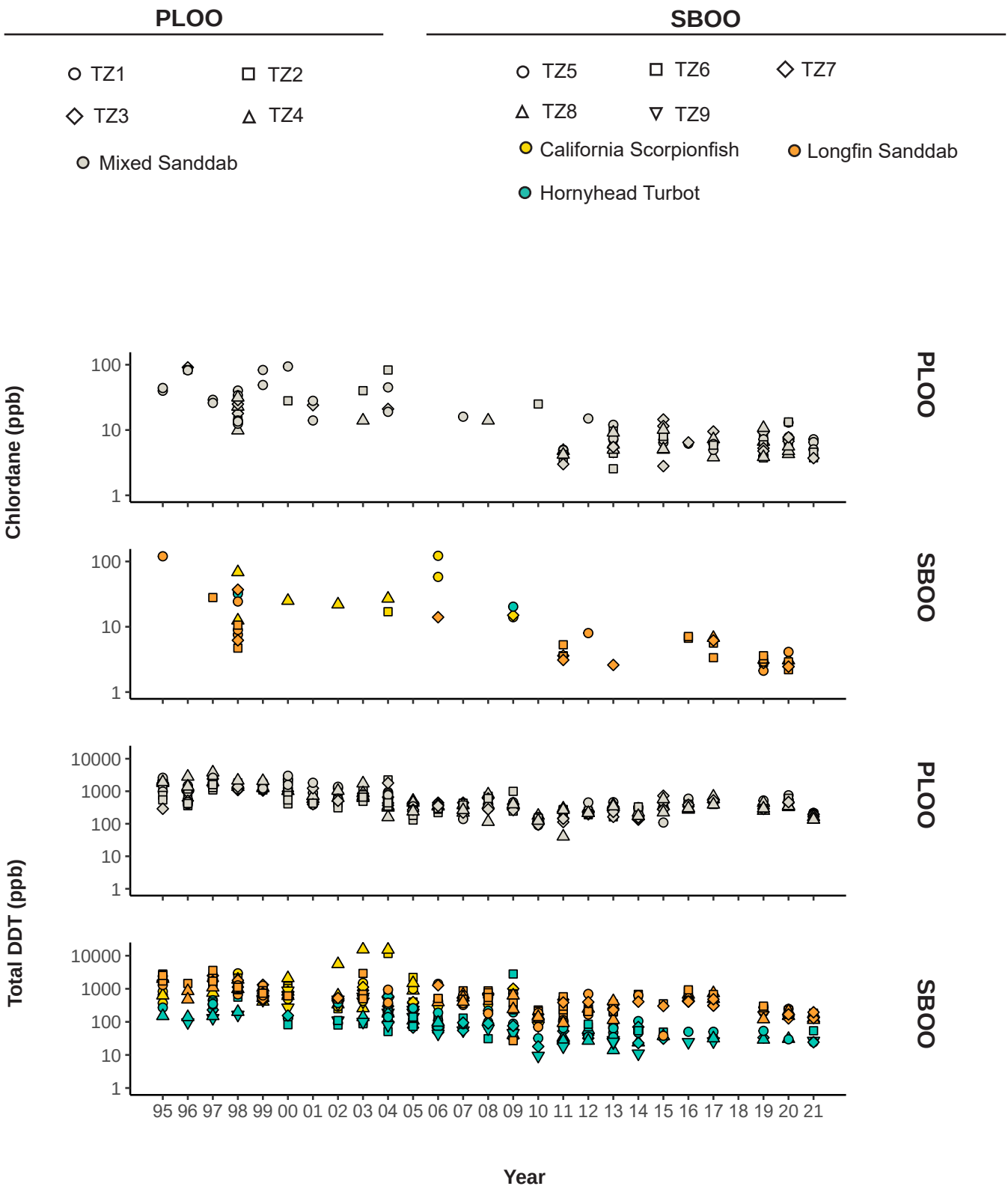

Figure 9.3

Concentrations of pesticides and total PCB in liver tissues of fishes collected from PLOO and SBOO trawl zones from 1995 through 2021. Zones TZ1 and TZ5 are considered nearfield. No samples were collected in 2018 as described in text.

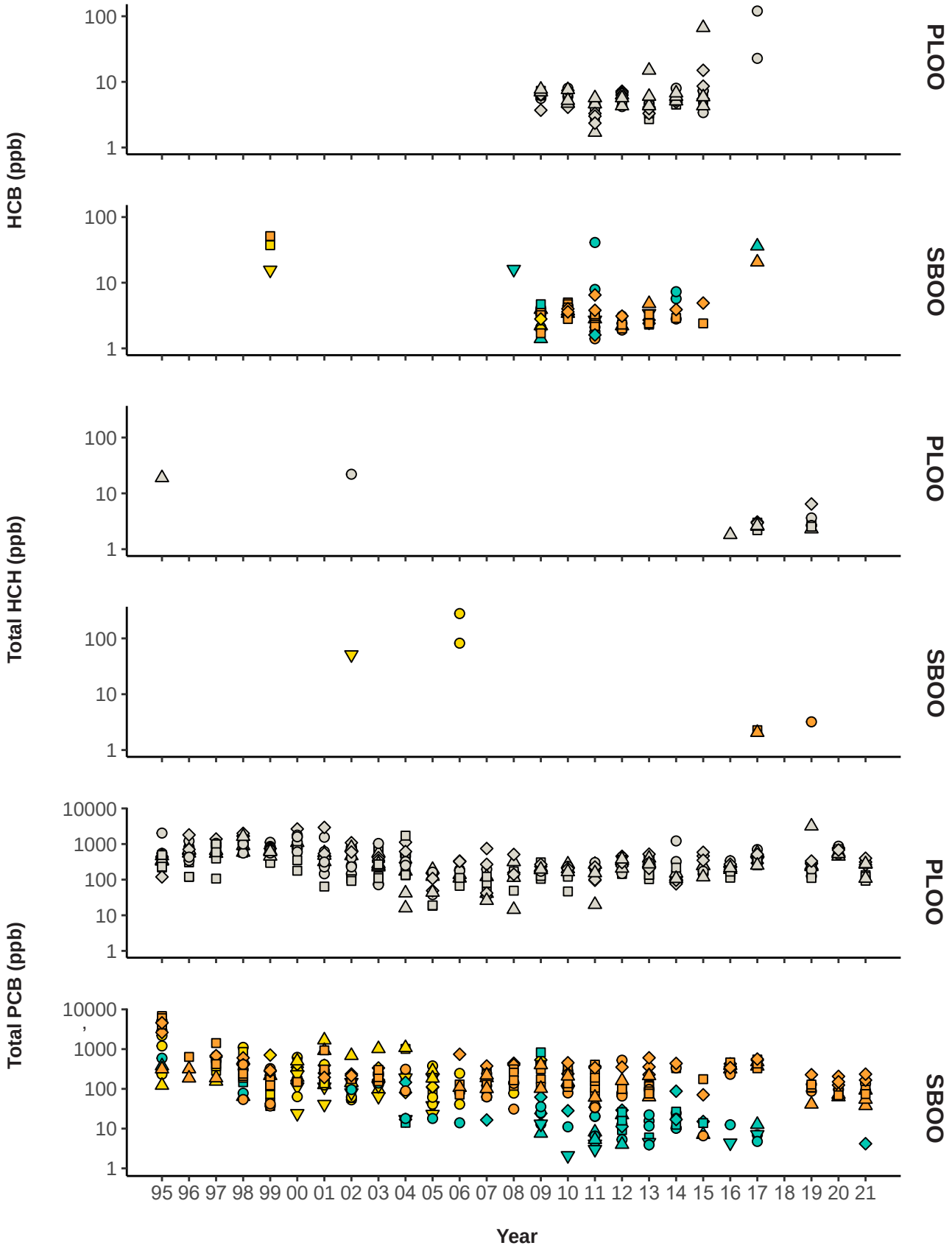

Figure 9.3 *continued*

Contaminants in Fish Muscle Tissues

Trace Metals

Ten of the 18 trace metals analyzed were detected in fish muscle tissue samples from PLOO and SBOO rig fishing zones in 2020–2021, including: aluminum, arsenic, cadmium, chromium, copper, iron, manganese, mercury, selenium, and zinc (Table 9.6). Arsenic, iron, mercury, and zinc were detected in all muscle samples. Detection rates for cadmium, copper, manganese, and selenium were 17–100% per region. Aluminum was found in 8% of the muscle tissue samples from the SBOO region but was not detected in muscle tissue samples from the PLOO region. Antimony, barium, beryllium, lead, nickel, silver, thallium, and tin were analyzed but not detected in any muscle tissue samples from either region during 2020–2021.

Detection rates have been relatively high for several different metals in muscle tissues of fishes captured at rig fishing zones since 1995 (Table 9.7). For example, arsenic, copper, iron, mercury, selenium, and zinc were detected in ≥61% of all California Scorpionfish and rockfish muscle samples analyzed from the PLOO and SBOO rig fishing over the past 27 years. Aluminum, barium, chromium, manganese, and tin were detected in 26–76% of all California Scorpionfish and rockfish muscle samples from both regions, while antimony, beryllium, cadmium, lead, nickel, silver, and thallium were detected in ≤26% of muscle samples from these species. In contrast to California Scorpionfish and mixed rockfish, iron, mercury, selenium, and zinc were the only metals detected in Barred Sand Bass muscle samples during the limited period this species was targeted. Metal concentrations in muscle tissues of San Diego fishes have been highly variable, but consistently lower than in liver tissues and within ranges reported elsewhere in the SCB (Mearns et al. 1991, CLA 2015, LACSD 2016, OCSD 2018, McLaughlin et al 2020). While relatively high values of various metals have been occasionally recorded in muscle tissues of fishes collected off San Diego, there were no discernable patterns at the rig fishing zones, which could be associated with proximity to either the PLOO or the SBOO (Figure 9.4, Appendix J.6).

Of the 24 rockfish muscle tissue samples collected from PLOO and SBOO rig fishing zones in 2020–2021, 75% exceeded the median international standard for arsenic (33–100% per zone) and 46% exceeded this standard for selenium (17–67% per zone) (Table 9.8). The OEHHA limit for mercury was exceeded in 33% of the samples from PLOO farfield zone RF2, but all samples were below the USFDA mercury action limit. All samples were also below the OEHHA limit for selenium. These rate of exceedances for the current reporting period were similar to those observed previously (1995–2019) (Table 9.8). Since 1995, median international standards were exceeded for arsenic (50–72% per zone), chromium (≤4% per zone), mercury (1–7% per zone), and selenium (31–76% per zone). Cadmium, copper, lead, tin, and zinc were never found at concentrations above their median international standards. The OEHHA fish contaminant goals were exceeded for mercury (10–21% per zone), but not for selenium. The USFDA action limit for mercury was exceeded for just 1% of the samples from SBOO farfield zone RF4.

Pesticides

Three chlorinated pesticides were detected in fish muscle tissue samples from PLOO and SBOO rig fishing zones in 2020–2021 (Table 9.9). Total DDT was detected in 100% of the PLOO samples and 75% of the SBOO samples, at concentrations ≤15.4 ppb. Dieldrin and endrin were detected in 8% of SBOO samples at concentrations ≤0.7 ppb. During the 2020–2021 surveys, these two pesticides were not detected in fish muscle tissue samples from PLOO rig fishing zones. Additionally, the pesticides (or pesticide constituents) aldrin, alpha endosulfan, beta-endosulfan, chlordane, HCH, HCB, endosulfan sulfate, endrin aldehyde, and mirex were not detected in any muscle samples from fishes collected from either region. None of the detected pesticide values from the past 2 years exceeded median international standards, OEHHA fish contaminant goal, or the USFDA action limits (Table 9.8).

Table 9.6

Summary of metals (ppm) in muscle tissues of fishes collected from PLOO and SBOO rig fishing zones during 2020–2021. Data include the number of detected values (n), minimum, maximum, and mean[a] detected concentrations per species and the total number of samples, detection rate (DR%), and maximum value for all species; nd = not detected.

		Al	Sb	As	Ba	Be	Cd	Cr	Cu	Fe
PLOO	Vermilion Rockfish									
	n	0	0	6	1	0	4	3	6	6
	Min	—	—	2.5	0	—	nd	nd	0.111	1.6
	Max	—	—	6.0	0.091	—	0.081	0.086	0.446	10.7
	Mean	—	—	3.9	0.091	—	0.046	0.066	0.240	3.8
	Mixed Rockfish									
	n	0	0	2	0	0	1	1	2	2
	Min	—	—	1.3	—	—	nd	nd	0.213	3.0
	Max	—	—	2.3	—	—	0.026	0.078	0.257	4.5
	Mean	—	—	1.8	—	—	0.026	0.078	0.235	3.8
	Starry Rockfish									
	n	0	0	4	0	0	1	2	2	4
	Min	—	—	1.0	—	—	nd	nd	nd	1.0
	Max	—	—	2.2	—	—	0.030	0.077	0.299	3.2
	Mean	—	—	1.4	—	—	0.030	0.077	0.284	1.9
	Total Samples	12	12	12	7	12	12	12	12	12
	DR%	0	0	100	14	0	50	50	83	100
	Max	0	0	6.0	0.091	0	0.081	0.086	0.446	10.7
SBOO	California Scorpionfish	0	0	6	0	0	3	2	6	6
	n	—	—	1.5	—	—	nd	nd	0.177	1.9
	Min	—	—	3.2	—	—	0.041	0.093	0.602	4.7
	Max	—	—	2.2	—	—	0.032	0.084	0.357	3.0
	Mean									
	Mixed Rockfish	1	0	4	0	0	1	1	4	4
	n	nd	—	1.1	—	—	nd	nd	0.182	1.3
	Min	2.1	—	3.2	—	—	0.042	0.093	0.602	2.7
	Max	2.1	—	1.9	—	—	0.042	0.093	0.346	1.9
	Mean									
	Gopher Rockfish	0	0	2	0	0	2	2	2	2
	n	—	—	2.0	—	—	0.024	0.074	0.145	1.8
	Min	—	—	2.4	—	—	0.033	0.097	0.170	2.6
	Max	—	—	2.2	—	—	0.029	0.086	0.158	2.2
	Mean	12	12	12	6	12	12	12	12	12
	Total Samples	12	12	12	12	12	12	12	12	12
	DR%	8	0	100	0	0	50	42	100	100
	Max	2.1	0	3.2	0	0	0.042	0.097	0.602	4.7

[a] Minimum and maximum values were based on all samples, whereas means were calculated from detected values only

Historically, only six pesticides have been found in muscle tissues from Barred Sand Bass, California Scorpionfish, and mixed rockfish samples from the PLOO or SBOO rig fishing zones (Table 9.10). Long term detection rates were 50–92% per species (or species group) for DDT, 0–10% for HCB, 0–2% for total chlordane, ≤1% for total HCH, and ≤2% for dieldrin and endrin. Other pesticides such as aldrin, endrin aldehyde, alpha-endosulfan, beta endosulfan,

Table 9.6 *continued*

		Pb	Mn	Hg	Ni	Se	Ag	Tl	Sn	Zn
PLOO	Vermilion Rockfish									
	n	0	2	6	0	4	0	0	0	6
	Min	—	nd	0.062	—	nd	—	—	—	3.2
	Max	—	0.164	0.120	—	0.817	—	—	—	4.3
	Mean	—	0.109	0.090	—	0.566	—	—	—	3.7
	Mixed Rockfish									
	n	0	0	2	0	2	0	0	0	2
	Min	—	—	0.122	—	0.437	—	—	—	3.0
	Max	—	—	0.136	—	0.878	—	—	—	3.6
	Mean	—	—	0.129	—	0.658	—	—	—	3.3
	Starry Rockfish									
	n	0	1	4	0	2	0	0	0	4
	Min	—	nd	0.132	—	nd	—	—	—	2.7
	Max	—	0.055	0.452	—	0.566	—	—	—	3.2
	Mean	—	0.055	0.255	—	0.543	—	—	—	2.9
	Total Samples	12	12	12	12	12	12	6	12	12
	DR%	0	25	100	0	67	0	0	0	100
	Max	0	0.164	0.452	0	0.878	0	0	0	4.3
SBOO	California Scorpionfish									
	n	0	1	6	0	0	0	0	0	6
	Min	—	nd	0.117	—	—	—	—	—	3.3
	Max	—	0.124	0.218	—	—	—	—	—	4.6
	Mean	—	0.124	0.163	—	—	—	—	—	4.1
	Mixed Rockfish									
	n	0	1	4	0	1	0	0	0	4
	Min	—	nd	0.059	—	nd	—	—	—	3.3
	Max	—	0.126	0.137	—	0.462	—	—	—	4.5
	Mean	—	0.126	0.098	—	0.462	—	—	—	4.1
	Gopher Rockfish									
	n	0	0	2	0	2	0	0	0	2
	Min	—	—	0.134	—	0.427	—	—	—	3.6
	Max	—	—	0.194	—	0.529	—	—	—	4.2
	Mean	—	—	0.164	—	0.478	—	—	—	3.9
	Total Samples	12	12	12	12	12	12	6	12	12
	DR%	0	17	100	0	25	0	0	0	100
	Max	0	0.126	0.218	0	0.529	0	0	0	4.6

endosulfan sulfate, and mirex have never been detected in muscle tissue samples from these species collected from the PLOO or SBOO regions over the past 27 years. As with metals, pesticides also typically occurred in lower concentrations in muscle tissues compared to liver tissue, and most were detected at levels within ranges reported elsewhere in the SCB (e.g., Allen et al. 1998, 2002, Mearns et al. 1991, CLA 2015, McLaughlin et al 2020). While relatively high values of various pesticides have been occasionally recorded in muscle tissues of fishes collected off San Diego, there were no discernable patterns at the rig fishing zones, which could be associated with proximity to either the PLOO or the SBOO (Figure 9.5, Appendix J.7).

Table 9.7

Summary of metals (ppm) in muscle tissues of fishes collected from PLOO and SBOO rig fishing zones from 1995 through 2021. Data include the total number of samples (n), detection rate (DR%), minimum, maximum, and mean[a] detected concentrations for each guild or species; nd = not detected.

		Al	Sb	As	Ba	Be	Cd	Cr	Cu	Fe	Pb	Mn	Hg	Ni	Se	Ag	Tl	Sn	Zn
PLOO	Mixed Rockfish																		
	n	142	142	142	98	142	142	142	142	142	142	142	140	142	142	142	130	142	142
	DR%	35	8	85	45	4	26	56	61	78	3	37	96	11	96	5	14	38	99
	min	nd	nd	nd	nd	nd	nd	nd	nd	nd	nd	nd	nd	nd	nd	nd	nd	nd	nd
	max	22.1	1.11	13.5	0.185	0.042	0.178	1.78	8.96	257.0	0.420	5.30	0.790	0.378	0.878	0.500	2.93	2.12	5.9
	mean	6.4	0.62	2.7	0.062	0.010	0.065	0.24	0.92	7.0	0.288	0.56	0.160	0.146	0.407	0.122	1.27	0.96	3.7
SBOO	Barred Sand Bass																		
	n	4	4	4	0	4	4	4	4	4	4	4	4	4	4	4	4	4	4
	DR%	0	0	0	—	0	0	0	0	100	0	0	100	0	75	0	0	0	75
	min	—	—	—	—	—	—	—	—	3.2	—	—	0.230	—	—	—	—	—	nd
	max	—	—	—	—	—	—	—	—	6.7	—	—	0.362	—	—	—	—	—	5.0
	mean	—	—	—	—	—	—	—	—	4.6	—	—	0.294	—	—	—	—	—	4.4
	California Scorpionfish																		
	n	82	82	82	49	82	82	82	82	82	82	82	82	82	82	82	76	82	82
	DR%	38	1	73	35	5	22	46	70	80	5	26	96	9	87	4	18	29	100
	min	nd	nd	nd	nd	nd	nd	nd	nd	nd	nd	nd	nd	nd	nd	nd	nd	nd	1.9
	max	19.4	0.23	5.4	0.151	0.025	0.083	2.21	5.11	21.2	0.380	1.85	1.540	0.221	0.630	0.113	2.74	1.96	6.8
	mean	6.5	0.23	2.4	0.060	0.013	0.044	0.28	1.03	5.2	0.276	0.18	0.196	0.103	0.263	0.094	1.06	0.84	3.9
	Mixed Rockfish																		
	n	63	63	63	54	63	63	63	63	63	63	63	63	63	63	63	58	63	63
	DR%	33	14	92	48	0	25	76	75	73	3	49	95	16	95	3	24	49	100
	min	nd	nd	nd	nd	—	nd	nd	nd	nd	nd	nd	nd	nd	nd	nd	nd	nd	1.4
	max	16.1	1.57	11.2	0.202	—	0.197	0.81	3.80	9.5	0.440	2.60	0.330	0.730	0.740	0.072	2.87	2.43	6.2
	mean	5.5	0.77	2.3	0.056	—	0.089	0.25	0.62	3.4	0.380	0.20	0.100	0.202	0.310	0.067	1.13	0.95	3.8

[a]Minimum and maximum values were based on all samples, whereas means were calculated from detected values only

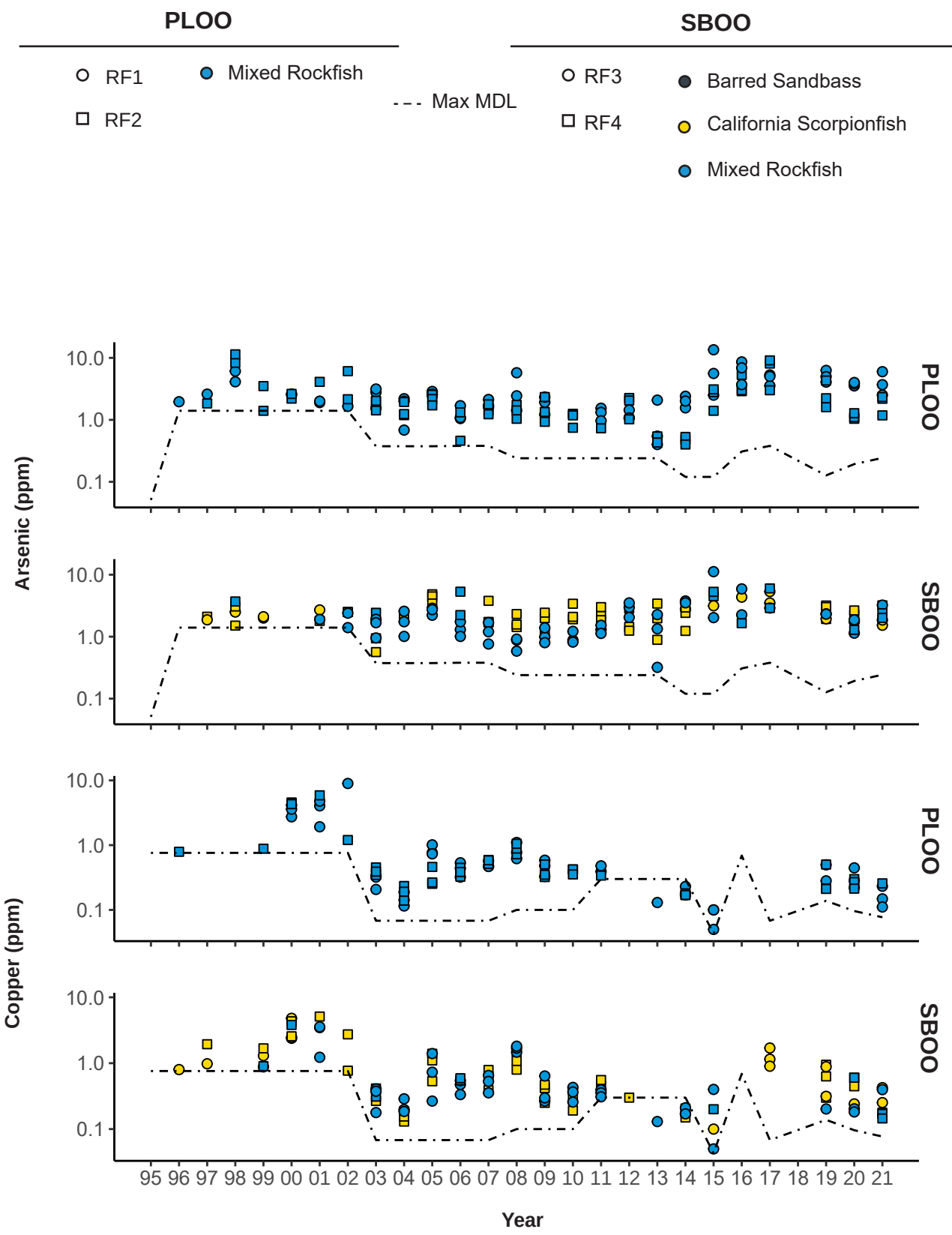

Figure 9.4
Concentrations of select metals detected in muscle tissues of fishes collected from PLOO and SBOO rig fishing zones from 1995 through 2021. Zones RF1 and RF3 are considered nearfield. No samples were collected in 2018 as described in text.

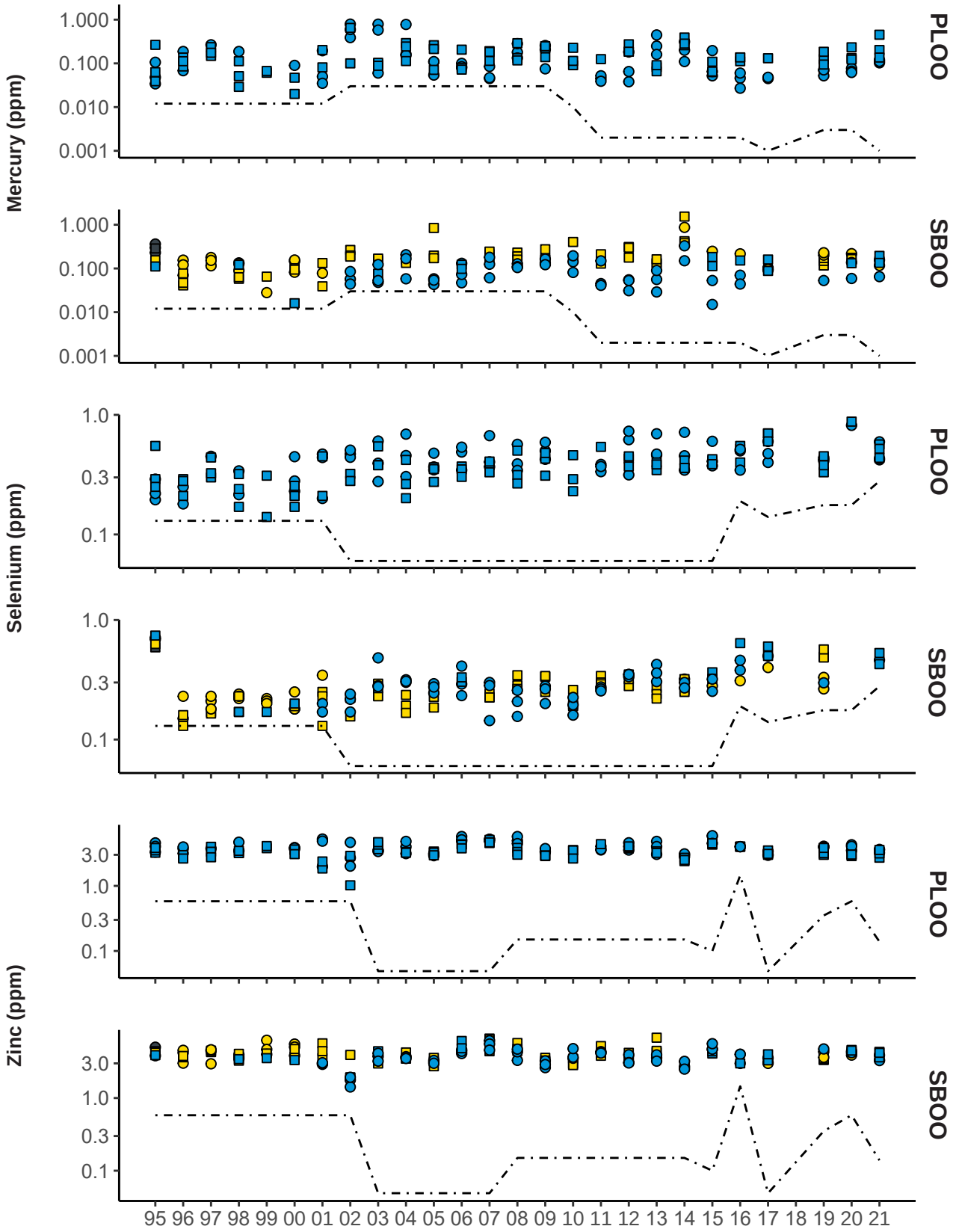

Figure 9.4 *continued*

Table 9.8

Summary of metals (ppm), pesticides (ppb), and total PCB (ppb) in fish muscle samples with chemistry concentrations that exceeded available thresholds (see Mearns et al 1991) from PLOO and SBOO rig fishing zones sampled historically (1995–2019) and during the current reporting period (2020–2021). Data include the percent of samples that exceeded thresholds during each time period. See Tables 9.2–9.7, 9.9–9.10 for total number of samples analyzed.

		PLOO				SBOO			
		1995–2019		2020–2021		1995–2019		2020–2021	
Threshold		RF1	RF2	RF1	RF2	RF3	RF4	RF3	RF4
Median International Standard [a]									
Arsenic	1	72	50	100	33	50	67	83	83
Cadmium	1	0	0	0	0	0	0	0	0
Chromium	1	1	1	0	0	4	0	0	0
Copper	20	0	0	0	0	0	0	0	0
Lead	2	0	0	0	0	0	0	0	0
Mercury	1	7	1	0	0	1	3	0	0
Selenium	0.30	76	70	67	67	31	35	17	33
Tin	175	0	0	0	0	0	0	0	0
Zinc	70	0	0	0	0	0	0	0	0
Total Chlordane	100	0	0	0	0	0	0	0	0
Total DDT	5000	0	0	0	0	0	0	0	0
Hexachlorobenzene	100	0	0	0	0	0	0	0	0
OEHHA [b]									
Mercury	0.22	19	21	0	33	10	18	0	0
Selenium	7.40	0	0	0	0	0	0	0	0
Total DDT	21	19	10	0	0	13	7	0	0
Total Chlordane	6	0	0	0	0	0	0	0	0
Total PCB	4	24	13	67	33	15	4	17	0
USFDA [a]									
Mercury	1	0	0	0	0	0	1	0	0
Total DDT	5000	0	0	0	0	0	0	0	0
Hexachlorobenzene	300	0	0	0	0	0	0	0	0

[a] From Mearns et al. 1991. USFDA action limits for mercury and all international standards are for shellfish, but are often applied to fish

[b] From the California OEHHA (Klasing and Brodberg 2008);

Among the various detected pesticides, the rate of threshold exceedances for the current reporting period were similar to those observed previously (1995–2019) (Table 9.8). Since 1995, median international standards for total chlordane, total DDT, and hexachlorobenze, the OEHHA fish contaminant goal for total chlordane, and the USFDA action limits for total DDT and hexachlorobenze were never exceeded, while the OEHHA fish contaminant goal for total DDT was exceeded in ≤19% of samples per zone.

PCBs

During 2020–2021 PCBs were detected in 58% of all muscle tissue samples from PLOO and 25% SBOO rig fishing zones, at concentrations ≤8.1 ppb (Table

Table 9.9

Summary of pesticides (ppb), total PCB (ppb), total PAH (ppb), and lipids (% weight) in muscle tissues of fishes collected from PLOO and SBOO rig fishing stations during 2020–2021. Data include the number of detected values (n), minimum, maximum, and mean [a] detected concentrations for each species, and the total number of samples, detection rate (DR%), and maximum value for all species; nd = not detected.

		Pesticide					
		tDDT	Dieldrin	Endrin	tPCB	tPAH	Lipids
PLOO	Mixed Rockfish						
	n	2	0	0	1	0	2
	Min	4.6	—	—	nd	—	0.2
	Max	5.7	—	—	1.2	—	0.4
	Mean	5.2	—	—	1.2	—	0.3
	Starry Rockfish						
	n	4	0	0	2	0	4
	Min	1.7	—	—	nd	—	0.1
	Max	15.4	—	—	8.1	—	0.4
	Mean	8.1	—	—	7.1	—	0.2
	Vermilion Rockfish						
	n	6	0	0	4	1	6
	Min	4.1	—	—	nd	nd	0.2
	Max	7.8	—	—	6.3	299	0.6
	Mean	5.6	—	—	5.1	299	0.4
	Total Samples	12	12	12	12	12	12
	DR%	100	0	0	58	8	100
	Max	15.4	0	0	8.1	299	0.6
SBOO	California Scorpionfish						
	n	5	0	0	3	0	6
	Min	nd	—	—	nd	—	0.1
	Max	13.1	—	—	6.0	—	0.8
	Mean	5.9	—	—	2.3	—	0.3
	Gopher Rockfish						
	n	2	0	0	0	0	1
	Min	0.9	—	—	—	—	nd
	Max	1.6	—	—	—	—	0.2
	Mean	1.3	—	—	—	—	0.2
	Mixed Rockfish						
	n	2	1	1	0	1	4
	Min	nd	nd	nd	—	nd	0.1
	Max	2.7	0.3	0.7	—	227	0.3
	Mean	2.3	0.3	0.7	—	227	0.2
	Total Samples	12	12	12	12	12	12
	DR%	75	8	8	25	8	92
	Max	13.1	0.3	0.7	6.0	227	0.8

[a] Minimum and maximum values were based on all samples, whereas means were calculated from detected values only

9.9). Several samples from PLOO zones RF1 and RF2 (67% and 33%, respectively), and from SBOO nearfield zone RF3 (17%), had total PCB levels in exceedance of the OEHHA threshold of 3.6 ppb (Table 9.8). Historically, PCB detection rates were 16–75% per species (or species group) in muscle tissue samples, with highly variable concentrations falling within ranges reported elsewhere in the SCB (e.g., Allen et al. 2002, Mearns et al. 1991, LACSD 2016, OCSD 2018, McLaughlin et al 2020) and

Table 9.10

Summary of pesticides (ppb), total PCB (ppb), total PAH (ppb), and lipids (% weight) in muscle tissues of fishes collected from PLOO and SBOO rig fishing zones from 1995 through 2021. Data include total number of samples (n), detection rate (DR%), minimum, maximum, and mean[a] detected concentrations per species; nd = not detected.

		Pesticides								
		tChlor	tDDT	Dieldrin	Endrin	HCB	tHCH	tPCB	tPAH	Lipids
PLOO	Mixed Rockfish									
	n	142	142	130	130	132	142	142	69	142
	DR (%)	2	92	0	0	10	1	41	7	98
	min	nd	nd	—	—	nd	nd	nd	nd	nd
	max	2.4	217.3	—	—	15	13.4	69	360.1	4.4
	mean	1.4	13.3	—	—	1.6	13.4	9.1	180.6	0.9
SBOO	Barred Sand Bass									
	n	4	4	4	4	4	4	4	4	4
	DR (%)	0	50	0	0	0	0	75	0	100
	min	—	nd	—	—	—	—	nd	—	0.7
	max	—	13	—	—	—	—	32	—	1.4
	mean	—	9.6	—	—	—	—	20	—	1
	California Scorpionfish									
	n	78	78	76	76	73	78	82	61	82
	DR (%)	0	92	0	0	0	0	39	3	100
	min	—	nd	—	—	—	—	nd	nd	0.05
	max	—	195.7	—	—	—	—	49.3	22.7	2.6
	mean	—	17.3	—	—	—	—	5.4	18.4	0.6
	Mixed Rockfish									
	n	61	61	54	54	57	61	63	59	63
	DR (%)	0	74	2	2	7	0	16	5	98
	min	—	nd	nd	nd	nd	—	nd	nd	nd
	max	—	15.1	0.3	0.7	7.2	—	5.6	227.0	3.0
	mean	—	3.4	0.3	0.7	2.0	—	1.7	92.4	0.6

[a] Minimum and maximum values were based on all samples, whereas means were calculated from detected values only

with no discernable patterns that could be associated with proximity to either outfall (Table 9.10, Figure 9.5). From 1995 through 2019, the OEHHA fish contaminant goal was exceeded in 4–24% of samples collected per zone (Table 9.8).

PAHs

During 2020–2021 PAHs were detected in 8% of the muscle tissue samples from PLOO and SBOO rig fishing zones, at concentrations ≤299 ppb (Table 9.9). Historically, PAH detection rates were 0–7% per species (or species group) in muscle tissue samples, with highly variable concentrations falling within ranges reported elsewhere in the SCB (e.g., Allen et al. 2002, Mearns et al. 1991, LACSD 2016, OCSD 2018) and with no discernable patterns that could be associated with proximity to either outfall (Table 9.10, Appendix J.7).

Discussion

Several trace metals, pesticides, PCBs, and PAHs were detected in liver tissues from various fish species collected in the Point Loma and South Bay

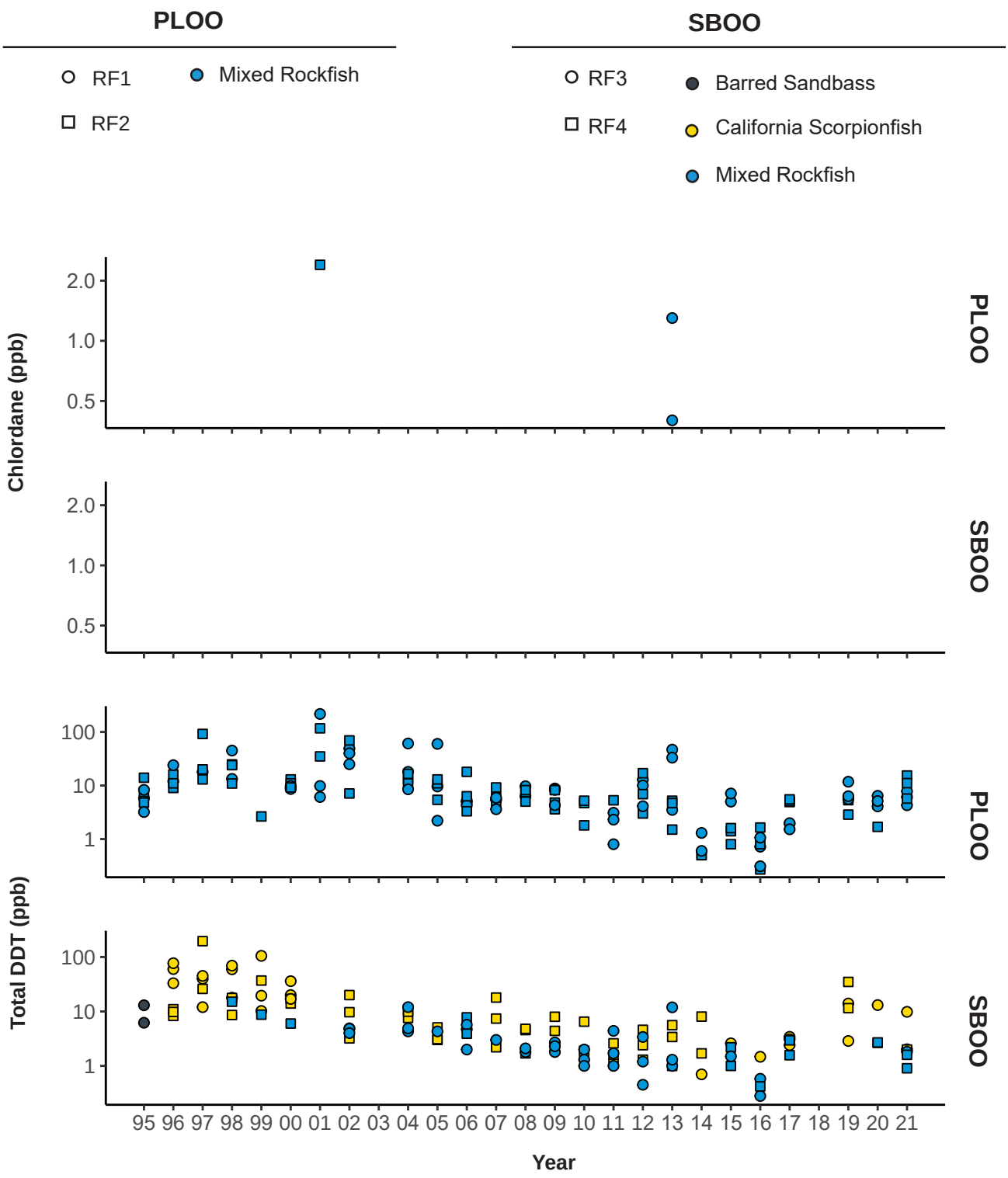

Figure 9.5
Concentrations of pesticides and total PCB in muscle tissues of fishes collected from PLOO and SBOO rig fishing zones from 1995 through 2021. Zones RF1 and RF3 are considered nearfield. No samples were collected in 2018 as described in text.

monitoring regions in 2020–2021. Many of the same metals, pesticides, PCBs, and PAHs were detected during this reporting period, as have been documented historically in California Scorpionfish and rockfish muscle tissues, albeit generally less frequently and/or in lower concentrations. Although tissue contaminant

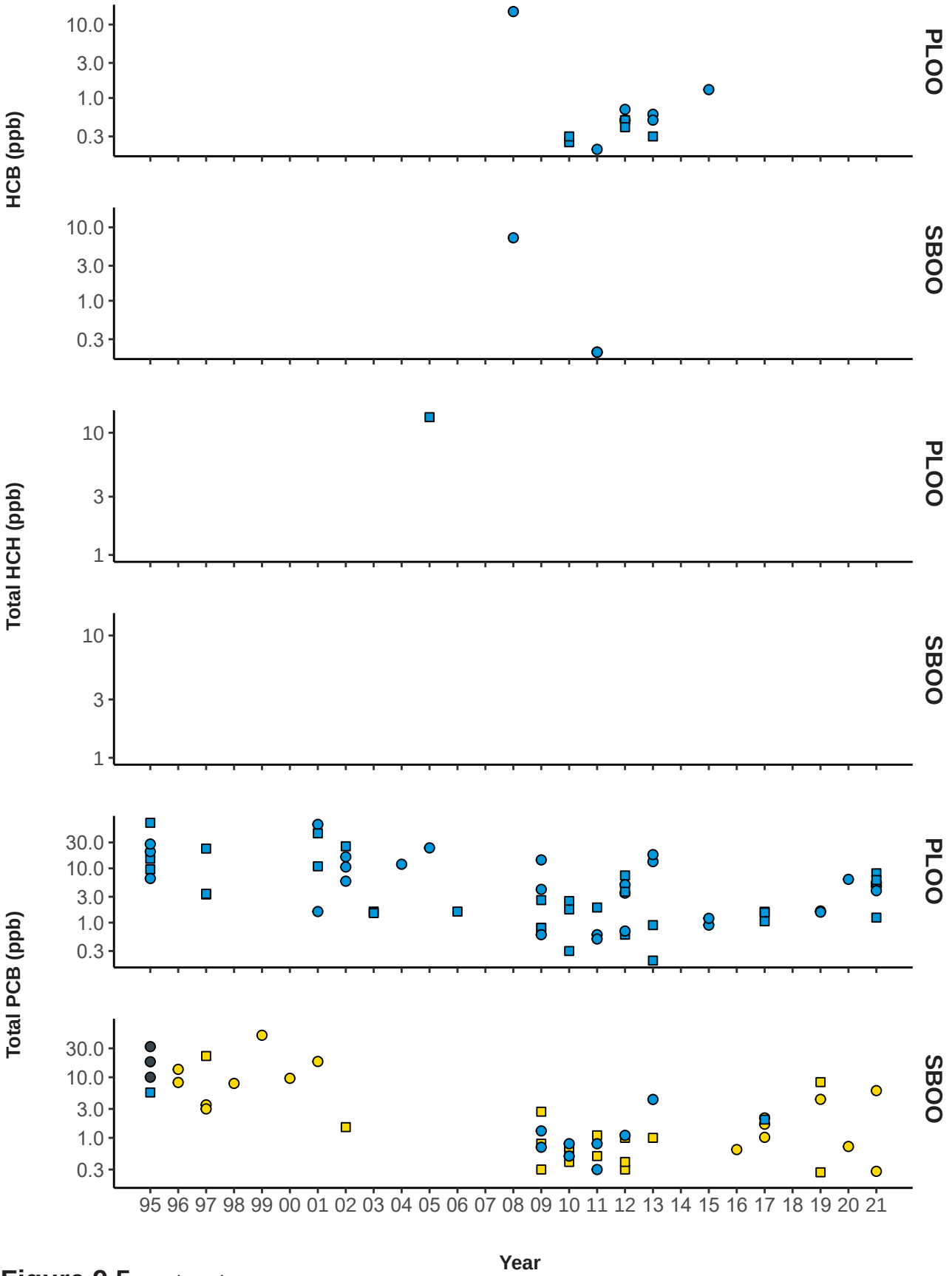

Figure 9.5 *continued*

concentrations varied among different species of fish and across stations, most values were within ranges reported previously for southern California fishes (e.g., Mearns et al. 1991, Allen et al. 1998, 2002, CLA 2015, LACSD 2016, OCSD 2018, McLaughlin et al 2020). Over the 2 years, arsenic and selenium were found to exceed their median international standards for human consumption in ≥17% of the muscle tissue samples from sport fish collected from PLOO and SBOO rig fishing zones. In contrast, all muscle tissue samples had concentrations of mercury, total chlordane, and total DDT below USFDA action limits. Historically, elevated levels of such contaminants have remained uncommon in sport fish collected from both survey areas.

The frequent occurrence of different trace metals and chlorinated hydrocarbons in the tissues of fish collected from the PLOO and SBOO regions is likely influenced by multiple factors. For example, many metals occur naturally in the environment, although little information is available on background levels in fish tissues. Brown et al. (1986) determined that there may be no area in the SCB sufficiently free of chemical contaminants to be considered a reference site, while Mearns et al. (1991) described the distribution of several contaminants, such as arsenic, mercury, DDT, and PCBs as being ubiquitous. The wide-spread distribution of contaminants in SCB fishes has been supported by more recent work regarding PCBs and DDT (e.g., Allen et al. 1998, 2002).

Other factors that affect contaminant loading in fish tissues include the physiology and life history of different species (see Groce 2002). Exposure to contaminants can also vary greatly between different species and among individuals of the same species depending on migration pathways (Otway 1991). Fishes may be exposed to contaminants in a highly polluted area and then move into areas free of contamination. For example, California Scorpionfish tagged in Santa Monica Bay have been recaptured as far south as the Coronado Islands (Hartmann 1987, Love et al. 1987). This is of particular concern for fishes collected in the vicinity of the PLOO and the SBOO, as there are many point and non-point sources that may contribute to local contamination in the region, including the San Diego River, San Diego Bay, Tijuana River, and offshore dredged material disposal sites (see Chapters 2–8 and Parnell et al. 2008). However, assessments of contaminant loading in San Diego offshore sediments have revealed no evidence to indicate that the PLOO or SBOO are major sources of pollutants in the region (see Chapters 5, 7, and Parnell et al. 2008).

Overall, there was no evidence of contaminant accumulation in PLOO or SBOO fishes during the 2020–2021 reporting period that could be associated with wastewater discharge from either outfall, which is consistent with historical findings. Concentrations of most contaminants were generally similar across trawl or rig fishing zones, and no relationships with the PLOO or SBOO were evident. These results are consistent with findings of other assessments of bioaccumulation in fishes off San Diego (Parnell et al. 2008, City of San Diego 2020a, 2022). Finally, there were no other indications of poor fish health in the region, such as the presence of fin rot or other indicators of disease (see Chapter 8).

Literature Cited

Allen, M.J., S.L. Moore, K.C. Schiff, D. Diener, S.B. Weisberg, J.K. Stull, A. Groce, E. Zeng, J. Mubarak, C.L. Tang, R. Gartman, and C.I. Haydock. (1998). Assessment of demersal fish and megabenthic invertebrate assemblages on the mainland shelf of Southern California in 1994. Southern California Coastal Water Research Project, Westminster, CA.

Allen, M.J., A.K. Groce, D. Diener, J. Brown, S.A. Steinert, G. Deets, J.A. Noblet, S.L. Moore, D. Diehl, E.T. Jarvis, V. Raco-Rands, C. Thomas, Y. Ralph, R. Gartman, D. Cadien, S.B. Weisberg, and T. Mikel. (2002). Southern California Bight 1998 Regional Monitoring Program: V. Demersal Fishes and Megabenthic Invertebrates. Southern California Coastal Water Research Project, Westminster, CA.

Brown, D.A., R.W. Gossett, G.P. Hershelman, C.G. Word, A.M. Westott, and J.N. Cross. (1986). Municipal wastewater contamination in the Southern California Bight: Part I — Metal and Organic Contaminations in Sediments and Organisms. Marine Environmental Research, 18:291–310

Cardwell, R. D. (1991). Methods for evaluating risks to aquatic life and human health from exposure to marine discharges of municipal wastewaters. Pages 253–252 in A. G. Miskiewicz (ed.). Proceedings of a Bioaccumulation Workshop: Assessment of the Distribution, Impacts, and Bioaccumulation of Contaminants in Aquatic Environments. Australian Marine Science Association, Inc./WaterBoard.

[CLA] City of Los Angeles, Environmental Monitoring Division. (2015). Marine Monitoring in Santa Monica Bay: Biennial Assessment Report for the Period January 2013 through December 2014. Report submitted to USEPA and RWQCB (Los Angeles). Department of Public Works, LA Sanitation, Hyperion Treatment Plant, Playa del Rey, California, pp. 1-264 + appendices.

City of San Diego. (2015). Point Loma Ocean Outfall Annual Receiving Waters Monitoring and Assessment Report, 2014. City of San Diego Ocean Monitoring Program, Public Utilities Department, Environmental Monitoring and Technical Services Division, San Diego, CA.

City of San Diego. (2020a). Biennial Receiving Waters Monitoring and Assessment Report for the Point Loma and South Bay Ocean Outfalls, 2018–2019. City of San Diego, Public Utilities Department, Environmental Monitoring and Technical Services Division, San Diego, CA.

City of San Diego. (2020b). Quality Assurance Project Plan for Coastal Receiving Waters Monitoring. City of San Diego Ocean Monitoring Program, Public Utilities Department, Environmental Monitoring and Technical Services Division, San Diego, CA.

City of San Diego. (2021). Interim Receiving Waters Monitoring Report for the Point Loma Ocean Outfall and South Bay Ocean Outfalls, 2020. City of San Diego Ocean Monitoring Program, Public Utilities Department, Environmental Monitoring and Technical Services Division, San Diego, CA.

City of San Diego. (2022). Appendix C5. Bioaccumulation Assessment. In: Application for Renewal of NPDES CA0107409 and 301(h) Modified Secondary Treatment Requirements Point Loma Ocean Outfall. Volume V, Appendix C. Public Utilities Department, Environmental Monitoring and Technical Services Division, San Diego, CA.

Connell, D. W. (1988). Bioaccumulation behavior of persistent organic chemicals with aquatic organisms. Review of Environmental Contamination and Toxicology, 101:117–154.

Groce, A.K. (2002). Influence of life history and lipids on the bioaccumulation of organo-chlorines in demersal fishes. Master's thesis. San Diego State University. San Diego, CA.

Hartmann, A.R. (1987). Movement of scorpionfishes (Scorpaenidae: Sebastes and Scorpaena) in the Southern California Bight. California Fish and Game, 73: 68–79.

Helsel, D.R. (2005a). More than obvious: better methods for interpreting nondetect data. Environmental Science & Technology (October 15, 2005), 419A-423A.

Helsel, D.R. (2005b). Nondetects and Data Analysis: Statistics for Censored Environmental Data. John Wiley, New York.

Helsel, D.R. (2006). Fabrication data: how substituting values for nondetects can ruin

results, and what can be done about it. Chemosphere 65: 2434-2439.

Kassambara, A. (2020). ggpubr: 'ggplot2' Based Publication Ready Plots. R package version 0.2.5 https://CRAN.R-project.org/package=ggpubr.

Klasing, S. and R. Brodberg. (2008). Development of Fish Contaminant Goals and Advisory Tissue Levels for Common Contaminants in California Sport Fish: Chlordane, DDTs, Dieldrin, Methylmercury, PCBs, Selenium, and Toxaphene. California Environmental Protection Agency, Office of Environmental Health Hazard Assessment, Sacramento, CA.

[LACSD] Los Angeles County Sanitation District. (2016). Joint Water Pollution Control Plant Biennial Receiving Water Monitoring Report 2014-2015. Los Angeles, CA.

Love, M.S., B. Axell, P. Morris, R. Collins, and A. Brooks. (1987). Life history and fishery of the California scorpionfish, Scorpaena guttata, within the Southern California Bight. Fisheries Bulletin, 85: 99–116.

McLaughlin, K., K. Schiff, B. Du, J. Davis, A. Bonnema, G. Ichikawa, B. Jakl, and W. Heim. 2020. Southern California Bight 2018 Regional Monitoring Program: Volume V. Contaminant Bioaccumulation in Edible Sport Fish Tissue. Technical Report 1155. Southern California Coastal Water Research Project. Costa Mesa, CA.

Mearns, A.J., M. Matta, G. Shigenaka, D. MacDonald, M. Buchman, H. Harris, J. Golas, and G. Lauenstein. (1991). Contaminant Trends in the Southern California Bight: Inventory and Assessment. NOAA Technical Memorandum NOS ORCA 62. Seattle, WA.

Oksanen, J., F.G. Blanchet, R. Kindt, P. Legendre, P.R. Minchin, R.B. O'Hara, G.L. Simpson, P. Solymos, M.H.H. Stevens, and H. Wagner. (2019). vegan: Community Ecology Package. R package version 2.5-6. http://CRAN.R-project.org/package=vegan.

[OCSD] Orange County Sanitation District. (2018). Ocean Monitoring Annual Report, Year 2016 – 2017. Marine Monitoring, Fountain Valley, CA.

Otway, N. (1991). Bioaccumulation studies on fish: choice of species, sampling designs, problems and implications for environmental management. In: A.G. Miskiewicz (ed.). Proceedings of a Bioaccumulation Workshop: Assessment of the Distribution, Impacts, and Bioaccumulation of Contaminants in Aquatic Environments. Australian Marine Science Association, Inc./Water Board.

Parnell, P.E., A.K. Groce, T.D. Stebbins, and P.K. Dayton. (2008). Discriminating sources of PCB contamination in fish on the coastal shelf off San Diego, California (USA). Marine Pollution Bulletin, 56: 1992–2002.

R Core Team. (2021). R: A language and environment for statistical computing. R Foundation for Statistical Computing, Vienna, Austria. URL https://www.R-project.org/

Rand, G.M., ed. (1995). Fundamentals of Aquatic Toxicology: Effects, Environmental Fate, and Risk Assessment. 2nd ed. Taylor and Francis, Washington, D.C.

Revelle, W. (2019) psych: Procedures for Personality and Psychological Research, Northwestern University, Evanston, Illinois, USA, https://CRAN.R-project.org/package=psych Version=1.9.12.31.

Schiff, K. and M.J. Allen. (1997). Bioaccumulation of chlorinated hydrocarbons in livers of flatfishes from the Southern California Bight. In: S.B. Weisberg, C. Francisco, and D. Hallock (eds.). Southern California Coastal Water Research Project Annual Report 1995–1996. Southern California Coastal Water Research Project, Westminster, CA.

[USEPA] United States Environmental Protection Agency. (2000). Bioaccumulation Testing and Interpretation for the Purpose of Sediment Quality Assessment. Status and Needs. EPA-823-R-00-001. U.S. Environmental Protection Agency. February 2000.

Wickham, H. (2007). Reshaping Data with the reshape Package. Journal of Statistical Software, 21(12), 1-20. URL http://www.jstatsoft.org/v21/i12/.

Wickham, H. (2011). The Split-Apply-Combine Strategy for Data Analysis. Journal of Statistical Software, 40(1), 1-29. URL http://www.jstatsoft.org/v40/i01/.

Wickham, H. (2019). Scales: Scale Functions for Visualization Rstudio. R package version 1.1.0. https://scales.r-lib.org/.

Wickham, H., M. Averick, J. Bryan, W. Chang, L. D'Agostino McGowan, R. François, G.Grolemund, A. Hayes, L. Henry, J. Hester, M. Kuhn, T. Lin Pedersen, E. Miller, S. Milton Bache, K. Müller, J. Ooms, D. Robinson, D. P. Seidel, V. Spinu, K. Takahashi, D. Vaughan, C. Wilke, K. Woo, H. Yutani. (2019). Welcome to the tidyverse. Journal of Open Source Software, 4(43), 1686, https://doi.org/10.21105/joss.01686.

Zeileis, A and G. Grothendieck. (2005). zoo: S3 Infrastructure for Regular and Irregular Time Series. Journal of Statistical Software, 14(6), 1-27. URL http://www.jstatsoft.org/v14/i06/.

Appendices

Appendix A

Evaluation of Anthropogenic Impacts on the San Diego Coastal Kelp Forest Ecosystem (Biennial Project Report)

2020 – 2021

Ed Parnell, PhD
Kristin Riser
Brenna Bulach, MS
Paul K. Dayton, PhD

Scripps Institution of Oceanography, UC San Diego
9500 Gilman Dr., La Jolla, CA 92093-0227

Submitted to City of San Diego
Public Utilities Department

March 31, 2022

Evaluation of Anthropogenic Impacts on the San Diego Coastal Kelp Forest Ecosystem (Biennial Project Report): 2020 to 2021

Prepared By:

Ed Parnell, PhD[1*]
Kristin Riser[1]
Brenna Bulach, MS[1]
Paul K. Dayton, PhD[1]

March 31, 2022

[*]Corresponding Author: edparnell@ucsd.edu
[1]Scripps Institution of Oceanography, UC San Diego
9500 Gilman Dr, Mail Code 0227, La Jolla, CA 92093-0227

EXECUTIVE SUMMARY

Kelp forests are among the most charismatic marine communities off the southern California coast. They are highly productive, characterized by the rapid growth of their structural species, *Macrocystis pyrifera* (commonly referred to as giant kelp), whose areal rate of primary production can exceed that of tropical rain forests (Towle and Pearse, 1973). Giant kelp forests provide habitat, food and shelter for a host of fishes and invertebrates, and competes with many other algal species. Kelp forests occupy the inner margins of the southern California continental shelf and offshore islands extending from the offshore edge of tidepools to depths as great as thirty meters off the mainland of southern California. Kelp forests also host a range of economically and aesthetically important consumptive and non-consumptive human activities including boating, recreational fishing, spearfishing, SCUBA diving, and the commercial harvest of finfishes, invertebrates, and algae. The kelp forests off Point Loma and La Jolla are among the most important commercial fishing grounds for the red sea urchin (*Mesocentrotus franciscanus*) and spiny lobster (*Panulirus interruptus*) fisheries off California. The kelp forests of La Jolla and Point Loma are the largest contiguous kelp forests off the western coast of the US.

Kelp forests off southern California are affected by both natural and human disturbances. The El Niño Southern Oscillation (ENSO) is the primary ocean climate mode that affects kelp abundance, growth, and reproduction along the west coast of the Americas. Positive ENSO's, known as El Niños, are associated with warm water, depressed concentrations of nitrate ,the principal nutrient limiting giant kelp, and a more energetic storm environment off southern California. Both phenomenon can severely stress giant kelp and accompanying species of algae. The opposite conditions occur during negative ENSO events, termed La Niñas, enhancing both the growth and reproduction of kelps. Together, the two ocean climate modes drive the greatest amount of annual variability in surface canopy cover of *M. pyrifera* off southern and Baja California. The periodicity of El Niño is variable, typically occurring at 3-5 year intervals and persisting for <1 year. Kelp forests wax and wane over these cycles, experiencing high mortality during El Niños with recovery afterwards. Rates of recovery depend on growth conditions after an El Niño ebbs. The kelp forests off San Diego have been studied by researchers at the Scripps Institution of Oceanography (SIO) since the 1950's, and baseline data collection began in the 1970's. Currently, kelps and associated animals are monitored at twenty permanent study sites located among the Pt. Loma, La Jolla, and North County kelp forests.

During the current reporting period (2020-2021), the kelp forests off southern California are experiencing a stalled recovery from a marine heat wave that began in 2014 and persisted until the spring of 2017. This lengthened period of heat stress was due to the combination of two consecutive ocean climate events. An anomalous warm pool extended across much of the NE Pacific from 2014-2015. This warm pool, unique in the climate record of the NE Pacific, was coined the BLOB and resulted from decreased wind mixing in the NE Pacific. The climatic forcing of the NE Pacific warm pool is different in nature and scale than ENSO cycles which are caused by anomalous winds along the equatorial Pacific. A strong El Niño occurred during fall of 2015 and the winter of 2016 just as the BLOB was dissipating along the US west coast. Together these consecutive warm events are now referred to as the NE Pacific marine heat wave (MHW) which was the longest and warmest heat event ever observed in the 110 year record of sea surface temperature at the Scripps Institution of Oceanography (SIO) pier. Cooler conditions returned to the equatorial eastern Pacific and the Southern California Bight by late 2016. The spring upwelling seasons of 2017-2021 brought cool nutrient-laden waters up onto the inner continental shelf of southern California creating favorable conditions for giant kelp recovery. However, this cooling is superimposed onto a larger scale trend of increasing ocean temperatures within the California Current System and the global ocean generally. As the ocean

absorbs ever more heat it becomes increasingly likely that conditions supportive of giant kelp growth and reproduction will decrease in frequency and duration over the next century. Because of this, risks to *M. pyrifera* persistence in southern California will likely increase. In fact, the failure of giant kelp to recover over much of its former range off San Diego despite favorable ocean conditions may be evidence that this risk is now manifest.

The marine heat wave and associated depressed nutrient conditions decimated *M. pyrifera* and cohabiting algae off San Diego. Pooled across 20 kelp forest sites, densities of adult *M. pyrifera* were reduced >90%. Unlike previous warm events attributed to El Niño, the coupled marine heat wave resulted in warming and low nutrient exposure of understory kelp species for prolonged periods of time leading to dramatic reductions of those species in addition to giant kelp. The BLOB persisted longer than a typical El Niño and kelps did not recover after the warm pool dissipated as a result of the stress induced by the following El Niño of 2016. The two events affected kelps at the study sites differently, and the historic pattern of areal synchronized mortality and recovery was disrupted. Growth conditions returned to normal with the onset of mild La Niña conditions in the spring of 2017. Rates of giant kelp recovery since then have been variable among study sites and were initially slower than previous recovery periods and non-existent at some study sites. Surface canopy cover in some areas was precluded by increases in understory species density. Some of these areas will likely remain devoid of giant kelp canopy for years since understory species are long-lived and competitively interfere with giant kelp recruitment. Favorable conditions for kelp growth and reproduction returned with the 2018 spring upwelling season and continued through 2021. Numerous study sites experienced significant giant kelp recruitment that successfully matured and became reproductive. However, the giant kelp canopy off San Diego County remains patchy due to a combination of competition with understory species in the shallower margins of the kelp forests and a lack of recruitment in many deeper areas through early 2018. The lack of recruitment in areas deeper than 18 m is possibly a result of decreased light levels caused by phytoplankton blooms. Giant kelp abundances and stipe densities are presently very low relative to historical levels, and recovery from the MHW persists at only five of our 20 study sites. Most other sites are now dominated by space-competitive understory species or are highly disturbed with very little algae.

An anomalously warm surface layer, limited to the upper 3-5 meters of the ocean's surface, bathed much of the southern California coast during the summer of 2018. Sea surface temperatures reached 27°C, exceeding the all time high temperature record for the SIO Pier sea surface temperature series by ~2°C . Summer surface temperature maxima in this record are typically ~23°C. This surface warm pool degraded the giant kelp canopy tissue which was mostly lost from the offshore forests and drifted onto nearby beaches. However, cooler temperatures persisted closer to the bottom, and most of the giant kelp plants in the initial recovery cohorts of 2017 and 2018 survived and regrew to the surface when the warm pool dissipated by the fall of 2018. However, the marine heat wave decimated what remained of the North County kelp forests and the warm surface anomaly resulted in almost total loss of giant kelp within these forests. Recruitment in these forests has been extremely limited and unsuccessful. Similar near-surface warming events have occurred over the last two summers but were not as strong as the 2018 event. The combination of understory overgrowth and summer surface warming may be leading to reduced giant kelp abundances over the long term where it will be limited to smaller patches within its historical footprint. This pattern may herald the eventual loss of giant kelp canopy throughout much of southern California as warming conditions increasingly favor understory kelps such that kelp forests off San Diego mirror those of central Baja California where giant kelp canopy cover is greatly reduced to ephemeral patches. Such a change reflects the initial stages of a poleward biogeographical shift for *M. pyrifera*.

Diseases in many invertebrates, including sea urchins (echinoids) and predatory seastars (asteroids), are common during warm events. Mass mortality of red (*Mesocentrotus franciscanus*) and purple sea urchins (*Strongylocentrotus purpuratus*) and seastars in the genus *Pisaster*, began off San Diego in 2014 and extended through 2017. Sea urchins are primary grazers of many kelp species, and can overgraze giant kelp and associated algal species given the right conditions. They are capable of limiting or even precluding giant kelp recovery, and overgrazed areas known as barrens, can persist in some areas for decades. The echinoderm epidemic associated with the MHW resulted in the disappearance or near-disappearance of seastars and the decimation of sea urchins at our study sites and from all San Diego kelp forests generally. Further, little to no recruitment of sea urchins was observed until the fall of 2017 which continued at many sites through the fall of 2021. Despite this recruitment, populations of adult animals have not yet increased and thus sea urchins have not likely contributed to the dampened giant kelp recovery from the MHW. However, these new cohorts of sea urchins may eventually overgraze some areas off San Diego as they emerge from cryptic nursery habitat and begin to actively forage. Sea urchin overgrazing has been a recurring problem off south Pt. Loma where a unique combination of topography and turbidity emanating from San Diego Bay contribute to resilient barrens. Some recruitment of the seastars *Pisaster giganteus* and *Patiria miniata*, two important kelp forest predators, has been observed off Pt. Loma and La Jolla. However, adult densities are presently still very low and it is unknown whether they will recover anytime soon.

Abalone, another important kelp forest grazer and the target of a once extensive fishery, depend primarily on giant kelp for food. Abalone once supported a large recreational and commercial fishery off southern California until all harvest was closed in 1996 due to depletion from overfishing and disease mainly associated with warm events. Abalone off San Diego County suffered further mortality during and after the 2014-2016 MHW due to disease and lack of food. Abundances of all abalone species at the study sites off La Jolla and Pt. Loma have since declined to near zero with the exception of pink abalone (*Haliotis corrugata*) where there has been some recovery at the two shallowest study sites off central Pt. Loma that began around 2010. Presently, pink abalone densities at these sites are at least an order of magnitude lower than their historical highs.

Sargassum horneri, an invasive algal species that has overwhelmed giant kelp in some sheltered forests off southern California, was first observed in the kelp forests off San Diego in 2014. By 2018, this species had been observed at 13 of 20 study sites, but has since not spread to the remaining sites. Densities of *S. horneri* at the sites where it has been observed have actually decreased over time with the exception of one study site off northern La Jolla where it covers ~3% of the bottom. Presently, this species does not appear to pose as great a risk to San Diego County kelp forests that it has to more sheltered kelp forests off the California Channel Islands.

The failed recovery of giant kelp at many of our study sites can not be due to any localized effects of treated wastewater discharge by the City of San Diego through the ocean outfalls offshore of Imperial Beach (South Bay Ocean Outfall) or Pt. Loma (Pt. Loma Ocean Outfall). The present patchy nature of giant kelp canopy cover is not related to any distance gradient from either outfall. The areas that have exhibited the poorest post-MHW recovery and whose algal communities are the most degraded, relative to their historical condition, include northern La Jolla and North County which are the sites furthest from these outfalls.

INTRODUCTION

Kelp forests are susceptible to human disturbance because of their proximity to urbanized coasts exposing them to overfishing, polluted surface and groundwater discharge, as well as the discharge of wastewater. Perhaps the largest effect is that due to increased turbidity which limits light penetration for kelps to grow, germinate, and reproduce (Clendenning and North, 1960). Dramatic reductions in kelp forest canopy off Palos Verdes have been attributed to the combined effects of wastewater disposal and an energetic El Niño in the late 1950's (Grigg, 1978). Nearshore turbidity due to wastewater discharge has since been mitigated by increasing the offshore distances and depths of discharge, and improved outfall design (Roberts, 1991). Beach replenishment can also negatively impact kelp forests via sedimentation and burial. This has been observed at kelp forests off northern San Diego County where replenished sediments erode from beaches and partially bury low relief habitat that forms the foundation for giant kelp.

The Point Loma Ocean Outfall (PLOO) discharges advanced primary treated wastewater through a deep water open ocean outfall. The Outfall was extended and deepened in 1993, and presently discharges treated wastewater ~7.3 km offshore in marine waters ~98 m deep. The PLOO is situated approximately 5 km offshore of the outer edge of the Point Loma kelp forest. Due to its proximity, wastewater discharge through the PLOO presents at least a perceived risk to the health of the nearby kelp forest community off Pt. Loma. Local human risks to kelp forests can magnify risks posed by larger scale natural disturbances by reducing the resilience of kelp forests after episodic natural disturbances.

Kelp forests in southern California are disturbed naturally by ocean climate variability that occurs at interannual (El Niño Southern Oscillation – ENSO; Fig. 1) and decadal (Pacific Decadal Oscillation - PDO) periods. Positive phases of both ocean climate modes are associated with a deepened thermocline limiting nutrient delivery to the inner shelf that is necessary for kelp growth and reproduction. These modes are also associated with increased storm energy which causes giant kelp mortality via plant detachment and abrasion (Seymour et al., 1989). The northeastern Pacific experienced a profound regime shift in the late 1970's in which the main ocean thermocline deepened, resulting in a step reduction in nitrate concentrations along the Southern California Bight (SCB) that persists at present (Parnell et al., 2010 and Fig. 2). Concentrations of nitrate, the main limiting nutrient for kelp growth in southern California switched from being conducive for kelp growth most years prior to the regime shift, with the exception of the most intense El Niños, to being generally less adequate (Parnell et al., 2010) with the exception of strong negative ENSO phases known as La Niñas. The ecology of kelp forests off San Diego has changed fundamentally due to the increased frequency of natural disturbance resulting in a demographic shift towards younger and smaller *Macrocystis pyrifera* individuals (Parnell et al., 2010).

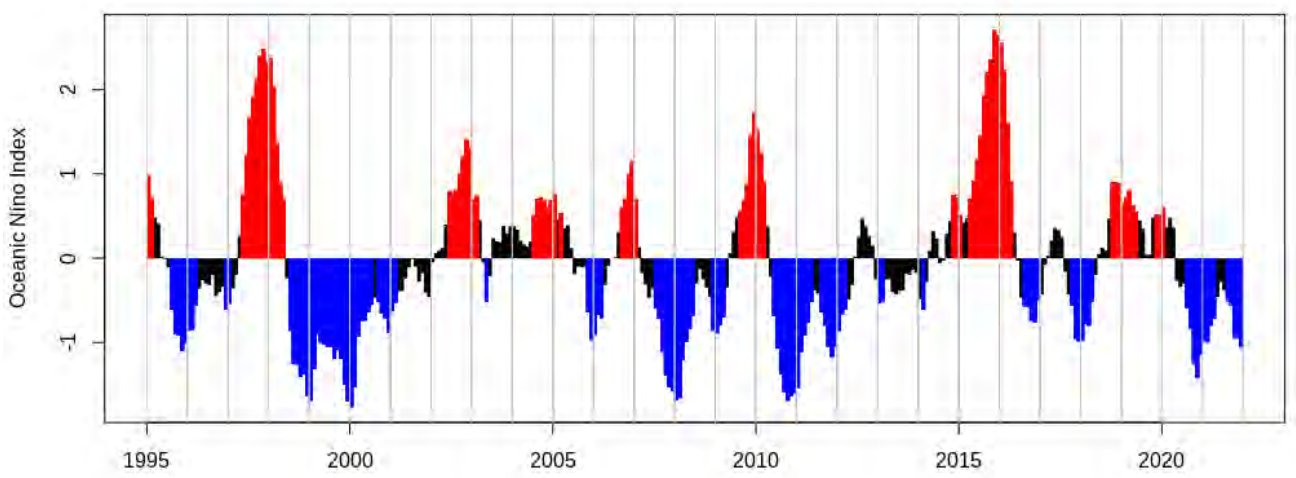

Figure 1. *Barplot of the Oceanic Niño Index (ONI) since 1995. Red bars indicate El Niño conditions, blue bars indicate La Niña conditions, and black bars indicate ENSO neutral conditions (data from NOAA, 2022). The ONI index is based on equatorial sea surface temperatures in the Eastern Pacific.*

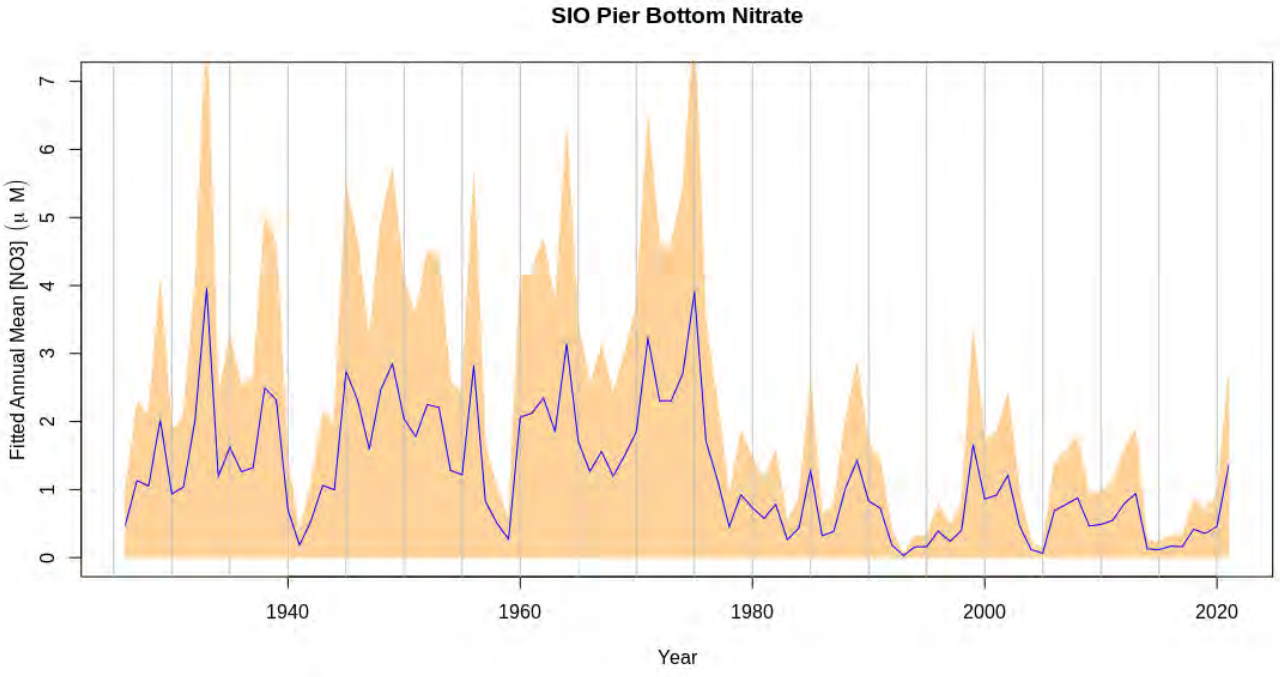

Figure 2. *Time series of annual mean nitrate concentrations estimated from daily temperature and salinity sampled at the base of the Scripps Institution of Oceanography Pier (see Parnell et al., 2010 for details). Dotted gray line indicates the minimum nitrate threshold for the growth and reproduction of giant kelp (M. pyrifera). Peach area indicates the 95% confidence limits.*

Sea urchin overgrazing is another form of natural disturbance within kelp forests (Leighton et al., 1966). Kelps are susceptible to overgrazing when sea urchin densities increase or when sea urchins aggregate into overgrazing fronts. Overgrazing can lead to areas denuded of most or all algae and have been termed barrens. Barrens can be frequent and resilient in some areas including the southern portion of the Pt. Loma kelp forest (Parnell, 2015), or can alternate with forested periods due to external forcing such as reductions in kelp standing stock as a result of El Niño, sea urchin disease epidemics, and indirectly from human activities including the harvest of important sea urchin predators (Steneck et al., 2002). Overfishing of sea urchin predators including spiny lobsters (*Panulirus interruptus*) and sheephead (*Semicossyphus pulcher*) in southern California can lead to outbreaks of sea urchin overgrazing.

A more recent source of disturbance has been the introduction of an invasive alga, *Sargassum horneri*, throughout southern California. This species competes with *Macrocystis pyrifera* for space and light, and is now seasonally dominant in some areas previously dominated by *M. pyrifera*. The most impacted areas include the protected low energy habitats in the lee of islands such as the northern Channel Islands and Santa Catalina Island (Miller et al., 2011). *S. horneri* is now establishing itself in many areas off San Diego County including the kelp forests, bays, and estuaries.

Researchers at the Scripps Institution of Oceanography (SIO) have partnered with the City of San Diego Ocean Monitoring Program to conduct regular surveys of the kelp forests off San Diego County including the kelp forests off Point Loma, La Jolla and North County. These surveys represent a continuation of ecological studies that began at SIO in the Point Loma (PLKF) and La Jolla (LJKF) kelp forests and continue at some of the sites established in the 1970's and 1980's (Dayton and Tegner, 1984). Additional study sites have been established more recently in both kelp forests and in kelp forests off northern San Diego County (North County - NCKF). PLKF and LJKF are the largest contiguous kelp forests off the western United States coast and are historically one of the most studied kelp forest systems in the world.

MATERIALS AND METHODS

Algae, invertebrates and bottom temperatures are monitored at twenty permanently established study sites (Fig. 3). Algae and invertebrates are monitored along four replicate parallel permanent band transects oriented perpendicular to shore (25 x 4 m bands separated 3-5 m apart) except at the DM study site where two sets of band transects are located ~1300 m apart due to the small size and fragmented shape of that forest. The main components of the kelp forest monitoring program include estimation of (1) algal density, growth, reproductive condition and recruitment, (2) invertebrate densities, (3) sea urchin demography (size distributions to monitor for episodic recruitment), and (4) ocean bottom temperature (which is a proxy of ocean nutrient status). The types of data collected and the frequency of collection are listed in Table 1.

Algae

Several life stages of *M. pyrifera* are enumerated to identify recruitment events and follow the fate of recruiting cohorts into adulthood. Survival of recruitment cohorts to adulthood is highly variable and a lack of successful maturation into adulthood indicates changes in the growth environment in the form of stress by temperature and nutrients, grazers, or/or reduced light. Giant kelp life stages include adults (def., ≥4 stipes), pre-adults (def., plants >1 m tall but with <4 stipes), bifurcates (a late post recruitment stage indicated by the presence of a split in the apical meristem which represents the primary dichotomous branching event), and pre-bifurcates (very early post

settlement stage lacking the initial dichotomous split). Stipe numbers are counted and recorded for each adult plant each visit.

Conspicuous macroalgal species/groups are enumerated or percent cover is estimated within 5 x 2 m (10 m^2) contiguous quadrats along the band transect lines at all sites. Reproduction and growth of *M. pyrifera*, and the understory kelps *Pterygophora californica* and *Laminaria farlowii,* are measured on permanently tagged plants along the central Pt. Loma study sites.

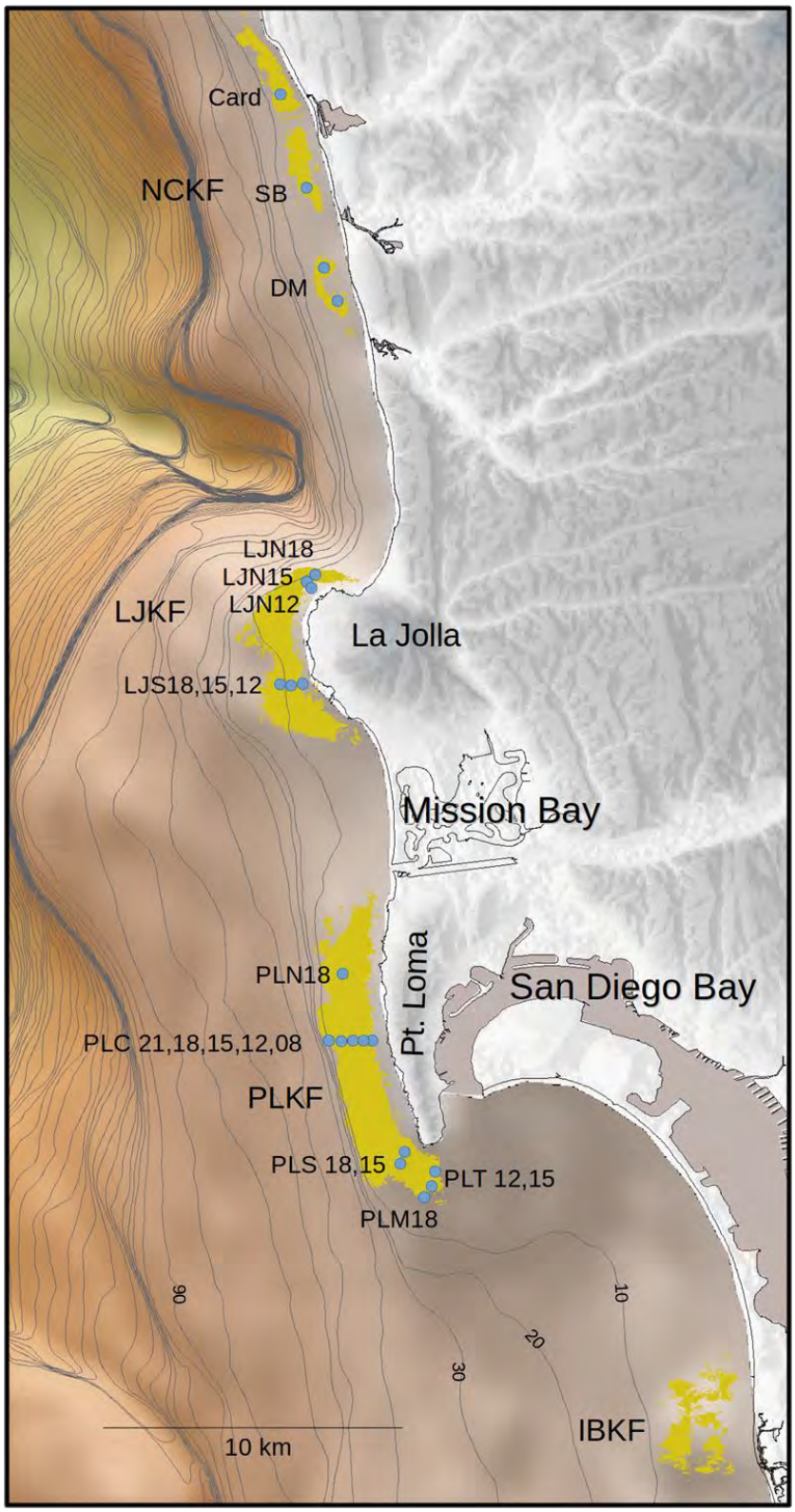

Figure 3. *Map of the San Diego inner shelf showing locations of the Point Loma, La Jolla, North County, and Imperial Beach kelp forests (indicated by PLKF, LJKF, NCKF, and IBKF, respectively). Permanent study site locations are indicated by blue circles and corresponding study site names. Depth contour units are meters.*

Growth of *M. pyrifera* is monitored by counting the number of stipes on each tagged plant one meter above the substratum. Reproductive state is represented by the size of the sporophyll bundle (germ tissue) at the base of each plant. Sporophyll volume is calculated as a cylinder based on the height and diameter of each bundle. This is an indirect measure of reproductive effort. Reed (1987) has shown that sporophyll biomass is closely related to zoospore production. Reproductive capacity, a derived parameter that represents the relative reproductive potential among plants by coupling sporophyll volume and reproductive state, is calculated as the product of sporophyll volume and squared reproductive state. Reproductive capacity is then standardized by division of each value by the maximal value observed among all sites. Reproductive state for each plant is ranked according to the ordinal scale in Table 2.

Growth of *Pterygophora californica* is determined by the method of DeWreede (1984). A hole (6 mm) is punched into the midrib of the terminal blade ~30 mm from the base of the blade, and another hole is punched monthly at the same location. The distance between the two holes represents the linear growth of each blade. Reproductive effort for *P. californica* is evaluated by a count of the total number of sporophyll blades on each plant and the number with active spore production (def., sori). Growth of *Laminaria farlowii* is determined in a similar manner to *P. californica*. A 13mm diameter hole is punched 100 mm from the base of each blade and is repeated each visit. The distance between the two holes represents the linear growth of each blade. The reproductive status of *L. farlowii* is evaluated as the percent of each blade covered by sori.

The distribution of algal species among all permanent sites was calculated using factor analysis in R (R Core Team, 2018). Factor analysis (Lawley and Maxwell, 1971) was used to reduce the multi-dimensional algal data. This technique facilitates the examination of entire algal communities in two or three dimensions that can then be plotted to assess changes in community composition among study sites and over time. Thirteen algal groups and derived bare space were analyzed among 20 sites. Relative bare space was derived by ranking the sum of rankings for individual algal groups among sampling units. Sampling units (individual $10m^2$ quadrats) with the least amount of total algae (density or percent cover) were ranked highest for bare space.

Invertebrates

All conspicuous sessile and mobile invertebrates are enumerated annually within the 10 m^2 quadrats during spring. Size frequencies of red (RSU - *Mesocentrotus franciscanus*) and purple (PSU - *Strongylocentrotus purpuratus*) sea urchins are recorded for >100 individuals when possible for each species located near all of the study sites except for the NCKF sites which do not have adequate densities of sea urchins.

Sea urchin recruitment is sampled semi-annually (spring and fall) at all of the Pt. Loma and La Jolla study sites. Sea urchins are exhaustively collected in haphzardly placed 1 m^2 quadrats in suitable substrate within 50m of each study site. Suitable substrate includes ledges and rocks which can be fully searched for sea urchins as small as 2mm. Sea urchins are measured using calipers and then returned to their place of capture.

Temperature and Sedimentation

Sea bottom temperatures are recorded at 10 min intervals using ONSET Tidbit recorders (accuracy and precision = 0.2˚C and 0.3˚C (respectively) at the permanent central Pt. Loma study sites

and an additional site located just offshore of PLC21 at a depth of 33 m. Additionally, a water column temperature profile is recorded utilizing a mooring located in south La Jolla at a depth 24 m. Sensors are located at 3 m depth intervals along the mooring.

Sedimentation of the north county kelp forests has historically been problematic at times. The most noticeable burial appeared to be related to beach sand replenishment activities in the early 2000's when large sections of hard bottom substrate supporting the Solana Beach kelp forest was covered by sediments as they migrated offshore from the beach (Parnell, pers. obs.) . With the establishment of kelp forest study sites in the area, sediment depths are monitored along all of the NCKF sites. Sedimentation is tracked by measuring the height of permanently established spikes at replicate locations within each of those forests.

Study Site	Depth (m)	Year Established	Work Conducted (frequency)
Card	17	2006	ABT(q), Inv(a), BT(10min), Sed(q)
SB	16	2006	ABT(q), Inv(a), BT(10min), Sed(q)
DM	16	2007	ABT(q), Inv(a), BT(10min), Sed(q)
LJN18	18	2004	ABT(q), Inv(a), USF(sa), BT(10 min)
LJN15	15	2004	ABT(q), USF(sa), Inv(a), BT(10 min)
LJN12	12	2004	ABT(q), USF(sa), Inv(a), BT(10 min)
LJS18	18	2004	ABT(q), USF(sa), Inv(a), BT(10 min)
LJS15	15	1992	ABT(q), USF(sa), Inv(a), BT(10 min)
LJS12	12	2004	ABT(q), USF(sa), Inv(a), BT(10 min)
PLN18	18	1983	ABT(q), USF(sa), Inv(a), BT(10 min)
PLC21	21	1995	ABT(q), USF(sa), Inv(a), AR(m), BT(10 min)
PLC18	18	1983	ABT(q), USF(sa), Inv(a), AR(m), BT(10 min)
PLC15	15	1983	ABT(q), USF(sa), Inv(a), AR(m), BT(10 min)
PLC12	12	1983	ABT(q), USF(sa), Inv(a), AR(m), BT(10 min)
PLC08	8	1997	ABT(q), USF(sa), Inv(a), AR(m), BT(10 min)
PLS18	18	1983	ABT(q), USF(sa), Inv(a), BT(10 min)
PLS15	15	1992	ABT(q), USF(sa), Inv(a), BT(10 min)
PLT12	12	1997	ABT(q), USF(sa), Inv(a), BT(10 min)
PLT15	15	1997	ABT(q), USF(sa), Inv(a), BT(10 min)
PLM18	18	1996	ABT(q), USF(sa), Inv(a), BT(10 min)

Table 1. *List of study sites including year of establishment and work conducted at each site. ABT = algal band transects, USF = sea urchin size frequency, Inv = Invertebrate censuses, AR = algal reproduction and growth measurements, and BT = bottom temperature. Frequencies are noted in parenthesis: a = annual, sa = semi-annual, q = quarterly, m = monthly.*

Reproductive Score	Description
0	No sporophylls present
1	Sporophylls present but no sori (sites of active reproduction) development
2	Sporophylls with sori only at the base of sporophylls
3	Sporophylls with sori over most of the sporophylls surface
4	Sporophylls with sori over all of the sporophylls surface
5	Sporophylls with sori over all of the sporophylls surface releasing zoospore

Table 2. *Ordinal ranking criteria for Macrocystis pyrifera reproductive st*ate.

Finfishes

Fish surveys were initiated in the fall of 2019 and continue semi-annually (fall/spring) at four sites within the LJKF and three sites within the PLKF (Figs. 4 and 5, respectively). Sites were chosen based on topographic features that fish are known to prefer and are as similar as possible in reef size and rugosity based on previously collected bathymetric data (Parnell, 2015). Sites were paired within the LJKF where a large marine protected area (MPA, South La Jolla State Marine Reserve) is located in the southern half (Fig. 4). The take of all species is prohibited within the MPA which went into effect in 2012. Study sites within the LJKF and PLKF were paired by depth (21 and 15 m) to facilitate comparisons of the fish communities inside and outside the MPA (Table 3). Fish counts are conducted along replicate 30x4 m band transects (up to 3 meters off the bottom) which include an initial swimming count for conspicuous species followed by a thorough search for cryptic species using a dive light. The 'UrFL' was discontinued in 2020 due to chronically poor visibility and was replaced by station 'VR' located at the same depth and situated just to the west of our permanent PLC15 algal study site.

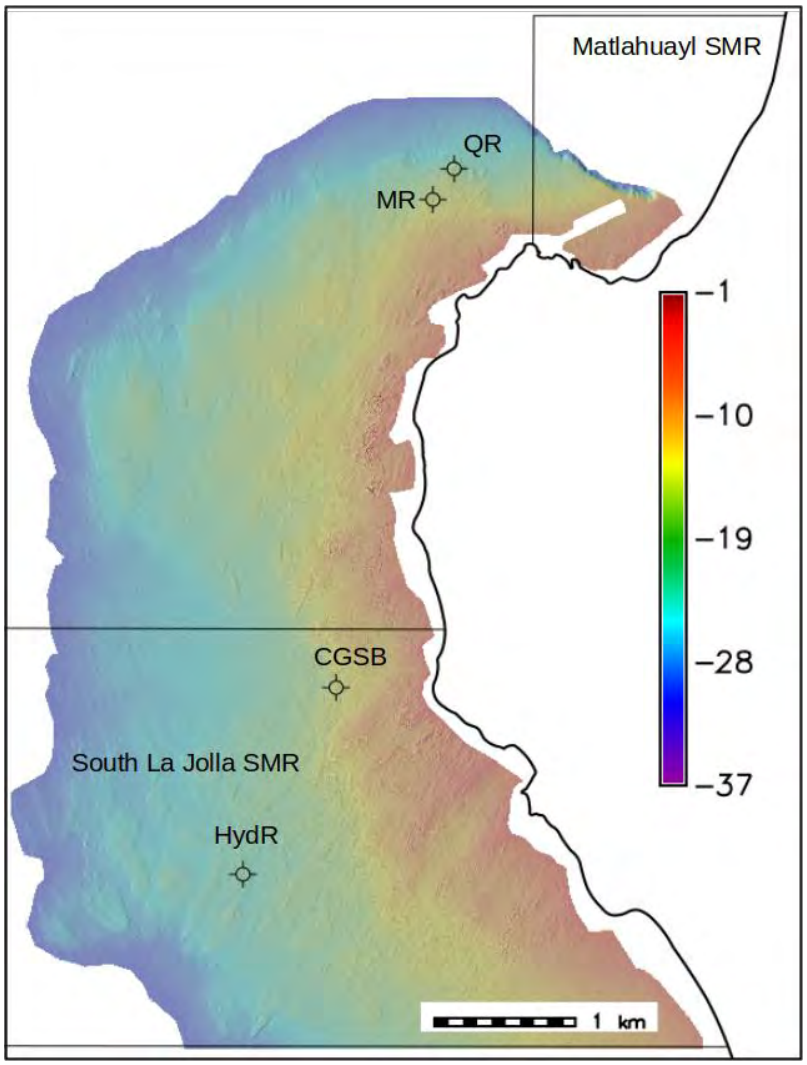

Figure 4. *Locations of fish survey study sites within the La Jolla kelp forest. Color legend indicates depth in meters.*

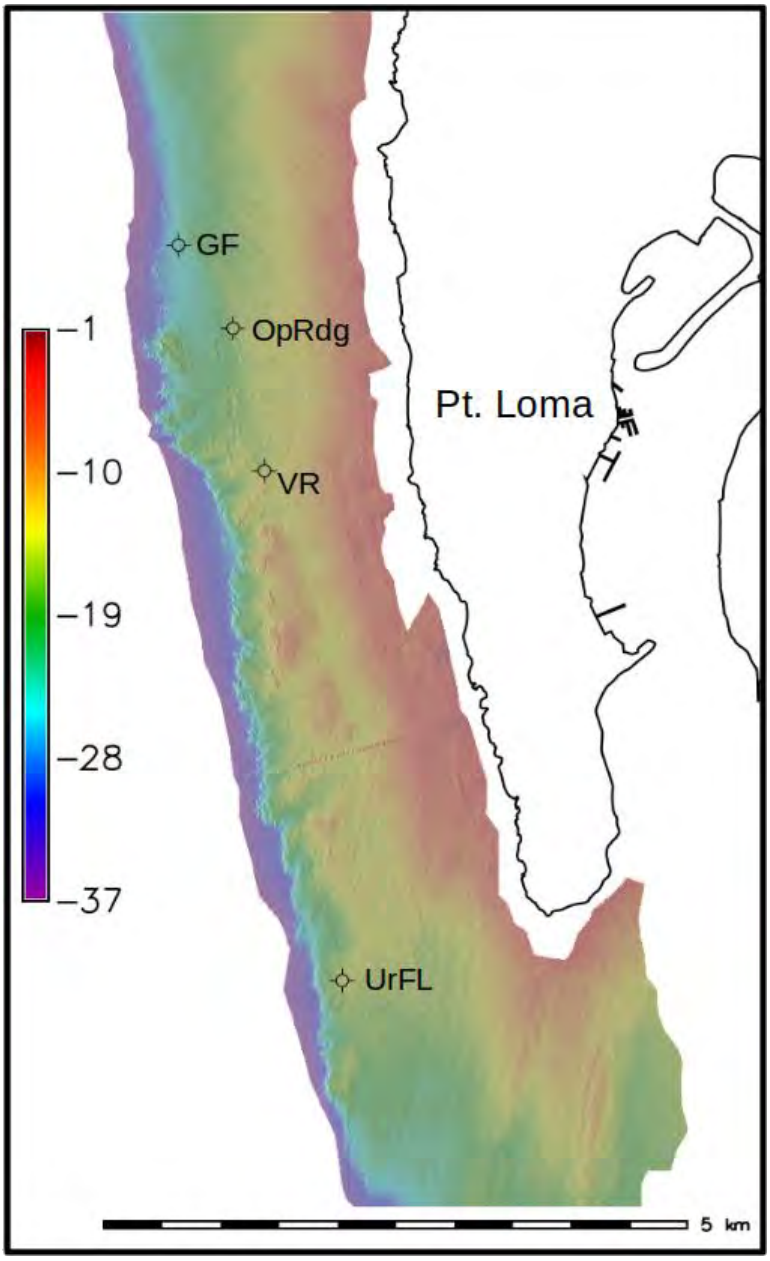

Figure 5. *Locations of fish survey study sites within the Pt. Loma kelp forest. Color legend indicates depth in meters. Site 'UrFL' was replaced by 'VR' in 2020 (see text).*

Site	Kelp Forest	Depth (m)	MPA	MPA Pairings	Species Richness
QR	La Jolla	21	No	A	27
HydR	La Jolla	21	Matlahuayl SMR	A	39
MR	La Jolla	15	No	B	30
CGSB	La Jolla	15	Matlahuayl SMR	B	23
VR	Pt. Loma	15	No	A	33
OpRdg	Pt. Loma	15	No	A	37
GF	Pt. Loma	21	No	B	33

Table 3. *Site details and species richness for fish surveys.*

Light

Marine algae are dependent on ambient light to support photosynthetic production enabling growth, reproduction, and recruitment. The aerial extent of where giant kelp can be found is mainly controlled by the availability of hard substrate at depths where light penetration is adequate for gametogenesis and growth since the plants must all recruit and begin growth at the bottom. Light is attenuated in a logarithmic fashion with ocean depth, and various wavelengths are attenuated differentially. Photosynthesis is facilitated by visible light having wavelengths between 400 and 700 nanometers. Light energy within this bandwidth is generally considered to be of primary importance for photosynthesis and is termed Photosynthetic Active Radiation (PAR). Longer wavelength red light is most rapidly attenuated with depth, while shorter wavelength blue light, most important for gametogenesis in Laminarian kelps including *M. pyrifera* (Lüning and Dring, 1975), penetrates further into the water column. Light availability limits the deepest depths that giant kelp can exist along the mainland shelf of southern California to ~25 m. The clearer offshore waters bathing many of the Channel Islands support kelp stands as deep as ~35 m. The main limiting factor for kelp recruitment at depth is the availability of light for gametogenesis, the lower limit of which has been estimated as a quantum dose of ~0.4 mol of photons $m^{-2}d^{-1}$ (Deysher and Dean, 1984), and ~0.7 mol of photons $m^{-2}d^{-1}$ for early sporophyte growth (Dean and Jacobsen, 1984). As light becomes more limiting with depth, the recovery of giant kelp from disturbances such as a MHW, is more limited due to the limited periods that bottom illumination is adequate for gametogenesis and the growth of the early sporophytes.

Bottom PAR was measured at three depths off central Pt. Loma along a cross-shore transect near the permanent algal study sites but in areas without giant kelp canopy. These areas are dominated by low growing understory algae thus precluding shading by nearby giant kelp canopy. The measurement sites off Pt. Loma are located at 24, 15, and 9 m deep. Submarine light is also measured off southern La Jolla at a depth of 24 m. PME miniPAR loggers equipped with LICOR LI-192 quantum sensors are used to measure bottom PAR. Sampling was conducted at 1 minute intervals and the sensors were wiped at 4 hour intervals using a PME miniWIPER to keep the sensor surface clear of marine growth.

RESULTS AND DISCUSSION

Ocean Climate

The ENSO index (ONI – Oceanic Niño Index, Fig. 1) is based on equatorial sea surface temperatures in the eastern Pacific Ocean. ENSO warming and cooling of the west coast of the Americas propagates poleward from the tropics, and the extent that individual El Niño or La Niña events propagate to higher latitudes varies greatly. Therefore, while correlated, the magnitudes of ENSO events at the equator and temperatures along the SCB can be somewhat decoupled.

The bottom temperature record along the central Pt. Loma study sites extends back to 1983 when the strong 1982/1983 El Niño was ebbing. Since then, the largest temperature signals in the time series include the 1997/98 El Niño and the extended warm period of 2014-2016 that was associated with a large scale anomalous NE Pacific warm event (DiLorenzo and Mantua, 2016) termed the BLOB but more recently referred to as a marine heat wave (MHW). This was immediately followed by a strong El Niño in 2015/2016 (Figs. 1, 6, and 7). The ONI (Fig. 1) and the Pt. Loma bottom temperature time series (Fig. 6) are highly concordant for the largest ocean climate events including the onset of the coupled BLOB/El Niño warm event beginning in late 2014 which began to ebb by the spring of 2016 and was immediately followed by cooler La Niña conditions in late 2016. Another cool period occurred between fall 2018 and summer of 2019 that continues to the present (through winter 2022). An anomalous warm event occurred during the summer of 2018 during which surface waters (upper 3-5 m) exceeded 27°C and stayed warm through most of the summer. This event was not observed at the bottom at any of the study sites as it was limited to near surface waters, but was evident in the Scripps Pier temperature time series (Fig. 7) and included the warmest temperatures ever observed in the time series. This warm event caused significant deterioration of the giant kelp surface canopy which virtually disappeared over the summer. However, most plants were still growing and healthy beneath the warm surface layer at the study sites where recovery from the MHW had occurred, because bottom temperatures remained relatively cool during the summer of 2018. Surface warming also occurred during the summers of 2020 and 2021 (Fig. 8, top panel). The recent trend of record and near-record surface temperatures and concomitant near-surface thermocline strengthening poses yet another risk to the health of giant kelp since most canopy biomass is located within the upper 3 meters of the water column. The bottom panel of Figure 8 shows the strength of stratification within the upper 5 meters of the water column. Recent increased near-surface stratification has been attributed to surface warming and exacerbates nutrient limitation as mixing of cooler more nutrient rich waters from below is weakened.

Less pronounced warm periods occurred between the 1997/98 and 2016/17 El Niños. Most notable was the 2005/2006 El Niño when much of the giant kelp canopy disappeared at the surface but plants still grew below the thermocline where nutrients were more abundant. Because bottom temperatures decrease with depth, nutrient stress during warming events also decreases with depth. This physical forcing is a fundamental mechanism that controls space competition between understory and canopy kelps. Strong El Niños such as the 1997/98 El Niño and the 2014-2016 marine heat wave penetrated to the bottom for extended periods even at the offshore edge of the forest stressing all kelps including understory species. By contrast, milder El Niños do not typically penetrate to the bottom of the forests for extended periods (e.g., >1 month), and therefore primarily stress the surface canopy kelps (mainly *M. pyrifera*) more than the understory kelps where temperatures are cooler. Repeated cycles of mild to moderate El Niño events over many years in the absence of large storm waves can lead to understory domination at the expense of giant kelp canopy cover.

Bottom temperatures have been cool since the spring of 2018 (<15°C at all sites except for the central Pt. Loma 8 m site) leading to recruitment and growth at many of the study sites. Warming occurred during the fall and winter of 2018/2019 but temperatures have since cooled with bottom temperatures at study sites deeper than 12 m typically <13°C much of the time. La Niña or near La Niña conditions have dominated the eastern equatorial Pacific since summer of 2020 and southern California by extension. La Niña conditions are predicted to ebb this spring (2022) when ENSO neutral conditions will dominate along the equator and spread to southern California by summer (NOAA, 2022). However, as of this writing, a NE Pacific warm pool is developing that is similar to the BLOB of 2016, and if it continues to develop, it could encroach upon the western U.S. coast by fall. This will likely be deleterious to the giant kelp of southern California if it develops into a major MHW. Giant kelp recovery at the few sites where it has persisted since the last MHW will once again decline precipitously.

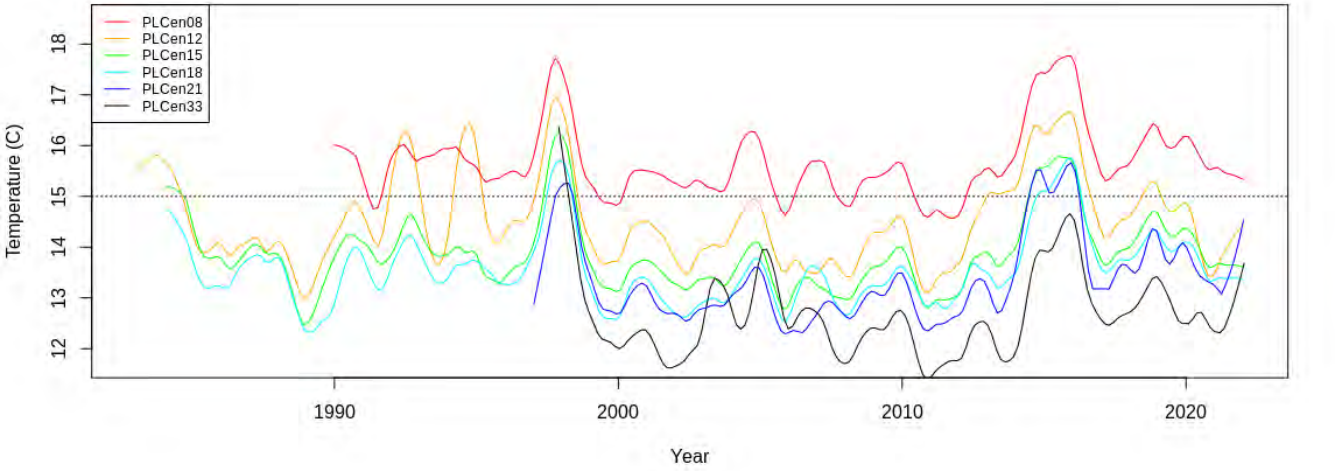

Figure 6. *Ocean bottom temperature trends along the central Pt. Loma study sites. Horizontal gray line indicates the temperature above which nitrate concentrations are typically limiting for giant kelp growth.*

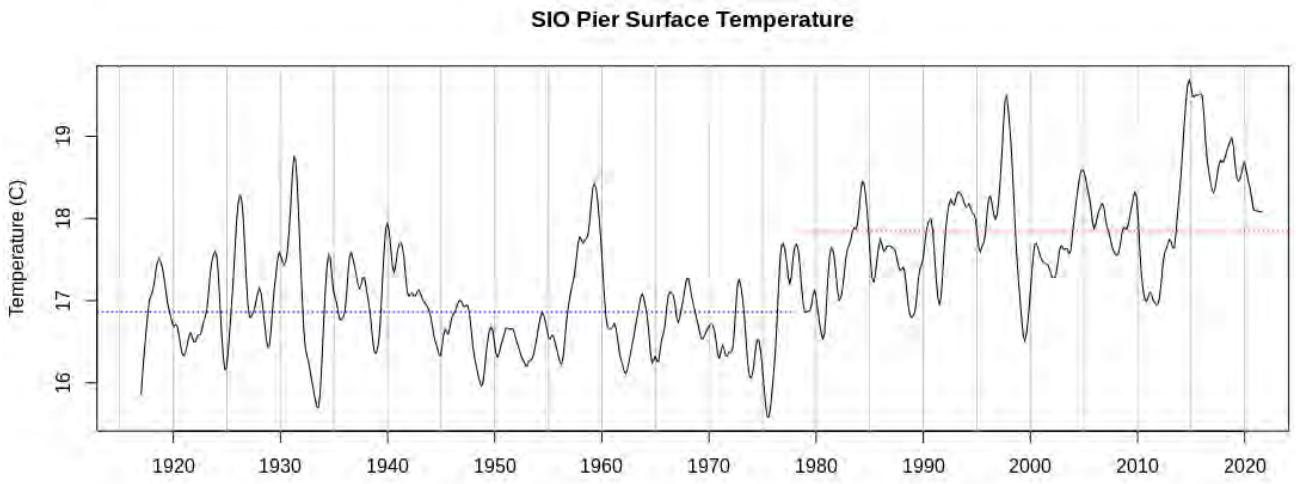

Fig. 7. *Trend of surface temperature at the Scripps Institution of Oceanography Pier. Data inclusive through Fall 2021. Dotted blue/red line indicates mean temperature prior/after to regime shift of the late 70's.*

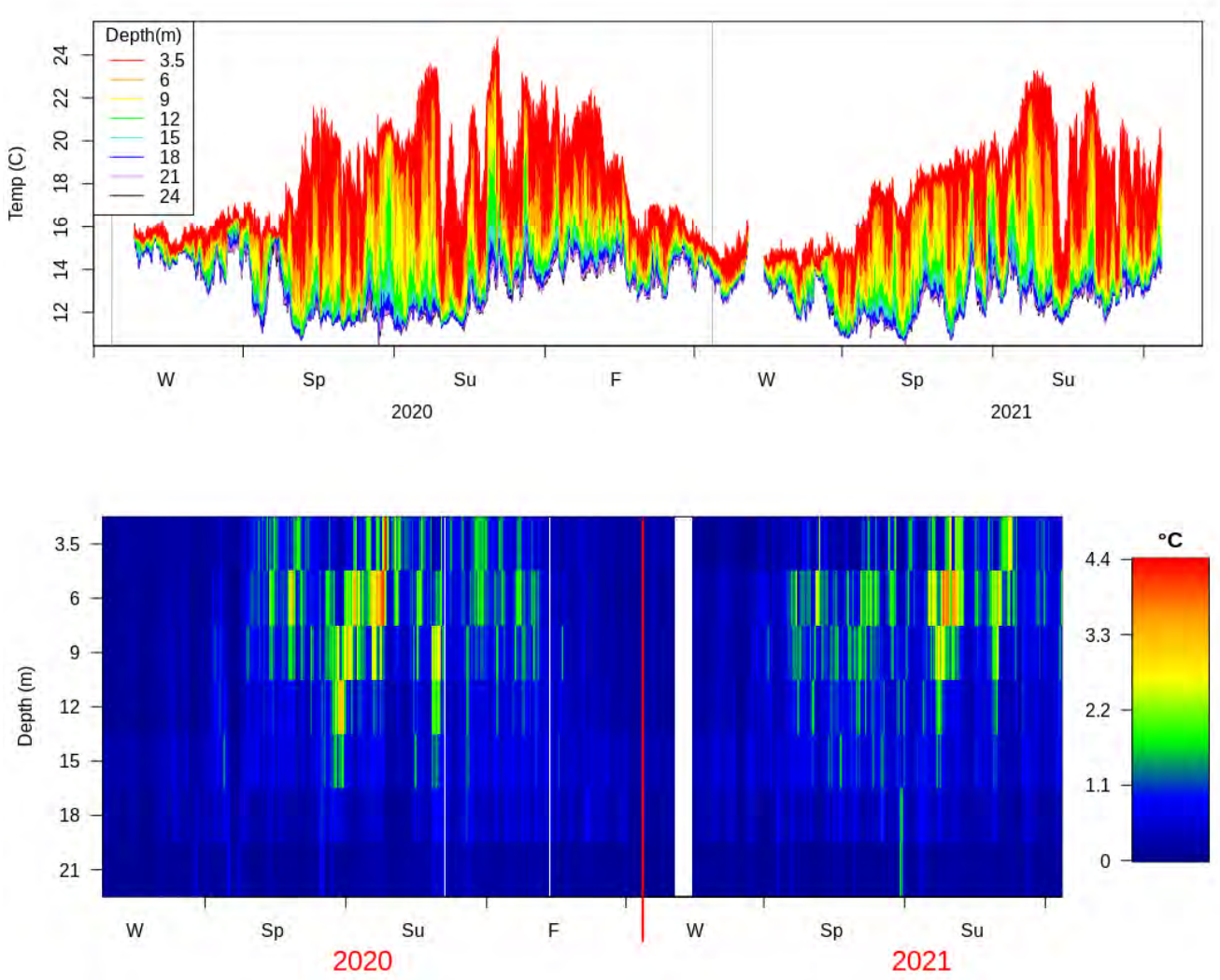

Figure 8. *Time series of temperature profiles off south La Jolla (top panel). Bottom panel shows near-surface temperature stratification (temperature difference among thermistors by depth) during spring and summer of 2020 and 2021.*

Light

Integrated daily PAR values for the three cross-shore study sites offshore of central Pt. Loma are shown in Fig. 9. Light levels were saturating at the 9m site most of the time with the exception of an intense red tide that dominated the coast of southern California during May of 2020. In contrast, light at the deeper end of the kelp forest at 24 m was well below the gametogenesis and growth thresholds for most of the time series except for a brief period of increased illumination during late winter early and early spring of 2021. Therefore, further recovery of giant kelp in the deeper portions of the Pt. Loma forest (20-25m) as part of any potential post-MHW recovery continues to be extremely limited. Recruitment periods are further limited by the need for a temporal match between kelp spore availability and periods of greater bottom illumination, a rare coincidence given the lack of kelp in the deeper areas of the kelp shelf off San Diego. The same is true for the La Jolla kelp forest. Light meter data from the southern portion of that forest at 24m (not shown) were similar to the data for the same depth off Pt. Loma.

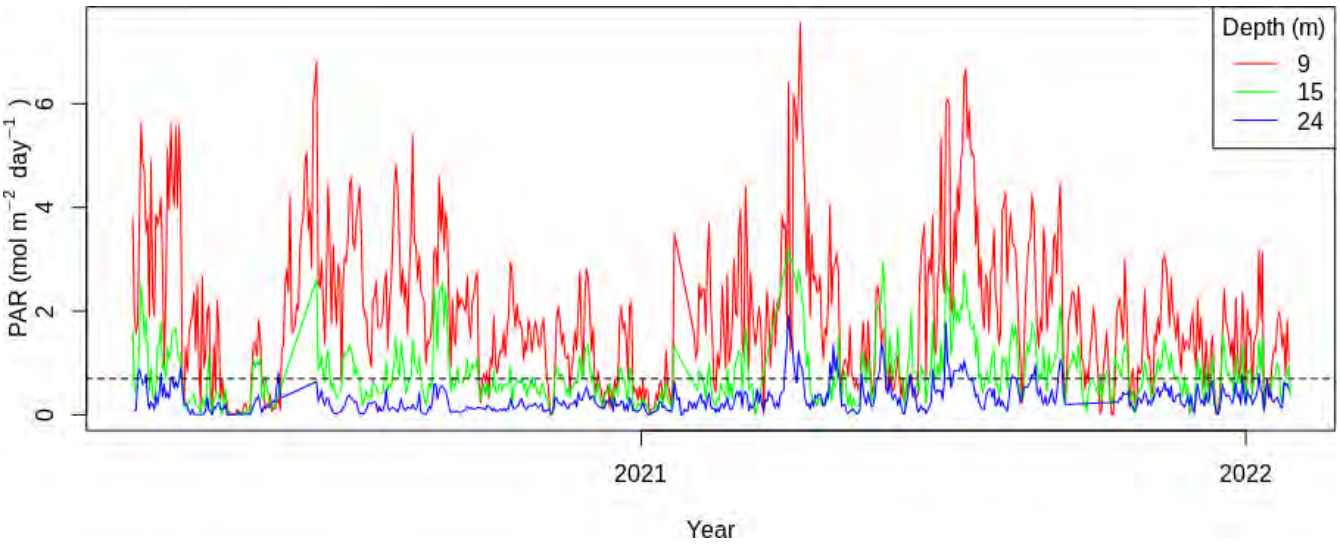

Fig. 9. *Daily PAR illuminating the bottom along the central Pt. Loma algal study sites. Horizontal dashed line indicates PAR threshold values for juvenile giant kelp growth (Dean and Jacobsen, 1984).*

Giant Kelp Status and Reproduction

The primary abundance pattern for *M. pyrifera* since the 1980's includes rapid declines associated with El Niños (Fig. 10) followed by step increases in plant and stipe density chiefly due to discrete pulses of recruitment leading to varying levels of recovery, or failed recovery if a cohort fails to reach adulthood or succumbs soon afterward. In addition to the temporal variation of regional ocean climate, the recruitment, maturation, and establishment of adult giant kelp plants are highly variable in space even within a single kelp forest. Densities of all life stages and stipes are shown in Figs. 10-13. Densities for these life stages at all of the 18 m deep sites off La Jolla and Pt. Loma are plotted in Fig. 14 for comparisons among the outer kelp forest sites where bottom temperatures are cool relative to shallower sites. Such conditions are typically more conducive for the recruitment and growth of early giant kelp life stages given adequate light.

The 2014-2016 MHW caused massive mortality of giant kelp off San Diego County mainly through a combination of nutrient and temperature stress. Giant kelp surface canopy was nearly entirely lost off most of San Diego, Orange, and Los Angeles counties during 2016 (MBC). Densities of adult *M. pyrifera* plants (Fig. 10) and stipes (Fig. 13) decreased dramatically at all study sites off San Diego. *M. pyrifera* recruited in some areas of the forests beginning as early as 2016 with subsequent recruitment observed in 2017 and 2018. Low levels of recruitment continued into the spring of 2019 (Figs. 11 and 12). Some of the 2016 site cohorts at least partially matured into pre-adults and adults at a subset of the sites.

The basic sawtooth pattern of giant kelp adult and stipe densities after major disturbances appears to have fundamentally changed since the recovery from the 1997 El Niño. Giant kelp recruitment still occurs after such events, but recovery to pre-disturbance densities has since been dampened to various degrees among the study sites. The only site where significant giant kelp recruitment has been observed during this reporting period occurred at PLM18 but is now failing to thrive. Generally, the status of giant kelp among the study sites in relation to the 2014-2016 MHW can be categorized as (1) recovery to giant kelp dominance, (2) recovery followed by collapse, (3) partial

recovery followed by collapse, (4) no recovery, and (5) not kelp dominated prior to the MHW nor afterward. Giant kelp has only maintained recovery at 3 of the 20 sites, all of which are 18 m deep (PLC18, PLS18, and LJS18). Collapsed recovery includes Cardiff, Solana Beach, LJN12, LJN15, LJS12, PLN18, PLC08, PLC12, PLC15, PLC21, PLS15, PLT15, and PLM18. LJS15 exhibited some recovery that has since collapsed. There has essentially been no giant kelp recovery at LJN18 where giant kelp was abundant prior to the MHW and at Del Mar where giant kelp is completely absent and was at very low density prior to the MHW. The reasons for such poor giant kelp performance when growth conditions have been supportive for recovery varies among the study sites, and is not understood at others, particularly LJN18. A combination of competition with understory species, low light conditions, and the lack of nearby reproductive plants all contribute to this pattern of limited giant kelp recovery. An early colonizing post disturbance brown alga, *Desmerestia ligulata*, dominated the PLT15 and PLM18 study sites until 2019, thus delaying giant kelp recovery via competitive exclusion at those sites.

The poor condition of *M. pyrifera* at most of the study sites is best exemplified in Table 4 which lists the quantiles of stipe sums at each of the sites for the latest sampling bout (Fall, 2021). The site that is currently in the best condition relative to historical data is PLM18 where the quantile for the present stand is ~0.95 for that site. The next greatest quantiles were observed at PLT15 and LJ18 which each exhibited >0.8 quantiles. These two sites are also doing well by historical standards. This was less true at PLC18 and PLC12 which are presently above the 0.5 quantiles indicating a moderate condition historically. Stipe numbers at the the remaining sites are not doing well, especially PLC21, LJN12, PLS15, LJN18, Cardiff, LJS12, PLC15, PLN18 and LJN15. Quantiles at these sites highlight the present reduced canopy of giant kelp off much of San Diego County despite the recent growth conditions that have now been favorable for nearly four years. This may herald the fundamental shift discussed in Parnell et al., (2010) in which the southern limit of *M. pyrifera* is suddenly shifted northward and kelp forests in southern California begin to mirror algal stands off central Baja California which are typically dominated by understory kelps, particularly *Eisena arborea*. The next El Niño or strong NE Pacific MHW will likely decimate giant kelp even more. One possible mechanism that might reverse this trend would be a very powerful storm effectively eliminating or significantly reducing understory species followed immediately by the onset of good growth conditions such as a La Niña.

Site	Stipe Sum Maximum	Date Maximum Observed	Fall 2021 Stipe Sum	Fall 2021 Stipe Quantile
PLM18	926	2008-12-17	570	0.95
PLT15	770	1999-10-20	245	0.82
LJS18	2114	2009-08-14	1648	0.81
PLC18	3336	1990-10-19	1519	0.66
PLC12	2665	1985-04-11	365	0.53
SB	2933	2011-11-10	574	0.44
LJS15	3341	1994-08-23	82	0.42
PLC08	2454	2018-08-09	294	0.41
PLS18	2483	1994-06-06	214	0.41
DM	519	2010-09-03	0	0.41
PLT12	1952	2008-08-19	0	0.40
PLC21	3274	2013-05-02	116	0.31
LJN12	607	2014-02-11	4	0.28
PLS15	2110	1994-08-25	66	0.17
LJN18	2093	2010-08-04	0	0.16
Card	3341	2014-02-13	8	0.16
LJS12	1013	2018-08-07	66	0.15
PLC15	3819	1989-06-29	114	0.10
PLN18	3083	2013-08-15	0	0.05
LJN15	2161	2013-11-13	0	0.05

Table 4. *Quantiles of giant kelp (M. pyrifera) stipe sums observed during the latest sampling bout (Fall, 2021) for stipe sum distributions over time by individual sites. Date indicates the day that each site maximum was observed. Rows are ordered by decreasing quantile values.*

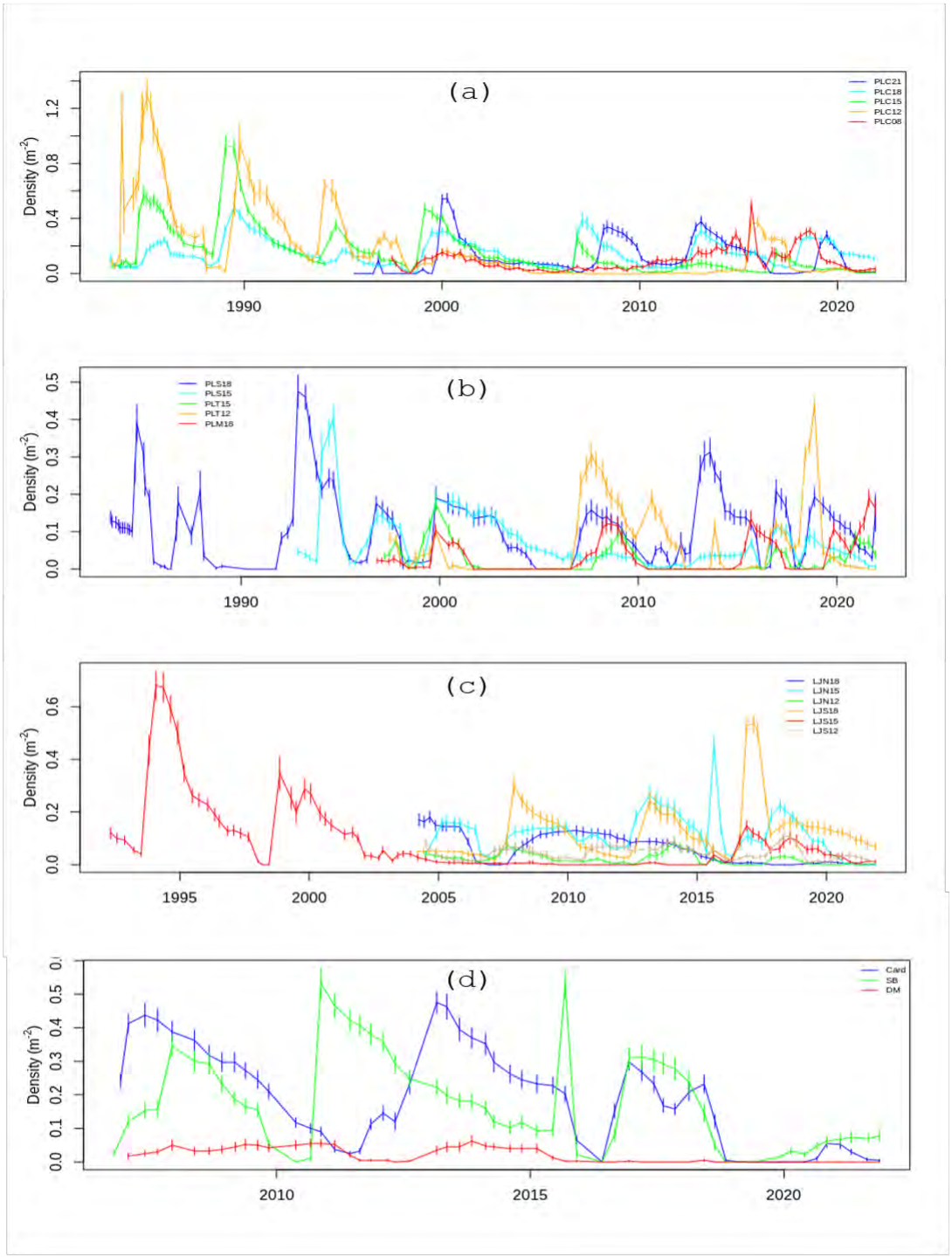

Figure 10. *Mean densities of adult Macrocystis pyrifera among study site groups: (a) central Pt. Loma, (b) south Pt. Loma, (c) La Jolla, and (d) North County. Error bars indicate standard errors.*

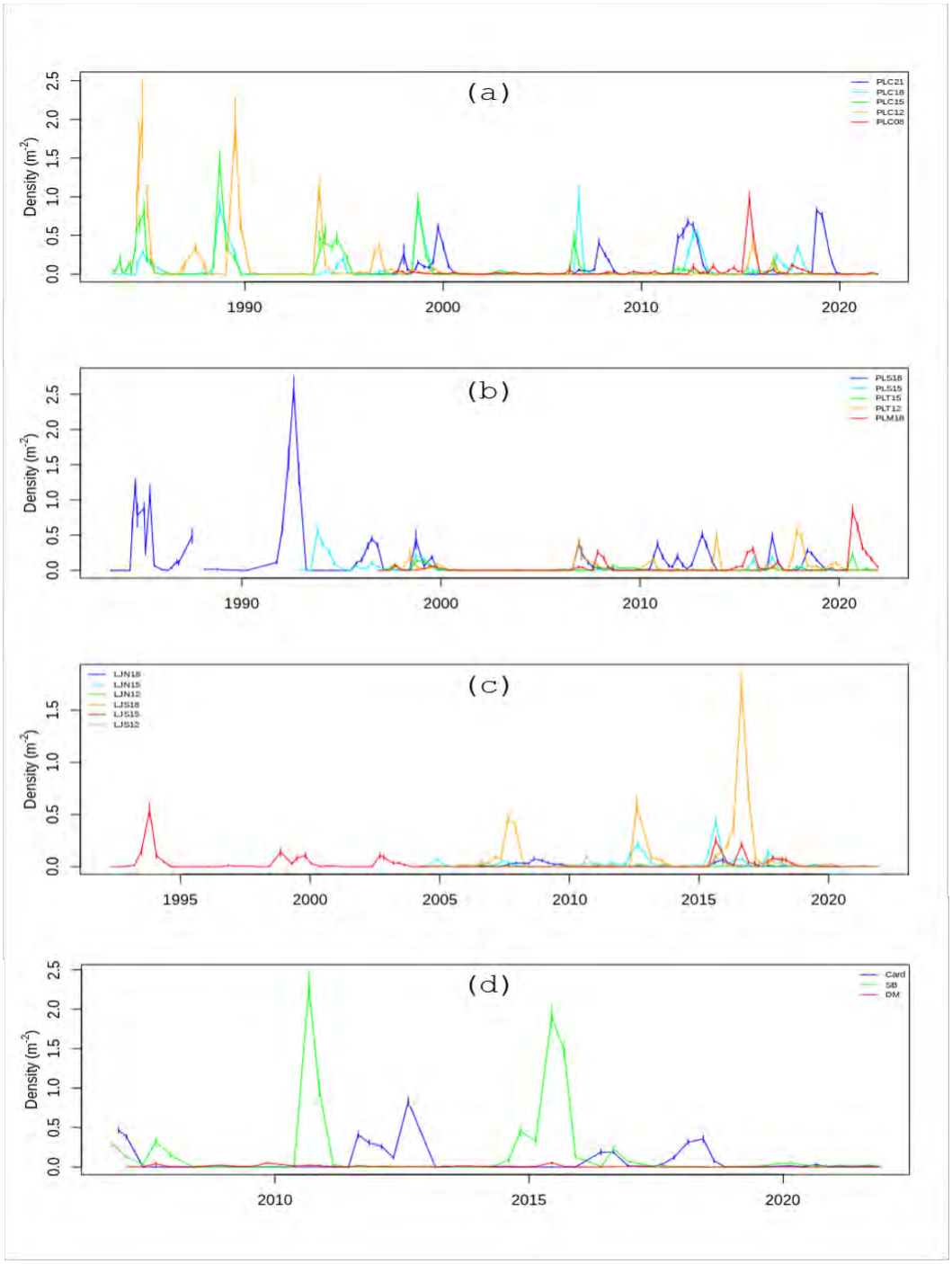

Figure 11. *Mean densities of Macrocystis pyrifera pre-adults (<4 stipes): (a) central Pt. Loma, (b) south Pt. Loma, (c) La Jolla, and (d) North County study sites. Error bars indicate standard errors.*

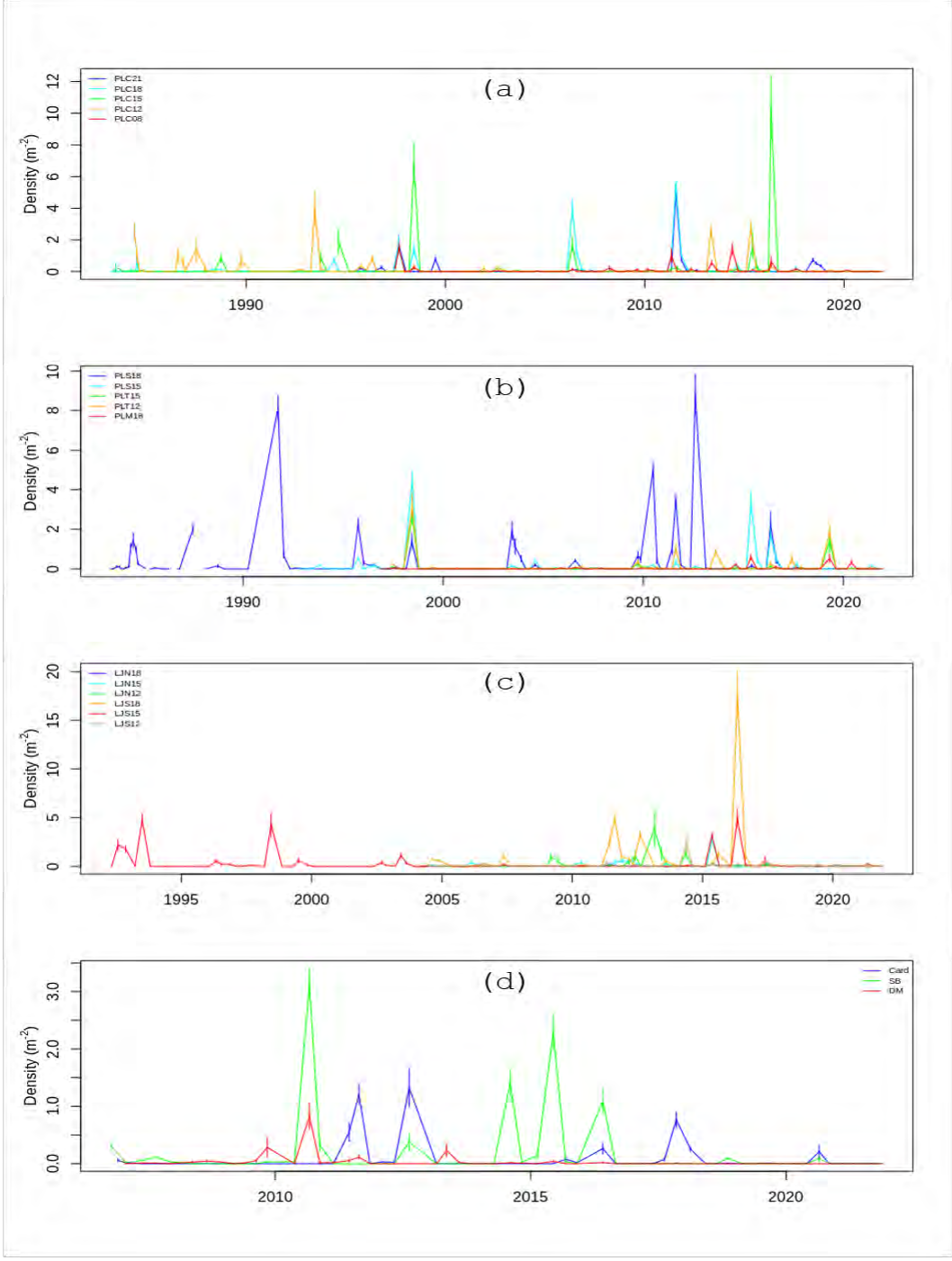

Figure 12. *Mean densities of Macrocystis pyrifera bifurcates: (a) central Pt. Loma, (b) south Pt. Loma, (c) La Jolla, and (d) North County study sites. Error bars indicate standard errors*

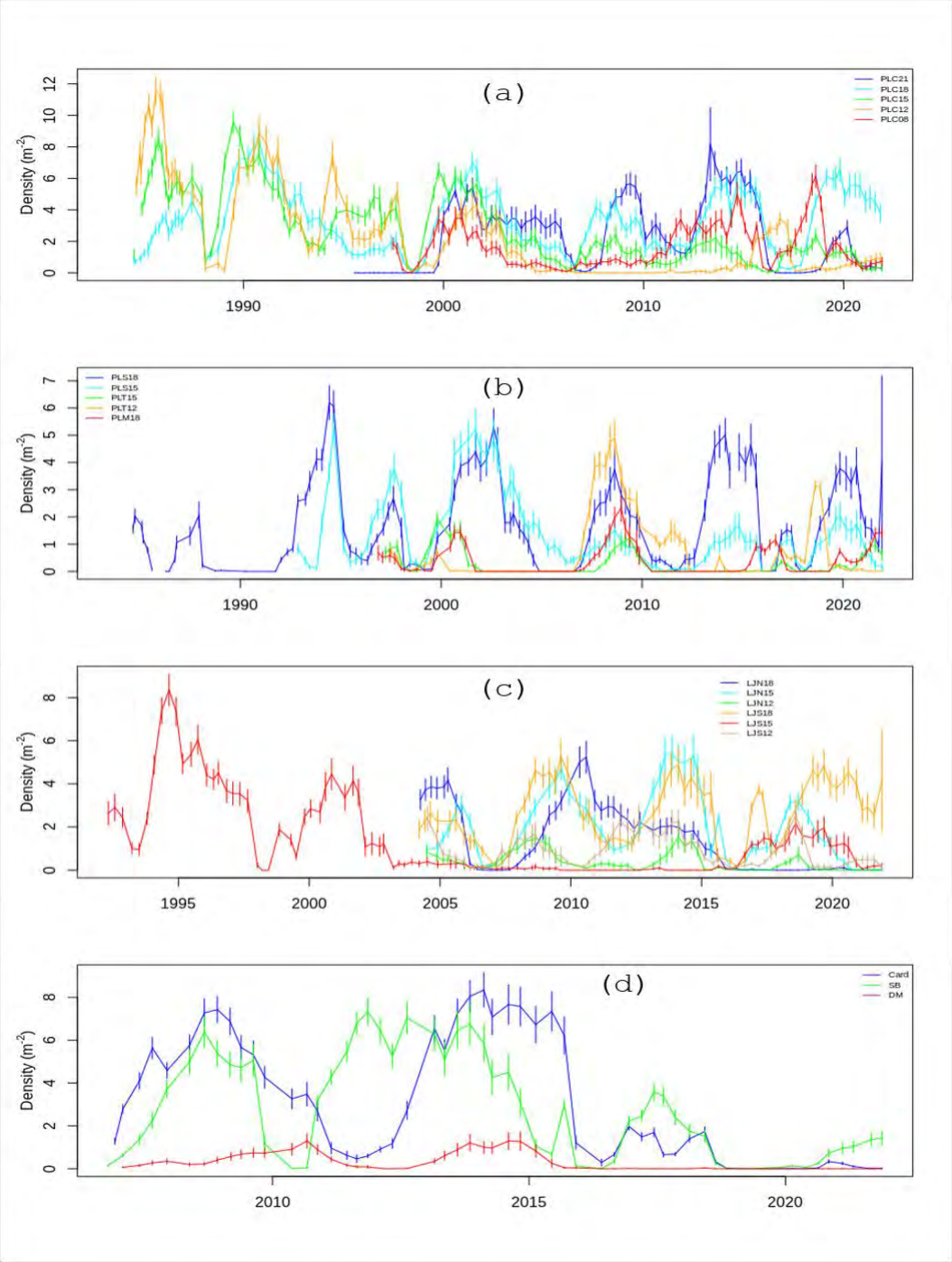

Figure 13. *Mean densities of Macrocystis pyrifera stipes: (a) central Pt. Loma, (b) south Pt. Loma, (c) La Jolla, and (d) North County study sites. Error bars indicate standard errors.*

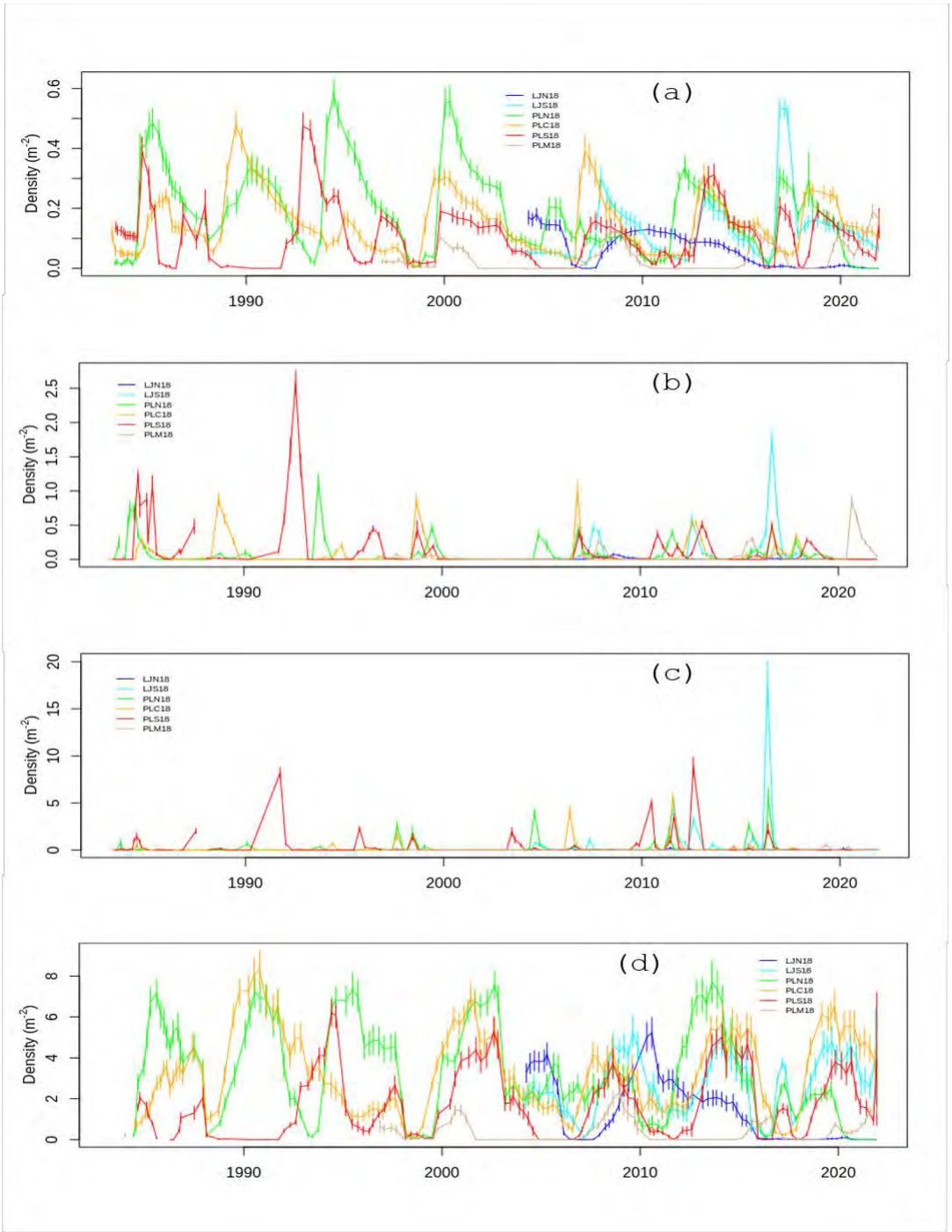

Figure 14. *Mean densities of Macrocystis pyrifera (a) adults, (b) pre-adults, (c) pre-bifurcates, and (d) stipes along the 18 m sites off La Jolla and Pt. Loma. Error bars indicate standard errors.*

The reproductive condition of giant kelp along the central Pt. Loma study sites was greatly diminished through the MHW and by the end of the 2016 El Niño (Fig. 14). Reproductive capacity was uniformly the lowest among all study sites over the entire time series dating back to before the 1997/98 El Niño. Sporophyll volumes were greatly reduced by the end of the 2016 El Niño and sporophylls were not reproductive at the PLC8 and PLC21 study sites where adult plants were the most abundant. Such greatly diminished reproductive capacity of giant kelp is both an indicator of how stressful the MHW of 2014-2016 was for *M. pyrifera*, but has also likely limited the rate at which giant kelp has been able to recover since that time given the relationship between reproductive capacity as a function of the number of stipes for individual plants (Fig. 15d). Figure 15d indicates that the reproductive output of individual plants relative to their biomass (stipes) has not returned to historical levels suggesting continued stress. The only study site where reproductive capacity has at least briefly recovered is the central Pt. Loma site at 15 m (PLC15) where densities of *M. pyrifera* are low relative to the historical record.

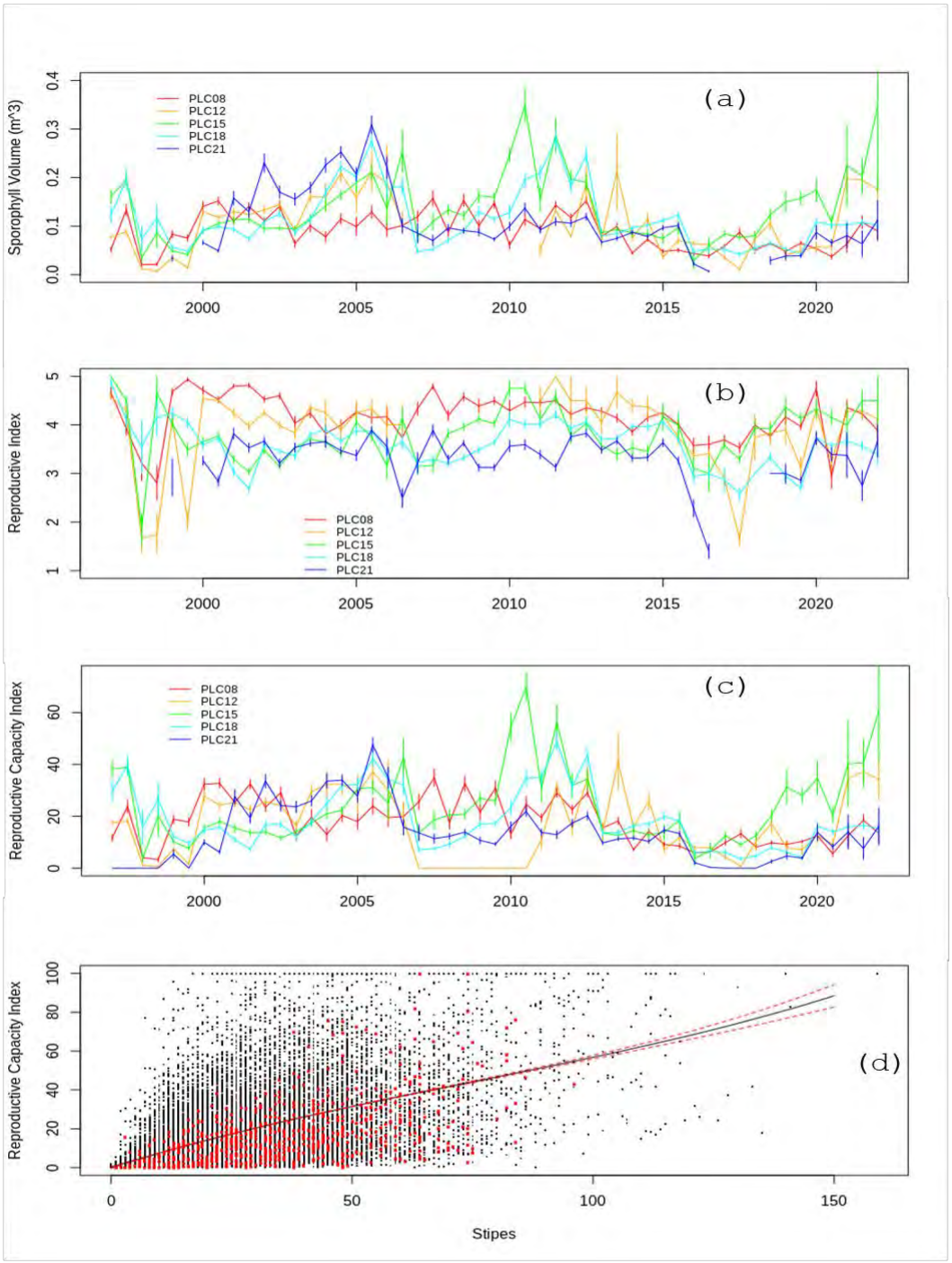

Figure 15. *Reproductive states of Macrocystis pyrifera at the central Pt. Loma study sites: (a) sporophyll volume, (b) reproductive index (see Table 2), (c) reproductive capacity (derived index of relative among-site reproductive potential - see Methods). Means are plotted and error bars indicate standard errors. (d) Reproductive capacity of Macrocystis pyrifera as a function of the number of stipes. Fit is a second order polynomial fit and dashed red curves indicate 95% confidence interval. Data are inclusive between 1997-2021. Red points indicate present study period (2020-2021).*

Understory Kelp Status and Reproduction

Understory kelps and turf algae grow close to the bottom, and unlike the local canopy forming kelps (*M. pyrifera*, *Egregia menziesii*, and *Pelagophycus porra*), do not have buoyant pneumatocysts to support photosynthetic tissue up in the water column where light is more abundant. Therefore, high densities of canopy forming kelps outcompete understory kelps and turf algae. El Niño events modulate this competition between the two types of canopy guilds. Buoyant, warm and nutrient depleted water is nearest the surface where most of the photosynthetic and nutrient absorbing tissue for giant kelp is distributed. Therefore, giant kelp is disproportionately stressed by El Niño events. By contrast the understory and turf canopy guilds are exposed to cooler and more nutrient replete waters. As the surface canopy begins to lose tissue and die, the light field for the lower canopy guilds increases leading to rapid growth and reproduction.

Pterygophora californica, a stipitate understory kelp has a central woody stipe that supports photosynthetic blades from below. Stipes can grow up to >2 m in height off the bottom and individuals can persist for decades. The growth form consists of a ribbed terminal blade that grows outward from the end of the stipe. Sporophyll blades grow horizontally outward from the narrowed margins of the stipe. Soral (reproductive) tissue develops on these side branching sporophyll blades. *Laminaria farlowii*, a prostrate understory kelp grows as a long blade along the bottom where it is attached by a small woody stipe and holdfast. Soral tissue develops along the length of the blade. Reproduction and growth is seasonally offset in both species with growth occurring during late spring and summer while reproductive tissue development peaks in winter.

Pterygophora californica and *Laminaria farlowii*, were affected differently by the consecutive warm periods that constituted the 2014-2016 MHW. The main effects on *P. californica* manifested into two groups of sites (Fig. 16). The first group included sites where densities decreased dramatically during the MHW and remained low during and after the 2016 El Niño (PLC21, PLC18, PLC12, PLC08, LJN15, LJN12, LJS12). Densities of *P. californica* at the second set of sites decreased during the BLOB then increased rapidly just after the 2016 El Niño (PLC15, LJS18, LJS15). Densities of *P. californica* at the North County sites have been persistently low and remain low at present with the exception of a 2017 cohort that died by late 2018. Presently, *P. californica* is present in at least moderate density (>1m^{-2}) at the LJS15, PLC15, and PLT12 study sites. The 2016 cohort is still thriving at the sites where post El Niño recruitment was greatest (PLC15 and LJS15). *P. californica* at LJS18 has nearly disappeared at LJS18 where *M. pyrifera* has begun to dominate.

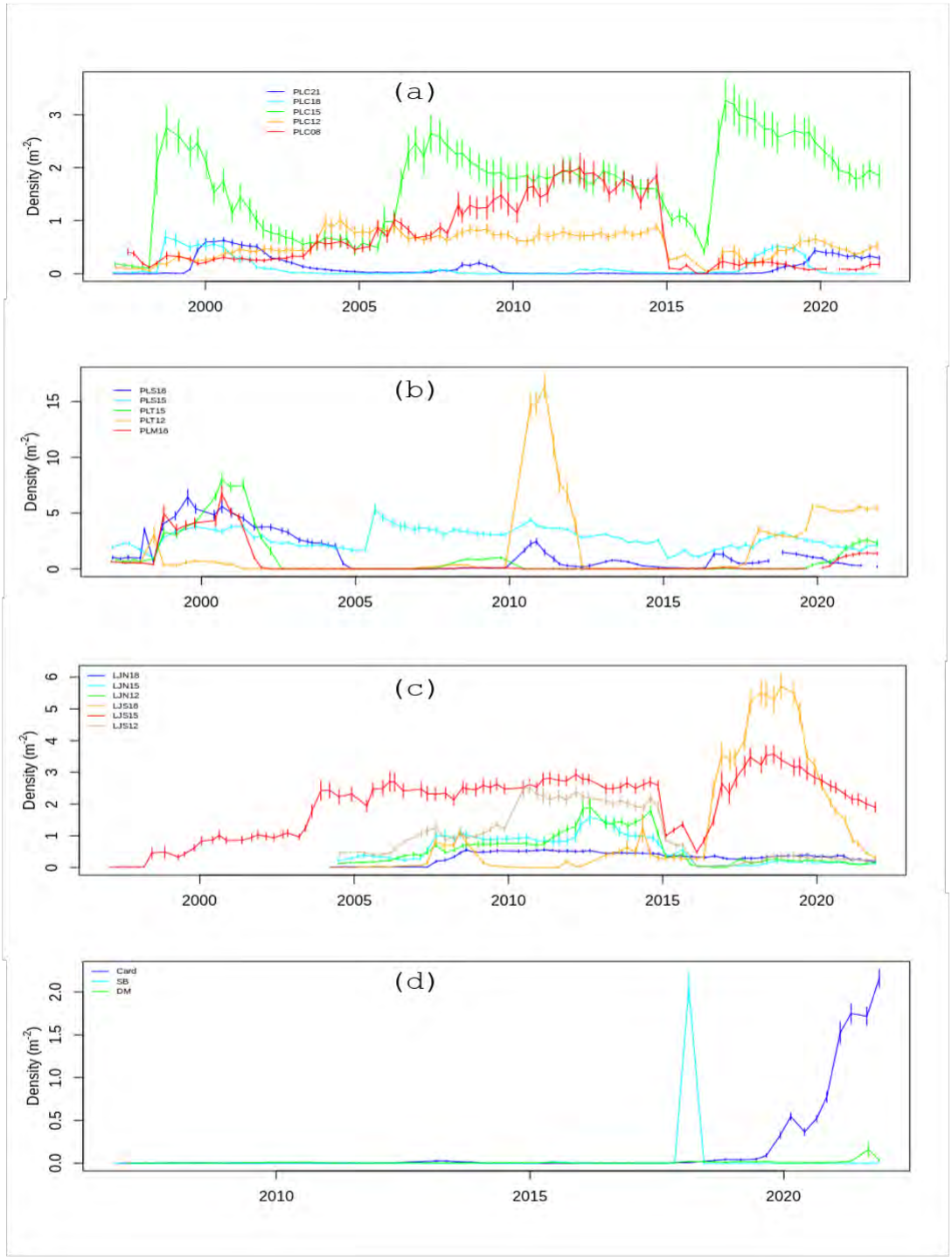

Figure 16. *Mean densities of the understory kelp Pterygophora californica: (a) central Pt. Loma, (b) south Pt. Loma, (c) La Jolla, and (d) North County study sites. Error bars indicate standard errors.*

The response of *L. farlowii* to the MHW also varied among study sites (Fig. 17). The most common pattern has been its increase in cover that was occurring at many sites prior to the MHW. These include all of the central Pt. Loma sites with the exception of PLC18 where *M. pyrifera* is now clearly dominant. *Laminaria farlowii* population trajectories within the south Pt. Loma and La Jolla study sites were generally relatively stable until the MHW but have recovered since with the exception of PLS18, LJN18, and LJS18. Densities within the north county kelp forests are low by comparison but are increasing, most rapidly at Cardiff.

Densities of *Cystoseira osmundacea* generally increased prior to and during the MHW. Densities have since decreased at some of the sites off La Jolla from their 2018/2019 peak, particularly at the LJN18 site. This was also true at the PLS15 study site where *C. osmundacea* was increasing prior to and after the MHW, but has since decreased rapidly with a new cohort of recruits leading to increasing densities since late 2020. *C. osmundacea* at PLT12 began to increase through the 2016 El Niño which continues at present. However, densities of *C. osmundacea* at all sites in south Pt. Loma are low in comparison with other areas. The most important pattern among most of the study sites has been the increase in understory, particularly *L. farlowii* and *C. osmundacea*, which has been facilitated, or has directly contributed to declines in *M. pyrifera* at many sites. The general resistance of understory to heat waves and storm disturbance relative to *M. pyrifera*, and their ability to outcompete giant kelp for space, means that this pattern of understory domination will likely continue well into the future barring the occurrence of a really large storm or strong MHW.

The complex trajectories of understory species during and after the consecutive warm periods appear to have switched states. These states can be defined by three canopy/understory modes and are forced by the shading effects of *M. pyrifera* surface canopy. The three modes include (1) lush to moderate surface canopy with less understory, (2) lush understory with reduced surface canopy, and (3) lush to moderate canopy with low fractional cover of understory. A fourth ephemeral mode was also observed during the MHW where both canopy and understory were sparse, forced by the unprecedented duration of nutrient stress during the combined warm periods. In contrast to previous warming events when the shading effect of giant kelp on understory decreases due to thinning of the surface canopy, warm temperatures during the BLOB penetrated to the bottom for an extended period of time (Fig. 6). This resulted in long periods of nutrient stress for these lower canopy species, and delayed their recovery even when bottom light levels increased during periods of low surface canopy.

The growth and reproductive condition of tagged *P. californica* (Figs. 19 and 20) and *L. farlowii* (Figs. 21 and 22) at the central Pt. Loma study sites decreased dramatically during the BLOB but have since increased. Growth and reproduction of *P. californica* remained depressed at the deeper central Pt. Loma sites until 2017 and has since decreased at PLC18. Decreased reproductive output by both species can delay understory recovery after El Niño disturbances (Dayton et al., 1984), and may contribute to the persistence of switched canopy/understory patch modes. Such forcing can result in long term dominance over giant kelp than can persist for several years until the occurrence of a new major disturbance. For both species, growth, and reproduction, to a more limited extent, have recovered at all the study sites off central Pt. Loma. Growth and reproduction of *P. californica* was clearly more affected than *L. farlowii* by the marine heat wave of 2014-2016 and has been somewhat slower to recover.

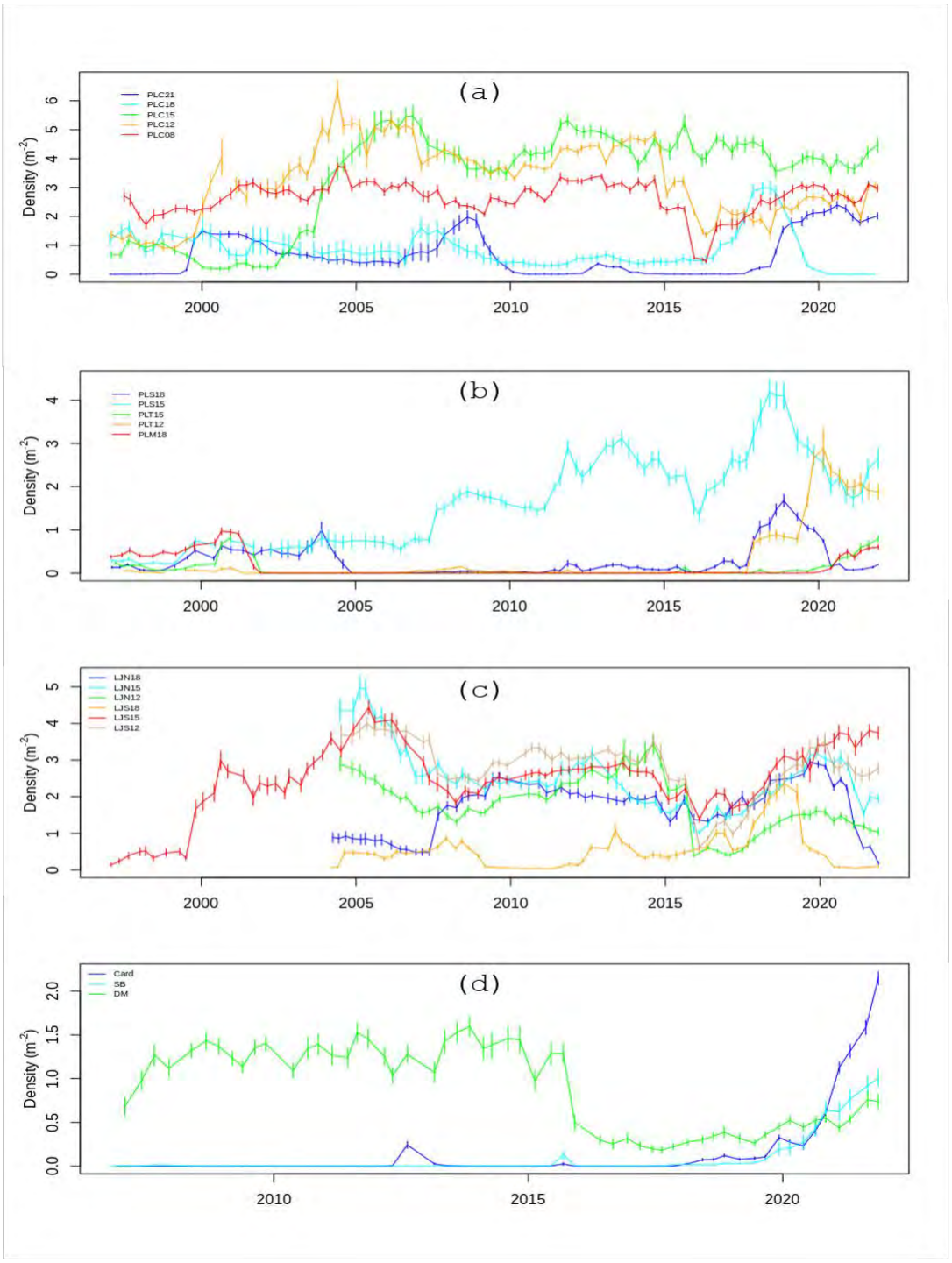

Figure 17. *Mean densities of the understory kelp Laminaria farlowii: (a) central Pt. Loma, (b) south Pt. Loma, (c) La Jolla, and (d) North County study sites. Error bars indicate standard errors.*

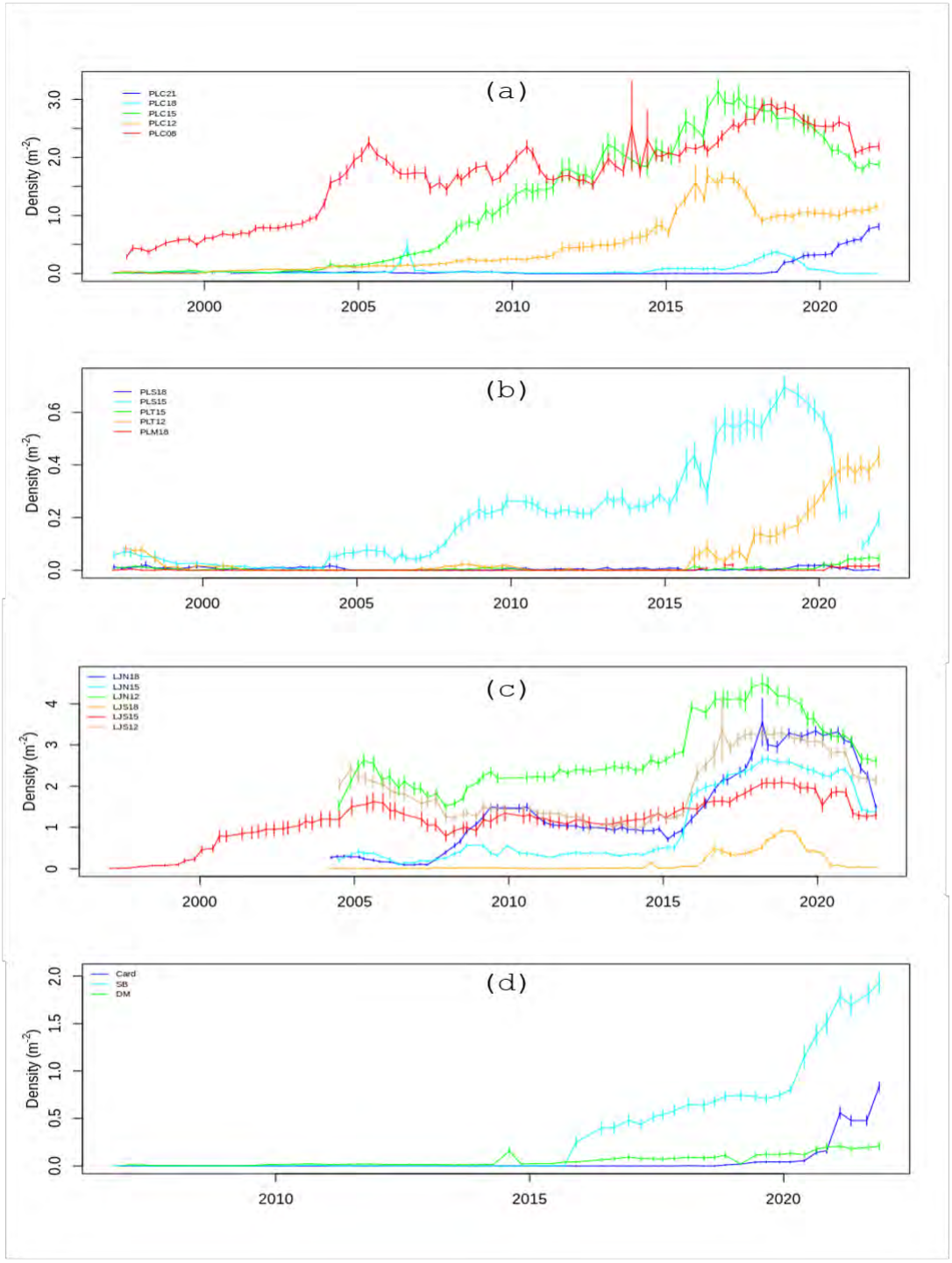

Figure 18. *Mean densities of the understory kelp Cystoseira osmundacea: (a) central Pt. Loma, (b) south Pt. Loma, (c) La Jolla, and (d) North County study sites. Error bars indicate standard errors.*

Figure 19. *Growth and reproduction of the understory kelp Pterygophora californica at the central Pt. Loma study sites: (a) growth, (b) # sporophylls, and (c) # reproductive (sexy) sporophylls. Means are plotted and error bars indicate standard errors.*

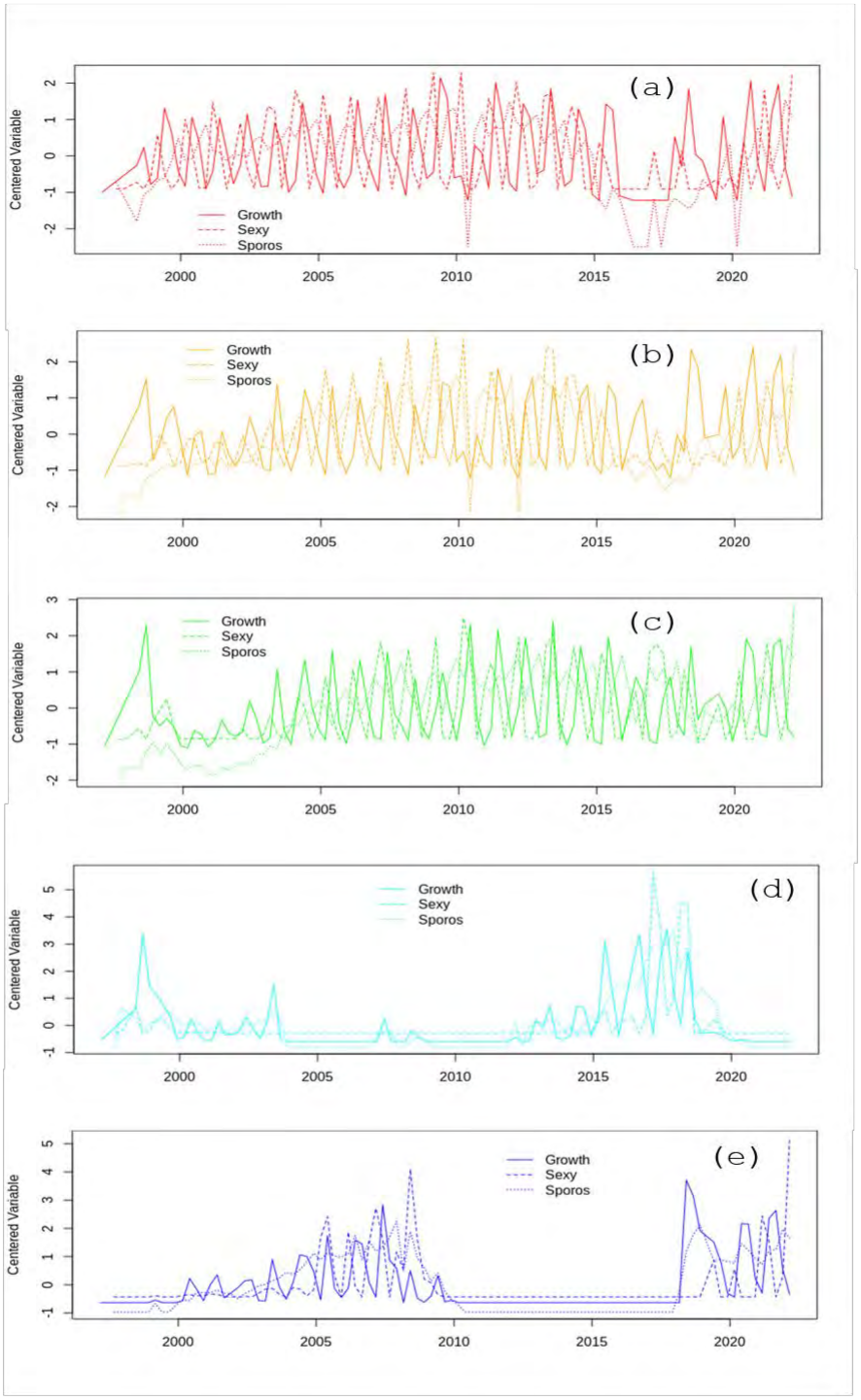

Figure 20. *Centered Pterygophora californica growth rates, sporophyll, and # of reproductive sporophylls for (a) PLC08, (b) PLC15, (c) PLC18, and (d) PLC21 study sites. Means are plotted and error bars indicate standard errors.*

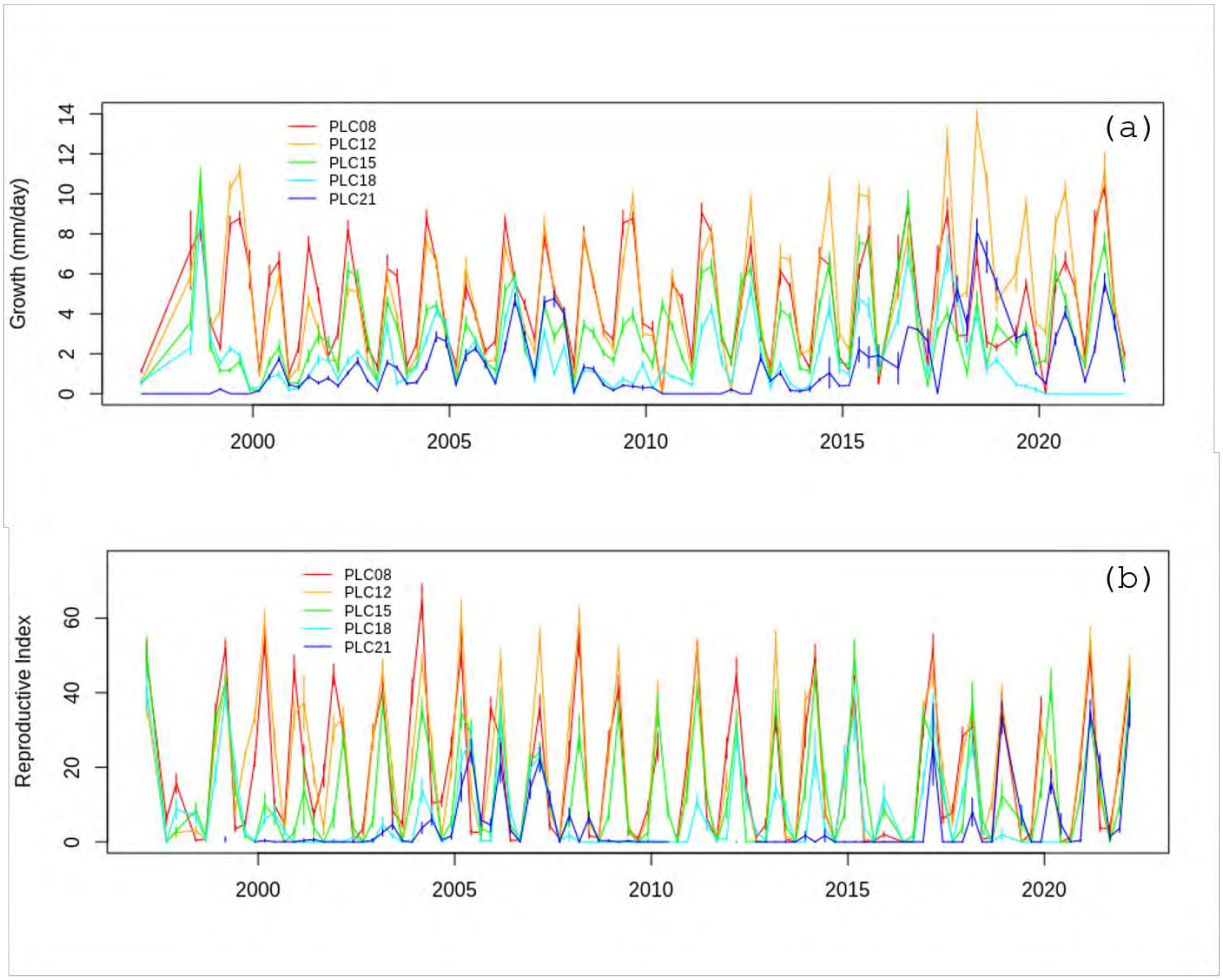

Figure 21. *Growth and reproduction of the understory kelp Laminaria farlowii at the central Pt. Loma study sites: (a) growth, and (b) % of blade that is sorus (reproductive), Means are plotted and error bars indicate standard errors.*

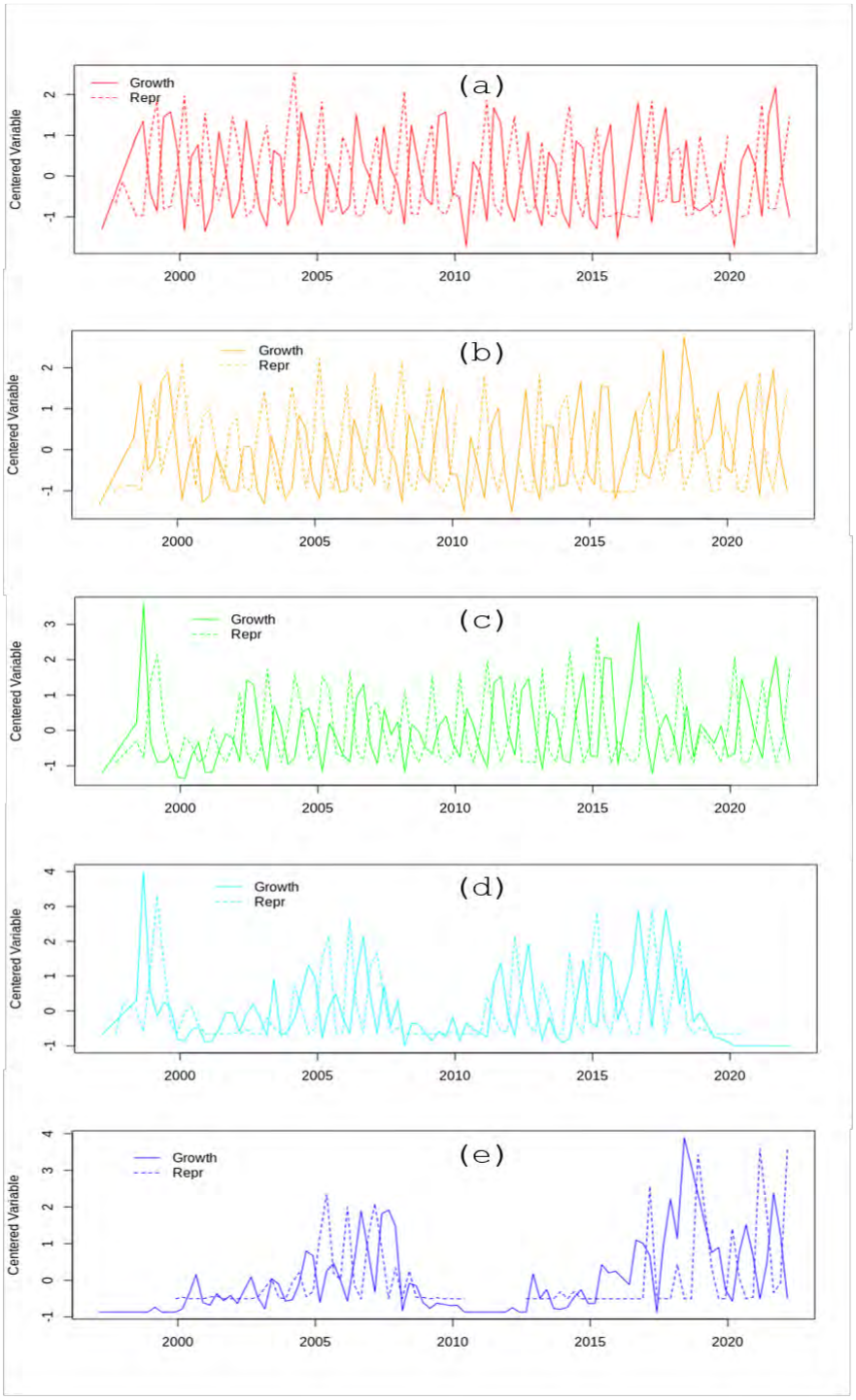

Figure 22. *Centered growth and reproduction of the understory kelp Laminaria farlowii at the central Pt. Loma study sites. (c) standardized growth and reproduction for the PLC8 and the (d) PLC12 study sites.*

Algal Community Analysis

Algal community composition among all of the study sites during the study period are shown in Figures 23 and 24 where the first two factors of the dimension-reducing factor analysis are plotted against one another. The most abundant algal species and groups were included in the analysis as well as bare space which was included as a derived ranked variable (see Methods). When plotted against one another, the first two factors graphically depict the community-wide state of algae among the study sites. Together, these factors account for ~34% of the overall variability in the dataset, and therefore provide a good representation of the algal communities over time. Factor 1 indicates a continuum of understory algal composition ranging (from positive to negative) from fleshy red and articulated coralline algae to the stipitate brown algal species, *Eisenia arborea*, and *P. californica*, the prostrate brown alga *L. farlowii*, to the post-disturbance pioneer brown alga *Desmerestia ligulata*, to bare space. This factor captures the depth gradient effect from shallow to deep (positive to negative), representing the gradient in benthic light availability. Shallower sites are typically saturated by adequate light thus facilitating algal domination, whereas deeper sites are light limited thereby reducing algal growth and reproduction, which forces a change from algal domination at shallower depths to domination by encrusting suspension feeders at depth. Factor 2 indicates the condition of *M. pyrifera*, whether sites are dominated by adults and abundant stipes (positive values) or young recruits and pre-adults (values near zero) to a virtual absence of surface canopy (negative values).

The major patterns of macroalgal community composition among the study sites are best contrasted by comparing the upper left quadrant of the plot, which indicates *M. pyrifera* domination and sparse understory and turf. The lower right quadrant represents understory and turf domination. PLC18, LJS18, and PLS18 are the only sites clearly dominated by giant kelp while most of the shallower sites are heavily dominated by understory (mainly *L. farlowii* and *C. osmundacea*) and turf algae. The lower left quadrant represents sites with reduced understory and *M. pyrifera*. The Del Mar and Cardiff study sites represent the extremes within this quadrant, characterized as poorly vegetated sites. PLT12 is sparsely covered with articulated coralline algae and *C. osmundacea*.

The forcing behind these patterns of algal cover among the sites not well understood at all of the study sites. *M. pyrifera* has failed to thrive during the cooler nutritive conditions of the last several years even after initially recovering to some extent at many of the sites where understory kelps have either remained steady or increased since the MHW. These patterns of reduced canopy cannot be attributed to sea urchin overgrazing as both locally common species crashed during the MHW and have yet to appreciably increase as recruitment has been present but limited at many of the study sites.

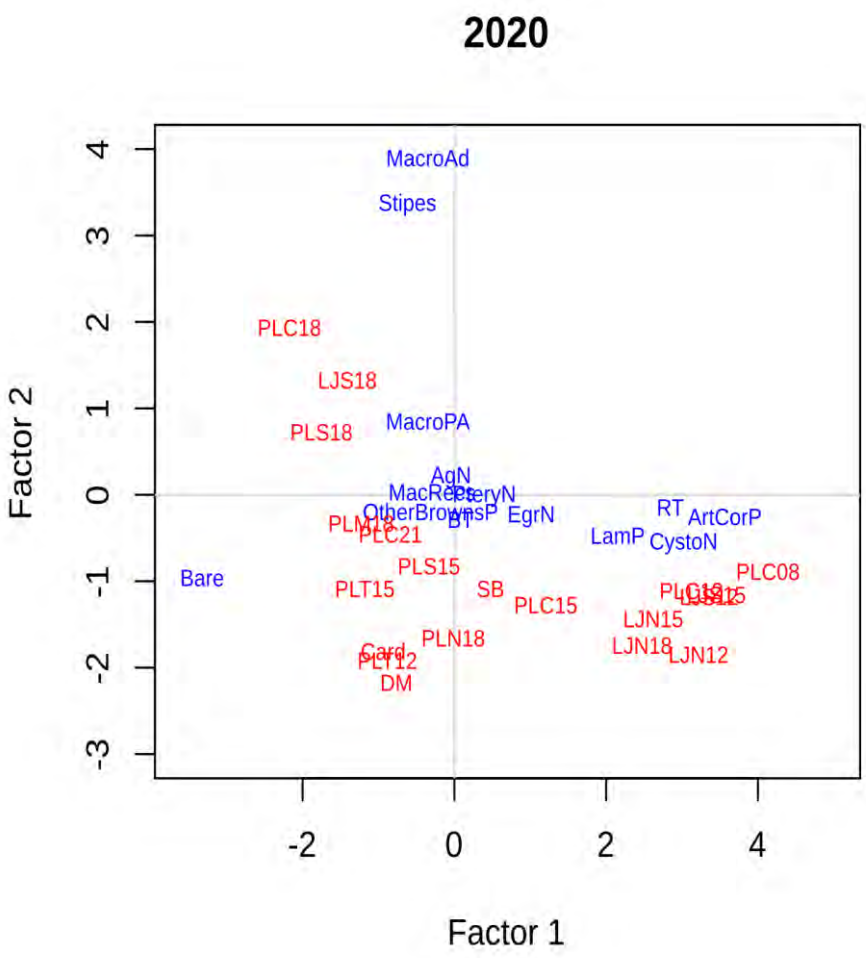

Figure 23. *Plot of first two factors resulting from the factor analysis of algal groups among the 20 permanent study sites in 2020. Algal group definitions: Bare = derived bare space, MacRecs = M. pyrifera recruit stage (pre-bifurcates + bifurcates), MacroAd = M. pyrifera adult density, Stipes = M. pyrifera stipe density, MacroPA = M. pyrifera pre-adults (<4 stipes), PteryN = Pteryogophora californica density, LamP = Laminaria farlowii percent cover, EisN = Eisenia arborea density, EgrN = Egregia menziesii density, AgN = Agarum fimbriatum density, DesP = Desmerestia ligulata percent cover, ArtCorP = articulated coralline algae percent cover, RT = foliose red algal percent cover, BT = brown algal turf percent cover.*

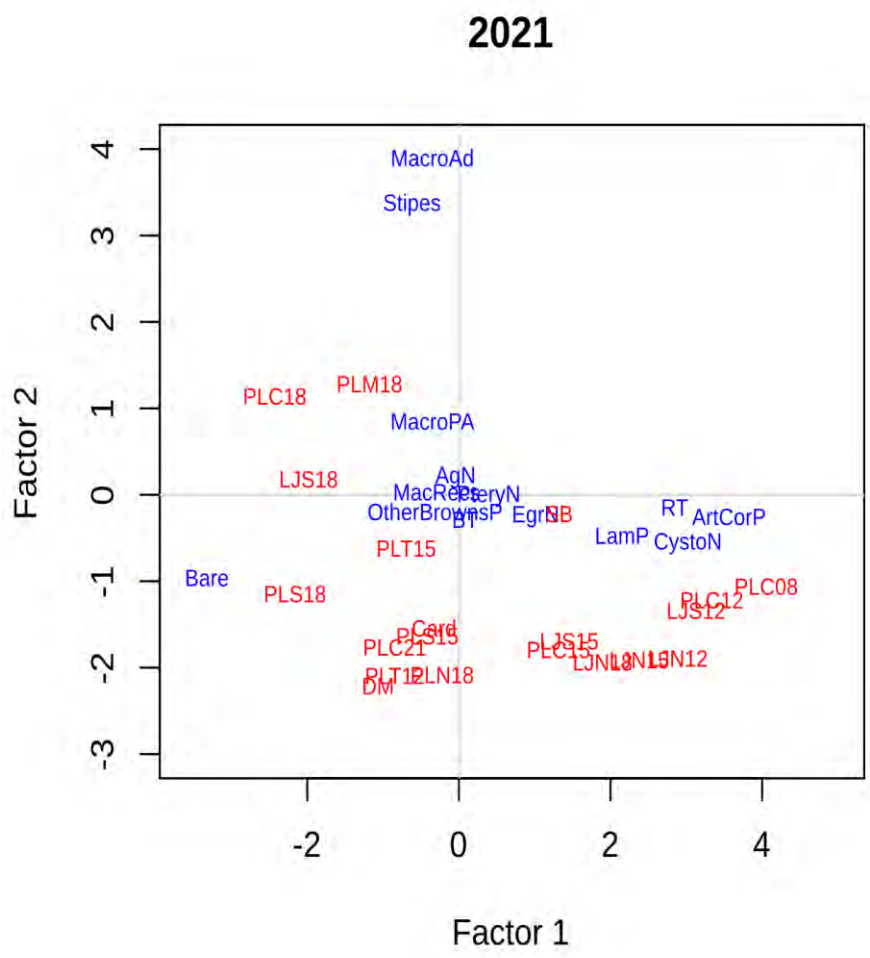

Figure 23. *Plot of first two factors resulting from the factor analysis of algal groups among the 20 permanent study sites in 2021. See Figure 23 for description of plot.*

Invasive Algal Species

Sargassum horneri is an algal species native to Japanese and Korean coastlines but has invaded southern California within the last couple of decades. *S. horneri* was first reported from Long Beach Harbor in 2006 (Miller et al., 2007) and has gradually spread along the southern California marine shelf. It was first observed in San Diego County in Mission Bay in 2008. *S. horneri* dominates some areas formerly dominated by *M. pyrifera* including areas off Santa Catalina Island and the Northern Channel Islands off Santa Barbara. *S. horneri* was first observed in the kelp forests off San Diego in early 2014. Since that time, it has spread to 13 of our study sites. Initially, it was only observed near some of the study sites, but has subsequently been consistently observed within the permanent band transects at several sites. Table 5 lists first sightings within the actual band transects, and Fig. 25 shows the relative observational frequencies among the study sites pooled over time. The greatest percent cover observed thus far has been at PLC08 (Fig. 26) in the fall of 2017 when mean percent cover exceeded 3.5%. This maximum was followed by a maximum percent cover of ~3% at LJN18 in the fall

of 2018 where it has varied in percent cover ever since. However, while *S. horneri* spread relatively quickly to many study sites by 2018, it has still not been observed at seven other sites (Cardiff, Del Mar, PLC15, PLC12, PLS15, PLM18, and PLT15). Rather, it has decreased or disappeared at many of the invaded sites, and presently persists at at very low cover at all sites with the exception of LJN18.

However, *S. horneri* clearly poses a risk to *M. pyrifera* and other algal species due to its potentially high seasonal growth rates. It is not implausible for it to take over some areas of San Diego kelp forests especially after a future major disturbance that reduces the densities and cover of native algal species. Presently, it is too sparsely distributed to be significantly affecting giant kelp with the exception of the LJN18 study site and the deeper portions of the northern La Jolla kelp forest.

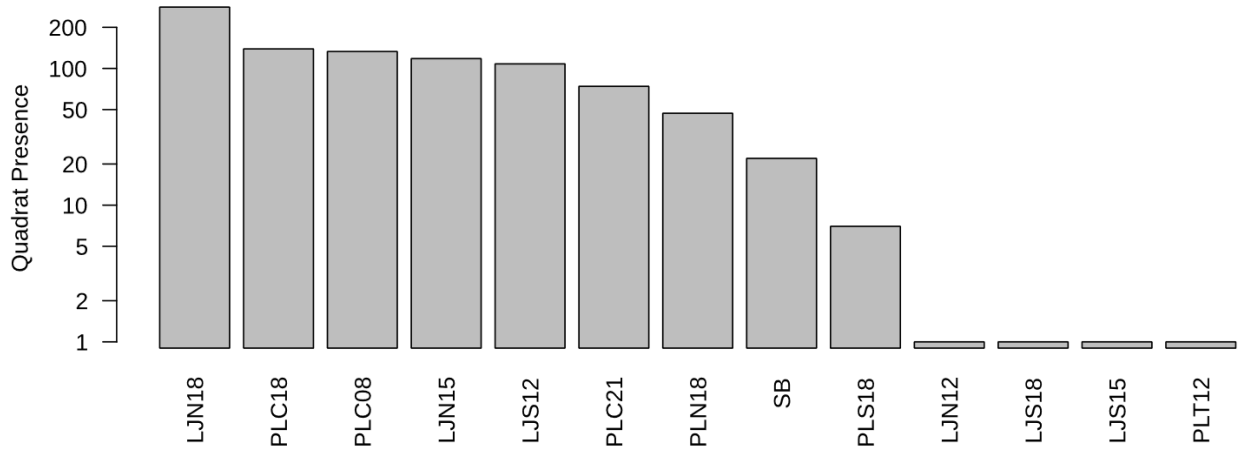

Figure 25. *Presence of the invasive alga, Sargassum horneri, among the study sites where it has been observed within the permanent band transects. Quadrant presence indicates the total number of 5x2 m quadrats along the transects where it has been observed over time since first sighting at each individual site.*

Study Site	Date 1st Observed
SB	Sept. 9, 2105
PLC18	Oct. 10, 2015
PLN18	Dec. 2, 2015
LJN15	Dec. 3, 2015
LJS12	Feb. 8, 2016
PLC08	Mar. 31, 2016
LJS18	May 3, 2016
LJS15	May 3, 2016
PLT12	May 11, 2016
LJN18	May 19, 2016
PLC21	April 18, 2017
LJN12	Jun. 30, 2017
PLS18	May 30, 2018

Table 5. *List of study sites where the invasive alga, Sargassum horneri, has been observed within the band transects and the dates it was first observed.*

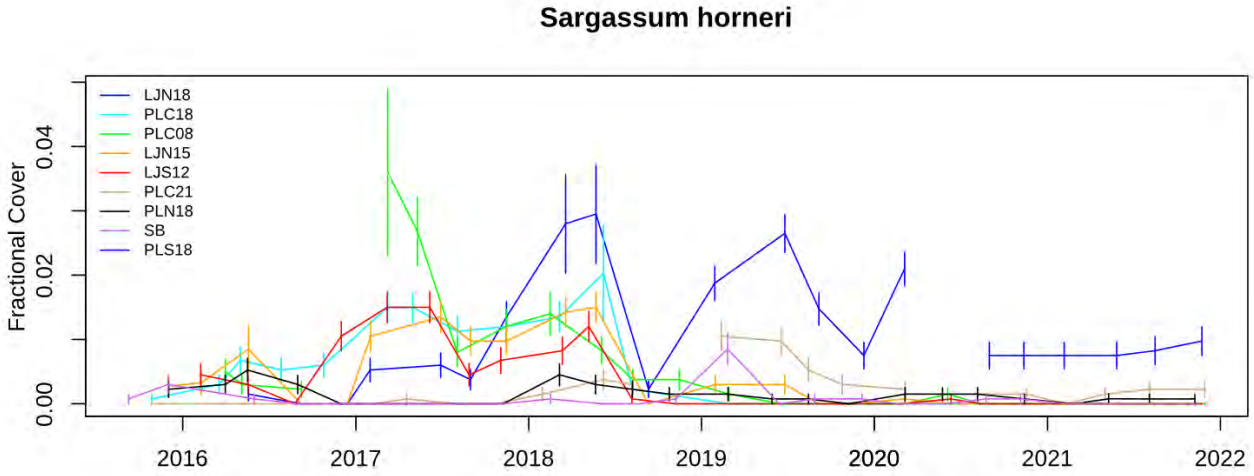

Figure 26. *Fractional cover of the invasive alga Sargassum horneri over time beginning when it was first observed in the kelp forests off San Diego (see Table 4). Some study sites where S. horneri has been observed were omitted because cover values approximate zero.*

Invertebrates

Many invertebrate species were negatively impacted by the 2014-2016 MHW. Sea urchins (Echinoids) and seastars (Asteroids) were most affected. Both groups play important functional roles within kelp forest communities. Sea urchins are major grazers of algae capable of overgrazing kelp forests if they become too numerous and mobile. Seastars are important benthic predators and are considered by many as keystone species whose predatory activities can control benthic community structure. Both groups suffered heavy mortality off San Diego during the warm event and remain depressed as of this writing (2022). Decimation of sea urchin populations off San Diego was a direct result of disease mortality and included the 'dark-blotch' disease. Disease epidemics commonly occur in echinoids (sea urchins - Lafferty, 2004) and asteroids ('sea star wasting disease' - Eckert et al., 2000) during periods of warm water stress.

Densities of both red (*Mesocentrotus franciscanus*) and purple (*Strongylocentrotus purpuratus*) sea urchins (RSU and PSU, respectively) either crashed in response to the consecutive warm periods or were already experiencing disease mortality. Sea urchin densities are shown in Figures 27-29 for a subset of the study sites. These sites were chosen as exemplary of the major population trajectories for red and purple sea urchins and where sea urchins have been most numerous historically. Presently, there are few sea urchins of either species at any of the study sites, even off south Pt. Loma where sea urchin overgrazing has been historically resilient (Parnell, 2015).

The two major patterns of sea urchin population trends among the sites include (1) dramatically reduced densities at sites where they have spiked in the past and (2) stability at sites where they have typically been observed at low densities. Red sea urchins at the central Pt. Loma study sites have been relatively stable but at low density. These animals are sparsely distributed in cryptic habitat and have not exhibited overgrazing during the entire time series. By contrast, red and purple sea urchin overgrazing associated with population spikes have been observed at several of the south Pt. Loma study sites. An example for red sea urchins is the dramatic spike beginning in 2012 at PLM18 when giant kelp densities crashed. The sea urchins then emerged into feeding fronts at high densities. The subsequent MHW decimated these feeding fronts mainly through disease, though population diffusion may have also contributed. Purple sea urchins are typically observed at higher densities than reds and have exhibited population spikes along some of the central Pt. Loma study sites. However, their densities at these sites have remained stable and cryptic over the last two decades and did not succumb in large numbers to the MHW event. That has not been the case in south Pt. Loma where densities have greatly varied and where urchin feeding lines have developed leading to episodic overgrazing fronts that remove young stands of giant kelp.

Sea urchin populations are typically cohort dominated with episodic periods of enhanced larval settlement and juvenile survival. Recruitment of both species was depressed during the MHW (Figs. 30-32), being absent or extremely limited at all study sites until the fall of 2017 when significant recruitment was observed once again. Patterns of recruitment then varied among sites and by species but the general pattern included increased levels of recruitment in 2017-2018 followed by a decrease in 2019-2020 and another increase in recruitment at some of the sites. However, the biggest pulse of recruitment for both species occurred in 2018 and winter of 2019. This cohort of red and purple sea urchins does not appear to have resulted in increased adult densities thus far, indicating that their post recruitment survival has been relatively low or they are remaining cryptic (likely a combination of both). Therefore it is highly likely that sea urchin overgrazing will not be problematic in the near future in most areas of the LJKF and PLKF.

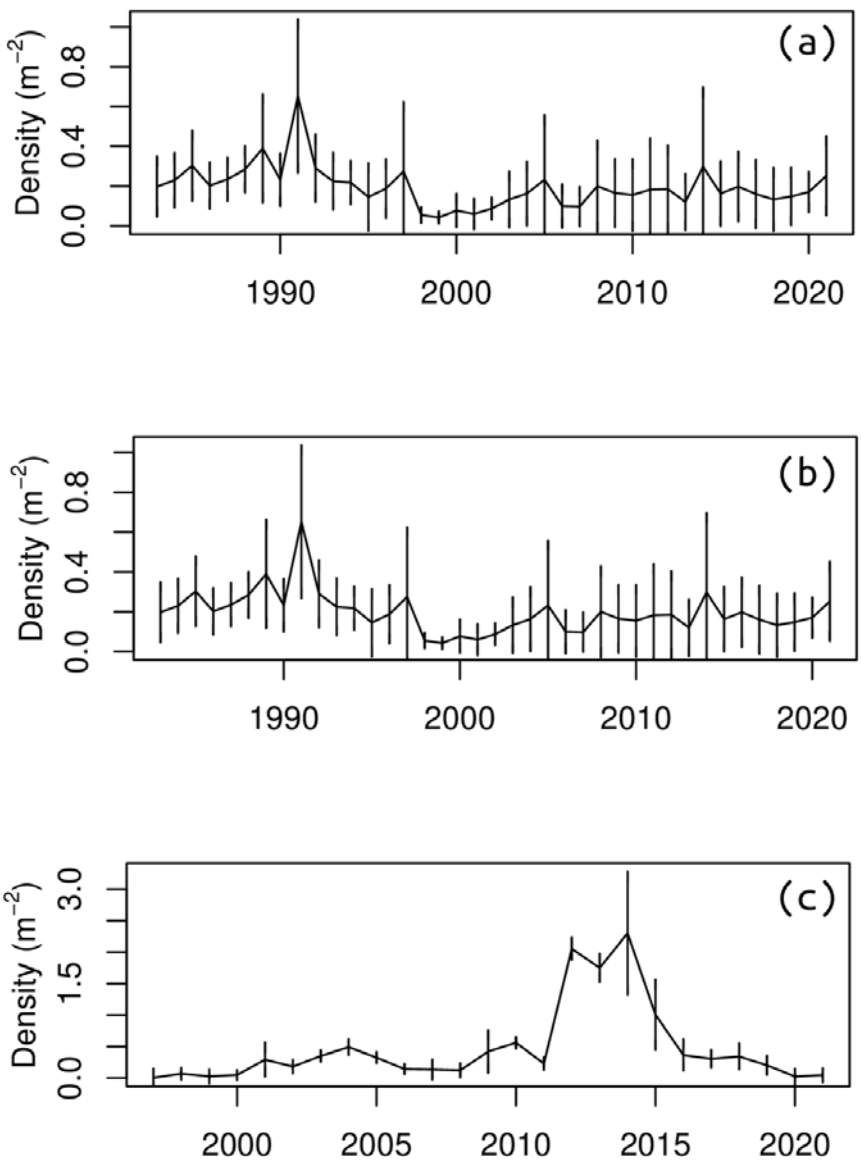

Figure 27. *Time series of the red sea urchin (Mesocentrotus franciscanus) mean densities at the (a) PLC15, (b) PLC18, and (c) PLM18 study sites. Error bars are standard errors.*

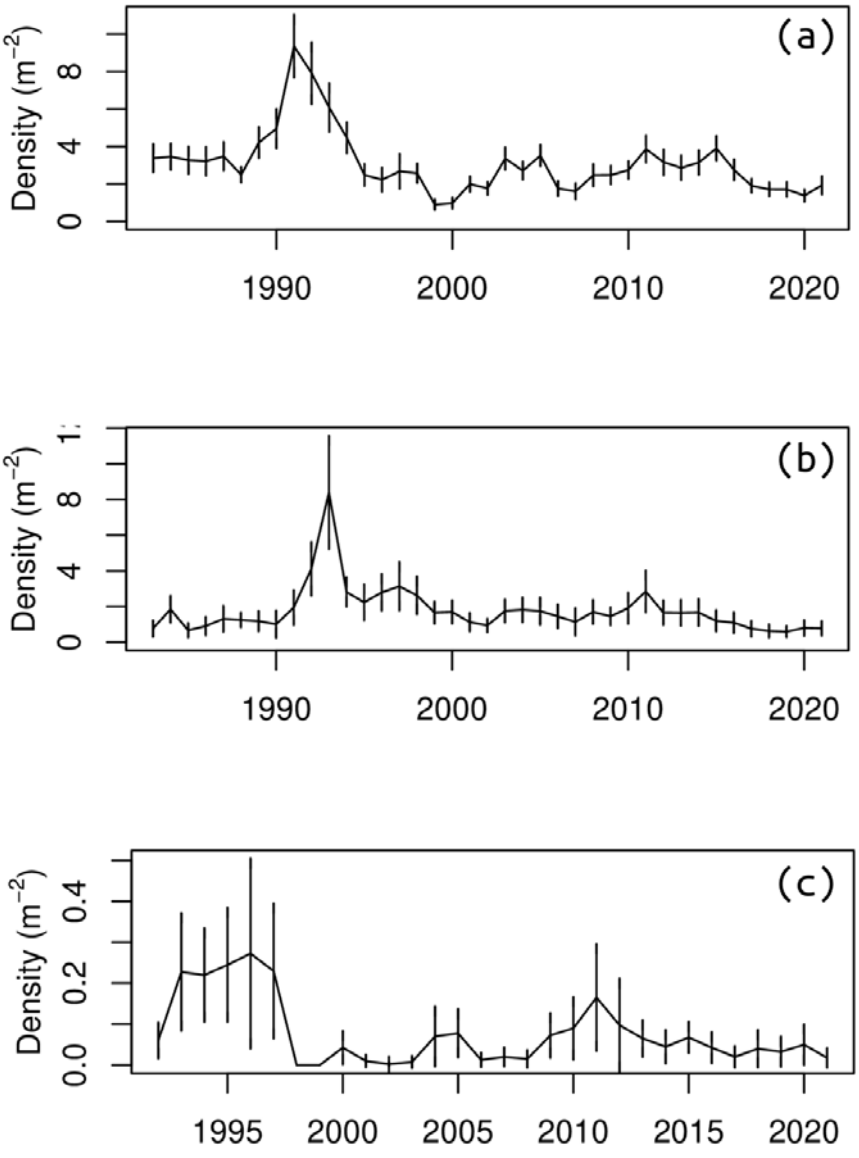

Figure 28. *Time series of purple sea urchin (Strongylocentrotus purpuratus) mean densities at the (a) PLC15, (b) PLN18, and (c) LJS15 study sites. Error bars are standard errors.*

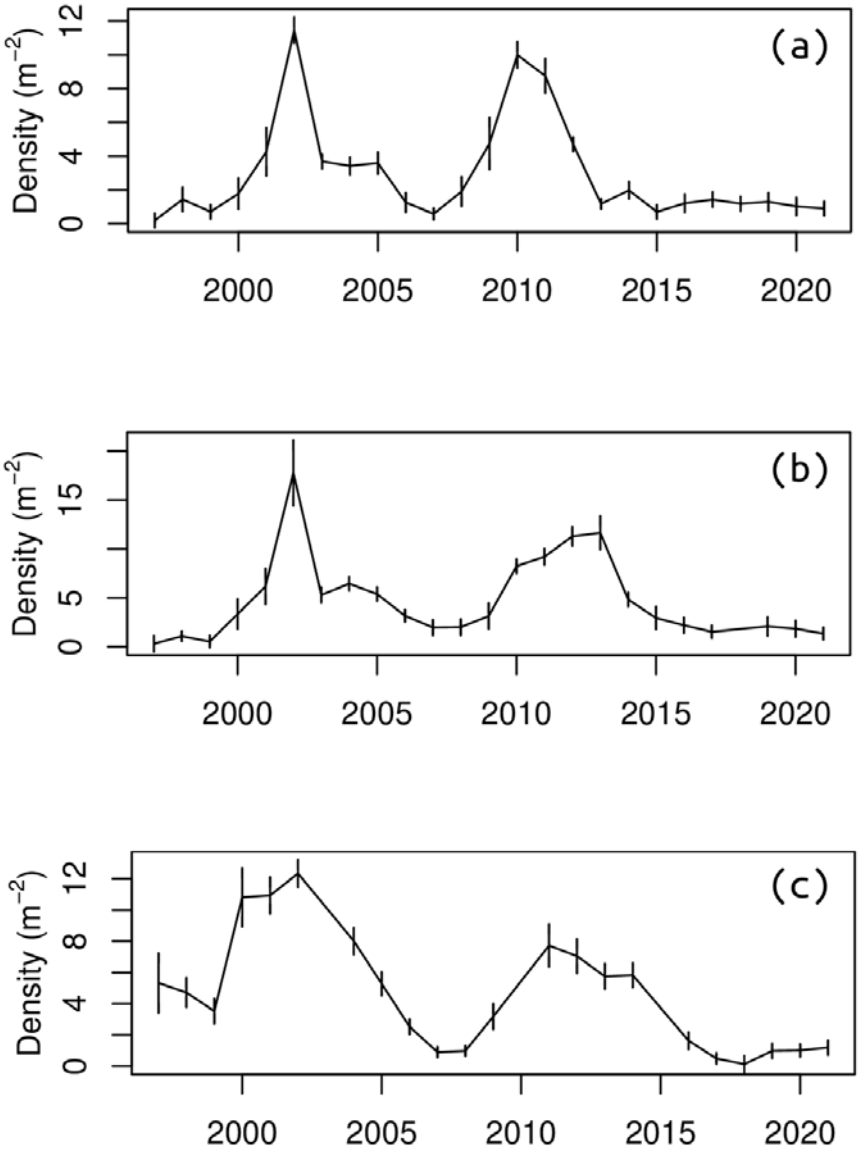

Figure 29. *Time series of purple sea urchin (Strongylocentrotus purpuratus) mean densities at the (a) PLM18, (b) PLT15, and (c) PLT12 study sites. Error bars are standard errors.*

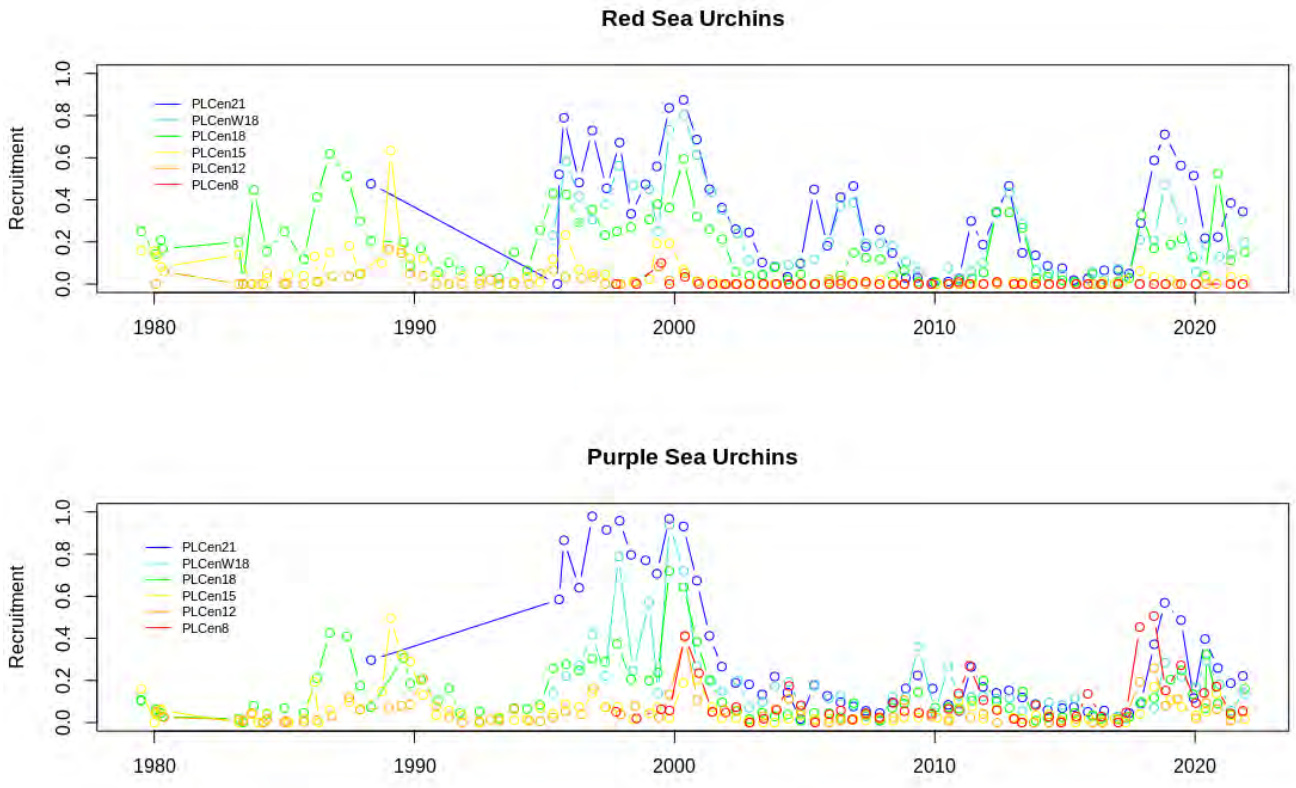

Figure 30. *Time series of red (top) and purple (bottom) sea urchin recruitment (fraction of the population considered in the first year class by size - see Methods) at the central Pt. Loma study sites.*

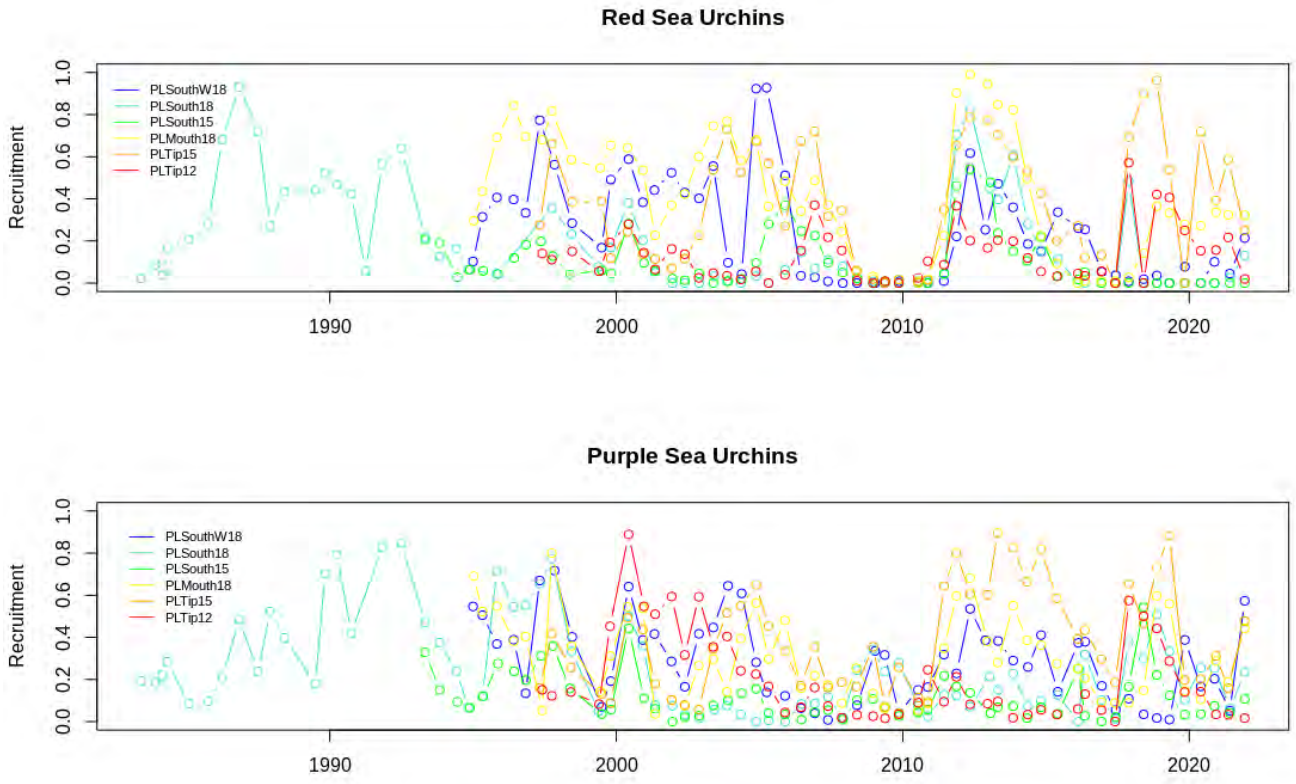

Figure 31. *Time series of red (top) and purple (bottom) sea urchin recruitment at the southern Pt. Loma study sites.*

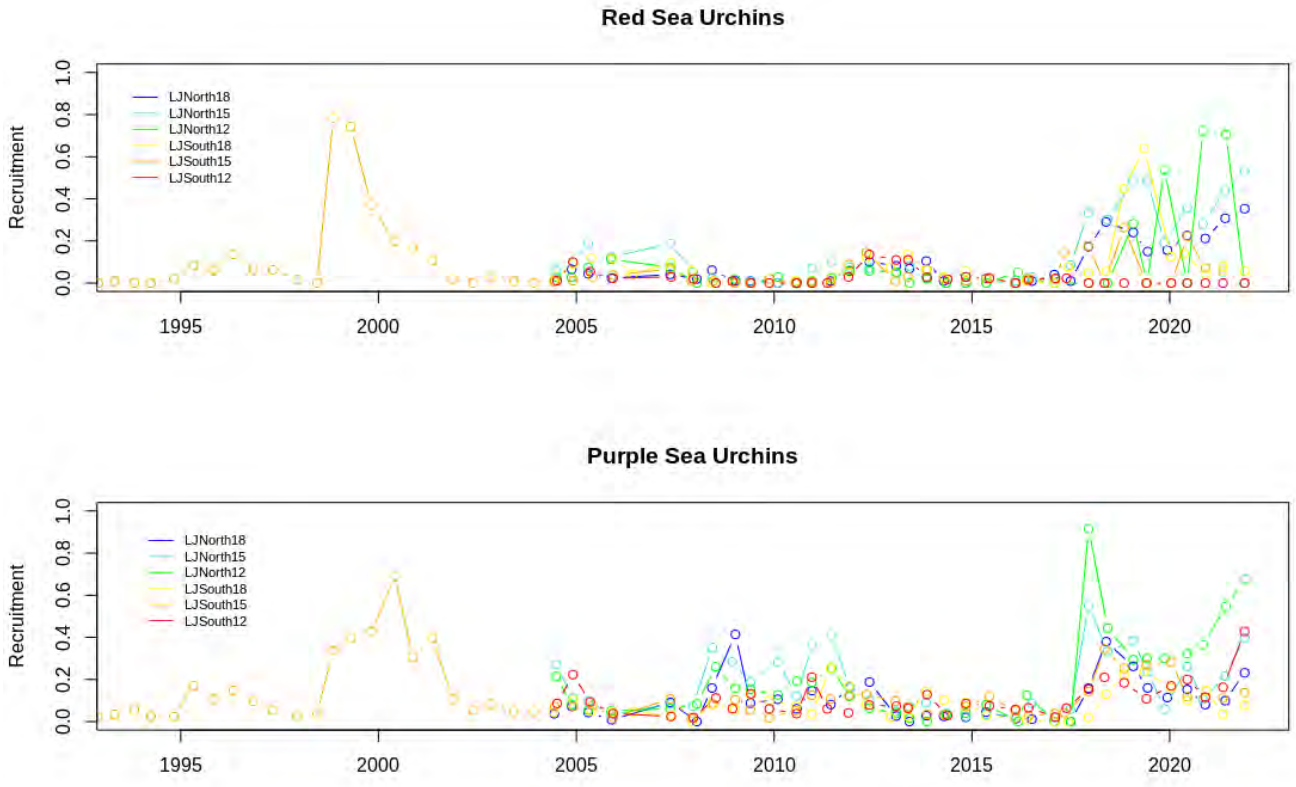

Figure 32. *Time series of red (top) and purple (bottom) sea urchin recruitment at the La Jolla study sites.*

Diseases and associated die-offs affected many other echinoderm species, mainly asteroids (seastars), throughout the Southern California Bight during the just prior to and during the MHW. Species that suffered the greatest mortality at our study sites included *Pisaster giganteus* (Fig. 33) and *P. brevispinus* where densities were reduced to zero for both species, even at sites where they were previously abundant. Disease induced mass mortality events of asteroids and echinoids are commonly followed by recovery at differing rates (Hewson et al., 2014). Juvenile *P. giganteus* were observed recruiting onto giant kelp fronds off Pt. Loma beginning in 2017 continuing into 2018, thus heralding their recovery. However this species is still very uncommon or absent at all of the study sites. *P. brevispinus* is virtually gone from all the south Pt. Loma study sites where they had been common in the past. Disease has also decimated *Pycnopodia helianthodes*, an important sea urchin predator (Moitoza et al., 1979). This species has not been observed anywhere off Pt. Loma since 2014 even in areas where they were commonly observed. *P. helianthodes* was in decline even prior to the BLOB event.

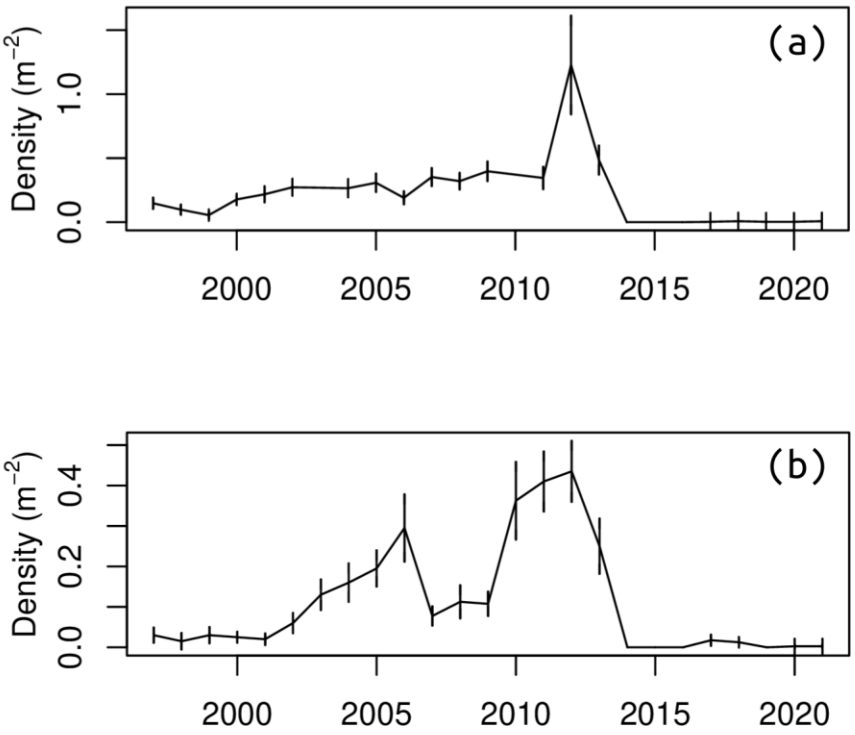

Figure 33. *Time series of the seastar Pisaster giganteus mean density at the (a) PLT12 and (b) PLM18 study sites. Error bars are standard errors.*

Abalones once supported an economically important commercial fishery throughout California until the 1980's. Their primary food in southern California is giant kelp. Therefore, when kelp populations are reduced, abalones become stressed both by the lack of food as well as diseases associated with warm water events (Vilchis et al., 2005). Historically, seven species of abalone have been common off San Diego. Two species, *Haliotis cracherodii* and *H. sorenseni*, are now on the federal endangered species list. Another species, *H. rufescens* has been in decline off southern California since the 1970's, and populations off Pt. Loma crashed in the 1980's (Tegner and Dayton, 1987). However, *H. rufescens* persisted in low numbers near PLS18 and LJS18. Those few were lost during the recent prolonged MHW. Presently, there are relatively few *H. rufescens* throughout San Diego County with the exception of a small population at the extreme western end of the southern Pt. Loma shelf where there has been an increase in kelp canopy cover since the MHW. However, densities of pink abalone (*H. corrugata*) have increased steadily at PLC8 beginning in the early 2000's (Fig. 34). *H. corrugata* has since increased in density even throughout the warm period reaching peak densities approaching 0.1 m^{-2} but have since been halved by 2021 indicating this population increase may have subsided. For comparison, densities of pink abalone in the early 70's at similar depths off Catalina were >1 m^{-2}. (Tutschulte, 1976).

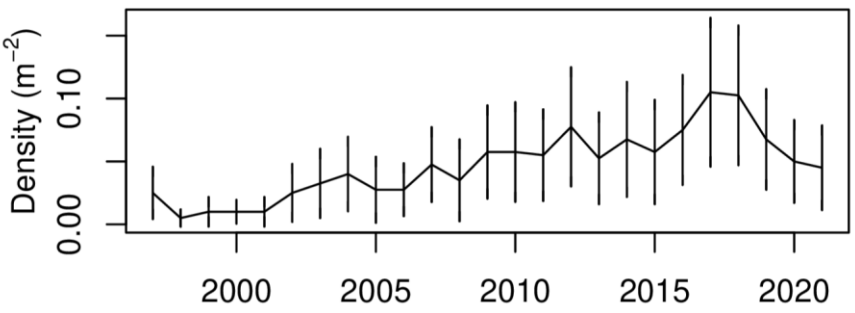

Figure 34. *Time series of pink abalone (Haliotis corrugata) mean densities at the PLC08 study site. Error bars are standard errors.*

North County Sedimentation

The grain size of sediments used for beach replenishment is an important determinant of beach stability. Finer sediments dredged from deeper waters offshore are more rapidly eroded from replenished beaches and are more likely to pose sedimentation risks to nearby kelp forest platforms off North County. The beaches from Carlsbad to Solana Beach were replenished with ~327,000 cubic meters of sand in 2012 using coarser sediments from the San Elijo Lagoon as part of a project to restore the estuary to more marine conditions. Sediments within the NCKF sites have been relatively stable since 2008 indicating that the 2012 replenishment has not been problematic for these kelp forests. Sediment horizons have varied less than 10 cm since 2008 when the sediment time series began. A 50 year replenishment project has recently (2021) been approved for the same area in which sediments will be augmented at 5 to 10 year intervals beginning as soon as 2024. The grain size composition of these sediments is not clearly defined but are anticipated to be from offshore dredging. Therefore, potential risks to north county kelp forests may be more pronounced than the 2012 based on source and replenishment volumes. The initial plan includes replenishing a 2.2 km stretch of Solana Beach with ~535,000 cubic meters of sediment in 2024.

LITERATURE CITED

Clendenning, K.A. and North, W.J. (1960). Effects of wastes on the giant kelp, Macrocystis pyrifera. In *Proceedings of the First International Conference on Waste Disposal in the Marine Environment University of California, Berkeley, July 22-25, 1959* (p. 82). Pergamon.

Dayton, P. K., and Tegner, M. J. (1984). Catastrophic storms, El Niño, and patch stability in a southern California kelp community. *Science*, *224*(4646), 283-285.

Dayton, P. K., Currie, V., Gerrodette, T., Keller, B. D., Rosenthal, R., and Tresca, D. V. (1984). Patch dynamics and stability of some California kelp communities. *Ecological Monographs*, *54*(3), 253-289.

Dayton, P. K., Tegner, M. J., Parnell, P. E., and Edwards, P. B. (1992). Temporal and spatial patterns of disturbance and recovery in a kelp forest community. *Ecological Monographs*, *62*(3), 421-445.

Dean, T. A., & Jacobsen, F. R. (1984). Growth of juvenile Macrocystis pyrifera (Laminariales) in relation to environmental factors. *Marine Biology*, 83(3), 301-311.

DeWreede, R. E. (1984). "Growth and age class distribution of Pterygophora *californica* (Phaeophyta)." *Marine Ecology Progress Series* 19: 93-100.

Deysher, L. E., and Dean, T. A. (1984). Critical irradiance levels and the ineractive effects of quantum irradiance and dose on gametogenesis in the giant kelp *Macrocystis pyrifera*. *Journal of Phycology*, *20*(4), 520-524.

Di Lorenzo, E., and Mantua, N. (2016). Multi-year persistence of the 2014/15 North Pacific marine heatwave. *Nature Climate Change*, *6*(11), 1042-1047.

Eckert, G. L., Engle, J. M., and Kushner, D. J. (2000). Sea star disease and population declines at the Channel Islands. In *Proceedings of the fifth California Islands symposium* (pp. 390-393).

Grigg, R. W. (1978). Long-term changes in rocky bottom communities off Palos Verdes. *Coastal Water Research Project, annual report for the year*, 157-184.

Hewson, I., Button, J. B., Gudenkauf, B. M., Miner, B., Newton, A. L., Gaydos, J. K., ... and Fradkin, S. (2014). Densovirus associated with sea-star wasting disease and mass mortality. *Proceedings of the National Academy of Sciences*, *111*(48), 17278-17283.

Lafferty, K. D. (2004). Fishing for lobsters indirectly increases epidemics in sea urchins. *Ecological Applications*, *14*(5), 1566-1573.

Lawley, D. N. and Maxwell, A. E. (1971). Factor Analysis as a Statistical Method. Second edition. Butterworths.

Leighton, D. L., Jones, L. G., and North, W. J. (1966). Ecological relationships between giant kelp and sea urchins in southern California. In *Proceedings of the Fifth International Seaweed Symposium, Halifax, August 25–28, 1965* (pp. 141-153).

Lüning, K., & Dring, M. J. (1975). Reproduction, growth and photosynthesis of gametophytes of Laminaria saccharina grown in blue and red light. *Marine Biology*, 29(3), 195-200.

Miller, K. A., Aguilar-Rosas, L. E., and Pedroche, F. F. (2011). A review of non-native seaweeds from California, USA and Baja California, Mexico. *Hidrobiológica*, *21*(3).

Moitoza, D. J., and Phillips, D. W. (1979). Prey defense, predator preference, and nonrandom diet: the interactions between Pycnopodia helianthoides and two species of sea urchins. *Marine Biology*, *53*(4), 299-304.

NOAA (2022). ENSO: Recent Evolution, Current Status and Predictions. Update prepared by: Climate Prediction Center/NCEP, 22 April 2019. Retrieved from NOAA website: https://www.cpc.ncep.noaa.gov/products/analysis_monitoring/laNiña/enso_evolution-status-fcsts-web.pdf

Parnell, P., Miller, E. F., Cody, C. E. L., Dayton, P. K., Carter, M. L., and Stebbinsd, T. D. (2010). The response of giant kelp (Macrocystis pyrifera) in southern California to low-frequency climate forcing. *Limnology and Oceanography*, *55*(6), 2686-2702.

Parnell, P. E. (2015). The effects of seascape pattern on algal patch structure, sea urchin barrens, and ecological processes. *Journal of experimental marine biology and ecology*, *465*, 64-76.

R Core Team (2022). R: A language and environment for statistical computing. R Foundation for Statistical Computing, Vienna, Austria. URL https://www.R-project.org/.

Reed, D. C. (1987). "Factors affecting the production of sporophylls in the giant kelp *Macrocystis pyrifera*." Journal of Experimental Marine Biology and Ecology 113: 61-69.

Roberts, P. J. (1991). Ocean outfalls. *Critical Reviews in Environmental Science and Technology*, *20*(5-6), 311-339.

Seymour, R. J., Tegner, M. J., Dayton, P. K., and Parnell, P. E. (1989). Storm wave induced mortality of giant kelp, Macrocystis pyrifera, in southern California. *Estuarine, Coastal and Shelf Science*, *28*(3), 277-292.

Steneck, R. S., Graham, M. H., Bourque, B. J., Corbett, D., Erlandson, J. M., Estes, J. A., and Tegner, M. J. (2002). Kelp forest ecosystems: biodiversity, stability, resilience and future. *Environmental conservation*, *29*(4), 436-459.

Tegner, M. J., and Dayton, P. K. (1987). El Niño effects on southern California kelp forest communities. In *Advances in Ecological Research* (Vol. 17, pp. 243-279). Academic Press.

Towle, D. W., and Pearse, J. S. (1973). Production of the giant kelp, Macrocystis, estimated by in situ incorporation of 14C in polyethylene bags. *Limnology and Oceanography*, *18*(1), 155-159.

Tutschulte, T.C. (1976). The comparative ecology of three sympatric abalones. Ph.D thesis,University of California, 335 pp.

Vilchis, L. I., Tegner, M. J., Moore, J. D., Friedman, C. S., Riser, K. L., Robbins, T. T., and Dayton, P. K. (2005). Ocean warming effects on growth, reproduction, and survivorship of southern California abalone. *Ecological Applications*, *15*(2), 469-480.

Appendix B

Ocean Imaging Annual Report

2020 – 2021

Jan Svejkovsky, Ph.D., Mark Hess

Ocean Imaging Corps
13976 West Bowles Avenue, Suite 100, Littleton CO 80127

Submitted to City of San Diego
Public Utilities Department

Satellite & Aerial Coastal Water Quality Monitoring in the San Diego / Tijuana Region

By Jan Svejkovsky, Ph.D., Mark Hess

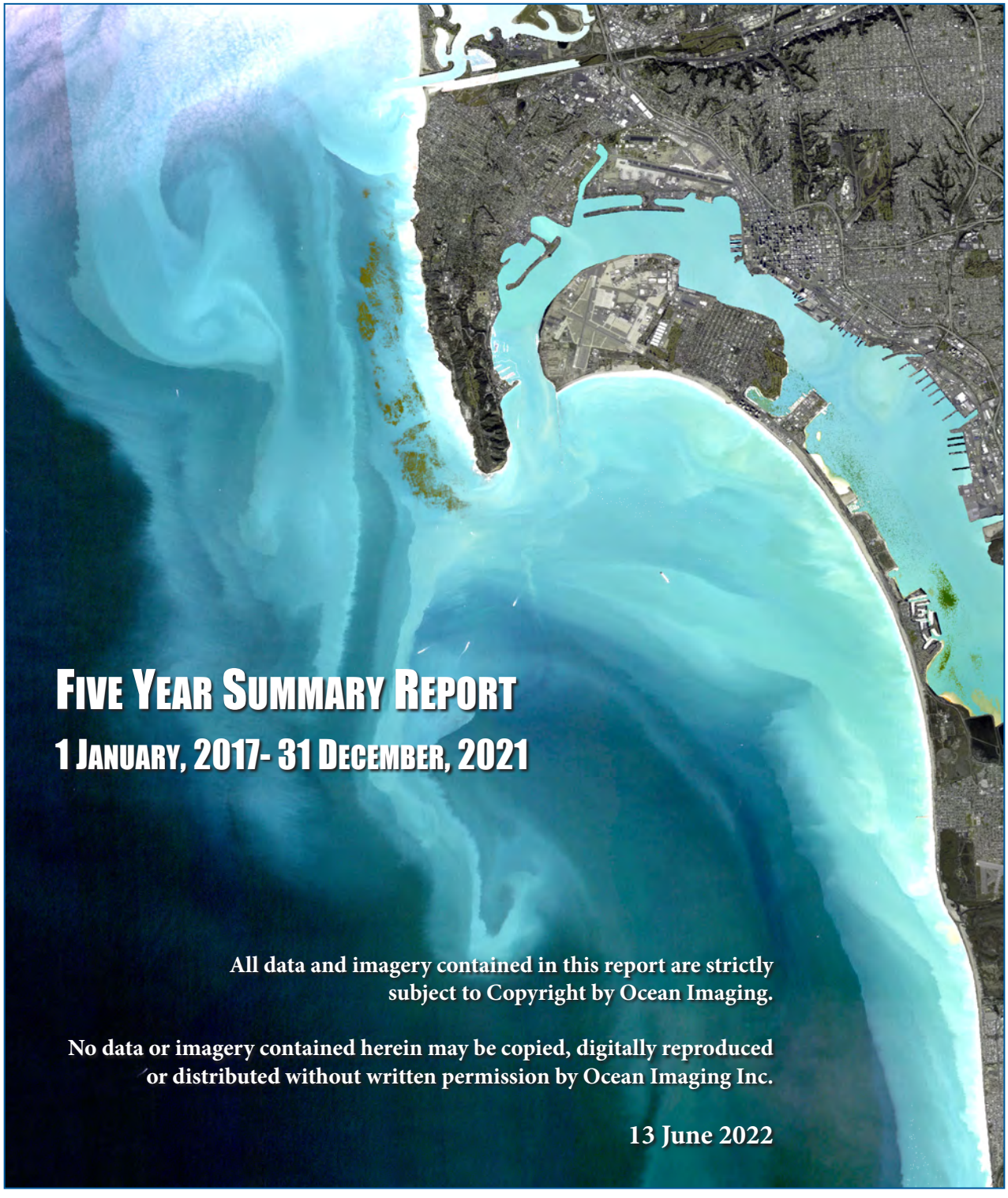

Five Year Summary Report

1 January, 2017- 31 December, 2021

13 June 2022

Ocean Imaging

13976 West Bowles Avenue, Suite 100, Littleton CO 80127 Phone: 303-948-5272 Fax: 303-948-2549 www.oceani.com

Table of Contents

EXECUTIVE SUMMARY 1

1. PROJECT BACKGROUND AND OBJECTIVES 5

2. STUDY AREA 6

2.1 Southern California and San Diego Regions 6

2.2 Climate and Oceanography 8

3. METHODS AND TECHNOLOGY OVERVIEW 9

3.1 Imaging in the UV-Visible-Near Infrared Spectrum 9

3.2 Imaging in the Thermal Infrared Spectrum 9

3.3 Satellites and Sensors Utilized 10

3.4 Recent Data Enhancements 12

3.5 Data dissemination and analysis 16

3.6 Field Sampling Data 17

4. HISTORICAL RESULTS 18

4.1 The Point Loma Ocean Outfall 18

4.2 The South Bay Ocean Outfall 20

4.3 The Tijuana River and San Antonio de los Buenos Creek 27

5. NOTABLE CONDITIONS AND EVENTS 2017 – 2021 29

5.1 Overall Atmospheric and Oceanographic Trends 29

5.1.1 Ocean Temperature Conditions 29

5.1.2 Ocean Chlorophyll and Plankton Levels 30

5.1.3 Regional Precipitation 30

5.2 Conditions in 2017 34

5.3 Conditions in 2018 37

5.4 Conditions in 2019 38

5.5 Conditions in 2020 41

5.6 Conditions in 2021 43

5.6.1 Atmospheric and Ocean Conditions in 2021 43

5.6.2 The South Bay Ocean Outfall Region in 2021 49

5.6.3 The Point Loma Ocean Outfall Region in 2021 50

5.7 Kelp Variability 52

6. RECENT AND FUTURE DEVELOPMENTS AND ADDITIONS TO THE PROJECT 54

7. REFERENCES 57

APPENDIX A – 2021 HIGH RESOLUTION SATELLITE IMAGERY SHOWING SBOO-RELATED WASTEWATER PLUME 60

EXECUTIVE SUMMARY

Following initial NASA-funded development in the 1990s and subsequent demonstration projects with the EPA and California State Water Resources Control Board, in October 2002 Ocean Imaging Corporation began providing regional ocean water quality monitoring for the City of San Diego and the International Boundary Waters Commission. The monitoring utilizes various aerial and satellite sensors in the visible, near-infrared and thermal infrared to detect patterns in the coastal ocean due to oceanographic variables as well as point and non-point terrestrial runoff, and anthropogenic sources such as the region's offshore sewage outfalls. These image data are utilized to spatially and temporally augment regular field sampling surveys, and to help interpret results from those surveys. In the early years of the project its focus was primarily on the detection and monitoring of the sewage outfall plumes and runoff from historically high contamination sources such as the Tijuana River and San Antonio de los Buenos Creek. The project's objectives later expanded to include the generation of multiple spatial data products on a larger, regional scale to provide information on oceanic variables affecting San Diego's coastal waters. The project's results include the determination of dispersal pattern trends of the South Bay Ocean Outfall plume when it reaches the ocean's surface layer, dispersal pattern trends of stormwater runoff from multiple shoreline point sources and their relation to beach contamination potential, as well as short term patterns and long-term trends of oceanic phenomena such as phytoplankton blooms and red tides, and growth cycles of the region's kelp beds. Some of the results have been published in peer-reviewed journals. This report provides a summary of the most important results and gives highlights of notable events in the last 5 years.

List of Abbreviations

ADCP	Acoustic doppler current profilers
AOI	Area of Interest
AVHRR	Advanced Very High Resolution Radiometer
CMML	City Marine Microbiology Laboratory
CORDC	Coastal Observing Research and Development Center
DMSC	Digital Multispectral Camera
EFF	Effluent
EPA	Environmental Protection Agency
ESA	European Space Agency
FC	Fresh Core (River plume components)
HAB	Harmful Algal bloom
HF Radar	High Frequency Radar-derived surface currents
HYCOM	Hybrid Coordinate Ocean Model
IBWC	International Boundary and Water Commission
INF	Influent
MGD	Millions of Gallons Per Day
mg/L	Milligrams per Liter
MODIS	Moderate Resolution Imaging Spectroradiometer
MSI	Multispectral Instrument
NASA	National Aeronautics and Space Administration
Near-IR	Near-Infrared
OC	Old Core (River plume components)
OI	Ocean Imaging Corporation
OLCI	Ocean and Land Color Instrument
ONI	Oceanic Niño Index
OP	Old Plume (River plume components)
PLOO	Point Loma Ocean Outfall
REST	Representational State Transfer
RTOMS	Real-time oceanographic mooring station
SAR	Synthetic Aperture Radar
SBIWTP	South Bay International Wastewater Treatment Plant
SBOO	South Bay Ocean Outfall
SCB	Southern California Bight
SDIA	San Diego International Airport (SDIA)
SDPUD	San Diego's Public Utilities Department
SDR	San Diego River
SDWQ	San Diego Water Quality
SLSTR	The Sea and Land Surface Temperature Radiometer
SPOT	Satellite Pour l'Observation de la Terre
SST	Sea Surface Temperature
SWRCB	State Water Resources Control Board
TIR	Thermal Infrared
TJR	Tijuana River
TM	Thematic Mapper
TSS	Total Suspended Solids
UV	Ultraviolet
VIIRS	Visible Infrared Imaging Radiometer Suite
WMS	Web Map Service

1. PROJECT BACKGROUND AND OBJECTIVES

Due to the economic benefits that accrue from access to ocean navigation, coastal fisheries, tourism and recreation, human settlements are often more concentrated in the coastal zone than elsewhere. Presently about 40% of the world's population lives within 100 kilometers of the coast (United Nations, 2017). The large population densities result in proportionately large volumes of municipal and industrial wastewater which, in large metropolitan areas, are most commonly disposed of through submarine wastewater outfalls. The practice of wastewater disposal into coastal environments in the U.S. has advanced tremendously over the past 50 years from discharging untreated or partly treated sewage effluent in shallow water close to shore to the discharge of highly treated effluent through deep ocean outfalls (Rogowski, Peter, et al, 2012). The actual efficiency of effluent treatment varies with outfall design, location, discharge depth and distance from shore, regional ocean current patterns, etc. A sub-efficient outfall can thus have significant negative consequences for both environmental impact and human health in the surrounding area. In the United States, municipal outfalls operate under permits issued by the Environmental Protection Agency (EPA). Often, permits allowing the discharge of effluent that has undergone only primary (large objects and some suspended sediment removed) or secondary (most organic matter removed) treatment require a regional water quality monitoring plan that includes regular sampling of biological, chemical and physical parameters around the outfall discharge site. This monitoring is typically done by field sampling performed at regular time intervals (e.g., monthly) at sampling locations comprising a predetermined sampling grid. In the case of the City of San Diego a total of 69 offshore water quality monitoring stations are sampled quarterly to assess coastal oceanographic conditions in the two outfall regions monitored. The City of San Diego Biennial reports summarize additional monitoring efforts such as the sampling of sediments and fish species (City of San Diego, 2020).

The position of the sampling grid usually includes the offshore outfall discharge location and the ocean area surrounding it to a sufficient distance as to be able to deduce the vertical and horizontal extents of the discharge plume through indicator measurements such as salinity, indicator bacteria, and the plume's dilution rate and hence mixing parameters as it expands from its discharge location. In some cases, additional sampling locations may be located outside the main grid at nearby ecologically important sites such as reefs or kelp beds. In most regions, the field-sampling strategy to monitor the near-term and long-term fate of the discharged wastewaters is compromised by several factors: First, both the number of sampling sites and the frequency of sampling is limited by the budget that is reasonably available for such work. Second, coastal regions where municipal wastewater outfalls are located tend to contain other point and non-point sources that discharge possible pollutants into ocean and estuarine waters, either continuously (e.g., rivers and streams) or episodically (e.g., storm drains). Plumes from these sources sometimes enter the outfall sampling grid areas, making it difficult to separate the outfall plume's true effects from other external influences.

Satellite remote sensing has been utilized in oceanography since the 1970s to detect and monitor oceanic processes. In recent decades satellite and aerial imaging have provided means to study coastal discharges such as river and stormwater runoff plumes using multispectral visible and thermal imagery (Ruddick et al. 1994, Ouillon et al. 1997, Walker et al. 2005, Nezlin et al. 2005, Warrick et al. 2007, Svejkovsky et al. 2010), and microwave-based synthetic aperture radar (SAR) for detection of surfactant films associated with natural processes (Svejkovsky and Shandley 2001) and plumes containing anthropogenic substances (Svejkovsky and Jones 2001, Gierach et al. 2016, Holt et al. 2017).

The unique advantage of such imaging is that if a particular process, event or discharge plume feature is detectable, the image data provide a synoptic view of it on a spatial scale and often at spatial resolution that is impossible to attain with ship-based field sampling. Because of this, such imagery also provides increased potential for accurately separating features from multiple discharge sources in the same area. Additionally, the revisit frequency of many satellite systems has the potential to provide data on a time frequency not economically possible with ship-based field sampling programs. On the other hand, satellite and aerial remote sensing instruments can sample only the surface or near-surface waters, thus not providing any three-dimensional information, or detection capabilities of phenomena not reaching the upper water column. Also, with the exception of SAR, imaging is blocked by clouds, so useful data acquisition cannot be relied upon during every satellite overpass. Imaging from aircraft is somewhat less compromised since imagery can be acquired by flying under the cloud layer when feasible.

The utilization of remote sensing specifically for the detection or monitoring of offshore wastewater outfall plumes has been significantly less common than for river and stormwater sources. With the exception of the Massachusetts Water Resources Authority who have utilized 1 km resolution satellite chlorophyll imagery since the mid 1990s as part of their Boston Harbor sewage outfall monitoring program (Werme and Hunt 2000, Hyde et al. 2007), other efforts tend to be short term studies or one-time technology demonstrations. In the early 1990s multispectral visible and thermal satellite imagery were used in studies linked to the installation of new deep-water outfalls in Sydney, Australia (Howden 1995). Axiak et al. (2000) utilized satellite SAR imagery to assess the spatial extent of coastal impact from the island of Malta's main wastewater outfall in the Mediterranean Sea. Keeler et al. (2005) utilized very high resolution (70 cm – 1 m) panchromatic satellite imagery to detect internal wave effects from a deep-water outfall in Hawaii, USA. Aerial multispectral and thermal imagery were used by Marmorino et al. (2010) to demonstrate the direct detection of a wastewater outfall in Florida, USA, and characterize its dilution patterns. More recently, multiple mid-resolution satellite instruments were used to monitor chlorophyll, sea surface temperature (SST) and surfactant distributions during two wastewater outfall diversion events in Southern California (Gierach et al. 2017, Trinh et al. 2017).

In the 1990s, Ocean Imaging Corporation (OI) received multiple research grants from NASA's Commercial Remote Sensing Program for the development and commercialization of novel remote sensing applications in the coastal zone. As part of these projects, OI developed methods to utilize various types of remotely sensed data for the detection and monitoring of stormwater runoff and wastewater discharges from offshore outfalls. The methodology was initially demonstrated with collaboration of the Orange County Sanitation District in California (Svejkovsky and Haydock 1998). The NASA-supported research led to a proof-of-concept demonstration project in the San Diego, California region co-funded by the EPA in 2000. Those results led, in 2002, to adding an operational remote sensing-based monitoring component to the San Diego region's established water quality monitoring program. The project continues as a joint effort between the Ocean Monitoring Program of the City of San Diego's Public Utilities Department (SDPUD). This report provides background information for the entire project, historical data and analyses as well as summarizes notable events from the period between 2017 through 2021.

2. STUDY AREA

2.1 Southern California and San Diego Regions

The San Diego coastal region lies within the Southern California Bight (SCB) – a broad ocean

embayment created by an indentation of the coastline south of Pt. Conception, California. Much of the Bight coastline is heavily urbanized, with estimates of as much as 90% of original coastal wetlands having been lost to development (Schiff et al. 2000). The related damming of rivers and streams emptying into the wetlands has resulted in drastic reductions of natural freshwater inputs to the ocean, and with it the loss of sand transport that has accelerated beach erosion (Bird and Lewis 2015). As is shown in **Figure 1,** this project's present monitoring efforts strive to provide remote sensing data on two main regional scales: 1) SCB image products spanning the entire Southern California Bight at spatial resolutions of approximately 250 m – 1000 m; 2) "Core" image products focusing on coastal waters around the Point Loma Ocean Outfall (PLOO) and South Bay Ocean Outfall (SBOO) and approximately 15 km to their North and South at spatial resolutions of 30 m and finer.

The PLOO discharges wastewater treated by the Point Loma Wastewater Treatment Plant under a 301(h) modified treatment permit. The PLOO average discharge in 2018 and 2019 was roughly 141 MGD (million gallons per day). It extends 7.2 km offshore from Pt. Loma (see Figure 1 above). The end of the pipeline connects to a perforated "Y" diffuser section of two legs, each 762 meters long. Wastewater is discharged through diffuser ports ranging in depth from 93.3 m to 97.5 m. At present only the south leg of the diffuser section is operational in order to maintain sufficient water pressure. (City of San Diego, 2020).

The Tijuana River (TJR) watershed is approximately 4465 km² in size. It straddles the United States and Mexico border, with about 72% in Mexico and 28% in the United States. During the dry season (approximately April through September) none or only minimal flow tends to reach the TJR Estuary and no appreciable discharge thus enters the ocean. Following rain events, however, the TJR discharges excess runoff into the ocean in a highly turbid

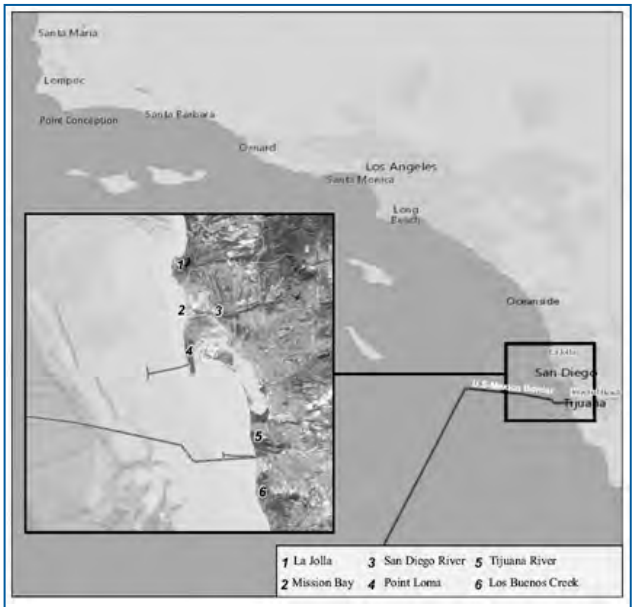

Figure 1. Coverage areas of satellite image products generated for San Diego's water quality monitoring program: 1) SCB products (large area); 2) "Core" area (inset); 2) "Core" area (inset).

plume, readily discernible in satellite imagery. In addition to high suspended solids concentrations, the runoff waters have been repeatedly shown to contain high levels of toxic contaminants (Gersberg et al., 2004), bacteria, and hepatitis and enteroviruses (Gersberg et al., 2006). Public health hazards posed by the TJR discharge result in beach advisory postings or closures northward along the U.S. shoreline and lasting from several days to months.

The frequent shoreline contamination problems associated with stormwater runoff from the TJR prompted the U.S. to construct the SBIWTP, which began operation in January of 1999. Each day the plant processes approximately 26 MGD of sewage from Tijuana's sewer system to advanced primary level (full secondary level since November 2010) and discharges it into the Pacific Ocean through the SBOO (Figure 1 above). In addition to receiving wastewater from Tijuana's municipal sewer system, the plant is connected to the TJR directly through a diverter channel system above the TJR Estuary, which diverts up to 13 MGD of flow from the river into the plant for treatment. The diverter system thus

delays somewhat the initial entry of runoff into the estuary and the ocean following a storm and lessens the total volume of effluent entering the ocean during the TJR active flow. The average SBOO discharge in 2018-2019 was approximately 28 MGD through a "Y" diffuser system approximately 5.6 km offshore at a depth of 27 meters. This included about 3 MGD of secondary and tertiary treated effluent from the SBWRP, and 25 MGD of secondary treated effluent from the SBIWTP (City of San Diego, 2020 and San Diego Regional Water Quality Control Board, 2020).

Although some studies have shown a possible slight decrease in the frequency of beach contamination after the SBOO began operation (as measured by fecal coliform and enterococci bacteria indicators), the shoreline contamination problem persists, primarily through continued discharge from the Tijuana River (Gersberg et al. 2008). This is particularly common during the rainy season when the SBIWTP reaches its full capacity and excess runoff is bypassed and allowed to flow out to sea (San Diego Regional Water Quality Control Board, 2020).

2.2 Climate and Oceanography

The climate of Southern California is of the Mediterranean type, with distinct dry (summer) and wet (winter) seasons. Aside from the outfall discharges, the majority of annual water and sediment loads entering the ocean from land sources are linked to winter storms (Inman and Jenkins 1999). The accumulation of pollutants on terrestrial surfaces occurs during the dry season, which then get swept into the ocean during the first few annual storms, resulting in a "First Flush Effect" that has been well documented with field measurements (Bertrand-Krajewski et al., 1998; Cristina and Sansalone, 2003; Tiefenthaler and Schiff, 2003) and even from space with satellite imagery (Svejkovsky and Jones, 2001). The "Core" study region around the PLOO and SBOO includes numerous sources of episodic stormwater runoff entering the coastal zone. The largest include the already-mentioned Tijuana River, the San Diego River (its dry season flow tends to be very low, less than 2 cubic meters per second), and the entrances to Mission and San Diego Bay. Stormwater runoff plumes flowing out of coastal lagoons and wetlands in San Diego's North County and Orange County further to the north are often also advected southward into the "Core" region after heavy rains. Additionally, a multitude of storm drains from city streets and other, non-point sources discharge seasonal runoff directly onto the shoreline.

The prevailing nearshore surface flow pattern along San Diego's coastline is southward, with a localized, headland-related upwelling zone south of Pt. Loma (Roughan et al. 2005). Plankton blooms and red tides (most common in the spring and summer months) periodically affect water clarity in the San Diego County region as well as the entire SCB. Occasional flow reversal episodes lasting up to several days occur throughout the year and advect nearshore waters from south of the US/Mexico border northward. One significant shoreline discharge source needs to be noted south of the US/Mexico border, as it is in relative proximity to US waters and the SBOO: San Antonio de los Buenos Creek located approximately 10 km south of the border (Figure 1 above) has no natural flow during the dry season, but receives a daily input of 20 – 30 MGD of minimally treated sewage effluent from the San Antonio de los Buenos Sewage Treatment Facility near Tijuana, Mexico. This volume can more than double during rain events. Treatment consists of passing part of the sewage influx through sedimentation and aeration ponds and, at least on some days, the addition of chlorine to the water. Due to capacity limitations, how¬ever, 6 MGD or more of untreated sewage can be diverted around the ponds and is left untreated. The untreated water is dis¬charged into the creek channel 1 km upstream from its mouth and flows into the surf zone over a rocky beach (Graf et al. 2005).

The variety of natural and anthropogenic discharge sources, coupled with a dynamic and varied oceanographic regime make San Diego's region-wide water quality monitoring quite challenging. Utilizing satellite and aerial remote sensing to augment traditional field sampling has provided additional capabilities to better spatially define the various effluent plumes and monitor their variability during both wet and dry season conditions.

3. METHODS AND TECHNOLOGY OVERVIEW

OI uses several remote sensing technologies to monitor San Diego's offshore outfalls and shoreline water quality. Their main principle is to reveal light reflectance and heat emission patterns that are characteristic of the different discharges, water masses, plankton blooms and suspended sediment loads. Most often this is due to specific substances contained in the effluent but absent in the surrounding water.

3.1 Imaging in the UV-Visible-Near Infrared Spectrum

This is the most common technique used with satellite and aerial images. Wavelengths (colors) within the range of the human eye are most often used but Ultraviolet (UV) wavelengths are useful for detecting fluorescence from petroleum compounds (oil, diesel, etc.) and near-IR wavelengths can be useful for correcting atmospheric interference from aerosols (e.g., smog and smoke). Near-IR wavelengths are also highly reflected from kelp seaweeds, so such data are very useful for delineating the region's kelp beds and monitor their extents through time.

The best detection capabilities are attained when several images in different wavelengths are acquired simultaneously. These "multispectral" data can be digitally processed to enhance features not readily visible in simple color photographs. For example, two such images can be ratioed, thus emphasizing the water features' differences in reflection of the two specific wavelengths. A multi-wavelength image set can also be analyzed with "multispectral classification algorithms" which separate different features or effluents based on the correlation relationships between the different color signals.

The depth to which the color sensors can penetrate depends on which wavelengths they see, their sensitivity and the general water clarity. In the San Diego region, green wavelengths tend to reach the deepest and, as elsewhere, UV and near-IR wavelengths penetrate the least. Generally, OI's satellite and aerial sensor data reveal patterns in the upper 15-40 feet.

3.2 Imaging in the Thermal Infrared Spectrum

Some satellite and aerial sensors image heat emanating from the ground and the ocean. They thus reveal patterns and features due to their differences in temperature. Since thermal infrared (TIR) wavelengths are strongly absorbed by water, the images reveal temperature patterns only on the water's surface. Such images can help detect runoff plumes when their temperatures differ from the surrounding ocean water. Runoff from shoreline sources tends to be warmer than the ocean water, although the reverse can be true during the winter. Plumes from offshore outfalls can sometimes also be detected with thermal imaging. Since the effluent contains mostly fresh water, it is less dense than the surrounding salt water and tends to rise towards the surface. How far it rises depends on outfall depth, ocean currents, and stratification conditions. If it makes it all the way, it is usually cooler than the surrounding sun-warmed surface water. A plume signature detectable in multispectral color imagery but not detectable in simultaneously collected TIR imagery indicates the rising plume has not reached the actual ocean surface and remains submerged.

3.3 Satellites and Sensors Utilized

In October 2002, the operational monitoring phase of the project was initiated. To date, this work utilizes 1100 m resolution Advanced Very High Resolution Radiometer (AVHRR)-derived imagery (available multiple times per day), 1000 m resolution chlorophyll and SST Moderate Resolution Imaging Spectroradiometer (MODIS)-derived imagery (available multiple times per day), 500 m resolution MODIS true color imagery (available near-daily), 750 m resolution Visible Infrared Imaging Radiometer Suite (VIIRS) chlorophyll and SST imagery (available multiple times per day), 300 m resolution Sentinel 3 color and thermal imagery (available daily), 30 m & 60 m Landsat 7 ETM+ , Landsat 8 OLI/TIRS and Landsat 9 OLI-2/TIRS color and thermal imagery (each available approximately every 16 days), 10 m resolution Sentinel 2 multispectral imagery (available 2-4 times per week), and 6 m resolution Satellite Pour l'Observation de la Terre (SPOT) 6 and SPOT 7 (available approximately every 4-5 days). Synthetic Aperture Radar (SAR) from the Sentinel 1A and 1B satellites (available every 3-6 days at a spatial resolution of 5m x 20 m) were added to the mix of remote sensing data in late 2021.

Until 2010, the project relied heavily on acquisition of multispectral color imagery with OI's DMSC-MKII aerial sensor and TIR imagery from a Jenoptik thermal imager integrated into the system (see details in the "Technology Overview" section). These aerial image sets were most often collected at 2 m resolution. The flights were done on a semi-regular schedule ranging from 1-2 times per month during the summer to once or more per week during the rainy season. The flights were also coordinated with the City of San Diego's regular offshore field sampling schedule so that the imagery was collected on the same day (usually within 2-3 hours) of the field data collection. Additional flights were done on an on-call basis immediately after major storms or other events such as sewage spills. In late 2010, OI negotiated a special data collection arrangement with Germany's RapidEye Corporation and this project began utilizing their multispectral imagery in lieu of most of the aerial Digital Multispectral Camera (DMSC) image acquisitions. The use of satellite as opposed to aerial data also enables a more regionally contiguous monitoring of events affecting the target areas. In late 2019 the RapidEye satellite constellation was decommissioned by the current operator Planet Labs. Subsequently, OI secured the regular acquisition of SPOT 6 and SPOT 7 satellite imagery covering the same geographical area beginning in 2020. **Table 1** lists the properties of the remote sensing image sources routinely used during the project.

The prime objectives of the project have expanded somewhat since its inception. Initially, emphasis was on utilizing the image data to discern and monitor surface and near-surface signatures from the SBOO and PLOO, separate them from other nearshore point and non-point runoff features, and monitor their locations, extents and potential impact on the shoreline. Prior to this project, the spatial extents of the plumes could only be estimated from a relatively sparse spatial grid of field samples, which made it very difficult to separate, for example, the SBOO near surface plume from the Tijuana River runoff plume. This ambiguity made it difficult, in turn, to objectively evaluate the potential contribution, if any, of the SBOO plume to beach contamination along the nearby shoreline. The satellite and aerial imagery helped directly establish the dispersal trajectories of the SBOO effluent during months when it reaches the near-surface layer and support the claim that it likely never reaches the surf zone.

Over the past five to ten years, the project's objectives have broadened from focusing primarily on the outfalls to also provide larger-scale, regional observations of the physical and biological patterns and processes affecting the San Diego County and Tijuana River discharge regions. It is this broader-view perspective that led to the creation of the

Table 1. Satellite sensors utilized in the project and their characteristics.

Sensor	Utilization Period	Resolution (m)	Utilized Wavelength Range
AVHRR	2003 - Present	1100	Channel 4: 10.30 – 11.39 um Channel 5: 11.50 – 12.50 um
MODIS	2003 - Present	250/500/1000	Band 1 (250 m): .620 – .670 um Band 2 (250 m): .841 – .876 um Band 3 (500 m): .459 – .479 um Band 4 (500 m): .545 – .565 um
Landsat TM/ETM+ 4-7	2013 - 2022	30 (visible - Near-IR) 60 (Thermal-IR)	Band 1: .450 - .520 um Band 2: .520 - .600 um Band 3: .630 - .690 um Band 4: .760 - .900 um Band 6: 10.40 - 12.50 um (TM5 Thermal not used due to noise)
Landsat 8 OLI-1, TIRS	2003 - Present	30 (visible - Near-IR) 100 (Thermal-IR)	Band 2: .452 - .512 um Band 3: .533 - .590 um Band 4: .636 - .673 um Band 5: .851 - .879 um Band 10: 10.60 - 11.19 um Band 11: 11.50 - 12.51 um
Landsat 9 OLI-2, TIRS	2022 - Present	30 (visible - Near-IR) 100 (Thermal-IR)	Band 2: .452 - .512 um Band 3: .533 - .590 um Band 4: .636 - .673 um Band 5: .851 - .879 um Band 10: 10.60 - 11.19 um Band 11: 11.50 - 12.51 um
Sentinel 2A/2B	2017 - Present	10 (visible - Near-IR) 60 (Vegetation Red Edge) 60 (UV, SWIR)	Band 1: .443 um Band 2: .490 um Band 3: .560 um Band 4: .665 um Band 5: .705 um Band 6: .740 um Band 7: .783 um Band 8: .842 um Band 8A: .865 um
Sentinel 3A/3B	2018 - Present	300 (all utilized bands)	Band Oa2: .412.5 um Band Oa3: .442.5 um Band Oa4: .490 um Band Oa5: .510 um Band Oa6: .560 um Band Oa7: .620 um Band Oa8: .665 um Band Oa10: .68125 um Band Oa11: .07875 um Band Oa17: .865 um
VIIRS	2019 - Present	750 (all utilized bands)	Band M1: 0.402 - 0.422 um Band M2: 0.436 - 0.454 um Band M3: 0.478 - 0.488 um Band M4: 0.545 - 0.565 um Band M5: 0.662 - 0.682 um Band M6: 0.739 - 0.754 um Band M7: 0.846 - 0.885 um Band M8: 1.23 - 1.25 um Band M9: 1.371 - 1.386 um Band M10: 1.58 - 1.64 um Band M11: 2.23 - 2.28 um Band M12: 3.61 - 3.79 um Band M13: 3.97 - 4.13 um Band M14: 8.4 - 8.7 um Band M15: 10.26 - 11.26 um Band M16: 11.54 - 12.49 um
SPOT 6/7	2019 - Present	6	Band 1: .450 - .745 um Band 2: .450 - .525 um Band 3: .530 - .590 um Band 4: .625 - .695 um Band 5: .760 - .890 um
Sentinel 1A/1B SAR	2021 - Present	5 x 20	C-band operating at a center frequency of 5.405 GHz

additional image products from additional sensors for the City.

In 2012, OI added additional broad-scale products to the datasets available to the City and project partners. These include two types of ocean current products: High Frequency Radar-derived surface currents (HF Radar) and Hybrid Coordinate Ocean Model (HYCOM) model-derived surface currents (http://hycom.org). The raw data for the HF Radar currents are retrieved from National HF Radar Network via the Scripps Coastal Observing Research and Development Center (CORDC) on an hourly basis and reformatted into ESRI-compatible shapefiles. The hourly products are averages of the previous 25 hours and generated at 1 km and 6 km spatial resolutions. Additional HYCOM model-based products include daily ocean salinity, mixed layer depth, and subsurface temperature at 50, 100, 150 and 200 meters. In 2016 these products were delivered in a Web Map Service (WMS) Representational State Transfer (REST) service format compatible with the City's now retired BioMap server. They are presently being generated and archived in preparation for delivery via a next generation WMS dashboard planned for the future. The existing high resolution (6-30 m) observation region extends from approximately La Jolla southward to Rosarita Beach, Mexico and out approximately 50 miles. The coarser-scale products (250-1000 m) such as chlorophyll, SST, ocean currents and HYCOM-derived products encompass the entire SCB.

3.4 Recent Data Enhancements

Beginning in 2017, OI also began processing and posting imagery from the Sentinel-2A satellite. Sentinel-2A is a satellite operated by the European Space Agency (ESA) and is the spaceborne platform for the Multispectral Instrument (MSI). The Sentinel 2 MSI samples 13 spectral bands: four bands at 10 meters, six bands at 20 meters and three bands at 60-meter spatial resolution. The green band focusing in the 560 nm wavelength is ideal for detecting turbidity plumes from the outfalls both at the surface and at depths down to 40 feet depending on ocean conditions. A second satellite carrying the MSI sensor, the Sentinel-2B (identical to 2A), was launched into orbit by the ESA and provided the first set of data from the MSI sensor as of March 17, 2017. In 2018, data from Sentinel 2B became a regular addition to the satellite imagery products posted to the OI San Diego Water Quality (SDWQ) web portal. On average the Sentinel 2A and 2B imagery processed to highlight anomalous turbidity signals emanating from the PLOO, SBOO, the discharge from the Tijuana River, as well as the Pt. Loma kelp bed are posted to the OI web portal within 24-36 hours of satellite data acquisition. In some cases, if the data are available to OI earlier, the image products are delivered as quickly as 12 hours after acquisition. During the 2017 to 2021 time period, the Sentinel 2A and 2B satellites provided the most temporarily comprehensive set of high-resolution satellite imagery. In total, 526 high resolution satellite images showing the offshore San Diego County region were acquired, processed, and delivered during that time span. Between 2012 and 2016 196 high resolution satellite images were used for the monitoring. This equates to a 168% increase in the high-resolution satellite data used to document the project area of interest (AOI) between 2017-2021 when compared to the previous five years. Of the 526 total images, 333 were from Sentinel 2A or 2B making up ~63% of the high-resolution satellite data used for analysis. On average, the addition of Sentinel 2 data effectively increased the number of high-resolution satellite observations of the San Diego region to ~105 per year, compared to the prior average of ~39/yr. 2021 showed the highest number of high-resolution datasets to date (135) used for the project.

In October 2018, OI incorporated imagery from Sentinel-3A into the program. Shortly thereafter, in December of 2018 imagery from Sentinel-3B was added. Just like Sentinel 2, Sentinel-3A and Sentinel-3B are earth observation satellites developed by the

ESA for the Copernicus Program. Sentinel-3A was launched on February 16, 2016, and Sentinel-3B followed on April 25, 2018. The 3A and 3B satellites are identical and deliver products in near-real time. The satellites include 4 different remote sensing instruments. The Ocean and Land Colour Instrument (OLCI) covers 21 spectral bands (400–1020 nm) with a swath width of 1270 km and a spatial resolution of 300 m. The Sea and Land Surface Temperature Radiometer (SLSTR) covers 9 spectral bands (550–12000 nm), using a dual-view scan with swath widths of 1420 km (nadir) and 750 km (backwards), at a spatial resolution of 500 m for visible and near-infrared, and 1 km for TIR channels. The Sentinel 3 mission's main objectives are to measure sea surface topography along with the measurement of ocean/land surface temperature and ocean/land surface color. One of the satellites' secondary missions is to monitor sea-water quality and marine pollution. The instrument on these satellites designed for these purposes is the OLCI. Ocean Imaging creates daily products dependent on cloud cover for the entire San Diego/Tijuana region using the OLCI instrument. Between the 3A and 3B satellites this results in better than daily coverage with 3A and 3B data occasionally both being available on the same day. True color, near infrared, products are posted bi-monthly along with the similar resolution MODIS products. Other possible, future products derived from the Sentinel 3 sensors being considered as additions to the monitoring data set include chlorophyll, sea surface temperature, total suspended matter (TSM), as well as cyanobacteria monitoring. Sentinel 3 carries the only satellite sensor package with the necessary spectral bands, spatial resolution, and coverage for near real-time detection of cyanobacteria. The results of these products may also be compared to the field sampling data in order to assess accuracy. **Figure 2** shows a time series of the offshore San Diego region using Sentinel 3 data between 11/24/20 and 12/04/20. During this period, a plankton bloom developed west of Pt. Loma and Coronado and forms a cyclonic eddy off the coast. The plankton bloom then dissipates but forms again towards the middle of December. This unique time series highlights the usefulness of how daily Sentinel 3 data at 300-meter resolution can provide informative temporal documentation of the oceanographic and biological conditions in the region. An animated version of this figure better illustrating the dynamics of the changing conditions through 12/30/20 can be found on the Ocean Imaging-San Diego Water Quality website at: https://oceani.com/SDWQ/2020-S3-Time-Series.gif.

As stated above, the RapidEye satellite data were discontinued as of late 2019 and replaced by data from the SPOT 6 and SPOT 7 satellites in January of 2020. SPOT 6 and SPOT 7 are identical in design and function. They both image in spectral bands similar to the RapidEye satellites at a slightly better ground sampling distance of six meters for the multispectral data. The dynamic range of these sensors is 12-bits per pixel. OI uses the blue, green, red, and near-infrared bands from these sensors. We have found that the SPOT data have a high signal to noise ratio and therefore produce a high-quality product for detecting wastewater surface manifestations and delineating the river run-off plumes. Because of the ability of these sensors to image from off-nadir viewing angles it is also possible to obtain imagery close together in time. **Figure 3** shows a set of SPOT and Sentinel 2 images from 03/01/21, 03/04/21, 03/05/21 and 03/06/21 highlighting the ability to obtain high-resolution imagery from multiple satellites on successive days. Note the relatively small TJR discharge moving offshore to the west on the 03/01 which develops into a large, turbid plume, first continuing its push to the northwest towards Pt. Loma then dying down and dissipating within a 24-hour period. 25-hour averaged HF Radar ocean currents from these days derived within one to two hours of the satellite data acquisition are overlaid on the imagery corroborate the shift in current direction seen in the imagery.

In 2021, there were 21 occurrences when either Sentinel 2A or 2B data were acquired within minutes

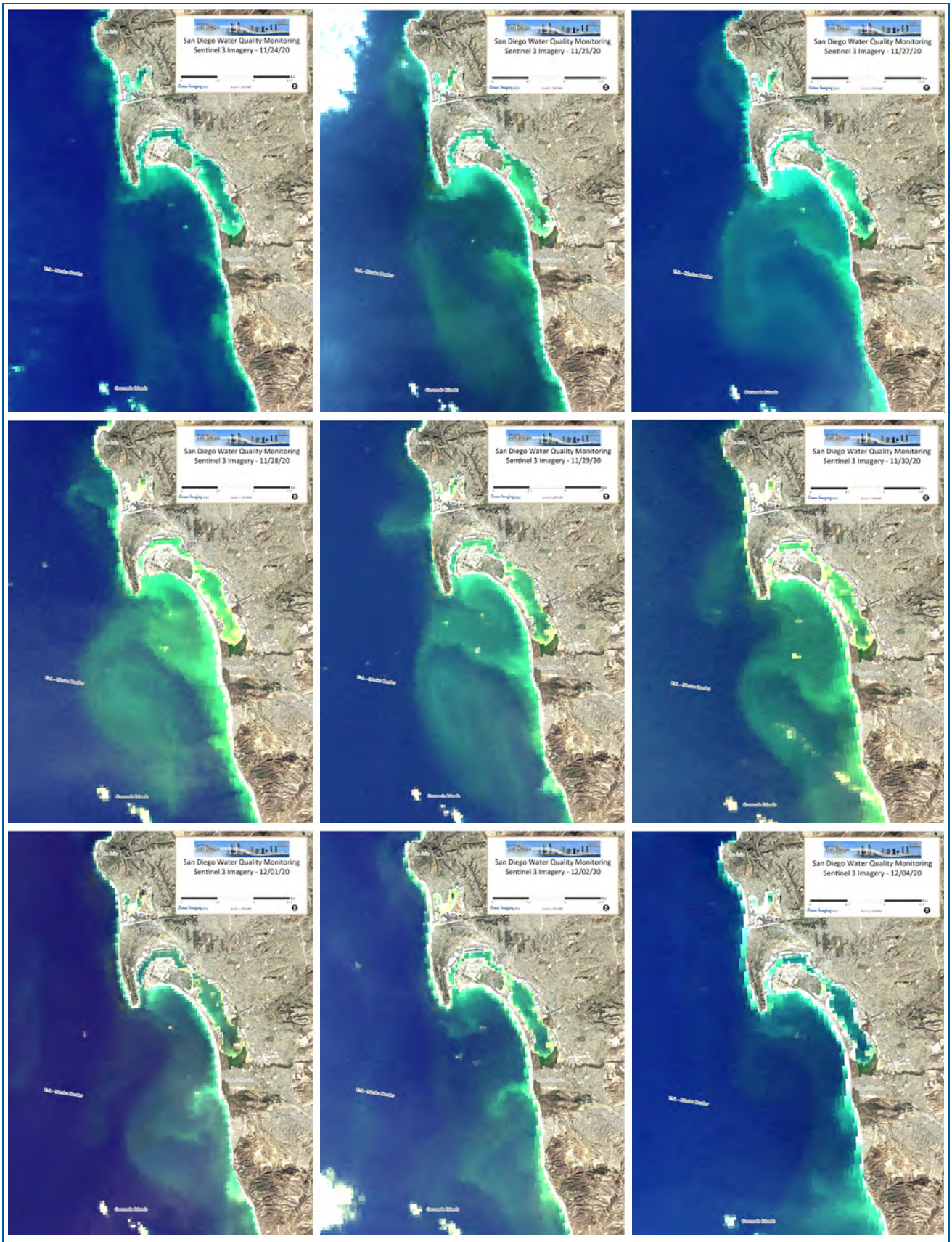

Figure 2. Sentinel 3 RGB Time series showing the development and dissipation of a phytoplankton bloom and large eddy west of San Diego. For a more complete time series presented as an animation visit: https://oceani.com/SDWQ/2020-S3-Time-Series.gif.

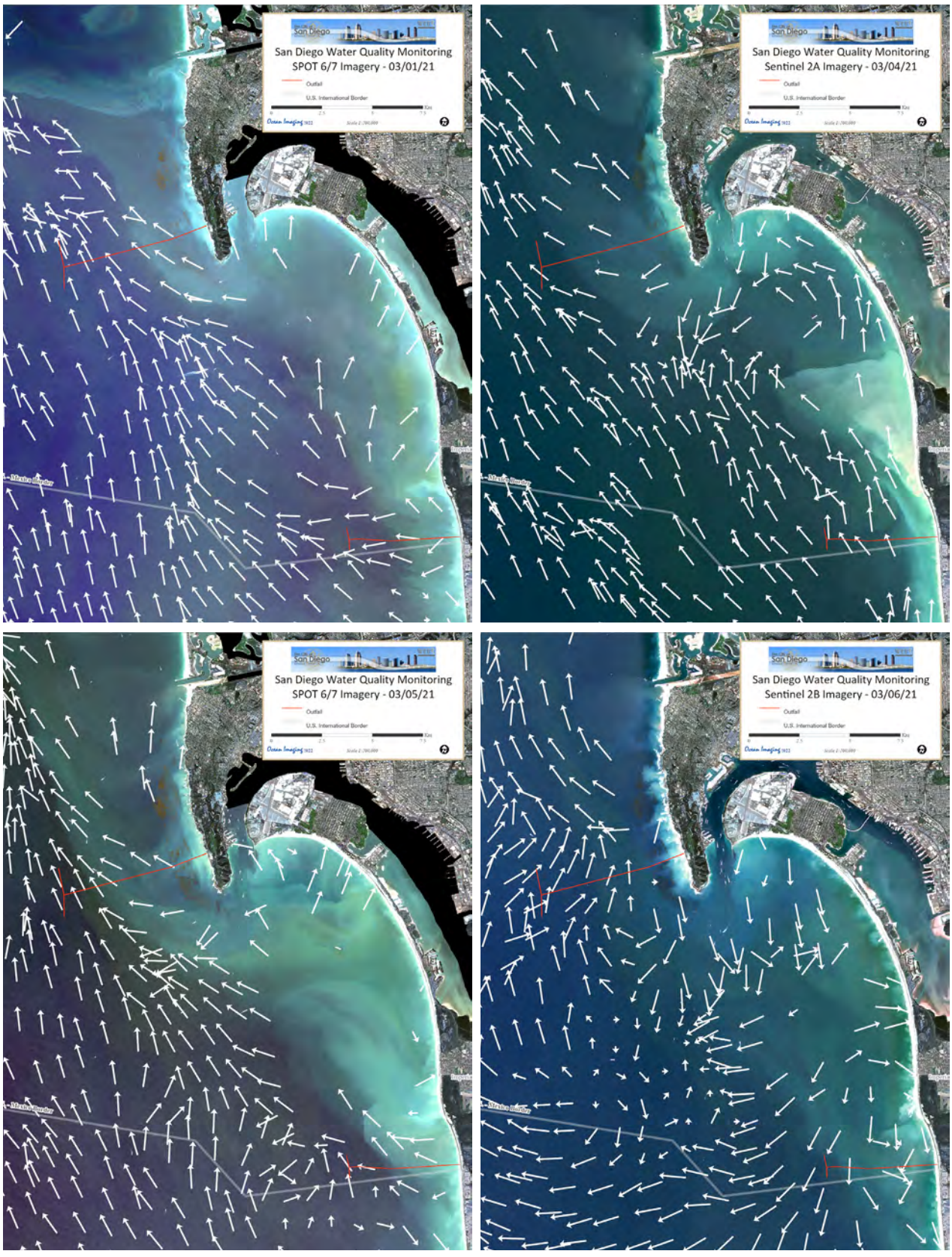

Figure 3. SPOT and Sentinel 2 imagery of the SBOO region between 03/01/21 and 03/06/21. Both satellite systems show the development and expansion of a large TJR discharge plume fist moving to the west, then northwest and finally dissipating over the 5-day period. 25-hour averaged HF Radar currents from the same day and time are overlaid on the image data.

to hours of either SPOT, Landsat TM7 or Landsat 8 OLI/TIRS data providing a near time-coincident validation of features (or lack thereof) observed in the imagery. There was one day on which all three satellite/sensors acquired data of the San Diego offshore region within hours of each other. **Figure 4** provides an example of the SBOO surface turbidity expression observed 28 minutes apart by SPOT 7 and the Landsat 8 satellite sensors on 01/04/21. The surface turbidity plume extending to the south from the SBOO is one of the largest/strongest observed that year. The Landsat thermal imagery reveals that the turbid water coming from the wye is cooler than the surrounding water. A relatively large turbidity plume emanating from the TJR and moving to the south is also readily apparent in the imagery.

3.5 Data dissemination and analysis

The satellite data are made available to the SDPUD and other project constituents through a dedicated, password-protected web site. Although it is possible to process most of the used data in near-real-time, earlier in the project it was decided that the emphasis of this project is not on providing real-time monitoring support and the extra costs associated with the rapid data turn-around are not warranted. Most satellite data is thus processed and posted within 1-2 days after acquisition. As noted above however, OI has in a number of cases made imagery available to the SDPUD in near-real time (within 12-24 hours) via email when observations appeared to be highly significant to the management of beach closures or other sudden/anomalous events.

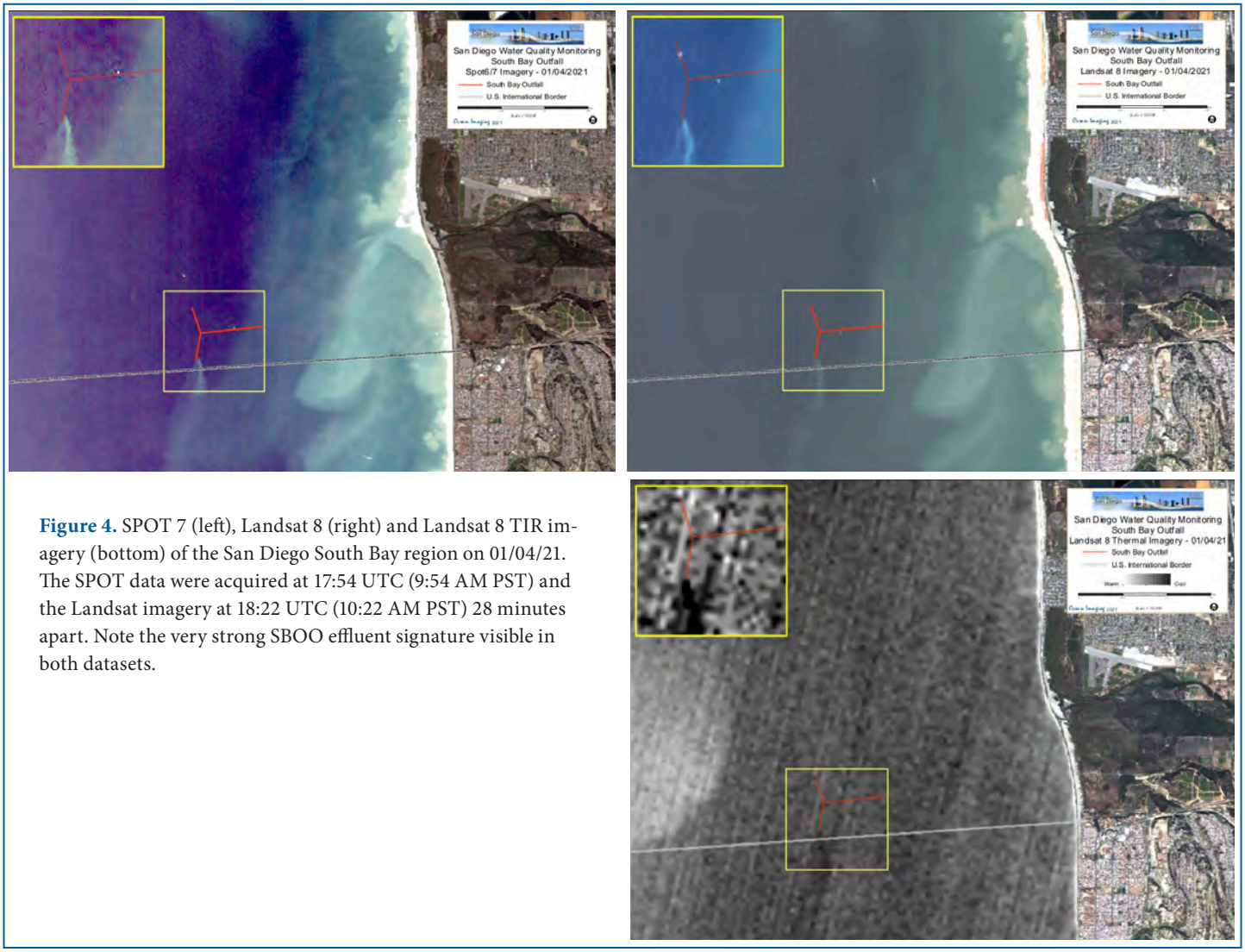

Figure 4. SPOT 7 (left), Landsat 8 (right) and Landsat 8 TIR imagery (bottom) of the San Diego South Bay region on 01/04/21. The SPOT data were acquired at 17:54 UTC (9:54 AM PST) and the Landsat imagery at 18:22 UTC (10:22 AM PST) 28 minutes apart. Note the very strong SBOO effluent signature visible in both datasets.

3.6 Field Sampling Data

A total of 19 shoreline stations, ranging from Mission Beach to northern Baja (across the US/Mexico border), are sampled weekly, by City of San Diego staff, to monitor the levels of three types of fecal indicator bacteria (i.e., total coliform, fecal coliform, and Enterococcus bacteria) in recreational waters (**Figure 5**). An additional 15 nearshore (kelp) stations are also sampled weekly to monitor Fecal Indicator Bacteria (FIB) and a range of water quality parameters (i.e., temperature, salinity, dissolved oxygen, pH, transmissivity, Chlorophyl-a, CDOM). Furthermore, 69 offshore stations are sampled quarterly to monitor both water quality conditions and one or more types of FIB. These stations are located from 9 to 55-m depth in the SBOO region, and 9 to 98-m depth in the PLOO region.

The City Marine Microbiology Laboratory (CMML) follows guidelines issued by the U.S. Environmental Protection Agency (USEPA) Water Quality Office, State Water Resources Control Board (SWRCB) including the 2019 Ocean Plan, the California Department of Public Health (CDPH),

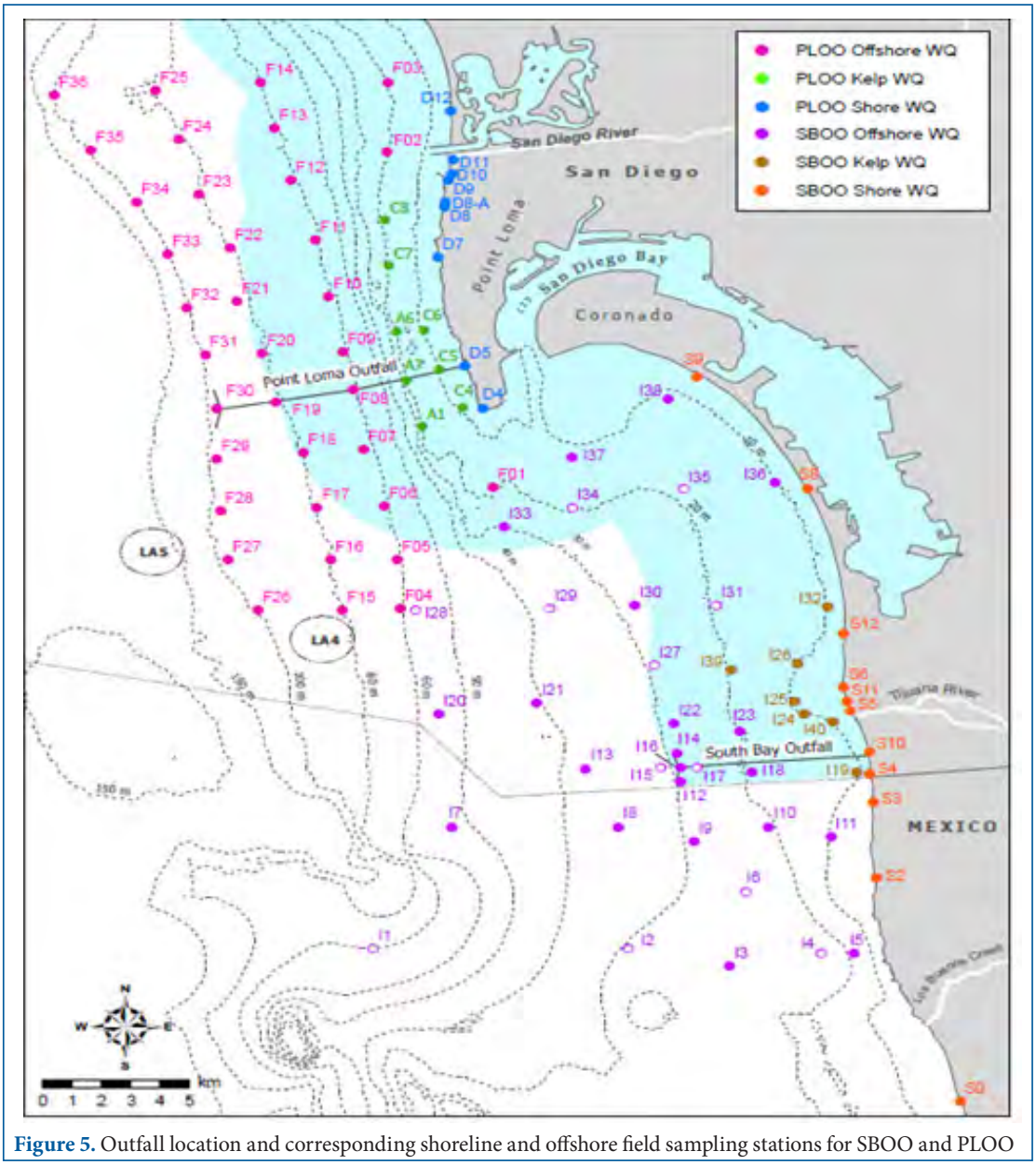

Figure 5. Outfall location and corresponding shoreline and offshore field sampling stations for SBOO and PLOO

and Environmental Laboratory Accreditation Program (ELAP) with respect to sampling and analytical procedures (Bordner et al. 1978, APHA 2012, CDPH 2000, USEPA 2009). All bacterial analyses were initiated within eight hours of sample collection and conformed to standard membrane filtration techniques, for which the laboratory is certified (ELAP Field of Testing 126). FIB densities were determined and validated in accordance with USEPA and APHA guidelines as follows. [APHA] American Public Health Association. (2012). Standard Methods for the Examination of Water and Wastewater, 22nd edition. American Public Health Association, American Water Works Association, and Water Environment Federation.

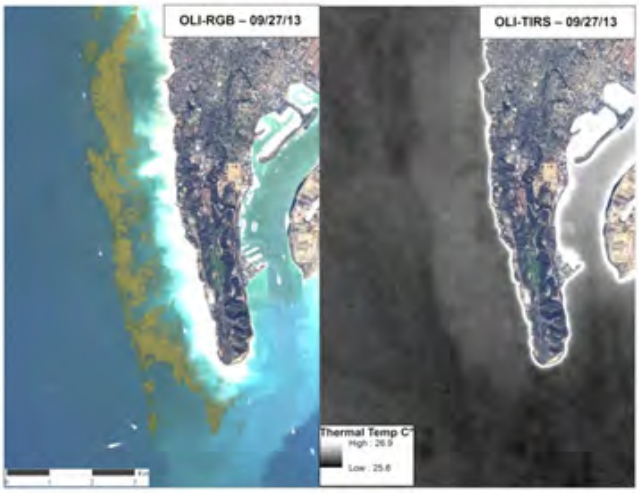

Figure 6. Satellite image of the Pt. Loma region showing the kelp bed (yellow) and corresponding thermal boundary patterns.

4. HISTORICAL RESULTS

4.1 The Point Loma Ocean Outfall

The PLOO represents a major contrast to the SBOO both in greater distance from shore (7.2 vs. 5.5 km) and primarily in depth of discharge (@95 vs. 27 m). Also, its daily discharge volume is nearly five times greater. During the 21 years of this project no satellite or aerial image was ever collected with a verifiable surface turbidity or thermal signature of the PLOO's effluent plume. Regular field sampling results also support the notion that the plume rarely, if ever, reaches the surface layer in concentrated or detectable form. This is likely due not only to the outfall's great depth but also to its location near the break in the mainland shelf. The shelf drops precipitously immediately offshore from the diffuser, and a significant portion of the discharged effluent is believed to be carried off into deep water by swift currents. Remote sensing work in the PLOO region has primarily concentrated on monitoring shoreline phenomena such as discharges from the San Diego River and Mission Bay to the north that affect water quality along Pt. Loma, and mesoscale phenomena such as plankton blooms and runoff events from the north and south that get swept over the PLOO location and thus affect offshore sampling results. High resolution imaging also provides a comprehensive means to monitor changes in the Pt. Loma kelp bed — one of the largest in California — which the PLOO bisects.

The PLOO transects three primary areas along its 7.2 km underwater length: 1) shallow waters with rocky and sandy bottom between the shoreline and the Pt. Loma kelp bed; 2) The kelp bed itself; 3) a bottom slope and deeper waters west of the kelp. Multispectral and thermal imagery acquired for this project shows that the offshore location of the PLOO wye often places it outside a relatively stable alongshore upper-column water mass boundary that is detectable in the imagery and tends to represent a current shear zone as well (as revealed in HF-Radar data). During the warmer months, surface waters between the shore and the kelp bed, and sometimes within the kelp bed itself tend to be warmer by a degree Celsius or more than the waters immediately west of the kelp bed. As is exemplified in **Figure 6**, a region 2-4 km wide with noticeably cooler SSTs often rounds the outside of the bed. We believe the cooler SST band represents upwelling associated with the drop-off in bottom topography outside the kelp bed. Since upwelled water could provide a mechanism to bring the submerged PLOO effluent to the surface and closer to shore, we have paid particular attention

in analyzing the thermal and turbidity/color patterns in that zone relative to time-coincident monthly and (more recently) quarterly field sampling done by the CMML. We have never identified a thermal or color anomaly similar to those from the SBOO, that was separate from larger scale patterns outside the region. Correspondingly, while some offshore sampling stations (e.g., F08/A17) occasionally show elevated bacteria counts at 60 m (rarely up to 25 m) and deeper, the elevated counts generally do not extend to shallower depths monitored by the remote imaging. (City of San Diego, 2020) An area of cool SSTs is also commonly seen in the region's thermal imagery just south of Pt. Loma, which we believe corresponds to locally driven upwelling modeled and field-validated by others (e.g., Roughan et al. 2005).

As is the case with much of the San Diego coastline, the most commonly occurring near-shore current regime along Pt. Loma is southward. Under such conditions, nearshore waters from San Diego's North County are swept southward, deflected offshore somewhat by the La Jolla peninsula, and thus often cover the area over the PLOO wye. During the rainy season those waters contain highly turbid runoff from North County's several lagoons, sweeping it over the offshore PLOO area along with (after heavy storms) turbid discharge from the San Diego River and Mission Bay (**Figure 7A**). Since the North County nearshore waters also tend to give rise to intense red tide (dinoflagellate) blooms during various times of year, the plankton-laden streams also tend to be advected over the PLOO wye area (**Figure 7B**). The area within and inside the Pt. Loma kelp bed tends to be more often affected by direct shore runoff, and discharges from the San Diego River and Mission Bay during the southward current regime. Unlike the TJR plume which contains heavy suspended sediment loads and very high indicator bacteria concentrations, the San Diego River and Mission Bay

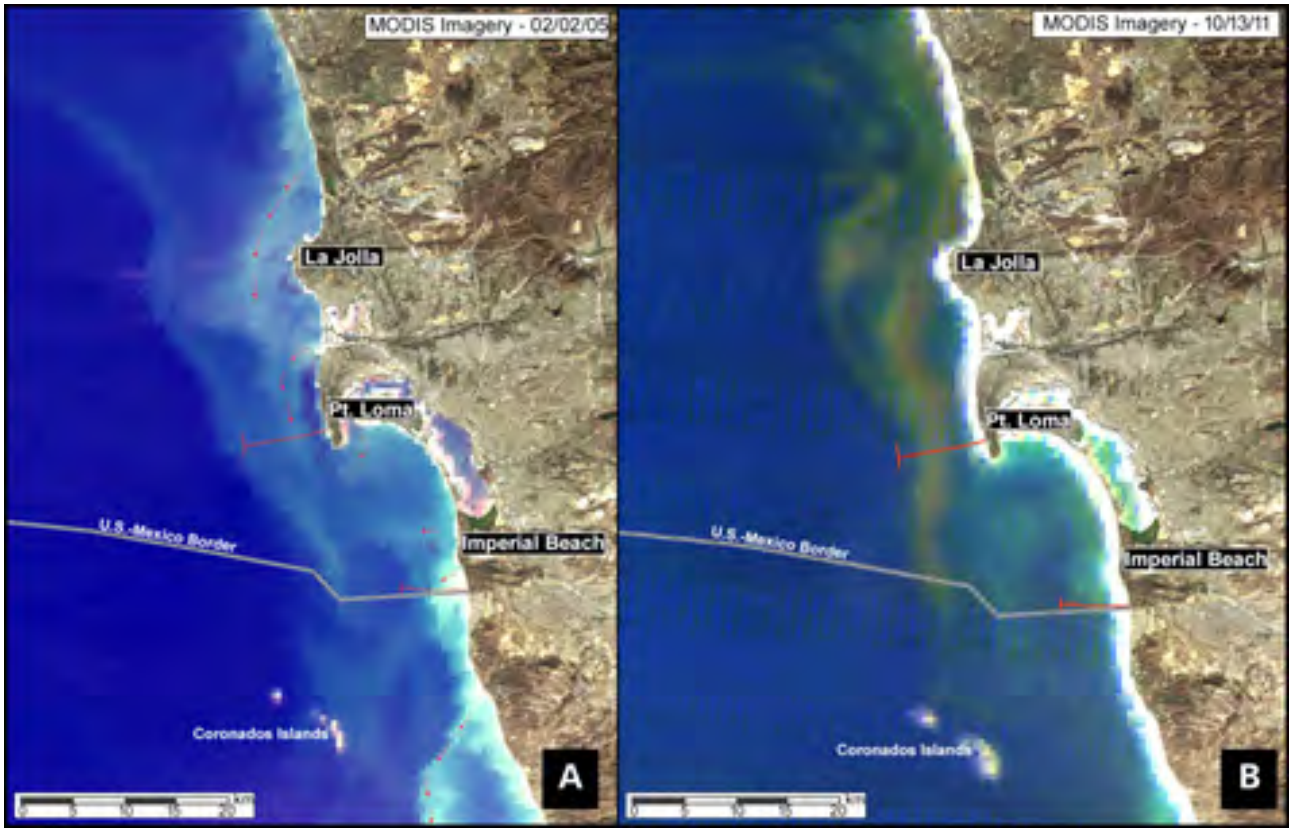

Figure 7. MODIS satellite imagery of the San Diego region showing (A) stormwater runoff from the north advecting over the PLOO region and (B) a north-originated dinoflagellate "red tide" bloom being advected over the region.

plumes tend to more commonly have only sub-exceedance bacteria levels. As was described above for the SBOO region, occasional northward flow regime episodes also affect the waters along Pt. Loma. Both tidal and storm runoff plumes from the San Diego River and Mission Bay are deflected northwestward under such conditions, and runoff outflow from San Diego Bay tends to round Pt. Loma and affect the southern section of the kelp bed, as well as the area between the kelp bed and the PLOO wye (**Figure 8**).

4.2 The South Bay Ocean Outfall

The wastewater plume emitted from the SBOO generally remains well below the surface between approximately late March and November due to vertical stratification of the water column. Seasonal breakdown of the vertical stratification results in the plume's rise closer to the surface or to actually reach the surface between approximately late November and late March, when it can sometimes be detected in near-surface field samples at sampling stations over the outfall wye. Prior to this project, regular field sampling at a preset station grid around the outfall (Figure 5 above) provided the only means to estimate its plume's trajectory and whether it had reached the surface. Since the SBOO wye is located relatively close to the TJR mouth, it was often difficult or impossible to positively separate plumes from the two sources with the field samples, especially during the rain seasons when the TJR plume was large and both plumes expanded in the ocean surface layer. This situation led to contentions by some that the SBOO effluent reaches the shoreline and is thus directly responsible for some beach contamination events. Remote sensing observations early in this project established that the two plumes are detectable in imagery with Landsat TM resolutions or better (≤30 m). The plumes are almost always spatially separated, allowing their identification and separation directly from their location. The rare exceptions occur immediately after extreme storm events when the TJR runoff plume can

Figure 8 – Sentinel 2 satellite imagery showing parts of the TJR plume being advected up and around the west side of Pt. Loma and up during a 12/30/2018 – 01/01/2019 northward current regime episode. The PLOO and SBOO are shown in red.

extend far offshore and overrun the SBOO wye region. Upon breaking the surface, the SBOO plume was also found to exhibit an identifiable thermal signature, distinctly cooler than the surrounding water (see Figures 4 above and 11 below).

Internally, the SBOO plume tends to exhibit a relatively homogenous spectral signature which decreases in intensity with distance from the wye, as the discharge progressively mixes into the surrounding ocean. Within the first few years of this project the characteristic SBOO plume extents and trajectories (when it reached the surface layer) were established through repeated imaging. The most common near-surface current pattern in the SBOO wye region is southward (Roughan et al. 2005). Under such circumstances, the plume tends to be directed from the wye toward the south-south-east (**Figure 9A**) or more directly southward (**Figure 9B**). The plume tends to have a sharply defined triangular shape, expanding with distance from the wye and decreasing in intensity for up to several kilometers, as its effluent dilutes through mixing into the surrounding water column. Except for station I9, the field sampling grid has no established stations in that area, and so the plume tends to remain mostly undetected in field data under southward current field conditions except for, occasionally, station I12 over the wye.

The SBOO outfall is also affected by periodic northward current episodes. These events usually last from less than 24 hours to 2-3 days. In such conditions, observations of the outfall plume show it to be most often advected northwestward (**Figure 10A**) and on rare occasions to the north or northeast, as is exemplified in **Figure 10B**. Acoustic doppler current profilers (ADCPs) near the SBOO indicate that the currents often alternate between a north northwest and southeast direction (City of San Diego 2020). During northward current episodes the high-resolution satellite observations have shown it to be detectable up to several kilometers from the outfall wye, often curving northwestward. We believe the reason for the westward motion component corresponds to the general offshore veering of the region's flow pattern as waters from the south become deflected by the shallower bottom topography of the TJR's alluvial fan (as seen in the protrusion of the bathymetric contour lines shown in Figure 5 above). More immediate mixing appears to occur along the plume's edges during northward flow, since they tend to be considerably less sharp than in the southward flowing patterns. During the northward flow conditions,

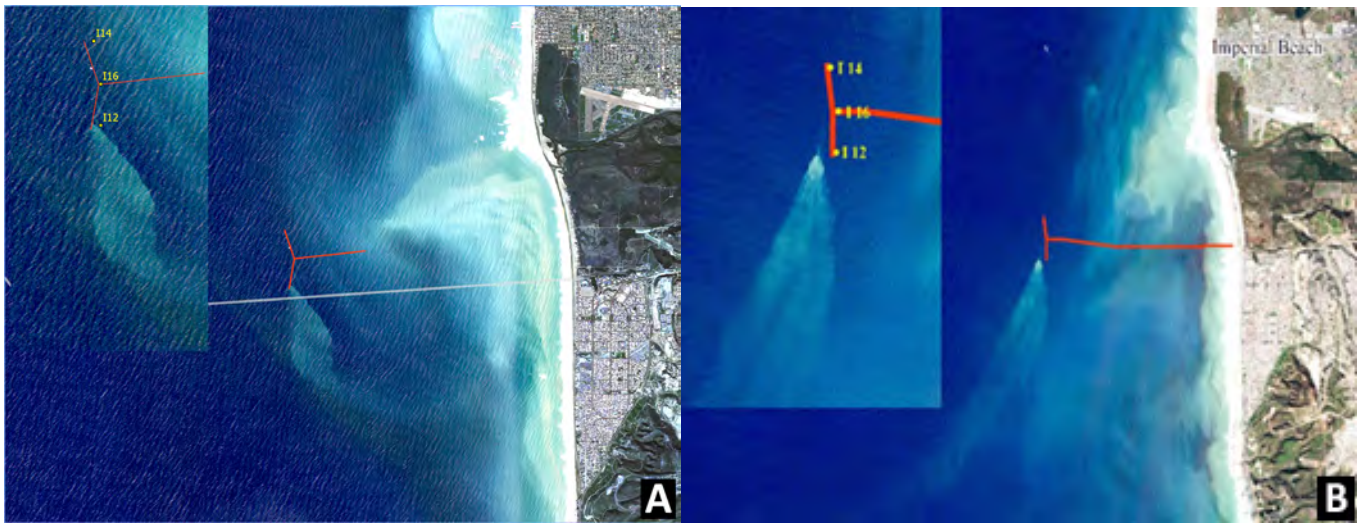

Figure 9. Typical SBOO plume dispersal patterns during southward current conditions on 02/03/2020 imaged with the Sentinel 2B (left), and on 01/04/2012 imaged with RapidEye satellite (right). Multi-depth field samples were taken at the three wye stations on the same day of the RapidEye image (01/04/2012) but showed no elevated bacteria values.

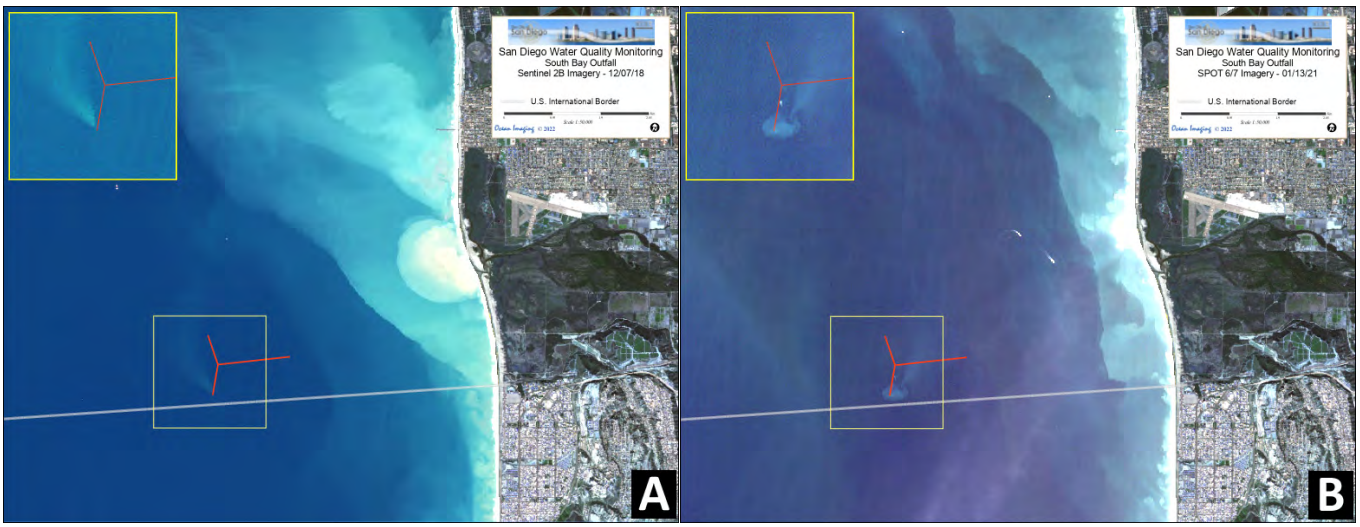

Figure 10. Unusual SBOO plume dispersal patterns during northward current conditions on 12/07/18 imaged with the Sentinel 2B (left), and a rare situation when the SBOO plume was pushed to the northeast on 01/13/2021 imaged with SPOT 6 (right).

evidence of the effluent's near-surface manifestation is also sometimes seen in time coincident field samples at stations I-12 and I-16 and/or I-14 to the north.

Under low to mild current conditions the higher resolution satellite and aerial images can sometimes discern separate plume components emanating from the different active diffuser groups along the SBOO wye. Examples are shown in **Figure 11**. The uneven intensity of some of them initially caused a concern to the outfall's designer – Parsons Corporation – when first such images were made available in 2003-2004. Parsons conducted an underwater video survey of the wye and found all risers operating normally. The effluent intensity pattern has remained the same since then throughout the project, providing rather novel information on the continuing functioning of the diffuser groups.

Since this project's inception, the collected imagery showed that under both current regimes (but especially the southward regime) the outfall plume tends to commonly have very sharp side boundaries. In relatively strong surface current conditions the apex of the plume is also often displaced 50 m or more from the actual wye location (indicating a diagonal vertical travel path due to the currents) but it tends to retain the sharp edge boundaries. This characteristic was found to have important ramifications on the interpretation of field samples collected around the outfall: Because the sampling site grid is fixed, near-time-coincident field sampling and aerial image data have shown cases where the plume clearly existed on the surface but, due to its particular orientation that day and its very sharp delineation at the wye, was entirely missed by the field sampling. On 1/4/2012, for example, the sharply defined plume was detectable in RapidEye satellite imagery for more than 4 km southward from its source (Figure 9B above). It did not breach any of the field sampling locations over the wye, however, where time-coincident samples showed no indicator bacteria between the surface and 27 m. An alternate situation is illustrated in **Figure 12** which shows an aerial image overlaid with the actual sampling vessel track during sampling at stations I12 and I16 over the outfall wye on 1/6/2004. The multi-depth samples were acquired while the vessel drifted (Global Positioning System ticks spaced closely together). The data show the vessel passed in and out of the "Wye Riser" plume while sampling at I16 and drifted out of the "S28-S85 Riser" plume at I12 during sampling. This resulted in an uneven vertical sampling profile, with plume indications at some depths but not others, potentially confusing interpretation without the imagery.

The SBOO area is also subject on occasion to practically no current flow. This is reflected in the imagery by the surfacing plume components being located directly over the wye, indicating direct vertical effluent rise. During such no-current conditions we have occasionally observed the outfall's effluent to create circular standing wave patterns around the wye. The plume then tends to spread in a more concentric pattern over the wye area – and thus also in the shoreward direction. The project's extensive image data base since 2003 shows it is only under such circumstances that portions of the surfacing SBOO plume reach any appreciable distance shoreward from the wye location. Generally, this extent is detectable with the multispectral and thermal sensors 1000 – 1500 meters eastward or northeastward.

Since this project's aerial and satellite image-based monitoring of the SBOO outfall began, we have observed the plume to disperse in the four patterns discussed above. We have also witnessed the plume's

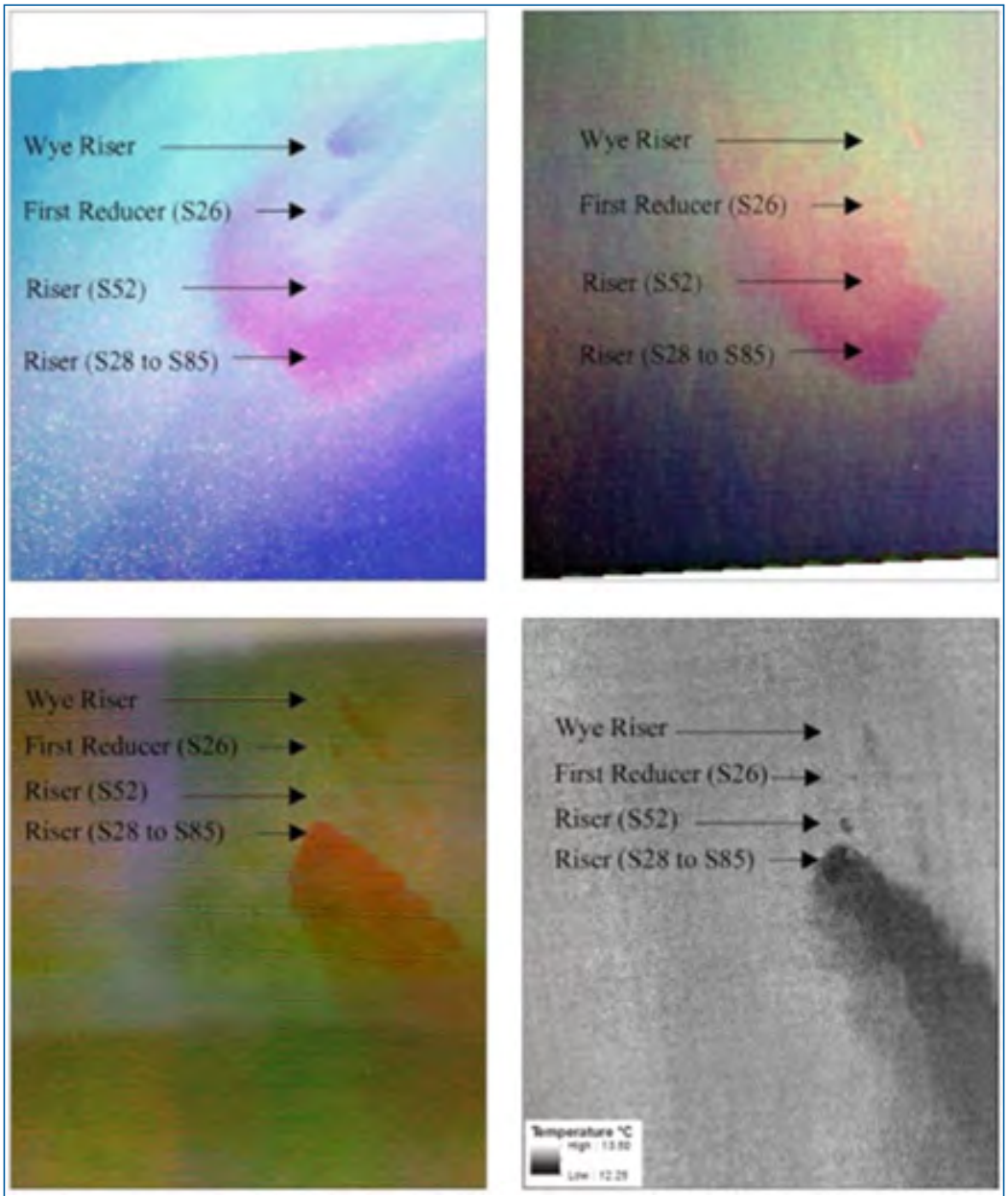

Figure 11. Examples of SBOO plume sub-components imaged during weak current conditions by the DMSC aerial sensor: (A) 2/6/2003, (B) 12/9/2003, (C) 12/14/2005, (D) 12/14/2005 (thermal).

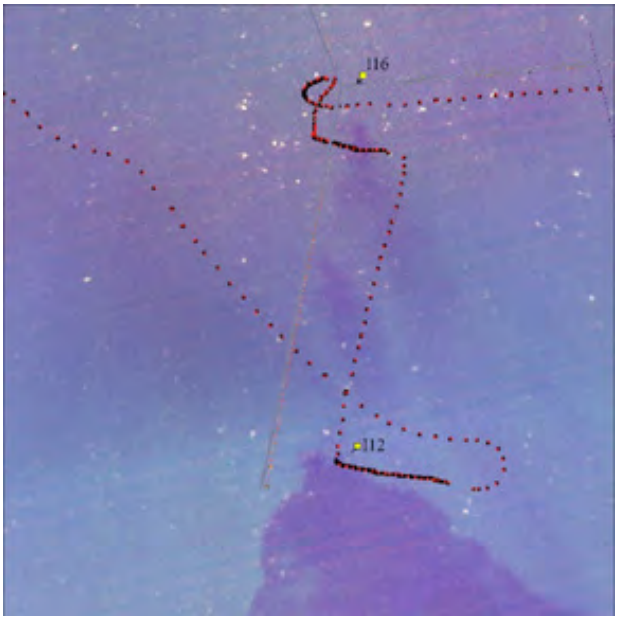

Figure 12. Time coincident DMSC imagery of the SBOO plume on 1/6/2004 and track of field sampling vessel during vertical sampling at stations I12 and I16. Each tick represents 10 seconds duration.

trajectory to be directly westward (offshore) on a few, rare occasions when offshore-directed Santa Ana winds caused a relatively anomalous strong offshore forcing of the surface waters. We have, however, never observed the SBOO plume trajectory to be directed east or shoreward past approximately 1500 m. It must be noted, however, that all of this project's SBOO plume trajectory observations reflect the plume's behavior during vertically unstratified conditions when it reaches the upper ocean layer. These observations cannot thus be extended to the summer months when the plume is undetectable with multispectral visible and thermal imaging. It must also be noted that detection of the surface or near-surface plume depends on sufficient thermal or turbidity contrast between the effluent and the surrounding waters. Hence it must be assumed that certain physical and biological components of the plume continue past the distance at which it becomes undetectable with OI's aerial and satellite imaging, albeit at an ever-increasingly diluted concentration.

Table 2 shows the number of high-resolution satellite images acquired and processed per year between 2012-2021 along with the number of instances when the SBOO effluent was observed in the remote sensing data at the ocean's surface. Over the past 10 years the number of high-resolution data sets acquired to monitor the region has increased by 400%. As noted above, there are often days when the SBOO plume is visible by more than one satellite. To account for duplicate datasets showing the SBOO plume on the same day, the number of days the SBOO region was imaged along with the number of SBOO observation days are listed in the table. The percent of SBOO observations per number of image days is shown, adjusting for the increasing number of satellite datasets used over the years. Rarely has the SBOO plume been observed at the surface prior to November or after April. This is most likely due to the seasonal water column stratification timing discussed above. It also coincides with California's rainy season. Therefore, the table also lists the observation data by the November to April, rain/vertical mixing season (lack of water column stratification). 2013 (and the 2012-2013 season) and 2016 (and the 2015-2016 season) stand out as the years during which the fewest and most SBOO surface plumes were seen in in the imagery respectively. All other years/seasons show the percentage of observations within one standard deviation of the mean.

Figure 13 shows monthly averages of Influent (INF) and effluent (EFF) volume and TSS for the SBIWTP since 2003. While the effluent volumes and intake TSS concentrations did not change appreciably through time (aside from a spike in the EFF Flow during 2020), there were two notable reductions and one spike in the exiting effluent's TSS concentrations. The first occurred through 2006-2007 when the TSS loads were reduced from approximately 90 mg/L to approximately 60 mg/L, and the second reduction was in November 2010 when the SBIWTP switched to full secondary treatment. Starting in 2012 the exiting TSS loads have been consistently below 20 mg/L. In the latter part of 2020 into the early months of 2021 there was an appreciable increase in the EFF

flow rate as well as extreme spikes in EFF TSS concentrations with the monthly EFF flow average peaking during the month of September and the average monthly EFF TSS levels peaking in November of 2020. Daily TSS numbers reached as high as 512 mg/L on 01/31/2021 (**Figure 14**). These dramatic increases have been attributed to excessive flows (>25 MGD) into the SBIWTP from the Mexican wastewater system that were not attributed to rains (Morgan Rogers, personal communication).

The plume's reflectance signature in the multispectral visible and near-IR imagery is dominated by reflectance spectrum characteristics of its suspended sediment. Hence a reduction in the sediment concentration should be expected to affect the detectability of the plume. However, analysis of the size and intensity of the plume patterns as well as the number of SBOO plume observations in the satellite data relative to the TSS reductions as seen between 2017 and 2021 does not show a direct correlation. In fact, some of the largest plume signatures have been imaged after the 2010 secondary treatment switch, such as 01/19/2019 when the EFF TSS amounts were recorded at 12.0 mg/L and on 04/11/20 when the EFF TSS level was only 7.4 mg/L. The median EFF TSS load between 2017 and 2021 was 10.4 mg/L. The median on days when the SBOO surface plume as observed in the remote sensing data was 11.6 mg/L. These plumes were identifiable more than 4.1 km and 5.6 km away from SBOO wye respectively (**Figure 15**). Other plume signatures imaged during 2013 through 2021 when TSS loads were approximately 16 mg/L or less show that such TSS amounts are sufficient for adequate distinction of the effluent from surrounding waters if the plume remains concentrated.

Table 2. SBOO Surface Observations in the High-Resolution Satellite Imagery

Year	Number of High-Res Images Processed and Reviewed	Number of Days Imaged	Number of SBOO Surface Observations	Number of Days SBOO Observed on Surface	Percent of SBOO Observations per Days Imaged
2012	26	25	6	6	24.0%
2013	32	31	1	1	3.2%
2014	50	46	10	9	19.6%
2015	46	44	12	12	27.3%
2016	42	42	13	13	31.0%
2017	60	54	10	8	14.8%
2018	82	75	19	15	20.0%
2019	122	109	19	17	15.6%
2020	133	111	34	27	24.3%
2021	134	112	19	16	14.3%
Season					
2012-2013	21	19	1	1	5.3%
2013-2014	33	31	6	5	16.1%
2014-2015	31	29	11	10	34.5%
2015-2016	35	34	16	16	47.1%
2016-2017	36	34	6	6	17.6%
2017-2018	56	49	17	13	26.5%
2018-2019	64	56	20	16	28.6%
2019-2020	76	68	22	20	29.4%
2020-2021	105	85	36	27	31.8%

Season = November through April. 2012-2021 mean observation ratio = 19.4% annually and 26.3% seasonally. 2012-2021 observation ratio standard deviation = 7.9% annually and 12.1% seasonally.

However, during those years, numerous instances also occurred when, on a given day, the plume was detectable with both the multispectral visible and thermal sensors but became detectable only with thermal imaging a day or two later. The existence of a thermal plume signature proves the effluent reached the ocean surface, but its simultaneous lack of a color signature implies it reached the surface in a significantly diluted state. Additionally, there are alternate situations during which a relatively clear (low TSS) plume is detected via remote sensing because the effluent breaks through surrounding turbid water caused by either an offshore extension of the TJR discharge or heavy plankton blooms over the SBOO wye. Therefore, our data thus suggest that on days with significant subsurface currents and/or vertical mixing the effluent is sufficiently dilute as it travels up through the water column and/or the EFF TSS levels are lower than ~12.0 mg/L, the effluent can still be detectable by the sensors utilized in this project. Also, analysis of the size and intensity of the plume patterns relative to the

Figure 13. Influent (INF) and effluent (EFF) volume and total suspended solids (TSS) concentrations for wastewater processed through the SBIWTP and released into the ocean through the SBOO.

TSS reductions does not show a direct correlation. Furthermore, no significant correlation was found, between color-based detection of the SBOO plume and high frequency radar-derived surface currents or nearby shore station wind measurements. Similarly, no correlation was found between plume detection and imaging time within the tidal cycle.

4.3 The Tijuana River and San Antonio de los Buenos Creek

Since its inception in 2003, this project has provided an extensive image data set of the TJR runoff plume under various oceanic and atmospheric conditions. This data set was utilized by Svejkovsky et al. (2010), to study the TJR plume's extents and resulting effects on shoreline contamination. Unlike the

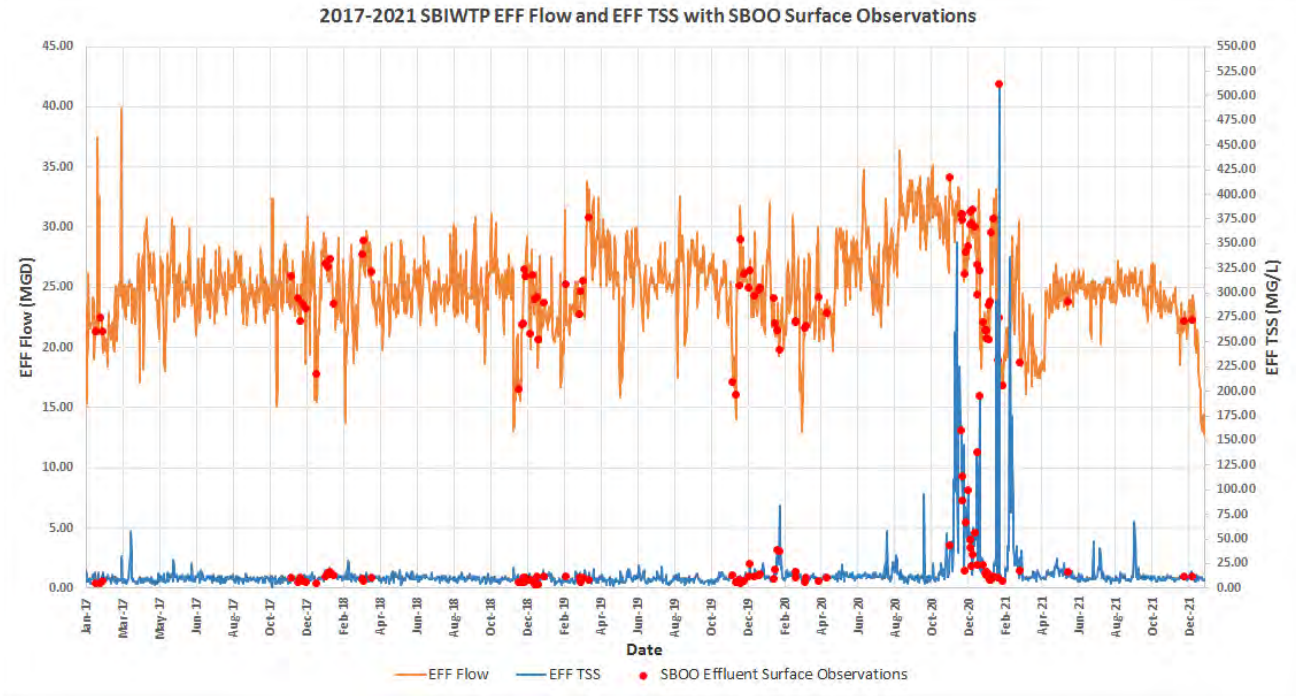

Figure 14. Daily EFF Flow volume EFF TSS concentrations for wastewater processed through the SBIWTP and released into the ocean through the SBOO from 2017 through 2021.

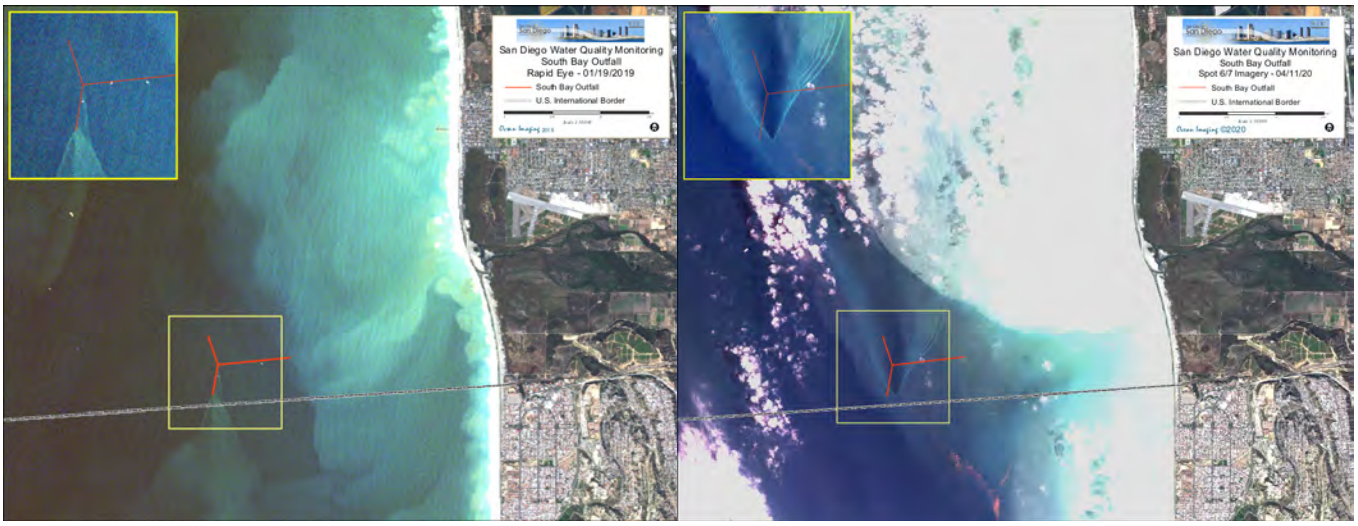

Figure 15. Examples of large SBOO effluent plumes at the oceans' surface observed in a RapidEye image acquired on 01/19/19 and a SPOT image from 04/11/20 when the measured EFF TSS levels were relatively low (12.0 mg/L and 7.4 mg/L respectively).

SBOO plumes spectrally homogenous reflectance signature, the investigators found the TJR plume to consist of 3 spectrally distinct components which they believe are related to different discharge ages within the plume. The Svejkovsky et al. (2010) study found that wave direction was the prime variable affecting the along-shore distribution of the TJR plume's core components (**Figure 16**).

Following heavy rains, the satellite and aerial imagery has shown the TJR plume to extend up to tens of kilometers offshore. When this occurs during a northward current regime, portions of the TJR's highly contaminated plume are advected northward and can reach Pt. Loma, potentially affecting water quality within the PLOO's field sampling grid more than 16 km to the Northwest. This was first noticed in October 2004 when satellite imagery acquired during a prolonged northward current episode and following intense rain events showed the TJR plume to reach the southern end of Pt. Loma. The image data indicated a possible explanation for anomalously high indicator bacteria concentrations in field samples taken in the area during the same time. This event is not common but has occurred several times in the 18 years since it was first observed. More recent examples are shown in Figures 3 and 8 above.

This project's monitoring of the San Antonio de los Buenos Creek discharge plume in Mexico revealed that the plume rarely reaches the U.S. border in concentrations sufficient for detection in the imagery. Its usual trajectory is southward. We have observed it to spread a considerable distance, as far south as past Rosarito Beach, Mexico. During northward flow events, its northward trajectory due to currents and south swell tends to be diminished by the coastal geography (the shore angles northwestward immediately north of the Creek mouth) and its usual size vs. the distance needed to reach the U.S. border in detectable concentrations. US-collected shoreline sampling has shown relatively regular elevated bacteria concentrations at stations south of and on the US/Mexico border, but these could have been caused by other localized point and non-point sources. OI has not collected any imagery directly linking such measurements to a detectable San Antonio de los Buenos plume crossing the border in the surf or immediate coastal zone, although the lack of such imagery does not preclude that possibility. Imagery showing the plume crossing the border shows most of it to travel in a northwestward (i.e., offshore) trajectory, and mixing with the TJR discharge once across the border.

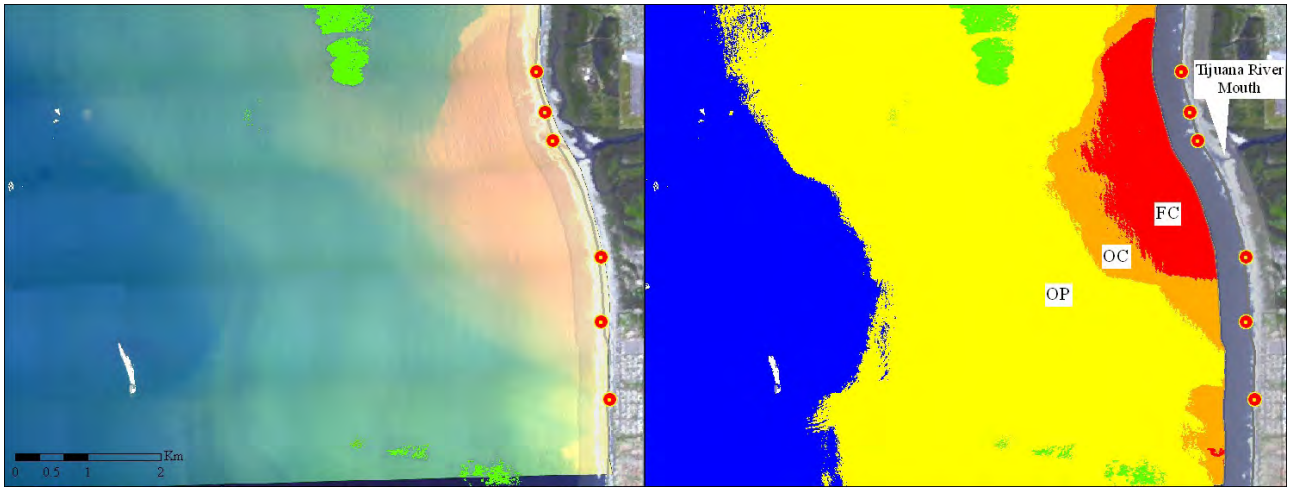

Figure 16. Example of the Tijuana River stormwater runoff plume as it appears in DMSC aerial multispectral color data (left) and after classification for various plume components with distinguishing spectral reflectance characteristics: "Fresh Core" (FC), "Old Core" (OC), and "Old Plume" (OP). Kelp is shown in green, and the locations of shoreline bacteriological sampling stations are also shown.

5. NOTABLE CONDITIONS AND EVENTS 2017 – 2021

5.1 Overall Atmospheric and Oceanographic Trends

San Diego's nearshore water quality gets affected by a combination of factors during the dry and wet seasons. In the absence of rain from late spring to fall, stormwater runoff is nonexistent, San Diego River (SDR) discharge is minimal (and generally uncontaminated), and discharges from North County's lagoons, Mission Bay and the TJR are primarily the result of tidal flushing. In the absence of rare events such as sewage spills or channel dredging of closed lagoon mouths, events affecting the nearshore waters are primarily of oceanic origin such as phytoplankton blooms and harmful algal blooms (HABs) - red tides included. Diatoms (primarily *Pseudo-nitzschia* spp) and dinoflagellates are largely responsible for the local HABs and red tides when they occur (Southern California Coastal Water Research Project, 2019). During the rainy season the most prominent factors are stormwater runoff from point and non-point sources along the shore, and sediment resuspension caused by strong winds and large waves in the surf zone. As is discussed below, our observations show that the sizes and extents (and hence also beach contamination potential) of the stormwater plumes is not simply related to the total amount of rainfall, but also to the intensity (i.e., amount within a time interval) with which it fell.

In the last five years (2017-2021) San Diego was subject to only moderately variable oceanographic conditions when compared to the past 10 years (2012-2021) in its entirety, but there were significant year-to-year differences in atmospheric and precipitation conditions. This includes a few extremes in high (2019) and low (2018) rainfall both annually and seasonally, heavy phytoplankton and red tide blooms, weak to moderate El Niño and La Niña conditions as well as a summer marine heat wave in 2019 commonly referred to as "The Blob 2.0" (Amaya, Dillon J., et al., 2020). Many of these episodes led to events and processes observed in the satellite and aerial imagery acquired for this project. The following is a summary of notable events through the latest 5-year period. Although the scope of this report is 2017-2021, we use conditions over the past 10 years as a "baseline" for comparison.

5.1.1 Ocean Temperature Conditions

Aside from the reoccurrence of a marine heat wave, termed the Blob 2.0, centered off central California and Oregon during the summer of 2019, the northeast Pacific and in particular the Southern California Bight region did not experience dramatic fluctuations in ocean temperature outside of climatic norms. The direct effect, if any, of the Blob 2.0 on regional conditions is not yet known (Amaya, Dillon J., et al., 2020). Figure 17 shows the average monthly temperatures recorded at the Scripps Institution of Oceanography pier between 2012 and 2021 along with the years experiencing either El Niño or La Niña conditions according to the Oceanic Niño Index (ONI). Note the average Scripps pier temperature for 2017-2021 differed by only 0.1 °C from the 2012-2021 average. The only El Niño period between 2017-2021 was during the late summer of 2018 through the late spring of 2019 and it was only considered a weak event. The fall to spring months of 2017 to 2019 and much of the latter part of 2020 through 2021 experienced weak to moderate La Niña conditions. The 2018-2019 El Niño event can be seen in a summer peak in the 2018 Scripps pier temperatures as can the 2020-2021 La Niña episode. These warmer and cooler periods are also apparent in the 2019 and 2021 NOAA sea surface temperature anomaly analyses (**Figure 18**). **Figure 19** shows a VIIRS-generated SST image from one of the warmest SST days in 2018 (left) and a MODIS SST image from the same day in 2021 (right). The satellite image data help illustrate the ~4.6°C difference between the warmest year on average (2018) and the coolest (2021) during the five-year period of this report – especially in the San Diego region.

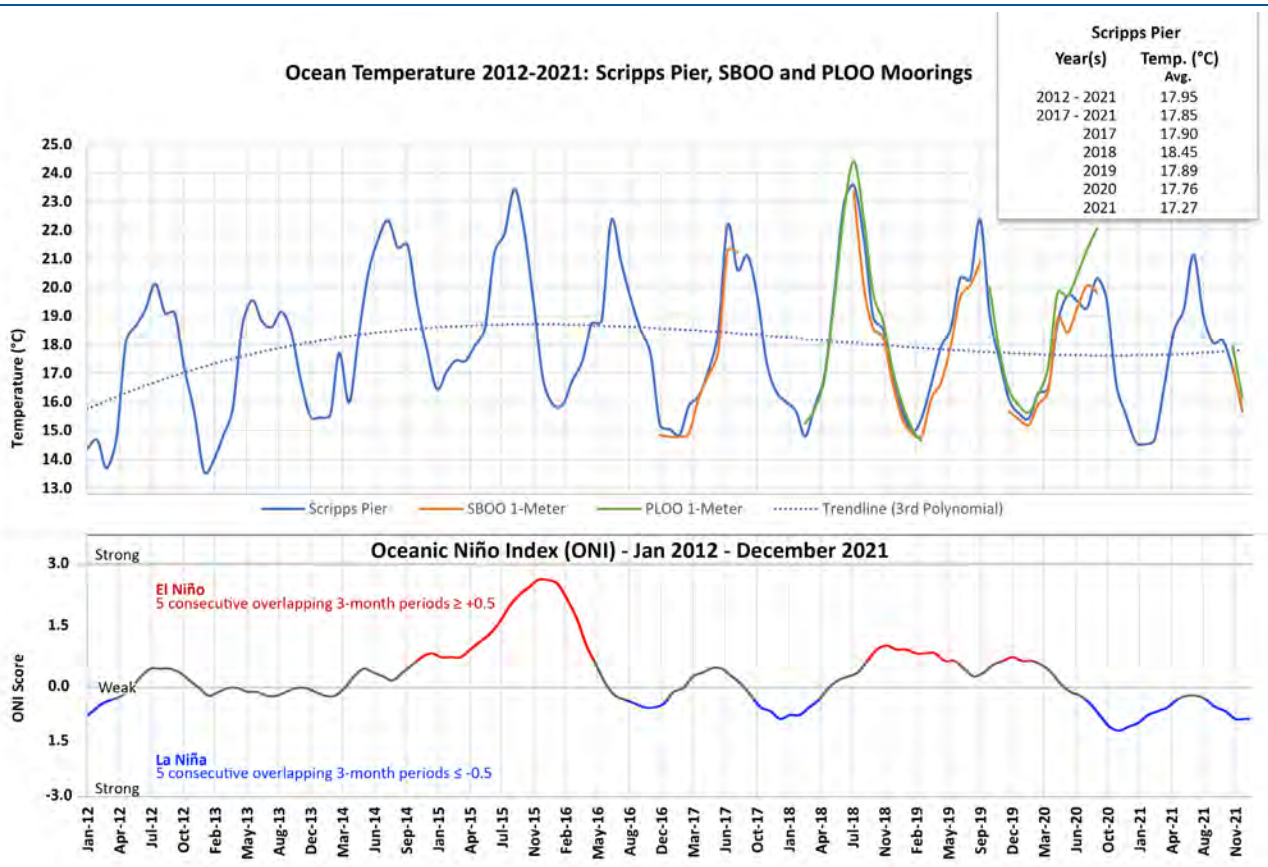

Figure 17. Average monthly ocean temperature from 2012 through 2021 as recorded at the Scripps Pier automated shore station, the PLOO real-time oceanographic mooring station (RTOMS) (1 meter depth) and the SBOO RTOMS (1 meter depth). Below the temperature data is a plot of the El Niño Southern Oscillation (ENSO) cycle for the same time period as represented by the Oceanic Niño Index (ONI). PLOO and SBOO data being in 2016 and are incomplete due to periods when the RTOMS were either inoperable or out of the water. Additional information on the City's RTOMS can be found in the City of San Diego 2018-2019 biannual report (City of San Diego, 2020).

5.1.2 Ocean Chlorophyll and Plankton Levels

Ocean chlorophyll levels generally followed seasonal norms over the past five years with levels indicative of phytoplankton blooms peaking in the spring to early summer months. A few exceptions in the San Diego region were a brief, but somewhat unusual, large phytoplankton bloom in September of 2018, frequent plankton blooms through September in 2019 and the extreme phytoplankton and red tide events which occurred during the months of April and May of 2020. **Figure 20** shows the chlorophyll levels measured at a depth of one meter at the SBOO and PLOO RTOMS from 2017 to 2021. Data gaps exist due to sensor issues or the moorings being out of the water (Stephanie Jaeger, personal communication). When the RTOMS data were available, however, the satellite data correspond well to the SBOO and PLOO measurements. **Figure 21** provides examples when the satellite data corresponded with the RTOMS data while providing a more synoptic view of the conditions recorded at the single stations. Additional details on the regional water clarity and quality for each year are provided in subsequent sections.

5.1.3 Regional Precipitation

As noted above the 5-year period between 2017-2021 experienced significant interannual rainfall totals both in terms of the amount of precipitation over a season or year as well as the intensity and duration of rainfall events. Table 3 shows the 2017-2021 monthly cumulative precipitation as recorded at the San Diego International Airport (SDIA) and

TJR Estuary stations (NOAA National Climactic Data Center). The average precipitation recorded at the SDIA over the past five years (8.34 in./yr.) was much the same as the past 10 years (8.13 in./yr.). The average at the TJR Estuary station between 2017-2021 (9.19 in./yr.) was 26% higher than the past 10 years (7.61 in./yr.). 2018 and 2019 were the outliers with 2018 having the lowest annual total of 4.99

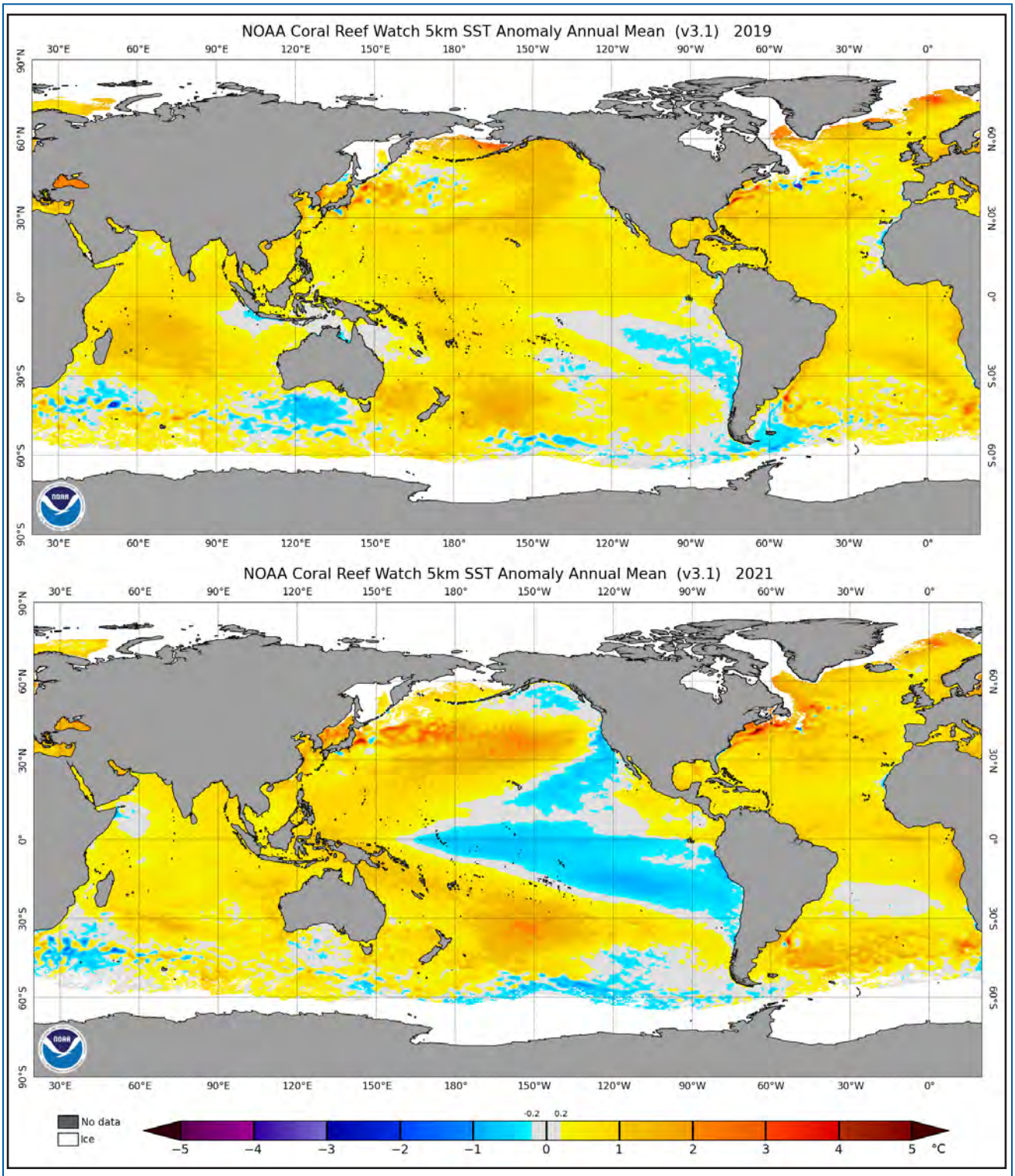

Figure 18. NOAA annual mean sea surface temperature anomaly analyses for the years 2019 (weak El Niño) and 2021 (weak La Niña).

inches recorded at SDIA and 2019 having the highest total rainfall of 15.52 inches. When approached seasonally with the period between November and April considered as the rainy season in California (although a recent study by Luković et al., 2021 suggests that the season should now be considered to start in December), the 2017-2018 season proved to be the lowest over the past 10 years (2.81 inches at SDIA) and the 2019-2020 season the highest (13.44 inches at SDIA) compared to the 10-year seasonal average of 6.89 inches. The data from the TJR Estuary were similar with the 2019-2020 rainy

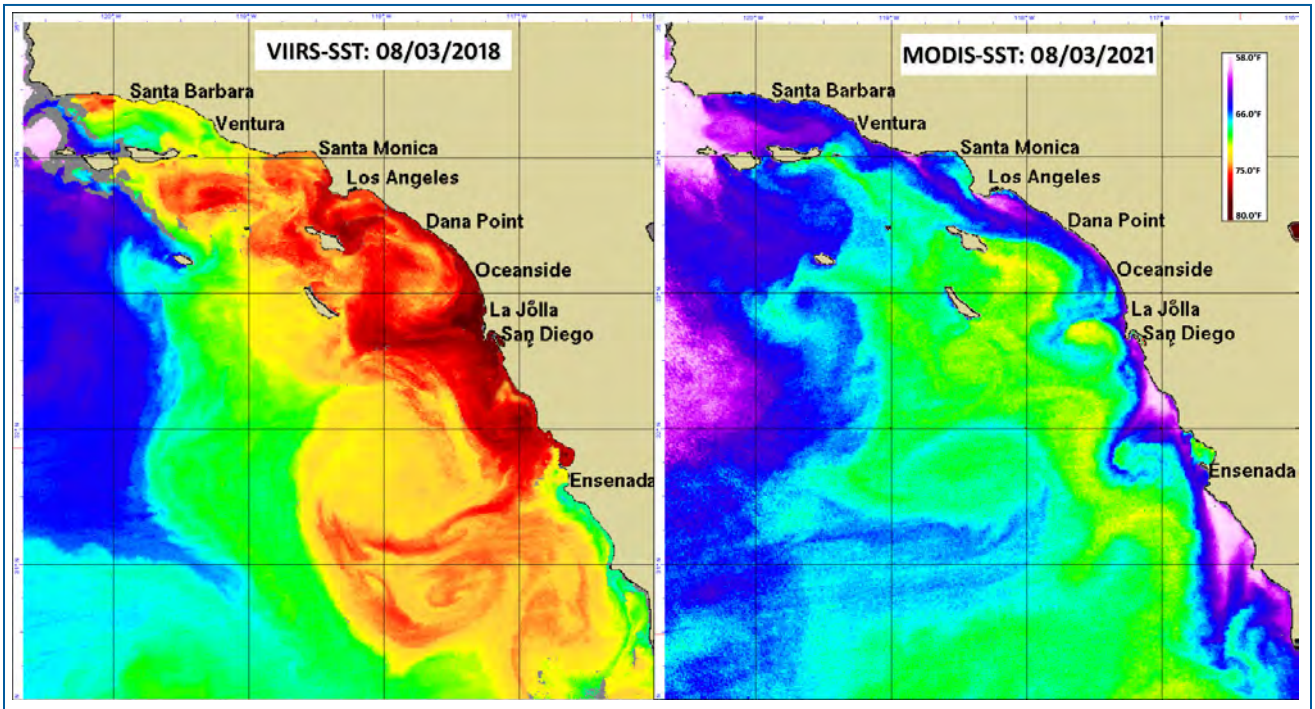

Figure 19. VIIRS SST image from 08/03/2018, one of the warmest SST days in 2018 (left) and a MODIS SST image from the same date in 2021 (right).

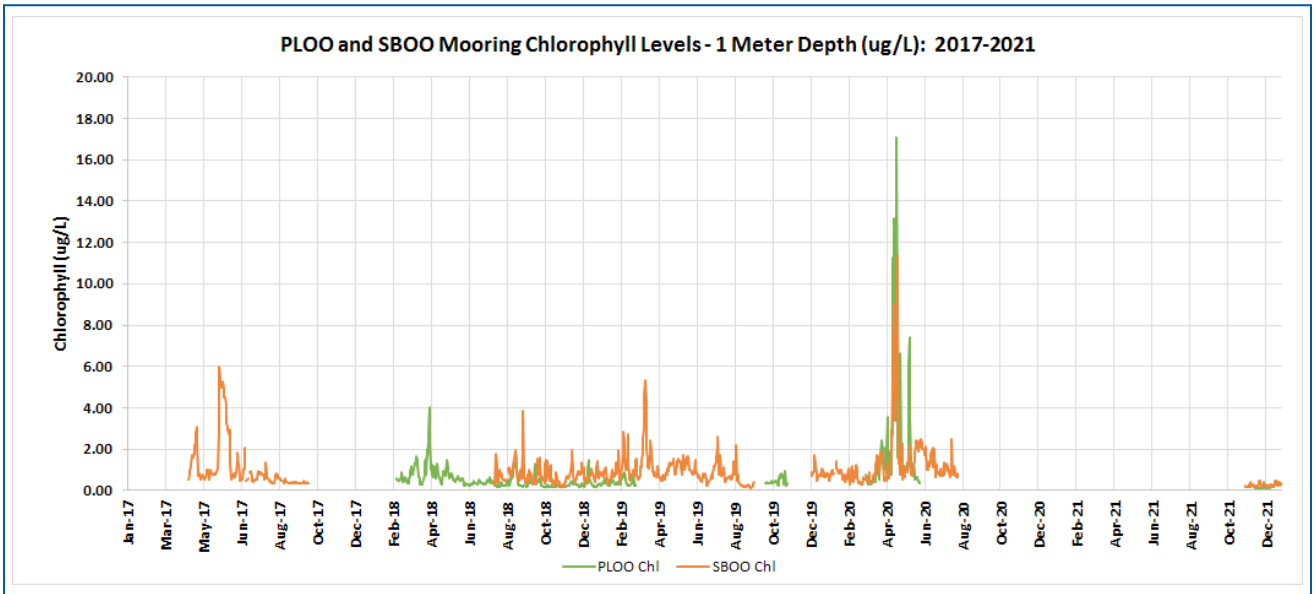

Figure 20. Average daily chlorophyll levels measured at the PLOO and SBOO moorings at the one-meter depth level between 2017 and 2021. Records flagged as "bad" or "suspect" were removed from the dataset. Gaps in the data record were either due to the moorings being out of the water or inoperable sensors. Note the spike the chlorophyll levels during the unusually strong red tide events in the spring of 2020.

season experiencing the most rain (16.04 inches), the 2017-2018 season the second lowest amount (2.71 inches), and the 2012-2013 season showing the lowest precipitation with a total of 1.63 inches. As discussed above rainfall has not been shown to have a direct effect on the surfacing of the SBOO effluent plume, however it does correlate well with the number of high volume TJR discharge events as well as the relative size of the plume entering the ocean as observed in the satellite data. All but one of the high-resolution satellite images acquired and processed for this project between 2017-2021 showed a significant TJR plume within 0-2 days of a rain event totaling 0.1 inches or more. A significant plume being defined as a clearly visible "Fresh Core" or "Old Core" plume (Svejkovsky, 2010) extending from the shoreline. There were many instances, however, when a relatively large TJR plume was visible in the image data during a period of no precipitation. These situations were likely the result of excess cross-boundary flow into the TJR Estuary caused by pump station failures, collection system overflows and/or debris obstructing the inlets (San Diego Regional Water Quality Control Board, 2020). These events and subsequent observations are discussed in more detail in the following sections.

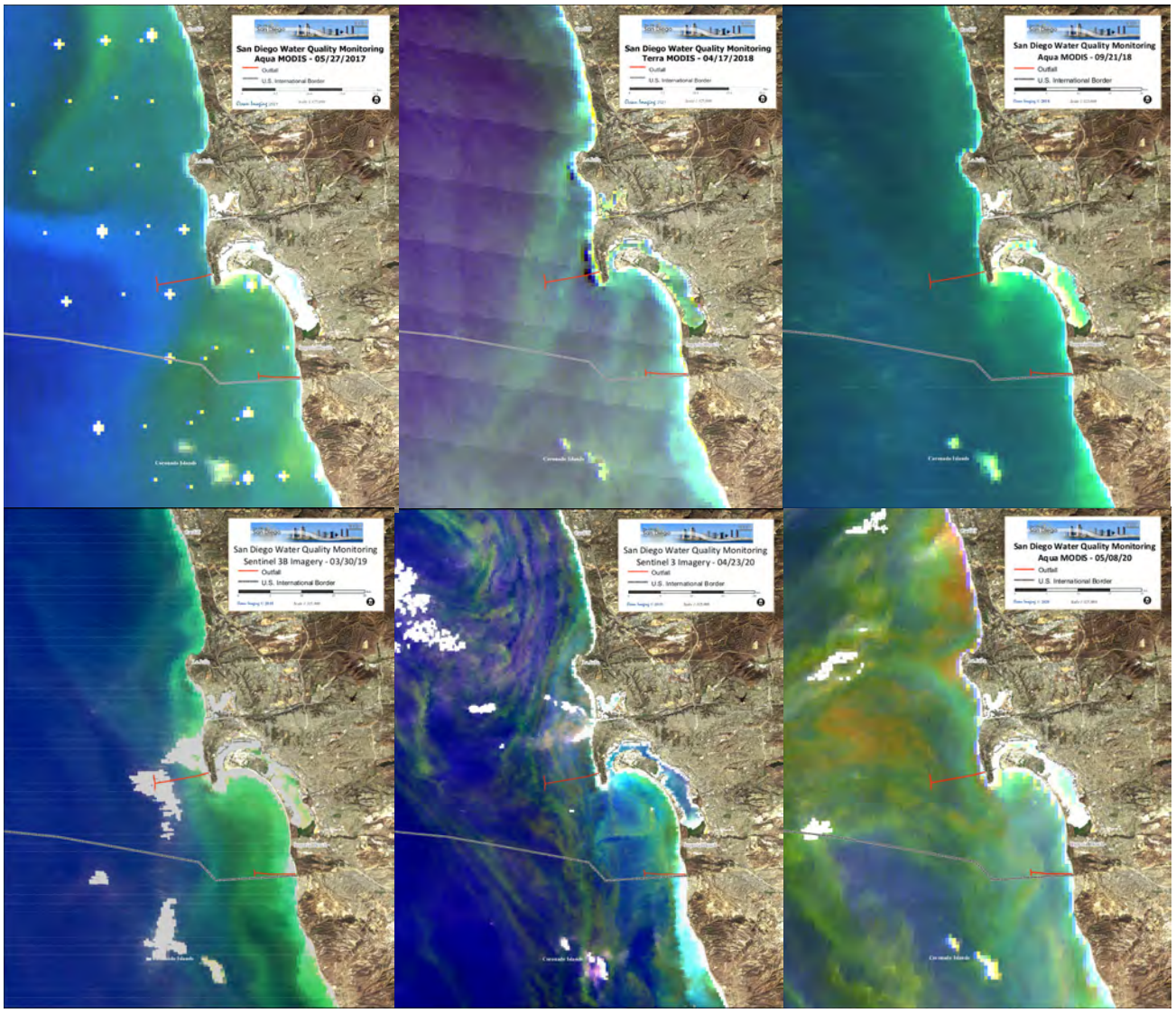

Figure 21. Representative Sentinel 3 and MODIS images showing plankton blooms during peaks seen in the chlorophyll measurements shown in Figure 20.

5.2 Conditions in 2017

The conditions in 2017 off the San Diego coast could perhaps be considered the most "average" when compared to the past ten years in the sense that the oceanic conditions were close to normal, and both annual and seasonal precipitation numbers did not deviate widely from the 10-year means. As seen in **Table 3**, 2017 had the lowest percentage of SBOO surface plume observations per imaged day compared to the 2017-2021 period. From a seasonal perspective the 2016-2017 season showed the fewest number of SBOO detections since 2013-2014. The few satellite detections of the SBOO surfacing were in January and then no plumes were seen in the data until December when vertical

Table 3. Sand Diego and Tijuana Estuary precipitation totals 2012-2021

San Diego International Airport Cumulative Monthly Precipitation in Inches

	2012	2013	2014	2015	2016	2017	2018	2019	2020	2021
January	0.40	0.70	0.01	0.42	3.21	2.99	1.77	2.42	0.48	1.80
February	1.19	0.63	1.00	0.28	0.05	1.58	0.35	4.04	0.38	0.10
March	0.97	1.22	1.28	0.93	0.76	0.08	0.65	1.23	2.15	1.48
April	0.88	0.01	0.54	0.02	0.55	0.01	0.02	0.10	3.68	0.07
May	0.02	0.26	--	2.39	0.44	0.87	0.09	0.86	0.02	0.07
June	--	--	--	0.04	--	0.02	--	0.01	0.14	0.01
July	--	0.05	--	1.71	--	--	--	--	--	--
August	--	--	0.08	0.01	--	--	0.02	--	--	0.23
September	--	--	--	1.24	0.32	0.06	--	0.11	--	0.50
October	0.70	0.25	--	0.43	0.07	--	0.57	--	0.12	1.01
November	0.28	1.48	0.37	1.54	0.61	0.02	0.69	2.72	0.14	--
December	2.19	0.46	4.50	0.88	4.22	--	0.83	4.03	0.60	2.58
Annual Total	**6.63**	**5.06**	**7.78**	**9.89**	**10.23**	**5.63**	**4.99**	**15.52**	**7.71**	**7.85**

Tijuana Estuary Cumulative Monthly Precipitation in Inches

	2012	2013	2014	2015	2016	2017	2018	2019	2020	2021
January	0.70	0.05	0.08	0.32	2.40	3.61	0.82	1.80	0.61	2.21
February	0.86	--	1.35	0.13	0.02	4.06	0.47	3.62	0.51	0.06
March	1.21	1.43	0.55	1.01	1.28	0.04	1.17	1.33	2.59	1.12
April	0.82	0.11	0.35	0.07	1.91	0.01	0.10	0.33	5.52	0.04
May	--	0.36	--	1.13	0.97	1.07	0.08	0.50	0.02	0.01
June	--	--	0.12	--	--	--	--	0.02	0.21	0.06
July	--	0.01	0.33	0.39	--	0.01	0.01	--	--	0.00
August	--	--	0.04	--	--	0.02	--	--	--	0.02
September	0.02	0.01	--	0.48	0.49	0.03	--	--	--	0.00
October	0.50	0.41	--	0.21	--	--	0.13	--	0.04	0.91
November	--	0.25	0.29	0.61	0.34	0.06	0.82	2.99	0.08	0.02
December	0.04	0.50	3.09	0.61	4.32	0.09	3.16	3.82	0.60	1.18
Annual Total	**4.15**	**3.13**	**6.20**	**4.94**	**11.73**	**8.99**	**6.76**	**14.41**	**10.18**	**5.63**

water column stratification likely weakened again. Offshore plankton blooms started earlier than usual. High levels of chlorophyll throughout the entire Southern California Bight developed as early as January and lasted through the end of March. As can be seen in the MODIS image archive locally high concentrations persisted into mid-July with intense blooms developing off the northern San Diego coast and TJR area and spinning off into plankton-rich eddies to the west. The vast January to March blooms can partially be attributed to heavy, region-wide rainfall events beginning in January introducing nutrients from coastal runoff into the ocean system. Nearshore blooms occurring after March were primarily fueled by coastal upwelling.

Station	Depth (M)	Entero	Fecal	Total
D11	NA	3400e	1000e	>=8600

Station	Depth (M)	Entero	Fecal	Total
I19	2	580	440	4000
	6	540	300e	3800e
	11	800	440	5600
I24	2	820	3400e	>16000
	6	480	220e	1400e
	11	50	200e	2000e
I25	2	260e	220e	1200e
	6	220e	220e	1300
	9	400e	76	800
I26	2	60	48	400e
	6	220e	50	700
	9	240e	60	960
I32	2	40	14e	200e
	6	110	36e	580
	9	220e	66	540
I39	2	1600e	1200e	>16000
	12	80	26e	160e
	18	160e	6e	320e
I40	2	4400	4400	>16000
	6	760	320e	2000e
	9	2200e	1300e	7800

Figure 22A. 2017 high resolution satellite image examples from the Landsat 8 sensors with the near-surface bacterial sampling data overlaid from the same day or within two days of image acquisition. Continued in Figure 22B.

Even though the 2017 total annual rainfall (7.87 inches - averaged between the SDIA and TJR Estuary stations) was very close to the 10-year mean (8.13 inches), a few strong, multi-day storms in January and February brought over 3.6 and 4.0 inches of rain to the TJ Estuary. This resulted in heavy TJR discharge and subsequent high bacteria counts at the SBOO stations. **Figures 22A & B** show examples of satellite data with the near-surface bacterial sampling data overlaid from the same day or within two days of image acquisition. The TJR plume can be seen extending for several kilometers offshore driven by the heavy and persistent rains. Aside from a few days in May, these rainy periods

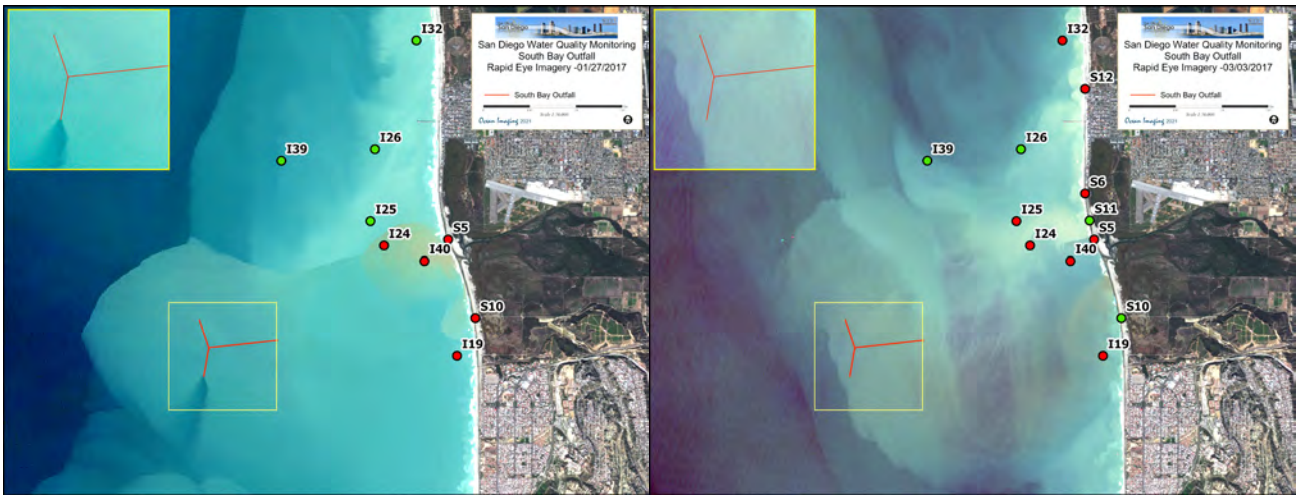

Station	Depth (M)	Entero	Fecal	Total
I19	2	10e	<2	34e
	6	6e	<2	14e
	11	160e	8e	180e
I24	2	140e	400	1100
	6	280e	700	3000e
	11	120	52	100e
I40	2	140e	180e	1800e
	6	700	660	5400
	9	180e	80e	300e
S5	NA	>12000	>12000	>16000
S10	2	3000e	NS	NS

Station	Depth (M)	Entero	Fecal	Total
I19	2	80e	150e	1900e
	6	150e	64	800
	11	540	120e	1900e
I24	2	40e	120	780
	6	840	150e	1800e
	11	140e	320e	2600e
I25	2	150e	52	620
	6	680	60e	2000e
	9	140e	180e	1600e
I32	2	12e	<2	4e
	6	110	44	840
	9	520	140e	1100
I40	2	82	92	360e
	6	68	38e	440
	9	260e	140e	1400
S5	NA	420	NS	NS
S6	NA	920	NS	NS
S12	NA	460	NS	NS

Figure 22B. 2017 high resolution satellite image examples from the RapidEye sensors with the near-surface bacterial sampling data overlaid from the same day or within two days of image acquisition. These images were acquired following multi-day storms bringing heavy rainfall resulting in heavy TJR runoff. Stations showing FIB measurements exceeding the single sample maximum as defined by the California Ocean Plan are shown as red dots (Total coliform density will not exceed 10,000 per 100 mL; or Fecal coliform density will not exceed 400 per 100 mL; or Total coliform density will not exceed 1,000 per 100 mL when the ratio of fecal/total coliform exceeds 0.1; or enterococcus density will not exceed 104 per 100 mL). Green dots identify stations at which the FIB levels were in compliance. The tables below each image show the measurement values by depth for each station with elevated bacteria levels.

were the only significant precipitation events for the year. This is evidenced by the mostly turbidity-free image data from April through the end of November and infrequent observations of significant TJR discharge. All other conditions exhibiting a lack of water clarity were related to the summer plankton blooms discussed previously. The 21 shoreline closures in San Diego County during 2017 was the second lowest in the 2017-2021 period. This is also likely related to the dry post-March conditions.

5.3 Conditions in 2018

2018 was a transitionary year in regard to the El Niño Southern Oscillation (ENSO) index. A mild La Niña phase was in place from September of 2017 through May of 2018. This shifted to an El Niño which lasted from August of 2018 to July of 2019. Typically, Southern California will experience less precipitation during a La Niña and more during an El Niño phase (NOAA Climate Prediction Center, 2012). Two predominant effects of the the La Niña and El Niño conditions were an overall decrease in precipitation and an increase in summer to fall ocean temperatures when compared to the past 10 years. While January of 2018 brought a decent amount of rainfall to the San Diego region, the county experienced very little additional precipitation until late November-early December, but even the totals for those months were below average. The SDIA gauge recorded the lowest annual rainfall in 2018 compared to 2012-2021 and while the TJR Estuary totals were above the 10-year average, it was only because of significant rain recorded at that station during the month of December. These conditions were likely related to the switching of the ENSO pattern during the summer. The average annual ocean temperature recorded at the Scripps Pier was 0.5°C warmer in 2018 than that of the past ten years. The average water temperatures during the month of August recorded at the Scripps Pier, the PLOO RTOMS (1 meter depth) and the SBOO RTOMS (1 meter depth) were near 24°C which were the highest temperatures recorded between 2012 and 2021. The warm ocean temperatures are well documented in

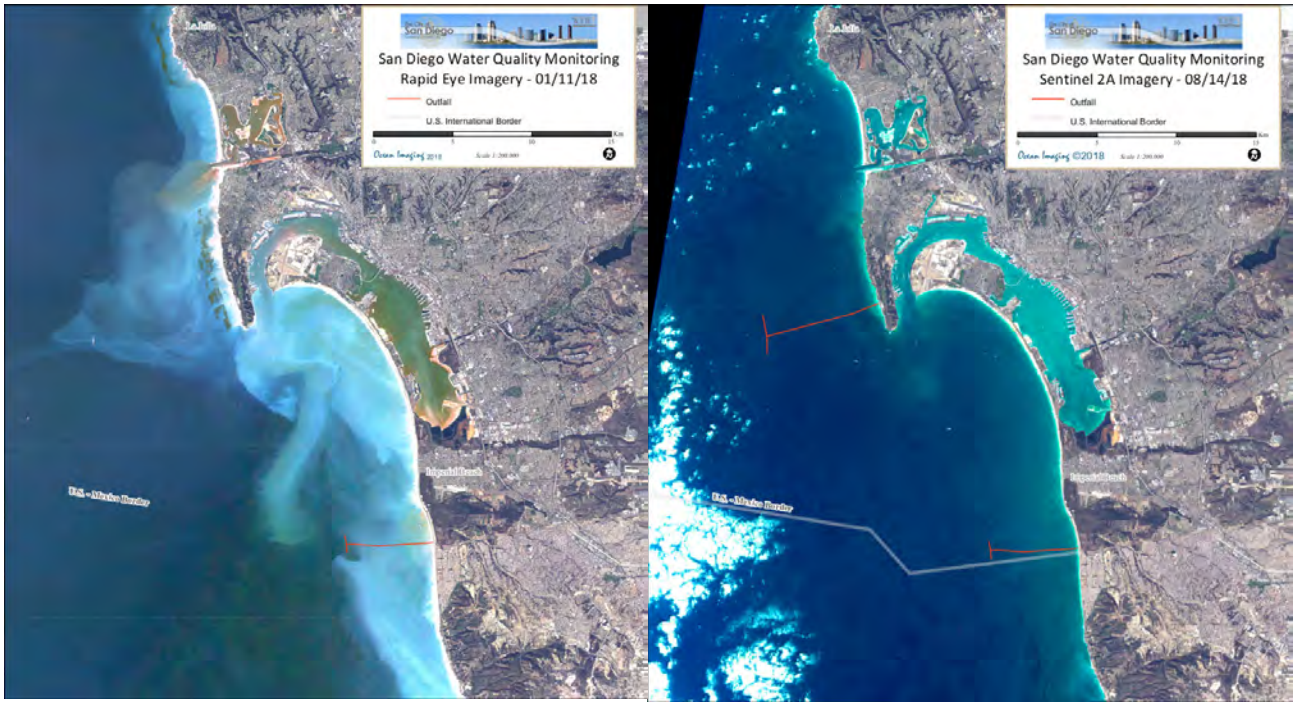

Figure 23. RapidEye image from 01/11/18 (left) one day after a significant rain event in which the strong San Deigo River discharge is evident. In contrast the Sentinel 2A image from 08/14/18 exhibits the clear water conditions resulting from a near rain-free summer.

the satellite data archive. A comparative example of the high August SSTs is shown in Figure 19 above. One result of the low annual rainfall in 2018 was that there were only 12 significant TJR discharge events seen in the satellite data over the entire year. One very heavy coastal turbidity event was seen in the RapidEye imagery acquired on 01/11/18 following 0.81 inches of rain measured at the TJR Estuary station between 01/08/18-01/10/18. The aftereffect was seen in the San Diego River discharge as well. Given that only 0.15 inches of rain had fallen since September of 2017 prior to that rain event, it was a good example of the "first flush effect" described in section 2.2 above. **Figure 23** highlights the RapidEye image from 01/11/18 in contrast to a Sentinel 2A image from 08/14/18 exhibiting the clear water conditions along the coast after only 0.02 inches of rain the entire summer. Between April and October of 2018 most other conditions affecting water clarity and quality were likely due to either wave action and/or phytoplankton blooms. Chlorophyll levels indicative of phytoplankton blooms in the Southern California Bight followed seasonal upwelling and California Current cycles, however higher chlorophyll/plankton levels persisted along the San Diego County coast for a greater portion of the year. Rainfall events in November and December and a reportedly large sewage spill into the TJR on 12/10/18 contributed to the increase in coastal turbidity and decreased water quality during those months.

5.4 Conditions in 2019

Heavy and persistent rainfall was the defining characteristic in 2019 related to offshore water quality. According to SDIA station records, in 2019 San Diego showed the highest cumulative annual precipitation total from the past 10 years (15.52 inches). This is almost double the average rainfall from that period and the 17th highest rainfall total recorded in San Diego since 1850. The largest total of 27.59 inches recorded in 1884. The average annual precipitation between 1850 and 2019 was 9.86 inches (NWS, San Diego). The TJR Estuary station reported a lower cumulative precipitation total in 2019 than San Diego station of 14.41 inches but was still higher than any of the TJR totals from past 10 years (Table 3). The monthly precipitation totals recorded for 2019 did follow expected seasonal patterns with the months of January, November and December recoding high amounts of precipitation and June through October following the typical dry season patterns. February, March and November, however, were atypical months, recording unusually high rainfall totals. The rains during January, February, November and December were not only intense at times (high amount within a short time interval), but persistent. Between the SDIA and TJR Estuary stations during the months of January and February there was measurable precipitation recorded on 30 out of the 59 days with eight of those days recording 0.5 inches of rain or more on a single day. As stated above, the sizes and extents (and hence the beach contamination potential) of the associated stormwater plumes correlate not only with rainfall amounts, but also the intensity with which it fell. As a result, the discharge from the TJR was abnormally strong throughout the month of February. **Figure 24** presents a satellite image time series during the month of February highlighting six days when the Tijuana River plume reached beyond its normal offshore extent. There were 27 significant TJR discharge events documented in the satellite data in 2019, more than twice that of the year prior and the most observed between 2017-2021.

In 2019 the county of San Diego issued 166 posted shoreline and/or rain advisories and 32 beach/shoreline closures. This is twice as many closures when compared to 2018 and the highest number of closures during the 5-year period summarized in this report. The longest contiguous 2019 closure lasting 164 days between January 1 and June 14 was in Border Field State Park along the south end of the Tijuana Slough Shoreline (California State Water Quality Control Board). This closure was an extension from 2018 and so in reality lasted 197 days.

As is typical for the region, almost all the closures were in the area between the Tijuana River mouth and Avenida Del Sol at the south end of North Island. With the exception of those during the June through September summer months, almost all of the closures can be attributed to a rain event prior to and/or during the closure period. All except two were associated with Tijuana River discharge. The satellite imagery available on the web portal on or around the closure dates and rainfall events visually correlate with the closure information. Imagery during those time periods show high turbidity and suspended solid levels along the coastline in the closed region as well as persistent, higher than normal TJR runoff, sometimes being carried north by the ocean currents. **Figure 25** provides an example of the Tijuana River plume extending north corresponding with shoreline closures during the same time period.

The coast of San Diego County, as well as a large percentage of the California Bight, experienced moderate to high chlorophyll levels for most of the year indictive of frequent and persistent phytoplankton blooms throughout 2019. Only for short periods of time in March and May did

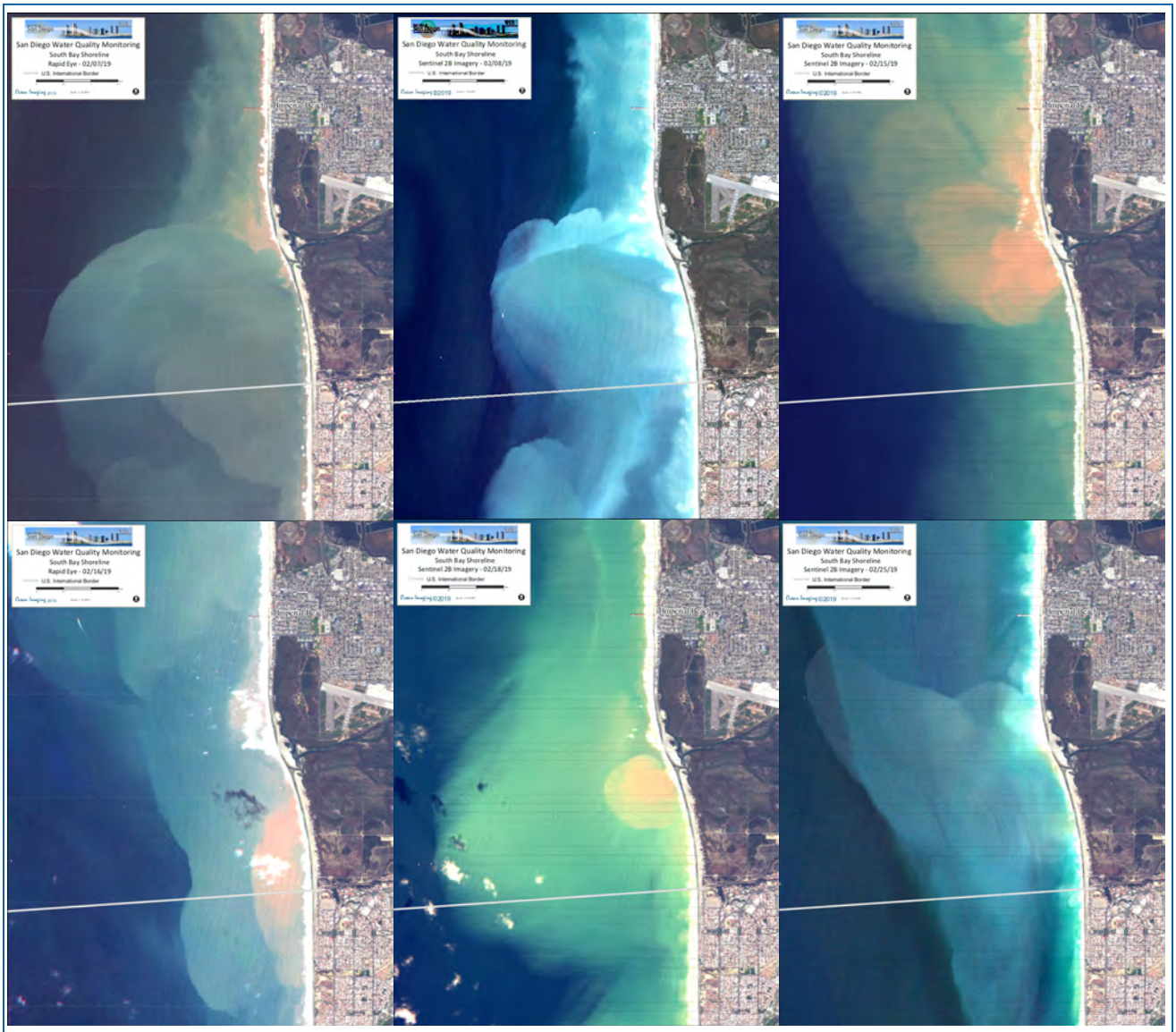

Figure 24. High resolution satellite time series between 02/07/19 and 02/25/19 showing strong TJR discharge events following a period of heavy precipitation.

the satellite data show relatively low levels of chlorophyll/phytoplankton or turbidity along the San Diego coastal region. The first half of 2019 was classified as being in a weak to moderate El Niño phase, however when averaged over the entire year, the ocean temperatures as recorded at the Scripps Pier, PLOO and SBOO RTOMS were actually 0.06 °C lower than the average of the past

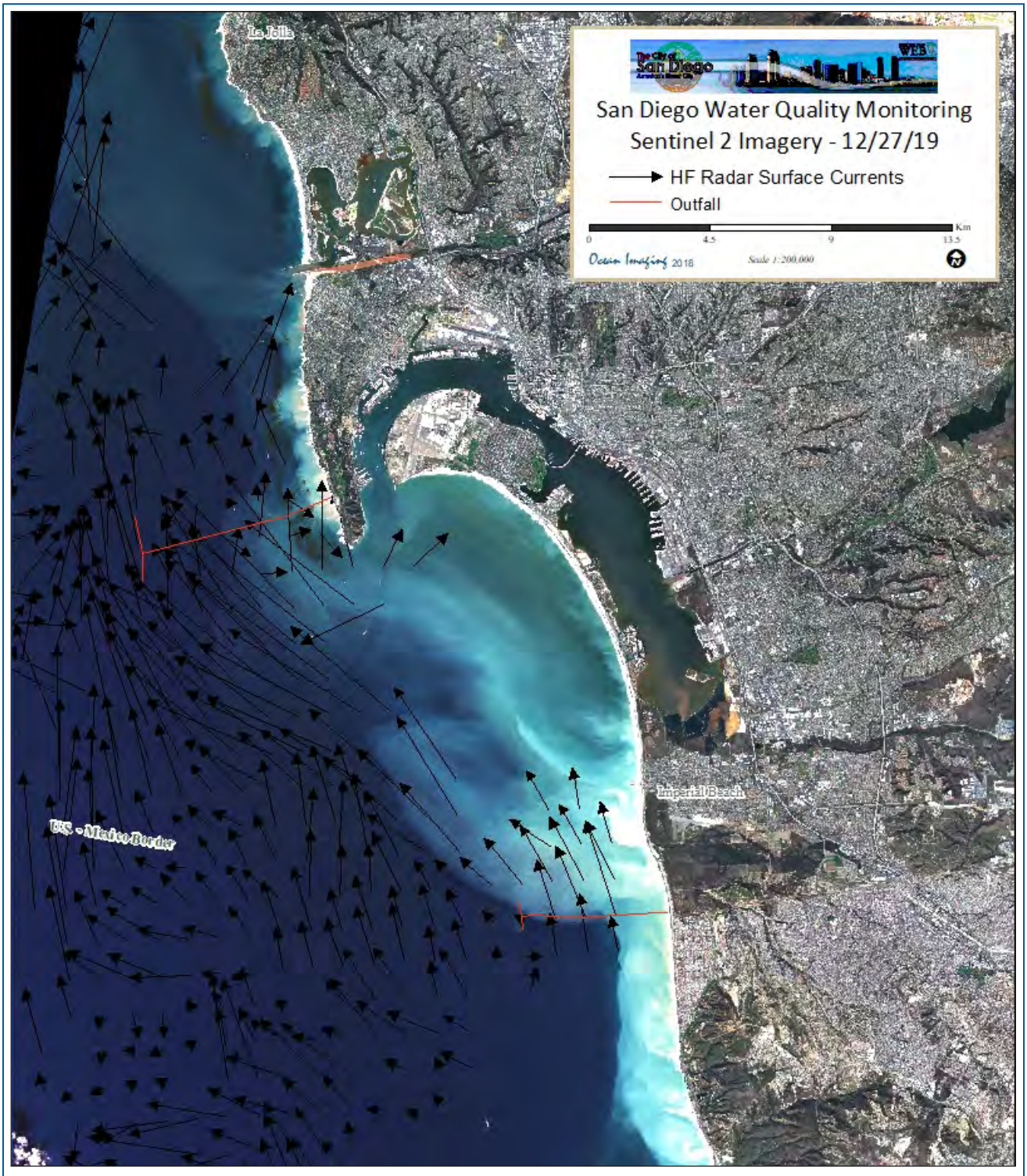

Figure 25. Sentinel 2 image with HF radar-derived surface currents showing the TJR plume extending north during a time of shoreline closures along San Diego.

10 years. The percentage of SBOO plume surface observations per days imaged from satellite was only 15.6% which is under the 10-year mean.

5.5 Conditions in 2020

2020 was marked by strong spring plankton blooms and red tide events. Besides the expected higher levels resulting from the California Current moving down past Point Conception, overall, the Southern California Bight experienced lower levels of chlorophyll during the months of January through early March. After mid-March the levels significantly increased region wide. A strong push of the California Current to the southeast along with coastal upwelling from May through December kept the chlorophyll in the bight high throughout the summer months and into winter. The coastal San Diego region showed normal to high coastal upwelling leading to phytoplankton blooms with the exception of months of March through May when large dense plankton blooms and red tide conditions existed for most of that three-month period from the border up past Oceanside. The blooms were unusually intense and were visible in all types of satellite data including observations in the relatively coarse resolution MODIS imagery. **Figure 26** provides a set of images from the Sentinel2 and SPOT satellites during April and May highlighting the anomalous conditions. The insets show the VIIRS- and MODIS-derived chlorophyll imagery on the same day or within one day of the high-resolution data. While red tides reflect strongly in the red wavelengths of the spectrum, they also reflect highly in the bands used to detect and quantify chlorophyll. In the MODIS and VIIRS imagery, the plankton blooms were so intense that chlorophyll levels surpassed normal cutoff values used to represent the data. Therefore, if examined closely the enhanced MODIS and VIIRs imagery for the months of April and May appear to show colors typically reserved for highly turbid water (as opposed to high chlorophyll). In these cases, the data are actually showing the unusually large and concentrated blooms.

The average ocean temperatures for 2020 recorded at the Scripps Pier, PLOO and SBOO RTOMS were about 0.2 °C below the 10-year mean, however a La Niña began to take hold in July of that year and lasted through June of 2021. This resulted in even lower overall water temperatures from fall into the following year.

Precipitation for the year was close to average at the SDIA station (7.71 inches for the year) and above average at the TJR Estuary station (10.18 inches). However, the majority of the rain fell in March and April while the rest of the year remained very dry. One extreme event was between 04/06/20 and 04/10/20 when a total of almost 5.4 inches were recorded at the TJR Estuary station during that five-day period. This unusually intense episode likely led to an influx of nutrients into the ocean system, sustaining and possibly exacerbating the strong plankton blooms and red tides documented in the satellite imagery during April and May. The number of significant TJR offshore plumes, SBOO effluent surfacings and beach closures were not necessarily high during this time period. The percentage of 2020 SBOO plume surface observations per days imaged was 24.3% which was above the 10-year mean, yet only two of those were in April and not necessarily linked to any storm event. The period of November 2020 through April of 2021 did show the second highest percentage of SBOO detections per image day at 31.8% but was more likely related to excessive flows (>25 MGD) into the SBIWTP from the Mexican wastewater system due to collection system overflows and pump failures later in 2020. These transboundary events were not solely responsible for the high effluent observations, but when they happened during the season when the ocean water column stratification weakened, the combination of factors probably resulted in the relatively frequent SBOO surface detections in the imagery. One such occurrence was on 12/11/20 shown in **Figure 27**. The Sentinel 2 data were acquired only a minute after the SPOT data. Both

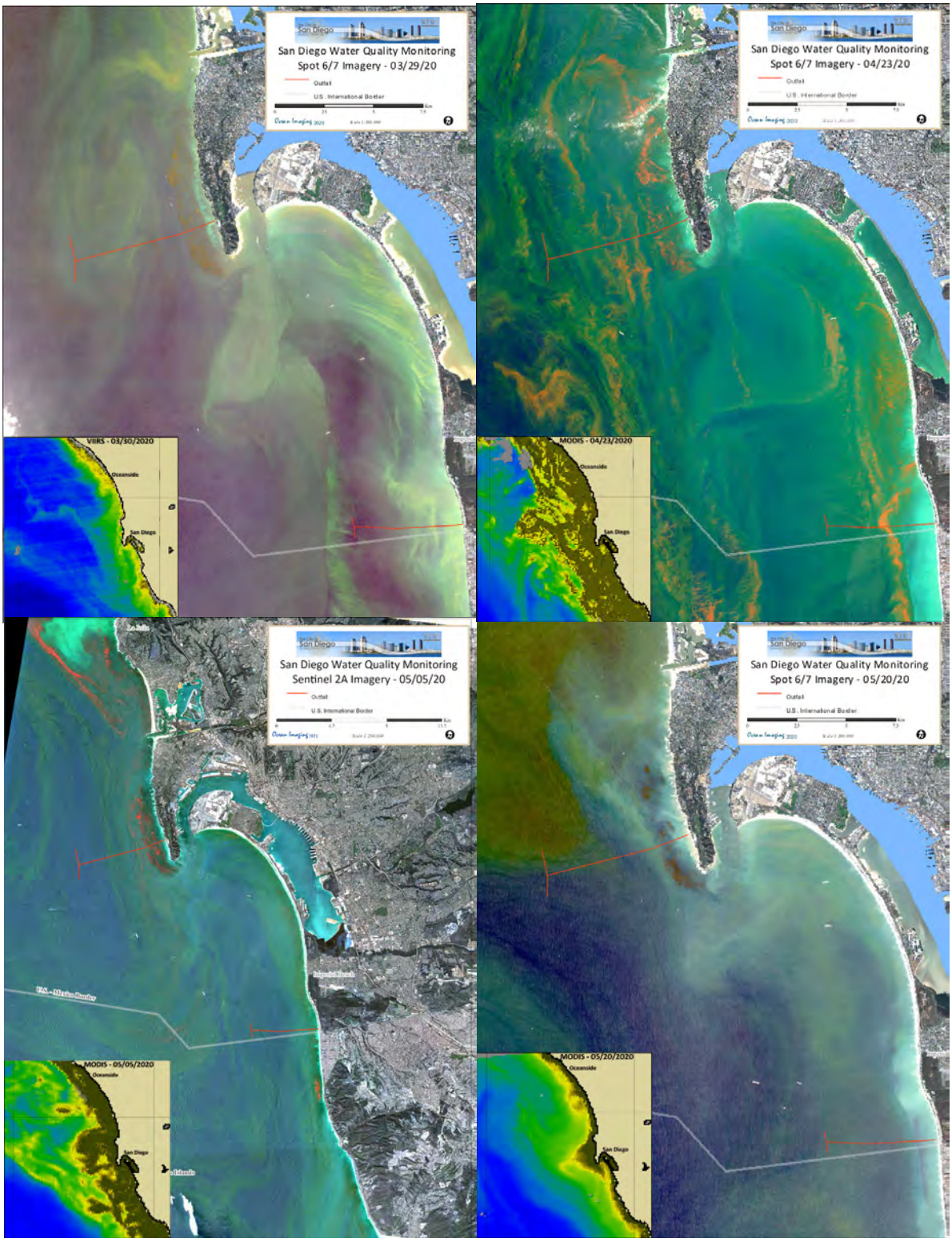

Figure 26. Plankton blooms visible in the SPOT and Sentinel 2 imagery on 03/29/20 (Red-Green-Blue), 04/23/20 (Red- Green-Near Infrared), 05/05/20 (Red-Green-Near Infrared) and 05/20/20 (Red-Green-Blue). Note the strong, probably coccolithophore bloom west of La Jolla in the 05/05/20 image as well as the intense reflectance in the Near-Infrared (NIR) channels (orange-red) in the imagery acquired on 04/23/20 and 05/05/20. The strong NIR signal illustrates the high levels of algae/phytoplankton in the blooms. Insets show MODIS- and VIIRS-derived chlorophyll imagery. Brown areas are where pixel value exceeded the 29.0 mg/L maximum typically used to represent the highest level of chlorophyll.

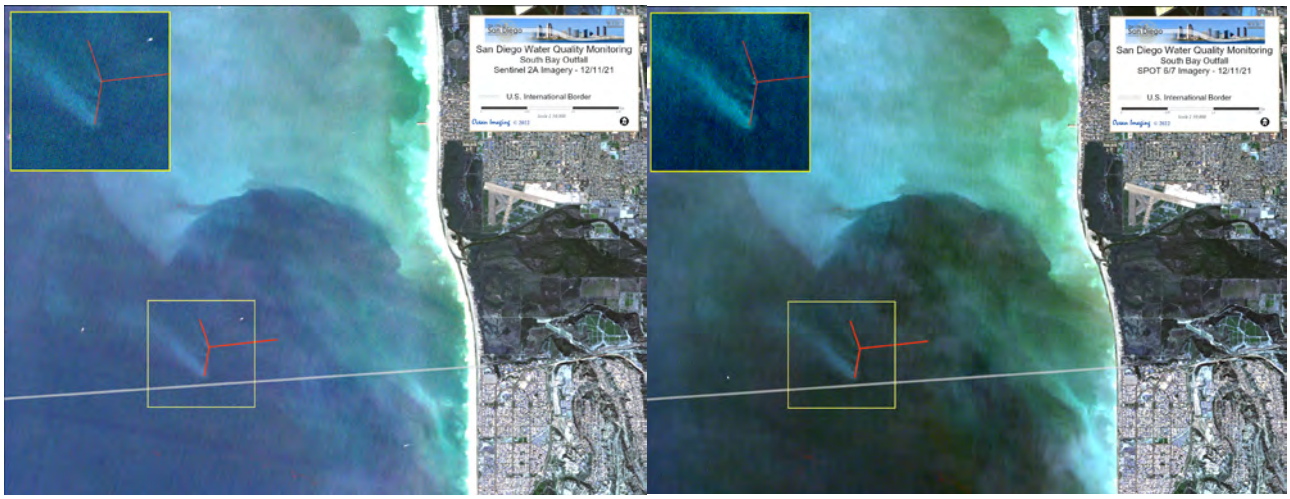

Figure 27. Sentinel 2A and SPOT imagery acquired within one minute of each other on 12/11/20 exhibiting a strong SBOO effluent plume.

images clearly depict the strong SBOO effluent plume emanating from at least three of the wye's risers. There was no storm or rainfall in the region prior to the date of these images. The most recent rainfall before these observations was on 11/09/20.

5.6 Conditions in 2021

While this report is a 5-year summary, it also serves as the 2021 annual report. Therefore, a more detailed discussion of 2021 follows.

5.6.1 Atmospheric and Ocean Conditions in 2021

Annual recorded precipitation for this year was close to the 10-year average for the region. The SDIA measured 7.85 inches and the TJR Estuary 5.63 inches, both a little lower than average (8.13 and 5.63 inches respectively – Table 3 above). The monthly rainfall followed normal patterns seasonally, with the winter and spring months matching the expected rainy season and the summer months being dry. Only 0.13 inches of rain were recorded at the TJR Estuary station from April through September. **Figure 28** shows cumulative daily precipitation in the estuary. The table to the side of the plot gives the dates for which there was measurable precipitation at that station.

The primary period of consistent and/or heavy precipitation occurred between mid-January and Mid-March. The vast majority (17 out of 22) of significant TJR discharge events seen in the remotely sensed data occurred from 01/04/21 to 03/05/21. **Figure 29** provides a dramatic example of the coastal turbidity and a large TJR plume following a long period of rain between 01/22/21 to 01/29/21.

River flow rates as shown in **Figure 30**, which plots the daily San Diego River flow rates in cubic feet per second (cfs) measured by the United States Geological Survey (USGS) Fashion Valley, gauge correspond with the rainfall data. Monthly precipitation totals at the San Diego International Airport station are displayed to the right of the plot. The flow rate of ~630 cfs on 01/29/21 correlates well the heavy coastal turbidity in the 01/30/21 Sentinel image in Figure 29.

In 2021 the county of San Diego issued 113 posted shoreline and/or rain advisories and 44 beach/shoreline closures. This is fewer postings, yet more closures compared to the previous year (151 and 28 respectively). The longest continuous 2021 closure lasting 142 days between January 1st and May 23rd was in Border Field State Park along the south end of the Tijuana Slough shoreline. This closure was an extension from 2020 and so in reality lasted 147

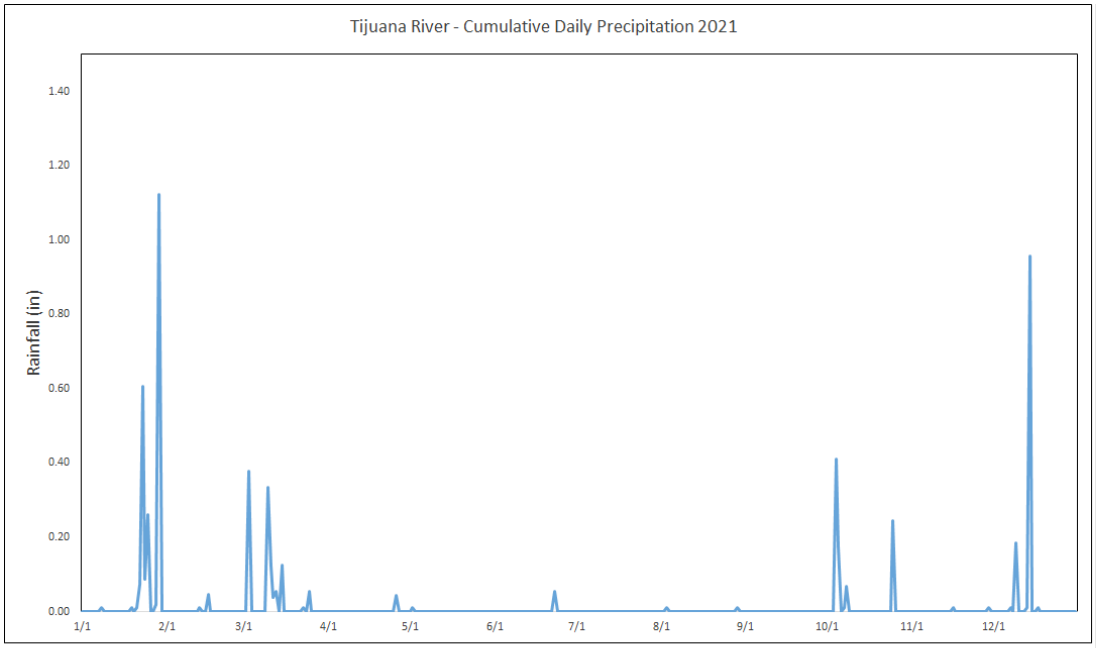

Date	CumPrcp (in)
01/08/21	0.01
01/19/21	0.01
01/21/21	0.01
01/22/21	0.07
01/23/21	0.61
01/24/21	0.09
01/25/21	0.26
01/28/21	0.02
01/29/21	1.12
02/13/21	0.01
02/16/21	0.05
03/03/21	0.38
03/10/21	0.33
03/11/21	0.12
03/12/21	0.04
03/13/21	0.06
03/15/21	0.13
03/23/21	0.01
03/25/21	0.06
04/26/21	0.04
05/02/21	0.01
06/23/21	0.06
08/03/21	0.01
08/29/21	0.01
10/04/21	0.41
10/05/21	0.17
10/07/21	0.01
10/08/21	0.07
10/25/21	0.24
11/16/21	0.01
11/29/21	0.01
12/07/21	0.01
12/09/21	0.19
12/13/21	0.01
12/14/21	0.96
12/17/21	0.01

Figure 28. Daily accumulated rainfall in the Tijuana Estuary

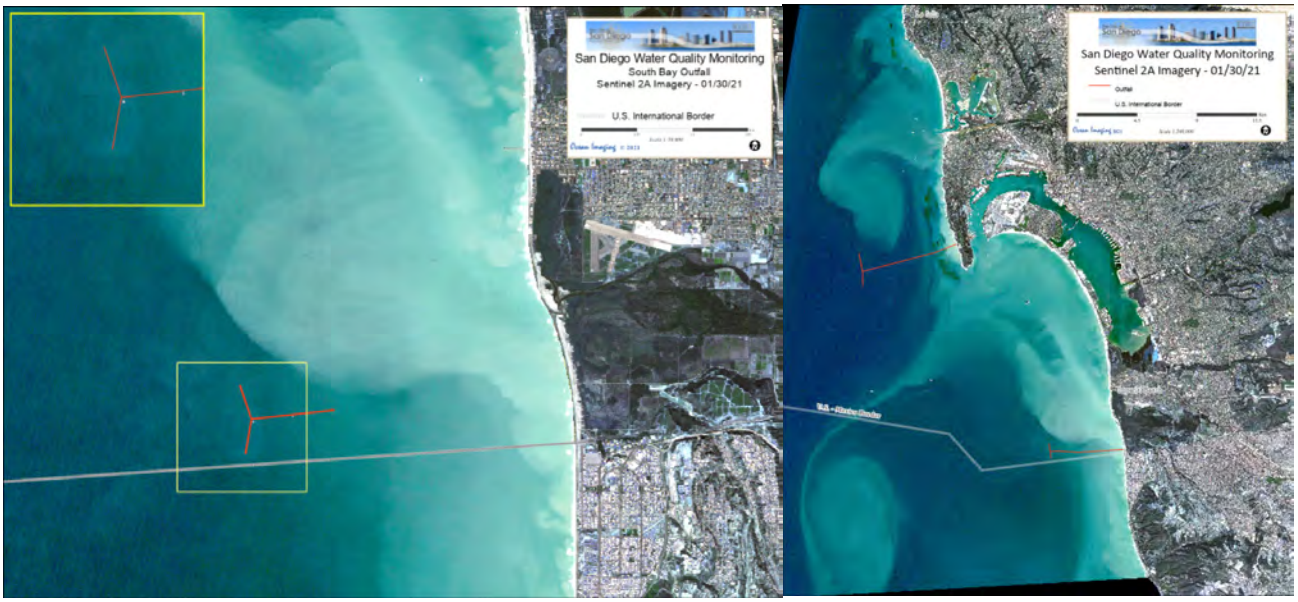

Figure 29. Sentinel 2A imagery from 01/30/21 showing heavy coastal turbidity resulting from heavy rains occurring during the previous seven days. The image on the left shows an expanded view of the TJR plume moving offshore and to the north.

days. As is typical for the region, all but one of the closures were in the area between the Tijuana River mouth and Avenida Del Sol at the south end of North Island and the result of contamination from the TJR runoff. The one exception was the beach to the west of Centennial Park which was closed due to a nearby sewage spill. In previous years most of the closures could be attributed to a rain event prior to and/or during the closure period. However, this was not necessarily the case in 2021 (**Table 4**). Many of the closures were likely the result of excess flow into the TJR Estuary caused by pump station failures and overflows in the TJR basin (San Diego Regional Water Quality Control Board, 2021, 2022 and Morgan Rogers, personal communication). Table 4 also shows the date of the high-resolution satellite data in the project's archive acquired closest in time to the start date of the closure and/or rain advisory.

2021 experienced consistently high chlorophyll/plankton levels throughout the year in the SCB and especially in the waters offshore of San Diego. **Figure 31** provides representative MODIS-derived chlorophyll images for each month of 2021. As is seen in the image data, the months of March, April and May experienced high chlorophyll levels along the Southern California coast with areas along the shoreline from Oceanside down past Pt. Loma often experiencing concentrations above 20 µg/L during the month of March. The California Current's southeastward push relaxed a bit in July, August and September allowing for clearer water between Oceanside and the islands, however the coastal waters in the San Diego region remained chlorophyll rich through December. Despite the dry spring and summer, there were several days during this period exhibiting exceptionally strong phytoplankton blooms. June and August displayed significant phytoplankton blooms in the image archive with dramatic plankton-rich eddies spinning off the coast and moving offshore.

The City of San Diego CTD sampling results correlated well with what was observed in the satellite data. Some of the highest chlorophyll levels recorded via CTD (as high as 27.3 µg/L) occurred between March and May during the series of ubiquitous phytoplankton blooms. **Figure 32** offers examples of the CTD fluorometry data in correlation with the

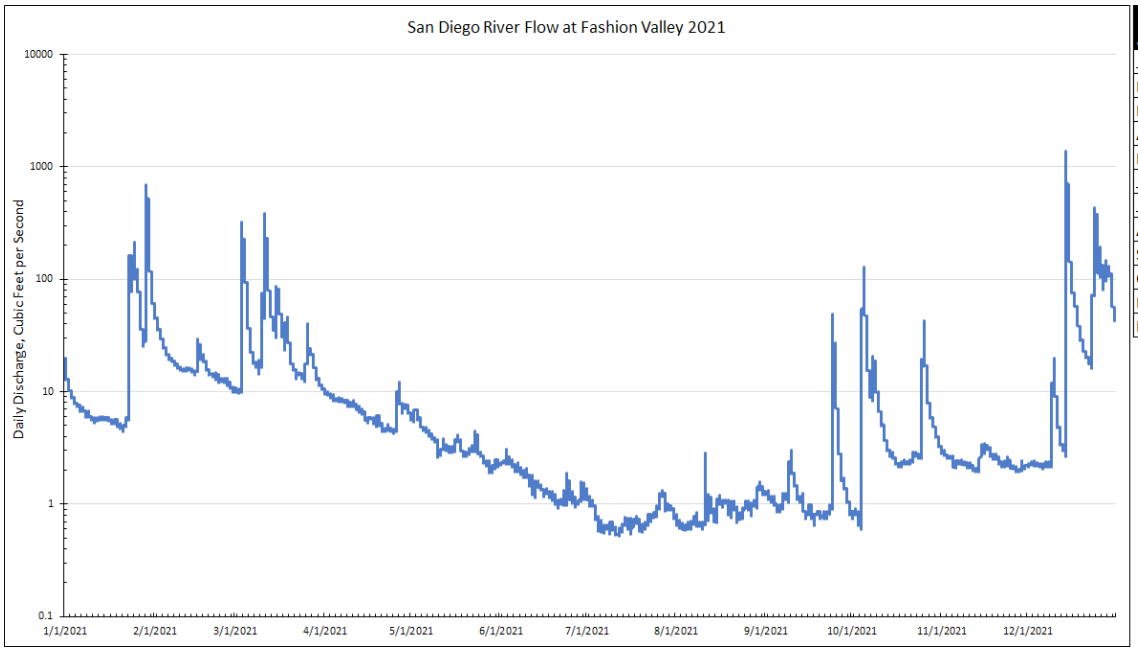

San Diego Intl. Airport Rainfall 2021	
Jan	1.80
Feb	0.10
Mar	1.48
Apr	0.07
May	0.07
Jun	0.01
Jul	--
Aug	0.23
Sep	0.50
Oct	1.01
Nov	--
Dec	2.58

Figure 30. Daily San Diego River flow rates in cubic feet per second measured by the USGS Fashion Valley gauge. Monthly precipitation totals at the San Diego International Airport station are displayed to the right of the plot.

Table 4. 2021 County of San Diego shoreline closures and advisories (courtesy of the County of San Diego Department of Environmental Health).

Station Description	Beach Name	Station Name	Type	Cause	Source	Start Date	End Date	Duration (days)	Nearest Rain Date	Time From Rain Event	Satellite Image Data
Border Fence N side	Border Field State Park	IB-010	Closure	TJR Associated	Sewage/Grease	1/1/2021	5/23/2021	142	1/8/2021	7	1/8/2021, 1/9/2021
All_SanDiego_County_Beaches	All_SanDiego_County	All_SanDiego_County_Beaches	Rain			1/23/2021	2/2/2021	10	1/23/2021	0	1/30/2021
All_SanDiego_County_Beaches	All_SanDiego_County	All_SanDiego_County_Beaches	Rain			1/23/2021	2/2/2021	10	1/23/2021	0	1/30/2021
All_SanDiego_County_Beaches	All_SanDiego_County	All_SanDiego_County_Beaches	Rain			1/23/2021	2/2/2021	10	1/23/2021	0	1/30/2021
All_SanDiego_County_Beaches	All_SanDiego_County	All_SanDiego_County_Beaches	Rain			1/23/2021	2/2/2021	10	1/23/2021	0	1/30/2021
All_SanDiego_County_Beaches	All_SanDiego_County	All_SanDiego_County_Beaches	Rain			1/23/2021	2/2/2021	10	1/23/2021	0	1/30/2021
All_SanDiego_County_Beaches	All_SanDiego_County	All_SanDiego_County_Beaches	Rain			1/23/2021	2/2/2021	10	1/23/2021	0	1/30/2021
Silver Strand N end (ocean)	Silver Strand State Beach	IB-070	Closure	TJR Associated	Sewage/Grease	1/29/2021	2/2/2021	4	1/29/2021	0	01/27/2021,01/28.2021, 01/30/2021
End of Seacoast Dr	Imperial Beach municipal beach, other	IB-050	Closure	TJR Associated	Sewage/Grease	1/29/2021	2/4/2021	6	1/29/2021	0	1/30/2021
End of Seacoast Dr	Imperial Beach municipal beach, other	IB-050	Closure	TJR Associated	Sewage/Grease	2/6/2021	2/7/2021	1	1/29/2021	-8	2/5/2022
Silver Strand N end (ocean)	Silver Strand State Beach	IB-070	Closure	TJR Associated	Sewage/Grease	2/10/2021	2/12/2021	2	1/29/2021	-12	2/11/2021
End of Seacoast Dr	Imperial Beach municipal beach, other	IB-050	Closure	TJR Associated	Sewage/Grease	2/10/2021	2/14/2021	4	1/29/2021	-12	02/11/2021, 02/12/2021, 02/14/2021
End of Seacoast Dr	Imperial Beach municipal beach, other	IB-050	Closure	TJR Associated	Sewage/Grease	2/25/2021	2/26/2021	1	2/16/2021	-9	2/25/2022
Silver Strand N end (ocean)	Silver Strand State Beach	IB-070	Closure	TJR Associated	Sewage/Grease	3/4/2021	3/19/2021	15	3/3/2021	-1	03/01/2021, 03/04/2021
End of Seacoast Dr	Imperial Beach municipal beach, other	IB-050	Closure	TJR Associated	Sewage/Grease	3/4/2021	3/19/2021	15	3/3/2021	-1	3/4/2021
End of Seacoast Dr	Imperial Beach municipal beach, other	IB-050	Closure	TJR Associated	Sewage/Grease	3/25/2021	3/27/2021	2	3/25/2021	0	3/26/2022
End of Seacoast Dr	Imperial Beach municipal beach, other	IB-050	Closure	TJR Associated	Sewage/Grease	3/30/2021	4/9/2021	10	3/25/2021	-5	3/31/2021
Avd. del Sol	Coronado City beaches	IB-080	Closure	TJR Associated	Sewage/Grease	4/3/2021	4/4/2021	1	3/25/2021	-9	4/3/2021
Silver Strand N end (ocean)	Silver Strand State Beach	IB-070	Closure	TJR Associated	Sewage/Grease	4/3/2021	4/5/2021	2	3/25/2021	-9	4/3/2021
End of Seacoast Dr	Imperial Beach municipal beach, other	IB-050	Closure	TJR Associated	Sewage/Grease	4/14/2021	4/15/2021	1	3/25/2021	-20	4/15/2022
End of Seacoast Dr	Imperial Beach municipal beach, other	IB-050	Closure	TJR Associated	Sewage/Grease	4/16/2021	4/18/2021	2	3/25/2021	-22	4/17/2021
Border Fence N side	Border Field State Park	IB-010	Closure	TJR Associated	Sewage/Grease	5/29/2021	5/30/2021	1	5/2/2021	-27	5/28/2021
Border Fence N side	Border Field State Park	IB-010	Closure	TJR Associated	Sewage/Grease	6/5/2021	6/11/2021	6	5/2/2021	-34	6/5/2021
Border Fence N side	Border Field State Park	IB-010	Closure	TJR Associated	Sewage/Grease	6/13/2021	6/22/2021	9	5/2/2021	-42	6/12/2021
Border Fence N side	Border Field State Park	IB-010	Closure	TJR Associated	Sewage/Grease	6/24/2021	7/1/2021	7	6/23/2021	-1	6/24/2021
Centennial Park, Beach To The West	Coronado north beach	EH-063	Closure	Sewage Spill	Unknown	6/30/2021	7/2/2021	2	6/23/2021	-7	6/26/2021
Border Fence N side	Border Field State Park	IB-010	Closure	TJR Associated	Sewage/Grease	7/15/2021	7/17/2021	2	6/23/2021	-22	7/16/2022
End of Seacoast Dr	Imperial Beach municipal beach, other	IB-050	Closure	TJR Associated	Sewage/Grease	7/15/2021	7/16/2021	1	6/23/2021	-22	7/16/2022
Border Fence N side	Border Field State Park	IB-010	Closure	TJR Associated	Sewage/Grease	7/25/2021	7/30/2021	5	6/23/2021	-32	07/22/2021, 07/29/2021
Border Fence N side	Border Field State Park	IB-010	Closure	TJR Associated	Sewage/Grease	8/8/2021	8/10/2021	2	8/3/2021	-5	8/8/2021
End of Seacoast Dr	Imperial Beach municipal beach, other	IB-050	Closure	TJR Associated	Sewage/Grease	8/9/2021	8/10/2021	1	8/3/2021	-6	8/11/2022
Border Fence N side	Border Field State Park	IB-010	Closure	TJR Associated	Sewage/Grease	8/20/2021	8/24/2021	4	8/3/2021	-17	08/23/2021, 08/24/2021
End of Seacoast Dr	Imperial Beach municipal beach, other	IB-050	Closure	Bacterial Standards Violation	Sewage/Grease	8/22/2021	8/24/2021	2	8/3/2021	-19	08/23/2021, 08/24/2021
Border Fence N side	Border Field State Park	IB-010	Closure	Bacterial Standards Violation	Sewage/Grease	9/2/2021	9/5/2021	3	8/29/2021	-4	9/2/2021
End of Seacoast Dr	Imperial Beach municipal beach, other	IB-050	Closure	TJR Associated	Sewage/Grease	9/2/2021	9/5/2021	3	8/29/2021	-4	09/02/2021, 09/05/2021
Border Fence N side	Border Field State Park	IB-010	Closure	Bacterial Standards Violation	Sewage/Grease	9/7/2021	9/11/2021	4	8/29/2021	-9	9/7/2021
Border Fence N side	Border Field State Park	IB-010	Closure	Bacterial Standards Violation	Sewage/Grease	9/15/2021	9/22/2021	7	8/29/2021	-17	09/14/2021, 09/15/2021
End of Seacoast Dr	Imperial Beach municipal beach, other	IB-050	Closure	Bacterial Standards Violation	Sewage/Grease	9/16/2021	9/19/2021	3	8/29/2021	-18	9/17/2021
Border Fence N side	Border Field State Park	IB-010	Closure	Bacterial Standards Violation	Sewage/Grease	9/28/2021	10/3/2021	5	8/29/2021	-30	09/29, 09/30
Border Fence N side	Border Field State Park	IB-010	Closure	TJR Associated	Sewage/Grease	10/5/2021	10/15/2021	10	10/5/2021	0	10/5/2021
End of Seacoast Dr	Imperial Beach municipal beach, other	IB-050	Closure	TJR Associated	Sewage/Grease	10/6/2021	10/11/2021	5	10/5/2021	-1	10/10/2021, 10/12/2021
Silver Strand N end (ocean)	Silver Strand State Beach	IB-070	Closure	TJR Associated	Sewage/Grease	10/9/2021	10/11/2021	2	10/8/2021	-1	10/12/2021
Border Fence N side	Border Field State Park	IB-010	Closure	TJR Associated	Sewage/Grease	10/26/2021	11/12/2021	17	10/25/2021	-1	10/26/2021
Border Fence N side	Border Field State Park	IB-010	Closure	TJR Associated	Sewage/Grease	12/3/2021	12/5/2021	2	11/29/2021	-4	11/28/2021
Border Fence N side	Border Field State Park	IB-010	Closure	TJR Associated	Sewage/Grease	12/8/2021	12/31/2021	23	12/7/2021	-1	11/28/2021
All_SanDiego_County_Beaches	All_SanDiego_County	All_SanDiego_County_Beaches	Rain			12/9/2021	12/12/2021	3	12/9/2021	0	12/11/2022
All_SanDiego_County_Beaches	All_SanDiego_County	All_SanDiego_County_Beaches	Rain			12/14/2021	12/18/2021	4	12/9/2021	-5	12/15/2021
End of Seacoast Dr	Imperial Beach municipal beach, other	IB-050	Closure	TJR Associated	Sewage/Grease	12/14/2021	12/18/2021	4	12/14/2021	0	12/15/2021, 12/16/2021
Silver Strand N end (ocean)	Silver Strand State Beach	IB-070	Closure	TJR Associated	Sewage/Grease	12/15/2021	12/18/2021	3	12/14/2021	-1	12/16/2022
End of Seacoast Dr	Imperial Beach municipal beach, other	IB-050	Closure	TJR Associated	Sewage/Grease	12/21/2021	12/31/2021	10	12/17/2021	-4	12/24/2022
All_SanDiego_County_Beaches	All_SanDiego_County	All_SanDiego_County_Beaches	Rain			12/24/2021	12/31/2021	7	12/17/2021	-7	
Silver Strand N end (ocean)	Silver Strand State Beach	IB-070	Closure	TJR Associated	Sewage/Grease	12/28/2021	12/31/2021	3	12/17/2021	-11	12/24/2022
Avd. del Sol	Coronado City beaches	IB-080	Closure	TJR Associated	Sewage/Grease	12/30/2021	12/31/2021	1	12/17/2021	-13	12/24/2022

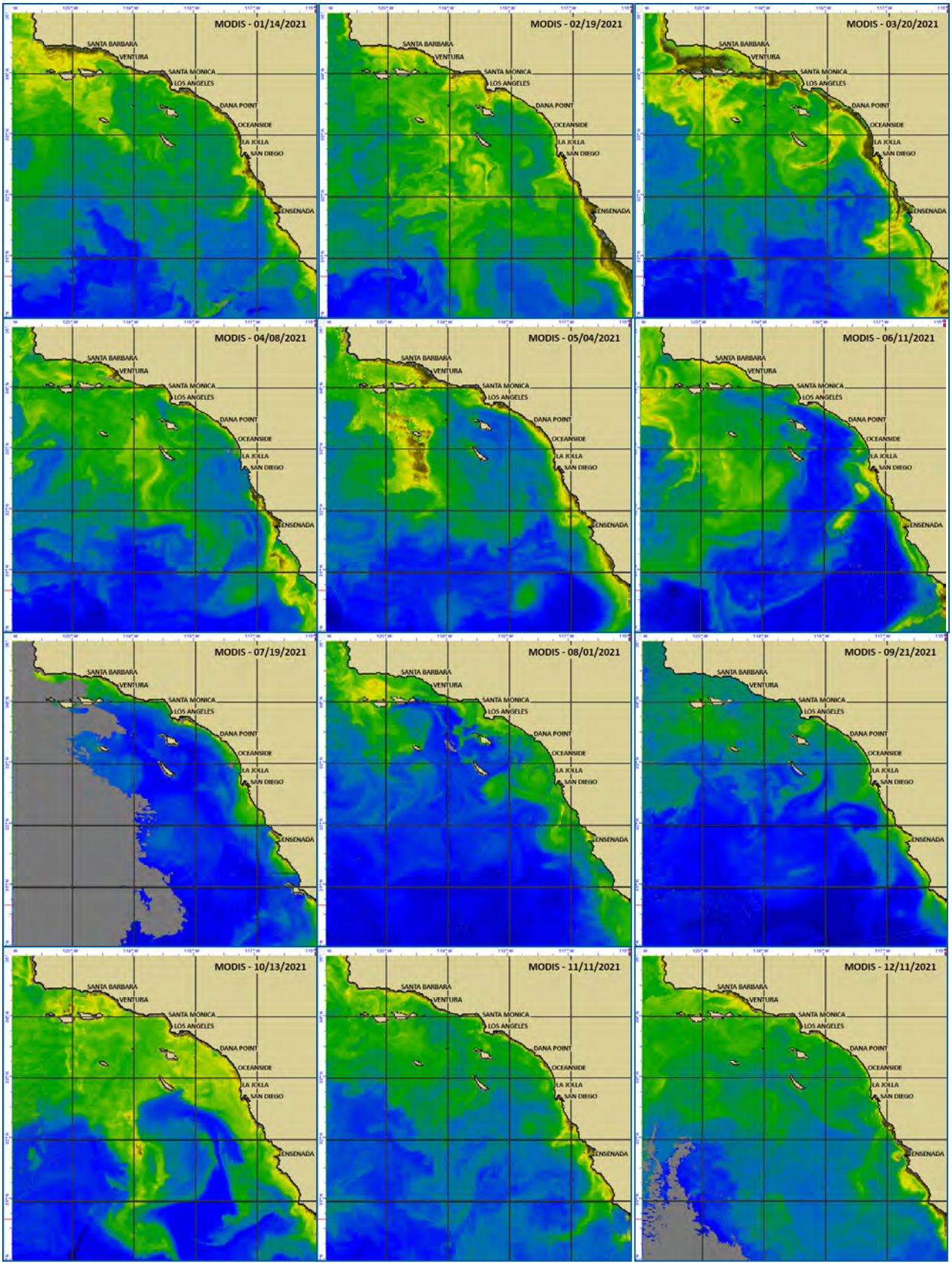

Figure 31. Representative MODS-derived chlorophyll images for each month of 2021 showing strong California Current southward push and significant phytoplankton blooms during nine months of the twelve months.

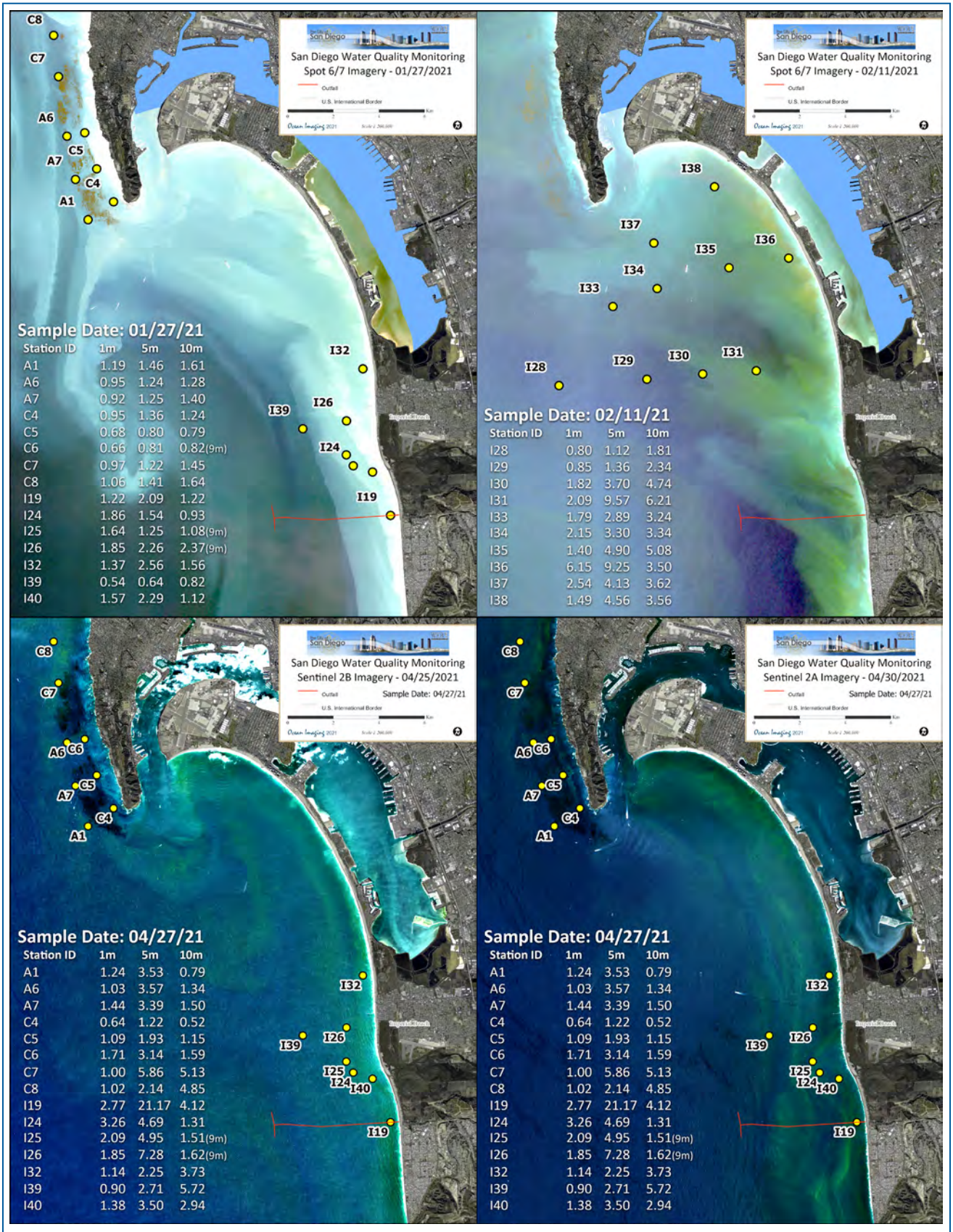

Figure 32. CTD fluorometry data plotted over Sentinel 2 and SPOT satellite imagery showing chlorophyll levels at sampling stations in correlation with the image data.

high-resolution satellite imagery on or near the same date as the field samples. While the remotely sensed data do not depict quantitative chlorophyll levels, the plankton blooms are self-evident in the imagery and correlate well with the CTD data – especially those taken on 02/11/21 and 04/27/21. One interesting day to note is the SPOT image from 01/27/2021. While the image shows very heavy coastal turbidity there is a relative lack of chlorophyll in the turbid water which is reflected in the CTD data. The image color appropriately represents the turbidity as being primarily suspended sediment as opposed to organics.

5.6.2 The South Bay Ocean Outfall Region in 2021

There were 19 instances during which the SBOO effluent plume was observed in 2021 out of the 134 high resolution satellite scenes acquired and processed (Appendix A). Of the 19, three were instances of the plume observed by different satellites on the same day. This equates to 16 days when the plume was visible in the high-resolution imagery. This is 11 fewer than observed in 2020 and below the average percentage when compared to the past 10 years. Accounting for the duplicate observations, the percentage of SBOO plume surface observations per days imaged in 2021 was 14.3% which is about five percentage points under the 10-year mean (19.4%).

The period between 11/11/20 and 01/30/21 exhibited the highest frequency of SBOO effluent plume observations in the satellite data within a period of less than three months. As noted above there were several instances during this time when the SBIWTP took on excess sewage from Tijuana exceeding the maximum allowed capacity of 25 MGD, but the EFF flow is not considered to be the primary factor linked to the high number of SBOO detections. Also discussed previously, the numerous effluent surface manifestations occurring during this time period were likely the result of two primary factors: the lack of strong vertical stratification during the winter months and relatively weak subsurface currents over the SBOO which allowed the undispersed effluent to reach the surface.

In 2021, the shoreline area of the SBOO/Tijuana River outflow region experienced 90 days on which the field sampling showed elevated bacteria levels as defined by the California Ocean Plan. The offshore SBOO region, which includes the stations over the SBOO wye experienced only three days of elevated bacteria levels at depths of six meters or shallower and the nearshore region (referred to as the "kelp" region in previous reports) experienced 20 days on which the bacteria levels were deemed elevated. There were 81 sampling days when at least one shore station showed elevated levels. The total number of sampling days for all three SBOO areas (either along the shoreline or offshore, but at six meters or shallower) totaled 122 in 2021 and 162 in 2020. Therefore, in 2021 for the three sampling regions combined, 73.8% of the sampling days resulted in elevated bacteria levels at one station or more which is close to 77.8% from 2020. However, as noted above, it should be emphasized that the vast majority of samples showing elevated levels were recorded at the shore stations and high levels offshore, near the SBOO wye, are rare. As with 2020, 2021 continued to experience a higher-than-normal number (86) of reports citing the transboundary flow of sewage, solid waste and sediment across the U.S.-Mexico border into the canyon collectors such as Stewart's Drain, the TJR main channel and thus into the Tijuana Estuary and U.S. coastal waters waters (San Diego Regional Water Quality Control Board, 2022). The satellite imagery showing substantial discharge from the TJR region compare well visually with times when the shoreline and kelp area sampling showed elevated bacteria levels (**Figure 33**). Heavy and/or persistent rainfall along with excess untreated flow into the TJR are the most plausible causes for the majority of the elevated bacteria samples and turbid waters seen in the remote sensing data. As is typical, the best water quality and clarity in the South Bay region in 2021 was observed from June through August.

5.6.3 The Point Loma Ocean Outfall Region in 2021

In 2021 the Pt. Loma region was affected by conditions already described for general San Diego County: significant seasonal rainfall during the months of January through mid-March and December with almost no rainfall from of April through November. Similar to past years, this compromised water clarity in the shoreline areas in January

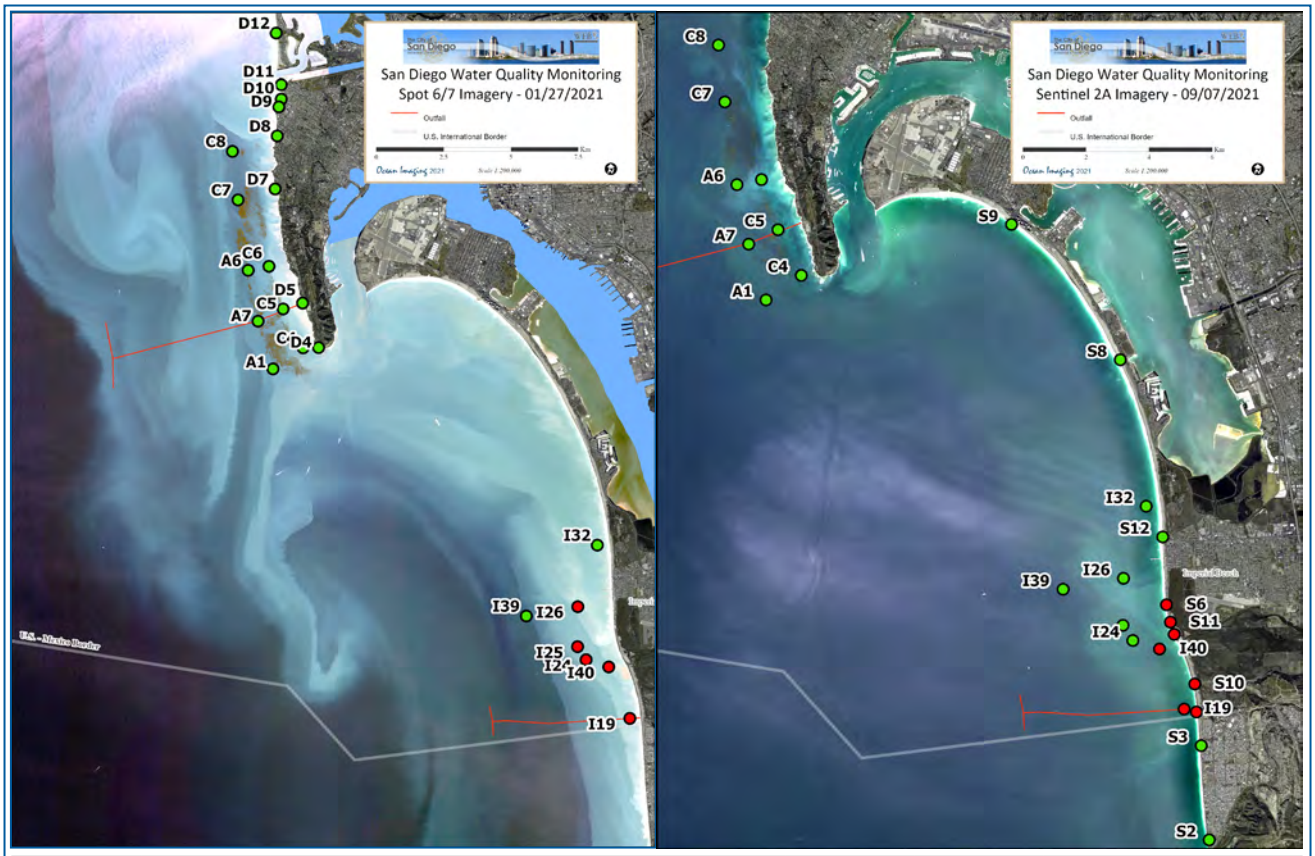

Station	Depth (M)	Entero	Fecal	Total
I19	11	140	220	800
	2	320	860	12000
	6	680	1000	12000
I24	2	400	880	8400
	6	62	82	540
	11	8	20	200
I25	2	360	560	4400
	6	28	62	200
	9	14	42	200
I26	2	340	840	3600
	6	200	860	2200
	9	100	280	2000
I40	2	200	580	5800
	6	440	920	8800
	9	72	88	600

Station	Depth (M)	Entero	Fecal	Total
I19	2	920	300	5200
	11	460	500	4000
	6	2400	160	11000
I40	2	160	220	800
	6	140	74	600
	9	140	100	1000
S5	NA	5200	1600	16000
S6	NA	720	420	6400
S10	NA	4600	880	16000
S11	NA	1800	1100	16000

Figure 33. Sentinel 2 and SPOT data with near-surface bacterial sampling data overlaid from the same day of image acquisition. Stations showing FIB measurements exceeding the single sample maximum as defined by the California Ocean Plan are shown as red dots. Green dots identify stations at which the FIB levels were in compliance. The tables below each image show the measurement values by depth for each station with elevated bacteria levels.

through March and in December as runoff from the San Diego River and Mission Bay brought sediment-laden water inside and outside the Pt. Loma kelp bed after the rain events described above.

The shoreline, kelp and offshore bacterial sampling resulted in a similar number of elevated bacteria measurements as in 2020. Shoreline field sampling yielded 3 days on which one or more stations experienced high bacteria counts. Offshore and kelp station sampling resulted in 8 days and 1 day respectively when stations recorded excessive FIBs. As expected, most of the high bacteria measurements were seen in winter months and attributed to rain events, however the offshore region did see a few days with elevated numbers in May and August on days prior to which there was no precipitation. **Figure 34** displays samples taken on 11/12/21 plotted over a SPOT image from 11/13/21. No obvious visual correlation to the slightly elevated bacteria data exists in the satellite data, yet it should be noted that all the elevated bacteria levels existed

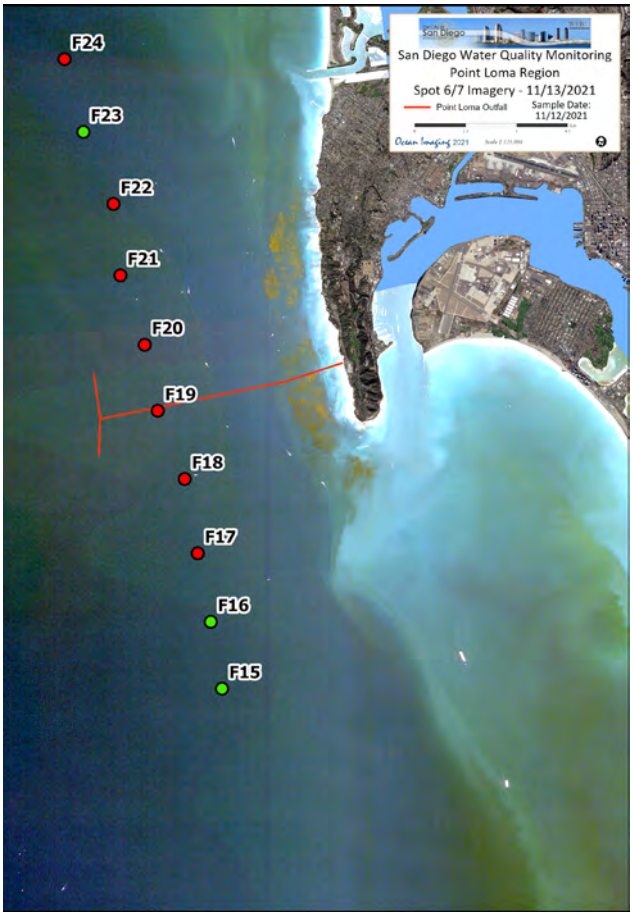

Station	Depth (M)	Entero	Fecal	Total	Station	Depth (M)	Entero	Fecal	Total
F17	1	2	NA	NA	F21	1	2	NA	NA
	25	2	NA	NA		25	2	NA	NA
	60	10	NA	NA		60	260	NA	NA
	80	280	NA	NA		80	220	NA	NA
F18	1	2	NA	NA	F22	1	2	NA	NA
	25	2	NA	NA		25	2	NA	NA
	60	52	NA	NA		60	16	NA	NA
	80	300	NA	NA		80	120	NA	NA
F19	1	2	NA	NA	F24	1	2	NA	NA
	25	2	NA	NA		25	2	NA	NA
	60	54	NA	NA		60	300	NA	NA
	80	260	NA	NA		80	110	NA	NA
F20	1	2	NA	NA					
	25	2	NA	NA					
	60	220	NA	NA					
	80	**180**	**NA**	**NA**					

Figure 34. SPOT image with bacterial sampling data overlaid from the day before image acquisition. Stations showing FIB measurements exceeding the maximum allowed as defined by the California Ocean Plan are shown as red dots. Green dots identify stations at which the FIB levels were in compliance. The tables below each image show the measurement values by depth for each station with elevated bacteria levels.

only at depths of 60 meters or deeper, which is beyond the depth reached with multispectral and thermal infrared remote sensing data.

5.7 Kelp Variability

One observation provided by the satellite image archive is the continuing variability in the size of the Pt. Loma kelp bed over time (**Figure 35**). **Table 5** shows the area in km2 of three notable kelp beds in the San Diego region over the past 14 years. The September and October dates were chosen to represent the kelp bed canopy coverage for each year since spring and fall are considered to be the time periods when the canopy size is thought to be at or near its peak. The size of the Pt. Loma bed

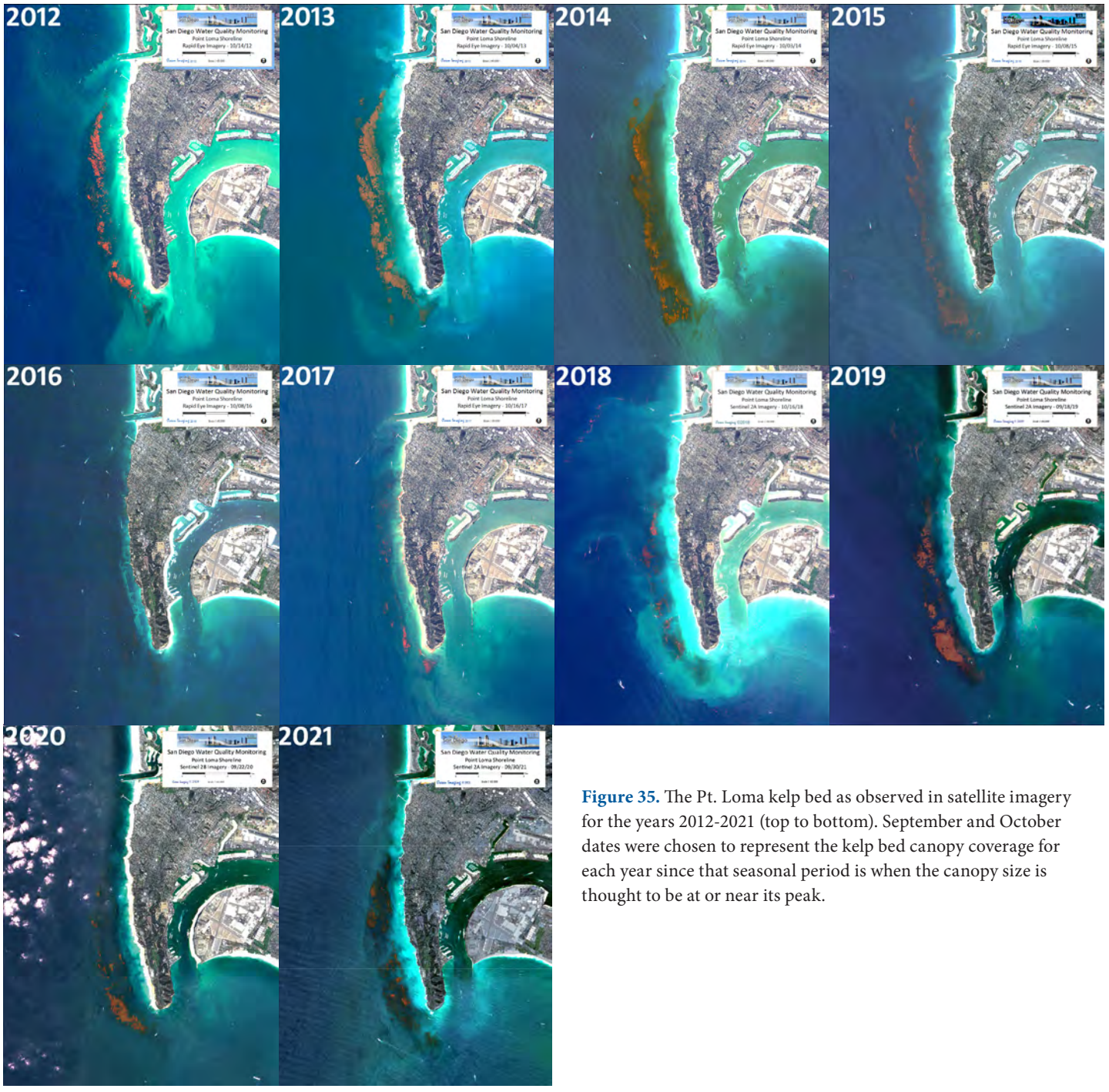

Figure 35. The Pt. Loma kelp bed as observed in satellite imagery for the years 2012-2021 (top to bottom). September and October dates were chosen to represent the kelp bed canopy coverage for each year since that seasonal period is when the canopy size is thought to be at or near its peak.

in the fall of 2021 (3.82 km2) was very close to the average canopy coverage for the 14-year period (4.04 km2). As has been reported in previous years, the satellite data show the bed begin to decrease in size during February of 2016, perhaps due to the storm events taking place during early to mid-January, effects from the 2014-2016 strong El Niño event and/or the Northeast Pacific marine heat wave (Di Lorenzo, 2016). Noted in the 2017 and 2018 annual reports, the kelp bed appeared to be coming back in January of 2017, but then decreased in size as the year progressed resulting in much smaller than average canopy coverage by the end of that year. As was also the case in 2018 and 2020, the relative high frequency of the satellite data of Pt. Loma available through this project revealed significant month-to-month variability in canopy coverage likely due to a combination of factors. In the beginning of 2021, the bed roughly held the same canopy size observed at the end of 2020, however the coverage of the exposed canopy decreased during the latter part of February through late March. Between April and October, the bed experienced several fluctuations in size showing a dramatic reduction for a few weeks in late October to early November. The bed then peaked in size in the November 28th imagery and held close to that coverage for the remainder of the year. While there were significant differences in tidal heights at the time of each satellite image acquisition, tides cannot be flagged as the primary reason for the difference in canopy coverage observed in the satellite data. There were days when the areal coverage was high, but the tide level was also high and vice versa when the imagery revealed smaller bed size, but the tides were relatively low. Additionally, passing storms that result in kelp bed damage can be considered factors, though not the sole cause of smaller kelp bed observations. The intra-annual variation as captured in the Near-IR, 6-meter SPOT imagery is visually documented in a year-long time series video in which the bed is imaged multiple times per month (https://oceani.com/SDWQ/2021_PointLomaKelpTimelapse.mp4).

It is important to point out that the canopy coverages shown in Table 5 may differ slightly from those provided in the Southern California Bight

Table 5. Kelp canopy areas of three San Diego kelp beds measured from satellite imagery collected for this project.

			Kelp (km²)		
Year	Date	Satellite	Point Loma	Imperial Beach	Tijuana
2021	09/30/21	Sentinel-2B	3.82	0.00	0.00
2020	09/22/20	Sentinel-2A	2.93	0.00	0.00
2019	09/18/19	Sentinel-2A	5.17	0.00	0.00
2018	10/16/2018	Sentinel-2A	2.44	0.00	0.00
2017	10/04/2017	RapidEye	1.05	0.00	0.00
2016	09/08/2016	RapidEye	0.22	0.00	0.00
2015	09/17/2015	Landsat 7	4.11	0.39	0.29
2014	09/14/2014	Landsat 8	5.42	0.59	0.30
2013	09/23/2013	RapidEye	5.89	0.19	0.05
2012	09/15/2012	RapidEye	2.91	0.00	0.00
2011	09/01/2011	RapidEye	1.99	0.00	0.00
2010	09/27/2010	Landsat 7	6.01	0.00	0.00
2009	09/16/2009	Landsat 5	5.96	1.01	0.21
2008	09/05/2008	Landsat 7	8.66	0.82	0.01

* Average surface canopy coverage 2008-2021 = 4.04 km2

Regional Arial Kelp Survey reports. This is because the canopy areas for the Pt. Loma bed computed for those reports are averages of four surveys performed throughout the year; while the coverage estimates shown in this report are taken from single satellite images acquired during the fall time period chosen to represent the maximum coverage seen during that time of year. Tide levels were not a factor in the inter-year comparison as there was little variability in tide level between the years (often approximately two feet or less). However, due to the overflight times of these satellites, the canopy areas could be under-represented compared to the kelp survey reports because the tide levels at the time of satellite data acquisition could vary significantly from the tides during the aerial surveys. The Imperial Beach and Tijuana beds have not been visible in the satellite data since 2015. It is being documented that kelp forests along the West Coast have been experiencing noteworthy variability in canopy size for the past several years, and thus warrants keeping a close watch on the health of the kelp beds in the San Diego region (Bell, et al., 2020; Schroeder, 2019).

6. RECENT AND FUTURE DEVELOPMENTS AND ADDITIONS TO THE PROJECT

During the period covered in this summary report OI has added several data products and capabilities to the daily offerings provided as part of the project. As discussed above, in 2016, OI began to generate ocean currents, subsurface temperature and salinity analyses along with other HYCOM-derived products in a WMS REST service format which is directly compatible with any WMS the City might be working to implement. It was intended that all the OI-delivered data products, including all the satellite imagery would be delivered via OI's ArcGIS Server for easy ingestion into the City's WMS by fall of 2017. OI is in discussion with the City about further developing the project web server into a WMS-driven dashboard style site that will facilitate the delivery of all of the existing data products, the HYCOM oceanographic products and any other data sets that the City choose to incorporate into an interactive platform. Not only will the server give the user the capability to overlay different data types on top of each other (i.e., ocean currents on top of satellite imagery) it will significantly enhance the information experience providing easy, near real-time access to the many data products delivered as part of this project. As part of this process, the historical imagery, data and reports will remain accessible via the existing web portal. If a more capable web server comes online, OI will progressively work backwards in time to make all historical data available via the City's online WMS, including the archived HYCOM data products.

In the meantime, OI has begun the process to update the project's existing web site in order to better present the various data products and hopefully increase end user interaction. **Figure 36** provides an example of what the data access page will look like. The upgrades to the site are intended to give the visitor quick, "at a glance" access to thumbnail images for a particular monitoring region from the most recent 15 days in an interactive carousel-style gallery. Clicking on a thumbnail image will open a page with access to the matching month and imaging region. The new site will also reduce excessive text links for the older data sets but provide one-click access to the data archive pages.

As discussed above, beginning in 2017, OI also began processing and posting imagery from the Sentinel-2A, 2B, 3A and 3B satellites. In 2020 OI transitioned from the now-decommissioned RapidEye Satellite constellation to the SPOT 6 and 7 satellites. Also mentioned above, in late 2021 SAR data from the Sentinel 1A and 1B satellites were added to the suite of products. SAR can detect surfactant films associated with natural processes (Svejkovsky and Shandley 2001) and

plumes containing anthropogenic substances (Svejkovsky and Jones 2001, Gierach et al. 2016, Holt et al. 2017) when optical sensors might be limited by cloud cover or heavy atmospheric haze. The primary purpose of these satellites for this project will be to provide another look at the TJR discharge plume to assess its extent and direction of flow. The runoff often contains the natural and anthropogenic surfactants that dampen the SAR signal and therefore make it detectable in the data. **Figure 37** shows a sample SAR image from 02/01/22 highlighting a potential surfactant signature from the TJR discharge. Note that the potentially contaminated water is moving northward.

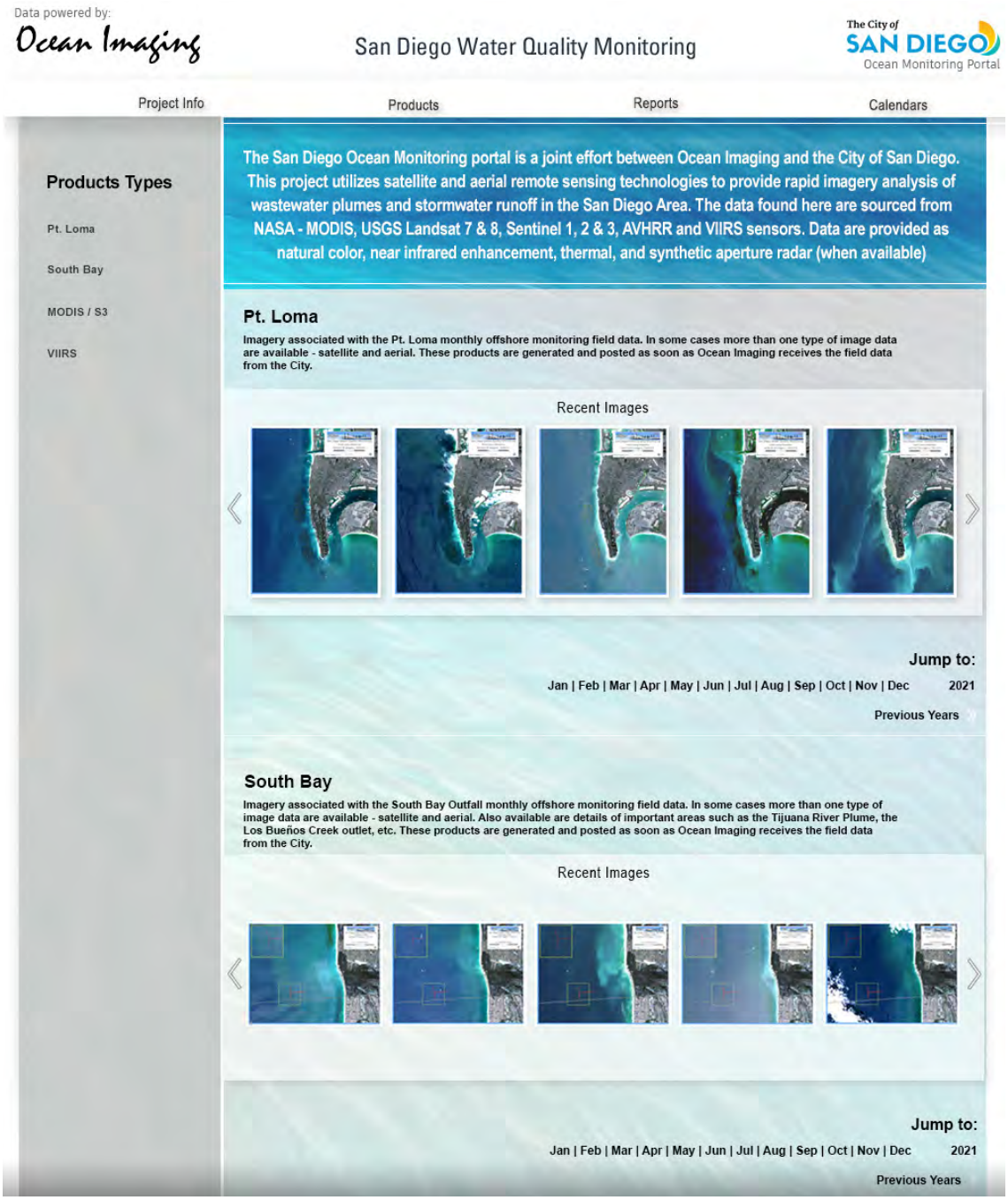

Figure 36. Sample front page of updated SDWQ web site providing near-real time access to the remote sensing data acquired and processed for this project. The new site is expected to be live in the summer of 2022.

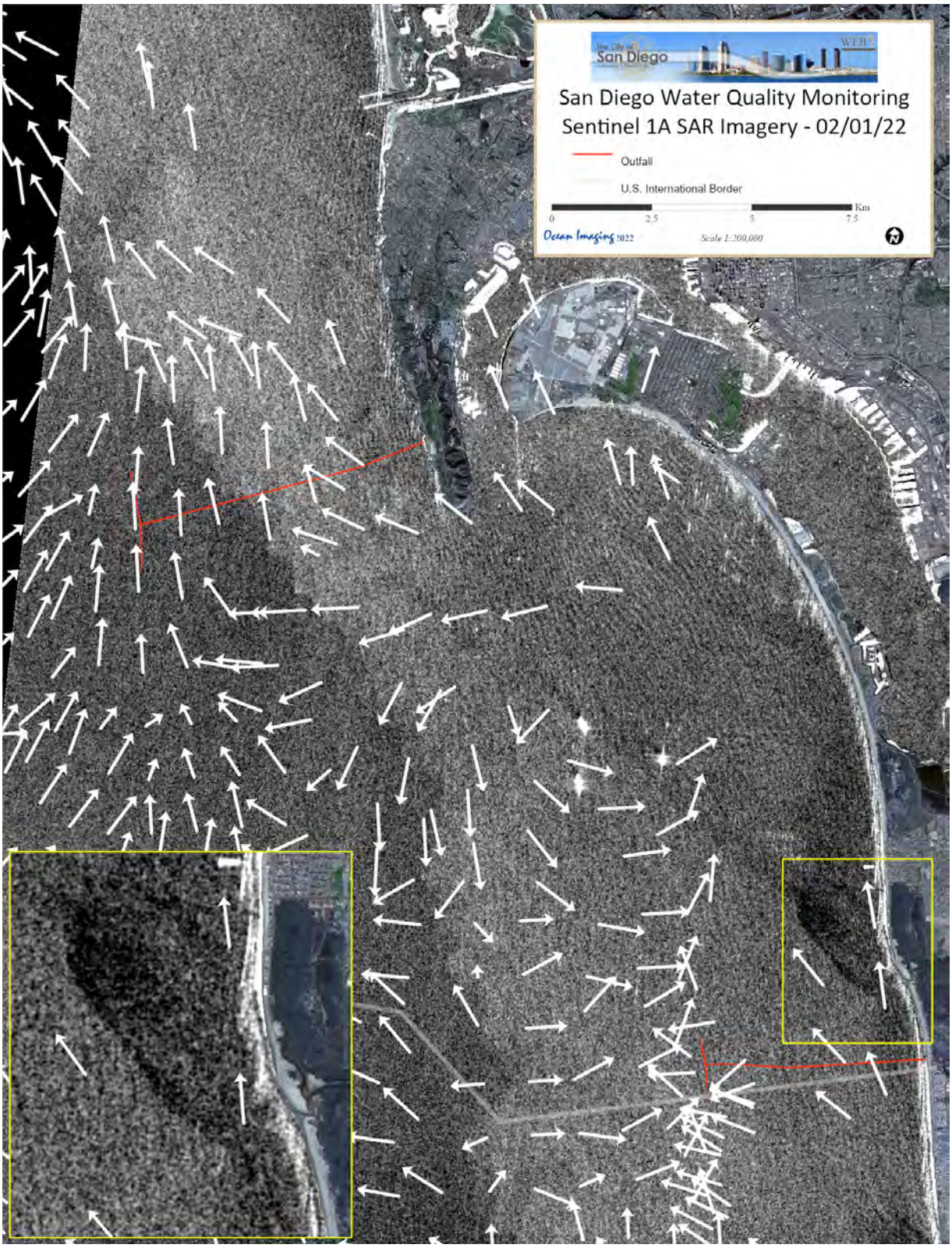

Figure 37 Sentinel 1A SAR image showing possibly contaminated TJR discharge plume moving north farther into San Diego Waters. The image was acquired on 02/01/21 at 13:45 UTC. The 25-hour averaged HF Radar currents from 14:00 UTC are overlaid to further document the northward surface flow. No other high resolution remote sensing data were available on this day, so this SAR dataset offers an additional observation of the core of the TJR plume's extent and direction.

7. REFERENCES

Amaya, Dillon J., et al. "Physical Drivers of the Summer 2019 North Pacific Marine Heatwave." Nature Communications, vol. 11, no. 1, 2020, https://doi.org/10.1038/s41467-020-15820-w.

[APHA] American Public Health Association. (2012). Standard Methods for the Examination of Water and Wastewater, 22nd edition. American Public Health Association, American Water Works Association, and Water Environment Federation.

Axiak, V., Pavlakis, P., Sieber, A. J., Tarchi, D., 2000. Re-assessing the extent of impact of Malta's (Central Mediterranean) major sewage outfall using ERS SAR. Marine Pollution Bulletin, 40(9), 734 – 738.

Bell, Tom W., et al. "Three Decades of Variability in California's Giant Kelp Forests from the Landsat Satellites." Remote Sensing of Environment, vol. 238, 2020, p. 110811., https://doi.org/10.1016/j.rse.2018.06.039.

Bertrand-Krajewski, J.-L., Chebbo, G., Saget, A., 1998. Distribution of pollutant mass vs volume in stormwater discharges and the first flush phenomenon. WaterResearch 32, 2341–2356.

Bird, E., Lewis, N., 2015. Beach Renourishment, Springer Briefs in Earth Sciences, pp. 135, DOI 10.1007/978-3-319-09728-2_2.

Bordner, R., Winter, J., Scarpino, P., eds., 1978. Microbiological Methods for Monitoring the Environment: Water and Wastes, EPA Research and Development, EPA-600/8-78-017.

California State Water Quality Control Board. "Search Beach Monitoring Data." SWRCB.gov, https://www.waterboards.ca.gov/water_issues/programs/beaches/search_beach_advisory.html.

[CDPH] California State Department of Public Health website. (2019). Regulations for Public Beaches and Ocean Water-Contact Sports Areas. Appendix A: Assembly Bill 411, Statutes of 1997, Chapter765. https://www.cdph.ca.gov/Programs/CEH/DRSEM/Pages/EMB/RecreationalHealth/Beaches-and-Recreational-Waters.aspx

City of San Diego. (2020). Biennial Receiving Waters Monitoring and Assessment Report for the Point Loma and South Bay Ocean Outfalls, 2018-2019. City of San Diego, Public Utilities Department, Environmental Monitoring and Technical Services Division, San Diego, CA.

Cristina, C.M., Sansalone, J.J., 2003. First flush, power law and particle separation diagrams for urban storm-water suspended particulates. Journal of Environmental Engineering-ASCE 129, 298–307.

Di Lorenzo, Emanuele, and Nathan Mantua. "Multi-Year Persistence of the 2014/15 North Pacific Marine Heatwave." Nature Climate Change, vol. 6, no. 11, 2016, pp. 1042–1047., https://doi.org/10.1038/nclimate3082. [ELAP] Environmental Laboratory Accreditation Program https://www.waterboards.ca.gov/drinking_water/certlic/labs/index.html

"Frequently Asked Questions About El Nino and La Nina." Climate Prediction Center - Enso FAQ, 26 Apr. 2012, https://origin.cpc.ncep.noaa.gov/products/analysis_monitoring/ensostuff/ensofaq.shtml#general.

Gersberg, R.M., Daft, D., Yorkey, D., 2004. Temporal pattern of toxicity in runoff from the Tijuana River Watershed. Water Research 38, 559–568.

Gersberg, R.M., Rose, M.A., Robles-Sikisaka, R., Dhar, A.K., 2006. Quantitative detection of hepatitis a virus and enteroviruses near the United States-Mexico border and correlation with levels of fecal indicator bacteria. Applied and Environmental Microbiology 72, 7438–7444.

Gersberg, R., Tiedge, J., Gottstein, D., Altmann, S., Watanabe, K., Luderitz, V., 2008. Effect of the South Bay Ocean Outfall (SBOO) on ocean beach water quality near the USA-Mexico border. International Journal of Environmental Health Research 18, 149–158.

Gierach, M. M., Holt, B., Trinh, R., Pan, B.J., Rains, C., 2017. Satellite detection

of wastewater diversion plumes in Southern California. Estuarine, Coastal and Shelf Science, 186, 171 – 182.

Graf, C., Tinney, C., Konner, T., 2005. Water and wastewater at the international boundary. Southwest Hydrology, September/October, 16-18.

"Harmful Algal Blooms." Southern California Coastal Water Research Project, 10 May 2019, https://www.sccwrp.org/about/research-areas/eutrophication/harmful-algal-blooms/.

Holt, B., Trinh, R., Gierach, M. M., 2017. Stormwater runoff plumes in the Southern California Bight: A comparison study with SAR and MODIS imagery. Marine Pollution Bull. Vol. 118, 141-154.

Howden, M., 1995. Application of remote sensing for monitoring the Sydney deepwater ocean outfalls. Trans. on Ecology and Environment,7, 269-276.

Hyde, K. J. W., O'Reilly, J.E., Oviatt, C.A., 2007. Validation of SeaWiFS chlorophyll a in Massachusetts Bay. Continental Shelf Research, 27(12), 1677 – 1691.

Inman, Douglas L., and Scott A. Jenkins. "Climate Change and the Episodicity of Sediment Flux of Small California Rivers." The Journal of Geology, vol. 107, no. 3, 1999, pp. 251–270., https://doi.org/10.1086/314346.

Keeler, R. N., Bondur, V.G., Gibson, C. H., 2005. Optical satellite imagery detection of internal wave effects from a submerged turbulent outfall in the stratified ocean. Geophys. Research Letters, 32, L12610.

Luković, Jelena, et al. "A Later Onset of the Rainy Season in California." Geophysical Research Letters, vol. 48, no. 4, 2021, https://doi.org/10.1029/2020gl090350.

Marmorino, G. O., Smith, G. B., Miller, W.D., Bowles, J., 2010. Detection of a buoyant coastal wastewater discharge using airborne hyperspectral and infrared imagery. J. of Applied Remote Sensing, 4(1), 043502.

MBS Applied Environmental Sciences, 2017. Status of the Kelp Beds in 2016. Annual Report, http://kelp.sccwrp.org/2016/Status_of_the_Kelp_Beds_2016_Ventura_Los%20Angeles_Orange_and_San_Diego_Counties.pdf

National Weather Service Corporate Image Web Team. "NWS San Diego." National Weather Service, 24 Oct. 2005, w2.weather.gov/climate/index.php?wfo=sgx.

Nezlin, N. P., DiGiacomo, P.M., Stein, E.D., Ackerman, D., 2005. Stormwater runoff plumes observed by SeaWiFS radiometer in the Southern California Bight. Remote Sensing of Environment, 98, 494 – 510.

[NOAA] National Oceanic and Atmospheric Administration. (2022). National Climatic Data Center. http://www7.ncdc.noaa.gov/CDO/cdo.

Ocean Fact Sheet Package - United Nations. https://www.un.org/sustainabledevelopment/wp-content/uploads/2017/05/Ocean-fact-sheet-package.pdf.

Ouillon, S., Forget, P., Froidefond, J-M., Naudin, J-J., 1997. Estimating suspended matter concentrations from SPOT data and from field measurements in the Rhone River plume. Marine Tech. Society Journal, 31(2), 15-20.

Rogowski, Peter, et al. "Mapping Ocean Outfall Plumes and Their Mixing Using Autonomous Underwater Vehicles." Journal of Geophysical Research: Oceans, vol. 117, no. C7, 2012, https://doi.org/10.1029/2011jc007804.

Roughan, M., Terrill, E.J., Largier, J.L., Otero, M.P., 2005. Observations of divergence and upwelling around Point Loma, California. J. Geophys. Res., 110, C04011.

Ruddick, K. G., Lahousse, L., Donnay, E., 1994. Location of the Rhine plume front by airborne remote sensing. Continental Shelf Res., 14(4), 325 – 332.

San Diego Regional Water Quality Control Board,2022. "International Boundary and Water Commission Transboundary Flow Reports." International Boundary and Water Commission Spill Reports | San Diego Regional Water Quality Control Board, https://www.waterboards.ca.gov/sandiego/water_issues/programs/

tijuana_river_valley_strategy/spill_report.html.
San Diego Regional Water Quality Control Board, 2020. "Sewage Pollution within the Tijuana River Watershed." Sewage Pollution within the Tijuana River Watershed | San Diego Regional Water Quality Control Board, https://www.waterboards.ca.gov/sandiego/water_issues/programs/tijuana_river_valley_strategy/sewage_issue.html.
Schiff, K. C., Allen, M.J., Zeng, E.Y., Bay, S.M., 2000. Southern California. Mar. Pollut. Bull. 41(1-6), 76-93.
Schroeder, S. B., C. Dupont, L. Boyer, F. Juanes, and M. Costa. 2019. Passive remote sensing technology for mapping bull kelp (Nereocystis luetkeana): a review of techniques and regional case study. Glob. Ecol. Conserv. 19, e00683.
SCCOOS Automated Shore Station, Institution: Scripps, University of California San Diego (Dataset ID: autoss) https://erddap.sccoos.org/erddap/tabledap/autoss.html?time,pressure,pressure_flagPrimary,temperature,temperature_flagPrimary,chlorophyll,chlorophyll_flagPrimary,salinity,salinity_flagPrimary&station=%22scripps_pier%22&time%3E=2020-12-30T08:00:00.000Z&time%3C2022-01-01T07:59:59.000Z&orderBy(%22time%22)
Svejkovsky, J., Haydock, I., 1998. Satellite remote sensing as part of an ocean outfall environmental monitoring program. In: Taking a Look at California's Ocean Resources: An Agenda for the Future, ASCE, Reston, VA (USA), 2, 1306.
Svejkovsky, J., Jones, B., 2001. Satellite Imagery Detects Coastal Stormwater and Sewage Runoff. EOS-Trans. American Geophys. Union, 82(50).
Svejkovsky, J., Shandley, J., 2001. Detection of offshore plankton blooms with AVHRR and SAR imagery. Int. J. of Remote Sensing, 22 (2&3), 471-485.
Svejkovsky, J., Nezlin, N. P., Mustain, N.M. Kum, J. B., 2010. Tracking storm water discharge plumes and water quality of the Tijuana River with multispectral aerial imagery. Estuarine, Coastal and Shelf Science. 87(3), 387-398.
Tiefenthaler, L.L., Schiff, K.C., 2003. Effects of rainfall intensity and duration on first flush of stormwater pollutants. In: Weisberg, S.B., Elmore, D. (Eds.).
Southern California Coastal Water Research Project Annual Report 2001–2002. Southern California Coastal Water Research Project Authority, Westminster, CA, pp. 209–215.
Trinh R.C., Fichot C.G., Gierach M.M., Holt B., Malakar N.K., Hulley G. Smith J., 2017. Application of Landsat 8 for Monitoring Impacts of Wastewater Discharge on Coastal Water Quality. Frontiers in Marine Science, 4:329
United Nations, 2009. Percentage of Total Population Living in Coastal Areas. http://www.un.org/esa/sustdev/natlinfo/indicators/methodology_sheets/oceans_seas_coasts/pop_coastal_areas.pdf
[USEPA] United States Environmental Protection Agency. (2014). Method 1600: Enterococci in Water by Membrane Filtration Using membrane-Enterococcus Indoxyl-β-D-Glucoside Agar (mEI). EPA Document EPA-821-R-14-011. Office of Water (4303T), Washington, DC.
Walker, N. D., Wiseman, W.J., Rouse, L.J., Babin, A., 2005. Effects of river discharge, wind stress, and slope eddies on circulation and satellite-observed structure of the Mississippi River plume. J. of Coastal Res., 21(6), 1228 – 1244.
Warrick, J.A., DiGiacomo, P.M., Weisberg, S.B., Nezlin, N.P., Mengel, M.J., Jones, B.H., Ohlmann, J.C., Washburn, L., Terrill, E.J., Farnsworth, K.L., 2007. River plume patterns and dynamics within the Southern California Bight. Continental Shelf Research 27, 2427–2448.
Werme, C., Hunt, C.D., 2000. 1998 Outfall monitoring overview. Boston: Massachusetts Water Resources Authority. Report ENQUAD 00-04. 66 pp.

APPENDIX A – 2021 HIGH RESOLUTION SATELLITE IMAGERY SHOWING SBOO-RELATED WASTEWATER PLUME

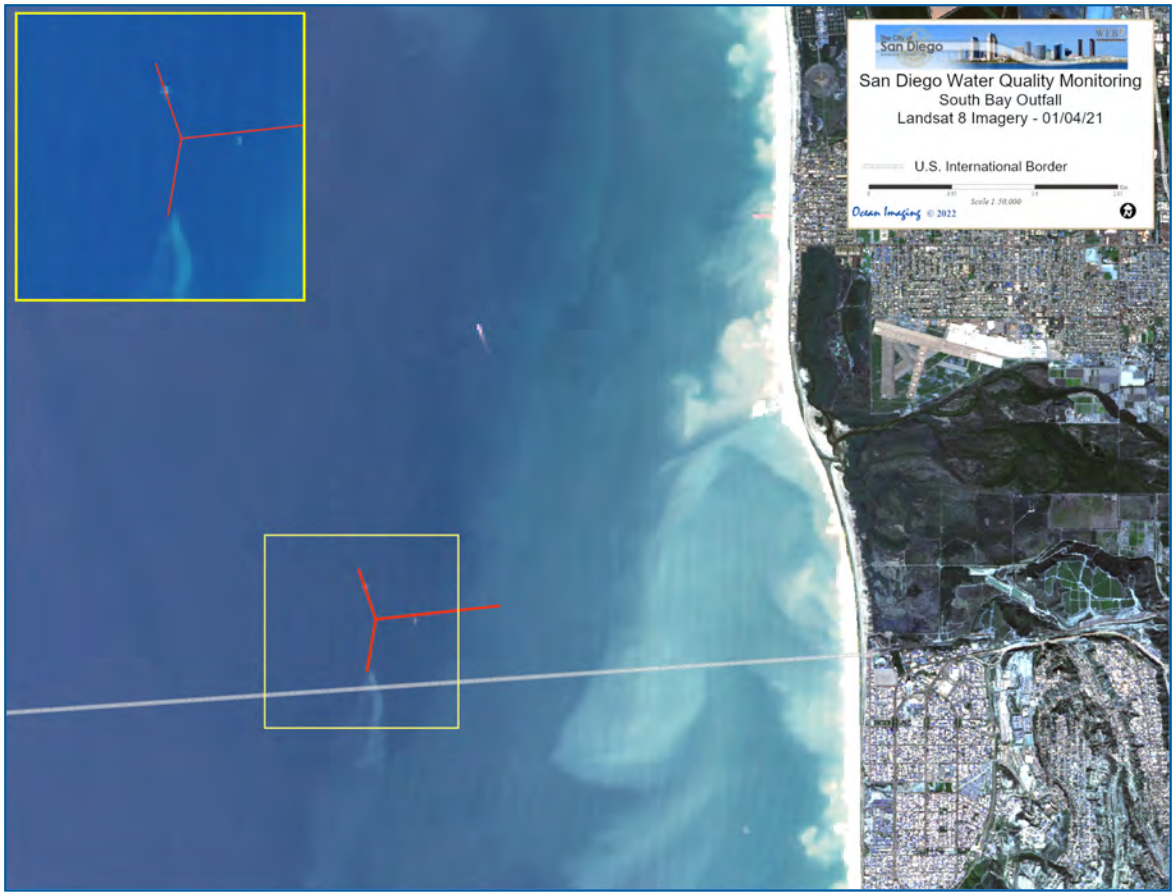

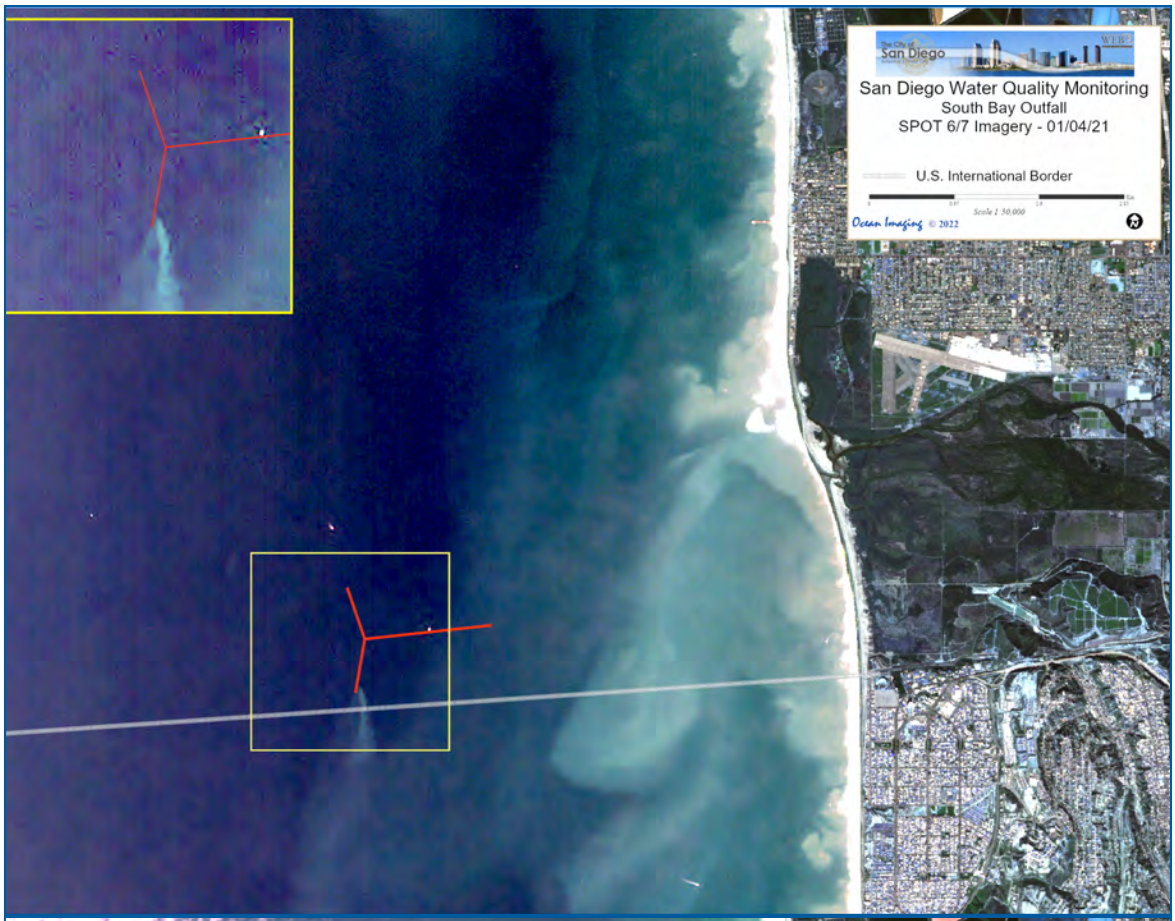
San Diego Water Quality Monitoring
South Bay Outfall
SPOT 6/7 Imagery - 01/04/21
U.S. International Border
Ocean Imaging © 2022

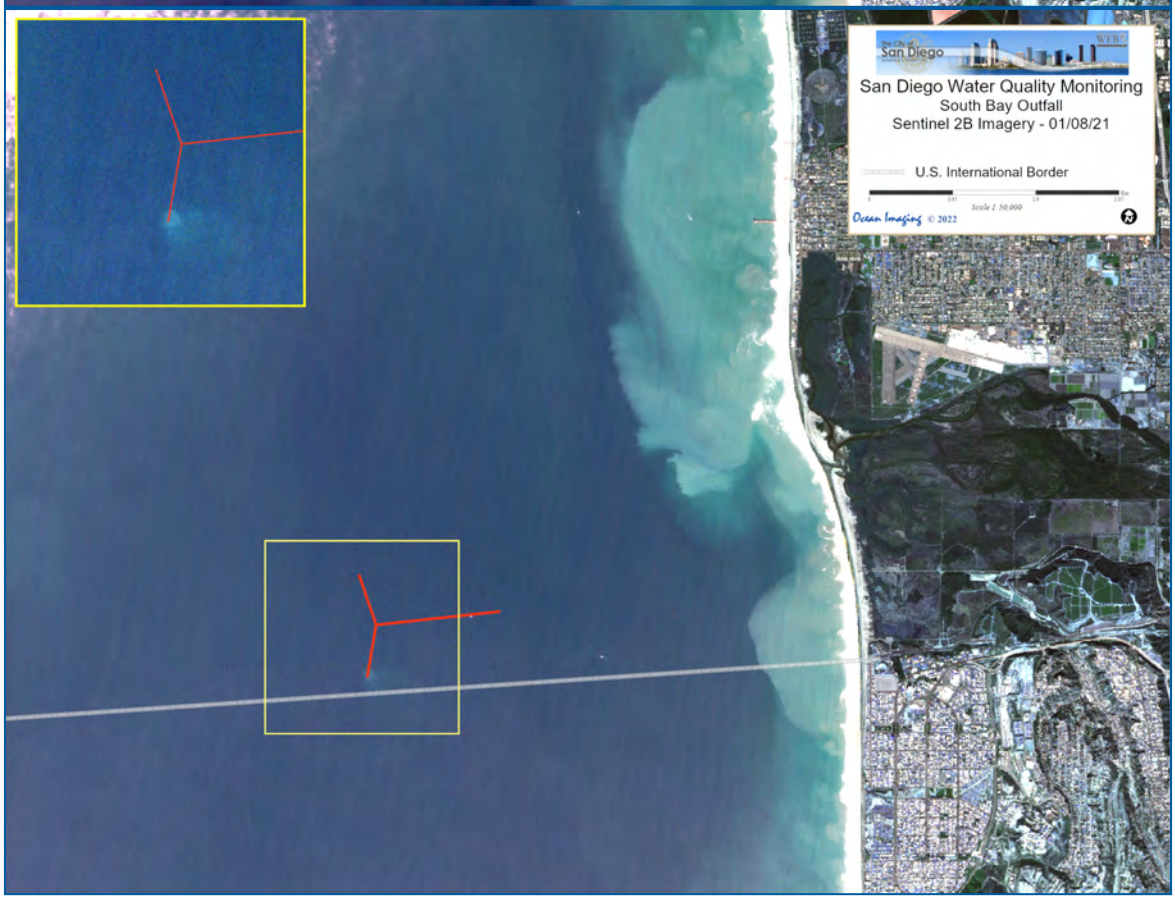
San Diego Water Quality Monitoring
South Bay Outfall
Sentinel 2B Imagery - 01/08/21
U.S. International Border
Ocean Imaging © 2022

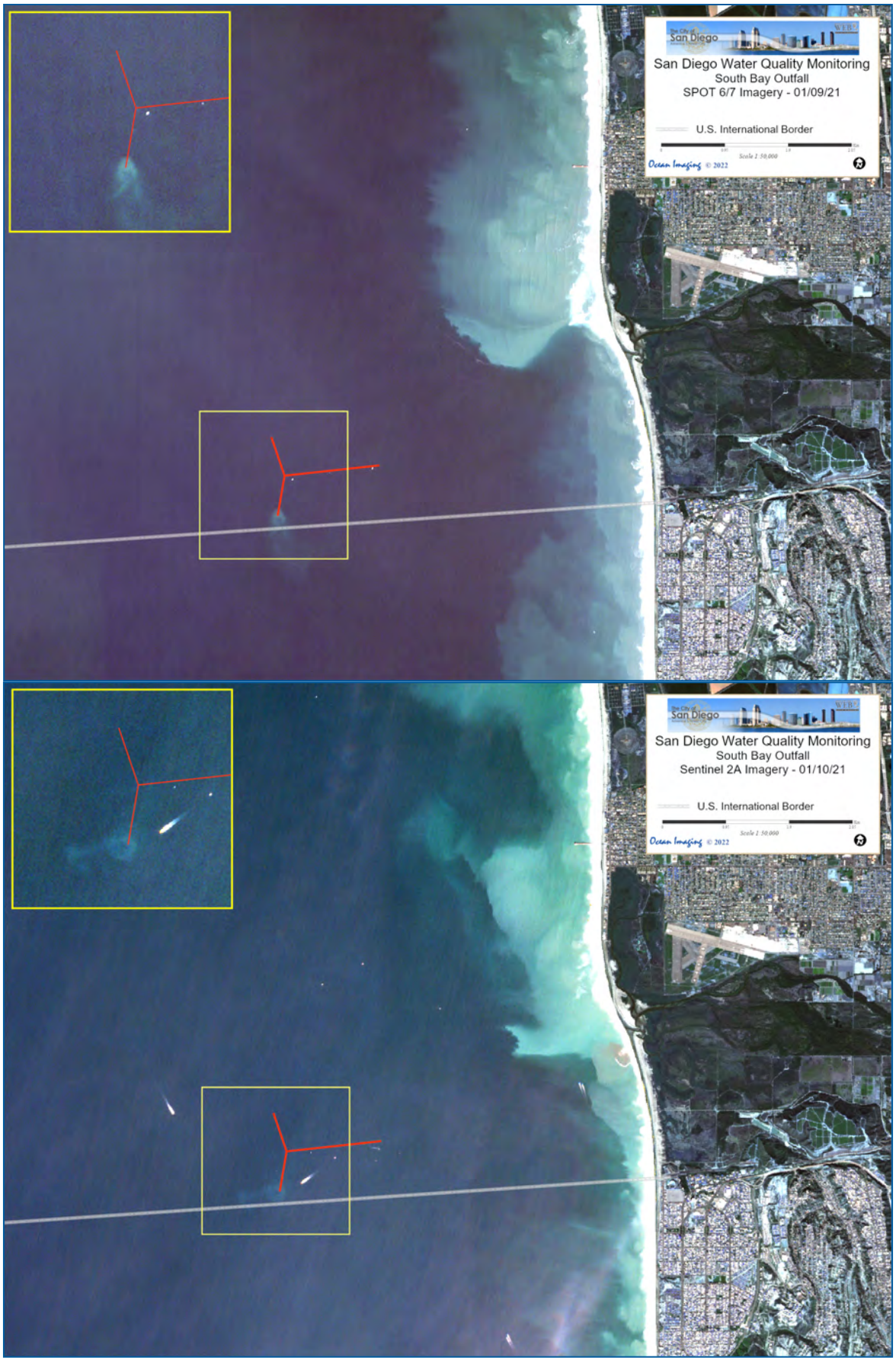
San Diego
San Diego Water Quality Monitoring
South Bay Outfall
SPOT 6/7 Imagery - 01/09/21
U.S. International Border
Ocean Imaging © 2022
San Diego
San Diego Water Quality Monitoring
South Bay Outfall
Sentinel 2A Imagery - 01/10/21
U.S. International Border
Ocean Imaging © 2022

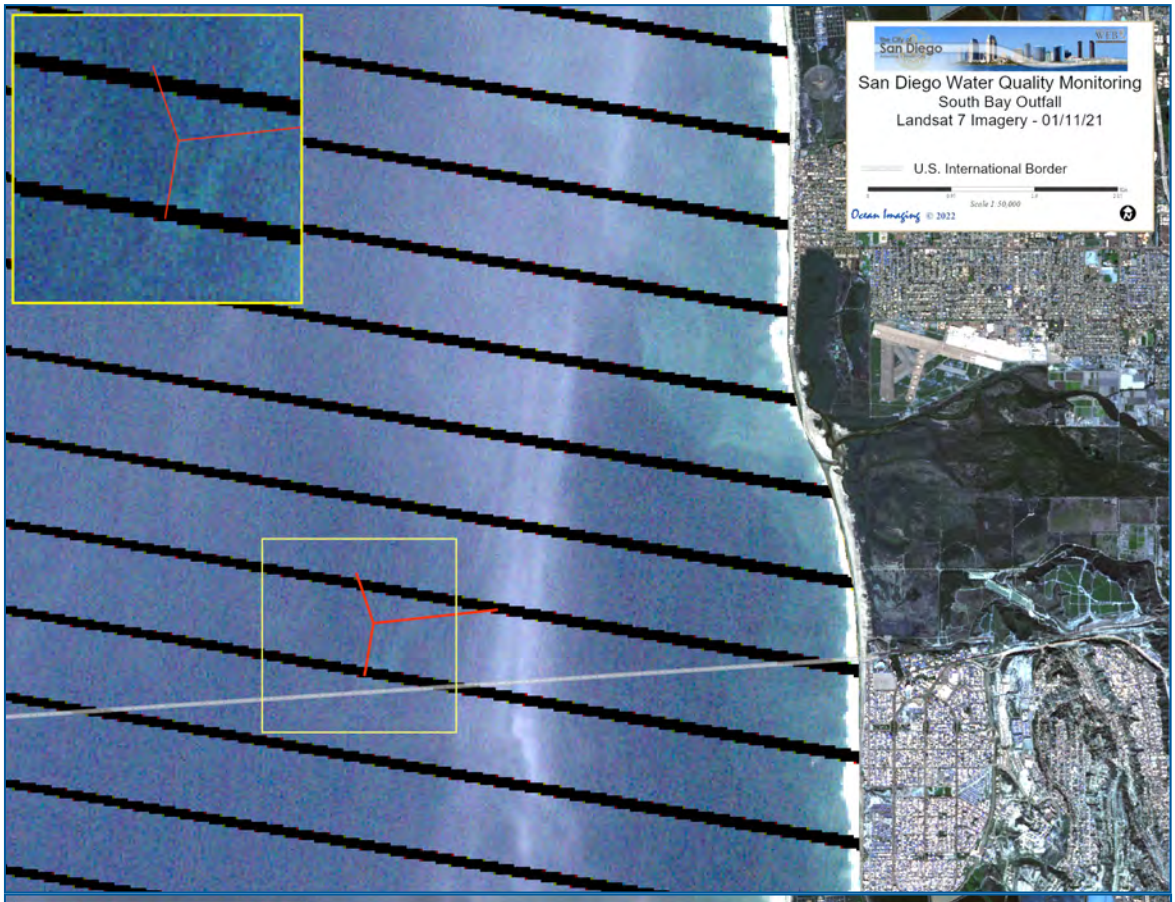
San Diego Water Quality Monitoring
South Bay Outfall
Landsat 7 Imagery - 01/11/21
U.S. International Border
Ocean Imaging © 2022

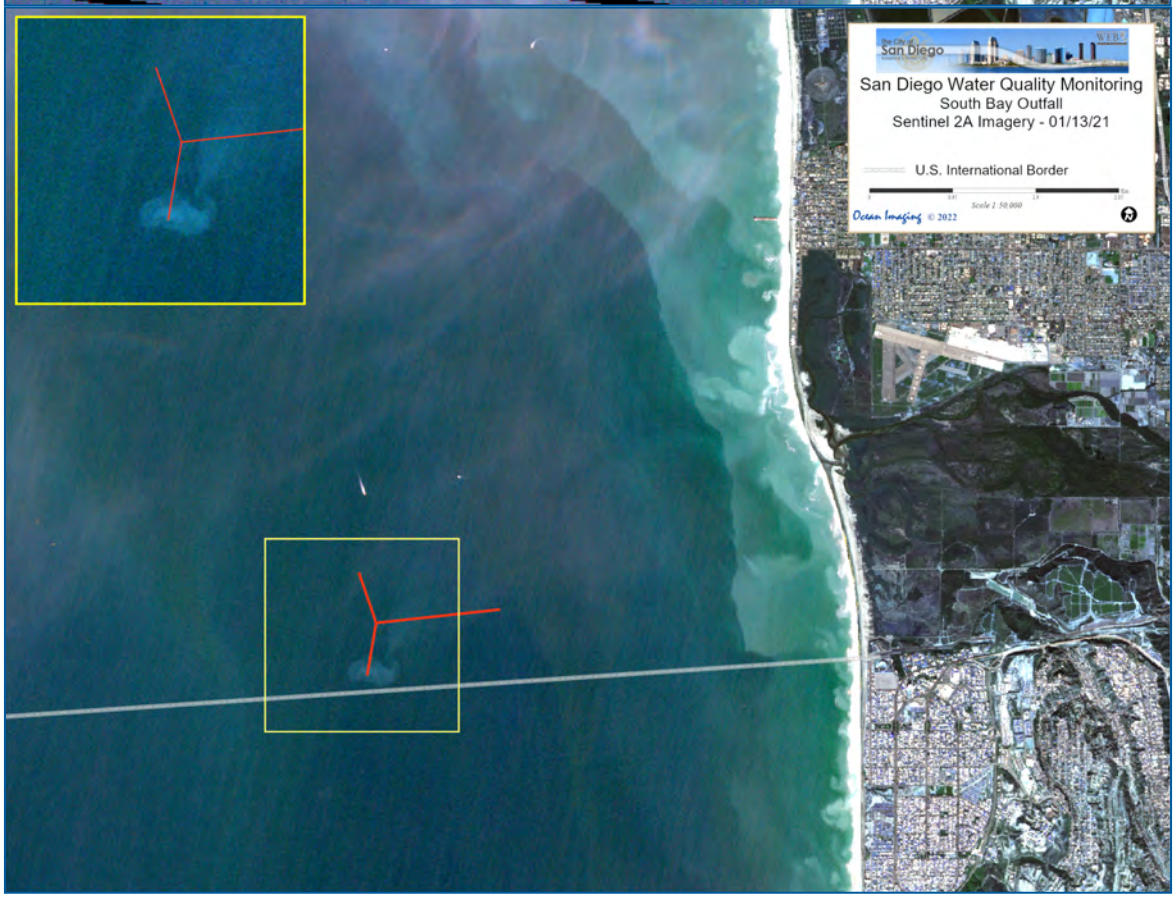
San Diego Water Quality Monitoring
South Bay Outfall
Sentinel 2A Imagery - 01/13/21
U.S. International Border
Ocean Imaging © 2022

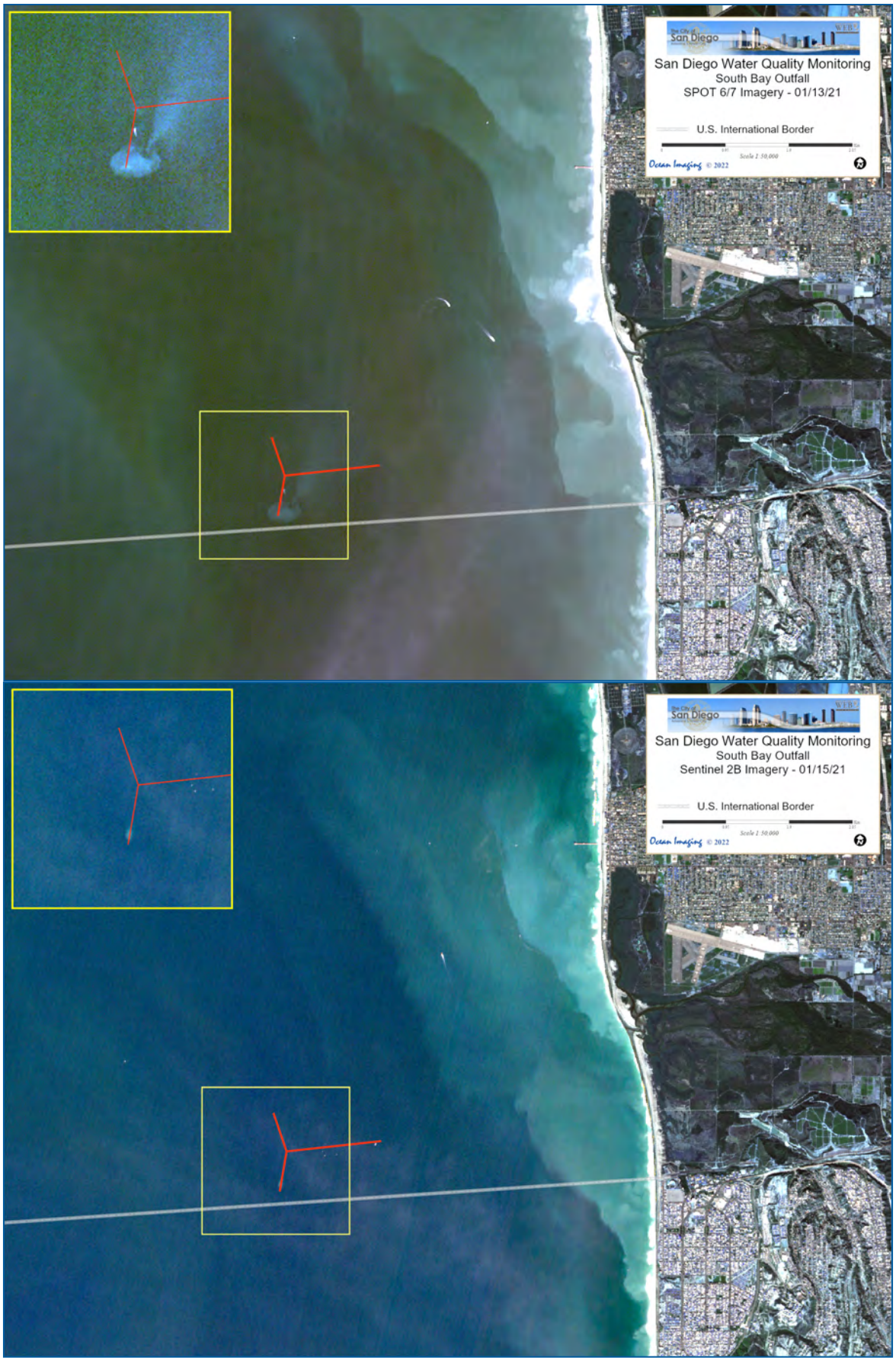
San Diego
San Diego Water Quality Monitoring
South Bay Outfall
SPOT 6/7 Imagery - 01/13/21
U.S. International Border
Ocean Imaging © 2022
San Diego
San Diego Water Quality Monitoring
South Bay Outfall
Sentinel 2B Imagery - 01/15/21
U.S. International Border
Ocean Imaging © 2022

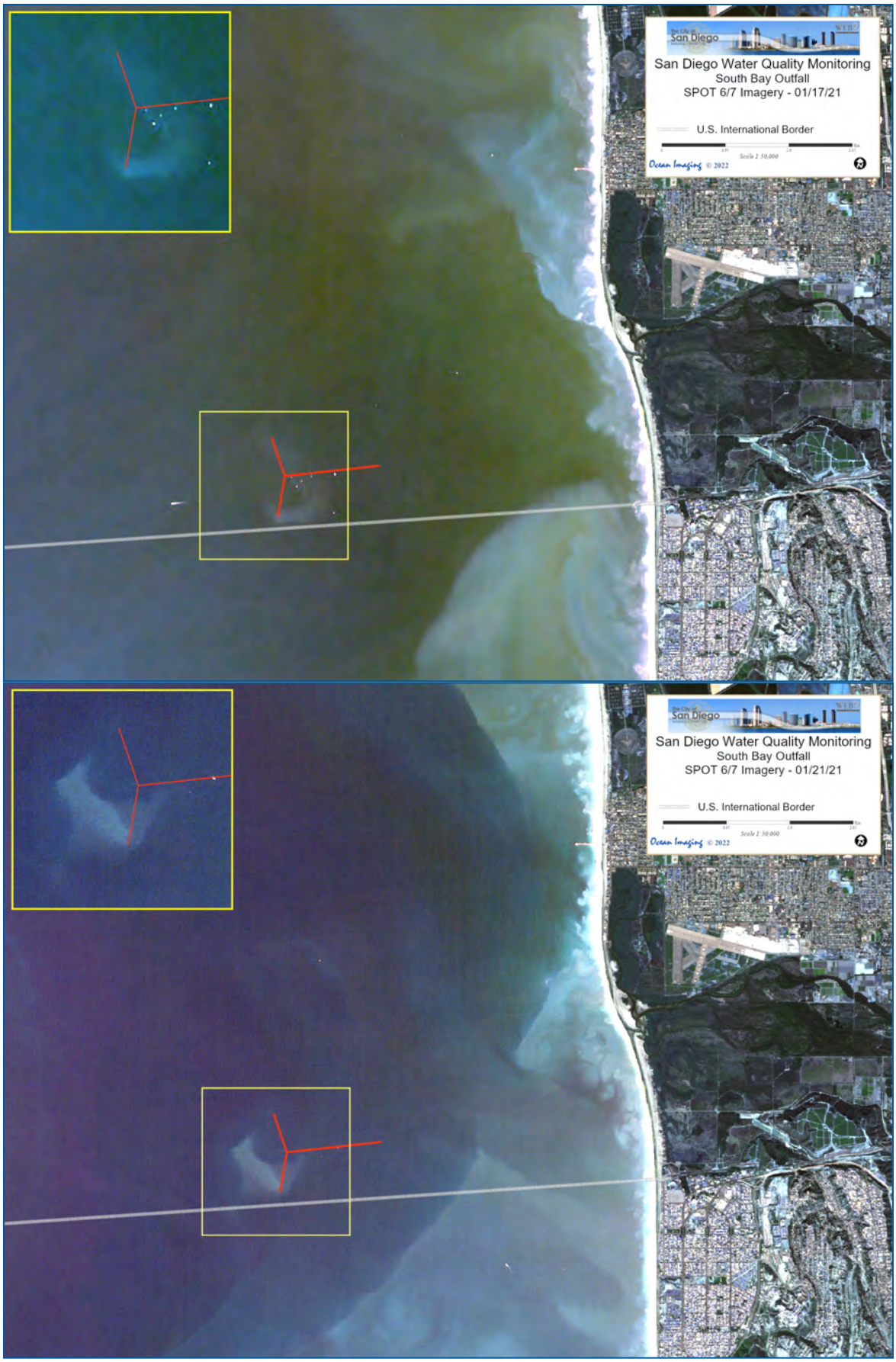
San Diego
San Diego Water Quality Monitoring
South Bay Outfall
SPOT 6/7 Imagery - 01/17/21
U.S. International Border
Ocean Imaging © 2022
San Diego
San Diego Water Quality Monitoring
South Bay Outfall
SPOT 6/7 Imagery - 01/21/21
U.S. International Border
Ocean Imaging © 2022

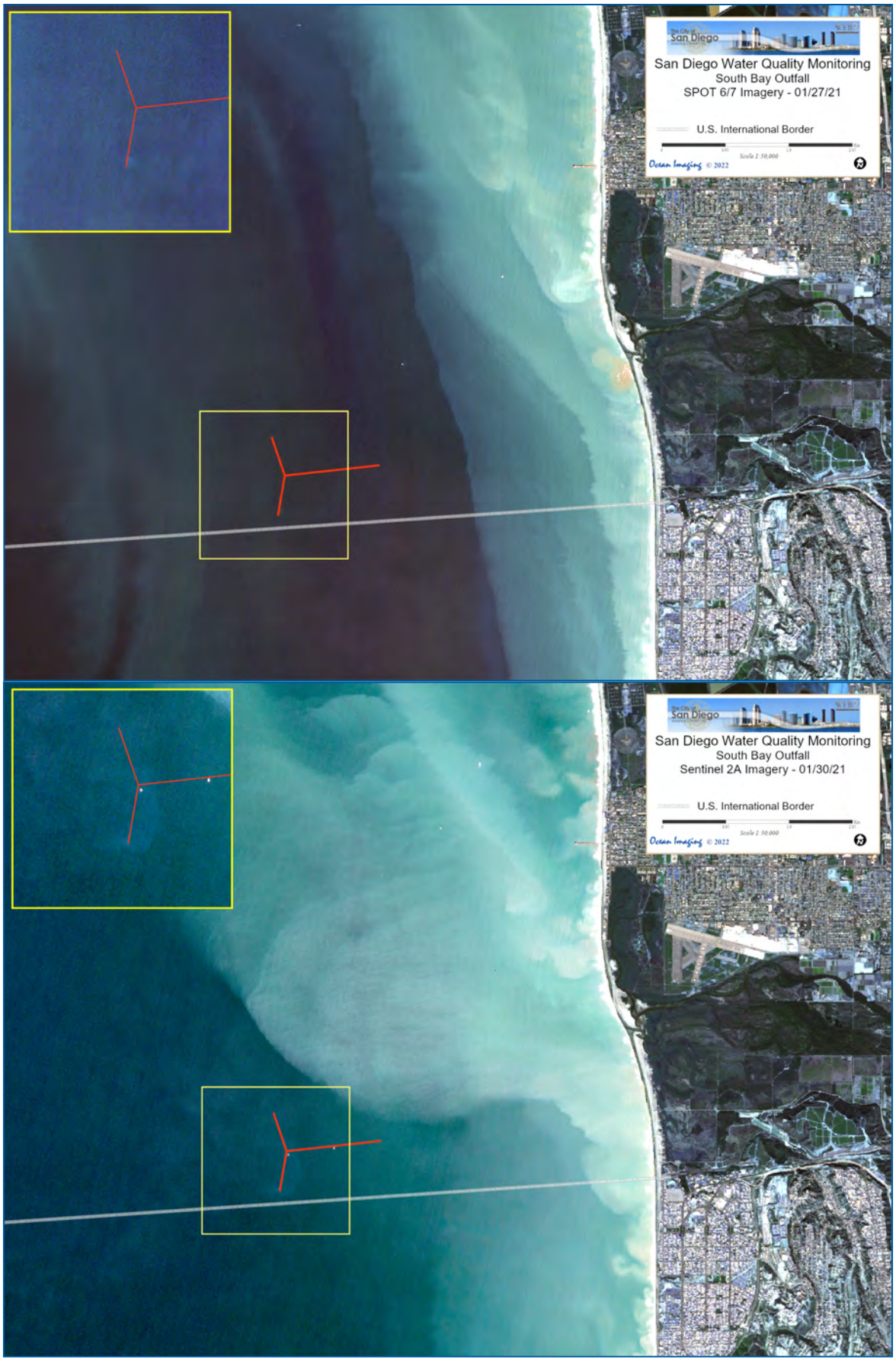
San Diego
San Diego Water Quality Monitoring
South Bay Outfall
SPOT 6/7 Imagery - 01/27/21
U.S. International Border
Ocean Imaging © 2022
San Diego
San Diego Water Quality Monitoring
South Bay Outfall
Sentinel 2A Imagery - 01/30/21
U.S. International Border
Ocean Imaging © 2022

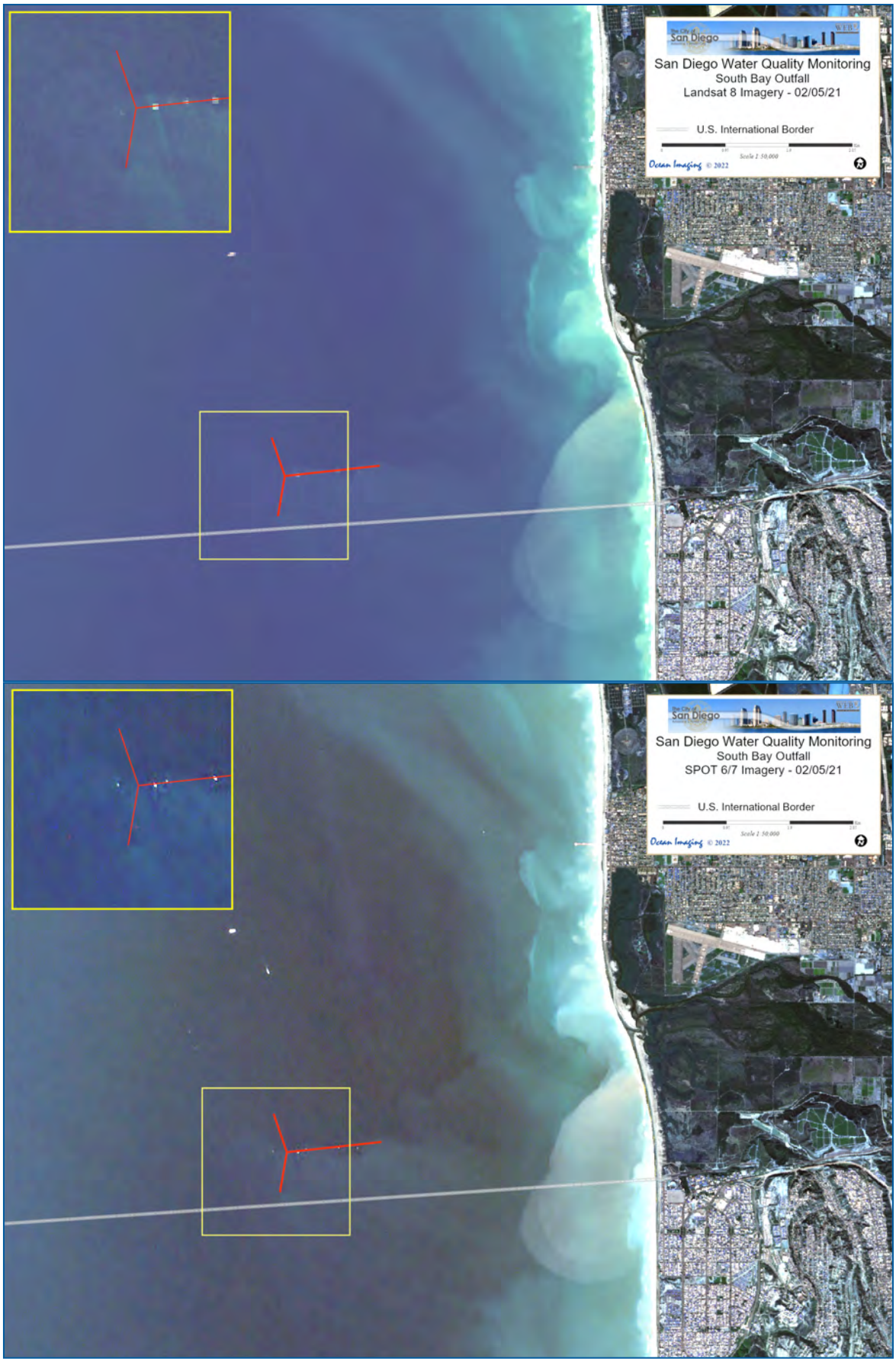
San Diego
San Diego Water Quality Monitoring
South Bay Outfall
Landsat 8 Imagery - 02/05/21
U.S. International Border
Ocean Imaging © 2022
San Diego
San Diego Water Quality Monitoring
South Bay Outfall
SPOT 6/7 Imagery - 02/05/21
U.S. International Border
Ocean Imaging © 2022

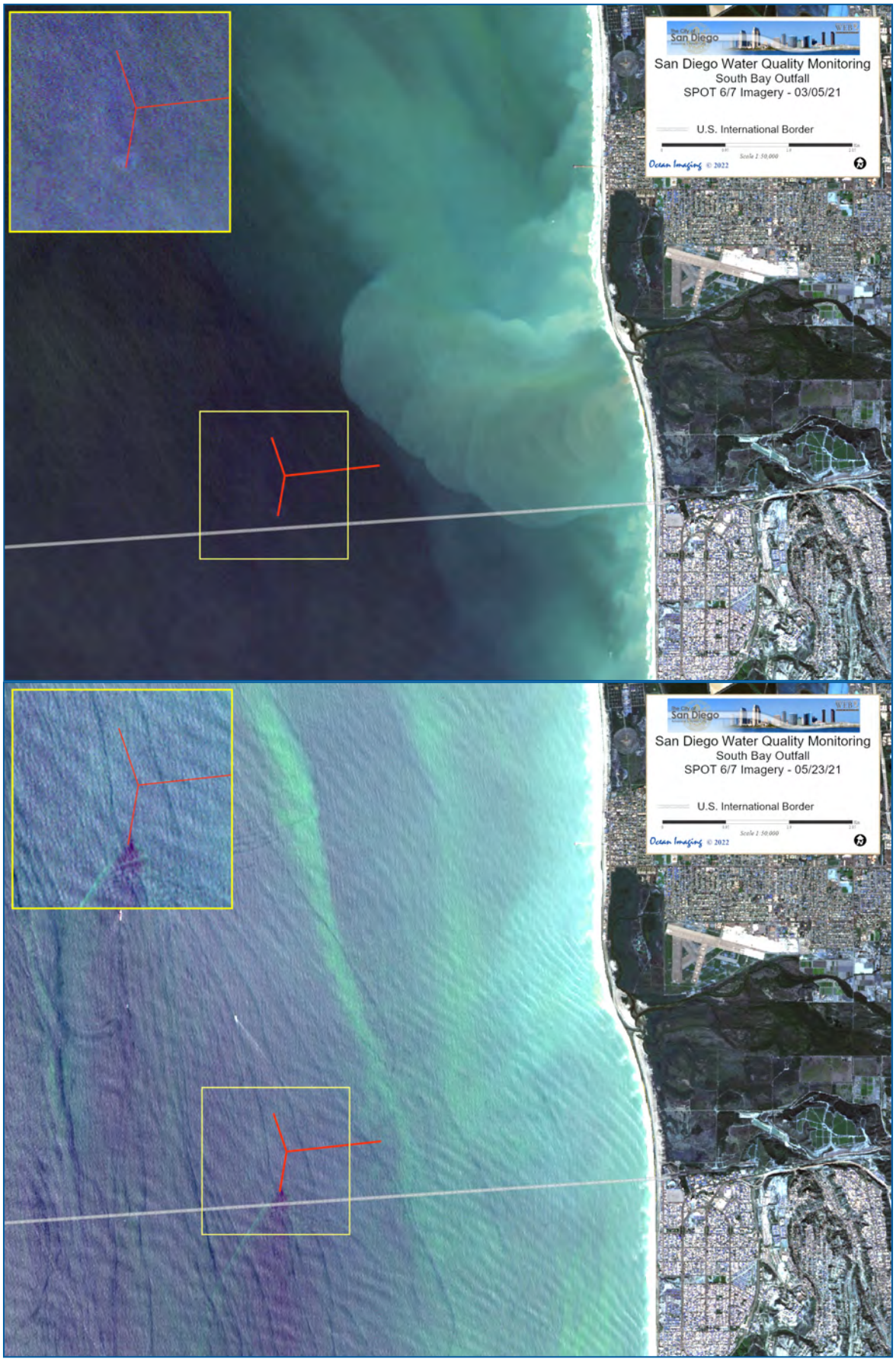
San Diego Water Quality Monitoring
South Bay Outfall
SPOT 6/7 Imagery - 03/05/21
U.S. International Border
Ocean Imaging © 2022
San Diego Water Quality Monitoring
South Bay Outfall
SPOT 6/7 Imagery - 05/23/21
U.S. International Border
Ocean Imaging © 2022

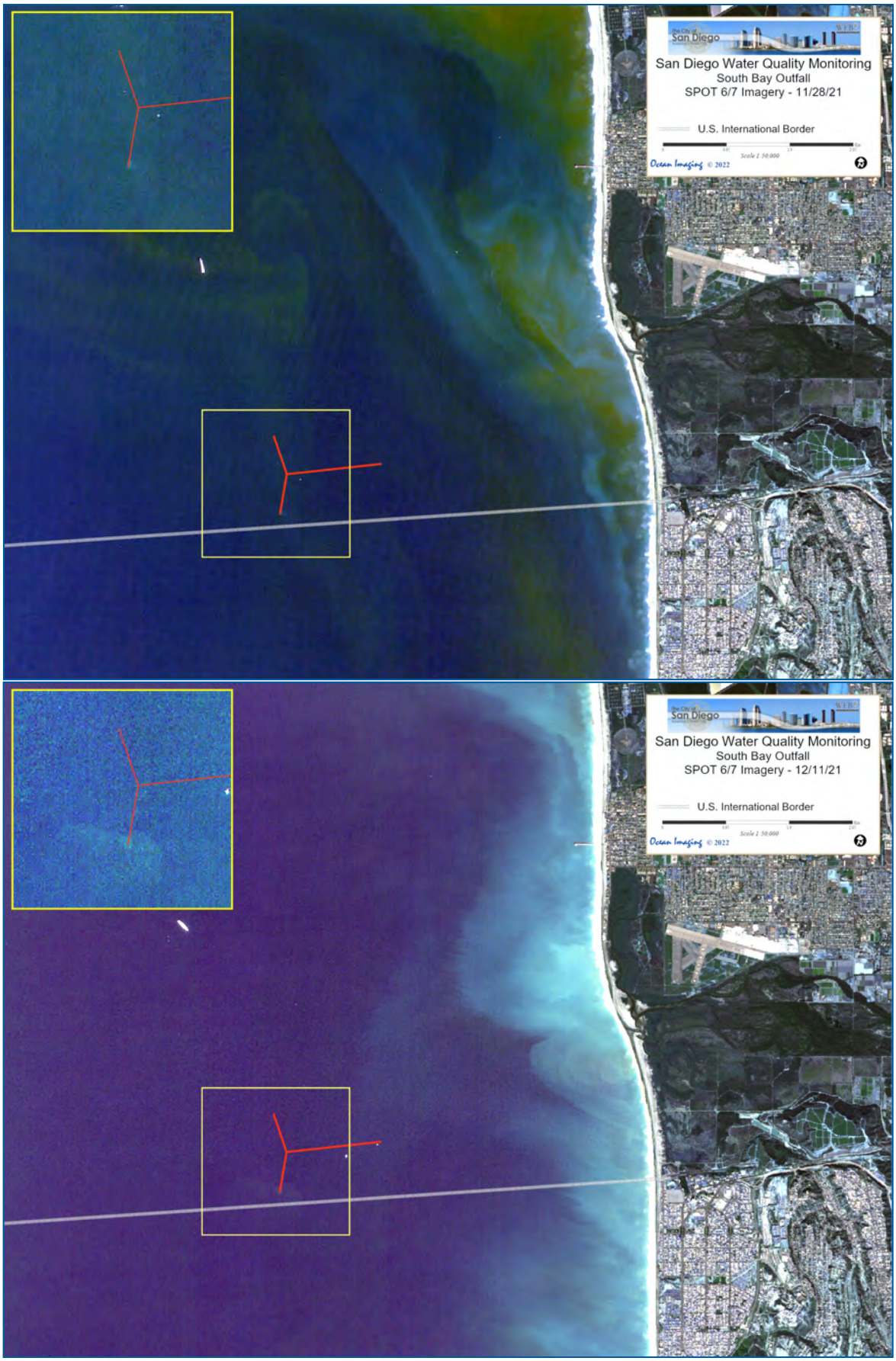
San Diego Water Quality Monitoring
South Bay Outfall
SPOT 6/7 Imagery - 11/28/21
U.S. International Border
Ocean Imaging © 2022
San Diego Water Quality Monitoring
South Bay Outfall
SPOT 6/7 Imagery - 12/11/21
U.S. International Border
Ocean Imaging © 2022

Appendix C

Coastal Oceanographic Conditions

2020 – 2021 Supplemental Analyses

Appendix C.1

Sample dates for quarterly oceanographic surveys conducted during 2020 and 2021. All stations in each station group were sampled on a single day (see Figure 2.1 for stations and locations).

	2020				2021			
	Winter	**Spring**	**Summer**	**Fall**	**Winter**	**Spring**	**Summer**	**Fall**
PLOO Station Group								
Kelp WQ	Feb-18	May-18	Aug-17	Nov-11	Feb-22	May-10	Aug-9	Nov-8
18 & 60-m WQ	Feb-20	May-22	Aug-19	Nov-12	Feb-24	May-12	Aug-11	Nov-10
80-m WQ	Feb-21	May-21	Aug-20	Nov-13	Feb-25	May-13	Aug-12	Nov-12
98-m WQ	Feb-19	May-20	Aug-18	Nov-10	Feb-23	May-11	Aug-10	Nov-9
SBOO Station Group								
Kelp WQ	Feb-10	May-26	Aug-27	Nov-8	Feb-11	May-3	Aug-2	Nov-2
North WQ	Feb-14	May-29	Aug-25	Nov-11	Feb-15	May-5	Aug-5	Nov-3
Mid WQ	Feb-13	May-28	Aug-24	Nov-10	Feb-13	May-6	Aug-4	Nov-4
South WQ	Feb-12	May-27	Aug-26	Nov-9	Feb-12	May-4	Aug-3	Nov-5

SBOO North (I28–I31, I33–I38); SBOO Mid (I12–I18, I20–I23, I27); SBOO South (I1–I11)

Appendix C.2

Location, depth, and dates for each year-long deployment of the PLOO and SBOO RTOMS. Dates are displayed by deployment, recovery, and period of real-time (RT) data availability. All times are Pacific Standard Time; DD = decimal degrees.

Site	Deployment #	Lat (DD)	Long (DD)	Total Depth (m)	Deployment	RTdata Start	RTdata End	Recovery
PLOO	2	32.66959	-117.32298	95	10/7/2019 12:40	10/7/2019 13:00	9/29/2020 15:00	9/29/2020
	3	32.66963	-117.32272	95	11/3/2021 9:23	11/3/2021 10:00	Present	—
SBOO	3	32.53185	-117.18644	31	12/18/2019 11:30	12/18/2019 12:30	12/17/2020 9:00	12/17/2020
	4	32.53177	-117.18628	31	11/3/2021 12:57	11/3/2021 14:00	Present	—

Appendix C.3

Summary of manual QA/QC review findings, including major sensor problems and data quality issues for the PLOO and SBOO RTOMS. Gaps in data resulted during time periods data were not collected or flagged as bad or suspect.

Parameter	Site	Depths	Time Period	Problem	Action Taken
pH_T	PLOO	75 m	11/20 - 12/31/21	SeaFET failure early in deployment where data became noisy and dropped to low unreasonable values	Data qualified as bad and not reported
xCO2	PLOO	1 m	11/29 - 12/31/21	ProOceanus sensor calculated incorrect values when blank sample was not completed for hourly data	Retained samples from every 12 hours when blank collected; remaining data qualified as suspect and not reported
BOD	PLOO	75 m	12/27 - 12/31/21	Uvilux sensor jumped high without corresponding change in any other parameters, then displayed noise	Data qualifed as suspect and not reported
Chlorophyll a, CDOM, and turbidity	PLOO and SBOO	1 m	11/5 - 12/31/21	Intermittent single large spikes from ECO triplet sensors, likely related to interference from buoy cage or wiper	Single point spikes qualified as suspect and not reported

Appendix C.4

Location, depth, and dates for each deployment of static moorings located at the PLOO and SBOO. DD = decimal degrees.

Site	Deployment #	Lat (DD)	Long (DD)	Total Depth (m)	Deployment
PLOO	ADCP (#2)	32.66697	117.3266	100	9/9/2021
SBOO	ADCP (#3)	32.53773	117.1987	36	9/15/2021
PLOO	Thermistor (#1) south	32.66106	117.3257	100	9/9/2021
PLOO	Thermistor (#2) north	32.66587	117.3264	100	9/9/2021
SBOO	Thermistor(#6)	32.53059	117.2013	36	9/14/2021

Appendix C.5

Data qualifier definitions for QC data flags. Follows national data standards for summary real-time data flagging (US IOOS 2017), and post-processing data flagging (ARGO 2020).

QC_Flag	Designation	Use
1	Pass/good	For data reviewed both automatically and manually
2	Provisional/unreviewed	For data that is not reviewed or unable to validate; or passed automated test only
3	Suspect/questionable	Failed automated test but not unreasonable (such as climatology test) or manually flagged as possible instrument drift (such as due to biofouling)
4	Bad	Failed automated test (such as out of range test) or manually flagged as clearly bad (such as due to instrument malfunction)
5	Value changed/drift-corrected	Used only in post-processing. Values have been corrected based on new information, such as water sample results to correct for drift or new calibration factors. For data use purposes, this flag can be treated as a “pass.” Original data are also retained separately.
9	Missing	Placeholder to show missing real-time data; may be able to be filled in later by downloaded data after mooring recovery

Appendix C.6

Ranges used for automated QC data flagging for each parameter for the gross range test. Values outside of these ranges were assigned a qualifier flag value of 4. Ranges were defined by manufacturers for each sensor configuration.

Parameter	Units	Min	Max	Deployments where applied
BOD equivalent	mg/L	0	50	All
CDOM - Eco triplet	ppb	0	375	All
Chl - Eco triplet	µg/L	0	30	PLOO_2 and SBOO_3
Chl - Eco triplet	µg/L	0	75	PLOO_3 and SBOO_4
xCO_2	ppm	0	2000	All
NO_3 (Nitrate + Nitrite)	µM	0	3000	All
NTU (Turbidity)	NTU	0	10	PLOO_2 and SBOO_3
NTU (Turbidity)	NTU	0	100	PLOO_3 and SBOO_4
O_2 (DO)	mg/L	0.1	20	All
pH (total scale; both internal and external)	pH_T	6.5	9	All
Sal (Salinity)	PSU	2	42	All
Temp (Temperature)	°C	-2.5	35	All

Appendix C.7

Annual ranges used for automated QC data flagging for each parameter, site, and depth for the climatological range test. Temperature, salinity, DO, and pH_T ranges were based on the minimum and maximum values recorded at each site and depth range where the sensors were found to be functional and in reasonable agreement with historical CTD ranges from the City's quarterly surveys. BOD ranges were based on the maximum value observed from all deployments, since that is a new parameter and historical data were not available. CDOM ranges were based on maximum of multiple readings recorded at the PLOO mooring due to proximity to plume. Chlorophyll *a* and turbidity ranges were based on the maximum sensor range for the ECO triplet. Nitrate ranges were based on values observed at both moorings where the sensors were found to be functional, and verified in a reasonable range compared to nearshore data collected by the California Cooperative Oceanic Fisheries Investigations (see: https://calcofi.org). Ranges for xCO_2 were based on values observed at both moorings, where the phytoplankton bloom in spring 2020 resulted in lower xCO_2 values than prior years, and comparable to ranges recorded by the closest NOAA/SIO carbon program mooring (CCE2, see: https://www.pmel.noaa.gov/c02/story/CCE2).

		PLOO RTOMS						SBOO RTOMS						
		1 m		Mid depths		Bottom depth (>70 m)		1 m		Mid depths		Bottom depth (>25 m)		Qualifer to assign if outside of site/ depth range
Parameter	**Units**	**Min**	**Max**	**Min**	**Max**	**Min**	**Max**	**Min**	**Max**	**Min**	**Max**	**Min**	**Max**	
BOD equivalent	mg/L	NA	NA	0	10	0	10	NA	NA	0	10	0	10	3
CDOM-ECO triplet	ppb	0	50	0	50	0	50	0	50	0	50	0	50	3
Chl-ECO triplet	µg/L	0	30	0	30	0	30	0	30	0	30	0	30	3
xCO_2	ppm	50	800	NA	NA	NA	NA	50	800	NA	NA	NA	NA	3
NO_3 (Nitrate + Nitrite)	µM	0	39	0	39	0	39	0	39	NA	NA	0	39	3
NTU (Turbidity)	NTU	0	10	0	10	0	10	0	10	0	10	0	10	3
O_2 (DO)	mg/L	5.5	24.0	3.0	9.5	2.0	7.5	5.5	24.0	3.0	11.0	2.5	11.0	3
pH (total scale; both internal and external)	pH_T	7.6	8.9	7.5	8.1	7.4	8.1	7.6	8.7	NA	NA	7.4	8.1	3
Sal (Salinity)	PSU	32.0	34.0	32.3	34.0	32.3	34.0	31.2	34.0	32.0	34.0	33.0	34.0	3
Temp (Temperature)	°C	11.0	26.5	9.0	24.5	9.0	15.0	12.0	26.5	10.0	26.0	9.0	19.0	3

Appendix C.8

Summary of temperature recorded by the PLOO thermistor array (100 m) at nearest depths to the PLOO RTOMS sensors, during seasons between 2020 to 2021 where RTOMS data were unavailable. Data include mean, minimum, and maximum values, sample size (n), and proportion recovered (n_prop) for each depth by season.

Parameter	Season		6 m	10 m	22 m	30 m	46 m	62 m	74 m	90 m
Temperature (°C)	*Fall 2020*	mean	17.2	16.4	14.5	13.6	12.7	12.0	11.7	11.4
		min	13.9	13.3	12.6	12.1	11.4	10.9	10.8	10.4
		max	21.8	20.8	17.3	16.2	14.8	13.5	12.9	12.5
		n	13,103	13,103	13,103	13,103	13,103	13,103	13,103	13,103
		n_prop	0.99	0.99	0.99	0.99	0.99	0.99	0.99	0.99
	Winter 2021	mean	14.7	14.4	13.4	12.6	11.8	11.2	11.0	10.8
		min	11.5	11.2	10.7	10.3	10.0	9.9	9.8	9.8
		max	16.3	16.2	16.1	15.9	15.0	14.5	13.2	13.0
		n	12,959	12,959	12,959	12,959	12,959	12,959	12,959	12,959
		n_prop	1	1	1	1	1	1	1	1
	Spring 2021	mean	17.2	15.8	12.7	11.9	10.9	10.5	10.3	10.3
		min	12.3	11.8	10.5	10.5	9.9	9.8	9.6	9.6
		max	20.4	19.7	16.2	14.4	12.9	12.0	11.5	11.3
		n	13,083	13,083	13,083	13,083	13,083	13,083	13,083	13,083
		n_prop	1	1	1	1	1	1	1	1
	Summer 2021	mean	18.4	16.2	13.3	12.6	11.6	11.2	11.0	10.9
		min	12.8	12.2	11.4	11.1	10.3	10.1	10.1	9.9
		max	22.7	22.0	16.9	14.9	13.2	12.6	12.2	11.9
		n	13,239	13,239	13,239	13,239	13,239	13,239	13,239	13,239
		n_prop	1	1	1	1	1	1	1	1

Appendix C.9

Summary of temperature recorded by the SBOO thermistor array (36 m) at nearest depths to the SBOO RTOMS sensors, during seasons between 2020 to 2021 where RTOMS data were unavailable. Data include mean, minimum, and maximum values, sample size (n), and proportion recovered (n_prop) for each depth by season.

Parameter	Season		6 m	10 m	18 m	26 m
Temperature (°C)	*Fall 2020*	mean	16.6	15.8	14.6	13.9
		min	13.8	13.3	12.9	12.5
		max	21.9	21.3	18.8	15.6
		n	13,080	13,080	13,080	13,080
		n_prop	0.99	0.99	0.99	0.99
	Winter 2021	mean	14.5	14.2	13.5	12.9
		min	11.4	11.2	11.0	10.8
		max	16.3	16.2	16.3	15.7
		n	12,959	12,959	12,959	12,959
		n_prop	1	1	1	1
	Spring 2021	mean	16.2	14.6	12.6	11.9
		min	11.5	11.1	10.7	10.6
		max	20.2	20.1	19.4	15.5
		n	13,087	13,087	13,087	13,087
		n_prop	1	1	1	1
	Summer 2021	mean	17.2	15.2	13.3	12.7
		min	13.0	12.3	11.6	11.3
		max	21.9	20.5	19.3	15.5
		n	13,095	13,095	13,095	13,095

Appendix C.10

Summary of temperature, salinity, DO, pH (total scale), chlorophyll a, CDOM, turbidity, nitrate + nitrite, BOD, and xCO2 recorded at various depths by the PLOO RTOMS in fall 2021. Seasonal summaries from 2020 are available in the interim report by City of San Diego (2021). Data include mean, minimum, and maximum values, sample size (n), and proportion recovered (n_prop) for each depth by season. Sample sizes differed due to variations in sampling interval, deployment date, and data quality (Appendix C.2—C.7); id = insufficient data (see text).

Parameter	Season		1 m	9 m	20 m	30 m	45 m	60 m	75 m	87 m
Temperature (°C)	*Fall*	mean	17.0	16.9	15.7	14.1	12.9	12.3	11.9	11.6
		min	15.1	15.1	13.2	12.5	11.8	11.1	10.7	10.5
		max	19.1	18.4	18.0	17.1	15.7	15.3	14.5	13.2
		n	7894	8266	8266	8192	8259	8253	8194	8180
		n_prop	0.60	0.62	0.62	0.62	0.62	0.62	0.62	0.62
Salinity (psu)	*Fall*	mean	33.53	33.51	33.43	33.37	33.42	33.50	33.53	33.62
		min	33.40	33.40	33.04	33.12	33.14	33.19	33.22	33.36
		max	33.64	33.63	33.61	33.63	33.61	33.70	33.79	33.87
		n	7894	8266	8252	8192	8258	8252	8194	8180
		n_prop	0.60	0.62	0.62	0.62	0.62	0.62	0.62	0.62
DO (mg/L)	*Fall*	mean	8.2	—	—	7.5	—	—	4.8	4.5
		min	7.9	—	—	6.0	—	—	3.4	3.1
		max	10.0	—	—	8.3	—	—	7.0	5.9
		n	7951	—	—	8254	—	—	8255	8241
		n_prop	0.60	—	—	0.62	—	—	0.62	0.62
pH_T	*Fall*	mean	8.05	—	—	7.97	—	—	id	—
(pH Total scale)		min	8.01	—	—	7.85	—	—	id	—
		max	8.15	—	—	8.07	—	—	id	—
		n	7952	—	—	8248	—	—	id	—
		n_prop	0.60	—	—	0.62	—	—	0.17	—
Chlorophyll *a*	*Fall*	mean	0.2	—	—	0.6	—	—	0.1	—
(µg/L)		min	0.04	—	—	0.2	—	—	0	—
		max	1.3	—	—	1.9	—	—	0.3	—
		n	7994	—	—	8162	—	—	8164	—
		n_prop	0.6	—	—	0.62	—	—	0.62	—
CDOM (ppb)	*Fall*	mean	1.0	—	—	0.7	—	—	0.5	—
		min	0.7	—	—	0.4	—	—	0.2	—
		max	2.5	—	—	1.0	—	—	1.4	—
		n	7986	—	—	8162	—	—	8164	—
		n_prop	0.60	—	—	0.62	—	—	0.62	—
Turbidity (NTU)	*Fall*	mean	0.02	—	—	0.1	—	—	0.13	—
		min	0	—	—	0.04	—	—	0.02	—

Appendix C.10 *continued*

Parameter	Season		1 m	9 m	20 m	30 m	45 m	60 m	75 m	87 m
		max	1.2	—	—	1.9	—	—	4	—
		n	7979	—	—	8162	—	—	8164	—
		n_prop	0.60	—	—	0.62	—	—	0.62	—
Nitrate +	*Fall*	mean	—	—	—	8.2	—	—	21.3	—
nitrite (µM)		min	—	—	—	1.0	—	—	9.7	—
		max	—	—	—	16.1	—	—	27.3	—
		n	—	—	—	1340	—	—	1335	—
		n_prop	—	—	—	0.61	—	—	0.60	—
BOD (mg/L)	*Fall*	mean	—	—	—	0.1	—	—	0.1	—
		min	—	—	—	0.07	—	—	0	—
		max	—	—	—	1.6	—	—	1	—
		n	—	—	—	8190	—	—	5659	—
		n_prop	—	—	—	0.62	—	—	0.43	—
xCO2 (ppm)	*Fall*	n	id	—	—	—	—	—	—	—
		n_prop	0.28	—	—	—	—	—	—	—

Appendix C.11

Summary of temperature, salinity, DO, pH (total scale), chlorophyll a, CDOM, turbidity, nitrate + nitrite, BOD, and xCO2 recorded at various depths by the SBOO RTOMS in fall 2021. Seasonal summaries from 2020 are available in the interim report by City of San Diego (2021). Data include mean, minimum, and maximum values, sample size (n), and proportion recovered (n_prop) for each depth by season. Sample sizes differed due to variations in sampling interval, deployment date, and data quality (Appendix C.2 to C.7); id = insufficient data (see text).

Parameter	Season		1 m	10 m	18 m	26 m
Temperature (°C)	*Fall*	mean	16.4	15.8	14.8	14.0
		min	13.4	12.8	12.5	12.3
		max	18.8	18.1	17.6	16.1
		n	8022	8101	8025	8031
		n_prop	0.61	0.61	0.61	0.61
Salinity (psu)	*Fall*	mean	33.48	33.45	33.42	33.41
		min	33.24	33.18	33.05	33.23
		max	33.59	33.55	33.58	33.59
		n	8020	8101	8023	8031
		n_prop	0.61	0.61	0.61	0.61
DO (mg/L)	*Fall*	mean	8.2	—	7.6	7.0
		min	6.8	—	5.8	5.6
		max	10.1	—	9.6	9.2
		n	8079	—	8077	8083
		n_prop	0.61	—	0.61	0.61
pH_T	*Fall*	mean	8.04	—	—	7.94
(pH Total scale)		min	7.88	—	—	7.83
		max	8.15	—	—	8.12
		n	8083	—	—	8088
		n_prop	0.61	—	—	0.61
Chlorophyll *a*	*Fall*	mean	0.3	—	0.7	0.6
(µg/L)		min	0.1	—	0.1	0.2
		max	4.9	—	3.5	2.8
		n	7870	—	7955	7957
		n_prop	0.59	—	0.60	0.60
CDOM (ppb)	*Fall*	mean	1.0	—	0.8	0.8
		min	0.6	—	0.6	0.5
		max	4.2	—	1.8	1.4
		n	7874	—	7955	7957
		n_prop	0.59	—	0.60	0.60
Turbidity (NTU)	*Fall*	mean	0.01	—	0.2	0.3
		min	0	—	0.05	0.07

Appendix C.11 *continued*

Parameter	Season		1 m	10 m	18 m	26 m
		max	1.1	—	4.9	3.8
		n	7871	—	7953	7957
		n_prop	0.59	—	0.60	0.60
Nitrate +	*Fall*	mean	3.4	—	—	5.9
nitrite (µM)		min	0.01	—	—	0.01
		max	8.0	—	—	13.6
		n	1049	—	—	1202
		n_prop	0.48	—	—	0.54
BOD (mg/L)	*Fall*	mean	—	—	—	0.1
		min	—	—	—	0.04
		max	—	—	—	1
		n	—	—	—	8045
		n_prop	—	—	—	0.61
xCO2 (ppm)	*Fall*	mean	375	—	—	—
		min	271	—	—	—
		max	449	—	—	—
		n	1271	—	—	—
		n_prop	0.94	—	—	—

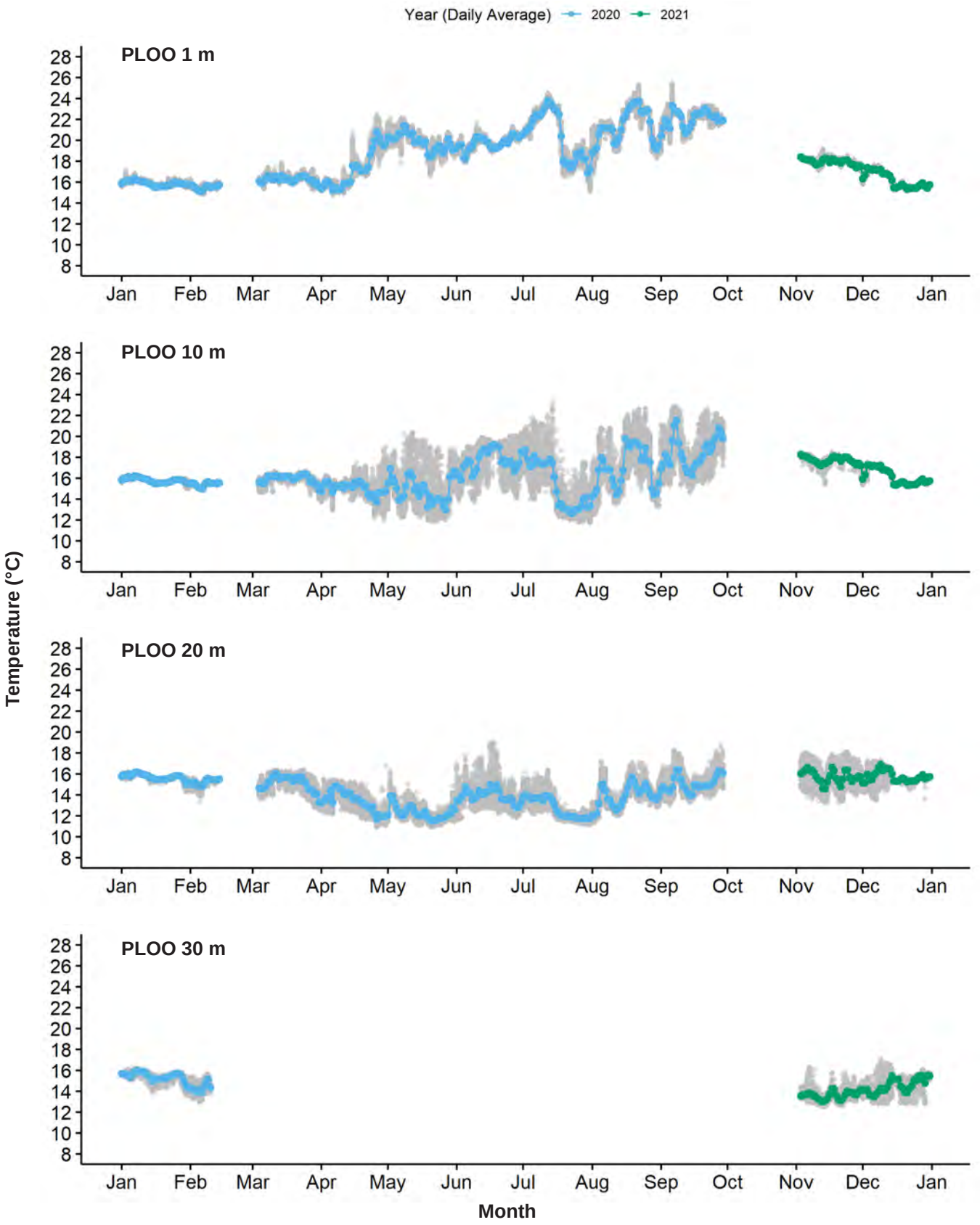

Appendix C.12

Temperature, salinity, DO, pH (total scale), chlorophyll a, CDOM, turbidity, nitrate + nitrite, BOD, and xCO2 recorded at various depths by the PLOO and SBOO RTOMS during 2020 and 2021. Grey points represent raw data and green points represent daily averaged data.

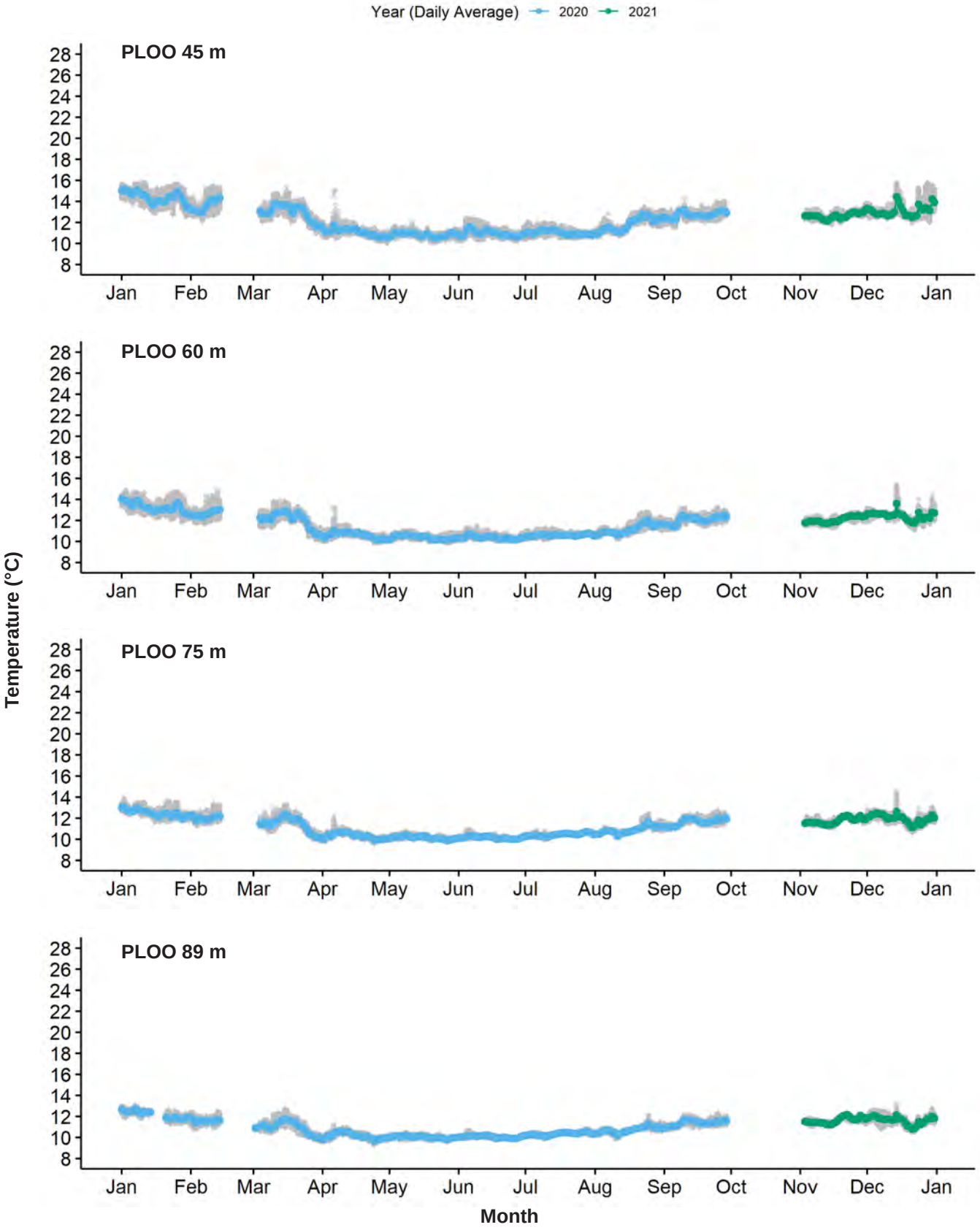

Appendix C.12 *continued*

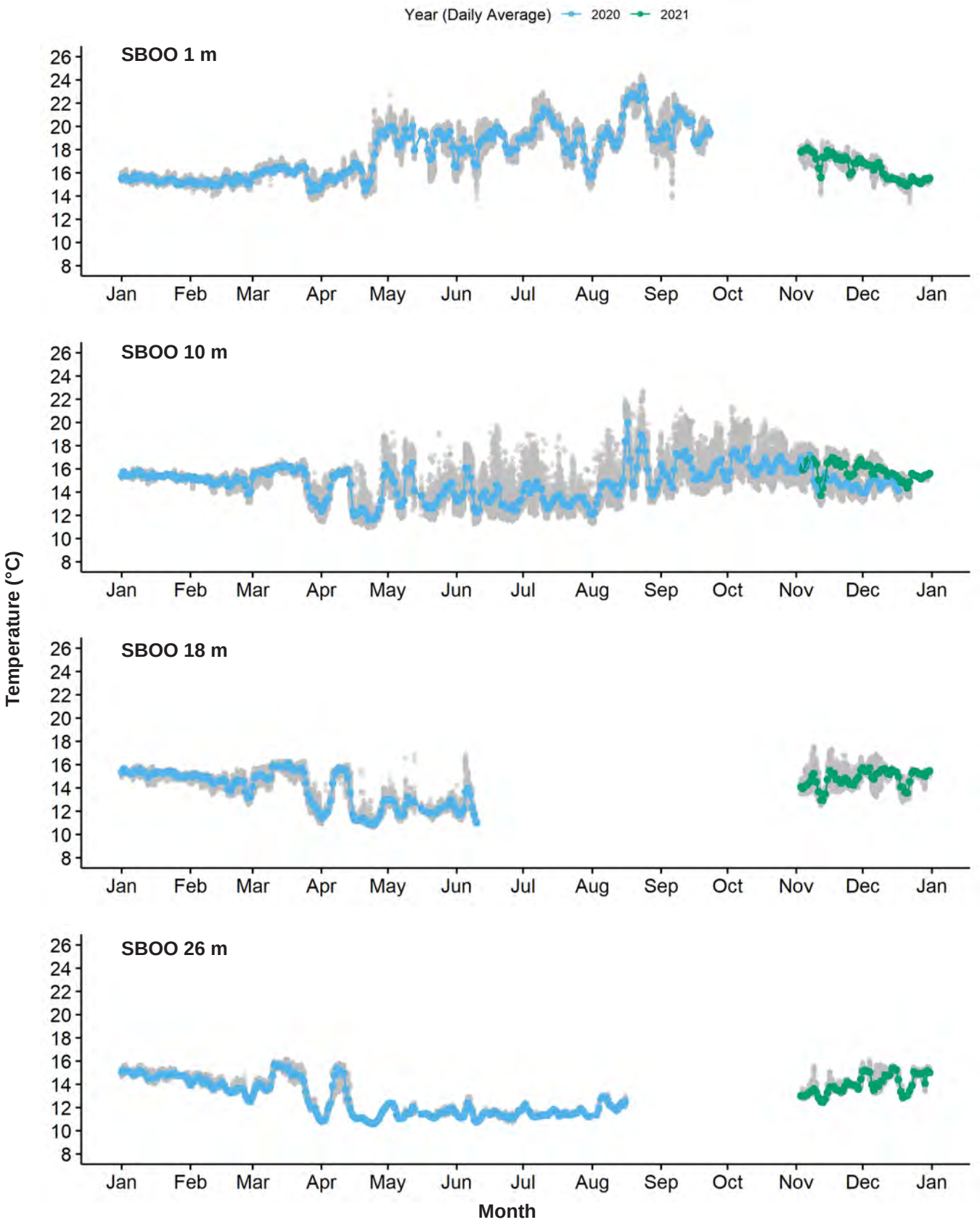

Appendix C.12 *continued*

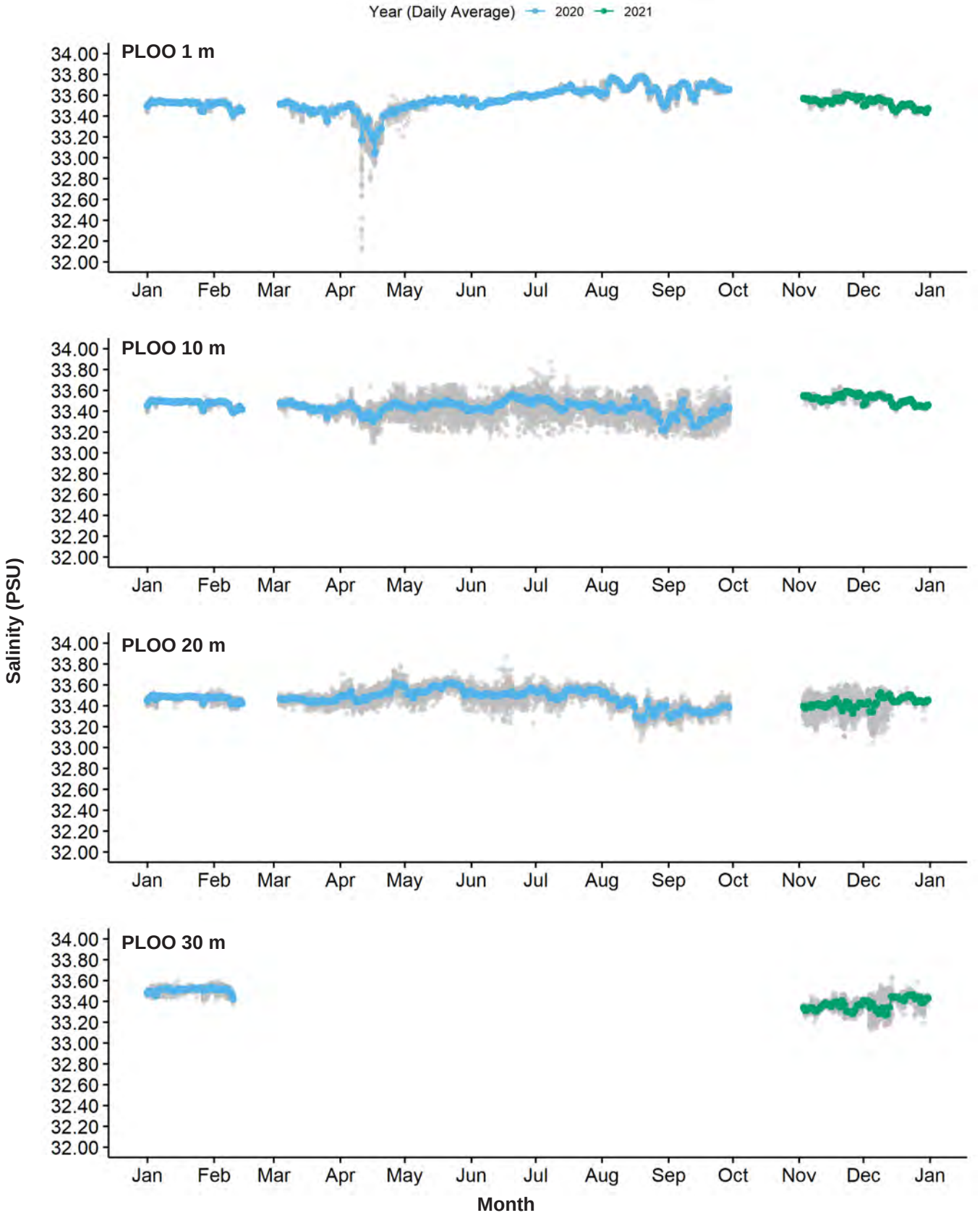

Appendix C.12 *continued*

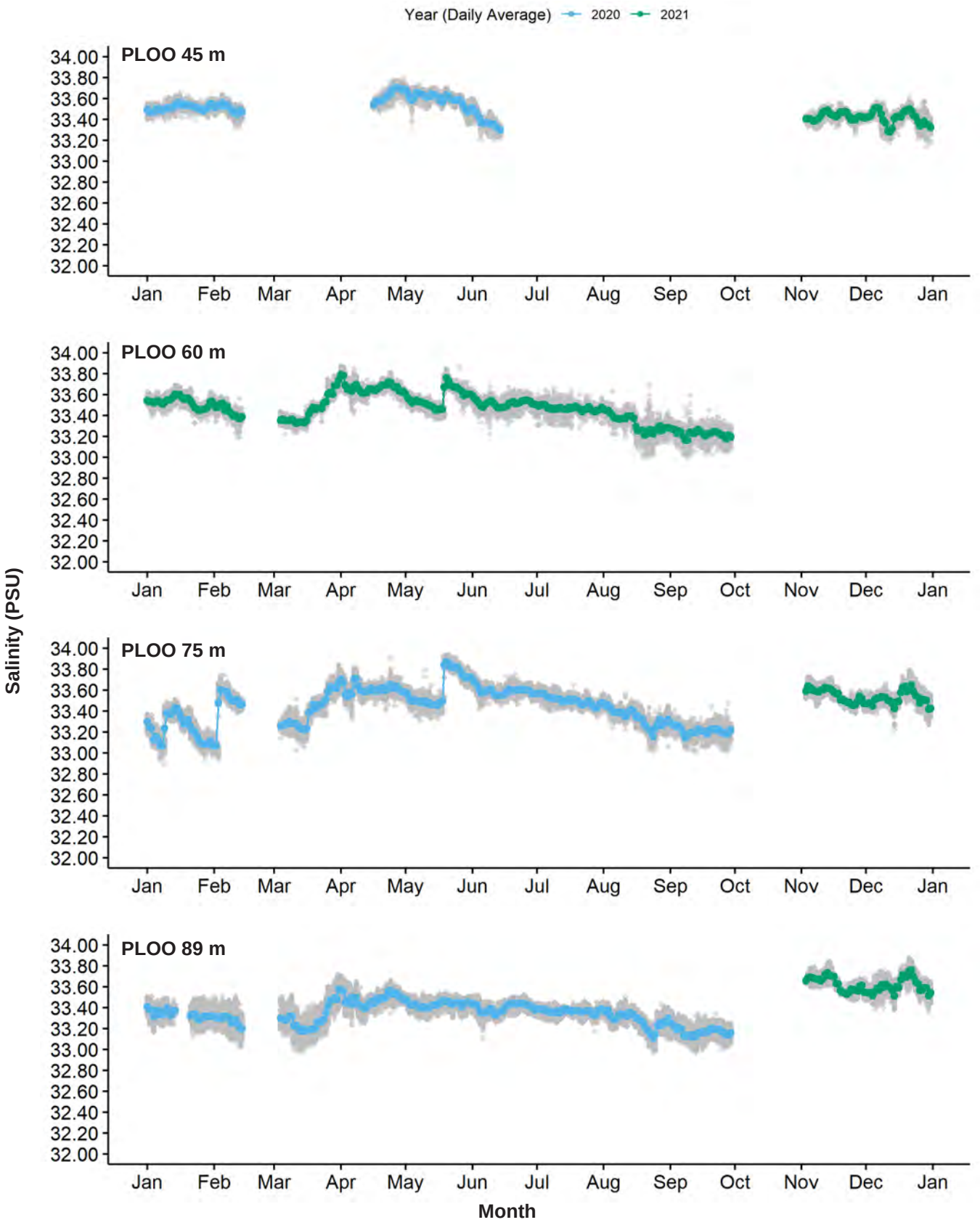

Appendix C.12 *continued*

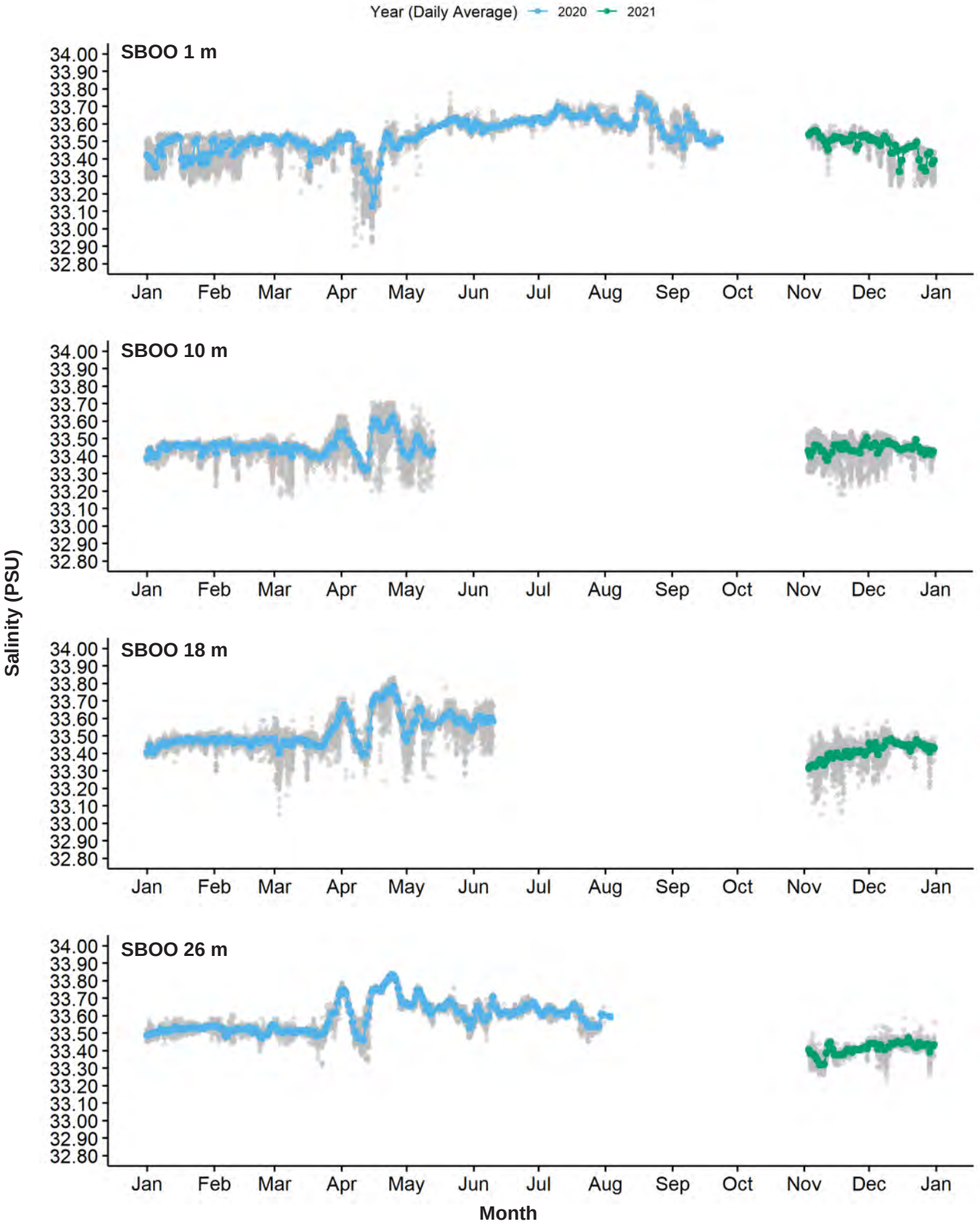

Appendix C.12 *continued*

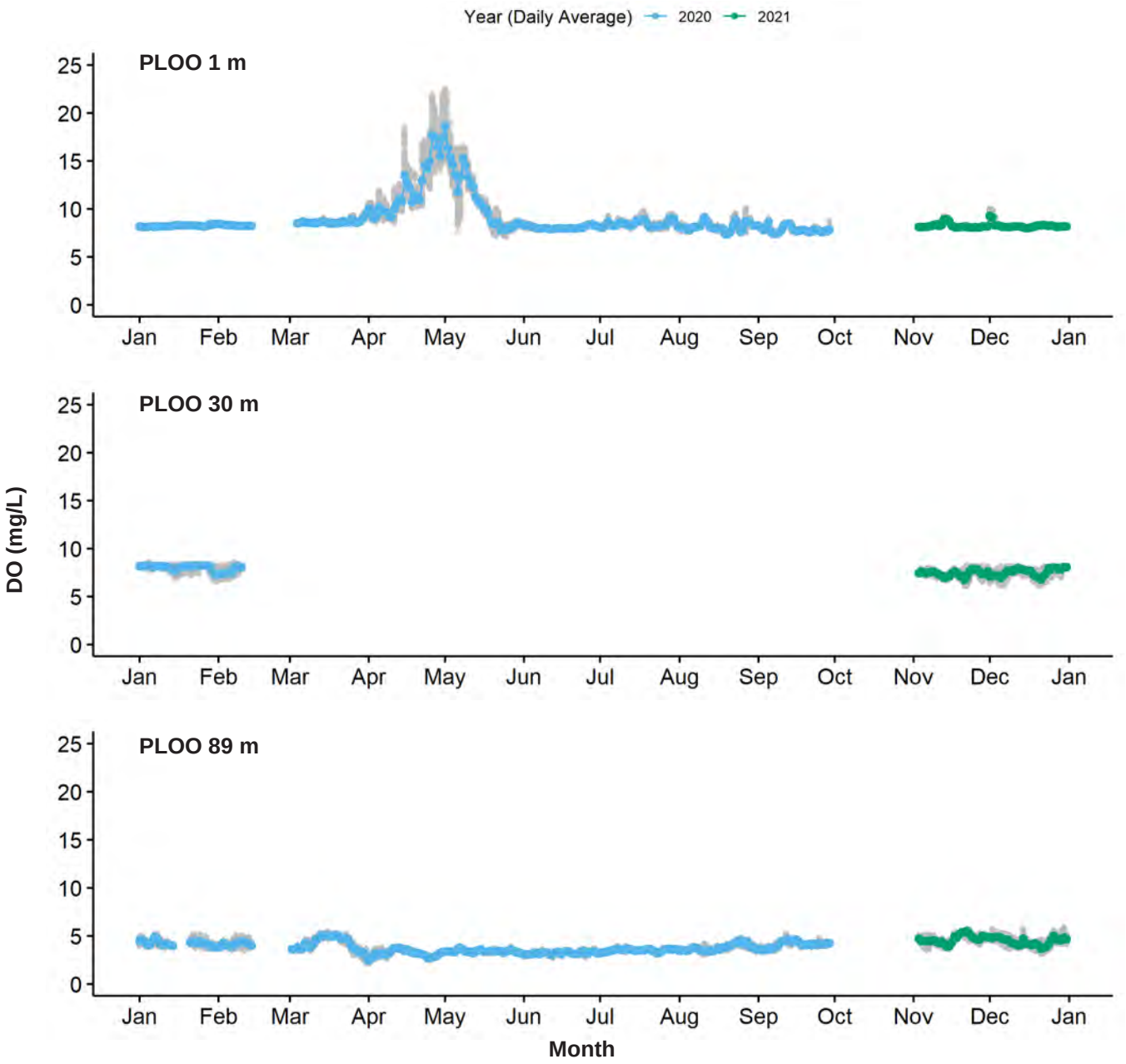

Appendix C.12 *continued*

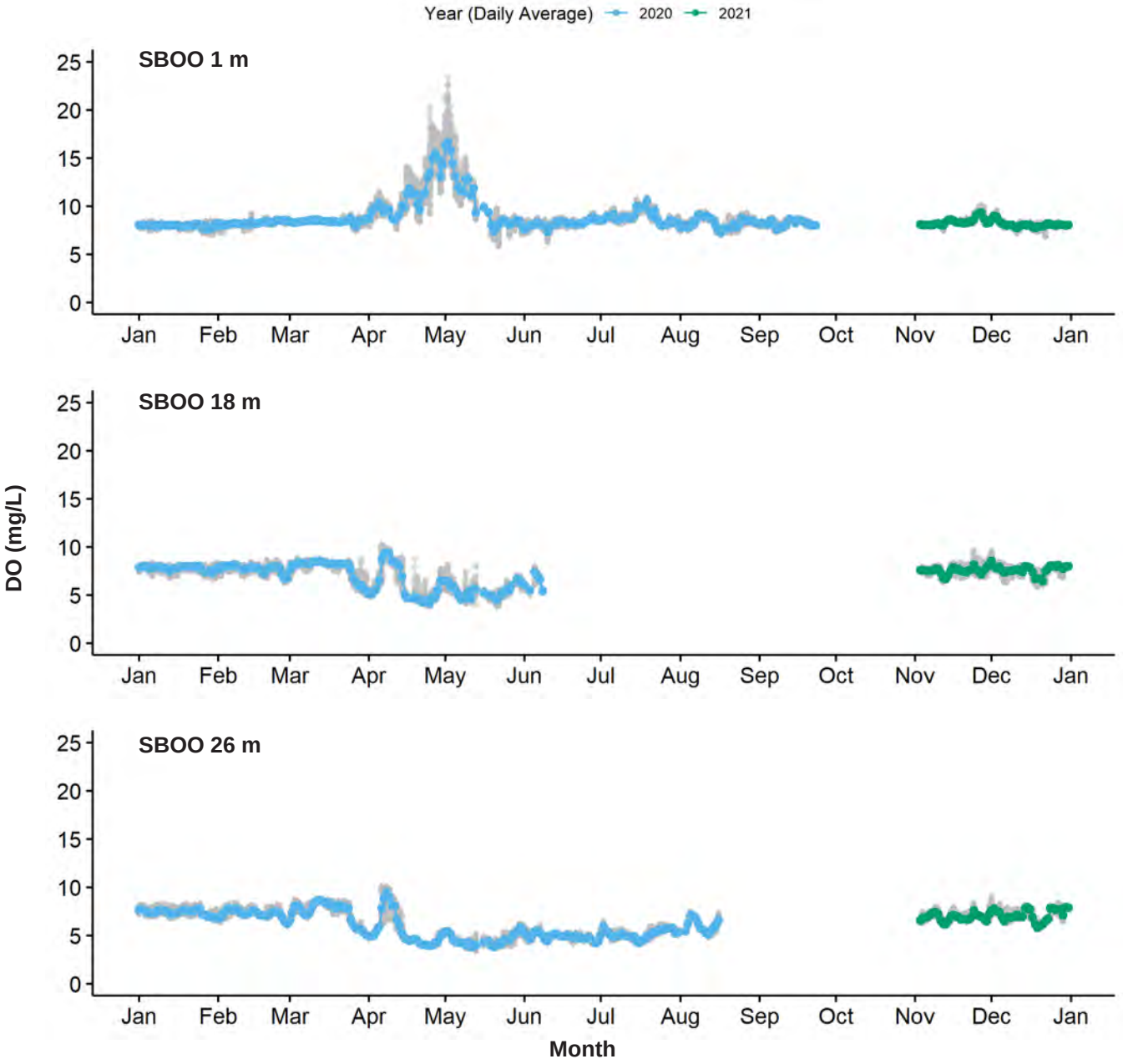

Appendix C.12 *continued*

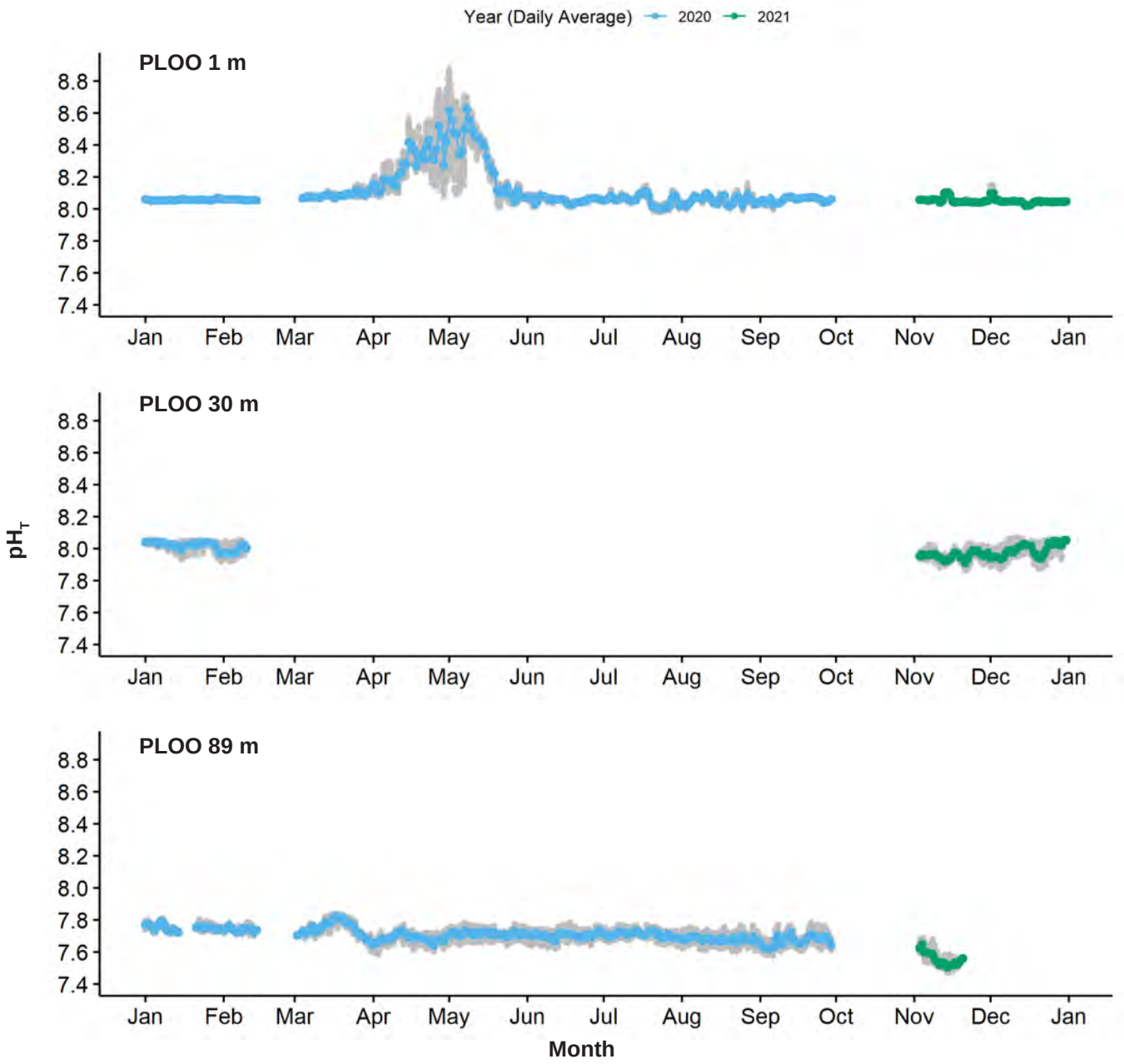

Appendix C.12 *continued*

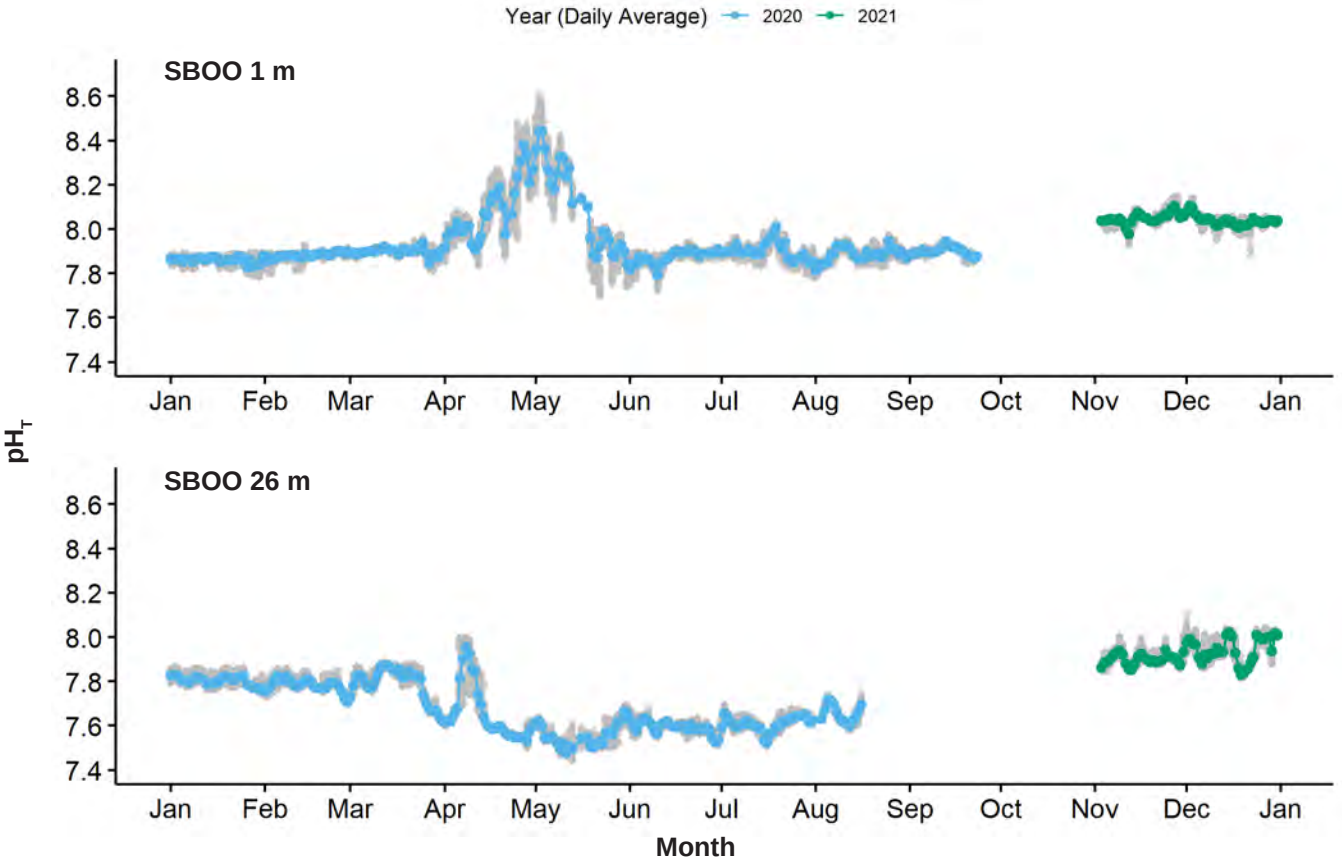

Appendix C.12 *continued*

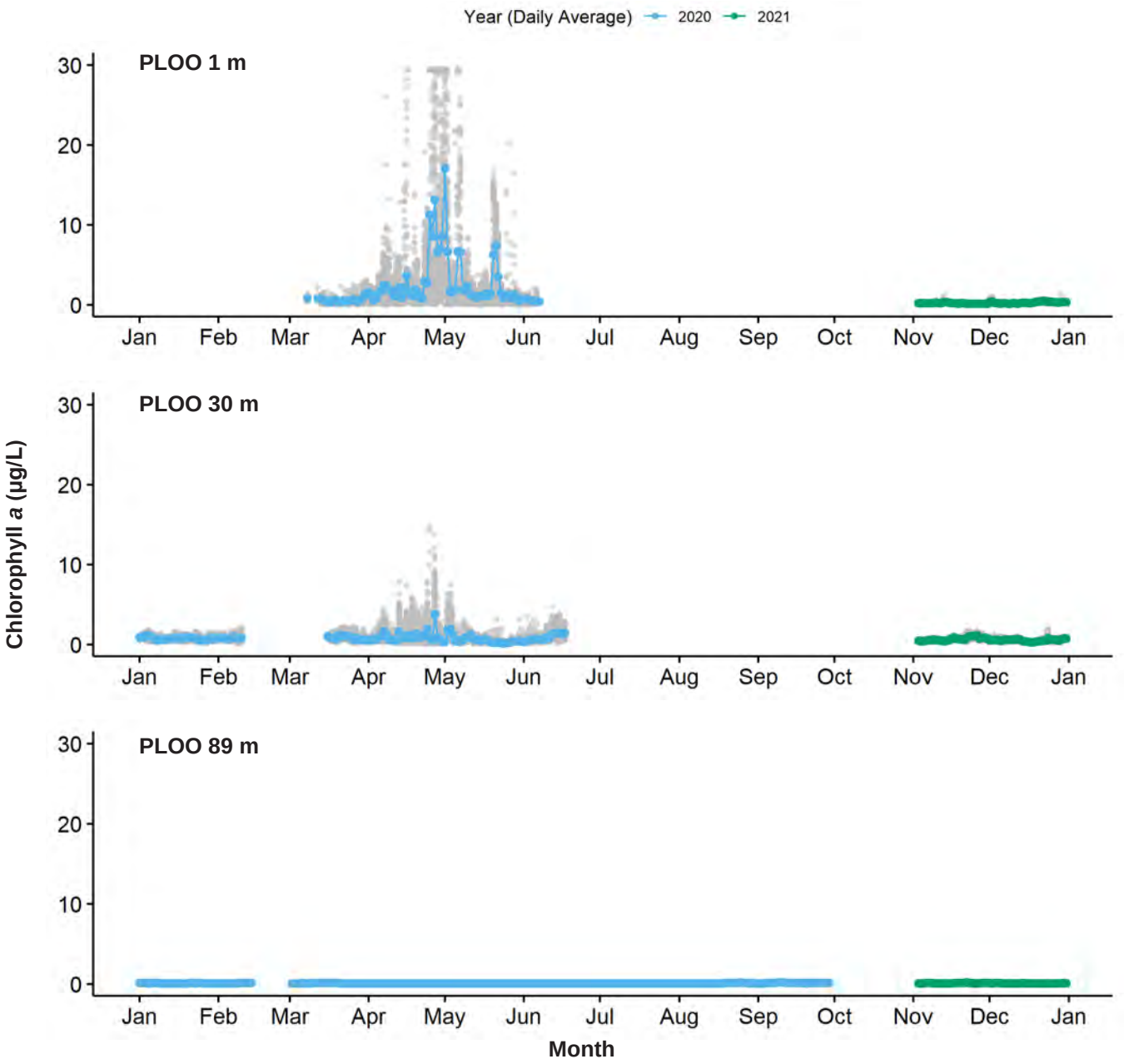

Appendix C.12 *continued*

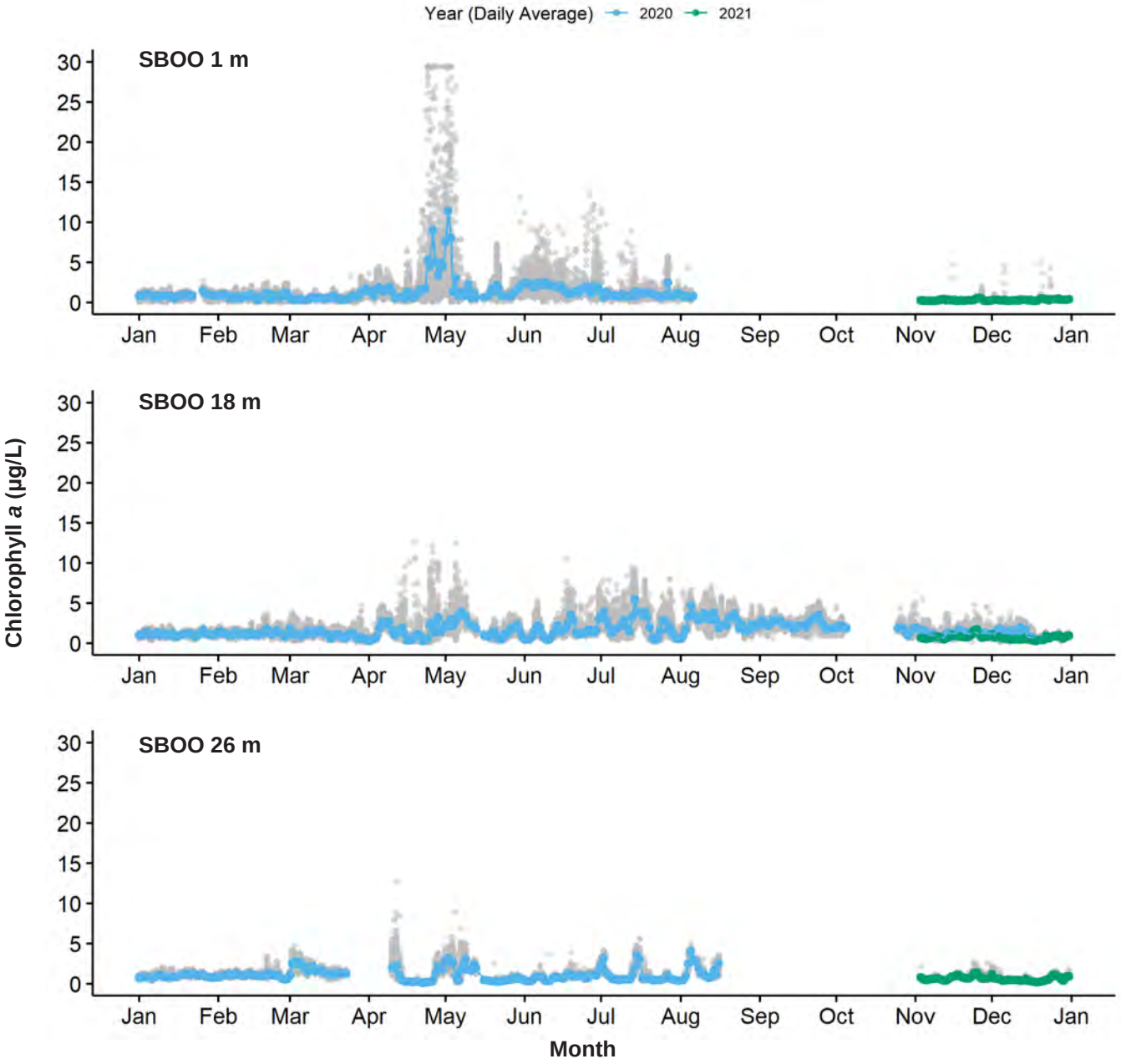

Appendix C.12 *continued*

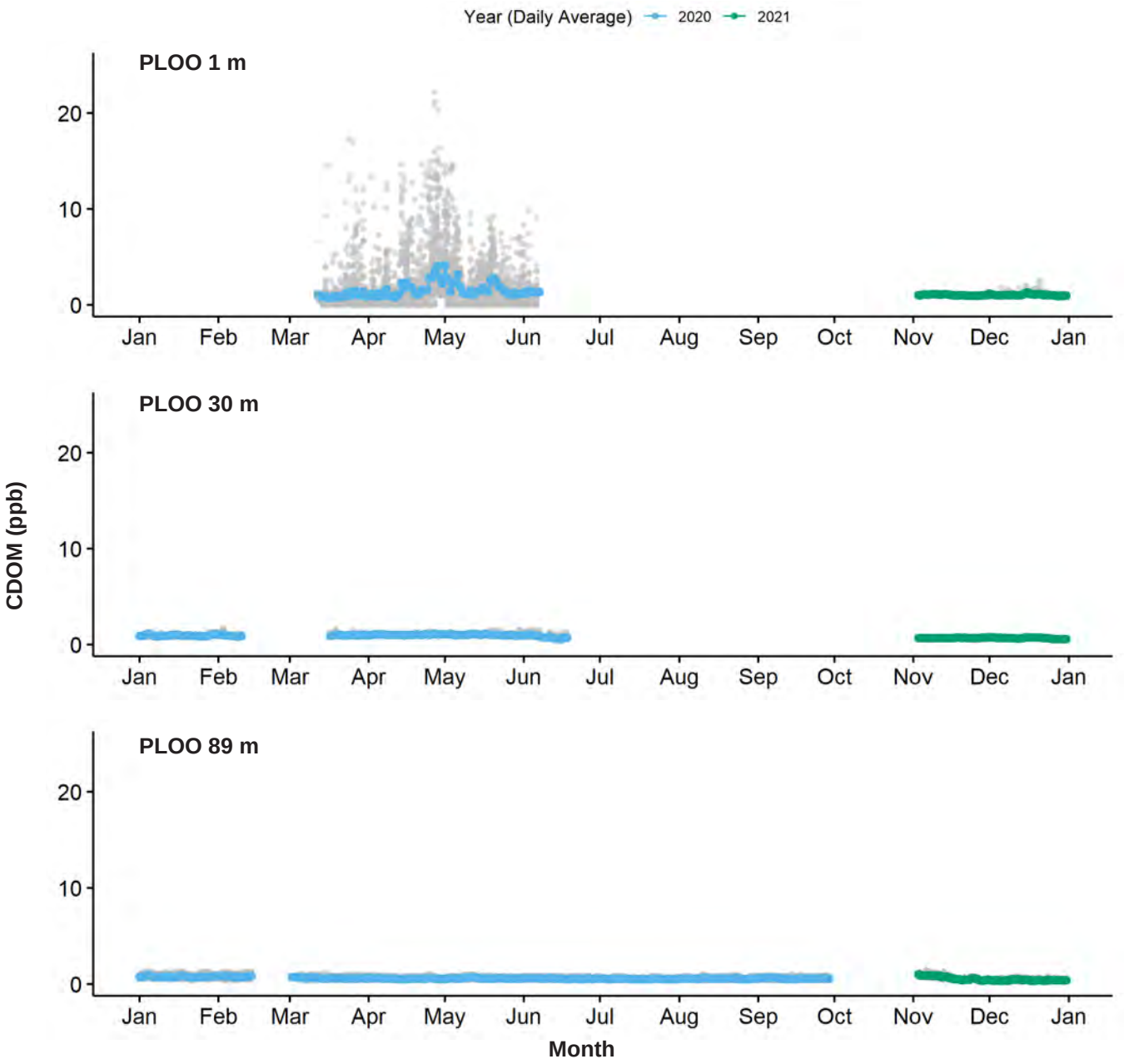

Appendix C.12 *continued*

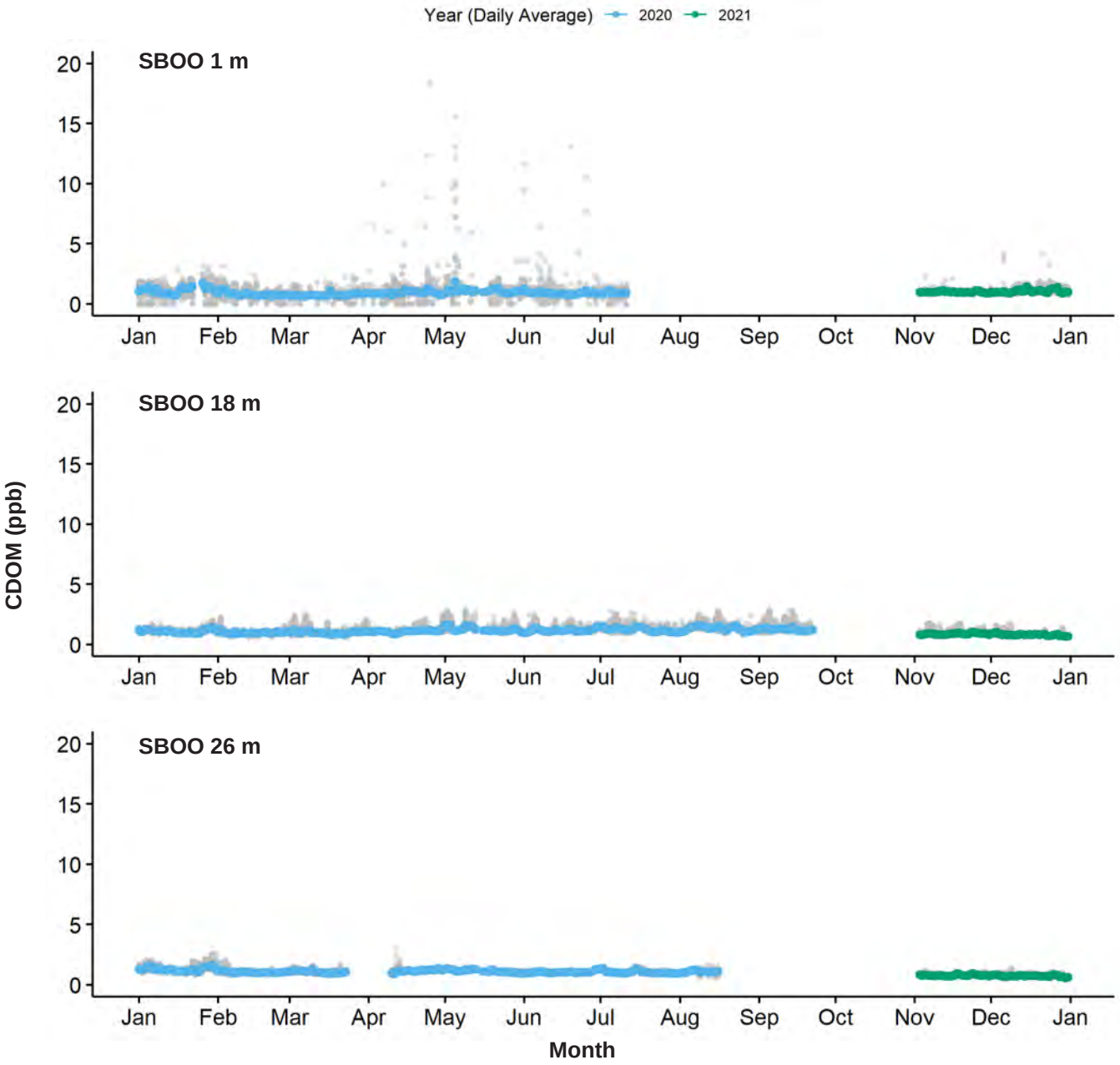

Appendix C.12 *continued*

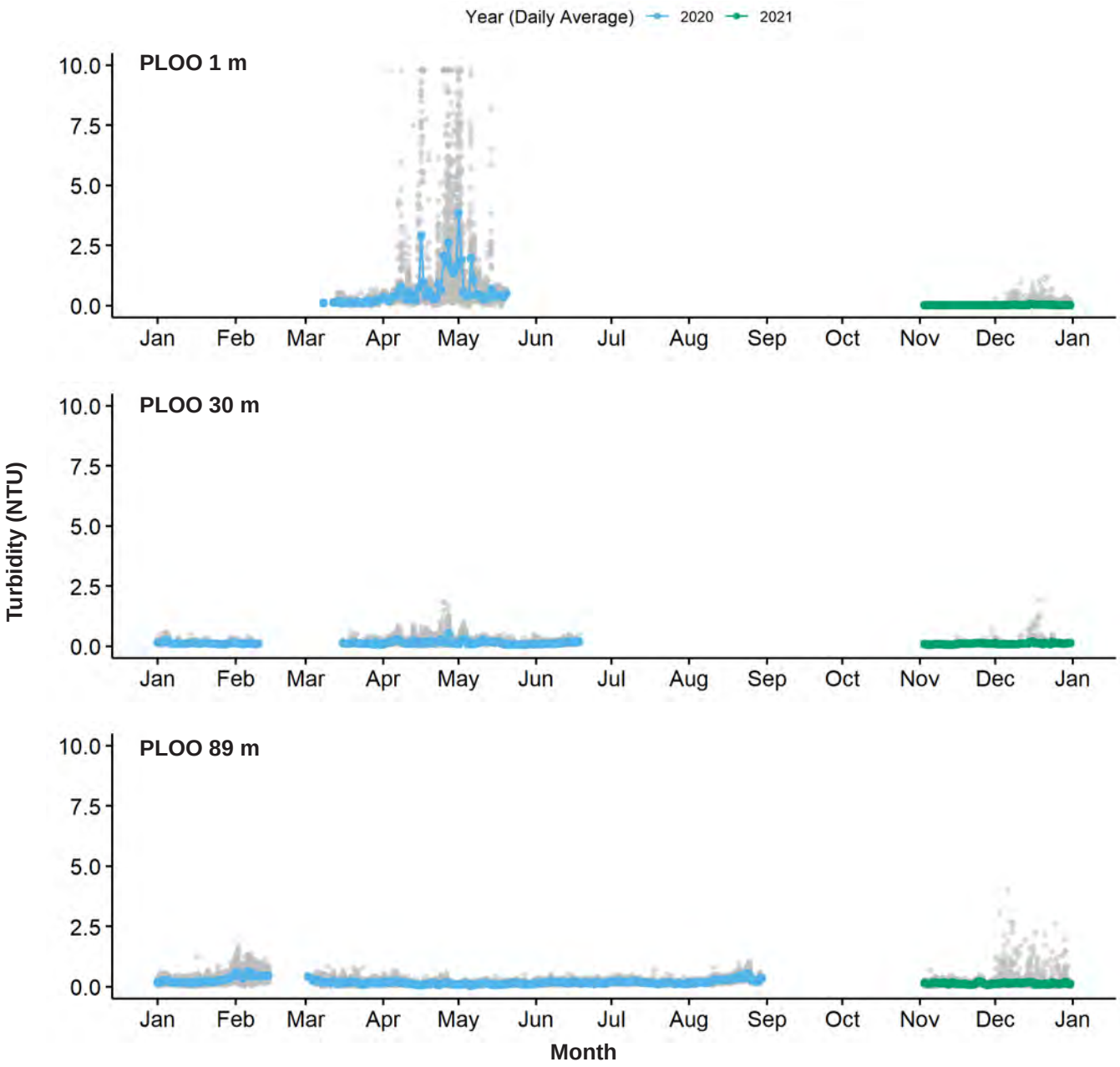

Appendix C.12 *continued*

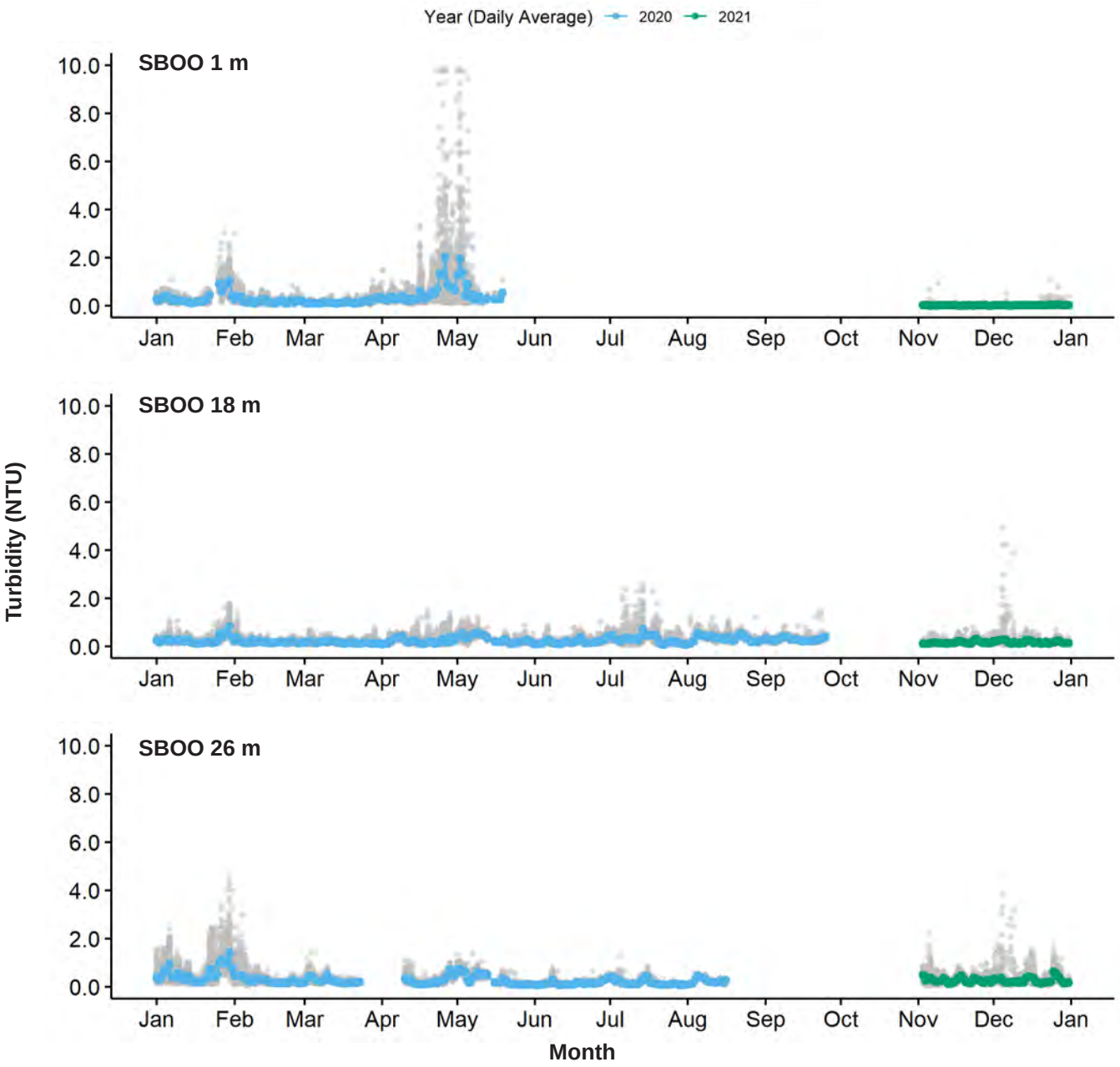

Appendix C.12 *continued*

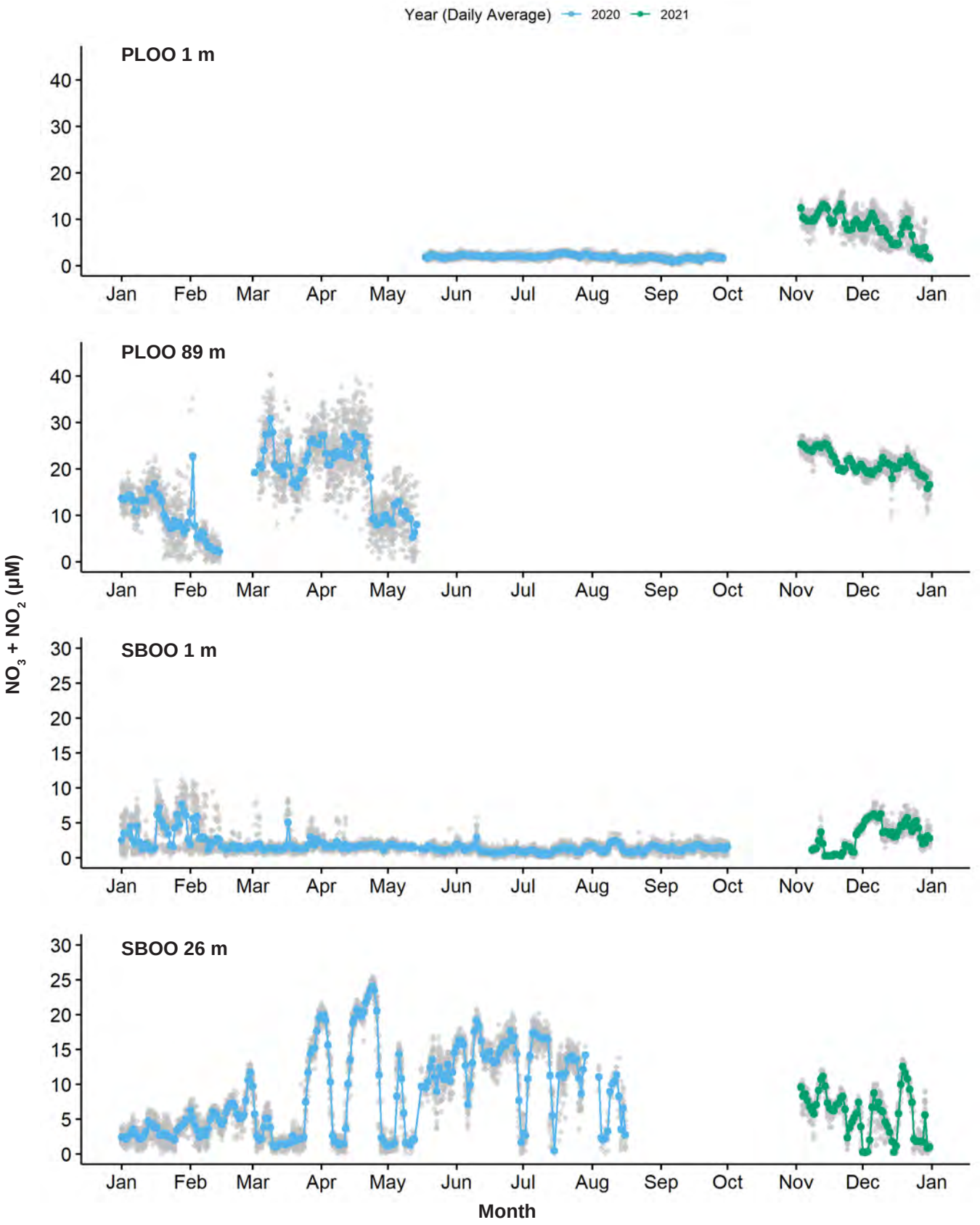

Appendix C.12 *continued*

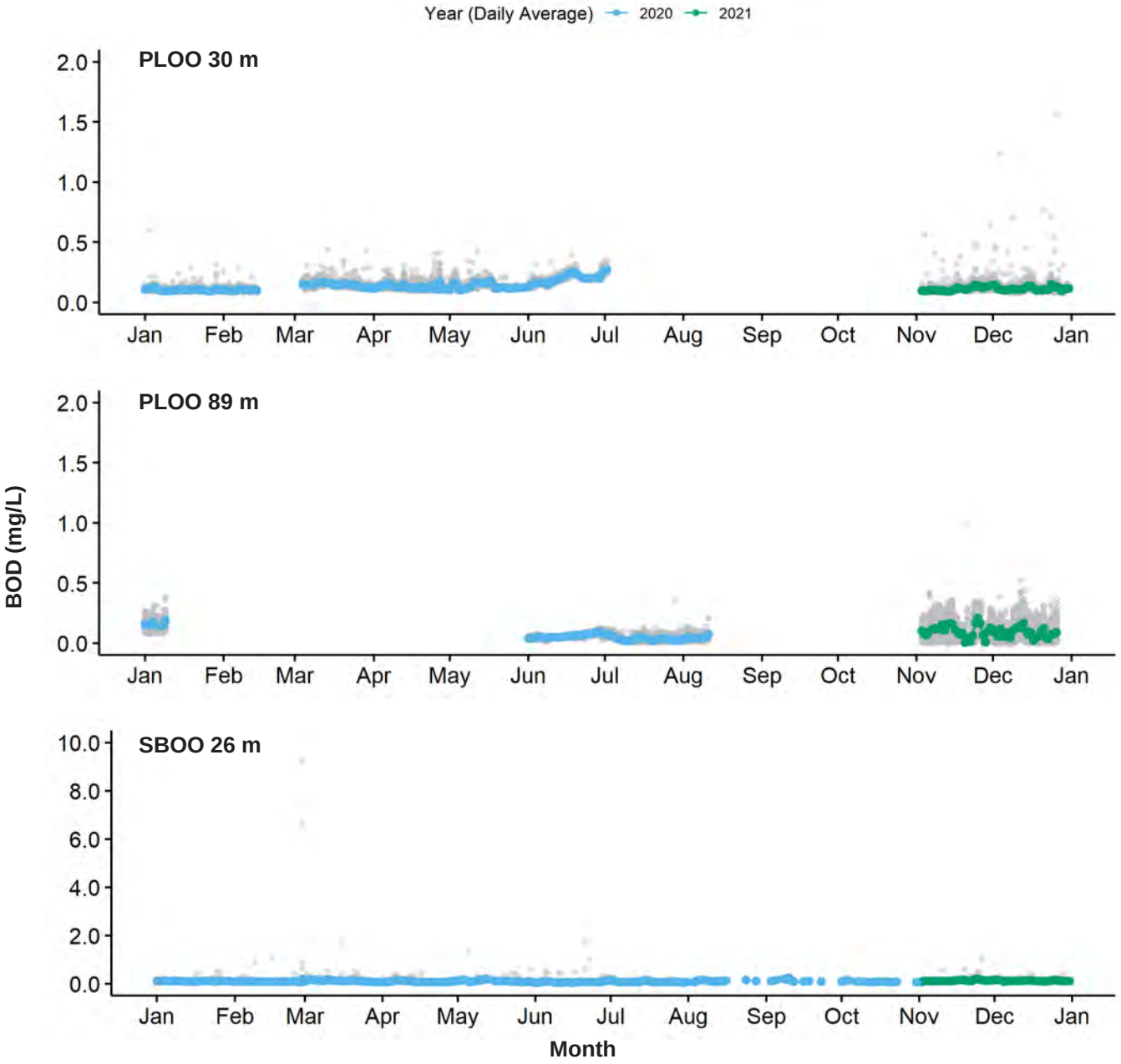

Appendix C.12 *continued*

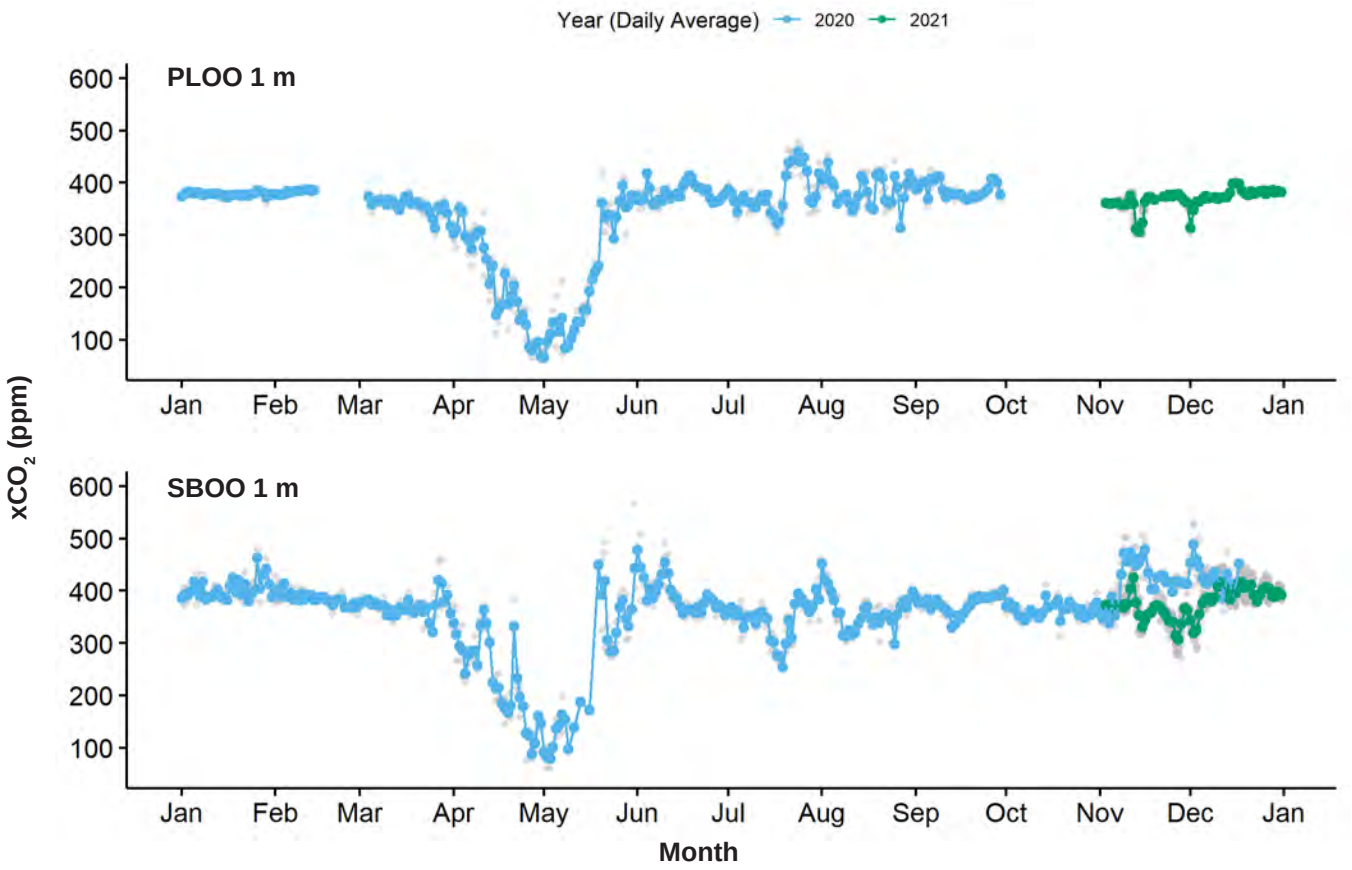

Appendix C.12 *continued*

Appendix C.13

Summary of seasonal buoyancy frequency in the PLOO and SBOO regions during 2020 and 2021. Depth refers to the depth of maximum buoyancy frequency. Max BF refers to the maximum buoyancy frequency, measured in cycles per second. For each quarter: n = 11 (PLOO), n = 13 (SBOO).

	2020		2021	
	Depth (m)	**Max BF (s^{-1})**	**Depth (m)**	**Max BF (s^{-1})**
PLOO Region				
Winter	36	5.93	19	6.68
Spring	8	15.74	9	9.39
Summer	5	14.36	9	12.83
Fall	14	9.38	27	8.72
SBOO Region				
Winter	25	5.27	17	4.92
Spring	6	14.84	6	11.48
Summer	10	14.60	2	11.42
Fall	4	8.56	6	9.20

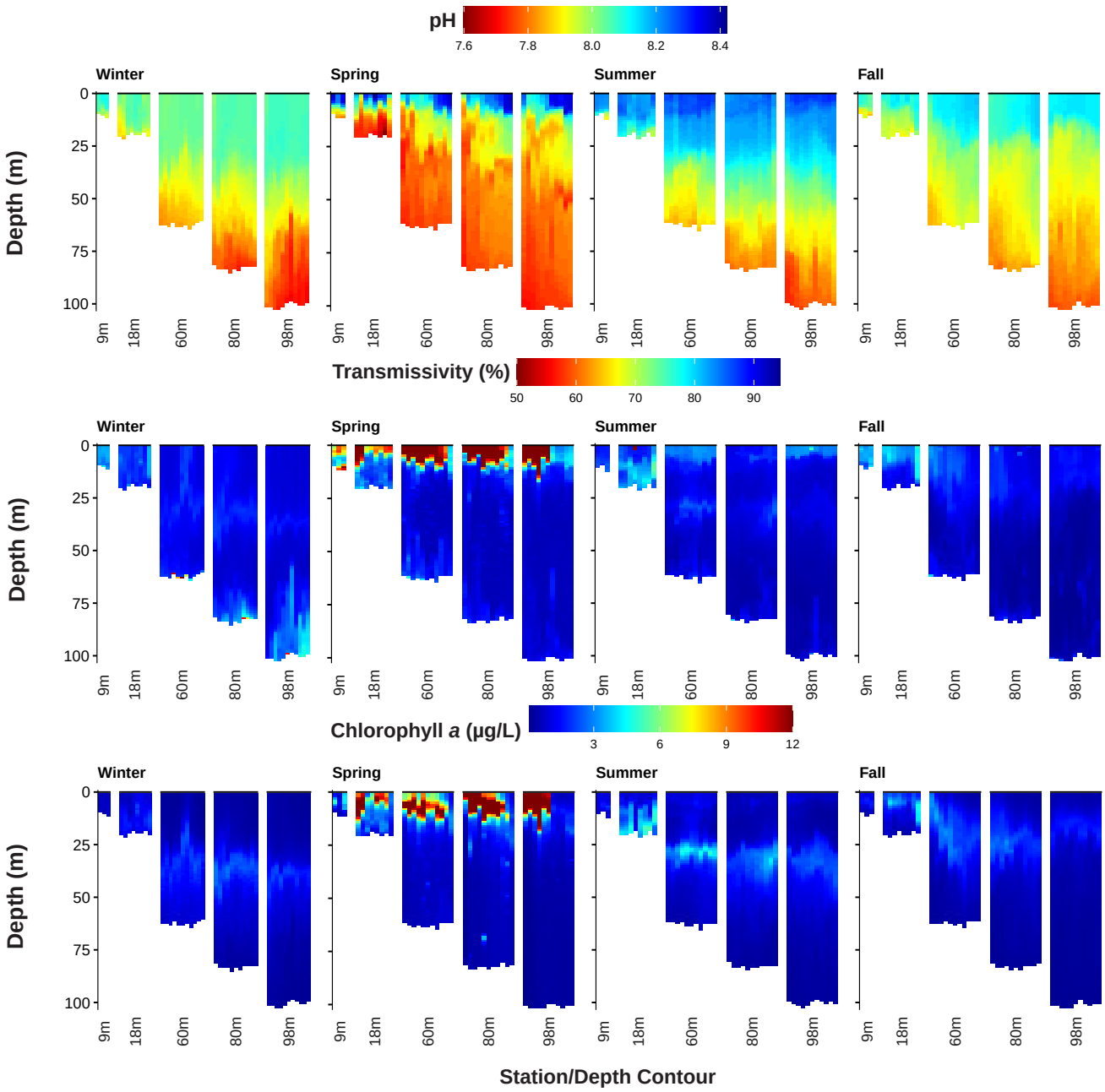

Appendix C.14

Values of pH, transmissivity, and chlorophyll *a* recorded in the PLOO region during 2020. Data are 1-m binned values per depth for each station and were collected over 4–5 days during each quarterly survey. Stations are depicted from north to south along each depth contour.

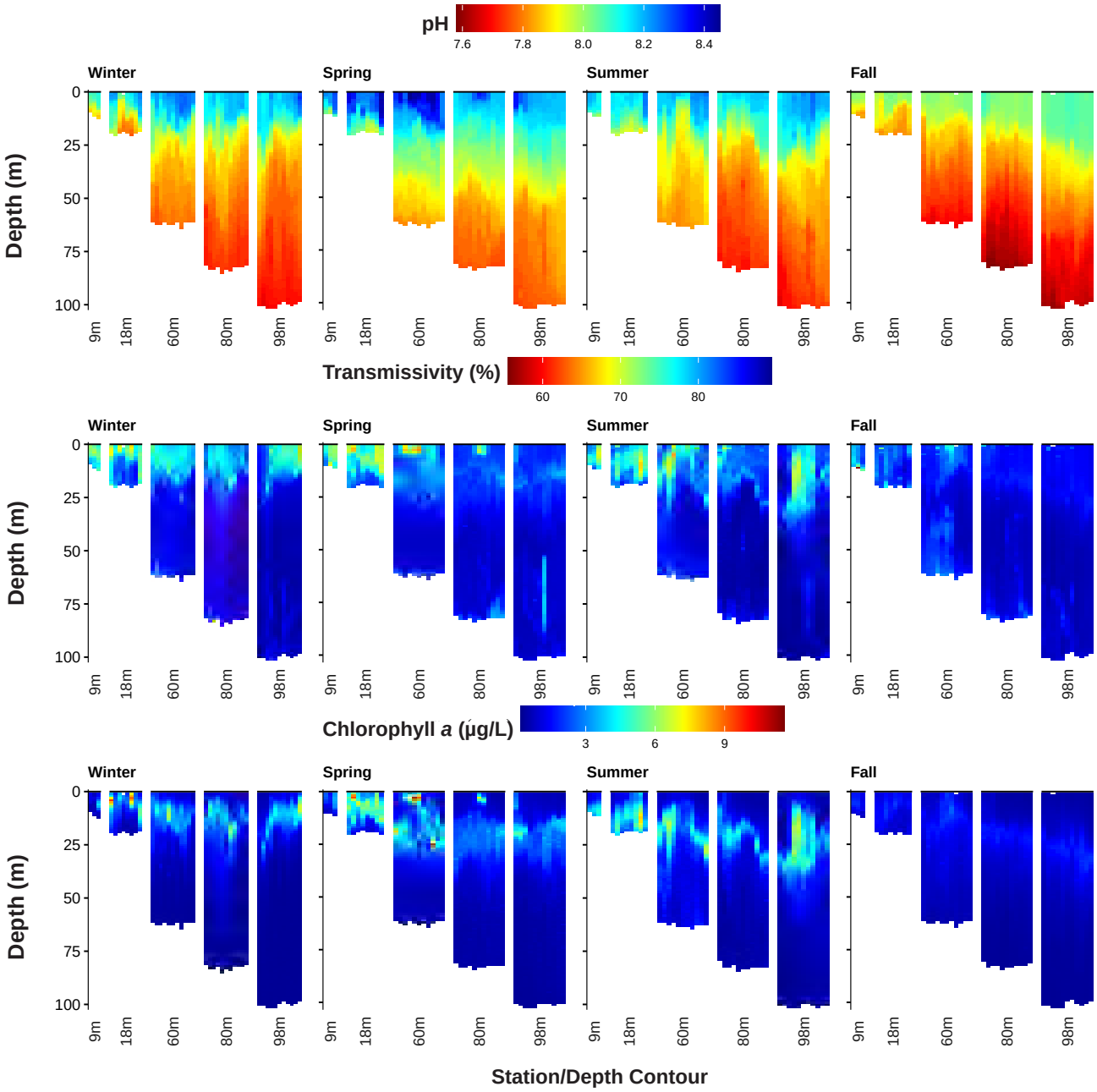

Appendix C.15

Values of pH, transmissivity, and chlorophyll *a* recorded in the PLOO region during 2021. Data are 1-m binned values per depth for each station and were collected over 4–5 days during each quarterly survey. Stations are depicted from north to south along each depth contour.

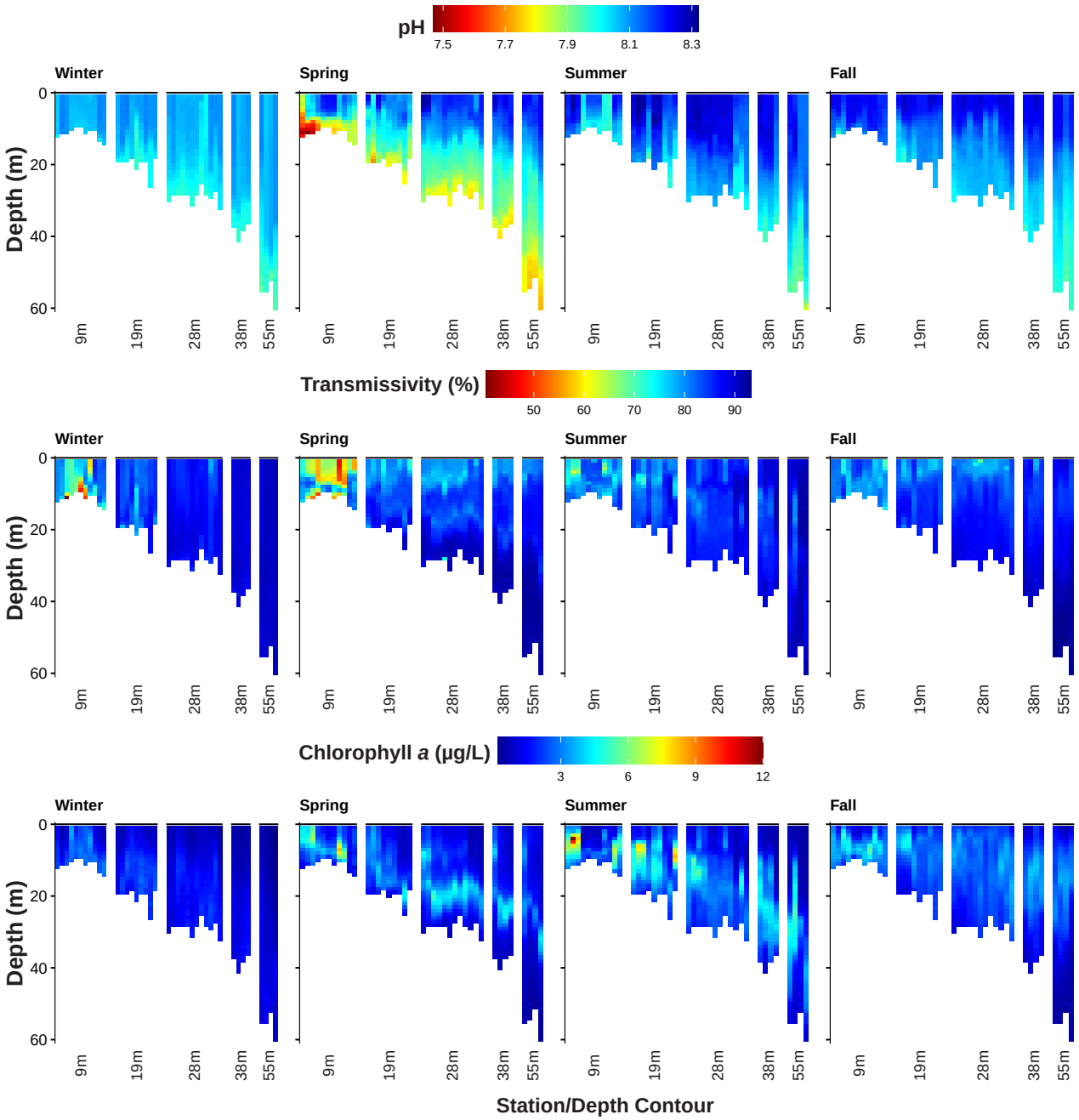

Appendix C.16

Values of pH, transmissivity, and chlorophyll *a* recorded in the SBOO region during 2020. Data are 1-m binned values per depth for each station and were collected over 4–5 days during each quarterly survey. Stations are depicted from north to south along each depth contour.

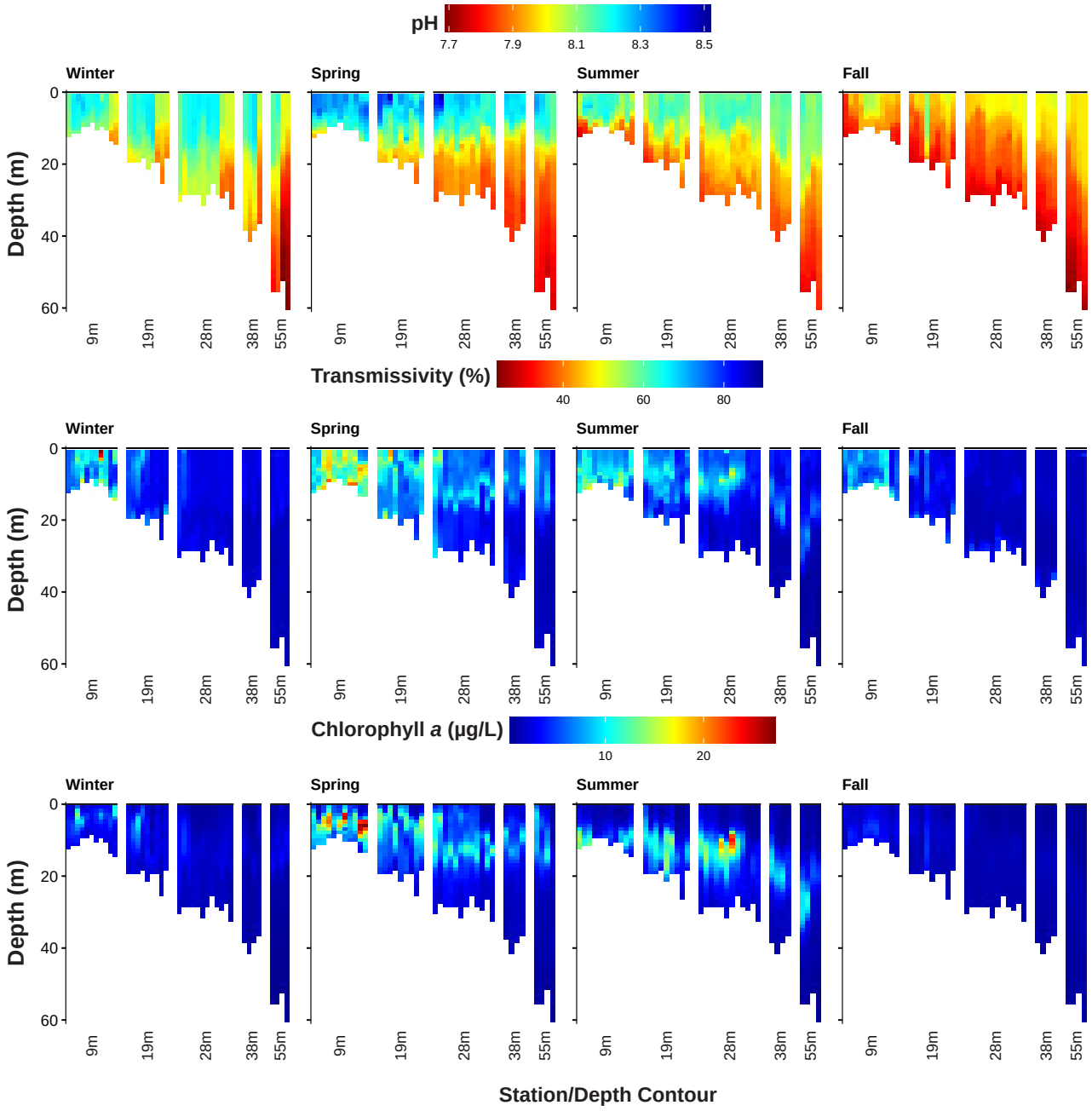

Appendix C.17

Values of pH, transmissivity, and chlorophyll *a* recorded in the SBOO region during 2021. Data are 1-m binned values per depth for each station and were collected over 4–5 days during each quarterly survey. Stations are depicted from north to south along each depth contour.

Appendix C.18

Summary of current velocity magnitude and direction from the PLOO RTOMS ADCP during 2021. The deployment began in November. Data are presented by depth bin as seasonal recovered observations (n), minimum (min), maximum (max), and means with 95% confidence intervals (CI). Proportion of recovered observations (n_prop) differed due to variations in data quality (see text). Minimum and maximum angles of velocity are not shown due to the circular nature of the measurement.

				Magnitude (mm/s)				Angle	
Season	**Depth (m)**	**n**	**n_prop**	**Min**	**Max**	**Mean**	**95% CI**	**Mean**	**95% CI**
Fall	3	8226	1.00	1	213	85	1	141	63
	4	8225	1.00	17	252	101	1	141	64
	5	8225	1.00	1	224	108	1	143	63
	6	8224	1.00	4	224	108	1	142	62
	7	8224	1.00	1	232	106	1	144	63
	8	8223	1.00	1	250	105	1	146	63
	9	8225	1.00	3	266	112	1	140	63
	10	8224	1.00	2	273	116	1	139	63
	11	8224	1.00	6	282	117	1	138	63
	12	8225	1.00	10	283	117	1	138	65
	13	8224	1.00	16	283	116	1	136	65
	14	8225	1.00	13	276	114	1	135	66
	15	8223	1.00	16	256	113	1	133	65
	16	8221	1.00	14	240	109	1	133	65
	17	8222	1.00	9	229	105	1	132	65
	18	8222	1.00	7	232	106	1	129	67
	19	8221	1.00	0	224	104	1	125	67
	20	8223	1.00	1	219	101	1	124	67
	21	8222	1.00	1	210	98	1	122	67
	22	8219	1.00	1	217	96	1	119	68
	23	8222	1.00	3	210	93	1	116	67
	24	8220	1.00	1	202	90	1	114	67
	25	8221	1.00	2	206	86	1	114	66
	26	8220	1.00	1	196	77	1	122	63
	27	8221	1.00	1	179	72	1	117	66
	28	8222	1.00	5	192	83	1	99	64
	29	8222	1.00	6	185	79	1	92	65
	30	8221	1.00	3	177	80	1	88	66
	31	8221	1.00	3	180	80	1	83	66
	32	8221	1.00	2	187	80	1	79	65
	33	8219	1.00	3	193	81	1	73	65
	34	8220	1.00	5	188	82	1	68	65
	35	8224	1.00	5	188	82	1	64	66
	36	8219	1.00	1	190	83	1	62	65
	37	8219	1.00	2	199	83	1	57	66
	38	8220	1.00	9	195	83	1	56	67
	39	8221	1.00	9	197	83	1	53	67

Appendix C.18 *continued*

				Magnitude (mm/s)				Angle	
Season	Depth (m)	n	n_prop	Min	Max	Mean	95% CI	Mean	95% CI
	40	8222	1.00	13	209	83	1	52	67
	41	8220	1.00	11	199	83	1	53	66
	42	8221	1.00	10	209	83	1	51	68
	43	8222	1.00	7	213	83	1	49	68
	44	8219	1.00	2	215	84	1	51	68
	45	8219	1.00	0	212	84	1	51	68
	46	8221	1.00	2	212	82	1	49	68
	47	8220	1.00	3	213	82	1	49	69
	48	8221	1.00	2	213	81	1	48	69
	49	8219	1.00	0	206	81	1	47	69
	50	8221	1.00	2	212	82	1	45	68
	51	8220	1.00	1	205	81	1	46	69
	52	8222	1.00	0	193	81	1	44	68
	53	8221	1.00	1	201	82	1	44	69
	54	8221	1.00	4	196	81	1	43	68
	55	8218	1.00	0	186	83	1	45	69
	56	8221	1.00	1	179	83	1	45	69
	57	8222	1.00	2	171	83	1	46	69
	58	8224	1.00	3	173	84	1	48	69
	59	8223	1.00	3	170	83	1	49	70
	60	8222	1.00	1	169	83	1	50	71
	61	8223	1.00	2	168	82	1	50	71
	62	8223	1.00	0	170	81	1	51	72
	63	8219	1.00	3	176	81	1	52	72
	64	8218	1.00	2	182	80	1	55	72
	65	8220	1.00	7	184	79	1	55	74
	66	8219	1.00	2	192	79	1	58	74
	67	8219	1.00	3	195	77	1	59	75
	68	8220	1.00	1	194	76	1	59	76
	69	8220	1.00	2	192	75	1	60	75
	70	8219	1.00	9	198	78	1	72	76
	71	8218	1.00	6	202	78	1	73	76
	72	8220	1.00	6	197	76	1	73	76
	73	8221	1.00	9	206	76	1	72	76
	74	8219	1.00	6	207	77	1	75	77
	75	8219	1.00	8	199	74	1	77	75
	76	8223	1.00	0	193	74	1	84	72
	77	8219	1.00	3	198	71	1	81	75
	78	8215	1.00	1	202	71	1	87	74
	79	8216	1.00	1	199	72	1	99	71
	80	8217	1.00	1	203	68	1	90	72

Appendix C.18 *continued*

				Magnitude (mm/s)				Angle	
Season	**Depth (m)**	**n**	**n_prop**	**Min**	**Max**	**Mean**	**95% CI**	**Mean**	**95% CI**
	81	8214	1.00	1	212	70	1	121	68
	82	8218	1.00	6	228	71	1	128	68
	83	8213	1.00	1	196	67	1	110	71
	84	8211	1.00	8	192	66	1	120	70
	85	8200	1.00	1	196	64	1	166	70
	86	8197	1.00	1	183	67	1	561	67
	87	8175	0.99	1	185	61	1	590	67
	88	8180	0.99	1	154	53	1	607	67
	89	8200	1.00	4	132	45	1	619	59
	90	8218	1.00	4	74	25	0	589	65
	91	8221	1.00	0	49	17	0	160	51
	92	8216	1.00	0	40	17	0	115	45

Appendix C.19

Summary of current velocity magnitude and direction from the SBOO RTOMS ADCP during 2021. The deployment began in November. Data are presented by depth bin as seasonal recovered observations (n), minimum (min), maximum (max), and means with 95% confidence intervals (CI). Proportion of recovered observations (n_prop) differed due to variations in data quality (see text). Minimum and maximum angles of velocity are not shown due to the circular nature of the measurement.

				Magnitude (mm/s)				Angle	
Season	**Depth (m)**	**n**	**n_prop**	**Min**	**Max**	**Mean**	**95% CI**	**Mean**	**95% CI**
Fall	3	8126	1.00	2	339	116	2	163	69
	4	8126	1.00	0	396	153	2	160	67
	5	8126	1.00	7	368	159	2	158	66
	6	8125	1.00	4	381	164	2	156	65
	7	8126	1.00	15	402	164	2	153	65
	8	8124	1.00	14	391	157	2	152	64
	9	8125	1.00	2	298	134	2	156	64
	10	8121	1.00	5	335	134	2	151	66
	11	8124	1.00	2	326	133	2	149	66
	12	8122	1.00	4	307	126	2	148	67
	13	8125	1.00	3	301	118	2	146	67
	14	8122	1.00	4	300	113	2	143	68
	15	8125	1.00	2	289	105	1	142	69
	16	8123	1.00	2	252	93	1	144	69
	17	8121	1.00	9	248	87	1	147	70
	18	8122	1.00	1	246	91	1	139	70
	19	8121	1.00	9	243	91	1	132	71
	20	8119	1.00	3	243	88	1	129	72
	21	8122	1.00	2	234	82	1	126	71
	22	8119	1.00	2	195	71	1	121	72
	23	8121	1.00	7	152	62	1	344	71
	24	8122	1.00	1	151	62	1	322	73
	25	8119	1.00	0	159	64	1	66	71
	26	8119	1.00	2	153	62	1	28	68
	27	8119	1.00	1	132	58	1	359	64

Appendix C.20

Summary of current velocity magnitude and direction from the PLOO static ADCP during 2020 and 2021. Data are presented by depth bin as seasonal recovered observations (n), minimum (min), maximum (max), and means with 95% confidence intervals (CI). Proportion of recovered observations (n_prop) differed due to variations in data quality (see text). Minimum and maximum angles of velocity are not shown due to the circular nature of the measurement.

				Magnitude (mm/s)				Angle	
Season	**Depth (m)**	**n**	**n_prop**	**Min**	**Max**	**Mean**	**95% CI**	**Mean**	**95% CI**
Winter	9	3130	0.74	2	352	129	3	157	63
	13	3434	0.81	1	491	155	3	170	63
	17	3695	0.87	4	496	150	3	169	64
	21	3928	0.93	1	497	143	3	170	64
	25	4074	0.96	1	498	135	3	170	65
	29	4168	0.98	3	494	126	2	169	66
	33	4204	0.99	0	492	118	2	168	66
	37	4222	1.00	1	471	109	2	168	66
	41	4225	1.00	2	455	100	2	167	65
	45	4225	1.00	1	415	91	2	162	65
	49	4224	1.00	1	354	83	2	155	64
	53	4226	1.00	1	326	75	2	121	63
	57	4230	1.00	1	304	70	1	8	63
	61	4232	1.00	1	288	65	1	355	62
	65	4231	1.00	0	276	62	1	352	62
	69	4231	1.00	0	274	61	1	354	62
	73	4232	1.00	1	298	61	1	1	63
	77	4232	1.00	1	309	59	1	16	64
	81	4232	1.00	1	309	57	1	48	66
	85	4232	1.00	3	303	54	1	101	68
	89	4232	1.00	1	288	53	1	139	66
	93	4232	1.00	1	257	45	1	164	62
Spring	9	2157	0.99	7	361	155	3	105	60
	13	2152	0.99	4	440	175	4	159	64
	17	2176	1.00	2	435	161	3	156	64
	21	2180	1.00	11	408	147	3	153	64
	25	2180	1.00	6	363	134	3	148	64
	29	2181	1.00	9	334	124	3	138	64
	33	2181	1.00	1	307	114	3	121	65
	37	2181	1.00	4	274	106	3	95	65
	41	2181	1.00	2	259	98	2	67	64
	45	2181	1.00	1	245	91	2	43	63
	49	2181	1.00	4	241	86	2	24	62
	53	2181	1.00	1	249	81	2	10	62
	57	2181	1.00	0	246	76	2	358	61
	61	2181	1.00	2	234	72	2	347	60
	65	2181	1.00	3	218	68	2	338	59

Appendix C.20 *continued*

				Magnitude (mm/s)				Angle	
Season	Depth (m)	n	n_prop	Min	Max	Mean	95% CI	Mean	95% CI
	69	2181	1.00	1	203	65	2	333	60
	73	2181	1.00	0	195	61	2	335	63
	77	2181	1.00	1	195	58	2	343	66
	81	2179	1.00	2	191	56	2	359	69
	85	2175	1.00	4	183	55	1	26	68
	89	2157	0.99	2	176	56	1	64	67
	93	2160	0.99	1	158	49	1	93	65
Summer	9	2265	0.97	1	299	110	2	104	57
	13	2291	0.98	3	435	128	4	157	66
	17	2333	1.00	1	423	121	4	116	66
	21	2339	1.00	2	375	113	4	355	65
	25	2341	1.00	6	350	107	3	349	64
	29	2342	1.00	1	354	102	3	348	64
	33	2342	1.00	1	346	98	3	349	64
	37	2342	1.00	4	331	95	3	349	65
	41	2342	1.00	2	317	92	3	348	66
	45	2342	1.00	3	310	90	3	349	67
	49	2342	1.00	3	297	87	3	348	66
	53	2342	1.00	1	279	83	3	345	66
	57	2342	1.00	0	269	80	3	341	65
	61	2342	1.00	1	266	76	2	337	65
	65	2342	1.00	1	259	73	2	333	66
	69	2342	1.00	2	246	70	2	332	66
	73	2342	1.00	2	228	67	2	334	65
	77	2342	1.00	1	207	61	2	338	66
	81	2342	1.00	0	184	56	2	346	67
	85	2336	1.00	0	167	52	1	1	67
	89	2314	0.99	1	141	49	1	43	66
	93	2306	0.98	0	116	42	1	128	62
Fall	9	4058	0.92	3	355	111	2	151	65
	13	4303	0.97	1	349	119	2	158	64
	17	4388	0.99	1	341	106	2	151	64
	21	4405	1.00	1	357	94	2	134	64
	25	4415	1.00	1	363	85	2	68	64
	29	4416	1.00	1	348	81	2	29	64
	33	4416	1.00	1	326	80	2	16	63
	37	4416	1.00	1	300	81	2	11	64
	41	4416	1.00	2	265	81	2	10	64
	45	4416	1.00	1	248	81	1	9	65
	49	4416	1.00	1	252	80	1	7	66
	53	4416	1.00	1	232	81	1	3	66

Appendix C.20 *continued*

				Magnitude (mm/s)				Angle	
Season	Depth (m)	n	n_prop	Min	Max	Mean	95% CI	Mean	95% CI
	57	4416	1.00	1	197	81	1	359	67
	61	4416	1.00	1	201	79	1	352	67
	65	4416	1.00	1	206	76	1	344	67
	69	4416	1.00	0	222	74	1	339	67
	73	4416	1.00	1	237	71	1	338	67
	77	4416	1.00	0	244	68	1	342	69
	81	4416	1.00	1	241	64	1	359	71
	85	4416	1.00	1	235	62	1	42	71
	89	4416	1.00	1	221	60	1	90	70
	93	4416	1.00	0	198	51	1	121	68

Appendix C.21

Summary of current velocity magnitude and direction from the SBOO static ADCP during 2020 and 2021. Data are presented by depth bin as seasonal recovered observations (n), minimum (min), maximum (max), and means with 95% confidence intervals (CI). Proportion of recovered observations (n_prop) differed due to variations in data quality (see text). Minimum and maximum angles of velocity are not shown due to the circular nature of the measurement.

				Magnitude (mm/s)				Angle	
Season	**Depth (m)**	**n**	**n_prop**	**Min**	**Max**	**Mean**	**95% CI**	**Mean**	**95% CI**
Winter	6	2914	0.99	1	396	133	3	149	62
	10	2941	1.00	3	391	113	3	167	68
	14	2942	1.00	2	367	101	2	158	68
	18	2943	1.00	2	298	89	2	152	69
	22	2948	1.00	3	220	74	1	149	71
	26	2949	1.00	1	193	58	1	146	70
	30	2949	1.00	1	165	42	1	139	66
Spring	6	2171	0.99	2	361	156	3	117	66
	10	2184	1.00	2	319	111	3	141	68
	14	2184	1.00	2	259	94	3	121	69
	18	2184	1.00	1	214	81	2	90	71
	22	2184	1.00	1	206	69	2	51	71
	26	2184	1.00	1	177	60	2	24	69
	30	2184	1.00	0	132	48	1	9	64
Summer	6	2184	1.00	20	311	114	2	125	69
	10	2186	1.00	0	231	79	2	139	69
	14	2186	1.00	1	227	75	2	74	70
	18	2186	1.00	2	198	70	2	20	73
	22	2186	1.00	1	168	63	2	8	74
	26	2186	1.00	1	146	53	1	3	73
	30	2186	1.00	1	115	41	1	352	71
Fall	6	2205	1.00	1	370	149	4	156	67
	10	2207	1.00	3	324	128	3	157	65
	14	2208	1.00	2	311	106	3	149	65
	18	2208	1.00	0	271	83	2	142	68
	22	2208	1.00	4	229	67	2	131	71
	26	2208	1.00	1	204	56	2	75	73
	30	2208	1.00	0	167	47	1	345	69

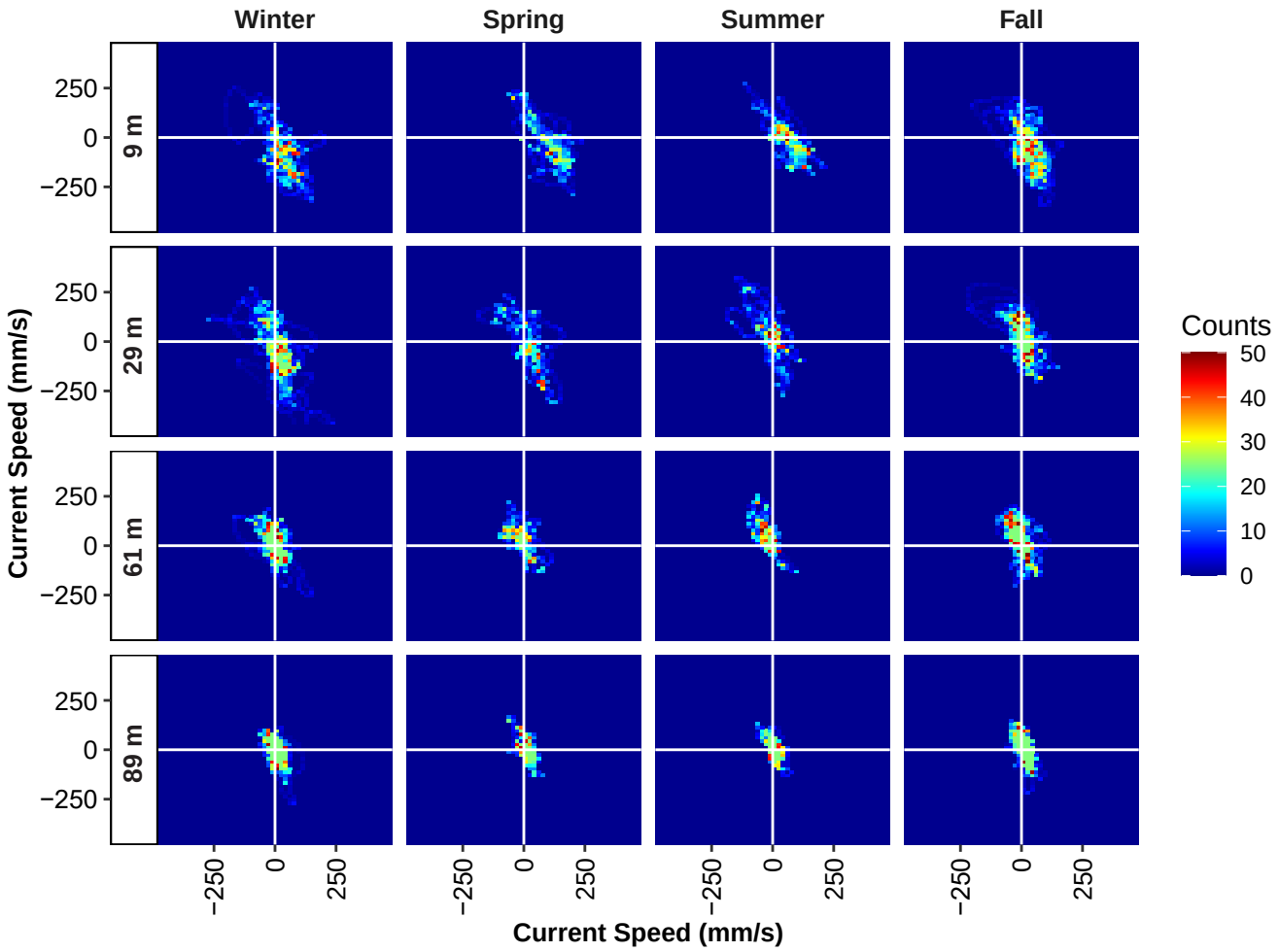

Appendix C.22

Frequency distribution (counts) by season of current speed (mm/s) and direction from 2020 and 2021 at the PLOO static ADCP location at representative depth bins. On the x-axis, positive values indicate an eastward direction while negative values indicate a westward direction. On the y-axis, positive values indicate a northward direction while negative values indicate a southward direction.

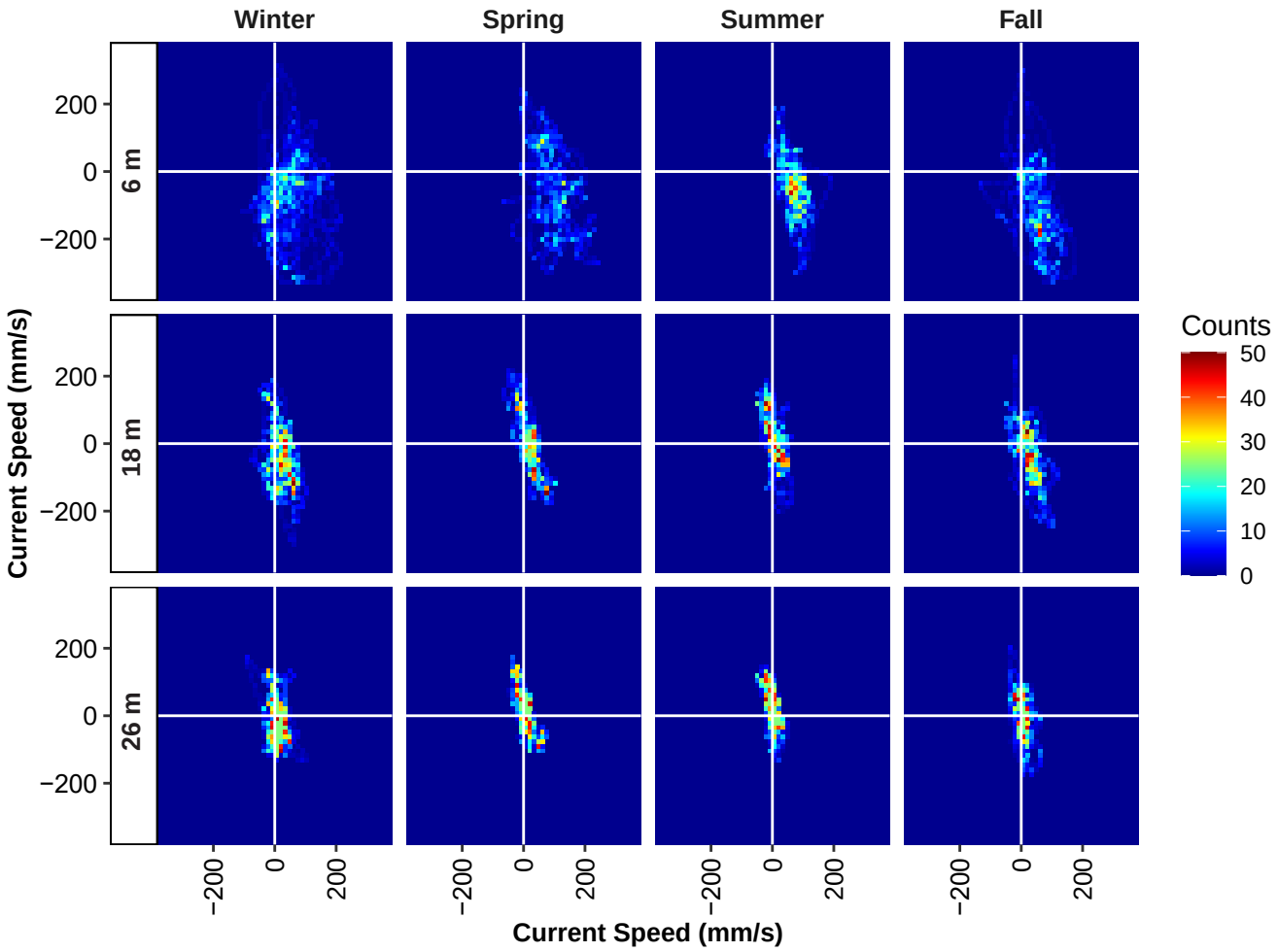

Appendix C.23

Frequency distribution (counts) by season of current speed (mm/s) and direction from 2020 and 2021 at the SBOO static ADCP location at representative depth bins. On the x-axis, positive values indicate an eastward direction while negative values indicate a westward direction. On the y-axis, positive values indicate a northward direction while negative values indicate a southward direction.

This page intentionally left blank

Appendix D

Water Quality: 2015 California Ocean Plan Objectives for the Point Loma Ocean Outfall

2020 – 2021 Supplemental Analyses

Appendix D. Water Quality: 2015 California Ocean Plan Objectives for the Point Loma Ocean Outfall

Introduction

NB: This appendix presents data analysis to meet the 2015 Ocean Plan water quality bacterial objectives as required by the National Pollutant Discharge Elimination System (NPDES) permit for the Point Loma Wastewater Treatment Plant (NPDES No. CA0107409; Order No. R9-2017-0007). However, additional analyses using current 2019 Ocean Plan Objectives are presented in Chapter 3.

The City of San Diego (City) conducts extensive monitoring along the shoreline (beaches), nearshore (e.g., kelp forests), and other offshore coastal waters surrounding the Point Loma Ocean Outfall (PLOO) to characterize regional water quality conditions and to identify possible impacts of wastewater discharge, or other contaminant sources, on the marine environment. Densities of fecal indicator bacteria (FIB), including total coliforms, fecal coliforms and *Enterococcus*, are measured and evaluated in context with various oceanographic parameters (see Chapter 2) to provide information about the movement and dispersion of wastewater discharged into the Pacific Ocean through the PLOO. Evaluation of these data may also help to identify other sources of bacterial contamination off San Diego. In addition, the City's water quality monitoring efforts are designed to assess compliance with the bacterial water contact standards and other physical and chemical water quality objectives specified in the California Ocean Plan (Ocean Plan) that are intended to help protect the beneficial uses of State ocean waters (herein utilizing 2015 objectives: see SWRCB 2015).

Multiple sources of bacterial contamination exist in the Point Loma region, and being able to separate any impact that may be associated with wastewater discharge from other point, or non-point, sources of contamination is often challenging. Examples include outflows from the San Diego River and San Diego Bay. Likewise, storm water discharges and terrestrial runoff from local watersheds during storms, or other wet weather events, can also flush sediments and contaminants into nearshore coastal waters (Noble et al. 2003, Reeves et al. 2004, Sercu et al. 2009, Griffith et al. 2010). Moreover, decaying kelp and seagrass (beach wrack), sediments and sludge accumulating in storm drains, and sandy beach sediments themselves can serve as reservoirs for bacteria until release into coastal waters by returning tides, rain events, or other disturbances (Gruber et al. 2005, Martin and Gruber 2005, Noble et al. 2006, Yamahara et al. 2007, Phillips et al. 2011). Further, the presence of shore birds and their droppings has been associated with high bacterial counts that may impact nearshore water quality (Grant et al. 2001, Griffith et al. 2010).

This appendix presents an analysis and assessment of bacterial distribution patterns, during 2020 and 2021, at more than 50 permanent water quality monitoring stations surrounding the PLOO. The primary goals are to: (1) document overall water quality conditions off of the San Diego, Point Loma region; and (2) assess compliance with the 2015 Ocean Plan water contact standards.

Materials and Methods

Field Sampling

Shore stations

Seawater samples were collected weekly at 8 shoreline stations to monitor concentrations of FIB in waters adjacent to public beaches (Appendix D.1). All of these stations are in California State waters and are therefore subject to Ocean Plan water contact standards (Appendix D.2) (SWRCB 2015). PLOO shoreline stations (D4, D5,

D7, D8-A/D8-B, D9, D10, D11, D12) are located from Mission Beach southward to the tip of Point Loma. Due to access issues, station D8-A replaced D8 in July 2016 and station D8-B replaced D8-A in March 2018. Sampling at station D8-A resumed in December 2020. However, due to further access issues at D8-A, sampling resumed at D8-B during February 2021.

Seawater samples were collected from the surf zone at each of the above stations in sterile 250 mL bottles, after which they were transported on blue ice to the City's Marine Microbiology Laboratory and analyzed to determine concentrations of three types of FIB (i.e., total coliform, fecal coliform, *Enterococcus* bacteria). In addition, weather conditions and visual observations of water color and clarity, surf height, and human or animal activity were recorded at the time of sample collection. Wind speed and direction were measured using a hand-held anemometer with a compass. These observations were previously reported in monthly receiving waters monitoring reports submitted to the San Diego Regional Water Quality Control Board (SDRWQCB) (see City of San Diego 2020–2022). These reports are available online (City of San Diego 2022a).

Kelp and offshore stations

Eight stations located in relatively shallow waters within or near the Point Loma kelp beds (referred to as "kelp" stations herein) were monitored weekly to assess water quality conditions and Ocean Plan compliance in nearshore areas used for recreational activities such as SCUBA diving, surfing, fishing, and kayaking (Appendix D.1). These included stations C4, C5, and C6 located along the 9-m depth contour near the inner edge of the Point Loma kelp forest, and stations A1, A6, A7, C7, and C8 located along the 18-m depth contour near the outer edge of the Point Loma kelp forest.

An additional 36 offshore stations were sampled quarterly over consecutive days in winter (February or March), spring (May), summer (August), and fall (November) to monitor water quality conditions. PLOO stations are designated F1–F36 and are located along or adjacent to the 18, 60, 80, and 98-m depth contours. Seawater samples for FIB were collected at all of these stations (see below). Additionally, 15 of the PLOO stations (F01–F03, F06–F14, F18–F20) are located within State jurisdictional waters (i.e., within 3 nautical miles of shore) and therefore subject to the Ocean Plan compliance standards.

Seawater samples for FIB analyses were collected from 3 to 5 discrete depths at the kelp and offshore stations as indicated in Appendix D.3. These samples were typically collected using a rosette sampler fitted with Niskin bottles surrounding a central Conductivity, Temperature, and Depth (CTD) instrument, although replacement samples due to misfires or other causes may have been collected from a separate follow-up cast using stand-alone Van Dorn bottles if necessary. All weekly kelp/nearshore samples were analyzed for all three types of FIB, while the quarterly offshore samples were only analyzed for *Enterococcus* per permit requirements. All samples were refrigerated at sea and then transported on blue ice to the City's Marine Microbiology Laboratory for processing and analysis. Oceanographic data were collected simultaneously with the water samples at each station (see Chapter 2). Visual observations of weather, sea conditions, and human or animal activity were also recorded at the time of sampling. These latter observations were also reported previously in monthly receiving waters monitoring reports submitted to the SDRWQCB (see City of San Diego 2020–2022). These reports are available online (City of San Diego 2022a).

Laboratory Analyses

The City Marine Microbiology Laboratory follows guidelines issued by the U.S. Environmental Protection Agency (USEPA) Water Quality Office, State Water Resources Control Board (SWRCB) including the 2015 Ocean Plan, and Environmental Laboratory Accreditation Program (ELAP) with respect to sampling and analytical procedures (Bordner et al. 1978, APHA 2012, USEPA 2014). All bacterial analyses were initiated within eight hours of sample collection and conformed to standard membrane filtration techniques, for which the laboratory is certified (ELAP Field of Testing 126).

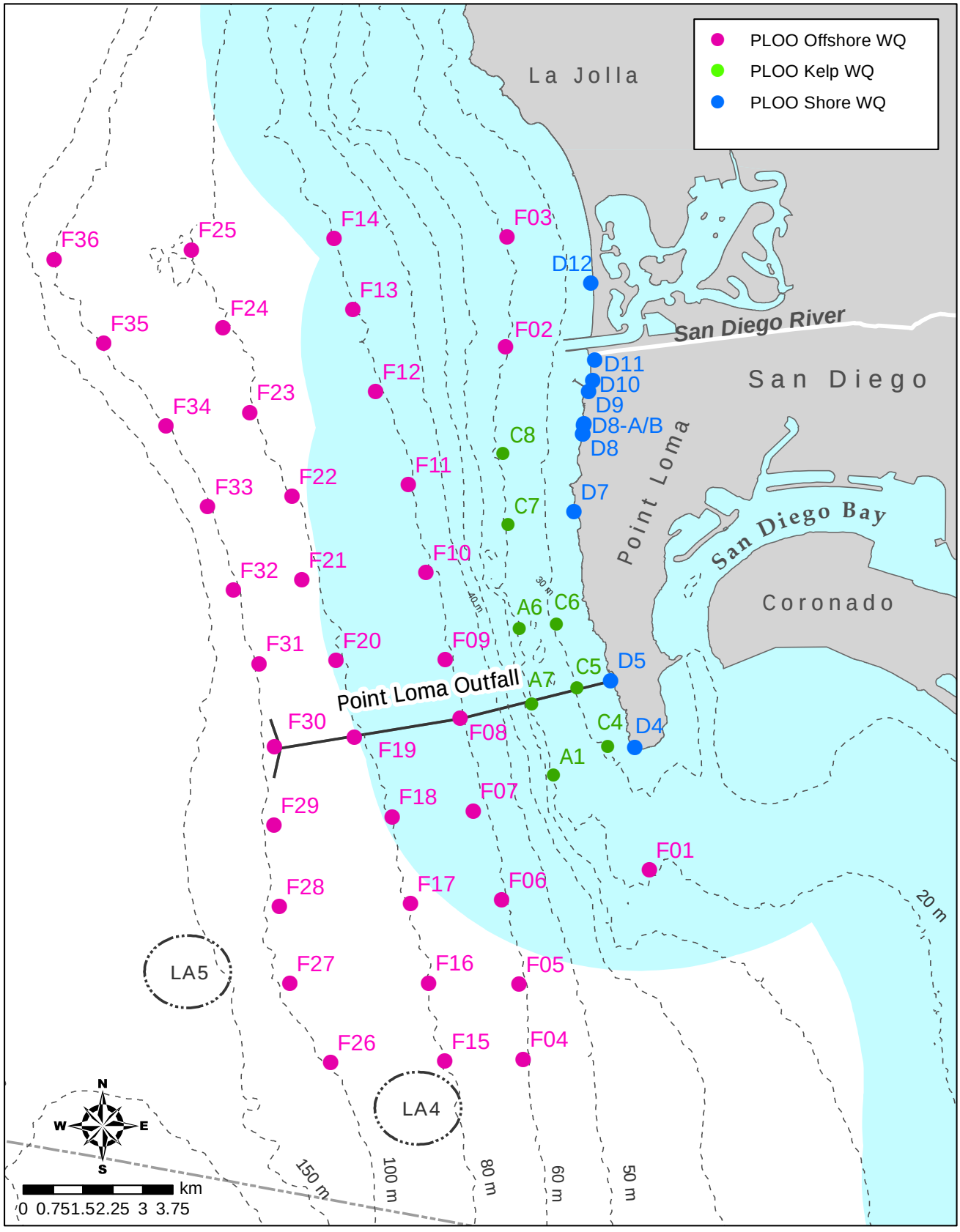

Appendix D.1

Water quality (WQ) monitoring station locations sampled around the PLOO as part of the City of San Diego's Ocean Monitoring Program. Light blue shading represents State jurisdictional waters.

Appendix D.2

Water quality objectives for water contact areas, California Ocean Plan (SWRCB 2015).

A. Bacterial Characteristics – Water Contact Standards; CFU = colony forming units.

(a) 30-day Geometric Mean – The following standards are based on the geometric mean of the five most recent samples from each site:

1) Total coliform density shall not exceed 1000 CFU/100 mL

2) Fecal coliform density shall not exceed 200 CFU/100 mL

3) Enterococcus density shall not exceed 35 CFU/100 mL

(b) Single Sample Maximum:

1) Total coliform density shall not exceed 10,000 CFU/100 mL

2) Fecal coliform density shall not exceed 400 CFU/100 mL

3) Enterococcus density shall not exceed 104 CFU/100 mL

4) Total coliform density shall not exceed 1000 CFU/100 mL when the fecal coliform:total coliform ratio exceeds 0.1

B. Physical Characteristics

(a) Floating particulates and oil and grease shall not be visible.

(b) The discharge of waste shall not cause aesthetically undesirable discoloration of the ocean surface.

(c) Natural light shall not be significantly reduced at any point outside of the initial dilution zone as the result of the discharge of waste.

C. Chemical Characteristics

(a) The dissolved oxygen concentration shall not at any time be depressed more than 10 percent from what occurs naturally, as a result of the discharge of oxygen demanding waste materials.

(b) The pH shall not be changed at any time more than 0.2 units from that which occurs naturally.

FIB densities were determined and validated in accordance with USEPA and APHA guidelines (Bordner et al. 1978, APHA 2012, USEPA 2014). Plates with FIB densities above or below the ideal counting range were given greater than (>), greater than or equal to (≥), less than (<), or estimated (e) qualifiers. However, all qualifiers were dropped, and densities were treated as discrete values, when determining compliance with Ocean Plan standards.

Quality assurance tests were performed routinely on bacterial samples to ensure that analyses and sampling variability did not exceed acceptable limits. Laboratory and field duplicate bacteriological samples were processed according to method requirements to measure analyst precision and variability between samples, respectively. Results of these procedures were reported under separate cover (City of San Diego 2021a, 2022b).

Data Analyses

Bacteriology

Compliance with Ocean Plan water contact standards was summarized as the number of times per sampling period that each shore, kelp, and offshore station within State waters exceeded geometric mean or single sample maximum (SSM) standards for total coliforms, fecal coliforms, and *Enterococcus* (Appendix D.2) (SWRCB 2015). Compliance calculations were limited to shore, kelp and offshore stations located within State waters. For shore stations, these calculations included resamples; no resamples are required to be collected at kelp or other offshore stations. To assess temporal and spatial trends, data were summarized as the number of samples in which FIB concentrations exceeded SSM benchmark levels. These calculations were performed for all shore, kelp and offshore stations located within and outside of State waters, but excluded resamples at shore stations.

Appendix D.3

Depths from which seawater samples are collected for bacteriological analysis from kelp and offshore stations.

Station Contour	PLOO Sample Depth (m)								
	1	3	9	12	18	25	60	80	98
Kelp Bed									
9-m	x	x	x						
18-m	x			x	x				
Offshore									
18-m	x			x	x				
60-m	x					x	x		
80-m	x					x	x	x	
98-m	x					x	x	x	x

Bacterial densities were compared to rainfall data from Lindbergh Field, San Diego, CA (NOAA 2022). Satellite images of the San Diego coastal region were provided by Ocean Imaging of Solana Beach, California and used to aid in the analysis and interpretation of water quality data (see Appendix B). All analyses were performed using R (R Core Team 2019) and various functions within the gtools, Hmisc, psych, reshape2, RODBC, tidyverse, ggpubr, quantreg, and openxlsx packages (Wickham 2007, 2017, Harrell et al. 2015, Warnppes et al. 2015, Revelle 2015, Ripley and Lapsley 2017, Kassambara 2019, Koenker 2019, Schauberger and Walker 2019). All raw data for the 2020–2021 sampling period have been submitted to either the Regional Water Quality Control Board or the California Environmental Data Exchange Network (CEDEN) and may be accessed upon request.

Results and Discussion

Bacteriological Compliance and Distribution

Shore stations

Overall compliance with the Ocean Plan water contact standards specified in Appendix D.2 was high at the PLOO shore stations in 2020–2021. Seawater samples collected from the eight PLOO shore stations were 100% compliant with the 30 day total coliform and fecal coliform geometric mean standards, while compliance with the 30 day *Enterococcus* geometric mean standard was 97–100% (Appendix D.4A). Compliance with the SSM standards at these sites was 100% for total coliforms, 100% for fecal coliforms, 93–100% for *Enterococcus*, and 100% for the fecal:total coliform ratio (FTR) (Appendix D.4B). Of the 838 sea water samples collected at the PLOO shore stations in 2020–2021 (not including resamples), only 1.2% (n = 10) had elevated FIB. Almost all of the shore samples with elevated FIB (90%) were collected during the wet seasons when rainfall totaled 10.96 inches over both years (Appendix D.5). This general relationship between rainfall and elevated bacterial levels at shore stations has been evident since water quality monitoring began.

Kelp bed stations

Overall compliance with Ocean Plan water contact standards was also high at the eight PLOO kelp stations in 2020–2021. Seawater samples from these stations were 100% compliant with each of the geometric mean standards and ≥ 99% compliant with the SSM standards for total coliform, fecal coliform, *Enterococcus*, and the FTR criterion (Appendix D.6). Of the 2520 samples collected at the PLOO kelp stations in 2020–2021, only 1 sample had elevated FIB, and that sample occurred in the wet season (Appendix D.7).

Offshore stations

Water quality was extremely high at all non-kelp offshore stations that were sampled quarterly in the PLOO region in 2020–2021. Of the 1127 samples collected at these stations over the past two years, only about 6% (n = 69) had elevated FIB, with approximately 50% occurring in the wet season (Appendix D.8). All most all of the offshore samples with elevated FIB (n = 68) in 2020–2021 occurred at stations located along the 80 or 98-m depth contours, and 25% were from stations F29, F30, and F31 located within 1000 m of the PLOO discharge site (i.e., nearfield stations). These results suggest that the PLOO wastewater plume continues to be restricted to relatively deep, offshore waters

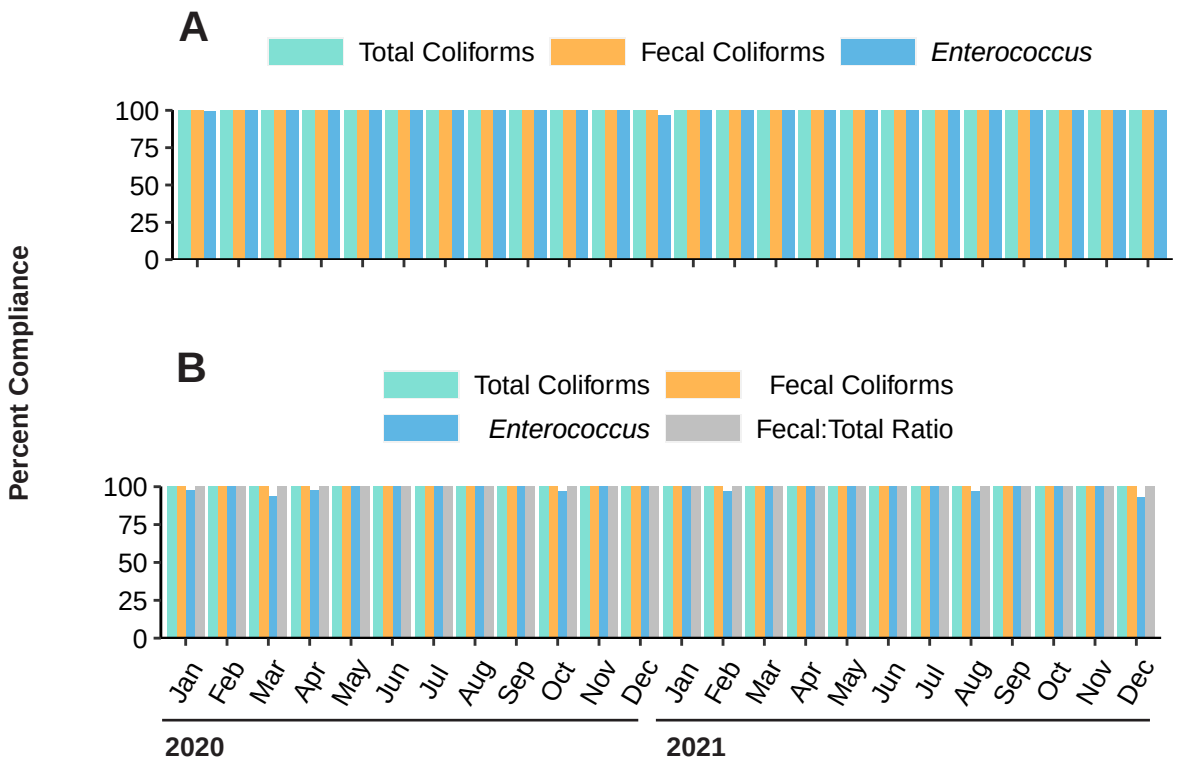

Appendix D.4
Compliance rates for (A) geometric mean and (B) single sample maximum water contact standards at PLOO shore stations during 2020 and 2021.

throughout the year. Additionally, there were no signs of wastewater at any of the 36 offshore PLOO stations based on visual observations of the surface. This conclusion is consistent with historical remote sensing observations that have provided no evidence of the PLOO plume reaching surface waters (see Appendix B: Svejkovsky and Hess 2022).

The above findings are consistent with historical ocean monitoring results, which revealed that <4% of samples collected at depths of ≤25 m from the PLOO 98-m (i.e., discharge depth) stations had elevated levels of *Enterococcus* during the pre-chlorination years (1993–2008). This percentage dropped to <1% at these depths following the initiation of partial chlorination at the Point Loma Wastewater Treatment Plant (PLWTP) in 2008 (City of San Diego 2009) and was zero during the current reporting period (Appendix D.9A). Overall, detection of elevated *Enterococcus* has been significantly more likely at the three nearfield stations (F29, F30, F31) than at any other 98-m site (20% versus 8%, respectively; n=7577, $\chi^2=48.91$, $p<0.0001$). The addition of chlorination significantly decreased the number of samples with elevated *Enterococcus* at these three stations (i.e., 26% before versus 10% after, n=2640, $\chi^2=330.9$, $p<0.0001$), and the other 98-m stations (11% before versus 4% after; n=4937, $\chi^2=156.64$, $p<0.0001$) (Appendix D.4B).

Summary

Overall water quality conditions were excellent throughout the PLOO monitoring region during 2020 and 2021. For example, overall compliance with Ocean Plan water contact standards was over 98%, which was similar to that observed during recent years (City of San Diego 2020). Compliance with both the SSM and geometric mean standards for fecal indicator bacteria was high at PLOO shore, kelp bed, and offshore stations. Reduced compliance at shore and kelp stations tended to occur during the wet season. However, offshore stations did not show an impact on compliance with increased rain fall, likely due to the distance of these stations from land based runoff. In addition, there was no evidence that wastewater

Appendix D.5

Number of samples with elevated FIB (eFIB) densities collected from PLOO shore stations during wet and dry seasons, and percent occuring in wet season (%wet), during 2020 and 2021. Rain data are from Lindbergh Field, San Diego, CA. Stations are listed north to south from top to bottom.

	Seasons		
Station	**Wet**	**Dry**	**% Wet**
PLOO			
D12	1	0	100
D11	3	1	75
D10	1	0	100
D9	1	0	100
D8-B	3	0	100
Rain (inches)	10.96	4.72	70
Total eFIB	9	1	90
Total Samples	486	352	58

discharged into the ocean reached nearshore waters. Historically, elevated FIB along the shore, or at the kelp bed stations, have typically been associated with storm activity (rain), heavy recreational use, the presence of seabirds, and decaying kelp or surfgrass (e.g., City of San Diego 2020). Exceptions to the above patterns have occurred over the years due to specific events. For example, the elevated bacteria that occurred at the PLOO shore and kelp stations during a few months in 1992 followed a catastrophic rupture of the outfall that occurred within the Point Loma kelp forest (Tegner et al. 1995).

The above results are also consistent with observations from remote sensing studies (i.e., satellite imagery) over several years that show a lack of shoreward transport of wastewater plumes from the PLOO (see Appendix B: Svejkovsky and Hess 2022), and with previous studies that have indicated the PLOO wastefield typically remains submerged in deep offshore waters (Rogowski et al. 2012a,b, 2013). The approximately 98 m depth of the PLOO discharge site is likely an important factor that inhibits the wastewater plume from reaching surface waters. Wastewater released into these deep, cold and dense waters does not appear to mix with the upper 25 m of the water column (Rogowski et al. 2012a,b, 2013).

Literature Cited

[APHA] American Public Health Association. (2012). Standard Methods for the Examination of Water and Wastewater, 22ndt edition. E.W. Rice, R. Baird, A. Eaton and L. Clesceri (eds.). American Public Health Association, American Water Works Association, and Water Pollution Control Federation.

Bordner, R., J. Winter, and P. Scarpino, eds. (1978). Microbiological Methods for Monitoring the Environment: Water and Wastes, EPA Research and Development, EPA-600/8-78-017.

City of San Diego. (2009). Annual Receiving Waters Monitoring Report for the Point Loma Ocean Outfall, 2008. City of San Diego Ocean Monitoring Program, Metropolitan Wastewater Department, Environmental Monitoring and Technical Services Division, San Diego, CA.

City of San Diego. (2020–2022). Monthly Receiving Waters Monitoring Reports for the Point Loma Ocean Outfall (Point Loma Wastewater Treatment Plant), January 2020–December 2021. City of San Diego Ocean Monitoring Program, Public Utilities Department, Environmental Monitoring and Technical Services Division, San Diego, CA.

City of San Diego. (2020). Biennial Receiving Waters Monitoring and Assessment Report for the Point Loma and South Bay Ocean Outfalls, 2018–2019. City of San Diego Ocean Monitoring Program, Public Utilities Department, Environmental Monitoring and Technical Services Division, San Diego, CA.

City of San Diego. (2021a). Annual Receiving Waters Monitoring and Toxicity Testing Quality Assurance Report, 2020. City of San Diego Ocean Monitoring Program, Public Utilities Department, Environmental Monitoring and Technical Services Division, San Diego, CA.

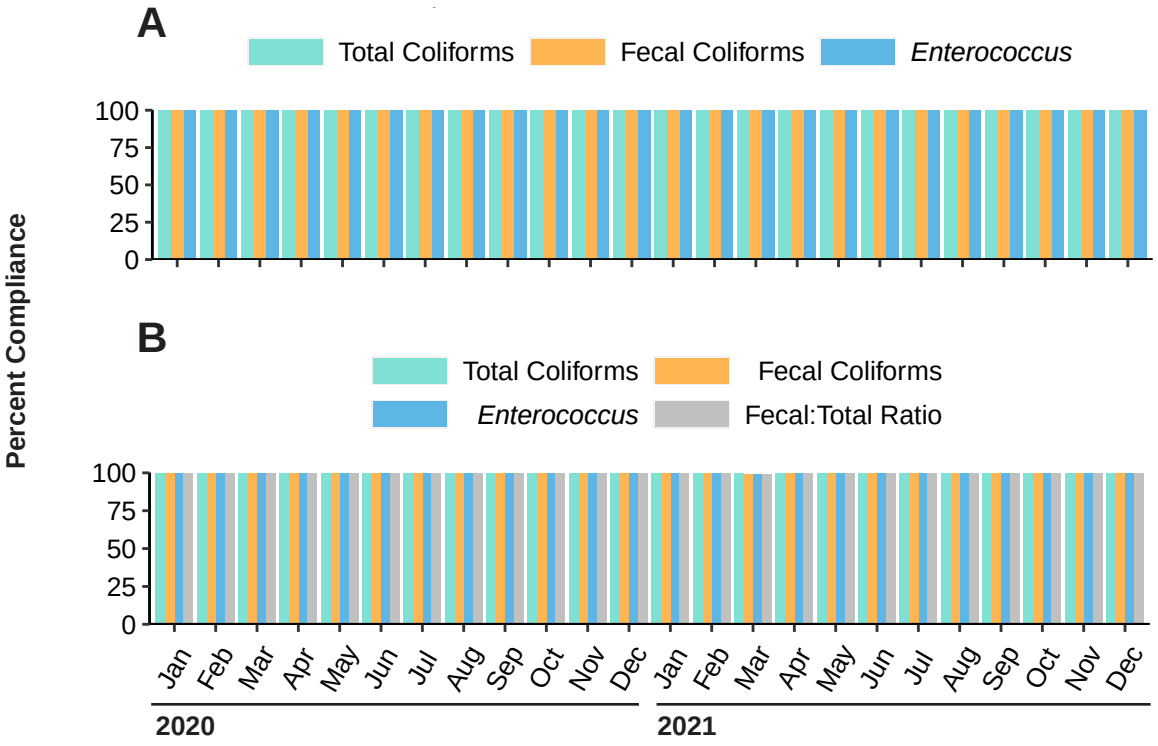

Appendix D.6

Compliance rates for (A) geometric mean and (B) single sample maximum water contact standards at PLOO kelp stations during 2020 and 2021.

City of San Diego. (2022a). Ocean Monitoring Reports. https://www.sandiego.gov/public-utilities/sustainability/ocean-monitoring/reports

City of San Diego. (2022b). Annual Receiving Waters Monitoring and Toxicity Testing Quality Assurance Report, 2021. City of San Diego Ocean Monitoring Program, Public Utilities Department, Environmental Monitoring and Technical Services Division, San Diego, CA.

Grant, S.B., B.F. Sanders, A. Boehm, J. Redman, R. Kim, A. Chu, M. Gouldin, C. McGee, N. Gardiner, B. Jones, J. Svejkovsky, and G. Leipzig. (2001). Generation of enterococci bacteria in a coastal saltwater marsh and its impact on surf zone water quality. Environmental Science Technology, 35: 2407–2416.

Griffith, J., K.C. Schiff, G. Lyon, and J. Fuhrman. (2010). Microbiological water quality at non-human influenced reference beaches in southern California during wet weather. Marine Pollution Bulletin, 60: 500–508.

Gruber, S., L. Aumand, and A. Martin. (2005). Sediments as a reservoir of indicator bacteria in a coastal embayment: Mission Bay, California, Technical paper 0506. Weston Solutions, Inc. Presented at StormCon 2005. Orlando, FL, USA. July 2005.

Harrell, F.E. Jr, C. Dupont and many others. (2015). Hmisc: Harrell Miscellaneous. R package version 3.17-0. http://CRAN.R-project.org/package=Hmisc.

Kassambara, A. (2019). ggpubr: 'ggplot2' Based Publication Ready Plots. R package version 0.2.4. https://CRAN.R-project.org/package=ggpubr.

Koenker, R. (2019). quantreg: Quantile Regression. R package version 5.52. https://CRAN.R-project.org/package=quantreg.

Appendix D.7

Number of samples with elevated FIB (eFIB) densities collected at PLOO kelp stations during wet and dry seasons, and percent occuring in wet season (%wet), during 2020 and 2021. Within each contour stations are listed from north to south. See Appendix D.5 for rain data. Stations not listed had no samples with elevated FIB concentrations during this time period.

	Seasons		
	Wet	**Dry**	**% Wet**
PLOO			
18-m Depth Contour			
C7	1	0	100
Total eFIB	1	0	100
Total Samples	1464	1056	58

Martin, A., and S. Gruber. (2005). Amplification of indicator bacteria in organic debris on southern California beaches. Technical Paper 0507. Weston Solutions, Inc. Presented at StormCon 2005. Orlando, FL, USA. July 2005.

[NOAA] National Oceanic and Atmospheric Administration. (2022). National Climatic Data Center. https://www.ncdc.noaa.gov/cdo-web/search

Noble, R.T., D.F. Moore, M.K. Leecaster, C.D. McGee, and S.B. Weisberg. (2003). Comparison of total coliform, fecal coliform, and *Enterococcus* bacterial indicator response for ocean recreational water quality testing. Water Research, 37: 1637–1643.

Noble, M.A., J.P. Xu, G.L. Robertson, and K.L. Rosenfeld. (2006). Distribution and sources of surfzone bacteria at Huntington Beach before and after disinfection of an ocean outfall–A frequency-domain analysis. Marine Environmental Research, 61: 494–510.

Phillips, C.P., H.M. Solo-Gabriele, A.J. Reneiers, J.D. Wang, R.T. Kiger, and N. Abdel-Mottaleb. (2011). Pore water transport of enterococci out of beach sediments. Marine Pollution Bulletin, 62: 2293–2298.

R Core Team. (2019). R: A language and environment for statistical computing. R Foundation for Statistical Computing, Vienna, Austria. URL https://www.R-project.org/.

Reeves, R.L., S.B. Grant, R.D. Mrse, C.M. Copil Oancea, B.F. Sanders, and A.B. Boehm. (2004). Scaling and management of fecal indicator bacteria in runoff from a coastal urban watershed in southern California. Environmental Science and Technology, 38: 2637–2648.

Revelle, W. (2015). psych: Procedures for Personality and Psychological Research, Northwestern University, Evanston, Illinois, USA, http://CRAN.R-project.org/package=psych version 1.5.8.

Ripley, B. and M. Lapsley. (2017). RODBC: ODBC Database Access. R package version 1.3-12. http://CRAN.R-project.org/package=RODBC.

Rogowski, P., E. Terrill, M. Otero, L. Hazard, S.Y. Kim, P.E. Parnell, and P. Dayton. (2012a). Final Report: Point Loma Ocean Outfall Plume Behavior Study. Prepared for City of San Diego Public Utilities Department by Scripps Institution of Oceanography, University of California, San Diego, CA.

Rogowski, P., E. Terrill, M. Otero, L. Hazard, and W. Middleton. (2012b). Mapping ocean outfall plumes and their mixing using Autonomous Underwater Vehicles. Journal of Geophysical Research, 117: C07016.

Rogowski, P., E. Terrill, M. Otero, L. Hazard, and W. Middleton. (2013). Ocean outfall plume characterization using an Autonomous Underwater Vehicle. Water Science & Technology, 67: 925–933.

Schauberger, P. and A. Walker (2019). openxlsx: Read, Write and Edit xlsx Files. R package version 4.1.4. https://CRAN.R-project.org/package=openxlsx.

Appendix D.8

Number of samples with elevated FIB (eFIB) densities collected at PLOO offshore stations during wet and dry seasons, and percent occuring in wet season (%wet), during 2020 and 2021. Within each contour stations are listed from north to south. See Appendix D.5 for rain data. Stations not listed had no samples with elevated FIB concentrations during this time period.

	Seasons		
	Wet	**Dry**	**% Wet**
PLOO			
60-m Depth Contour			
F11	0	1	0
80-m Depth Contour			
F25	2	2	50
F24	2	2	50
F23	0	1	0
F22	1	2	33
F21	2	2	50
F20	3	3	50
F19	2	4	33
F18	2	0	100
F17	1	1	50
F15	1	0	100
100-m Depth Contour			
F36	1	0	100
F34	1	0	100
F33	4	2	67
F32	2	3	40
F31	2	3	40
F30	3	6	33
F29	1	2	33
F28	1	1	50
F27	2	0	100
F26	1	0	100
Total eFIB	34	35	49
Total Samples	563	564	50

Sercu, B., L.C. Van de Werfhorst, J. Murray, and P.A. Holden. (2009). Storm drains are sources of human fecal pollution during dry weather in three urban southern California watersheds. Environmental Science and Technology, 43: 293–298.

Svejkovsky, J. and Hess, M. (2022). Satellite & Aerial Coastal Water Quality Monitoring in the San Diego/Tijuana Region: Five Year Summary Report: 1 January 2017 – 31 December 2021. Littleton, CO.

[SWRCB] California State Water Resources Control Board. (2015). California Ocean Plan, Water Quality Control Plan, Ocean Waters of California. California Environmental Protection Agency, Sacramento, CA.

Tegner, M.J., P.K. Dayton, P.B. Edwards, K.L. Riser, D.B. Chadwick, T.A. Dean, and L. Deysher. (1995). Effects of a large sewage spill on a kelp forest community: Catastrophe or disturbance? Marine Environmental Research, 40: 181–224.

[USEPA] United States Environmental Protection Agency. (2014). Method 1600: Enterococci in Water by Membrane Filtration Using membrane-*Enterococcus* Indoxyl-β-D-Glucoside Agar (mEI). EPA Document EPA-821-R-14-011. Office of Water (4303T), Washington, DC.

Warnes, G., B. Bolker, and T. Lumley. (2015). gtools: Various R Programming Tools. R package version 3.5.0. http://CRAN.R-project.org/package=gtools.

Wickham, H. (2007). Reshaping Data with the reshape Package. Journal of Statistical Software, 21(12), 1-20. URL http://www.jstatsoft.org/v21/i12/.

Wickham, H. (2017). tidyverse: Easily Install and Load the 'Tidyverse'. R package version 1.2.1. https://CRAN.R-project.org/package=tidyverse.

Yamahara, K.M., B.A. Layton, A.E. Santoro, and A.B. Boehm. (2007). Beach sands along the California coast are diffuse sources of fecal bacteria to coastal waters. Environmental Science and Technology, 41: 4515–4521.

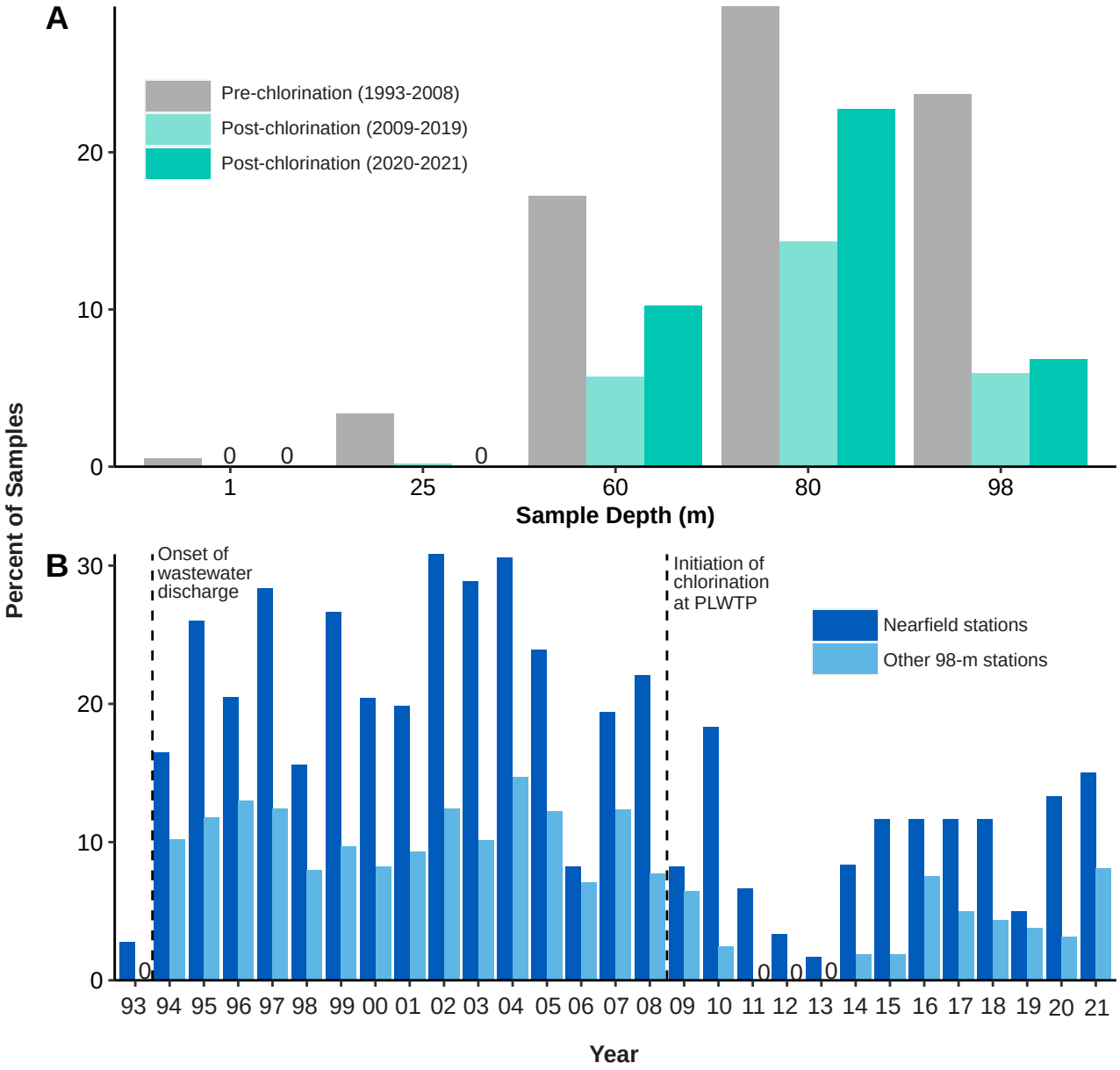

Appendix D.9

Percent of samples collected from PLOO 98-m offshore stations with elevated FIB. Samples from 2020 and 2021 are compared to those collected from 1993 through 2019 by (A) sampling depth and (B) year.

This page intentionally left blank

Appendix E

Plume Dispersion

2020 – 2021 Supplemental Analyses

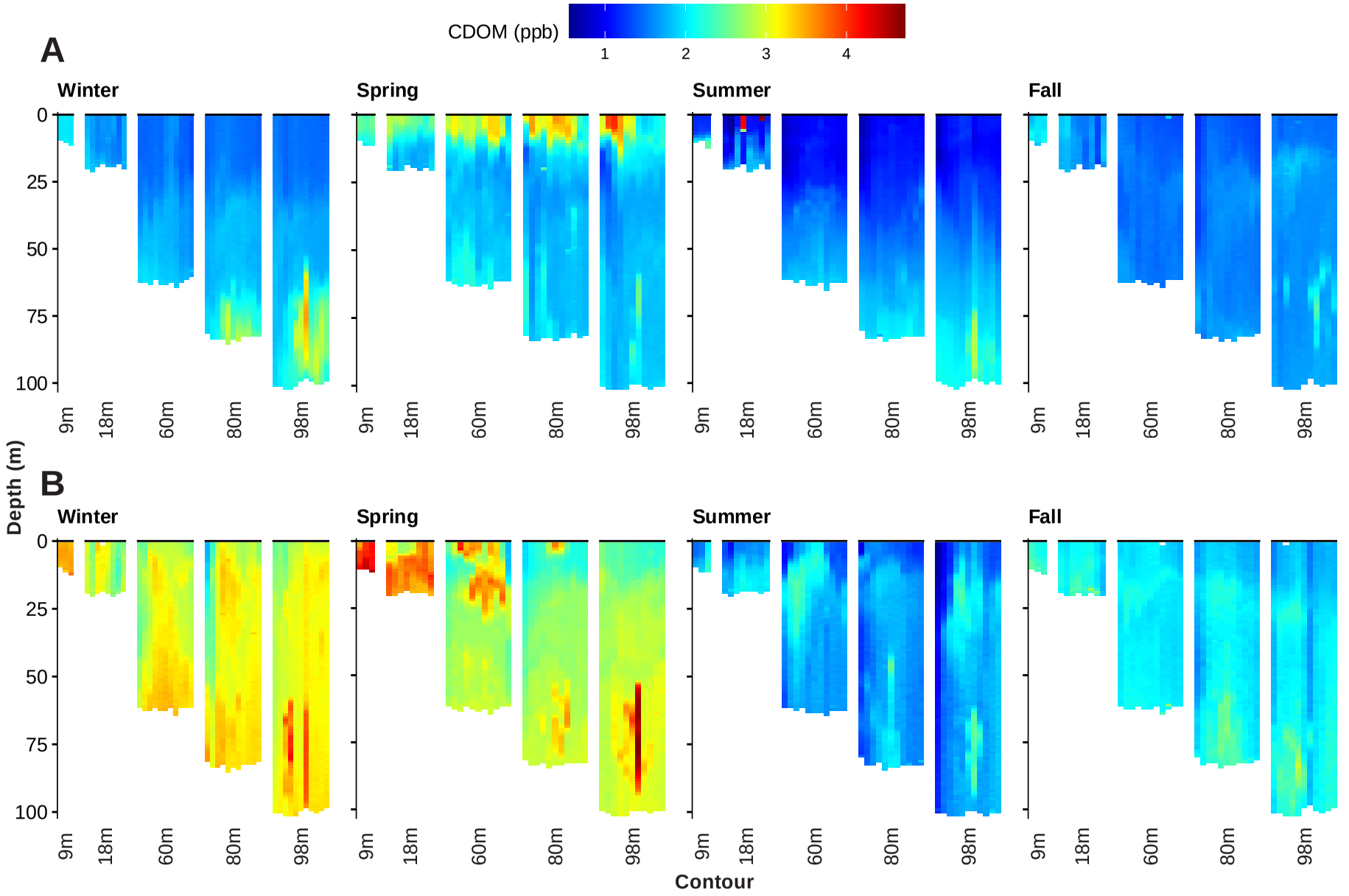

Appendix E.1

Concentrations of CDOM recorded in the PLOO region during (A) 2020 and (B) 2021. Data are 1-m binned values per depth for each station during each quarterly survey. Stations depicted from north to south along each depth contour. See Chapter 2 for additional sampling details.

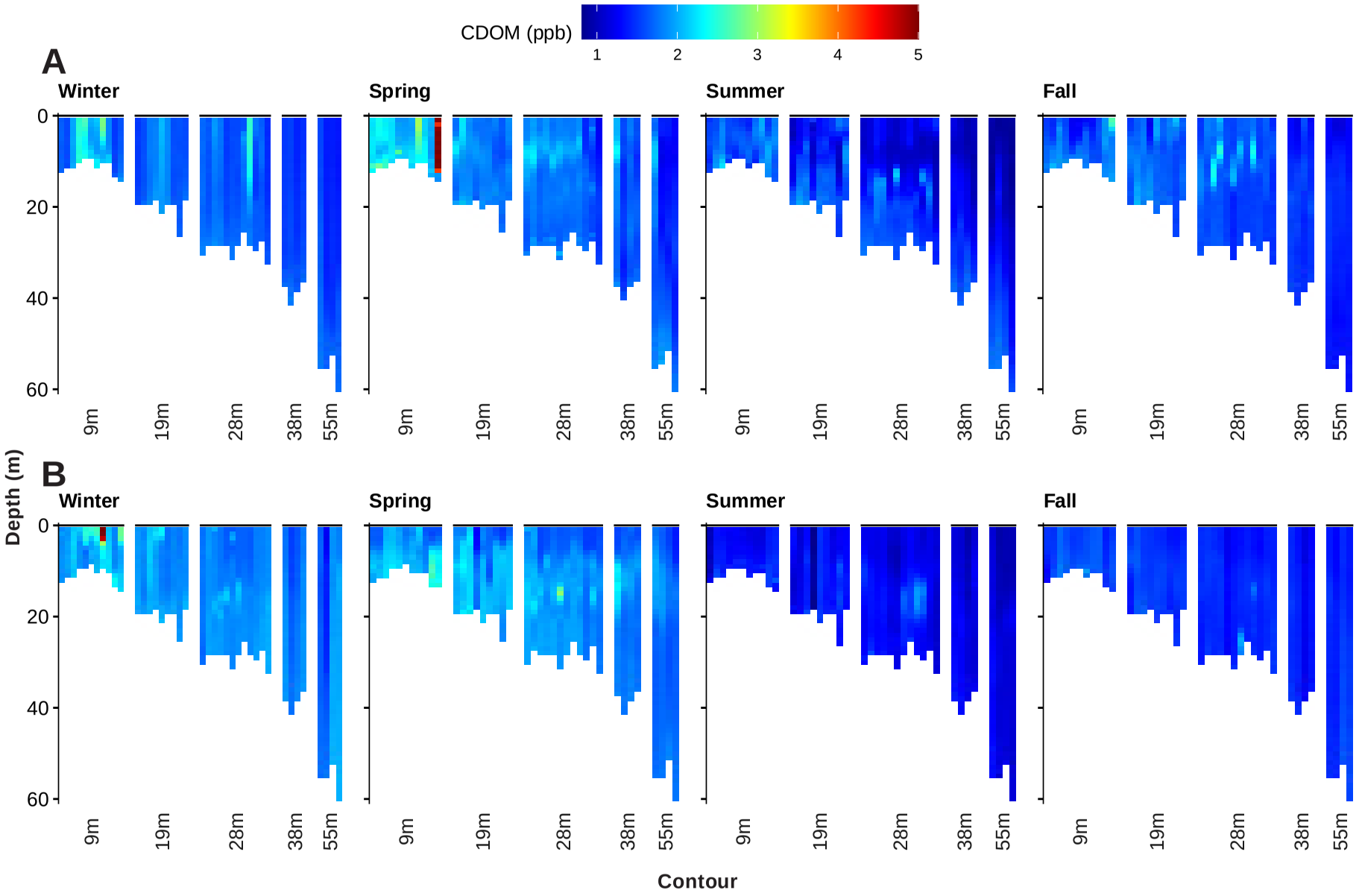

Appendix E.2

Concentrations of CDOM recorded in the SBOO region during (A) 2020 and (B) 2021. Data are 1-m binned values per depth for each station during each quarterly survey. Stations depicted from north to south along each depth contour. See Chapter 2 for additional sampling details.

Appendix E.3

Summary of oceanographic data within potential detected plume at PLOO offshore stations and corresponding reference values during 2020 and 2021. Plume depth is the minimum depth at which CDOM exceeds the 95th percentile while plume width is the number of meters across which that exceedance occurs. Out-of-range values are indicated with an asterisk. DO = dissolved oxygen (mg/L); XMS = transmissivity (%); SD = standard deviation; CI = confidence interval.

		Potential Plume					Reference [b]		
Station	Date	Width (m)	Depth (m)	Mean DO	Mean pH	Mean XMS	DO (Mean - SD)	pH (Mean)	XMS (Mean - 95% CI)
F27	19-Feb-20	21	72	4.3*	7.7	85	5.5	7.8	77
F28	19-Feb-20	16	82	4.2*	7.7	81*	5.8	7.8	91
F29	19-Feb-20	10	87	4.4*	7.7	84*	5.6	7.8	91
F30	19-Feb-20	36	59	4.3*	7.7	83	5.7	7.9	83
F31	19-Feb-20	24	71	4.5*	7.7	85	5.5	7.8	78
F32	19-Feb-20	10	78	4.5*	7.8	86	5.9	7.9	86
F19 [a]	21-Feb-20	4	78	4.4*	7.7	84	5.8	7.9	79
F21	21-Feb-20	12	71	4.7*	7.8	87	5.4	7.8	70
F30	20-May-20	15	61	3.5	7.8	89	—	—	—
F31	20-May-20	8	86	3.4	7.8	90	—	—	—
F27	18-Aug-20	13	84	4.3	7.8	92	—	—	—
F28	18-Aug-20	15	83	4.3	7.8	93	—	—	—
F29	18-Aug-20	12	85	4.3	7.8	92	—	—	—
F30	18-Aug-20	24	72	4.4	7.8	90	—	—	—
F31	18-Aug-20	16	81	4.6	7.8	92	—	—	—
F26	10-Nov-20	12	62	5.1	7.9	93	5.1	7.9	93
F27	10-Nov-20	8	55	5.0	7.9	93	5.1	7.9	92
F28	10-Nov-20	10	55	5.0	7.9	93	5.2	7.9	92
F29	10-Nov-20	27	61	4.7*	7.8	93	5.0	7.9	92
F30	10-Nov-20	8	64	4.8	7.8	92*	5.2	7.9	93
F34	10-Nov-20	9	61	4.6	7.8	93	5.5	7.9	92
F30	23-Feb-21	36	60	3.6	7.7	86*	3.4	7.7	87
F33	23-Feb-21	35	59	3.5	7.7	87	3.4	7.7	87

[a] Station located within State jurisdictional waters

[b] No reference stations available in May 2020; all reference stations in August 2020 were shallower than plume depths

Appendix E.3 *continued*

Station	Date	Potential Plume					Reference[b]		
		Width (m)	Depth (m)	Mean DO	Mean pH	Mean XMS	DO (Mean - SD)	pH (Mean)	XMS (Mean - 95% CI)
F34	23-Feb-21	19	64	3.6	7.7	87	3.4	7.8	87
F22	25-Feb-21	5	73	3.8	7.8	87	3.4	7.7	87
F25	25-Feb-21	3	76	3.4	7.7	86	3.3	7.7	86
F30	11-May-21	40	54	4.4	7.8	80*	4.4	7.8	87
F31	11-May-21	7	64	4.5	7.8	86*	4.4	7.8	87
F32	11-May-21	2	62	4.6	7.8	87*	4.5	7.8	88
F18[a]	13-May-21	2	65	4.7	7.8	86*	4.4	7.8	87
F29	10-Aug-21	4	70	4.3	7.8	87*	4.2	7.8	88
F30	10-Aug-21	30	63	4.1	7.8	85*	4.1	7.8	88
F31	10-Aug-21	4	79	4.3	7.8	88	5.0	7.8	86
F20[a]	12-Aug-21	6	44	4.5	7.7	87*	4.9	7.8	88
F31	09-Nov-21	6	85	4.5	7.7	86	4.3	7.7	86
F32	09-Nov-21	16	77	4.5	7.7	86	4.4	7.7	85
F33	09-Nov-21	13	74	4.5	7.7	87	4.4	7.7	85
F34	09-Nov-21	4	71	4.8	7.7	87	4.6	7.7	86
F35	09-Nov-21	5	86	4.3	7.7	87	4.3	7.7	86
F19[a]	12-Nov-21	8	72	4.5	7.6	87	4.5	7.7	85
F20[a]	12-Nov-21	21	57	4.5	7.6	87	4.8	7.7	86
F21	12-Nov-21	20	61	4.5	7.6	88	4.6	7.7	86

[a] Station located within State jurisdictional waters

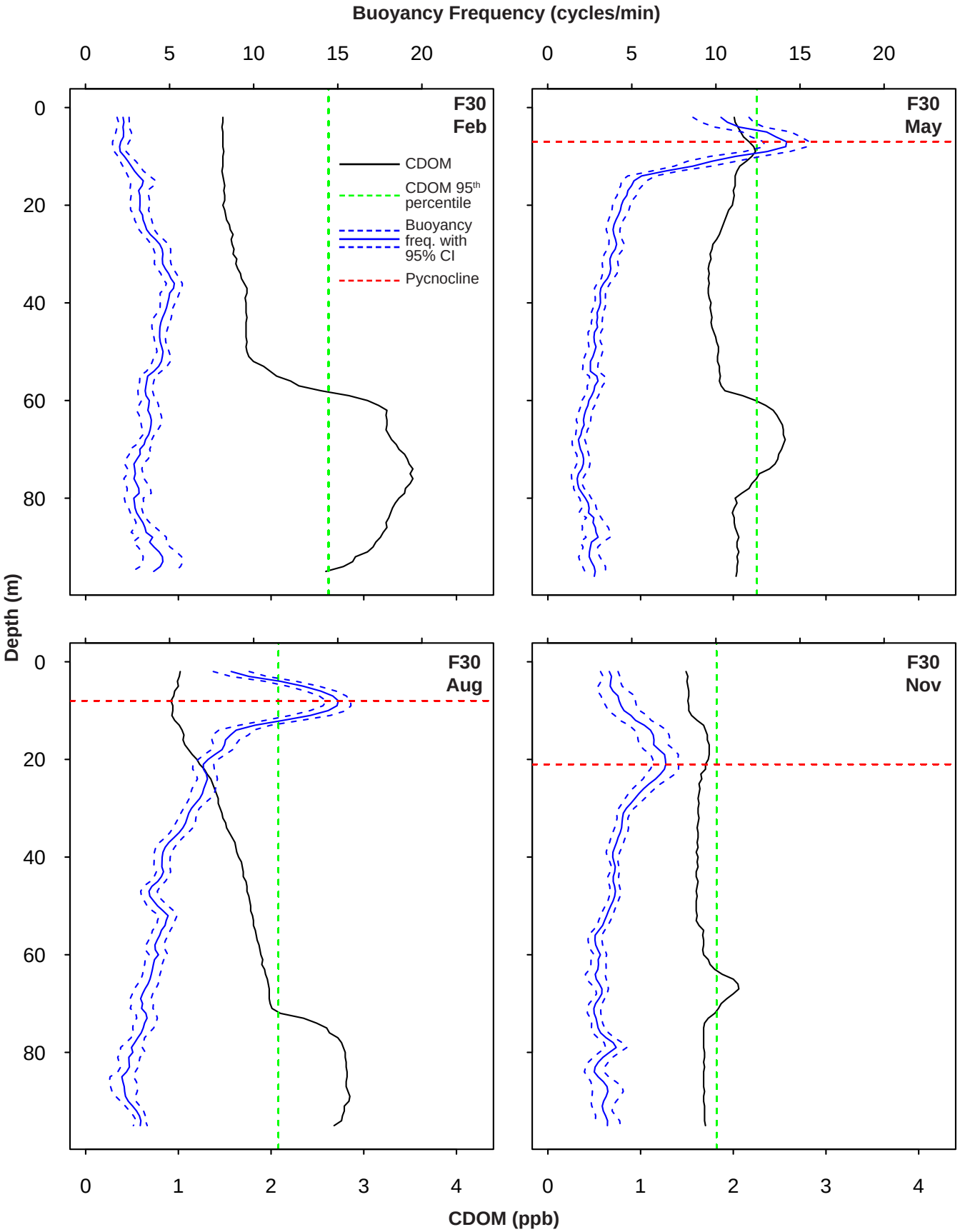

Appendix E.4

Representative vertical profiles of CDOM and buoyancy frequency from PLOO nearfield station F30 during 2020.

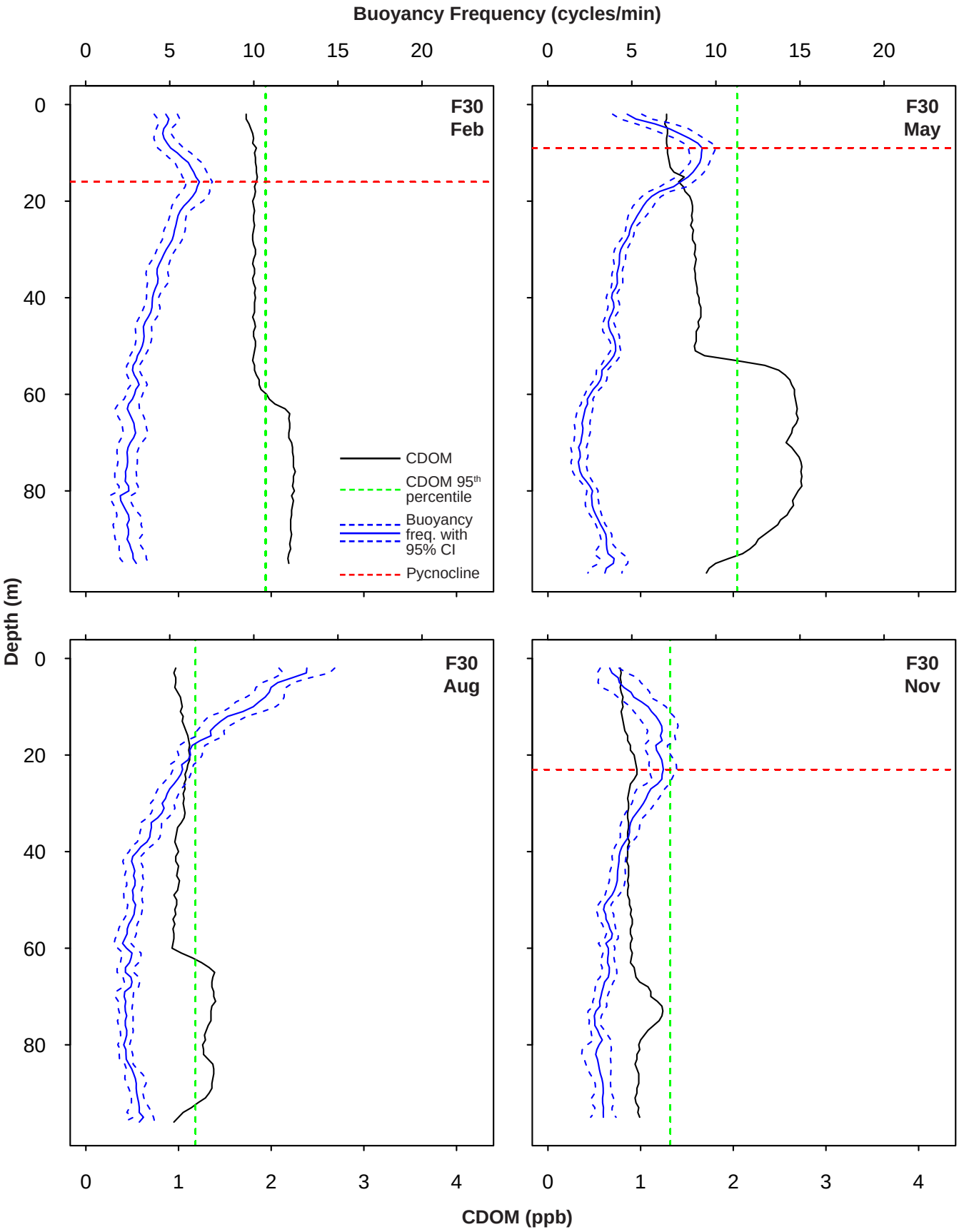

Appendix E.5

Representative vertical profiles of CDOM and buoyancy frequency from PLOO nearfield station F30 during 2021.

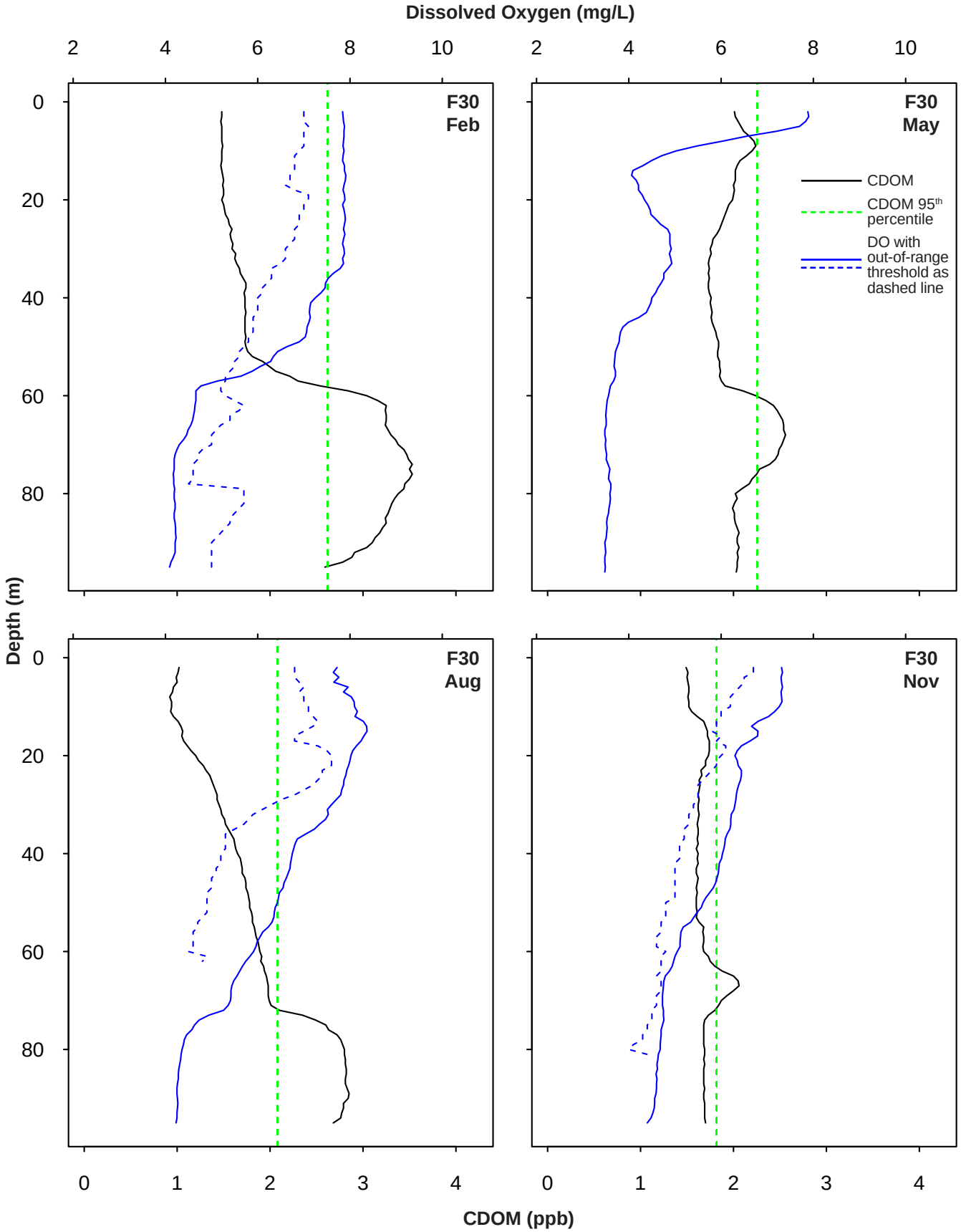

Appendix E.6

Representative vertical profiles of CDOM and DO from PLOO nearfield station F30 during 2020.

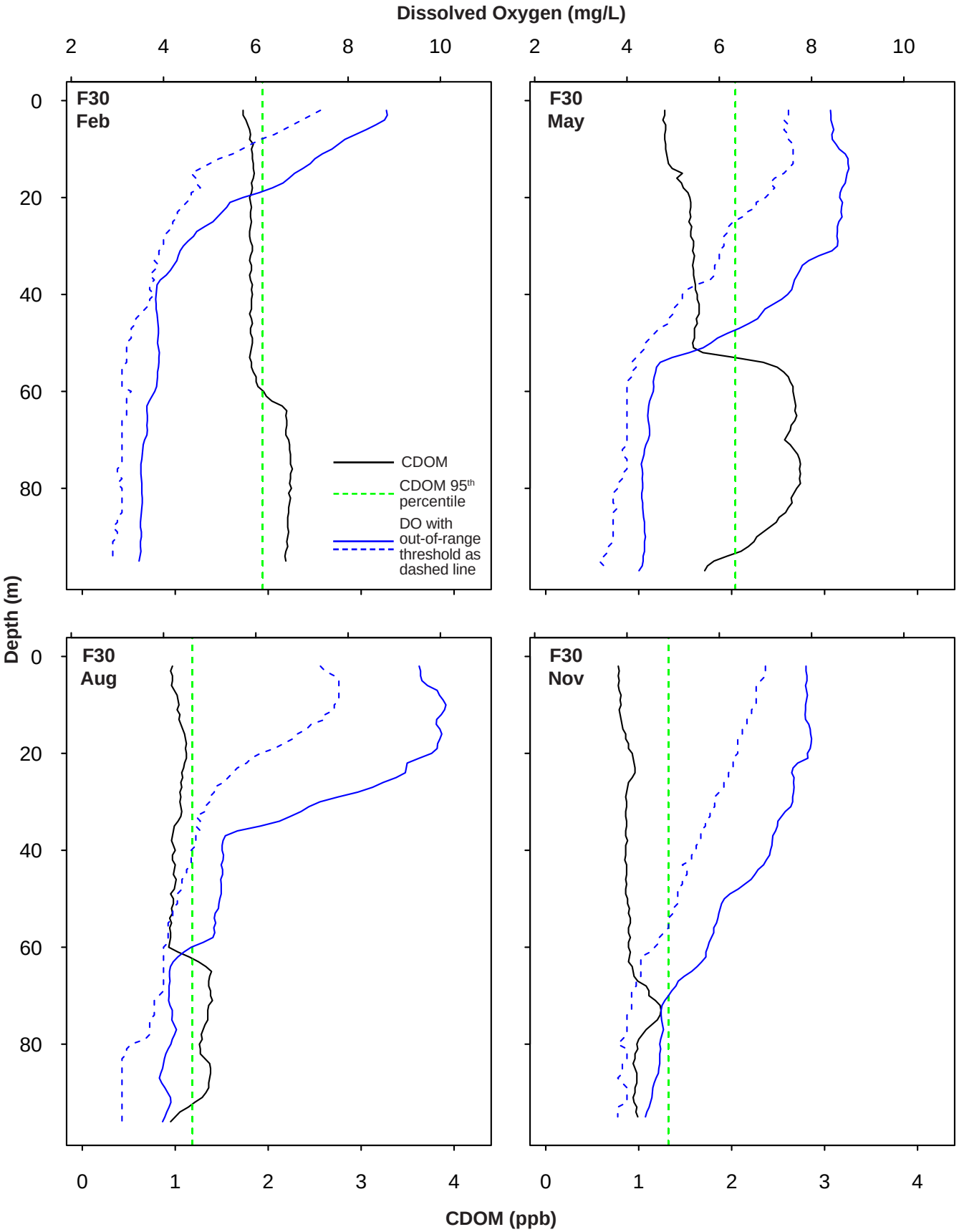

Appendix E.7

Representative vertical profiles of CDOM and DO from PLOO nearfield station F30 during 2021.

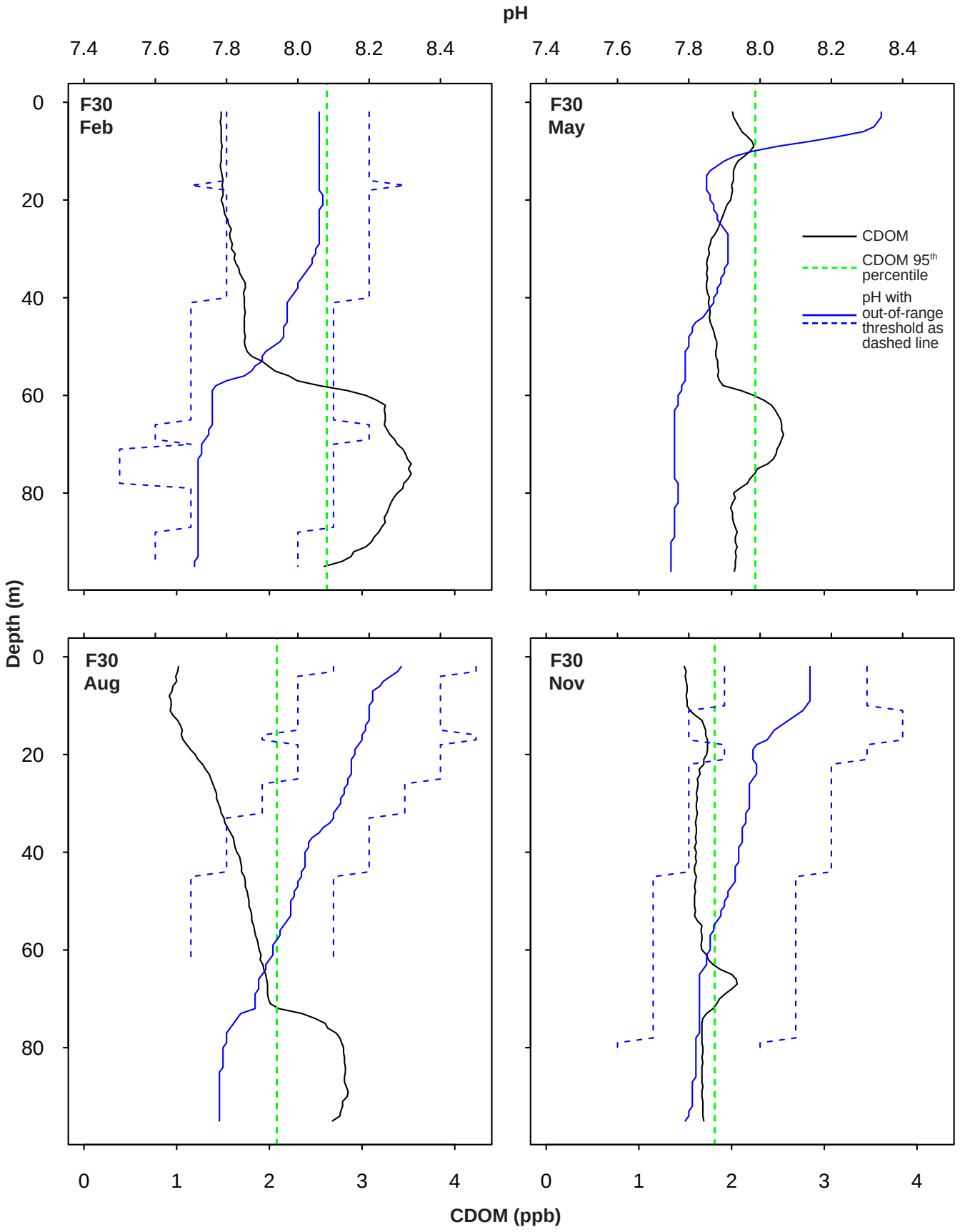

Appendix E.8

Representative vertical profiles of CDOM and pH from PLOO nearfield station F30 during 2020.

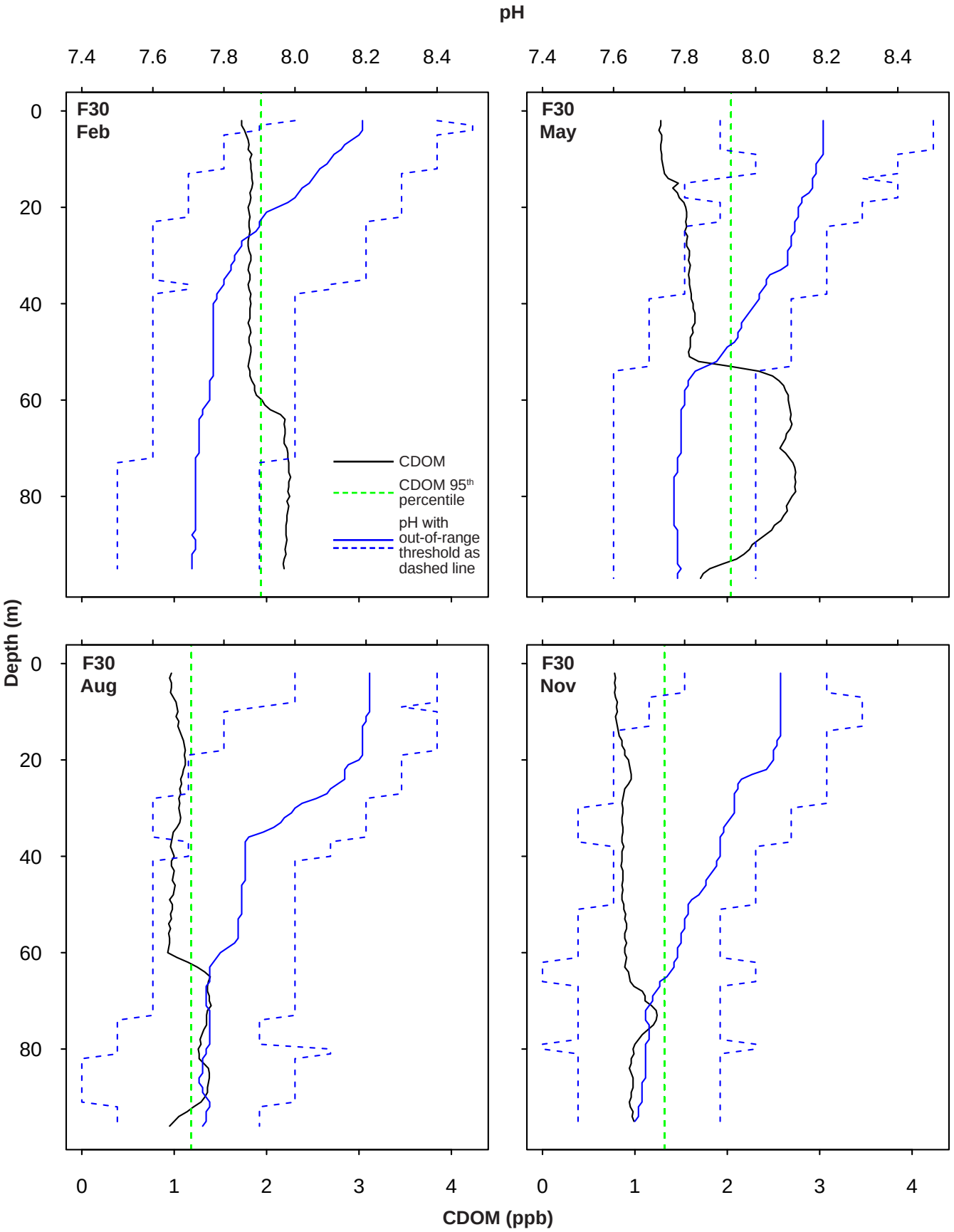

Appendix E.9

Representative vertical profiles of CDOM and pH from PLOO nearfield station F30 during 2021.

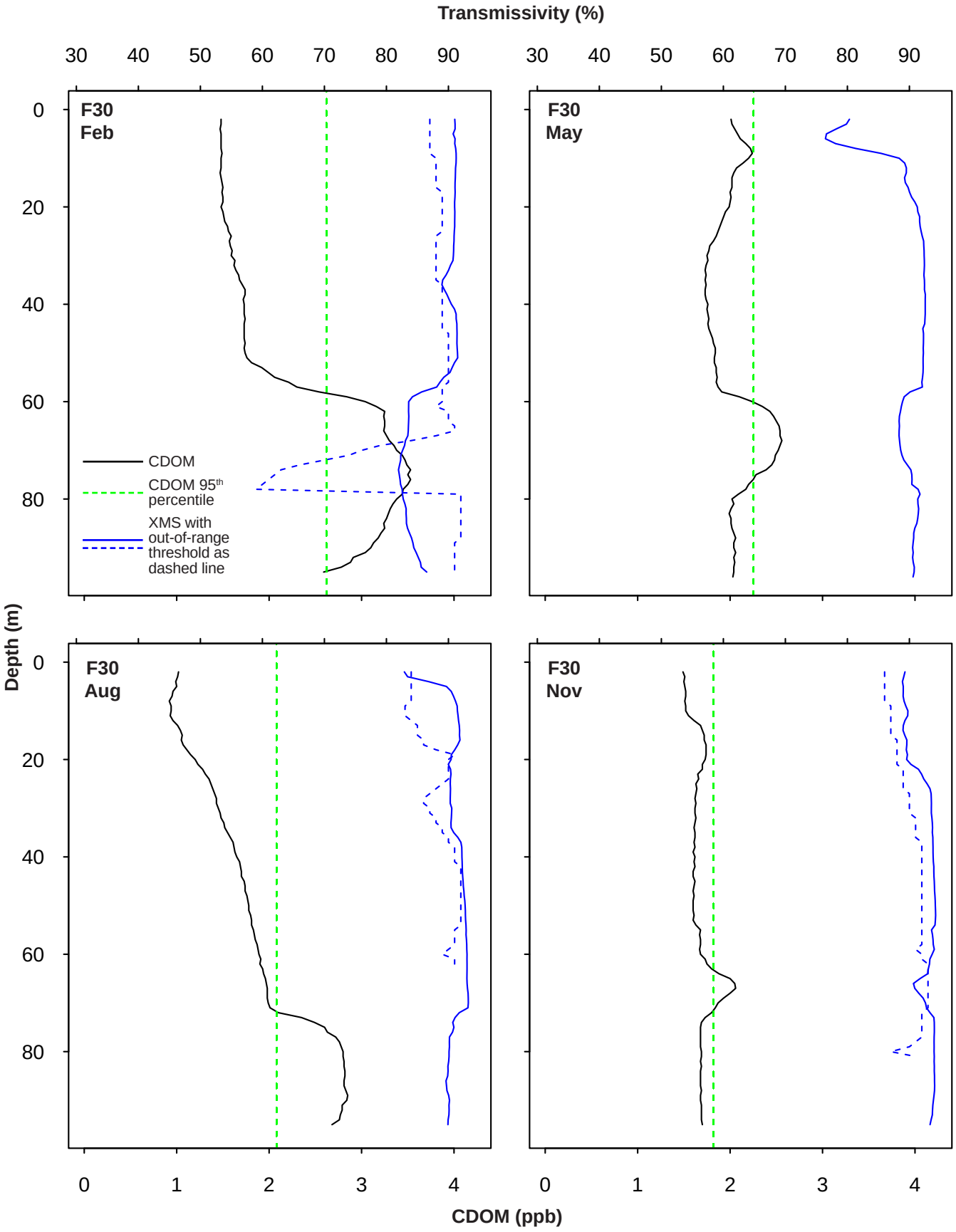

Appendix E.10

Representative vertical profiles of CDOM and transmissivity (XMS) from PLOO nearfield station F30 during 2020.

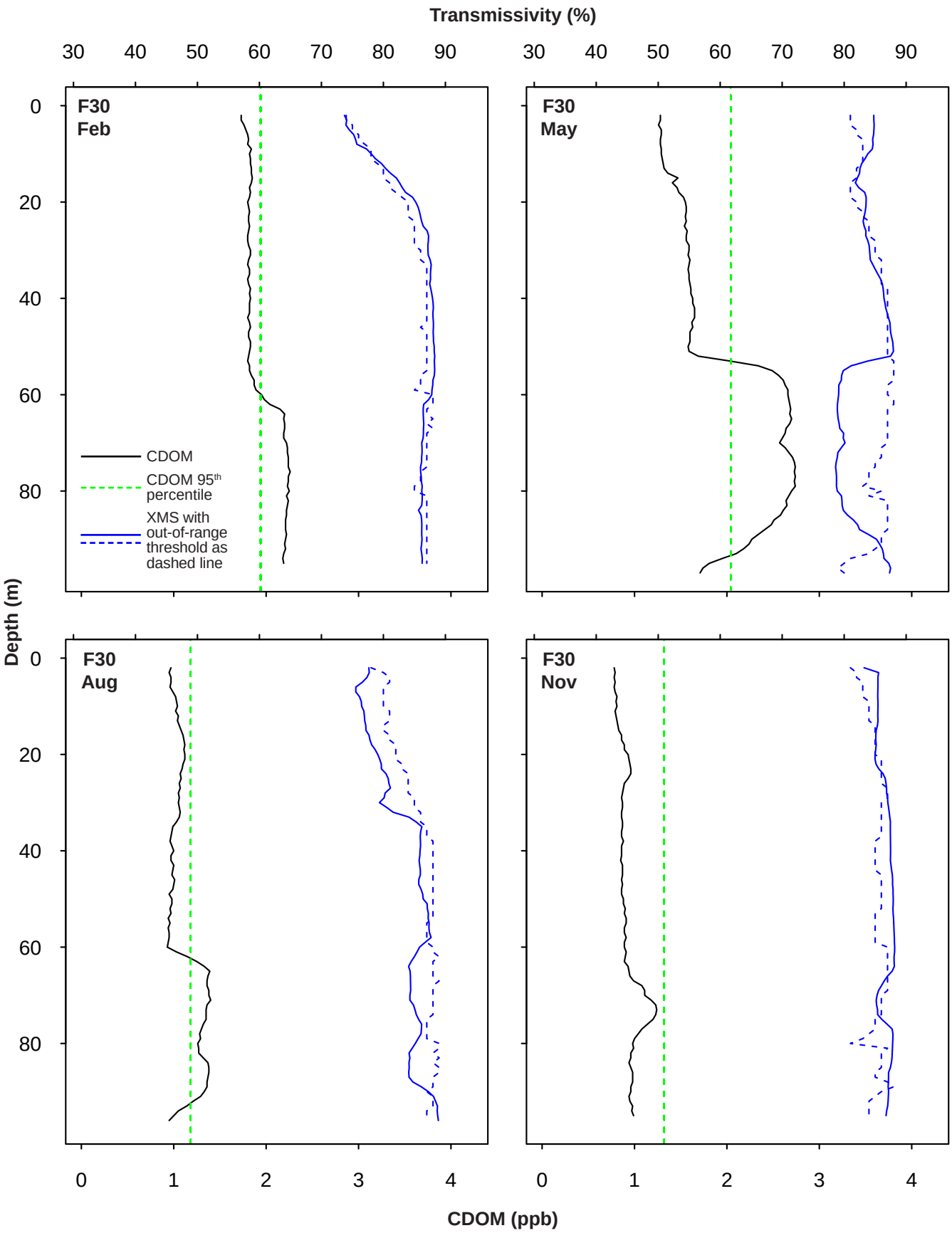

Appendix E.11

Representative vertical profiles of CDOM and transmissivity (XMS) from PLOO nearfield station F30 during 2021.

Appendix E.12

Summary of oceanographic data within potential detected plume at SBOO offshore stations and corresponding reference values during 2020 and 2021. Plume depth is the minimum depth at which CDOM exceeds the 95th percentile while plume width is the number of meters across which that exceedance occurs. Out-of-range values are indicated with an asterisk. DO = dissolved oxygen (mg/L); XMS = transmissivity (%); SD = standard deviation; CI = confidence interval.

		Potential Plume					Reference		
Station	Date	Width (m)	Depth (m)	Mean DO	Mean pH	Mean XMS	DO (Mean - SD)	pH (Mean)	XMS (Mean - 95% CI)
I12[a]	13-Feb-20	16	2	7.3	8.0	87	7.7	8.1	86
I23[a]	13-Feb-20	11	2	7.5	8.0	78*	7.8	8.1	86
I12[a]	28-May-20	1	6	7.6	8.1	79*	7.5	8.2	82
I14[a]	28-May-20	2	9	7.5	8.1	77*	7.2	8.1	84
I28	29-May-20	4	7	7.1	8.1	82*	7.4	8.1	84
I34[a]	29-May-20	3	6	6.2*	8.0	79*	7.5	8.2	83
I15	24-Aug-20	3	12	8.4	8.2	85	8.1	8.2	84
I22[a]	24-Aug-20	5	14	8.2	8.2	83*	8.0	8.2	84
I31[a]	25-Aug-20	3	14	8.0	8.1	83*	8.0	8.2	84
I9	26-Aug-20	2	13	8.0	8.1	89	8.1	8.2	84
I12[a]	04-Nov-20	7	5	7.1	8.1	85	7.8	8.2	83
I15	04-Nov-20	4	11	7.3	8.1	85	7.4	8.2	84
I16[a]	04-Nov-20	4	6	6.9*	8.1	86	7.8	8.2	83
I22[a]	04-Nov-20	5	6	7.1	8.1	85	7.8	8.2	83
I27[a]	04-Nov-20	7	9	7.2	8.1	85	7.4	8.2	84
I35[a]	05-Nov-20	2	15	5.6*	8.0	87	7.0	8.1	85
I14[a]	10-Feb-21	2	15	7.1	8.1	84	7.1	8.1	83
I16[a]	10-Feb-21	4	13	7.2	8.1	85	7.3	8.1	83
I22[a]	10-Feb-21	2	16	7.5	8.1	85	6.7	8.1	83

[a] Station located within State jurisdictional waters

Appendix E.12 *continued*

Station	Date	Potential Plume					Reference		
		Width (m)	Depth (m)	Mean DO	Mean pH	Mean XMS	DO (Mean - SD)	pH (Mean)	XMS (Mean - 95% CI)
I27[a]	10-Feb-21	2	17	7.7	8.1	83	6.7	8.1	83
I29	05-May-21	9	9	6.6	8.0	77	6.8	8.1	72
I30	05-May-21	2	17	5.7	7.9	82	5.8	8.0	80
I15	06-May-21	3	14	6.5	8.0	75	6.2	8.0	74
I6	03-Aug-21	4	9	7.1	8.0	82	7.2	8.1	75
I9	03-Aug-21	7	13	6.5	8.0	85	6.7	8.0	77
I12[a]	04-Aug-21	9	12	6.3	8.0	84	6.7	8.0	77
I16[a]	04-Aug-21	5	15	6.6	8.0	83	6.6	8.0	78
I17[a]	04-Aug-21	3	15	6.5	8.0	83	6.4	8.0	78
I12[a]	04-Nov-21	4	13	7.4	7.9	86	7.3	7.9	86
I16[a]	04-Nov-21	3	23	6.3	7.8	82*	6.9	7.8	87
I7	05-Nov-21	1	29	7.4	7.9	87*	6.8	7.8	88

[a]Station located within State jurisdictional waters

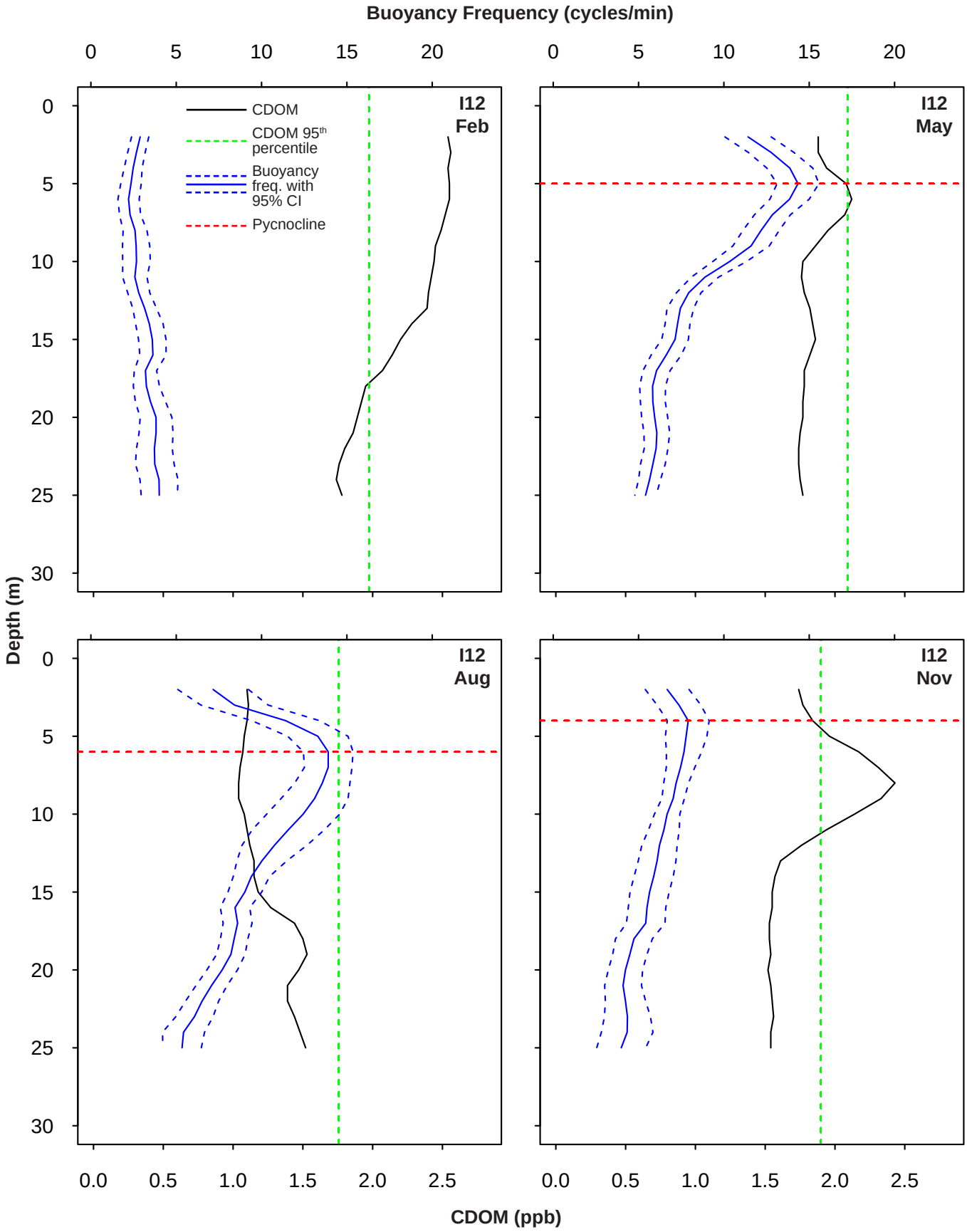

Appendix E.13

Representative vertical profiles of CDOM and buoyancy frequency from SBOO nearfield station I12 during 2020.

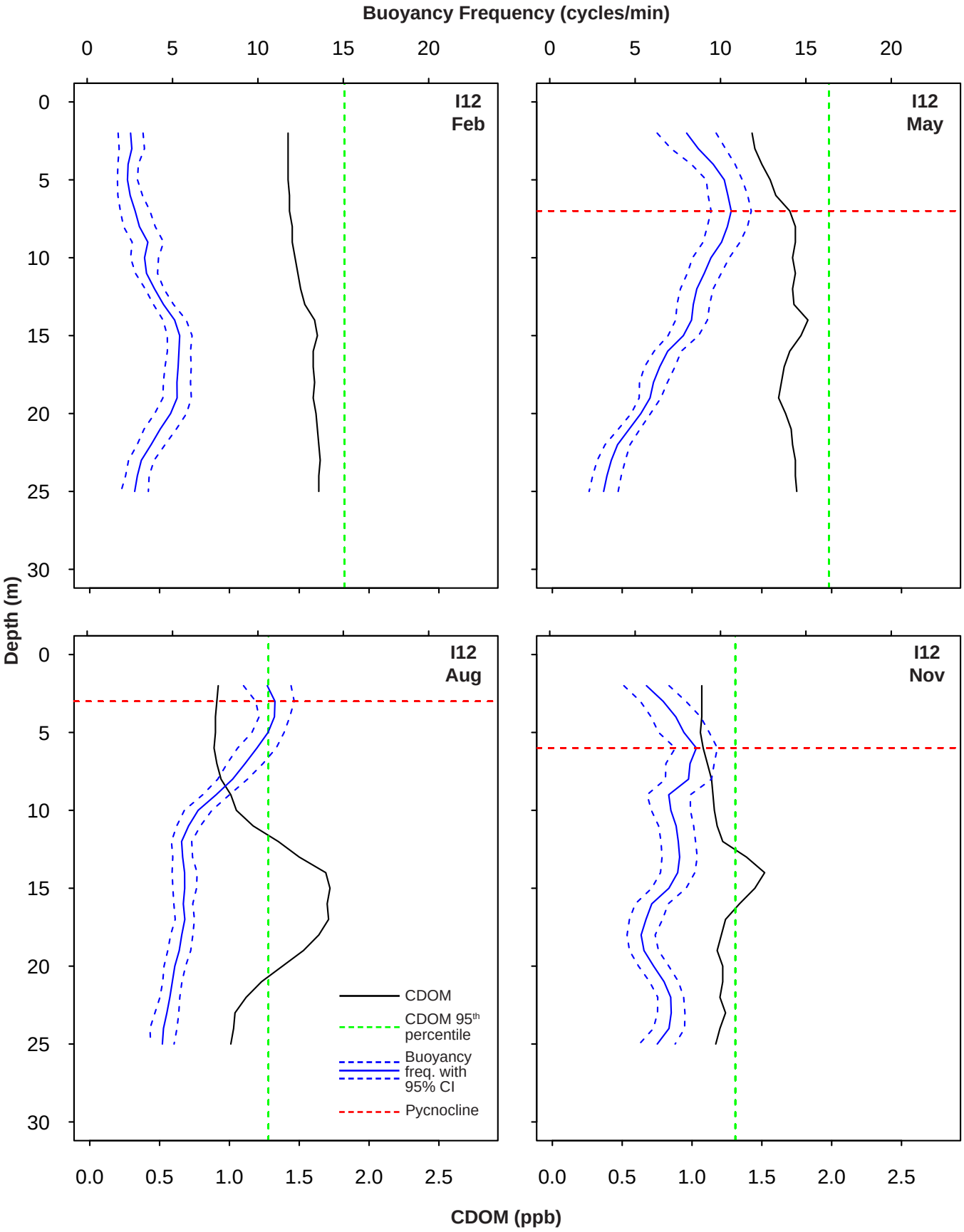

Appendix E.14

Representative vertical profiles of CDOM and buoyancy frequency from SBOO nearfield station I12 during 2021.

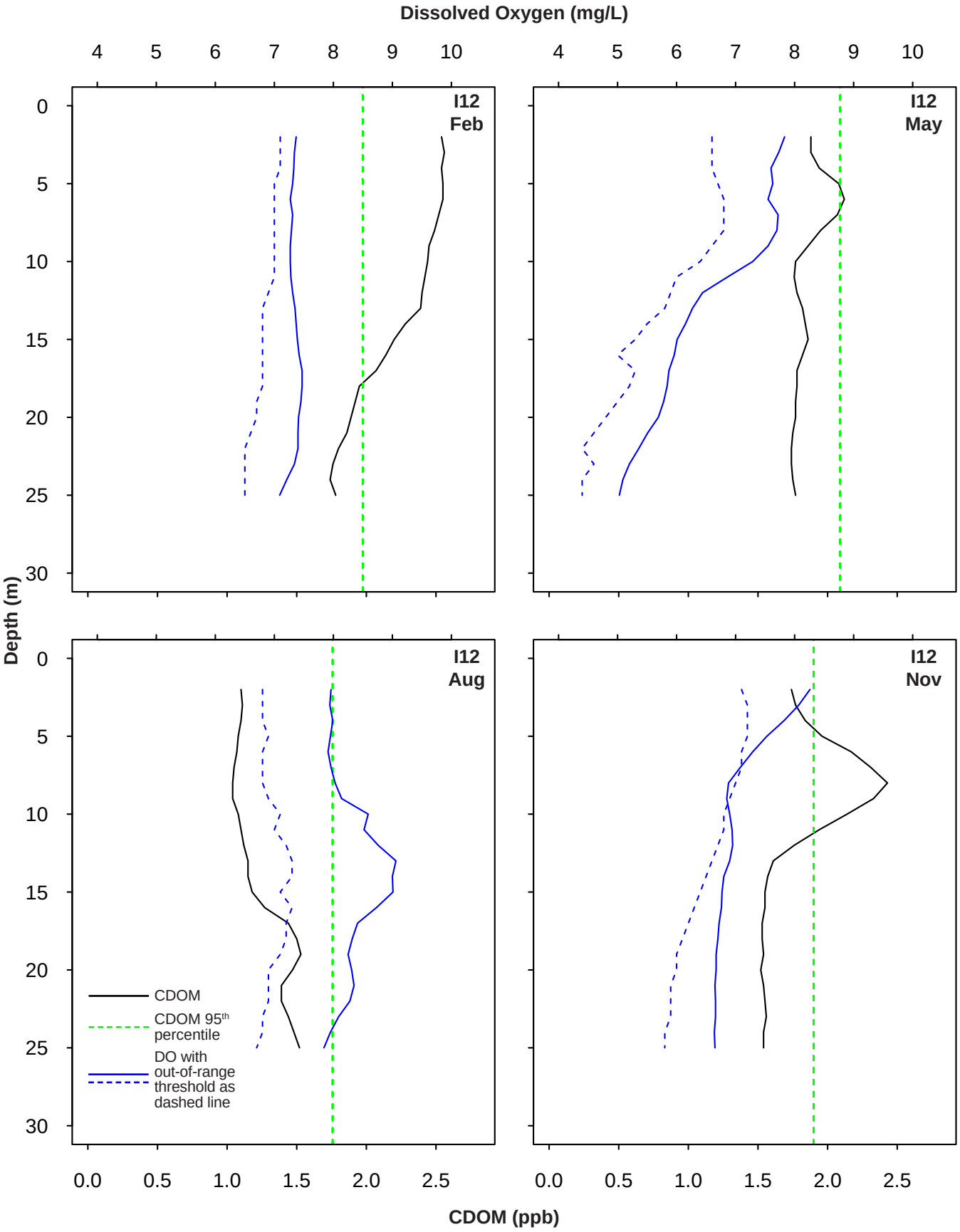

Appendix E.15

Representative vertical profiles of CDOM and DO from SBOO nearfield station I12 during 2020.

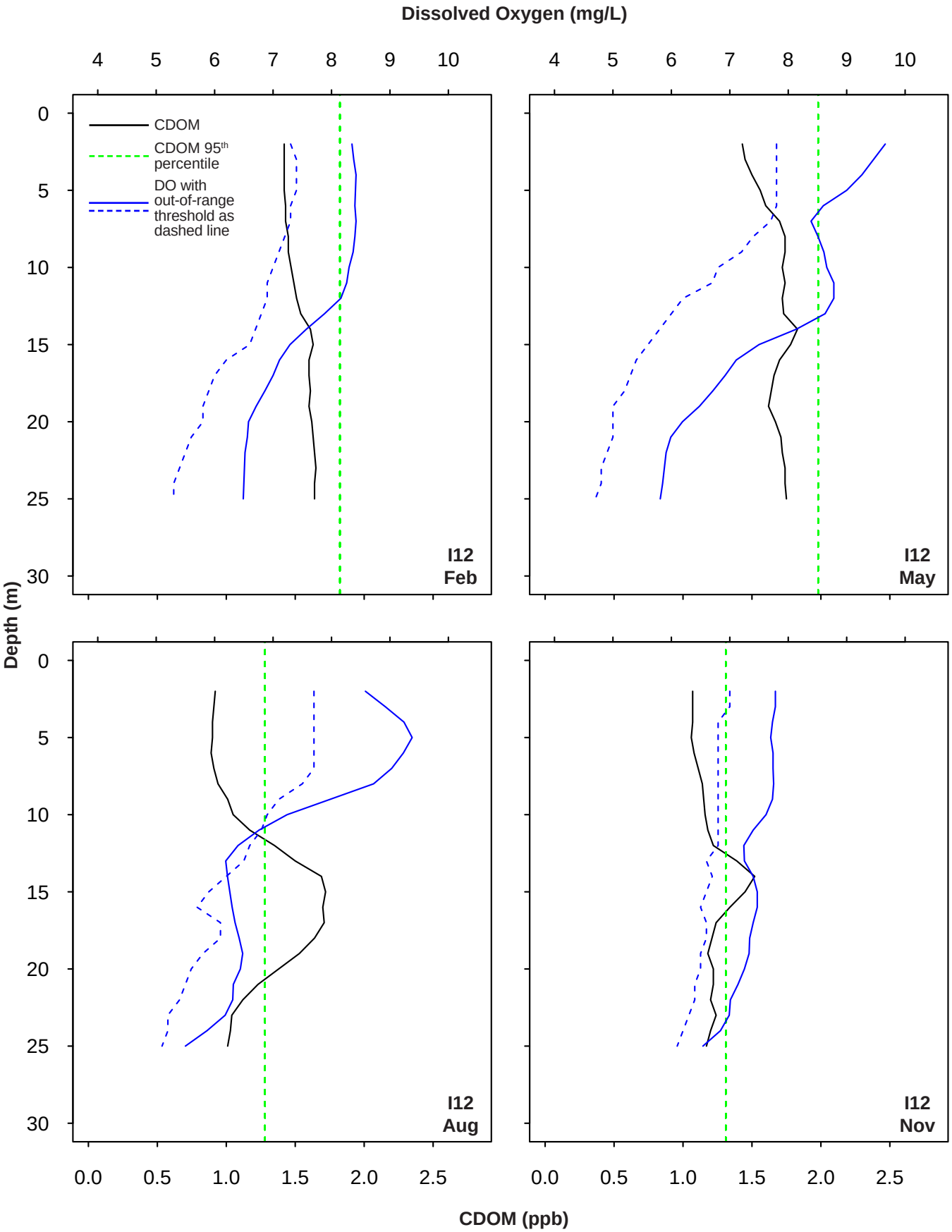

Appendix E.16

Representative vertical profiles of CDOM and DO from SBOO nearfield station I12 during 2021.

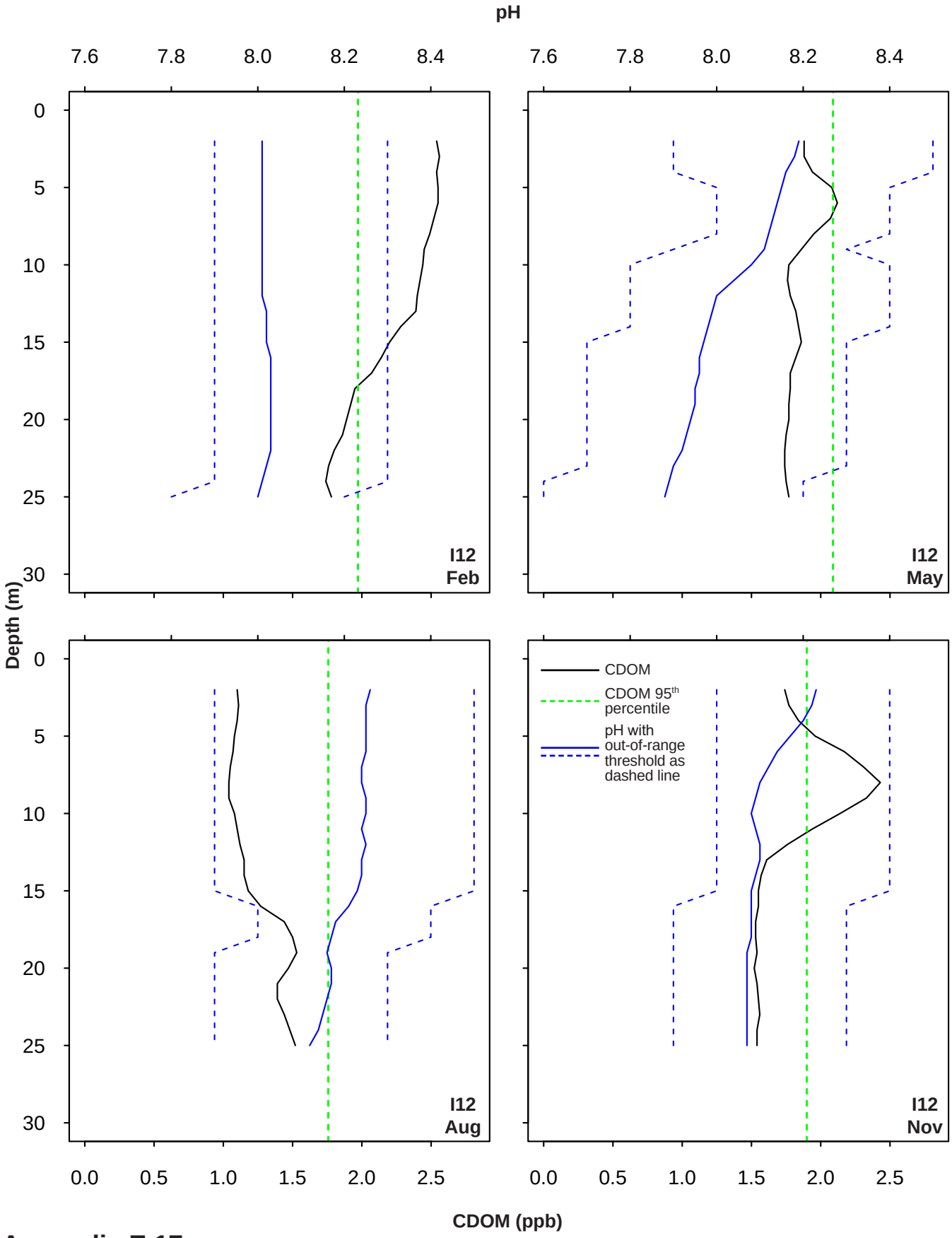

Appendix E.17

Representative vertical profiles of CDOM and pH from SBOO nearfield station I12 during 2020.

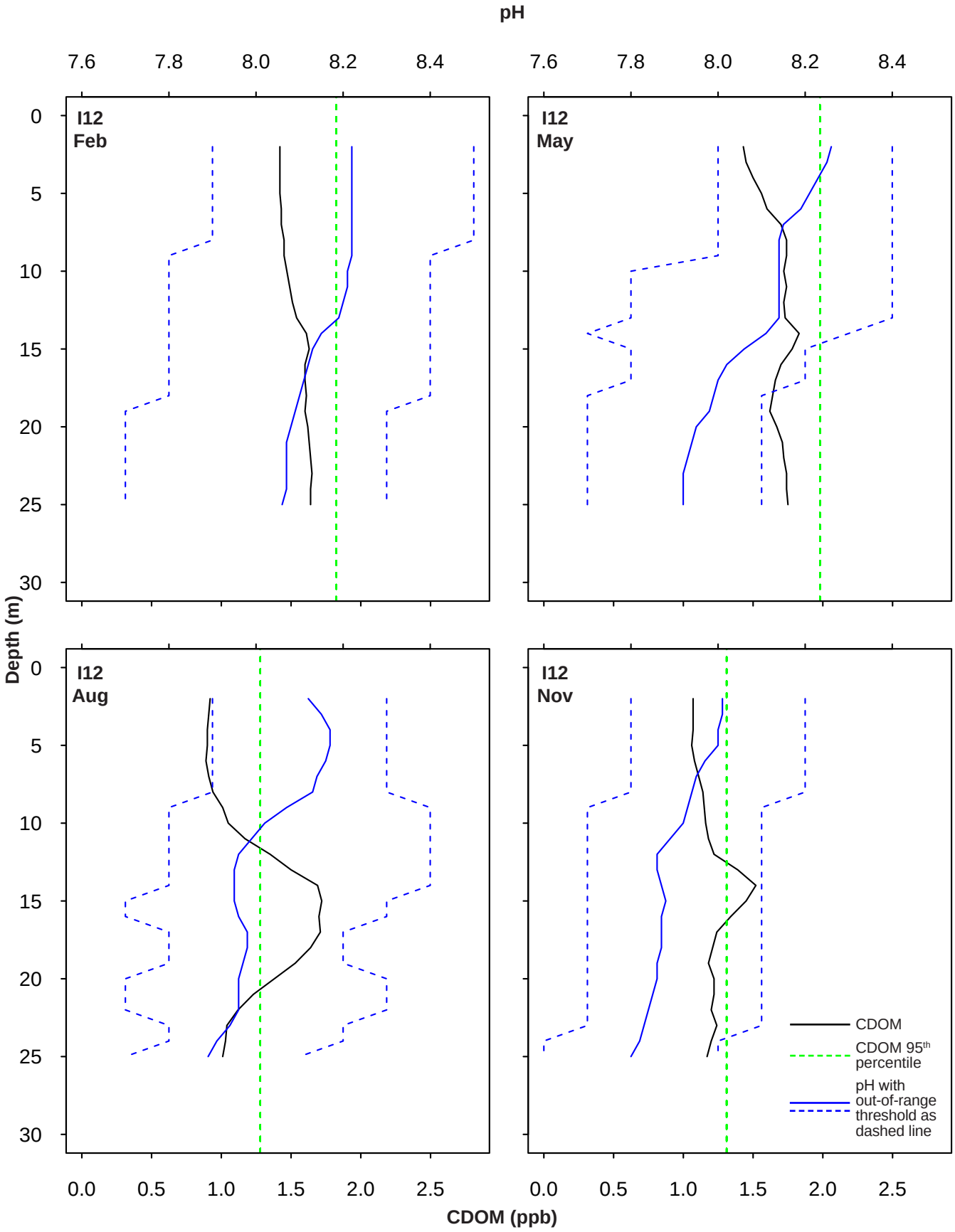

Appendix E.18

Representative vertical profiles of CDOM and pH from SBOO nearfield station I12 during 2021.

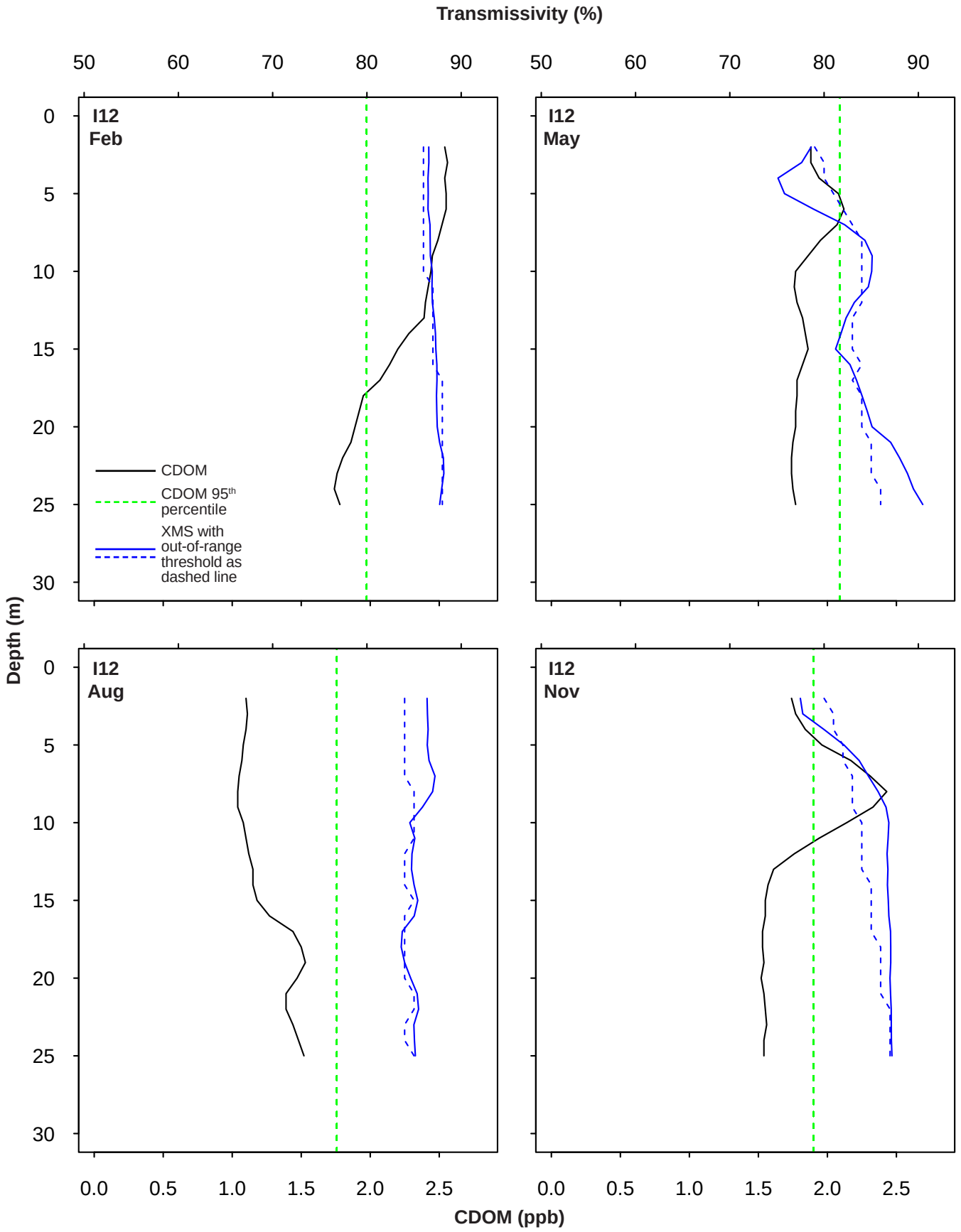

Appendix E.19

Representative vertical profiles of CDOM and transmissivity (XMS) from SBOO nearfield station I12 during 2020.

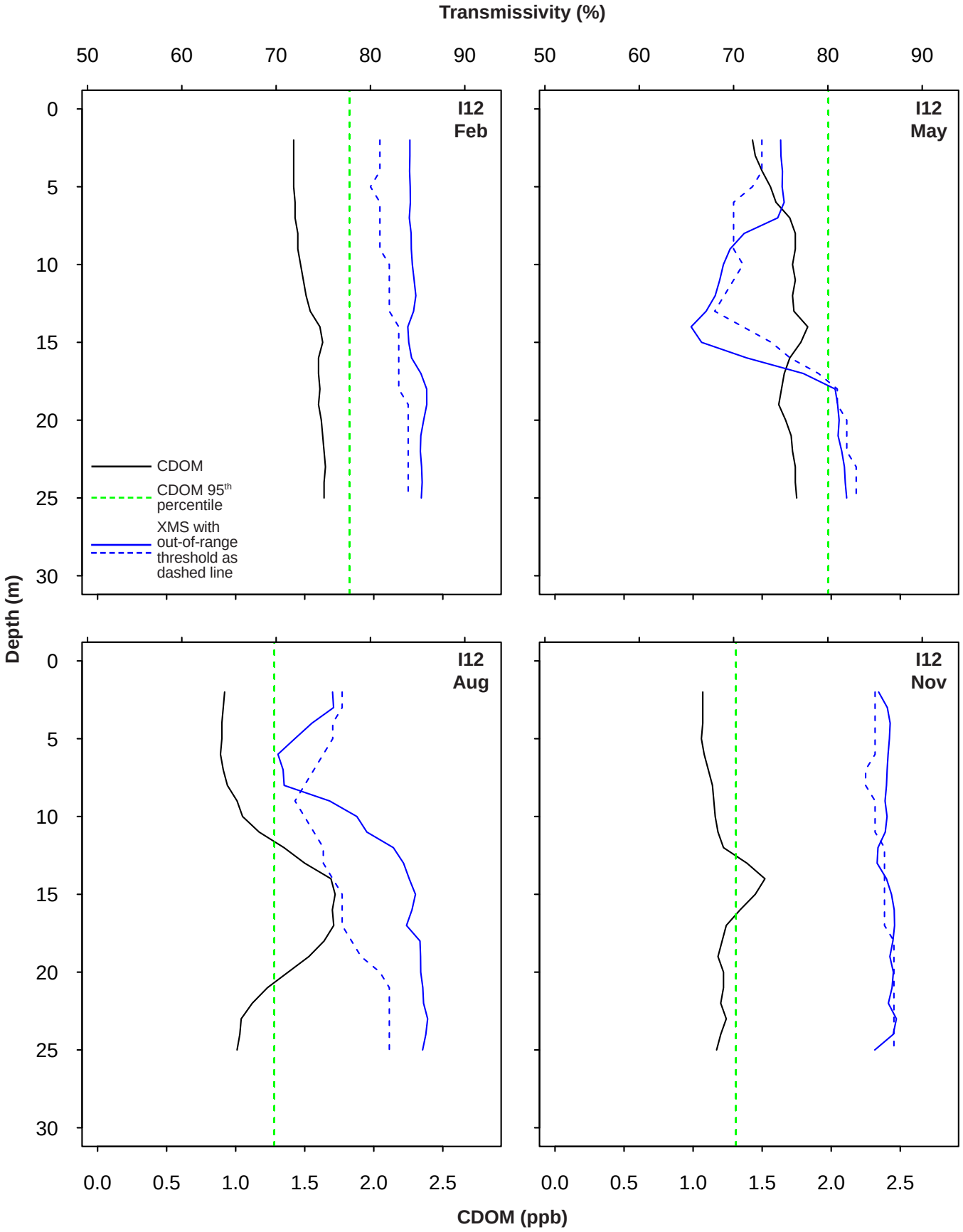

Appendix E.20

Representative vertical profiles of CDOM and transmissivity (XMS) from SBOO nearfield station I12 during 2021.

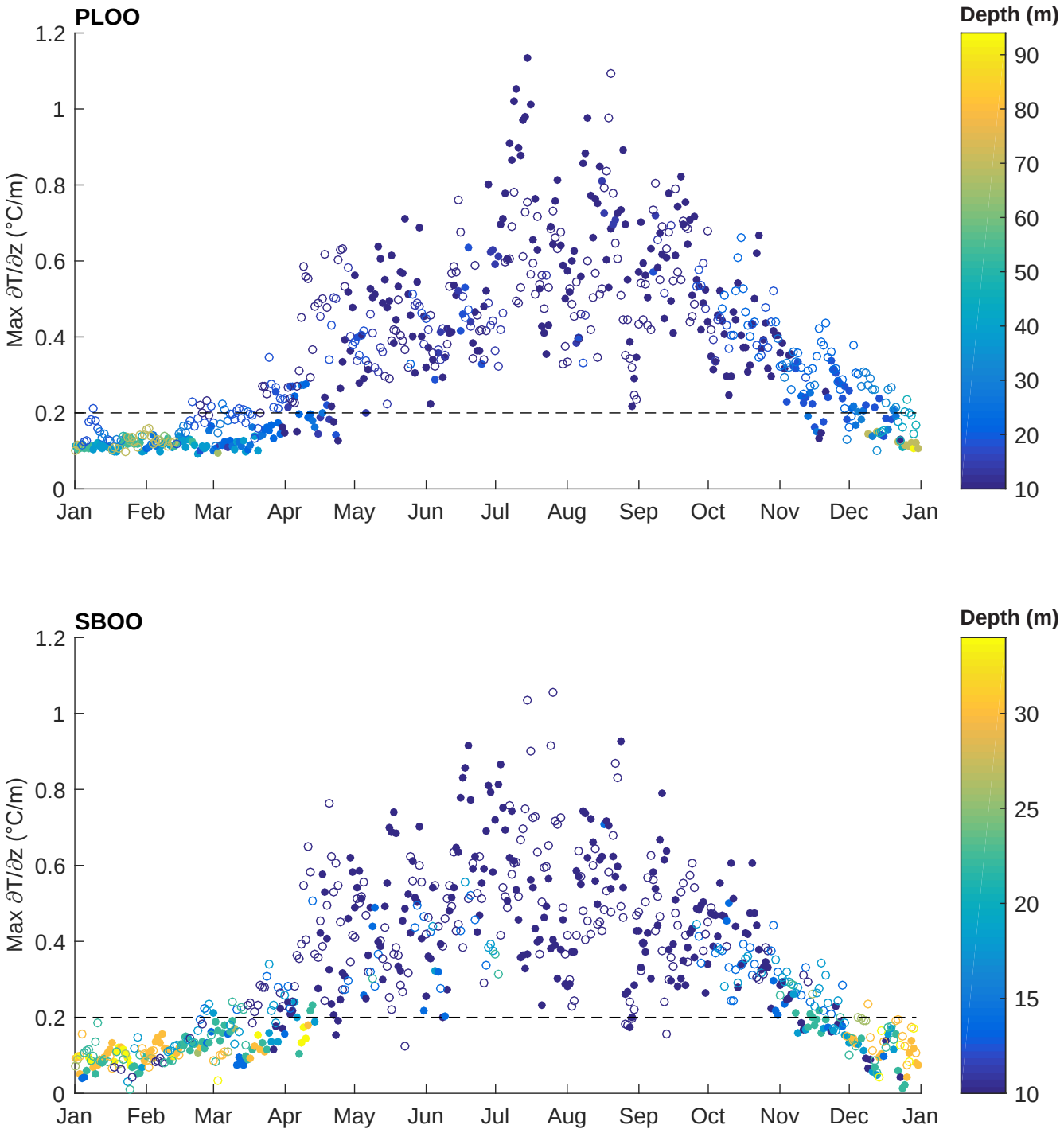

Appendix E.21

Maximum daily averaged thermal gradients (δT/δz) by depth of occurrence collected by thermistor arrays near PLOO (100 m) and SBOO (36 m) in 2020 (filled circles) and 2021 (open circles). Dashed line indicates moderate relative stratification (0.2°C/m), with values below line showing more weakly stratified conditions.

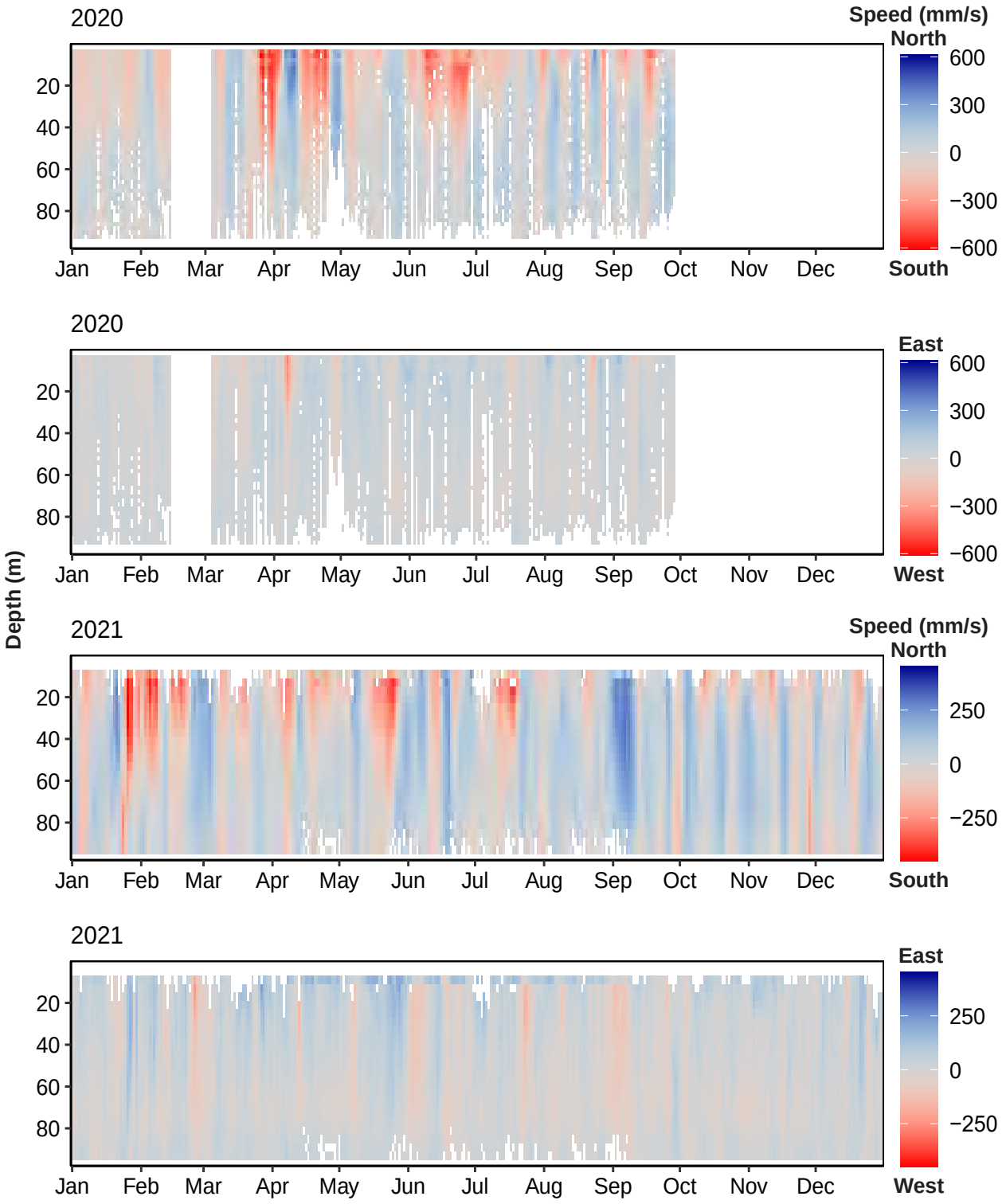

Appendix E.22

North-south and east-west daily averaged current speeds (tides removed) from the PLOO RTOMS in 2020 and the static ADCP in 2021. White areas indicate loss of data due to instrumentation issues or failure to meet data quality criteria (see text).

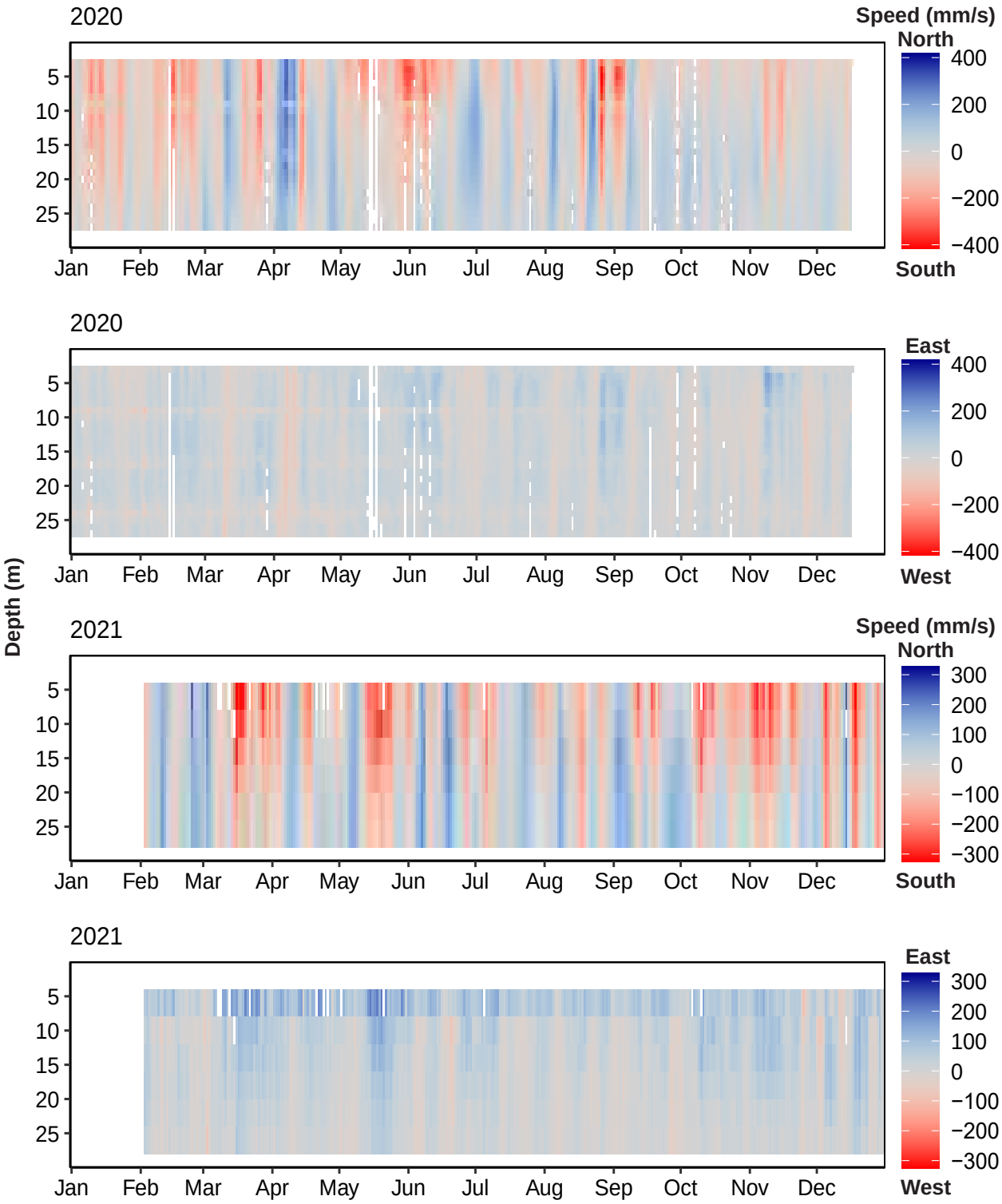

Appendix E.23

North-south and east-west daily averaged current speeds (tides removed) from the SBOO RTOMS in 2020 and the static ADCP in 2021. White areas indicate loss of data due to instrumentation issues or failure to meet data quality criteria (see text).

This page intentionally left blank

Appendix F

Sediment Quality

2020 – 2021 Supplemental Analyses

Appendix F.1

Constituents and method detection limits (MDL) used for the analysis of sediments during 2020 and 2021. MDLs are summarized as minimum, and maximum values over the two years.

	MDL			MDL	
Parameter	**Min**	**Max**	**Parameter**	**Min**	**Max**
Organic Indicators					
BOD (ppm)	2	2	Sulfides (ppm)	0.68	2.2
TN (% wt.)	0.008	0.026	TVS (% wt.)	0.11	0.11
TOC (% wt.)	0.07	0.178			
Metals (ppm)					
Aluminum (Al)	1.52	3.1	Lead (Pb)	0.1	0.1
Antimony (Sb)	0.17	0.385	Manganese (Mn)	0.061	0.151
Arsenic (As)	0.152	0.152	Mercury (Hg)	0.003	0.0145
Barium (Ba)	0.155	0.43	Nickel (Ni)	0.1	0.28
Beryllium (Be)	0.003	0.009	Selenium (Se)	0.213	0.434
Cadmium (Cd)	0.018	0.073	Silver (Ag)	0.133	0.133
Chromium (Cr)	0.049	0.102	Thallium (Tl)	0.122	0.122
Copper (Cu)	1.19	1.19	Tin (Sn)	0.059	0.059
Iron (Fe)	1.88	9.4	Zinc (Zn)	0.384	0.384
Chlorinated Pesticides (ppt)					
Chlordanes					
Alpha (cis) Chlordane	46.1	95	Heptachlor epoxide	31.5	67.9
Cis Nonachlor	44	95.1	Methoxychlor	91.1	847
Gamma (trans) Chlordane	27	126	Oxychlordane	66.3	143
Heptachlor	79.4	344	Trans Nonachlor	29.3	125
Dichlorodiphenyltrichloroethane (DDT)					
o,p–DDD	36.4	143	p,p–DDE	17.2	138
o,p–DDE	14.1	115	p,p–DDMU	35.5	76.6
o,p–DDT	29.2	96.2	p,p–DDT	21.3	130
p,p–DDD	30.3	69.7			
Endrin					
Endrin	92.4	200	Endrin aldehyde	153	613
Endosulfan					
Alpha-Endosulfan	78.2	329	Endosulfan sulfate	41.5	308
Beta-Endosulfan	50.9	1130			
Hexachlorocyclohexane (HCH)					
HCH, Alpha isomer	24.4	110	HCH, Delta isomer	68	147
HCH, Beta isomer	37.6	148	HCH, Gamma isomer	14.1	147
Miscellaneous Pesticides					
Aldrin	28.8	62.1	Hexachlorobenzene (HCB)	50.9	350
Dieldrin	50.6109		Mirex	26.4	57.1

Appendix F.1 *continued*

Parameter	MDL Min	MDL Max	Parameter	MDL Min	MDL Max
Polychlorinated Biphenyl Congeners (PCBs) (ppt)					
PCB 8	40.9	85	PCB 126	53.7	116
PCB 18	52.2	113	PCB 128	41.1	80
PCB 28	23.7	122	PCB 138	46.7	101
PCB 37	26.1	150	PCB 149	20.6	125
PCB 44	22.3	87.8	PCB 151	36	70.2
PCB 49	27.2	117	PCB 153/168	87	312
PCB 52	25.4	123	PCB 156	29.7	146
PCB 66	21.9	97.4	PCB 157	18.8	174
PCB 70	18.9	106	PCB 158	30.5	184
PCB 74	13.2	98.3	PCB 167	17.5	106
PCB 77	25.8	114	PCB 169	39.8	85.9
PCB 81	28.5	61.5	PCB 170	33.4	65
PCB 87	23.8	83.9	PCB 177	21.4	83.8
PCB 99	19.6	80.6	PCB 180	36.1	70.4
PCB 101	38.3	82.6	PCB 183	24.5	52.1
PCB 105	37.9	159	PCB 187	30.5	65.8
PCB 110	32.6	104	PCB 189	17	167
PCB 114	47.9	103	PCB 194	21.4	91.7
PCB 118	17.6	97.7	PCB 195	29.2	60.7
PCB 119	29.6	142	PCB 201	40.6	87.7
PCB 123	20.4	134	PCB 206	20.6	107
Polycyclic Aromatic Hydrocarbons (PAHs) (ppb)					
1-methylnaphthalene	2.22	14.5	Benzo[G,H,I]perylene	5.12	21.1
1-methylphenanthrene	2.72	9.74	Benzo[K]fluoranthene	4.69	14.7
2-methylnaphthalene	2.42	10.5	Biphenyl	5.76	12.8
2,3,5-trimethylnaphthalene	2.58	12.6	Chrysene	4.97	9.95
2,6-dimethylnaphthalene	2.23	13.5	Dibenzo(A,H)anthracene	4.77	20.6
3,4-benzo(B)fluoranthene	4.14	9.89	Fluoranthene	2.31	9.37
Acenaphthene	1.98	18.1	Fluorene	2.28	18.4
Acenaphthylene	3.46	13.1	Indeno(1,2,3-CD)pyrene	4.44	16.1
Anthracene	3.6	17.9	Naphthalene	3.33	11
Benzo[A]anthracene	2.51	9.1	Perylene	5.16	13.5
Benzo[A]pyrene	4.6	10.4	Phenanthrene	2.51	14.6
Benzo[e]pyrene	4.49	11.6	Pyrene	2.37	12.1

Appendix F.2

Particle size classification schemes (based on Folk 1980) used in the analysis of sediments during 2020 and 2021. Included is a subset of the Wentworth scale presented as “phi” categories with corresponding Horiba channels, sieve sizes, and size fractions.

Wentworth Scale

	Horiba[a]				
Phi size	**Min µm**	**Max µm**	**Sieve Size**	**Sub-Fraction**	**Fraction**
-1	—	—	SIEVE_2000	Granules	Coarse Particles
0	1100	2000	SIEVE_1000	Very coarse sand	Coarse Particles
1	590	1000	SIEVE_500	Coarse sand	Med-Coarse Sands
2	300	500	SIEVE_250	Medium sand	Med-Coarse Sands
3	149	250	SIEVE_125	Fine sand	Fine Sands
4	64	125	SIEVE_75	Very fine sand	Fine Sands
4	64	125	SIEVE_63	Very fine sand	Fine Sands
5	32	62.5	SIEVE_0[b]	Coarse silt	Fine Particles[c]
6	16	31	—	Medium silt	Fine Particles[c]
7	8	15.6	—	Fine silt	Fine Particles[c]
8	4	7.8	—	Very fine silt	Fine Particles[c]
9	≤	3.9	—	Clay	Fine Particles[c]

[a] Values correspond to Horiba channels; particles > 2000 µm measured by sieve

[b] SIEVE_0 = sum of all silt and clay, which cannot be distinguished for samples processed by nested sieves

[c] Fine particles also referred to as percent fines

Appendix F.3

Summary of visual observations for each PLOO and SBOO station sampled during 2020–2021. Visual observations are from sieved "grunge" (i.e., particles retained on 1-mm mesh screen and preserved with infauna for benthic community analysis).

		Winter 2020	Summer 2020	Winter 2021	Summer 2021
PLOO					
88-m Stations	B11	shell hash; gravel; cobble	gravel; shell hash	coarse sand and shell hash	gravel and cobble
	B8	—	—	—	—
	E19	—	worm tubes; shell hash	—	—
	E7	—	shell hash	—	—
	E1	shell hash; coarse sand	coarse sand; shell hash	coarse sand and shell hash	coarse sand and shell hash
98-m Stations	B12	shell hash; gravel; cobble	coarse black sand; shell hash	coarse sand and shell hash	coarse sand and shell hash
	B9	pea gravel	pea gravel; shell hash	—	gravel
	E26	shell hash; coarse sand	shell hash	shell hash	shell hash and organic debris
	E25	shell hash; gravel	shell hash	coarse sand and shell hash	—
	E23	—	shell hash	—	coarse sand and shell hash
	E20	—	worm tubes; shell hash	—	—
	E17[a]	—	worm tubes; shell hash	—	coarse sand and shell hash
	E14[a]	coarse sand; gravel	coarse black sand; shell hash	shell hash and gravel	coarse sand, shell hash, and organic debris
	E11[a]	coarse black sand; organic debris	—	—	shell hash and organic debris
	E8		—	—	shell hash and gravel
	E5	—	—	coarse sand and shell hash	coarse sand and shell hash
	E2	shell hash; coarse sand; gravel; organic debris	coarse sand; shell hash	coarse sand and shell hash	coarse sand and shell hash
116-m Stations	B10	shell hash	shell hash	shell hash and gravel	shell hash and gravel
	E21	—	—	—	—
	E15[a]	coarse sand; organic debris	worm tubes; coarse sand; shell hash	—	shell hash and gravel
	E9	—	coarse sand; shell hash	coarse sand and shell hash	shell hash and gravel
	E3	shell hash; coarse sand; gravel; organic debris	coarse sand; shell hash	coarse sand and shell hash	coarse sand and shell hash

[a] Near-ZID station

Appendix F.3 *continued*

		Winter 2020	Summer 2020	Winter 2021	Summer 2021
SBOO					
19-m Stations	I35	coarse sand; organic debris	organic debris	—	—
	I34	red relict sand; shell hash	red relict sand; shell hash	shell hash	relict red sand and shell hash
	I31	—	—	—	—
	I23	—	—	—	shell hash and cobble
	I18	—	coarse sand; shell hash	—	sea grass
	I10	—	worm tubes	—	—
	I4	shell hash	coarse sand; shell hash	—	shell hash
28-m Stations	I33	—	worm tubes	—	coarse sand
	I30	—	—	—	—
	I27	—	—	—	—
	I22	—	—	—	—
	I14[a]	—	—	—	–
	I16[a]	gravel; shell hash	shell hash	coarse sand and shell hash	—
	I15[a]	—	—	—	—
	I12[a]	shell hash	—	coarse sand and shell hash	—
	I9	—	organic debris	—	—
	I6	shell hash	shell hash	red relict sand and shell hash	shell hash
	I2	—	—	—	—
	I3	shell hash	red relict sand; shell hash	red relict sand and shell hash	—
38-m Stations	I29	red relict sand; gravel	organic debris	—	—
	I21	—	shell hash	—	–
	I13	shell hash	shell hash	coarse sand and shell hash	coarse sand and shell hash
	I8	—	—	—	—
55-m Stations	I28	black gravel; shell hash	black gravel	coarse black sand and organic debris	coarse black sand, organic debris, and pea gravel
	I20	red relict sand	red relict sand	red relict sand and shell hash	relict red sand and shell hash
	I7	red relict sand; shell hash	red relict sand; shell hash	red relict sand	relict red sand
	I1	—	—	—	—

[a] Near-ZID station

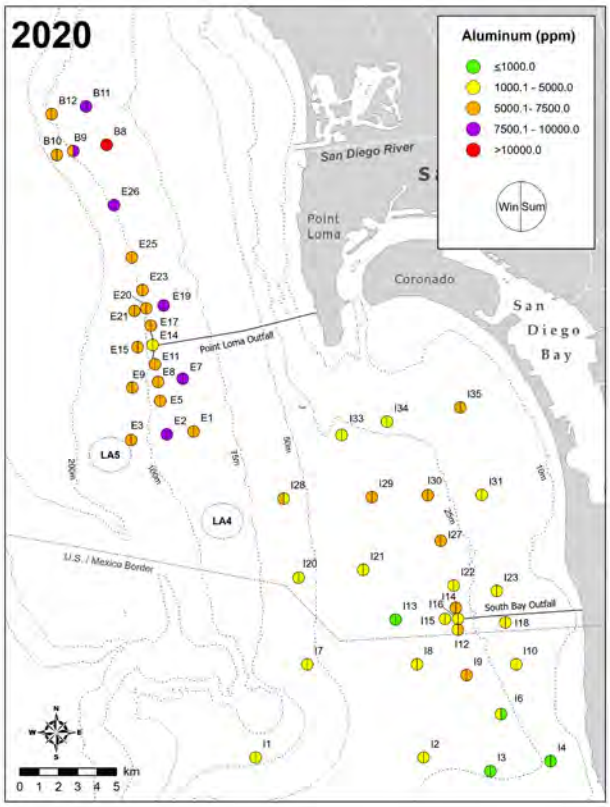

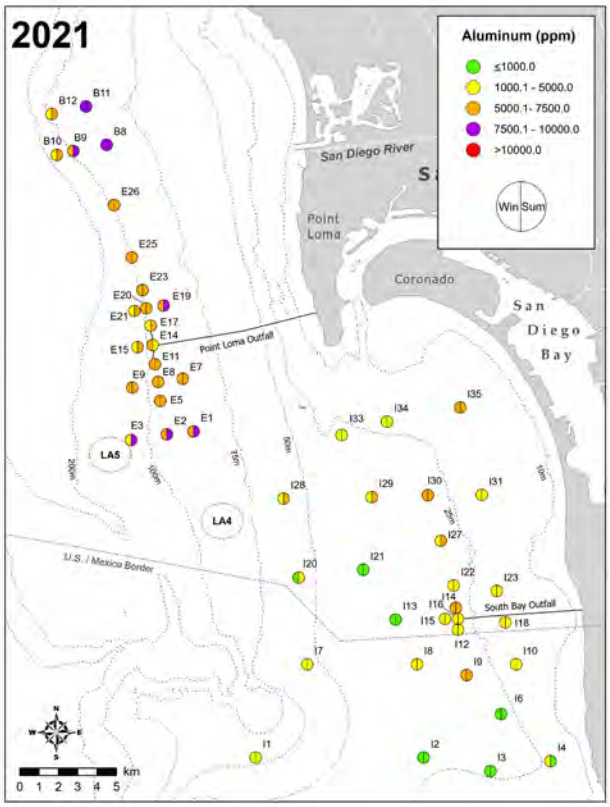

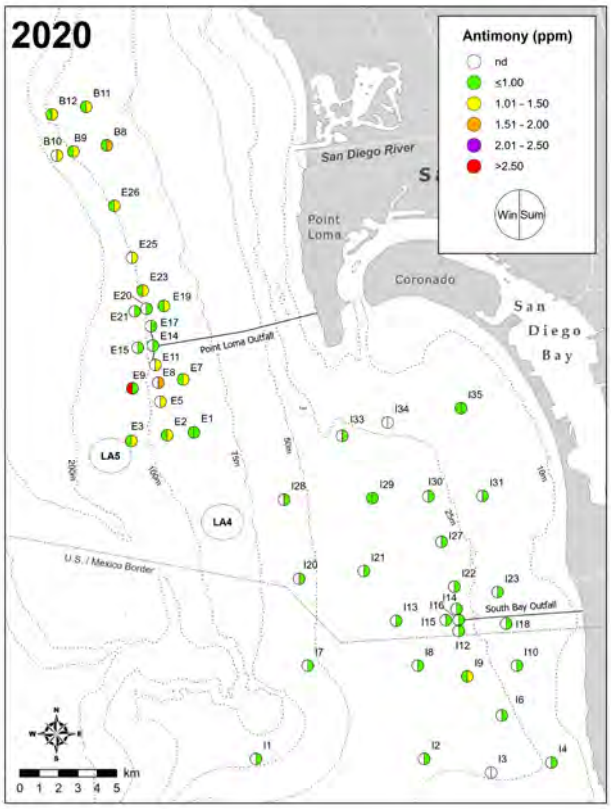

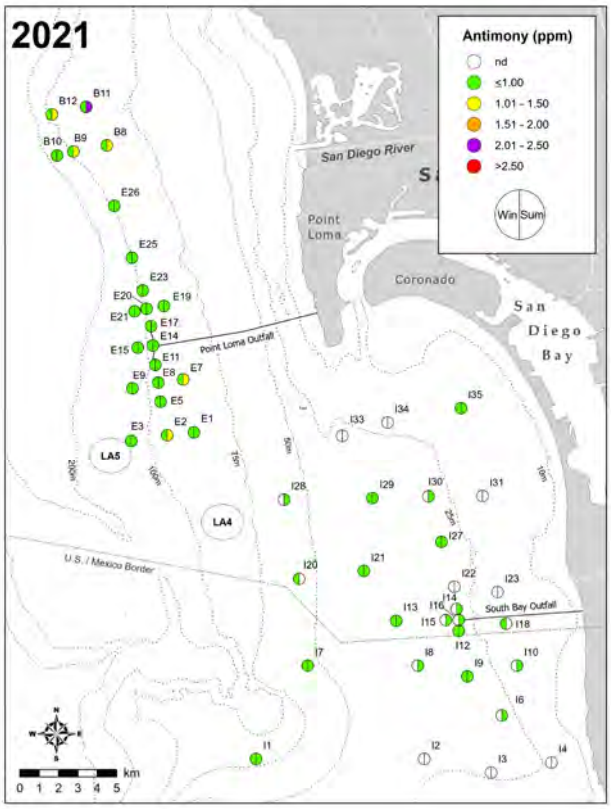

Appendix F.4

Distribution of select metals (ppm) in sediments from the PLOO and SBOO regions during winter and summer surveys of 2020 and 2021.

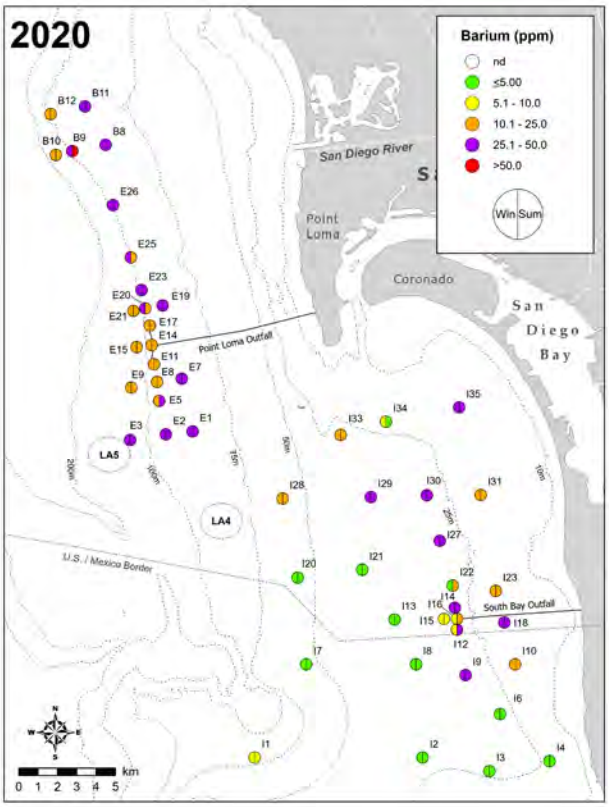

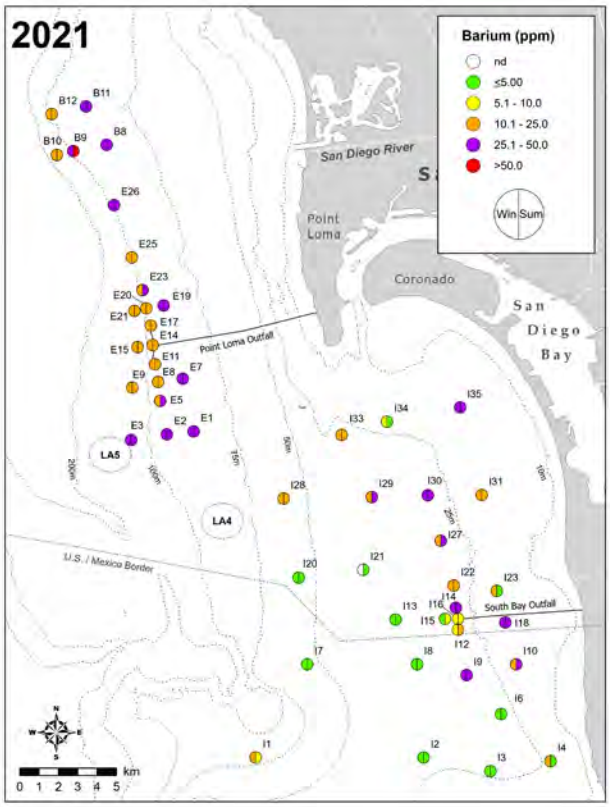

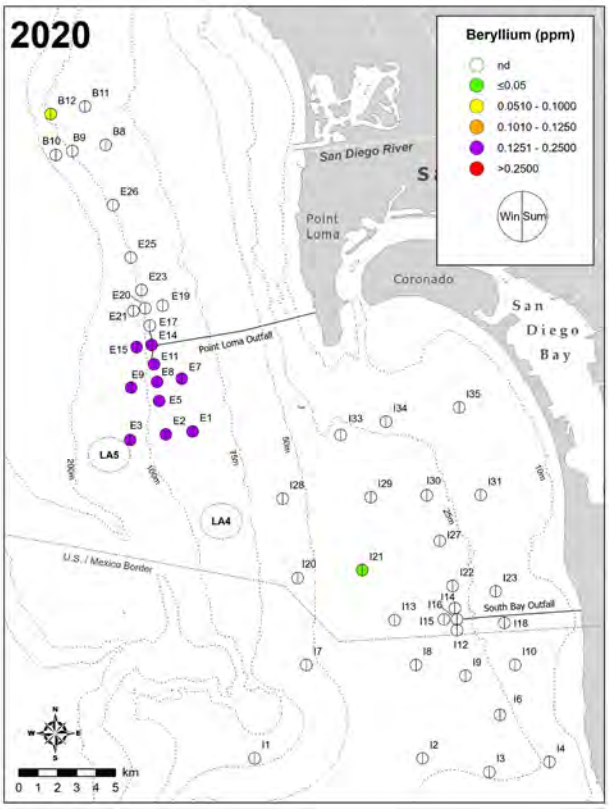

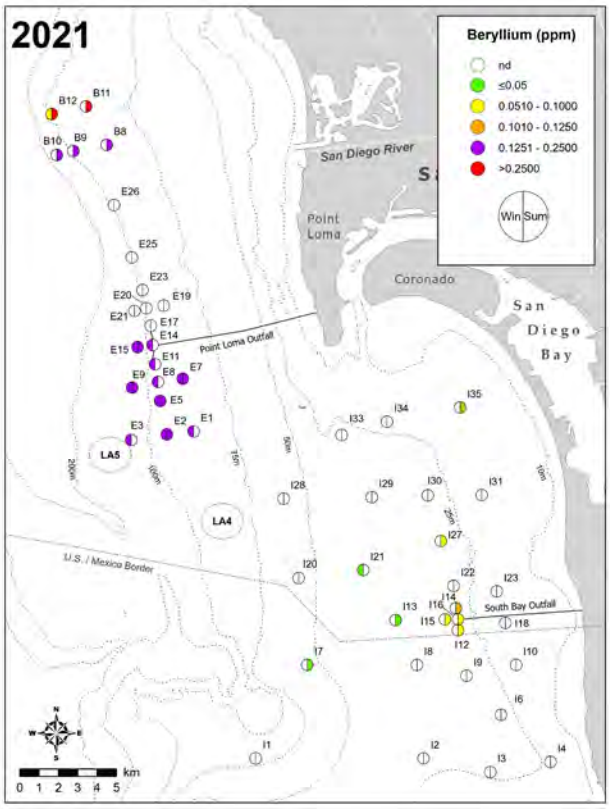

Appendix F.4 *continued*

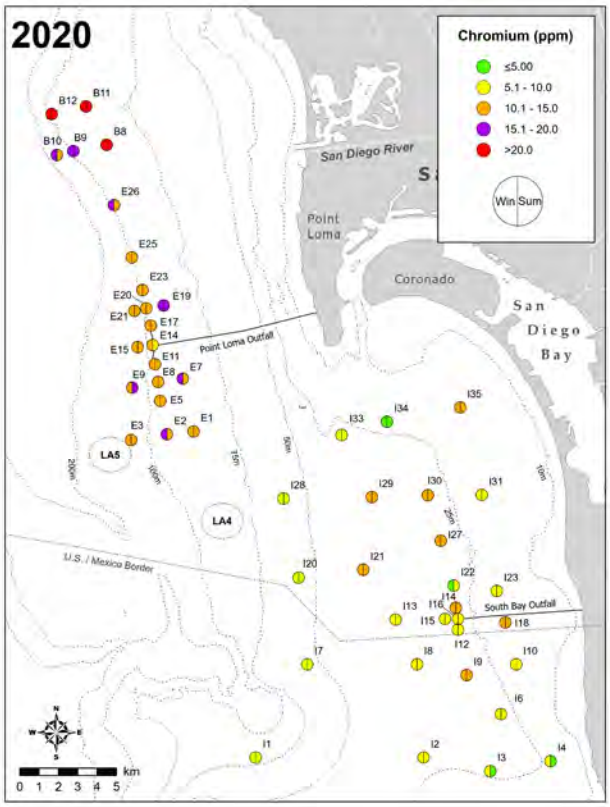

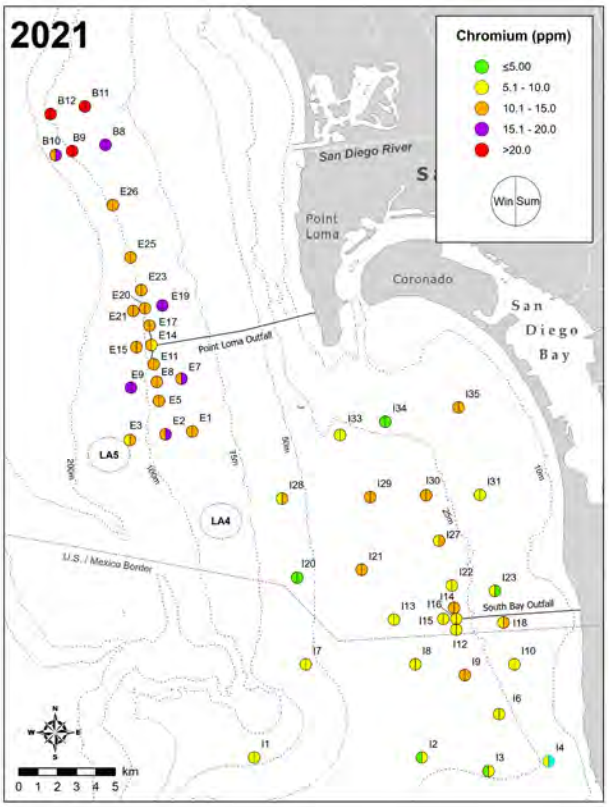

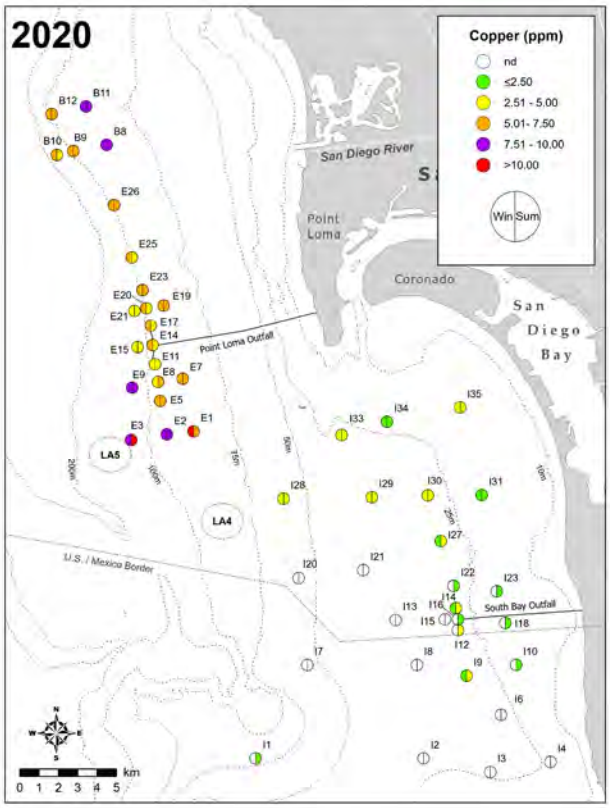

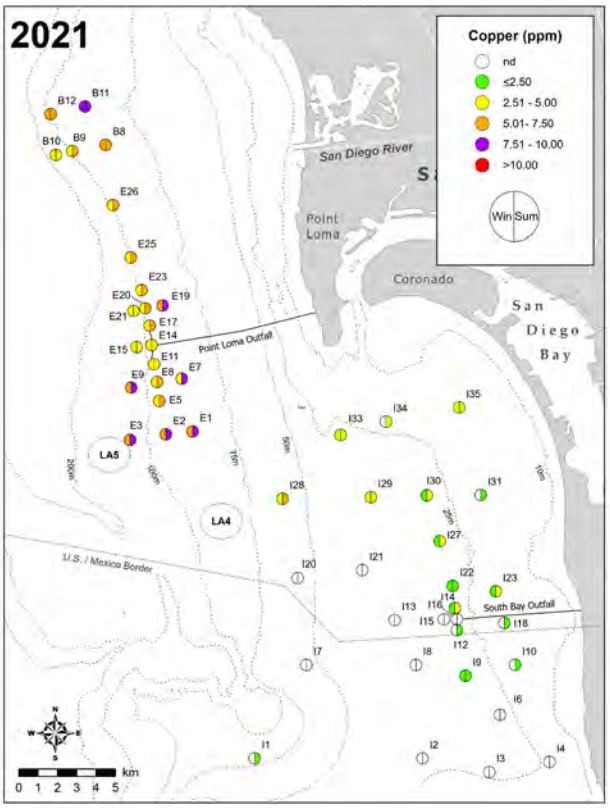

Appendix F.4 *continued*

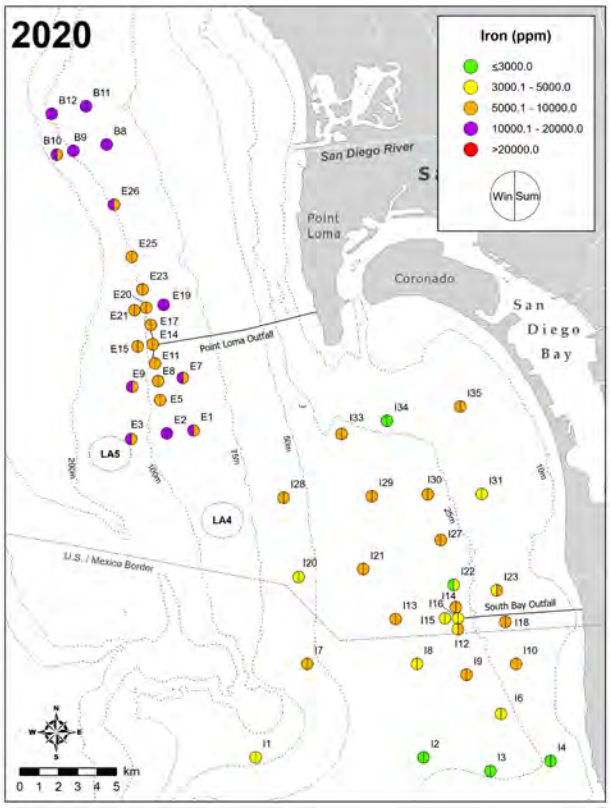

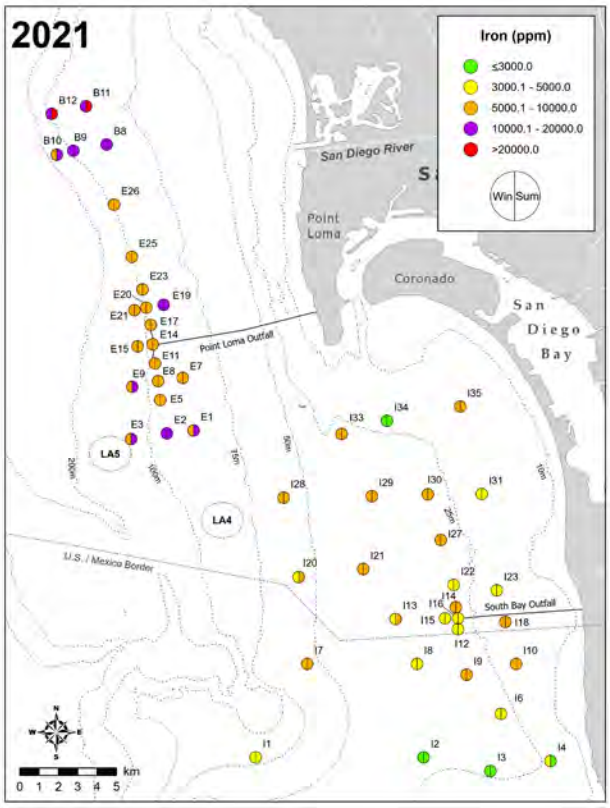

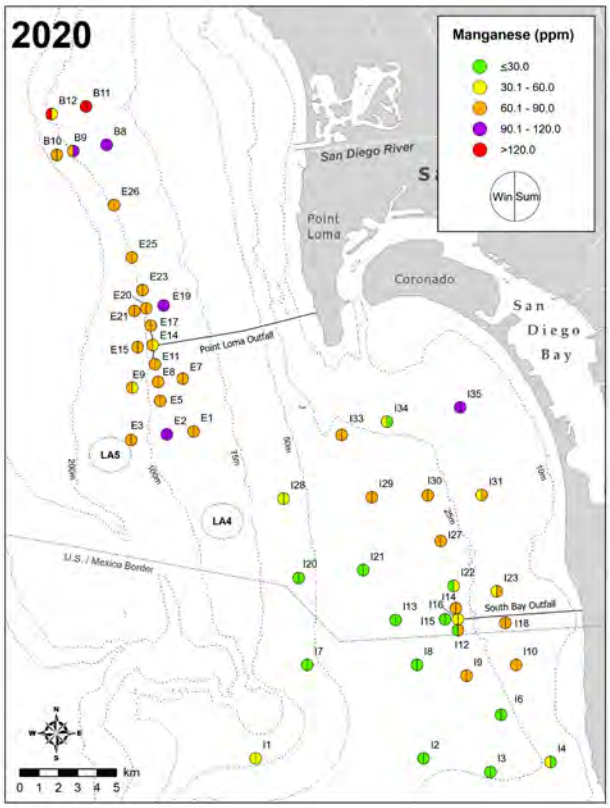

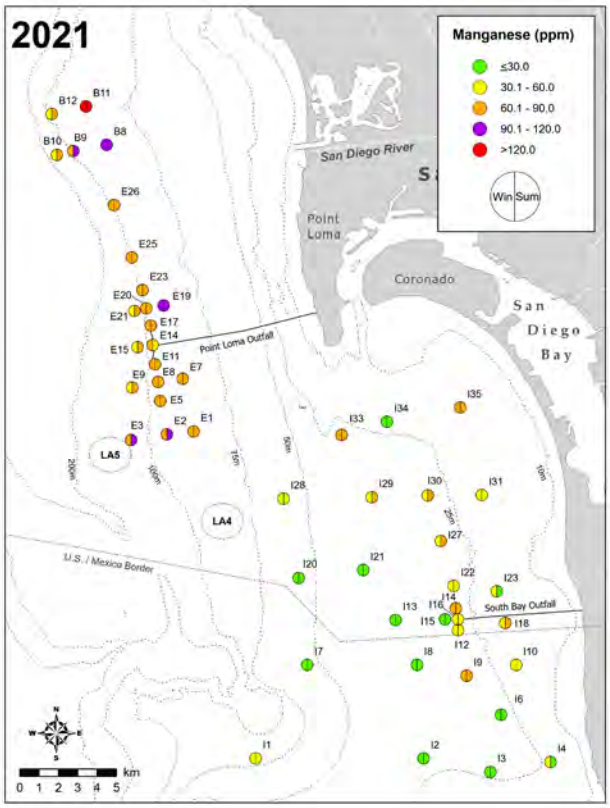

Appendix F.4 *continued*

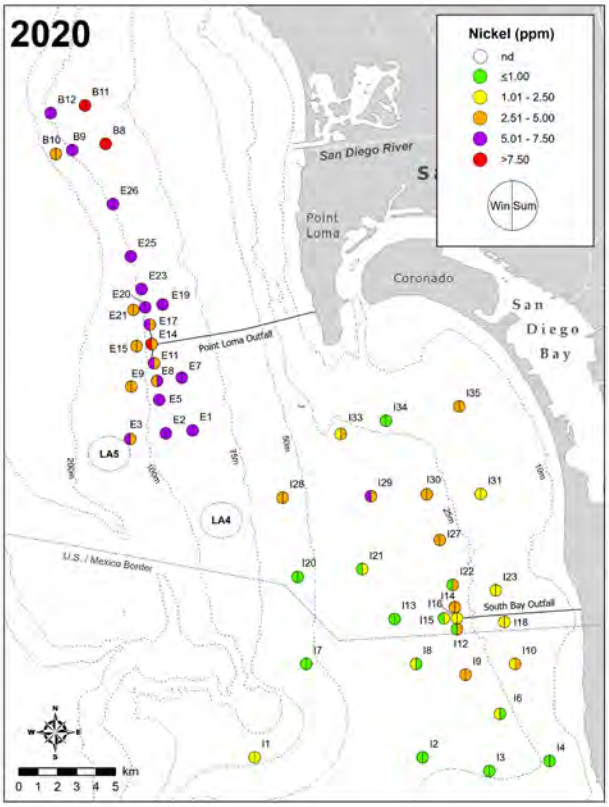

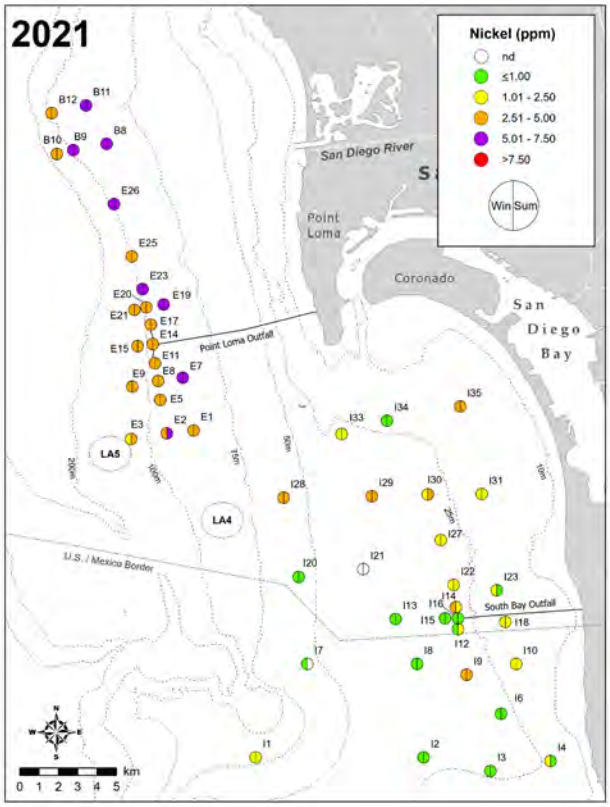

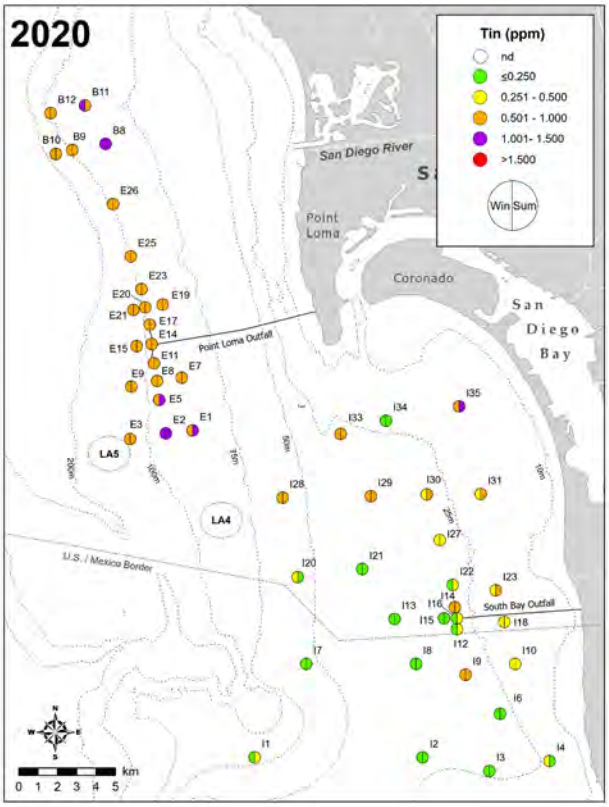

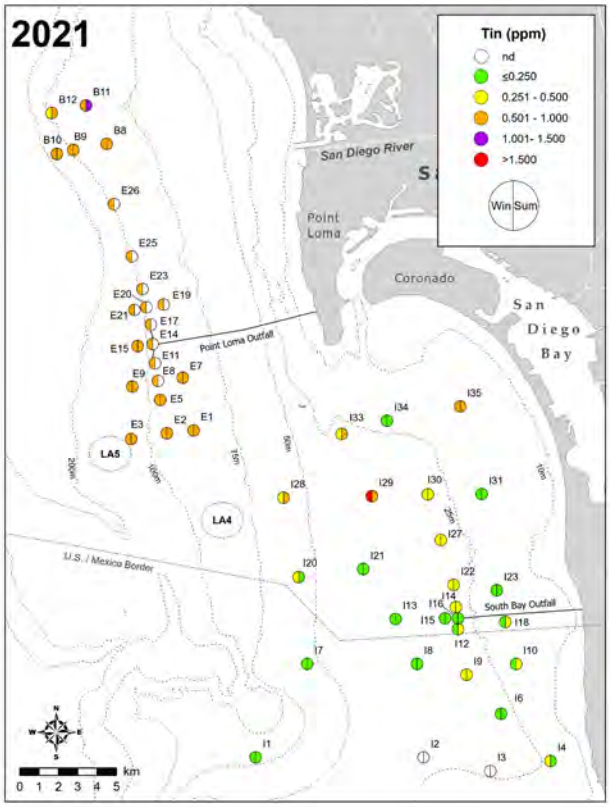

Appendix F.4 *continued*

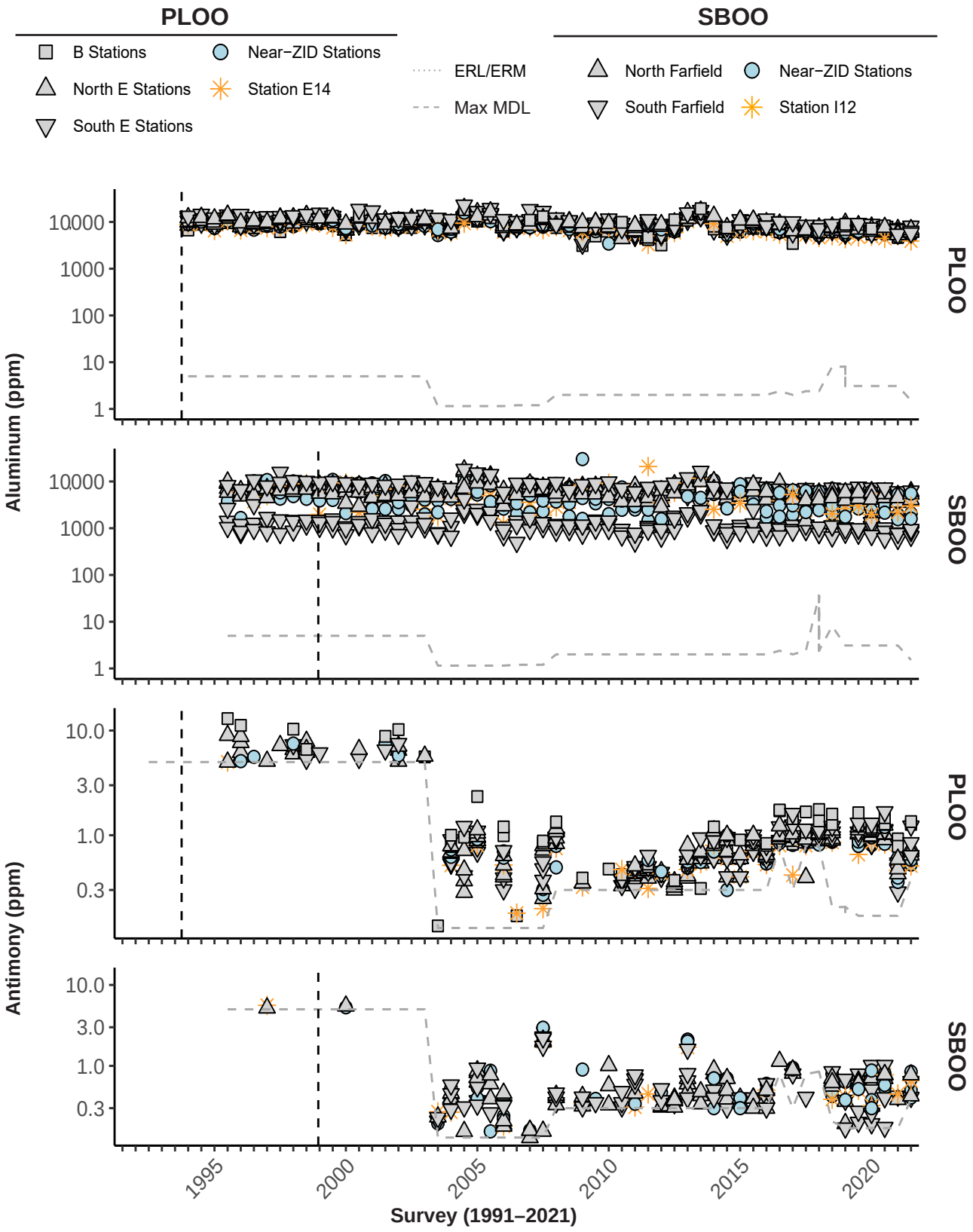

Appendix F.5

Concentrations of select metals in sediments sampled during winter and summer surveys at PLOO primary core stations from 1991 through 2021 and at SBOO primary core stations from 1995 through 2021. Data represent detected values from each station, n ≤ 12 samples per survey. Vertical dashed lines indicate onset of discharge from the PLOO or SBOO. Thresholds included (ERLs, ERMs) when relevant (see Table 5.3), along with the maximum MDL per survey.

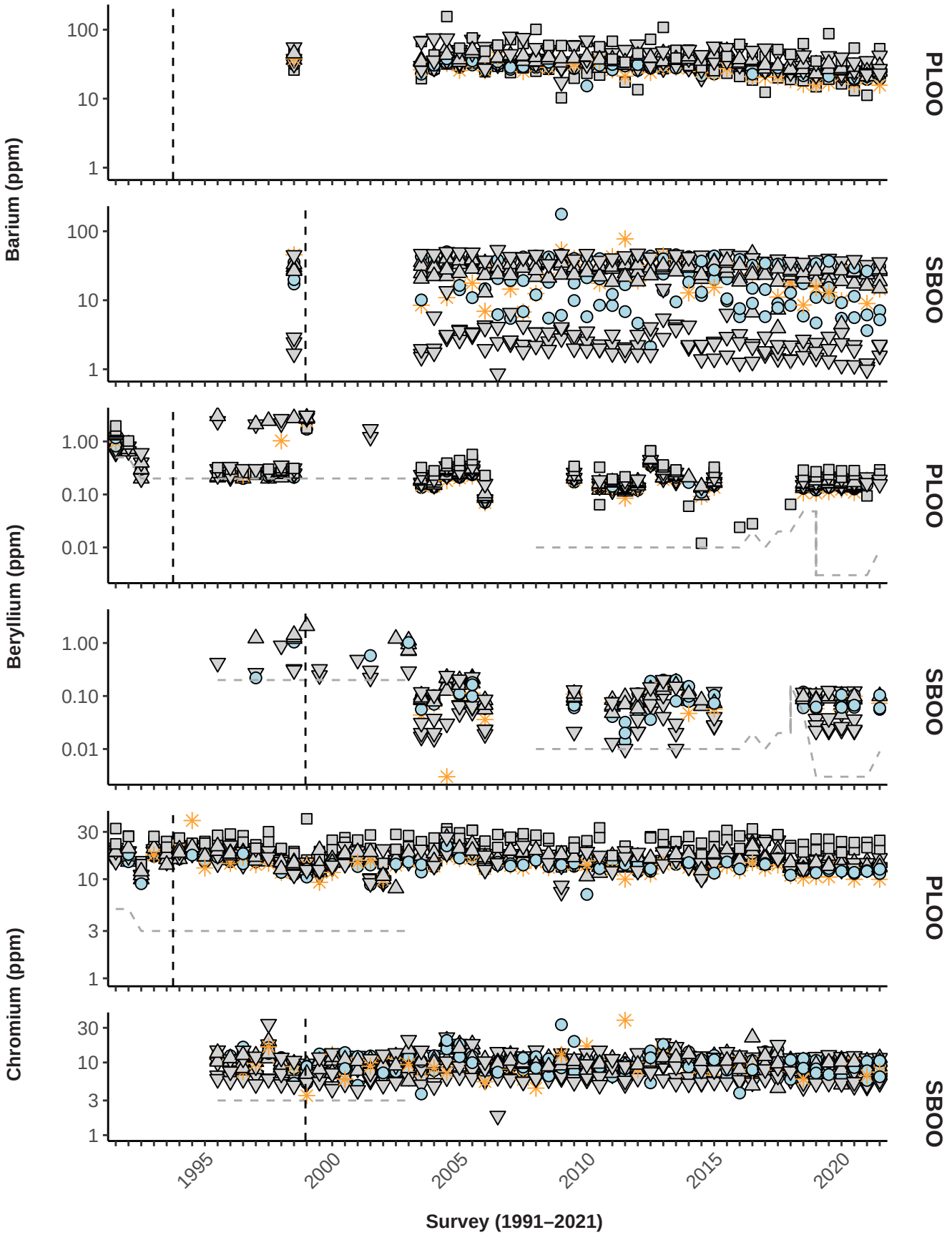

Appendix F.5 *continued*

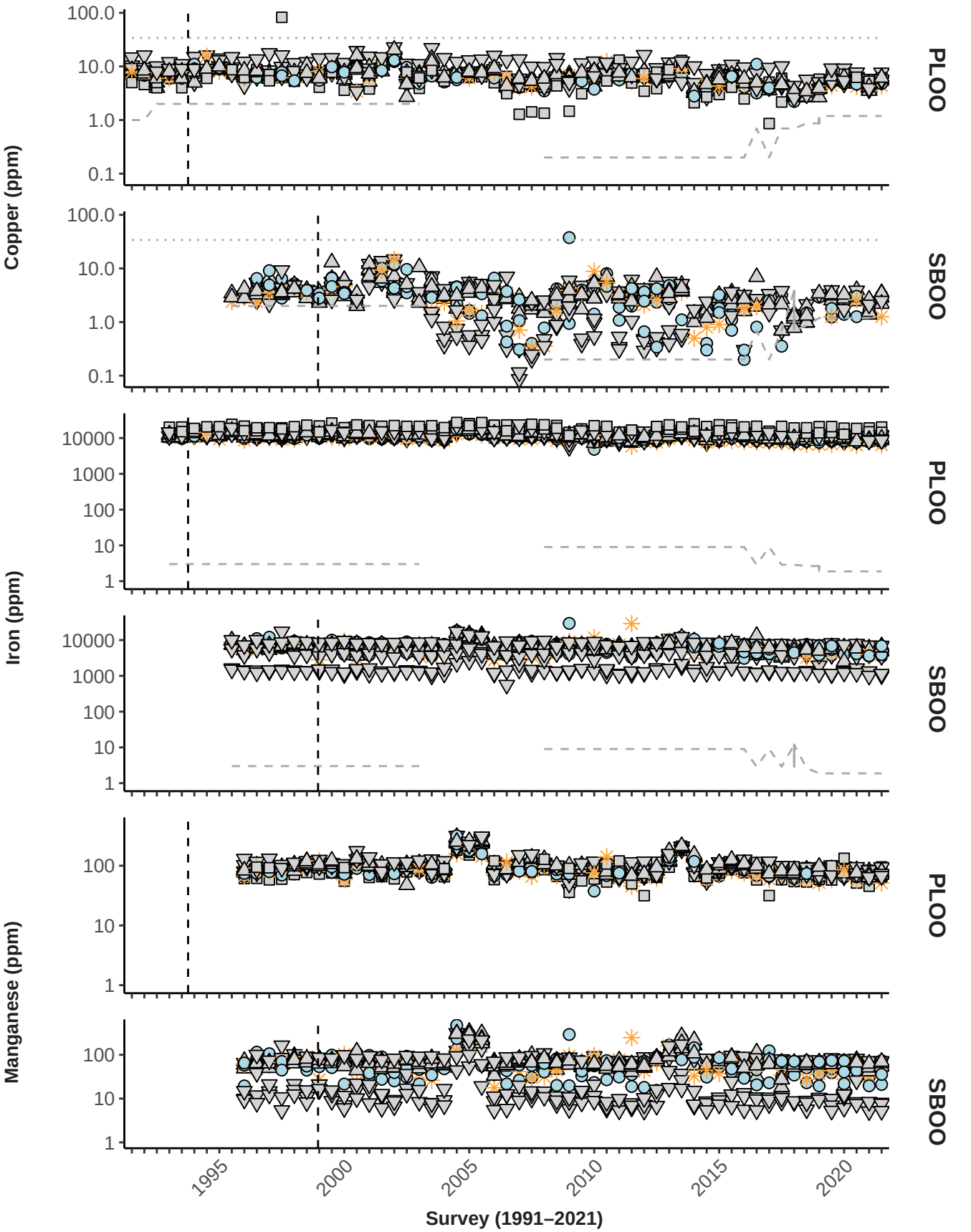

Appendix F.5 *continued*

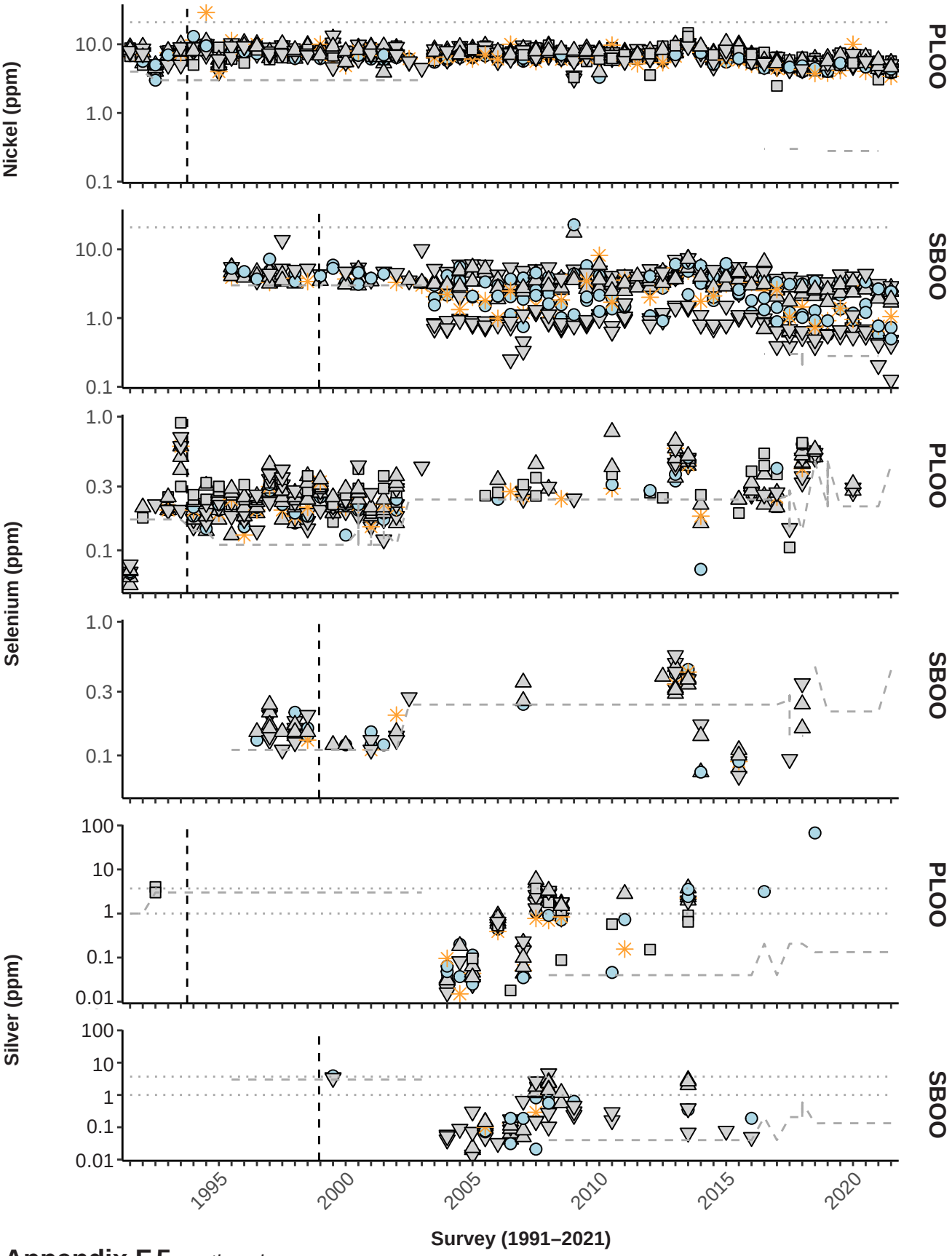

Appendix F.5 *continued*

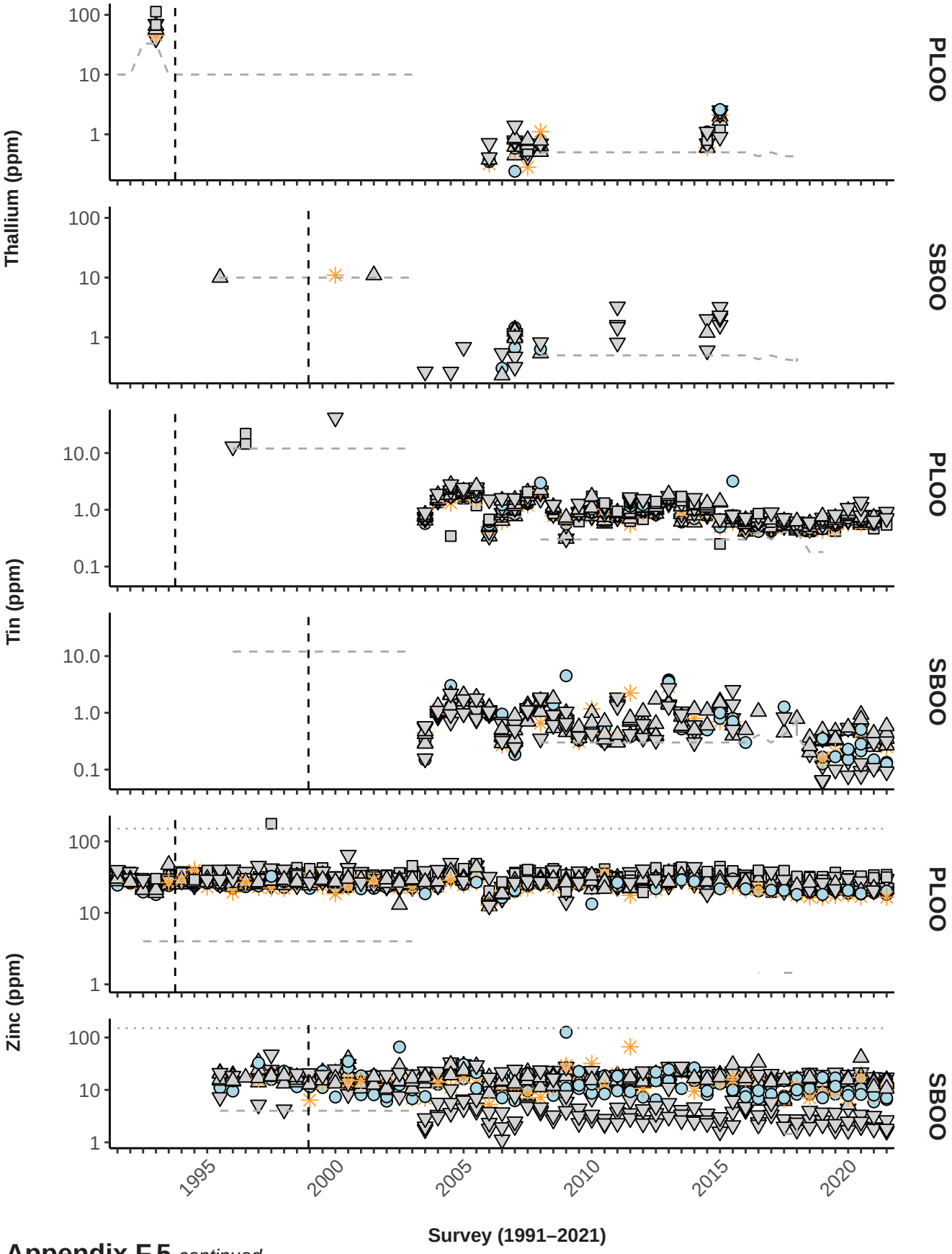

Appendix F.5 *continued*

This page intentionally left blank

Appendix G

Macrobenthic Communities

2020 – 2021 Supplemental Analyses

Appendix G.1

Macrofaunal community parameters by grab for PLOO benthic stations sampled during 2021. SR = species richness; Abun = abundance; H' = Shannon diversity index; J' = Pielou's evenness; Dom = Swartz dominance; BRI = Benthic Response Index.

Depth Contour	Station	Survey	SR	Abun	H'	J'	Dom	BRI
88-m	B11	winter	108	367	4.2	0.90	40	11
		summer	122	311	4.3	0.90	49	9
	B8	winter	83	300	3.9	0.87	28	4
		summer	65	249	3.6	0.86	25	7
	E19	winter	92	510	3.5	0.78	17	11
		summer	79	433	3.5	0.79	18	11
	E7	winter	91	350	3.8	0.83	27	15
		summer	93	293	4.1	0.90	35	12
	E1	winter	98	414	3.9	0.85	29	9
		summer	104	389	3.9	0.84	27	7
98-m	B12	winter	105	283	4.2	0.91	42	12
		summer	118	382	4.3	0.90	46	11
	B9	winter	87	329	3.9	0.87	30	10
		summer	94	257	4.1	0.91	37	10
	E26	winter	99	491	3.9	0.85	30	12
		summer	95	375	3.9	0.87	31	13
	E25	winter	87	555	3.5	0.79	19	9
		summer	82	534	3.3	0.74	17	13
	E23	winter	90	568	3.7	0.82	22	9
		summer	83	384	3.7	0.84	25	11
	E20	winter	95	554	3.8	0.85	27	11
		summer	78	399	3.6	0.82	19	15
	E17[a]	winter	103	645	3.6	0.78	24	14
		summer	84	376	3.7	0.84	24	13
	E14[a]	winter	75	453	3.4	0.78	18	28
		summer	90	562	3.6	0.79	22	30
	E11[a]	winter	93	645	3.7	0.81	22	13
		summer	75	360	3.8	0.88	27	16
	E8	winter	90	470	3.9	0.86	27	9
		summer	106	359	4.2	0.90	39	8
	E5	winter	105	461	3.8	0.82	29	9
		summer	88	385	3.9	0.86	28	9
	E2	winter	95	402	3.9	0.86	32	10
		summer	109	406	3.9	0.82	34	10

[a] Near-ZID station

Appendix G.1 *continued*

Depth Contour	Station	Survey	SR	Abun	H'	J'	Dom	BRI
116-m	B10	winter	86	334	3.9	0.89	31	14
		summer	96	269	4.0	0.88	37	12
	E21	winter	75	407	3.3	0.77	18	11
		summer	61	215	3.6	0.87	23	12
	E15[a]	winter	78	463	3.4	0.79	18	13
		summer	74	336	3.7	0.86	24	16
	E9	winter	92	330	4.0	0.88	33	10
		summer	101	311	4.1	0.88	40	13
	E3	winter	116	274	4.3	0.91	48	12
		summer	114	328	4.3	0.91	46	10

[a] Near-ZID station

Appendix G.2

Macrofaunal community parameters by grab for SBOO benthic stations sampled during 2021. SR = species richness; Abun = abundance; H' = Shannon diversity index; J' = Pielou's evenness; Dom = Swartz dominance; BRI = Benthic Response Index.

Depth Contour	Station	Survey	SR	Abun	H'	J'	Dom	BRI
19-m	I35	winter	65	263	3.6	0.86	22	29
		summer	57	129	3.6	0.90	25	24
	I34	winter	31	115	2.9	0.84	12	3
		summer	68	913	2.8	0.67	8	21
	I31	winter	57	147	3.6	0.89	23	18
		summer	36	126	2.7	0.75	10	18
	I23	winter	66	200	3.8	0.90	27	21
		summer	64	501	2.9	0.70	9	21
	I18	winter	44	100	3.4	0.90	20	13
		summer	63	307	3.3	0.80	19	14
	I10	winter	37	70	3.3	0.93	20	20
		summer	55	136	3.5	0.89	23	15
	I4	winter	27	48	3.0	0.91	16	19
		summer	32	63	3.2	0.92	17	6
28-m	I33	winter	90	260	4.0	0.88	37	24
		summer	97	227	4.2	0.91	41	21
	I30	winter	55	167	3.5	0.87	22	26
		summer	65	154	3.9	0.93	31	22
	I27	winter	59	169	3.6	0.88	24	24
		summer	65	179	3.7	0.89	25	19
	I22	winter	72	180	3.7	0.88	31	25
		summer	56	144	3.6	0.90	25	22
	I14[a]	winter	75	180	3.9	0.91	33	24
		summer	83	255	3.9	0.87	30	21
	I16[a]	winter	61	200	3.6	0.88	24	19
		summer	49	148	3.3	0.85	21	13
	I15[a]	winter	46	83	3.6	0.95	26	14
		summer	50	265	2.7	0.68	10	15
	I12[a]	winter	46	115	3.4	0.88	19	12
		summer	41	189	2.6	0.69	8	17
	I9	winter	58	160	3.7	0.90	25	25
		summer	70	207	3.6	0.85	25	23
	I6	winter	26	114	2.4	0.73	7	12
		summer	45	120	3.3	0.87	18	11
	I2	winter	30	83	3.0	0.89	14	19
		summer	46	207	2.7	0.70	10	24
	I3	winter	33	95	2.8	0.80	13	10
		summer	31	112	2.7	0.78	9	6

[a] Near-ZID station

Appendix G.2 *continued*

Depth Contour	Station	Survey	SR	Abun	H'	J'	Dom	BRI
38-m	I29	winter	125	449	4.4	0.90	46	16
		summer	128	392	4.3	0.89	47	14
	I21	winter	30	121	2.7	0.81	9	-6
		summer	57	147	3.7	0.92	29	9
	I13	winter	45	114	3.3	0.87	18	8
		summer	46	167	3.3	0.87	18	8
	I8	winter	44	110	3.3	0.87	18	17
		summer	42	120	3.2	0.86	17	11
55-m	I28	winter	163	597	4.5	0.88	53	14
		summer	135	372	4.4	0.90	55	15
	I20	winter	47	180	3.3	0.86	17	6
		summer	64	314	2.6	0.63	12	9
	I7	winter	34	80	3.0	0.85	15	7
		summer	59	219	3.2	0.79	19	7
	I1	winter	63	211	3.6	0.87	24	15
		summer	87	264	4.0	0.89	33	11

Appendix G.3

Summary taxonomic listing of benthic infauna taxa identified from PLOO stations during 2021. Data are total number of individuals (n). Taxonomic arrangement follows SCAMIT (2018).

Phylum	Class	Family	Taxon	n
Cnidaria	Hydrozoa	Corymorphidae	*Corymorpha bigelowi*	1
			Euphysa sp A	1
	Anthozoa			1
		Virgulariidae	*Stylatula* sp A	2
			Virgularia sp	1
		--	Ceriantharia	2
			Actiniaria	3
		Edwardsiidae		21
			Edwardsia juliae	1
			Edwardsia olguini	6
			Edwardsia sp SD1	1
			Scolanthus triangulus	86
		Halcampidae	*Halcampa decemtentaculata*	1
			Halianthella sp A	11
Platyhelminthes	Rhabditophora	Plehniidae	*Diplehnia caeca*	4
		Leptoplanidae		1
Nemertea	Anopla	Cephalotrichidae	*Cephalothrix* sp	1
		--	Palaeonemertea	3
		Carinomidae	*Carinoma mutabilis*	6
		Tubulanidae		7
			Tubulanus cingulatus	7
			Tubulanus polymorphus	37
			Tubulanus sp A	1
		--	Heteronemertea	2
		Lineidae		84
			Cerebratulus californiensis	4
			Cerebratulus sp	1
			Lineidae sp SD1	11
			Lineus bilineatus	47
			Zygeupolia rubens	7
		--	Heteronemertea sp SD2	123
	Enopla		Hoplonemertea	10
		Emplectonematidae	*Paranemertes californica*	19
		--	Hoplonemertea sp A	2
			Hoplonemertea sp D	1
Mollusca	Caudofoveata	Chaetodermatidae	*Chaetoderma pacificum*	2
			Falcidens longus	1
	Polyplacophora	Leptochitonidae	*Leptochiton rugatus*	1
	Gastropoda	Solariellidae	*Solariella peramabilis*	10
		Cerithiidae	*Lirobittium rugatum* Cmplx	3
		Caecidae	*Caecum crebricinctum*	9
		Epitoniidae	*Epitonium sawinae*	1
		Mangeliidae		1
			Kurtzia arteaga	7
			Kurtzina beta	8
		Pseudomelatomidae	*Antiplanes catalinae*	1
		Acteonidae	*Rictaxis punctocaelatus*	1
		Aplustridae	*Parvaplustrum cadieni*	1

Appendix G.3 *continued*

Phylum	Class	Family	Taxon	n
		Pyramidellidae	*Odostomia* sp	6
			Turbonilla chocolata	1
			Turbonilla santarosana	6
			Turbonilla sp A	4
			Turbonilla sp SD5	1
			Turbonilla sp	2
		Rhizoridae	*Volvulella californica*	6
			Volvulella catharia	1
			Volvulella cylindrica	1
		Acteocinidae	*Acteocina cerealis*	22
		Philinidae	*Philine auriformis*	20
		Aglajidae	*Aglaja ocelligera*	4
		Gastropteridae	*Gastropteron pacificum*	1
		Cylichnidae	*Cylichna diegensis*	24
		Diaphanidae	*Diaphana californica*	1
	Bivalvia			4
		Nuculidae	*Acila castrensis*	2
			Ennucula tenuis	30
		Solemyidae	*Solemya pervernicosa*	4
		Nucinellidae	*Huxleyia munita*	2
		Nuculanidae	*Nuculana hamata*	2
			Nuculana sp A	131
		Mytilidae	*Amygdalum pallidulum*	4
		Limidae	*Limatula saturna*	1
		Pectinidae		1
		Lucinidae	*Parvilucina tenuisculpta*	91
			Lucinoma annulatum	37
		Thyasiridae	*Adontorhina cyclia*	15
			Axinopsida serricata	1138
			Thyasira flexuosa	9
		Lasaeidae	*Kurtiella mortoni*	1
			Kurtiella tumida	5
			Kurtiella sp D	8
		Cardiidae	*Keenaea centifilosum*	30
		Tellinidae	*Tellina carpenteri*	168
			Tellina sp B	226
			Tellina sp	1
			Macoma sp	1
		Hiatellidae	*Hiatella arctica*	1
		Veneridae	*Compsomyax subdiaphana*	3
		Lyonsiidae		3
			Lyonsia californica	2
		Thraciidae		1
			Asthenothaerus diegensis	1
			Thracia trapezoides	1
		Cuspidariidae	*Cardiomya pectinata*	2
			Cuspidaria parapodema	9
	Scaphopoda			1
		Dentaliidae	*Dentalium neohexagonum*	1
		Gadilidae	*Polyschides quadrifissatus*	28

Appendix G.3 *continued*

Phylum	Class	Family	Taxon	n
Sipuncula				8
	Sipunculidea	Golfingiidae	*Nephasoma diaphanes*	6
			Thysanocardia nigra	5
		Phascolionidae	*Phascolion* sp A	25
	Phascolosomatidea	Phascolosomatidae	*Apionsoma misakianum*	2
Annelida	Polychaeta	Amphinomidae	*Chloeia pinnata*	118
		Dorvilleidae		1
			Dorvillea (Schistomeringos) sp	1
			Protodorvillea gracilis	1
		Eunicidae		1
			Marphysa disjuncta	1
			Marphysa sp	2
		Lumbrineridae		3
			Eranno lagunae	11
			Lumbrineris cruzensis	59
			Lumbrineris index	1
			Lumbrineris latreilli	18
			Lumbrineris ligulata	10
			Lumbrineris limicola	3
			Lumbrineris sp Group I	24
			Lumbrineris sp Group II	2
			Ninoe tridentata	4
			Scoletoma tetraura Cmplx	37
			Scoletoma sp	2
		Oenonidae	*Drilonereis falcata*	17
			Drilonereis mexicana	2
			Drilonereis sp	8
			Notocirrus californiensis	3
		Onuphidae		14
			Diopatra sp	1
			Hyalinoecia juvenalis	1
			Mooreonuphis exigua	19
			Mooreonuphis nebulosa	4
			Mooreonuphis segmentispadix	4
			Mooreonuphis sp SD2	1
			Mooreonuphis sp	19
			Nothria occidentalis	9
			Nothria sp	2
			Onuphis affinis	1
			Onuphis iridescens	7
			Onuphis sp A	20
			Onuphis sp	5
			Paradiopatra parva	684
			Rhamphobrachium longisetosum	2
		Acoetidae	*Acoetes pacifica*	1
		Aphroditidae		2
			Aphrodita sp	5
		Polynoidae	*Malmgreniella baschi*	3
			Malmgreniella liei	1
			Malmgreniella sanpedroensis	2

Appendix G.3 *continued*

Phylum	Class	Family	Taxon	n
			Malmgreniella sp A	21
			Malmgreniella sp	2
			Subadyte mexicana	9
			Tenonia priops	3
		Pholoidae	*Pholoe glabra*	71
		Sigalionidae	*Pholoides asperus*	10
			Pisione sp	1
			Sigalion spinosus	46
			Sthenelais tertiaglabra	6
			Sthenelais verruculosa	3
			Sthenelanella uniformis	55
		Glyceridae	*Glycera americana*	9
			Glycera nana	103
			Glycera oxycephala	2
			Hemipodia borealis	1
		Goniadidae	*Glycinde armigera*	57
			Goniada brunnea	7
			Goniada maculata	60
		Hesionidae	*Podarkeopsis glabrus*	5
			Podarkeopsis sp	1
		Nereididae	*Nereis* sp A	27
			Nereis sp	4
		Pilargidae	*Sigambra tentaculata*	1
		Syllidae	*Syllides mikeli*	2
			Eusyllis blomstrandi Cmplx	2
			Eusyllis transecta	2
			Eusyllis sp SD2	1
			Paraehlersia articulata	3
			Exogone lourei	36
			Parexogone molesta	2
			Syllis gracilis Cmplx	3
			Syllis heterochaeta	5
			Syllis sp SD2	1
		Nephtyidae	*Aglaophamus verrilli*	8
			Bipalponephtys cornuta	1
			Nephtys caecoides	19
			Nephtys ferruginea	16
			Nephtys simoni	1
			Nephtys sp SD2	1
			Nephtys sp	2
		Sphaerodoridae	*Sphaerodoropsis biserialis*	1
		Phyllodocidae	*Eteone pigmentata*	1
			Eulalia levicornuta Cmplx	2
			Eulalia sp SD4	2
			Eulalia sp	1
			Eumida longicornuta	4
			Sige sp A	13
			Sige sp	2
			Nereiphylla sp 2	1
			Phyllodoce groenlandica	8

Appendix G.3 *continued*

Phylum	Class	Family	Taxon	n
			Phyllodoce hartmanae	37
			Phyllodoce longipes	25
			Phyllodoce pettiboneae	13
		Oweniidae	*Galathowenia pygidialis*	6
			Myriochele gracilis	44
			Myriochele olgae	3
			Myriochele striolata	9
			Myriowenia californiensis	1
		Sabellidae	*Acromegalomma* sp*lendidum*	1
			Dialychone albocincta	28
			Dialychone trilineata	114
			Dialychone veleronis	2
			Euchone arenae	2
			Euchone hancocki	17
			Euchone incolor	44
			Euchone sp A	24
			Euchone sp	1
			Jasmineira sp B	8
			Myxicola sp	3
			Paradialychone bimaculata	7
			Paradialychone eiffelturris	1
			Paradialychone harrisae	4
			Paradialychone paramollis	6
			Potamethus sp A	6
		Longosomatidae	*Heterospio catalinensis*	1
		Magelonidae	*Magelona berkeleyi*	7
			Magelona hartmanae	2
			Magelona hobsonae	1
			Magelona longicornis	2
			Magelona sp B	7
			Magelona sp	1
		Spionidae		1
			Dipolydora socialis	4
			Laonice cirrata	29
			Laonice nuchala	38
			Microspio pigmentata	47
			Paraprionospio alata	27
			Prionospio dubia	377
			Prionospio jubata	345
			Prionospio lighti	7
			Spio filicornis	3
			Spiophanes berkeleyorum	22
			Spiophanes duplex	1199
			Spiophanes kimballi	359
			Spiophanes wigleyi	8
			Spiophanes sp	2
		Cirratulidae	*Aphelochaeta glandaria* Cmplx	157
			Aphelochaeta monilaris	57
			Aphelochaeta phillipsi	30
			Aphelochaeta tigrina	12

Appendix G.3 *continued*

Phylum	Class	Family	Taxon	n
			Aphelochaeta williamsae	5
			Aphelochaeta sp LA1	17
			Aphelochaeta sp SD5	1
			Aphelochaeta sp	4
			Chaetozone columbiana	1
			Chaetozone hartmanae	72
			Chaetozone sp SD3	7
			Chaetozone sp SD5	2
			Chaetozone sp SD7	8
			Chaetozone sp	1
			Kirkegaardia cryptica	12
			Kirkegaardia serratiseta	1
			Kirkegaardia siblina	103
			Kirkegaardia tesselata	19
			Kirkegaardia sp SD9	10
			Kirkegaardia sp	4
		Fauveliopsidae	*Fauveliopsis* sp SD1	8
		Flabelligeridae	*Brada pilosa*	7
			Brada pluribranchiata	2
			Pherusa neopapillata	3
			Trophoniella harrisae	3
		Sternaspidae	*Sternaspis affinis*	76
		Ampharetidae		12
			Amage anops	6
			Amage scutata	32
			Amage sp	1
			Ampharete finmarchica	14
			Ampharete labrops	4
			Ampharete sp	1
			Ampharetidae sp SD1	11
			Amphicteis scaphobranchiata	14
			Amphisamytha bioculata	1
			Anobothrus gracilis	24
			Asabellides lineata	5
			Eclysippe trilobata	335
			Lysippe sp A	28
			Lysippe sp B	44
			Sabellides manriquei	2
			Samytha californiensis	3
			Schistocomus sp	1
			Sosane occidentalis	19
			Melinna oculata	8
		Pectinariidae	*Pectinaria californiensis*	101
		Terebellidae	*Amaeana occidentalis*	7
			Polycirrus californicus	111
			Polycirrus sp I	1
			Polycirrus sp A	221
			Polycirrus sp OC1	114
			Polycirrus sp	64
			Lanassa venusta venusta	312

Appendix G.3 *continued*

Phylum	Class	Family	Taxon	n
			Lanice conchilega	1
			Phisidia sanctaemariae	443
			Pista brevibranchiata	10
			Pista estevanica	93
			Pista moorei	1
			Pista pacifica	2
			Pista wui	4
			Proclea sp A	34
		Trichobranchidae		2
			Terebellides californica	4
			Terebellides sp Type D	1
			Trichobranchus hancocki	1
		Chaetopteridae		1
			Phyllochaetopterus limicolus	2
			Phyllochaetopterus prolifica	4
			Spiochaetopterus costarum Cmplx	42
		Capitellidae	*Capitella teleta*	164
			Decamastus gracilis	37
			Mediomastus sp	1029
			Notomastus hemipodus	60
			Notomastus latericeus	3
			Notomastus sp	8
		Cossuridae	*Cossura candida*	6
			Cossura sp A	1
		Maldanidae		133
			Euclymeninae	37
			Axiothella sp	3
			Clymenella sp A	1
			Clymenura gracilis	153
			Euclymeninae sp *A*	449
			Isocirrus longiceps	1
			Petaloclymene pacifica	65
			Praxillella gracilis	5
			Praxillella pacifica	485
			Maldaninae	8
			Maldane sarsi	71
			Metasychis disparidentatus	5
			Rhodine bitorquata	129
		Opheliidae	*Armandia brevis*	8
			Ophelina acuminata	2
			Ophelina sp A	1
			Ophelina sp SD1	2
		Orbiniidae	*Leitoscoloplos pugettensis*	1
			Scoloplos armiger Cmplx	361
		Paraonidae	*Aricidea (Acmira) catherinae*	77
			Aricidea (Acmira) lopezi	45
			Aricidea (Acmira) rubra	1
			Aricidea (Acmira) simplex	27
			Aricidea (Acmira) sp	5
			Aricidea (Aricidea) wassi	4

Appendix G.3 *continued*

Phylum	Class	Family	Taxon	n
			Aricidea (Aricidea) sp SD3	3
			Aricidea (Strelzovia) antennata	45
			Aricidea (Strelzovia) hartleyi	6
			Aricidea (Strelzovia) sp A	25
			Levinsenia gracilis	20
			Levinsenia kirbyae	14
			Paradoneis sp SD1	1
		Scalibregmatidae	*Scalibregma californicum*	8
		Travisiidae	*Travisia brevis*	88
Arthropoda	Ostracoda	Cylindroleberididae	*Xenoleberis californica*	9
		Philomedidae	*Euphilomedes carcharodonta*	13
			Euphilomedes producta	102
			Scleroconcha tritubercula	2
		Rutidermatidae	*Rutiderma lomae*	1
	Malacostraca	Mysidae	*Pseudomma californica*	1
			Mysidella americana	1
			Inusitatomysis insolita	1
		Caprellidae	*Caprella verrucosa*	3
			Caprella sp	1
			Mayerella banksia	1
		Photidae	*Photis bifurcata*	1
			Photis californica	14
			Photis lacia	12
			Photis sp SD10	10
			Photis sp	5
			Podoceropsis ociosa	1
		Aoridae	*Aoroides* sp A	3
			Aoroides sp	2
		Corophiidae	*Protomedeia articulata* Cmplx	5
		Oedicerotidae	*Americhelidium shoemakeri*	8
			Americhelidium sp SD1	1
			Americhelidium sp	3
			Bathymedon pumilus	38
			Deflexilodes norvegicus	11
			Monoculodes emarginatus	15
			Westwoodilla tone	15
		Eusiridae	*Rhachotropis* sp A	7
		Liljeborgiidae		1
			Listriella goleta	4
		Melphidippidae	*Melphisana bola* Cmplx	1
		Pardaliscidae	*Halicoides synopiae*	4
			Nicippe tumida	12
		Ampeliscidae	*Ampelisca agassizi*	3
			Ampelisca brevisimulata	40
			Ampelisca cf *brevisimulata*	16
			Ampelisca careyi	163
			Ampelisca cristata microdentata	5
			Ampelisca hancocki	51
			Ampelisca indentata	1
			Ampelisca lobata	1

Appendix G.3 *continued*

Phylum	Class	Family	Taxon	n
			Ampelisca pacifica	80
			Ampelisca pugetica	95
			Ampelisca romigi	4
			Ampelisca sp	31
			Byblis millsi	5
		Argissidae	*Argissa hamatipes*	1
		Urothoidae	*Urothoe elegans* Cmplx	3
		Phoxocephalidae		9
			Foxiphalus obtusidens	5
			Foxiphalus similis	2
			Rhepoxynius bicuspidatus	300
			Rhepoxynius lucubrans	2
			Rhepoxynius menziesi	104
			Eyakia robusta	26
			Paraphoxus sp 1	1
			Heterophoxus ellisi	2
			Heterophoxus oculatus	36
			Heterophoxus sp	5
		--	Lysianassoidea	1
		Lysianassidae	*Aruga holmesi*	2
			Aruga oculata	2
		Opisidae	*Opisa tridentata*	1
		Uristidae	*Anonyx lilljeborgi*	5
		Tryphosidae	*Hippomedon zetesimus*	3
			Hippomedon sp A	3
		Acidostomatidae	*Acidostoma hancocki*	1
		Pakynidae	*Pachynus barnardi*	5
			Prachynella lodo	2
		Cirolanidae	*Eurydice caudata*	4
		Gnathiidae	*Caecognathia crenulatifrons*	85
		Anthuridae	*Haliophasma geminata*	12
		Serolidae	*Heteroserolis carinata*	1
		--	Tanaidacea	12
		Akanthophoreidae	*Chauliopleona dentata*	6
		Anarthruridae	*Siphonolabrum californiensis*	6
		Leptocheliidae	*Chondrochelia dubia* Cmplx	97
		Tanaellidae	*Araphura breviaria*	124
			Araphura sp SD1	3
			Araphura sp	4
			Tanaella propinquus	36
		Typhlotanaidae	*Typhlotanais williamsae*	4
		Tanaopsidae	*Tanaopsis cadieni*	9
		Leuconidae	*Eudorella pacifica*	1
		Nannastacidae	*Campylaspis blakei*	1
			Campylaspis canaliculata	3
			Campylaspis rubromaculata	2
			Procampylaspis caenosa	8
		Diastylidae	*Diastylis crenellata*	32
			Leptostylis abditis	1
		Diogenidae	*Paguristes turgidus*	1

Appendix G.3 *continued*

Phylum	Class	Family	Taxon	n
		Paguridae	*Pylopagurus holmesi*	2
		Cyclodorippidae	*Deilocerus decorus*	2
			Deilocerus sp	2
		Calappidae	*Platymera gaudichaudii*	1
		Pinnotheridae	*Pinnixa longipes*	1
			Pinnixa occidentalis Cmplx	6
Nematoda				39
Echinodermata	Asteroidea			80
		Astropectinidae	*Astropecten californicus*	6
			Astropecten sp	3
	Ophiuroidea			29
		Ophiuridae	*Ophiura luetkenii*	4
		Amphiuridae		448
			Amphichondrius granulatus	32
			Amphiodia digitata	39
			Amphiodia urtica	841
			Amphiodia sp	372
			Amphioplus sp	1
			Amphipholis squamata	1
			Amphiura arcystata	5
			Dougaloplus amphacanthus	11
			Dougaloplus sp A	2
	Echinoidea			1
		Toxopneustidae	*Lytechinus pictus*	2
		Brissidae	*Brissopsis pacifica*	1
		Spatangidae	*Spatangus californicus*	2
	Holothuroidea	Phyllophoridae	*Pentamera rigida*	1
			Thyone benti	1
		Synaptidae	*Leptosynapta* sp	32
		Chiridotidae	*Chiridota* sp	20
		Molpadiidae	*Molpadia intermedia*	3
Phoronida				3
		Phoronidae	*Phoronis* sp SD1	6
			Phoronis sp	11
Chordata	Enteropneusta			4
		Ptychoderidae	*Balanoglossus* sp	1
		Harrimaniidae	*Stereobalanus* sp	19
	Ascidiacea	Molgulidae		1

Appendix G.4

Summary taxonomic listing of benthic infauna taxa identified from SBOO stations during 2021. Data are total number of individuals (n). Taxonomic arrangement follows SCAMIT (2018).

Phylum	Class	Family	Taxon	n
Cnidaria	Hydrozoa	Corymorphidae		1
			Corymorpha bigelowi	15
			Euphysa sp A	4
	Anthozoa	Virgulariidae	*Stylatula* sp A	2
			Stylatula sp	6
			Virgularia sp	1
		--	Ceriantharia	9
		Arachnactidae	*Arachnanthus* sp A	2
		--	Actiniaria	5
		Edwardsiidae		23
			Edwardsia juliae	35
			Edwardsia olguini	4
			Scolanthus triangulus	10
		Halcampidae	*Halcampa decemtentaculata*	13
			Pentactinia californica	2
		Isanthidae	*Zaolutus actius*	5
		Limnactiniidae	Limnactiniidae sp A	2
Platyhelminthes	Rhabditophora	--	Polycladida	1
		Stylochidae	*Stylochus exiguus*	3
		--	Rhabditophora sp C	3
Nemertea				5
	Anopla	Cephalotrichidae	*Cephalothrix* sp	28
		--	Palaeonemertea	21
		Carinomidae	*Carinoma mutabilis*	63
		Tubulanidae		23
			Tubulanus cingulatus	13
			Tubulanus polymorphus	122
			Tubulanus sp A	2
			Tubulanus sp	1
			Tubulanidae sp B	3
		--	Heteronemertea	11
		Lineidae		102
			Cerebratulus sp	1
			Lineidae sp SD1	16
			Lineus bilineatus	17
			Maculaura alaskensis Cmplx	3
			Zygeupolia rubens	8
		Valenciniidae	*Baseodiscus princeps*	1
		--	Heteronemertea sp SD2	27
	Enopla			1
			Hoplonemertea	15
		Emplectonematidae	*Cryptonemertes actinophila*	6
			Paranemertes californica	10
		Oerstediidae	*Oerstedia dorsalis* Cmplx	8
		Amphiporidae	*Amphiporus flavescens*	1
		Tetrastemmatidae	*Quasitetrastemma nigrifrons*	3
			Tetrastemma candidum	39
			Tetrastemma sp HYP1	2

Appendix G.4 *continued*

Phylum	Class	Family	Taxon	n
		--	Hoplonemertea sp A	1
			Hoplonemertea sp D	7
Mollusca	Caudofoveata		Chaetodermatida	1
	Polyplacophora	Mopaliidae	*Dendrochiton thamnoporus*	1
	Gastropoda			1
		Trochidae	*Halistylus pupoideus*	4
		Calyptraeidae	*Calyptraea fastigiata*	7
		Naticidae	*Neverita draconis*	1
			Neverita recluziana	4
		Caecidae	*Caecum crebricinctum*	23
		Eulimidae		1
			Balcis oldroydae	5
			Eulima raymondi	5
			Polygireulima rutila	33
		Nassariidae	*Caesia perpinguis*	3
		Olivellidae	*Callianax baetica*	37
		Conidae	*Californiconus californicus*	1
		Borsoniidae	*Ophiodermella inermis*	5
		Mangeliidae	*Kurtzia arteaga*	1
			Kurtziella plumbea	5
		Pseudomelatomidae	*Crassispira semiinflata*	1
			Megasurcula carpenteriana	1
		Terebridae	*Terebra hemphilli*	2
			Terebra pedroana	3
		Pyramidellidae	*Odostomia* sp	1
			Turbonilla santarosana	3
			Turbonilla sp SD7	2
		Arminidae	*Armina californica*	1
		--	Cephalaspidea	1
		Rhizoridae	*Volvulella catharia*	2
			Volvulella cylindrica	2
			Volvulella sp	1
		Acteocinidae	*Acteocina cerealis*	1
			Acteocina culcitella	1
			Acteocina harpa	1
		Philinidae	*Philine auriformis*	28
		Aglajidae	*Aglaja ocelligera*	1
		Philinoglossidae	*Philinoglossa* sp A	3
		Cylichnidae	*Cylichna diegensis*	5
		Diaphanidae	*Diaphana californica*	2
	Bivalvia			6
		Nuculidae	*Ennucula tenuis*	2
		Solemyidae	*Solemya pervernicosa*	4
		Nuculanidae	*Nuculana hamata*	1
			Nuculana taphria	5
		Mytilidae		1
			Crenella decussata	13
			Solamen columbianum	2
			Modiolinae	11
			Amygdalum pallidulum	2

Appendix G.4 *continued*

Phylum	Class	Family	Taxon	n
		Pectinidae	*Leptopecten latiauratus*	90
		Lucinidae	*Lucinisca nuttalli*	1
			Parvilucina tenuisculpta	11
			Lucinoma annulatum	6
		Thyasiridae	*Axinopsida serricata*	3
			Thyasira flexuosa	2
		Lasaeidae	*Kurtiella grippi*	7
			Kurtiella mortoni	1
			Kurtiella tumida	28
		Cardiidae	*Keenaea centifilosum*	11
		Tellinidae	*Tellina carpenteri*	3
			Tellina modesta	37
			Tellina sp B	9
			Macoma yoldiformis	13
			Macoma sp	27
			Psammotreta obesa	2
		--	Solenoidea	3
		Solenidae	*Solen sicarius*	2
		Pharidae	*Ensis myrae*	7
			Siliqua lucida	2
		Veneridae	Venerinae	1
			Compsomyax subdiaphana	7
		Petricolidae	*Cooperella subdiaphana*	62
		Mactridae		1
			Simomactra falcata	15
		Lyonsiidae		6
			Entodesma navicula	2
			Lyonsia californica	2
		Thraciidae	*Thracia trapezoides*	2
	Scaphopoda	Dentaliidae	*Dentalium vallicolens*	3
		Gadilidae	*Polyschides quadrifissatus*	37
			Gadila aberrans	81
Sipuncula				13
	Sipunculidea	Golfingiidae	*Thysanocardia nigra*	10
		Phascolionidae	*Phascolion* sp A	8
		Sipunculidae	*Siphonosoma ingens*	1
	Phascolosomatidea	Phascolosomatidae	*Apionsoma misakianum*	77
Annelida	Polychaeta	Amphinomidae	*Chloeia pinnata*	35
			Paramphinome sp	66
		Amphinomidae	*Pareurythoe californica*	87
		Dorvilleidae	*Dorvillea (Dorvillea)* sp	2
			Parougia caeca	5
			Protodorvillea gracilis	245
		Eunicidae		3
			Leodice americana	4
			Marphysa disjuncta	2
			Marphysa sp	2
		Lumbrineridae		5
			Lumbrinerides platypygos	46
			Lumbrineris cruzensis	16

Appendix G.4 *continued*

Phylum	Class	Family	Taxon	n
			Lumbrineris japonica	3
			Lumbrineris latreilli	64
			Lumbrineris ligulata	19
			Lumbrineris limicola	1
			Lumbrineris sp Group I	5
			Lumbrineris sp Group II	1
			Lumbrineris sp	1
			Scoletoma tetraura Cmplx	26
			Scoletoma sp	1
		Oenonidae		1
			Arabella iricolor Cmplx	4
			Drilonereis falcata	6
			Drilonereis sp A	1
			Drilonereis sp	1
		Onuphidae		21
			Diopatra ornata	8
			Diopatra splendidissima	2
			Diopatra tridentata	4
			Diopatra sp	2
			Hyalinoecia juvenalis	1
			Mooreonuphis nebulosa	11
			Mooreonuphis sp SD1	69
			Mooreonuphis sp SD2	1
			Mooreonuphis sp	18
			Nothria occidentalis	1
			Onuphis affinis	6
			Onuphis eremita parva	4
			Onuphis iridescens	11
			Onuphis sp A	20
			Onuphis sp	3
			Paradiopatra parva	37
			Rhamphobrachium longisetosum	1
		Aphroditidae		1
		Polynoidae		1
			Lepidasthenia longicirrata	2
			Hesperonoe laevis	1
			Malmgreniella baschi	2
			Malmgreniella macginitiei	2
			Malmgreniella nigralba	1
			Malmgreniella scriptoria	2
			Malmgreniella sp A	1
			Tenonia priops	8
		Pholoidae	*Pholoe glabra*	4
		Sigalionidae	*Pholoides asperus*	1
			Pisione sp	102
			Sigalion spinosus	145
			Sthenelais tertiaglabra	5
			Sthenelais verruculosa	4
			Sthenelanella uniformis	80
		Glyceridae	*Glycera macrobranchia*	2

Appendix G.4 *continued*

Phylum	Class	Family	Taxon	n
			Glycera nana	19
			Glycera oxycephala	109
			Glycera sp	1
			Hemipodia borealis	6
		Goniadidae	*Glycinde armigera*	95
			Goniada littorea	10
			Goniada maculata	29
			Goniada sp	1
		Hesionidae	*Heteropodarke heteromorpha*	6
			Microphthalmus hystrix	9
			Micropodarke dubia	12
			Oxydromus pugettensis	16
			Podarkeopsis glabrus	1
		Nereididae		2
			Nereis sp A	57
			Nereis sp SD1	2
			Platynereis bicanaliculata	30
		Syllidae	*Syllides mikeli*	1
			Syllides reishi	2
			Syllides sp SD1	3
			Eusyllis habei	4
			Eusyllis transecta	14
			Eusyllis sp SD2	74
			Odontosyllis phosphorea	25
			Odontosyllis sp SD1	1
			Opisthodonta sp SD2	3
			Exogone dwisula	20
			Exogone lourei	19
			Exogone sp	1
			Parexogone acutipalpa	2
			Parexogone breviseta	3
			Salvatoria brevipharyngea	1
			Salvatoria californiensis	1
			Sphaerosyllis californiensis	20
			Sphaerosyllis ranunculus	2
			Syllis farallonensis	11
			Syllis gracilis Cmplx	6
			Syllis heterochaeta	70
			Syllis sp SD1	51
		Nephtyidae	*Aglaophamus verrilli*	1
			Bipalponephtys cornuta	3
			Nephtys caecoides	27
			Nephtys ferruginea	3
			Nephtys simoni	14
			Nephtys sp SD2	5
			Nephtys sp	1
		Sphaerodoridae	*Sphaerodoropsis biserialis*	1
		Phyllodocidae		1
			Eteone pigmentata	2
			Eteone sp	1

Appendix G.4 *continued*

Phylum	Class	Family	Taxon	n
			Eulalia levicornuta Cmplx	3
			Eulalia sp SD1	8
			Eumida longicornuta	25
			Hesionura coineaui difficilis	89
			Mystides sp	25
			Sige sp A	15
			Nereiphylla sp 2	2
			Nereiphylla sp SD1	1
			Paranaitis polynoides	1
			Phyllodoce groenlandica	12
			Phyllodoce hartmanae	44
			Phyllodoce longipes	48
			Phyllodoce medipapillata	13
			Phyllodoce pettiboneae	28
		Fabriciidae	*Pseudofabriciola californica*	1
		Oweniidae	*Galathowenia pygidialis*	7
			Myriochele gracilis	14
			Myriochele olgae	1
			Myriochele striolata	12
			Owenia collaris	28
		Sabellidae		1
			Acromegalomma pigmentum	2
			Dialychone albocincta	2
			Dialychone trilineata	2
			Dialychone veleronis	26
			Euchone arenae	14
			Euchone hancocki	2
			Euchone incolor	51
			Euchone sp A	1
			Jasmineira sp B	251
			Paradialychone bimaculata	10
			Paradialychone ecaudata	6
			Paradialychone harrisae	34
			Paradialychone paramollis	7
			Potamethus sp A	2
		Apistobranchidae	*Apistobranchus ornatus*	1
		Longosomatidae	*Heterospio catalinensis*	1
		Magelonidae	*Magelona berkeleyi*	2
			Magelona hartmanae	5
		Poecilochaetidae	*Poecilochaetus johnsoni*	17
			Poecilochaetus sp	1
		Spionidae	*Aonides* sp SD1	5
			Dipolydora socialis	21
			Dispio sp SD1	10
			Laonice cirrata	6
			Laonice nuchala	4
			Malacoceros indicus	6
			Microspio pigmentata	14
			Paraprionospio alata	55
			Polydora cornuta	4

Appendix G.4 *continued*

Phylum	Class	Family	Taxon	n
			Polydora nuchalis	1
			Prionospio dubia	23
			Prionospio jubata	52
			Prionospio lighti	4
			Prionospio pygmaeus	76
			Spio maculata	33
			Spiophanes berkeleyorum	12
			Spiophanes duplex	632
			Spiophanes kimballi	2
			Spiophanes norrisi	667
			Spiophanes wigleyi	3
		Acrocirridae	*Macrochaeta* sp A	1
		Cirratulidae	*Aphelochaeta glandaria* Cmplx	10
			Aphelochaeta monilaris	7
			Aphelochaeta petersenae	1
			Aphelochaeta phillipsi	1
			Aphelochaeta tigrina	2
			Aphelochaeta williamsae	8
			Aphelochaeta sp LA1	5
			Aphelochaeta sp SD5	2
			Aphelochaeta sp	2
			Caulleriella hamata	12
			Chaetozone corona	23
			Chaetozone hartmanae	27
			Chaetozone lunula	10
			Chaetozone sp SD2	21
			Chaetozone sp SD5	28
			Chaetozone sp SD7	1
			Chaetozone sp	20
			Kirkegaardia cryptica	2
			Kirkegaardia siblina	115
			Kirkegaardia tesselata	40
			Kirkegaardia sp SD9	3
			Protocirrineris sp B	15
		Flabelligeridae	*Brada pilosa*	1
			Pherusa neopapillata	2
			Trophoniella harrisae	3
		Sternaspidae	*Sternaspis affinis*	4
		Ampharetidae		4
			Amage anops	5
			Amage scutata	6
			Amage sp	1
			Ampharete acutifrons	2
			Ampharete finmarchica	1
			Ampharete labrops	61
			Ampharete sp	1
			Ampharetidae sp SD1	1
			Amphicteis mucronata	3
			Amphicteis scaphobranchiata	12
			Anobothrus gracilis	15

Appendix G.4 *continued*

Phylum	Class	Family	Taxon	n
			Asabellides lineata	7
			Eclysippe trilobata	32
			Lysippe sp A	28
			Lysippe sp B	3
			Sabellides manriquei	80
			Schistocomus hiltoni	3
			Schistocomus sp A	2
			Schistocomus sp	3
			Melinna oculata	45
			Melinna sp	1
		Pectinariidae	*Pectinaria californiensis*	7
		Terebellidae	*Amaeana occidentalis*	15
			Polycirrus californicus	7
			Polycirrus sp I	6
			Polycirrus sp V	2
			Polycirrus sp A	82
			Polycirrus sp OC1	9
			Polycirrus sp SD3	180
			Polycirrus sp	16
			Eupolymnia heterobranchia	4
			Lanassa venusta venusta	84
			Phisidia sanctaemariae	13
			Pista brevibranchiata	1
			Pista elongata	1
			Pista estevanica	27
			Pista pacifica	3
			Pista wui	7
			Pista sp	2
			Proclea sp A	13
			Streblosoma crassibranchia	3
			Streblosoma sp B	9
			Streblosoma sp C	26
			Streblosoma sp SF1	1
		Trichobranchidae	*Terebellides californica*	2
			Trichobranchus hancocki	10
		Chaetopteridae		1
			Phyllochaetopterus prolifica	3
			Spiochaetopterus costarum Cmplx	55
		Capitellidae	*Anotomastus gordiodes*	1
			Capitella teleta	11
			Mediomastus acutus	1
			Mediomastus sp	261
			Notomastus latericeus	26
			Notomastus tenuis	2
			Notomastus sp	2
		Cossuridae	*Cossura* sp	1
		Maldanidae		36
			Euclymeninae	5
			Clymenella complanata	3
			Clymenella sp SD1	1

Appendix G.4 *continued*

Phylum	Class	Family	Taxon	n
			Clymenura gracilis	2
			Euclymeninae sp A	104
			Isocirrus longiceps	2
			Petaloclymene pacifica	43
			Praxillella gracilis	3
			Praxillella pacifica	42
			Maldane sarsi	1
			Metasychis disparidentatus	23
			Praxillura maculata	3
			Rhodine bitorquata	5
		Opheliidae		2
			Armandia brevis	2
			Ophelia pulchella	24
		Orbiniidae		1
			Leitoscoloplos pugettensis	4
			Naineris uncinata	3
			Naineris sp	2
			Scoloplos acmeceps	16
			Scoloplos armiger Cmplx	121
			Scoloplos sp	1
		Paraonidae	*Aricidea (Acmira) catherinae*	12
			Aricidea (Acmira) cerrutii	13
			Aricidea (Acmira) lopezi	6
			Aricidea (Acmira) rubra	1
			Aricidea (Acmira) simplex	16
			Aricidea (Acmira) sp SD1	1
			Aricidea (Acmira) sp SD3	2
			Aricidea (Aedicira) pacifica	4
			Aricidea (Aricidea) wassi	2
			Aricidea (Aricidea) sp	2
			Aricidea (Strelzovia) antennata	3
			Aricidea (Strelzovia) hartleyi	4
			Aricidea (Strelzovia) sp A	1
			Cirrophorus furcatus	3
			Levinsenia gracilis	6
			Levinsenia sp SD1	2
			Paradoneis lyra	3
			Paradoneis sp SD1	42
			Paradoneis sp	5
		Scalibregmatidae	*Scalibregma californicum*	19
		Travisiidae	*Travisia brevis*	1
		Saccocirridae	*Saccocirrus* sp	22
	Clitellata		Oligochaeta	3
Arthropoda	Pycnogonida			1
		Phoxichilidiidae	*Anoplodactylus erectus*	4
	Ostracoda	Cylindroleberididae	*Leuroleberis sharpei*	1
			Xenoleberis californica	1
		Philomedidae	*Euphilomedes carcharodonta*	125
		Sarsiellidae	*Eusarsiella thominx*	1
	Malacostraca	Nebaliidae	*Nebalia daytoni*	3

Appendix G.4 *continued*

Phylum	Class	Family	Taxon	n
			Nebalia pugettensis Cmplx	3
			Nebalia sp	2
		Mysidae	*Acanthomysis californica*	1
			Neomysis kadiakensis	8
		Caprellidae	*Caprella californica* Cmplx	3
			Caprella mendax	13
			Mayerella banksia	7
			Tritella laevis	2
			Hemiproto sp A	1
		Ischyroceridae	*Ericthonius brasiliensis*	30
			Ericthonius sp	1
			Microjassa bousfieldi	1
			Notopoma sp A	27
		Kamakidae	*Amphideutopus oculatus*	12
		Photidae	*Ampelisciphotis podophthalma*	7
			Gammaropsis thompsoni	6
			Photis bifurcata	6
			Photis brevipes	27
			Photis californica	59
			Photis lacia	7
			Photis macinerneyi	15
			Photis sp C	12
			Photis sp OC1	115
			Photis sp	54
		Aoridae	*Aoroides exilis*	2
			Aoroides sp A	1
			Aoroides sp	1
			Bemlos audbettius	2
		Unciolidae	*Rudilemboides stenopropodus*	2
		Corophiidae	*Laticorophium baconi*	31
		Megaluropidae	*Gibberosus myersi*	10
			Megaluropidae sp A	5
		Oedicerotidae	*Americhelidium shoemakeri*	20
			Americhelidium sp SD1	10
			Americhelidium sp SD4	2
			Americhelidium sp	4
			Bathymedon pumilus	1
			Deflexilodes norvegicus	4
			Hartmanodes hartmanae	23
			Westwoodilla tone	4
		Liljeborgiidae	*Listriella goleta*	2
			Listriella melanica	1
			Listriella sp	1
		Melphidippidae	*Melphisana bola* Cmplx	2
		Pardaliscidae	*Halicoides synopiae*	4
		Ampeliscidae	*Ampelisca agassizi*	30
			Ampelisca brachycladus	42
			Ampelisca brevisimulata	84
			Ampelisca cf *brevisimulata*	5
			Ampelisca careyi	55

Appendix G.4 *continued*

Phylum	Class	Family	Taxon	n
			Ampelisca cristata cristata	93
			Ampelisca cristata microdentata	88
			Ampelisca hancocki	1
			Ampelisca indentata	3
			Ampelisca pugetica	38
			Ampelisca sp	21
			Byblis millsi	22
		Synopiidae	*Metatiron tropakis*	6
		Argissidae	*Argissa hamatipes*	5
		Haustoriidae	*Eohaustorius barnardi*	4
		Platyischnopidae	*Tiburonella viscana*	3
		Urothoidae	*Urothoe elegans* Cmplx	20
		Phoxocephalidae		2
			Foxiphalus golfensis	4
			Foxiphalus obtusidens	45
			Foxiphalus sp	1
			Metharpinia jonesi	7
			Rhepoxynius fatigans	2
			Rhepoxynius heterocuspidatus	145
			Rhepoxynius lucubrans	33
			Rhepoxynius menziesi	87
			Rhepoxynius stenodes	34
			Rhepoxynius variatus	4
			Rhepoxynius sp	3
			Metaphoxus frequens	4
			Heterophoxus oculatus	1
		Tryphosidae	*Hippomedon zetesimus*	5
			Lepidepecreum gurjanovae	2
			Lepidepecreum serraculum	6
			Orchomenella pacifica	2
		Pakynidae	*Pachynus barnardi*	6
		Cirolanidae	*Eurydice caudata*	29
		Gnathiidae	*Caecognathia crenulatifrons*	20
		Anthuridae	*Haliophasma geminata*	13
		Arcturidae	*Neastacilla californica*	7
		Idoteidae	*Edotia sublittoralis*	34
			Synidotea magnifica	1
		Serolidae	*Heteroserolis carinata*	7
		--	Tanaidacea	1
		Anarthruridae	*Siphonolabrum californiensis*	3
		Leptocheliidae	*Chondrochelia dubia* Cmplx	238
		Tanaopsidae	*Tanaopsis cadieni*	5
		Bodotriidae	*Cyclaspis nubila*	11
		Nannastacidae	*Campylaspis canaliculata*	3
			Campylaspis maculinodulosa	1
			Campylaspis rubromaculata	1
			Procampylaspis caenosa	2
		Lampropidae		1
			Hemilamprops californicus	48
			Mesolamprops bispinosus	15

Appendix G.4 *continued*

Phylum	Class	Family	Taxon	n
		Diastylidae	*Anchicolurus occidentalis*	2
			Diastylis californica	7
			Diastylis crenellata	1
			Diastylopsis tenuis	2
			Leptostylis abditis	1
			Oxyurostylis pacifica	5
		Crangonidae		1
			Crangon alba	2
		Paguridae	*Parapagurodes laurentae*	1
		Albuneidae	*Lepidopa californica*	1
		Blepharipodidae	*Blepharipoda occidentalis*	1
		Cyclodorippidae	*Deilocerus planus*	2
			Deilocerus sp	2
		Inachoididae	*Pyromaia tuberculata*	2
		Parthenopidae	*Latulambrus occidentalis*	1
		Cancridae	*Metacarcinus gracilis*	2
		Pinnotheridae	*Pinnixa occidentalis* Cmplx	1
			Pinnixa sp	8
Nematoda				231
Echinodermata	Asteroidea			20
		Luidiidae	*Luidia armata*	1
			Luidia foliolata	1
		Astropectinidae	*Astropecten californicus*	27
			Astropecten sp	2
	Ophiuroidea			4
		Ophiuridae	*Ophiura luetkenii*	4
		Ophioscolecidae	*Ophiuroconis bispinosa*	66
		Amphiuridae		37
			Amphichondrius granulatus	1
			Amphiodia digitata	2
			Amphiodia urtica	9
			Amphiodia sp	18
			Amphioplus sp A	2
			Amphipholis squamata	11
	Echinoidea			2
		Toxopneustidae	*Lytechinus pictus*	15
		Dendrasteridae	*Dendraster terminalis*	46
		Loveniidae	*Lovenia cordiformis*	10
	Holothuroidea	Phyllophoridae		4
			Pentamera sp	1
			Phyllophoridae sp A	1
		Synaptidae	*Leptosynapta* sp	40
		Chiridotidae	*Chiridota* sp	8
Phoronida				8
		Phoronidae	*Phoronis* sp SD1	2
			Phoronis sp	18
			Phoronopsis sp	2
Brachiopoda	Lingulata	Lingulidae	*Glottidia albida*	37
Chordata	Enteropneusta			6
		Ptychoderidae	*Balanoglossus* sp	8

Appendix G.4 *continued*

Phylum	Class	Family	Taxon	n
		Harrimaniidae	*Saccoglossus* sp	1
			Stereobalanus sp	1
	Ascidiacea	Agneziidae	*Agnezia septentrionalis*	1
		Styelidae	*Cnemidocarpa rhizopus*	19
		Molgulidae	*Molgula regularis*	1
	Leptocardii	Branchiostomatidae	*Branchiostoma californiense*	16

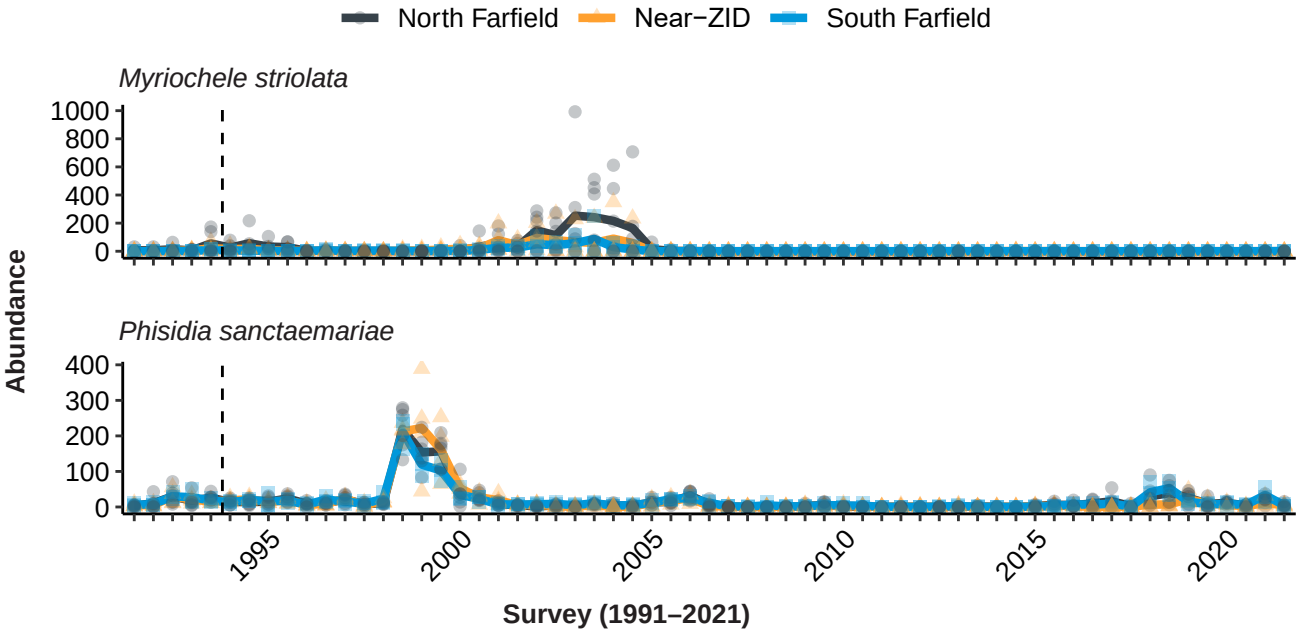

Appendix G.5

Two of the five historically most abundant species recorded from 1991 through 2021 at PLOO north farfield, near-ZID, and south farfield primary core stations. The other historically dominant taxa, *Amphiodia urtica, Spiophanes duplex,* and *Proclea* sp A, are shown in Figures 6.4 and 6.5. For each station group, mean abundance per survey is shown by the solid line ($n \leq 8$) while abundance per station is shown by the symbols. Dashed lines indicate onset of wastewater discharge.

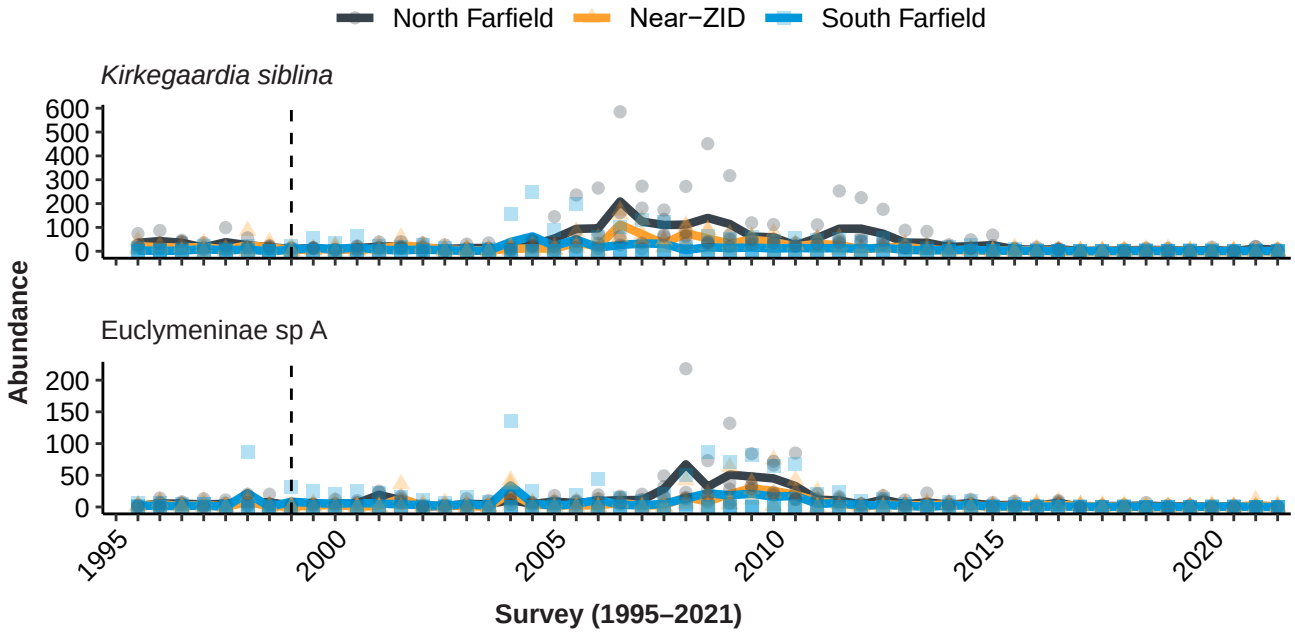

Appendix G.6

Two of the five historically most abundant species recorded from 1995 through 2021 at SBOO north farfield, near-ZID, and south farfield primary core stations. The other historically dominant taxa, *Spiophanes norrisi, Spiophanes duplex,* and *Mediomastus* sp, are shown in Figure 6.6. For each station group, mean abundance per survey is shown by the solid line ($n \leq 8$) while abundance per station is shown by the symbols. Dashed lines indicate onset of wastewater discharge.

This page intentionally left blank

Appendix H

San Diego Regional Benthic Condition Assessment

2020 – 2021 Supplemental Analyses

Appendix H.1

Summary of visual observations for each regional station sampled during 2020-2021. Visual observations are from sieved "grunge" (i.e., particles retained on 1-mm mesh screen and preserved with infauna for benthic community analysis).

	Summer 2020			Summer 2021		
Strata	Station	Depth (m)	Vis Obs	Station	Depth (m)	Vis Obs
Inner Shelf	8929	7	—	9241	10	relict red sand and shell hash
	8944	7	—	9244	10	coarse sand
	8918	8	coarse sand; shell hash	9213	12	—
	8946	15	—	9219	12	—
	8915	16	gravel; shell hash	9233	14	coarse sand and shell hash
	8907	18	—	9231	15	—
	8943	19	—	9239	19	—
	8914	20	—	9201	20	—
	8911	24	—	9214	20	—
	8938	28	organic debris	9243	26	—
	8901	29	—	9242	28	—
				9229	29	relict red sand, cobble and shell hash
Mid Shelf	8913	31	—	9209	34	—
	8906	41	—	9232	34	—
	8939	65	—	9202	38	coarse sand and organic debris
	8903	66	—	9234	42	organic debris and shell hash
	8912	67	organic debris	9236	58	coarse sand and shell hash
	8925	67	—	9238	58	—
	8919	68	gravel; shell hash	9211	60	gravel, shell hash, and organic debris
	8909	73	shell hash	9215	61	—
	8931	74	—	9222	62	—
	8933	80	—	9206	82	shell hash
	8930	83	—	9221	84	—
	8949	83	—	9227	93	shell hash
	8924	85	organic debris	9210	95	coarse sand and shell hash
	8926	87	—	9235	98	coarse black sand
	8932	89	gravel; organic debris	9230	104	coarse sand and shell hash
	8940	108	gravel	9224	120	—
	8921	116	—			
Outer Shelf	8905	134	shell hash	9208	131	relict red sand and gravel
	8937	137	cobble; worm tubes	9216	136	—
	8910	169	organic debris	9207	170	coarse sand and organic debris
	8922	185	organic debris; worm tubes	9220	170	chitinous worm tubes
	8916	189	organic debris; worm tubes	9225	171	organic debris
	8908	194	organic debris; shell hash	9212	203	cobble, shell hash, and gravel
Upper Slope	8928	223	organic debris; shell hash	9205	228	organic debris and shell hash
	8920	270	—	9218	292	cobble and coarse black sand
	8936	292	—	9228	296	organic debris
	8927	460	—	9237	327	coarse sand and organic debris
	8934	491	—	9223	437	—
	8923	523	—	9240	501	sea grass

Appendix H.2

Summary taxonomic listing of benthic infauna taxa identified from regional stations during 2021. Data are total number of individuals (n). Taxonomic arrangement follows SCAMIT (2018).-- indicates taxon is not within previous family.

Phylum	Class	Family	Taxon	n
Cnidaria	Hydrozoa	Corymorphidae	*Corymorpha bigelowi*	3
			Euphysa sp A	4
		Campanulariidae	*Laomedea calceolifera*	1
	Anthozoa	Virgulariidae	*Stylatula* sp A	2
			Stylatula sp	1
			Virgularia californica	1
			Virgularia sp	3
		--	Actiniaria	8
		Edwardsiidae		14
			Edwardsia juliae	7
			Edwardsia olguini	7
			Scolanthus triangulus	40
		Halcampidae	*Halcampa decemtentaculata*	1
			Halianthella sp A	2
			Pentactinia californica	3
		Isanthidae	*Zaolutus actius*	1
		Limnactiniidae	Limnactiniidae sp A	1
Platyhelminthes	Rhabditophora	Plehniidae	*Diplehnia caeca*	1
		Stylochoplanidae	*Phaenoplana longipenis*	1
		--	Rhabdocoela sp A	4
			Rhabditophora sp A	1
Nemertea	Anopla			1
		Cephalotrichidae	*Cephalothrix* sp	10
		--	Palaeonemertea	11
		Carinomidae	*Carinoma mutabilis*	51
		Tubulanidae		6
			Tubulanus cingulatus	5
			Tubulanus polymorphus	71
			Tubulanus sp A	6
			Tubulanus sp	1
			Tubulanidae sp B	5
		--	Heteronemertea	5
		Lineidae		66
			Lineidae sp SD1	11
			Lineus bilineatus	25
			Maculaura alaskensis Cmplx	5
			Zygeupolia rubens	5
		--	Heteronemertea sp SD2	46
	Enopla			2
			Hoplonemertea	10
		Emplectonematidae	*Cryptonemertes actinophila*	3
			Paranemertes californica	6
		Prosorhochmidae	*Prosorhochmus albidus*	2
		Oerstediidae	*Oerstedia dorsalis* Cmplx	2
		Tetrastemmatidae	*Tetrastemma candidum*	4
		--	Hoplonemertea sp D	4
			Enopla sp B	1

Appendix H.2 *continued*

Phylum	Class	Family	Taxon	n
Mollusca	Caudofoveata		Chaetodermatida	2
		Chaetodermatidae	*Chaetoderma marinelli*	3
			Chaetoderma pacificum	5
			Falcidens longus	6
		Limifossoridae	*Limifossor fratula*	5
	Gastropoda	Trochidae	*Halistylus pupoideus*	4
			Lirularia sp	1
		Solariellidae	*Solariella peramabilis*	4
		Caecidae	*Caecum crebricinctum*	1
		Eulimidae	*Balcis micans*	1
			Balcis oldroydae	1
			Eulima raymondi	1
			Polygireulima rutila	1
		Nassariidae	*Caesia perpinguis*	1
		Olivellidae	*Callianax baetica*	1
		Borsoniidae	*Ophiodermella inermis*	4
		Mangeliidae		2
			Kurtzia arteaga	1
			Kurtziella plumbea	1
			Kurtzina beta	8
		Terebridae	*Terebra hemphilli*	1
		Acteonidae	*Rictaxis punctocaelatus*	2
		Pyramidellidae	*Odostomia* sp	3
			Turbonilla chocolata	1
			Turbonilla santarosana	5
			Turbonilla sp SD9	1
		--	Nudibranchia	1
		Arminidae	*Armina californica*	1
		Rhizoridae	*Volvulella californica*	2
			Volvulella cylindrica	3
			Volvulella panamica	3
		Acteocinidae	*Acteocina cerealis*	2
		Philinidae	*Philine auriformis*	18
		Gastropteridae	*Gastropteron pacificum*	6
		Cylichnidae	*Cylichna diegensis*	9
	Bivalvia			4
		Nuculidae	*Acila castrensis*	4
			Ennucula tenuis	11
		Nucinellidae	*Huxleyia munita*	3
		Nuculanidae	*Nuculana taphria*	10
			Nuculana sp A	22
		Yoldiidae	*Yoldia seminuda*	1
			Yoldiella nana	18
		Mytilidae	*Crenella decussata*	2
			Solamen columbianum	1
			Dacrydium pacificum	2
			Modiolinae	6
			Amygdalum pallidulum	4
		Pectinidae		2

Appendix H.2 *continued*

Phylum	Class	Family	Taxon	n
			Leptopecten latiauratus	227
		Carditidae	*Cyclocardia ventricosa*	3
		Lucinidae	*Parvilucina tenuisculpta*	27
			Lucinoma annulatum	5
		Thyasiridae	*Adontorhina cyclia*	6
			Axinopsida serricata	288
			Thyasira flexuosa	5
		Lasaeidae		1
			Kurtiella tumida	9
			Kurtiella sp D	1
		Cardiidae	*Keenaea centifilosum*	5
			Trachycardium quadragenarium	1
		Tellinidae	*Tellina carpenteri*	34
			Tellina modesta	4
			Tellina nuculoides	1
			Tellina sp B	81
			Tellina sp	2
			Macoma carlottensis	1
			Macoma yoldiformis	10
			Macoma sp	4
			Psammotreta obesa	1
		Pharidae	*Siliqua lucida*	5
		Hiatellidae	*Saxicavella pacifica*	2
		Veneridae	Venerinae	3
			Compsomyax subdiaphana	10
		Petricolidae	*Cooperella subdiaphana*	16
		Mactridae		6
		Myidae	*Sphenia* sp	3
		Spheniopsidae	*Grippina californica*	1
		Pandoridae	*Pandora bilirata*	1
		Lyonsiidae		6
		Thraciidae		2
		Periplomatidae	*Periploma discus*	5
			Periploma planiusculum	1
		Cuspidariidae	*Cuspidaria parapodema*	12
	Scaphopoda			2
		Rhabdidae	*Rhabdus rectius*	2
		Gadilidae	*Polyschides quadrifissatus*	10
			Cadulus californicus	3
			Gadila aberrans	51
		uncertain	*Compressidens stearnsii*	2
Sipuncula				6
	Sipunculidea	Golfingiidae	*Golfingia margaritacea*	1
			Nephasoma diaphanes	1
			Thysanocardia nigra	2
		Phascolionidae	*Phascolion* sp A	34
		Sipunculidae		1
	Phascolosomatidea	Phascolosomatidae	*Apionsoma misakianum*	186
Annelida	Polychaeta	Bonelliidae	*Nellobia eusoma*	1

Appendix H.2 *continued*

Phylum	Class	Family	Taxon	n
		Thalassematidae	*Listriolobus hexamyotus*	2
		Amphinomidae	*Chloeia pinnata*	81
			Paramphinome sp	7
			Pareurythoe californica	9
		Dorvilleidae		1
			Parougia caeca	2
			Pettiboneia sanmatiensis	1
			Protodorvillea gracilis	18
		Eunicidae		3
			Leodice americana	4
			Marphysa disjuncta	24
			Marphysa sp	1
		Lumbrineridae	*Eranno bicirrata*	1
			Eranno lagunae	8
			Lumbrinerides platypygos	41
			Lumbrineris cruzensis	25
			Lumbrineris japonica	11
			Lumbrineris latreilli	69
			Lumbrineris ligulata	10
			Lumbrineris limicola	12
			Lumbrineris sp Group I	15
			Scoletoma tetraura Cmplx	33
			Scoletoma sp	1
		Oenonidae	*Drilonereis falcata*	13
			Drilonereis sp	13
			Notocirrus californiensis	1
		Onuphidae		16
			Diopatra ornata	5
			Diopatra splendidissima	1
			Hyalinoecia juvenalis	1
			Mooreonuphis nebulosa	15
			Mooreonuphis segmentispadix	5
			Mooreonuphis sp SD1	1
			Mooreonuphis sp SD2	1
			Mooreonuphis sp	6
			Nothria occidentalis	8
			Nothria sp	1
			Onuphis iridescens	23
			Onuphis sp A	15
			Paradiopatra parva	347
		Acoetidae	*Acoetes pacifica*	1
		Aphroditidae		3
			Aphrodita sp	4
		Polynoidae	*Lepidasthenia berkeleyae*	1
			Eucranta anoculata	1
			Hesperonoe laevis	1
			Malmgreniella baschi	1
			Malmgreniella macginitiei	6
			Malmgreniella sanpedroensis	4

Appendix H.2 *continued*

Phylum	Class	Family	Taxon	n
			Malmgreniella scriptoria	8
			Malmgreniella sp A	7
			Malmgreniella sp	1
			Subadyte mexicana	1
			Tenonia priops	3
		Pholoidae	*Pholoe glabra*	27
		Sigalionidae	*Pholoides asperus*	9
			Pisione sp	42
			Sigalion sp*inosus*	56
			Sthenelais tertiaglabra	13
			Sthenelais verruculosa	4
			Sthenelanella uniformis	61
		Glyceridae	*Glycera americana*	7
			Glycera macrobranchia	1
			Glycera nana	47
			Glycera oxycephala	22
			Hemipodia borealis	1
		Goniadidae	*Glycinde armigera*	72
			Goniada brunnea	8
			Goniada littorea	13
			Goniada maculata	44
			Goniada sp	2
		Chrysopetalidae	*Chrysopetalum occidentale*	1
		Hesionidae	*Heteropodarke heteromorpha*	1
			Microphthalmus hystrix	2
			Micropodarke dubia	1
			Oxydromus pugettensis	3
			Podarkeopsis glabrus	4
		Nereididae		1
			Nereis sp A	39
			Platynereis bicanaliculata	10
		Pilargidae	*Ancistrosyllis groenlandica*	2
			Hermundura fauveli	1
			Hermundura ocularis	2
			Sigambra setosa	3
		Syllidae		1
			Syllides japonicus	2
			Epigamia-Myrianida Cmplx	1
			Eusyllis habei	4
			Eusyllis longicirrata	1
			Eusyllis transecta	3
			Eusyllis sp SD2	1
			Odontosyllis phosphorea	10
			Odontosyllis sp SD1	1
			Opisthodonta sp	1
			Exogone dwisula	2
			Exogone lourei	10
			Parexogone breviseta	2
			Parexogone molesta	2

Appendix H.2 *continued*

Phylum	Class	Family	Taxon	n
			Salvatoria brevipharyngea	1
			Sphaerosyllis californiensis	4
			Plakosyllis americana	3
			Syllis farallonensis	1
			Syllis gracilis Cmplx	4
			Syllis heterochaeta	76
			Syllis sp SD1	5
			Syllis sp SD2	1
		Nephtyidae	*Aglaophamus erectans*	2
			Aglaophamus verrilli	3
			Bipalponephtys cornuta	17
			Nephtys caecoides	18
			Nephtys ferruginea	11
			Nephtys simoni	3
			Nephtys sp SD2	1
			Nephtys sp	1
		Phyllodocidae	*Eulalia californiensis*	3
			Eulalia sp SD1	3
			Eulalia sp SD4	1
			Eumida longicornuta	7
			Hesionura coineaui difficilis	264
			Protomystides sp SD2	1
			Sige sp A	10
			Nereiphylla ferruginea Cmplx	1
			Nereiphylla sp SD1	2
			Paranaitis polynoides	1
			Phyllodoce groenlandica	7
			Phyllodoce hartmanae	26
			Phyllodoce longipes	22
			Phyllodoce pettiboneae	25
		Fabriciidae	*Pseudofabriciola californica*	1
		Oweniidae	*Galathowenia pygidialis*	3
			Myriochele gracilis	10
			Myriochele striolata	10
			Myriowenia californiensis	5
			Owenia collaris	2
		Sabellariidae	*Neosabellaria cementarium*	1
			Sabellaria gracilis	1
		Sabellidae	*Acromegalomma pigmentum*	14
			Acromegalomma splendidum	4
			Acromegalomma sp	1
			Dialychone albocincta	7
			Dialychone trilineata	17
			Dialychone veleronis	7
			Euchone arenae	4
			Euchone hancocki	10
			Euchone incolor	20
			Euchone sp A	11
			Euchone sp	1

Appendix H.2 *continued*

Phylum	Class	Family	Taxon	n
			Jasmineira sp B	17
			Myxicola sp	1
			Paradialychone bimaculata	2
			Paradialychone ecaudata	2
			Paradialychone harrisae	16
			Paradialychone paramollis	3
			Potamethus sp A	5
		Longosomatidae	*Heterospio catalinensis*	4
		Magelonidae	*Magelona berkeleyi*	5
			Magelona hartmanae	1
			Magelona sp A	1
			Magelona sp B	2
		Poecilochaetidae	*Poecilochaetus johnsoni*	3
			Poecilochaetus martini	1
		Spionidae	*Dipolydora socialis*	13
			Dispio sp SD1	1
			Laonice cirrata	14
			Laonice nuchala	41
			Microspio pigmentata	14
			Paraprionospio alata	77
			Prionospio dubia	157
			Prionospio ehlersi	18
			Prionospio jubata	130
			Prionospio lighti	20
			Prionospio pygmaeus	35
			Spio filicornis	1
			Spio maculata	2
			Spiophanes berkeleyorum	14
			Spiophanes duplex	670
			Spiophanes fimbriata	3
			Spiophanes kimballi	201
			Spiophanes norrisi	92
			Spiophanes wigleyi	1
			Spiophanes sp	1
		Acrocirridae	*Macrochaeta* sp A	1
		Cirratulidae		1
			Aphelochaeta glandaria Cmplx	35
			Aphelochaeta monilaris	53
			Aphelochaeta phillipsi	4
			Aphelochaeta tigrina	2
			Aphelochaeta williamsae	1
			Aphelochaeta sp HYP2	2
			Aphelochaeta sp LA1	17
			Aphelochaeta sp SD5	1
			Aphelochaeta sp	6
			Caulleriella hamata	3
			Chaetozone armata	3
			Chaetozone commonalis	1
			Chaetozone corona	1

Appendix H.2 *continued*

Phylum	Class	Family	Taxon	n
			Chaetozone hartmanae	42
			Chaetozone hedgpethi	3
			Chaetozone setosa Cmplx	3
			Chaetozone sp SD2	11
			Chaetozone sp SD5	8
			Chaetozone sp SD7	2
			Chaetozone sp	6
			Kirkegaardia cryptica	29
			Kirkegaardia siblina	99
			Kirkegaardia tesselata	18
			Kirkegaardia sp SD9	12
			Protocirrineris sp B	1
		Fauveliopsidae	*Fauveliopsis* sp SD1	10
		Flabelligeridae	*Brada pilosa*	15
			Lamispina schmidtii	1
			Pherusa neopapillata	5
			Pherusa sp SD2	1
			Trophoniella harrisae	1
			Trophoniella sp	1
		Sternaspidae	*Sternaspis affinis*	39
		Ampharetidae		8
			Amage anops	2
			Amage scutata	17
			Ampharete acutifrons	10
			Ampharete finmarchica	9
			Ampharete labrops	18
			Ampharetidae sp SD1	12
			Amphicteis scaphobranchiata	14
			Amphisamytha bioculata	1
			Anobothrus gracilis	8
			Asabellides lineata	7
			Eclysippe trilobata	100
			Lysippe sp A	28
			Lysippe sp B	11
			Sabellides manriquei	99
			Samytha californiensis	1
			Schistocomus sp A	3
			Sosane occidentalis	15
			Melinna heterodonta	6
			Melinna oculata	40
		Pectinariidae	*Pectinaria californiensis*	37
		Terebellidae	*Amaeana occidentalis*	6
			Polycirrus californicus	7
			Polycirrus sp A	31
			Polycirrus sp OC1	14
			Polycirrus sp SD3	1
			Polycirrus sp	13
			Lanassa venusta venusta	15
			Leaena caeca	2

Appendix H.2 *continued*

Phylum	Class	Family	Taxon	n
			Phisidia sanctaemariae	47
			Pista brevibranchiata	4
			Pista estevanica	44
			Pista moorei	1
			Pista wui	1
			Pista sp	1
			Proclea sp A	4
			Streblosoma crassibranchia	25
			Streblosoma sp B	3
			Streblosoma sp C	1
		Trichobranchidae		1
			Terebellides sp C	2
			Terebellides californica	7
			Terebellides reishi	1
			Trichobranchus hancocki	1
		Chaetopteridae	*Phyllochaetopterus limicolus*	311
			Phyllochaetopterus prolifica	2
			Spiochaetopterus costarum Cmplx	129
		Capitellidae	*Anotomastus gordiodes*	1
			Capitella teleta	21
			Decamastus gracilis	9
			Dodecamastus mariaensis	2
			Mediomastus sp	354
			Notomastus hemipodus	12
			Notomastus latericeus	3
			Notomastus magnus	1
			Notomastus sp	2
		Cossuridae	*Cossura bansei*	3
			Cossura candida	26
			Cossura sp A	1
		Maldanidae		85
			Clymenella complanata	4
			Clymenella sp SD1	1
			Clymenella sp	1
			Clymenura gracilis	28
			Euclymeninae sp A	198
			Petaloclymene pacifica	136
			Praxillella gracilis	3
			Praxillella pacifica	98
			Notoproctus pacificus	1
			Maldaninae	6
			Maldane sarsi	64
			Metasychis disparidentatus	55
			Praxillura maculata	5
			Rhodine bitorquata	22
		Opheliidae	*Armandia brevis*	2
			Ophelina acuminata	4
		Orbiniidae	*Leitoscoloplos pugettensis*	8
			Leitoscoloplos sp A	2

Appendix H.2 *continued*

Phylum	Class	Family	Taxon	n
			Naineris uncinata	3
			Phylo felix	1
			Scoloplos acmeceps	5
			Scoloplos armiger Cmplx	41
		Paraonidae	*Aricidea (Acmira) catherinae*	24
			Aricidea (Acmira) cerrutii	1
			Aricidea (Acmira) lopezi	2
			Aricidea (Acmira) rubra	5
			Aricidea (Acmira) simplex	15
			Aricidea (Acmira) sp	1
			Aricidea (Aedicira) pacifica	1
			Aricidea (Aricidea) pseudoarticulata	1
			Aricidea (Aricidea) wassi	3
			Aricidea (Strelzovia) antennata	8
			Aricidea (Strelzovia) hartleyi	6
			Aricidea (Strelzovia) sp A	5
			Cirrophorus branchiatus	4
			Levinsenia gracilis	19
			Levinsenia kirbyae	6
			Paradoneis spinifera	5
			Paradoneis sp SD1	292
			Paradoneis sp	5
		Scalibregmatidae	*Scalibregma californicum*	37
		Travisiidae	*Travisia brevis*	30
			Travisia pupa	1
		Saccocirridae	*Saccocirrus* sp	2
	Clitellata	--	Oligochaeta	2
Arthropoda	Pycnogonida	Phoxichilidiidae	*Anoplodactylus erectus*	14
	Ostracoda			1
		Cylindroleberididae	*Xenoleberis californica*	8
		Philomedidae	*Euphilomedes carcharodonta*	10
			Euphilomedes producta	16
			Euphilomedes sp	1
		Sarsiellidae	*Eusarsiella thominx*	1
		Rutidermatidae	*Rutiderma lomae*	2
	Malacostraca	Nebaliidae	*Nebalia daytoni*	4
			Nebalia pugettensis Cmplx	2
		Mysidae	*Neomysis kadiakensis*	2
			Metamysidopsis elongata	1
			Mysidopsis intii	1
		Caprellidae		2
			Caprella mendax	1
			Mayerella banksia	12
			Tritella laevis	1
		Ischyroceridae	*Ericthonius brasiliensis*	3
			Notopoma sp A	12
		Kamakidae	*Amphideutopus oculatus*	17
		Photidae	*Ampelisciphotis podophthalma*	14
			Photis bifurcata	1

Appendix H.2 *continued*

Phylum	Class	Family	Taxon	n
			Photis brevipes	6
			Photis californica	100
			Photis lacia	9
			Photis macinerneyi	3
			Photis macrotica	1
			Photis sp C	8
			Photis sp OC1	2
			Photis sp	10
		Aoridae	*Aoroides inermis*	2
			Aoroides sp A	4
			Aoroides sp	3
		Corophiidae	*Laticorophium baconi*	2
			Protomedeia articulata Cmplx	2
		Hornelliidae	*Hornellia occidentalis*	1
		Megaluropidae	*Gibberosus myersi*	5
		Oedicerotidae	*Americhelidium shoemakeri*	12
			Americhelidium sp SD1	2
			Americhelidium sp SD4	3
			Americhelidium sp	1
			Bathymedon pumilus	15
			Deflexilodes norvegicus	4
			Hartmanodes hartmanae	7
			Monoculodes emarginatus	6
			Monoculodes sp	1
			Westwoodilla tone	10
		Eusiridae	*Rhachotropis* sp A	2
		Liljeborgiidae	*Listriella albina*	1
			Listriella goleta	12
			Listriella sp	1
		Pleustidae		1
		Stenothoidae	*Stenothoides bicoma*	1
		Pardaliscidae	*Halicoides synopiae*	5
			Nicippe tumida	4
		Ampeliscidae	*Ampelisca agassizi*	31
			Ampelisca brachycladus	1
			Ampelisca brevisimulata	48
			Ampelisca cf *brevisimulata*	3
			Ampelisca careyi	41
			Ampelisca cristata cristata	3
			Ampelisca cristata microdentata	14
			Ampelisca hancocki	8
			Ampelisca indentata	22
			Ampelisca pacifica	23
			Ampelisca pugetica	49
			Ampelisca romigi	4
			Ampelisca unsocalae	2
			Ampelisca sp	7
			Byblis millsi	13
		Synopiidae	*Bruzelia tuberculata*	1

Appendix H.2 *continued*

Phylum	Class	Family	Taxon	n
			Tiron biocellata	3
		Platyischnopidae	*Tiburonella viscana*	4
		Urothoidae	*Urothoe elegans* Cmplx	8
		Phoxocephalidae		2
			Foxiphalus obtusidens	14
			Rhepoxynius abronius	2
			Rhepoxynius bicuspidatus	36
			Rhepoxynius fatigans	1
			Rhepoxynius heterocuspidatus	5
			Rhepoxynius lucubrans	5
			Rhepoxynius menziesi	27
			Rhepoxynius stenodes	2
			Rhepoxynius variatus	2
			Rhepoxynius sp	1
			Eyakia robusta	10
			Heterophoxus ellisi	6
			Heterophoxus oculatus	4
			Heterophoxus sp	1
		Lysianassidae	*Aruga holmesi*	1
			Aruga oculata	1
		Uristidae	*Anonyx lilljeborgi*	1
		Tryphosidae	*Hippomedon columbianus*	1
			Hippomedon zetesimus	1
			Hippomedon sp A	2
			Lepidepecreum serraculum	2
		Acidostomatidae	*Acidostoma hancocki*	3
		Pakynidae	*Prachynella lodo*	1
		Gnathiidae	*Caecognathia crenulatifrons*	31
		Anthuridae	*Haliophasma geminata*	17
		Arcturidae	*Neastacilla californica*	1
		Idoteidae	*Edotia* sp B	4
		Sphaeromatidae		1
		Serolidae	*Heteroserolis carinata*	1
		Janiridae	*Caecianiropsis* sp	4
		Munnopsidae	*Ilyarachna acarina*	1
		--	Tanaidacea	8
		Akanthophoreidae	*Chauliopleona dentata*	2
		Anarthruridae	*Siphonolabrum californiensis*	2
		Leptocheliidae	*Chondrochelia dubia* Cmplx	67
		Tanaellidae	*Araphura breviaria*	25
			Araphura cuspirostris	12
			Araphura sp SD1	1
			Tanaella propinquus	6
		Typhlotanaidae	*Typhlotanais williamsae*	1
		Tanaopsidae	*Tanaopsis cadieni*	5
		Bodotriidae	*Cyclaspis nubila*	1
		Leuconidae		1
		Nannastacidae	*Campylaspis canaliculata*	2
			Campylaspis rubromaculata	1

Appendix H.2 *continued*

Phylum	Class	Family	Taxon	n
			Procampylaspis caenosa	9
		Lampropidae	*Alamprops quadriplicatus*	2
			Hemilamprops californicus	18
			Mesolamprops bispinosus	2
		Diastylidae	*Anchicolurus occidentalis*	3
			Diastylis californica	4
			Diastylis crenellata	6
			Diastylis pellucida	4
			Diastylopsis tenuis	5
		Sicyoniidae	*Sicyonia penicillata*	1
		--	Caridea	1
		Crangonidae	*Neocrangon zacae*	1
		Callianassidae	*Neotrypaea gigas*	1
		Paguridae	*Pagurus* sp	1
		Blepharipodidae	*Blepharipoda occidentalis*	1
		Cyclodorippidae	*Deilocerus* sp	1
		Pinnotheridae	*Pinnixa longipes*	1
			Pinnixa occidentalis Cmplx	2
Nematoda				70
Echinodermata	Asteroidea			36
		Luidiidae	*Luidia foliolata*	1
		Astropectinidae	*Astropecten californicus*	5
	Ophiuroidea			12
		Ophioscolecidae	*Ophiuroconis bispinosa*	7
		Amphiuridae		88
			Amphichondrius granulatus	6
			Amphiodia digitata	19
			Amphiodia urtica	237
			Amphiodia sp	113
			Amphioplus strongyloplax	3
			Amphioplus sp A	1
			Amphioplus sp	1
			Amphipholis squamata	16
			Amphiura arcystata	1
			Amphiura diomedeae	2
			Dougaloplus amphacanthus	7
			Dougaloplus sp A	8
	Echinoidea	Toxopneustidae	*Lytechinus pictus*	7
		Dendrasteridae	*Dendraster terminalis*	3
		--	Spatangoida	1
		Schizasteridae	*Brisaster* sp	1
		Brissidae	*Brissopsis pacifica*	4
		Spatangidae	*Spatangus californicus*	4
		Loveniidae	*Lovenia cordiformis*	1
	Holothuroidea	Phyllophoridae	*Phyllophoridae*	1
			Pentamera sp	1
		Synaptidae	*Leptosynapta* sp	14
		Chiridotidae	*Chiridota* sp	8
		Molpadiidae	*Molpadia arenicola*	3

Appendix H.2 *continued*

Phylum	Class	Family	Taxon	n
		Caudinidae	*Paracaudina chilensis*	1
Phoronida				6
		Phoronidae	*Phoronis* sp SD1	6
			Phoronis sp	37
Brachiopoda	Lingulata	Lingulidae	*Glottidia albida*	35
Bryozoa	Gymnolaemata	Clavoporidae	*Ascorhiza occidentalis*	4
Chordata	Enteropneusta			1
		Ptychoderidae	*Balanoglossus* sp	6
		Spengeliidae	*Schizocardium* sp	2
		Harrimaniidae	*Saccoglossus* sp	3
			Stereobalanus sp	23
	Ascidiacea	Molgulidae	*Eugyra glutinans*	1
			Eugyra sp	1

Appendix H.3

Results of Spearman Rank correlation analyses of various sediment parameters from San Diego regional and core benthic stations sampled during summer 2020 and 2021. Data include the correlation coefficient (r_s) for all parameters with detection rates ≥50% (see Table 7.1). Correlation coefficients $r_s \geq 0.70$ are highlighted; ns=not significant ($p > 0.05$).

	Depth	Fines	Sul	TN	TOC	TVS	Al	Sb	As	Ba	Be	Cr	Cu	Fe	Pb	Mn	Hg	Ni	Sn	Zn	tDDT
Fines	0.64																				
Sul	ns	ns																			
TN	0.65	0.78	ns																		
TOC	0.62	0.54	ns	0.88																	
TVS	0.79	0.74	ns	0.92	0.79																
Al	0.68	0.73	ns	0.82	0.61	0.92															
Sb	0.55	0.51	ns	0.48	0.56	0.68	0.73														
As	0.41	0.28	ns	0.46	0.54	0.38	0.30	0.44													
Ba	0.50	0.63	ns	0.69	0.52	0.82	0.93	0.63	0.18												
Be	0.74	0.65	ns	0.85	0.78	0.92	0.91	0.89	0.48	0.77											
Cr	0.78	0.74	ns	0.88	0.71	0.94	0.93	0.74	0.44	0.84	0.93										
Cu	0.77	0.81	ns	0.85	0.65	0.92	0.91	0.62	0.55	0.77	0.82	0.92									
Fe	0.78	0.73	ns	0.88	0.74	0.95	0.92	0.74	0.49	0.83	0.93	0.98	0.93								
Pb	0.75	0.73	ns	0.83	0.63	0.88	0.86	0.61	0.51	0.75	0.80	0.89	0.94	0.91							
Mn	0.53	0.68	0.19	0.71	0.53	0.84	0.94	0.66	0.22	0.95	0.82	0.84	0.81	0.85	0.79						
Hg	0.67	0.77	ns	0.80	0.61	0.85	0.84	0.47	0.40	0.70	0.70	0.82	0.92	0.82	0.93	0.78					
Ni	0.78	0.76	ns	0.87	0.64	0.94	0.95	0.65	0.34	0.84	0.87	0.93	0.91	0.91	0.88	0.86	0.88				
Sn	0.66	0.68	ns	0.74	0.54	0.87	0.92	0.67	0.32	0.82	0.82	0.84	0.87	0.85	0.87	0.89	0.87	0.91			
Zn	0.73	0.73	ns	0.82	0.67	0.93	0.94	0.72	0.34	0.87	0.88	0.94	0.93	0.94	0.88	0.88	0.82	0.92	0.89		
tDDT	0.44	0.72	ns	0.81	0.67	0.80	0.78	0.38	0.35	0.71	0.70	0.80	0.81	0.77	0.79	0.69	0.78	0.82	0.69	0.74	
tPAH	0.36	0.41	ns	0.43	0.30	0.44	0.57	0.37	0.27	0.51	0.46	0.43	0.62	0.45	0.61	0.54	0.69	0.52	0.63	0.46	0.56

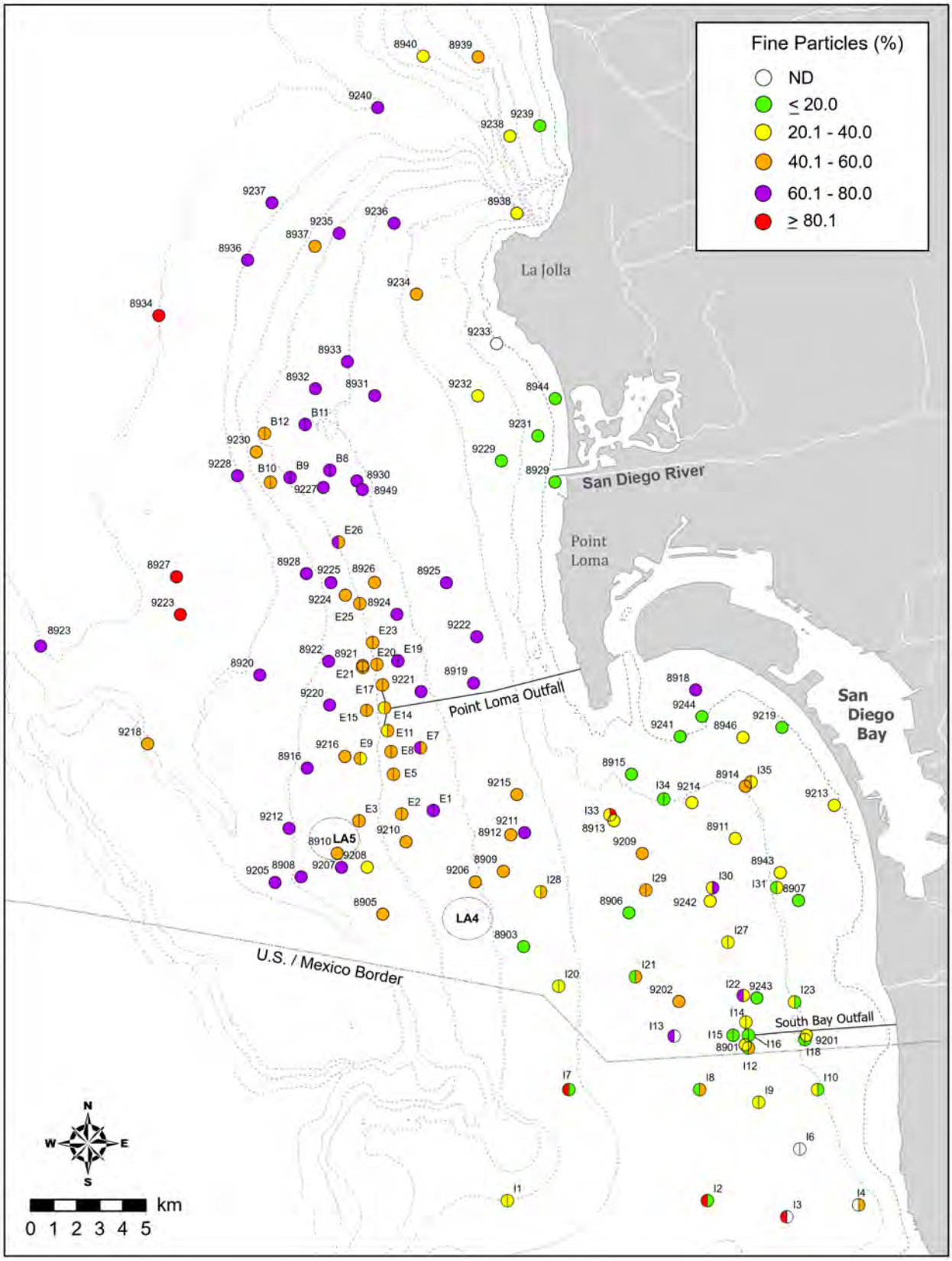

Appendix H.4

Distribution of fine particles in sediments from San Diego regional and core benthic stations sampled during summer 2020 and 2021; ND = not detected.

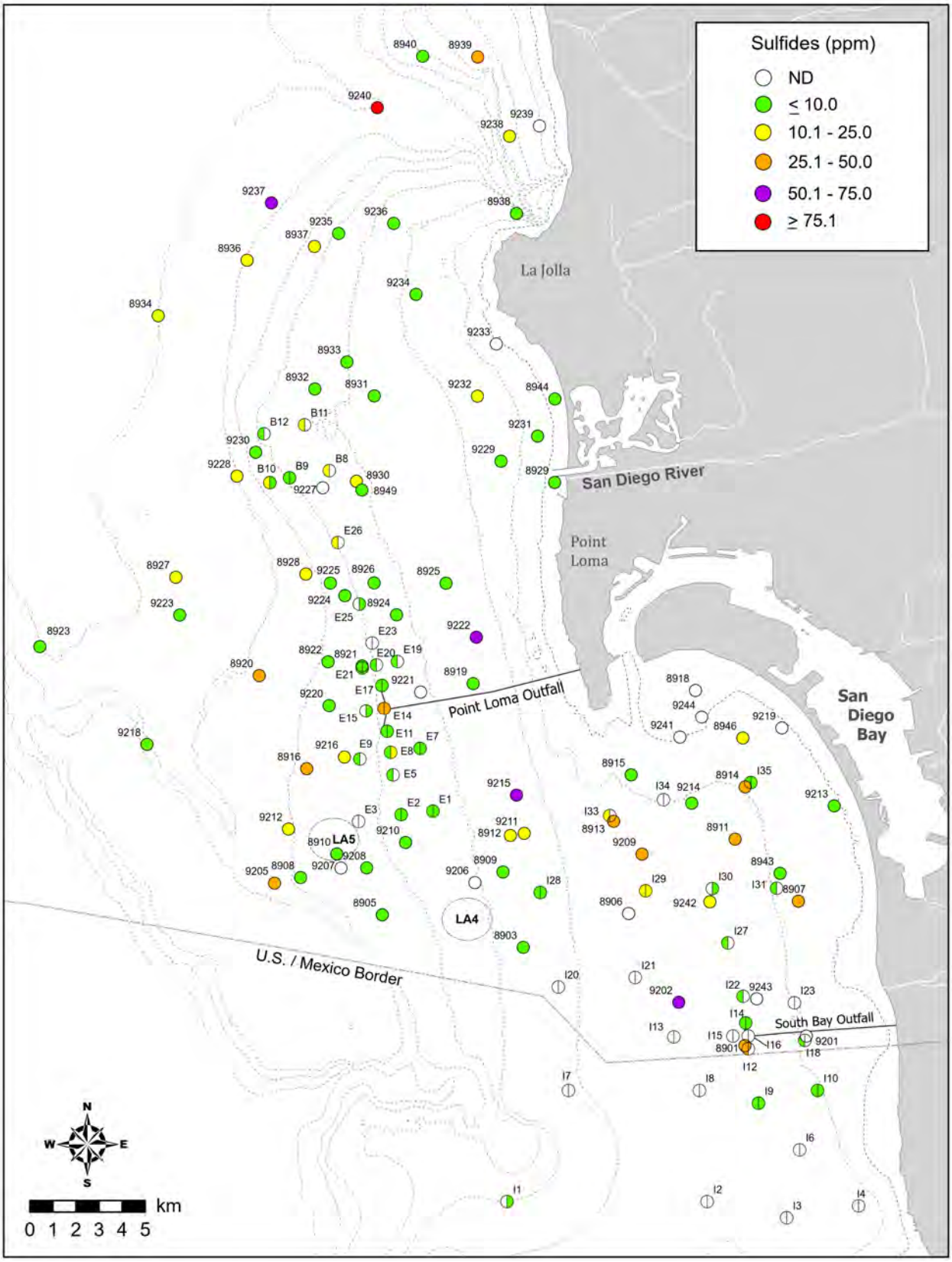

Appendix H.5

Distribution of select parameters in sediments from San Diego regional and core benthic stations sampled during summer 2020 and 2021; ND = not detected.

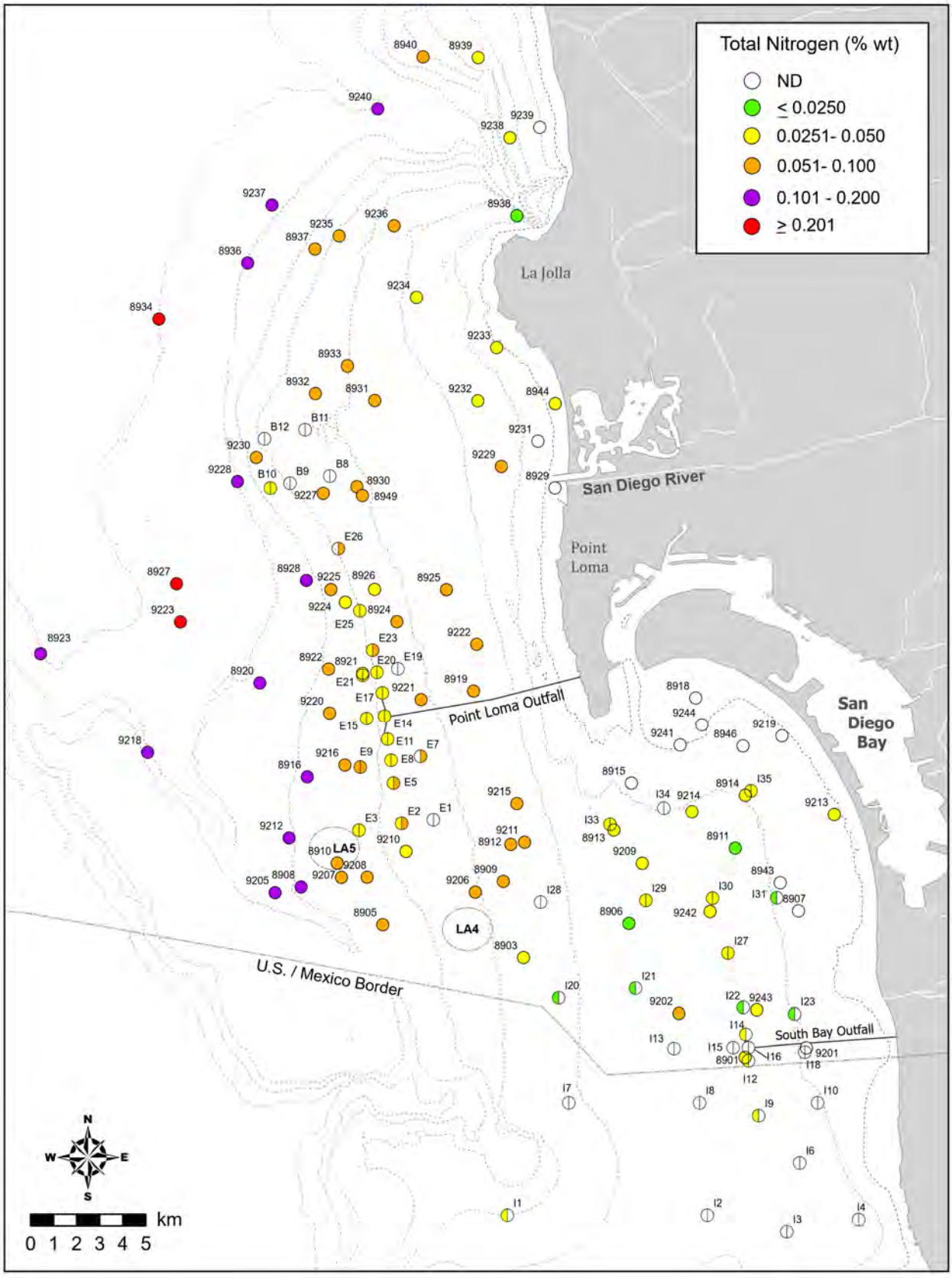

Appendix H.5 *continued*

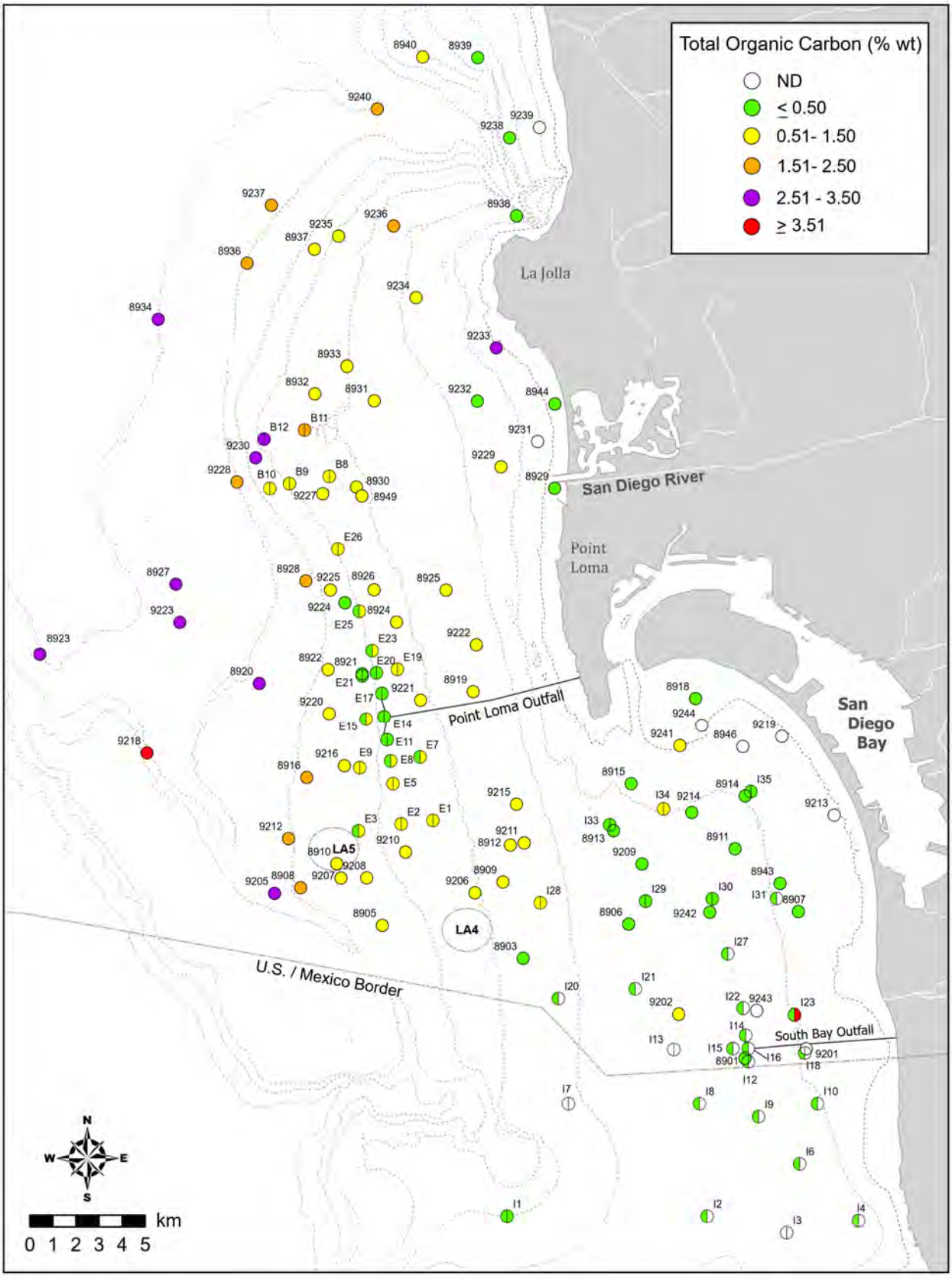

Appendix H.5 *continued*

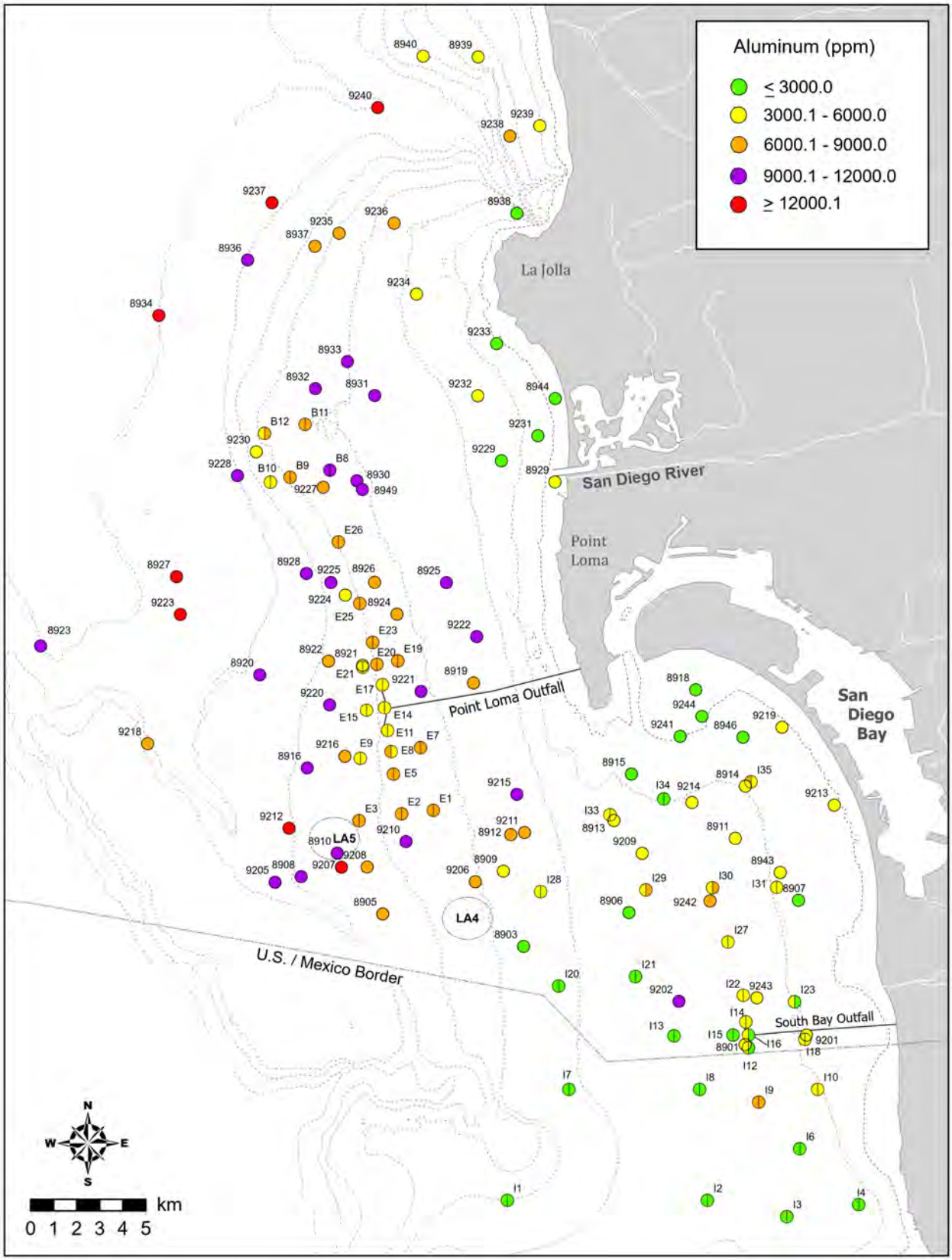

Appendix H.5 *continued*

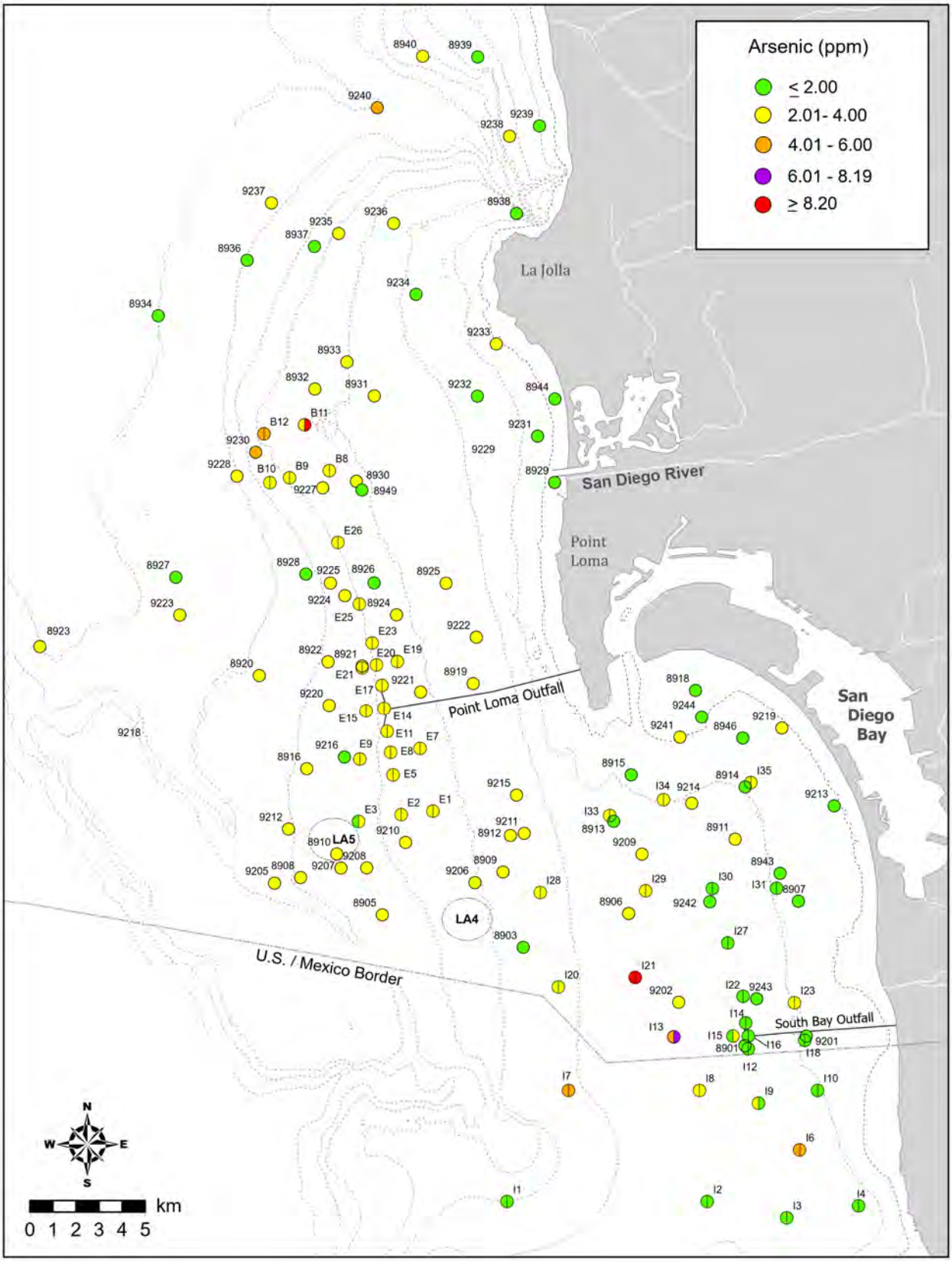

Appendix H.5 *continued*

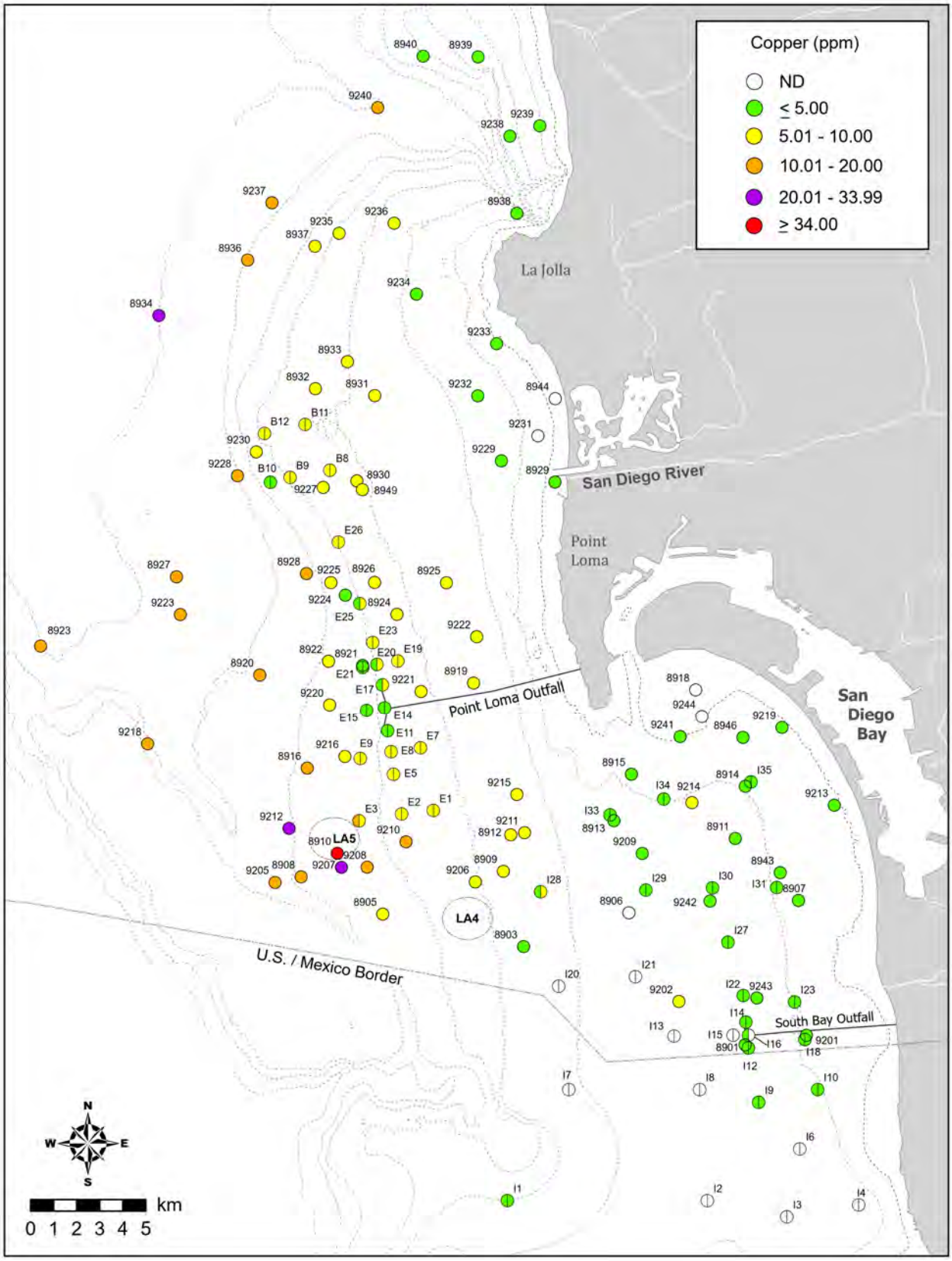

Appendix H.5 *continued*

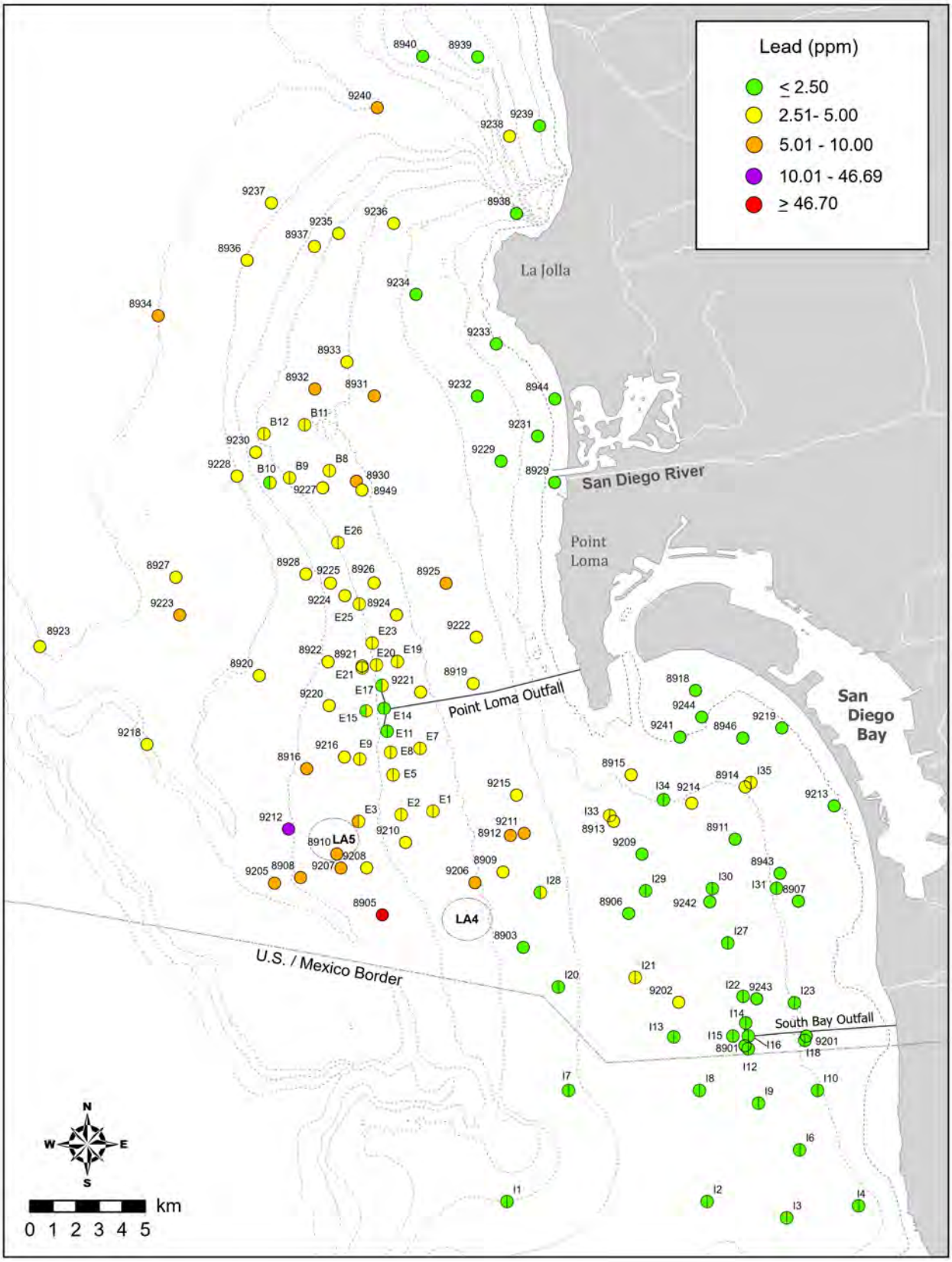

Appendix H.5 *continued*

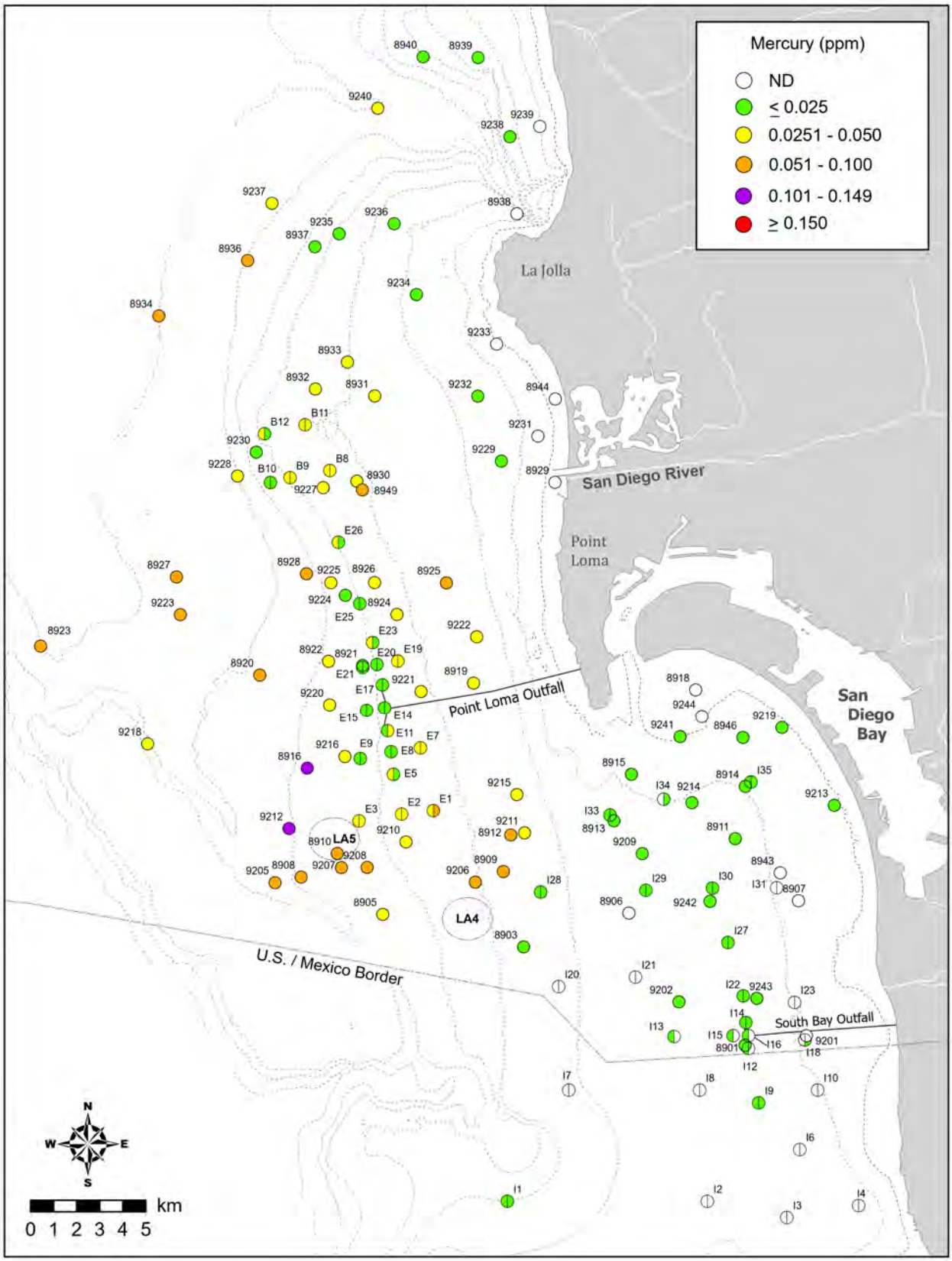

Appendix H.5 *continued*

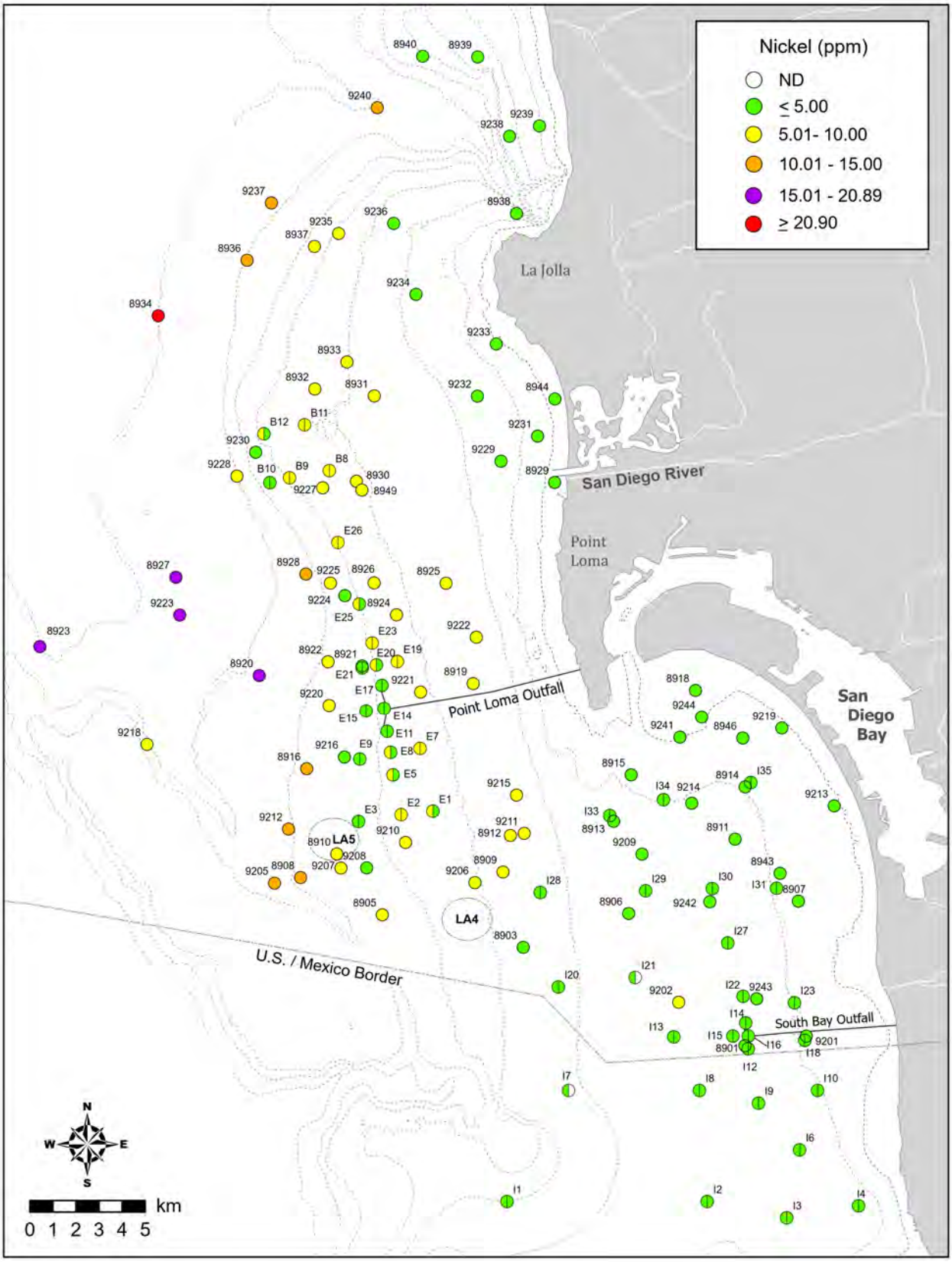

Appendix H.5 *continued*

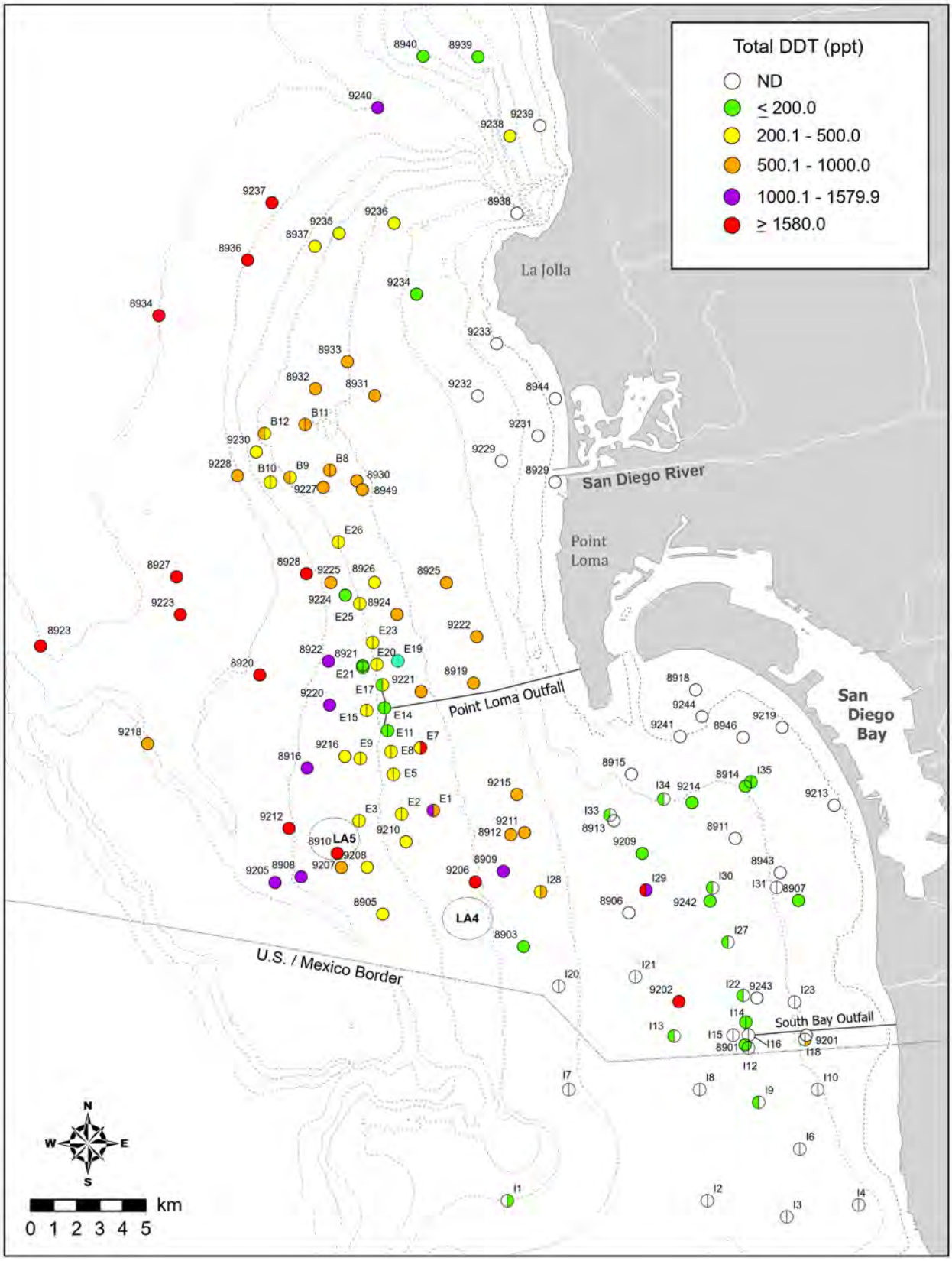

Appendix H.5 *continued*

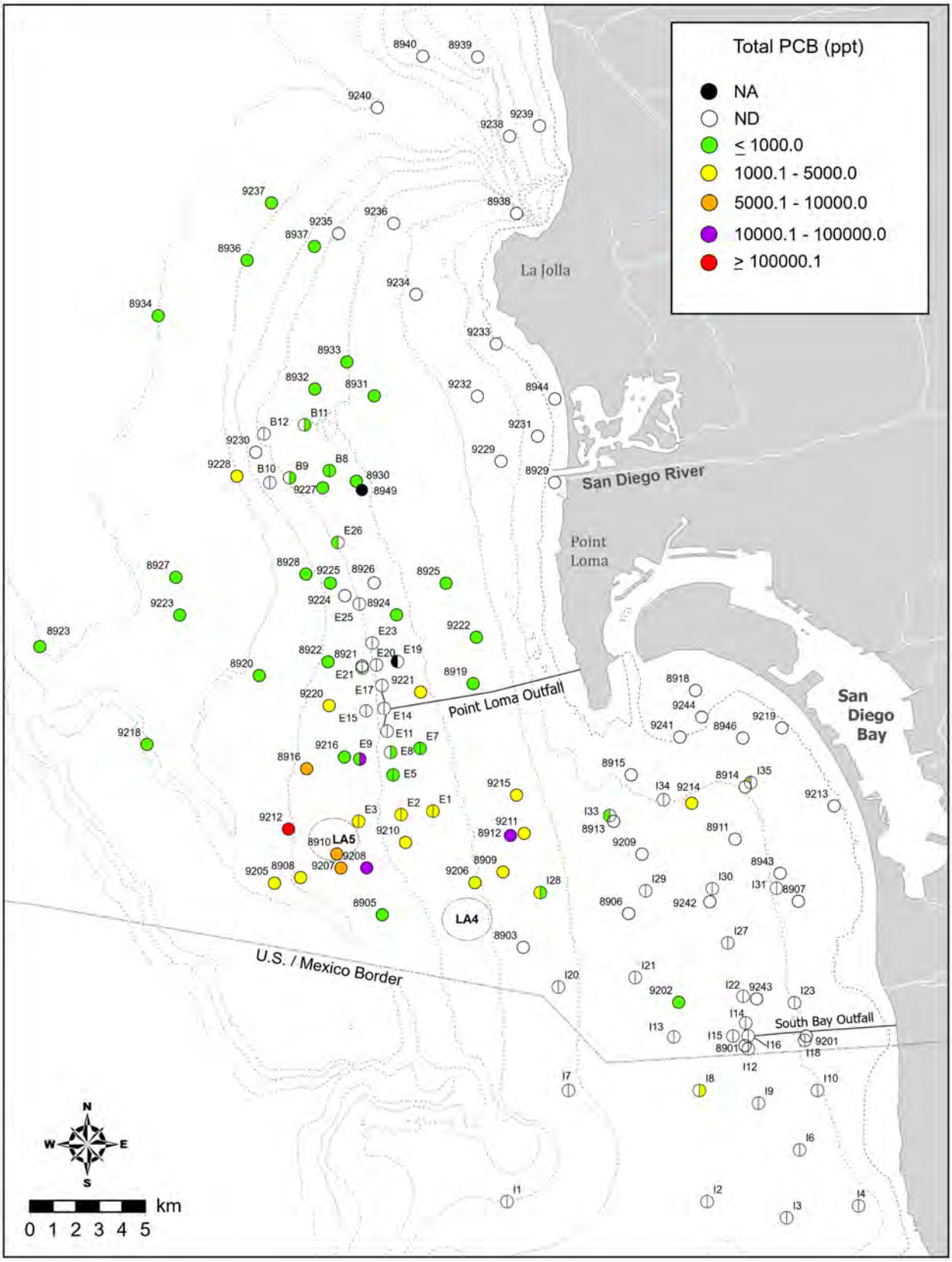

Appendix H.5 *continued*

Appendix H.6

Sediment chemistry summary for each sediment chemistry cluster group A–F (defined in Figure 7.4). Data include detection rate (DR; %), means, and ranges calculated over all samples within a cluster group (total samples). With the exception of fine particles, minimum and maximum values were calculated using all samples, whereas means were calculated with detected values only; nd = not detected.

		Sediment Chemistry Cluster Group					
		A	**B**	**C**	**D**	**E**	**F**
Total samples	n	1	1	1	1	161	13
Depth (m)	Mean	203	83	134	169	64	338
	Range	—	—	—	—	(7-327)	(189-523)
Fine Particles (%)	Mean	75.2	71.1	59.4	55.7	42.5	73.6
	Range	—	—	—	—	(0-100.1)	(50.4-87.7)
Organic Indicators							
Sulfides (ppm)	DR	100	100	100	100	62	100
	Mean	20.5	6.7	3.4	3.5	11.3	23.0
	Range	—	—	—	—	(nd-70.9)	(2.3-87.6)
TN (% weight)	DR	100	100	100	100	72	100
	Mean	0.154	0.072	0.060	0.051	0.050	0.170
	Range	—	—	—	—	(nd-0.136)	(0.120-0.270)
TOC (% weight)	DR	100	100	100	100	81	100
	Mean	2.04	0.75	0.94	0.60	0.65	2.55
	Range	—	—	—	—	(0-4.37)	(1.74-3.65)
TVS (% weight)	DR	100	100	100	100	100	100
	Mean	5.5	3.1	2.8	2.5	1.7	6.6
	Range	—	—	—	—	(0.4-5.5)	(4.6-9.5)
Trace Metals (ppm)							
Aluminum	DR	100	100	100	100	100	100
	Mean	13,700	9930	6560	10,300	5196	11,479
	Range	—	—	—	—	(597-13,200)	(7400-15,700)
Antimony	DR	100	100	100	100	88	100
	Mean	1.96	0.69	0.54	0.91	0.78	1.08
	Range	—	—	—	—	(nd-2.38)	(0.75-1.42)
Arsenic	DR	100	100	100	100	100	100
	Mean	3.2	1.64	2.21	3.21	2.55	2.90
	Range	—	—	—	—	(0.78-9.31)	(1.23-5.35)
Barium	DR	100	100	100	100	100	100
	Mean	63.9	44.7	28.0	62.4	23.9	68.3
	Range	—	—	—	—	(0.3-67.1)	(35.4-120.0)
Beryllium	DR	100	0	100	100	63	38
	Mean	0.426	—	0.124	0.131	0.130	0.270
	Range	—	—	—	—	(nd-0.400)	(nd-0.384)
Cadmium	DR	100	0	100	100	37	46
	Mean	0.160	—	0.094	0.106	0.070	0.240
	Range	—	—	—	—	(nd-0.223)	(nd-0.467)
Chromium	DR	100	100	100	100	100	100
	Mean	28.3	20.2	15.6	19.4	12.0	30.2
	Range	—	—	—	—	(2.3-28.7)	(24.2-41.9)

Appendix H.6 *continued*

		Sediment Chemistry Cluster Group					
		A	**B**	**C**	**D**	**E**	**F**
Copper	DR	100	100	100	100	84	100
	Mean	29.8	8.8	8.0	34.5	5.3	16.0
	Range	—	—	—	—	(nd-31.2)	(10.7-21.5)
Iron	DR	100	100	100	100	100	100
	Mean	17,800	13,300	9790	18,000	8007	17,408
	Range	—	—	—	—	(1030-24,300)	(13,700-24,100)
Lead	DR	100	100	100	100	100	100
	Mean	12.0	4.3	72.7	7.8	2.6	5.0
	Range	—	—	—	—	(0.7-7.4)	(3.8-7.6)
Manganese	DR	100	100	100	100	100	100
	Mean	144	113	75.9	128	66	122
	Range	—	—	—	—	(5-142)	(55-191)
Mercury	DR	100	100	100	100	75	100
	Mean	0.134	0.075	0.041	0.081	0.020	0.060
	Range	—	—	—	—	(nd-0.098)	(0.026-0.107)
Nickel	DR	100	100	100	100	99	100
	Mean	12.0	8.6	7.5	6.7	3.7	14.1
	Range	—	—	—	—	(nd-11.1)	(7.1-21.7)
Selenium	DR	0	0	0	0	1	85
	Mean	—	—	—	—	0.29	0.66
	Range	—	—	—	—	(nd-0.29)	(nd-1.07)
Silver	DR	100	0	0	0	1	0
	Mean	0.102	—	—	—	0.070	—
	Range	—	—	—	—	(0-0.072)	—
Thallium	DR	0	100	0	0	3	15
	Mean	—	0.175	—	—	0.180	0.170
	Range	—	—	—	—	(nd-0.223)	(nd-0.173)
Tin	DR	100	0	100	100	88	85
	Mean	3.08	—	0.87	1.13	0.57	1.24
	Range	—	—	—	—	(nd-1.46)	(nd-2.75)
Zinc	DR	100	100	100	100	100	100
	Mean	58.4	33.9	25.7	55.4	19.04	49.48
	Range	—	—	—	—	(1.64-52.5)	(30.8-79.2)
Pesticides (ppt)							
tDDT	DR	100	100	100	100	64	100
	Mean	2930	884	492	1823	489	2021
	Range	—	—	—	—	(nd-3984)	(789-4072)
tHCH	DR	0	100	0	0	0	0
	Mean	—	61	—	—	—	—
	Range	—	—	—	—	—	—
tChlordane	DR	100	100	0	100	3	0
	Mean	1058	73	—	918	111	—
	Range	—	—	—	—	(nd-170)	—

Appendix H.6 *continued*

		Sediment Chemistry Cluster Group					
		A	**B**	**C**	**D**	**E**	**F**
Total PCB (ppt)	DR	100	0	100	100	31	92
	Mean	167,680	—	808	7988	4158	1367
	Range	—	—	—	—	(nd-76,260)	(nd-5777)
Total PAH (ppb)	DR	100	0	100	100	57	100
	Mean	736.9	—	33.0	290.0	48.1	91.1
	Range	—	—	—	—	(nd-683.6)	(11.2-251.6)

Appendix H.7

Bioassay results (10-day amphipod survival tests) for sediment toxicity testing conducted for San Diego regional and core benthic stations sampled during summer 2020 and 2021. Percent fines = percentage of silt + clay combined. Test results (% Survival) are expressed as mean percent survival ± 1 standard deviation.

Survey	Site/Sample	Depth Stratum	Station Depth (m)	Percent Fines	Sample Date	Test Initiation	% Survival (Mean ± SD)
Summer 2020	Lab Control	—	—	—	—	7/21/2020	95 ± 6.1
	8943	Inner Shelf	19	37.0	7/13/2020	7/21/2020	98 ± 2.7
	8938	Inner Shelf	28	54.2	7/14/2020	7/21/2020	99 ± 2.2
	8906	Mid Shelf	41	13.6	7/13/2020	7/21/2020	96 ± 4.2
	8930	Mid Shelf	83	55.1	7/14/2020	7/21/2020	98 ± 4.5
	8910	Outer Shelf	169	51.7	7/13/2020	7/21/2020	93 ± 6.7
	8916	Outer Shelf	189	53.3	7/13/2020	7/21/2020	96 ± 8.9
	8908	Outer Shelf	194	51.1	7/13/2020	7/21/2020	92 ± 8.4
	8920	Upper Slope	270	55.9	7/14/2020	7/21/2020	97 ± 4.2
Summer 2021	Lab Control	—	—	—	—	7/27/2021	99 ± 2.2
	E11	Mid Shelf	98	47.1	7/20/2021	7/27/2021	98 ± 2.7
	E14	Mid Shelf	98	51.1	7/20/2021	7/27/2021	95 ± 6.1
	E15	Mid Shelf	98	48.7	7/20/2021	7/27/2021	98 ± 2.7
	E17	Mid Shelf	98	48.5	7/20/2021	7/27/2021	89 ± 6.5
	I12	Inner Shelf	28	54.5	7/19/2021	7/27/2021	98 ± 2.7
	I14	Inner Shelf	28	20.1	7/19/2021	7/27/2021	97 ± 6.7
	I15	Inner Shelf	28	4.0	7/19/2021	7/27/2021	99 ± 2.2
	I16	Inner Shelf	28	6.8	7/19/2021	7/27/2021	98 ± 2.7

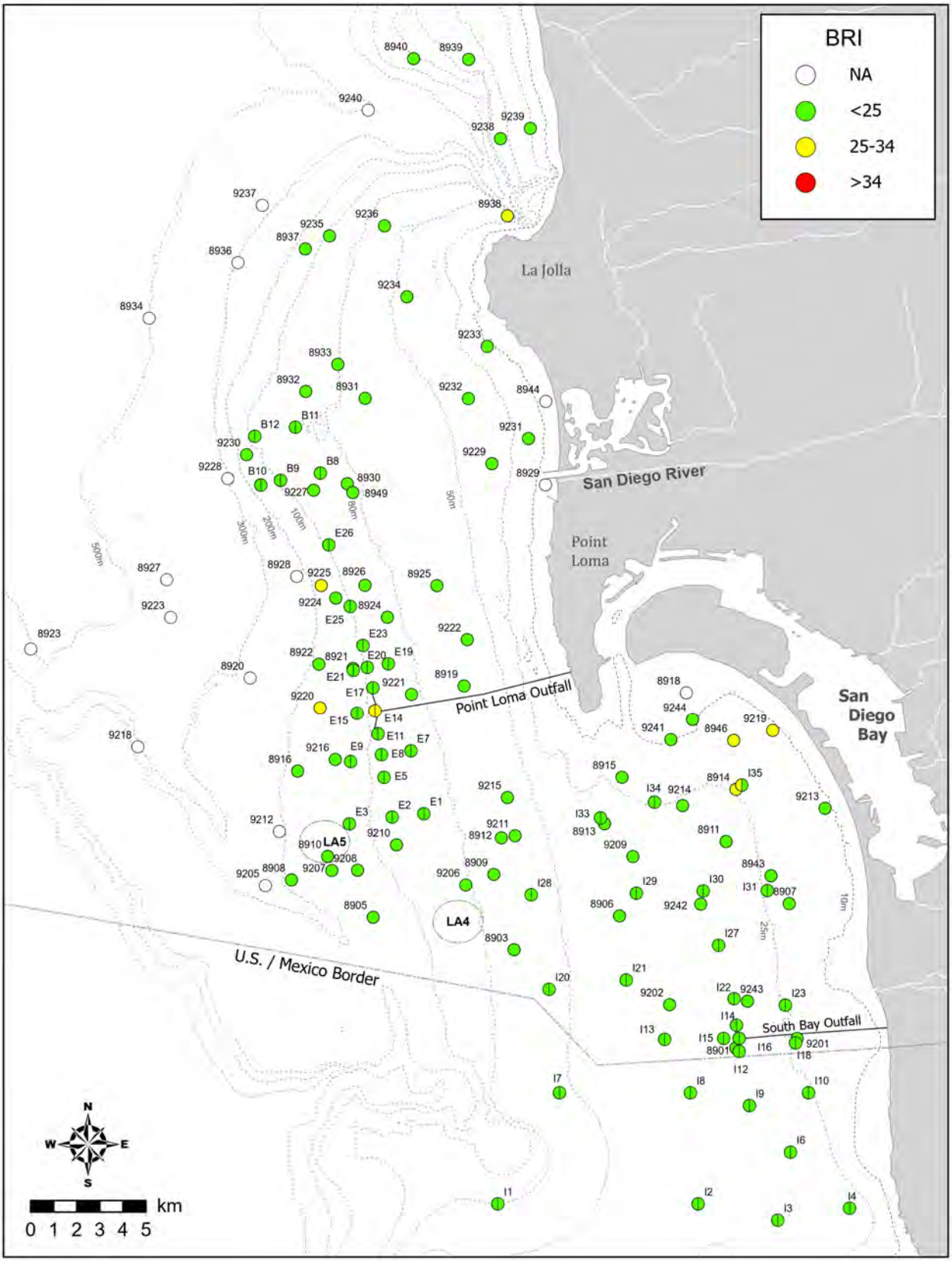

Appendix H.8

Distribution of BRI values from San Diego regional and core benthic stations sampled during summer 2020 and 2021; NA=not applicable.

Appendix H.9

Particle size summary for each macrofauna cluster group A–M (defined in Figure 7.5). Data are presented as means (ranges) calculated over all grabs within a cluster group. VF = very fine; F = fine; M = medium; C = coarse; VC = very coarse.

Cluster		Particle Size (%)						
Group	n	Fines	VFSand	FSand	MSand	CSand	VCSand	Granules
A	5	79.7 (67.3-87.7)	13.7 (9.4-17.1)	5.9 (2.7-13.0)	0.7 (0.1-2.6)	0 —	0 —	0 —
B	4	27.0 (1.0-63.8)	21.2 (4.7-53.8)	26.5 (11.5-46.0)	15.9 (0.8-29.8)	7.0 (0-22.7)	2.3 (0-9.1)	0 —
C	1	46.1	4.9	4.0	32.2	12.9	0	0
D	4	3.1 (2.2-4.3)	2.3 (0.3-7.0)	5.2 (0.6-9.0)	20.7 (13.2-31.1)	30.2 (20.4-43.9)	21.9 (16.7-25.8)	16.7 (11.7-27.0)
E	2	1.0 (0-1.9)	0.8 (0-1.6)	3.3 (0.4-6.2)	18.2 (9.0-27.4)	59.5 (33.8-85.2)	10.4 (5.4-15.4)	6.9 (0-13.8)
F	2	10 (9.8-10.2)	34.1 (29.8-38.5)	39.2 (33.7-44.8)	11.7 (9.0-14.4)	3.6 (1.2-5.9)	1.3 (0-2.7)	0 —
G	38	27.7 (6.9-84.7)	44.6 (3.7-68.8)	22.3 (3.0-40.1)	4.1 (0-16.3)	1.1 (0-10.1)	0.2 (0-4.7)	0 (0-1.5)
H	4	40.1 (0.6-100.1)	1.6 (0-3.6)	1.3 (0-2.7)	8.5 (0-13.1)	43.4 (0-81.4)	5.1 (0-7.9)	0 —
I	19	22.5 (0-93.8)	3.8 (0.2-13.9)	10.1 (0.9-40.9)	32.6 (0-57.2)	28.1 (0-59.4)	2.8 (0-8.1)	0 —
J	1	50.4	8.4	10.2	10.6	16.8	3.6	0
K	84	53.9 (17.8-73.3)	28.5 (7.9-44.6)	10.5 (3.8-43.0)	1.9 (0.1-9.7)	3.5 (0-45.7)	1.6 (0-25.5)	0.1 (0-2.9)
L	1	77	19	4	0.1	0	0	0
M	13	69.1 (55.7-75.2)	23.1 (17.4-30.5)	7 (4.3-17.5)	0.8 (0.1-5.8)	0 —	0 —	0 —

Appendix H.10

Mean abundance of the characteristic species found in each macrofauna cluster group A–M (defined in Figure 7.6). Highlighted values indicate the top five most characteristic species according to SIMPER analysis.

	Cluster Group												
Taxa	**A**	**B**	**C[a]**	**D**	**E**	**F**	**G**	**H**	**I**	**J[a]**	**K**	**L[a]**	**M**
Prionospio ehlersi	7	0	0	0	0	0	0	0	0	0	0	3	1
Yoldiella nana	5	0	0	0	0	0	0	0	0	0	0	0	0
Bipalponephtys cornuta	4	0	0	0	0	0	<1	0	0	0	<1	0	<1
Eclysippe trilobata	3	0	0	0	0	0	<1	1	0	0	6	0	2
Rhabdus rectius	1	0	0	0	0	0	0	0	0	0	0	0	<1
Prionospio pygmaeus	0	154	0	0	0	7	4	0	1	0	<1	0	<1
Goniada littorea	0	3	0	0	0	1	1	0	0	0	0	0	<1
Spiophanes duplex	0	2	0	2	0	26	18	6	4	1	39	0	8
Carinoma mutabilis	0	2	0	<1	4	8	2	<1	1	0	<1	0	0
Nephtys caecoides	0	1	0	<1	0	1	<1	0	<1	0	<1	0	<1
Dendraster terminalis	0	1	9	2	0	0	0	0	7	0	0	0	0
Cnemidocarpa rhizopus	0	0	6	2	0	0	0	2	0	0	0	0	0
Nematoda	0	1	4	54	20	0	1	0	<1	0	1	0	1
Scoloplos acmeceps	0	1	4	1	0	0	<1	0	1	0	0	0	0
Protodorvillea gracilis	0	0	4	76	7	0	0	2	3	0	0	0	0
Rhepoxynius lucubrans	0	0	3	0	0	0	<1	<1	0	0	<1	0	0
Lineidae	<1	1	2	4	0	3	1	2	1	0	2	0	1
Cephalothrix sp	0	0	2	3	5	0	<1	0	1	0	0	0	0
Lumbrinerides platypygos	0	0	2	6	20	0	<1	3	1	0	0	0	0
Mesolamprops bispinosus	0	0	2	0	0	0	<1	0	0	0	<1	0	0
Oligochaeta	0	0	2	<1	0	0	<1	0	0	0	0	0	<1
Ophelia pulchella	0	0	2	0	0	0	0	<1	1	0	0	0	0
Simomactra falcata	0	0	2	<1	0	0	<1	<1	1	0	0	0	0
Hesionura coineaui difficilis	0	<1	0	57	132	0	0	0	<1	0	0	0	0
Pisione sp	0	0	0	54	14	0	0	0	<1	0	0	0	0
Lumbrineris latreilli	0	<1	0	28	0	0	<1	0	<1	0	<1	0	0
Callianax baetica	0	<1	0	1	0	16	1	0	1	0	0	0	0
Gibberosus myersi	0	0	0	1	2	7	<1	0	<1	0	0	0	0
Spiophanes norrisi	0	1	1	18	0	6	11	3	38	0	1	0	0

[a] SIMPER analyses not conducted on cluster groups that contain only one grab. For these groups, shading indicates five most abundant taxa.

Appendix H.10 *continued*

Taxa	Cluster Group												
	A	B	C[a]	D	E	F	G	H	I	J[a]	K	L[a]	M
Mediomastus sp	0	<1	0	5	0	1	13	<1	<1	10	16	3	14
Gadila aberrans	0	0	0	0	0	0	6	0	<1	1	1	0	0
Sigalion spinosus	0	1	0	<1	0	0	6	1	2	0	1	0	0
Jasmineira sp B	0	0	0	0	0	0	<1	72	<1	0	1	0	<1
Mooreonuphis sp SD1	0	0	0	0	1	0	0	15	1	0	0	0	0
Byblis millsi	0	0	0	0	0	0	0	4	0	0	<1	0	0
Polycirrus sp A	0	0	1	<1	0	0	<1	3	3	0	2	0	<1
Rhepoxynius heterocuspidatus	0	1	0	0	0	0	<1	1	8	0	0	0	0
Ampelisca cristata cristata	0	0	0	0	0	0	<1	1	4	0	0	0	0
Spiochaetopterus costarum Cmplx	0	0	0	1	1	6	3	5	4	0	2	0	9
Phyllochaetopterus limicolus	0	0	0	0	0	0	0	0	0	13	<1	10	39
Fauveliopsis sp SD1	1	0	0	0	0	0	0	0	0	8	<1	0	0
Ampharete acutifrons	0	0	0	0	0	0	<1	0	0	5	0	0	<1
Amphiodia digitata	0	0	0	0	0	0	<1	0	0	5	1	0	1
Kirkegaardia siblina	0	1	0	<1	0	0	3	0	<1	2	2	0	1
Pectinaria californiensis	5	0	0	0	0	1	<1	0	0	2	2	0	2
Aricidea (Aricidea) wassi	0	0	0	0	0	0	<1	0	0	2	<1	0	0
Drilonereis falcata	0	0	0	0	0	0	<1	0	0	2	<1	0	<1
Ascorhiza occidentalis	0	0	0	0	1	0	0	0	0	2	0	0	0
Decamastus gracilis	0	0	0	<1	0	0	0	0	0	2	1	0	1
Amphiodia urtica	0	0	0	0	0	0	0	0	<1	0	20	0	<1
Paradiopatra parva	0	0	0	0	0	1	<1	1	1	0	13	0	10
Prionospio jubata	0	1	0	0	0	0	1	1	<1	0	8	0	4
Paraprionospio alata	2	0	1	0	0	0	2	0	<1	0	1	33	11
Scoletoma tetraura Cmplx	0	<1	0	0	0	1	<1	2	<1	0	1	3	3
Compressidens stearnsii	0	0	0	0	0	0	0	0	0	1	0	2	<1
Cossura sp A	0	0	0	0	0	0	<1	0	0	0	0	2	0
Goniada brunnea	<1	0	0	0	0	0	0	0	0	0	<1	1	<1
Axinopsida serricata	<1	0	0	0	0	0	0	0	0	0	25	0	22
Spiophanes kimballi	0	0	0	0	0	1	<1	0	2	1	12	0	10

[a] SIMPER analyses not conducted on cluster groups that contain only one grab. For these groups, shading indicates five most abundant taxa.

Appendix I

Demersal Fishes and Megabenthic Invertebrates

2020 – 2021 Supplemental Analyses

Appendix I.1

Taxonomic listing of demersal fish species collected at PLOO trawl stations during 2020 and 2021. Data are reported as total number of fish (n), biomass (BM, wet weight, kg), minimum, maximum, and mean length (standard length, cm unless otherwise noted). Taxonomic arrangement follows Eschmeyer and Herald (1998) and Page et al. (2013).

Taxonomic Classification		Common Name	n	Bm	Length (cm) Min	Max	Mean
RAJIFORMES							
Rajidae	*Raja inornata*	California Skate[a]	7	3.5	19	55	36
ARGENTINIFORMES							
Argentinidae	*Argentina sialis*	Pacific Argentine	11	0.3	5	11	8
AULOPIFORMES							
Synodontidae	*Synodus lucioceps*	California Lizardfish	22	2.2	17	34	23
GADIFORMES							
Merlucciidae	*Merluccius productus*	Pacific Hake	1	0.1	–	–	27
OPHIDIIFORMES							
Ophidiidae	*Chilara taylori*	Spotted Cusk-eel	11	1	11	19	15
BATRACHOIDIFORMES							
Batrachoididae	*Porichthys myriaster*	Specklefin Midshipman	10	0.1	4	12	8
	Porichthys notatus	Plainfin Midshipman	105	2.8	8	18	12
SCORPAENIFORMES							
Scorpaenidae	*Scorpaena guttata*	California Scorpionfish	40	6.6	10	25	17
Sebastidae	*Sebastes chlorostictus*	Greenspotted Rockfish	1	0.1	–	–	8
	Sebastes elongatus	Greenstriped Rockfish	10	0.7	5	10	7
	Sebastes goodei	Chilipepper	15	0.3	10	12	11
	Sebastes helvomaculatus	Rosethorn Rockfish	4	0.4	8	10	9
	Sebastes hopkinsi	Squarespot Rockfish	17	0.6	9	12	11
	Sebastes miniatus	Vermilion Rockfish	4	0.9	15	26	19
	Sebastes rosenblatti	Greenblotched Rockfish	1	0.1	–	–	8
	Sebastes rubrivinctus	Flag Rockfish	1	0.1	–	–	7
	Sebastes saxicola	Stripetail Rockfish	174	2.4	5	13	7
	Sebastes semicinctus	Halfbanded Rockfish	894	18.4	5	18	10
	Sebastes sp	Rockfish Unidentified	12	0.7	3	5	4
Hexagrammidae	*Zaniolepis frenata*	Shortspine Combfish	229	3.2	5	18	12
	Zaniolepis latipinnis	Longspine Combfish	295	4.2	6	16	11
Cottidae	*Chitonotus pugetensis*	Roughback Sculpin	2	0.1	8	8	8
	Icelinus quadriseriatus	Yellowchin Sculpin	265	1.1	2	7	5
	Icelinus tenuis	Spotfin Sculpin	1	0.1	–	–	3
Agonidae	*Xeneretmus latifrons*	Blacktip Poacher	2	0.2	14	14	14

[a] measured as total length (cm)

Appendix I.1 *continued*

Taxonomic Classification			Common Name	n	Bm	Length (cm) Min	Max	Mean
PERCIFORMES								
	Sciaenidae	*Genyonemus lineatus*	White Croaker	7	0.7	16	20	17
	Embiotocidae	*Zalembius rosaceus*	Pink Seaperch	57	1.9	5	12	9
	Bathymasteridae	*Rathbunella alleni*	Stripefin Ronquil	1	0.1	–	–	10
		Rathbunella hypoplecta	Bluebanded Ronquil	3	0.3	11	14	13
	Zoarcidae	*Lycodes cortezianus*	Bigfin Eelpout	3	0.1	17	18	17
		Lycodes pacificus	Blackbelly Eelpout	3	0.3	18	21	19
	Anarhichadidae	*Anarrhichthys ocellatus*	Wolf-eel	1	7.3	–	–	118
	Uranoscopidae	*Kathetostoma averruncus*	Smooth Stargazer	1	0.1	–	–	8
PLEURONECTIFORMES								
	Paralichthyidae	*Citharichthys sordidus*	Pacific Sanddab	3404	77.3	3	26	10
		Citharichthys xanthostigma	Longfin Sanddab	355	11.3	4	24	12
		Hippoglossina stomata	Bigmouth Sole	74	3.5	6	23	15
		Paralichthys californicus	California Halibut	1	1.8	–	–	52
		Xystreurys liolepis	Fantail Sole	2	1.2	25	35	30
	Pleuronectidae	*Lyopsetta exilis*	Slender Sole	49	0.9	8	17	12
		Microstomus pacificus	Dover Sole	704	17.9	6	21	12
		Parophrys vetulus	English Sole	306	18.6	8	23	15
		Pleuronichthys decurrens	Curlfin Sole	3	0.2	11	16	14
		Pleuronichthys verticalis	Hornyhead Turbot	79	3.1	10	19	13
	Cynoglossidae	*Symphurus atricaudus*	California Tonguefish	68	2	9	16	13

Appendix I.2

Taxonomic listing of demersal fish species collected at SBOO trawl stations during 2020 and 2021. Data are reported as total number of fish (n), biomass (BM, wet weight, kg), minimum, maximum, and mean length (standard length, cm unless otherwise noted). Taxonomic arrangement follows Eschmeyer and Herald (1998) and Page et al. (2013).

					Length (cm)		
Taxonomic Classification		**Common Name**	**n**	**Bm**	**Min**	**Max**	**Mean**
RAJIFORMES							
Rhinobatidae	*Rhinobatos productus*	Shovelnose Guitarfish[a]	3	1.3	32	55	43
Rajidae	*Raja inornata*	California Skate[a]	1	0.3	–	–	30
Platyrhynidae	*Platyrhinoidis triseriata*	Thornback[a]	4	1.5	35	47	40
MYLIOBATIFORNES							
Urolophidae	*Urobatis halleri*	Round Stingray[a]	4	1.4	24	33	30
CLUPEIFORMES							
Engraulidae	*Engraulis mordax*	Northern Anchovy	613	4.2	6	12	9
Clupeidae	*Sardinops sagax*	Pacific Sardine	62	1	11	14	12
AULOPIFORMES							
Synodontidae	*Synodus lucioceps*	California Lizardfish	707	6.1	8	27	11
BATRACHOIDIFORMES							
Batrachoididae	*Porichthys myriaster*	Specklefin Midshipman	18	1.2	6	29	12
	Porichthys notatus	Plainfin Midshipman	25	1	3	6	5
GASTEROSTEIFORMES							
Syngnathidae	*Syngnathus californiensis*	Kelp Pipefish	1	0.1	–	–	24
	Syngnathus exilis	Barcheek Pipefish	7	0.4	13	20	18
	Syngnathus sp	Pipefish Unidentified	19	0.6	12	24	17
SCORPAENIFORMES							
Scorpaenidae	*Scorpaena guttata*	California Scorpionfish	4	0.7	13	22	17
Hexagrammidae	*Zaniolepis latipinnis*	Longspine Combfish	1	0.1	–	–	16
Cottidae	*Chitonotus pugetensis*	Roughback Sculpin	15	0.8	7	9	8
	Icelinus quadriseriatus	Yellowchin Sculpin	54	0.8	6	7	7
	Leptocottus armatus	Pacific Staghorn Sculpin	1	0.1	–	–	13
PERCIFORMES							
Malacanthidae	*Caulolatilus princeps*	Ocean Whitefish	1	0.1	–	–	4
Sciaenidae	*Genyonemus lineatus*	White Croaker	73	3.5	9	18	14
	Seriphus politus	Queenfish	3	0.2	14	14	14
Embiotocidae	*Cymatogaster aggregata*	Shiner Perch	1	0.1	–	–	10
Clinidae	*Heterostichus rostratus*	Giant Kelpfish	2	0.2	12	24	18
Gobiidae	*Lepidogobius lepidus*	Bay Goby	1	0.1	–	–	7
Stromateidae	*Peprilus simillimus*	Pacific Pompano	2	0.2	8	9	8
PLEURONECTIFORMES							
Paralichthyidae	*Citharichthys sordidus*	Pacific Sanddab	34	0.7	3	10	6

[a] measured as total length (cm)

Appendix I.2 *continued*

Taxonomic Classification		Common Name	n	Bm	Length (cm) Min	Max	Mean
	Citharichthys stigmaeus	Speckled Sanddab	2051	12.8	4	12	8
	Citharichthys xanthostigma	Longfin Sanddab	610	18.6	4	20	11
	Hippoglossina stomata	Bigmouth Sole	4	0.3	17	24	21
	Paralichthys californicus	California Halibut	31	24.7	23	63	35
	Xystreurys liolepis	Fantail Sole	10	2.4	10	31	21
Pleuronectidae	*Parophrys vetulus*	English Sole	35	2.8	9	26	16
	Pleuronichthys ritteri	Spotted Turbot	13	1.3	13	19	16
	Pleuronichthys verticalis	Hornyhead Turbot	45	2.1	5	18	11
Cynoglossidae	*Symphurus atricaudus*	California Tonguefish	129	2.3	5	16	11

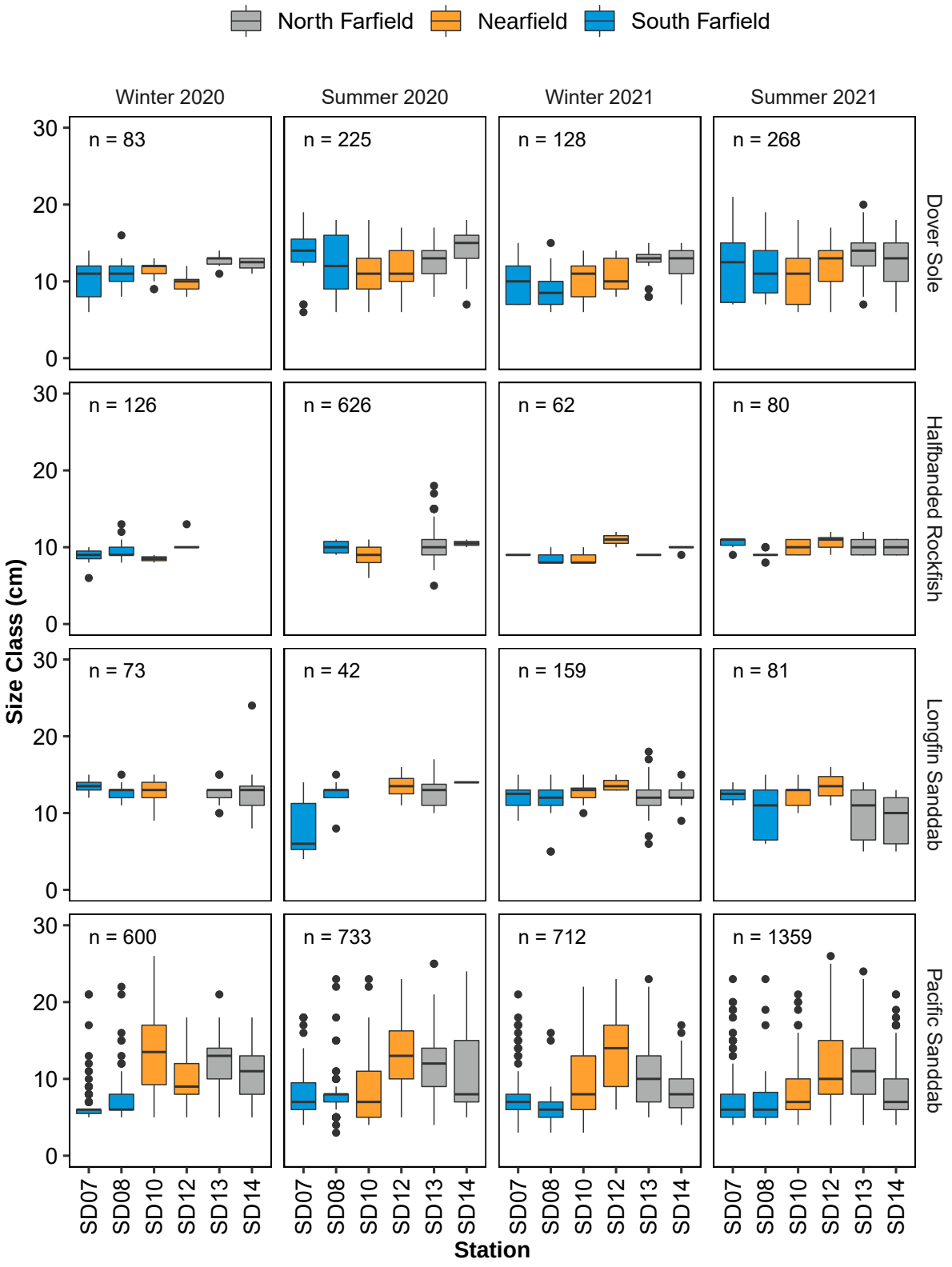

Appendix I.3

Summary of fish lengths by survey and station for the four most abundant species collected in the PLOO region during 2020 and 2021. Data are median, upper and lower quartiles, 1.5 times the interquartile range (whiskers), and outliers (open circles).

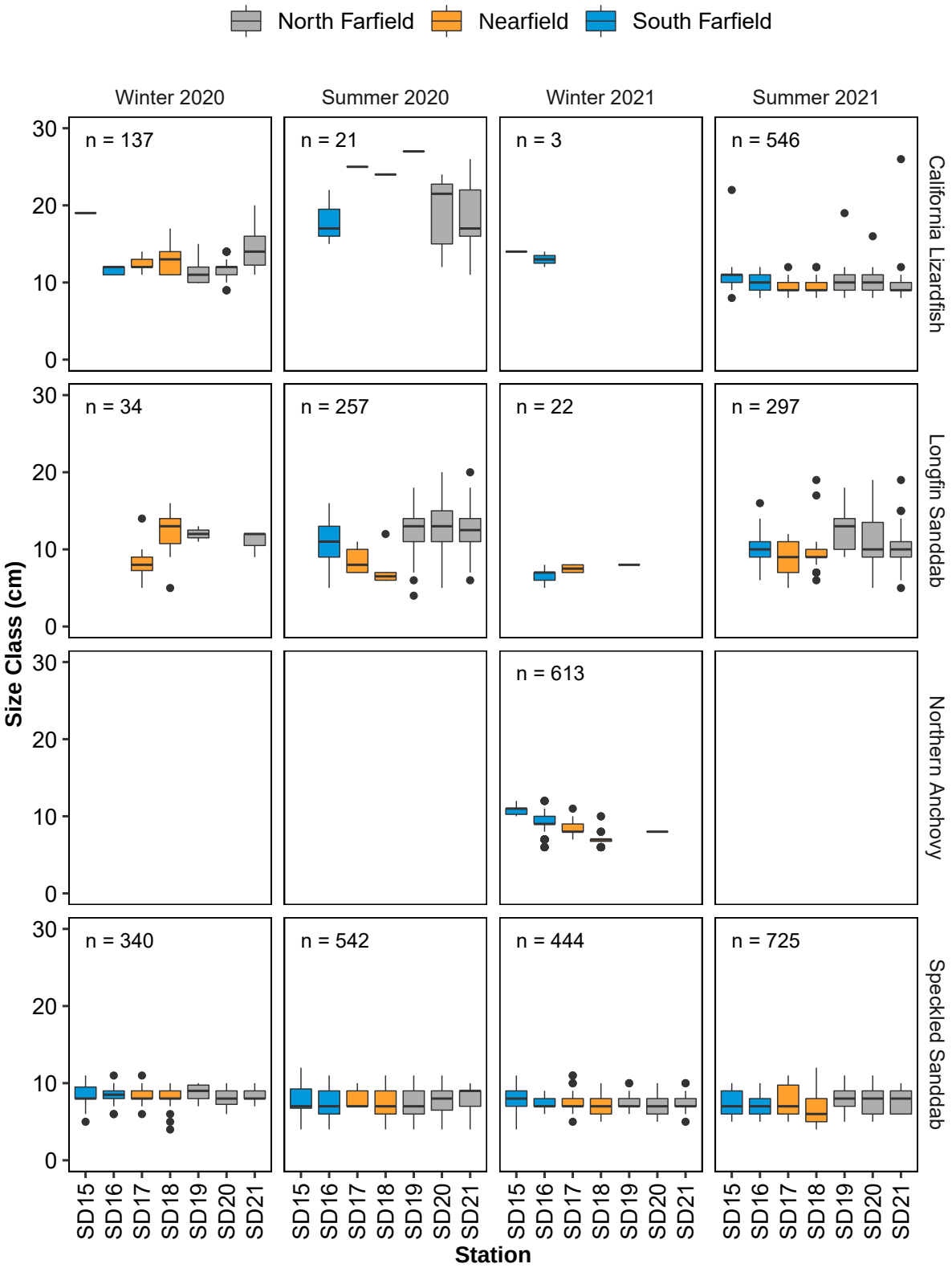

Appendix I.4

Summary of fish lengths by survey and station for the four most abundant species collected in the SBOO region during 2020 and 2021. Data are median, upper and lower quartiles, 1.5 times the interquartile range (whiskers), and outliers (open circles).

Appendix I.5

Summary of demersal fish abnormalities and parasites at PLOO and SBOO trawl stations during 2020 and 2021.

Region	Year	Survey	Station	Species	AbnormalitiesParasite	n
PLOO	**2020**	Winter	SD10	Pacific Sanddab	*Phrixocephalus cininnatus*	1
			SD12	Pacific Sanddab	*Phrixocephalus cininnatus*	1
			SD7	Pacific Sanddab	*Phrixocephalus cininnatus*	1
			SD8	Fantail Sole	*Phrixocephalus cininnatus*	1
			SD8	Pacific Sanddab	*Phrixocephalus cininnatus*	5
		Summer	SD12	Pacific Sanddab	*Elthusa vulgaris*	1
			SD13	Pacific Sanddab	*Phrixocephalus cininnatus*	1
			SD14	Pacific Sanddab	*Phrixocephalus cininnatus*	2
			SD8	Dover Sole	*Phrixocephalus cininnatus*	1
	2021	Winter	SD10	Dover Sole	Tumor	1
			SD10	Hornyhead Turbot	*Phrixocephalus cininnatus*	2
			SD10	Pacific Sanddab	*Phrixocephalus cininnatus*	5
			SD12	Pacific Sanddab	*Phrixocephalus cininnatus*	3
			SD13	Pacific Sanddab	*Phrixocephalus cininnatus*	5
			SD13	Pacific Sanddab	*Phrixocephalus cininnatus*, *Elthusa vulgaris*	2
			SD14	Pacific Sanddab	*Phrixocephalus cininnatus*	3
			SD8	Dover Sole	Tumor	1
		Summer	SD12	California Scorpionfish	*Elthusa vulgaris*	3
			SD12	Pacific Sanddab	*Elthusa vulgaris*	1
			SD12	Pacific Sanddab	*Elthusa vulgaris*	1
			SD13	Pacific Sanddab	*Phrixocephalus cininnatus*	1
			SD13	Pacific Sanddab	*Elthusa vulgaris*	1
			SD14	Pacific Sanddab	*Phrixocephalus cininnatus*	1
SBOO	**2020**	Winter	SD17	Speckled Sanddab	*Elthusa vulgaris*	1
			SD18	California Halibut	Leech	1
			SD21	Speckled Sanddab	Skeletal Deformity	1
		Summer	SD19	California Tonguefish	Other	1
			SD20	Speckled Sanddab	Tumor	1
	2021	Winter	SD20	Thornback	Leech	1
			SD21	Speckled Sanddab	*Elthusa vulgaris*	1
		Summer	SD18	Speckled Sanddab	*Elthusa vulgaris*	1

Appendix I.6

Description of PLOO demersal fish cluster groups A–D defined in Figure 8.6. Data are mean abundance of the characteristic species. Highlighted/bold values indicate the most characteristic species according to SIMPER analysis.

	Cluster Groups			
Species	**A**[a]	**B**	**C**	**D**
Pacific Sanddab	**75**	**212**	**86**	**30**
Plainfin Midshipman	**116**	6	**16**	0
Dover Sole	**36**	**26**	**10**	1
Halfbanded Rockfish	0	**27**	1	8
Longspine Combfish	**7**	**18**	2	0
Longfin Sanddab	0	4	**5**	1
Shortspine Combfish	0	**6**	2	0
Gulf Sanddab	**5**	< 1	< 1	< 1

[a] SIMPER analysis only conducted on cluster groups that contain more than one haul. For these groups, shading indicates five most abundant species.

Appendix I.7

Description of SBOO demersal fish cluster groups A–F defined in Figure 8.7. Data are mean abundance of the characteristic species. Highlighted/bold values indicate the most characteristic species according to SIMPER analysis.

	Cluster Groups					
Species	**A**	**B**	**C**	**D**	**E**[a]	**F**
Speckled Sanddab	**17**	**111**	**53**	**35**	**26**	**157**
California Lizardfish	**13**	4	2	< 1	**75**	**81**
Longspine Combfish	< 1	< 1	< 1	< 1	**79**	3
White Croaker	< 1	< 1	5	< 1	**22**	< 1
Longfin Sanddab	**7**	< 1	**10**	< 1	**8**	**25**
Hornyhead Turbot	**2**	4	**5**	**7**	3	5
Yellowchin Sculpin	< 1	< 1	< 1	< 1	5	19
Spotted Turbot	1	2	1	**3**	0	< 1

[a] SIMPER analysis only conducted on cluster groups that contain more than one haul. For these groups, shading indicates five most abundant species.

Appendix I.8

Taxonomic listing of megabenthic invertebrate taxa collected at all PLOO trawl stations during 2020 and 2021. Data are total number of individuals (n). Taxonomic arrangement follows SCAMIT (2018). -- indicates taxon is not within previous family.

Taxonomic Classification				n
SILICEA	Demospongiae	Halichondriidae	*Halichondria* sp	1
CNIDARIA	Anthozoa	Plexauridae	*Thesea* sp B	5
		Virgulariidae	*Acanthoptilum* sp	3
		Parazoanthidae	*Savalia lucifica*	1
MOLLUSCA	Gastropoda	Calliostomatidae	*Calliostoma turbinum*	1
		Naticidae	*Neverita draconis*	1
		Nassariidae	*Tritia insculpta*	3
		Muricidae	*Austrotrophon catalinensis*	1
		Pseudomelatomidae	*Megasurcula carpenteriana*	1
		Pleurobranchidae	*Pleurobranchaea californica*	3
	Cephalopoda	Octopodidae	*Octopus rubescens*	7
			Octopus veligero	8
ANNELIDA	Polychaeta	Aphroditidae	*Aphrodita refulgida*	2
ARTHROPODA	Malacostraca	Sicyoniidae	*Sicyonia ingentis*	1347
		Crangonidae	*Neocrangon zacae*	13
		--	Paguroidea	32
		Diogenidae	*Paguristes bakeri*	16
		Paguridae	*Pagurus armatus*	1
			Phimochirus californiensis	2
		Munididae	*Pleuroncodes planipes*	151,616
		Calappidae	*Platymera gaudichaudii*	466
		Epialtidae	*Loxorhynchus crispatus*	2
			Loxorhynchus grandis	1
		Cancridae	*Metacarcinus anthonyi*	1
ECHINODERMATA	Asteroidea	Luidiidae	*Luidia armata*	13
			Luidia asthenosoma	30
			Luidia foliolata	35
		Astropectinidae	*Astropecten californicus*	48
			Astropecten ornatissimus	1
	Ophiuroidea	Gorgonocephalidae	*Gorgonocephalus eucnemis*	1
		Ophiuridae	*Ophiura luetkenii*	14
		Amphiuridae	*Amphichondrius granulatus*	1
		Ophiopholidae	*Ophiopholis bakeri*	10
		Ophiotrichidae	*Ophiothrix spiculata*	28
	Echinoidea	Toxopneustidae	*Lytechinus pictus*	10,342
		Strongylocentrotidae	*Strongylocentrotus fragilis*	3
	Holothuroidea	Stichopodidae	*Apostichopus californicus*	16

Appendix I.9

Taxonomic listing of megabenthic invertebrate taxa collected at all SBOO trawl stations during 2020 and 2021. Data are total number of individuals (n). Taxonomic arrangement follows SCAMIT (2018).

Taxonomic Classification				n
SILICEA	Demospongiae	Suberitidae	*Suberites* sp	9
CNIDARIA	Anthozoa	Renillidae	*Renilla koellikeri*	4
		Virgulariidae	*Stylatula elongata*	4
MOLLUSCA	Gastropoda	Calliostomatidae	*Calliostoma gloriosum*	3
		Turbinidae	*Megastraea undosa*	1
		Naticidae	*Neverita lewisii*	3
			Neverita recluziana	1
			Sinum scopulosum	2
		Bursidae	*Crossata ventricosa*	8
		Buccinidae	*Kelletia kelletii*	5
		Muricidae	*Pteropurpura festiva*	1
		Olivellidae	*Callianax baetica*	1
		Pseudomelatomidae	*Crassispira semiinflata*	2
		Onchidoridiidae	*Acanthodoris brunnea*	3
			Acanthodoris rhodoceras	5
		Arminidae	*Armina californica*	3
		Dendronotidae	*Dendronotus iris*	1
		Flabellinopsidae	*Flabellinopsis iodinea*	1
		Philinidae	*Philine auriformis*	148
	Bivalvia	Pectinidae	*Leptopecten latiauratus*	1
	Cephalopoda	Octopodidae	*Octopus rubescens*	2
ARTHROPODA	Malacostraca	Hemisquillidae	*Hemisquilla californiensis*	8
		Penaeidae	*Farfantepenaeus californiensis*	4
		Sicyoniidae	*Sicyonia penicillata*	71
		Hippolytidae	*Eualus subtilis*	1
			Heptacarpus palpator	1
			Heptacarpus stimpsoni	33
			Spirontocaris prionota	1
		Crangonidae	*Crangon alba*	68
			Crangon nigromaculata	732
		Diogenidae	*Paguristes bakeri*	1
		Paguridae	*Pagurus spilocarpus*	13
		Munididae	*Pleuroncodes planipes*	1
		Dromiidae	*Moreiradromia sarraburei*	4
		Calappidae	*Platymera gaudichaudii*	4
		Leucosiidae	*Randallia ornata*	1
		Epialtidae	*Pugettia richii*	1
			Loxorhynchus grandis	5

Appendix I.9 *continued*

Taxonomic Classification				n
		Inachidae	*Ericerodes hemphillii*	2
		Inachoididae	*Pyromaia tuberculata*	20
		Parthenopidae	*Latulambrus occidentalis*	4
		Cancridae	*Metacarcinus anthonyi*	3
			Metacarcinus gracilis	3
		Portunidae	*Portunus xantusii*	46
ECHINODERMATA	Asteroidea	Luidiidae	*Luidia armata*	26
		Astropectinidae	*Astropecten californicus*	365
	Ophiuroidea	Amphiuridae	*Amphiodia psara*	1
		Ophiotrichidae	*Ophiothrix spiculata*	183
	Echinoidea	Toxopneustidae	*Lytechinus pictus*	105
		Dendrasteridae	*Dendraster terminalis*	36
		Loveniidae	*Lovenia cordiformis*	67

Appendix I.10

Description of PLOO megabenthic invertebrate cluster groups A–F defined in Figure 8.11. Data are mean abundance of the characteristic species. Highlighted/bold values indicate most characteristic species according to SIMPER analysis.

	Cluster Groups					
Species	**A**	**B**	**C[a]**	**D**	**E**	**F**
Pleuroncodes planipes	3	**7514**	0	2	< 1	2
Ophiura luetkenii	0	0	**2640**	47	17	1
Lytechinus pictus	**5**	124	**102**	**2126**	**230**	**11**
Strongylocentrotus fragilis	0	26	**442**	5	**134**	**40**
Acanthoptilum sp	0	0	0	41	36	**69**
Sicyonia ingentis	**49**	71	0	6	2	**11**
Luidia foliata	**2**	0	**11**	4	5	0
Astropecten californicus	< 1	< 1	**1**	5	3	**5**
Octopus veligero	**1**	0	0	< 1	< 1	0

[a] SIMPER analysis only conducted on cluster groups that contain more than one haul. For these groups, shading indicates five most abundant species.

Appendix I.11

Description of SBOO megabenthic invertebrate cluster groups A–D defined in Figure 8.12. Data are mean abundance of the characteristic species. Highlighted/bold values indicate most characteristic species according to SIMPER analysis.

	Cluster Groups			
Species	**A**	**B[a]**	**C**	**D**
Ophiura luetkenii	0	**72**	< 1	0
Astropecten californicus	0	0	**30**	< 1
Lytechinus pictus	0	0	12	**2**
Ophiothrix spiculata	0	**3**	< 1	2
Dendraster terminalis	0	**3**	1	< 1
Crangon alba	0	**2**	< 1	0
Crangon nigromaculata	**2**	0	< 1	< 1
Crossata ventricosa	0	0	< 1	**1**
Megastraea turbanica	0	**1**	0	0
Kelletia kelletii	0	0	< 1	**< 1**
Platymera gaudichaudii	0	0	< 1	**< 1**
Pisaster brevispinus	0	0	**< 1**	0

[a] SIMPER analysis only conducted on cluster groups that contain more than one haul. For these groups, shading indicates five most abundant species.

Appendix J

Contaminants in Marine Fishes

2020 – 2021 Supplemental Analyses

Appendix J.1

Lengths and weights of fishes used for each composite (Comp) tissue sample from PLOO trawl and rig fishing zones during 2020–2021. Data are summarized as number of individuals (n), minimum, maximum, and mean values.

					Length (cm, size class)			Weight (g)		
	Zone	Comp	Species	n	Min	Max	Mean	Min	Max	Mean
2020	RF1	1	Vermilion Rockfish	3	22	26	24	282	479	358
	RF1	2	Vermilion Rockfish	3	24	27	26	360	629	525
	RF1	3	Vermilion Rockfish	3	24	27	25	372	545	438
	RF2	1	Starry Rockfish	3	18	26	21	197	595	331
	RF2	2	Starry Rockfish	3	22	24	23	224	377	326
	RF2	3	Mixed Rockfish[a]	3	21	28	25	242	574	423
	TZ1	1	Pacific Sanddab	4	16	24	20	74	252	168
	TZ1	2	Pacific Sanddab	6	17	20	19	74	134	105
	TZ1	3	Pacific Sanddab	10	14	20	16	33	123	60
	TZ2	1	Pacific Sanddab	7	13	21	17	30	155	88
	TZ2	2	Pacific Sanddab	8	13	21	18	22	155	84
	TZ2	3	Pacific Sanddab	6	16	24	19	51	211	118
	TZ3	1	Pacific Sanddab	6	11	20	16	26	177	90
	TZ3	2	Pacific Sanddab	7	12	19	16	23	121	69
	TZ3	3	Pacific Sanddab	7	14	21	17	41	131	77
	TZ4	1	Pacific Sanddab	5	14	20	17	46	163	99
	TZ4	2	Pacific Sanddab	7	14	21	16	30	135	62
	TZ4	3	Longfin Sanddab	6	13	18	16	32	125	76
2021	RF1	1	Vermilion Rockfish	3	27	28	28	469	591	544
	RF1	2	Vermilion Rockfish	3	24	29	27	402	596	498
	RF1	3	Vermilion Rockfish	3	19	33	25	178	965	478
	RF2	1	Starry Rockfish	3	23	26	25	282	385	343
	RF2	2	Starry Rockfish	3	27	32	29	567	1044	740
	RF2	3	Mixed Rockfish[b]	3	23	29	27	324	675	529
	TZ1	1	Pacific Sanddab	10	15	21	18	44	151	79
	TZ1	2	Pacific Sanddab	13	12	23	16	28	200	81
	TZ1	3	Pacific Sanddab	11	13	22	17	38	228	84
	TZ2	1	Pacific Sanddab	9	13	21	17	27	140	82
	TZ2	2	Pacific Sanddab	8	14	21	17	40	150	82
	TZ2	3	Pacific Sanddab	5	15	22	19	55	176	107
	TZ3	1	Pacific Sanddab	4	17	23	20	80	223	144
	TZ3	2	Pacific Sanddab	7	15	22	18	45	171	103
	TZ3	3	Pacific Sanddab	12	14	22	17	33	163	80
	TZ4	1	Pacific Sanddab	5	18	21	20	75	142	113
	TZ4	2	Pacific Sanddab	5	18	23	21	86	233	164
	TZ4	3	Pacific Sanddab	8	18	20	19	83	128	108

[a]Includes Flag, Speckled, and Starry Rockfish; [b]includes Vermilion and Flag Rockfish

Appendix J.2

Lengths and weights of fishes used for each composite (Comp) tissue sample from SBOO trawl and rig fishing zones during 2020–2021. Data are summarized as number of individuals (n), minimum, maximum, and mean values.

					Length (cm, size class)			Weight (g)		
	Zone	Comp	Species	n	Min	Max	Mean	Min	Max	Mean
2020	RF3	1	California Scorpionfish	3	26	27	26	587	705	642
	RF3	2	Mixed Rockfish[a]	3	22	26	25	287	585	484
	RF3	3	Mixed Rockfish[b]	3	18	27	21	172	458	268
	RF4	1	Mixed Rockfish[c]	3	21	26	23	252	390	326
	RF4	2	California Scorpionfish	3	25	29	27	567	812	686
	RF4	3	California Scorpionfish	3	24	26	25	424	571	521
	TZ5	1	Longfin Sanddab	11	12	20	14	26	145	50
	TZ5	2	Hornyhead Turbot	6	14	20	17	51	177	130
	TZ5	3	Spotted Turbot	12	15	20	16	57	169	94
	TZ6	1	Longfin Sanddab	7	12	16	14	26	91	52
	TZ6	2	Longfin Sanddab	7	12	16	14	35	94	58
	TZ6	3	Longfin Sanddab	11	12	14	13	28	62	40
	TZ7	1	Longfin Sanddab	10	12	15	13	29	70	40
	TZ7	2	Longfin Sanddab	9	12	15	13	24	67	37
	TZ7	3	Longfin Sanddab	10	11	15	13	24	71	37
	TZ8	1	Hornyhead Turbot	8	13	19	14	60	178	94
	TZ8	2	Longfin Sanddab	9	11	15	12	32	85	47
	TZ8	3	California Scorpionfish	3	20	23	22	278	320	299
	TZ9*	1	Spotted Turbot	5	12	23	17	40	335	137
2021	RF3	1	California Scorpionfish	3	15	35	23	108	831	378
	RF3	2	California Scorpionfish	3	17	26	21	158	462	305
	RF3	3	Mixed Rockfish[d]	3	19	31	23	162	838	390
	RF4	1	Gopher Rockfish	3	20	25	23	270	453	378
	RF4	2	Gopher Rockfish	3	20	22	21	223	375	289
	RF4	3	California Scorpionfish	3	18	28	23	176	651	400
	TZ5	1	Longfin Sanddab	12	14	20	17	59	122	83
	TZ5	2	Longfin Sanddab	14	14	15	14	47	70	57
	TZ5	3	Hornyhead Turbot	12	13	19	15	44	172	90
	TZ6	1	Longfin Sanddab	30	11	14	12	19	73	30
	TZ6	2	Longfin Sanddab	31	10	13	11	17	45	25
	TZ6	3	Hornyhead Turbot	5	12	15	13	31	74	49
	TZ7	1	Longfin Sanddab	19	11	16	12	22	71	37
	TZ7	2	Longfin Sanddab	32	10	14	11	19	47	28
	TZ7	3	Hornyhead Turbot	13	12	21	15	38	249	83
	TZ8	1	Longfin Sanddab	17	11	16	12	21	87	36
	TZ8	2	Longfin Sanddab	24	11	16	12	21	100	33
	TZ8	3	Longfin Sanddab	14	11	16	12	19	73	30
	TZ9	1	Hornyhead Turbot	5	12	19	16	38	173	109
	TZ9	2	English Sole	5	19	20	20	97	143	121
	TZ9	3	Spotted Turbot	3	14	19	16	56	147	87

*insufficient fish collected (see text); [a] includes Treefish and Gopher Rockfish; [b] includes Brown and Olive Rockfish; [c] includes Treefish and Gopher Rockfish; [d] includes Brown and Vermilion Rockfish

Appendix J.3

Constituents and method detection limits (MDL) used for the analysis of liver and muscle tissues of fishes collected during 2020–2021. MDLs are summarized as minimum and maximum values over the two years.

	Liver		Muscle			Liver		Muscle	
Parameter	**Min**	**Max**	**Min**	**Max**	**Parameter**	**Min**	**Max**	**Min**	**Max**
Metals (ppm)									
Aluminum (Al)	5.02	5.45	1.51	1.72	Lead (Pb)	0.261	0.278	0.076	0.092
Antimony (Sb)	0.531	0.57	0.157	0.179	Manganese (Mn)	0.307	0.526	0.09	0.142
Arsenic (As)	0.579	0.881	0.193	0.277	Mercury (Hg)	0.002	0.008	0.001	0.003
Barium (Ba)	1.07	1.07	0.357	0.357	Nickel (Ni)	0.104	0.11	0.03	0.036
Beryllium (Be)	0.011	0.015	0.004	0.005	Selenium (Se)	0.952	2.35	0.176	0.318
Cadmium (Cd)	0.053	0.06	0.017	0.019	Silver (Ag)	0.304	0.524	0.089	0.175
Chromium (Cr)	0.185	0.449	0.054	0.15	Thallium (Tl)	0.392	0.392	0.082	0.082
Copper (Cu)	0.258	0.287	0.077	0.096	Tin (Sn)	3.49	7.96	1.02	2.65
Iron (Fe)	2.82	3	0.827	0.988	Zinc (Zn)	0.476	1.74	0.139	0.581
Chlorinated Pesticides (ppb)									
Chlordanes									
Alpha (cis) chlordane	3.11	4.06	0.33	0.406	Heptachlor epoxide	2.09	3.24	0.25	0.324
Cis nonachlor	2.39	3.14	0.262	0.32	Methoxychlor	1.88	8.53	0.22	0.854
Gamma (trans) chlordane	2.52	3.3	0.3	0.33	Oxychlordane	2.66	3.53	0.32	0.353
Heptachlor	2.25	3.93	0.247	0.4	Trans nonachlor	1.95	3.77	0.23	0.377
Dichlorodiphenyltrichloroethane (DDT)									
o,p-DDD	2.94	5.7	0.323	0.57	p,p-DDD	3.43	7.45	0.38	0.75
o,p-DDE	2.48	3.78	0.271	0.38	p,p-DDE	2.84	14.9	0.312	1.52
o,p-DDT	2.7	3.51	0.296	0.35	p,p-DDT	3.43	6.34	0.376	0.63
p,-p-DDMU	2.76	3.78	0.33	0.378					
Endrin									
Endrin	4.15	5.08	0.49	0.51	Endrin aldehyde	5.89	9.26	0.646	0.93
Endosulfan									
Alpha-Endosulfan	3.45	4.22	0.389	0.42	Endosulfan sulfate	2.39	5.05	0.28	0.505
Beta-Endosulfan	6.45	9.7	0.707	0.97					
Hexachlorocyclohexane (HCH)									
HCH, Alpha isomer	2.26	2.8	0.26	0.28	HCH, Delta isomer	2.94	4.93	0.323	0.5
HCH, Beta isomer	2.95	6.11	0.324	0.61	HCH, Gamma isomer	2.11	2.77	0.231	0.28
Miscellaneous Pesticides									
Aldrin	4.11	6.07	0.455	0.61	Hexachlorobenzene (HCB)	8.28	466	0.908	46.6
Dieldrin	1.14	4.6	0.14	0.46	Mirex	2.86	8.07	0.314	0.81

Appendix J.3 *continued*

Parameter	Liver Min	Liver Max	Muscle Min	Muscle Max	Parameter	Liver Min	Liver Max	Muscle Min	Muscle Max
Polychlorinated Biphenyls Congeners (PCBs) (ppb)									
PCB 8	1.95	2.17	0.213	0.217	PCB 126	1.76	4.07	0.21	0.407
PCB 18	2.62	6.43	0.287	0.64	PCB 128	3.15	5.94	0.345	0.6
PCB 28	2.31	3.13	0.253	0.31	PCB 138	2.34	6.4	0.257	0.65
PCB 37	2.12	3.95	0.25	0.395	PCB 149	3.12	5.02	0.342	0.51
PCB 44	2.56	3.13	0.298	0.31	PCB 151	4.53	7.53	0.502	0.75
PCB 49	2.51	3.76	0.29	0.376	PCB 153/168	9.24	15.1	1.01	1.54
PCB 52	2.52	4.02	0.29	0.402	PCB 156	2.23	3.73	0.26	0.373
PCB 66	2.51	5.1	0.49	4.8	PCB 157	2.67	4	0.29	0.4
PCB 70	2.14	5	0.48	3.7	PCB 158	1.68	6.44	0.184	0.65
PCB 74	2.67	5.01	0.49	4	PCB 167	3.08	4.59	0.341	0.46
PCB 77	2.53	3.13	0.3	6	PCB 169	2.65	3.25	0.31	0.33
PCB 81	2.45	4.41	0.271	0.44	PCB 170	2.77	3.34	0.322	0.34
PCB 87	2.06	3.54	0.24	0.354	PCB 177	3.92	5.96	0.43	0.6
PCB 99	2.7	5.55	0.296	0.56	PCB 180	2.8	6.5	0.307	0.66
PCB 101	2.19	2.95	0.27	0.295	PCB 183	2.51	6.98	0.275	0.7
PCB 105	3.72	4.48	0.409	0.45	PCB 187	2.94	7.19	0.323	0.328
PCB 110	3.59	5.06	0.393	0.5	PCB 189	2.42	4.47	0.268	0.45
PCB 114	4.7	6.6	0.56	5.1	PCB 194	3.22	7.67	0.353	0.77
PCB 118	2.62	6.24	0.287	0.64	PCB 195	2.87	3.2	0.315	0.32
PCB 119	3.58	5.13	0.392	0.51	PCB 201	3.25	9.48	0.356	0.95
PCB 123	3.41	6.18	0.374	0.62	PCB 206	3.15	7.3	0.71	14.9
Polycyclic Aromatic Hydrocarbons (PAHs) (ppb)									
1-methylnaphthalene	212	233	213	231	Benzo[G,H,I]perylene	404	443	404	440
1-methylphenanthrene	276	303	277	301	Benzo[K]fluoranthene	399	438	400	435
2-methylnaphthalene	175	192	175	190	Biphenyl	205	225	205	222
2,3,5-trimethylnaphthalene	298	327	299	325	Chrysene	176	193	176	192
2,6-dimethylnaphthalene	229	251	229	249	Dibenzo(A,H)anthracene	352	386	352	383
3,4-benzo(B)fluoranthene	422	463	423	460	Fluoranthene	228	250	228	248
Acenaphthene	187	205	187	203	Fluorene	112	123	112	122
Acenaphthylene	171	188	172	187	Indeno(1,2,3-CD)pyrene	326	358	327	355
Anthracene	199	218	199	216	Naphthalene	205	225	205	222
Benzo[A]anthracene	217	238	217	236	Perylene	303	333	304	330
Benzo[A]pyrene	335	368	336	365	Phenanthrene	400	439	401	436
Benzo[e]pyrene	409	449	410	446	Pyrene	215	236	215	234

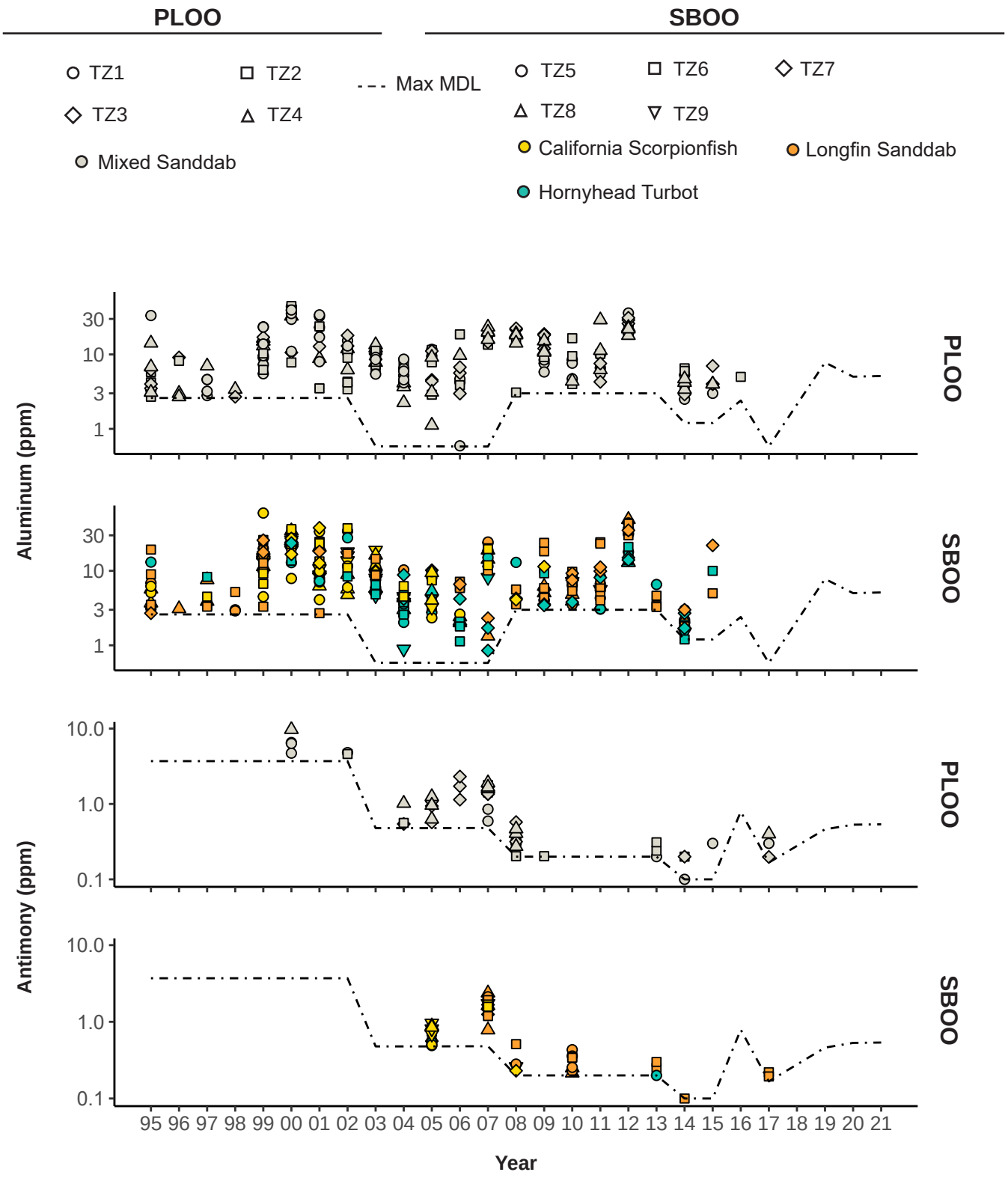

Appendix J.4

Concentrations of select metals in liver tissues of fishes collected from PLOO and SBOO trawl zones from 1995 through 2021. Zones TZ1 and TZ5 are considered nearfield. No samples were collected in 2018 as described in text.

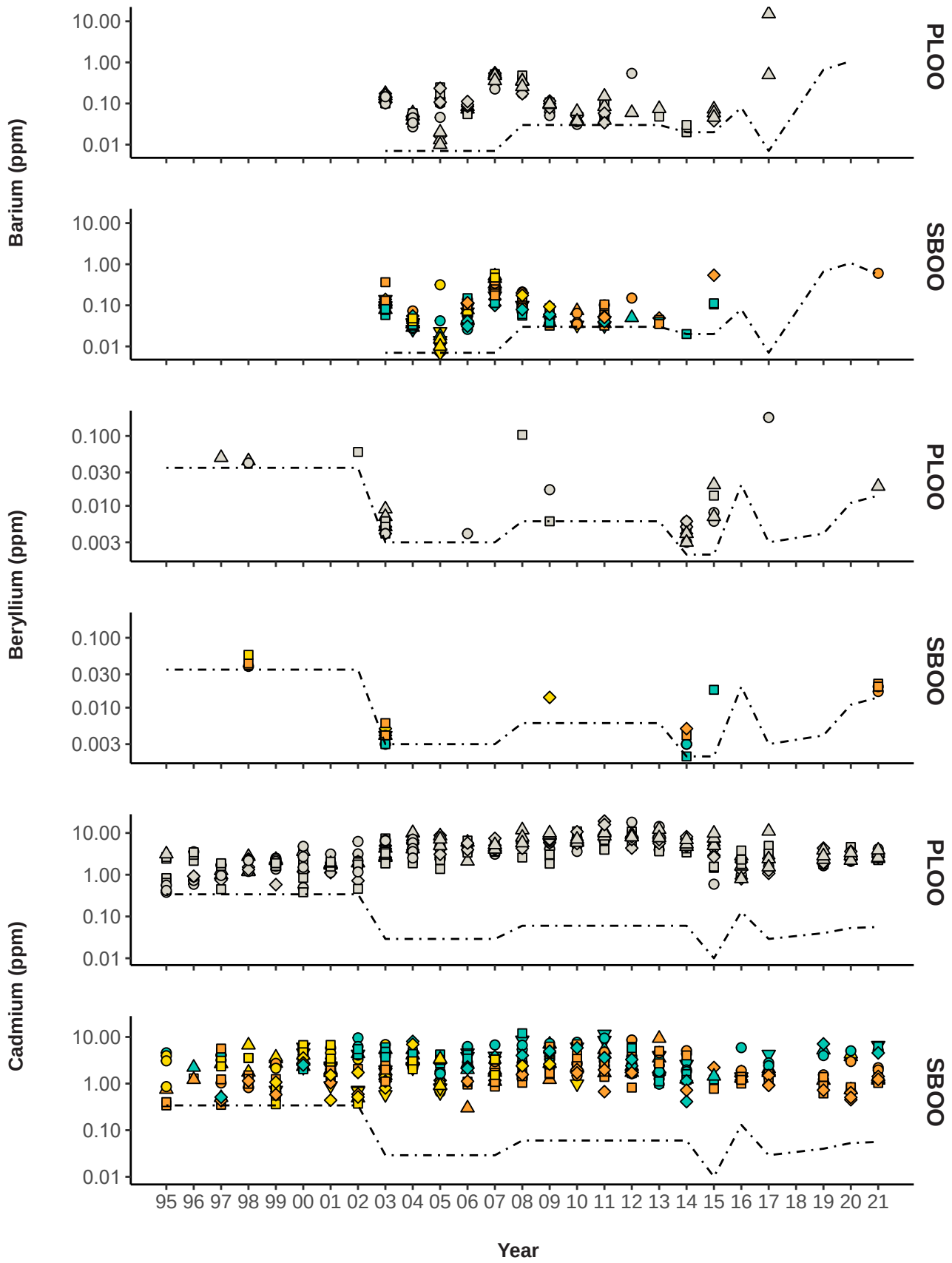

Appendix J.4 *continued*

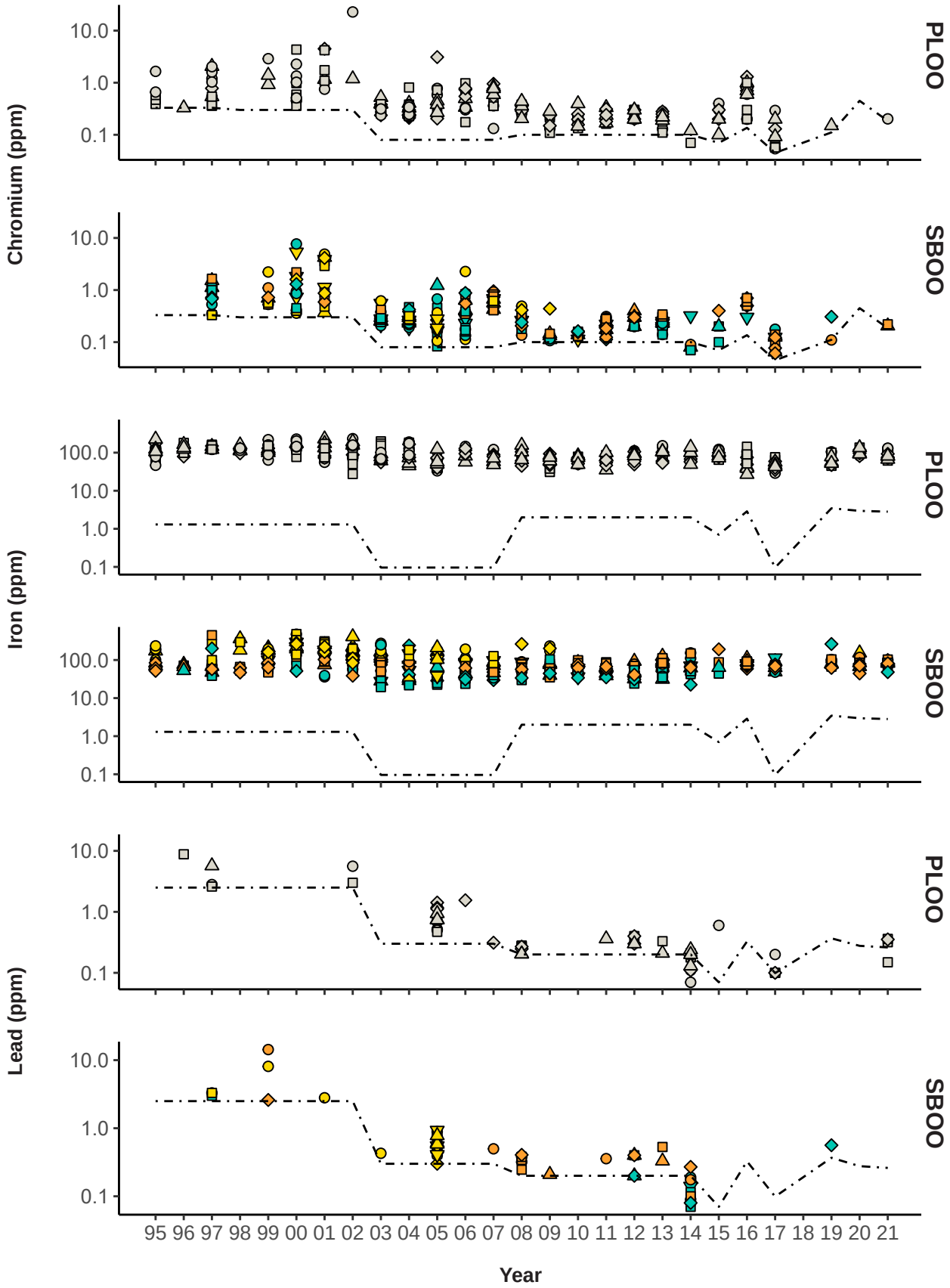

Appendix J.4 *continued*

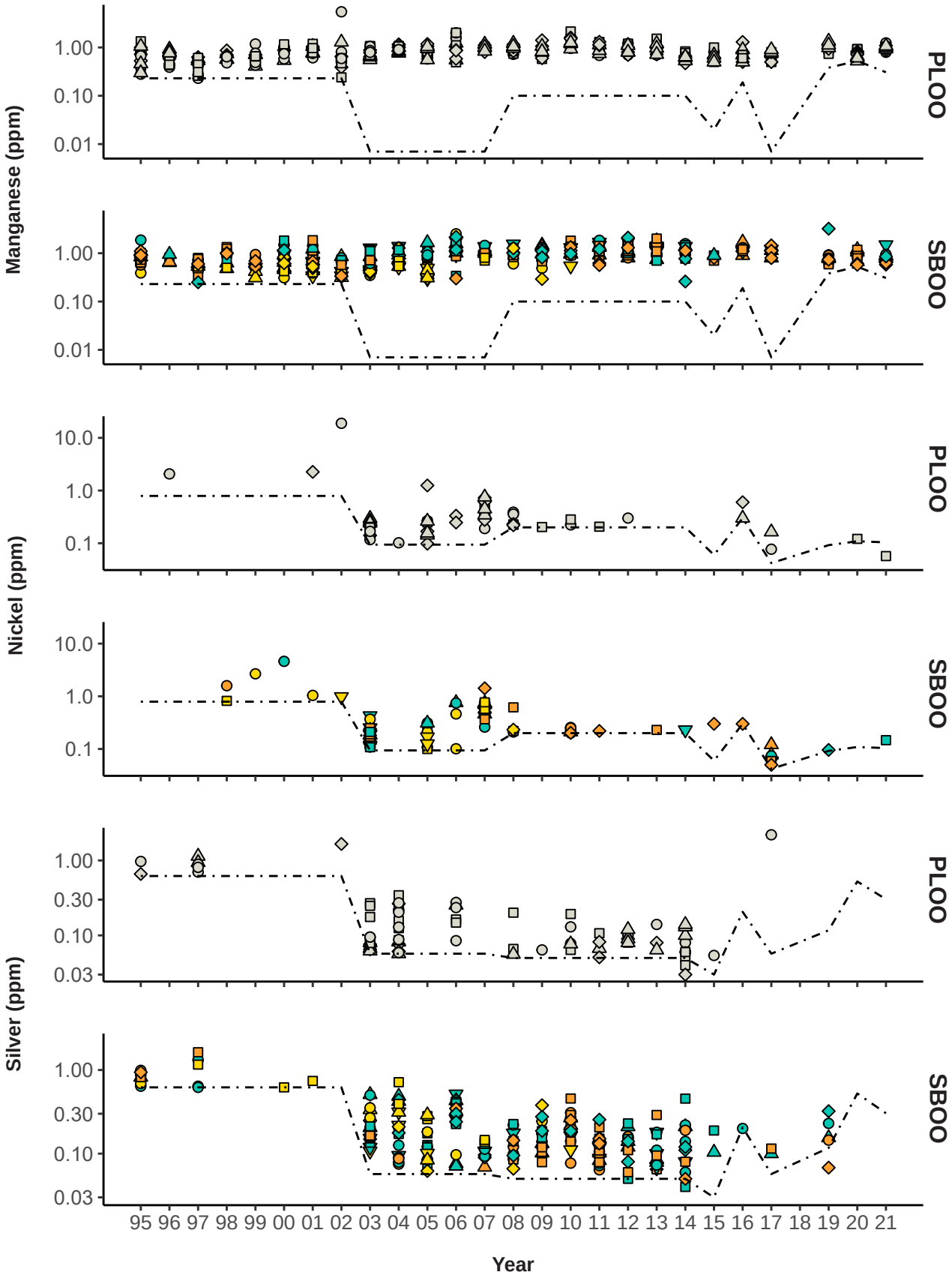

Appendix J.4 *continued*

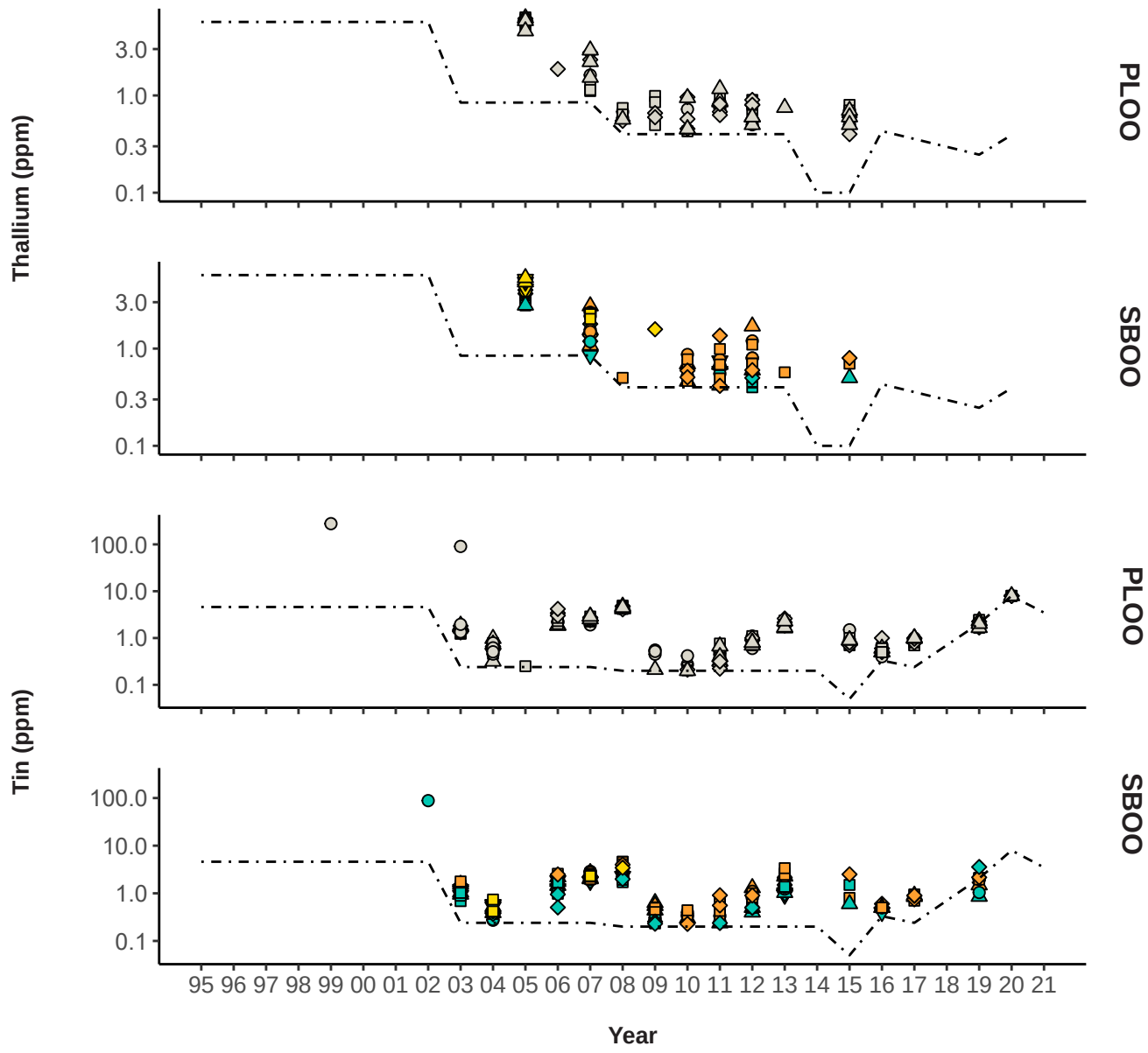

Appendix J.4 *continued*

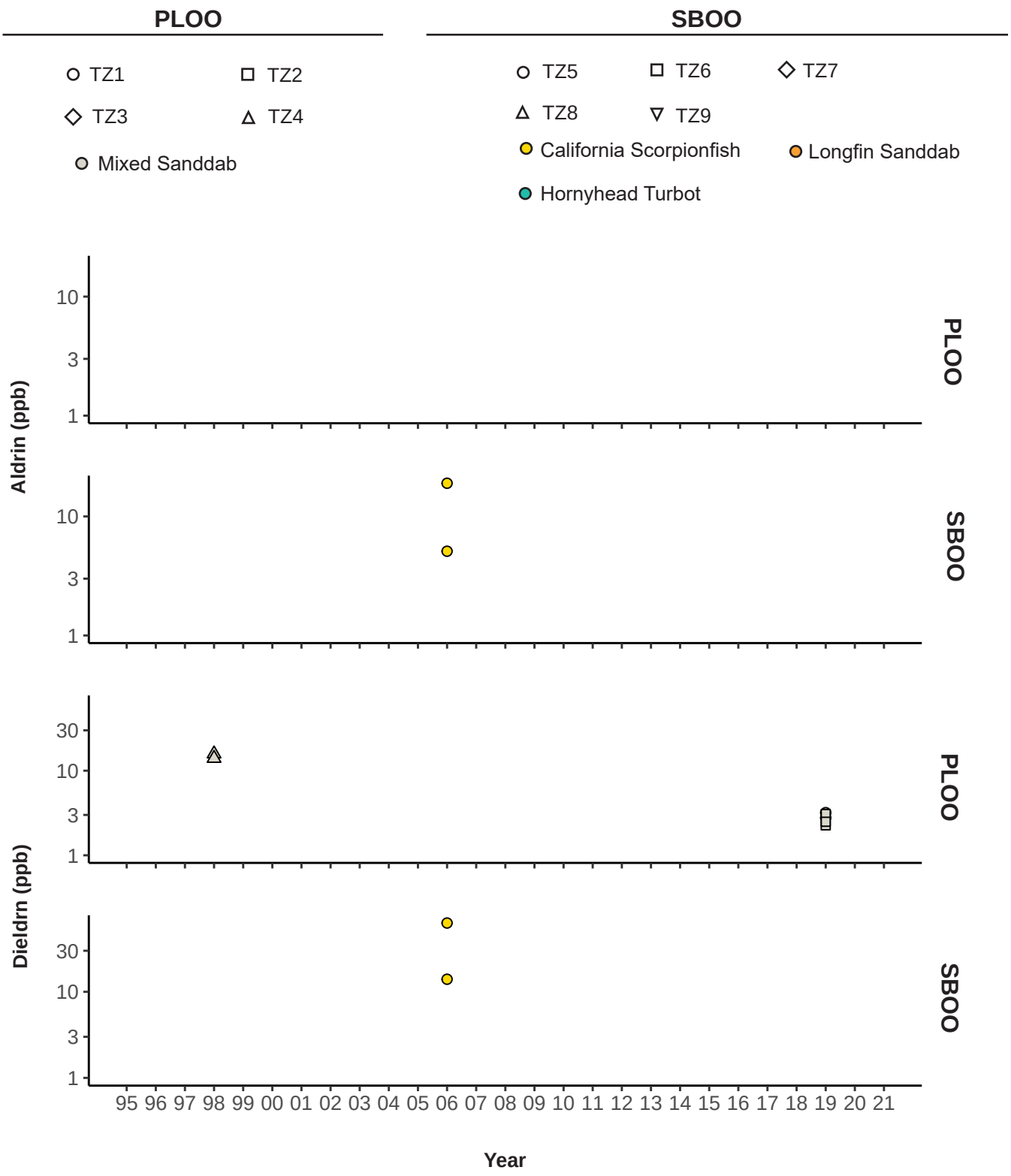

Appendix J.5

Concentrations of pesticides and total PAH in liver tissues of fishes collected from PLOO and SBOO trawl zones from 1995 through 2021. Zones TZ1 and TZ5 are considered nearfield. No samples were collected in 2018 as described in text.

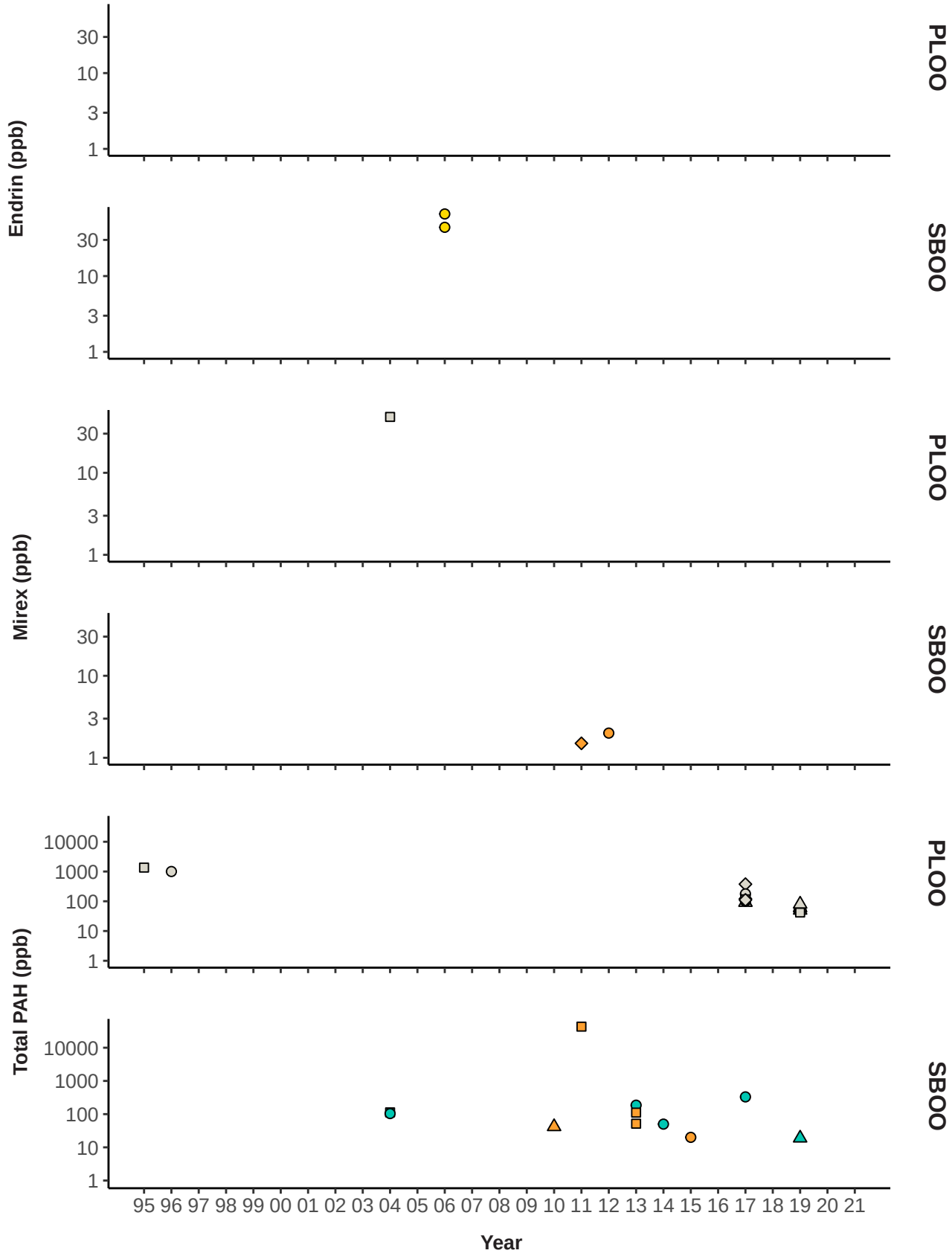

Appendix J.5 *continued*

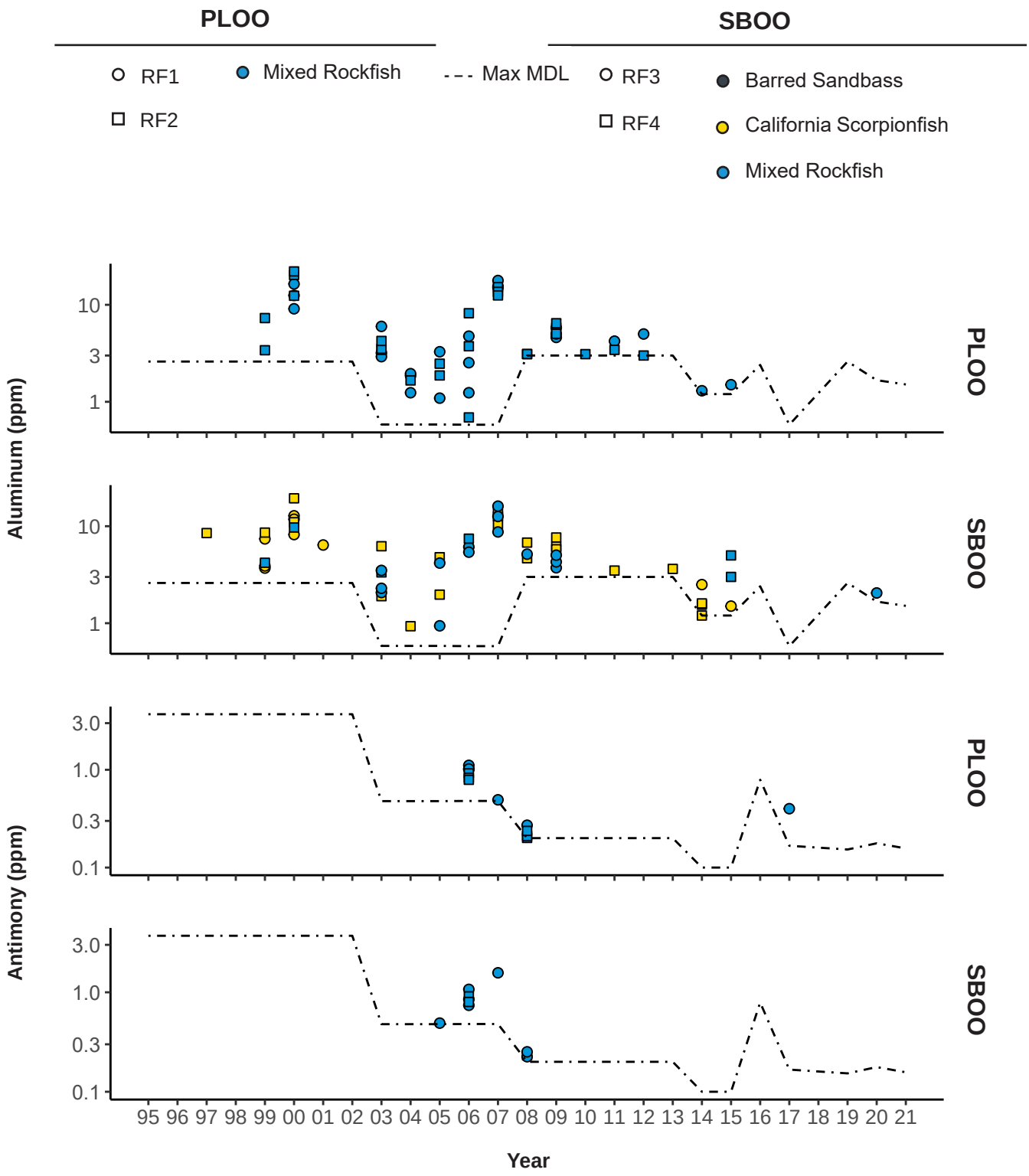

Appendix J.6

Concentrations of select metals in muscle tissues of fishes collected from PLOO and SBOO rig fishing zones from 1995 through 2021. Zones RF1 and RF3 are considered nearfield. No samples were collected in 2018 as described in text.

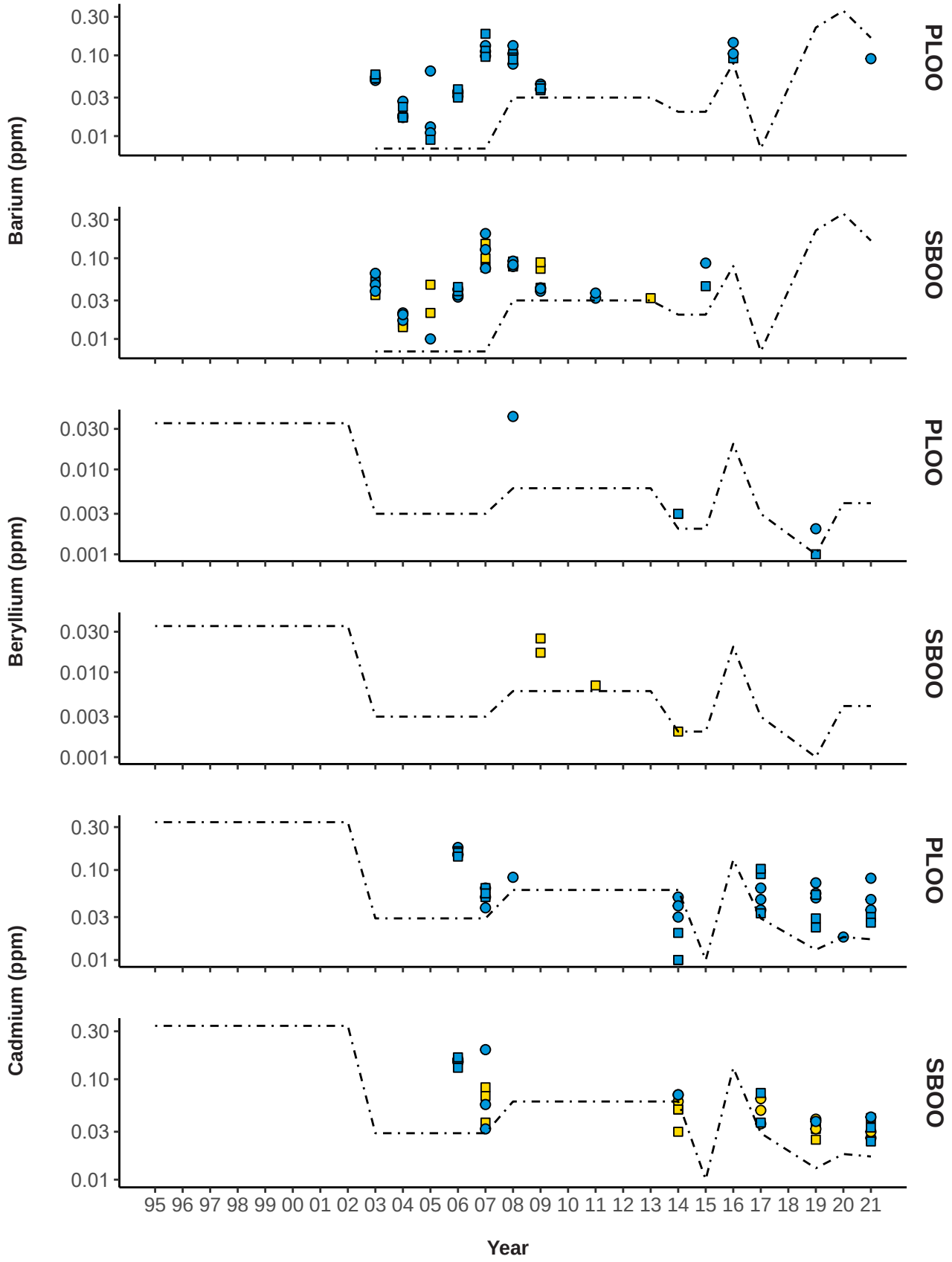

Appendix J.6 *continued*

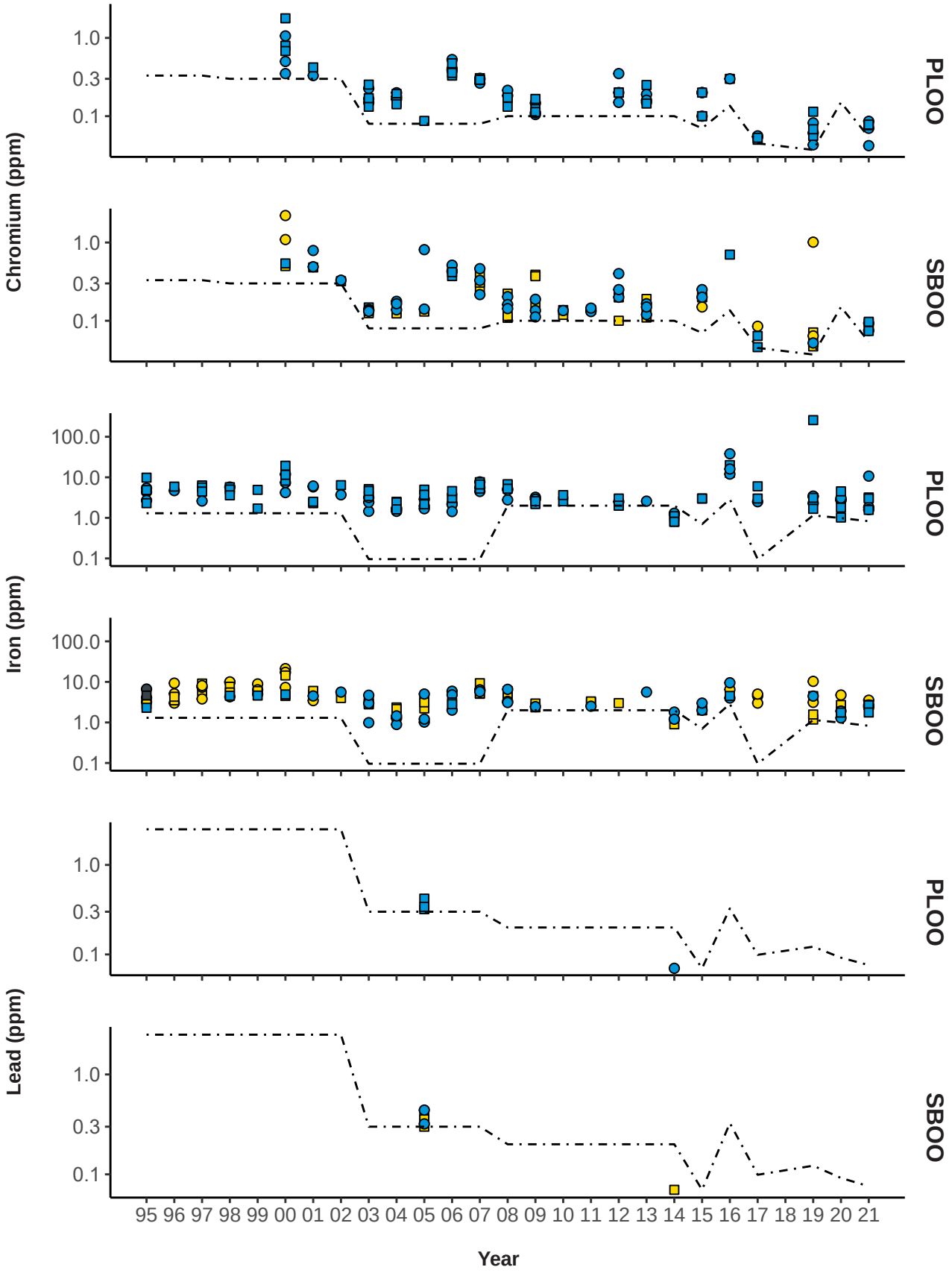

Appendix J.6 *continued*

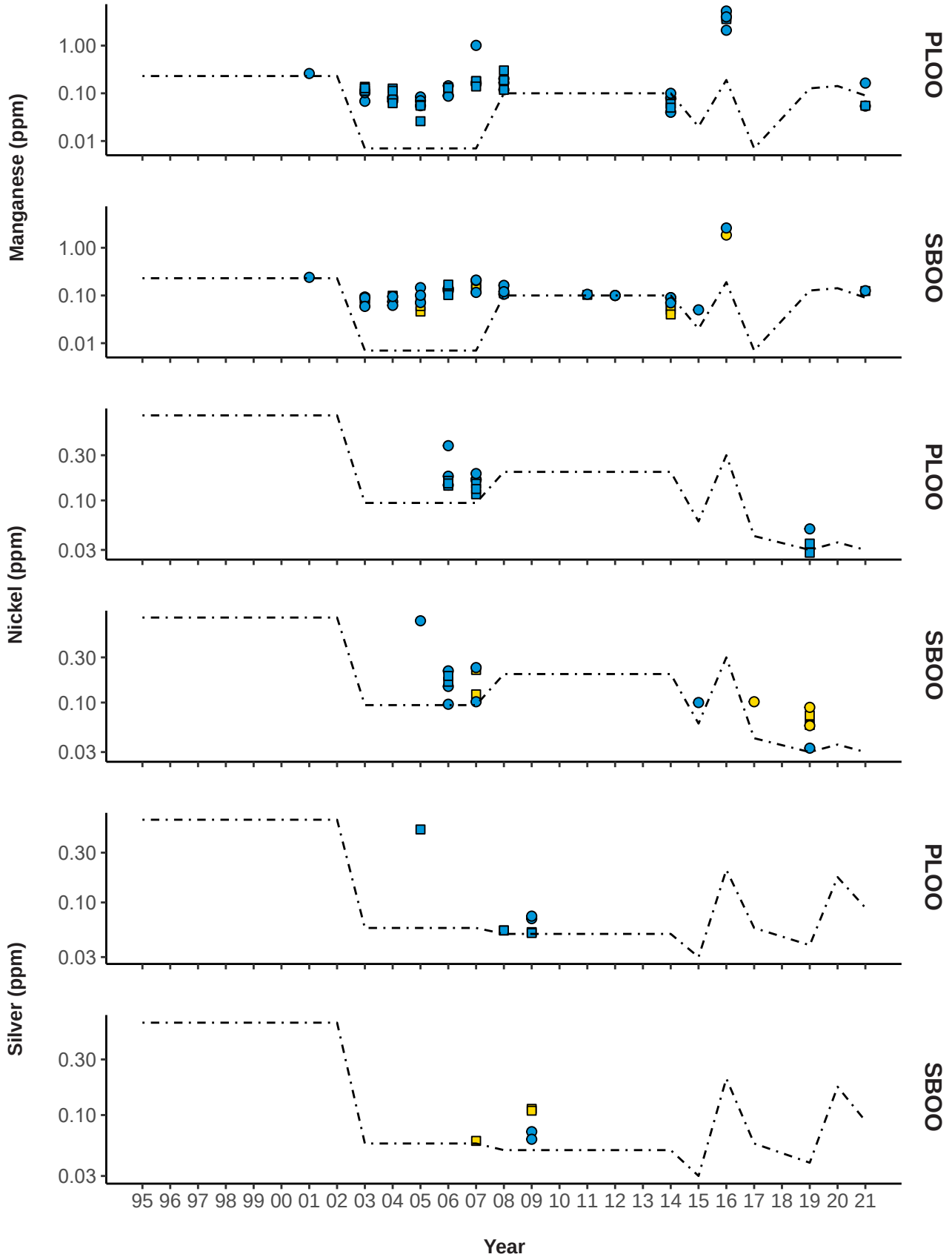

Appendix J.6 *continued*

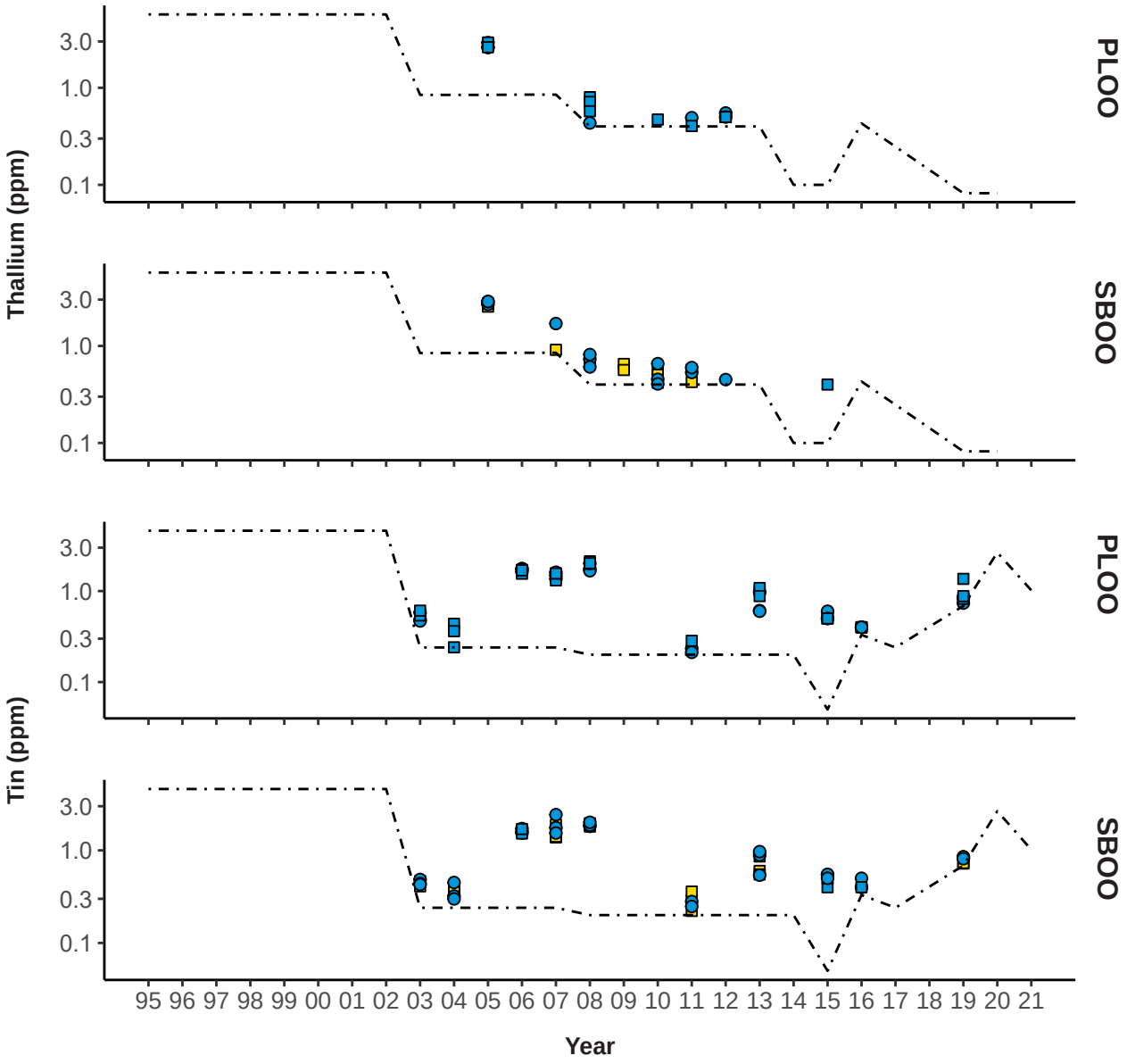

Appendix J.6 *continued*

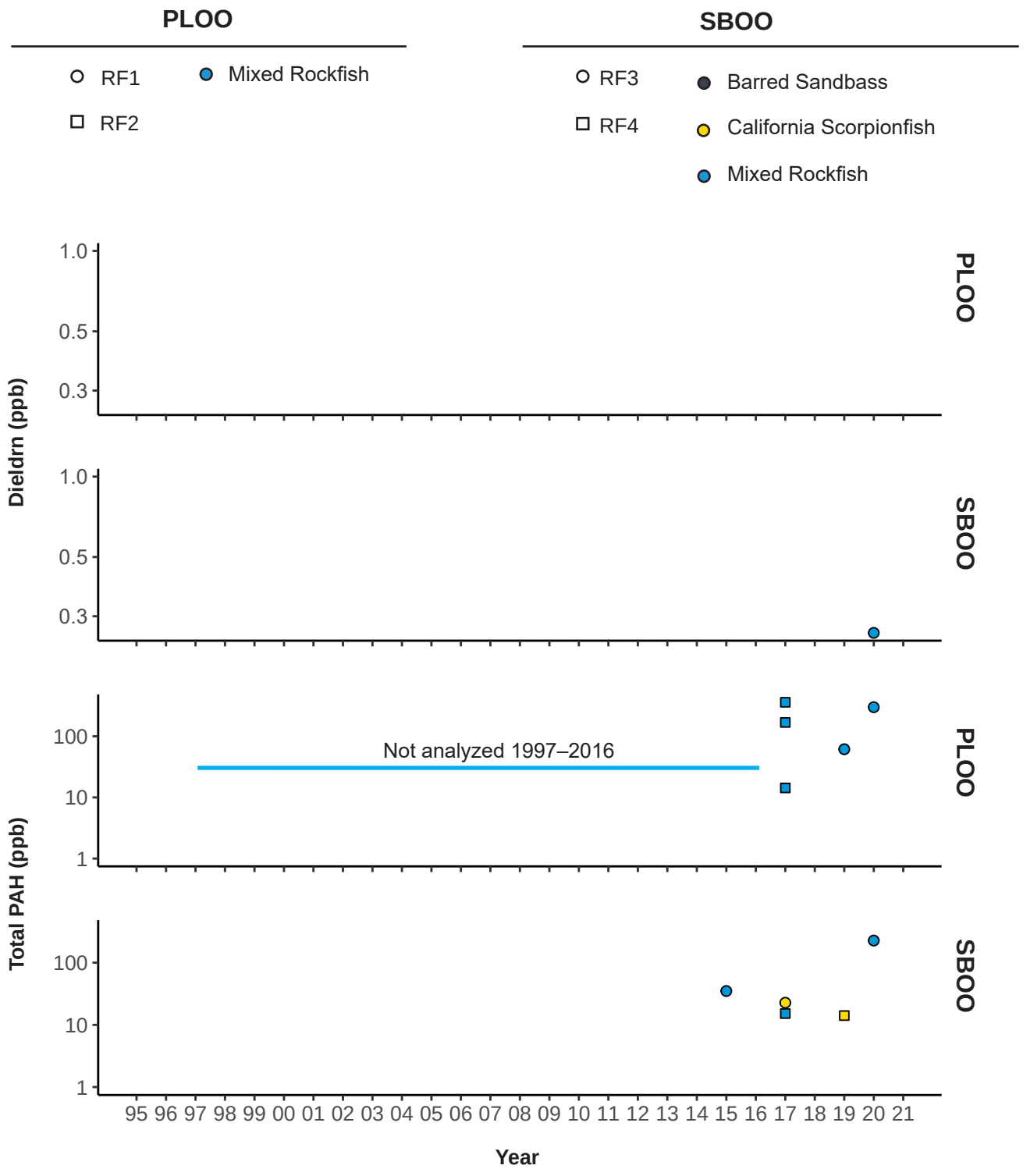

Appendix J.7

Concentrations of dieldrin and total PAH in muscle tissues of fishes collected from PLOO and SBOO rig fishing zones from 1995 through 2021. Analysis of Total PAH was not a permit requirement from 1997–2016. Zones RF1 and RF3 are considered nearfield. No samples were collected in 2018 as described in text.

This page intentionally left blank